9774-103-29

THE

LONDON, EDINBURGH AND DUBLIN

PHILOSOPHICAL MAGAZINE

AND

JOURNAL OF SCIENCE

CONDUCTED BY

SIR LAWRENCE BRAGG, O.B.E., M.A., D.Sc., F.R.S.
SIR GEORGE THOMSON, M.A., D.Sc., F.R.S.
AND
ALLAN FERGUSON, M.A., D.Sc.

> "Nec aranearum sane textus ideo melior quia ex se fila gignunt, nec noster vilior quia ex alienis libamus ut apes."
>
> JUST. LIPS. *Polit.* lib. i. cap. 1. Net.

VOL. XXXVI.—SEVENTH SERIES

JANUARY—DECEMBER 1945

LONDON:
TAYLOR & FRANCIS, LTD., RED LION COURT, FLEET STREET, E.C. 4.
Agents: WM. DAWSON & SONS, LTD., 129 CANNON STREET, E.C 4

"Meditationis est perscrutari occulta; contemplationis est admirari perspicua . . . . Admiratio generat quæstionem, quæstio investigationem, investigatio inventionem."—*Hugo de S. Victore.*

—— "Cur spirent venti, cur terra dehiscat.
Cur mare turgescat, pelago cur tantus amaror,
Cur caput obscura Phœbus ferrugine condat,
Quid toties diros cogat flagrare cometas,
Quid pariat nubes, veniant cur fulmina cœlo,
Quo micet igne Iris, superos quis conciat orbes
Tam vario motu."

J. B. Pinelli ad Mazonium.

ALERE FLAMMAM.

CONTENTS OF VOL. XXXVI. (Nos. 252–263)

(SEVENTH SERIES)

NUMBER 252—JANUARY

Page

I. On the Energy and Mechanical Relations of the Magnetic Field. By G. H. Livens 1

II. The Behaviour of Liquids in a Vibrating Air Column. By A. F. Howatson, M.A., Natural Philosophy Department, The University, Glasgow. (Plates I. & II.) 20

III. An Historical Note on a Paradox in Electrodynamics. By Ian A. Robertson, M.A., B.Sc., Assistant in Natural Philosophy in the University of Glasgow 32

IV. Construction of Groups of Commutative Functions. By Ludwik Silberstein, Ph.D. 43

V. Study of the Relative Intensities of Lines in Fibre X-ray Camera Photographs. By Professor E. A. Owen and Dr. I. G. Edmunds. (Plate III.) 54

VI. Direct Determination of Stresses from the Stress Equations in some Two-Dimensional Problems of Elasticity.—Part IV. Problems of Wedges. By Bibhutibhusan Sen 66

NUMBER 243—FEBRUARY

VII. The Measurement of Surface and Interfacial Tensions at Fresh Surfaces by the Vibrating Jet Method. By C. C. Addison, Ph.D., F.R.I.C. (Plate IV.) 73

VIII. Spin in the Universe. By Sir Edmund Whittaker, F.R.S. 101

IX. Kinematic Relativity. By R. A. Newing 113

X. On the Pseudo-Plastic State. By Walther Deutsch, F.Inst.P. .. 115

XI. Notes on the Evaluation of Zeros and Turning Values of Bessel Functions.—I. Introductory. By W. G. Bickley, D.Sc., Imperial College of Science and Technology, and J. C. P. Miller, Ph.D., University of Liverpool 121

XII. Notes on the Evaluation of Zeros and Turning Values of Bessel Functions.—II. The McMahon Series. By W. G. Bickley, D.Sc., Imperial College of Science and Technology, and J. C. P. Miller, Ph.D., University of Liverpool 124

Page

XIII. Notes on the Evaluation of Zeros and Turning Values of Bessel Functions.—III. Interpolation by Taylor Series. By W. G. Bickley, D.Sc., Imperial College of Science and Technology 131

XIV. Kinematic Relativity: a Reply to Prof. W. Wilson. By E. A. Milne, F.R.S. 134

XV. Comments on Dr. Silberstein's Paper in Phil. Mag., June 1944. 143

XVI. The Whipple Collection of Historic Scientific Instruments. By Allan Ferguson, M.A., D.Sc. 144

XVII. Notices respecting New Books:—

Five-figure Logarithm Tables 145

Prof. G. N. Watson's A Treatise on the Theory of Bessel Functions 146

Mathematical Tables and Other Aids to Computation 147

Mr. Erwin Schrödinger's What is Life? 147

Dr. Martin Davidson's From Atoms to Stars 149

Sound Insulation and Acoustics..................... 150

Mr. S. L. Green's An Introduction to Differential Equations.. 150

Mr. N. Ernest Dorsey's The Velocity of Light.............. 151

NUMBER 254—MARCH

XVIII. Ten Two-Dimensional Electrostatic Problems. By N. Davy, University College, Nottingham 153

XIX. On the Vectors and Invariants of Kinematic Relativity. By G. J. Whitrow 170

XX. Tension of Semi-Infinite Plate with Notched Boundary. By A. C. Stevenson..................... 178

XXI. Chance Effects and the Gaussian Distribution. By J. B. S. Haldane, F.R.S. 184

XXII. The Energies of Uniformly Accelerated Particles in a Gas. By Rev. G. D. Yarnold, M.A., D.Phil., University College, Nottingham 185

XXIII. Notes on the Evaluation of Zeros and Turning Values of Bessel Functions.—IV. A New Expansion. By J. C. P. Miller, Ph.D., and C. W. Jones, B.Sc., University of Liverpool 200

XXIV. Notes on the Evaluation of Zeros and Turning Values of Bessel Functions.—V. Checks. By W. G. Bickley, D.Sc., Imperial College, London, and J. C. P. Miller, Ph.D., University of Liverpool 206

XXV. Stresses in an Infinite Plate due to Isolated Forces and Couples acting near a Circular Hole. By Bibhutibhusan Sen 211

XXVI. Coefficients for Mid-Interval Numerical Integration with Central Differences. By Herbert E. Salzer 216

XXVII. A Note on the Charge produced by Spraying Liquids with a Jet of Air. By Dr. Gao Chih-En, Physics Dept., Fukien Union University, Shaown, China..................... 218

XXVIII. Heat Conduction in Semi-Infinite Cylinders. By J. W. Craggs, B.Sc. 220

XXIX. Gyroscopic Coupling Terms. By H. Jefferson 223

XXX. A Certain Multiple Integral. By Harold Simpson 224

NUMBER 255—APRIL

Page

XXXI. New Contributions to Interferometry. Part V.—New Multiple Beam White Light Interference Fringes and their Applications. By S. Tolansky, Ph.D., D.I.C., The University, Manchester. (Plate V.) 225

XXXII. New Contributions to Interferometry. Part VI.—White Light Fabry-Perot Fringes. By S. Tolansky, Ph.D., D.I.C., The University, Manchester. (Plate VI.) 236

XXXIII. The Stress Distribution in a Long Circular Cylinder when a Discontinuous Pressure is Applied to the Curved Surface. By C. J. Tranter, M.A., and J. W. Craggs, B.Sc. 241

XXXIV. Entropy and Irreversible Processes. By Dr. W. Ehrenberg. 250

XXXV. The Application of the Characteristic Equation of a Matrix to the Evaluation of the Range of Frequencies for which Currents are passed through networks with four or more terminals without attenuation. By H. V. Lowry 255

XXXVI. Spectrum of Radium (B+C) Gamma-Rays. By J. E. Roberts, D.Sc., F.Inst.P., Barnato Joel Laboratories, Middlesex Hospital. 264

XXXVII. Phase Space in Eddington's Theory. By A. J. Coleman .. 269

XXXVIII. The Electromotive Force of the Selenium Barrier-Layer Photo-Cell. By R. A. Houstoun, D.Sc., and A. F. Howatson, M.A., University of Glasgow 279

XXXIX. The Surface Tension of Molecular Solutions. By Henry McCormick 288

XL. On the Accumulation of Chance Effects and the Gaussian Frequency Distribution. By A. H. R. Grimsey 294

XLI. Notices respecting New Books :—

F. Emde's Tables of Elementary Functions 296

H. Brandenburg's Sechsstellige trigonometrische Tafel 296

NUMBER 256—MAY

XLII. The Magnetic Potentiometer Study of Permanent Magnets. By Professor L. F. Bates, University College, Nottingham 297

XLIII. The Probable Number of Aggregates in Random Distributions of Points. By Ludwig Silberstein, Ph.D. 319

XLIV. Aggregates in One- and Two-Dimensional Random Distributions. (Developability of Silver Specks of Known Dimensions and the Size of Photographic Sensitivity Specks.) By W. F. Berg 337

XLV. The Effect of Grain or Particle Size on X-ray Reflections from Mixed Powders and Alloys, considered in relation to the Quantitative Determination of Crystalline Substances by X-ray Methods. By G. W. Brindley, M.Sc., Ph.D., Physics Laboratories, University of Leeds 347

XLVI. Notices respecting New Books :—

Messrs. R. Belcher and A. L. Godbert's Semi-Micro Quantitative Organic Analysis 369

Messrs. A. W. Stewart and C. L. Wilson's Recent Advances in Physical and Inorganic Chemistry 370

NUMBER 257—JUNE

Page

XLVII. A new Type of Electrical Resonance. By ERICH E. SCHNEIDER, Dr.phil.nat., A.Inst.P. 371

XLVIII. Derivation of the Lorentz Transformations. By HERBERT E. IVES 392

XLIX. Computation of the Solution of Mathieu's Equation. By N. W. MCLACHLAN, D.Sc. 403

L. Second Note on Condensation in the Form of Clouds and Dew. By J. W. ARCHBOLD, M.A., University College, London 414

LI. On Thermal Stresses in Circular Cylinders. By J. C. JAEGER 418

LII. The Accumulation of Chance Effects and the Gaussian Frequency Distribution. By L. S. GODDARD, St. John's College, Cambridge 428

LIII. The Primary and Secondary Scattering of Sunlight in a Plane-stratified Atmosphere of Uniform Composition.—Part II. Numerical Tables and Discussion of the Directional Distribution of the Primary Scattered Light. By A. HAMMAD, Ph.D., Department of Applied Mathematics, The Egyptian University, Cairo 434

LIV. Systems with Gyroscopic Coupling Terms. By A. BLOCH 440

LV. Notices respecting New Books:—

Building Research Board's Report on the Lighting of Buildings . 441

ANSELM TALALAY and MICHEL MAGAT'S Synthetic Rubber from Alcohol 442

NUMBER 258—JULY

LVI. Compatibility of Stress and Strain in Yielded Metals By K. H. SWAINGER, Ph.D., B.Sc.(Eng.) 443

LVII. The Application of the Helmholtz Resonator to the Measurement of Sound Absorption. By W. S. TUCKER, D.Sc., A.R.C.Sc 473

LVIII. A Summary Statement of the Principles of Measurement. By D. P. DALZELL 485

LIX. The Behaviour of Liquids in Shear. By E. G. RICHARDSON, B.A., Ph.D., D.Sc. (King's College, University of Durham, Newcastle-upon-Tyne) 490

LX. Expansion in Series of the Exact Solution for Compressible Flow past a Circular or an Elliptic Cylinder. By A. R. MANWELL, now at Department of Mathematical Physics, Queen's University, Belfast 499

LXI. On the Theory of Light-Scattering.—A Note. By S. PARTHASARATHY, D.Sc., F.Inst.P., F.I.C. 510

LXII. Notice respecting New Book:—

The Advancement of Science (British Association) 514

NUMBER 259—AUGUST

LXIII. The Precision of Measurement of Broad Spectrum Lines, with Special Reference to Electron-Diffraction Photographs. By T. B. RYMER, Ph.D., and C. C. BUTLER, B.Sc., The University, Reading 515

Page

LXIV. Some Criticisms of the Theory of Point Electrons. By T. Lewis 533

LXV. Note on the Helmholtz Make-and-Break Theorem and an Application to the Wheatstone Net. By G. F. Freeman, M.Sc. (Eng.), M.I.E.E., A.M.I.Mech.E., of West Ham Municipal College 541

LXVI. Monochromatic Lens Aberration Theory. By H. H. Hopkins, Ph.D., F. Inst. P., W. Watson and Sons, High Barnet, Herts 546

LXVII. An Application of the Method of Finite Difference Equations to a Problem of Bending Moments.—Continuous Beam of N equal Spans under Transverse Loading and an Axial Force. By N. J. Durant 569

LXVIII. Struts of Variable Flexural Rigidity. By N. J. Durant 572

LXIX. A Relation between some Natural Constants and the Lesser Particles. By H. D. K. Drew 577

LXX. Drainage of a Vertical Plate. By George Wyllie, B.Sc., Assistant to the Professor of Applied Physics, Glasgow University 581

LXXI. Notice respecting New Book:—

C. W. Bunn's Chemical Crystallography 586

NUMBER 260—SEPTEMBER

LXXII. Calculations concerning Theoretical Values of Boundary-Layer Thickness and Coefficients of Friction and of Heat Transfer for steady Two-Dimensional Laminar Flow in an incompressible Boundary-Layer with Mainstream Velocity $U \propto x^m$ or $U \propto e^{ax}$. By J. G. Oldroyd, B.A., Trinity College, Cambridge 587

LXXIII. Heat Conduction in Elliptical Cylinder and an Analogous Electromagnetic Problem. By N. W. McLachlan, D.Sc. 600

LXXIV. An Expression for following the Process of Refinement in X-ray Structure Analysis using Fourier Series. By A. D. Booth 609

LXXV. Factorization of a Class of Determinants and Applications to Dynamical Chains. By W. J. Duncan, D.Sc., M.I.Mech.E., F.R.Ae.S., Wakefield Professor of Aeronautics at University College, Hull 615

LXXVI. On the Change in the Dielectric Constants of Liquids Flowing Through Narrow Separations. By B. N. Singh, D.Sc., and B. D. Singh, M.Sc. 622

LXXVII. A Note on the Equations of Plane Plastic Flow. By Ian N. Sneddon 629

LXXVIII. Quantum Equations and Nuclear Field Theories. By H. T. Flint, Professor of Physics, Bedford College, University of London 635

LXXIX. Switching Problems and Instantaneous Impulses. By J. C. Jaeger 644

LXXX. Theory of Ground-Water Accumulation. By H. Löwy, Dr.Phil. 651

LXXXI. Notices respecting New Books:—

Table of Arcsin x: prepared by the Mathematical Tables Project 657

A. Weissberger's Physical Methods of Organic Chemistry 658

NUMBER 261—OCTOBER

Page

LXXXII. The Buckling of Flat Rectangular Plywood Plates. By A. E. Green and R. F. S. Hearmon 659

LXXXIII. An Extension of Campbell's Theorem of Random Fluctuations. By R. S. Rivlin 688

LXXXIV. The Two-Dimensional Electric Field of a Single Semi-Infinite Rectangular Conductor. By N. Davy, University College, Nottingham 694

LXXXV. A Power Law of the Viscosity of Liquids. By W. J. Jones and S. T. Bowden 705

LXXXVI. Orientation Effect in Powder Photographs of Graphite. By J. B. Nelson and D. P. Riley, Crystallographic Laboratory, Cambridge. (Plate VII.) 711

LXXXVII. The Principal Directions of Loading and the Principal Directions of Forced Oscillation at a Point of an Elastic Body or System. By Prof. W. J. Duncan, D.Sc., M.I.Mech.E. 715

LXXXVIII. Crystalline Sheen of Moonstones. By B. V. Thosar, M.Sc., A.Inst.P., College of Science, Nagpur, India 719

LXXXIX. Notices respecting New Books:—

- Messrs. R. E. Burk and O. Grummitt's Frontiers in Chemistry 728
- Dr. E. I. Rabinowitch's Photosynthesis and Related Processes 728
- Tables of Associated Legendre Functions. Prepared by the Mathematical Tables Project 729
- Mr. F. B. Puddick's Currents in Aerials and High Frequency Networks 730

NUMBER 262—NOVEMBER

XC. Viscosity and the Hydrogen Bond. Hydroxyl and Ortho Effects. By J. Newton Friend and William D. Hargreaves 731

XCI. A Viscometer with Constant Working Volume suitable for Measurements over a Wide Range of Viscosities. By William D. Hargreaves, M.Sc. 756

XCII. Determination of the Electric Intensity near an Aerial Cage. By J. C. Simmonds, Ph.D., M.Sc. 758

XCIII. On the Solid Solutions of Chromium and Manganese in Aluminium. By G. V. Raynor, M.A., D.Phil., The Department of Metallurgy, The University of Birmingham 770

XCIV. The Behaviour of Glass under Impact and Static Loading. By R. N. Haward, B.Sc., Ph.D. (Plates VIII.–X.) 777

XCV. The Lattice Spacings of Lithium at 20° C. and $-183°$ C. By Kathleen Lonsdale, F.R.S., and William Hume-Rothery, F.R.S. .. 799

XCVI. Notices respecting New Books:—

- The Committee for the Calculation of Mathematical Tables: Circular and Hyperbolic Functions (B. A. Mathematical Tables, Vol. 1) 801
- Dr. Alexander Wood's The Cavendish Laboratory 802

NUMBER 263—DECEMBER

Page

XCVII. The Demagnetizing Factors for Ellipsoids. By EDMUND C. STONER, Sc.D., F.R.S., Professor of Theoretical Physics at the University of Leeds.......... 803

XCVIII. The Technique of Precise Electron-Diffraction Measurements with Polycrystalline Specimens. By T. B. RYMER, Ph.D., and C. C. BUTLER, B.Sc., The University, Reading. (Plate XI.)............ 821

XCIX. The Equilibrium Diagrams of Certain Alloys of Iron. By W. HUME-ROTHERY, F.R.S., and J. W. CHRISTIAN.............. 835

C. The Lattice Spacing of Rubidium between −183° C. and +19° C. By W. HUME-ROTHERY, F.R.S., and KATHLEEN LONSDALE, F.R.S. 842

CI. A New Form of Chart for Determining Temperature in Bodies of Regular Shape during Heating or Cooling. By A. J. EDE. (Low Temperature Station for Research in Biochemistry and Biophysics, University of Cambridge and Department of Scientific and Industrial Research.) .. 845

CII. A Closer Approximation to the Theory of the Field of Gerlach-Stern Magnets. By N. DAVY, University College, Nottingham 852

CIII. A Note on a Particular Type of Asymptotic Series. By R. A. RANKIN, Clare College, Cambridge 860

CIV. The Use of the Impedance Concept as Applied to Wave Guides. By GORDON WILLIAMS and H. C. BOLTON, King's College, London...... 862

CV. Notices respecting New Books:—
    BERTRAND RUSSELL's Physics and Experience................ 873
    The Advancement of Science. Vol. III., No. 11.............. 873

Index.. 875

PLATES

I. & II. Illustrative of Mr. A. Howatson's Paper on the Behaviour of Liquids in a Vibrating Air Column.

III. Illustrative of Prof. E. A. Owen and Dr. I. G. Edmund's Paper on the Relative Intensities of Lines in Fibre X-ray Camera Photographs.

IV. Illustrative of Dr. C. C. Addison's Paper on the Measurement of Surface and Interfacial Tensions at Fresh Surfaces by the Vibrating Jet Method.

V. Illustrative of Dr. S. Tolansky's Paper on New Contributions to Interferometry. Part V.—New Multiple Beam White Light Interference Fringes and their Applications.

VI. Illustrative of Dr. S. Tolansky's Paper on New Contributions to Interferometry. Part VI.—White Light Fabry-Perot Fringes.

VII. Illustrative of Messrs. J. B. Nelson and D. P. Riley's Paper on Orientation Effect in Powder Photographs of Graphite.

VIII.–X. Illustrative of Dr. R. N. Haward's Paper on the Behaviour of Glass under Impact and Static Loading.

XI. Illustrative of Dr. T. B. Rymer and Mr. C. C. Butler's Paper on the Technique of Precise Electron-Diffraction Movements with Polycrystalline Specimens.

THE

PHILOSOPHICAL MAGAZINE

A JOURNAL OF THEORETICAL EXPERIMENTAL AND APPLIED PHYSICS

First published in 1797

[SEVENTH SERIES—VOL. 36]

I. *On the Energy and Mechanical Relations of the Magnetic Field.*

By G. H. LIVENS*.

[Received April 26, 1944.]

1. THERE still seems to be considerable reluctance in many quarters to accept the, perhaps rather revolutionary, consequences of the logical development of the energy relations of the magnetic field. The apparent similarity in the form of the results relating to two quite distinct cases in the familiar forms of the discussion, and their general (but not complete) agreement with experience in the limited directions in which they have been tried, seem at first to disarm all criticism, and it is only occasionally that doubt has been cast on the validity of the familiar results. The persistent adherence to a supposed analogy with the electrostatic case, which does not exist, and to frequently fanciful analogies of the stress-strain type, which have introduced more confusion than they have saved, seem to have blinded to the real solution those few authors who were able to see clearly that there are anomalies in the usual discussion; and the usual dimensional treatment which starts by assuming—again on the basis of some supposed stress-strain analogy—that the nature of the vectors of force and induction in the field must be different, has perhaps not helped in any way to clear the air for a more satisfactory treatment.

Several recent discussions with friends and colleagues have helped me to clarify somewhat my own views on this subject, and have suggested a restatement of them in an amplified and perhaps improved form.

---

* Communicated by the Author.

2. In the usual treatment, when magnetism is first introduced statically, the *potential* energy associated with a field of intensity **H** is shown, usually by presuming an analogy with the dielectric case, to be the same as if it were distributed throughout the field with density $\mu\mathbf{H}^2/8\pi$, at least when the induction follows a linear isotropic law. And the energy so defined is such that the mechanical body forces on the magnets, acting to counterbalance the magnetic attractions and to maintain the static field, tend to move the magnets in directions in which their energy increases, the work done by the forces adding to the store. Thus this measure of the energy, properly interpreted, serves also as a potential function from which these applied forces can be derived by differentiation.

On the introduction of linear currents with their associated magnetic fields no attempt is ever made to revaluate the energy in the field, the formula $\mu\mathbf{H}^2/8\pi$ being assumed without further question to define the density of its distribution. And in the absence of permanent polarity the total defined by this distribution is then shown to be equivalent to the familiar expression

$$\frac{1}{2c}\Sigma(\mathrm{L}_{ss}i_s^2+2\mathrm{L}_{rs}i_ri_s)$$

in terms of the currents i_s and the coefficients L_{ss}, L_{rs} of self and mutual induction of the circuits. Now, however, it is found that the mechanical forces on the currents, applied to balance the magnetic attractions between them, tend to move the circuits in the directions in which the energy decreases, so that now it is the negative value of this energy which serves as the potential function of the applied forces.

This different relation of the same energy function to the body forces in the two cases does not seem to create any surprise, much less criticism, although it clearly suggests inconsistency somewhere, as one or two authors have suggested. It leads, for example, to the anomaly that, when a current and a magnet exist together in the same field, the force on the magnet exerted by the current tends to increase the energy, whilst the equal and opposite reactions on the current would tend to decrease it.

3. The underlying cause of the discrepancy is not, however, far to seek. It is involved in the change of ideas which accompany the gradual development of the theory and which are never adequately regarded in their influence on the discussions. When first introduced, on the electrostatic analogy, magnetic forces are quite legitimately regarded as the end aspects of a state of stress in the surrounding aethereal field, so that naturally we associate with them a potential energy function representing energy of something like elastic stress; and the calculation of this energy, using the potential (energy) function of the field from which its intensity derives, conforms to this view of the energy as potential energy.

Later on in the discussions, however, when it is found that magnetic fields are equally, if not essentially, the accompaniment of electric flow, a more detailed picture becomes necessary, in which the energy of the magnetic field appears as an integral part of the kinetic energy of the electric motions involved in the currents and polarizations. But this change of ideas involves another important consequence which is usually overlooked in these discussions. In its original conception the potential energy of the static field is determined as the function associated with the forces on the masses in the field, and the fact that it is conserved with other mechanical types of energy is taken more or less for granted. This procedure is, of course, quite justifiable and cannot lead to inconsistencies. But at a later stage, when magnetism is shown to be a kinetic affair of the currents, the transfer of the formula for the energy is made without realising that an entirely different conception is now necessary and, what is perhaps more important, that a distinction must now be made between the energy function as a force function and the energy as an entity which enters into the conservation principle.

4. Once it is assumed that the energy of the magnetic field is, at least in part, kinetic, the whole discussion—as Maxwell shows quite clearly—of the mechanical and electrical relations of the field must be based on more involved principles, on the lines of Lagrange's method in dynamics, before a complete picture can be obtained. The principle of energy ceases to be even nearly sufficient for our purposes.

On Lagrange's method, when a mechanical system with co-ordinates $q_1, q_2, \ldots, q_n$ is in motion with kinetic energy T and potential energy V, under the influence of externally applied forces $Q_1, Q_2, \ldots$ in these co-ordinates, the relations between the forces and energies are

$$Q_s = \frac{d}{dt}\left(\frac{\partial L}{\partial \dot{q}_s}\right) - \frac{\partial L}{\partial q_s}, \quad s=1, 2, \ldots n,$$

where $L = T - V$ is the kinetic potential or Lagrangian function of the system, the excess of the kinetic over the potential energy.

In our electromagnetic discussions the determination of L is always, in the first instance, made for a statical system, at least as far as the palpable material co-ordinates are concerned. For such a co-ordinate the general equation of Lagrange reduces to

$$Q_s = -\frac{\partial L}{\partial q_s},$$

so that the work done by the mechanical forces in any small displacement of the system, viz.

$$\Sigma Q_s \delta q_s = -\Sigma \frac{\partial L}{\partial q_s} \delta q_s = -\delta L$$

is equal, not directly to the variation of either the potential or kinetic energy of the system, but rather to the variation $-\delta L$ of the Lagrangian function (with the negative sign), or at least that part of it which is concerned with the geometrical co-ordinates, which is the only part with which we are really concerned.

Of course, if we know definitely that the energy is entirely of the potential type or that $L = -V$, then

$$\Sigma Q_s \delta q_s = \delta V,$$

and the external forces may thus be said to act to increase V. Whilst if, on the other hand, the energy is entirely kinetic or L=T, then

$$\Sigma Q_s \delta q_s = -\delta T,$$

and the external forces thus tend to decrease T. The operations of the forces in the two cases mentioned in paragraph 2 are, therefore, quite properly related to the energies of the field if in the first case the energy is assumed to be potential and in the second case to be kinetic. But the satisfaction caused by this agreement is dispelled at once by a realization of the fact that in transferring energy from the first case, where it is potential, to the second, where it is kinetic, complete dynamical consistency can only be obtained when a change of sign accompanies the transfer. In fact, as the forces depend ultimately on the Lagrangian function L, the inclusion of a particular measure of the energy in T and its inclusion in V can only give the same forces if opposite signs are attached to the measure in the two cases.

5. The freedom to call energy kinetic or potential as we choose may be readily granted—what is in a name, after all?—but it would appear at first sight that the necessity for changing the sign when the designation is altered can hardly conform to the fundamental principle of conservation which is a necessary implication of the whole concept of energy. A closer examination will, however, show that the whole procedure is consistent not only with the principle of energy but with the more general principles of which it is the outcome.

From the general equations of motion in Lagrange's form we derive at once, by multiplication by $\dot{q}_s$ and addition over all the co-ordinates, the equation of energy in the form

$$\begin{aligned}\Sigma Q_s \dot{q}_s &= \Sigma \frac{d}{dt}\left(\frac{\partial L}{\partial \dot{q}_s}\right)\dot{q}_s - \Sigma \frac{\partial L}{\partial q_s}\dot{q}_s \\ &= \frac{d}{dt}\left(\Sigma \dot{q}_s \frac{\partial L}{\partial \dot{q}_s}\right) - \Sigma\left\{\frac{\partial L}{\partial \dot{q}_s}\ddot{q}_s + \frac{\partial L}{\partial q_s}\dot{q}_s\right\} \\ &= \frac{d}{dt}\left\{\Sigma \dot{q}_s \frac{\partial L}{\partial \dot{q}_s} - L\right\}.\end{aligned}$$

when L does not contain the time explicitly. But if, as is usually the case in all elementary problems, L divides itself naturally into two parts, the first T which is a homogeneous quadratic function of the velocities, and the second V, which is independent of these velocities, then we know that

$$\Sigma \dot{q}_s \frac{\partial L}{\partial \dot{q}_s} = 2T,$$

so that the equation of energy reduces to

$$\Sigma Q_s \dot{q}_s = \frac{d}{dt}(T+V),$$

expressing that the rate of working of the external forces is fully accounted for by the growth of the total energy, kinetic plus potential.

In certain problems, however, we have to deal with a more general case where L divides itself into three parts

$$L=L_0+L_1+L_2,$$

L_2 being a homogeneous quadratic function of some or all of the velocities, L_1 a homogeneous linear function of these same velocities, and L_0 a part independent of the velocities. In this general case it is not difficult to see that

$$\Sigma\dot{q}_s\frac{\partial L}{\partial\dot{q}_s}-L=L_2-L_0,$$

so that the equation of energy now assumes the form

$$\Sigma Q_s\dot{q}_s=\frac{d}{dt}(L_2-L_0),$$

and now the work of the external forces is accounted for by the growth of a total energy, including kinetic energy of amount L_2 and potential energy of amount $-L_0$. The interesting point is that the term L_1 in the Lagrangian function—an integral part of one of the energies—has no influence on the conservation principle.

If in this last case L_1 and L_2 both belong to the kinetic energy and L_0 to the potential energy, then $L_2+L_1=T$ and $L_0=-V$, but we might equally imagine that the whole or any part of T, with the opposite sign, was counted as potential energy ; or the whole or any part of V, with the opposite sign, as kinetic energy ; if each part carries its appropriate sign the function L is unaltered and the equation of motion and of energy will be unaffected.

This last remark illustrates clearly the sort of difficulties and uncertainties that beset any interpretation of any particular measure of energy as kinetic or potential. We know from the physical interpretation of Routh's process of modifying the Lagrangian function by the ignoration of some of the co-ordinates of the system that any assumption as to the character of any particular part of the total energy of the system is purely arbitrary and in a way quite gratuitous. In any calculation of the kinetic and potential energies of a mechanical system there is, in fact, no guarantee that some assumption has not been made which is equivalent to the ignoration of certain unknown or unspecified co-ordinates, resulting in the partial conversion of some of the associated kinetic energy to the potential type, with the necessary reversal of sign ; the assumption, for example, to be made later, of the existence of permanent magnetic polarity is probably of this type. Fortunately, however, the equations of motion and energy are independent of any such assumptions, and all that matters is the determination of the Lagrangian function which defines the proper motions in the palpable co-ordinates. It is true, of course, that under certain conditions the Lagrangian function L itself will be identical with the kinetic energy of the system, whilst under others it will, with the reversed sign, be identical with the potential energy, but we may regard these merely as irrelevant accidents of interpretation.

6. The whole of this discussion seems, however, almost to be belied by the fact that an energy function which determines quite properly the *potential* energy of the magnetic field in the simple case, when the field is due to permanent magnets alone, proves equally suitable when used, without reversal of sign, for the *kinetic* energy function when the field arises from linear currents. But energy cannot be at the same time both kinetic and potential, and there is the problem of its character when there are both permanent magnets and currents in the field.

This difficulty is, however, resolved at once if simple and independent calculations are made in the two cases of the energy as a force function, as distinct from the energy which enters into the conservation principle. It will then be seen that:

(i) While the formula $\mu\mathbf{H}^2/8\pi$ for the density of the energy in the simple static cases does determine correctly the total potential energy of the field which can be used as a force function when there are no currents, it is not by any means the only formula which satisfies this condition. We know, in fact, that in the absence of finite currents from the field, the integral

$$\int(\mathbf{BH})\,dv,$$

when taken over the field is zero. It follows, therefore, that we can redistribute the energy without in any way altering its total by adding or subtracting from the density $\mu\mathbf{H}^2/8\pi$ at each place any multiple of $(\mathbf{BH})$. In particular the density

$$\frac{1}{8\pi}\mu\mathbf{H}^2-\frac{1}{4\pi}(\mathbf{BH})$$

gives exactly the same total as the original formula for the potential energy associated with the field.

(ii) When the field is due at least in part to finite linear currents the distribution of energy, still regarded as potential, cannot properly be represented by the density $\mu\mathbf{H}^2/8\pi$, but is in fact represented by

$$\frac{1}{8\pi}\mu\mathbf{H}^2-\frac{1}{4\pi}(\mathbf{BH}),$$

the formula quoted in (i) above.

Since
$$\mathbf{B}=\mu\mathbf{H}+4\pi\mathbf{I}_0,$$

where $\mathbf{I}_0$ represents the intensity of the permanent polarity, the new formula for the potential energy density is equivalent to

$$-\frac{1}{8\pi}\mu\mathbf{H}^2-(\mathbf{I}_0\mathbf{H}),$$

so that in parts of the field where $\mathbf{I}_0=0$ it agrees with the previous result except that it has the opposite sign consistent with its interpretation as potential energy.

(iii) Assuming that this new formula, with the reversed sign, gives on integration the appropriate Lagrangian function for the system, it will be proved that the part of the energy which enters into the conservation principle is of such amount that it may be regarded as distributed through the field with a density $\mu\mathbf{H}^2/8\pi$ in all cases, at least when the induction follows the linear isotropic law. This accounts for the fact that conclusions derived by the use of this formula have not in fact proved to be inconsistent with the energy principle. It is only in connection with the derivation of the force that troubles have arisen.

It will also appear, in accordance with the hints given in the general dynamical discussions above, that the conserved energy of the magnetic field contains no part of the mutual energy of the permanent magnets and currents. This is the explanation of the astonishing conclusion drawn in some books that the mutual energy of a rigid magnet and a current is zero, a result derived by using the conserved energy as a Lagrangian function.

7. Before proceding to the actual analysis we must, however, justify by one further remark the methods which we propose to adopt and the conclusions which we shall ultimately draw from them. Some readers may find some difficulty in distinguishing between the energy equation

$$\Sigma \mathrm{Q}_s\dot{q}_s=\frac{d}{dt}(\mathrm{T}+\mathrm{V}),$$

which when multiplied by *dt* seems to take the form

$$\Sigma \mathrm{Q}_s\,dq_s=d(\mathrm{T}+\mathrm{V})$$

and the equation of virtual work

$$\Sigma \mathrm{Q}_s\delta q_s=-\delta \mathrm{L}.$$

The difference between these two is really of the essence of Lagrange's method, distinguishing as it does between a general *virtual* displacement, typified by δq_s, which is restricted only in so far as it must be consistent with the geometrical conditions of the system at the moment under consideration, and the actual displacement dq_s undertaken by the system in the next small stage of its motion.

In the virtual work equation the δq's are a series of quite arbitrary and independent variations, so that in reality the equation itself is equivalent to as many different equations of the type

$$\mathrm{Q}_s=-\frac{\partial \mathrm{L}}{\partial q_s}$$

as there are independent co-ordinates, which are, however, for some purposes conveniently grouped together in the one general equation. In the equation of energy, on the other hand, the dq's are definite variations resulting from a specified motion of the system, and there is therefore no question of their independence or therefore also of the equation itself being capable of resolution into a series of equations of the type

$$\mathrm{Q}_s=\frac{\partial}{\partial q_s}(\mathrm{T}+\mathrm{V}).$$

Moreover, in the equation of energy every conceivable co-ordinate must be represented, whereas in the equation of virtual work it is only necessary to retain those that interest us, the others being eliminated by taking the corresponding variations, which can be chosen at will, to be zero. This remark is important because it implies that in the present problems we must, in forming the energy equation, take complete account of the applied forces acting not only in the material co-ordinates (mechanical forces of ordinary type) but also those acting in the electrical co-ordinates as well (electromotive forces), whereas the latter are quite unnecessary for the determination of the relevant part of the Lagrangian function.

We thus see that the virtual work method determines in the first place merely the Lagrangian function of the system, and this is all it can in fact determine. The conserved energy is then represented by a subsidiary function derivable in a definite and prescribed manner from this Lagrangian function, and not directly from the virtual work equation unless it is certain that this equation contains terms representative of all the forces acting either directly or indirectly on the system.

In our analysis we shall equate to the sum $\Sigma Q_s \delta q_s$, relating only to the externally applied mechanical forces the variation of the field function which results from a completely arbitrary change in the distribution of the masses giving rise to the field; the result must therefore include the possibility of any arbitrary set of changes in the material co-ordinates q_s (in which there are no finite velocities) interpreted, of course, as changes in the field distribution; it is therefore the change in the part of L, the Lagrangian function, which is concerned with these material co-ordinates, which is all that we are really concerned with, that is determined. The conserved energy will then be determined after proper interpretation of L by the procedure outlined above.

8. We commence then by proving the formulæ of paragraph 6. For this we adopt a familiar procedure in calculating the relevant part of the Lagrangian function or kinetic potential L as the negative integral of the work done by the external forces in building up the system from infinite dispersion in a completely arbitrary manner. In actual fact the variation of L as we have defined it is the variation of this function when the completed system undergoes a small virtual displacement—in a small variation of the geometrical co-ordinates—but this is the same as the variation of the function to be calculated. In fact, in the complete cycle starting from infinite dispersion, building up the system to state 1, moving it then to state 2 and then finally dispersing it to infinity again, a zero total of work will be done on the whole so that in an obvious notation

$$W_1+\Sigma Q_s \delta q_s - W_2 = 0,$$

assuming reversibility, of course, and the impossibility of perpetual motions. Thus

$$\begin{aligned}\Sigma Q_s \delta q_s &= W_2 - W_1 = \delta W\\ &= -\delta L\end{aligned}$$

as stated.

We determine then the function W associated with two simple static magnetic fields. In the first of these (*a*) we assume that the static field is due solely to a distribution of permanent polarity $\mathbf{I}_0$ accompanied perhaps by certain induced polarity $\mathbf{I}$. In the second (*b*) we assume that there is, in addition to this distribution of polarity, also a series of circuits the typical one of which carries a current i_s and encloses induction N_s. We use **B** and **H** in their usual significance and assume as usual in the first case (*a*), where **H** is derived from an acyclic potential, that

$$\int(\mathbf{BH})\,dv=\int(\mathbf{B}\delta\mathbf{H})\,dv=\int(\mathbf{H}\delta\mathbf{B})\,dv=0,$$

where the integrals are extended over the whole field. In case (*b*), on the other hand, where the potential is cyclic with respect to each finite current circuit, we have

$$\frac{1}{4\pi}\int(\mathbf{HB})\,dv=\frac{1}{c}\Sigma i_s N_s. \quad \frac{1}{4\pi}\int(\mathbf{B}\delta\mathbf{H})\,dv=\frac{1}{c}\Sigma N_s\delta i_s.$$

Let us now build up the system in small stages and calculate the work done by the external forces in each stage; simple addition or integration will then give the complete result. We consider then the steps which involve bringing up to each point of the field additional permanent polarity $\delta\mathbf{I}_0$ and, in addition in case (*b*), bringing up to each circuit an additional current filament δi_s; in both cases the induced polarity is assumed to take its appropriate value as the field is built up. In case (*a*) then work is done on the system of amount

$$\delta W=-\int(\mathbf{H}\delta\mathbf{I}_0)\,dv,$$

being that required to bring from infinity the polarity $\delta\mathbf{I}_0$ against the action of the magnetic forces on the constituent bi-poles. In case (*b*) additional work is required to bring up the current filaments δi_s, and this amounts to

$$-\frac{1}{c}\Sigma N_s\delta i_s=-\frac{1}{4\pi}\int(\mathbf{B}\delta\mathbf{H})\,dv,$$

representing work done by the reactions to the attractions on the filaments by the field as they move up. In this more general case then

$$\delta W=-\int(\mathbf{H}\delta\mathbf{I}_0)\,dv-\frac{1}{4\pi}\int(\mathbf{B}\delta\mathbf{H})\,dv,$$

the result in the first case being identical with this when the second term due to the currents is zero.

As the conditions are statical in so far as the masses containing the polarizations and currents are concerned, the work done in this stage of the process of building up results in a corresponding diminution of the kinetic potential or Lagrangian function, so that

$$\delta L=\int(\mathbf{H}\delta\mathbf{I}_0)\,dv+\frac{1}{4\pi}\int(\mathbf{B}\delta\mathbf{H})\,dv.$$

9. The rest of the argument now depends on the process adopted for separating the complete function L into its two parts, magnetic and molecular. The usual procedure is to write

$$\delta\mathbf{I}_0 = \frac{1}{4\pi}(\delta\mathbf{B} - \delta\mathbf{H}) - \delta\mathbf{I},$$

and then in (a)

$$\delta L = \frac{1}{4\pi}\int(\mathbf{H}\delta\mathbf{B})\,dv - \frac{1}{4\pi}\int(\mathbf{H}\delta\mathbf{H})\,dv - \int(\mathbf{H}\delta\mathbf{I})\,dv,$$

whilst in (b)

$$\delta L = \frac{1}{4\pi}\int\{(\mathbf{H}\delta\mathbf{B}) + (\mathbf{B}\delta\mathbf{H})\}\,dv - \frac{1}{4\pi}\int(\mathbf{H}\delta\mathbf{H})\,dv - \int(\mathbf{H}\delta\mathbf{I})\,dv.$$

In both of these equations the last term on the right is recognized at once as the part of the Lagrangian function corresponding to the work done against the quasi-elastic forces holding the induced polarizations. This may be regarded, therefore, as internal (molecular) potential energy stored in the media of the field, which admit of the induced polarizations. This leaves the purely magnetic part in (a) as

$$\delta L_m = \frac{1}{4\pi}\int(\mathbf{H}\delta\mathbf{B})\,dv - \frac{1}{4\pi}\int(\mathbf{H}\delta\mathbf{H})\,dv,$$

and in (b)

$$\delta L_m - \frac{1}{4\pi}\int\delta(\mathbf{HB})\,dv - \frac{1}{4\pi}\int(\mathbf{H}\delta\mathbf{H})\,dv.$$

The second of these is immediately integrable and gives

$$L_m = \frac{1}{8\pi}\int\{2(\mathbf{HB}) - \mathbf{H}^2\}\,dv.$$

With the first there are various possibilities and it is here that the familiar theory goes astray. It assumes, in fact, that the first integral is zero, which in itself is perfectly justifiable, of course, but it leads to the result that L_m is distributed over the field with a density $-\mathbf{H}^2/8\pi$, which is very different from that suggested for the more general case, so that it cannot under any conditions be used under the general conditions of case (b). There is, however, an alternative procedure which makes the first form integrable by adding another zero integral, the one that has been omitted because the currents are not there, viz.

$$\frac{1}{4\pi}\int(\mathbf{B}\delta\mathbf{H})\,dv,$$

and then the form obtained is identical with that obtained for case (b).

Our conclusion, therefore, is that while the formula

$$L_m = -\frac{1}{8\pi}\int\mathbf{H}^2\,dv$$

agrees on total, in the special case to which it applies, with the result given by the more general formula

$$L_m = -\frac{1}{8\pi}\int\{\mathbf{H}^2 - 2(\mathbf{HB})\}\,dv,$$

it is the latter form alone that can be employed under all conditions to define the purely magnetic part of the Lagrangian function of the system.

With this form for L_m we have

$$\delta L = \frac{1}{4\pi}\int\{\delta(\mathbf{BH}) - (\mathbf{H}\delta\mathbf{H})\}\,dv + \int(\mathbf{H}\delta\mathbf{I})\,dv,$$

which, when the induction follows a linear law or $\mathbf{I} = \kappa\mathbf{H}$ $(\mu = 1 + 4\pi\kappa)$, is equivalent to

$$L = \frac{1}{4\pi}\int\left\{(\mathbf{BH}) - \frac{1}{2}\mu\mathbf{H}^2\right\}dv,$$

the formula quoted in the previous paragraph 6 but with the reversed sign, as it was then treated as potential energy.

As
$$\mathbf{B} = \mu\mathbf{H} + 4\pi\mathbf{I}_0,$$

this result can also be written in the form

$$L = \frac{1}{8\pi}\int(\mathbf{BH}) + \frac{1}{2}\int(\mathbf{HI}_0)\,dv,$$

and then, by applying the usual transformation to the first term, in the familiar form

$$L = \frac{1}{2c}\Sigma i_s N_s + \frac{1}{2}\int(\mathbf{HI}_0)\,dv.$$

This completes the first part of our thesis. It is the expression

$$\mu\mathbf{H}^2/8\pi - (\mathbf{BH})/4\pi$$

rather than the simpler expression $\mu\mathbf{H}^2/8\pi$ which represents in all cases the distribution of the energy in the magnetic field which must serve as the force-function, but then only when it is treated as potential energy.

10. We next prove, maintaining the assumption of a linear law of induction, that the more familiar formula $\mu\mathbf{H}^2/8\pi$ does, in fact, represent under all conditions the part of the energy of the field which is conserved. For this purpose we introduce $\mathbf{H}_0$ and $\mathbf{B}_0$ to denote the force intensity and induction vectors in the field of the permanent magnets alone, with a similar suffix notation for other quantities as required. The vector $\mathbf{H}_0$ will now, of course, be the gradient of an acyclic potential, so the last integral in the expression for L can be written in the form

$$\begin{aligned}\frac{1}{2}\int(\mathbf{HI}_0)\,dv &= \frac{1}{8\pi}\int(\mathbf{HB}_0)\,dv - \frac{1}{8\pi}\int\mu(\mathbf{HH}_0)\,dv\\ &= \frac{1}{2c}\,\Sigma i_s N_{s0} - \frac{1}{8\pi}\int(\mu\mathbf{H} - \mu\mathbf{H}_0 \,.\, \mathbf{H}_0)\,dv\\ &\qquad - \frac{1}{8\pi}\int\mu\mathbf{H}_0^2\,dv,\end{aligned}$$

and since

$$\begin{aligned}\operatorname{div}(\mu\mathbf{H} - \mu\mathbf{H}_0) &= \operatorname{div}(\mu\mathbf{H} + 4\pi\mathbf{I}_0) - \operatorname{div}(\mu\mathbf{H}_0 + 4\pi\mathbf{I}_0)\\ &= \operatorname{div}\mathbf{B} - \operatorname{div}\mathbf{B}_0\\ &= 0,\end{aligned}$$

the second integral is zero, so that

$$\mathrm{L}=\frac{1}{2c}\,\Sigma \boldsymbol{i}_s\mathrm{N}_s+\frac{1}{2c}\,\Sigma i_s\mathrm{N}_{s0}-\frac{1}{8\pi}\int\mu\mathbf{H}_0{}^2\,dv,$$

N_{s0} denoting the flux through the circuit of i_s due to the field of the permanent magnets alone. Writing this in the form

$$\mathrm{L}=\frac{1}{2c}\,\Sigma \boldsymbol{i}_s(\mathrm{N}-\mathrm{N}_{s0})+\frac{1}{c}\,\Sigma \boldsymbol{i}_s\mathrm{N}_{s0}-\frac{1}{8\pi}\int\mu\mathbf{H}_0{}^2\,dv,$$

we see that it divides itself into three distinct parts. The first term involves the currents and their own fields alone, and is therefore by the usual argument a homogeneous quadratic function of the currents i_s. The second term, representing the mutual energy of the currents and permanent magnets, is a linear function of the current strengths i_s; whilst the last term of all represents the intrinsic energy of the field of the permanent magnets alone, and is therefore independent of the currents.

As the system is assumed to be statical in so far as the geometrical co-ordinates are concerned, the currents in the circuits are the only palpable velocities in the system. The fact that the magnetic polarities may ultimately be the equivalent of a continuous distribution of currents is for the moment ignored, it being assumed that it is possible to apply restraints sufficient to keep them rigidly permanent. This is the assumption, referred to above, which is equivalent to the ignoration of the co-ordinates defining the molecular current whirls which are the equivalent of the permanent magnetism. But with a Lagrangian function of this mixed character we have associated a conserved energy function

$$\mathrm{E}=\left(\Sigma \boldsymbol{i}_s\frac{\partial\mathrm{L}}{\partial i_s}-\mathrm{L}\right)=\mathrm{L}_2-\mathrm{L}_0,$$

L_2 representing the quadrate terms in L and L_0 the terms independent of the velocities i_s. Thus

$$\mathrm{E}=\frac{1}{2c}\,\Sigma i_s(\mathrm{N}_s-\mathrm{N}_{s0})+\frac{1}{8\pi}\int\mu\mathbf{H}_0{}^2\,dv,$$

and by the usual argument this is

$$=\frac{1}{8\pi}\int(\mathbf{H}\,.\,\mathbf{B}-\mathbf{B}_0)\,dv+\frac{1}{8\pi}\int\mu\mathbf{H}_0{}^2\,dv.$$

But since

$$\begin{aligned}\mathbf{B}-\mathbf{B}_0&=\mu\mathbf{H}+4\pi\mathbf{I}_0-\mu\mathbf{H}_0-4\pi\mathbf{I}_0\\&=\mu(\mathbf{H}-\mathbf{H}_0),\end{aligned}$$

we have

$$\mathrm{E}=\frac{1}{8\pi}\int\mu\mathbf{H}^2\,dv+\frac{1}{8\pi}\int(\mathbf{H}_0\,.\,\mu\mathbf{H}-\mu\mathbf{H}_0)\,dv;$$

but as H_0 is derived from an acyclic potential and

$$\operatorname{div}(\mu\mathbf{H}-\mu\mathbf{H}_0=\operatorname{div}(\mathbf{B}-\mathbf{B}_0)=0,$$

the last integral is zero and we have finally

$$E=\frac{1}{8\pi}\int \mu \mathbf{H}^2 \, dv.$$

This is then the second part of our thesis. The function $\mu\mathbf{H}^2/8\pi$ does, in every case where the law of induction is linear isotropic, properly represent the density of that part of the energy which enters into the conservation principle, although it does not in the general case represent the density of the energy which forms the function from which the forces can be derived by differentiation.

It must of course be emphasised that the whole argument of this paragraph depends on the linear law of induction, and that the expressions derived have no validity under any more general conditions. The results cannot therefore be applied in the most important practical applications of the subject involving ferromagnetic materials. In such cases it is necessary to go back to the general differential formulæ of paragraph 8, which are valid under the most general conditions, although these only provide us with an expression for the force or Lagrangian function ; this alone has significance in this more general case. The whole magnetization process in ferromagnetic materials being an irreversible affair, there is no question of a conservation principle in the strict sense being applicable, so there can be no question of a simple expression representing a conserved energy function.

11. Let us now apply these general results to the details of some special cases bearing on our earlier remarks.

Whether the energy itself is interpreted as potential or kinetic the forces derive properly from the Lagrangian function, which in the general case is

$$L=\frac{1}{2c}\Sigma \boldsymbol{i}_s N_s+\frac{1}{2}\int (\mathbf{H}\mathbf{I}_0) \, dv.$$

(*a*) Omitting induced magnetism from the argument, we first examine the relations between two parallel circuits fixed at a distance x apart on the same axis, carrying currents i_1 and i_2 driven by internal electromotive forces E_1, E_2 against resistances R_1, R_2. The self and mutual induction coefficients for the circuits being L_{11}, L_{22} and L_{12} (the last alone depends on x), the kinetic potential for the field is

$$L=\frac{1}{2c}L_{11}i_1^2+2L_{12}i_1i_2+L_{22}i_2^2).$$

The coils are held at rest by equal and opposite forces X, which in any small relative displacement along the axis do work of amount $X\delta x$. As the Lagrangian function is quadratic in the only velocities i_1 and i_2 which appear, it represents itself the total of the conserved energy, so that the principle of energy in this case assumes the form

$$X+E_1i_1+E_2i_2=R_1i_1^2+R_2i_2^2+\frac{dL}{dt},$$

the second and third terms on the left being the rates of working of the applied electromotive forces in the electrical co-ordinates, and the first two terms on the right the rates of dissipation of energy into heat in the two circuits.

But in this equation

$$\begin{aligned}c\frac{dL}{dt}&=(L_{11}i_1+L_{12}i_2)\frac{di_1}{dt}+(L_{12}i_1+L_{22}i_2)\frac{di_2}{dt}+i_1i_2\frac{\partial L_{12}}{\partial x}\dot{x}\\&=i_1\frac{d}{dt}(L_{11}i_1+L_{12}i_2)+i_2\frac{d}{dt}(L_{12}i_1+L_{22}i_2)-i_1i_2\frac{\partial L_{12}}{\partial x}\dot{x}\\&=i_1\frac{dN_1}{dt}+i_2\frac{dN_2}{dt}-i_1i_2\frac{\partial L_{12}}{\partial x}\dot{x},\end{aligned}$$

N_1, N_2 denoting the inductions through the currents. The energy equation can therefore be written in the form

$$X\dot{x}+E_1i_1+E_2i_2=R_1i_1^2+R_2i_2^2+\frac{i_1}{c}\frac{dN_1}{dt}+\frac{i_2}{c}\frac{dN_2}{dt}-\frac{i_1i_2}{c}\frac{\partial L_{12}}{\partial x}\dot{x}.$$

But the currents themselves are determined by

$$E_1=R_1i_1+\frac{1}{c}\frac{dN_1}{dt},\quad E_2=R_2i_2+\frac{1}{c}\frac{dN_2}{dt},$$

so that this equation reduces to

$$X\dot{x}=-\frac{i_1i_2}{c}\frac{\partial L_{12}}{\partial x}\dot{x},$$

whence

$$X=-\frac{i_1i_2}{c}\frac{\partial L_{12}}{\partial x}=-\frac{\partial L}{\partial x}.$$

The forces acting to keep the currents in position thus tend to decrease the kinetic potential, that is, to decrease the energy when reckoned as kinetic or to increase it when reckoned as potential.

(*b*) The next case we examine is the one in which the second of the coils is replaced by a rigid magnetic shell, of strength equivalent to that of the current i_2 in the circuit. This shell will act as a magnet and we have the apparently anomalous case mentioned at the outset.

Still, in the absence of induced magnetism, the kinetic potential of the field is

$$\begin{aligned}L&=\frac{1}{2c}i_1N_1+\frac{1}{2}\int(\mathbf{I}_0\mathbf{H})\,dv\\&=\frac{1}{2c}(i_1N_1+i_2N_2)\\&=\frac{1}{2c}(L_{11}i_1^2+2L_{12}i_1i_2+L_{22}i_2^2),\end{aligned}$$

the symbols N_1 and N_2 and the geometrical constants L_{11}, L_{12}, L_{22} having the same values as before.

Now, however, we have a case in which i_2, the strength of the rigid shell, is constant, so that i_1 is the only (electric) velocity represented in L, which therefore is of the mixed type, with quadratic linear and a constant term. The conserved energy is not therefore represented by the complete function, but by

$$i_1\frac{\partial L}{\partial i_1}-L=\frac{1}{2c}(L_{11}i_1{}^2-L_{22}i_2{}^2),$$

the second term of which is an absolute constant. The equation of energy now becomes simply

$$X\dot{x}+E_1i_1=R_1i_1{}^2+\frac{1}{2c}\frac{d}{dt}(L_{11}i_1{}^2),$$

the terms in E_2 and R_2 having no significance in regard to the shell. This can again be written in the form

$$X\dot{x}+E_1i_1=R_1i_1{}^2+\frac{i_1}{c}\frac{dN_1}{dt}-\frac{i_1i_2}{c}\frac{\partial L_{12}}{\partial x}\cdot$$

And then, assuming the relation for the current, we derive again that

$$X=-\frac{i_1i_2}{c}\frac{\partial L_{12}}{\partial x}=-\frac{\partial L}{\partial x},$$

as before.

(*c*) Finally, let us consider the case when both currents are replaced by their equivalent shells of constant strengths i_1, i_2. Again, the kinetic potential of the field amounts on the aggregate to

$$L=\frac{1}{2c}(L_{11}i_1{}^2+2L_{12}i_1i_2+L_{22}i_2{}^2),$$

the coefficients having their previous geometrical significance. But now as i_1 and i_2 are constants of the system the function L contains no velocity at all, and the conserved energy is now therefore represented simply by —L, and the equation of energy is

$$X\dot{x}=-\frac{d}{dt}\frac{1}{2c}\{L_{11}i_1{}^2+2L_{12}i_1i_2+L_{22}i_2{}^2\}$$

$$=-\frac{i_1i_2}{c}\frac{\partial L_{12}}{\partial x}\dot{x},$$

so that still $$X=-\frac{\partial L}{\partial x}\cdot$$

In each of these three cases, therefore, the total kinetic potential of the two elements and force between them are all exactly the same. This we should really expect because the magnetic fields—distributions of B and H—are identical in the three cases, and therefore the kinetic potential defined by a distribution with density

$$\frac{1}{4\pi}(\mathrm{BH})-\frac{\mu}{8\pi}\mathrm{H}^2;$$

and the magnetic forces between them, which can be expressed in terms of a stress in the field defined in a similar way, are bound to be the same quite independently of the origin of the field. But the conserved energies in the three cases are all different, although in each case they correspond to a distribution throughout the field with density $\mu\mathbf{H}^2/8\pi$.

12. In the main we have so far been concerned to obtain consistency in the mechanical relations of the field, using as a basis such of the familiar relations and formulæ as are necessary. Apart from matters of interpretation the only changes necessary in the usual procedure are, firstly that a clear distinction must be drawn between the energy to be used as a force function, Lagrangian function or kinetic potential, which exists under all conditions, and that to be used in the conservation principle, which exists in fact only when the law of induction follows a linear law; and secondly, in the formula for the force function the usual and familiar expression $\mathbf{H}^2/8\pi$ for the purely magnetic part of the total density has to be replaced by the expression

$$\frac{1}{8\pi}\mathbf{H}^2-\frac{1}{4\pi}(\mathbf{HB})=-\frac{1}{8\pi}\mathbf{B}^2-\frac{1}{2}(\mathbf{I}+\mathbf{I}_0)^2.$$

Unfortunately, this spoils the one apparently satisfactory feature of the older discussion. In a theory in which **H** is the fundamental (æthereal) force vector the usual expression for the æthereal energy density suggests itself as the most natural result, corresponding exactly to the formula in electric theory, where there still seems to be every justification for it, and fitting in to the stress-strain picture of magnetic actions. The new and more complicated expression suggested by our discussions seems, on the contrary, to be very involved and even unnatural, making as it does the æthereal part of the energy depend not only on the æthereal vector **H**, but also on the induced and therefore partly material vector **B**. And it is this dilemma which forces us to make another and probably, as regards its significance, the most important change in the theoretical discussion in order to secure simplicity with consistency.

This last step in our thesis involves a complete inversion of the rôles of **B** and **H**, and as a consequence also the complete abandonment of the analogy with the electrostatic case, This change, as we shall soon see, results in the formulation of a theory which has all the advantages of simplicity of the earlier formulæ with all the consistency of the new and rather more involved formulæ derived above. We need not here elaborate on the difficulty of defining the magnetic force at a point inside a continuous distribution of polarity where alone the distinction between **B** and **H** is apparent, but there is ample evidence on both the experimental and theoretical aspects of our subject to support the suggested inversion. We mention briefly :—

(i) The formula for the force on an element of current involves **B** rather than **H**.

(ii) If the current distribution which is the real equivalent of the magnetic polarity is introduced in Maxwell's equations it is the **H** and not the **B** vector that disappears.

(iii) The experimental evidence on the Hall and allied effects in metals suggests that, in the ferromagnetic metals, where the effect is most marked, the results are all more nearly proportional to **B** than to **H**. This is important because it is just in such phenomena that we see the internal force in operation.

These and other points of detail in the theory suggest, at least, that a much greater degree of consistency and agreement with experience is secured by taking **B** as the fundamental force vector. Then of course the vector **H** must become the induced vector, but it is now the induction of mechanically effective force, that is, the part of the total force without the local part $4\pi\mathbf{I}$, which is implied, this being the vector to use in determining the action of the field on a finite magnet.

13. Assuming the inversion, we should have to replace **H** by **B** in the first term of our general result in paragraph 8, when it would be

$$\begin{aligned}\delta \mathrm{W} &= -\int(\mathbf{B}\delta\mathbf{I}_0)\,dv - \frac{1}{4\pi}\int(\mathbf{B}\delta\mathbf{H})\,dv \\ &= \int(\mathbf{B}\delta\mathbf{I})\,dv - \frac{1}{4\pi}\int(\mathbf{B}\delta\mathbf{B})\,dv.\end{aligned}$$

The form of this relation suggests at once that if we identify the first term with the energy of the induced polarizations, then the other integral determines the purely magnetic part of the potential energy in the field and it corresponds to a distribution for the complete field with a density $-\mathbf{B}^2/8\pi$, the natural expression in a theory in which **B** is the fundamental force vector. This formula for the density differs from the rather involved one previously obtained only by the local term $-(\mathbf{I}+\mathbf{I}_0)^2/2$.

With this form for W we have associated the formula for the kinetic potential or Lagrangian function of the field

$$\delta \mathrm{L} = \frac{1}{4\pi}\int\{(\mathbf{B}\delta\mathbf{B}) - 4\pi(\mathbf{B}\delta\mathbf{I})\}\,dv,$$

and in the case of a linear isotropic law of induction, when $\mathbf{I}=\kappa'\mathbf{B}$ this is equivalent to

$$\begin{aligned}\mathrm{L} &= \frac{1}{8\pi}\int\{\mathbf{B}^2 - 4\pi(\mathbf{BI})\}\,dv \\ &= \frac{1}{8\pi}\int(\mathbf{BH})\,dv + \frac{1}{2}\int(\mathbf{BI}_0)\,dv \\ &= \frac{1}{2c}\Sigma i_s \mathrm{N}_s + \frac{1}{2}\int(\mathbf{BI}_0)\,dv,\end{aligned}$$

as before, except that now the last term represents the proper contribution in terms of the induction to the sum $\Sigma i\mathrm{N}$, relating to the molecular current whirls which are the equivalent of the permanent magnets.

Associated with this new function we have, of course, also a slightly modified conserved energy function. On the assumption of a linear law of induction, and it is only then that conserved energy exists, so that, if $\mu' = 1 - 4\pi\kappa'$,

$$\mathbf{H}' = \mu'\mathbf{B} - 4\pi\mathbf{I}_0, \quad \mathbf{H}_0 = \mu'\mathbf{B}_0 - 4\pi\mathbf{I}_0,$$

the last integral in the formula for L can be seen to be equal to

$$\begin{aligned} \frac{1}{2}\int(\mathbf{B}\mathbf{I}_0)\,dv &= \frac{1}{8\pi}\int(\mathbf{B}\,.\,\mu'\mathbf{B}_0 - \mathbf{H}_0)\,dv \\ &= \frac{1}{8\pi}\int\mu'(\mathbf{B}\mathbf{B}_0)\,dv \\ &= \frac{1}{8\pi}\int(\mathbf{H} + 4\pi\mathbf{I}_0\,.\,\mathbf{B}_0)\,dv \\ &= \frac{1}{2c}\Sigma i_s \mathrm{N}_{s0} + \frac{1}{2}\int(\mathbf{I}_0\mathbf{B}_0)\,dv. \end{aligned}$$

Thus L now assumes the form

$$\frac{1}{2c}\Sigma i_s(\mathrm{N}_s - \mathrm{N}_{s0}) + \frac{1}{c}\Sigma i_s \mathrm{N}_{s0} + \frac{1}{2}\int(\mathbf{I}_0\mathbf{B}_0)\,dv,$$

in which the different types of energy are immediately recognised. The associated conserved energy function is therefore, by the usual argument, equal to

$$\frac{1}{2c}\Sigma i_s(\mathrm{N}_s - \mathrm{N}_{s0}) - \frac{1}{2}\int(\mathbf{I}_0\mathbf{B}_0)\,dv,$$

which differs from our previous estimate by the amount

$$\frac{1}{8\pi}\int(\mathbf{B}_0 - \mathbf{H}_0\,.\,\mathbf{I}_0)\,dv,$$

which, in the only type of case to which our analysis really applies, represents the contribution of a small localized distribution depending on the density of the permanent polarity in the field. The formula for the conserved energy is therefore effectively the same as in the older form of the theory.

14. One difficulty might seem to stand in the way of the acceptance of the suggested inversion of the rôles of **B** and **H**, and that is the fact that in static fields at least it is the old force vector **H**, and not the induction, which is desirable from a potential function. A closer examination of the physical argument by which the dependence of the force on a potential is derived shows, however, that this is a natural result even if **B** is the fundamental force vector of the field. The argument, as we remember, depends on the calculation of the work done in moving a magnetic pole slowly along a path between two points in the field: if the path passes through magnetic media, where alone the difference between **B** and **H** is significant, we should really have to make a small tunnel through which to move the particle; and in a tunnel of this kind we know that it is precisely the vector **H** which measures the force; it is therefore still quite

natural to expect that the potential function of the field relates to the vector **H** rather that the vector **B**.

The mathematical-physical argument here is somewhat akin to that used in the earlier discussions in the treatment of the relations of a field of a current and a magnetic system. This treatment as we know starts on the assumption that the mutual energy of a current i and a magnetic pole is $i\omega/c$, ω being the solid angle of the cone subtended by the circuit at the position of the pole. On interpreting this as $i\mathrm{N}/c$, the N appears naturally as the number of tubes of force (**H**) threading the circuit; but in generalizing the result by addition for any magnetic system we have suddenly to change the significance of N so that it measures the number of tubes of induction (**B**) rather than force (**H**). And the only possible justification for this procedure is based on the argument that the original result has been established only for parts of the field free from magnetic or magnetizable matter. If then we want to, or have to, calculate N by taking a surface abutting on the circuit, which passes either wholly or partly through magnetic matter, we must really clear a thin layer of the media out of the way so that the surface still passes through free space; but in such a layer we know that the magnetic force is measured not by **H** but by **B**, so that generally we should expect to have to count tubes of induction (**B**) rather than tubes of force (**H**).

The whole of the theoretical relations of the theory thus seem to be entirely consistent with the new point of view, which assumes that the vector **B** measures the fundamental force vector of the field under the most general circumstances.

15. If this new form of the theory is finally accepted considerable modifications may be required in the interpretation of the properties of magnetic materials, but this is a matter for the future. One thing becomes certain, however, the presumed analogy with the electrostatic field, which has been used as the bases of much of the argument in this theory, will have to be abandoned as being completely incompatible with the logical development of the relations of the magnetic field. And the fact that, when reckoned as potential energy, the purely magnetic part of the field energy turns out to be measured by the density $-\mathbf{B}^2/8\pi$, disposes of all possibility of any simple stress-strain picture of the affairs of the field. All that we are left with then is the picture of a field of activity of unspecified type defined in terms of two vectors **H** and **B** connected together by a relation which, in its Maxwellian form, is

$$\mathbf{B}=\mathbf{H}+4\pi\mathbf{I},$$

so that naturally the two vectors are necessarily of the same physical nature. The only difference is that one of them is a simple entity in the strict physical sense, while the other is a vector compounded of this one and the vector $4\pi\mathbf{I}$, which depends on the polarization. And the fact that $4\pi\mathbf{I}$ is a measure of the *force* intensity in a certain shaped cavity merely verifies this implication of the relation. The only question remaining is, which vector measures the simpler and therefore more fundamental of these physical or mechanical entities ? The conclusion of the above discussion is, I think indisputably, that the only theory of these affairs which is completely consistent in all its details assumes its simplest and most natural form if **B** is taken as the fundamental force vector in the field, in the sense in which this term is usually applied, and **H** is then the induction, although now it is the induction of mechanically effective force that is implied.

If this thesis is accepted, then we must prepare for a complete inversion of the whole of our traditional notions on this subject, that is, of course, if we admit that the claims of theoretical consistency must ultimately take precedence over those of traditional and almost universal and long-standing practice.

University College,
Cardiff.
April, 1944.

II. *The Behaviour of Liquids in a Vibrating Air Column.*

By A. F. Howatson, M.A., Natural Philosophy Department, The University, Glasgow *.

[Received July 3, 1944.]

[Plates I. & II.]

I. *Introduction.*

The characteristic striations and figures formed in dust or powder strewn along the bottom of a tube in which the air is set into stationary vibration as in the classical experiments of Kundt⁽¹⁾, are well known and have more recently been studied by Irons⁽²⁾, Hutchisson and Morgan⁽³⁾, and, in particular, by Andrade⁽⁴⁾. The last-mentioned has given an explanation of the phenomena occurring inside the tube in terms of a general circulation of the air between adjacent nodes and antinodes, as predicted mathematically by Rayleigh⁽⁵⁾ and verified experimentally by Andrade⁽⁶⁾, and of separate vortex systems set up round any obstacle when the vibrations exceed a certain intensity. A distinctive feature of such experiments, unnoticed by the earlier observers because of the unsteady and intermittent nature of the vibrations produced by the apparatus at their disposal, is the formation of sharp and almost complete disks of dust at the antinodes at certain intensities and frequencies.

---

* Communicated by Professor E. Taylor Jones.

Equally striking effects occur when a layer of liquid on the bottom of the tube is substituted for the dust, but these do not appear to have been investigated or described in detail, although, as early as 1874, Dvorak⁽⁷⁾ in the course of some experiments on sound-waves in tubes, seems to have employed such an arrangement. Dvorak, using the old method of stroked rod and disk to excite the vibrations and a short length of tubing containing a layer of water, succeeded in producing a movement of the liquid at the antinodes, which he illustrated by the sketch reproduced in fig. 1.

Dvorak attributed the motion of the liquid to a small excess mean pressure at the nodes due to second order effects, which are appreciable when the amplitude of vibration is not negligible compared with the wave-length. The observations, as in the dust-tube experiments, were greatly hampered by the unsatisfactory nature of the source of vibration.

More recently Brandt and Freund⁽⁸⁾, using a magnetostriction oscillator as the source of vibration and working at three fixed frequencies in the upper audible region (6·5, 10·6 and 25 k.c./sec.), have given a brief description of some effects of this nature obtained in narrow tubes containing liquid. No explanation of the observed phenomena is given, though one appears to be promised by the authors. The writer has been unable to trace any such explanation.

Fig. 1.

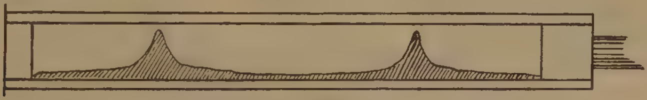

The present experiments were designed to investigate the effect of stationary air-waves on a liquid layer in more detail. The frequencies employed were in the lower audible region (c. 300–1500 c.p.s.) and the source of sound was continuously variable in both frequency and intensity. This has the advantage of enabling the experiments to be carried out under steady and controlled conditions and greatly facilitates the observation and elucidation of the various phenomena. The more important features of the latter are described in some detail with photographic illustrations and the explanation of the striking behaviour of the liquid discussed in the light of recent knowledge.

II. *Apparatus.*

The source of sound was a loudspeaker unit driven by a valve oscillator and power amplifier. The oscillator, which was of the beat-frequency type, produced a reasonably pure sine-wave output of continuously variable frequency within the limits of about 100–10,000 c.p.s. The frequency could be determined, when required, with sufficient accuracy from the calibrated scale of the variable condenser, and the amplitude of the oscillations adjusted by means of a rheostat volume-control. The amplifier was of conventional design and consisted of a single valve followed by an output stage of two power valves in push-pull. The loudspeaker which was found most satisfactory for the purpose of the experiments was of the attracted diaphragm or telephone-receiver type. The diaphragm was covered and clamped at the edge by means of a metal plate, which had at its centre a circular hole and cylindrical projection of diameter 2·0 cm. and length 2·5 cm. The original front of the instrument (an Amplion type AR 15 loud sounding unit), slightly modified, was found quite suitable. The tubes used in the experiments were of glass and varied in diameter from 1·5 to 2·6 cm. and in length from 25 to 150 cm. The most convenient method of attaching the tube to the loudspeaker was by means of a short length of thick rubber tubing which fitted over the cylindrical projection of the latter and one end of the tube, the other end being either sealed off or else closed by a cork, or, occasionally, a glass disc. The speaker was given a slight upward tilt to prevent the liquid from running on to the diaphragm. The tubes were illuminated by a projection lantern housing a 500 watt tungsten lamp, the projecting lens being for most purposes removed.

A number of different liquids was used, the principal ones being acetone, methylated spirits, ether, liquid paraffin, and water. Differences in such physical properties of the liquids as surface tension, viscosity, and density cause certain differences in behaviour which will be considered in due course. The general movements, however, are common to all the liquids used, and are described first.

III. *General Behaviour.*

A quantity of the liquid under observation, sufficient to produce a layer of maximum depth of about half a centimetre, was introduced into the tube and the speaker attached to one end as described. The tube was carefully adjusted to a horizontal position to ensure that the layer of liquid was of uniform depth.

On switching on the source of sound no visible effect takes place at any frequency if the sound is of low or even of moderate intensity. If the intensity of the sound is increased, however, and the frequency is slowly varied, a movement of the liquid becomes apparent at each resonant frequency, *i. e.*, whenever the frequency is such that the air column contains an integral number of half-wave-lengths. The surface of the liquid then assumes a wavy appearance, the crests of the waves being at the antinodes and the troughs at the nodes of the vibrating air column. The diaphragm coincides very nearly with a vibration node as does also, of course, the closed end of the tube, the remaining nodes and antinodes being equally spaced in between. The general arrangement of the apparatus showing the appearance of the tube at this stage is illustrated in fig. 2 (Pl. I.).

On further increasing the intensity, the curvature of the liquid surface increases until a certain limiting value of intensity is reached. At this point the surface of the liquid is suddenly broken at the antinodes, the liquid spurting up with considerable violence into a thin sheet which, with tubes of the diameters used, almost fills the whole cross-section. The exact nature of the disturbance depends on the physical properties of the liquid in use, but a good idea of its appearance can be obtained from figs. 4, 5 and 6 (Pl. II.), which show a typical antinodal sheet or spout from three different viewpoints, the frequency in this case being 1200 c.p.s. Fig. 4 shows an oblique view, fig. 5 is a view from the side, fig. 6 from above. The general appearance of the tube when the antinodal spouts are in action is illustrated in fig. 3 (Pl. I.), the number of spouts shown being five. With a long tube and with careful adjustment a greater number of spouts can be produced simultaneously, the number being limited only by the intensity of sound available. At frequencies much greater than 2000 c.p.s., owing to the diminishing efficiency of the speaker, the intensity was not sufficient to initiate the spouts, but pronounced curvature of the liquid surface continued to be noticeable at each resonant frequency.

As can be seen from figs. 4–6 the antinodal spouts are remarkably sharp and localised, the liquid sheet being only two or three millimetres thick at its base but extending transversely across the whole section. With proper adjustment the spouts remain stable and their positions remain unaltered over long periods, except at the lowest frequencies when irregular fluctuations take place and multiple spouts are, in general, formed. At moderate frequencies the spouts may therefore be used as convenient and accurate indicators for measuring the wave-length of sound in the tube, fig. 6 showing especially well how sharply the antinodes are defined. They are also very suitable for demonstrating to an audience in a striking manner the different modes of oscillation of a column of air.

The photographs in figs. 2–6 were obtained with acetone which was, in fact, the liquid most frequently used in these experiments because of its suitable physical properties, such as low viscosity, surface tension and density, and high refractive index for photographic purposes. It also gave particularly steady spouts at all except the lowest frequencies. The behaviour of acetone will therefore be described in somewhat more detail as being typical of liquids of low viscosity and surface tension.

IV. *Acetone.*

The inception of the spurting motion is so sudden that it cannot readily be followed by the eye. Occasionally, however, a small ridge can be seen on the surface of the liquid transverse to the axis of the tube. The ridge increases in height very rapidly, especially at the walls of the tube, until it forms a sheet of liquid which almost fills the cross-section. Any irregularity on the surface of the liquid, such as the presence of liquid drops thrown off by a neighbouring spout already in action, assists the formation of the sheet. If the conditions are steady the spout continues in action as long as the sound is maintained at the necessary intensity, the liquid moving up the sheet and falling back, in the main, down the sides of the tube. With liquids such as acetone the sheet is never complete, but (as may be seen from figs. 4 and 5) breaks up on its upper half into small drops which are thrown upwards and outwards with considerable violence.

The paths of several of these drops are clearly visible in fig. 5. The spouts form at a small range of frequencies around each resonant frequency, being steadiest at a frequency slightly higher than that for maximum disturbance. This is evidently an intensity effect due to the falling off in intensity at frequencies removed from the resonant frequency, as the same result can be obtained by reducing the intensity at resonance somewhat below the maximum value.

At low frequencies the antinodal region extends over a considerable length of the tube, and several spouts are usually formed in the vicinity of each antinode. These are generally short-lived, tending if close together to coalesce, their place being taken by newly-formed spouts. If the spouts are somewhat farther apart they are carried outward from the antinodal position towards the nearest node, but collapse before travelling very far. At higher frequencies a general unsteadiness and tendency for multiple spout formation is also evident when the intensity is very high, but, as already mentioned, on lowering the intensity or altering the frequency slightly the spouts become perfectly steady. At low frequencies, however, single, steady spouts do not form at any intensity.

Though multiple spouts formed at a single antinode are generally short-lived, it is occasionally possible to excite near a single antinode two spouts which remain stable for some time at a fixed distance apart. This occurrence appears to be associated with irregularities in the vibratory motion, as the note emitted by the speaker is noticeably impure when double spouts are formed.

V. *Methylated Spirits.*

Spouts form in this liquid in a manner similar to that described for acetone, but they are slightly more difficult to excite and do not attain quite the same stability. They also show a greater tendency to break up into little drops, many of which on regaining the surface of the liquid remain floating for some time as small liquid spheres. The phenomenon of liquid drops floating on a liquid surface occurs elsewhere*, and has been the subject of several investigations, but has not been fully explained. Explanations involving either (*a*) electrical charges, or (*b*) films of adsorbed air or vapour have been suggested, but, according to Hazelhurst and Neville(9), the chief factor is the molecular structure of the liquid as it effects the character and stability of the surface film.

The only liquid other than methylated spirits which showed the effect to any extent was melted paraffin wax, in which the stability of the drops was most marked.

The behaviour of such liquid spheres under the influence of the air vibrations is very interesting, and affords considerable insight into the nature of the forces involved in tube phenomena. They invariably tend to arrange themselves in parallel rows transverse to the axis of the tube on each side of the antinodal spout. The rows may consist of a single line of spheres apparently in close contact, but more often the spheres mount up to form a wall or ridge two or three spheres in height, but never more than one sphere in width. When the antinodal spouts are in action the ridges are naturally disturbed by the constant addition of fresh drops, but if the intensity is then reduced to a value insufficient to maintain the spouts the ridge formation becomes well defined, though there is always a slight to and fro motion of the ridges as a whole. A photograph showing a number of such ridges is reproduced in fig. 9 (Pl. II.) The number of ridges gradually decreases as the spheres coalesce with the main body of the liquid until only one or two remain at each antinode. The last ridge or two, however, persist almost indefinitely provided the sound is maintained at the necessary intensity, but disappear almost immediately when the sound is cut off. Fig. 7 (Pl. II.) shows a single ridge of liquid spheres, the spheres being two deep along the greater part of its length; fig. 8 (Pl. II.) shows two such ridges at a single antinode. The single ridge moves only slightly relative to the tube, but when two ridges are present they usually oscillate to and fro parallel to the axis, maintaining a constant average distance apart. This behaviour is interesting as it disproves conclusively the earlier theory of König[(10)], put forward to account for the formation of the ridges in Kundt's tubes. On this theory the force between the ridges is one of repulsion only—a result obviously incompatible with the behaviour described.

---

* See, for example, two recent letters to 'Nature,' vol. cliii. pp. 80 and 109 1944).

VI. *Other Liquids of Low Viscosity.*

The behaviour of other liquids of low viscosity does not differ markedly from that already described for acetone and methylated spirits. Such variations as occur are due chiefly to differences in surface tension and may be illustrated by the liquids ether and water.

Ether, with its low surface tension and density, forms antinodal spouts very easily, the sound intensity required for excitation being lower for ether than for any other liquid used. The liquid sheets break up readily into a profusion of droplets which are thrown off as previously described but which do not, however, remain floating on the surface for any length of time.

With water, on the other hand, owing to its relatively high surface tension, the antinodal spouts are difficult to excite; nor do they break up readily into drops, taking the form rather of thin sheets of liquid. These films or sheets, extending as they do across practically the whole cross-section, reduce considerably the intensity of vibration on the side remote from the speaker, so that it is difficult to maintain more than two or three spouts in action simultaneously. The addition of a little ammonia solution, however, by reducing the surface tension, facilitates the formation of the antinodal spouts.

VII. *Viscous Liquids.*

Liquids of high viscosity, such as petroleum oil or liquid paraffin, are considered in this section. At moderate intensities such liquids assume the appearance shown in fig. 2, the curvature of the surface at any particular intensity and frequency depending on the density; but their subsequent behaviour is rather different. When an intensity sufficient to rupture the surface is reached the liquid rises up at an antinode to form a thin film, which stretches right across the tube if the diameter is not too great. The film effectively seals the tube, altering the resonant conditions to such an extent that the intensity is not sufficient for the formation of further antinodal films. The single film so formed persists at a large range of frequencies apart from the original frequency. The spouting motion characteristic of the liquids previously described is absent, the film remaining for the most part completely inert. In wider tubes, however, the film is not complete and does break up to some extent into drops which are projected against the upper surface of the tube. The liquid which adheres to this surface has a peculiar corrugated structure, the bands running round the tube normal to the axis. The corrugations persist as long as the vibration is maintained, but disappear slowly when the sound is cut off. They are present but not so clearly defined with other liquids of lower viscosity.

VIII. *Theoretical.*

The form of the liquid surface at the stage shown in fig. 2 indicates that the mean pressure is greater at a node than at an antinode. The value of the mean pressure difference in terms of the maximum particle velocity at an antinode can be deduced from the general hydrodynamical equation

$$\int \frac{dp}{\rho} + \frac{1}{2}\mathrm{U}^2 + \mathrm{V} - \frac{\partial \phi}{\partial t} = \text{constant},$$

where p=pressure, ρ=density, U=particle velocity, V=potential of external forces, ϕ=velocity potential, t=time.

In dealing with sound-waves external forces may be neglected and the term $\frac{1}{2}\mathrm{U}^2$ is usually negligible. In the present instance, because of the high intensities involved, we retain this term. Consequently the expression

$$\int \frac{dp}{\rho} + \frac{1}{2}\mathrm{U}^2 - \frac{\partial \phi}{\partial t}$$

has a constant value at all points inside the tube.

To evaluate the integral the adiabatic relation between p and ρ, $\rho = \kappa p^{1/\gamma}$ is assumed, giving

$$\int \frac{dp}{\rho} = \frac{p^{1-1/\gamma}}{\kappa(1-1/\gamma)}.$$

Hence
$$\frac{p^{1-1/\gamma}}{\kappa(1-1/\gamma)} + \frac{1}{2}\mathrm{U}^2 - \frac{\partial \phi}{\partial t} = \text{constant}. \quad \ldots \ldots \quad (1)$$

By evaluating the L.H.S. of (1) first at an antinode and then at a node, equating, and integrating over a complete period of the oscillations, we have, since U=0 at a node,

$$\frac{1}{\kappa(1-1/\gamma)}\int_0^T p_a^{1-1/\gamma}\,dt+\frac{1}{2}\int_0^T \mathrm{U}_a^2\,dt=\frac{1}{\kappa(1-1/\gamma)}\int_0^T p_n^{1-1/\gamma}\,dt, \quad . \quad (2)$$

where subscripts a and n refer to antinodal and nodal values respectively.

Rearranging (2),

$$\int_0^T (p_n^{1-1/\gamma}-p_a^{1-1/\gamma})\,dt=\frac{\kappa(1-1/\gamma)}{2}\int_0^T \mathrm{U}_a^2\,dt.$$

Expanding the L.H.S. in powers of (p_n-p_a),

$$\int_0^T\left\{(1-1/\gamma)\frac{(p_n-p_a)}{p_a^{1/\gamma}}+\frac{(1-1/\gamma)(-1/\gamma)}{2}\frac{(p_n-p_a)^2}{p_a^{1+1/\gamma}}\right\}dt=\frac{\kappa(1-1/\gamma)}{2}\int_0^T \mathrm{U}_a^2\,dt,$$

$$\therefore \quad \int_0^T (p_n-p_a)\,dt=\frac{1}{2\gamma}\int_0^T\frac{(p_n-p_a)^2}{p_a}\,dt+\frac{\kappa p_a^{1/\gamma}}{2}\int_0^T \mathrm{U}_a^2\,dt. \quad . \quad . \quad (3)$$

Since the expressions under the integral signs on the R.H.S. are of the second order in small quantities, in evaluating them it is sufficient to write

$$p_n-p_a=\rho_0\left(\frac{\partial\phi}{\partial t}\right)_n, \quad \mathrm{U}_a=\left(\frac{\partial\phi}{\partial x}\right)_a, \quad p_a=p_0, \quad \rho_a=\rho_0.$$

The velocity potential is of the form

$$\phi=\cos\frac{s\pi x}{l}\cos\frac{s\pi ct}{l},$$

so that $\left(\frac{\partial\phi}{\partial t}\right)_n=c^2\left(\frac{\partial\phi}{\partial x}\right)_a$, where c is the velocity of sound in air.

Hence
$$\int_0^T\frac{(p_n-p_a)^2}{p_a}\,dt=\gamma\rho_0\int_0^T \mathrm{U}_a^2\,dt,$$

and from (3)
$$\int_0^T (p_n-p_a)\,dt=\rho_0\int_0^T \mathrm{U}_a^2\,dt,$$

i. e.,
$$\overline{p_n-p_a}=\rho_0\overline{\mathrm{U}_a^2},$$

the bars indicating mean values over a complete period.

The mean pressure difference between each node and antinode is therefore

$$\tfrac{1}{2}\rho_0\hat{\mathrm{U}}_a^2, \quad . \quad . \quad . \quad . \quad . \quad . \quad . \quad . \quad . \quad . \quad (4)$$

where $\hat{\mathrm{U}}_a=\sqrt{2}\overline{\mathrm{U}}_a$ is the maximum particle velocity at an antinode.

IX. *Experimental Verification.*

In order to test the adequacy of the above explanation, experiments were carried out to determine the amplitude of vibration and hence the particle velocity at an antinode when the intensity was such as to produce a marked curvature of the liquid surface. The value of the pressure difference deduced from expression (4) was then compared with that obtained by direct measurement of the liquid levels. The amplitude of the vibrations was observed by means of smoke particles. It can be shown * that particles of tobacco smoke take up the full amplitude of the air vibrations at audible frequencies and are therefore suitable for use as tracing points.

Smoke from an ordinary cigarette was introduced into a tube containing a layer of liquid. The condensing and projecting lens systems of an optical lantern were removed, and light from the 500 watt tungsten lamp which it housed brought to a focus inside the tube by means of a photographic lens of effective aperture 5 cm. and focal length 10 cm., stray light being excluded by suitable screens. The beam of light was horizontal and at right-angles to the axis of the tube. The smoke particles were observed by means of a travelling microscope, the eyepiece of which was fitted with a divided millimetre graticule. The axis of the microscope was inclined at an angle of about 60° to the axis of the illuminating beam, as the scattered light was found to be stronger in this than in the vertical direction. The tube was adjusted so that the beam passed near its centre at an antinode of the air vibrations.

When the air is set into vibration the smoke particles appear as bright, horizontal lines against a dark background, the length of the lines being twice the amplitude of vibration. Owing to the general circulations of the air, which always take place in Kundt tubes when the intensity is great, there is a general movement of the particles across the field of view. This makes accurate measurement of the amplitude at high intensities difficult, but appears to be unavoidable. It is possible, however, by selecting a region of the cross-section where the motion is a minimum, to estimate fairly accurately the length of the lines as they cross the millimetre scale. For a particular tube of diameter 2·6 cm. and a frequency of 1360 c.p.s., the maximum double amplitude which could be measured was very nearly 1 mm. At this intensity there was a slight but noticeable curvature of the liquid surface. Measurements at higher intensities were not possible owing to the rapid movement of the particles across the field of view. However, from consideration of the relative intensity as it effects the curvature of the surface, it appears a reasonable estimate that the limiting amplitude at which the surface of the liquid is broken at the antinodes is of the order of twice this value, or 2 mm. double amplitude.

Using the value 1 mm. for the amplitude (a), we have for the maximum particle velocity

$$\hat{U}_a = 2\pi n a = 854 \text{ cm./sec.}$$

From expression (4), taking the standard value for atmospheric density, we obtain for the mean pressure difference 4·8 mm. of water. This value is of the same order but somewhat in excess of that obtained by measurements of the maximum difference in level of a layer of water in the same tube, made with a travelling microscope at an intensity just insufficient to cause the formation of antinodal spouts.

---

* See, *e. g.*, reference (6), p. 448.

It appears from the above that consideration of second order effects is sufficient to account for the distribution of pressure inside the tube to the correct order of magnitude. This is essentially the explanation suggested by Dvorak to account for the movement of the liquid as observed by him (see fig. 1), but he made no attempt to calculate the magnitude of the effect and his explanation is not complete. In particular it is not clear how the small excess pressure at the nodes causes the uprush of liquid at the antinodes, as illustrated in Dvorak's sketch. In any complete explanation of the formation of the spouts two additional factors must be considered: (1) the constricting action of the liquid at the antinodes, (2) viscosity effects (including vortex circulations). These are discussed in turn in the next section.

X. *Formation of Spouts.*

So far the effect of the air vibrations on the free surface of the liquid has been considered, but the movement of the liquid must also affect the air vibrations by its constricting action in the region of the antinodes. It may reasonably be assumed that the rate of volume displacement across any section of the tube is unaltered by the movement of the liquid, that is, the product of the particle velocity and the cross-sectional area at, say, an antinode is not altered. The action of the liquid in rising at the antinode is therefore to increase the particle velocity, which in turn increases the pressure difference between node and antinode, causing a further rise in level of the liquid. A stage might clearly be reached at which this state of affairs would become unstable with a consequent abrupt change in the behaviour of the liquid. This would explain in a general manner the antinodal disturbance, but the explanation is not entirely satisfactory. Values of the pressure difference required to initiate the disturbance, calculated on the above basis, are much higher than those observed experimentally. Moreover, the antinodal spouts form, or tend to form, even when the quantity of liquid in the tube is very small.

It appears that although the first factor plays some part, the second factor, the viscosity of the air, is of much greater importance in the actual formation of the spouts. Owing to viscous forces the air in the immediate vicinity of the wall of the tube and the liquid surface does not partake of the full oscillatory motion, so that the particle velocity and amplitude cannot be assumed uniform over any cross-section. The variation in amplitude with distance from the walls has been measured by Carrière (11) for a tube excited at a frequency of 50 c.p.s. The results, as might be expected, show that the amplitude rises rapidly from zero to a maximum at a short distance from the wall of the tube. In the present instance a similar variation in amplitude and particle velocity will occur normal to the liquid surface and will be most marked in the vicinity of the antinodes. This implies, by the general hydrodynamical equation, a rapid pressure gradient normal to the surface, the pressure decreasing in the vertical direction. It is to this pressure gradient that the formation of the antinodal spouts is to be chiefly attributed. If it becomes sufficiently great to overcome the surface and gravitational resistance of the liquid, the surface is ruptured at the antinode, the liquid moving upwards from the region of relatively high pressure to the region of lower pressure. The constricting action of the liquid column so formed increases rather than diminishes the pressure difference, so that in the case of viscous liquids the whole cross-section is rapidly filled by a sheet of liquid with consequent disturbance of the vibratory conditions. With liquids of smaller cohesion and surface tension the column breaks up into little drops in the upper half of the section, thus enabling the vibrations to continue at much their original intensity and the spouts to remain in action.

The vortices which form round obstacles in a vibrating gas, and which are responsible for the formation of the striations and antinodal disks in the dust-tube experiments, probably do not play such an important part in the action of the antinodal spouts, since the movement of the drops would tend to prevent the establishment of stable vortices. Moreover, at the intensities required to produce the spouts the general circulation of the air (from node to antinode down the centre of the tube, the current returning along the walls) is very vigorous and tends to prevail over the vortex circulations. It should be noted that the spouts differ from the antinodal discs in that the movement of the liquid in the spouts is upwards, whereas the general movement of the dust particles in the disks is downwards. The characteristic shape of the liquid sheets, however, with their narrow longitudinal section, suggests that the vortices do exert some influence once the spouts have been formed.

Nor do the general circulations appear to have any great part in the formation of the spouts, but they are responsible for several minor effects such as the movement of spouts formed some little distance from an antinode towards the nearest node, observed at lower frequencies ; the current along the walls being more effective in moving the spouts than the opposing central current.

XI. *Vortex Effects.*

The influence of the vortices is best seen at somewhat lower intensities, when the general circulation is relatively much weaker. The behaviour of the liquid drops and the formation of the corrugations described in sections V. and VII. respectively are due to their action.

Observations on the behaviour of the floating drops under the influence of the air vibrations confirm the views of Andrade based on experiments with small pith spheres and ivory cylinders *. The explanation of the ridge formation on his theory is briefly as follows :—Round any isolated object in a vibrating gas is formed a vortex system with four loops arranged symmetrically. For a drop on the surface of the liquid the two lower loops are naturally absent. If two drops are present close together a common vortex system is formed, and the drops approach each other, moving round into the equilibrium position, in which the line of centres is normal to the direction of vibration. If several drops are close together they are therefore drawn into a line transverse to the axis of the tube with a common cylindrical vortex on each side. The tendency for the drops to mount up into a ridge two or three deep is probably due to forces of the same nature as those responsible for the formation of antinodal spouts. The drops appear to be in close contact and once formed into a ridge show no tendency to separate, but there is, owing to recombination with the liquid, a gradual loss, which is greatly accelerated in the absence of vibration. If, on the other hand, two drops are farther apart, separate vortex systems are formed round each, and if constrained to move in a longitudinal direction the drops approach or recede from each other until the adjacent vortices touch, when they are in equilibrium. Similarly, for a line of drops there is an equilibrium position in which the cylindrical vortices just touch, the distance between them depending on the size of the vortices, which in turn depends chiefly on the frequency and intensity. The force between ridges is attractive for greater and repulsive for smaller distances than the critical distance. This explains the regular spacing of the ridges and also the behaviour of the two isolated ridges described in section V., the to and fro movement being probably initiated by the general circulations.

---

* See reference (4).

Owing to the ease of their formation and their great mobility on the liquid surface, the drops provide an especially suitable means of studying the vortex effects outlined above.

The experiments were carried out in the Research Laboratories of the Natural Philosophy Department in the University of Glasgow. The writer wishes to acknowledge his indebtedness to Professor E. Taylor Jones for constant help and encouragement during the investigation, and also to Professor T. Alty and Dr. G. Green for their interest in the work.

References.

(1) Kundt, *Ann. Physik*, vol. cxxvii. p. 497 (1866); vol. cxxviii. p. 337 (1866).
(2) Irons, Phil. Mag. (7) vol. vii. p. 523 (1929).
(3) Hutchisson and Morgan, Phys. Rev., vol. xxxvii. p. 1155 (1931).
(4), Andrade, Phil. Trans. A, vol. ccxxx. p. 413 (1932).
(5) Rayleigh, Phil. Trans. A, vol. clxxv. p. 1 (1883).
(6) Andrade, Proc. Roy. Soc. A, vol. cxxxiv. p. 443 (1932).
(7) Dvorak, *Ann. Physik*, vol. iii. p. 102 (1874); vol. vii. p. 42 (1876).
(8) Brandt and Freund, *Zeits. Phys.* vol. xcii. p. 385 (1934); vol. xcv. p. 415 (1935).
(9) Hazelhurst and Neville, J. Phys. Chem. vol. xli. p. 1205 (1937).
(10) König, *Ann. Physik*, vol. xlii. pp. 353 and 549 (1891); vol. xliii. p. 43 (1891).
(11) Carrière, *J. de Physique*, vol. x. p. 198 (1929).

III. *An Historical Note on a Paradox in Electrodynamics.*

By Ian A. Robertson, M.A., B.Sc., Assistant in Natural Philosophy in the University of Glasgow *.

[Received July 5, 1944.]

An investigation of the forces between two electrons, or charged particles, leads to a paradox concerning these forces. As this paradox has been the subject of two recent papers, one in the 'Philosophical Magazine,' August 1941, and the other in the 'American Journal of Physics,' December 1942, and an editorial in the 'Wireless Engineer,' March 1944, it may be of interest to consider this problem in relation to its historical background. In this note it will be shown that the problem was present from the beginning of electrodynamics, that Ampère considered it and used it in his fundamental formula, and that Ampère's theory is still superior to any given in the recent papers considered in connection with this problem.

The paradox will now be given in terms of the classical theory of electricity, as is given in Joos' Theoretical Physics. According to the Biot–Savart Law, a current element or slowly moving electron gives rise at a position r to a magnetic field H. This field is given by

$$\mathrm{H}=\frac{i(ds\times r)}{r^3}=\frac{e(v\times r)}{r^3}, \quad . \quad . \quad . \quad . \quad . \quad . \quad . \quad . \quad (1)$$

where an electron of charge e moving with velocity v corresponds to a current element ids, and where $(v\times r)$ represents the vector product of v and r. This field H acts upon another electron e' having velocity v' with a force given by

$$\mathrm{F}=e'(v'\times \mathrm{H})=\frac{ee'(v'\times(v\times r))}{r^3}. \quad . \quad . \quad . \quad . \quad . \quad (2)$$

Now consider two electrons moving at a certain instant, in mutually perpendicular directions, as shown in fig. 1.

The electron at A is moving with velocity v and the electron at B is moving with velocity v', perpendicular to v. When the above formula is applied it is found that there is a force on the electron at B of magnitude $\frac{ee'\,vv'}{r^2}$ acting in a direction normal to the velocity, but that there is no corresponding force on the electron at A. Hence there is a failure of Newton's Third Law when the Biot–Savart Law is applied to electrons.

Now this problem was present from the beginning of electrodynamics.

---

* Communicated by Professor E. Taylor Jones.

In 1823 Ampère published his *Mémoire* on the law of force between current elements, or as they could now be called, electrons. This theory was based on postulates which Ampère attempted to establish by experiment, but as Maxwell said of these experiments : " We can scarcely believe that Ampère really discovered the law of action by means of the experiments which he describes. We are led to suspect, what, indeed, he tells us himself, that he discovered the law by some process which he has not shown to us. . . ." The postulate which concerns our problem is given on p. 202 of the 'Mémoire de L'Académie' (1823), and may be translated thus : *an element of one current has no effect on an element of another current which lies in the plane bisecting the former at right angles.* Thus for electrons or current elements in the special case under consideration, there is, according to Ampère, who assumed Newton's Laws, no force on either of the electrons and therefore no failure of the action–reaction law. The reasons that Ampère gave for using this postulate can hardly be considered satisfactory. He stated on p. 202 : " En effet, les deux moitiés du premier élément produisent sur le second des actions égales, l'une attractive et l'autre répulsive, parce que dans l'une de ces moitiés le courant va en s'approchant et dans l'autre en s'éloignant de la perpendiculaire commune. Or, ces deux forces égales font un angle qui tend vers deux angles droits à mesure que l'élément tend vers zéro. Leur résultante est donc infiniment petite par rapport à ces forces, et doit par conséquent être négligeé dans le calcul."

Fig. 1.

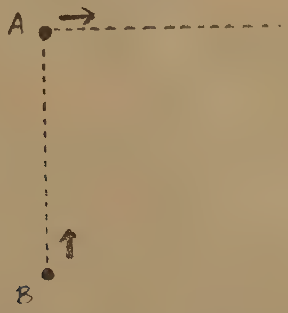

Yet it was from postulates like this, that Ampère deduced the law of force between two current elements, namely :

$$\mathrm{F}=\mathrm{C}\times\frac{ii'\,ds\,ds'}{r^2}(2\sin\theta\sin\theta'\cos w-\cos\theta\cos\theta'), \quad . \quad . \quad . \quad (3)$$

where the force F acts entirely along the line joining the elements, and where θ and θ' are the angles between the directions of ds *and* ds' and the line r joining them, and w is the angle between the plane containing ds and r and the plane containing ds' and r, and C is a constant depending upon the units chosen. This formula has borne the test of experiment. Clerk Maxwell described it as " perfect in form and unassailable in accuracy and it (Ampère's theory) is summed up in a formula from which all the phenomena may be deduced, and which must always remain the cardinal formula of electrodynamics" (vol. ii. p. 175).

If we apply Ampère's formula to our particular problem we have $\theta=\pi/2$, $\theta'=\pi$ or 0, and therefore $F=0$, showing again that if Ampère's formula is used no paradox arises. It has already been pointed out that Ampère's formula gives results in keeping with experiment, the paradox arises because Biot's rule and not Ampère's is used in classical electrodynamics. In his *Mémoire* of 1823, on p. 280, Ampère begins his criticism of Biot's formula, which gives the magnitude and direction of the force exerted by an element of a circuit on a magnetic pole, on the grounds that a magnetic pole is more complex than a simple element of a circuit and a fundamental law should be between elements of the same nature ; moreover, the force acting on the pole is at right angles to the plane containing the element and the line joining it to the pole, whereas the reaction to this force is an equal and opposite force on the element of the circuit, but acting in a direction parallel to the force on the pole, thus giving rise to a couple. Ampère goes on to state, p. 326 : " J'ai toujours regardé cette hypothèse des couples primitifs comme absolument contraire aux premières lois de la mécanique." On the other hand, Ampère was aware that Biot's rule agreed with his own, when integrated around a closed circuit. Now Biot's law leads to a violation of Newton's laws for isolated elements, yet it is Biot's law which is usually applied to electrons even to this day (*cf.* Jeans' ' Electricity,' par. 628).

Fig. 2.

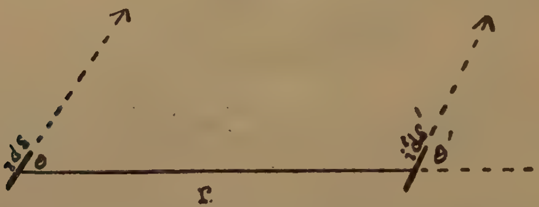

There is another interesting difference between Ampère's formula and the Biot–(Savart) law which requires consideration in the light of modern theories, and that is the force between two electrons moving in the same straight line. If Ampère's formula, given above, is applied with $\theta=\theta'=0$, we find that there is an electromagnetic force of repulsion between the elements equal to

$$-C\times\frac{ii'\,ds\,ds'}{r^2}, \qquad \ldots \ldots \ldots \quad (4)$$

while Biot's law gives no force at all between the electrons in that position.

Ampère devised an experiment to demonstrate this repulsion. The description of his apparatus is given on p. 211 of his *Mémoire*, and may be summarized thus :

A horizontal vessel PQ is divided by an insulating partition MN into two compartments. These compartments are filled with mercury and are connected by means of the wire ABCDE. This wire has two branches, AB and DE, floating on the surface of the mercury, and joined by the part BCD, which crosses over the partition MN. The wire is covered with insulating material except at its ends A and E. When the mercury-filled compartments are joined at H and K with the terminals S and T of a battery, a current flows, partly through the mercury, partly through the wire ABCDE, and the wire glides over the surface of the mercury away from the points H and K. Ampère concludes: " Quelle que soit la direction du courant, on voit toujours les deux fils AB, ED marcher parallèlement à la cloison MN en s'éloignant des points H et K, ce qui indique une répulsion pour chaque fil entre le courant établi dans le mercure et son prolongement dans le fil lui-même." This experiment is not conclusive proof that there is a magnetic repulsion between elements moving in the same straight line. The experimental fact that the wire glides away from the points H and K is usually explained thus:—" the circuit will so arrange itself as to include the maximum flux, the current being kept constant." Of course, such a statement in no way disproves Ampère's theory that a repulsion exists.

Fig. 3.

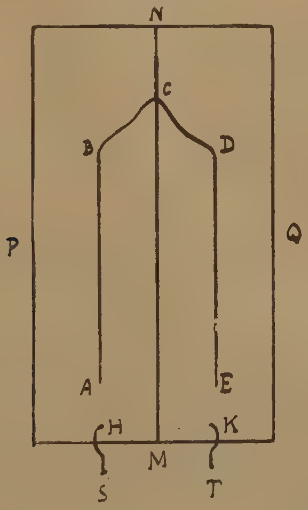

A somewhat similar experiment was described by W. F. Dunton in 'Nature,' August 1937. In this case a current is sent round a rectangle ABCD (fig. 4 (*a*)).

M and N are mercury cups which allow MBCN to move, while the portion NDAM is firmly held. Dunton attached the middle of BC to a beam balance and measured the outward force exerted upon it. Dunton devised this experiment in the hope of deciding between Neumann's and Faraday's law of induction, but that controversy does not concern this paper. Nevertheless Dunton's experiment has been used by S. B. L.

Mathur ('Philosophical Magazine,' August 1941) as experimental evidence that Biot's law is correct and that Newton's third law is wrong. However, on careful examination of Mathur's paper, excellent reasons can be deduced for discarding Biot's law. Mathur begins by stating the paradoxical case considered in this note, pointing out that by Biot's law action is not always equal and opposite to reaction, and hence if Biot's law is used, it is wrong to use Newton's third law. Ignoring Newton's laws, Mathur calculates by Biot's law the outward force on the side BC of the rectangle ABCD. If $AB=180r$, $BC=60r$, where r is the radius of the conductor of which the circuit is made, Mathur finds this force to be $6{\cdot}9i^2$, where i is the current flowing round the rectangle. Then it is pointed out that Dunton had found experimentally that under the same conditions the force is $8{\cdot}7i^2$. One would think that the difference between $6{\cdot}9i^2$ and $8{\cdot}7i^2$ would arouse suspicion that there was something wrong either with Biot's law or Dunton's experiment, but Mathur concludes "However, as it is evident, it is not the Biot–Savart law that is in error; but it leads to wrong results when the inapplicability of Newton's third law is not recognized."

Fig. 4.

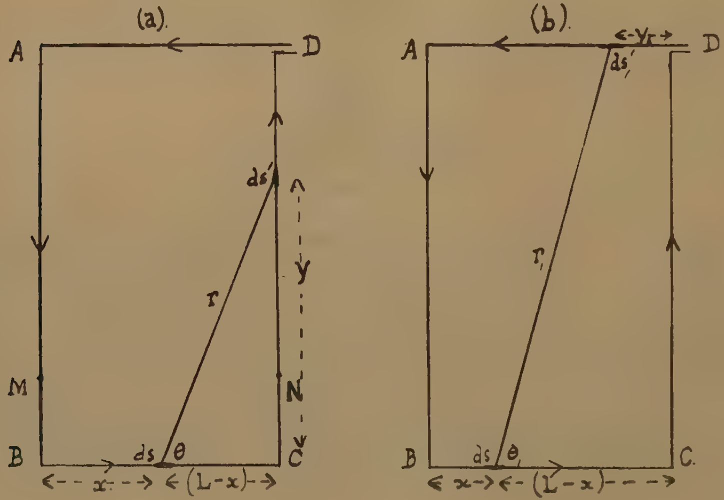
(a). (b).

As the problems connected with the forces in a rectangular circuit, one side of which is mechanically separable from the other three, are of practical importance, and have aroused a large amount of discussion in connection with the laws of induction, it may not be out of place to calculate the outward force on one side by Ampère's formula; after all, Ampère was the first of the "circuit-breakers." Ampère's formula, as given above, is

$$F=C\times ii'\,\frac{ds\,ds'}{r^2}\,(2\sin\theta\sin\theta'\cos w-\cos\theta\cos\theta').$$

Now $\cos\epsilon=\cos\theta\cos\theta'+\sin\theta\sin\theta'\cos w$, where ϵ is the angle between the directions of ds and ds'.

Hence $$F=C\times\frac{ii'\,ds\,ds'}{r^2}(2\cos\epsilon-3\cos\theta\cos\theta'). \quad . \quad . \quad . \quad . \quad . \quad (3)$$

Referring again to fig. 4, consider an element of current ds in BC and another element ds' in CD (the mercury cups M and N being placed at B and C), the force between these two elements lies along the line r joining them. Now BC is perpendicular to CD, therefore $\cos\epsilon=0$, and from the geometry of the figure $\theta'=\left(\theta+\frac{3}{2}\pi\right)$; hence there is a force of repulsion between the elements equal to

$$F_1=C\times\frac{i^2\,ds\,ds'}{r^2}[-3\cos\theta\sin\theta]$$

if we take $C=-1$, then $F_1=+\frac{i'\,ds\,ds'}{r^2}3\cos\theta\sin\theta$. Thus the outward force on ds, that is, the component force acting perpendicular to ds, due to ds', is equal to

$$\frac{i'\,ds\,ds'}{r^2}3\cos\theta\sin^2\theta.$$

Therefore, the outward force on BC due to CD is equal to

$$i^2\int_0^d ds'\int_a^{L-a}\frac{3\cos\theta\sin^2\theta}{r^2}ds, \quad . \quad . \quad . \quad . \quad . \quad . \quad (5)$$

where d is the length of the side BA, L is length of the side BC, and a is the radius of the wire, which is assumed small compared with d and L. Similarly, the outward force on BC due to AB is likewise given by the same integral, while the outward force on BC due to AD is given by

$$i^2\int_a^{L-a}ds_1'\int_a^{L-a}\frac{(2\sin\theta_1-3\cos^2\theta_1\sin\theta_1)}{r_1^2}ds, \quad . \quad . \quad . \quad (6)$$

where ds lies along BC and ds_1' along AD, and r_1 is the distance between ds and ds_1' (fig. 4 (*b*)). Thus the total outward force on BC due to the other three sides is given by

$$6i^2\int_a^d ds'\int_a^{L-a}\frac{\cos\theta\sin^2\theta}{r^2}ds+i^2\int_a^{L-a}ds'\int_a^{L-a}\frac{(2\sin\theta_1-3\sin^2\theta_1\cos\theta_1)\,ds}{r_1^2}, \quad . \quad . \quad . \quad (7)$$

where $\cos\theta=\frac{L-x}{r}$, $\cos\theta_1=\frac{L-x-y_1}{r_1}$,

$\sin\theta=\frac{y}{r}$, $\sin\theta_1=\frac{d}{r}$,

$r_2=(L-x)^2+y^2$, $r_1^2=(L-x-y_1)^2+d^2$,

$ds=dx,\ ds'=dy$, $ds=dx,\ ds'=dy_1$.

Substituting these values in the above integral (7) we obtain

$$6i^2\int_0^d y^2\,dy\int_a^{L-a}\frac{(L-x)\,dx}{[(L-x)^2+y^2]^{5/2}}$$
$$+i^2\int_a^{L-a}dy_1\int_a^{L-a}\frac{\left[2\left(\frac{d}{r}\right)-3\left(\frac{L-x-y}{r_1}\right)^2\frac{d}{r_1}\right]dx}{{r_1}^2},$$

that is

$$6i^2\int_0^d y^2\,dy\int_a^{L-a}\frac{(L-x)\,dx}{[(L-x)^2+y^2]^{5/2}}$$
$$+2i^2\int_a^{L-a}dy_1\int_a^{L-a}\frac{d\,.\,(dx)}{{r_1}^3}-3i^2\int_a^{L-a}dy_1\int\frac{[(L-x-y)^2.\,d]\,(dx)}{{r_1}^5},$$

and when this is integrated, we obtain

$$2i^2\left[\log\frac{L-a}{a}+\log\frac{d+\sqrt{d^2+a^2}}{d+\sqrt{d^2+(L-a)^2}}-\left(1+\frac{a^2}{d^2}\right)^{-\frac{1}{2}}\right.$$
$$\left.+\left(1-\frac{(L-a)^2}{d^2}\right)^{-\frac{1}{2}}+\left(1+\frac{(L-2a)^2}{d^2}\right)^{\frac{1}{2}}-\left(1+\frac{(L-2a)^2}{d^2}\right)^{-\frac{1}{2}}\right]. \quad . \quad . \quad . \quad (8)$$

If $d=180a$ and $L=60a$, we obtain the outward force on BC, due to the other three sides, equal to $8{\cdot}24i^2$, which is fairly close to Dunton's value $8{\cdot}7i^2$.

It may well be remarked that the calculation of such expressions by Ampère's original formula is laborious, but there is only one other method for calculating such forces on the sides of a rectangle, and that can only be accomplished by calculating the self-inductance of the rectangle, a process quite as complicated as the above calculation, and involving artifices which seem hardly satisfactory (*cf.* Jeans' 'Electricity,' par. 505).

Other experiments on the forces of rectangular circuits have been described by F. F. Cleveland ('Philosophical Magazine,' 1936). These experiments prove conclusively that action and reaction are equal and opposite for the mechanically separable parts of a rectangular circuit, thus showing again that the Biot–Savart law is wrong in this instance. Cleveland suggests that more use should be made of Ampère's formula and gives the expression for the force, on one side of a rectangular circuit, exerted by the other three sides. Unfortunately the expression given by Cleveland is invalidated by algebraic slips, and the expression as it stands would give the impression that the outward force on BC (fig. 4) tends to infinity as the sides AB and CD increase in length, whereas for a very long rectangle the force on the side BC is equal to

$$2i^2\log\frac{L-a}{a}. \quad . \quad . \quad . \quad . \quad . \quad . \quad . \quad . \quad . \quad (8a)$$

as can be seen at once from expression (8).

In calculating the outward force on the side BC (fig. 4), no account has been taken of the "corner effect" at B and C. This question and many others of a similar nature were studied, fourteen years before Dunton's experiment, in a most interesting paper on Electromagnetic Forces in the 'Transactions of the American Institute of Electrical Engineers' (Feb. 1923), by Carl Hering. Part of Hering's work can be stated in his own words, thus: "Researches with high current densities in such mobile conductors as liquids and arcs, have brought out some heretofore unnoticed forces, the existence of some of which had been denied." One of the conclusions of Hering's researches, which is of special interest in connection with this paper, is the longitudinal electromagnetic force acting on current elements or electrons. Now, it has already been shown that such a force was one of the basic principles of Ampère's theory, and further experiments tending to prove the existence of such a force are of the greatest importance. Hering devised many experiments to demonstrate this longitudinal force, but there is one, so simple and yet so extraordinary, that it might well rank alongside Ampère's original experiments. Here is a description of the experiment.

Fig. 5.

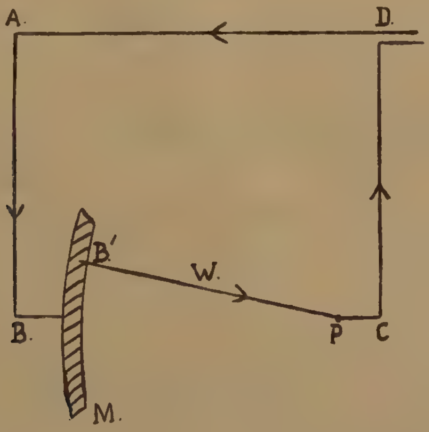

A current flows round a circuit ABCD (fig. 5). Part of the side BC is the horizontal wire W, pivoted at P, the other end of W being free to move over mercury in a curved trough M.

When Hering asked numerous physicists what would be the direction of motion of the wire W, they stated without exception that the wire would move outwards, the reason of course being "the circuit will arrange itself so as to include the maximum flux," but this, however, is contrary to experimental fact, the wire moves inwards. Indeed, the fact that the wire moves inwards is so contrary to preconceived notions, that one almost invariably suspects a trick, and soon Carl Hering had plenty of critics, but there was not one who repeated his experiment who did not also find that the wire W moves inwards, provided that the sides AB and DC are not small compared with AD.

The result can be readily explained by Ampère's theory. There is a longitudinal repulsion between the elements of the current (*i. e.* the electrons) in a metallic wire; these forces practically cancel each other, but in a liquid like mercury this longitudinal repulsion is able to push the free end of the wire W inwards. The wire W will eventually be in equilibrium under the repulsive force inwards from the forces in the mercury, and the outward force due to the rest of the circuit CDAB. When the wire W is placed on the other side of the "dead point" B, it is moved outwards under the action of two forces, one due to the mutual repulsion of the electrons in the mercury, the other due to the rest of the circuit.

There is one comment on Hering's experiment from the same journal, by John Mills, which is worth quoting: "Imagine billions of electrons rushing along from the negative terminal of the battery, along the connecting wire and plunging into the liquid of the trough. Then remember that each of these electrons is about $\frac{1}{1845}$ of the mass of the hydrogen atom. Remember that for the currents used there would be about a thousand billion billion of these electrons taking that plunge each second. Now I simply raise the question: is it inconceivable that, as they do plunge, they would kick back on the slider? I do not believe it is inconceivable and I cannot see—and here is where I differ and am unpopular—I cannot see that flux and other Maxwellian concepts enter into the problem at all."

However, there were very few of Hering's critics who agreed with his views on longitudinal magnetic forces, although not one of them could show that no longitudinal forces existed; there were many, however, who attempted to explain Hering's experimental facts in terms of electromagnetic induction, etc. John H. Morecroft was without doubt successful in giving an alternative explanation to this experiment of Hering. Morecroft repeated the experiment using heavy currents and observed the equilibrium position of the wire W; then he measured the self-inductance of the circuit by a resonance method, using a frequency of four million cycles per second. Morecroft found that the self-inductance of the circuit decreased as the wire W was varied from its original equilibrium position; and hence the problem could be explained in terms of self-inductance, but this in no way disproves the first explanation based on the assumption that a longitudinal force exists.

As already stated, no account was taken of the "corner effect" at B and C, in fig. 4, in the calculation of the outward force on BC. If there were mercury cups at B and C (neglecting those at M and N), there would be an extra outward force on BC due to longitudinal repulsive forces arising in the mercury.

The paradox under consideration was considered in great detail in a long mathematical investigation, involving the special theory of relativity, time of propagation of the field, etc., by J. M. Keller in the 'American Journal of Physics,' December 1942. Concerning this problem Keller states "one can restore the third law to complete respectability and validity by introducing the artifice of the electromagnetic field, to which one attributes a momentum density $\frac{1}{4\pi c}$ E×H. The field has just as much claim to reality as the original concept of momentum." Keller accepts the classical results, *i. e.* the Biot–Savart law; this, of course, leads to the paradox described at the beginning of this paper, but Keller attempts to surmount that difficulty by the use of a "field" which is solely due to the electrons themselves! One may well ask what is the difference between the charge on a particle and the "field" due to that charge; but that difference is not explained by Keller. Keller's argument may be all right for two vortex filaments in a liquid like water, which has inertia, but if it is to hold for charged particles in free space, then these particles must be assumed to be imbedded in an æther, also having inertia. Poynting believed that such an æther existed and derived an expression for its momentum density, and it is on this momentum density that Keller has based his paper. Now Poynting's theorem is a useful mathematical expedient for calculating energy radiated from wireless ærials, etc., but the large number of experiments devised during the last fifty years, for the purpose of detecting such an æther, leave no shadow of doubt that Poynting's method is devoid of any physical reality. The fact that Keller showed that the force on the electron at B is equal to $-\frac{1}{4\pi c}\frac{\partial}{\partial t}(\mathrm{E}\times\mathrm{H})$, where E and H are the electrical and magnetic fields at B, in no wise solves the paradox. One rather remarkable feature of Keller's paper is the great use made of the notation of the special theory of relativity, despite the fact that an æther is implied although not stated; however, towards the end of this paper the assumption is made that the electrons are going very slowly with uniform velocity, and hence all factors such as $\left(1-\left(\frac{v}{c}\right)^2\right)^{-\frac{1}{2}}$ can be equated to unity.

While investigating the difficulties arising from these problems, I mentioned the paradoxical case to Professor G. W. O. Howe, who published an account of the problem and his conclusions upon it as an Editorial in the 'Wireless Engineer,' March 1944. Professor Howe concluded that there was no magnetic force on either electron in the particular position, by virtue of displacement currents surrounding each electron and causing the electron to act similarly to a toroidal magnet. This conclusion satisfies the particular problem, because if there is no magnetic force on either electron there is no failure of Newton's third law, and it also agrees with Ampère's original postulate. As can be gathered from the article, Professor Howe does not regard his explanation as final, but rather as an attempt to arouse interest in a paradox which is not easily solved. It is only right to remark that Professor Howe's conclusion is a direct contradiction of the Biot–Savart law, which is the one used by electrical engineers.

It has already been noted in this paper that Ampère also had difficulty in giving reasons to justify his postulate on this particular problem, but as he used this postulate to derive a formula which gives results in keeping with experiment, it can be safely said that Ampère's postulate is in keeping with experimental evidence. One cannot divorce this paradox from the rest of electrodynamics, as Professor Howe seems to imply in his Editorial (p. 107): "It must be emphasised that we are not here concerned with forces between moving electrons in general, but only with the special case illustrated in fig. 1."

Ampère was anxious that his law of force between elements of currents should be in keeping with Newton's law of motion, and in that he was almost completely successful, but in the year 1823, the Conservation of Energy was not known as a universal principle of nature, and Ampère did not consider his theory in terms of that important concept. For instance, if we try to find the energy of a system consisting of two Ampèrean elements, we are driven to conclude that the energy depends upon the angles which the elements make with the line joining them; yet, if this is so, couples will arise between the elements, when the angles are varied; and this is contrary to Ampère's original postulate that between two elements there is only a force along the line joining them. Nevertheless, the potential energy of two closed circuits is correctly given by Ampère's formula, as F. E. Neumann showed in 1845; and it is only fair to say that Biot's formula, likewise, gives the same result for two closed circuits.

Now, although Ampère's formula is not perfect, it is surely superior to Biot's, the one at present in use. It is indeed strange why Ampère's formula is so often misrepresented; for example, in Jeans' 'Electricity,' par. 497, we find: "Clearly the resultant is a force at right angles both to OP and to ds and of amount

$$\frac{i\,ds\sin\theta}{r^2},$$

where θ is the angle between OP and ds. [OP$=r$.]

"Thus the total force at P may be regarded as made up of contributions such as $\frac{i\,ds\sin\theta}{r^2}$ for each element of the circuit. This is known as Ampère's law." Now, from an historical point of view, the law given is not Ampère's but Biot's, and moreover it was severely criticised by Ampère. In the light of modern theories this criticism by Ampère is worth reading. The reason why Biot's formula has been preferred to Ampère's may be due to the fact that Biot's formula lends itself to simpler calculations, and, over closed circuits, where both formulæ give identical results, that is an advantage.

The object of this paper has been to draw attention to a formula in existence since the beginning of electrodynamics, superior to, although a little more complicated than, the one at present in use, and particularly suited to dealing with this paradox which has aroused a great deal of discussion. Moreover, this formula suggests that the magnetic force between electrons has a component parallel to the direction of the motion of the electrons, and although there are many who do not like this idea, it does not appear to have ever been proved wrong, and there are many experiments which can be much more easily explained in terms of this force, but further research is urgently required into that important aspect of the problem.

I wish to express my thanks to Professor Taylor Jones for much encouragement and advice, and also to Professor G. W. O. Howe for the loan of many papers and for valuable criticism. I wish it to be understood that I am solely responsible for the opinions and criticism expressed in this paper.

References.

A. Ampère, *Mémoire de L'Académie royale des sciences de L'Institut de France*, vol. vi. p. 175 (1823).
F. F. Cleveland, Phil. Mag. vol. xxi. p. 416 (Feb. 1936).
W. F. Dunton, 'Nature,' vol. cxl. p. 245 (Aug. 1937).
C. Hering, Trans. A.I.E.E. vol. xlii. p. 139 (Feb. 1923).
G. W. O. Howe, 'Wireless Engineer,' vol. xxi. Editorial (March 1944).
J. H. Jeans, 'Electricity and Magnetism,' § 497 (1925).
G. Joos, 'Theoretical Physics,' p. 447.
J. M. Keller, 'American Journal of Physics,' vol. x. p. 302 (Dec. 1942).
S. B. L. Mathur, Phil. Mag. vol. xxxii. p. 171 (1941).
Clerk-Maxwell, 'Electricity and Magnetism' (1873).
A. O'Rahilly, 'Electromagnetism,' chap. iv.
I. A. Robertson, "Magnetic Moments," Phil Mag. vol. xxxiv. p. 182 (March 1943).
J. J. Thomson, British Association Report, p. 98 (1885).

IV. *Construction of Groups of Commutative Functions.*

By Ludwik Silberstein, Ph.D.*

[Received January 11, 1944.]

Two functions, f and g, of a single variable x are said to be *commutative* or to commute with each other if, operationally,

$$fg=gf,$$

that is, $f[g(x)]=g[f(x)]$, for all x.

Let $g(x)$ be given and let it be required to find $f(x)$ as an analytical function commuting with $g(x)$. If we write $y=g(x)$, then the equation to be solved for f is

$$f(y)=g[f(x)],$$

whence, assuming the differentiability of both functions,

$$f'(y)\,g'(x)=g'[f(x)]f'(x),$$

$$f''(y)\,g'^2(x)+f'(y)\,g''(x)=g''[f(x)]f'^2(x)+g'[f(x)]f''(x),$$

---

* Communicated by the Author.

and so on. Let $x=\lambda$ be a fixed point of g, that is, $g(\lambda)=\lambda$. Then $f(\lambda)=g[f(\lambda)]$, which can be satisfied by $f(\lambda)=\lambda$. Thus the first derivative equation becomes at the fixed point an identity, $f'(\lambda)g'(\lambda)=g'(\lambda)f'(\lambda)$ leaving, so far, $f'(\lambda)$ free. The second derivative equation, with $g'(\lambda)$, $g''(\lambda)$ as known numbers, expresses $f''(\lambda)$ in terms of $f'(\lambda)$. Similarly, the third and higher derivative equations will either be satisfied identically at the fixed point or give some relations between $f'''(\lambda)$, etc., and the lower derivatives of the unknown function at the fixed point, and so on. Account being taken of all these necessary relations, the analytical solution of the proposed equation will become

$$f(x)=\lambda+f'(\lambda)(x-\lambda)+\frac{1}{2!}f''(\lambda)(x-\lambda)^2+\ldots,$$

where some of the coefficients $f^{(n)}(\lambda)$ may remain free, as so many parameters of $f(x)$, while others are completely determined by these parameters, according to the nature of the given function g. If this be such that $f'(\lambda)=1$, while $f''(\lambda)$, $f'''(\lambda)$, etc., are all nil, we are left with the trivial solution $f=1$, that is, $f(x)=x$. (Of course, $1g=g1$ for every g.) Such a function $g(x)$ would then be said to admit no commuting mate at all. Otherwise, the series, provided that it converges, will give an actual solution valid, at least, in some neighbourhood of the point $x=\lambda$.

The following two general properties will be helpful for the sequel.

Let g^{-1}, as operator, be the inverse of g. Apply it to $fg=gf$. Then $g^{-1}fg=f$ and $g^{-1}fgg^{-1}=g^{-1}f$, so that

$$fg^{-1}=g^{-1}f. \qquad \ldots\ldots\ldots \quad (1)$$

That is to say, if a function commutes with $g(x)$, it will commute also with *the inverse* function, $g^{-1}(x)$.

Again, let f_1 and f_2 be any two functions commutative with g, that is,

$$f_1g=gf_1 \text{ and } f_2g=gf_2.$$

From the second assumption follows $g^{-1}f_2g=f_2$; by the first assumption, $f_1g.g^{-1}f_2g=gf_1.f_2$, and since the product of functions (as operators) is associative, we have

$$f_1f_2.g=g.f_1f_2. \qquad \ldots\ldots\ldots \quad (2)$$

In words, if two functions (operators) commute with a third, so does their *product*, that is, the function $f_1[f_2(x)]$ and, of course, also $f_2[f_1(x)]$.*

After these generalities, let us consider in detail two special cases of $g(x)$ which have seemed to offer some points of particular interest. Each of these cases will be seen to give rise to a whole set of functions $f(x)$ of noteworthy properties.

I. *Logarithmic Group of Functions.*

Let our given function be

$$g(x)=e^x-1.$$

We have chosen the truncated exponential, instead of e^x itself, since it is convenient to have $x=0$ as a fixed point; $g(0)=0$. The inverse function is $g^{-1}(x)=\log(1+x)$.

---

* Notice, however, that f_1 and f_2 (may, but) need not necessarily commute with each other. This will depend on the nature of g.

With $y=g(x)$, the equation $fg=gf$ to be solved for f becomes

$$f(y)=e^{f(x)}-1.$$

For $x=0$ we have $y=0$ and $e^{f(0)}=1+f(0)$. Let us take the only real root of this transcendental equation, viz.,

$$f(0)=0.$$

Differentiating with respect to x, we have

$$f'(y)\,e^{x}=e^{f(x)}f'(x),$$

whence, at $x=0$, the identity $f'(0)=f'(0)$, leaving $f'(0)$ free. Next,

$$f''(y)\,e^{2x}+f'(y)\,e^{x}=e^{f(x)}[f'^{2}(x)+f''(x)].$$

At $x=0$, f'' drops out, leaving $f'^{2}(0)=f'(0)$, so that $f'(0)=0$ or 1. Let us take

$$f'(0)=1.$$

The third-order equation, which is

$$f'''(y)\,e^{3x}+3f''(y)\,e^{2x}+f'(y)\,e^{x}=e^{f(x)}\{f'^{3}(x)+3f'(x)f''(x)+f'''(x)\},$$

becomes, at $x=0$, an identity, imposing no restrictions upon f'', f'''. In fact, with $f=0$, $f'=1$, both sides of the equation are reduced to $f'''+3f''+1$. The next higher equation is

$$f^{\mathrm{IV}}(y)e^{4x}+6f'''(y)e^{3x}+7f''(y)e^{2x}+f'(y)e^{x}=e^{f}\{f'^{4}+6f'^{2}f''+4f'f'''+3f''^{2}+f^{\mathrm{IV}}\},$$

with x as argument throughout in the second member. For $x=0$ the coefficient f^{IV} cancels out and we have the relation

$$f'''(0)=\frac{1}{2}f''(0)\,[3f''(0)-1],$$

while $f''(0)$ is left undetermined and will remain unrestricted by all higher equations, say $f''(0)=a$, a free parameter of the function $f(x)$. The fifth-order equation, written down for $x=0$, leaves f^{V} free and leads to a unique value of the fourth coefficient, viz.,

$$f^{\mathrm{IV}}(0)=\frac{1}{2}a(2a-1)(3a-1).$$

Similarly, the sixth-order equation gives

$$f^{\mathrm{V}}(0)=\frac{a}{3}\left\{\frac{45}{2}a^{3}-\frac{65}{2}a^{2}+15a-2\right\},$$

and so on. All higher coefficients are completely determined by the parameter a. Generally, $f^{(n)}(0)$ is a polynomial in a of degree $n-1$, vanishing for $a=0$. A more convenient method of evaluating the higher polynomials will be given presently.

In the meantime we may write down the leading terms of the series,

$$f(x)=x+a\frac{x^{2}}{2}+\frac{a}{2}(3a-1)\frac{x^{3}}{3!}+\frac{a}{2}(2a-1)(3a-1)\frac{x^{4}}{4!}+f^{\mathrm{V}}(0)\frac{x^{5}}{5!}+\dots, \qquad (3)$$

which will give a sufficiently good idea of the nature of the function $f(x)$ commuting with $g(x)$.

A convenient check of the correctness of any coefficient found by the differential method readily suggests itself. The function $f(x)$ is the most general analytical solution of the equation $gf=fg$, with the conditions $f(0)=0$ and $f'(0)=1$. Since g certainly commutes with itself and $g(0)=0$, $g'(0)=1$, the function $g(x)$ must be contained in the set of functions $f(x)=f(x, a)$, which is possible only for $a=1$, since $g(x)=x+\frac{x^2}{2!}+\ldots\ldots$ Hence, for $a=1$, every coefficient $f^{(n)}(0)$ in (3) must be equal to 1. Such, in fact, is the case. We have

$$f'''(0)=\frac{1}{2}(3-1)=1, \quad f^{\text{IV}}(0)=\frac{1}{2}(2-1)(3-1)=1, \quad f^{\text{V}}(0)=\frac{1}{3}(13-10)=1.$$

There seems to be no royal road to the coefficients of the series, but they are all virtually expressible as unique polynomials of the parameter a. A general recurrency formula for $f^{(n)}(0)$ would be very hard, if at all possible, to find. Under such circumstances, a rigorous convergency criterion of the series (3), within a given range of the parameter a and the variable x, cannot be contemplated. Yet, apart from formal rigour, one can see that the series will converge, at least, within a certain range of a, namely, $0<a<1$. For, at its lower limit we have $f(x)=x$ and, at its upper limit, $f(x)$ reduces to $g(x)=x+\frac{x^2}{2!}+\ldots$, which is always convergent, so that the f-series can be plausibly expected to converge, at least, for fractional values of its parameter. (For an extension to $a>1$ *vide infra.*)

In this connection it may not be amiss to consider one or two numerical examples.

Thus, let $a=\frac{1}{2}$. Then the fourth coefficient vanishes,

$$f'''(0)=\frac{1}{8}, \quad f^{\text{V}}(0)=\frac{1}{32},$$

and we have up to x^6,

$$f(x)=x+\left(\frac{x}{2}\right)^2+\frac{1}{3!}\left(\frac{x}{2}\right)^3+\frac{1}{5!}\left(\frac{x}{2}\right)^5+\ldots\ldots \qquad (3, \tfrac{1}{2})$$

These first four terms alone turn out to give a remarkably close approach to the requirement $fg=gf$, not only for fractional x, but even for $x=1$. In fact, to four decimals,

$$f(1)=1{\cdot}2711, \quad gf(1)=2{\cdot}5647$$

and, on the other hand,

$$g(1)=1{\cdot}71828, \quad fg(1)=2{\cdot}5659.$$

The excess of the latter value amounts only to 0·0012. Again, as we saw under (1), our function must commute with the inverse function, $g^{-1}(x)=\log(1+x)$, that is to say,

$$f[\log(1+x)]=\log[1+f(x)]. \qquad (4)$$

Let us test this on the same special function $(3, \frac{1}{2})$. We now have

$$f(1)=1\cdot2711, \quad \log[1+f(1)]=0\cdot8200\,;$$

on the other hand,

$$\log(1+1)=0\cdot6931, \quad f(0\cdot6931)=0\cdot8201,$$

remarkably close to $\log[1+f(1)]$. These four decimals, moreover, are contributed by the first three terms alone (the fourth contributes only 0·00004). The approximation is even more close than in the preceding example.

Another noteworthy subcase of (3) is that for $a=\frac{1}{3}$, when both $f'''(0)$ and $f^{\mathrm{IV}}(0)$ vanish and the function is reduced to

$$f(x)=x+\frac{1}{6}x^2+\frac{1}{20}\left(\frac{x}{3}\right)^5+\ldots\ldots \qquad \ldots\ldots \quad \mathbf{(3,\ \tfrac{1}{3})}$$

This gives, for instance, $f(1)=1\cdot16688$, $\log[1+f(1)]=0\cdot77328$, against $f[\log(1+1)]=0\cdot77320$. Even the first two terms alone would satisfy the requirement of commutativity to four decimals.

The formula (3) defines a one-parametric set of functions or operators which contains the idem factor $f=1$, that is, $f(x)=x$, and the generating operator g itself. Every operator of the set commutes with g and thus also with g^{-1}. They have, moreover, remarkable properties among themselves.

In fact, by (2), the product of any two operators of the set commutes with g. And since the corresponding function manifestly vanishes at $x=0$ and has there the derivative 1, the product is again an operator of the set. We shall see presently that the inverse of any f also belongs to the set. Thus the set (3) forms a one-parametric *group* of operators (transformations) $f=f_a$ or of corresponding functions $f(x, a)=f_a(x)$, with $a=f''(0)$ as its free parameter. Since it contains also $\log(1+x)$, it may be called *the logarithmic group* of functions or operators.

If a_1 and a_2 be the parameters of two operators, then we must have

$$f_{a_1}f_{a_2}=f_a,$$

where a will depend in a certain way on a_1 and a_2. Let us find the form of this dependence and, at the same time, test explicitly the equivalence. By (3),

$$f_{a_1}(x)=x+\frac{1}{2}a_1x^2+b_1\frac{x^3}{6}+\ldots\ldots,$$

$$f_{a_2}(x)=x+\frac{1}{2}a_2x^2+b_2\frac{x^3}{6}+\ldots\ldots,$$

where

$$b_i=\frac{1}{2}a_i(3a_i-1).$$

Thus, up to x^4-terms,

$$f_{a_1}f_{a_2}(x)=x+\frac{1}{2}(a_1+a_2)x^2+\left(\frac{1}{2}a_1a_2+\frac{1}{6}b_1+\frac{1}{6}b_2\right)x^3+\ldots\ldots$$

$$=x+\frac{1}{2}ax^2+b\frac{x^3}{6}+\ldots\ldots,$$

whence $a=a_1+a_2$ and

$$b=b_1+b_2+3a_1a_2=\frac{3}{2}(a_1+a_2)^2-\frac{1}{2}(a_1+a_2)=\frac{a}{2}(3a-1).$$

This, then, verifies the expected equivalence up to x^4. (In much the same way the reader may extend the test to higher terms.) At the same time we have the property of simple *additivity* of parameters, $a=a_1+a_2$, that is to say,

$$f_{a_1}f_{a_2}=f_{a_1+a_2}. \quad \ldots\ldots\ldots \quad (5)$$

Thus also any two operators f commute with each other. Our logarithmic group is an *Abelian group* of operators or transformations *. Manifestly, the additivity of parameters holds also for any number of operators of the group and, in particular, for the n-fold iteration of an operator f_a,

$$f_a^n=f_{na}. \quad \ldots\ldots\ldots \quad (6)$$

This holds for any positive integer n and for any value of the parameter. In particular, for $a=1$, f is g, and therefore,

$$f_n=g^n,$$

that is to say, $f(x, 2)=gg(x)$, $f(x, 3)=ggg(x)$, and so on, $f(x, n)$ an n-fold iteration of $g(\lambda)=x+\frac{x^2}{2!}+\ldots.$ Now, all these iterations of the series are certainly convergent. Thus $f(x, a)$, as defined by (3), must converge for $a=2$, 3, 4, etc., and the series (3) can hardly diverge for some intermediate values of the parameter.

If f_a^{-1} be the inverse of f_a, we have

$$f_a^{-1}f_a=1=f_0=f_a f_{-a},$$

by (5). Consequently,

$$f_a^{-1}=f_{-a}. \quad \ldots\ldots\ldots \quad (7)$$

That is to say, to *invert* our function $f(x, a)$ it is enough to change the sign of its parameter,

$$f^{-1}(x)=x-\frac{1}{2}ax^2+\frac{1}{2}a(1+3a)\frac{x^3}{3!}+\text{etc.}$$

Now, this function commutes with g, vanishes at $x=0$, and has there 1 for its first derivative. It belongs, therefore, to the contemplated set of functions. The set contains the inverse of any of its elements. This, then, supplies the outstanding part of the proof that the set forms a group.

In particular, for $a=1$, we have, by (7), $f_1^{-1}=f_{-1}$. But $f_1(x)=g(x)$. Thus we must have

$$f_{-1}(x)=g^{-1}(x)=\log(1+x).$$

In fact, by (3),

$$f_{-1}(x)=x-\frac{1}{2}x^2+\frac{1}{3}x^3-\frac{1}{4}x^4+\ldots,$$

---

* From (5) follows, by one of Lie's well-known theorems, that $\frac{df_a(x)}{da}$ must be a function of $f_a(x)$ alone, not containing a explicitly. A direct test of the series (3) for this fundamental property is given below.

the familiar expansion of $\log(1+x)$. This, by the way, gives also one more check for the evaluation of any coefficients $f^{(n)}(0)$.

By (6), the relation of any operator f with a fractional parameter, such as $\frac{1}{2}$, to the operator g is given by

$$f_{\frac{1}{2}}^2=f_1=g,$$

so that $f_{\frac{1}{2}}$ may be said to be, operationally, the "square-root" of g and may be denoted by $g^{1/2}$. Similarly, $f_{1/3}=g^{1/3}$, the "cube-root" of g, and so on. Thus, *e.g.*, a twofold application of the transformation $(3, \frac{1}{2})$ should give $g(x)$. This is readily tested. As we saw, $f(1)=1{\cdot}2711$. Now, $ff(1)=1{\cdot}7187$, which is close enough to $g(1)=1{\cdot}7183$.

The whole group of operators may be briefly expressed by $f_a=f_1^a=g^a$, any operator of the group a "power" of g. The actual meaning or evaluation of this merely symbolic statement is given by the series expansion (3).

The simple sub-case of (6), $f_{2a}=f_a f_a$, can be utilized as a method for determining the higher coefficients $f^n(0)$, more convenient than the differential one. The details of this method will be seen in working out our second example. In the present case it may suffice to quote only the result. Applying this method *ab initio*, I have verified all the coefficients given above and found, for the next higher one,

$$f^{\mathrm{VI}}(0)=\frac{a}{2}\left\{45a^4-\frac{385}{4}a^3+\frac{445}{6}a^2-\frac{91}{4}a+\frac{11}{6}\right\}. \quad . \quad . \quad . \quad (8)$$

The function $f(x)$, formula (3), is thus evaluated up to x^7. We may mention that the last term in (8) is found by claiming $f^{\mathrm{IV}}(0)=1$ for $a=1$, so that the $a=1$ test is no longer available. There remains, however, the $a=-1$ test mentioned a moment ago. Now, for $a=-1$, formula (8) gives

$$f^{\mathrm{VI}}(0)=-120 \quad \text{or} \quad \frac{1}{6!}f^{\mathrm{VI}}(0)=-\frac{1}{6},$$

which is the correct coefficient of x^6 in the expansion of $\log(1+x)$.

For $a=\frac{1}{2}$, formula (8) gives the small negative coefficient $-\frac{7}{128}$, which makes the expansion $(3, \frac{1}{2})$ available up to x^7.

The whole logarithmic group of functions or transformations is now explicitly determined up to the seventh power of the operand.

The *infinitesimal* transformation which, together with the identity, is contained in the group, is found by retaining of each coefficient

$$f^{(n)}(0)=c_n(a)$$

only its lowest term in a, which is $ac_n'(0)$, thus:

$$f(x)=x+a\sum_{n=2} c_n'(0)\frac{x^n}{n!},$$

or, explicitly,

$$f(x)=x+a\left\{\frac{x^2}{2}-\frac{1}{2}\frac{x^3}{3!}+\frac{1}{2}\frac{x^4}{4!}-\frac{2}{3}\frac{x^5}{5!}+\frac{11}{12}\frac{x^6}{6!}-\ldots\right\}. \quad . \quad . \quad (9)$$

The coefficients of $\frac{x^n}{n!}$ in the bracketed series are, so far, simple proper fractions.

Returning to any transformation of the group, let us write, for brevity, $y=f(x, a)$. Then, according to Lie's theorem mentioned in the last footnote,

$$\frac{dy}{da}=\mathrm{F}(y), \quad \text{. . . . .} \quad \text{(L)}$$

a function of y alone, not containing the parameter a explicitly. Let us test our solution for this fundamental property. The expansion (3) is

$$y=x+a\frac{x^2}{2}+c_3(a)\frac{x^3}{3!}+c_4(a)\frac{x^4}{4!}+\dots, \quad \text{. . . . .} \quad \text{(A)}$$

whence

$$\frac{dy}{da}=\frac{1}{2}x^2+c_3'(a)\frac{x^3}{3!}+c_4'(a)\frac{x^4}{4!}+\dots, \quad \text{. . . . . .} \quad \text{(B)}$$

where the derivatives $c_3'(a)$, etc. are known functions (polynomials) of a. Apparently, then, $\frac{dy}{da}$ depends on x and a. But, by (7), the inversion of (A) is

$$x=y-a\frac{y^2}{2}+c_3(-a)\frac{y^3}{3!}+c_4(-a)\frac{y^4}{4!}+\dots..$$

Now, substitute this value of x in (A) and collect all terms in y^2, y^3, and so on. The coefficient of y^2 is directly seen to be just $\frac{1}{2}$, independent of a. The coefficient of y^3 is

$$-\frac{a}{2}+\frac{1}{3!}c_3'(a)=-\frac{a}{2}+\frac{1}{6}\left(3a-\frac{1}{2}\right)=-\frac{1}{2.3!};$$

a has dropped out leaving the pure number $\frac{1}{3!}c_3'(0)$. The coefficient of y^4 is

$$a^2\left(\frac{1}{8}+\frac{1}{4}-\frac{9}{12}+\frac{9}{24}\right)+a\left(\frac{1}{12}+\frac{1}{8}-\frac{5}{24}\right)+\frac{1}{4!}c_4'(0)=\frac{1}{4!}c_4'(0)=\frac{1}{2.4!}.$$

In much the same way the reader will find that the terms in a^3, a^2, a of the coefficient of y^5 all drop out and what is left is

$$\frac{1}{5!}c_5'(0)=-\frac{2}{3}\cdot\frac{1}{5!},$$

and similarly for the coefficient of y^6.

Thus our solution (3) is tested for the property (L). At the same time we have found for the function $\mathrm{F}(y)$ the expansion

$$\mathrm{F}(y)=\sum_{n=2}^{\infty} c_n'(0)\frac{y^n}{n!},$$

that is to say,

$$\frac{dy}{da}-\mathrm{F}(y)=\frac{1}{2}\left[y^2-\frac{y^3}{3!}+\frac{y^4}{4!}-\frac{4}{3}\frac{y^5}{5!}+\frac{11}{6}\frac{y^6}{6!}-\dots\right], \quad . \quad \text{(10)}$$

a function of $y=f(x, a)$ alone, with purely numerical coefficients.

Notice that exactly the same function, with x as argument, appears in the infinitesimal transformation (9), which may be rewritten

$$y = x + a\mathrm{F}(x). \quad \dots\dots\dots \quad (9')$$

No wonder. For, since in the infinitesimal transformation terms in a^2, etc. are to be neglected, it may as well be written $y = x + a\mathrm{F}(y)$, whence $\frac{dy}{da} = \mathrm{F}(y)$, which is the original definition of F.

The expansion (10) of the function $\mathrm{F}(y)$, which characterizes the contemplated group of functions or transformations, shows a comparatively simple structure.

II. *Trigonometric Group of Functions.*

Let us now try to find an analytical function $f(x)$ commuting with $\sin x$. The equation to be solved becomes

$$f(\sin x) = \sin f(x)$$

or, with $y = \sin x$,

$$f(y) = \sin f(x),$$

whence $f(0) = \sin f(0)$. As before, let us take the only real root of this equation, $f(0) = 0$. The first two derivative equations, with f written for $f(x)$, are

$$f'(y)\cos x = \cos f . f'$$

and

$$f''(y)\cos^2 x - f'(y)\sin x = -\sin f . f'^2 + \cos f . f''.$$

At $x = 0$, the former gives the identity $f' = f'$ and the latter, the identity $f'' = f''$. The third-order equation, which need not be rewritten here, is more informative. It gives, at $x = 0$, $f'^3 = f'$, and thus, $f' = 0$ or ± 1. Let us choose

$$f'(0) = 1.$$

The fourth derivative equation, which consists of eight terms, reduces at the origin to $f^{\mathrm{IV}} - 4f'' = -6f'' + f^{\mathrm{IV}}$, leaving f^{IV} free and claiming

$$f''(0) = 0.$$

The fifth-order equation which, of course, is yet more unwieldy, gives, at $x = 0$, the identity $f^{\mathrm{V}} - 10f''' = -10f''' + f^{\mathrm{V}}$, refusing all information about f''', f^{V} and f^{IV} as well. Nor is the sixth derivative equation more enlightening, as the reader may find for himself. The differential method becomes prohibitively cumbersome and will, therefore, be replaced by a more convenient one, mentioned above.

Let us put $f'''(0) = -a$, leaving its value undetermined. Since $f'(0) = 1$ and $f''(0) = 0$, we may, at any rate, write

$$f_a(x) = x - a\frac{x^3}{6} + c_4 x^4 + c_5 x^5 + \dots, \quad \dots\dots \quad (11)$$

where the constant coefficients c_4, etc., are to be determined. If we assume, tentatively, that the value of a will remain unrestricted by the conditions of the problem (as in the preceding case) and that all c_κ will be completely determined by a, then $f(x)$ will be a one-parametric set of functions commuting with $\sin x$ and vanishing at $x=0$. Thus also $f_a f_b(x)$ will be a function of the set, and its parameter is readily found to be $a+b$, or $f_a f_b = f_{a+b}$. In particular, $f_{2a}=f_a f_a$ or, by (11), with $c_\kappa = c_\kappa(a)$ and $c'_\kappa = c_\kappa(2\,a)$,

$$x-2a\frac{x^3}{6}+c'_4x^4+c'_5x^5+\ldots=f_a(x)-\frac{a}{6}f_a^3(x)+c_4f_a^4(x)+c_5f_a^5(x)+\ldots.$$

$$=x-\frac{a}{6}x^3+c_4x^4+\ldots-\frac{a}{6}x^3\left[1-\frac{a}{6}x^2+c_4x^3+\ldots\right]^3+c_4x^4\,[\text{idem}]^4+\ldots,$$

which reduces at once to

$$-\frac{a}{3}+c'_4x+c'_5x^2+\ldots$$

$$=-\frac{a}{6}+c_4x+c_5x^2+\ldots-\frac{a}{6}\left[1-\frac{a}{6}x^2+c_4x^3+\ldots\right]^3+c^4x\,[\text{idem}]^4+\ldots..$$

The constant terms are the same on both sides, $-\frac{a}{3}$ and $-\frac{a}{6}-\frac{a}{6}$, leaving a free, as expected. A comparison of the coefficients of x gives

$$c'_4=2c_4 \quad \text{or} \quad c_4(2a)=2c_4(a),$$

so that $c_4=ma$, where m is independent of a. But for $a=1$ we must have

$$f_1(x)=\sin x=x-\frac{x^3}{3!}+\frac{x^5}{5!}-\ldots,$$

so that $m=0$ and $c_4=0$ for any a. Next, the coefficients of x^2 give

$$c'_5=c_5+\frac{1}{12}a^2+c_5,$$

or

$$c'_5-2c_5=\frac{a^2}{12}.$$

Put $c_5=\alpha a+\beta a^2$. Then $2\beta a^2=\frac{a^2}{12}$ and

$$c_5(a)=\frac{1}{24}a^2+\alpha a,$$

where α is, so far, undetermined. But $c_5(1)=1/5!$ Thus, $\alpha=-4/5!$ and the required coefficient is

$$5!\;c_5=5a^2-4a.$$

Next, by comparing the coefficients of x^3, we find $c'_6=2c_6$ or $c_6(2a)=2c_6(a)$, whence, as before, $c_6=0$. Such also will be the case of all higher "even" c_κ. The comparison of the coefficients of x^4 gives

$$c'_7-2c_7=-\frac{a^3}{72}-\frac{4}{3}ac_5.$$

Proceeding as before and noticing that $c_7(1)=-1/7!$, we find

$$7!\;c_7=-\frac{175}{3}a^3+112a^2-\frac{164}{3}a.$$

In much the same way c_9 and higher coefficients can be evaluated with comparative ease, but those found above ought to suffice for the present.

Thus the one-parametric set of functions or transformations commutative with $\sin x$ becomes, up to x^9,

$$f(x, a)=x-a\frac{x^3}{3!}+(5a^2-4a)\frac{x^5}{5!}-\frac{1}{3}(175a^3-336a^2+164a)\frac{x^7}{7!}+\ldots\ldots \quad (12)$$

This set contains the function upon which it has been based, $f(x, 1)=\sin x$, the identical transformation, $f(x, 0)=x$, and the inverse of any transformation, $f^{-1}(x, a)=f(x,-a)$. The product of any two elements of the set is again an element of the set, and since its parameters are simply additive, $f_a f_b=f_{a+b}$, all elements of the set commute with each other. Thus, as in the preceding case, based on e^x-1, the set forms an *Abelian group* of functions or transformations* which may be called *the trigonometric* group, since $\sin x$ belongs to it.

In fact, since $f_1=\sin$, the whole group may be expressed, symbolically, by $f_a=\sin^a$.

In particular, for $a=n$, any positive integer, f becomes an iteration of the operator sin. Thus, *e. g.*, for $n=2$, by formula (12),

$$f_2(x)=\sin\sin x=x-\frac{1}{3}x^3+\frac{1}{10}x^5-\frac{23}{630}x^7+\ldots\ldots \quad . \quad (12, 2)$$

These few terms of the series give a tolerably close approximation, even for a whole radian. We have, to three decimals, $f_2(1)=0{\cdot}730$, against the actual value $\sin\sin(1)=0{\cdot}745_6$. The bulk of the defect $0{\cdot}016$ would, no doubt, be made up by the x^9 term which is, presumably, positive. At half that angle the approximation is, of course, much closer, $f_2(\tfrac{1}{2})=0{\cdot}4609$ against $\sin\sin(\tfrac{1}{2})=0{\cdot}4613$, with a defect of $0{\cdot}0004$ only.

For $a=\dfrac{1}{n}$ we have the (operational) n-th "root" of the sine. Thus, for instance,

$$f_{\frac{1}{2}}(x)=\sqrt{\sin}\,(x)=x-\frac{1}{2}\frac{x^2}{3!}-\frac{3}{4}\frac{x^5}{5!}-53\frac{x^7}{7!}-\ldots\ldots, \quad . \quad (12, \tfrac{1}{2})$$

where $\sqrt{\sin}$ stands for the operator whose iteration is the ordinary sine. This gives, *e. g.*, for $x=\dfrac{\pi}{6}$ or 30 degrees, $\sqrt{\sin}\left(\dfrac{\pi}{6}\right)=0{\cdot}5112$ (to which the first three terms alone contribute $0{\cdot}5113$). Now, $\sqrt{\sin}\,(0{\cdot}5112)=0{\cdot}4989$, against $\sin\dfrac{\pi}{6}=\dfrac{1}{2}$.

---

* The *infinitesimal* transformation is

$$f(x)=x-a\mathrm{F}(x)=x-a\left\{\frac{x^3}{3!}+4\frac{x^5}{5!}+\frac{164}{3}\frac{x^7}{7!}+\ldots\right\}.$$

For $a=-1$, our function should be the inverse of the sine or arc sin x. Now, by (12),

$$f_{-1}(x)=x+\frac{x^3}{3!}+9\frac{x^5}{5!}+225\frac{x^7}{7!}+\dots$$

$$=x+\frac{1}{2}\frac{x^3}{3}+\frac{1.3}{2.4}\frac{x^5}{5}+\frac{1.3.5}{2.4.6}\frac{x^7}{7}+\dots,$$

which is the well-known expansion of arc sin x. This is, incidentally, one more test of the correctness of the coefficients of the series (12) representing (up to x^9) the whole " trigonometric " group of functions.

129 Seneca Parkway,
Rochester, N.Y.
December 8, 1943.

V. *Study of the Relative Intensities of Lines in Fibre X-ray Camera Photographs.* By Professor E. A. OWEN and Dr. I. G. EDMUNDS *.

[Received June 21, 1944.]

[Plate III.]

1. *Introduction.*

As a preliminary † to the study of the change in the intensity of lines in X-ray structure-spectra with the change in temperature of the specimen, it was necessary to choose the camera most suitable for the purpose and to establish a reliable method of procedure. Of the types of camera available the fibre camera possesses certain obvious advantages over the others. For instance, the specimen used with this camera is small and can, for that reason, be more easily heated uniformly ; also a much wider range of reflecting angles is possible than with, say, the focusing type of camera, but with both of these cameras there is uncertainty regarding the absorption correction, and in this respect the flat powder plate camera, of the type described by Brentano (1) and by Brindley and Spiers (2), is more satisfactory, but this, on the other hand, cannot easily be adapted for high temperature work.

After considering all aspects of the problem it appeared to us that the fibre camera would be the most suitable for the investigation provided a fibre could be produced which would yield reliable results that could readily be interpreted. It has been our aim to prepare such fibres and this paper contains an account of some observations made with them at ordinary temperatures.

---

* Communicated by the Authors.

† This work was completed before the outbreak of war.

The order of procedure was to measure firstly the lines in photographs obtained with a flat plate camera in order to find how closely the relative intensities of the lines repeated those with the same material, recorded by other workers, and then, if agreement could be established, to proceed to the measurement of the intensity of the lines in fibre camera photographs which had been taken with the special fibres prepared for the purpose.

2. *Preliminary Work.*

i. *Previous Work.*

It is essential in work of this nature to know exactly the relation between the intensity of the X-rays falling on the photographic film and the blackening which the rays produce, and so the first part of the investigation deals with this point. Other workers have examined the laws of blackening of a film exposed to X-rays, but as there seems to be some disagreement in their findings, due largely no doubt to varying conditions of experiment since the blackening may vary with the film and the method of development as well as with the quantity and quality of the X-rays, it was decided to make a thorough investigation of the law of blackening under conditions which would obtain in future work carried out in this laboratory.

The density of blackening of the film (D) is defined as $\log_{10}(L_0/L)$, where L and L_0 are the intensities of light transmitted through the blackened and unblackened (or unexposed) parts of the film. Bouwers ⁽³⁾ found that the relation $D = c \log\left(\frac{It}{a}+1\right)$ is satisfied for values of D up to 3. In this equation, a and c are constants, I the intensity of the incident X-rays, and t the time of exposure. The constant c was found to be independent of wave-length but to increase asymptotically with the time of development. Bouwers worked with heterogeneous radiation as well as with the Kα radiations of molybdenum, platinum, and copper, the Kβ radiations having been removed by appropriate filters.

Using molybdenum Kα radiation reflected from a cleavage face of calcite, Brindley and Spiers ⁽⁴⁾ have also made investigations of the blackening of X-ray films; they employed Ilford double-coated films which they developed under standard conditions. The conclusion they reached was that for values of blackening up to 1·4, the relation between the blackening (D) and the quantity of X-rays (It) falling on the film, is a linear one, that is, $D = kIt$, where k is a constant. For greater values of D, the curve departs from a linear course and bends over towards the (It)-axis, in general agreement with Bouwers. In both investigations however, the blackening is found to be a function of the quantity of X-rays falling on the film.

ii. *Relation between blackening and quantity of X-rays falling on the film.*

For the measurement of the blackening of the X-ray film there was available a Moll microphotometer, the traces obtained with which were employed to arrive at the values of the intensities of blackening. This procedure was altered later, but for the whole of the measurements referred to in this paper the microphotometer traces recorded with the instrument were measured.

In the first attempts at calibration, X-ray films processed in a fine-grain developer were employed. The films were exposed to direct radiation from a cobalt-target, a filter of iron being used to remove the β-radiation as well as some of the general radiation. Each film, in the form of a strip about one inch wide, was encased in a black envelope which was held in position behind a lead screen. The rays fell on a small part of the film through a hole in this screen and could be cut off by a lead shutter. The edges of the hole were bevelled to reduce the amount of X-rays scattered by the lead on to the film. Exposures ranging from 2 to 100 seconds were made, a fresh part of the film being moved opposite the aperture in the screen for each exposure. As the output of the tube varied appreciably, standard exposures were frequently interposed as a check on this variation.

Fig. 1.

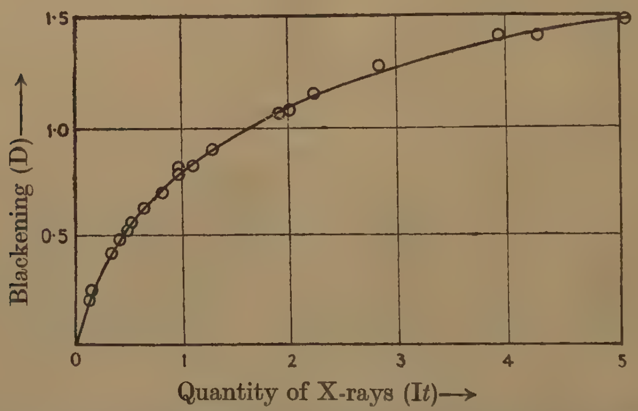

Relation between blackening of the film and quantity of X-rays falling upon it under initial conditions specified in text.

When the blackening was plotted against time of exposure a different curve was obtained for each series of readings depending upon the thickness of filter used and the running of the X-ray tube. If, however, the curve for one series be plotted and the time intervals for any other series be multiplied by a factor which brings one point on this curve, then *all* the points of the series lie on the curve (fig. 1). This is evidence that blackening is a function of the product It, the quantity of X-rays falling on the film—a result in agreement with previous investigations—but under the conditions of experiment the blackening is not a linear function of this quantity. The curve in fig. 1 agrees more nearly with Bouwers' results.

Owing to the presence of a considerable amount of general radiation and to the unsteadiness of the X-ray tube, this curve was not considered satisfactory, and an attempt was next made to calibrate the blackening of the film by a method similar to that described by Brindley and Spiers (4) in which a bank of films was used. For this purpose a flat powder plate camera, which will be described in detail later, was employed. A plate of copper filings was mounted at the centre of this camera and six strips of film were placed one behind the other on its circumference. Radiation from a copper target, filtered through nickel, fell on the powder plate and the reflections from the (111) and (200) planes were approximately in focus. The films, held in a small rack, were all developed together at 65° F. and the developer was continually stirred. The fine-grain developer was again used. When the logarithm of the blackening (D), after allowing for the background, was plotted against the number of the film (*n*), in order of sequence, the resulting graph showed curvature both for the (111) and for the (200) reflections. It was definite evidence that log D was not, in this case, a linear function of n, and therefore the blackening was not a linear function of the intensity of the X-ray beams falling on the films.

It was suspected that the difference between these findings and those of Brindley and Spiers might be due to the developer used; a more accurate method of exposure was also desirable. So the work was repeated using Ilford double coated X-ray films processed in the standard Ilford developer, developing for five minutes at 65° F., and employing a rotating sector wheel so constructed that a number of areas on a film could be exposed to X-rays for periods of time in the ratios 1, 2,...., 8. With this wheel characteristic radiation from silver or copper filings could be used; the chief difficulty was to obtain a reflected beam of sufficiently uniform intensity to cover an opening measuring 1″ by 0·25″. A satisfactory reflected beam was obtained from the (311) planes of silver, using copper radiation filtered through nickel, when a large flat plate of silver filings was mounted about six inches from the window of the tube and eight inches from the sector wheel. All the edges on the sector wheel were bevelled as before to diminish the amount of radiation scattered on to the film. The exposures were made when the film, in its black envelope, was situated immediately behind the wheel and backed by a sheet of lead. Exposures, when the wheel was stationary and the whole film opening was exposed to radiation, were made alternately with those made when the wheel was rotating; the measurement of traces of the exposures made when the wheel was stationary enabled small corrections to be applied for the lack of uniformity of the intensity of the beam over the whole film-opening. These corrections have been entered in Table I. as changes in the unit of time, assuming that $D=f(It)$ over these small ranges.

Plotting for each film the values of the blackening and the corrected time ratios, the graphs show that within experimental error the blackening varies linearly with time up to $D=0\cdot8$; above this value the blackening does not increase so fast with time. The final calibration curve is shown in fig. 2.

On the results of these experiments it was considered safe to assume a linear relation between the blackening (D) and the quantity of X-rays (It) falling on the film up to D=0·8 units, when Ilford X-ray films and developer were used.

In the later stages of the work, Kodak Duplitized Safety X-ray films, developed under standard conditions in the Kodak X-ray developer, were employed. The calibration curve in this case was similar in form to that obtained with the Ilford films, the linear portion extending to a blackening of about the same value as before.

TABLE I.

Actual Time ratios.	Film 3.		Film 5.		Film 7.		Film 10.	
	Corrected Time ratios (t).	Blackening (D).	t.	D.	t.	D.	t.	D.
1.	1·04	0·053	1·00	0·096	0·97	0·110	0·98	0·365
2.	2·04	0·110	2·00	0·195	1·86	0·217	1·96	0·700
3.	3·06	0·175	3·08	0·311	3·08	0·346	3·09	1·059
4.	4·08	0·227	4·14	0·418	4·11	0·464	4·09	1·345
5.	4·98	0·278	5·03	0·507	5·06	0·577	5·06	1·605
6.	5·89	0·315	5·82	0·603	6·07	0·685	5·92	1·851
7.	6·80	0·364	6·68	0·684	6·70	0·769	—	—
8.	7·87	0·424	7·42	0·756	—	—	—	—

Fig. 2.

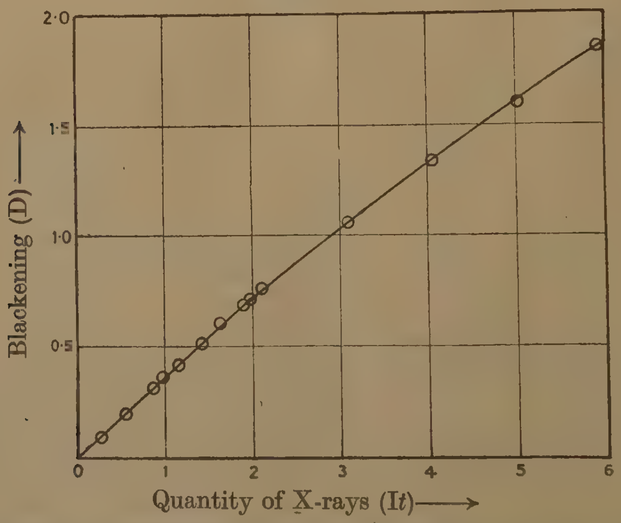

Relation between blackening of the film and quantity of X-rays falling upon it. Curve shows approximately linear relation between these two quantities for values of blackening up to about 0·8.

3. *Flat Powder Plate X-ray Camera.*

In this method of crystal examination, the X-rays are reflected from a stationary flat plate of powder or filings of considerable thickness, which is placed at the centre of a cylindrical camera, the axis of the camera lying in the surface of the powder plate. The method has been fully described by Brentano (1) and by Brindley and Spiers (2); it has advantages over other methods in that the absorption factor can be accurately calculated and the variation of focusing along the film can be utilised to facilitate the measurement of the intensity of the lines.

The intensity of X-rays reflected from an incident beam of unit intensity by a given crystal plane is

$$I=\frac{\lambda^3N^2e^4}{16\pi m^2c^4}\cdot\frac{l}{r}\cdot p\,.\,F_t^2\cdot\frac{1+\cos^2 2\theta}{\sin\theta\,.\sin 2\theta}\cdot\frac{\rho'}{\rho\mu'}\cdot\frac{\sin(2\theta-\alpha)}{\sin(2\theta-\alpha)+\sin\alpha}, \quad . \quad (1)$$

where the symbols λ, e, m and c have their usual meanings, N is the number of unit cells per unit volume of the crystal, l the length of line recorded on the film, r the radius of the camera, F the amplitude scattered per unit cell at the temperature of the experiment in terms of the amplitude scattered by a single electron, p the multiplicity factor of reflection, θ the glancing angle, ρ and ρ' the true and apparent density of the substance under examination, μ' the linear coefficient of absorption for the powder and α the angle between the incident beam and the surface of the powder.

As we shall be concerned only with relative intensity measurements, we may write

$$I=\text{constant}\,.\,p\,.\,F_t^2\cdot\frac{1+\cos^2 2\theta}{\sin\theta\,.\sin 2\theta}\cdot A, \quad . \quad . \quad . \quad . \quad . \quad . \quad (2)$$

where A, the absorption factor for the plate,

$$=\frac{\sin(2\theta-\alpha)}{\sin(2\theta-\alpha)+\sin\alpha},$$

so that

$$\left|\frac{\delta A}{A}\right|=\frac{\sin 2\theta}{\sin(2\theta-\alpha)}\cdot\frac{\delta\alpha}{\sin(2\theta-\alpha)+\sin\alpha}. \quad . \quad . \quad . \quad . \quad (3)$$

Equation (3) shows that for values of 2θ a little greater than α, that is, for a reflected beam making only a small angle with the plate, errors in α will produce serious errors in the intensity calculation. For values of $(2\theta-\alpha)$ greater than 20°, the error in A will be less than one per cent if $\delta\alpha$ is not greater than $0^\circ{\cdot}2$.

In order to use to full advantage the focusing effect of the powder plate camera, a fairly large area of powder should be irradiated. The divergence of the incident beam which this entails, will not produce an appreciable error in A provided the mean value for α can be measured accurately. This can be done if the slit system is such as to produce a beam with well defined edges.

Another factor to be considered in designing the slit system is the distribution of the intensity of blackening across a line on the film. Brentano (2) points out that a line of uniform blackening over its whole width, and whose blackening falls off abruptly at its edges, will give the more accurate values of intensity when measured with the microphotometer. It is found that such lines are obtained if the arrangements, described below, are adopted to produce a well-defined incident beam.

The radius of the camera was 4·5 cm. The slit system consisted of two parts ; the first part was a cylindrical brass tube, stopped at one end with a piece of brass plate 3 mm. thick, in which was cut a rectangular aperture 1 mm. wide by 2·5 mm. high. This cylinder was detachable and was held firmly in a hole in the camera by a spring, the slit being then situated on the circumference of the camera. When the camera was placed close up to the X-ray tube, the beam, falling on the powder plate through this slit, appeared uniform over a width of 3 mm. The second part of the slit, consisting of another rectangular slit 2·5 mm. wide by 3·5 mm. high, and situated about 1 cm. from the surface of the powder plate, restricted the beam still further. This slit system gave a well-defined beam and the microphotometer traces of reflection lines were satisfactory for measurement. The inside surfaces of the second slit were bevelled outwards to reduce the amount of scattered radiation ; the actual slit was situated about 3 mm. inside the outer edge of the opening.

Fig. 3.

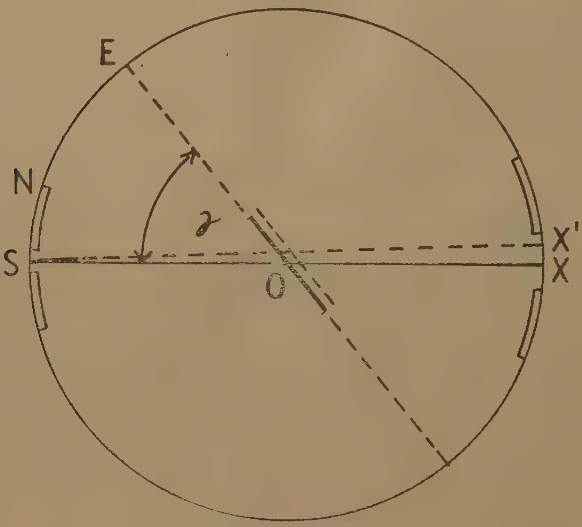

The angle α was determined by measuring the distance from the slit S to the edge of the blackening at E produced by the general radiation reflected from the plate, correction of course being made for any shrinkage of the film during processing. A reference to fig. 3 will show the possible sources of error in α. The two main sources of error are (1) the dissymetry of the X-ray beam in relation to the centre of the camera, and (2) the displacement of the powder surface from the central axis. These two factors were carefully examined and it was concluded that the value of the angle α could be determined to an accuracy which did not introduce an appreciable error into intensity measurements.

Special attention was given to the production of a suitable powder plate. Copper powder and copper Kα radiation were used, since the work of Brindley (5) had established the F-values for this reflector and radiation. Finely divided copper, prepared by precipitation from copper sulphate solution, proved unsatisfactory because the lines were ill-defined owing to particle scattering and also the powder rapidly became oxidised when exposed to the atmosphere. Afterwards filings of the pure metal were used. Brindley and Spiers had found that filings of copper gave lower F-values than the precipitated metal due to distortion of the lattice. If, however, the filings are annealed for the appropriate time, this distortion can be removed. Finally, the following procedure was adopted. Copper filings were annealed at about 350° C. for $5\frac{1}{2}$ hours, and then sieved through a gauze of 320 mesh to the inch. A photograph taken with these filings on a focusing X-ray camera gave lines that were sharp, indicating that the heat treatment had been sufficient to remove the effect of cold work done on the filings. In addition to the necessity of using undistorted particles, it is also necessary for intensity measurements that the particles should be small in order to reduce the errors due to primary extinction. To ensure this, the filings were made by filing very lightly with a small warding file and sieved through a gauze of 350 mesh ; the first filings to fall through the sieve were used for the surface layer of the powder plate.

The freedom of the lines in the photographs from spottiness when the specimen was not rotated, provides a rough criterion of the degree to which primary extinction has been eliminated. The lines in photographs taken under these conditions were usually quite free from this defect.

4. *Results obtained with the Flat Powder Plate.*

Several photographs were taken with the powder plate at different angles with the X-ray beam and with powder plates prepared at different times. The results of the measurements of the microphotometer traces are collected in Table II.

Since there are four atoms to the unit cell in copper, f_t, the scattering factor for an atom at the temperature of the experiment is $F_t/4$, where F_t is the value calculated from equation (1). To obtain the scattering factor for an atom at rest, the f_t-values must be multiplied by a term e^{M}, where

$$M = \frac{6h^2}{mk\Theta} \cdot \left[\frac{\Phi(x)}{x} + \frac{1}{4}\right]\left(\frac{\sin\theta}{\lambda}\right)^2,$$

h and k are the Planck and the Boltzmann constants respectively, and Θ is the characteristic temperature of the reflector. Values of $\Phi(x)$ for different values of x have been calculated by Debye.

To compare the results of the different photographs, the f_t-values have been tabulated on such a scale that their sum for all the lines in each photograph is the same. It is more satisfactory to adopt this procedure than to assume a value for any one reflection in each photograph. It will be observed that the maximum difference between any single value of f_t and the mean value is less than 4 per cent. The table also includes the relative f_t-values deduced from the absolute f_t-values published by Brindley (5); the agreement with these values is good and proves that the technique adopted in the present work is capable of yielding reliable results. It was essential to obtain this agreement with results obtained in another laboratory before proceeding to examine the case of the cylindrical fibre.

TABLE II.

Relative f_t-values for copper obtained with a flat powder plate camera and copper Kα radiation.

Film No.	a.	$(h^2+k^2+l^2)$ for reflecting planes.					
		8.	11.	12.	16.	19.	20.
1.	35° 56′	—	9·58	8·81	7·43	6·58	6·23
4.	34° 18′	11·27	9·71	8·46	7·84	6·55	6·16
5.	34° 18′	11·53	9·48	9·00	7·64	6·42	5·94
6.	33° 15′	11·44	9·83	8·76	7·52	6·33	6·11
11.	32° 27′	11·25	9·54	8·75	7·74	6·43	6·29
Mean f_t-values		11·37	9·63	8·76	7·63	6·46	6·15
Brindley, relative f_t-values ..		11·55	9·55	8·83	—	6·44	6·05
$(\sin\theta)/\lambda \times 10^8$		0·392	0·460	0·480	0·554	0·604	0·620

5. *Preparation of a Suitable Cylindrical Fibre.*

Some difficulty was experienced in producing a fibre that would yield lines, the intensities of which could be satisfactorily interpreted. Solid specimens, such as wires, are unsuitable for two reasons : firstly, it would not be possible to obtain all substances to be examined in this form, and secondly, the drawing process produces preferred orientation of the crystals. Some workers have coated the metal filings to be examined on a hair, using an adhesive, but previous experience with similar fibres of glass or silica in this laboratory decided us against this form, as it would be difficult to prepare, in this way, a fibre of accurately circular cross-section, and in addition the adhesive would introduce an error which could not be allowed for in the absorption factor. It was necessary, if possible, to produce fibres of uniform circular cross-section composed entirely of small particles (without a central core of any other material), orientated at random, but not small enough to produce particle scattering, and holding together without adhesive of any kind. After many attempts, satisfactory powder rods of copper conforming to these requirements were produced. The method consists in compressing together metallic filings in a steel mould so as to form a solid rod. The rods were about 10 mm. long and 0·86 mm. in diameter and were fixed at the base to a steel pin to facilitate their mounting in the specimen holder of the camera. In this condition the rods are very fragile and an X-ray photograph taken with a powder rod at this stage gave broad unresolved doublets at the precision end of the camera, indicating that the crystals were distorted. After annealing for two hours at about 500° C., well resolved doublets were obtained; moreover, the lines were not "spotty" even when the rod was not rotated. The annealing treatment had therefore been adequate. After annealing, the rods were not quite so fragile and could be more easily handled.

6. *Relative f_t-values for Copper obtained with the Fibre X-ray Camera and Copper* Kα *Radiation.*

Two photographs, with different rods, were taken at room-temperature and the blackening of the lines measured with the microphotometer. Fig. 4 (Pl. III.) shows structure-spectra of copper, obtained with the flat powder plate and fibre cameras, and a fibre camera spectrum of gold, together with typical microphotometer traces. It will be noted that the background in these photographs is fairly uniform and light; this helped to increase the accuracy of measurement of line-intensity.

In the case of a fibre camera of radius r, the energy of X-rays diffracted in a unit time from an incident beam of unit intensity by a given crystal plane and giving rise to a line of length l on the film is

$$\mathrm{I}=\frac{\lambda^3\mathrm{N}^2e^4}{16\pi m^2c^4}.\frac{l}{r}.p.\mathrm{F}_t^2.\frac{1+\cos^2 2\theta}{\sin\theta.\sin 2\theta}.\mathrm{A}, \quad . \quad . \quad . \quad . \quad . \qquad (4)$$

where the symbols have the same meanings as in equation (1), and A is the absorption factor. Since we are dealing only with relative values of intensity, the expression becomes similar to (2) only that A, the absorption factor, is different. The values of A have been tabulated by Bradley(6) for different angles of reflection and different values of weight and dimensions of specimen and mass absorption coefficient of the material of the specimen. These quantities are known for the specimens used in the investigation.

The results of the measurements are summarized in Table III., which contains the relative f_t-values for copper calculated from data obtained with the rods. Two films were measured and the mean f_t-values from the two halves of each film are given for the same planes as were included in Table II.

The relative f_t-values for copper calculated from measurements made on lines in photographs obtained with the fibre camera agree well with those obtained with the flat powder plate camera, and both agree with the results recorded by Brindley. The agreement is considered sufficiently good to justify the use of the fibre camera to study the intensities of

X-ray reflections from powdered crystals. This has been done for aluminium, copper, and gold, in an investigation on the variation of the intensity of reflection with temperature, an account of which will be published in a separate paper.

TABLE III.

Relative f_t-values for copper obtained with a fibre camera and copper Kα radiation.

Film No.	$(h^2+k^2+l^2)$ for reflecting planes.				
	8.	11.	12.	19.	20.
5.	11·43	9·34	9·04	6·45	6·10
6.	11·67	9·44	8·87	6·30	6·08
Mean relative f_t-values.	11·55	9·39	8·95	6·37	6·09
Brindley, relative f_t-values.	11·55	9·55	8·83	6·44	6·05

TABLE IV.

Relative f_t-values for gold obtained with a fibre camera, and copper Kα radiation.

Film No.	$(h^2+k^2+l^2)$ for reflecting planes.								
	3	4	8	11	12	19	20	24	27
6.	64·3	61·8	53·1	49·3	47·9	40·6	40·1	36·3	32·8
8.	63·4	59·8	52·3	49·7$_5$	48·4	41·3	40·1	36·7	33·9
Mean relative f_t-values	63·9	60·8	52·7	49·5	48·1	40·9	40·1	36·5	33·3
$(\sin\theta)/\lambda\times 10^8$.	0·213	0·246	0·348	0·408	0·436	0·535	0·549	0·602	0·638

7. *Relative f_t-values for Gold obtained with a Fibre Camera and Copper Kα Radiation.*

Gold was examined at room temperature in the present investigation to apply the technique that had been developed with copper to a material, the F-values of which had not previously been experimentally determined. One great advantage of using gold instead of copper is, that errors arising from tarnishing will be almost entirely absent.

Two gold powder rods, made in a mould as previously indicated, were examined after annealing *in vacuo* for 3 hours at about 450° C. After measuring the blackening of the lines with the microphotometer, the relative f_t-values, which are included in Table IV., were calculated.

No account of a previous experimental determination of F-values for gold has been found, but an F-curve has been plotted for comparison with the present results, using the theoretical values calculated by James and Brindley (7) from the Thomas model of the atom and corrected to room-temperature. These values hold strictly only in the case when the wave-length of the radiation is short; they would probably not apply to a wave-length as long as that of the Kα radiation from copper, which was the radiation used to obtain the photographs, the lines of which were measured. It is, however, interesting to note from fig. 5 that there is not much difference between the two curves; the experimental f_t-values fall off with $(\sin\theta)/\lambda$ only a little less rapidly than do the calculated values, but the experimental curve shows slightly less curvature than the theoretical curve over the range of values of $(\sin\theta)/\lambda$ investigated.

Fig. 5.

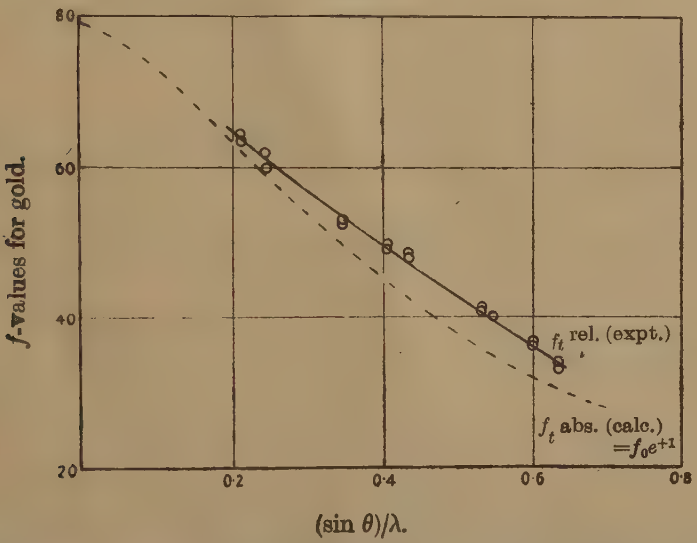

Experimental and theoretical f-values for gold plotted against $(\sin\theta)/\lambda$.

8. *Conclusion.*

The preliminary work described in this paper shows that by taking particular care in the preparation of the powder specimen, it is possible to use a fibre camera for the investigation of the relative intensity of lines in structure-spectra. The method of procedure adopted, enables one to apply an absorption correction with some confidence that it is approximately correct, as in making the fibre no adhesive or central core is used which can introduce errors into the calculations. The particles in the powder specimen are not small enough to produce particle scattering and not large enough to interfere, to an appreciable extent, with primary extinction; they are also in random arrangement.

The agreement found between the relative f_t-values for copper calculated from the measurements of lines in fibre camera photographs, and those calculated from the measurements of lines in flat powder plate photographs, is satisfactory at room temperatures, and there is no reason to doubt that reliable values will be obtained with the fibre camera when the specimen is heated, provided precautions are taken to avoid tarnishing of the specimen at the higher temperatures.

References.

1. J. C. M. Brentano, Proc. Phys. Soc. xlvii. p. 932 (1935).
2. G. W. Brindley and F. W. Spiers, Proc. Phys. Soc. xlvi. p. 841 (1934).
3. A. Bouwers, *Zeits. f. Physik*, xiv. p. 374 (1923).
4. G. W. Brindley and F. W. Spiers, Phil. Mag. xvi. p. 686 (1933).
5. G. W. Brindley, Phil. Mag. xxi. p. 778 (1936).
6. A. J. Bradley, Proc. Phys. Soc. xlvii. p. 879 (1935).
7. R. W. James and G. W. Brindley, *Zeits. f. Krist.* lxxviii. p. 470 (1931).

VI. *Direct Determination of Stresses from the Stress Equations in some Two-Dimensional Problems of Elasticity.*—Part IV. *Problems of Wedges.*

By Bibhutibhusan Sen.*

[Received November 16, 1943.]

Introduction.

In the previous parts (Sen, 1938, 1939), it has been shown that in two-dimensional problems of elasticity connected with a circular plate or a semi-infinite plate with a straight edge, the stress equations can be reduced with the help of consistency relations to such simple forms that the stresses at any point in the plate can be at once written down when their boundary values are known. The object of this paper is to extend this method to problems of thin plates having two intersecting straight edges. Some problems of such wedges have been discussed by other investigators, who have invariably used stress functions. In this paper these problems will not be considered in detail; but a general method of solving problems of different types without the use of stress functions will be given. As an illustration, a particular problem connected with a wedge of ælotropic material of the type discussed in a previous part (1939) will be completely solved.

---

* Communicated by the Author.

1. *The Method of Solution for an Isotropic Wedge.*

If we assume the plate of unit thickness to be in a state of generalized plane stress, we know that the mean stresses $\breve{xx}$, $\breve{xy}$, $\breve{yy}$ satisfy the equation

$$\left.\begin{aligned} \frac{\partial \breve{xx}}{\partial x}+\frac{\partial \breve{xy}}{\partial y}=0, \\ \frac{\partial \breve{xy}}{\partial x}+\frac{\partial \breve{yy}}{\partial y}=0. \end{aligned}\right\} \quad \ldots\ldots\ldots \quad (1.1)$$

In this type of problem, the only equation of compatibility to be satisfied is

$$\left.\begin{aligned} &\nabla_1^2\odot=0, \\ \text{where} \qquad &\odot=\breve{xx}+\breve{yy}, \quad \text{and} \quad \nabla_1^2\equiv\frac{\partial^2}{\partial x^2}+\frac{\partial^2}{\partial y^2} \end{aligned}\right\} \quad \ldots\ldots \quad (1.2)$$

If $\breve{\theta x}$, $\breve{\theta y}$ be the x and y components of the stress at the point $(r,\ \theta)$ on the edge $\theta=$constant, we have

$$\left.\begin{aligned} r\breve{\theta x}=-y\breve{xx}+x\breve{xy}, \\ r\breve{\theta y}=-y\breve{xy}+x\breve{yy}. \end{aligned}\right\} \quad \ldots\ldots\ldots \quad (1.3)$$

Using the stress equations (1.1) we get

$$\frac{\partial}{\partial x}(r\breve{\theta x})+\frac{\partial}{\partial y}(r\breve{\theta y})=0, \quad \ldots\ldots\ldots \quad (1.4)$$

$$\left.\begin{aligned} \frac{\partial}{\partial x}(r\breve{\theta y})-\frac{\partial}{\partial y}(r\breve{\theta x})&=r\frac{\partial\odot}{\partial r}+\odot \\ &=\mathrm{F}\ (\text{say}) \end{aligned}\right\} \quad \ldots\ldots \quad (1.5)$$

Since $\odot$ is a harmonic function, F will also be so. Let G be the function conjugate to F such that $\mathrm{F}+i\mathrm{G}$ is a function of $x+iy$. Then from (1.4) and (1.5) we obtain

$$\left.\begin{aligned} \nabla_1^2(r\breve{\theta x})&=-\frac{\partial \mathrm{F}}{\partial y}, \\ \nabla_1^2(r\breve{\theta y})&=\quad\frac{\partial \mathrm{G}}{\partial y}. \end{aligned}\right\} \quad \ldots\ldots\ldots \quad (1.6)$$

Assuming that the line $y=0$ (corresponding to $\theta=0$) is one of the edges, we can put

$$\left.\begin{aligned} r\breve{\theta x}&=-\tfrac{1}{2}y\mathrm{F}+\phi_1, \\ r\breve{\theta y}&=\quad\tfrac{1}{2}y\mathrm{G}+\phi_2, \end{aligned}\right\} \quad \ldots\ldots\ldots \quad (1.7)$$

where ϕ_1 and ϕ_2 are harmonic functions such that

$$\left.\begin{aligned}[\phi_1]_{y=0}&=[r\overset{\smile}{\theta x}]_{y=0},\\ \text{and}\qquad [\phi_2]_{y=0}&=[r\overset{\smile}{\theta y}]_{y=0},\end{aligned}\right\} \quad . \; . \; . \; . \; . \; . \; . \; . \quad (1.8)$$

Let

$$\left.\begin{aligned}\phi_1&=\mathrm{Re}f_1(z),\\ \text{and}\qquad \phi_2&=\mathrm{Re}f_2(z),\end{aligned}\right\} \quad . \; . \; . \; . \; . \; . \; . \; . \; . \quad (1.9)$$

where $z=x+iy$ and Re denotes the real part.

Substituting these values in (1.7) we have from (1.4) and (1.5)

$$\left.\begin{aligned}G&=-2\,\mathrm{Re}[f_1'(z)+if_2'(z)],\\ F&=2\mathrm{Re}[f_2'(z)-if_1'(z)],\end{aligned}\right\} \quad . \; . \; . \; . \; . \; . \quad (1.10)$$

and

$$\odot=\;2\mathrm{Re}\frac{[f_2(z)-if_1(z)]}{z}, \quad . \; . \; . \; . \; . \; . \; . \quad (1.11)$$

where $f_1'(z)$ and $f_2'(z)$ denote the derivatives of $f_1(z)$ and $f_2(z)$ with respect to z.

Hence we have finally

$$\left.\begin{aligned}r\overset{\smile}{\theta x}&=\mathrm{Re}[-y\{f_2'(z)-if_1'(z)\}+f_1(z)],\\ r\overset{\smile}{\theta y}&=\mathrm{Re}[-y\{f_1'(z)+if_2'(z)\}+f_2(z)].\end{aligned}\right\}. \quad . \; . \; . \quad (1.12)$$

2. *Solution of Some Problems of Isotropic Wedge.*

(a) Suppose that the two edges are $\theta=0$ and $\theta=\beta$ or that the equations of the straight lines forming the edges are $y=0$ and $y=x\tan\beta$. If on the edge $y=0$, $\overset{\smile}{\theta x}=0$ and $\overset{\smile}{\theta y}=-qr^n$, where q is a constant and n is a positive integer, we can obtain the solution by putting

$$\left.\begin{aligned}f_2(z)&=-qz^{n+1}+A_n iz^{n+1},\\ f_1(z)&=\phantom{-qz^{n+1}+}B_n iz^{n+1},\end{aligned}\right\} \quad . \; . \; . \; . \; . \; . \; . \quad (2.1)$$

A_n and B_n being real constants. These satisfy the conditions on the edge $y=0$ as stated above. Remembering that

$$z^n=r^n(\cos n\theta+i\sin n\theta),$$

we find

$$\left.\begin{aligned}r\overset{\smile}{\theta x}&=r^{n+1}[A_n(n+1)\sin\theta\sin n\theta-B_n\{(n+1)\sin\theta\cos n\theta+\sin(n+1)\theta\}\\ &\qquad\qquad+(n+1)q\sin\theta\cos n\theta],\\ r\overset{\smile}{\theta y}&=r^{n+1}[A_n\{(n+1)\sin\theta\cos n\theta-\sin(n+1)\theta\}+B_n(n+1)\sin\theta\sin n\theta\\ &\qquad\qquad-q\{(n+1)\sin\theta\sin n\theta+\cos(n+1)\theta\}].\end{aligned}\right\}. \quad (2.2)$$

If the other edge $\theta=\beta$ be free from stress, the constants A_n and B_n are found from the equations

$$\left.\begin{aligned}&A_n(n+1)\sin\beta\sin n\beta-B_n[(n+1)\sin\beta\cos n\beta+\sin(n+1)\beta]\\ &\qquad\qquad+(n+1)q\sin\beta\cos n\beta=0,\\ &A_n[(n+1)\sin\beta\cos n\beta-\sin(n+1)\beta]+B_n(n+1)\sin\beta\sin n\beta\\ &\qquad\qquad-q[(n+1)\sin\beta\sin n\beta+\cos(n+1)\beta]=0.\end{aligned}\right\}. \quad (2.3)$$

(*b*) The above solution fails only when $n=0$, *i. e.* when

$$[\overset{\smile}{\theta x}]_{y=0}=0 \quad\text{and}\quad [\overset{\smile}{\theta y}]_{y=0}=-q.$$

In this case we can get the solution by putting

$$\left.\begin{aligned} f_2(z)&=-qz+\mathrm{A}iz\log z,\\ f_1(z)&=\quad \mathrm{B}iz. \end{aligned}\right\} \quad \dots\dots\dots \quad (2.4)$$

These values of $f_1(z)$ and $f_2(z)$ substituted into (1.12) give

$$\begin{aligned} r\overset{\smile}{\theta x}&=y[q+\mathrm{A}\theta-2\mathrm{B}],\\ r\overset{\smile}{\theta y}&=[\mathrm{A}y-\mathrm{A}x\theta-qx]. \end{aligned}$$

These expressions will be zero when $\theta=\beta$, *i. e.* when $y=x\tan\beta$ if

$$\mathrm{A}=q/(\tan\beta-\beta) \quad\text{and}\quad 2\mathrm{B}=q\tan\beta/(\tan\beta-\beta).$$

Hence we get

$$r\overset{\smile}{\theta x}=\frac{qy(\theta-\beta)}{\tan\beta-\beta}, \quad\text{and}\quad r\overset{\smile}{\theta y}=\frac{qx[\tan\theta-\theta-(\tan\beta-\beta)]}{\tan\beta-\beta}. \quad . \quad . \quad (2.5)$$

This problem was solved by Levy (1898) in a different manner.

(*c*) If we put $f_1(z)=\mathrm{A}i$ and $f_2(z)=\mathrm{B}i$ we have $\overset{\smile}{\theta x}=\overset{\smile}{\theta y}=0$.

Since $\overset{\smile}{r\theta}=\overset{\smile}{\theta x}\cos\theta+\overset{\smile}{\theta y}\sin\theta$ and $\overset{\smile}{\theta\theta}=-\overset{\smile}{\theta x}\sin\theta+\overset{\smile}{\theta y}\cos\theta$, $\overset{\smile}{r\theta}=\overset{\smile}{\theta\theta}=0$.
From (1.11) we have

$$\odot=\overset{\smile}{rr}=2\mathrm{Re}\frac{\mathrm{A}i+\mathrm{B}}{z}=\frac{2\mathrm{A}\sin\theta}{r}+\frac{2\mathrm{B}\cos\theta}{r}. \quad . \quad . \quad . \quad (2.6)$$

If there be a single force F acting at the apex, making an angle α with the axis of x, we can find A and B from the relations

$$\int_0^\beta \overset{\smile}{rr}\cos\theta\, r d\theta=-\mathrm{F}\cos\alpha \quad\text{and}\quad \int_0^\beta \overset{\smile}{rr}\sin\theta\, r d\theta=-\mathrm{F}\sin\alpha.$$

When the force is directed along the internal bisector of the wedge, $\alpha=\frac{\beta}{2}$, and we get $\mathrm{A}=-\mathrm{F}\sin\frac{\beta}{2}\Big/(\beta+\sin\beta)$ and $\mathrm{B}=-\mathrm{F}\cos\frac{\beta}{2}\Big/(\beta+\sin\beta)$.

Then

$$\overset{\smile}{rr}=-\frac{2\mathrm{F}\cos\left(\theta-\frac{\beta}{2}\right)}{r(\beta+\sin\beta)}. \quad \dots\dots\dots \quad (2.7)$$

This result was obtained by Michell (1902) by using stress function.

Another simple solution is obtained by putting

$$f_1(z)=\frac{\mathrm{A}i}{z} \quad\text{and}\quad f_2(z)=\frac{\mathrm{B}i}{z}.$$

These substituted into (1.12) give

$$r\overset{\smile}{\theta x}=\frac{2xy}{r^4}(\mathrm{A}x+\mathrm{B}y),$$

$$\overset{\smile}{r\theta y}=\frac{2y^2}{r^4}(\mathrm{A}x+\mathrm{B}y).$$

If the edges be free we shall have $\mathrm{A}\cos\beta+\mathrm{B}\sin\beta=0$, *i. e.*

$$\frac{\mathrm{A}}{\sin\beta}=-\frac{\mathrm{B}}{\cos\beta}=\mathrm{Q}\ (\text{say}).$$

Then

$$\left.\begin{aligned}\overset{\smile}{r\theta x}&=-\frac{2\cos\theta\sin\theta}{r}\mathrm{Q}\sin(\theta-\beta),\\ \overset{\smile}{r\theta y}&=-\frac{2\sin^2\theta}{r}\mathrm{Q}\sin(\theta-\beta).\end{aligned}\right\}\quad . \quad . \quad . \quad . \quad . \quad (2.8)$$

Also

$$\overset{\smile}{\theta\theta}=0,\quad\text{and}\quad\overset{\smile}{r\theta}=\overset{\smile}{\theta x}\cos\theta+\overset{\smile}{\theta y}\sin\theta$$

$$=-\frac{\mathrm{Q}}{r^2}[\cos\beta-\cos(2\theta-\beta)].$$

If

$$\int_0^\beta\overset{\smile}{r\theta}\,r^2d\theta=-\mathrm{M}$$

we shall have

$$\mathrm{Q}=\frac{\mathrm{M}}{\beta\cos\beta-\sin\beta}.\quad . \quad . \quad . \quad . \quad . \quad . \quad . \quad (2.9)$$

This is the case of a couple of moment M applied at the apex, and the result was obtained in a different manner by Inglis (1922).

(*d*) Sometimes it is advantageous to express F and G in (1.6) in terms of infinite integrals. As for example, if in a quadrantal wedge the edge $y=0$ is free from stress while the stresses on the edge $x=0$ can be expressed as

$$\left.\begin{aligned}[\overset{\smile}{rx\theta}]_{x=0}&=y\psi_1(y)=y\int_0^\infty \mathrm{C}\sin m(\log y)dm,\\ \text{and}\qquad [\overset{\smile}{ry\theta}]_{x=0}&=y\psi_2(y)=y\int_0^\infty \mathrm{D}\cos m(\log y)dm,\end{aligned}\right\}\quad . \quad . \quad . \quad (2.10)$$

where C and D are functions of m and the integrals are convergent, then we can put the results of (1.7) in the forms

$$\left.\begin{aligned}\overset{\smile}{rx\theta}&=-\tfrac{1}{2}y\int_0^\infty[\mathrm{L}\cosh m\theta+\mathrm{M}\sinh m\theta]\sin mp\,dm,\\ \overset{\smile}{ry\theta}&=\ \tfrac{1}{2}y\int_0^\infty[\mathrm{L}\sinh m\theta+\mathrm{M}\cosh m\theta]\cos mp\,dm,\end{aligned}\right\}\quad . \quad . \quad (2.11)$$

in which ρ stands for $\log r$ and L and M are functions of m. When $x=0$, *i.e.* $\theta=\frac{\pi}{2}$, we have from (2.10) and (2.11)

$$\left.\begin{aligned}\mathrm{L}\cosh\frac{m\pi}{2}+\mathrm{M}\sinh\frac{m\pi}{2}&=-2\mathrm{C},\\ \mathrm{L}\sinh\frac{m\pi}{2}+\mathrm{M}\cosh\frac{m\pi}{2}&=\ 2\mathrm{D}.\end{aligned}\right\}\quad . \quad . \quad . \quad . \quad . \quad (2.12)$$

C and D being known, these equations give L and M. The above types of infinite integrals were used by Shepherd (1935), who used stress functions to deduce the stresses in a sector under different edge loads.

3. *The Wedge of a Non-Isotropic Material.*

We shall now consider the case of a wedge of non-isotropic material of the type discussed in a previous paper (1939). It is supposed that the ælotrophy is such as to make the Poisson's ratios and Young's moduli for two rectangular axes satisfy the relations

$$\frac{\sigma_1}{\sigma_2}=\frac{E_2}{E_1}=k^2. \qquad (3.1)$$

In this case we shall have

$$\odot=Re\odot(z_1), \qquad (3.2)$$

where $z_1=x+iy_1$ and $y_1=\frac{y}{k}$.

The equations (1·4) and (1.5) now stand as

$$\frac{\partial}{\partial x}(\overset{\smile}{r\theta x})+\frac{\partial}{\partial y}(\overset{\smile}{r\theta y})=0, \qquad (3.3)$$

$$\frac{\partial}{\partial x}(\overset{\smile}{r\theta y})-\frac{\partial}{\partial y}(\overset{\smile}{r\theta x})=x\frac{\partial\odot}{\partial x}+y_1\frac{\partial\odot}{\partial y_1}+\odot. \qquad (3.4)$$

If and

$$\left.\begin{aligned}[\overset{\smile}{r\theta x}]_{y=0}&=[Ref_1(z)]_{y=0},\\ [\overset{\smile}{r\theta y}]_{y=0}&=[Ref_2(z)]_{y=0},\end{aligned}\right\} \qquad (3.5)$$

we can put

$$\left.\begin{aligned}\overset{\smile}{r\theta x}&=\mathrm{Re}\left[-\frac{i}{k-1}\{\psi(z_1)-\psi(z)\}+f_1(z)\right],\\ \overset{\smile}{r\theta y}&=\mathrm{Re}\left[\frac{k}{k-1}\{\psi(z_1)-\psi(z)\}+f_2(z)\right],\end{aligned}\right\} \qquad (3.6)$$

where

$$\psi(z)=f_2(z)-if_1(z), \qquad (3.7)$$

and

$$\odot(z_1)=\frac{(k+1)\psi(z_1)}{kz_1}=\frac{k+1}{kz_1}[f_2(z_1)-if_1(z_1)]. \qquad (3.8)$$

As an example, suppose that the edge $y=0$ has a normal pressure of intensity q while the edge $y=x\tan\beta$ $(\theta=\beta)$ is free from stress.

We assume in 2 (*b*)

$$\left.\begin{aligned}f_2(z)&=-qz+A_1iz\log z,\\ f_1(z)&=B_1iz.\end{aligned}\right\} \qquad (3.9)$$

Putting now

$$\left.\begin{aligned}&y=x\tan\theta,\quad y_1=x\tan\theta_1,\quad \tan\theta=k\tan\theta_1,\\ &r=\sqrt{x^2+y^2}=x\sec\theta,\ \text{and}\ r_1=\sqrt{x^2+y_1{}^2}=k\sec\theta_1,\end{aligned}\right\} \qquad (3.10)$$

we get

$$\left.\begin{aligned} r\overset{\smile}{\theta x} &= \frac{x}{k-1}[q(\tan\theta-\tan\theta_1)+A_1(\log\sec\theta_1-\log\sec\theta+\theta\tan\theta-\theta_1\tan\theta_1) \\ &\qquad\qquad -B_1(k\tan\theta-\tan\theta_1)], \\ r\overset{\smile}{\theta y} &= \frac{x}{k-1}[A_1\{\tan\theta\,(\log\sec\theta-\log\sec\theta_1)+\theta-k\theta_1\}-q(k-1)]. \end{aligned}\right\} \quad . \quad . \quad . \quad (3.11)$$

Finding the values of A_1 and B_1 from the conditions that $(\overset{\smile}{\theta x})_{\theta=\beta}=0$ and $(\overset{\smile}{\theta y})_{\theta=\beta}=0$, we obtain finally

$$\left.\begin{aligned} r\overset{\smile}{\theta x} &= \frac{qx}{\Delta}[\log\sec\theta_1-\log\sec\theta+\theta\tan\theta-\theta_1\tan\theta_1 \\ &\qquad -\tan\theta_1\cot\beta_1(\log\sec\beta_1-\log\sec\beta+\beta\tan\beta-\beta_1\tan\beta_1)], \\ r\overset{\smile}{\theta y} &= \frac{qx}{\Delta}[\tan\theta(\log\sec\theta-\log\sec\theta_1)+\theta-k\theta_1-\Delta], \\ \text{where}\quad \beta_1 &= \tan^{-1}(\tan\beta/k), \\ \text{and}\quad \Delta &= \tan\beta(\log\sec\beta-\log\sec\beta_1)+\beta-k\beta_1. \end{aligned}\right\} \quad . \quad (3.12)$$

References.

Inglis, C. E., Trans. Inst. Naval Architects, lxiv. (1922).
Levy, M., C. R., Paris, cxxvi. p. 1235 (1898).
Michell, J. H., London Math. Soc. Proc. xxxiv. p. 134 (1902).
Sen, B., Phil. Mag. (ser. 7) xxvi. pp. 98–119 (1938); xxvii. pp. 596–604 (1939).
Shepherd, W. M., Proc. Roy. Soc. London, A, cxlviii. pp. 284–303 (1935).

Bengal Engineering College,
Sibpore, Bengal.

[*The Editors do not hold themselves responsible for the views expressed by their correspondents.*]

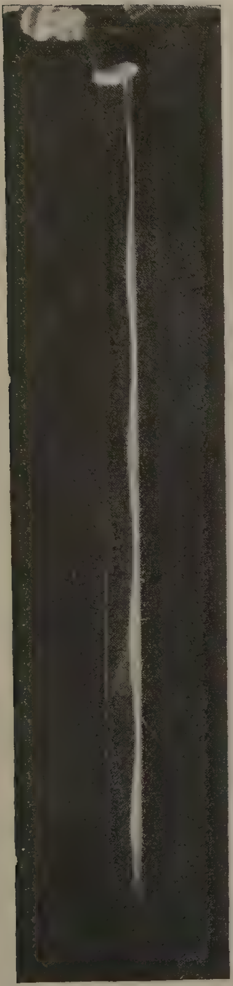

Fig. 2.

Fig. 3.

VII. *The Measurement of Surface and Interfacial Tensions at Fresh Surfaces by the Vibrating Jet Method.*

By C. C. Addison, Ph.D., F.R.I.C.*

[Received October 2, 1944.]

[Plate IV.]

Summary.

The paper describes a simplified practical and mathematical technique designed to bring the vibrating jet method within the scope of routine laboratory work. The method is extended to include liquid/liquid interfaces, and previous work on freshly formed surfaces is summarized. The paper is subdivided as follows :—

1. Introduction.
2. Review of available methods.
3. Previous work on vibrating jets.
4. Practical technique for vibrating jet measurement.
5. Interpretation of results.
6. Influence of form of orifice tube on wave-length.
7. The use of vertical jets.
8. Application to the study of dynamic tensions of solutions.
9. Liquid/liquid interfacial jets.

1. *Introduction.*

When a liquid surface is freshly formed, the constitution and structure of the surface layer of molecules do not differ from that of any theoretical plane in the bulk of the liquid. Molecular rearrangements then take place, and the tension at the surface at any age below that at which equilibrium is established is termed the dynamic tension. Therefore although the term surface tension (which is widely accepted as an abbreviation for static or equilibrium tension) has significance alone, the term dynamic surface tension has no significance unless related directly to surface age. If the liquid is pure and the air phase free from contamination, the only change at the surface with age is the orientation of the surface molecules, which proceeds to an extent depending on the molecular structure. The experiments described below indicate that such orientation must take place almost instantaneously. Hiss (1),

---

* Communicated by the Author.

Schmidt and Steyer⁽²⁾ and Buchwald and Konig⁽³⁾ described determinations which suggested that the surface tension of a fresh water surface is much higher than the accepted value. In view of the quantity of evidence to the contrary, the findings require confirmation by an independent method, and no established case is known where the actual development of surface orientation in a pure liquid has been measured. Therefore while surface-tension measurements at fresh surfaces of pure liquids have the great advantage of eliminating surface contamination (and in the case of liquid/liquid interfaces, the drifts in tension due to the mutual solubility of the liquids), the values obtained should not be termed dynamic. In the case of solutions, one component may be preferentially adsorbed at the surface, and the diffusion of this component to the surface from the bulk⁽⁴⁾ can be measured. Although Dupre's experiments⁽⁵⁾ on the rise of soap solutions up very narrow capillary tubes had indicated an unexpectedly high initial tension, Rayleigh⁽⁶⁾ first showed directly from vibrating jet measurements that the tension of a freshly formed soap solution is considerably higher than the equilibrium value.

Surface tension measurements made while adsorption is proceeding have a wide significance. A knowledge of the actual rate at which surface active molecules migrate to the surface can lead directly to valuable information on the forces operating between molecules. Again, the matter has practical as well as academic significance, since in many detergent processes the surface is never sufficiently old for equilibrium to be established. Although the chemical and physical properties of equilibrium surfaces have received extensive study, there is at present no information on the rate of development of this equilibrium. This may be due to the lack of a method capable of measuring the tension over a sufficiently wide range of known surface ages, which utilizes readily available apparatus and lends itself to simple mathematical interpretation. It is the purpose of this paper to describe the adaption of the vibrating jet technique to such studies.

2. *Review of Available Methods.*

The methods available for surface-tension measurement are usually classified as static or dynamic, but it should be emphasized that dynamic methods cannot necessarily be used to measure dynamic tensions; in any method capable of doing this it must be possible to measure the surface age also. The ring method, the sessile drop method and the capillary height method (with its variants) are static methods in which no attempt is usually made to measure or reduce surface age. The drop weight and maximum bubble pressure methods are dynamic in that the system is at no time at rest, but the results obtained are static values. The ripple method, a truly dynamic method, operates by alternately stretching and compressing an equilibrium surface, and again the results are static. The oscillating drop method could perhaps be adapted to the measurement of dynamic tensions if the drop could be released to oscillate at the instant it was formed, but the practical difficulty of combining true oscillation with this instantaneous release has not yet been overcome. Satterly and co-workers (7), (8), (9) measured the vibrations which develop along a vertical jet of liquid of circular cross-section when the jet strikes a solid barrier, and these vibrations have also been studied by Leniham (10). It should be possible to adapt this very useful method to the measurement of dynamic surface tension. Bond (11) has designed an attractive liquid sheet method for measuring the tension at a fresh surface. The impact of two cylindrical jets of water gives rise to a disk of liquid at right angles to the axis of the jets, and the diameter of this disk was found to depend on the surface tension of the liquid. Puls (12) applied the technique with success to mercury. Bond and Puls (13) extended the measurements to a series of aqueous solutions, and developed theoretical formulæ for the "characteristic time" (the time when the adsorption is halfway complete) and also for the fraction of the transition to equilibrium which has occurred at any given time. However, the theoretical predictions in most cases agree with experiment in order only, and the characteristic time has little physical significance. In the study of the development of surface equilibrium the liquid sheet method is limited in application, since the range of surface ages is confined to very narrow limits and cannot be determined with accuracy. Worthington (14), (15) studied the rebound of liquid from a surface when a liquid drop or solid object falls into it. This involves the formation of a fresh surface, but again the difficulty arises that the true surface age cannot be measured, nor is a range available.

Of all the available methods, the vibrating jet produced by an elliptical orifice has been found to be most suited to dynamic studies. It provides stationary waves bounded by a continually renewed surface; the wave-length at any point along the jet is an index of the surface tension, and the surface age at any point along the jet can be deduced from the flow rate. The range of surface age available is approximately 0·001–0·1 seconds, which is the range within which many adsorption processes are complete.

3. *Previous Work on Vibrating Jets.*

The fact that the cross-sectional form of a jet of liquid issuing from an unsymmetrical orifice will oscillate between that of the orifice and the circular, thus giving rise to a series of waves, was first observed by Bidone (16) and Magnus (17), who worked with large orifices of various shapes. Only a few waves were obtained, and the experiments served only as illustrations of the phenomenon. Neither author offered an explanation of the recurrent return of the jet to the original cross-sectional shape, and the fact that it was due to surface tension (or "capillary force") was first suggested by Buff (18). Rayleigh (19) first developed a mathematical relationship (referred to later) connecting surface tension, wave-length and jet velocity, which assumed two-dimensional oscillation in the jet. The experiments reported were designed to illustrate the theory rather than to prove its quantitative application, but were sufficient to confirm that the wave-length increases more rapidly than the flow rate, and that the wave-length must be much greater than the jet diameter before the oscillations are confined to two dimensions. Piccard (20) and Meyer (21) used the method for direct comparative measurements only. Pederson (22) first developed a practical technique for accurate wave-length measurement in a jet produced from a capillary orifice, and considered that to obtain true vibrations the orifice should depart only slightly from the circular, and should conform exactly to the theoretical equation for an ellipse. The waves obtained could not be measured visually, and a photographic method was used. The mathematical treatment was based on that of Rayleigh, and the results obtained for aniline, toluene, water and some aqueous solutions are in reasonable agreement with accepted static values. A highly accurate treatment of the method from both theoretical and practical aspects was made by Bohr (23), who related the dimensions of a jet of water from an elliptical orifice with the surface tension by a formula which took into full account the atmospheric inertia, the viscosity of the jet liquid, and the changing amplitude of oscillation in the jet. The practical measurements were limited to pure water, but the result obtained (72·23 dynes/cm. at 20°) indicates that for water at least, no other complicating factors play a major part. However, as with Pederson's technique, neither the apparatus nor the mathematical treatment is readily applicable to routine laboratory work. Bohr's method was applied by Stocker (24) to a range of inorganic salt solutions, and Bond and Puls (13) made a few approximate determinations on a commercial soap solution for comparison with the liquid sheet method.

It is clear, therefore, that throughout the development of the vibrating jet method no apparatus has been described which is capable of being assembled by the physicist in any laboratory from readily available components. The method has therefore been little used, and the mathematical treatment necessary to determine surface tension from wave-length has been almost prohibitive where large numbers of measurements are contemplated. In the study of dynamic tensions, the highest accuracy is not essential, since changes in tension can occur over a range of up to 50 dynes/cm. The apparatus described below is readily assembled, and while suitable for determinations on pure liquids, finds very ready application where changes in tension are more important than high accuracy in the values themselves. Tensions calculated by this method deviate from the true value if the test liquid has a high viscosity. True results are obtained at all viscosities below 0·02 c.g.s. units, and the deviations which occur above this limit increase with increasing viscosity. These deviations are being studied quantitatively. However, as all the aqueous solutions used, and the majority of common organic liquids, fall inside this range, the present viscosity limit imposes no undue restriction on the applicability of the method.

4. *Practical Technique for Vibrating Jet Measurements.*

The apparatus used for horizontal jets is shown in fig. 1. A 2-litre aspirator A was fitted with water manometer M and a fine capillary tube BB_1. This tube was coated with a film of vaseline where it passed through the rubber bung, so that it could be readily adjusted to any required position. The liquid under test was led from the tubulure down a glass tube C, and both A and C were fixed rigidly in position. The lower end of tube C was connected to the jet tube D by a small piece of rubber tubing, so that C and D made glass-to-glass contact. The jet tube, which was about 10 cm. long, was clamped at about 10° to the horizontal, and a millimetre scale E was fixed immediately behind the jet, so that the tip of tube D lay on the zero of the scale. By this means the part of the jet of liquid to be measured flowed horizontally in front of the scale. The liquid was received in vessel F, which carried a 50 ml. calibration mark on the narrow neck immediately above the bulb. The jet was illuminated by a striplight G placed horizontally over the jet. This gives the most efficient illumination, although with practice accurate readings can be obtained using a point source of light (*e. g.* a small torch) moved along the jet.

Fig. 1.

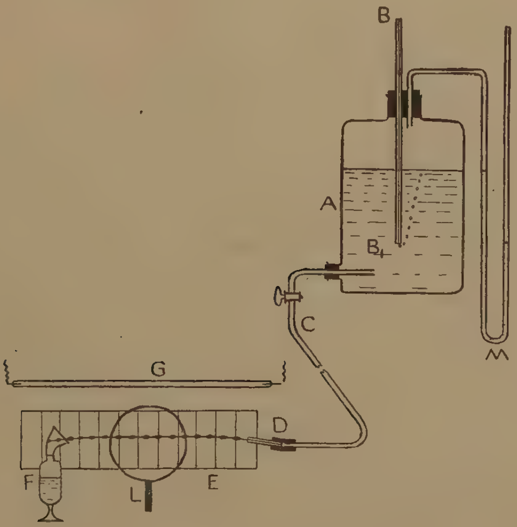

Arrangement for Constant Liquid Flow.—It is necessary to maintain a steady and constant flow of liquid over a period of several minutes for each determination. The jet is very sensitive to disturbances in the reservoir, and most of the standard types of constant-head equipment were unsuitable due to the pulsing action which was reflected in the jet. Pederson and Bohr both described arrangements based on the distribution of test liquid between several reservoirs, which are only applicable when an unlimited supply of test liquid is available. When supplies of liquid were limited, Pederson had to determine wave-lengths under a falling head of pressure. In this work, a constant flow rate has been found to be essential. Using the capillary tube orifice, true vibration takes place over part only of the jet length, and the selection of the appropriate section of the jet involves measurement over the full length ; this is only possible under constant flow. The head of pressure (h) is equal to the vertical distance from D to the lower tip of B (fig. 1) irrespective of the liquid level in A. If B has a large diameter, the bubbling of air from B_1 to replace liquid flowing from the aspirator gives rise to a regular pulsing of the jet stream. Under these conditions the operative head of pressure fluctuates over a range equal to the diameter of each air bubble. As the internal diameter of B is reduced, the pulsing action diminishes ; when the bore of B is sufficiently fine the air issues as a continuous stream of small bubbles, and a steady jet stream is obtained. If reservoir A is rigidly fixed so that it cannot transmit mechanical vibration to D, the jet is not influenced by the slight disturbances on the surface of the liquid in A. The tube B used had an internal radius of 0·03 cm.

The length of tube C was adjusted (for liquids of different densities) to give appropriate flow rates, and delicate adjustment obtained by moving B. As the resistance of the system is thereby altered, the jet velocity does not vary in proportion to $\sqrt{2gh}$, and the flow rate was measured directly in every case. The vessel F was used for this purpose, and the flow rate (ml./sec.) was measurable to an accuracy of approx. 0·2 per cent. by taking the time required for the liquid to rise to the 50 ml. graduation mark. (A similar instrument, with unbent neck, was used in conjunction with the vertical jet.) The flow rate was confirmed by measurements taken both before and after reading the jet.

Preparation of Orifice Tube.—The shape of the glass tube, and the sharpness of the orifice edge, have pronounced effect on the stability of the jet. Any form of grinding damages this edge, and the tube used in these experiments was prepared by first softening, and then slightly drawing out and flattening the end of a piece of capillary tubing approximately 0·2 cm. internal diameter. The end of this tube was then broken off at such a position that the major/minor axis ratio of the ellipse so formed was as small as possible consistent with the formation of visible waves. The ratio used was 1·25.

Measurement of Wave Lengths.—A section of the jet is shown diagrammatically in fig. 2. The jet can be regarded for present purposes as composed of a series of interlocking lenses in alternate vertical and horizontal planes. The true " nodes " are at A, B, C and D, where the cross-section passes through the circular form. However, the jet liquid must pass from A to C before completing one full oscillation, and this distance is the wave length λ. When a strip-light is placed vertically over the jet, and the jet viewed in a horizontal plane, no reflection is seen in the horizontal lenses, but the lower boundary of the vertical lenses is outlined by a band of reflected light. As the light source is raised away from the jet, this strip of light is shortened. The limits are clearly defined, so that the mean values (*i. e.* points E and F) can be accurately determined, and EF equals one wave length. By viewing the jet through the fixed lens L against a millimetre scale, individual wave-lengths could be measured with an accuracy of 0·01 cm. The accuracy increases beyond this as the number of uniform waves available for measurement increases. In order to include the length of the first wave, the orifice tube can be rotated with respect to the light source until half a band of light shows beyond the orifice. Similar illumination, with vertical strip lights, was used in conjunction with vertical jets, and photographs of the effect obtained are shown in figs. 3 *a* and 3 *b* (Pl. IV.) Fig. 3 *a* ($\frac{2}{3}$ actual size) shows a vertical jet of ethyl alcohol at 20° produced from a capillary tube orifice, and fig. 3 *b* a jet of distilled water from the same orifice, magnified ×2·5 and superimposed on a millimetre scale. The illumination required for photography was not exactly that used in reading wave lengths (for instance for optimum clarity the distance of light source from jet requires slight adjustment as the amplitude of oscillation diminishes), so that the clarity of the light bands during measurement was better than that indicated in the photographs. Similar comments apply to the interfacial jet shown in fig. 3 *c* (Pl. IV).

Fig. 2.

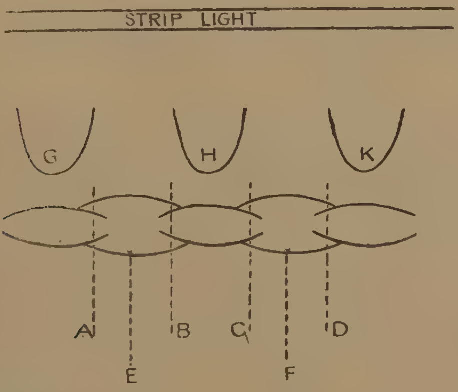

In certain positions of the light source, the rays of light are reflected and doubly refracted by the jet, and a wave image of exaggerated amplitude is thrown on the background scale. Pederson(22) utilized this effect to throw images on to a photographic plate. The position of the image with respect to the jet is shown at G, H and K in fig. 2. The lowest point of each parabola of light corresponds exactly with the centre of a horizontal lens, and the distance between these points again represents one wave length. It has not been necessary to utilize this effect during the present work.

Temperature Measurement.—Determinations were carried out over a range of temperature by enclosing the whole apparatus in a large wooden box 2 ft. deep, kept by thermostat at approximately the required air temperature. The upper half of the front was formed of glass, and the lower part was open while readings were being taken. Liquid at approximately the correct temperature was filled into the reservoir, and the liquid allowed to flow for a while before each determination to reach an even temperature. The temperature of the jet was then obtained by allowing it to impinge directly on to the bulb of a thermometer.

Quantity of Test Liquid Required.—Although the above arrangement of apparatus has been found to be most easily manipulated where ample supplies of test liquid are available, it can be reduced to a semi-micro scale if necessary. During work on interfacial jets it was found that the equations given below are applicable to minute orifices. Vibrating jets can therefore be maintained on a much smaller reservoir capacity, and measurements have been carried out using no more than 100 mls. of test liquid.

Fig. 4.

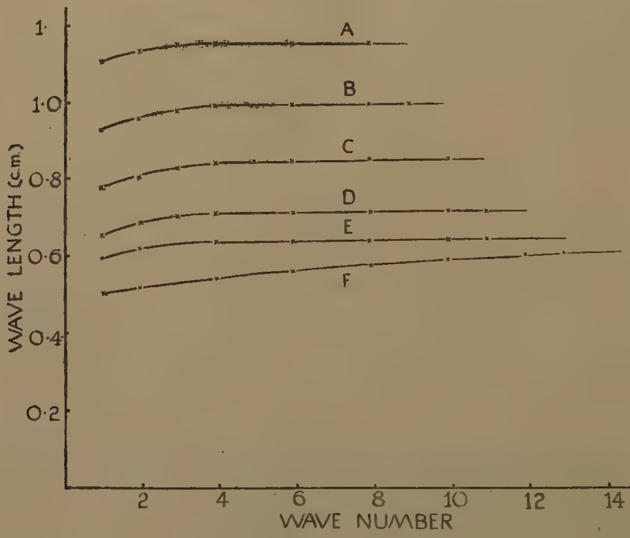

Flow rates (ml./sec.).
A 2·565, B 2·240, C 1·950,
D 1·670, E 1·515, F 1·380.

5. *Interpretation of Results.*

The change in wave-length along the jet in a horizontal position was first studied for distilled water at 20° at various flow rates. The results are shown graphically in fig. 4, in which " wave number " represents the serial number of the wave, counting along the jet from the orifice. The minimum flow rate for visible waves gives rise to a jet having a gradually increasing wave-length. In an ideal jet (in which wave-length varies directly as flow rate) the oscillations are two-dimensional, and this only holds true if the wave-lengths are considerable in comparison with the jet diameter. For small flow rates (and thus small wave-lengths) the oscillations become three-dimensional, and the oscillation frequency depends upon the wave-length also. At all flow rates but the smallest, increase in wave-length takes place over the first four waves, and is constant thereafter. It has therefore been necessary, whenever the capillary tube orifice was used, to ignore the first four wave-lengths as representing the period necessary for the establishment of fluid equilibrium. An orifice designed to eliminate this irregularity will be described later.

Fig. 5.

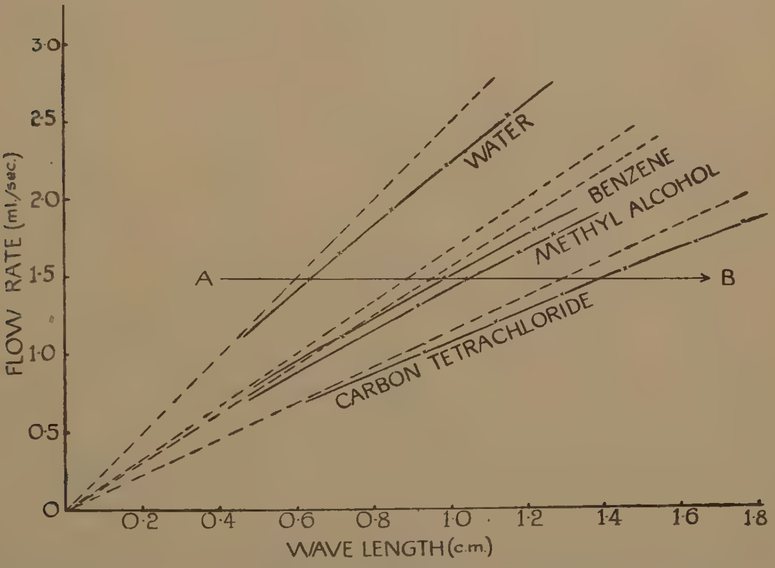

The flow rate f has been plotted against the equilibrium wave-length λ for four different liquids in fig. 5. Rayleigh (19) and Bohr (23) observed that λ for water increases more rapidly than f. This effect has been found to occur with all liquids tested, irrespective of type of orifice.

Relation between Wave-Length, Flow Rate and Surface Tension.— Rayleigh (19) has shown that for an ideal jet, the expression for the time of oscillation takes the form

$$t = K_1(dr^3/\gamma)^{1/2},$$

where d is the density of the liquid, γ its surface tension, and r the radius (in cm.) of the jet where its cross-section is circular. If λ is expressed in cm. and f in ml./second, then

$$t = \pi r^2 \lambda / f,$$

whence $$\gamma = (K_1^2/\pi^2 r) d (f/\lambda)^2.$$

As the apparatus is to be calibrated, using liquids of known surface tension, the term r can be conveniently incorporated in the constant in the above equation. Again, the value for λ/f for an ideal jet and any liquid is given by the slope of the tangent to the λ–f curve at the origin (fig. 5) and can thus be replaced by $\tan\theta$.

Hence $$\gamma = \mathrm{K}_2 d/\tan^2\theta, \qquad (1)$$

θ has, of course, no significance as an angle, and is significant only when referred directly to its tangent in the appropriate units. Tan θ for water was found by accurate construction to be 0·400 at 20°. By substituting the values $\gamma = 72{\cdot}8$ dynes/cm. and $d = 0{\cdot}9982$ at 20°, we find $\mathrm{K}_2 = 11{\cdot}68$. This value varies with the particular jet used, but when once determined is a fixed property of the apparatus.

Determination of tan θ.—The large number of measurements required before $\tan\theta$ can be obtained by geometrical construction prohibits the use of this method for routine measurements, and where changes in λ occur along the jet the method is not possible. It is therefore essential to obtain $\tan\theta$ from a single measurement of λ and f. The lower range of flow rates over which λ–f proportionality holds varies with the size of orifice and nature of liquid, but in no case does two-dimensional oscillation operate until the flow rate is so large that λ is appreciably deviated from proportionality. There are therefore no practical conditions under which $\tan\theta$ can be obtained as the direct ratio of measured values of λ and f. It can, however, be obtained as follows :—

TABLE I.

λ, cm.	f, ml./sec.	K_3 assuming $n=2$.	K_3 assuming $n=3$.	Approx. ratio λ/jet diameter.
0·640	1·515	87·3	143	8
0·714	1·670	79·2	143	9
0·850	1·950	68·8	146	10
0·990	2·240	68·8	168	12
1·150	2·565	68·5	192	14

When referred to the tangent as ordinate, the equations for the curves in fig. 5 have the general form $y^n = \mathrm{K}_3 x$. When referred to the f and λ axes, the equation becomes

$$(\lambda\sin\theta + f\cos\theta)^n = \mathrm{K}_3(\lambda\cos\theta - f\sin\theta), \qquad (2)$$

where θ is the angle between the tangent and the f axis. The value for $\tan\theta$ for water (0·400) was substituted in the above equation to determine appropriate values for K_3 and n. Table I. shows that as λ increases, the value to be given to n in order to maintain K_3 constant changes from 3 to 2, which is consistent with the change from three- to two-dimensional oscillation which takes place as λ increases with respect to jet diameter. The table also indicates that for orifices of this order of size, the ratio λ/jet diameter should be above 10 in order that true two-dimensional oscillation can operate.

The relationship between λ, θ, and f for water is therefore

$$(\lambda \sin \theta + f \cos \theta)^2 = K_3(\lambda \cos \theta - f \sin \theta),$$

K_3 is 68·7 for the apparatus used, and θ then remains the only unknown quantity.

Variation of K_3 with Properties of Test Liquid.—Equation (1) provides a suitable means of determining the variations which take place in K_3 when equation (2) is applied to various liquids. Fig. 5 shows the relation between λ and f for benzene, carbon tetrachloride and methyl alcohol under similar experimental conditions. The known values for the surface tension being assumed, the value of θ was calculated for each of the three liquids, using equation (1). This value was substituted in equation (2), with $n=2$, and the values obtained for K_3 compared with K_3 for water, three separate values of λ and f being used in each case. The results are given in Table II , where K_4 is defined by $K_3 = K_4 d/\tan \theta$. The value of K_3 is a measure of the extent to which λ departs from ideal proportionality with f, and the results in col. 6 indicate that there are considerable variations from liquid to liquid.

TABLE II.

Liquid.	γ assumed (dynes/cm. at 20°).	tan θ.	λ cm.	f ml./sec.	K_3.	K_4.
Water	72·8	0·400	1·150	2·565	68·5	27·5
	72·8	0·400	0·990	2·240	68·8	27·6
	72·8	0·400	0·850	1·950	68·8	27·6
Benzene	28·9	0·596	1·220	1·820	40·9	27·8
	28·9	0·596	0·980	1·495	41·1	27·9
	28·9	0·596	0·800	1·240	41·5	28·2
Carbon tetrachloride.	26·7	0·835	1·728	1·875	51·8	27·6
	26·7	0·835	1·606	1·750	51·4	27·4
	26·7	0·835	1·422	1·570	51·9	27·8
Methyl alcohol	22·6	0·640	1·312	1·790	34·8	27·9
	22·6	0·640	1·206	1·660	34·4	27·5
	22·6	0·640	1·062	1·480	34·0	27·3

The tangents in fig. 5 represent the ideal λ f ratio for each of the four liquids. The major causes of deviation from these lines, *i. e.*, air phase inertia, velocity gradient in the jet, viscosity, and variations in wave amplitude, are each functions of the flow rate, and their influence upon wave-length must necessarily depend upon the frequency of vibration. As the wave-length increases for any given flow rate (say along the line

AB in fig. 5) the rate of oscillation decreases and the factors causing deviation will play a less significant part. It was therefore to be expected that the value K_3/d would decrease with increase in $\tan\theta$. The respective values given in Table II. show that, in fact, a clear inverse proportionality exists, and that if K_3 in equation (2) be replaced by $K_4d/\tan\theta$, then the value of K_4 is constant for all four liquids.

Determination of Surface Tension of any Liquid.—The procedure can be summarized as follows :—

1. Accurate determination of wave-length and flow rate in horizontal jet.

2. Substitution of these results in the expression

$$(\lambda \sin\theta + f\cos\theta)^2 - K_4d(\lambda\cos\theta - f\sin\theta)/\tan\theta.$$

3. d, λ, and f being known, and K_4 determined as above for the apparatus used, it is possible to find the value of θ at which the expression has zero value. This is readily done by substituting into the expression near values of θ, plotting the value for the expression against the angle, and reading off the value of θ. $\tan\theta$ then has direct significance in terms of wave-length per unit flow rate.

TABLE III.

Liquid.	λ cm.	*f* ml./sec.	tan θ.	γ dynes/cm. at 20°.
Ethyl ether	1·320	1·640	0·700	17·0
Heptane	1·060	1·495	0·630	20·1
Ethyl alcohol	1·060	1·480	0·640	22·5
Acetone	1·104	1·580	0·620	23·8
Chloroform	1·480	1·690	0·801	27·2
Toluene	1·206	1·815	0·595	28·5
m-xylene	1·000	1·510	0·594	28·7

4. Substitution of the value of $\tan\theta$ so obtained into the expression

$$\gamma = K_2d/\tan^2\theta.$$

Adsorption processes are usually followed in dilute solution. Where a series of determinations are to be carried out on dilute solutions of similar density, it is convenient to use the same flow rate throughout. A calibration curve can then be drawn connecting wave-length directly with surface tension.

This simple procedure, which had so far been shown to give true surface tension values for four liquids of widely different density, surface tension and chemical nature, was then applied to the surface tensions of other liquids. The results are given in Table III., and the good agreement with results obtained by other methods indicates that K_2 in equation (1) is constant for all liquids tested.

Influence of Temperature.—Surface-tension measurements have been made for four liquids over a range of temperature. The flow rates chosen were such that at the lowest temperature the wave-lengths were still sufficiently long to ensure two-dimensional oscillation. The results are given in Table IV. The height of the capillary air inlet B (fig. 1) was adjusted at each temperature so that the flow rate was constant during the tests on any one liquid. Thus the variation of wave-length with temperature is immediately available from Table IV.

Thermal agitation was responsible for a progressive shortening of the unbroken jet as temperature increased. It was possible in each case to shorten the jet to less than five readable waves, and the highest temperature recorded in Table IV. represents the limit to which the temperature could be raised without reducing the unbroken jet to less than five waves. The results obtained indicate that the method can be applied over a range of temperature, and that the constants as defined above are independent of temperature.

TABLE IV.

Liquid.	Temperature. °C.	f ml./sec.	λ cm.	tan θ.	γ dynes/cm.	$-d\gamma/dt$.
Water	13	2·025	0·874	0·398	73·8	0·150
	33	2·025	0·900	0·406	70·6	0·160
	45	2·025	0·916	0·410	68·7	0·166
	60	2·025	0·940	0·417	66·0	0·180
Carbon tetrachloride	7	1·620	1·432	0·816	28·3	0·120
	32	1·620	1·520	0·854	25·1	0·135
	48	1·620	1·580	0·884	23·0	0·140
Benzene	11	1·690	1·106	0·587	30·0	0·120
	35	1·690	1·180	0·611	27·0	0·130
	50	1·690	1·240	0·630	24·9	0·140
Methyl alcohol ..	8	1·715	1·214	0·628	23·8	0·080
	18	1·715	1·238	0·635	23·0	0·085
	38·5	1·715	1·304	0·656	21·0	0·105
	50	1·715	1·340	0·671	19·8	0·115

Influence of Size and Shape of Orifice Ellipse.—The work described above was carried out using an orifice approx. 0·1 cm. mean radius, and major/minor axis ratio 1·25. In the liquid/liquid interfacial work described below it was necessary to use a much smaller orifice, 0·017 cm. mean radius and axis ratio 3. In view of the emphasis laid by Pederson and Bohr on the importance of having this ratio as near unity as possible, it was considered possible that the general calculations set out above might not hold true for minute orifices of exaggerated elliptical form. This aspect has not been studied exhaustively, but some of the determinations above have been repeated at 20° using this small orifice in a horizontal position. Abstracted results for three liquids are given in Table V. With this orifice, the same illuminating and reading equipment was used as for the large orifice. The experimental error is therefore increased, and any error in tan θ is squared in determining K_2. Nevertheless, the agreement in the values found for K_2 indicate that the general method of calculation is applicable over a wide range of orifice sizes and axis ratios. Greater accuracy with these small orifices could readily be achieved by refining the apparatus, and this may bring the values for K_2 into even closer accord.

Table V.

Liquid.	γ assumed (dynes/cm.).	tan θ.	K_2 (equation 1).
Water	72·8	0·65	30·8
Carbon tetrachloride ..	26·7	1·35	30·4
Methyl alcohol	22·6	1·02	29·1

6. *Influence of form of Orifice Tube on Wave-Length.*

A capillary tube orifice is very easily constructed, and the initial variation in wave-length in the jet (fig. 4) is not a disadvantage in the measurement of surface tensions of pure liquids, or where adsorption of surface active molecules from the liquid to the surface is slow. It is essential, however, that these variations should be reduced to a minimum where surface equilibrium is established rapidly; for instance, (25) in a 0·325 per cent. solution of iso-amyl alcohol in water, surface equilibrium is established over a period represented by the first four waves in the jet. Various forms of orifice tube have been used by previous workers, but no attempt appears yet to have been made to determine the influence which the type of orifice has on the change of wave length along the jet. Preliminary work with liquids of high viscosity indicated that wave-lengths in the early part of the jet from a capillary orifice diminished, in contrast to the increase found for mobile liquids. These viscous systems were not studied in detail, since the damping of the oscillations which also occurred reduced the accuracy of measurement. However, in view of the fact that horizontal jets of eleven mobile liquids all showed an initial increase (Tables III. and IV.), it was clear that viscosity was a major factor. The jets obtained for aniline (fig. 6) are of particular interest, since the range of viscosity available by temperature variation appears to be in the critical range for the capillary tube used. Table VI. gives the data relevant to the curves.

The increase in average wave-length with temperature is due to falling surface tension and increasing flow rate through the apparatus as viscosity falls, and the curves show a gradual change from increasing to decreasing λ as viscosity increases. Apart from its influence in the liquid stream, viscosity also plays an important part in determining the type of fluid motion set up in the liquid during its passage through the capillary tube. If the latter effect is predominant, variation in the length of capillary tube might be expected to influence the early wave-lengths in the jet. An elliptical orifice (mean radius 0·053 cm. and axis ratio 1·25) was therefore prepared at the end of a capillary tube 10 cm. long, and the horizontal jet of distilled water obtained at 20° under a flow rate of 2·25 ml./sec. was measured. The tube was then shortened in several stages, and the influence of this reduction on the form of the jet was studied at each stage. The results are shown graphically by the broken lines B, C and D in fig. 7. As the length of the tube was reduced, the initial deviation in wave-length from the constant value given later in the jet was reduced also. In each case the wave-length reached the same constant value, and variation in the length of capillary tube had no influence on the length of unbroken liquid jet available for measurement, which was equivalent to about 16 waves throughout these experiments.

Fig. 6.

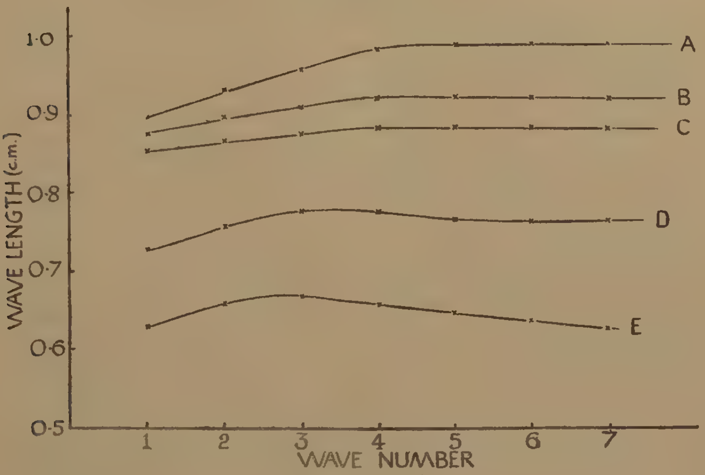

TABLE VI.

Curve (fig. 6).	Temperature °C.	c.g.s. units.	Flow rate ml./sec.	Linear velocity cm./sec.
A	55	0·018	1·67	378
B	40	0·024	1·57	356
C	32	0·030	1·50	340
D	20	0·044	1·32	300
E	10	0·065	1·14	258

In order to obtain a limiting case, an orifice was then prepared as shown in fig. 8, in which the length of narrow tube through which the jet liquid passes is reduced to the thickness of the orifice plate A, 0·02 cm. (For convenience this type of orifice will be termed a " plate " orifice.) The orifice was prepared to the required dimensions by gentle rubbing with a length of fine copper wire passed through the hole. This method has the advantage that the edges so produced are smooth. The size and shape of the orifice were made as identical with those of the capillary orifice as was experimentally possible. The steel sheet containing the

Fig. 7.

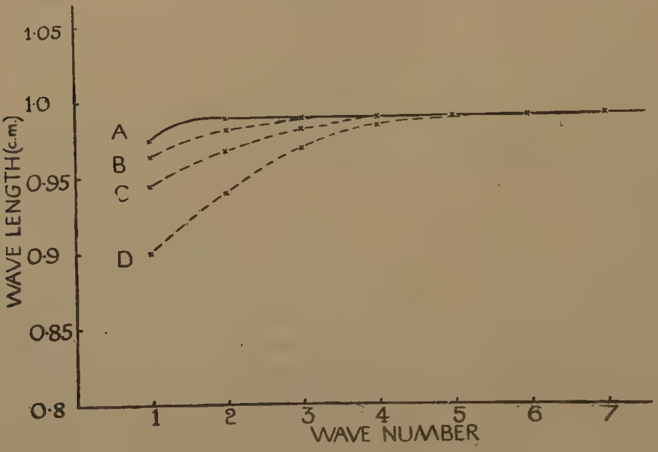

A Plate orifice.
B Capillary orifice, 0·4 cm. tube.
C ,, ,, 1·5 ,, ,,
D ,, ,, 3·5 ,, ,, and longer.

Fig. 8.

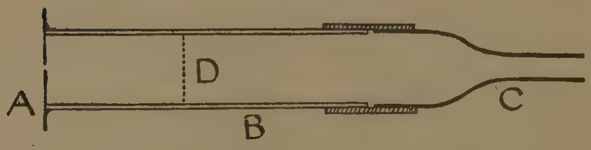

orifice was then soldered over the end of a piece of annealed copper tube B (6 cm. long, 1·5 cm. diameter and wall thickness 1 mm.). so that the orifice was on the axis of the copper tube. The tube was then attached by a piece of rubber tubing to a glass tube C which was narrowed to fit the lead from the liquid reservoir. When the tube was used in this condition, an unsteady horizontal jet was obtained whose direction wandered over several degrees and upset wave-length measurement. In the vertical position, the jet developed a natural spin which again prevented measurement of the jet. However, the insertion of a fine gauze D into the tube near the orifice regulated the flow of liquid in B, and stationary jets were obtained horizontally and vertically. The gauze was bronze, 20 mesh/cm. and was situated 2·5 cm. from the orifice.

Using a flow rate identical with that used in the capillary orifice, the type of jet obtained is shown by the unbroken line A in fig 7. The wave-lengths after the first were constant, and the length of unbroken jet available for measurement was similar to that given by the capillary orifice. This constancy in wave-length has been found to hold for all the pure liquids mentioned in this paper. It is well known that the coefficient of discharge of a plate orifice, and to a lesser extent that of a capillary nozzle, depends not only on the size and shape of the cross-section, but also on the curvature of the edges. On this account alone it was to be expected that early waves from the plate orifice would differ in length from those produced by capillary orifices B, C, and D (fig. 7), but the appreciable differences existing between B, C, and D themselves indicate that the nature of the motion set up inside the liquid by its passage through the capillary tube is also an important factor. Again, it is significant that the later waves from both types of orifice have the same constant value. This, and the difference existing between curves B, C, and D, lend support to the belief that beyond a certain distance from the orifice (which with the present orifice diameter is equivalent to four waves), fluid motion inside the jet has reached an equilibrium state which is irrespective of type of orifice.

Fig. 9.

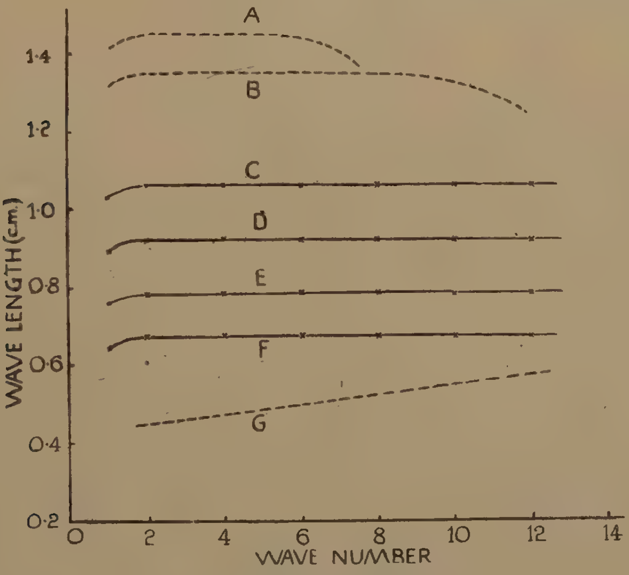

Flow rates (mls./sec.).
C 2·54, E 1·95,
D 2·25, F 1·71.

It has been confirmed that this constancy in the horizontal waves from a plane orifice holds over the workable range of flow rates. The results for distilled water at 20° are shown in fig. 9, and similar sets of curves have been obtained for carbon tetrachloride and ethyl alcohol. The wave-length is steady after the first wave irrespective of flow rate, provided that the wave-length is not so small that three-dimensional oscillation operates. As with the capillary orifice, this limit is indicated by a gradual increase in wave-length (line G, fig. 9). The maximum linear flow rate permissible theoretically will be approximately that at which a drop of the liquid with radius equal to that of the orifice can pass through air under pressure equal to that of the total head at the orifice. Flow rates in excess of this cause early break-up of the jet, and a reduction in the length of the waves immediately before the point of break-up. These conditions are represented by the broken lines A and B in fig. 9, without reference to the λ axis.

7. *The Use of Vertical Jets.*

Although a horizontal jet will normally provide sufficient waves for an accurate determination of surface tension on a pure liquid, it suffers from the disadvantage that the jet is appreciably curved at the lower flow rates. As this curvature varies with flow rate, measurement of λ may be hindered. Again, with either the capillary or plate orifice, the unbroken jet is as much as 20–30 per cent. longer in the vertical than the horizontal position. This may be due to the fact that the gravity force, although uniform along a horizontal jet, acts in the same plane as the oscillations, and may gradually upset their purity. The wave-lengths in vertical jets from capillary orifices are influenced by both gravity and the fluid motion set up in the tube. The form of wave-length/number curves thus varies with flow rate (26), and it has not yet been possible to interpret this system. However, by using the plate orifice described above in the vertical position, the elongation in wave-length which takes place under constant surface tension is caused by gravity alone. Vertical jets of distilled water at 20° produced by the plane orifice have been measured over a range of flow rates (fig. 10). Similar curves are given by carbon tetrachloride and methyl alcohol. The lower limit of available flow rate is again that at which three-dimensional oscillation commences, and the practical upper limit will not be more than that at which a drop, with radius equal to that of the orifice, can pass through air under gravity. The form of curve given under these limiting conditions is shown by broken lines A, B and G (fig. 10) again without reference to the λ axis. Between these limits the wave-length (after the first wave) increases very slightly and regularly along the jet under gravity, and the slope increases with flow rate.

In the absence of a suitable method of assessing this increase, previous work has been confined to horizontal jets, with the exception of a qualitative statement by Rayleigh (19) that “ most of this augmentation is compensated by a change in the frequency of vibration due to the attenuation which is the necessary concomitant of the increased velocity." The very slight increase in λ under gravity found experimentally (fig. 10) supports this statement. The method given below enables the vertical wave-length at any position in the jet to be converted to the corresponding horizontal jet value, thus enabling the equations already given to be applied to vertical jets also. The coefficient increase under gravity (a) deviates only slightly from unity. For this reason a number of mathematical approximations can be made in its determination, and a more rigorous mathematical treatment would have theoretical interest only.

In order to deduce a relationship which holds throughout the jet, the irregular fluid motion in the first wave is neglected below and is regarded as being superimposed on the theoretical jet. Equation (4) below therefore applies directly to all waves but the first. As the extension under gravity is a function of the wave-length, the influence of gravity may be deduced by considering the vertical jet as a stationary body of liquid with perfectly elastic properties, supported in space by the orifice. A body falling from rest under gravity for time t travels a distance $\frac{1}{2}gt^2$ irrespective of its mass, and thus the centre of gravity of any given section of the jet will advance beyond the position determined by the flow rate alone to an extent also in accord with this law. If the mass be one wave, then the time (t seconds) during which gravity acts is equal to the period of oscillation. It has been shown above that in order to

Fig. 10.

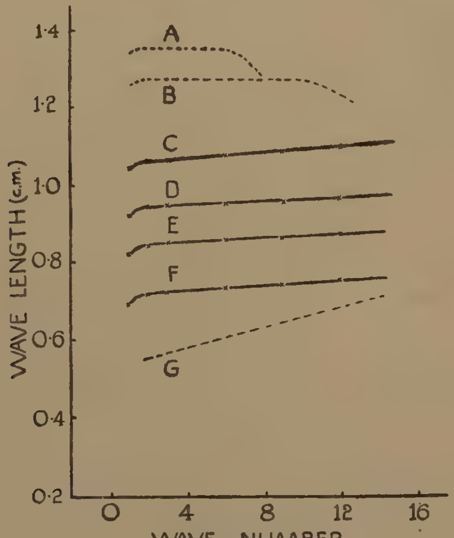

Flow rates (mls./sec.).
C 2·51, E 2·08,
D 2·27, F 1·80.

ensure true two-dimensional oscillation, the wave-length should be at least ten times the jet diameter. Under these conditions the extension of the first vertical wave (λ_{v_1}) under gravity can be considered to be gt^2. As this wave is not advancing against the gaseous phase, but is preceded by another wave moving with similar velocity, the air resistance is negligible. Again, the extension gt^2 should be independent of the mass of the wave (and therefore of the density of the liquid) and should vary only with t. As a result of this extension, the radius r_2 of the circle equivalent to the ellipse at the end of the first vertical wave will be less than the initial radius r. The wave can then be regarded as the frustum of a cone, and

$$r_2^2 = r^2(\lambda_{\mathrm{H}} - gt^2)/(\lambda_{\mathrm{H}} + gt^2)$$

where λ_{H} represents the wave-length in the corresponding horizontal jet. While this reduction in radius is proceeding evenly throughout the wave, it is accompanied by a reduction in the period of oscillation t, and for present purposes the value of t can be regarded with sufficient accuracy as dependent upon the mean radius r_1 of the wave. As a result of this factor, the original wave-length λ_{H} will be reduced to the value $\lambda_{\mathrm{H}}t_1/t$, where t_1 represents the period of oscillation corresponding to the mean radius r_1. Since the net alteration is very small, then

$$\lambda_{v_1} = \lambda_{\mathrm{H}}t_1/t + gt^2.$$

Now since

$$t = \mathrm{K}_1(dr^3/\gamma)^{1/2} = \mathrm{K}_5 r^{3/2}$$

for any given liquid, then

$$t_1/t = (r_1/r)^{3/2}$$

for all liquids, whence

$$\lambda_{v_1} = \lambda_{\mathrm{H}}\left(0{\cdot}5 + 0{\cdot}5\sqrt{\frac{\lambda_{\mathrm{H}} - gt^2}{\lambda_{\mathrm{H}} + gt^2}}\right)^{3/2} + gt^2. \quad . \quad . \quad . \quad . \quad . \qquad (3)$$

The ratio $\lambda_{v_1}/\lambda_{\mathrm{H}}$ given by this equation represents the influence of gravity on a single wave. As the relationship is expressed in general terms, then the second wave of a vertical jet will bear the same relation to the first as does the first wave to λ_{H}; the results given below indicate that the small drift in the value of t which takes place along the jet causes a negligible change in the value of $\lambda_{v_1}/\lambda_{\mathrm{H}}$. The waves in a vertical jet from a plate orifice can therefore be represented by the terms of the geometric progression:

$$\lambda_{\mathrm{H}}, \quad \lambda_{v_1}, \quad \lambda_{v_1}a, \quad \lambda_{v_1}a^2 \ldots \lambda_{v_n}(=\lambda_{\mathrm{H}}a^n)$$

where n is the wave number, and a has the value $\lambda_{v_1}/\lambda_{\mathrm{H}}$ given in equation (3). The first vertical wave is the second term of the series, and the nth wave is given by

$$\lambda_{v_n} = \lambda_{\mathrm{H}}\left\{\left(0{\cdot}5 + 0{\cdot}5\sqrt{\frac{\lambda_{\mathrm{H}} - gt^2}{\lambda_{\mathrm{H}} + gt^2}}\right)^{3/2} + \frac{gt^2}{\lambda_{\mathrm{H}}}\right\}^n \quad . \quad . \quad . \quad . \quad . \qquad (4)$$

From this expression it is possible to calculate the value of λ_{H} corresponding to each wave of a vertical jet, and thus to determine the surface tension by equations (1) and (2). Again, where changes in λ_H occur along a horizontal jet due to changing surface tension, the application of equation (4) enables the true λ_H/wave number curve to be obtained from vertical jet measurements. λ_H is most readily determined by substituting near values into the expression for λ_{v_n} in equation (4), and plotting the value of the expression against the value of λ_H taken. When a series of determinations is to be carried out at a constant flow rate, calibration curves can be drawn which considerably simplify the calculations. Since equation (4) has the general form $\lambda_v = Ka^n$, the curve relating λ_v and n at any given flow rate (fig. 10) should show an increasing slope with increasing value of n. In practice, the value of a is so slightly above unity that the line is virtually straight over the major part of the jet.

Fig. 11.

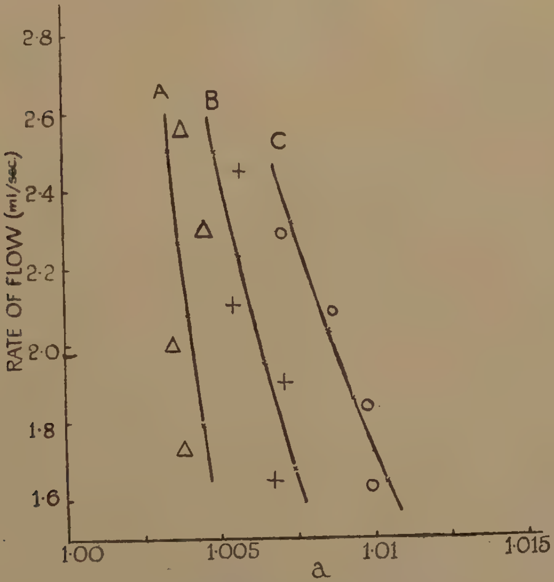

×—×—×— Calculated values of a for
A Distilled water,
B Ethyl alcohol,
C Carbon tetrachloride.
△ △ Experimental values for water.
+ + ,, ,, ,, alcohol.
○ ○ ,, ,, ,, carbon tetrachloride.

Equation (4) has been used to calculate values for a over a range of conditions, and its validity has been confirmed. Horizontal jets of water, ethyl alcohol and carbon tetrachloride were measured at 20°, and the values of a calculated from equation (4) are plotted against flow rate in fig. 11. The slight decrease in a with increasing f is the result of the disproportionate increase in λ_H which also occurs with increasing f

Vertical jets of the same three liquids were then measured at four separate flow rates. Knowing λ_H at the same flow rates, the value of a was obtained by direct measurement at several points along each jet. The mean values obtained are superimposed in fig. 11 on the values calculated by equation (4). As all values of λ_v determined during this work have varied only slightly from the corresponding λ_H, the experimental error of measurement is not inappreciable when compared with $\lambda_v - \lambda_H$. This error is further magnified in calculating a from practical results, but nevertheless the good agreement obtained indicates that any error in the calculation of λ_H from λ_v by applying equation (4) will be less than the experimental error in wave-length measurement.

In general, therefore, a jet from a capillary orifice is available for the measurement of surface tension (and over a restricted part of the jet, for rate of adsorption) in a horizontal, but not in a vertical position. Since it is possible to derive mathematically the extension in λ under gravity in a jet from a plate orifice, such jets are now available in either vertical or horizontal positions.

Fig. 12.

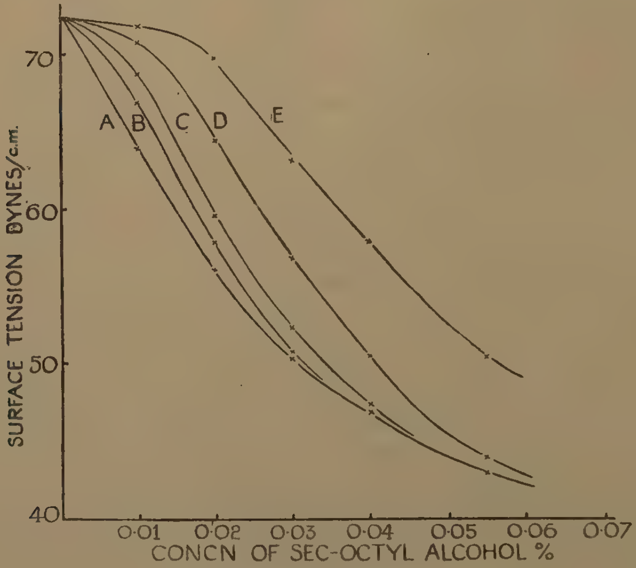

Surface ages (seconds).
A 0·12 and over. D 0·02,
B 0·06 E 0·01.
C 0·04.

8. *Application of Vibrating Jet Method to the Study of Dynamic Tensions of Solutions.*

Rayleigh (6) found that the dynamic surface tension of a soap solution was little below that for pure water. Pederson (22) used the vibrating jet method to measure the surface tension of aqueous ethyl alcohol solutions, but in this case the values obtained have been found to agree well with accepted static values. The rate of development of surface equilibrium therefore varies with the nature of the solute, and the author's experiments (25) (26) on aqueous alcohol solutions represent, as far as is known, the first study of the actual rate at which the solute collects in the surface. The order of results obtained is illustrated in fig. 12, which represents the γ-concentration relation at 20° for solutions of sec-octyl alcohol in water at various surface ages. The waves in a vibrating jet of such solutions lengthen as adsorption proceeds, and reach a constant value only when adsorption is complete. The surface tensions represented by these constant values of λ form the limiting curve A, and this curve has been found to agree exactly with results obtained by static methods.

Since the solutions used are very dilute, the activity of the alcohol can be equated to its concentration c, and the amount of alcohol adsorbed at equilibrium can be obtained from the approximate form of the Gibbs Theorem (28) (29)

$$\Gamma = -c(d\gamma/dc)/\mathrm{RT},$$

where $d\gamma/dc$ represents the tangent to curve A. R has the value $83{\cdot}2 \times 10^6 (=\mathrm{K}_6)$ for one gram molecule of adsorbate, whence

$$\Gamma = -c\mathrm{M}(d\gamma/dc)/\mathrm{K}_6\mathrm{T},$$

where M is the molecular weight of the adsorbate. If the terms of this equation are expressed in c.g.s. units, the value of Γ so obtained represents the mass of adsorbate in grams attached to 1 cm.^{2} of surface. Since the mass concerned is minute, it can be regarded as being drawn by surface forces from a disk 1 cm.^{2} in cross-section, placed with one face in the surface, and having thickness d cm. Although d is appreciable in terms of molecular dimensions, it is very small in comparison with the diameter of the disk. Surface equilibrium will thus be complete when the whole of the original solute content of the disk reaches the surface. The time, t_2 seconds, indicated by experiment as being necessary, will decrease with increasing concentration (fig. 12) and can be equated to the time taken for the last migrating molecules (*i. e.* those from the opposite face of the disk) to travel d cm. As concentration is expressed as per cent. by weight,

$$d = 100\Gamma/c = -100\mathrm{M}(d\gamma/dc)/\mathrm{K}_6\mathrm{T}.$$

The *mean* velocity at which adsorbate molecules travel to the surface has been found to provide a very useful index on which to compare surface activity of dissolved molecules, and has been termed the "migrational velocity." As this equals d/t_2 cm./sec., then

$$\text{Migrational velocity} = \mathrm{V} = -100\mathrm{M}(d\gamma/dc)/\mathrm{K}_6\mathrm{T}t_2.$$

Relevant figures used to determine this value for sec-octyl alcohol are given in Table VII.

The migrational velocity has been found to increase with length of carbon chain. However, the distance d also increases with chain length due to the enhanced surface activity (and thus greater Γ) and the smaller concentrations required to produce the necessary fall in surface tension. The rate of increase in d with chain length is greater than the rate of increase in migrational velocity, with the result that the time t_1 required for the establishment of equilibrium actually increases with increasing chain length. This explains the results of Rayleigh and Pederson referred to above; t_2 for the long-chain soap solution used by Rayleigh would be much greater than the range of surface age in the jet, whereas the adsorption of the ethyl alcohol used by Pederson would be complete within the first wave.

The vibrating jet technique is now being extended with success to the study of the actual rate of travel of various adsorbing molecules.

9. *Liquid—Liquid Interfacial Jets.*

The extension of the vibrating jet technique to liquid interfaces opens up a wide field of study, but the production of a vibrating jet of one liquid in another liquid of similar density with which it is immiscible has hitherto presented great practical difficulties. No record is known in the literature of this method having been applied to liquid/liquid systems. Rayleigh $^{(19)}$ made certain qualitative observations on the electrical properties of a jet of mercury discharged into sulphuric acid, but in this case the production of the jet presents no difficulty because of its high density. Jets of water from both the capillary and plate orifices described above were immersed in various liquids of lower density, but in each case the jet broke up before the end of the first wave. A similar failure was experienced with jets of denser liquids (carbon tetrachloride, chloroform) directed into water. (The liquid into which the jet is directed will be termed the "liquid phase" to distinguish it from the "jet liquid"; and "water→benzene" represents a jet of water directed into benzene.) Attempts were made to overcome the resistance of the liquid phase by arranging the orifice tube along the axis of a wider glass tube through which the liquid phase flowed in the direction of the jet. A slight improvement was obtained, but no more than one wave was readable. If the velocity of the liquid phase was increased to that of the jet, the turbulent motion in the outer tube was itself sufficient to break up the jet. However, the resistance of the liquid phase was successfully reduced by appreciably reducing the radius

TABLE VII.

c per cent.	$-d\gamma/dc$.	$\Gamma \times 10^8$ gram./cm^2.	$d \times 10^6$ cm.	t_2 secs.	$V \times 10^4$ cm./sec.
0·01	800	4·30	43·0	0·120	36·0
0·02	640	6·90	34·5	0·095	36·2
0·03	490	7·90	26·5	0·070	37·6

of the jet. It was necessary to reduce this to below 0·02 cm., and to use a tapered orifice tube (fig. 3 *c*). By this means it has been possible to obtain sufficient waves to determine the interfacial tension between a number of liquids, and in some cases to follow the process of adsorption to an interface.

The liquid reservoir and constant level device were the same as in fig. 1. The arrangement of apparatus round the jet is shown in fig. 13. The orifice tube A was attached by elastic bands B to a scale C marked in 0·5 mm. divisions, which stood on the bottom of the glass vessel D (a 250 ml. soft glass beaker is suitable). The jet liquid collected at the bottom of the vessel, thus displacing the liquid phase, which overflowed down tube E into graduated flask F. A copper wire G was placed in the neck of tube E as shown to prevent build up of liquid phase at the lip of E, ensuring regular flow of liquid down E. The flow rate from orifice O was therefore obtained directly by measuring the time taken to fill flask F to the 25 ml. graduation mark. The vessel was closed by a cork, in which was bored one hole to admit scale and orifice tube, in such a position that the orifice was about 1 cm. from the wall of vessel D. This hole, and flask F, were plugged with cotton wool to minimise evaporation. A photograph (with magnification ×2·5) of a vertical jet of carbon tetrachloride in water is shown in fig. 3 *c*, in which the orifice has been removed a little from the scale along which it laid during an experiment, for better illumination. The waves in the jet (overall length only about 2 cm.) are not visible without suitable magnification and illumination. Strip lighting was again found satisfactory, although a point source of light, such as a 2·5 volt torch bulb, could be used.

Fig. 13.

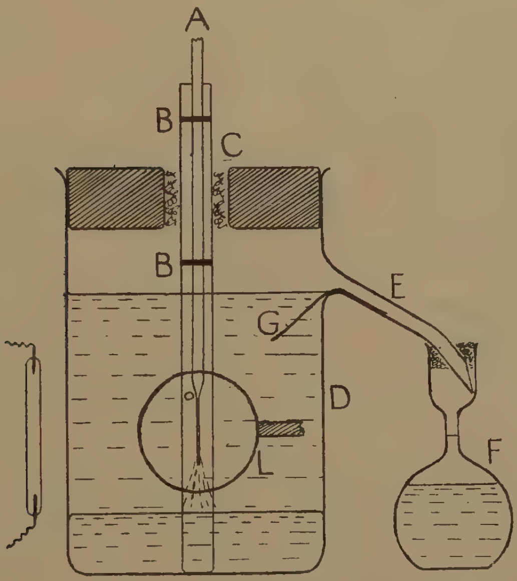

The clarity of the light bands on the jet depends on the relative positions of light source, lens L (which was outside the beaker), jet and scale. The adjustment of their positions was found to be a delicate operation, and the apparatus should be arranged so that any part can be easily moved. The orifice tube was prepared by drawing down a glass tube 0·5 cm. diameter to a taper 2 cm. long. The elliptical orifice was then obtained by gentle lateral compression of the tip in a bunsen flame. Using this orifice and a jet of carbon tetrachloride directed into water, a trace of dye solution was introduced into the water near the orifice. It was clear from the movement of the coloured liquid that when this shape of orifice was used a steady circulatory motion was set up in the liquid phase. The water immediately in contact with the jet moved at approximately the same velocity, though there was a steep velocity gradient away from the jet. When a plate orifice of the same radius was tested, the motion of the water was confused and a poor jet obtained.

The form of the wave-length/wave number curve from this jet is intermediate between those given by the plate and the capillary orifice in air. With all liquid pairs tested, the first wave was shorter, and the second wave slightly shorter, than the remaining waves. Thereafter, the wave-length was constant for pure liquids. The curvature in the jet when used in a horizontal position was a great inconvenience, and it has been possible to use the jet in a vertical position without the application of the correction factors necessary with larger orifices, in air. The extension in wave-length under gravity depends upon the difference in density between the two liquids rather than on the density of the jet liquid itself. This smaller extending force acts against a liquid phase rather than air; the length of the interfacial jet is smaller, and it is therefore reasonable that wave-lengths after the second are constant within experimental error.

The orifice used had a mean radius 0·017 cm. With an axis ratio of 1·25, the bands of light defining the waves were indistinct, and satisfactory readings were not obtained until the ratio was increased to 3. With this orifice, four interfacial systems have been studied, and the $\lambda - f$ relation for each is shown in fig. 14. In each case the heavier jet liquid was directed vertically downwards into the lighter phase, and the number of readable waves obtained appears to increase with the density of the jet liquid, and the difference in density between the two liquids. Thus up to ten good waves were obtained with carbon tetrachloride → water, whereas with water → benzene, petroleum ether or ethyl ether the fifth wave was indistinct. It is also significant that attempts to obtain a jet by directing the less dense liquid upwards into a more dense liquid phase failed completely; all jets broke up before the end of the first wave. The results in fig. 14 indicate that the $\lambda - f$ relation for liquid/liquid systems is in general linear over the experimental range of flow rates, and even in the extreme case, water → ethyl ether, where there is slight departure from linearity at the higher flow rates, points have been obtained on the linear portion of the curve (compare fig. 5).

The slopes of the lines in fig. 14 thus yield tan θ directly. Assuming that the operative density factor in applying equation (1) to liquid/liquid systems is the density difference between the two liquids, then

$$\gamma = K_7(d_1 - d_2)/\tan^2\theta, \qquad (5)$$

where d_1 and d_2 are the densities of the jet liquid and liquid phase respectively, γ is the interfacial tension, and $\tan\theta = \lambda/f$. Data for the four systems at 20°, and values of K_7 obtained using equation (5), are given in Table VIII.

Fig. 14.

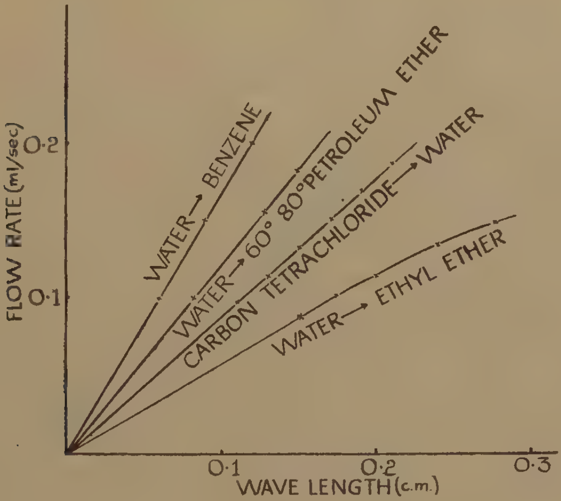

TABLE VIII.

System.	$d_1 - d_2$.	γ assumed dynes/cm.	tan θ.	K_7.
Carbon tetrachloride ⟶ water	0·602	45·0	1·15	98·8
Water ⟶ ethyl ether	0·284	10·4	1·62	96·1
Water ⟶ 60°–80° petroleum ether ..	0·327	50·2	0·81	100·7
Water ⟶ benzene	0·120	36·0	0·59	101·0

As the values given in the literature for the interfacial tension of water against ethyl ether vary, the value quoted in Table VIII. was determined by the drop weight method on the sample used. The life of the drop was 12 seconds. Since ethyl ether is slightly soluble in water, the value of the tension so obtained may be rather less than that operating in the jet, and may account for the lower value of K_7 in this case. However, the general constancy in K_7 indicates that equation (5) is probably applicable to all interfaces. Since tan θ is available from single measurements of λ and f, equation (5) can be used to show the variation in interfacial tension during adsorption to the interface, and experiments on these lines are now being conducted for comparison with rates of adsorption to surfaces.

Acknowledgment.

The author's thanks are due to Dr. G. O. Stephens, F.Inst.P., who kindly undertook the difficult task of photographing the jets.

References.

(1) Hiss, Diss. Heidelberg, 1913.
(2) Schmidt and Steyer, *Ann. d. Phys.* lxxvi. p. 442 (1926).
(3) Buchwald and König, *Ann. d. Phys.* xxvi. p. 659 (1936).
(4) Milner, Phil. Mag. (6) xiii. p. 102 (1907).
(5) Dupre, 'Théorie Méchanique de la Chaleur,' Paris, 1869.
(6) Rayleigh, Proc. Roy. Soc. xlvii. p. 281 (1890).
(7) Satterly and Strachan, Trans. Roy. Soc. Canada, xxix. p. 105 (1935).
(8) Satterly and McPherson, Trans. Roy. Soc. Canada, xxviii. p. 177 (1934).
(9) Satterly and Levitt, Trans. Roy. Soc. Canada, xxx. p. 129 (1936).
(10) Leniham, Phil. Mag. xxxii. p. 393 (1941).
(11) Bond, Proc. Phys. Soc. xlvii. p. 549 (1935).
(12) Puls, Phil. Mag. (7) xxii. p. 970 (1936).
(13) Bonds and Puls, Phil. Mag. xxiv. p. 864 (1937).
(14) Worthington, Proc. Roy. Soc. xxiii. p. 347 (1881).
(15) Worthington, Proc. Roy. Soc. xxiv. p. 217 (1882).
(16) Bidone, 'Expériences sur la Forme et sur la Direction des Veines et des Courans c'Eau lancés par diverses Ouvertures,' 1854.
(17) Magnus, Pogg. *Ann.* p. 95 (1855).
(18) Buff, Pogg. *Ann.* Bd. C. 1857.
(19) Rayleigh, Proc. Roy. Soc. xxix. p. 71 (1879).
(20) Piccard, Arch. Sci. Phys. Nat. xxvi. p. 561 (1890).
(21) Meyer, *Wied. Ann.* lxvi. p. 523 (1898).
(22) Pederson, Phil. Trans. (A) ccvii. p. 341 (1907).
(23) Bohr, Phil. Trans. (A) ccix. p. 281 (1909).
(24) Stocker, *Z. Phys. Chem.* xciv. p. 149 (1920).
(25) Addison, J. Chem. Soc. p. 252 (1944).
(26) Addison, J. Chem. Soc. p. 535 (1943).
(27) Addison, J. Chem. Soc. p. 477 (1944), p. 98 (1945).
(28) Willard Gibbs, 'Collected Papers,' i. p. 233 (1913).
(29) Langmuir, J. Amer. Chem. Soc. xxxix. p. 1848 (1917).

Harris Institute Technical College,
Preston.

VIII. *Spin in the Universe.*

By Sir Edmund Whittaker, F.R.S.*

(*Address of the President at the Annual Statutory Meeting of the Royal Society of Edinburgh, October* 23, 1944.)

[Received April 3, 1945.]

The session which is now beginning will complete a hundred years from the first discovery of a spiral nebula, an event from which can be dated all modern researches on the structure of the cosmos.

The discovery was made by a great Anglo-Irish nobleman, William, third Earl of Rosse (1800–1867), at the private observatory adjoining his mansion of Birr Castle. Like many other discoveries in astronomy, it was made possible by improvements in technical equipment. Lord Rosse, who for many years had devoted himself to increasing the power of reflecting telescopes, completed in 1844 the construction of one of 6 feet aperture and 54 feet focal length, by far the largest instrument then known; and with it, in the spring of 1845, he examined a nebula in the constellation of the Hounds, *Canes Venatici*, numbered 51 in Messier's catalogue.

This object had been examined previously by several astronomers, especially by Sir John Herschel, who had noticed a division in the nebulosity, which he compared to the bifurcation of the Milky Way. With the vastly greater resolving power now available, Lord Rosse saw to his intense astonishment that the nebula had the form of a spiral, of more than one convolution, and of remarkable regularity. The great telescope was at once applied to the study of other nebulæ: in the following spring an arrangement, also spiral but of a different character, was detected in Messier 99; and by 1850, fourteen spiral nebulæ had been found and described in a memoir read to the Royal Society, with the author's comment, "Much as the discovery of these strange forms may be calculated to excite our curiosity, and to awaken an intense desire to learn something of the laws which give order to their wonderful systems, as yet, I think, we have no fair ground even for plausible conjecture; and as observations have accumulated the subject has become, to my mind at least, more mysterious and more inapproachable."

The mystery is by no means completely solved even after a hundred years of unremitting labour; but there has been an enormous accession of knowledge, and there is now an extensive science of cosmology, based chiefly on investigations relating to the spiral nebulæ. On the occasion of the centenary, I propose to discourse this afternoon on one group of problems arising out of Lord Rosse's discovery. A spiral nebula obviously suggests a Catherine-wheel, which is a rotating system. Do spiral nebulæ rotate? And what is the cosmological significance of rotation and spin?

---

* Communicated by the Author.

Rotation is a universal phenomenon; the earth and all the other members of the solar system rotate on their axes, the satellites revolve round the planets, the planets revolve round the Sun, and the Sun himself is a member of the galaxy or Milky Way system which, as we shall see later, revolves in a very remarkable way. How did all these rotatory motions come into being? What secures their permanence or brings about their modification? And what part do they play in the system of the world?

One obvious fact is that a motion such as the earth's rotation on its axis can persist with little or no change for very long periods of time. This is an instance of what is called the *principle of conservation of spin* —that the spin, or angular momentum, of a body relative to its centre of mass remains permanently unaltered so long as there are no external forces whose resultant tends to rotate the body about the centre of mass. For example, the spin of the earth is not affected by the activities of man on its surface, or by the eruptions of volcanoes, or dislocations due to earthquakes, or by evaporation and the fall of rain. This principle of conservation might be thought to lead to the conclusion, that the spin in the universe is something whose total amount is invariable, and that nothing can happen to it except transference from one place or body to another, so that there is nothing to be discovered except the occasions and manner of these transferences. Such a conclusion, however, would be somewhat misleading, at any rate if we ignore the fact that spin can be communicated to visible bodies from that invisible storehouse of mystery which we call the æther. A simple experiment showing this is to take a circular vessel containing any liquid which conducts electricity, and to lead an electric current into it by an upright rod in the centre, the other electrode being formed by the circular wall of the vessel, so that the current flows through the liquid radially from the centre to the circumference. If now a vertical magnetic field is set up in any way, *e. g.* by sending the current through a coil surrounding the vessel, then every particle of liquid is acted on by a force transverse to the radius, and the liquid is set in rotation in the vessel—that is, the liquid acquires spin, or angular momentum, which was not previously possessed by any visible body *. What is essentially the same effect would be realized if electrons or ionized particles, shot out from an incandescent star, or repelled from it by light-pressure, had to pass through a magnetic field such as would exist if the star were a magnet like the earth; the particles would acquire a motion of revolution round the star.

---

* An equal and opposite amount of angular momentum is communicated by the æther to matter other than the liquid, so actually the total spin of visible bodies is conserved.

It is probable that electromagnetic actions more or less resembling this have played a considerable part in generating the spin which is now observable in the cosmos. Thus, in order to account for the angular momentum possessed by the planets of the solar system, H. Alfvén of Stockholm has put forward † the following theory. Suppose that a uniformly magnetized sphere, which is a conductor of electricity, rotates about its axis of magnetization with constant angular velocity: then in the surrounding space there is set up an electrostatic field, the equipotential surfaces being those obtained by rotating the lines of magnetic force about the axis of the sphere; and a charged particle moving in space would be acted on by both electric and magnetic forces. Alfvén applies this by taking the magnetized sphere to be the Sun, and considering the motion, under its influence, of a cloud of ionized matter which has fallen in towards the Sun from interstellar space, say to the distance of Jupiter. Electric currents will be set up, carried by charged particles moving spirally round the lines of magnetic force: a typical circuit would be from the part of the ion-cloud nearest the Sun to a point of the solar surface, thence to another point in the solar surface in a higher latitude, thence back to the farther side of the cloud, and lastly within the cloud from its farther to its nearer side. The mechanical forces due to these currents will tend to retard the Sun's rate of rotation, slowing it down more in high than in low latitudes; and thus an explanation is provided of the well-known fact that the Sun does not rotate as a whole, the rotation being slower near the pole than near the equator. The angular velocity lost by the Sun is transferred to the ion-cloud, which thus tends to assimilate its motion to the solar rotation; and when, later on, the cloud condenses to form a planet, the planet will have an orbital velocity and an axial rotation. Alfvén's theory would apply to the stars in general as well as to our Sun, and would therefore lead us to expect that a star would in most cases be accompanied by a family of planets: examples of this have actually been discovered during the last year or two.

Since spin can be acquired by material bodies under the action of electric and magnetic fields—or, as a physicist of the last generation would have put it, since spin or angular momentum can be transferred from æther to matter—it is natural to inquire whether anything is known about angular momentum existing invisibly in the æther. As a matter of fact, the concept occurs very frequently in the writings of the second half of the nineteenth century. In 1856 W. Thomson (Kelvin) formed the opinion (based on a study of the magnetic rotation of the plane of polarization of light) that magnetism possesses a rotatory character. This idea was taken up by Maxwell and embodied in the model which led him to the electromagnetic theory of light. The belief that the stresses in the æther are due in part to rotations can, however, be traced even farther back, to 1839, when MacCullagh devised a model of optical phenomena on this principle; and it appeared repeatedly in the last decade of the century, when Hicks, FitzGerald, and others represented electric and magnetic phenomena by the interactions of vortices in a liquid.

---

† *Arkiv för Mat., Astr., och Fys.*, 28 A, No. 6 (1942).

Since the discovery of the theory of relativity in the early years of the present century, the æther has been discarded except as the name of a supposed invisible transmitter of actions at a distance; and the æther theories have been replaced by the new science of atomic physics, in which the fundamental entities are elementary wave-particles or corporundals of certain kinds—electrons, protons, positrons, neutrons, and mesons. We must therefore inquire how the change has affected our conceptions of invisible spin. As a matter of fact, within the last nineteen years it has been found that each of the elementary particles possesses a certain definite quantity of spin, which is of great importance in determining the behaviour of the particle. The story of the discovery is one of the most remarkable chapters in the history of quantum mechanics.

To tell it, we recall that an atom of a chemical element may exist in its normal or fundamental state and also in various excited states or *levels*, and these levels are indicated by numbers. Now, when objects are described by numbers, it sometimes happens that more than one number is used to describe each object: thus a particular telephone may be described as No. 56132, Extension 36; or the home of a friend in an American city might be described as No. 231, 59th Street, 16th Floor, Flat 7. The numbers 56132 and 36 in the case of the telephone, or the set of numbers 231, 59, 16, 7 in the case of the flat, are what in atomic physics would be called *quantum numbers*. The state or level of an atom at any instant, then, is described by a set of quantum numbers.

There is, of course, no logical necessity to use four numbers in order to specify the flat; the municipal authorities might, if they pleased, number all the flats in the city in a single serial order, leaving out all mention of streets, house-numbers, and floors, so the flat might be simply No. 11,672. But the four numbers correspond to real features of the location, and are helpful to the stranger trying to find it. Similarly in quantum mechanics, it would be possible to number all the levels of an atom in a single serial order; but their physical behaviour shows that they fall naturally into groups and sub-groups, and a level is therefore best described by a set of several quantum numbers. Twenty years ago only two were used (for each electron): for definiteness we can picture the atom as consisting of an electron circulating in an orbit round a nucleus, and we can think of one of the numbers as corresponding to the energy of the system, and the other as corresponding to the spin, or angular momentum, of the orbital motion.

What happened in 1925 was the discovery that a third quantum number was needed in order to describe an electronic level. It was as if the houses in a street, which had hitherto been supposed to accommodate one family apiece, had been found to be divided into flats, so that in order to have an address precisely, it would be necessary to know not only the number of the street and the number of the house in the street, but also the number of the flat within the house. The question was at once asked, to what physical character in the atom does this new third quantum number correspond ? Spectroscopic evidence showed that it must be of the same nature as the second quantum number ; and reasons were found for believing that while the second number represented the angular momentum or spin of the orbital motion of the electron, the third number corresponded to the total spin of the whole atom. The further question had then to be settled, what was the character of the additional spin, which when compounded with the orbital spin, yielded the total spin ? There were two possibilities—it might be a spin of the nucleus, or it might be a spin of the circulating electron. The former alternative was soon shown to be impossible ; and so the final conclusion was that *the electron has a spin*—that is, an intrinsic mechanical angular momentum.

The next problem to be solved was to determine the amount of this electron-spin, which must evidently be a universal constant of Nature. The obvious suggestion was to inquire if it was connected with the only physical constant then known which had the dimensions of spin, namely the " constant of Action " as it was called, which had been introduced by Planck in 1900 in his theory of radiation, and which entered into all the formulæ of quantum-theory. The solution of this question was found by a study of the Zeeman effect (that is, the separation of single spectral lines into multiple sets of lines when the emitting atoms are subjected to a strong magnetic field) and the gyromagnetic effect (that is, the twist observed in a bar of iron which is suddenly magnetised). The final conclusion was that if Planck's constant of Action, divided by 2π, is denoted by $\hbar$, then the angular momentum or spin of the electron is $\frac{1}{2}\hbar$, and the electron has also, associated with the spin, a certain fixed magnetic moment—that is, it behaves like a small bar-magnet. With these assumptions, the extremely intricate results which had been found by workers on the Zeeman effect could now be explained completely.

Although the values just given for the spin and magnetic moment are now unquestioned, it is a curious fact that they cannot be verified by direct observation ; thus the magnetic moment cannot be measured by a magnetometer experiment ; for, as Bohr pointed out, the uncertainty principle of quantum mechanics imposes an uncertainty on the position and velocity of the electron, and this in turn gives rise to an uncertainty in the magnetic field due to the motion of the electron ; and this latter uncertainty is greater than the magnetic field due to the spin magnetic moment, which therefore cannot be measured.

This fact reminds us that the phenomenon of electron-spin belongs to quantum-theory. and hence may be expected to have peculiarities which are not met with in classical dynamics. When the spin was first discovered, the electron was pictured in the classical way as being like a spinning-top, or like the earth revolving on her axis. But the spin of a top, or of the earth, behaves like a vector—that is to say, its component in any direction is obtained by projecting the total spin on this direction. Electron-spin, on the other hand, behaves quite differently; it is a quantum-mechanical entity, and if an inquiry is made as to its component in any direction, say the axis of z, then the only statement that can be made is that there is a certain probability that the axis of spin will be parallel to the z-axis, and the spin-component of amount $\frac{1}{2}\hbar$, and also a certain probability that the axis of spin will be antiparallel to the z-axis—that is to say, in the opposite direction, the spin component being now $-\frac{1}{2}\hbar$. Thus in general it is not possible to attach any meaning to the phrase "direction of the axis of spin" of an electron which is in a given stationary state.

Since the discovery of electron-spin it has been found that each of the other elementary particles possesses a definite amount of spin. The proton, the neutron, and the positron, each have the same spin as the electron, namely $\frac{1}{2}\hbar$; the photon, or light-corpuscle, has the spin $\hbar$; the spin of the meson may have either of the two values 0 or h.

The spin of the elementary particles is a concept of fundamental importance in the order of Nature, as can be seen, for instance, by reference to the part it plays in chemical combination. Let us take as a very simple example the combination of two hydrogen atoms to form a hydrogen molecule. Each hydrogen atom consists of one proton and one electron, and when the two atoms are bound together as a molecule, the electrons are no longer attached each to its own proton, but both of them are, so to speak, shared between the two protons; and it can be shown that in this state *the two electrons must have antiparallel spins.* But this is not all. Each of the protons also has a spin, and consideration of the various possibilities with regard to the proton-spins led the mathematical physicists in 1927 to predict the existence of two different kinds of hydrogen molecule, and consequently two kinds of ordinary hydrogen gas, to which the names *para-hydrogen* and *ortho-hydrogen* were given. These have different physical properties (as regards specific heat, boiling-point, etc.) but are identical in their chemical properties, which explains why the chemists had never distinguished them.

The spin has a decisive influence on what is called the *statistical* behaviour of the elementary particles—that is, their behaviour when a crowd of them is present. A simple illustration of statistical behaviour is afforded by considering an ordinary gas, say nitrogen; the gas actually consists of billions of nitrogen molecules rushing hither and thither and frequently colliding with each other. Any particular molecule at any particular instant will have a definite velocity, and therefore will possess a definite amount of energy; not all particles will have the same energy—some will have very little, and some a great deal; and a graph, in which quantity of energy is plotted against the number of particles which possess that amount of energy, is said to describe the statistical behaviour of the molecules, so far as energy is concerned. The statistical behaviour of the molecules of an ideal gas was discovered by Clerk Maxwell, and is known as *Maxwellian statistics.*

Now turn to another field in physics—the conduction of an electric current through a metal. The reason why a metal is able to conduct electricity is that it contains in its pores, so to speak, an enormous number of electrons; if we fix our attention on these "conducting electrons" and ignore the rest of the metal, we can regard them as a kind of gas—an electron gas, as it is called. The electrons in this electron gas will, like the molecules in the nitrogen gas, possess energies distributed according to a certain statistical law; but it is not the Maxwellian distribution; it follows an altogether different law, known from its discoverer as *Fermi statistics.*

Altogether there are three kinds of statistics that are commonly found in assemblages of particles: the Maxwellian statistics, the Fermi statistics, and a third kind called *Bose* statistics *. The differences between them may be explained roughly in this way. Suppose an empty railway train is standing at a platform and passengers are getting into it. If we make the assumption that every passenger chooses his compartment blindfold, so to speak, without noticing whether other passengers are getting into it or not, then it would be possible to calculate the probability of any particular allocation of the passengers among the compartments. This set of probabilities would constitute a statistics, and we may compare it to the Maxwellian statistics. If, however, we make the assumption that passengers like to have compartments to themselves, or at any rate like to have corner seats, then the probabilities of the different distributions of passengers among compartments would be altered; the probability would be raised for those distributions in which every compartment has at least one occupant and no compartment is crowded. This set of probabilities may be compared to the Fermi statistics. If, lastly, we make the contrary assumption that the passengers are very friendly and gregarious people, who don't like to be alone and who choose by preference compartments into which a lot of other people are going, then the probabilities of the different distributions would again be modified, this time in favour of those distributions in which some compartments are crowded and others quite empty. This set of probabilities may be regarded as analogous to the Bose statistics. The Maxwellian statistics is a kind of limiting case, between the Fermi statistics and the Bose statistics, just as the parabola is the limiting case between the ellipse and the hyperbola; Fermi statistics and Bose statistics deviate from Maxwellian statistics in opposite directions, and tend to Maxwellian statistics in the limit when the temperature increases indefinitely.

We are now in a position to enunciate the surprising law which connects statistics with spin. It is very straightforward—just this, that all particles (elementary or composite) whose spin is an odd multiple of $\frac{1}{2}\hbar$ (that is, $\frac{1}{2}\hbar$, $\frac{3}{2}\hbar$, $\frac{5}{2}\hbar$, and so on) obey the statistics of Fermi ; while all particles whose spin is an even multiple of $\frac{1}{2}\hbar$ (that is, 0, $\hbar$, $2\hbar$, $3\hbar$, and so on) obey the statistics of Bose. Simple though this statement is, its proof is by no means easy, and it leaves one with the feeling that we have not as yet reached the true foundations on which ultimate physics should be grounded. The theorem, however, provides an explanation of many facts which perplexed the last generation of physicists. Since light, when regarded in its corpuscular aspect, has the spin $\hbar$, it must obey Bose statistics, and this accounts for the discovery, made early in the century, that black-body radiation obeys Planck's law rather than the law which had been deduced from classical theory. Also, since electrons have the spin $\frac{1}{2}\hbar$, they obey Fermi statistics, and this explains why the specific heat of the electrons in metals is exceedingly small, and why the paramagnetism of the alkali metals is feeble and nearly independent of the temperature. Fermi statistics also explains why the "white dwarf" stars have such extraordinarily high densities. All these things depend in the last resort on spin.

---

* The contributions of other workers are generally recognized by the composite titles *Maxwell-Boltzmann*, *Fermi-Dirac*, and *Bose-Einstein.*

Let us now examine the concept of spin somewhat more closely. The spin of elementary particles is essentially a quantum-mechanical phenomenon, and can therefore be understood only in connection with the quantum-mechanical concept of a particle, which differs fundamentally from the classical concept. It cannot be pictured as being at any instant located at a definite point and moving with a definite velocity ; indeed, many of its properties resemble rather those of a wave. We can arrive at it by starting with the classical particle, and "quantizing" it, thereby introducing the wave character ; or we can start from the other end with a classical wave, and by a different kind of quantization we can introduce the particle-character. Now when we regard it as a particle it has certain attributes—mass, velocity, energy, momentum ; and when we regard it as a wave it has a different set of attributes—wave-length, frequency, amplitude, and direction of propagation. What correspondences exist between the particle attributes and the wave attributes ? The question is of importance in our present investigation because we have found that the electron, when regarded as a particle, has yet another attribute, namely spin, which we picture as being like the rotation of a spinning-top ; and we want to know what corresponds to spin when the electron is regarded as a wave.

So far as concerns energy, momentum, and velocity, the correlation between the particle and wave properties of the elementary particles has long been known ; the energy of the particle is proportional to the frequency of the wave, the momentum of the particle is inversely proportional to the wave-length of the wave, and the velocity of the particle is equal to the group-velocity of the waves.

What feature of the waves is to be interpreted as spin ? In the earlier attempts to answer this question it was thought that a spinning wave might be obtained by applying a process of quantization to a spinning particle; but this method of attack failed. The true solution was discovered in 1927 by Sir Charles Darwin, who at that time occupied the Chair of Mathematical Physics in Edinburgh University. He went back to the original reason for introducing spin, namely that a knowledge of the energy and the orbital angular momentum of the active electron in an atom is insufficient to specify the state completely; there exist two different states for which the energy and orbital angular momentum have the given values, and these two states are accounted for by assuming that the electron has a spin of its own, which has opposite directions in these two states. Hence when we regard the electron in its wave-aspect, the assertion that it possesses spin must be equivalent to the assertion that there are two distinct waves which possess the same value of the energy and the same value of the momentum. But this at once suggests an analogy with the polarization of light; for we can have two distinct light-quanta which have the same energy (*i. e.* frequency) and the same momentum (which implies the same wave-length and the same direction of propagation), but which differ in respect of their polarization. Darwin thus concluded that the wave-aspect of spin was simply the capacity to exist in different states (analogous to differently polarized waves of light) possessing the same energy and momentum; and this principle is the basis of the modern wave theory of spin. If, when the energy and momentum are prescribed, there are $(2s+1)$ independent plane-wave states, then the spin is $s\hbar$; a rule which may be stated in the form, that in the wave-picture each independent state of plane-polarization, after the first, makes a contribution $\frac{1}{2}\hbar$ to the spin *.

As we have seen, the spin of every electron is invariable, but its component in any direction can have either of the two values $\frac{1}{2}\hbar$ and $-\frac{1}{2}\hbar$; the component in any direction of the resultant spin of an aggregate of electrons can therefore take many different values. The gyromagnetic effect shows that changes in this resultant, due to changes in the orientation of the axes of spin of the electrons, are capable of generating changes in the angular momentum of an ordinary molar body; and thus it is possible that the spin of the elementary particles may be concerned in rotatory phenomena even of the cosmic order.

Another aspect of spin was revealed in the following year, 1928, when Dr. Dirac of Cambridge succeeded in finding the wave equation of the electron in a form which was completely relativistic—that is to say, which was invariant under all the transformations that are associated with the Principle of Relativity. In the process of deriving his equation Dirac took no account of spin; his sole aim was to secure that the equation should be relativistically invariant. But when this was achieved, the surprising fact emerged, that the equation necessitated the spin effect—that is to say, the existence of electron-spin followed automatically from the condition that the equations of the electron must satisfy the Principle of Relativity. Spin is thus seen to be a consequence of the symmetry of the cosmos with respect to space and time. This discovery placed the concept of spin in an entirely new light; it had originated in atomic physics—the study of small-scale happenings—but it was now lifted into a new context, that of relativity theory, whose greatest triumphs had been won in the domain of astronomy and cosmology, the study of the universe in the large.

---

* For simplicity, the non-relativistic case is here considered. Moreover, the rule admits of an exception when the particle which corresponds to the wave has zero mass: in this case only two independent plane-wave states exist.

Some questions connected with spin had indeed engaged the attention of relativists for many years, especially that relating to the remarkable difference which exists, as regards relativity, between motions of rotation and motions of translation. According to the Principle of Relativity, a uniform motion of translation possessed by any system cannot be detected by observations of any phenomena—mechanical, optical, electrical, or gravitational—which take place wholly within the system. Hence if there were only one body in the universe, we could not speak of its velocity—the word would have no meaning; we can speak only of the velocity of one body *relative to another body*. If we consider two frameworks of reference, one of which is moving with a uniform velocity of translation relative to the other, then all the laws of Nature have the same form with respect to the two frameworks. But the case is quite different with regard to rotations: a motion of rotation possessed by a system can be detected by observations taking place wholly within the system. Thus if water contained in a pail is made to rotate rapidly, the surface of the water is not plane, but is depressed at its centre and elevated round the rim where it is in contact with the pail; this is an objective fact which could, in principle, be perceived even by an observer who was in the water and was being carried round by it. An interesting optical experiment carried out in 1925 by Michelson and Gale shows that the angular velocity of rotation of the earth on her axis can be determined by observations made, if desired, entirely underground. A pipe, over a mile long, was laid in the form of a rectangle and exhausted of air. Light from a carbon arc was divided at one corner by a half-silvered mirror into transmitted and reflected beams, which travelled in opposite senses—one clockwise and the other counter-clockwise—round the rectangle, being reflected by mirrors at the corners. On account of the earth's rotation, the optical lengths of the two paths were not equal, so on completing their circuits the interference fringes produced by the two beams showed displacements, by measurement of which it was possible to deduce the angular velocity of the earth *.

Thus it is allowable to speak of velocities of rotation in an absolute manner, without the necessity of specifying any framework with respect to which the angular displacement takes place. The statement that some particular body is at rest as regards rotation is a statement that has a meaning, although the statement that a particular body is at rest as regards translation is, taken by itself, meaningless.

---

* Actually the experiment was made in order to verify relativity theory.

The further question may, however, be asked, whether these propositions would still be true if the body were the only body in the world—in other words, is the absolute character of a body's rotation an inseparable concomitant of its mere existence, or does it depend on the co-existence of other bodies in the universe? We cannot settle the matter by an observational test, since we cannot remove all other bodies from the universe in order to perform the experiment; if an answer to the question is to be given at all, it must be provided by some general cosmical theory.

The application of relativity theory to problems of spin has, however, led to discordances which are not yet entirely resolved. An example of this is furnished by the problem of the revolving disk. As long ago as 1909 Ehrenfest drew attention to a paradox connected with the motion of a circular disk which is rotating with constant speed about an axis through its centre perpendicular to its plane. A point on the circumference will move in the direction of the tangent to the circle at the point, and we can therefore regard a small element of the periphery as a short rod which is instantaneously moving in the direction of its own length. Now a fundamental result of relativity theory is that the linear dimensions of bodies which are in motion (with respect to an observer at rest) are contracted in the direction of their motion (this is FitzGerald's celebrated theorem); and therefore every element of the periphery (as measured by the stationary observer) is shortened by the rotation. On the other hand, if we consider an element of a radius of the disk, its instantaneous motion is perpendicular to its own direction, and therefore its length does not suffer any contraction. Hence, argued Ehrenfest, since the circumference of the disk is shortened while the radius is unaffected, the ratio of the circumference to the diameter must be altered from the value π which it has when the disk is at rest—in other words, the geometry of the disk is no longer Euclidean.

The reasoning is somewhat crude; and a fuller investigation was made later by Lorentz, who concluded that the geometry does remain Euclidean, although the disk as a whole is contracted, the linear contraction in any direction being one-quarter of that which Ehrenfest had found for the circumference. A remarkable consequence is that if two equal disks are mounted on the same axis, and one is made to rotate while the other is at rest, then, to a stationary observer, the rotating disk will be smaller than the other. Eddington concurred with Lorentz's result, but other investigators, including Einstein, dispute it and claim to have proved the necessity for non-Euclidean geometry on the disk.

There are many other difficult problems in the relativity theory of spin, such as the behaviour of a clock which is at rest on a rotating disk, or the very fundamental question of how we can formulate geometrically the condition that two different bodies should have equal rotatory motions. In Euclidean space the answer to the last inquiry is simple : let a straight line be taken, fixed in the first body and moving with it ; and let a straight line also be taken, fixed in the second body, and such that at some instant it is parallel to the first straight line. Then if throughout the motion the two straight lines remain constantly parallel to each other, and if this is true whatever was the original choice of the first straight line, we can say that the two bodies have equal rotatory motions.

The condition thus formulated depends on the notion of parallelism, which in Euclidean space is a simple and familiar notion. If, however, the universe is not Euclidean, but is a closed space with curvature, it becomes difficult to define the parallelism of directions at two points which are at a considerable distance from each other, and consequently when we try to define the equality of rotatory motions at distant points we get into deep waters. And we have further to inquire whether the geometrical condition which we finally obtain is dependent on, or modified by, the existence of matter elsewhere in the universe. Thus we see that the study of rotation is essentially a cosmical problem ; our attempt to solve the mystery of spin brings us back to our starting-point, the spiral nebulæ. Let us now return to the consideration of their status and rotation.

The importance of the spiral nebulæ in the system of the world was first fully recognized in 1919, when the distances of many of them were approximately determined. It was found that even the nearest of them are millions of light-years away, and that they are therefore outside the system of the Milky Way or galaxy, to which our own sun belongs : each of these vast and immensely remote systems is of the same order of size as the whole galaxy.

In recent years much work has been done on the rotations of the galaxies, and especially of our own galactic system. Since the first investigations of Lindblad and Oort there has been no doubt that the whole aggregate of celestial objects associated with the Milky Way has a general motion of rotation. The system does not, however, rotate as if rigidly connected, with the same period of revolution for all its members ; on the contrary, their behaviour is more like that of the planets in the solar system, each having a period appropriate to its distance from the centre of the galaxy. Quantitative determinations are still somewhat uncertain, but the period of galactic revolution for stars in the neighbourhood of the Sun is about 200,000,000 years. Our galaxy is roughly of the same size as the average of the extra-galactic nebulæ, its diameter being about 100,000 light-years. It may perhaps be classified as a rather over-ripe spiral—that is, a spiral in which the process of condensation of nebulosity into stars is very far advanced. The suggestion has been made that it no longer possesses a large bright unresolved nucleus such as is found in early-type spirals ; but this is only conjecture, since the central parts of our galaxy, which are in the direction of the constellation Sagittarius, are probably hidden from us by obscuring clouds. The Sun is situated in the outer galactic regions, at a distance of about 30,000 light-years from the centre; in this neighbourhood the rotational velocity decreases with increasing central distance.

Knowledge concerning rotation is naturally more fragmentary as regards the extra-galactic nebulæ; but it seems probable that their inner regions rotate as if rigidly connected, the linear velocity increasing with the distance, while the outer parts behave like a planetary system, the linear velocity decreasing with increasing distance. In spirals, the sense of rotation is such that the arms trail behind the central regions. There is a suspicion that the period of rotation of the inner regions increases as the process of condensation of nebulosity into stars progresses.

An interesting explanation of the rotation of the extra-galactic nebulæ, and of the possession of spin by most large objects and groups of objects in the universe, has been proposed by Professor E. A. Milne, who has deduced from the theory of kinematical relativity that the angular momentum of any cosmical system increases proportionally to the time *; a spin which was initially small will therefore grow continually greater, and the existence of large accumulations of angular momentum is no longer a matter for surprise. It cannot be said, however, that any of the mathematical-physical theories that have been put forward to explain spin in the universe has as yet won complete and universal acceptance: but progress has been so rapid in recent years that it is reasonable to hope for a not long-delayed solution of this fundamental problem of cosmology.

IX. *Kinematic Relativity.*

By R. A. Newing †.

[Received November 30, 1944.]

In a recent paper (Phil. Mag. xxxv. p. 241 (1944)), Professor W. Wilson has given an account of a difficulty he has encountered in considering Milne's theory of Kinematical Relativity. He gives three independent discussions of Milne's equation for the motion of a free particle, and, in each case, is led to the conclusion that Milne's equation requires that $\mathbf{P}=\mathbf{V}t$, and therefore that the free particle must have zero acceleration This difficulty may be resolved if it is realized that the term $\mathbf{V}t$ occurring in Milne's equation is not the space part of a 4-vector.

---

* That is, to what Milne calls *kinematic time*, which is time as measured by atomic vibrations and radioactive clocks.

† Communicated by the Author.

Let the position and velocity of the particle be $\mathbf{P}$ and $\mathbf{V}$ as observed by an observer O at time t; and $\mathbf{P}^*$ and $\mathbf{V}^*$ as observed by an equivalent observer O* at the corresponding time t^*.

Then
$$t^* = \left(t - \frac{\mathbf{P}.\mathbf{u}}{c^2}\right)\left(1 - \frac{u^2}{c^2}\right)^{-\frac{1}{2}},$$

where $\mathbf{u}$ is the velocity of O* relative to O.

Also, if $\mathbf{V}_\perp$ is the component of $\mathbf{V}$ perpendicular to $\mathbf{u}$,

$$\mathbf{V}^*_\perp = \mathbf{V}_\perp\left(1 - \frac{u^2}{c^2}\right)^{\frac{1}{2}}\left(1 - \frac{\mathbf{V}.\mathbf{u}}{c^2}\right)^{-1}.$$

Thus
$$\mathbf{V}^*_\perp t^* = \mathbf{V}_\perp t\left(1 - \frac{\mathbf{P}.\mathbf{u}}{tc^2}\right)\left(1 - \frac{\mathbf{V}.\mathbf{u}}{c^2}\right)^{-1}.$$

Now $\mathbf{V}t$ can only be the space part of a 4-vector if $\mathbf{V}^*_\perp t^* = \mathbf{V}_\perp t$. This requires that $(\mathbf{P} - \mathbf{V}t).\mathbf{u} = 0$, for any $\mathbf{u}$ not parallel to $\mathbf{V}$, and therefore that $\mathbf{P} = \mathbf{V}t$. This condition also follows when $\mathbf{u}$ and $\mathbf{V}$ are parallel, as may be seen by considering the transformation law for the resolute of $\mathbf{V}t$ parallel to $\mathbf{u}$. We are thus led to the theorem "$\mathbf{V}t$ does not transform like the space part of a 4-vector unless $\mathbf{P} = \mathbf{V}t$." This result is quite independent of Milne's equation for the motion of a free particle.

Wilson first discusses Milne's equation in the form

$$\frac{1}{\mathrm{Y}}\frac{d\mathbf{V}}{dt} = -\frac{1}{\mathrm{X}}(\mathbf{P} - \mathbf{V}t),$$

where
$$\mathrm{X} = t^2 - \mathrm{P}^2/c^2, \quad \mathrm{Y} = 1 - \mathrm{V}^2/c^2.$$

He starts off with the assumption that $\mathbf{P} - \mathbf{V}t$ is the space part of a 4-vector. This implies that $\mathbf{V}t$ is itself the space part of a 4-vector, but it follows from our theorem that this is equivalent to assuming that $\mathbf{P} = \mathbf{V}t$. Wilson's first discussion is therefore invalid because, in effect, he assumes the result he seeks to establish. It should also be noted that the identities used by Wilson are not true identities. His identity (2)

$$\frac{1}{\mathrm{Y}^2}\frac{d\mathbf{V}}{dt} = \frac{1}{\mathrm{Y}^{\frac{1}{2}}}\frac{d}{dt}\left(\frac{\mathbf{V}}{\mathrm{Y}^{\frac{1}{2}}}\right)$$

is valid only if $\mathbf{V}$ is parallel to $d\mathbf{V}/dt$; there is therefore no need for the left-hand side of this equation to be covariant. In the same way, his identity (6) is valid only if the vectors $\mathbf{P}$ and $\mathbf{Q}$ are parallel. In this same discussion, Wilson makes use of the equation

$$\mathbf{P} - \frac{\mathbf{V}}{\mathrm{Y}}\left(t - \frac{\mathbf{P}.\mathbf{V}}{c^2}\right) = \frac{1}{\mathrm{Y}}(\mathbf{P} - \mathbf{V}t),$$

but this equation is valid only if $\mathbf{V}$ is parallel to $\mathbf{P}$.

Wilson's remaining lines of argument are also based upon the claim that $\mathbf{V}t$ is the space part of a 4-vector, but in these discussions he justifies this claim by saying that $\mathbf{V}t$ is the space part of a 4-vector because "it is the displacement of a particle moving with a velocity $\mathbf{V}$ in the system of reference of some observer O, during the time t, as reckoned by O."

His discussion, however, is invalid, because $\mathbf{V}t$, so defined, cannot be identified with the $\mathbf{V}t$ occurring in Milne's equation. This may be seen as follows. Consider a *fundamental* particle moving through the point P_0 with velocity $\mathbf{V}_0$ at time t_0 as observed by O. Let the *free* particle move through the point P_1 with velocity $\mathbf{V}_1$ at time t_1, and suppose that, at the instant $t_0=t_1=t$, $\mathbf{V}_0=\mathbf{V}_1=\mathbf{V}$. In our present notation, Milne's equation is

$$\frac{1}{Y_1}\frac{d}{dt_1}\mathbf{V}_1=-\frac{1}{X_1}(\mathbf{P}_1-\mathbf{V}_1t_1).$$

The quantity $\mathbf{V}t$ occurring in this equation is $(\mathbf{V}_1t_1)_{t_1=t}$. The quantity defined by Wilson is $(\mathbf{V}_0t_0)_{t_0=t}$, and is certainly the space part of a 4-vector, since $\mathbf{P}_0=\mathbf{V}_0t_0$. These two quantities are both equal to $\mathbf{V}t$ at the instant considered, but this does not mean that they must transform in the same way. For an observer O*, $(\mathbf{V}_0^*)_{t_0=t}=(\mathbf{V}_1^*)_{t_1=t}=\mathbf{V}^*$, but $t_0^*\neq t_1^*$ when $t_0=t_1=t$.

The quantity $(\mathbf{V}_1^*t_1^*)_{t_1=t}$ is the displacement of the fundamental particle as observed by O* at the instant t_1^*, where

$$t_1^*=\left(t-\frac{\mathbf{P}_1\cdot\mathbf{u}}{c^2}\right)\left(1-\frac{u^2}{c^2}\right)^{-\frac{1}{2}};$$

while $(\mathbf{V}_0^*t_0^*)_{t_0=t}$ is the displacement of the fundamental particle as observed by O* at the instant t_0^*, where

$$t_*=\left(t-\frac{\mathbf{P}_0\cdot\mathbf{u}}{c^2}\right)\left(1-\frac{u^2}{c^2}\right)^{-\frac{1}{2}}.$$

These two quantities are not the same for all observers O* unless P_0 and P_1 are coincident. It is therefore not permissible to identify $(\mathbf{V}_0t_0)_{t_0=t}$ with $(\mathbf{V}_1t_1)_{t_1=t}$. No difficulty arises if this identification is not made. We then have the satisfactory result that for O, the acceleration of the free particle at time t is towards the instantaneous position of the fundamental particle P_0, while for O*, the acceleration of the free particle, at the corresponding time t_1^*, is towards the instantaneous position of the fundamental particle as observed by O* himself.

X. *On the Pseudo-Plastic State.*

By Walther Deutsch, F.Inst.P. *†.

[Received June 12, 1944.]

Viscous liquids and solids are commonly divided into substances which follow the law of Newton ("Newtonian liquids," substances with "pure viscosity," "pure plastics" etc.) and those substances which do not follow it (" non-Newtonian-liquids," " pseudo-plastics," substances with " abnormal viscosity ").

---

* Communicated by the Author.

† Dr. Rosin Industrial Research Company, Ltd.

The purpose of the following analysis is to give a simple explanation of the mechanical behaviour of a substance in the pseudo-plastic state, making use of the well-founded view of Maxwell's law of relaxation in connection, of course, with the geometry of the pure elastic state in the body.

The experiment on which most of the phenomena in question are apparent, consists of shearing a layer of material between two parallel plates with different uniform velocities, and of measuring the resistance at each velocity. With uniform velocity most of the substances show a stationary state and the concept of " relaxation " in this state meets with difficulties. It now has to be asked whether this commonly assumed continuous flow of the substance is a real fact or whether this stationary flow proceeds by a succession of steps, too small to be discovered. Indeed, in another sphere of frictional problems—the sliding friction between two solid, dry and highly clean and smooth surfaces—the discovery was made that this motion under certain circumstances does *not* proceed smoothly but by jerks [*].

Our assumption concerns steps of an infinitesimal order only, two steps forming an iteration-element. The first step of this element consists of an infinitesimal additive change of *elastic strength*, impressed instantaneously by a sudden increase $d\sigma$ of the shear deformation σ. The second step occurs in the time dt without change of $\sigma+d\sigma$. In this time *relaxation* takes place up to a point where the original elastic strength and therefore the original state is reached again.

This idea of shearing by jerks in viscous substances is not a new one ; W. Kuhn [†] has already made use of it and has found a relation between the rigidity, the time of relaxation and the viscosity.

According to Maxwell's law of relaxation, we have, if τ is the shear stress, n the rigidity, η the true viscosity :

$$d\tau=-\tau\frac{n}{\eta}dt, \qquad (1)$$

and if g is the constant rate of shear and $\frac{d\sigma}{dt}$, the mean value in a finite time t, $dt=\frac{1}{g}d\sigma$, and therefore during the second step (relaxation).

$$d\tau=-\tau\frac{n}{g\eta}d\sigma. \qquad (2)$$

Here τ means the total elastic shear stress, according to the gradient g.

Now we have to resolve this elastic shear stress into the elastic stress inside the substance. This task was solved in principle as early as 1909 by Ludwik * who reduced the phenomenon of increase of strength of metals by extension to the orientation of the forces inside the metal (changing the angle α between shear direction and the direction of elongation) and to the summing up of the instantaneous "specific dilatations" to a finite total dilatation. In this way he found the so-called "diagram of flow" ("*Fliesskurve*"), a relation between the "inner friction" of the metal and the specific rate of shear †.

---

[*] Robert Schnurmann, 'Report on Progress in Physics,' Phys. Soc. vol. viii. p. 79 (1941).

[†] W. Kuhn, *Naturwiss. H.* vol. xl. p. 661 (Oct. 1938).

Since in an elastic body the tensile and the compressive forces (orthogonal principal stresses P_1 and P_2) are equal with opposite sign, the shear is

$$\tau = P_1 \sin 2\alpha, \qquad \qquad (3)$$

α being the angle between the tensile direction and the shear direction ("angle of action," "*Wirkungswinkel*" of Ludwik). Using for the increase $d\sigma$ of the elastic shear deformation σ the relation of Ludwik

$$d\sigma = 2\frac{d \lg a}{\sin 2\alpha}, \qquad \qquad (4)$$

where $\lg a = \int_1^a \frac{da}{a}$ the "total dilatation" in the direction of maximum elongation, and considering the tensile-force P_1 according to Hooke's law being

$$P_1 = \gamma \lg a,$$

we get, from (3) and (4),

$$\tau = \gamma \frac{d}{d\sigma} (\lg a)^2. \qquad \qquad (5)$$

In this formula the relation between the strain of shear (the mutual displacement of two planes unit distance apart) and the dilatation a ($a = 1 + \lambda$, where λ is the specific dilatation in the direction of maximum elongation relative to a state, in which the substance is without elastic energy) can easily be found by the rules of hydrodynamics (stationary flow between two planes). We obtain

$$\sin 2\alpha = \frac{1}{\sqrt{1+\sigma^2/4}}. \qquad \qquad (6)$$

Thus, according to (4):

$$2\int_{a=1}^{a} d \lg a = \int_{\sigma=0}^{\sigma} \frac{d\sigma}{\sqrt{1+\sigma^2/4}} = 2 \lg (\sigma/2 + \sqrt{1+\sigma^2/4}) = 2 \lg a,$$

---

* Ludwik, *Elemente d. technolog. Mechanik*, 1909, S. 18; see also, W. Deutsch, "*Plastizität*" *Handbuch d. phys. u. techn. Mechanik*, 4, 1931.

† K. Weissenberg has also systematically developed the relations between stress and finite strain and, in the framework of a general theory of the continua, applied them to the theory of the mechanical behaviour of a plasto-elastic substance.

K. Weissenberg, *Arch. des Sc. Phys. et Nat.* 5$^{\text{me}}$ Période, vol. xvii. p. 98 (1935).

and therefore $a=\sigma/2+\sqrt{1+\sigma^2/4}$, and from (5) and (4)

$$\tau=2\gamma\lg\left(\sigma/2+\sqrt{1+\sigma^2/4}\right)\frac{d\lg a}{d\sigma}=\gamma\frac{\lg\left(\sigma/2+\sqrt{1+\sigma^2/4}\right)}{\sqrt{1+\sigma^2/4}}\quad .\ .\ .\ (7)$$

Now, during the first step of the iteration element, the short elastic jerk $d\sigma$ generates an increase $d\tau$ of the elastic shear τ * :

$$d\tau=\frac{\gamma}{2}\frac{\sqrt{1+\sigma^2/4}-\sigma/2\lg\left(\sigma/2+\sqrt{1+\sigma^2/4}\right)}{(1+\sigma^2/4)^{3/2}}d\sigma.\quad .\ .\ .\ (8)$$

The connection between the constants γ and n can easily be determined in the neighbourhood of the original state (state without elastic energy). Thus,

$$\tau=\mathrm{P}_1=n\sigma=\lim_{\sigma\to 0}\gamma\lg a=\gamma\frac{\sigma}{2},$$

and therefore,

$$n=\gamma/2.\quad .\ .\ .\ .\ .\ .\ .\ (9)$$

Thus, comparing the elastic increase of τ during the first step (eq. 8) with the decrease caused by relaxation in the second step (eq. 2). we get in connection with (7) and (9) the following pair of equations, in which the abbreviations μ and q are used and wherein the value τ/g is denoted by η_a, this ratio being the measured value of viscosity, the "abnormal viscosity," and $\mu=\eta_a/\eta\leq 1$.

In the resulting equations

$$\left.\begin{aligned}\mu=\eta_a/\eta&=\frac{\sqrt{1+\sigma^2/4}-\sigma/2\lg\left(\sigma/2+\sqrt{1+\sigma^2/4}\right)}{(1+\sigma^2/4)^{3/2}},\\ q=\frac{\mu g\eta}{2n}&=\frac{\lg\left(\sigma/2+\sqrt{1+\sigma^2/4}\right)}{\sqrt{1+\sigma^2/4}},\end{aligned}\right\}\quad .\ .\ .\ (\mathrm{I})$$

σ can be considered as a parameter only. and therefore the abnormal viscosity η_a is expressed as a function of the gradient g.

The diagram (fig. 1) shows the result : according to the experiments with plasto-elastic substances the "apparent" viscosity η_a decreases with increasing rate of shear and shows an initial value, equal to the true viscosity η. The initial slope is greatest (point of inflexion) at about

$$g\eta/2n=0{\cdot}4.\quad .\ .\ .\ .\ .\ .\ .\ .\ .\ (10)$$

The agreement with experimental results is as good as can be expected from the data hitherto obtained for these substances, especially for the rigidity n.

In fig. 2 the values obtained with a Couette apparatus for a special liquid are plotted, a liquid for which the rigidity was found to be approximately 480 dynes/sq. cm. With this value and $\eta=300$ poise the 'calculated" curve has been drawn.

---

* Though in this infinitesimal time a variation of the angle a occurs, this variation is small and was neglected.

Up to the point $g\eta/2n \sim 7/100$ (fig. 1, curve (2)), the initial viscosity remains constant within a variation of 1 per cent. Say, a substance would have the true viscosity of 4 poise and the high rigidity of $n=5000$; then we would have to expect practically a normal viscosity up to the rate of shear.

$$g_0=\frac{0{\cdot}14n}{\eta}=\frac{0{\cdot}14.5000}{4}=175.$$

Fig. 1.

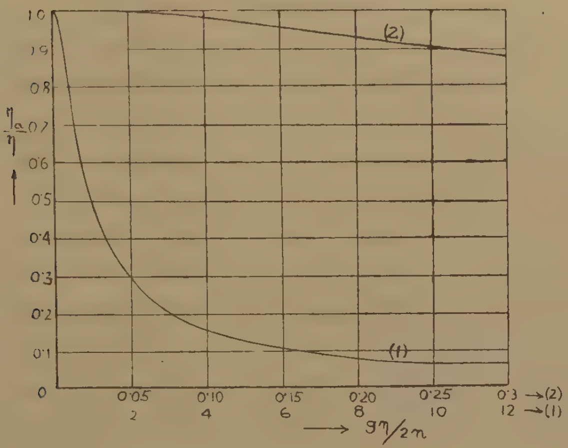

Fig. 2.

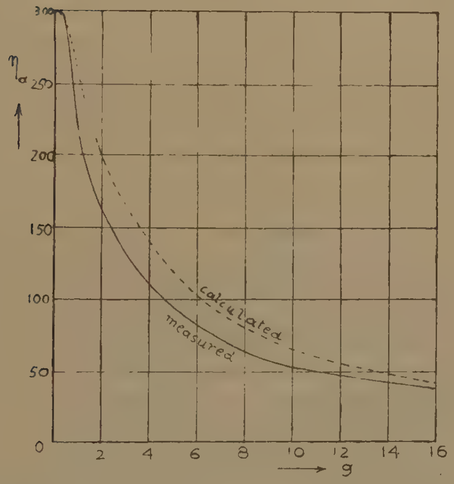

Since commonly measurement is not extended up to so high a value, we would call this substance a *Newtonian*. But, as results from eq. (10), a breakdown occurs in the neighbourhood of

$$g_1=\frac{0{\cdot}8n}{\eta}=1000.$$

Thus we come to the same conclusion as Miss R. Weltmann*, who recently found by experiment for a great number of oils (range of true viscosities from about 1 up to 790 poise), that a breakdown (limiting rate of shear) occurs in all cases, when the shearing force reaches a value of about 7000 dynes/sq. cm., the limiting rates of shear being not very sharply defined. Above the limiting rate of shear the curves obtained by Weltmann are very similar to the curves describing the plasto-elastic behaviour.

The shearing force (eq. (7)) does not increase unlimitedly with σ; it has a *maximum value*, corresponding to σ=about 3 ($g=\infty$), this value being

$$\tau_{\text{max.}}=2n\,.\,0{\cdot}66=1{\cdot}32n. \qquad \text{(11)}$$

If approximately the point of the breakdown τ_B is considered to be according to eq. (10), then $\tau_B=g_B\eta=0{\cdot}8n$ instead of $1{\cdot}32n$ according to eq. (11).

Identifying this value with the value obtained by Weltmann:

$$\tau_B=7000, \text{ we would have}$$

$$n=8700 \text{ dynes/sq. cm.}$$

Thus, we get the impression of these oils having a certain *form-elasticity* (rigidity) of the order of 8000 dynes/sq. cm., and possibly this fact concerns all the other liquids as well.

The fact that form-elasticity is involved in these oils would mean, according to definition, that either such liquids are not "true liquids" at all, or, that all liquids have in a certain degree *form-elasticity* which at ordinary shearing strains or by impressed oscillations cannot be observed in general. If, *e. g.* the Form Modulus (Kirchhoff's constant $K=n$) had the value $K=8700$ also in the case of *Glycerine*, the volume modulus (Helmholtz's Constant H) would be $H=4{\cdot}5\,.\,10^{10}$ and, since the following relation holds for all isotropic elastic bodies (μ .... Poisson's number),

$$\mu=\frac{3/2H-K}{3H+K},$$

$$\mu=\frac{6{\cdot}81\,.\,10^{10}-8700}{13{\cdot}65\,.\,10^{10}+8700}\sim\frac{1}{2};$$

thus the lateral contraction μ is almost *independent* of K.

Furthermore, the order of the time of relaxation t_R gives an approximate limit for the observable time T of oscillation of a pure elastic lateral vibrating layer h of the material. We shall have

$$T\leq t_R,$$

whereby $T=4h\sqrt{\rho/n}$ (ρ ... density), and $t_R=\eta/n$;

therefore $$h\leq\eta/4\sqrt{\rho n}. \qquad \text{(12)}$$

This gives, in the case of that material ($n=500$), on which fig. 2 is based, $h=3$ cm., but in case of, say, castor oil, with the assumed value $n=8700$,

---

* R. N. Weltmann, Ind. and Eng. Chem. (analyt. ed.), p. 424 (July, 1943).

$h=0\cdot1$ millimetre, and for water a fraction of one micron. The corresponding values of the time of one oscillation are

	0·6 sec.,	0·0005 sec.,	10^{-6} sec.,
for	pseudo-plastic.	castor-oil.	water.

This would explain the fact that such elastic oscillations have evaded hitherto the possibility of observation. Mineral oils of very high viscosity (*e. g.* 780 poise) which are assumed to be Newtonian liquids are between the obvious pseudo-plastics and the Newtonian liquids, and therefore they could offer a suitable test object in order to decide this important question. Some experiments are still in progress.

The equations (I) are based on Maxwell's relaxation law and there may exist pseudo-plastics with other laws of relaxation, more complicated than the first one. If, in such cases, the connection between strain and stress and their time-derivatives are known, the following way may lead also for those substances to a relation between η_a and g similar to that shown in fig. 1 :—

(i) This relation will adopt a simple form, if we take into account only those derivatives which at a sudden jerk rise to a large amount whilst the others are neglected. (Law of elasticity.) Then Hooke's law, $P_1=\lg a$, has to be replaced by this expression.

(ii) Another relatively simple form can be obtained from the said relation if no motion occurs (relaxation). Then all the time-derivatives of strain have to be cancelled, the remaining equation replacing the simple Maxwell relaxation law (eq. (2)).

Since the same state has to be reached after performing the iteration element (jerk and relaxation), all the stress derivatives have to be compensated by relaxation.

XI. *Notes on the Evaluation of Zeros and Turning Values of Bessel Functions.—I. Introductory.*

By W. G. Bickley, D.Sc., Imperial College of Science and Technology, and J. C. P. Miller, Ph.D., University of Liverpool *.

[Received May 3, 1944.]

1.1. One of the problems confronting those members of the British Association Committee for the Calculation of Mathematical Tables who are concerning themselves with the preparation and collection of material for the projected series of volumes of tables of Bessel functions is the computation of the zeros, turning values, and related numbers, of the J and

---

* Communicated by the Authors.

Y functions of orders other than 0 and 1. Difficulties have been encountered which do not exist for the functions of orders zero and unity, difficulties which increase progressively with the order. Efforts to overcome these difficulties have included a considerable amount of exploration, both numerical and formal, and have resulted in extensions to some existing formulæ, and novel uses of others, and also in what are believed to be entirely new methods and formulæ. Although it is certain that much of the computation remains to be done, probable that improvements in technique may still be made, and possible that additional methods await discovery, the difficulties have, at least in principle, been overcome.

War conditions have, of course, drastically curtailed the Committee's computational programme, and have made it impossible to predict how long the publication of the tables may be delayed. It has therefore seemed desirable to prepare and publish this series of Notes. Their main objects are: firstly, to give an account of work done, much of which is of intrinsic interest; secondly, to make generally available additions to formulæ and improvements in technique; and thirdly, by the provision, where possible, of compact ancillary tables, to facilitate the computation of zeros, etc., from the formulæ.

1.2. In these Notes $J_n(x)$ is the Bessel function of order n as usually defined, and $Y_n(x)$ denotes Weber's function as defined by Watson (W64)* and as already used (for orders zero and unity) in the British Association Mathematical Tables, vol. **VI**. The sth positive zeros (excluding 0) of $J_n(x)$, $Y_n(x)$, $J_n'(x)$ and $Y_n'(x)$, for positive n, will be denoted respectively by $j_{n,s}$, $y_{n,s}$, $j'_{n,s}$, and $y'_{n,s}$.

The general cylinder function,

$$\mathscr{C}_n(x)=J_n(x)\cos\alpha-Y_n(x)\sin\alpha,$$

where α is independent both of n and of x, will be used, and that zero of $\mathscr{C}_n(x)$ for which the first term of the McMahon expansion [(W 506), or Note II., p. 124 *infra*] is $\pi a/4$ will be denoted by $c_{n,a}$. Thus

$$y_{n,s}=c_{n,2n+4s-3},\quad j_{n,s}=c_{n,2n+4s-1}.$$

2. For the zeros of the functions of orders zero and unity two methods of computation have been used. Within the range over which the tabular interval is small (0–25 for J_n, 0–20 for Y_n), inverse interpolation; for the larger zeros, the McMahon asymptotic expansion [(W 506), or Note II., *infra*, p. 124]. To the order of accuracy (10 or 8 decimals, involving computation to two more), ample overlap was obtained. It is, however, known that

$$j_{n,1}>y_{n,1}>n,$$

so that as n increases, fewer zeros are accessible by inverse interpolation within the tabular ranges. Moreover, the McMahon expansion is asymptotic; the accuracy obtainable is limited by the magnitude of the smallest term. There is also the practical limitation that the coefficients of only a few leading terms have been determined—and the labour in obtaining additional terms would be very considerable; nothing approaching a recurrence formula for these very complicated coefficients has been obtained. The numerically smallest term increases, for fixed s, with n decreasing. It follows that, as n increases, a gap between the zeros obtainable by inverse interpolation and those given (to sufficient accuracy) by the McMahon expansion appears and widens. The ultimate magnitude of the gap may be seen when it is remarked that the *first* zero of $J_{20}(x)$ lies outside the tabular range

---

* References in this form are to pages of G. N. Watson's 'Theory of Bessel Functions' (Cambridge, 1922, 1944).

$$j_{20,1}=25{\cdot}41714\ldots,$$

while 8 terms of the McMahon expansion do not yield the required accuracy until x is greater than 100.

It is this gap which must be bridged.

3.1. In the first place the range of usefulness of the McMahon expansion has been increased by the determination of three terms additional to those given by Watson. These are given in Note II., along with tables whose use will facilitate the computation of zeros.

Secondly, a method of interpolation by Taylor's series, applicable to a wide interval, is described and illustrated in Note III.

Note IV. describes a method, believed to be new, which replaces inverse interpolation or successive approximation by direct computation and so allows a zero to be calculated by a single process based on a first approximation. Note V. is concerned with methods of checking these computations, and indicates a number of possibilities which lie open to us.

3.2. The McMahon expansion has the advantage of being entirely independent of computed values of the functions, but this advantage is shared by no other method so far devised or explored. Bridging the gap would therefore seem to entail the computation of $J_n(x)$ and $Y_n(x)$ at (say) unit interval in x up to $x=80$ or 100, for integral values of n up to about 25. Such a table for $J_n(x)$, up to $x=80$, has been computed by J. C. P. Miller and C. E. Gwyther, and some progress has been made with the corresponding table of $Y_n(x)$.

3.3. Methods depending on the use of the Debye expansions (W 244) have been advocated by Airey (1), (2). These, and the use of the equivalent Meissel expansion (W 228), are being further explored. Convenience in their use, however, demands a table of $\tan^{-1} x$ to many decimals and at a small interval. Such a table has been prepared by the Mathematical Tables Project of the W. P. A. of New York City at the instance of one of us, and further progress may now be expected.

3.4. So far it is the zeros of the functions which have mainly received attention but, as Airey (1) remarks, those of the derivatives are of almost equal importance to the physicist. It is clear, however, that any method available for the zeros of the functions is available, with modifications in detail, for zeros of the derivatives. For instance, Watson (W 507) gives three terms (only!) of the McMahon expansion for the zeros of $J_n'(x)$ and $Y_n'(x)$. Several additional terms of this series have been calculated and have been published along with a number of cognate results $^{(3)}$.

Within the tabulated range the maxima and minima of $J_n(x)$ and $Y_n(x)$, and the corresponding zeros of their derivatives, can be found by interpolation. Again, the method of Note III., and the new referred to in 3.1, can be applied to the zeros of $\mathscr{C}_n'(x)$—and since

$$\mathscr{C}_n'(x)=\tfrac{1}{2}\{\mathscr{C}_{n-1}(x)-\mathscr{C}_{n+1}(x)\},$$

no additional tabulation would be necessary.

As and when substantial progress is made in any of these directions, it is hoped that this may be recorded in further Notes of this series.

References.

(Additional to G. N. Watson, 'Theory of Bessel Functions.' Cambridge, 1922, 1944, concerning which see footnote on p. .)

(1) J. R. Airey, "The Roots of Bessel and Neumann Functions of High Order," Phil. Mag. (6) xxxii. pp. 7–14 (1916).

(2) J. R. Airey, "The Numerical Calculation of the Roots of the Bessel Function $J_n(x)$ and its First Derivative $J_n'(x)$," Phil. Mag. (6) xxxiv. pp. 187–195 (1917).

(3) W. G. Bickley, "Formulæ relating to Bessel Functions of Moderate or Large Argument and Order," Phil. Mag. (7) xxxiv. pp. **37–49** (1943).

(4) 'Table of Arc tan x,' W. P. A., New York City, Mathematical Tables Project, MT 16 (1942).

XII. *Notes on the Evaluation of Zeros and Turning Values of Bessel Functions.—II. The McMahon Series.*

By W. G. Bickley, D.Sc., Imperial College of Science and Technology, and J. C. P. Miller, Ph.D., University of Liverpool *.

[Received May 3, 1944.]

1. The method by which the additional terms were obtained is that described by Watson (W 505) and the analysis is not repeated here. Watson also outlines the history of this series.

Writing for brevity μ in place of $4n^2$, and using

$$\beta=(s+\tfrac{1}{2}n-\tfrac{1}{4})\pi-\alpha=\tfrac{1}{4}\pi a, \quad . \quad . \quad . \quad . \quad . \qquad (1.1)$$

---

* Communicated by the Authors.

where s is an integer and $a=4s+2n-1-4\alpha/\pi$, the larger zeros of

$$\mathscr{C}_n(x)=J_n(x)\cos\alpha-Y_n(x)\sin\alpha$$

are given by the asymptotic expansion

$$c_{n,\alpha}\sim\beta-\frac{A_1}{2^3\,1!}\beta^{-1}-\frac{A_3}{2^6\,3!}\beta^{-3}-\frac{A_5}{2^9\,5!}\beta^{-5}-\ldots, \tag{1.2}$$

where

$$\left.\begin{aligned}
A_1&=(\mu-1)\\
A_3&=(\mu-1)\ (7\mu-31)\\
A_5&=2^2(\mu-1)\ (83\mu^2-982\mu+3779)\\
A_7&=2.3(\mu-1)\ (6949\mu^3-1\ 53855\mu^2+15\ 85743\mu-62\ 77237)\\
A_9&=2^4.3^2(\mu-1)\ (70197\mu^4-24\ 79316\mu^3+480\ 10494\mu^2\\
&\qquad -5120\ 62548\mu+20921\ 63573)\\
A_{11}&=2^4.3^2.5(\mu-1)\ (55\ 92657\mu^5-2871\ 49133\mu^4+89039\ 61290\mu^3\\
&\qquad -17\ 92896\ 28602\mu^2+198\ 26114\ 56181\mu\\
&\qquad -824\ 97257\ 36393)\\
A_{13}&=2^6.3^2(\mu-1)\ (41489\ 44183\mu^6-29\ 12453\ 57370\mu^5\\
&\qquad +1317\ 20036\ 34537\mu^4-42635\ 39468\ 85548\mu^3\\
&\qquad +8\ 92948\ 93331\ 08377\mu^2-100\ 84747\ 20930\ 88506\mu\\
&\qquad +423\ 74844\ 36255\ 64327)
\end{aligned}\right\}. \tag{1.3}$$

2. The coefficients assume a form involving smaller numbers if we write

$$\lambda=(\mu-1)/24=(4n^2-1)/24 \quad . \quad . \quad . \quad . \quad . \quad . \quad . \tag{2.1}$$

We then find

$$\left.\begin{aligned}
A_1&=2^3.3\lambda\\
A_3&=2^6.3^2\lambda(7\lambda-1)\\
A_5&=2^{11}.3^3\lambda(83\lambda^2-34\lambda+5)\\
A_7&=2^{13}.3^5\lambda(6949\lambda^3-5542\lambda^2+2255\lambda-350)\\
A_9&=2^{19}.3^6\lambda(2\ 10591\lambda^4-2\ 74816\lambda^3+2\ 13509\lambda^2-91840\lambda+14700)\\
A_{11}&=2^{22}.3^7.5\lambda(167\ 77971\lambda^5-323\ 98231\lambda^4+406\ 83809\lambda^3\\
&\qquad -334\ 73245\lambda^2+149\ 16300\lambda-24\ 25500)\\
A_{13}&=2^{27}.3^9\lambda(41489\ 44183\lambda^6-1\ 10979\ 87178\lambda^5+2\ 04479\ 35782\lambda^4\\
&\qquad -2\ 72349\ 10810\lambda^3+2\ 32886\ 32375\lambda^2\\
&\qquad -1\ 05764\ 50500\lambda+17342\ 32500)
\end{aligned}\right\}. \tag{2.2}$$

For numerical work this may sometimes be less convenient than (1.3), since, for integral n, 24λ is an odd integer, but for determining the coefficients A_r in polynomial form, the use of λ has many advantages. This parameter λ is particularly convenient for numerical work when the order n is half an odd integer.

3. The results were checked by independent developments with the particular values $n=0$, $n=2$ and $n=20$. The two latter give

$$\left.\begin{aligned} n=2,\ c_{2,a}\sim\beta-\frac{15}{2^3}\beta^{-1}-\frac{405}{2^7}\beta^{-3}-\frac{9315}{2^{10}}\beta^{-5}-\frac{81\,70875}{2^{15}\,7}\beta^{-7} \\ -\frac{2116\,67175}{2^{18}\,7}\beta^{-9}-\frac{36\,34194\,70125}{2^{22}\,77}\beta^{-11} \\ +\frac{50560\,74657\,28125}{2^{25}\,1001}\beta^{-13}-\dots \end{aligned}\right\}, \qquad (3.1)$$

$$\left.\begin{aligned} n=20,\ c_{20,a}\sim\beta-\frac{1599}{2^3}\beta^{-1}-\frac{59\,53077}{2^7}\beta^{-3}-\frac{11\,24164\,04607}{2^{10}\,5}\beta^{-5} \\ -\frac{14\,96225\,13374\,63079}{2^{15}\,35}\beta^{-7} \\ -\frac{79951\,75366\,25157\,90003}{2^{18}\,35}\beta^{-9} \\ -\frac{1\,00910\,07098\,82542\,91588\,99777}{2^{22}\,385}\beta^{-11} \\ -\frac{30375\,49525\,00613\,85181\,77293\,40423}{2^{25}\,1925}\beta^{-13}-\dots \end{aligned}\right\}, \qquad (3.2)$$

The cases $n=1\frac{1}{2}$ and $n=2\frac{1}{2}$ are of special interest and have also been used for checking. When $n=1\frac{1}{2}$, the zeros given by (1.2) are solutions of the equation

$$\tan(x+\alpha)=x \quad \dots\dots\dots \quad (3.3)$$

and so correspond to maxima and minima of the function $(1/x)\sin(x+\alpha)$. The method to be described in a later note (IV.) gives a simple means for obtaining the McMahon series in this case, by taking β as a first approximation to the zero.

We find that

$$A_{2r-1}/2^{3r}(2r-1)!=\sum_{k=0}^{r-1}(-1)^k D_{r,k}, \quad \dots\dots \quad (3.41)$$

where we use $D_{r,k}$ in place of $C_{r+k,k}$ of note IV., so that

$$(r+k+1)D_{r+1,k}=(r+k-1)D_{r,k-1}+(3r+k-1)D_{r,k}, \quad . \quad (3.42)$$

with the initial conditions

$$D_{r,-1}=D_{1,k}=0,\ (k\geqslant 1);\quad D_{1,0}=1, \text{ whence } D_{r,r}=0. \quad . \quad (3.43)$$

The resulting expansion, as far as it has been determined, gives

$$\left.\begin{aligned} n=1\tfrac{1}{2},\ c_{1\frac{1}{2},a}\sim\beta-\beta^{-1}-\frac{2}{3}\beta^{-3}-\frac{13}{15}\beta^{-5}-\frac{146}{105}\beta^{-7}-\frac{781}{315}\beta^{-9} \\ -\frac{16328}{3465}\beta^{-11}-\frac{63\,16012}{6\,75675}\beta^{-13}-\frac{387\,59594}{20\,27025}\beta^{-15} \\ -\frac{96557\,14457}{2412\,15975}\beta^{-17}-\frac{5\,01345\,71594}{5875\,77375}\beta^{-19}-\dots \end{aligned}\right\}. \qquad (3.5)$$

Likewise, with $n=2\frac{1}{2}$, (1.2) gives solutions of the equation

$$\tan(x+\alpha)=3x/(3-x^2). \quad \dots\dots\dots \quad (3.6)$$

We find, again with β as a first approximation, that

$$A_{2r-1}/2^{3r}(2r-1)!=3^r\sum_{k=0}^{r-1}(-3)^k D_{r,k}, \quad . \quad . \quad . \quad . \quad . \qquad (3.71)$$

where

$$(r+k+1)D_{r+1,k}=(r+k-1)D_{r,k-1}+(5r+3k-1)D_{r,k}, \quad . \qquad (3.72)$$

with initial conditions as in (3.43). The resulting expansion is

$$\left.\begin{aligned} n=2\tfrac{1}{2},\ c_{2\frac{1}{2},a}\sim\beta-3\beta^{-1}-9\beta^{-3}-\frac{243}{5}\beta^{-5}-\frac{11178}{35}\beta^{-7}-\frac{81162}{35}\beta^{-9} \\ -\frac{68\,86863}{385}\beta^{-11}-\frac{35963\,81532}{25025}\beta^{-13} \\ -\frac{2\,97489\,25566}{25025}\beta^{-15}-\frac{2993\,39151\,19569}{29\,77975}\beta^{-17} \\ -\frac{24\,46082\,91926\,17956}{2829\,07625}\beta^{-19}-\ldots \end{aligned}\right\} . \qquad (3.8)$$

The expansions (3.5) and (3.8) have each been checked by independent evaluations with vulgar and decimal fractions.

4.1. The details of the application of the McMahon series to the numerical evaluation of a zero or set of zeros are not without interest. We proceed as follows:

Each coefficient A_r is calculated by use of the appropriate formula (1.3 or 2.2) for all relevant values of n; if, as in the B.A. calculations, the values of n are integers or simple fractions in arithmetical progression, the results can be checked *exactly* by differencing, since the coefficients A_r are polynomials with integer coefficients.

Next the ratios A_{2r+1}/A_{2r-1} for $r \geqslant 1$ are evaluated with an accuracy sufficient to give the desired number of decimals in the terms for $c_{n,a}$ with the smallest value of β to be used.

We now note that, for the zeros of $J_n(x)$ and $Y_n(x)$, *i.e.* when α is respectively zero or $\frac{1}{2}\pi$,

$$a=4\beta/\pi=2n+4s-1-4\alpha/\pi \quad . \quad . \quad . \quad . \quad . \quad . \qquad (4.11)$$

is an integer. The relation (1.2) may thus be written

$$c_{n,a}\sim\frac{\pi}{4}a-\frac{A_1}{2\pi}a^{-1}-\frac{A_3}{6\pi^3}a^{-3}-\frac{A_5}{60\pi^5}a^{-5}-\ldots. \quad . \quad . \qquad (4.12)$$

The next step is to divide A_1, A_3/A_1, $A_5/A_3, \ldots$ respectively by 2π, $3\pi^2$, $10\pi^2, \ldots$ (the ratios of the successive denominators in (4.2)) giving quantities which we shall denote by B_1, B_3, $B_5, \ldots$. In place of (4.2) we thus obtain

$$c_{n,a}\sim\frac{\pi}{4}a-\frac{B_1}{a}-\frac{B_1}{a}\cdot\frac{B_3}{a^2}-\frac{B_1}{a}\cdot\frac{B_3}{a^2}\cdot\frac{B_5}{a^2}-\ldots, \quad . \quad . \qquad (4.13)$$

where B_1, B_3, $B_5, \ldots$ are numerical coefficients depending, of course, on the value of n. The results of these processes for the case $n=2$ ($\mu=16$ or $\lambda=4/3$) are set out below.

TABLE I.

BESSEL FUNCTION ZEROS. MCMAHON FORMULA.

n	B_1	B_3	B_5	B_7	B_9	B_{11}	B_{13}
0	− 0·15915 49430 92	− 1·04698 55643	− 4·94055 165	− 12·02164 37	− 22·51314 2	− 36·32047	− 53·3782
1	+ 0·47746 48292 76	− 0·10132 11836	− 15·92769 007	− 11·97739 04	− 23·24185 0	− 36·84876	− 53·7945
2	2·38732 41463 78	+ 2·73567 19583	+ 4·66077 445	+ 6·34830 71	+ 5·24946 7	+ 15·81475	− 21·6866
3	5·57042 30082 16	7·46399 38617	13·93647 665	16·72537 82	18·50301 5	19·53967	+ 20·5554
4	10·02676 14147 89	14·08364 45263	27·30073 781	33·15014 64	36·42038 5	38·58232	40·1098
5	+ 15·75633 93660 98	+ 22·59462 39522	+ 44·56187 441	+ 54·73085 21	+ 60·36652 7	+ 63·94556	+ 66·4527
6	22·75915 68621 41	32·99693 21395	65·68595 297	81·26990 79	90·04686 7	95·57594	99·3769
7	31·03521 39029 20	45·29056 90881	90·66273 913	112·70618 65	125·32126 0	133·31462	138·7794
8	40·58451 04884 33	59·47553 47981	119·48822 722	149·01562 66	166·12725 9	177·06369	184·5565
9	51·40704 66186 82	75·55182 92693	152·16057 542	190·18714 79	212·43448 1	226·76881	236·6369
10	+ 63·50282 22936 66	+ 93·51945 25019	+188·67883 721	+236·21505 47	+ 264·22683 1	+ 282·39917	+ 294·9752
11	76·87183 75133 85	113·37840 44958	229·04248 451	287·09616 94	321·49516 8	343·93655	359·5429
12	91·51409 22778 40	135·12868 52510	273·25120 340	342·82860 34	384·23399 0	411·36968	430·3216
13	107·42958 65870 29	158·77029 47675	321·30479 759	403·41117 61	452·43983 2	484·69135	507·2991
14	124·61832 04409 54	184·30323 30454	373·20313 915	468·84311 81	526·11041 9	563·89675	590·4671
15	+143·08029 38396 14	+211·72750 00846	+428·94614 177	+539·12391 05	+ 605·24421 0	+ 648·98259	+ 679·8200
16	162·81550 67830 09	241·04309 58851	488·53374 549	614·25319 28	689·84013 3	739·94657	775·3537
17	183·82395 92711 39	272·25002 04470	551·96590 758	694·23070 83	779·89742 0	836·78702	877·0651
18	206·10565 13040 04	305·34827 37701	619·24259 695	779·05627 00	875·41551 0	939·50274	984·9521
19	229·66058 28816 05	340·33785 58546	690·36379 051	868·72973 91	976·39398 9	1048·09281	1099·0132
20	+254·48875 40039 41	+377·21876 67004	+765·32947 083	+963·25101 10	+1082·83254 1	+1162·55655	+1219·2469

TABLE II.

BESSEL FUNCTION ZEROS. MCMAHON FORMULA.

n	B_1	B_3	B_5	B_7	B_9	B_{11}	B_{13}
$0\frac{1}{2}$	+ 0	− 0·81056 94691	− 4·86341 681	− 12·15854 20	− 22·69594 5	− 36·47563	− 53·4976
$1\frac{1}{2}$	1·27323 95447 35	+ 1·08075 92922	+ 2·10748 062	+ 2·60094 82	+ 2·89066 1	+ 3·08113	+ 3·2159
$2\frac{1}{2}$	3·81971 86342 05	4·86341 68148	8·75415 027	10·65319 87	11·77087 8	12·50536	13·0242
$3\frac{1}{2}$	7·63943 72684 11	10·53740 30988	20·12706 343	24·26801 08	26·68518 5	28·28934	29·4301
$4\frac{1}{2}$	12·73239 54473 52	18·10271 81441	35·44729 171	43·31389 21	47·66255 2	50·46925	52·4549
$5\frac{1}{2}$	+19·09859 31710 27	+ 27·55936 19507	+ 54·64191 833	+ 67·38578 65	+ 74·50136 1	+ 78·98866	+ 82·0976
$6\frac{1}{2}$	26·73803 04394 38	38·90733 45187	77·69308 362	96·37785 15	106·98979 3	113·68920	118·2756
$7\frac{1}{2}$	35·65070 72525 85	52·14663 58479	104·59454 035	130·25263 31	145·03517 5	154·44199	160·8763
$8\frac{1}{2}$	45·83662 36104 66	67·27726 59385	135·34361 637	168·99406 38	188·59444 3	201·17406	209·8121
$9\frac{1}{2}$	57·29577 95130 82	84·29922 47904	169·93900 678	212·59429 18	237·64569 9	253·84469	265·0259
$10\frac{1}{2}$	+70·02817 49604 34	+103·21251 24037	+208·38001 086	+261·04910 06	+ 292·17690 6	+ 312·43031	+ 326·4817
$\frac{1}{3}$	− 0·08841 94128 29	− 0·94191 17442	− 4·88126 800	− 12·07064 76	− 22·59339 9	− 36·39092	− 53·4326
$\frac{2}{3}$	+ 0·12378 71779 60	− 0·62669 02840	− 5·01385 484	− 12·31251 97	− 22·83672 7	− 36·58676	− 53·5831
$1\frac{1}{3}$	+ 0·97261 35411 17	+ 0·63419 55569	+ 2·14326 612	− 2·05631 50	− 39·87858 5	− 35·84450	− 54·1300
$1\frac{2}{3}$	+ 1·60923 33134 85	+ 1·57985 99375	+ 2·69867 863	+ 4·36798 71	− 0·04555 536	−3118·313	− 48·3595
$\frac{1}{4}$	− 0·11936 62073 19	− 0·98788 15405	− 4·90316 589	− 12·04669 89	− 22·55795 0	− 36·36036	− 53·4091
$\frac{3}{4}$	+ 0·19894 36788 65	− 0·51504 93502	− 5·28780 308	− 12·39998 23	− 22·91771 2	− 36·64961	− 53·6319
$1\frac{1}{4}$	+ 0·83556 34512 32	+ 0·43061 50305	+ 2·80898 081	− 5·56719 11	− 26·72927 9	− 36·73908	− 53·9868
$1\frac{3}{4}$	+ 1·79049 31097 84	+ 1·84911 16015	+ 3·11250 348	+ 4·87857 51	+ 1·12198 8	+ 112·88475	− 45·2208

Table I. gives the numerical values of B_r for integral n up to 20, and Table II. gives the coefficients for certain non-integral values of n; for a duplicate calculation of the majority of these values the writers are indebted to Mr. C. E. Gwyther.

EXAMPLE.—*Calculation of B_r when $n=2$.*

r.	A_r	A_r/A_{r-2}	B_r
1	15		+ 2·38732 41463 78
3	1215	+ 81	2·73567 19583
5	5 58900	460	4·66077 445
7	7353 78750	1315·76087 0..	6·34830 71
9	137 16032 94000	1865·16580 ..	5·24946 7
11	+11 77479 08320 50000	+ 8584·6913.	+15·81475
13	−1 96580 18267 50950 00000	−16695·01..	−21·6866

In order to check the coefficients in Tables I. and II. we may evaluate in succession the products B_1B_3, $B_1B_3B_5, \ldots$ and multiply these, and B_1, by the corresponding denominators in (4.12), namely 2π, $6\pi^3$, $60\pi^5, \ldots$ which gives again the more easily checked quantities A_1, A_3, $A_5, \ldots$.

4.2. To evaluate a particular zero, we now compute in succession the terms of (4.13). The first two are evaluated independently; each of the later terms is deduced from the preceding one by multiplication by B_r and division by a^2 (or multiplication by a^{-2}, if a^2 is not an integer or a simple terminating decimal)—this is a continuous process on modern calculating machines.

As an illustration we consider $j_{2,4}$ with $a=19$ (by (4.11), since $\alpha=0$); we find

$$\begin{array}{rlr}
\frac{1}{4}\pi a & + & 14{\cdot}92256\ 51045\ 515 \\
-B_1/a & - & 0{\cdot}12564\ 86392\ 831 \\
\times B_3/a^2 & - & 95\ 21702\ 468 \\
\times B_5/a^2 & - & 1\ 22932\ 154 \\
\times B_7/a^2 & - & 2161\ 804 \\
\times B_9/a^2 & - & 31\ 436 \\
\times B_{11}/a^2 & - & 1\ 377 \\
\times B_{13}/a^2 & + & 83 \\
j_{2,4} & = & 14{\cdot}79595\ 17823\ 528
\end{array}$$

Inverse interpolation in 12-decimal tables gives

$$j_{2,4} = 14{\cdot}79595\ 17823\ 56$$

The agreement is satisfactory.

For mass computation of zeros with integral values of a, a modified procedure may be used, since tables of a^{-n} for integral a not exceeding 100 and integral n are available (Peters, *Zehnstellige Logarithmen*, Bd. 1, Anhang, p. 36, 1922); it may be easier to set, *e. g.* the product $B_1B_3B_5$

on a calculating machine and to multiply in succession by the various values of a^{-5} so long as a does not exceed 100. For the B.A. calculations, however, a exceeds 100 in the majority of cases, and the process exemplified has been used extensively.

4.3. In the numerical calculation of successive terms of a series, it is frequently possible to estimate one or more terms *beyond* those which have been calculated accurately, by making a difference table of the ratios of successive terms and a rough extrapolation. This can be done with the McMahon series for most values of n given in the tables; although difficulties evidently arise with the smaller values of n, for instance, $n=2$ or $n=1\frac{3}{4}$. As an example consider $n=17$: it is easy to estimate that B_{15} and B_{17} will be respectively about 907 and 930—with sufficient accuracy to give almost 3 extra decimals in the value of a zero.

The extra terms should, of course, be used with considerable caution, but are valuable when the McMahon series is used as one of two independent methods of calculation, at least with the smaller values of a.

XIII. *Notes on the Evaluation of Zeros and Turning Values of Bessel Functions.—III. Interpolation by Taylor Series.*

By W. G. Bickley, D.Sc.,
Imperial College of Science and Technology *.

[Received May 3, 1944.]

1. The first stage in the tabulation of $J_n(x)$ and $Y_n(x)$ was the computation of these functions at interval 0·1 in x. For $J_n(x)$ this was done by a method due to Comrie, using Meissel's values at unit interval in x and interpolating by Taylor series. This is simple and convenient in view of the formulæ

$$\left.\begin{aligned} J_n'(x)&=\tfrac{1}{2}[J_{n-1}(x)-J_{n+1}(x)] \\ J_n''(x)&=\tfrac{1}{4}[J_{n-2}(x)-2J_n(x)+J_{n+2}(x)] \\ J_n'''(x)&=\tfrac{1}{8}[J_{n-3}(x)-3J_{n-1}(x)+3J_{n+1}(x)-J_{n+3}(x)] \end{aligned}\right\}, \quad . \quad . \quad . \quad (1)$$

whence it appears that the $2r$th *derivative* of $J_n(x)$ is obtained from the $2r$th *difference* of the sequence $J_{n+2p}(x)$, and similarly for the derivatives of odd orders. Such differences can readily be obtained on the National machine, for large-scale routine computation; for our present purpose the few which are needed can easily be calculated on a hand machine.

---

* Communicated by the Author.

2. If a sequence of values of $J_n(x)$ or $Y_n(x)$ for constant x and at unit interval in n is available, interpolation for x can proceed simply, since the coefficients in the Taylor series can be derived from it. In such a sequence, a small value of $J_n(x)$ implies that x is an approximation to a zero of $J_n(x)$. Thus, after computing $J_n(30)$ we find

$$J_{20}(30)=+0{\cdot}00483\ 10199\ 934,$$

so that there is a zero (the second) of $J_{20}(x)$ near (slightly less than) 30. The values of $J_n(30)$ are ranged in sets of even and odd order, and the appropriate differences are calculated. Negative values are conveniently entered as complements *, and in view of (1), odd differences are given the sign opposite to that of the usual convention—a fact indicated by a bar thus, $\bar{\delta}$.

n	$J_n(30)$	δ^2	δ^4
16	..9·91093 49237 330		
18	0·15847 53060 222	..9·59881 53317	
20	0·00483 10199 934	..9·97250 36844	..9·97887 692
22	..9·82369 04183 981	0·32506 89589	
24	..9·96761 87757 230		

n	$J_n(30)$	$\bar{\delta}$	$\bar{\delta}^3$	$\bar{\delta}^5$
15	..9·84375 29316 096			
		..9·78250 86112 374		
17	0·06124 43203 722			
		..9·93231 82735 178	0·16298 2798	
19	0·12892 60468 544			
		0·25141 07337 176	..9·44311 4819	1·28683
21	..9·87751 53131 368			
		0·01361 80126 230	0·00377 9268	
23	..9·86389 73005 138			
		..9·77960 45598 708		
25	0·08429 27406 430			

Now by (1) we have the Taylor series

$$J_{20}(30-h)=J_{20}(30)-\frac{h}{2}\bar{\delta}+\frac{h^2}{8}\delta^2-\frac{h^3}{48}\bar{\delta}^3+\frac{h^4}{384}\delta^4\ldots, \quad . \quad . \quad (2)$$

in which all the differences are centred at $n=20$. Using the h^2 term to correct a first approximation $(h_1=2J_{20}(30)/\bar{\delta})$ we obtain, as the value of h corresponding to the zero,

$$h=0{\cdot}03839\ldots.$$

(In order that linear interpolation may suffice in the next stage, it is desirable here to get within one or two units in the fifth decimal ; hence the use of the h^2 term.)

We now compute, by (2), values of $J_{20}(30-h)$ for the values

0·03838, ...39, ...40, ...41 of h.

---

* One has then no further worry with sign.

A typical computation is

$$\begin{array}{rr} h = & 0{\cdot}03839 \\ h/2 = & 0{\cdot}01919\ 5 \\ h^2/8 = & 18\ 42240\ 125 \\ h^3/48 = & 11787\ 266 \\ h^4/384 = & 56\ 564 \\ h^5/3840 = & 217 \end{array} \qquad \begin{array}{rr} J_{20}(30) = & +0{\cdot}00483\ 10199\ 934 \\ -h\bar{\delta}/2 = - & 482\ 58290\ 337 \\ h^2\delta^2/8 = - & 50654\ 816 \\ -h^3\bar{\delta}^3/48 = + & 6564\ 154 \\ h^4\delta^4/384 = - & 1\ 195 \\ -h^5\bar{\delta}^5/3840 = - & 279 \\ \hline J_{20}(29{\cdot}96161) = & +0{\cdot}00000\ 07817\ 461 \end{array}$$

The values so computed are tabulated and differenced, the result being

x	$J_{20}(x)$	δ	δ^2
29·96159	$-0{\cdot}0^5$ 17366 145		
		12591 805	
60	− 4774 340		−4
		12591 801	
61	+ 7817 461		−5
		12591 796	
62	+ 20409 257		

Linear interpolation now suffices to give the zero at

$$\begin{aligned} x &= 29{\cdot}96160 + \frac{4774\ 340}{12591\ 801} \times 10^{-5} \\ &= 29{\cdot}96160\ 37916\ 26. \end{aligned}$$

3. Thirteen decimals have been kept in the calculations, and twelve are given for the zero, but they are not all reliable. An error up to 3 in the thirteenth decimal is *possible* in $J_{20}(29{\cdot}96159)$, etc. (although the second differences misleadingly suggest reliability to one unit !), so that the result can be regarded as accurate to within two or three units in the twelfth decimal.

A computation, by the same method, of $J_{20}(x)$ gives zero to the thirteenth decimal. As a check this is not independent, since it uses the same $\bar{\delta}$, δ^2, . . ., so that it is not entirely conclusive.

An additional check lies in the numerical equality of $J_{19}(x)$ and $J_{21}(x)$; we find

$$\begin{aligned} J_{19}(x) &= +0{\cdot}12591\ 80091\ 126 \\ J_{21}(x) &= -0{\cdot}12591\ 80091\ 124, \end{aligned}$$

and the agreement is satisfactory.

In addition to being a check on the zero, these values have an importance of their own, since (*cf.* I., p. 121).

$$J'_{20}(x) = 0{\cdot}12591\ldots$$

at this zero. The value of the derivative is of use, not only *qua* derivative, but also in the determination of the corresponding coefficient in a Fourier-Bessel expansion.

XIV. *Kinematic Relativity: a Reply to Prof. W. Wilson.*

By E. A. MILNE, F.R.S.*

[Received October 10, 1944.]

IN a recent number of this Journal †, Professor W. Wilson has published some criticisms of my work in relativity. I thank him for the courtesy with which he formulated his difficulties, and for his invitation to me to reply. The present reply has been delayed owing to war-time occupations. I value Prof. Wilson's interest, for his paper is, I think, the first critical paper which, using my notation, investigates my results from the inside. At the same time, I think it can readily be shown that he is wrong in his contentions.

Prof. Wilson's difficulties arise in connection with my equation of motion of a free particle P, as reckoned by an observer at the origin O. This has the form

$$\frac{1}{\mathrm{Y}}\frac{d\mathbf{V}}{dt}=-\frac{\mathbf{P}-\mathbf{V}t}{\mathrm{X}}, \qquad (1)$$

where

$$\mathrm{X}=t^2-\mathbf{P}^2/c^2, \quad \mathrm{Y}=1-\mathbf{V}^2/c^2, \qquad (2)$$

and $\mathbf{V}$ is the instantaneous velocity of the force particle at the instant t. I derived the equation of motion (1) as holding good in the presence of the *substratum*, or set of moving *fundamental* particles. distributed according to the particle-density law

$$n(\mathbf{P},t)\,dx\,dy\,dz=\frac{\mathrm{B}t\,dx\,dy\,dz}{c^3(t^2-\mathbf{P}^2/c^2)^2}, \qquad (3)$$

each moving with its appropriate velocity given by

$$\mathbf{V}=\mathbf{P}/t. \qquad (4)$$

Equation (1) is the form which the more general equation of motion

$$\frac{1}{\mathrm{Y}}\frac{d\mathbf{V}}{dt}=\frac{\mathbf{P}-\mathbf{V}t}{\mathrm{X}}\mathrm{G}(\xi) \qquad (5)$$

takes when the *statistical* system to which (5) relates reduces to a substratum. Here

$$\xi=\mathrm{Z}^2/\mathrm{XY}, \qquad (6)$$

$$\mathrm{Z}=t-\mathbf{P}.\mathbf{V}/c^2, \qquad (7)$$

---

* Communicated by the Author.

† Phil. Mag. ser. 7, vol. xxxv. p. 241 (April 1944).

and $G(\xi)$ is connected with $\psi(\xi)$, the function specifying the statistical system in question, by the relation

$$G(\xi)\equiv-1-\frac{C}{(\xi-1)^{3/2}\psi(\xi)}, \quad . \quad . \quad . \quad . \quad . \quad . \quad . \quad (8)$$

C being an arbitrary constant. The function $\psi(\xi)$ describes the population of the statistical system through the spatio-velocity distribution law

$$N(\mathbf{P},\ \mathbf{V},\ t)dx\,dy\,dz\,dx\,dv\,dw=\frac{\psi(\xi)}{c^6X^{3/2}Y^{5/2}}da\ .\ .\ .\ dw. \quad . \quad . \quad (9)$$

The proofs of these statements were given in 'World-Structure'* and in later papers †. One proof-sequence involved the use of functional equations, another the use of 4-vectors.

Prof. Wilson remarks that the set of functional equations are in fact satisfied by

$$G(\xi)\equiv0, \quad . \quad . \quad . \quad . \quad . \quad . \quad . \quad . \quad . \quad (10)$$

which would imply

$$\frac{d\mathbf{V}}{dt}=0 \quad . \quad . \quad . \quad . \quad . \quad . \quad . \quad . \quad . \quad . \quad (11)$$

for all particles. I will only say, in answer to this remark, that $G(\xi)\equiv0$ would be incompatible with (8), which flows from a study of the Boltzmann equation applied to the statistical system; (8) is the condition that the motion (5) is compatible with the distribution law (9). A system for which $G(\xi)\equiv0$ would exhibit no gravitational effects whatever, although (3) is a non-homogeneous system in the reckoning of any fundamental observer such as O.

But Professor Wilson has an apparently more weighty analytical difficulty with equation (1): he concludes, as a result of various arguments involving 4-vector calculus—arguments which I shall show are erroneous—that for any particle considered by the theory, $\mathbf{P}-\mathbf{V}t$ must vanish, and so $d\mathbf{V}/dt=0$; *i. e.*, that the only free particles possible would have constant velocities, and be indistinguishable from fundamental particles, and that other free particles could apparently only be accelerated in a continuum with some other (*e. g.* Riemannian) kind of metric.

My answer to this is that if a free particle is projected in any arbitrary manner, *i. e.* from an arbitrary point P with an arbitrary velocity **V** at the arbitrary epoch *t*, all reckoned with reference to a given fundamental observer O, then it will certainly have some motion relative to the particles of the substratum, and so there must be a relation describing its acceleration as a function of its **P**, **V** and *t*. Hence, to deny the possibility of contemplating free particles other than the fundamental particles is to impose a purely arbitrary restriction on the development of the kinematic calculus. In Newtonian theory, and in Einstein's theory, a fundamental line of enquiry is to determine what is the motion of a free particle, in the presence of a given system of gravitating masses or a given metric, respectively ; and I do not see why I should be denied the same enquiry in the presence of an expanding substratum of given particles. The notion of the *test-particle* is basic in dynamics, gravitation and electrodynamics ; small wonder that if you remove it, as Prof. Wilson states, you cut away the foundation of my theory of gravitation and of rational electrodynamics. You would cut away the foundations of any theory—of all existing physics—if you stultified its development in this way. Actually, in my theory, as soon as one admits the notion of a test-particle, one can have, and indeed in the general case must have, $\mathbf{V}\neq\mathbf{P}/t$.

---

* 'Relativity, Gravitation and World-Structure,' Oxford, 1935.

† Quart. Journ. Math. (Oxford), viii. p. 22 (1937); Proc. Roy. Soc. 156 A, lxix. p. 136.

Of course, in our ordinary experience, located (as we are) not far (in comparison with ct) from what is presumably a fundamental particle, namely the centre of our own galaxy *, we should expect our empirical dynamics to agree with that resulting from putting $\mathbf{P}=\mathbf{V}t$. I pointed out that my t-dynamics reduces to Einstein's *locally*, *i. e.* when $\mathbf{P}\sim\mathbf{V}t$, in my first paper † in my ' Royal Society Proceedings ' sequence, in conformity with Prof. Wilson's statements. But one of the objects of kinematic relativity is to derive a more general dynamics than our own local empirical dynamics, namely one holding good for particles ($\mathbf{P}$, $\mathbf{V}$, t) for which $\mathbf{V}\neq\mathbf{P}/t$.

Nevertheless, I am bound to pay attention to Prof. Wilson's analytical considerations, based on 4-vector calculus. I think it can be seen very simply that Prof. Wilson has committed certain errors in his vector analysis.

Prof. Wilson argues that $\mathbf{P}-\mathbf{V}t$ is the space part of a 4-vector, and thus that since X is a scalar invariant, the right-hand side of (1) is the space part of a 4-vector ; whilst the left-hand side is not. Hence he suspects a " fundamental weakness." He admits that my equation of motion in the form

$$\frac{1}{\mathrm{Y}^{\frac{1}{2}}}\frac{d}{dt}\left(\frac{\mathbf{V}}{\mathrm{Y}^{\frac{1}{2}}}\right)=-\frac{1}{\mathrm{X}}\left(\mathbf{P}-\mathbf{V}\frac{\mathrm{Z}}{\mathrm{Y}}\right) \quad . \quad . \quad . \quad . \quad . \quad . \quad (12)$$

preserves its form under a Lorentz transformation, and that it follows of necessity from (1). And so he asks, " How has this real, or apparent, contradiction slipped in ? "

The answer is that there is no contradiction, for $\mathbf{P}-\mathbf{V}t$ is *not* the space part of a 4-vector ; $\mathbf{P}$ is the space part of the 4-vector ($\mathbf{P}$, ct), but $\mathbf{V}t$ is not the space part of a 4-vector. This can be seen by writing it in the form $(\mathbf{V}/\mathrm{Y}^{\frac{1}{2}})(\mathrm{Y}^{\frac{1}{2}}t)$ and noting that whilst $\mathbf{V}/\mathrm{Y}^{\frac{1}{2}}$ is the space part of a 4-vector, $\mathrm{Y}^{\frac{1}{2}}t$, unlike $\mathrm{Y}^{\frac{1}{2}}dt$, is *not* an invariant.

---

* Apart from a possible " proper motion " of our own galaxy in the substratum.

† Proc. Roy. Soc. 154 A, pp. 32, 33, 34 (1936), " On the Foundations of Dynamics."

It is as well to be clear what we mean by a 4-vector. Temporarily using Cartesian components, we have that if (x_1, x_2, x_3, x_4) is a 4-vector, then referred to an observer O′ moving with velocity (U, O, O) relative to the first observer O and parting company from him at $t=0$, the new components $(x_1', x_2'\ x_3', x_4')$ are given by the Lorentz transformation

$$x_1'=\frac{x_1-(\mathrm{U}/c)x_4}{(1-\mathrm{U}^2/c^2)^{\frac{1}{2}}}, \quad x_2'=x_2, \quad x_3'=x_3, \quad x_4'=\frac{x_4-(\mathrm{U}/c)x_1}{(1-\mathrm{U}^2/c^2)^{\frac{1}{2}}}. \quad . \quad (13)$$

Alternatively and more fundamentally, in the way in which they emerge in Whitrow's and my discussion of signal functions, the first and last of these may be written in the equivalent form

$$x_1'-x_4'=(x_1-x_4)\left(\frac{1+\mathrm{U}/c}{1-\mathrm{U}/c}\right)^{\frac{1}{2}}, \quad x_1'+x_4'=(x_1+x_4)\left(\frac{1-\mathrm{U}/c}{1+\mathrm{U}/c}\right)^{\frac{1}{2}}. \quad (14)^*$$

If now the left- and right-hand sides of (1) are severally transformed, using the fact that $(\mathbf{P}, ct)$ and $(\mathbf{V}/\mathrm{Y}^{\frac{1}{2}}, c/\mathrm{Y}^{\frac{1}{2}})$ are 4-vectors, it will be found, as a simple algebraic result, that the new relation between the primed symbolts is of precisely the same form as the original relation (1) between the unprimed symbols. The transformation is slightly tedious, and I do not propose to reproduce it here. Nevertheless, I think that Prof. Wilson might have assumed that before building the extensive structure which I have in fact built on (1), I had actually verified for myself, by pedestrian methods, its conservation of form under the Lorentz transformation.

It must of course be possible to show at a glance, by non-pedestrian methods, that (1) conserves its form under a Lorentz transformation, and I propose, before going further, to do this. One way of showing this is to show that both (12) can be deduced from (1) and (1) from (12), by suitable vector operations, and then noting that both sides of (12) are the space parts of 4-vectors; this latter result follows since on the left-hand side $\mathbf{V}/\mathrm{Y}^{\frac{1}{2}}$ is the space part of a 4-vector and $\mathrm{Y}^{\frac{1}{2}}dt$ a scalar invariant, whilst on the right-hand side $\mathbf{V}\mathrm{Z}/\mathrm{Y}$ is the space part of a 4-vector since $\mathbf{V}/\mathrm{Y}^{\frac{1}{2}}$ is so, and $\mathrm{Z}/\mathrm{Y}^{\frac{1}{2}}$ is an invariant.

But a more satisfactory demonstration starts by noting that

$$\left(c\frac{\mathbf{P}-\mathbf{V}t}{\mathrm{Y}^{\frac{1}{2}}}, \ \frac{\mathbf{P}\wedge\mathbf{V}}{\mathrm{Y}^{\frac{1}{2}}}\right)$$

is what is perversely called a 6-vector †, that is to say, the non-zero part of an antisymmetrical tensor of rank 2 in four dimensions. To see this, we construct out of the 4-vectors $(\mathbf{P}, ct)$, $(\mathbf{V}/\mathrm{Y}^{\frac{1}{2}}, c/\mathrm{Y}^{\frac{1}{2}})$, which we temporarily call $(\mathrm{P}_1, \mathrm{P}_2, \mathrm{P}_3, \mathrm{P}_4)$ $(\mathrm{V}_1, \mathrm{V}_2, \mathrm{V}_3, \mathrm{V}_4)$, the antisymmetrical tensor $\mathrm{A}_{\alpha\beta\gamma\delta}\mathrm{P}_\gamma\mathrm{V}_\delta$, where $\mathrm{A}_{\alpha\beta\gamma\delta}$ is the *alternate* tensor, or tensor of rank 4 whose components are zero when any two suffixes are equal and equal to plus or minus unity when they are all unequal, according to the parity of the number of inversions in the order $\alpha\beta\gamma\delta$. If $A_{\alpha\beta\gamma\delta}P_\gamma V_\delta = T_{\alpha\beta}$, we have on carrying out the summations implied by the repeated suffix convention

---

* Incidentally, the form (14) shows that Dingle is misled, when he insists, as he so often has done, that the advance made in the Lorentz transformation consists in introducing the factor $(1-\mathrm{U}^2/c^2)^{-\frac{1}{2}}$.

† *Cf.* Proc. Roy. Soc. 165 A, p. 316 (1938).

$$T_{23} = P_1V_4 - P_4V_1 = c\frac{(\mathbf{P}-\mathbf{V}t)_1}{Y^{\frac{1}{2}}},$$

$$T_{14} = P_2V_3 - P_3V_2 = \frac{(\mathbf{P}\wedge\mathbf{V})_1}{Y^{\frac{1}{2}}}.$$

It now suggests itself that (1) can be exhibited in 6-vector form, and this is readily shown to be so. For, carrying out the differentiation indicated, and then using (1) whenever necessary, we have

$$\begin{aligned}\frac{1}{Y^{\frac{1}{2}}}\frac{d}{dt}\left(\frac{\mathbf{P}-\mathbf{V}t}{Y^{\frac{1}{2}}}\right) &= -\frac{t}{Y}\frac{d\mathbf{V}}{dt} + \frac{\mathbf{P}-\mathbf{V}t}{Y^2}\left(\frac{\mathbf{V}}{c^2}\cdot\frac{d\mathbf{V}}{dt}\right)\\ &= \frac{\mathbf{P}-\mathbf{V}t}{X}\left[t - \frac{1}{Y}\left(\frac{\mathbf{P}.\mathbf{V}}{c^2} - \frac{\mathbf{V}^2}{c^2}t\right)\right]\\ &= \frac{\mathbf{P}-\mathbf{V}t}{X}\left[t - \frac{1}{Y}\Big(t - Z + t(Y-1)\Big)\right]\\ &= \frac{\mathbf{P}-\mathbf{V}t}{Y^{\frac{1}{2}}}\frac{Z}{Y^{\frac{1}{2}}}\frac{1}{X}. \qquad \text{(15)}\end{aligned}$$

Both sides of this being corresponding parts of 6-vectors, without more ado we see that it conserves its form under Lorentz transformations. It is easy to reverse the steps, and so to deduce (1) from (15). Likewise we have, on multiplying (1) vectorially by **P**,

$$\frac{1}{Y}\frac{d}{dt}(\mathbf{P}\wedge\mathbf{V}) = \frac{(\mathbf{P}\wedge\mathbf{V})t}{X},$$

whence

$$\begin{aligned}\frac{1}{Y^{\frac{1}{2}}}\frac{d}{dt}\left(\frac{\mathbf{P}\wedge\mathbf{V}}{Y^{\frac{1}{2}}}\right) &= \frac{1}{Y}\mathbf{P}\wedge\frac{d\mathbf{V}}{dt} + \frac{\mathbf{P}\wedge\mathbf{V}}{Y^2}\left(\frac{\mathbf{V}}{c^2}\cdot\frac{d\mathbf{V}}{dt}\right)\\ &= \frac{\mathbf{P}\wedge\mathbf{V}}{X}t + \frac{\mathbf{P}\wedge\mathbf{V}}{XY}\left[-\frac{\mathbf{P}.\mathbf{V}}{c^2} + \frac{\mathbf{V}^2}{c^2}t\right]\\ &= \frac{\mathbf{P}\wedge\mathbf{V}}{X}\left[t + \frac{1}{Y}(Z - t + t(1-Y))\right]\\ &= \frac{\mathbf{P}\wedge\mathbf{V}}{Y^{\frac{1}{2}}}\frac{Z}{Y^{\frac{1}{2}}}\frac{1}{X}, \qquad \text{(16)}\end{aligned}$$

which again is in 6-vector form. It is probable that these forms of the equation of motion of a free particle can be usefully employed in electrodynamical researches, where (**H**, **E**) is also a 6-vector.

Before I pass on, it may be noted that since

$$\frac{Z}{X} = \frac{d}{dt}(\log X^{\frac{1}{2}}),$$

equations (15) and (16) admit the integrating factor $X^{-\frac{1}{2}}$, and thus possess the integrals

$$\frac{\mathbf{P}-\mathbf{V}t}{Y^{\frac{1}{2}}X^{\frac{1}{2}}}=\text{const.}, \quad . \quad . \quad . \quad . \quad . \quad . \quad . \quad . \qquad (17)$$

$$\frac{\mathbf{P}\wedge\mathbf{V}}{Y^{\frac{1}{2}}X^{\frac{1}{2}}}=\text{const.} \quad . \quad . \quad . \quad . \quad . \quad . \quad . \quad . \qquad (18)$$

Since (1) is known to admit the integral $\xi=\text{const.}$, integral (18) is simply my integral

$$\mathbf{P}\wedge\mathbf{V}=\text{const. } Z, \quad . \quad . \quad . \quad . \quad . \quad . \quad . \quad . \qquad (19)$$

which I have derived elsewhere; it gives the secular increase of angular momentum in t-measure.

I now come to the ungrateful task of showing just where Prof. Wilson has been misled. His first error, after falsely supposing $\mathbf{P}-\mathbf{V}t$ to be the space part of a 4-vector (p. 243 of his paper), is to write as an identity

$$\frac{1}{Y^2}\frac{d\mathbf{V}}{dt}=\frac{1}{Y}\frac{d}{dt}\left(\frac{\mathbf{V}}{Y^{\frac{1}{2}}}\right). \quad . \quad . \quad . \quad . \quad . \quad . \quad . \qquad (20)$$

This is false, for on differentiating out we have

$$\frac{1}{Y^{\frac{1}{2}}}\frac{d}{dt}\left(\frac{\mathbf{V}}{Y^{\frac{1}{2}}}\right)=\frac{1}{Y}\frac{d\mathbf{V}}{dt}+\frac{\mathbf{V}}{Y^2}\left(\frac{\mathbf{V}}{c^2}\cdot\frac{d\mathbf{V}}{dt}\right). \quad . \quad . \quad . \quad . \quad . \qquad (21)$$

If we multiply the correct identity (21) scalarly by $\mathbf{V}$, we get indeed

$$\frac{\mathbf{V}}{Y^{\frac{1}{2}}}\cdot\frac{d}{dt}\left(\frac{\mathbf{V}}{Y^{\frac{1}{2}}}\right)=\frac{1}{Y^2}\left(\mathbf{V}\cdot\frac{d\mathbf{V}}{dt}\right), \quad . \quad . \quad . \quad . \quad . \quad . \qquad (22)$$

so that the *components* of the two sides of (20) along $\mathbf{V}$ are equal. But this is quite a different thing from asserting (20). Relation (20) is in fact only true if $\mathbf{V}$ and $d\mathbf{V}/dt$ are parallel. In this connection, I wonder whether Prof. Wilson has misled himself by his omission of the dot for the sign of scalar multiplication; for this dot is omitted from the product $\mathbf{P}.\mathbf{V}$ in the equation preceding his (7), yet when it is restored it is by no means true that the right-hand side of my (1) can be written in the form he gives. The form he gives, when the dot is restored, is that of the right-hand side of my (12), but it must be understood clearly that whilst (12) is equivalent to (1), this does not mean that the right-hand side of (12) is another way of writing the right-hand side of (1).

Prof. Wilson's argument resting on his (7′) fails again, $\mathbf{V}t$ being once more falsely supposed to be the space part of a 4-vector.

On p. 245 of his paper, Prof. Wilson uses another argument, which depends on his enunciation of the Lorentz transformation in the form

$$\mathbf{D}=\frac{\mathbf{D}'+\mathbf{U}t'}{(1-\mathbf{U}^2/c^2)^{\frac{1}{2}}}. \quad . \quad . \quad . \quad . \quad . \quad . \quad . \quad . \qquad (23)$$

But surely this is an inaccurate statement of the Lorentz transformation.

For on taking the particular case $\mathbf{U}=(U, 0, 0)$, it gives that the y- and z-components of D are connected with those of $\mathbf{D}'$ by

$$D_y=\frac{D_y'}{(1-U^2/c^2)^{\frac{1}{2}}}, \qquad D_z=\frac{D_z'}{(1-U^2/c^2)^{\frac{1}{2}}},$$

whereas the true relations are

$$D_y=D_y', \qquad D_z=D_z'.$$

Thus (23) is false as a vector form of the Lorentz transformation. The correct form is

$$\mathbf{D}=\mathbf{D}'+\mathbf{U}\frac{\mathbf{D}'.\mathbf{U}}{U^2}\left[\frac{1}{(1-U^2/c^2)^{\frac{1}{2}}}-1\right]+\frac{\mathbf{U}t'}{(1-U^2/c^2)^{\frac{1}{2}}}, \quad . \quad . \quad (24)$$

with

$$t=\frac{t'+\mathbf{U}.\mathbf{D}'/c^2}{(1-U^2/c^2)^{\frac{1}{2}}}. \quad . \quad . \quad . \quad . \quad . \quad . \quad . \quad (24')$$

Even so, the formula does not apply to the 3-vector $\mathbf{V}t$, which is not the space part of a 4-vector, as shown above. In any case, the arguments put forward by Prof. Wilson in the middle paragraph of his p. 245 have no connection with my equation of motion: the contradiction at which he arrives is merely due to his mismanagement of the Lorentz transformation.

Prof. Wilson concludes by denying my claim that the ideas of kinematic relativity " form a clean break with the traditional method of approach to a question of physical science—the method of inductive generalization from experiment." He admits at the outset that the ideas develop " a completely new kind of relativity," but I doubt whether he has fully realized wherein the newness lies. He would realize it at once if he sought to enrich the theory by some new type of kinematic argument, for he would then see that in the development of the argument no actual appeal to any experimental result is ever involved. I fully admit that the idea of the substratum was suggested by the expanding universe of nebulæ. But in the construction of, and development of the properties of, the expanding substratum, *empirical* appeals are avoided. The whole of kinematic relativity could be developed by a pure mathematician out of the resources of his own mind, with no actual results of experiments to work on whatever. The concept of the substratum is like the concept of the Euclidian plane: suggested by experience, but constructed as an essay in logic. When I claim that the ideas form a clean break with the traditional method of approach to a question of physical science, I mean that whereas the usual paper on a physical problem begins by making physical assumptions, kinematic relativity proceeds without making physical assumptions. It does not assume, for example, Newton's laws of motion; it does not assume Einstein's postulate (essentially a physical assumption) of the constancy of the velocity of light to observers in uniform relative motion—I am glad to see in this connection that Prof. Wilson describes the Lorentz transformation as a *convention*, thereby recognizing that though these famous formulæ originated in physical appeals, their status really derives from the possibility of our being acquainted with the external world through sense-data. When I speak of no physical assumptions whatever, I do not mean to deny the empirical appeal involved in the assumption of the possession of a temporal experience by each observer; or that of the existence of three spatial dimensions. The former is the condition that there is an external world-history for each observer to describe; the latter I cannot claim to have yet fathomed. Nor, again, do I wish to deny the empirical appeal involved in the possibility of perception by *seeing* *. These appeals, empirical as they may be, are concerned rather with the theory of knowledge, with epistemology rather than with physics. The appeals to empirical quantitative laws, which are a feature in the development of usual physical theories, are absent from a proper kinematic argument.

I do not wish to overstate the claim. One may afterwards appeal to the external world, to identify the things represented by symbols or to evaluate parameters like t and M; but one does not need these identifications or evaluations in order to develop their relations. Whether or not the universe of mutually receding galaxies is built on the model of the substratum is a fascinating and fundamental problem; but it has no bearing on the properties of, or on the relations holding good in, the substratum as defined. What is novel in the resulting theory is that it establishes results about *motion*, whereas previously the same deductive method had been confined to the *static* assemblages of geometry.

We may acquire knowledge of theorems of a geometry from experience, but the status of a geometrical theorem is not its basis in experience, but its having been deduced from the definitions and axioms, the axioms being in turn concealed definitions of the subject of discourse; and kinematic relativity has to all intents and purposes the status of a geometry. The *axioms* of a geometry are not the same kind of thing as the *assumptions* of an investigation in theoretical physics: an assumption in a physical investigation is a contingent proposition—something which might have been otherwise, something fresh to, additional to, the march of the investigation as it has proceeded up to that point, something either plausibly suggested or believed on grounds of empirical evidence. The development of the investigation encounters an obstacle; and the obstacle is surmounted by an assumption or hypothesis. All the famous hypotheses of physics or chemistry, or indeed of pure mathematics in such cases as the Riemann hypothesis in the theory of the zeta-function, are of this kind. You can deny an assumption or a hypothesis; it may be false. You cannot deny a definition, except by showing that it involves an internal self-contradiction. The traditional type of physical investigation has elements in it which can be denied or modified; modified conclusions then follow. But, as a logical structure, you cannot deny a geometry except by finding logical flaws in its deduction. Similarly you may, with Prof. Wilson, claim to establish logical flaws in the establishment of kinematic relativity; but when these objections are answered, it has to be accepted.

---

* *Cf.*, on this point, my remarks in my James Scott Lecture, Proc. Roy. Soc. Edinburgh, lxii. pp. 19–20 (Pt. I. No. 2) (1943).

The cosmological principle may be regarded as an *assumption* if we are simply investigating the universe of nebulæ: whether the universe obeys it or not becomes a question of fact, concerning which evidence may be examined. But in kinematic relativity I use the cosmological principle as a way of constructing the substratum, as a way of conceiving a structure whose properties are of interest; weaker forms of the same principle, *i. e.* forms defining less and deducing more, have been given by Whitrow and Walker. What I claim to be novel about this type of investigation is that it leads to theorems about *moving* particles in the presence of other collections of particles which have the same degree of inevitableness that theorems about triangles and circles have when these triangles and circles are located on a Euclidean plane. It would, for example, be quite foreign to the method of kinematic relativity to *posit* the law of motion of a free particle, or to *posit* the law of gravitation; it has to ascertain such laws (if they exist) as theorems deduced as properties of the substratum.

A possible misconception may be cleared away. Suppose we knew all the motions of the external galaxies, or made some assumption tantamount to a knowledge of their motions; then a sufficiently powerful mathematician could presumably deduce the law of gravitation they are obeying; or, conversely, experiment in thought with divers kinds of laws till one emerged which fitted. Such was, in fact, Newton's method in connection with the lunar and planetary motions—a method in his case triumphantly directed by the insight of genius. But the method of kinematic relativity is essentially different. It constructs a certain system of moving particles, and then demonstrates that these will in fact, in one another's presence, move in the way prescribed; that the system will go on of itself, is self-perpetuating. The method produces, out of purely kinematic elements, propositions of a dynamical character. The *particle in motion* plays the part of the *point* in a geometry. This may be assessed by critics as "not physics"; but it is a legitimate branch of scientific enquiry.

That this dynamics reduces, in the neighbourhood of fundamental particles, as Professor Wilson agrees, to Einstein's earlier relativity, is of course pleasing confirmation of the relevancy of the investigation to Nature. But this, instead of diminishing its significance, gives a new sanction to Einstein's relativity. So long as this sanction was purely empirical, or rested on empirical postulates, it was always possible for refined experiment to alter the form of Einstein's relativity; but when the same equations are thrown up from a purely logical starting-point, they become evidence of the rationality of Nature. But I have laboured elsewhere this aspect of the origin of Laws of Nature.

To summarize, I must emphasize that I deny that Prof. Wilson's conclusion (that we must necessarily put $\mathbf{P}=\mathbf{V}t$ in my equations) has any basis. His arguments rest on a faulty use of 4-vector calculus; and his conclusion is incompatible with the obvious circumstance that we can contemplate a test-particle with arbitrary values of **P**, **V** at an arbitrarily chosen t.

Wadham College, Oxford.
October 1944.

XV. *Comments on Dr. Silberstein's Paper in Phil. Mag., June* 1944.

To the Editors of the Philosophical Magazine.

Gentlemen,—

Dr. Silberstein's paper in the 'Philosophical Magazine' for June 1944 on "The Accumulation of Chance Effects and the Gaussian Frequency Distribution" gives a discussion of certain integrals (equation 11) which are of importance in connection with the effect of non-linear circuits on fluctuation voltages.

It is therefore of interest to note that K. Fränz, in a paper in 'Elektrische Nachrichten-Technik,' October 1940, xvii. pp. 215–230, has discussed in detail these integrals, which he terms the "normal spectra."

He derived the discontinuous polynomial representation and also the asymptotic form whose accuracy was demonstrated numerically to be very striking even for $n=2$.

Regarding the integrals

$$P_n=\frac{2}{\pi}\int_0^\infty\left(\frac{\sin v}{v}\right)^n.dv,$$

it may be noted that these are evaluated in Whittaker and Watson's 'Modern Analysis' (4th edition, p. 123) and that the result may be written

$$P_n=\frac{1}{(n-1)\,!}\sum_{r=0}(-1)^r\binom{n}{r}\left(\frac{n}{2}-r\right)^{n-1},$$

where the upper limit of r in the summation is $\frac{n}{2}$ for n even and $\frac{n-1}{2}$ for n odd. The values given by Dr. Silberstein for P_6 and P_7 on p. 399 are in error, for they should be respectively $\frac{11}{20}$ instead of $\frac{83}{160}$ and 0·511 instead of "a little below $\frac{1}{2}$."

Yours faithfully,
R. E. Burgess.

Radio Division,
National Physical Laboratory.
December 1st, 1944.

XVI. *The Whipple Collection of Historic Scientific Instruments.*

The war in Europe moves towards its destined end, and the minds of men are turning to those problems of post-war reconstruction which urgently demand consideration and solution if our civilization is not to collapse under the burdens laid on it. Education takes a high place among these post-war problems, and the place of science in any ordered scheme of education is a matter of prime importance. Whether we like it or not—and there are those who, most emphatically, do not like it—the results of scientific discoveries play an ever increasingly important part in the shaping of the lives of men, and no scheme of education may be regarded as satisfactory which neglects the consideration of the aims and methods of science, the " how," if not the " why," of some of the multitude of phenomena which are presented to our senses in our daily lives.

These remarks are not intended to apply specially to the pupil who is training for a career in which science is designed to play a major part ; his (or her) interests are well considered in existing curricula, though even here the angle of outlook might be altered with advantage ; it is the interests of the ninety-five per cent. of the pupils in our schools who do not proceed to the universities, and of those who have embarked on a university career in some faculty other than that of science, which urgently demand attention ; and it is becoming increasingly clear that, at whatever level of teaching, primary, secondary or university, the instruction of such pupils in the aims, methods and results of science is best carried out by courses which are founded on a study of the history of science.

That being so, it is evident that science museums will play a much more important part in the educational future than they have done in the past, and any contribution to the foundation or development of such a museum is, at this stage of our national life, most welcome and timely.

Mr. R. S. Whipple, himself an eminent maker of scientific instruments, has recently presented to the University of Cambridge his magnificent collection of historic scientific instruments. The formal occasion of the presentation was the opening of an exhibition, in the East Room of the Old Schools, of a portion of the collection. The exhibition was opened on November 4th, 1944, by Sir Henry Dale, O.M., President of the Royal Society, and the exhibits remained on view for a fortnight.

Dials of all sorts and ages, astrolabes, nocturnals, orreries, armillary spheres, telescopes, microscopes, surveying and calculating instruments—these formed the main body of the exhibition, and many rare and very beautiful examples were shown. It was clear, on inspection of the collection, that the examples of each type of instrument were not chosen solely for their beauty of form or ingenuity of construction ; the word *evolution* must ever have been present in the mind of their collector. This is specially manifest in the remarkable collection of microscopes.

Which is as it should be, for if a museum of scientific instruments is to be a factor of any importance in the educational life of the community, it must be a living and a growing thing, with its constituents succinctly and clearly described (was it not Sir William Flower who said that a museum should consist of a series of labels, with specimens attached ?), and illustrating, as completely as possible, the development of an instrument from its primitive to its most modern form.

This impressive and comprehensive collection is intended to form the nucleus of a History of Science Museum which, to attain its full measure of usefulness, must be developed in close connection with a department of the History, Principles and Methods of Science, whose inception will, we trust, not long be delayed.

The donor has increased the value of his generous and timely gift by the addition of some 1,500 volumes of rare and important early books, thus forming the nucleus of that library which, itself living and growing, is an indispensable part of a living and growing museum. To give a list of either instruments or books would, by reason of space-limit, be impossible. One can but sample; and it must suffice to ask: How many libraries are likely to possess a work of such value and association as Ben Jonson's autographed copy of Gilbert's *De Magnete*? The Whipple collection has the volume; *ex uno disce omnes.*

Allan Ferguson.

XVII. *Notices respecting New Books.*

Five-figure Logarithm Tables. Published for the Ministry of Supply by H.M. Stationery Office, 1944. [Pp. 73+xx+90.] Price 7*s.* 6*d.* net.

It appears that a need has been felt for a set of five-figure tables of logarithms of numbers and of the trigonometrical functions, and the Ministry of Supply has filled the gap by producing a volume which contains reprints of tables from different sources.

If we regard existing tables of five-figure logarithms as covering the range from 1 to 10, they differ only in the fineness of the tabulation and in the provision made for interpolation. The commonest interval is 0·001, and this is adopted in the tables of Silberstein, Schlömilch, Hall and Rideal, Burington, Inman and Hoüel, among others. Chappell's tables adopt this interval for the greater part of the range, but they subdivide to a further decimal place in the part from 1 to 4, and thus keep the maximum difference down to 11. Differences are given throughout, and proportional parts in the later part of the table. This superiority has led to their selection for the present volume. The tables are printed from the stereos, and thus no new errors need be feared.

When it comes to the trigonometrical functions, the question of interval is complicated by that of units of angle. We may use the traditional degrees, minutes and seconds, or take either the right angle or the radian as unit, and use a decimal subdivision of the selected unit.

The demand among optical designers appears, however, to be for the hybrid system in which the right angle is divided into 90 degrees and these are then subdivided decimally; the only really good table on this basis is that of Bremiker, which has accordingly been reproduced here, by a photo offset process. Five-figure values of log sin and log tan are given at intervals of 0·01°, with differences and proportional parts, the latter having the useful feature of an extra decimal place. The difficulty near 0 and 90° is partially met by the inclusion of von Rohr's addition to Bremiker's table, in which values are given every 0·001° for the first and last five degrees of the quadrant. Even this, of course, does not entirely overcome difficulties at the extremes of the table, and a useful alternative might have been the inclusion of the S and T functions ($\log \sin x = \log x^\circ - S$), which Bremiker himself gave. These functions run smoothly to their limit as the angle decreases. In their absence, of course, both direct and inverse interpolation can be carried out with the ordinary logarithm table and the expansion of sin and tangent in series.

A Treatise on the Theory of Bessel Functions. By Prof. G. N. WATSON, Sc.D., F.R.S. [Pp. viii+804.] (Cambridge: University Press, Second Edition, 1944.) Price 60*s*. net.

THE second edition of this standard work differs only slightly from that of 1922. Professor Watson has not undertaken the task of including the discoveries of the last twenty years because this would mean rewriting the second half of the book. Attention has been confined to the correction of minor errors and misprints and to the emendation of a few assertions, the truth of which has changed since 1922. One of these relates to the unproven character of Bourget's conjecture (made in 1866) that, *when* ν *is a positive integer or zero, the functions* $J_\nu(z)$ *and* $J_{\nu+m}(z)$ *have no common zeros, other than the origin, for all positive integral values of m.* Except in some special cases it seems that this result was not proved before 1929 when Siegel proved that $J_\nu(z)$ is not an algebraic number when ν is rational and z is an algebraic number other than zero. From this the truth of Bourget's conjecture follows, since it is easy to show that the common zeros of $J_\nu(z)$ and $J_{\nu+m}(z)$ must be algebraic numbers.

Regarding the subject-matter, the first eleven chapters (about half the book) are devoted to an exposition of the intrinsic properties of Bessel Functions. Chapters are included on Integral Representations and Asymptotic Expansions and on functions associated with Bessel Functions (for example, the polynomials of Neumann and Lommel and the functions $\mathbf{J}_\nu(z)$ and $\mathbf{E}_\nu(z)$ defined by

$$\mathbf{J}_\nu(z) \pm i\mathbf{E}_\nu(z) = \frac{1}{\pi}\int_0^\pi e^{\pm i(\nu\theta - z\sin\theta)}\,d\theta,$$

where ν is non-integral). A chapter is devoted to Bessel Functions of large order n, which are of importance in various problems of Mathematical Physics It contains, *inter alia*, a description of the method of steepest descents. This was used by Debye to obtain integral representations which readily yield asymptotic expansions when n is large. Chapters XII., XIII. and XIV. are concerned with the evaluation of various integrals involving Bessel Functions. Infinite integrals, which are so important in Mathematical Physics, are dealt with in Chapter XIII. (nearly seventy pages in length). Chapter XV. is devoted to a study of the zeros of Bessel Functions, including the numerical calculation of these, and references are made to numerous Physical applications. In Chapters XVI. to XVIII. various series are studied. One chapter is given to Kapteyn series which arise in some astronomical problems and in the theory of Electromagnetic Radiation. Another treats the series of Fourier-Bessel which are perhaps better known amongst physicists than the Neumann series and the Schlömilch series.

In the final chapter an historical account is given of previously published Tables of Bessel Functions. This is followed by a comprehensive collection of those tables which seem to be of most value to the physicist. Those of $J_0(x)$, $Y_0(x)$, $J_1(x)$ and $Y_1(x)$ are not so complete as the corresponding British Association Tables but, on the other hand, other functions which are sometimes needed in numerical work are tabulated; for example, $J_{1/3}(x)$ and $Y_{1/3}(x)$ are tabulated to 7 decimal places over the range of values 0·00 (0·02) 16·00 for x, and short tables of $J_n(x)$ for $n=2$, 3, 4 and 5 are given over the range 0·0 (0·1) 5·0. The Fresnel integrals

$$\frac{1}{2}\int_0^x J_{-\frac{1}{2}}(t)\,dt \quad \text{and} \quad \frac{1}{2}\int_0^x J_{\frac{1}{2}}(t)\,dt$$

are tabulated over the ranges 0·00 (0·02) 1·00 and 1·0 (0·5) 50·0. The values of $J_n(n)$ and $Y_n(n)$ are given for $n=1, 2, 3, \ldots, 50$, and the numerical values of the zeros of various Bessel Functions are tabulated.

The printing of the book, by the photo-offset process, is clear and the paper is as good as can be expected in these austere times. Nevertheless, it has not the finish one would expect in times of peace and it does seem a real pity that high quality paper has not been made available for the printing of such important and permanent books as the one under review. L. S. GODDARD.

Mathematical Tables and Other Aids to Computation. Edited by R. A. ARCHIBALD and D. H. LEHMER. Vol. 1, No. 7 (July 1944) and No. 8 (October 1944). [Pp. 104 and 28 respectively.] (Published by the National Research Council, Lancaster, Pa., and Washington, D.C.) Price of No. 7, $1.75; of No. 8, $1.00.

NUMBER 8 of this useful publication is of the type to which we are becoming accustomed, with articles on recent tables, on errata, and on unpublished tables.

Number 7 is a special number, for which many workers have been waiting a long time. It lists all tables of Bessel functions known to its compilers, H. Bateman and R. A. Archibald, and vastly increases its usefulness by copious explanatory notes and expository sections. Beginning with the most familiar functions, it lists 39 tables of J_0 and J_1; it then proceeds to list tables of either J_0 or J_1 and such functions of them as $\log J_0(x)$, $J_0(\pi x)$, $1-J_1(2x)/x$. Then follow tables of the zeros of J_0 and J_1 and functions related to these zeros. Next we have functions of $J_n(x)$, where n is not restricted to the values 0 and 1; there are 34 such tables in the list, which is again followed by those of related functions and of zeros.

After dealing thus thoroughly with the functions of the first kind, the guide proceeds to those of the second kind. Here a useful introduction clarifies the tangled web of nomenclature which has been woven by various writers in the past. The letter Y is adopted for Weber's form of the function, in conformity with the usage in Watson's Treatise and in the B.A. Mathematical tables. The function $-\pi Y_n/2$ is called G_n, so that G_n is the same as that used by Gray and Matthews and is Heine's K_n.

The next section lists the functions $I_n(x)=i^{-n}J_n(ix)$ and the corresponding function of the second kind, $K_n(x)$, with the Hankel functions. The ber and bei functions occur much later in the book, which contains altogether 13 sections, of which the above summarizes only the first three.

Most of the references included in the guide are to tables actually calculated and first published by the authors cited, and it is not clear how far it is intended to quote tables which are merely reprinted. References from Jahnke and Emde and from Dale are included, so it is perhaps by an oversight that the tables of J_0 and J_1 and the small table of G_0 in Bell's 'Mathematical Tables' (Silberstein, 1922) have been omitted.

The Bessel functions present themselves in so many branches of physics, and tables relating to them are consequently so scattered, that a guide such as this must be of frequent value to every mathematical physicist, and, even if there are a few omissions, it will save many people from computing tables which they believe to be required, when, in fact, they are already in existence.

J. H. A.

What is Life? By ERWIN SCHRÖDINGER. [Pp. viii+91.] (Cambridge University Press, 1944.) Price 6*s*.

IN spite of the variety of topics, physical and biological, which are surveyed in this book, it is intended, like the course of public lectures from which it arose, "to convey one idea only—one small comment on a large and important question," that question being, "How can the events in space and time which take place within the spatial boundary of a living organism be accounted for by physics and chemistry ?" The comment explicitly indicated is that "the obvious inability of present-day physics and chemistry to account for such events is no reason at all for doubting that they can be accounted for by those sciences." There is, however, a great deal more than would be suggested by this particular comment, as may perhaps best be conveyed by summarizing some of the main lines of thought running through the book.

The orderly working of an organism, it is maintained, requires exact physical laws. From a classical standpoint the exactness might have seemed attainable on the basis of the ordinary laws of physics, which are almost invariably statistical, being an expression of the order arising from atomic disorder. Although the precision of these statistical laws decreases with decrease in the number of atoms involved, it might well have been argued some forty years ago that the number of atoms involved in any observed physiological process, the number even in a single cell, was amply large enough to ensure the required degree of exactness in the statistical laws. Investigations on genetics, however, particularly on the cytological side, have shown conclusively that relatively small groups of atoms play a dominating rôle in connection with the orderliness of the organism. These small groups are the parts or sections of the chromosomes, the "genes," with which can be associated definite hereditary characteristics of the organism. Various direct and indirect methods of estimating the effective size of genes, including the study of mutations induced by X-rays, lead to the conclusion that the number of constituent atoms lies in the range from a few thousand to a few million, a number far too small, if the atoms are in any sense independent individuals, to ensure that degree of uniformity in statistical behaviour which is required. The physical aspect of the situation leaves no other possibility of accounting for the permanence of hereditary characteristics, as localized in the genes, but to suppose, following the hypothesis of Delbrück, that genes are in fact huge molecules, in which the atoms are stably organized into the more complex structures. Although there is nothing new in the idea of large molecules, a physical understanding of the formation of stable molecules has become possible only through quantum mechanics, as has also the essentially discontinuous character of changes of molecular configuration. The identification of the basic mechanism of a mutation with the jump-like transition of a molecule from one isomeric form to another finds strong support from the biological evidence on both spontaneous and induced mutations.

In the light of present knowledge a molecule, a solid, and a crystal are virtually the same. Starting from a small molecule there are two ways of building up larger associations, one by the formation of periodic aggregates, which have been so extensively studied in physics, the other without using "the dull device of repetition." It is the second method which seems to be of such high biological significance. Schrödinger expresses his essential hypothesis by saying, "We believe a gene—or perhaps the whole chromosome fibre—to be an aperiodic solid."

Living matter, while not eluding the known laws of physics, is likely to involve other laws, still physical, but as yet unknown. The remarkable characteristic of a living organism, in the orderly unfolding of life, is that it avoids rapid decay into the inert state of equilibrium. Orderly events can arise from a "statistical mechanism" which produces order from disorder; for life, a new mechanism is required which produces order from order—the organism feeds on negative entropy. Order from order is not alien to physics, for it is characteristic of pure mechanism, but such resemblances as there are between a clockwork and an organism are much less striking than the fundamental differences.

Schrödinger's outlook on the physical aspect of the living cell is then, in briefest outline, as follows. In the physico-chemical interpretation of living matter, quantum mechanics is fundamental, though quantum indeterminacy, which has often been invoked, plays only an insignificant rôle. The physical scheme, however, is still inadequate. There are laws of the functioning of living matter yet to be discovered concerned with the production of order from order, laws different from those which are familiar, because the structure of living matter, particularly the aperiodic solid of the chromosome, is different from those material structures which hitherto have been almost exclusively the subject of physical investigation.

This indeed goes only a very small way towards answering the question of the book's title. Even in the immediate field of discourse there is no hint of an explanation of the remarkable phenomena involved in cell division, in mitosis and meiosis. But it is as a clear statement, in narrow compass, of the problem of living matter reduced to its simplest terms that the book will be valued; the presentation of the relevant physical and biological facts, and the exposition of the leading ideas are admirable. For the rest, a sketch is given of a way of looking at things which may help towards clearer understanding. And if the attitude, to some, seems too deterministic, an epilogue on free will and determinism gives a personal confession of an almost mystic faith which suggests that, to the author, a physico-chemical interpretation of life would never be more than one side of the story. E. C. S.

From Atoms to Stars. By Martin Davidson, D.Sc., F.R.A.S. [Pp. 188.] (Hutchinson's Scientific and Technical Publications.) Price 15*s*.

The author of a popular book on astronomy has a choice between obtaining the awed admiration of his reader by making play with the vastness of the distances and times with which his science deals, or trying to give the reader a notion of the arguments by which we conclude that these multi-ciphered numbers do represent reality. Dr. Davidson has chosen the harder—and far more valuable—course, and has attained great success.

Knowing that a description of the experimental work will lead to the conclusion that white dwarfs have densities thousands of times greater than any materials known to us, and that the search for an explanation of stellar energy will involve an appeal to nuclear chemistry, the author opens his book with a chapter on atomic physics. This may be of help to some readers, though it is hardly up to the standard of the rest of the book; in particular, there is a tendency to state facts (*e. g.*, that the masses of the neutron and proton are approximately equal) without any attempt to explain why we believe them.

The remainder of the book is astronomical, and is fascinatingly written. There is no description of the Heavens as observed from the earth, or of how to identify particular constellations, but there is an excellent account of the galactic system, and how it has been mapped, as also of the wider stellar universe. Preceding this is a good account of the solar system, with due attention paid to planetary temperatures (deduced from the heat balance, and not from observations).

In dealing with the stars themselves, all that is important in modern theory seems to be touched on. The effects of radiation pressure are described, the mass-luminosity relation is introduced and its applications well explained, and the current theory of stellar evolution is expounded.

The book is well produced (exceptionally so for war time) and is one to be highly recommended.

Sound Insulation and Acoustics. [Pp. 80.] (London : H.M. Stationery Office.) Price 1*s*. net.

The brochure under review is No. 14 in a series of post-war building studies, and has been produced under the ægis of the Ministry of Works by the Acoustics Committee of the Building Research Board of the Department of Scientific and Industrial Research. This Committee, composed mainly of architects leavened by a few physicists, was charged with the duty of reviewing existing scientific information on the sound insulation and acoustics of buildings, with making recommendations for post-war building practice, and with indicating the need for any further research. The Committee has performed its task well and recorded its findings in this easily comprehended report comprising four parts (headed respectively Sound Insulation, Acoustics of Auditoria, Proposals for Future Research and Investigation, and A Summary of Standards and Treatments for Sound Insulation and Acoustics) and six appendices, one of which, on Sound Transmission through Timber Floors, contains the results of previously unpublished work. While the reviewer cannot help wondering how nearly field measurements support the suggestion that an intensity reduction of 6 db. occurs every time the distance from a source (such as a bus) is doubled, he has no hesitation in asserting that the report will repay the study of those who cherish the hope that quietude may have some place in the brave new post-war world. E. J. I.

An Introduction to Differential Equations. By S. L. Green, M.Sc. [Pp. 138.] (London : University Tutorial Press, Ltd., Clifton House, Euston Road, N.W. 1. 1945. Price 7*s*. 6*d*.)

The author, who is lecturer in Mathematics at Queen Mary College, London, states that his book is intended to meet the needs of students reading for the Pass, and General and Special Honours Degrees of the Universities in Arts, Science and Engineering. If this list is not to be read as including those who will take honours in mathematics, the intention seems to be well fulfilled. The commonest types of ordinary differential equation are treated, together with the simpler partial differential equations, and there is a little on total equations and on systems of equations.

The problem of solution in power series is left to the last chapter, and is particularly well done. It is satisfying to find an elementary treatment which at once extends the problem to the domain of complex numbers, so that it is from the beginning possible to explain precisely the nature of ordinary points and of regular points. Without this, the reasons why expansions can be established for some but not for others must of necessity be obscure. Another matter on which the author is to be congratulated is his treatment of the Laplace equation, particularly in two dimensions, where he shows clearly how the method of conjugate functions arises naturally.

There is a chapter on geometrical applications, but we do not find here anything about envelopes, which are presumably beyond the scope of the author's design ; in fact, the only reference to singular solutions is in connection with Clairaut's form. Other matters which lie outside the scope of the book are numerical methods, the method of variation of parameters, and Jacobi's and Monge's methods for partial differential equations.

The book is, of course, " produced in complete conformity with the authorized economy standards," and this no doubt is responsible for the poor paper and for the small type, which makes it difficult in places to decipher whether an exponent is a 2 or a 3, and whether a letter carries a dot over it.

There are probably a few slips, excusable in the first edition of a mathematical work, but the only ones I have found were revealed by working out the miscellaneous exercises, in which No. 3 has a negative sign which should be positive, and the answer to No. 26 has $\frac{3x^4}{7}$, which should be $\frac{3x^4}{11}$.

J. H. A.

The Velocity of Light. By N. Ernest Dorsey. Transactions of The American Philosophical Society, vol. xxxiv. pt. 1. Price $2.25.

Since the publication of Clerk Maxwell's electromagnetic theory the determination of the velocity of light *in vacuo*, with all the precision that may be attainable, has been the ambition of some of the most distinguished experimentalists—the great Michelson among others. The importance of an accurate knowledge of the propagation of Light, and especially of its velocity, has increased since the advent of the theory of relativity. Both theory and observation indicate that there is no dispersion *in vacuo*—so that phase and group velocity are identical—and further that the velocity of light *in vacuo* is the upper limit for the velocity of a massive particle, or the velocity of convection of convected energy. According to existing theory (special theory of relativity) this velocity has a unique value, independent of which one of any number of coordinates systems, moving relatively to one another with constant velocities, it may be referred to (confirmed by the interferometer experiments of Michelson and his associates, with the exception of Miller). It is therefore rather disconcerting to hear of the suggestion of a secular variation of the velocity of light. and indeed a rather superficial examination of the results of the long sequence of measurements is apt to evoke this suggestion.

The author of the present work, D. Ernest Dorsey, was at first concerned, as he tells us, with the objective value of the data on which the suggestion of a possible secular variation of the velocity of light *in vacuo* rests ; but later expanded the scope of his work "to arrive at an objective estimate of the accuracy that might validly be ascribed to the work covered by each of the reports" ; *i. e.* the reports of measurements made by Fizeau, Foucault, Cornu, Newcomb, Michelson and the still more recent ones mentioned below. The author has devoted much care and labour to this investigation and comes to the final conclusion that "the data give no indication of any secular change in the velocity of light." The obvious competence and thoroughness manifested in the work will probably convince most of those who study it that this final conclusion is the only one compatible with the available data. Dorsey thinks it "probable that the best value that can be derived from the data now available is

Velocity of light in a vacuum $299{\cdot}77_3$ km./sec.
Dubiety *, perhaps, but probably less than 1_0 km./sec.

This final value is derived from the reports of

Michelson, Pease and Pearson, 1935.
Karolus and Mittelstaedt, 1929.
Anderson, 1937.
Anderson, 1941.
Hüttel, 1940.

---

* The author defines "dubiety," as also all or most of the other technical terms he uses, with clarity and precision.

The general plan of the work includes a section on the theory of errors, method of least squares, averaging, etc. This is followed by a study of the work of Fizeau, Foucault and Cornu and his associates. Then comes a similar study of the work of Newcomb and of Michelson and his collaborators, who used the rotating mirror (which method, the present reviewer believes, was first suggested by Fizeau, who was prevented by death from carrying it out). Then come Karolus and Mittelstaedt, Anderson and Hüttel, all of whom used what were virtually toothed-wheel methods much elaborated and endowed with immensely greater precision in the measurements of distances and times —the toothed wheel being replaced by inertialess devices, *i. e.* modulation of the beam of light by Kerr cells.

There are two appendices, one of them, which is entitled "Experimental Methods for Determining the Velocity of Light," being of very great merit. An interesting point is raised in the final paragraph of this appendix: the method of Karolus and Mittelstaedt "differs from Fizeau's in that the light between the [Kerr] cells does not consist of a series of discontinuous groups of waves, but of an uninterrupted pencil of light, of which the polarization varies continuously and periodically from plane to elliptical and to plane again, but of which the intensity does not undergo periodic fluctuations." Dorsey thinks it probable that the velocity measured in this case is the *phase* velocity, while Anderson would pronounce it to be the *group* velocity. This interesting question cannot be discussed here; but the present reviewer thinks there are compelling grounds for the view that *all* the methods discussed so ably by the author yield the *group* velocity. WM. WILSON.

[*The Editors do not hold themselves responsible for the views expressed by their correspondents.*]

FIG. 3*a*.

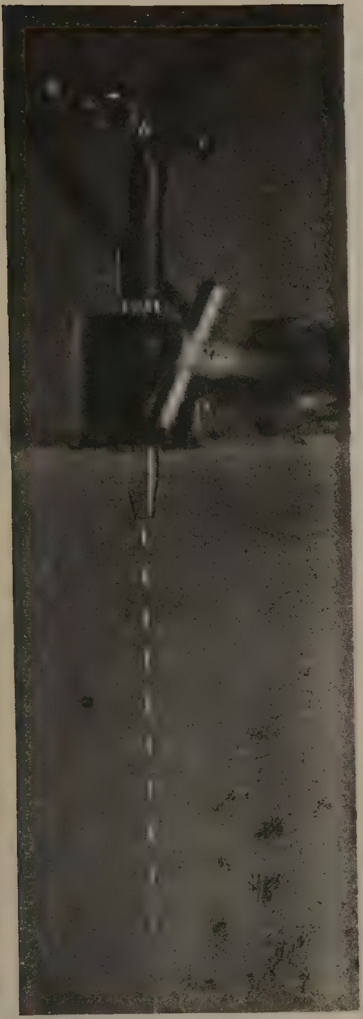

FIG. 3*b*.

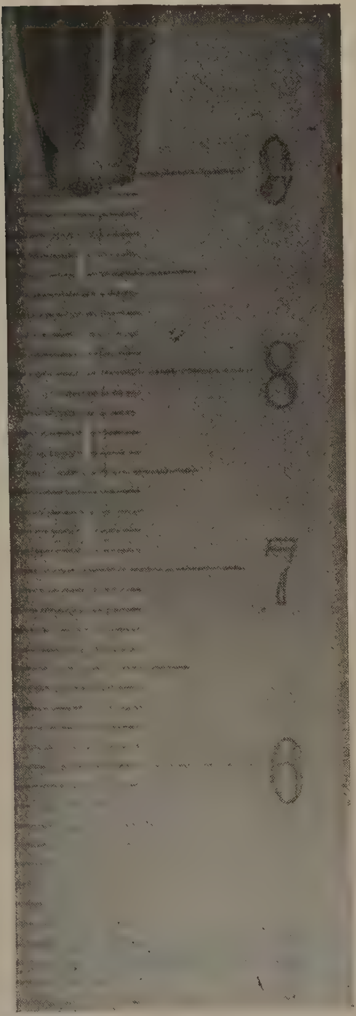

FIG. 3*c*.

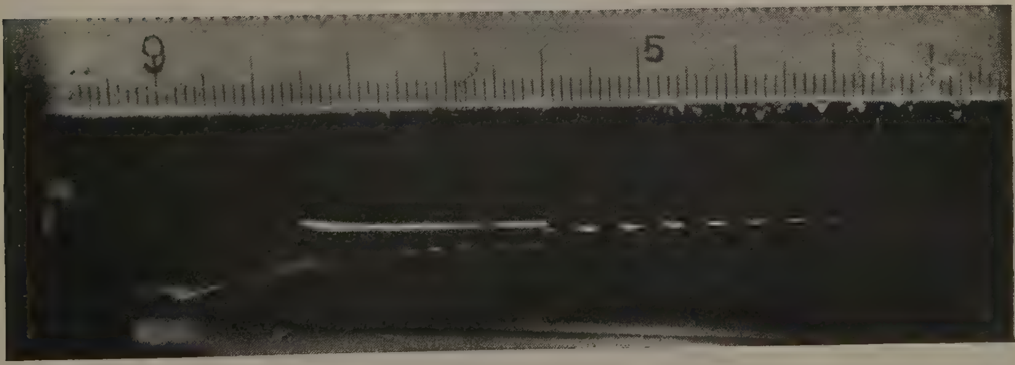

XVIII. *Ten Two-Dimensional Electrostatic Problems.*

By N. Davy, University College, Nottingham *.

[Received May 11, 1945.]

Abstract.

Ten different two-dimensional electrostatic problems, seven of which involve semi-infinite rectangular electrodes, are solved. The Schwarz-Christoffel method is used in all cases except the last. Only the results, with the necessary explanations, are given. These results include (1) the transformations, (2) the field strengths, (3) the surface densities at points on electrodes, (4) the total charges on parts of electrodes, (5) the capacities between parts of electrodes, and (6) expressions proportional to the forces on small para- or diamagnetic bodies at any point in the field. Elliptic functions are used in seven cases. Diagrams showing equipotentials obtained experimentally are shown. As usual, the results apply to magnetism, hydrodynamics, heat flow, electric current flow, and other branches of physics.

§ 1. *Introduction.*

Nine electrostatic problems are solved by the Schwarz-Christoffel method, and one by starting with a given equation of transformation. Since the method has been used before, only a summary of results is given in the first nine cases. In each, the section of the electrode or electrodes concerned is represented first in a z-plane. A transformation is found, whereby a line forming parts of the edges of the electrodes and one or more lines of force becomes the real axis in the t-plane. Another transformation links t with $W=U+iV$, where V and U are the potential and stream function, respectively, or *vice versa*. From W are calculated the various electrical quantities of interest, viz. the electric intensity or field strength F, the surface density σ, the total charge Q per cm. depth on any part of an electrode, and the capacity C per cm. depth between corresponding parts of two electrodes. In a magnetic system the force per gram on a small para- or diamagnetic body is $\frac{(\chi_2-\chi_1)}{2}\frac{dF^2}{dz}$, where χ_1 and χ_2 are the mass susceptibilities of the body and of the surrounding medium, respectively, and F is now the magnetic field, the electrodes now being regarded as polepieces. Here only values of $\frac{dF^2}{dz}$ are quoted in each case. Experimentally obtained equipotential diagrams are exhibited at the end of each section.

---

* Communicated by Professor L. F. Bates, D.Sc.

§ 2. *Semi-Infinite Rectangular Electrode at Potential* V_0, *in line with a Semi-Infinite Thin Plate at Potential Zero.*

Fig. 1.

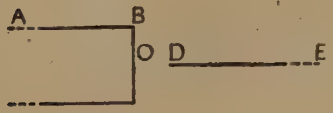

Fig. 2.

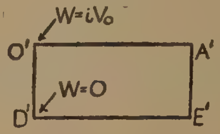

Fig. 1 represents the z-plane. The width of the semi-infinite electrode is $2a$ cm., and the width of the gap OD is b cm. The line ABODE is to be transformed into the real axis of t.

Table I. (See fig. 1.)

Point.	A.	B.	O.	D.	E.
z	$-\infty+ia$	ia	0	$+b$	$+\infty$
t	$-\infty$	-1	0	$+\alpha$	$+\infty$

Transformations.

$$dz=\frac{C_1.dt.(t+1)^{\frac{1}{2}}}{t^{\frac{1}{2}}},\quad t=\sinh^2\phi.$$

$$z=2C_1\{\sinh\phi.\cosh\phi+\phi\}+C_2.$$

$$C_2=0,\quad C_1=\frac{a}{\pi}.$$

$$z=\frac{2a}{\pi}\{t^2(1+t)^{\frac{1}{2}}+\sinh^{-1}t^{\frac{1}{2}}\}.$$

$$\alpha=\frac{-1+\left(1+\frac{2\pi b}{a}\right)^{\frac{1}{2}}}{2},$$

omitting the negative value as not wanted.

(See fig. 2.) $$dW=\frac{C_3.dt}{t^{\frac{1}{2}}(t-\alpha)^{\frac{1}{2}}},\quad t=\alpha\cosh^2\theta.$$

$$W=2C_3\theta+C_4,\quad C_4=0,\quad C_3=\frac{V_0}{\pi}.$$

$$W=\frac{2V_0}{\pi}\cosh^{-1}\left(\frac{t}{\alpha}\right)^{\frac{1}{2}},\quad t=\alpha\cosh^2\frac{\pi W}{2V_0}.$$

$$F=\left|\frac{dW}{dz}\right|=\left|\frac{C_3}{C_1(t-\alpha)^{\frac{1}{2}}(t+1)^{\frac{1}{2}}}\right|.$$

$$\sigma=\frac{F}{4\pi}=\left|\frac{C_3}{4\pi C_1(t-\alpha)^{\frac{1}{2}}(t+1)^{\frac{1}{2}}}\right|.$$

$$Q=\left|\frac{W_2-W_1}{4\pi}\right|=\frac{V_0}{2\pi^2}\left|\left\{\cosh^{-1}\left(\frac{t_2}{\alpha}\right)^{\frac{1}{2}}-\cosh^{-1}\left(\frac{t_1}{\alpha}\right)^{\frac{1}{2}}\right\}\right|.$$

$$Q_{AB}=\infty. \qquad Q_{BO}=\frac{V_0}{2\pi^2}\left|\left\{\cosh^{-1}\left(\frac{-1}{\alpha}\right)^{\frac{1}{2}}-\frac{i\pi}{2}\right\}\right|.$$

Effective capacity of the end per cm. depth

$$=\frac{V_0}{\pi^2}\left|\left\{\cosh^{-1}\left(\frac{-1}{\alpha}\right)^{\frac{1}{2}}-\frac{i\pi}{2}\right\}\right|.$$

$$\frac{dF^2}{dz}=-\frac{\pi V_0{}^2t^{\frac{1}{2}}(2t+1-\alpha)}{a^3(t-\alpha)^2(t+1)^{5/2}}.$$

Equipotentials are shown in fig. 3.

Fig. 3.

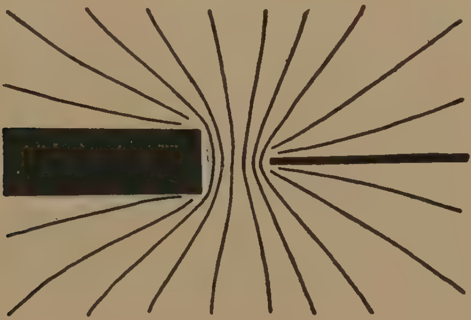

§ 3. *Semi-Infinite Rectangular Conductor at Potential* V_0 *in line with a Finite Thin Plate at Potential Zero.*

Fig. 4.

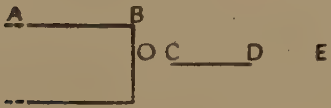

Fig. 5.

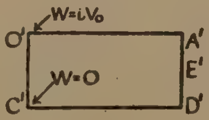

Fig. 4 represents the z-plane. The width of the semi-infinite electrode is $2\,a$ cm. The width of the gap OC is b cm., and the length of the finite plate is $c-b$ cm. The line ABOCDE is to be transformed into the real axis of t.

Table II.

Point.	A.	B.	O.	C.	D.	E.
t	$-\infty$	-1	0	k^2	α^2	$+\infty$
z ...	$-\infty+ia$	$+ia$	0	$+b$	$+c$	$+\infty$

Transformations. (See fig. 4.)

$$dz=\frac{C_1(t+1)^{\frac{1}{2}}.dt}{t^{\frac{1}{2}}},\quad t=\sinh^2\phi.$$

$$z=C_1\{\sinh\phi.\cosh\phi+\phi\}+C_2.$$

$$C_1=\frac{2a}{\pi},\quad C_2=0,\quad z=\frac{2a}{\pi}\{t^{\frac{1}{2}}(1+t)^{\frac{1}{2}}+\sinh^{-1}t^{\frac{1}{2}}\}.$$

k is obtained from $$b=\frac{2a}{\pi}\{k(1+k^2)^{\frac{1}{2}}+\sinh^{-1}k\}.$$

α is obtained from $$c=\frac{2a}{\pi}\{\alpha(1+\alpha^2)^{\frac{1}{2}}+\sinh^{-1}\alpha\}.$$

(See fig. 5.)

$$dW=\frac{C_3\,dt}{t^{\frac{1}{2}}(t-k^2)^{\frac{1}{2}}(t-\alpha^2)^{\frac{1}{2}}},\quad t=\frac{1}{\mathrm{sn}^2\,(u,\,k)},\quad \mathrm{sn}\,u=s,\ \mathrm{cn}\,u=c.$$

$$\mathrm{dn}\,u=d,\quad dt=-\frac{2c.d.du}{s^3},\quad dW=-\frac{2C_3c.du}{(1-\alpha^2s^2)^{\frac{1}{2}}}.$$

$$W=-\frac{2C_3}{\alpha}\mathrm{sn}^{-1}\left(\frac{\alpha}{t^{\frac{1}{2}}},\ \frac{k}{\alpha}\right)+C_4,\quad C_3=\frac{i\alpha V_0}{2K},\quad C_4=iV_0.$$

Note that K is to modulus $\frac{k}{\alpha}$.

$$F=\left|\frac{dW}{dz}\right|=\left|\frac{C_3}{C_1(t+1)^{\frac{1}{2}}(t-k^2)^{\frac{1}{2}}(t-\alpha^2)^{\frac{1}{2}}}\right|.$$

$$\sigma=\frac{F}{4\pi}.\quad Q=\left|\frac{W_2-W_1}{4\pi}\right|=\left|\frac{C_3}{2\pi\alpha}\left\{\mathrm{sn}^{-1}\left(\frac{\alpha}{t_1^{\frac{1}{2}}},\ \frac{k}{\alpha}\right)-\mathrm{sn}^{-1}\left(\frac{\alpha}{t_2^{\frac{1}{2}}},\ \frac{k}{\alpha}\right)\right\}\right|,$$

$$Q_{OB}=\left|\frac{C_3}{2\pi\alpha}\mathrm{sn}^{-1}\left(i\alpha,\ \frac{k}{\alpha}\right)\right|.$$

Total charge per cm. on the end $=2Q_{OB}$.

Total charge on each electrode $=2Q_{CD}=\frac{K'V_0}{2\pi K}$.

Capacity per cm. between the electrodes $=\frac{K'}{2\pi K}$.

Resistance per cm. between the electrodes $=\frac{\rho}{4\pi C}=\frac{\rho K}{2K'}$,

where ρ is the resistivity of the medium in the gap. K and K′ are both to modulus $\frac{k}{\alpha}$.

$$\frac{dF^2}{dz}=-\frac{C_3{}^2t^{\frac{1}{2}}}{C_1{}^3(t+1)^{3/2}(t-k^2)(t-\alpha^2)}\left\{\frac{1}{t+1}+\frac{1}{t-k^2}+\frac{1}{t-\alpha^2}\right\}.$$

Equipotentials are shown in fig. 6.

Fig. 6.

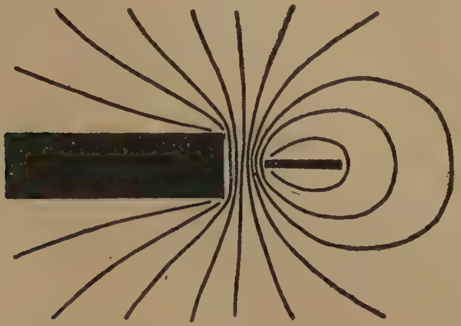

§ 4. *Single Semi-Infinite Rectangular Electrode with a Thin Finite Central Projecting Plate at Potential* V_0.

Fig. 7.

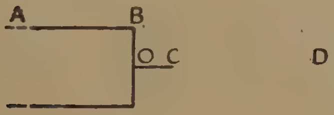

Fig. 8.

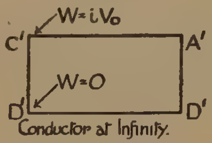

(See fig. 7.) The semi-infinite electrode is of width $2a$ and the length of the projection is b. The line ABOCD is to be transformed into the real axis in the t-plane.

TABLE III.

Points.	A.	B.	O.	C.	D.
t	$-\infty$	-1	0	α^2	$+\infty$
z	$-\infty+ia$	$+ia$	0	$+b$	$+\infty$

Transformations. (See fig. 7.)

$$dz=\frac{C_1 dt(t+1)^{\frac{1}{2}}}{t^{\frac{1}{2}}}, \quad t=\sinh^2\theta.$$

$$z=C_1\{\sinh\theta.\cosh\theta+\theta\}+C_2, \quad C_1=\frac{2a}{\pi}, \quad C_2=0.$$

$$z=\frac{2a}{\pi}\{t^{\frac{1}{2}}(1+t)^{\frac{1}{2}}+\sinh^{-1}t^{\frac{1}{2}}\}.$$

α is obtained from

$$b=\frac{2a}{\pi}\{\alpha(1+\alpha^2)^{\frac{1}{2}}+\sinh^{-1}\alpha\}.$$

$$dW=\frac{C_3 . dt}{(t-\alpha^2)^{\frac{1}{2}}},\quad W=2C_3(t-\alpha^2)^{\frac{1}{2}}+C_4,\quad C_4=iV_0.$$

$$W=2C_3(t-\alpha^2)^{\frac{1}{2}}+iV_0,\quad C_3 \text{ is indeterminate.}$$

$$F=\left|\frac{dW}{dz}\right|=\left|\frac{C_3 t^{\frac{1}{2}}}{C_1(t+1)^{\frac{1}{2}}(t-\alpha^2)^{\frac{1}{2}}}\right|,\quad \sigma=\frac{F}{4\pi}.$$

$$Q=\left|\frac{W_2-W_1}{4\pi}\right|=\left|\frac{C_3}{2\pi}\{(t_2-\alpha^2)^{\frac{1}{2}}-(t_1-\alpha^2)^{\frac{1}{2}}\}\right|.$$

$$Q_{BO}=\left|\frac{C_3}{2\pi}\{i(1+\alpha^2)^{\frac{1}{2}}-i\alpha\}\right|=\frac{C_3}{2\pi}\{(1+\alpha^2)^{\frac{1}{2}}-\alpha\}.$$

$$Q_{OC}=\left|\frac{C_3 i\alpha}{2\pi}\right|=\frac{C_3\alpha}{2\pi}.$$

Total charge on the end including the projection $=2Q_{BC}=\dfrac{C_3(1+\alpha^2)^{\frac{1}{2}}}{\pi}$.

Effective capacity of the end only $=\dfrac{C_3(1+\alpha^2)^{\frac{1}{2}}}{\pi V_0}$.

$$\frac{dF^2}{dz}=-\frac{C_3{}^2 t^{\frac{1}{2}}(t^2+\alpha^2)}{C_1{}^3(t+1)^{3/2}(t-\alpha^2)}.$$

Equipotentials are shown in fig. 9.

Fig. 9.

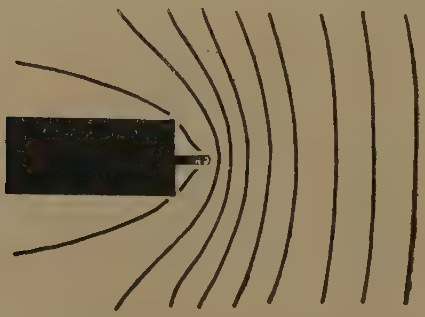

§ 5. *Semi-Infinite Rectangular Electrode with a Thin Central Finite Projecting Plate at Potential* V_0 *in line with a Semi-Infinite Thin Plate at Potential Zero.*

Fig. 10.

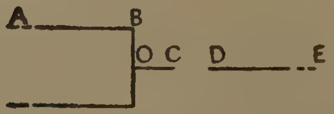

F. 11.

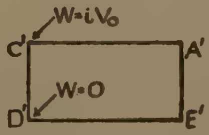

(See fig. 10.) The semi-infinite conductor is of width $2a$ cm., the length of the projection is b cm., and the width of the gap is $c-b$ cm. The line ABOCDE is to be transformed into the real axis in the t-plane,

TABLE 4.

Points.	A.	B.	O.	C.	D.	E.
t	$-\infty$	-1	0	$+k^2$	$+\alpha^2$	$+\infty$
z	$-\infty+ia$	$+ia$	0	$+b$	$+c$	$+\infty$

Transformations. (See fig. 10.)

$$dz=\frac{C_1 dt.(t+1)^{\frac{1}{2}}}{t^{\frac{1}{2}}},\quad t=\sinh^2\phi.$$

$$z=C_1\{\sinh\phi.\cosh\phi+\phi\}+C_2,\quad C_1=\frac{2a}{\pi},\quad C_2=0.$$

$$z=\frac{2a}{\pi}\{t^{\frac{1}{2}}(1+t)^{\frac{1}{2}}+\sinh^{-1}t^{\frac{1}{2}}\}.$$

k is obtained from $b=\frac{2a}{\pi}\{k(1+k^2)^{\frac{1}{2}}+\sinh^{-1}k\}.$

α is obtained from $c=\frac{2a}{\pi}\{\alpha(1+\alpha^2)^{\frac{1}{2}}+\sinh^{-1}\alpha\}.$

(See fig. 11.) $dW=\frac{C_3.dt}{(t-k^2)^{\frac{1}{2}}(t-\alpha^2)^{\frac{1}{2}}}.$

$$W=2C_3\log\{(t-k^2)^{\frac{1}{2}}+(t-\alpha^2)^{\frac{1}{2}}\}+C_4.$$

$$C_3=\frac{V_0}{\pi},\quad C_4=-\frac{2V_0}{\pi}\log(\alpha^2-k^2)^{\frac{1}{2}},\quad W=\frac{2V_0}{\pi}\log\left\{\frac{(t-k^2)^{\frac{1}{2}}+(t-\alpha^2)^{\frac{1}{2}}}{(\alpha^2-k^2)^{\frac{1}{2}}}\right\}.$$

$$F=\left|\frac{dW}{dz}\right|=\left|\frac{C_3 t^{\frac{1}{2}}}{C_1(t-k^2)^{\frac{1}{2}}(t-\alpha^2)^{\frac{1}{2}}}\right|,\quad \sigma=\frac{F}{4\pi}.$$

$$Q=\left|\frac{W_2-W_1}{4\pi}\right|=\left|\frac{V_0}{2\pi^2}.\log\left\{\frac{(t_2-k^2)^{\frac{1}{2}}+(t_2-\alpha^2)^{\frac{1}{2}}}{(t_1-k^2)^{\frac{1}{2}}+(t_1-\alpha^2)^{\frac{1}{2}}}\right\}\right|.$$

$$Q_{BC}=\frac{V_0}{2\pi^2}\log\left\{\frac{(1+k^2)^{\frac{1}{2}}+(1+\alpha^2)^{\frac{1}{2}}}{(\alpha^2-k^2)^{\frac{1}{2}}}\right\},\quad Q_{OC}=\frac{V_0}{2\pi^2}\log\frac{(k+\alpha)}{(\alpha^2-k^2)^{\frac{1}{2}}}.$$

Total charge on the end of the rectangular conductor, including the projection is

$$2Q_{OC}=\frac{V_0}{\pi^2}\log\frac{(k+\alpha)}{(\alpha^2-k^2)^{\frac{1}{2}}}.$$

Capacity per cm. depth between the end of the rectangular conductor and the corresponding part of the semi-infinite plate is

$$C_1=\frac{1}{\pi^2}\log\frac{(1+k^2)^{\frac{1}{2}}+(1+\alpha^2)^{\frac{1}{2}}}{(\alpha^2-k^2)^{\frac{1}{2}}}.$$

$$\frac{dF^2}{dz}=\frac{C_3{}^2t^{3/2}}{C_1{}^3(t-k^2)(t-\alpha^2)(t+1)^{\frac{1}{2}}}\left\{\frac{1}{t}-\frac{1}{t-k^2}-\frac{1}{t-\alpha^2}\right\}.$$

Equipotentials are shown in fig. 12.

Fig. 12.

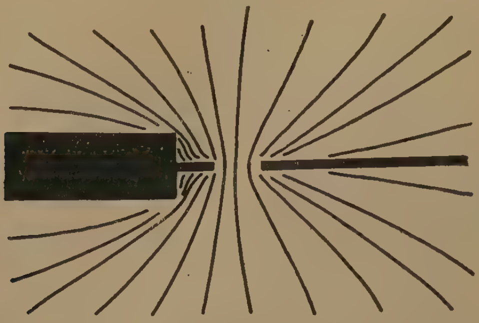

§ 6. *Two Equal Semi-Infinite Rectangular Conductors with Thin Finite Central Projecting Plates at Equal and Opposite Potentials facing each other. (Or One such Conductor at Potential* V_0 *facing an Infinite Plane Conductor at Potential Zero.)*

Fig. 13.

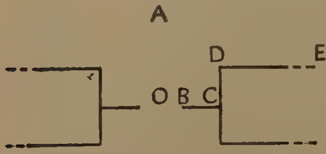

Fig. 14.

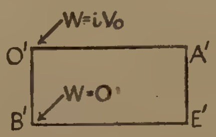

(See fig. 13.) Each rectangular conductor is of width $2a$ cm., the length of each projecting plate is $b-c$ cm., and the width of the gap is $2c$ cm. Noting that the central plane of symmetry is an equipotential, the line AOBCDE is transformed into the real axis in the t-plane.

Table V.

Points.	A.	O.	B.	C.	D.	E.
t	$-\infty$	0	α^2	k^2	$+1$	$+\infty$
z	$+i\infty$	0	$+c$	$+b$	$b+ia$	$+\infty$

Transformations. (See fig. 13.)

$$dz=\frac{C_1(t-1)^{\frac{1}{2}}\,dt}{t^{\frac{1}{2}}(t-k^2)^{\frac{1}{2}}},\quad t=\frac{1}{\operatorname{sn}^2(u,k)}.$$

$$\operatorname{sn} u=s,\quad \operatorname{cn} u=c,\quad \operatorname{dn} u=d,\quad dz=-C_1\frac{c^2}{s^2}\,\mathrm{dn}.$$

$$z=C_1\left\{\frac{Eu}{K}+Z(u)+\frac{\operatorname{cn} u\,.\operatorname{dn} u}{\operatorname{sn} u}\right\}+C_2$$

in terms of Jacobian elliptic functions.

$$C_1=\frac{aK}{\frac{\pi}{2}-EK'},\quad C_2=b+ia+\frac{aEK}{\frac{\pi}{2}-EK'}.$$

k is obtained from

$$b=C_1\left\{\frac{E(K+iK')}{K}-\frac{i\pi}{2K}\right\}+C_2, \text{ using tables.}$$

α is obtained from

$$c=C_1\left\{\frac{Eu_1}{K}+Z(u_1)+\frac{\operatorname{cn} u_1 . \operatorname{dn} u_1}{\operatorname{sn} u_1}\right\}+C_2,$$

where $\operatorname{sn} u_1=\frac{1}{\alpha}$.

(See fig. 14.) $dW=\frac{C_3 . dt}{t^{\frac{1}{2}}(t-\alpha^2)^{\frac{1}{2}}}$, $t=\alpha^2\cosh^2\theta$.

$$W=2C_3\theta+C_4=2C_3\cosh^{-1}\left(\frac{t^{\frac{1}{2}}}{\alpha}\right)+C_4.$$

$$C_3=\frac{V_0}{\pi},\quad C_4=0,\quad W=\frac{2V_0}{\pi}\cosh^{-1}\left(\frac{t^{\frac{1}{2}}}{\alpha}\right).$$

$$F=\left|\frac{dW}{dz}\right|=\left|\frac{2C_3(t-k^2)^{\frac{1}{2}}}{C_1(t-1)^{\frac{1}{2}}(t-\alpha^2)^{\frac{1}{2}}}\right|,\quad \sigma=\frac{F}{4\pi}.$$

$$Q=\left|\frac{W_2-W_1}{4\pi}\right|=\left|\frac{V_0}{2\pi^2}\left\{\cosh^{-1}\left(\frac{t_2^{\frac{1}{2}}}{\alpha}\right)-\cosh^{-1}\left(\frac{t_1^{\frac{1}{2}}}{\alpha}\right)\right\}\right|.$$

$$Q_{BD}=\left|\frac{V_0}{2\pi^2}\cosh^{-1}\left(\frac{1}{\alpha}\right)\right|.$$

Total charge on the end of an electrode$=2Q_{BD}$.

Effective capacity of the condenser formed by the two ends only

$$=\frac{1}{2\pi^2}\cosh^{-1}\left(\frac{1}{\alpha}\right).$$

Effective capacity of the condenser formed by one end and the central plane conductor

$$=\frac{1}{\pi^2}\cosh^{-1}\left(\frac{1}{\alpha}\right).$$

$$\frac{dF^2}{dz}=\frac{8C_3^2t^{\frac{1}{2}}(t-k^2)^{3/2}}{C_1^3(t-1)^{3/2}(t-\alpha^2)}\left\{\frac{1}{t-k^2}-\frac{1}{t-1}-\frac{1}{t-\alpha^2}\right\}.$$

Equipotentials are shown in fig. 15.

Fig. 15.

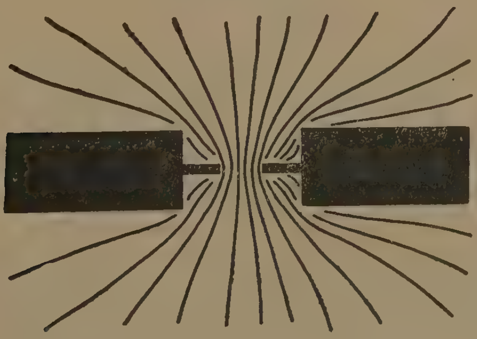

§ 7. *Single Semi-Infinite Rectangular Conductor with Equal Finite Thin Projecting Plates at Potential* V_0.

Fig. 16.

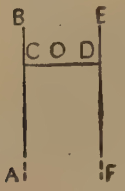

Fig. 17.

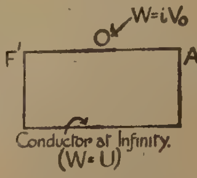

(See fig. 16.) This problem can also be regarded as that of a two-dimensional ice-pail standing on a semi-infinite conducting support of equal width, the whole system forming a single conductor at potential V_0. The width of the rectangular conductor is $2a$ cm., and the length of the equal projecting plates is b cm. The line ABCODEF is to be transformed into the real axis in the t-plane.

TABLE VI. (See fig. 16.)

Points.	A.	B.	C.	O.	D.	E.	F.
t	$-\infty$	-1	$-k$	0	$+k$	$+1$	$+\infty$
z	$-a-i\infty$	$-a+ib$	$-a$	0	$+a$	$+a+ib$	$a-i\infty$

Transformations.

$$dz=\frac{C_1\,dt(t^2-1)}{(t^2-k^2)^{\frac{1}{2}}},\qquad t=\frac{1}{\operatorname{sn}(u,k)}.$$

$$dt=-\frac{\operatorname{cn}u.\operatorname{dn}u.du}{\operatorname{sn}^2u},\qquad dz=-C_1\frac{\operatorname{cn}^3u.du}{\operatorname{sn}^3u}.$$

$$z=C_1\left\{\frac{(1+k'^2)}{2}\log\frac{1-\operatorname{dn}u}{\operatorname{sn}u}+\frac{\operatorname{dn}u}{2\operatorname{sn}^2u}\right\}+C_2.$$

$$C_1=\frac{i4a}{\pi(1+k'^2)}=\frac{i.2b}{(1+k'^2)\log\frac{1-k'}{k}+k'}.$$

$$C_2=a+\frac{ib\log k}{\log\frac{1-k'}{k}+\frac{k'}{1+k'^2}}=a+i\frac{2a}{\pi}\log k.$$

k and k' are obtained from

$$\frac{b}{a}=2\left\{\log\frac{1-k'}{k}+\frac{k'}{1+k'^2}\right\}.$$

(See fig. 17.)

$$dW=C_3.dt,\quad W=C_3t+C_4=\frac{C_3}{\operatorname{sn}u}+C_4.$$

$_4=iV_0$, C_3 is indeterminate, as yet.

$$F=\left|\frac{dW}{dz}\right|=\left|\frac{C_3(t^2-k^2)^{\frac{1}{2}}}{C_1(t^2-1)}\right|, \quad \sigma=\frac{F}{4\pi}.$$

$$Q=\left|\frac{W_2-W_1}{4\pi}\right|=\left|\frac{C_3}{4\pi}\left(\frac{1}{\operatorname{sn} u_2}-\frac{1}{\operatorname{sn} u_1}\right)\right|=\left|\frac{C_3}{4\pi}(t_2-t_1)\right|.$$

$$Q_{OD}=\left|\frac{C_3k}{4\pi}\right|.$$

Total charge on the bottom (inside the ice pail) $=\left|\frac{C_3k}{2\pi}\right|$.

$$Q_{DE}=\left|\frac{C_3}{4\pi}(1-k)\right|.$$

$2Q_{OE}$ = Total charge on the inside (bottom and two sides) $=\left|\frac{C_3}{2\pi}\right|$.

Hence $C_3=\alpha\pi\times$ total internal charge per cm. depth.

$$\frac{dF^2}{dz}=\frac{C_3{}^2 2t(2k^2-t^2-1)(t^2-k^2)^{\frac{1}{2}}}{C_1{}^3(t^2-1)^4}.$$

Equipotentials are shown in fig. 18.

Fig. 18.

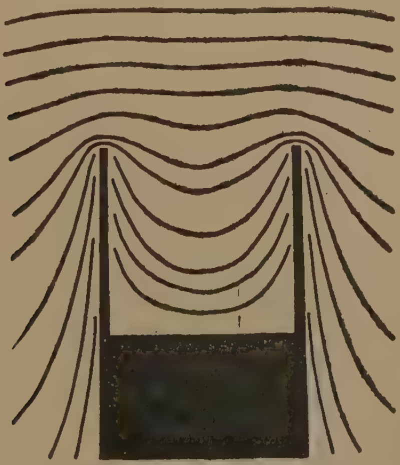

§ 8. *Single Semi-Infinite Rectangular Electrode with Equal Thin Lateral Projecting Plates at the end, at Potential* V_0.

Fig. 19.

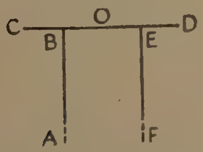

Fig. 20.

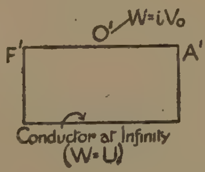

The width of the rectangular electrode is $2a$ cm., and the length of each projecting plate is $b-a$. The line ABCODEF is to be transformed into the real axis in the t-plane.

TABLE VII. (See fig. 19.)

Points.	A.	B.	C.	O.	D.	E.	F.
t	$-\infty$	-1	$-k$	0	$+k$	$+1$	$+\infty$
z	$-a-i\infty$	$-a$	$-b$	0	$+b$	$+a$	$+a+\infty$

Transformations. (See fig. 19.)

$$dz=\frac{C_1.dt.(t^2-k^2)}{(t^2-1)^{\frac{1}{2}}},\quad t=\frac{1}{\operatorname{sn}(u,k)}.$$

$$dz=-C_1\frac{\operatorname{dn}^3u.du}{\operatorname{sn}^3u},\quad z=C_1\left\{\frac{(k^2-k'^2)}{2}\log\frac{1-\operatorname{cn}u}{\operatorname{sn}u}+\frac{\operatorname{cn}u}{2\operatorname{sn}^2u}\right\}+C_2.$$

$$C_1=\frac{i2a}{\pi(k^2-k'^2)},\quad C_2=a.$$

k is obtained from

$$\frac{b}{a}=1-\frac{1}{\pi}\tan^{-1}\frac{k'}{k}+\frac{kk'}{\pi(k^2-k'^2)}$$

$$=1-\frac{\phi}{\pi}+\frac{\tan 2\phi}{2\pi},\text{ where }\tan\phi=\frac{k'}{k}.$$

(See fig. 20.)

$$dW=C_3dt,\quad W=C_3t+C_4,\quad C_4=iV_0,\quad W=\frac{C_3}{\operatorname{sn}u}+iV_0.$$

C_3 is indeterminate, as yet.

$$F=\left|\frac{dW}{dz}\right|=\left|\frac{C_3(t^2-1)^{\frac{1}{2}}}{C_1(t^2-k^2)}\right|,\quad \sigma=\frac{F}{4\pi}.$$

$$Q=\left|\frac{W_2-W_1}{4\pi}\right|=\left|\frac{C_3(t_2-t_1)}{4\pi}\right|,\quad Q_{OD}=\left|\frac{C_3k}{4\pi}\right|,\quad Q_{DE}=\left|\frac{C_3(1-k)}{4\pi}\right|.$$

$$Q_{OE}=\frac{C_3}{4\pi}\Big|,\quad Q_{BE}=\left|\frac{C_3}{2\pi}\right|.$$

This gives a meaning to $C_3=2\pi\times Q_{BE}$.

$$\frac{dF^2}{dz}=\left|\frac{C_3{}^2 2t(t^2-1)^{\frac{1}{2}}(2-t^2-k^2)}{C_1{}^3(t^2-k^2)^4}\right|.$$

Equipotentials are shown in fig. 21.

Fig. 21.

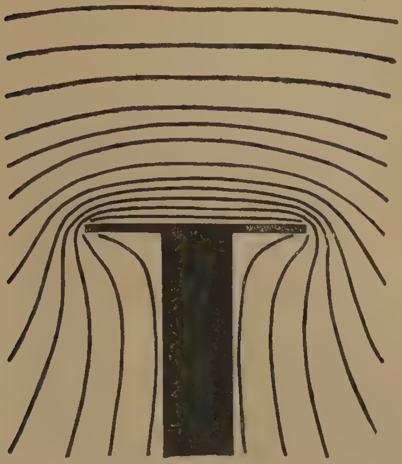

§ 9. *Thin Semi-Infinite Plate at Potential V_0 in line with a Thin Finite Plate at Potential Zero.*

Fig. 22.

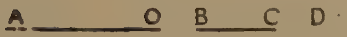

Fig. 23..

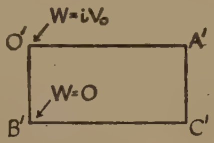

(See fig. 22.) The semi-infinite plate extends from $z=-\infty$ to $z=0$ along the real axis in the z-plane. The width of the gap is b cm., and the finite plate extends from $z=b$ to $z=c$ along the real axis in the z-plane. The line AOBCD is to be transformed into the real axis in the t-plane.

TABLE VIII.

Points.	A.	O.	B.	C.	D.
t	$-\infty$	0	k^2	1	$+\infty$
z	$-\infty$	0	b	c	$+\infty$

Transformations. (See fig. 22.)

$$dz=C_1\,dt, \quad z=C_1t+C_2.$$

$$C_1=c, \quad C_2=0, \quad k^2=\frac{b}{c}, \quad z=ct.$$

(See fig. 23.)

$$dW=\frac{C_3\,.\,dt}{t^{\frac{1}{2}}(t-k^2)^{\frac{1}{2}}(t-1)^{\frac{1}{2}}}, \quad t=\frac{1}{\operatorname{sn}^2(u,\,k)}.$$

$$W=-2C_3u+C_4,\quad C_3=+\frac{iV_0}{2K},\quad C_4=+\frac{iV_0}{K}(K+iK').$$

$$W=\frac{iV_0}{K}\left\{-\mathrm{sn}^{-1}\left(\frac{1}{t^{\frac{1}{2}}}\right)+K+iK'\right\}.$$

$$F=\left|\frac{dW}{dz}\right|=\left|\frac{C_3}{C_1t^{\frac{1}{2}}(t-k^2)^{\frac{1}{2}}(t-1)^{\frac{1}{2}}}\right|=\left|\frac{C_3\,\mathrm{sn}^3\,u}{C_1\,\mathrm{cn}\,u\,\mathrm{dn}\,u}\right|.$$

$$\sigma=\left|\frac{1}{4\pi}\frac{dW}{dz}\right|,\quad Q=\left|\frac{W_2-W_1}{4\pi}\right|=\left|\frac{iV_0}{4\pi K}\left\{\mathrm{sn}^{-1}\left(\frac{1}{t_1^{\frac{1}{2}}}\right)-\mathrm{sn}^{-1}\left(\frac{1}{t_2^{\frac{1}{2}}}\right)\right\}\right|$$

Total charge per cm. depth on each plate$=\dfrac{K'V_0}{2\pi K}$ e.s.u.

Capacity per cm. depth between the plates$=\dfrac{K'}{2\pi K}$ e.s.u.

$$\frac{d^2F}{dz^2}=\left|\frac{C_3{}^2\{3t^2-2(k^2+1)t+k^2\}}{C_1{}^3t^2(t-1)^2(t-k^2)^2}\right|.$$

Equipotentials are shown in fig. 24.

Fig. 24.

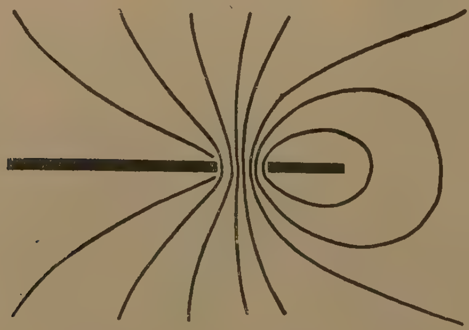

§ 10. *Central Finite Thin Plate at Potential $-V_0$ between two other Collinear Thin Plates at Potential $+V_0$.*

Fig. 25.

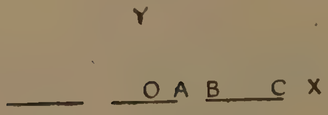

Fig. 26.

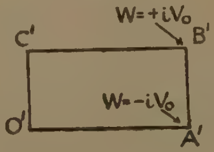

The outer plates are equal in length to each other and are symmetrically situated relative to the central plate, which is of a different length. The middle of the central plate is at the origin of co-ordinates in the z-plane. Its ends are at $z=+a$ and $z=-a$, respectively. The gaps are of width $b-a$, and the outer plates are each of length $c-b$. The line YOABCX in fig. 25 is to be transformed into the real axis in the t-plane.

TABLE IX. (See fig. 25.)

Points.	Y.	O.	A.	B.	C.	X.
t	$-\infty$	0	k^2	1	α^2	$+\infty$
z	$+i\infty$	0	a	b	c	$+\infty$

Transformations.

$$dz=\frac{C_1dt}{t^{\frac{1}{2}}},\quad z=2C_1t^{\frac{1}{2}}+C_2.$$

$$C_1=\frac{b}{2},\quad C_2=0,\quad \alpha=\frac{c}{b},\quad z=bt^{\frac{1}{2}}.$$

$$dW=\frac{C_3\,.\,dt}{t^{\frac{1}{2}}(t-k^2)^{\frac{1}{2}}(t-1)^{\frac{1}{2}}(t-\alpha^2)^{\frac{1}{2}}},\quad t=\frac{1}{\mathrm{sn}^2(u,\,k)},\quad k=\frac{a}{b}.$$

$$W=-\frac{2C_3}{\alpha\gamma}\mathrm{sn}^{-1}\left(\frac{p}{k'},\,\frac{k'}{\gamma}\right)+C_4,\text{ where } p=\mathrm{dn}\,(u,\,k),\quad \gamma=\frac{(\alpha^2-k^2)^{\frac{1}{2}}}{\alpha}.$$

(See fig. 26.) Let $W=-iV_0$ when $t=k^2$

and $W=+iV_0$ when $t=1$.

$$C_4=-iV_0,\quad C_3=-\frac{i(\alpha^2-k^2)^{\frac{1}{2}}V_0}{K},\text{ where K is to modulus }\frac{k'}{\gamma}.$$

$$W=\frac{2iV_0}{K}\,.\,\mathrm{sn}^{-1}\left(\frac{p}{k'},\,\frac{k'}{\gamma}\right)-iV_0.$$

$$F=\left|\frac{dW}{dz}\right|=\left|\frac{C_3}{C_1(t-k^2)^{\frac{1}{2}}(t-1)^{\frac{1}{2}}(t-\alpha^2)^{\frac{1}{2}}}\right|.\quad \sigma=\frac{F}{4\pi}.$$

Q, the charge per cm. depth

$$=\left|\frac{W_2-W_1}{4\pi}\right|=\left|\frac{iV_0}{4\pi K}\left\{\mathrm{sn}^{-1}\left(\frac{p_2}{k'}\right)-\mathrm{sn}^{-1}\left(\frac{p_1}{k'}\right)\right\}\right|.$$

These elliptic functions are all to modulus $\frac{k'}{\gamma}$.

The charge on the upper face of the outer plate BC or on half the upper face of the central plate, per cm. depth, is

$$Q_{OA}=Q_{BC}=\frac{V_0K'}{4\pi K}.$$

The negative charge on the whole of the centre plate and the positive charge on the whole of the other two, upper and lower faces included, is

$$4Q_{OA}=\frac{V_0K'}{\pi K}.$$

The potential difference is $2V_0$, so the capacity between the whole of the central plate regarded as one conductor, and the whole of the other two plates regarded as another single conductor, is $\frac{K'}{2\pi K}$ e.s.u.

$$\frac{dF^2}{dz}=\frac{-C_3{}^2t^{\frac{1}{2}}}{C_1{}^3(t-k^2)(t-1)(t-\alpha^2)}\left\{\frac{1}{(t-k^2)}+\frac{1}{(t-1)}+\frac{1}{(t-\alpha^2)}\right\}.$$

Fig. 27.

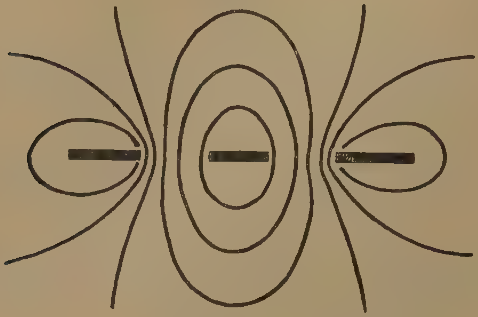

§11. *Two Unequal Thin Collinear Plates at Potentials* $\pm V_0$.

Fig. 28.

The problem of the field of two equal collinear plates was solved by J. J. Thomson.

Here an attempt is made to solve the problem of two unequal plates. Consider the transformation formula

$$z=(b\ \mathrm{sn}\ W+c)^2, \text{ where } b \text{ and } c \text{ are constants,}$$
$$=\{b\ \mathrm{sn}\ (U+iV)+c\}^2.$$

Let U be regarded as the potential here, V as the stream function. First consider what range of values of z corresponds to $U=+K=+V_0$.

$$z=\{b\ \mathrm{sn}\ (iV+K)+c\}^2$$
$$=\left\{\frac{b}{\mathrm{dn}\,(V, k')}+c\right\}^2.$$

For real values of V, dn (V, k') fluctuates between 1 and k, so that z is real and varies between $z_1=\left(c+\frac{b}{k}\right)^2$ and $z_2=(c+b)^2$. Thus $U=+K=+V_0$ corresponds to a thin conducting plate extending from $z_1=\left(c+\frac{b}{k}\right)^2$ to $z_2=(c+b)^2$ along the real axis in the z-plane.

Similarly, if we put $U=-K=-V_0$, $z=\{b\ \mathrm{sn}\ (iV-K)+c\}^2$, *i. e.*

$$z=\left\{\frac{-b}{\mathrm{dn}\,(V, k')}+c\right\}^2.$$

Hence, since dn (V, k') fluctuates between 1 and k as V varies, z is real and varies between $z_3=(c-b)^2$ and $z_4=\left(c-\frac{b}{k}\right)^2$. $U=-K=-V_0$ therefore corresponds to a thin conducting plate extending from $z_3=(c-b)^2$ to $z_4=\left(c-\frac{b}{k}\right)^2$. Since z_3-z_4 is not equal to z_1-z_2 the two plates are unequal in length. The numerical value of k is derived from

$$z_1=\left(c+\frac{b}{k}\right)^2,\quad z_2=(c+b)^2,\quad z^3=(c-b)^2,\quad \text{and}\quad z_4=\left(c-\frac{b}{k}\right)^2.$$

Thus $$2b=z_2^{\frac{1}{2}}-z_3^{\frac{1}{2}},\quad \frac{2b}{k}=z_1^{\frac{1}{2}}-z_4^{\frac{1}{2}},\quad \text{and}\quad k=\frac{z_2^{\frac{1}{2}}-z_3^{\frac{1}{2}}}{z_1^{\frac{1}{2}}-z_4^{\frac{1}{2}}}.$$

From this, using tables, $K=V_0$ is found.

Other electrical quantities of interest are the following :—

$$F=\left|\frac{dW}{dz}\right|=\left|\frac{1}{2b\,\mathrm{cn}\,W\,\mathrm{dn}\,W(b\,\mathrm{sn}\,W+c)}\right|$$

$$=\left|\frac{b}{2z^{\frac{1}{2}}\{b^2-(z^{\frac{1}{2}}-c)^2\}^{\frac{1}{2}}\{b^2-k^2(z^{\frac{1}{2}}-c)^2\}^{\frac{1}{2}}}\right|.$$

$$\sigma=\left|\frac{1}{4\pi}\frac{dW}{dz}\right|=\infty \text{ at the corners } z=z_1,\ z_2,\ z_3 \text{ and } z_4.$$

$$Q=\left|\frac{W_2-W_1}{4\pi}\right|=\left|\frac{1}{4\pi}\left\{\mathrm{sn}^{-1}\left(\frac{z_5^{\frac{1}{2}}-c}{b}\right)-\mathrm{sn}^{-1}\left(\frac{z_6^{\frac{1}{2}}-c}{b}\right)\right\}\right|,$$

using 5 and 6 to indicate any two points.

Hence, on the two plates the total charges are $+\frac{K'}{2\pi}$ and $-\frac{K'}{2\pi}$, respectively. The potential difference is $2K=2V_0$. Hence the mutual capacity is $\frac{K'}{4\pi K}$.

$$\frac{dF^2}{dz}=\left|\frac{b^2}{4z\{b^2-(z^{\frac{1}{2}}-c)^2\}\{b^2-k^2(z^{\frac{1}{2}}-c)^2\}}\right.$$
$$\left.\times\left[-\frac{1}{z}+\frac{z^{\frac{1}{2}}-c}{z^{\frac{1}{2}}\{b^2-(z^{\frac{1}{2}}-c)^2\}}+\frac{k^2(z^{\frac{1}{2}}-c)}{z^{\frac{1}{2}}\{b^2-k^2(z^{\frac{1}{2}}-c)^2\}}\right]\right|.$$

Equipotentials are shown in fig. 29.

Fig. 29.

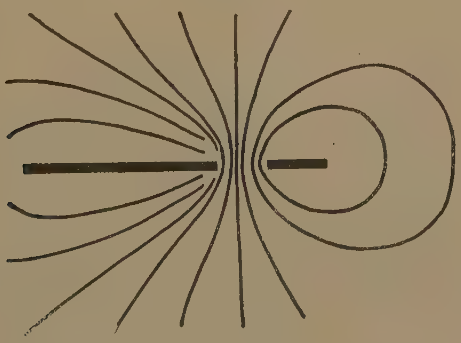

XIX. *On the Vectors and Invariants of Kinematic Relativity.*

By G. J. Whitrow *.

[Received October 16, 1944.]

1. *Introduction.*

In a recent article in this journal (1) Professor W. Wilson has objected to Milne's formula for the equation of motion of a free particle moving in the uniformly expanding substratum. In general, previous criticism has been concerned with the manner in which the equation has been derived, rather than with its form, and the misunderstandings involved have been mainly of a physical and philosophical character. However, unlike most previous critics, Wilson is sympathetic to the point of view adopted in Kinematical Relativity ; his difficulties are of a mathematical character. These difficulties seem to be due to a mistake in his 4-vector analysis.

The characteristic difference between classical and relativistic kinematics concerns the rôle of the time co-ordinate in transformations from one set of axes to another in uniform relative motion. In classical kinematics, time is an invariant. Hence, the appropriate vector analysis is that of three-dimensional Euclidean space. In relativistic kinematics, both in the form developed by Einstein (1905) and in the form due to Milne (1933), transformation of time involves reference to a spatial co-ordinate as well. There is no public Euclidean space, but, as Minkowski first pointed out (1908), there is a public space-time. This is of quasi-Euclidean form, but is four-dimensional and of signature -2. The appropriate vector analysis is known as 4-vector analysis. It was first developed by Sommerfeld (1910).

In Special Relativity, as in Newtonian kinematics, *all* frames in uniform relative motion are equivalent, so that at each of the ∞^3 points of infinite space there are, at any instant, ∞^3 Lorentz covariant frames. However, in Kinematic Relativity, there is, at any given instant, at any one of the ∞^3 points inside a certain uniformly expanding sphere, a *unique* fundamental "observer." Consequently, the 4-vector analysis of Kinematic Relativity is sharper than that of Special Relativity. In mathematics, as I believe A. N. Whitehead has remarked, generalization needs to be tempered with the fruitful restriction. The new 4-vector analysis of the limited system of fundamental observers of Kinematic Relativity has proved far more powerful than the old 4-vector analysis of Special Relativity. In fact, it is a distinct discipline. Possibly, this distinction has not been sufficiently stressed heretofore. In this short

---

* Communicated by the Author.

note, after refuting Wilson's recent criticism, the opportunity is taken to supplement a brief discussion on 4-vectors with a few comments on some of the invariants and 6-vectors of Kinematic Relativity and their physical interpretation. Some hitherto unpublished results are included.

2. *Refutation of Wilson's Criticism.*

In the presence of a system of equivalent observers, moving, in the Euclidean private space of each, according to the law,

$$\mathbf{V}=\mathbf{P}/t, \quad \ldots \quad (1)$$

Milne has found that a free particle moves so that

$$\frac{d\mathbf{V}}{dt}=-(\mathbf{P}-\mathbf{V}t)\frac{\mathrm{Y}}{\mathrm{X}}. \quad \ldots \quad (2)$$

Although he has not pointed out any flaw in the actual derivation of this equation, Wilson believes that it cannot be correct, because, although the left-hand side is not the space-part of a 4-vector, he maintains that the right-hand side is. The most convincing proof of the validity of equation (2) is to show that it can be translated into 4-vector form. At first sight, it is remarkable that equation (2) is Lorentz invariant, although not of 4-vector form. However, no contradiction arises, for, as will be seen, *neither* side is the space-part of a 4-vector, and Wilson's criticism is fallacious. Before considering this point, it is convenient to find the 4-vector equivalent of (2). This may be done in a number of ways. One method, not previously published, is as follows :—

With the usual notation, the 4-vector form, if it exists, must be of the type,

$$\left.\begin{aligned}\frac{1}{\mathrm{Y}^{\frac{1}{2}}}\frac{d}{dt}\left(\frac{\mathbf{V}}{\mathrm{Y}^{\frac{1}{2}}}\right)&=\lambda(\mathrm{X},\,\xi)\mathbf{P}+\mu(\mathrm{X},\,\xi)\frac{\mathbf{V}}{\mathrm{Y}^{\frac{1}{2}}},\\ \frac{1}{\mathrm{Y}^{\frac{1}{2}}}\frac{d}{dt}\left(\frac{c}{\mathrm{Y}^{\frac{1}{2}}}\right)&=\lambda(\mathrm{X},\,\xi)ct+\mu(\mathrm{X},\,\xi)\frac{c}{\mathrm{Y}^{\frac{1}{2}}}.\end{aligned}\right\} \quad \ldots \quad (3)$$

When $\mathbf{P}=0$, equation (2) reduces to

$$\frac{d\mathbf{V}}{dt}=\mathrm{Y}\frac{\mathbf{V}}{t},$$

or, putting the left-hand side in 4-vector form,

$$\frac{1}{\mathrm{Y}^{\frac{1}{2}}}\frac{d}{dt}\left(\frac{\mathbf{V}}{\mathrm{Y}^{\frac{1}{2}}}\right)=\frac{\mathbf{V}}{t\mathrm{Y}}.$$

Comparing this with the first equation in (3), when $\mathbf{P}=0$, it is seen that

$$\mu(t^2,\,1/\mathrm{Y})=1/t\mathrm{Y}^{\frac{1}{2}},$$

whence

$$\mu(\mathrm{X},\,\xi)=\xi^{\frac{1}{2}}/\mathrm{X}^{\frac{1}{2}}=\mathrm{Z}/\mathrm{X}\mathrm{Y}^{\frac{1}{2}}.$$

Similarly, by putting $\mathbf{V}=0$ in equations (2) and (3) it is seen that

$$\lambda(\mathrm{X},\,t^2/\mathrm{X})=-1/\mathrm{X},$$

whence

$$\lambda(\mathrm{X},\,\xi)=-1/\mathrm{X}.$$

Consequently, equations (3) must be of the form

$$\left.\begin{aligned} \frac{1}{Y^{\frac{1}{2}}}\frac{d}{dt}\left(\frac{\mathbf{V}}{Y^{\frac{1}{2}}}\right) &= -\frac{1}{X}\left(\mathbf{P}-\mathbf{V}\frac{Z}{Y}\right), \\ \frac{1}{Y^{\frac{1}{2}}}\frac{d}{dt}\left(\frac{c}{Y^{\frac{1}{2}}}\right) &= -\frac{1}{X}\left(ct-c\frac{Z}{Y}\right). \end{aligned}\right\} \quad \ldots \ldots \quad (4)$$

To refute Wilson's claim, it is sufficient to prove that equation (2) can be deduced from equations (4). From the first equation in (4), it follows that

$$\frac{1}{Y}\frac{d\mathbf{V}}{dt} = -\frac{1}{X}\left(\mathbf{P}-\mathbf{V}\frac{Z}{Y}\right)+\frac{\mathbf{V}}{2Y^{2}}\left(\frac{dY}{dt}\right). \quad \ldots \ldots \quad (5)$$

From the second equation, it follows that

$$\frac{1}{2Y^{2}}\left(\frac{dY}{dt}\right) = \frac{1}{X}\left(t-\frac{Z}{Y}\right). \quad \ldots \ldots \quad (6)$$

Hence, combining (5) and (6), it is seen that

$$\frac{1}{Y}\frac{d\mathbf{V}}{dt} = -\frac{1}{X}(\mathbf{P}-\mathbf{V}t), \quad \ldots \ldots \quad (7)$$

and thus equation (2) is recaptured.

3. *Discussion of Wilson's Difficulties concerning* 4-*Vectors.*

Wilson is correct in pointing out that the left-hand side of (2) is not the space part of a 4-vector. Moreover, X is a Lorentz invariant. Wilson's fallacy thus turns on his identification of ($\mathbf{P}-\mathbf{V}t$) as the space part of a 4-vector; or, since **P** is the space part of such a vector, by definition, in maintaining that **V***t* is of this character. Wilson argues that " **V***t* is indubitably the space part of a 4-vector, being, indeed, the displacement of a particle moving with velocity **V** in the system of reference of some observer O during the time, *t*, as reckoned by O "(2). This argument is invalid, since it assumes that a 3-vector in O's *private* Euclidean space is *necessarily* the space part of a 4-vector in the *public* Minkowskian space-time of the fundamental observers, O, O′, ... etc. In general this is not true.

A 4-vector in this space-time is, by definition(3), a set of four physical magnitudes, the respective measurements of which, according to O, O′ . . ., etc. are related in the same way as are the respective measurements of a typical position vector (**P**, *ct*). Thus, for example,

$$\left(\frac{\mathbf{V}}{Y^{\frac{1}{2}}},\ \frac{c}{Y^{\frac{1}{2}}}\right),$$

where $Y \equiv 1-\mathbf{V}^2/c^2$, is a 4-vector, since it is related to the corresponding vector, in the co-ordinates of O′, viz. :—

$$\left(\frac{\mathbf{V}'}{Y'^{\frac{1}{2}}},\ \frac{c}{Y'^{\frac{1}{2}}}\right),$$

where **V**′ is the transform of V, and $Y'=1-\mathbf{V}'^2/c^2$, by equations of the same algebraic form as those connecting $(\mathbf{P}', t')$ to $(\mathbf{P}, t)$, where $(\mathbf{P}', t')$ are the space and time co-ordinates assigned by O′ to an event $(\mathbf{P}, t)$ in the co-ordinates of O.

It is readily seen that $\mathbf{V}t$ is not the space part of a 4-vector, for if

$$\xi \equiv t\frac{dx}{dt}, \quad \eta \equiv t\frac{dy}{dt}, \quad \zeta \equiv t\frac{dz}{dt},$$

the transforms (ξ', η', ζ') of the quantities (ξ, η, ζ), by the Lorentz rules for transforming the spatial part of a 4-vector, do not satisfy the identities,

$$\xi' \equiv t'\frac{dx'}{dt'}, \quad \eta' \equiv t'\frac{dy'}{dt'}, \quad \zeta' \equiv t'\frac{dz'}{dt'},$$

except in the *particular case* in which

$$\xi \equiv x, \quad \eta \equiv y; \quad \zeta \equiv z.$$

Thus, only for the restricted type of motion, governed by the differential equations,

$$x = t\frac{dx}{dt}, \quad y = t\frac{dy}{dt}, \quad z = t\frac{dz}{dt}, \qquad \text{. . . . . . . (8)}$$

is $\mathbf{V}t$ the space part of a 4-vector.

This result can be immediately verified by transforming $t\frac{dx}{dt}$, etc. according to the Lorentz rules for transforming x, etc., and equating the results to $t'\frac{dx'}{dt'}$, etc., respectively, where (x', y', z', t') are the Lorentz transforms of (x, y, z, t). Alternatively, the argument may be developed as follows :—The element $d\mathbf{P}$ is the space part of a 4-vector, and the magnitude,

$$\mathbf{V}t \equiv \frac{d\mathbf{P}}{dt}t$$

will also be the space part of a 4-vector, if, and only if, dt/t is a Lorentz invariant. If the relative velocity of O and O′ is $\mathbf{U}$, and if they part company at zero epoch,

$$\frac{dt'}{t'} = \frac{d(t - \mathbf{U}.\mathbf{P}/c^2)}{t - \mathbf{U}.\mathbf{P}/c^2} = \frac{dt(1 - \mathbf{U}.\mathbf{V}/c^2)}{t(1 - \mathbf{U}.\mathbf{P}/c^2t)}.$$

Hence, for any $\mathbf{U}$,

$$\frac{dt'}{t'} = \frac{dt}{t},$$

if, and only if, $\mathbf{V} = \mathbf{P}/t,$

as before.

We have thus recaptured the principal result, in effect, of Wilson's paper, namely, that the equation of motion of a free particle would reduce to the equation of motion of a fundamental particle, if $\mathbf{V}t$ were the space part of a 4-vector. However, to assume, as Wilson does, that $\mathbf{V}t$ is the space part of a 4-vector, in order to prove that the motion of *any* free particle reduces to that of a fundamental particle is a *petitio principii.* In general, $\mathbf{V}t$ is not the space-part of a 4-vector for, as we have seen, equation (2) can be deduced from a 4-vector equation without making the additional restriction that $\mathbf{V}=\mathbf{P}/t$.

I think that Wilson's difficulty has arisen in the following way. *He has confused, at least implicitly, the transformation of two distinct 4-vectors.* If the transform of (x, y, z, ct) from O to O′ is (x', y', z', ct'), and if O′ has speed U away from O in the x-direction, then

$$t'=\frac{t-\mathrm{U}x/c^2}{(1-\mathrm{U}^2/c^2)^{\frac{1}{2}}}.$$

However, the transform of (ξ, η, ζ, ct) is not, in general, some

$$(\xi', \eta', \zeta', ct'),$$

but some

$$(\xi', \eta', \zeta', ct^*),$$

where t^* *differs from* t', owing to the fusion of spatial and temporal co-ordinates in the Lorentz transformation. Thus, if

$$\xi=t\,dx/dt, \quad \eta=t\,dy/dt, \quad \zeta=t\,dz/dt,$$

then

$$\xi'=\frac{t(dx/dt)-\mathrm{U}t}{(1-\mathrm{U}^2/c^2)^{\frac{1}{2}}}, \quad \eta'=\eta, \quad \zeta'=\zeta, \quad t^*=\frac{t-\mathrm{U}t(dx/dt)/c^2}{(1-\mathrm{U}^2/c^2)^{\frac{1}{2}}},$$

and hence,

$$\xi'=\frac{t-\mathrm{U}(dx/dt)t/c^2}{(1-\mathrm{U}^2/c^2)^{\frac{1}{2}}}\left(\frac{dx/dt-\mathrm{U}}{1-\mathrm{U}(dx/dt)/c^2}\right)=t^*(dx'/dt').$$

Consequently,

$$\xi'=t'(dx'/dt'),$$

if, and only if,

$$t^*=t'.$$

For this to be true, it is necessary that

$$x=t\,dx/dt.$$

Similarly, by considering the special cases of O′ moving in the directions of O's y and z axes, we find that

$$y=t\,dy/dt, \quad z=t\,dz/dt.$$

Since, in general, t^* is not the same as t' for any two fundamental observers O and O′, it follows that, in general, it is false to assert that *any* free particle must move according to the law,

$$x=t\,dx/dt, \quad y=t\,dy/dt, \quad z=t\,dz/dt.$$

It is accordingly not true that, unless $x=t\dfrac{dx}{dt}$, etc., equation (2) is invalid. It is certainly valid in this case, but it is also valid for any undefined velocity $\mathbf{V}$, assigned to the particle at $\mathbf{P}$ at epoch t.

4. *The Invariants of Kinematic Relativity.*

In view of the distinction between Kinematic Relativity and Special Relativity, stressed in the introduction, I conclude this note with a few comments on some invariants and 6-vectors of the former subject, and their application to the derivation of some fundamental physical laws.

The Lorentz transform, t', according to O′, of the temporal part of $(\mathbf{P}, t)$ is

$$t' = \frac{t - \mathbf{P}.\mathbf{U}/c^2}{(1 - \mathbf{U}^2/c^2)^{\frac{1}{2}}},$$

if O′ has velocity $\mathbf{U}$, relative to O. Consequently, if

$$\mathbf{P} = \mathbf{U}t,$$

then

$$t' = t(1 - \mathbf{U}^2/c^2)^{\frac{1}{2}} = (t^2 - \mathbf{P}^2/c^2)^{\frac{1}{2}}.$$

We thus deduce that

$$\mathrm{X} = t^2 - \mathbf{P}^2/c^2 \quad . \quad . \quad . \quad . \quad . \quad . \quad . \quad . \quad . \quad . \quad . \quad (9)$$

is an invariant, being the square of the local time corresponding to the event $(\mathbf{P}, t)$.

Since the Lorentz transformation is linear, it follows that, if λ and μ are invariants, the expression,

$$(\lambda t_1 + \mu t_2)^2 - (\lambda \mathbf{P}_1 + \mu \mathbf{P}_2)^2/c^2, \quad . \quad . \quad . \quad . \quad . \quad . \quad . \quad (10)$$

is invariant, where $(\mathbf{P}_1, t_1)$ and $(\mathbf{P}_2, t_2)$ are the co-ordinates of any two events according to O. By taking $\lambda = 1$, $\mu = -1$ and

$$t_2 = t_1 + dt, \quad \mathbf{P}_2 = \mathbf{P}_1 + d\mathbf{P},$$

we obtain the differential invariant,

$$ds^2 = dt^2 - d\mathbf{P}^2/c^2. \quad . \quad . \quad . \quad . \quad . \quad . \quad . \quad . \quad (11)$$

Writing

$$ds = \mathrm{Y}dt,$$

where

$$\mathrm{Y} = 1 - \mathbf{V}^2/c^2,$$

it follows that Y is *not* an invariant, but since

$$\mathrm{Z} = t - \mathbf{P}.\mathbf{V}/c^2 = \tfrac{1}{2}\, d\mathrm{X}/dt,$$

we find that

$$\frac{\mathrm{Z}}{\mathrm{Y}^{\frac{1}{2}}} = \frac{1}{2}\left(\frac{d\mathrm{X}/dt}{ds/dt}\right) = \frac{1}{2}\left(\frac{d\mathrm{X}}{ds}\right)$$

is an invariant. (We note that $\mathrm{Z}/\mathrm{Y}^{\frac{1}{2}}$ is the invariant generalization in Kinematic Relativity of t.) Combining X and $\mathrm{Z}/\mathrm{Y}^{\frac{1}{2}}$ we obtain the *dimensionless* invariant,

$$\xi^{\frac{1}{2}} \equiv \mathrm{Z}/\mathrm{X}^{\frac{1}{2}}\mathrm{Y}^{\frac{1}{2}} \equiv d\mathrm{X}^{\frac{1}{2}}/ds.$$

It is easily proved that the only invariants of $\mathbf{P}$, t and $\mathbf{V}$ are functions of X and ξ. For, if $\phi(\mathbf{P}, t, \mathbf{V})$ is invariant, then

$$\phi(\mathbf{P}, t, \mathbf{V}) = \phi(\mathrm{O}, t', \mathbf{V}'),$$

where primed symbols relate to the observer at the event $(\mathbf{P}, t)$, according to O. It is clear that $\phi(\mathrm{O}, t', \mathbf{V}')$ must reduce to a function of t' and $|\mathbf{V}'|$. Hence, since

$$\mathrm{X} = t^2 - \mathbf{P}^2/c^2 = t'^2,$$

and

$$\xi = \frac{(t - \mathbf{P}.\mathbf{V}/c^2)^2}{(1 - \mathbf{V}^2/c^2)(t^2 - \mathbf{P}^2/c^2)} = \frac{1}{1 - \mathbf{V}'^2/c^2)^{\frac{1}{2}}}, \quad . \quad . \quad . \quad . \quad (12)$$

we see that ϕ must be a function of X and ξ. Similarly, the only invariants of $(\mathbf{P}, t)$ are functions of X.

Incidentally, we deduce from (10) that the invariance of $X \equiv t^2 - \mathbf{P}^2/c^2$ implies the invariance of

$$X_{12} \equiv t_1 t_2 - \mathbf{P}_1 . \mathbf{P}_2 / c^2. \quad . \quad . \quad . \quad . \quad . \quad . \quad . \quad . \quad . \qquad (13)$$

Similarly *,

$$ds_{12} \equiv dt_1\, dt_2 - d\mathbf{P}_1 . d\mathbf{P}_2/c^2 \equiv dt_1\, dt_2 (1 - \mathbf{V}_1 . \mathbf{V}_2/c^2), \quad . \quad . \quad . \qquad (14)$$

where $\qquad \mathbf{V}_1 = d\mathbf{P}_1 dt_1, \quad \mathbf{V}_2 \equiv d\mathbf{P}_2/dt_2,$

is invariant. In fact, X_{12} is the scalar product of $(t_1, \mathbf{P}_1/c)$ and $(t_2, \mathbf{P}_2/c)$. If in X_{12} we replace t_2 by dt_2 and $\mathbf{P}_2$ by $d\mathbf{P}_2 = \mathbf{V}_2 dt_2$, we find that

$$(t_1 - \mathbf{P}_1 . \mathbf{V}_2/c^2) dt_2$$

is invariant. Similarly,

$$(t_2 - \mathbf{P}_2 . \mathbf{V}_1/c^2)\, dt_1$$

is invariant. Combining these results with the invariance of ds_{12}, we find that

$$\frac{(t_1 - \mathbf{P}_1 . \mathbf{V}_2/c^2)(t_2 - \mathbf{P}_2 . \mathbf{V}_1/c^2)}{1 - \mathbf{V}_1 . \mathbf{V}_2/c^2} \quad . \quad . \quad . \quad . \quad . \quad . \quad . \qquad (15$$

is invariant. This is the "generalization to two events" of Z^2/Y. The "generalization" of ξ is seen to be

$$\xi_{12} \equiv \frac{(t_1 - \mathbf{P}_1 . \mathbf{V}_2/c^2)\,(t_2 - \mathbf{P}_2 . \mathbf{V}_1/c^2)}{(t_1 t_2 - \mathbf{P}_1 . \mathbf{P}_2/c^2)\,(1 - \mathbf{V}_1 . \mathbf{V}_2/c^2)}. \quad . \quad . \quad . \quad . \quad . \qquad (16)$$

We note that ξ_{12} is unity, if *either* $\mathbf{P}_1 = \mathbf{V}_1 t_1$ *or* $\mathbf{P}_2 = \mathbf{V}_2 t_2$.

Similarly, since the reciprocal of the transformation from O to O′ is of the same form, except for the trivial replacement of $\mathbf{U}$ by $-\mathbf{U}$, it follows that

$$\left(\frac{\partial}{\partial x'}, \frac{\partial}{\partial y'}, \frac{\partial}{\partial z'}, \frac{\partial}{c\, dt'}\right)$$

are the same functions, respectively, of

$$\left(\frac{\partial}{\partial x}, \frac{\partial}{\partial y}, \frac{\partial}{\partial z}, \frac{\partial}{c\, \partial t}\right),$$

as (x', y', z', ct') are of (x, y, z, ct), except for the replacement of $\mathbf{U}$ by $-\mathbf{U}$. We thus can deduce, *without further calculation*, that

$$\frac{1}{c^2} \frac{\partial^2}{dt'^2} - \nabla'^2 \equiv \frac{1}{c^2} \frac{\partial^2}{\partial t^2} - \nabla^2, \quad . \quad . \quad . \quad . \quad . \quad . \quad . \qquad (17)$$

i. e. that the D'Alembertian is invariant. Similarly, it can be shown that

$$\frac{1}{c^2} \frac{\partial^2}{\partial t_1 \partial t_2} - \left(\frac{\partial^2}{\partial x_1 \partial x_2} + \frac{\partial^2}{\partial y_1 \partial y_2} + \frac{\partial^2}{\partial z_1 \partial z_2}\right),$$

operating on an invariant function of $(\mathbf{P}_1, \mathbf{P}_2, t_1, t_2)$, is also invariant.

5. *Six-vectors in Kinematic Relativity.*

The equation of motion of a free particle (2) can also be thrown into 6-vector form, which again justifies its correctness.

---

* For justification, *cf.* the argument by which (11) is derived.

The vector product of two 4-vectors is an instance of a 6-vector. In Kinematic Relativity two " basic " 4-vectors are $(\mathbf{P}, ct)$ and $\left(\frac{\mathbf{V}}{Y^{\frac{1}{2}}}, \frac{c}{Y^{\frac{1}{2}}}\right)$. Their vector product is immediately seen to be

$$\left(\frac{\mathbf{P}\wedge\mathbf{V}}{Y^{\frac{1}{2}}}, c\frac{\mathbf{P}-\mathbf{V}t}{Y^{\frac{1}{2}}}\right), \quad \ldots \ldots \ldots \quad (18)$$

which is thus a " basic " 6-vector.

The equation of motion of a free particle can now be expressed in 6-vector form. For, since

$$\frac{d\mathbf{V}}{dt}=-\frac{(\mathbf{P}-\mathbf{V}t)Y}{X},$$

it follows that

$$\frac{d}{dt}(\mathbf{P}\wedge\mathbf{V})=\mathbf{P}\wedge\frac{d\mathbf{V}}{dt}=(\mathbf{P}\wedge\mathbf{V})\frac{tY}{X},$$

whence

$$\left.\begin{aligned}\frac{\mathbf{P}\wedge\mathbf{V}}{Y^{\frac{1}{2}}}&=\left(\frac{X}{tY^{3/2}}\right)\frac{d}{dt}(\mathbf{P}\wedge\mathbf{V}),\\ c\frac{\mathbf{P}-\mathbf{V}t}{Y^{\frac{1}{2}}}&=c\left(\frac{X}{tY^{3/2}}\right)\frac{d}{dt}(\mathbf{P}-\mathbf{V}t),\end{aligned}\right\} \quad \ldots \ldots \quad (19)$$

using the fact that

$$\frac{d\mathbf{V}}{dt}=-\left(\frac{1}{t}\right)\frac{d}{dt}(\mathbf{P}-\mathbf{V}t).$$

From the first equation of (19) it is seen that

$$\frac{d}{dt}(\mathbf{P}\wedge\mathbf{V})=\frac{tY^{3/2}}{X}\left(\frac{\mathbf{P}\wedge\mathbf{V}}{Y^{\frac{1}{2}}}\right).$$

Using this result in differentiating the product of $\mathbf{P}\wedge\mathbf{V}$ and $Y^{-\frac{1}{2}}$, we find that

$$\begin{aligned}\frac{d}{dt}\left(\frac{\mathbf{P}\wedge\mathbf{V}}{Y^{\frac{1}{2}}}\right)&=(\mathbf{P}\wedge\mathbf{V})\left(\frac{V^2t-\mathbf{P}.\mathbf{V}}{c^2XY^{\frac{1}{2}}}\right)+\frac{tY}{X}\left(\frac{\mathbf{P}\wedge\mathbf{V}}{Y^{\frac{1}{2}}}\right)\\ &=\frac{Z}{X}\left(\frac{\mathbf{P}\wedge\mathbf{V}}{Y^{\frac{1}{2}}}\right).\end{aligned}$$

Similarly,

$$\frac{d}{dt}\left(\frac{\mathbf{P}-\mathbf{V}t}{Y^{\frac{1}{2}}}\right)=\frac{Z}{X}\left(\frac{\mathbf{P}-\mathbf{V}t}{Y^{\frac{1}{2}}}\right).$$

Consequently,

$$\left.\begin{aligned}\left(\frac{1}{Y^{\frac{1}{2}}}\right)\frac{d}{dt}\left(\frac{\mathbf{P}\wedge\mathbf{V}}{Y}\right)&=\frac{Z}{XY^{\frac{1}{2}}}\left(\frac{\mathbf{P}\wedge\mathbf{V}}{Y^{\frac{1}{2}}}\right),\\ \left(\frac{c}{Y^{\frac{1}{2}}}\right)\frac{d}{dt}\left(\frac{\mathbf{P}-\mathbf{V}t}{Y^{\frac{1}{2}}}\right)&=\frac{cZ}{XY^{\frac{1}{2}}}\left(\frac{\mathbf{P}-\mathbf{V}t}{Y^{\frac{1}{2}}}\right).\end{aligned}\right\}. \quad \ldots \ldots \quad (20)$$

In virtue of (18) and the invariance of X, $Z/Y^{\frac{1}{2}}$, it follows that equations (20) are in 6-vector form.

6. *The Fundamental Properties of a Free Particle.*

Since

$$Z=\frac{1}{2}\left(\frac{dX}{dt}\right),$$

equations (20) can be integrated to give

$$\left.\begin{aligned}\frac{\mathbf{P}\wedge\mathbf{V}}{\mathrm{Y}^{\frac{1}{2}}}&=\mathbf{A}\mathrm{X}^{\frac{1}{2}},\\ \frac{\mathbf{P}-\mathbf{V}t}{\mathrm{Y}^{\frac{1}{2}}}&=\mathbf{B}\mathrm{X}^{\frac{1}{2}},\end{aligned}\right\} \quad \ldots\ldots\ldots \quad (21)$$

where **A** and **B** are constant vectors, for a given free particle. Hence, if $|\mathbf{V}|\ll c$ and $|\mathbf{P}|\ll ct$, then

$$\left.\begin{aligned}\mathbf{P}\wedge\mathbf{V}&=\mathbf{A}t,\\ \mathbf{V}-\mathbf{P}/t&=-\mathbf{B}\end{aligned}\right\} \quad \ldots\ldots\ldots \quad (22)$$

By the Einstein velocity addition formulæ, it is seen from the second equation of (22) that the velocity of a slowly moving "near" particle, relative to the observer whom it is passing at any epoch, is the same for all epochs. Combining this result with (12) and with the identification of $mc^2\xi^{\frac{1}{2}}$ as the "energy" of a free particle(4), it follows that :—

(i) the "energy," in the t-scale, of a free particle, moving slowly in the neighbourhood of the observer, is conserved.

Also from equations (22) we deduce immediately that :—

(ii) the "linear momentum," in the t-scale, of such a particle, *relative to its immediate surroundings*, is conserved(5) ; and

(iii) the "angular momentum" is fixed in direction, but increases secularly in magnitude(6).

References.

(1) W. Wilson, Phil. Mag. xxxv. p. 241 (1944).
(2) W. Wilson, *ibid.* p. 245.
(3) E Cunningham, 'The Principle of Relativity' p. 90 (1914).
(4) E. A. Milne, Proc. Roy. Soc. A, cliv. pp. 31–34 (1936).
(5) E. A. Milne, *ibid.* p. 27.
(6) E. A. Milne, Proc. Roy. Soc. A, clviii. p. 336 (1937).

Christ Church, Oxford.

XX. *Tension of Semi-Infinite Plate with Notched Boundary.*

By A. C. STEVENSON *.

[Received June 2, 1944.]

THERE are few exact solutions in two-dimensional elasticity for a plate with a boundary containing one or more notches. This note is devoted to a relatively simple example of a semi-infinite plate bounded by a certain cubic curve, which gives a single smooth notch whose shape can be varied within limits, the plate being under tension in the direction asymptotic to the boundary. This curve has the polar equation

---

* Communicated by the Author.

$$r = c \sec\theta - \lambda c \cos\theta, \quad \lambda \leqslant 1, \quad \ldots\ldots \quad (1)$$

and, although it is obtained in a slightly different manner, is identical with the boundary used in a recent hydrodynamical problem investigated by Dean ⁽¹⁾ on the flow past a certain projection.

The method employed here is the complex potential method recently discussed by the present writer ⁽²⁾.

1. *The Conformal Transformations.*

We use the successive conformal transformations

$$z = c\{\tfrac{1}{2}\lambda\sigma + 2\sigma^{-1} - 1\}, \quad \sigma = \zeta + 1, \quad \zeta = e^{it}, \quad t = \xi + i\eta, \quad \ldots \quad (2)$$

Fig. 1.

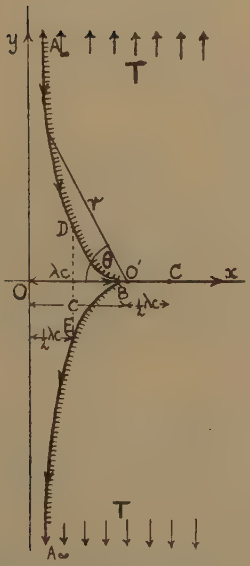

Boundary in z-plane ($\lambda = 0{\cdot}9$).

Fig. 2.

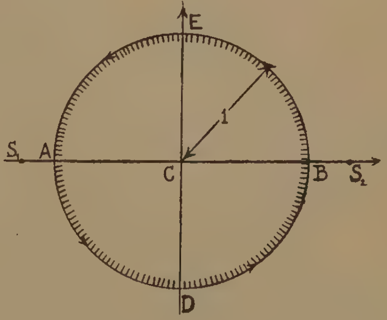

Boundary in ζ-plane.

in which λ is real and less than or equal to unity, and in figs. 1 and 2 we have the boundaries in the z- and ζ-planes corresponding to the boundary $\eta = 0$ in the t-plane.

From (2) we have

$$\frac{dz}{d\zeta} = \frac{dz}{d\sigma} = c\{\tfrac{1}{2}\lambda - 2\sigma^{-2}\}, \quad \ldots\ldots \quad (3)$$

which vanishes for $\sigma = \pm 2\lambda^{-\frac{1}{2}}$, and in the ζ-plane the corresponding critical points S_1, S_2 of the transformation are given by

$$\zeta_1 = -1 - 2\lambda^{-\frac{1}{2}}, \quad \zeta_2 = -1 + 2\lambda^{-\frac{1}{2}}.$$

Clearly S_1 lies outside the unit circle $|\zeta|=1$; S_2 will also lie outside the circle if $\lambda<1$. The unit circle in the ζ-plane transforms to the boundary $\eta=0$ in the t-plane and to a curve in the σ-plane for which

$$\sigma=2e^{i\xi/2}\cos\tfrac{1}{2}\xi. \quad . \quad . \quad . \quad . \quad . \quad . \quad . \quad . \quad . \quad . \qquad (4)$$

In the z-plane, changing axes temporarily for convenience to O′, given by $z=c$, we have

$$X+iY=Z=z-c=c\{\lambda\cos\tfrac{1}{2}\xi e^{i\xi/2}+\sec\tfrac{1}{2}\xi e^{-i\xi/2}-2\},$$

whence $\qquad Y=X\tan\tfrac{1}{2}\xi, \quad X=c\{\lambda\cos^2\tfrac{1}{2}\xi-1\}$

gives the cartesian equation of the boundary as

$$(X^2+Y^2)(X+c)=\lambda cX^2. \quad . \quad . \quad . \quad . \quad . \quad . \quad . \quad . \quad . \qquad (5)$$

From this, writing $X=-r\cos\theta$, $Y=r\sin\theta$, to conform with fig. 1, we have the polar equation of the curve in the z-plane as given in equation (1). Also from (5) the cubic has the asymptote $X=-c$ or $x=0$, and putting $Y=0$ we see that the depth of the notch is given by $x=X+c=\lambda c$; hence the limitation $\lambda\leqslant 1$ restricts us to a notched boundary for which the depth is less than or equal to c. For $\lambda=1$ the cubic has a cusp, for $\lambda>1$ the point O′ becomes a double point with real tangents and the curve has a loop. These cases $\lambda>1$ are not considered here.

2. *The Boundary Problem.*

Taking the problem of the semi-infinite plate to the right of the curve in the z-plane under tension T parallel to the y-axis as a problem of generalized plane stress under no body force, the solution for the displacements and stresses is known to be given by ⁽²⁾

$$8\mu(u+iv)=8\mu D=\kappa\Omega(z)-z\bar{\Omega}'(\bar{z})-\bar{\omega}'(\bar{z}), \quad \kappa=(3-\eta)/(1+\eta), \quad . \qquad (6)$$

$$\Theta=\widehat{xx}+\widehat{yy}=\tfrac{1}{2}\{\Omega'(z)+\bar{\Omega}'(\bar{z})\}, \quad . \quad . \quad . \quad . \quad . \quad . \quad . \quad . \quad . \qquad (7)$$

$$\Phi=\widehat{xx}-\widehat{yy}+2i\widehat{xy}=-\tfrac{1}{2}\{z\bar{\Omega}''(\bar{z})+\bar{\omega}''(\bar{z})\}, \quad . \quad . \quad . \quad . \quad . \qquad (8)$$

in terms of two complex potentials $\Omega(z)$, $\omega(z)$, the symbol η in equation (6) being Poisson's ratio (not to be confused with the curvilinear coordinate of equation (2)) and μ is the rigidity.

The complex potentials have to give the required direct tension T parallel to the y-axis and also give zero stresses over the notched boundary, the condition for this latter being (see ⁽²⁾, p. 772).

$$\bar{\Omega}(\bar{z})+\bar{z}\Omega'(z)+\omega'(z)=\text{const}. \quad . \quad . \quad . \quad . \quad . \quad . \qquad (9)$$

We can take the constant to be zero without loss of generality here.

If the boundary were $x=0$, the solution would be

$$\Omega(z)=Tz, \quad \omega(z)=Tz^2$$

Since the point at infinity in the z-plane corresponds to $\sigma=0$ in the σ-plane, the most important terms in z, z^2 are $2c\sigma^{-1}$, $4c^2(\sigma^{-2}-\sigma^{-1})$ respectively, and we assume tentatively

$$\Omega(z)=2Tc\{\sigma^{-1}+A\zeta+B\}, \quad \omega(z)=4Tc^2\{\sigma^{-2}-\sigma^{-1}+f(\sigma)\},$$

where A and B are real constants, and $f(\sigma)$ is to contain no singularities which give rise to non-physical displacements and stresses. These complex potentials then have the required form at infinity.

The boundary condition (9) can be written

$$\frac{dz}{d\sigma}\bar{\Omega}(\bar{z})+\bar{z}\frac{d\Omega}{d\sigma}+\frac{d\omega}{d\sigma}=0,$$

and along the boundary $\zeta\bar{\zeta}=1$, we have

$$\bar{\sigma}=\frac{1}{\zeta}+1=\frac{\sigma}{\zeta},\quad \frac{1}{\bar{\sigma}}=1-\frac{1}{\sigma},$$

so that from (2)

$$\bar{z}=c\left\{\frac{\lambda\sigma}{2\zeta}+1-\frac{2}{\sigma}\right\}.$$

Hence, using (3) we can write the boundary condition as

$$2f'(\sigma)+\mathrm{A}+\tfrac{1}{2}\lambda(\mathrm{A}+\mathrm{B}+1)+\lambda\mathrm{A}\zeta^{-1}-(\tfrac{1}{2}\lambda+2\mathrm{A})\sigma^{-1}$$
$$-(1+2\mathrm{B})\sigma^{-2}-\frac{\lambda}{2\sigma\zeta}-\frac{2\mathrm{A}}{\sigma^{2}\zeta}=0.$$

Also, since

$$\frac{1}{\sigma\zeta}=\frac{1}{\zeta}-\frac{1}{\sigma},\quad \frac{1}{\sigma^{2}\zeta}=\frac{1}{\zeta}-\frac{1}{\sigma}-\frac{1}{\sigma^{2}},$$

the boundary condition reduces still further to

$$f'(\sigma)+\frac{1}{2}\mathrm{A}+\frac{1}{4}\lambda(\mathrm{A}+\mathrm{B}+1)+\frac{1}{2\zeta}\left\{\mathrm{A}(\lambda-2)-\frac{1}{2}\lambda\right\}+\left\{\mathrm{A}-\mathrm{B}-\frac{1}{2}\right\}\frac{1}{\sigma^{2}}=0.$$

The terms in $1/\zeta$ and $1/\sigma^{-2}$ would give rise to infinite stresses and displacements at infinity and alter the conditions already satisfied there, so we choose A and B to make their coefficients vanish. This leads to

$$\mathrm{A}=-\frac{\lambda}{2(2-\lambda)},\quad \mathrm{B}=-\frac{1}{2-\lambda},$$

and the boundary equation becomes

$$f'(\sigma)=\frac{3\lambda^{2}}{8(2-\lambda)}\quad\text{or}\quad f(\sigma)=\frac{3\lambda^{2}\sigma}{8(2-\lambda)},$$

and, after dropping an irrelevant constant in $\Omega(z)$ corresponding to a rigid body displacement only, our final solution for the complex potentials is

$$\Omega(z)=2\mathrm{T}c\left\{\frac{1}{\sigma}-\frac{\lambda\sigma}{2(2-\lambda)}\right\}, \quad \ldots\ldots\ldots \quad (10)$$

$$\omega(z)=4\mathrm{T}c^{2}\left\{\frac{1}{\sigma^{2}}-\frac{1}{\sigma}+\frac{3\lambda^{2}\sigma}{8(2-\lambda)}\right\}. \quad \ldots\ldots \quad (11)$$

3. *The Peripheral Stress.*

It is of interest to obtain explicitly the mean stress $\overset{\smile}{\xi\xi}$ at points of the notched boundary, and in particular the stress concentration factor $(\overset{\smile}{\xi\xi}/\mathrm{T})_{\sigma=2}$ at the bottom of the notch, Over the boundary $\eta=0$ we have $\widetilde{\eta\eta}=0$, so that

$$\widetilde{\xi\xi}_{\eta=0}=\{\widetilde{\xi\xi}+\widetilde{\eta\eta}\}_{\eta=0}=\{\widetilde{xx}+\widetilde{yy}\}_{\eta=0}=\tfrac{1}{2}\{\Omega'(z)+\bar{\Omega}'(\bar{z})\}$$

$$=\text{real part of } \frac{d\Omega}{d\sigma}\Big/\frac{dz}{d\sigma}$$

$$=\text{real part of T}\ \frac{1+\dfrac{\lambda\sigma^2}{2(2-\lambda)}}{1-\dfrac{\lambda}{4}\sigma^2}, \qquad (12)$$

and using (4), we have, after a little reduction,

$$\widetilde{\xi\xi}_{\eta=0}=\frac{\mathrm{T}\left\{1-\dfrac{\lambda^2}{2-\lambda}\cos^2\tfrac{1}{2}\xi\right\}}{1-2\lambda\cos\xi\cos^2\tfrac{1}{2}\xi+\lambda^2\cos^4\tfrac{1}{2}\xi}. \qquad (13)$$

Fig. 3.

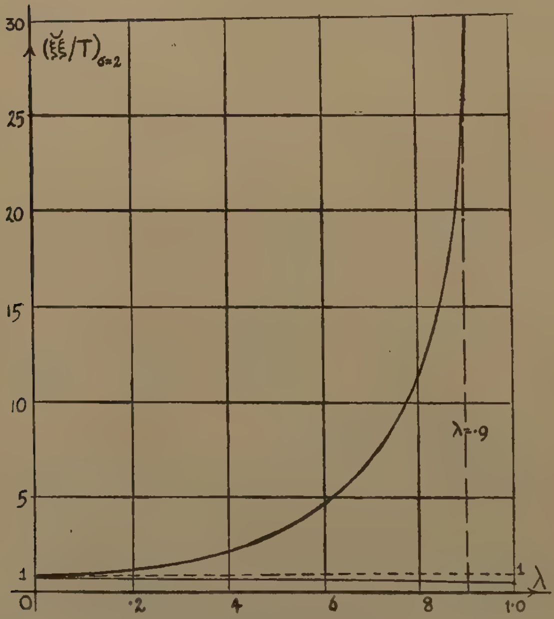

Variation of stress concentration factor at B with depth of notch.

For the stress concentration factor at the bottom of the notch, put $\xi=0$ in (13) or put $\sigma=2$ in (12); we have

$$(\widetilde{\xi\xi}/\mathrm{T})_{\sigma=2}=\frac{2+\lambda}{(2-\lambda)(1-\lambda)}, \qquad (14)$$

which is plotted against λ in fig. 3. For the sharp notch $\lambda=9/10$ of fig. 1, this stress concentration factor has the value $26\frac{4}{11}$.

For the points D, E on the boundary $\eta=0$ at half the depth of the notch, where $\zeta=\pm i$ or $\xi=\pm\pi/2$, the stress concentration factor is

$$(\widetilde{\xi\xi}/\mathrm{T})_{\xi=\pm i}=\frac{1-\dfrac{\lambda^2}{2(2-\lambda)}}{1+\frac{1}{4}\lambda^2},$$

from which $1\geqslant(\widetilde{\xi\xi}/\mathrm{T})_{\zeta=\pm i}\geqslant\frac{2}{5}$ for $0<\lambda<1$.

This also is indicated as the lower curve in fig. 3, and consideration of the ordinate to the two curves for a given λ reveals how marked the variation in peripheral stress is in the lower half of the notch.

Correction.

The writer is indebted to Dr. A. E. Green for pointing out that the solution for the unstressed n-sided curvilinear polygonal hole in an infinite plate under simple tension at infinity in a direction inclined at an angle β to the x-axis (see $^{(2)}$, p. 786) should be restricted to $n\geqslant3$, not $n\geqslant2$, since putting $n=2$ alters the assumed stresses at infinity.

The case $n=2$ gives the elliptic hole of semi-axes a, b corresponding to the unit circle $|\sigma|=1$, from

$$z=c(\sigma+\lambda\sigma^{-1}) \text{ with } 2c=a+b, \quad 2\lambda c=a-b,$$

and it might perhaps be added that the most simple method for this case is to assume tentative complex potentials

$$\Omega_0(\sigma)=\mathrm{T}c\{\sigma+\mathrm{A}\sigma^{-1}\}, \quad \omega_0(\sigma)=-\mathrm{T}c^2\{e^{-2i\beta}\sigma^2+\mathrm{B}\log\sigma+\mathrm{C}\sigma^{-2}\},$$

which have the required form at infinity, and follow the same process as before to obtain the complex constants A, B, C from the boundary condition. This leads easily to

$$\Omega_0(\sigma)=\mathrm{T}c\{\sigma+(2e^{2i\beta}-\lambda)\sigma^{-1}\},$$
$$\omega_0(\sigma)=-\mathrm{T}c^2\{e^{-2i\beta}\sigma^2+e^{2i\beta}\sigma^{-2}+2(1-2\lambda\cos 2\beta+\lambda^2)\log\sigma\}.$$

As a partial check, consider the stress concentration factor at the end of the major axis given by $\sigma=1$. We have

$$(\widetilde{\eta\eta})_{\sigma=1}=\text{real part of }\frac{\Omega_0'(1)}{z'(1)}=\mathrm{T}.\frac{1+\lambda-2\cos 2\beta}{1-\lambda},$$

whence $(\widetilde{\eta\eta}/\mathrm{T})_{\sigma=1}=\dfrac{a}{b}-\left(1+\dfrac{a}{b}\right)\cos 2\beta,$

and this is -1 for $\beta=0$ and $1+2a/b$ for $\beta=\pi/2$, agreeing with the known results (see $^{(3)}$, p. 544) from Airy stress function analysis.

References.

(1) Dean, Proc. Camb. Phil. Soc. xl. p. 19 (1944).
(2) Stevenson, Phil. Mag. xxxiv. p. 766 (1943).
(3) Coker and Filon, 'Photo-Elasticity,' C.U.P. (1931).

XXI. *Chance Effects and the Gaussian Distribution.*

By J. B. S. Haldane, F.R.S.*

[Received April 6, 1945.]

Dr. Silberstein's (1) recent paper on this subject, although containing some interesting and original features, appears to ignore a good deal of earlier work. He is concerned with the distribution of $X=x_1+x_2+\dots x_n$, where x_1, x_2, etc. are random variates which are equally likely to assume any values between 0 and 1. This problem has already been solved by Irwin (2) and Hull (3). Irwin gives graphs up to $n=4$. Their solution, however, gives the distribution of the mean $\frac{X}{n}$, rather than the sum X. The general frequency distribution is :—

$$f(X)=\frac{1}{(n-1)!}\sum_{r=0}^{k}(-1)^r\binom{n}{r}(X-r)^{n-1}dX \quad (k\leqslant X\leqslant k-1).$$

The frequency curve thus consists of a series of arcs of algebraic curves approximating very closely to the normal curve when n is of the order of 5 or larger.

To examine the closeness of the approximation we apply a Laplace transformation and obtain the moment-generating function of the distribution of x, namely

$$m(t)=\int_0^1 e^{tx}\,dx=\frac{e^t-1}{t}.$$

That of X is therefore $\quad M(t)=\left(\frac{e^t-1}{t}\right)^n,$

the value of the rth moment $\overline{X^r}$ being the coefficient of $\frac{t^r}{r!}$. The cumulant-generating function is therefore

$$K(t)=\log_e M(t)=\tfrac{1}{2}nt+n\log_e\left(\frac{\sinh\frac{1}{2}t}{\frac{1}{2}t}\right)$$

$$=\tfrac{1}{2}nt+\frac{n}{12}\frac{t^2}{2!}-\frac{n}{120}\frac{t^4}{4!}+\frac{n}{252}\frac{t^6}{6!}-\frac{n}{240}\frac{t^8}{8!}+.$$

Now transform to a variate $Y=\frac{X-\frac{1}{2}n}{\sqrt{\frac{n}{12}}}$, with mean zero and unit standard deviation. The cumulant-generating function becomes

$$\frac{t^2}{2!}-\frac{6}{5n}\frac{t^4}{4!}+\frac{48}{7n^2}\frac{t^6}{6!}-\frac{432}{5n^3}\frac{t^8}{8!}-\dots$$

---

* Communicated by the Author.

The frequency function of Y is then given by a Gram-Charlier Type A series

$$\frac{1}{\sqrt{2\pi}}e^{-\frac{1}{2}Y^2}\left[1-\frac{1}{20n}H_4(Y)+\frac{1}{105n^2}H_6(Y)-\frac{12n-7}{5600n^3}H_8(Y)+\dots\right],$$

where $H_{2r}(Y)$ is the $2r$th Hermitian polynomial $e^{\frac{1}{2}Y^2}\left(\frac{d}{dx}\right)^{2r}e^{-\frac{1}{2}Y^2}$.

To take numerical examples, when $n=10$, and $Y=1$, the term within the square bracket is about 1·01, when $Y=2$, about 1·03. Exact calculation is impossible, as the series is an asymptotic expansion.

Putting the matter in another way, the measure of kurtosis, γ_2 or β_2-3, of the distribution is $\frac{6}{5n}$. The variance of the estimate of γ_2 from a sample of N members of a normal population is

$$\frac{24N(N-1)^2}{(N-3)(N-2)(N+3)(N+5)},\text{ according to Fisher}^{(4)}.$$

We may therefore ask how many members of a normal population we should have to examine to be reasonably sure that it was not really derived from the sum of n rectangular distributions. Taking twice the standard error as our test of significance, we have

$$\frac{24N(N-1)^2}{(N-3)(N-2)(N+3)(N+5)}<\frac{9}{25n^2},\quad\text{or}\quad(N+5)\left[1-\frac{2(5N-9)}{N(N-1)^2}\right]>\frac{200n^2}{3}.$$

Thus when $n=1$, $N=62$, when $n=10$, $N=6{,}662$. That is to say, in the majority of statistical investigations we should not hesitate to regard the distribution as normal, and there would be no practical objection to doing so.

References.

(1) Phil. Mag. vol. xxxv. p. 395 (1944).
(2) Irwin, *Biometrika*, vol. xix. p. 225 (1928).
(3) Hull, *Biometrika*, vol. xix. p. 240 (1928).
(4) 'Statistical Methods for Research Workers,' p. 79, 6th edn. (Edinburgh, 1936.)

XXII. *The Energies of Uniformly Accelerated Particles in a Gas.*

By Rev. G. D. Yarnold, M.A., D.Phil.,
University College, Nottingham *.

[Received April 9, 1945.]

A knowledge of the energies of electrons and positive ions, under various conditions of pressure and electric-field strength, is of the utmost importance in the investigation of the passage of an electric discharge

---

* Communicated by Professor L. F. Bates, D.Sc.

through a gas. Electron energies have been widely studied during the past thirty years, whilst the equally important though much more difficult study of the energies of positive ions has received but scant attention. Thus, the mean energy of electrons under equilibrium conditions in many gases has been determined by Townsend's well-known diffusion experiment; and the distribution of the energies about the mean value, though not directly observed, has been the subject of a number of theoretical investigations.

The theoretical problem is considerably simplified if the gas is supposed to be ideal, the electron concentration to be small and the frequency of inelastic collisions to be negligible. Two important theoretical investigations of the problem may be noted, in which these simplifications have been made. Townsend (1930) confined his investigation to electrons having energies in excess of the mean energy $\overline{\mathrm{E}}$, and derived the following expression for the fraction dn/n of the electrons per cubic centimetre of a gas, having energies between E and E+dE :

$$\frac{dn}{n}=\frac{1}{\sqrt{\pi}}\epsilon^{-\left(\frac{\mathrm{E}}{\overline{\mathrm{E}}}-0{\cdot}85\right)^2}\frac{d\mathrm{E}}{\overline{\mathrm{E}}} \quad . \quad . \quad . \quad . \quad . \quad . \quad . \quad . \quad (1)$$

Druyvesteyn (1930), following an entirely different procedure, obtained an expression for the fraction dn/n of the electrons per cubic centimetre, which, under equilibrium conditions, have random velocities between u and $u+du$. Thus,

$$\frac{dn}{n}=\mathrm{C}u^2\epsilon^{-\frac{3\lambda}{8\bar{l}^2\gamma^2}u^4}du, \quad . \quad . \quad . \quad . \quad . \quad . \quad . \quad . \quad (2)$$

where λ is the fraction of its kinetic energy lost, on the average, by an electron in collision with a gas molecule; $\bar{l}$ is the mean free path of the electrons; γ is the acceleration of the electrons in the electric field, and C is a constant. These two expressions, however, are by no means in good agreement with one another in the range of energies which is common to both investigations. Subsequent attempts to allow for the effects of inelastic collisions and the variation of the mean free path with the velocity of an electron have generally been based on the Druyvesteyn solution of what may be called the "classical" form of the problem. (Druyvesteyn, 1936; Smit, 1937.)

Unfortunately, there is as yet no experimental means of discriminating between the different distributions which have been suggested, except as regards the fastest electrons, which are responsible for excitation and ionization. Nor is such evidence as exists for the faster electrons in any way decisive. For instance, calculations of the coefficient of ionization for electrons, made by Emeléus, Lunt and Meek (1936), appear to support the assumption of a Maxwellian distribution for the faster electrons. On the other hand, measurements of the intensities of different spectral lines emitted by the positive column of a discharge apparently support a distribution proposed by Llewellyn Jones (1936), which is a combination of the Druyvesteyn and Maxwellian distributions.

(More recently, Llewellyn Jones (1944) has used this combined distribution to derive values of the mobilities of electrons in helium, which are in good agreement with experimental data.)

In the circumstances, therefore, it has appeared to be worth while to attempt a solution of the classical form of the problem by a new, if somewhat laborious, method, involving the computation of the actual energy changes of a large number of particles over definite periods of time. A statistical study of the results of these calculations then leads to the required distribution. Provided the number of particles considered is sufficiently great, the final distribution can be accepted with certainty, since it represents in effect the result of direct observation of a model obeying the same laws as the electrons are assumed to obey in the classical form of the problem. The prolonged calculations have been made as time has allowed over a period of several years, and it is hoped to extend the investigation to the energies of positive ions in due course.

Statement of the Problem.

A uniform electric field of strength X is maintained in the space between two plane parallel metal electrodes of great extent and wide separation. The space between these electrodes contains an ideal gas which is assumed to be at ordinary temperature, so that the random molecular velocities are of the order of 10^4 cm. per sec. By some suitable agency, for example ultra-violet light, electrons are liberated from the negative electrode. The number of electrons emitted per sq. cm. per sec. is the same for all parts of the electrode and is independent of time. Steady conditions having been established, the number n of electrons per c.c. at any point in the gas is independent of time, and, except near the boundaries of the space, independent of position.

In their random motion through the gas, the electrons gain kinetic energy from the electric field and lose energy in collisions with gas molecules. It is well known that, under such conditions, electrons frequently attain energies greatly in excess of the mean kinetic energy of the molecules of the gas. At low pressures of the order of from 1 to 10 millimetres of mercury, and under electric fields of several volts per centimetre, the mean energy of electrons may be as great as several hundred times the mean molecular energy. Thus the electrons attain velocities of an order a thousand times greater than the molecular velocities.

Except in the neighbourhood of the negative electrode, where the velocities of the electrons are smaller, the gas molecules may conveniently be regarded as at rest compared with the electrons. The problem then reduces to the motion of a swarm of electrons in a space containing stationary molecules distributed at random throughout the space. Since the number of electrons in unit volume is small compared with the number of molecules, collisions between two electrons may be disregarded. Collisions of electrons with molecules are assumed to be perfectly elastic and to take place in accordance with the laws of classical mechanics

The small number of inelastic collisions, made by the fastest electrons, is completely disregarded. The theory of the motion is developed below in a form convenient for statistical study.

Mechanics of a Collision.

Consider then the impact of an elastic sphere of mass m, representing an electron, with an elastic sphere of mass M, representing a molecule. Let the initial and final directions of motion of the electron make angles α and β respectively with the line of centres at the moment of impact, as shown in fig. 1. Let the velocities of the electron immediately before and immediately after impact be u_1 and u_2 respectively, and let the molecule, initially at rest, have a velocity v after the collision. The laws of the conservation of momentum and energy give the equations :

Fig. 1.

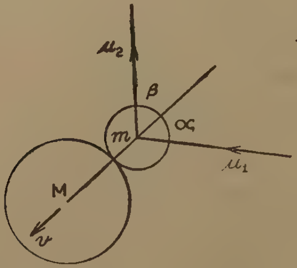

$$mu_1 \cos\alpha = -mu_2 \cos\beta + \mathrm{M}v \quad . \quad . \quad . \quad . \quad . \quad . \quad . \quad (3)$$

$$mu_1 \sin\alpha = mu_2 \sin\beta \quad . \quad . \quad . \quad . \quad . \quad . \quad . \quad . \quad . \quad . \quad (4)$$

$$mu_1^2 = mu_2^2 + \mathrm{M}v^2 . \quad . \quad . \quad . \quad . \quad . \quad . \quad . \quad . \quad . \quad (5)$$

Eliminating β from equations (3) and (4), we obtain

$$m^2u_2^2 = m^2u_1^2 - 2\mathrm{M}mu_1v_1 \cos\alpha + \mathrm{M}^2v^2,$$

which, on substitution from equation (5), gives, for the kinetic energy of the molecule after impact,

$$\tfrac{1}{2}\mathrm{M}v^2 = \frac{2\mathrm{M}m^2u_1^2 \cos^2\alpha}{(\mathrm{M}+m)^2} .$$

Writing $\mathrm{E} = \frac{1}{2}mu_1^2$ for the kinetic energy of the electron before impact, and $\Delta\mathrm{E} = \frac{1}{2}\mathrm{M}v^2$ for the energy lost by the electron to the molecule, and neglecting m in comparison with M, we have,

$$\Delta\mathrm{E} = \frac{4m}{\mathrm{M}} \mathrm{E} \cos^2\alpha .$$

The probability that the angle of impact in a particular collision lies between α and $\alpha + d\alpha$ is $\sin 2\alpha . d\alpha$. This is therefore the probability of an energy loss equal to ΔE above. Hence the average energy loss suffered by an electron of energy E in colliding with a molecule is

$$\frac{4mE}{M}\int_0^{\frac{\pi}{2}}\sin 2\alpha\,.\cos^2\alpha\,.\,d\alpha=\frac{2mE}{M}.$$

Writing $\lambda=\frac{2m}{M}$ for the mean fractional energy loss suffered by an electron, the energy loss in a collision where the angle of impact is α is given by

$$\Delta E=2\lambda E\cos^2\alpha. \quad . \quad . \quad . \quad . \quad . \quad . \quad . \quad . \qquad (6)$$

Directions of Successive Free Paths.

Since the energy loss in a collision is small, it follows that $u_1 \simeq u_2$ and hence that $\alpha \simeq \beta$, *i. e.* the path of the electron is deflected through an angle approximately equal to $(\pi-2\alpha)$. An electron, colliding with a molecule so that the angle of impact lies between α and $\alpha+d\alpha$, leaves the molecule in a direction lying between two cones of semi-angles 2α and $2(\alpha+d\alpha)$, having the initial direction of motion of the electron as axis.

Fig. 2.

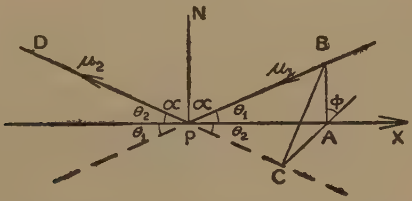

The solid angle between the two cones is $4\pi\sin 2\alpha\,.\,d\alpha$, and the probability of colliding in such a way as to leave the molecule in a direction lying within this solid angle is $\sin 2\alpha\,.\,d\alpha$. Hence, the probability of leaving the molecule in unit solid angle is the same in all directions, namely $\frac{1}{4\pi}$. Thus, immediately after a collision, all directions of motion are equally probable, no matter what the previous direction of motion of the electron.

However, it is convenient to express the angle of impact α in terms of the angles of inclination of the directions of motion of the electron, immediately before and immediately after the collision, to the direction of the electric field. Let BP and PD, the directions of motion of the electron before and after impact, be inclined at angles θ_1 and θ_2 respectively to the negative direction of the electric field X (fig. 2). Let PN be the line of centres of the molecule and electron at the moment of impact at the point P. The plane of impact BPD is the plane in which the deflection $(\pi-2\alpha)$ of the path of the electron takes place. The plane BPA, in which the motion takes place before impact, does not in general coincide with the plane CPA, in which the motion takes place after impact. Let ϕ be the angle between the two planes of motion. All values of ϕ are equally probable. From a point A, at unit distance from P along the direction of the electric field X, construct AB perpendicular to AP such that B lies on the path of the electron before impact, and AC perpendicular to AP such that C lies on the path of the electron after impact. Then in the triangle ABC,

$$BC^2=\tan^2\theta_1+\tan^2\theta_2+2\tan\theta_1.\tan\theta_2.\cos\phi.$$

In the triangle BPC,

$$BC^2=\sec^2\theta_1+\sec^2\theta_2+2\sec.\theta_1.\sec.\theta_2.\cos 2\alpha.$$

Hence,

$$\tan\theta_1.\tan\theta_2.\cos\phi=1+\sec.\theta_1.\sec.\theta_2.\cos 2\alpha.$$

From which we obtain,

$$\cos 2\alpha=\frac{-1+\tan\theta_1.\tan\theta_2.\cos\phi}{\sec\theta_1.\sec\theta_2}$$

and $$2\cos^2\alpha=1-\cos\theta_1.\cos\theta_2+\sin\theta_1.\sin\theta_2.\cos\phi. \quad . \quad . \quad . \quad (7)$$

This result is of value, in that it enables the energy loss in a collision to be expressed in terms of the inclinations θ_1 and θ_2 of the directions of motion before and after impact.

Energy Change in a Free Path.

Consider now an electron which commences a free path with a velocity u in a direction making an angle θ with the negative direction of the electric field X. The component of its velocity in the negative direction of the field is initially $u\cos\theta$. During the free path, the electron experiences an acceleration Xe/m in the negative direction of the field, in virtue of which the free path is curved. It is assumed that the curvature is small and that the length l of the path is unaffected by the curvature, being determined only by the distribution of molecules in space. Let the time occupied in the free path be t. Then the distance moved by the electron in the negative direction of X during the free path is

$$s=ut\cos\theta+\frac{1}{2}.\frac{Xe}{m}t^2,$$

and the corresponding increase in its kinetic energy is

$$Xes=Xeut\cos\theta+\frac{1}{2}\frac{X^2e^2}{m}t^2.$$

Except in the case of long free paths inclined at small angles to the direction of the field, the increase in energy is generally a small fraction of the kinetic energy of the electron at the commencement of the path. Thus the time t can be written as l/u with sufficient accuracy, giving

$$Xes=Xel\cos\theta+\frac{(Xel)^2}{4E}, \quad . \quad . \quad . \quad . \quad . \quad . \quad . \quad (8)$$

writing $E=\frac{1}{2}mu^2$, for the kinetic energy of the electron at the commencement of the path. Clearly the change in kinetic energy may be either positive or negative.

The Steady State of Motion.

The kinetic energy of an electron at a distance d from the negative electrode is equal to Xed, minus the sum of all the energy losses suffered in collisions before reaching the distance d. Thus

$$\mathrm{E}=\mathrm{X}ed-\Sigma 2\lambda\mathrm{E}\cos^2\alpha.$$

The sum $\Sigma 2\lambda\mathrm{E}\cos^2\alpha$ is not readily determinate, but it is clearly different for different electrons at the same distance d from the negative electrode. Thus the energies of the n electrons in one cubic centimetre at the mean distance d are distributed over a range of values, and the mean energy $\Sigma\mathrm{E}/n$ may be written as $\overline{\mathrm{E}}$. At distances d sufficiently great for a steady state of motion to have been established, both the mean energy $\overline{\mathrm{E}}$ and the form of the distribution of the individual energies E about the mean are independent of both time and position.

Consider next the motion of an electron from a plane at distance d_1 to a plane at distance d_2 from the negative electrode. Suppose that N collisions occur in the course of this motion and that the distance (d_2-d_1) is very large in comparison with the mean free path $\bar{l}$ of the electron. The energy gained from the electric field is

$$\mathrm{X}e(d_2-d_1)=\Sigma\mathrm{X}es=\Sigma\mathrm{X}el\cos\theta+\Sigma\frac{(\mathrm{X}el)^2}{4\mathrm{E}}.$$

Since the number N of free paths is very large, the term $\Sigma\mathrm{X}el\cos\theta$ approaches the value zero on the average and may be neglected. The balance of energy may be expressed by the equation

$$\Sigma\frac{(\mathrm{X}el)^2}{4\mathrm{E}}=\Sigma 2\lambda\mathrm{E}\cos^2\alpha.$$

Writing the length l of a free path in terms of the mean free path $\bar{l}$, and the instantaneous energy E in terms of the mean energy $\overline{\mathrm{E}}$, *i. e.*

$$l=b.\bar{l}\quad\text{and}\quad\mathrm{E}=c\overline{\mathrm{E}},$$

we obtain

$$\frac{(\mathrm{X}e\bar{l})^2}{4\overline{\mathrm{E}}}\Sigma\frac{b^2}{c}=\lambda\overline{\mathrm{E}}\,\Sigma\,2c.\cos^2\alpha.$$

The mean energy of the electrons is therefore given by the expression

$$\overline{\mathrm{E}}=\frac{\mathrm{X}e\bar{l}}{2\sqrt{\lambda}}\left(\frac{\Sigma\frac{b^2}{c}}{\Sigma\,2c\cos^2\alpha}\right)^{\frac{1}{2}}\quad\text{. . . . . (9)}$$

In this expression, $\mathrm{X}e\bar{l}/2\sqrt{\lambda}$ has the dimensions of energy, while the factor in the brackets is purely numerical and can be determined only if the form of the distribution of the energies E about the mean energy $\overline{\mathrm{E}}$ is known. It is convenient from now onwards to express the instantaneous energy E of an electron in terms of the quantity

$$\mathrm{E}_1=\frac{\mathrm{X}e\bar{l}}{2\sqrt{\lambda}}\quad\text{. . . . . (10)}$$

Thus, $E=aE_1$ and $\bar{E}=\bar{a}E_1$, where $\bar{a}$ represents the numerical factor in brackets in equation (9).

The energy change suffered by an electron during a single free path traversed at an inclination θ to the negative direction of the electric field X may now be obtained from equation (8) in the form

$$(\Delta E)_{\text{path}}=b(Xe\bar{l})\cos\theta+\frac{b^2(Xe\bar{l})^2}{4aE_1}$$

or

$$(\Delta E)_{\text{path}}=E_1\left(2\sqrt{\lambda}b\cos\theta+\frac{b^2\lambda}{a}\right). \quad . \quad . \quad . \quad . \quad (11)$$

The energy loss in a collision made with an angle of impact α is given by

$$(\Delta E)_{\text{collision}}=E_1(2\lambda a\cos^2\alpha), \quad . \quad . \quad . \quad . \quad . \quad . \quad (12)$$

in which $2\cos^2\alpha$ is given in terms of the inclinations θ_1 and θ_2 of the two successive free paths by equation (7). In equations (11) and (12) the energy changes are expressed only in terms of E_1 and purely numerical parameters, a, b, λ, θ and α. They are therefore in a form suitable for the computation of the energy changes suffered by a number of electrons over given intervals of time, the time occupied in a free path $l=b\bar{l}$, traversed with average energy $E=aE_1$, being expressed in appropriate units as

$$t=\frac{b}{\sqrt{a}}. \quad . \quad . \quad . \quad . \quad . \quad . \quad . \quad . \quad . \quad (13)$$

The Statistical Experiments.

In any actual gas, the average energy loss λ of an electron in an elastic collision is of the order of 10^{-3} or 10^{-4}. With this slow rate of loss, it would be necessary to follow the motion of an electron through a great many free paths before the resultant change in its energy became appreciable. For the purposes of computation, λ has been taken as 0·01. This means that the calculations have been made for an imaginary system of particles each of mass one two-hundredth of the mass of a gas molecule. The effect of this adjustment is only to speed up the rate of interchange of particles between the different energy groups. It can have no effect whatever on the final distribution of energies about the mean energy, since this is determined by the purely numerical factor of equation (9).

Tables were compiled which give the numerical values of the different terms occurring in equations (7), (11), (12) and (13), as follows :—

Table I. gives $2\sqrt{\lambda}b\cos\theta$ (equation 11) for values of b in steps of 0·2 from 0 to 8, and values of θ in steps of 5° from 0° to 180°.

Table II. gives $b^2\lambda/a$ (equation 11) for values of b in steps of 0·2 from 0 to 8, and values of a in steps of 0·2 from 0 to 6.

Table III. gives $b/\sqrt{a}$ (equation 13) for the same values of b and a as in Table II.

Table IV. gives $\sin\theta_1.\sin\theta_2$ and $\cos\theta_1.\cos\theta_2$ (equation 7) for values of both θ_1 and θ_2 in steps of 5° from 0° to 180°.

Table V. gives $\sin\theta_1.\sin\theta_2.\cos\phi$ (equation 7) for values of $\sin\theta_1.\sin\theta_2$ in steps of 0·05 from 0 to 1, and values of ϕ in steps of 5° from 0° to 180°. ($2\cos^2\alpha$ is quickly obtained from Tables IV. and V.)

Table VI. gives $2\lambda a\cos^2\alpha$ (equation 12) for values of $2\cos^2\alpha$ in steps of 0·1 from 0 to 2, and values of a as above.

By the aid of these tables the energy changes suffered by a particle in a succession of free paths and collisions are readily determined, given a series of values of b, θ and ϕ and the initial value of a.

Appropriate values of each of the three independent parameters b, θ and ϕ, having the correct distribution, were selected by drawing suitably marked cards at random from a large bowl, in which they had been vigorously stirred.

Selection of b.—The probability that a given free path exceeds a length $l=b\bar{l}$, is $\epsilon^{-l/\bar{l}}=\epsilon^{-b}$. A thousand small cards were divided among the ranges $b=0$ to $b=0{\cdot}2$, $b=0{\cdot}2$ to $b=0{\cdot}4$, etc., in accordance with this distribution law, and suitably marked. The probability of a free path greater than eight times the mean free path is less than one in a thousand. Hence, the values assigned to the parameter b were restricted to the range 0 to 8 as above.

Selection of θ.—The probability that a given inclination to the direction of the field should be less than an angle θ is $\frac{1}{2}(1-\cos\theta)$. A thousand cards were divided among the ranges $\theta=0°$ to $\theta=5°$, $\theta=5°$ to $\theta=10°$, etc., in accordance with this distribution law, and suitably marked.

Selection of φ.—All values of ϕ are equally probable. Equal numbers of cards were allotted to the ranges $\phi=0°$ to $\phi=5°$, $\phi=5°$ to $\phi=10°$, etc., making 360 cards in all. The actual distribution of a large number of cards, individually drawn in this way, was tested and found to be in satisfactory agreement with the corresponding theoretical distribution in each case. Altogether, for the purposes of the energy calculations, rather more than twelve thousand individual cards were drawn in the selection of values of each of the parameters b, θ and ϕ.

The energy changes were studied for five distinct groups, each of two hundred particles. The initial energies allotted to the individual particles comprising each group were equally spaced throughout the energy range covered by the group; *e. g.*, the initial energies assigned to the particles of the first group were 0·400 E_1, 0·401 E_1, 0·402 E_1, etc. The final energy reached by each particle was computed at the end of a time interval such that the terms $b/\sqrt{a}$ in equation (13) give a total of ten units, which is the time required by a particle of constant energy E_1 to travel a distance equal to ten times the mean free path. The energy distributions of the five groups of particles after this interval of time are given in Table A.

As will be seen, the energies of the particles after ten units of time cover a wide range. Thus, of the two hundred particles initially in the range $a=1{\cdot}2$ to $a=1{\cdot}4$, twenty-five only have energies lying within the initial range, eighty-one have energies in higher ranges, and ninety-four have energies in lower ranges; while the highest energy reached lies in the range $a=2{\cdot}6$ to $a=2{\cdot}8$ and the lowest energy in the range $a=0{\cdot}2$ to $a=0{\cdot}4$. The final energies of this group are fairly equally spread above and below the initial range. On the other hand, in a group of low initial energy, many more particles have suffered energy gains than energy losses; and in a group of high initial energy the reverse is the case. These figures, then, illustrate the general tendency of the mean energy of a group to move towards a value for which the gains and losses of energy are, on the average, approximately equal.

TABLE A.

Showing the observed energy distributions of various groups of particles after a time interval of ten units. (The asterisk, marking the initial energy range of each group, facilitates the interpretation of the Table.)

Energy range in terms of a.	Initial Energy of Group (in terms of a).				
	0·4–0·6.	0·8–1·0.	1·2–1·4.	1·6–1·8.	2·2–2·4.
0 –0·2	11	3			
0·2–0·4	32	8	2		
0·4–0·6	52*	19	4		
0·6–0·8	37	35	20	9	1
0·8–1·0	31	41*	36	14	0
1·0–1·2	18	25	32	18	5
1·2–1·4	13	30	25*	25	14
1·4–1·6	3	16	24	30	24
1·6–1·8	3	11	23	27*	16
1·8–2·0		7	14	25	27
2·0–2·2		4	12	20	27
2·2–2·4		1	3	13	26*
2·4–2·6			4	9	22
2·6–2·8			1	5	15
2·8–3·0				3	13
3·0–3·2				1	5
3·2–3·4				0	4
3·4–3·6				1	2

Before it is possible to determine the equilibrium distribution of energies, it is necessary to obtain the intermediate distributions, after the time of ten units, for all the relevant initial energy groups. These intermediate distributions may be derived by interpolation from the results given in Table A, by means of the graphs shown in fig. 3. The full curves show the fraction of the particles, initially in a particular energy range, which, after ten units of time, have energies greater than a certain value. The broken curves are drawn so as to pass through the points of intersection of the full curves with corresponding ordinates; *e.g.* the points of intersection of the five distribution curves with the ordinates $a=0{\cdot}6$, $a=1{\cdot}0$, $a=1{\cdot}4$, $a=1{\cdot}8$ and $a=2{\cdot}4$ respectively, which mark the upper limits of the initial energies of the five groups. By means of the broken curves, it is then possible to construct the distribution curves for other groups of particles having different initial energies. This has been done in fig. 3 for the group having initial energies lying in the range $a=2{\cdot}6$ to $a=2{\cdot}8$. The distributions for all the groups covering the range $a=0$ to $a=3{\cdot}0$ are given in Table B, which shows the probability that a particle, of a given initial energy, shall have an energy lying in a particular range, after an interval of ten units of time.

Fig. 3.

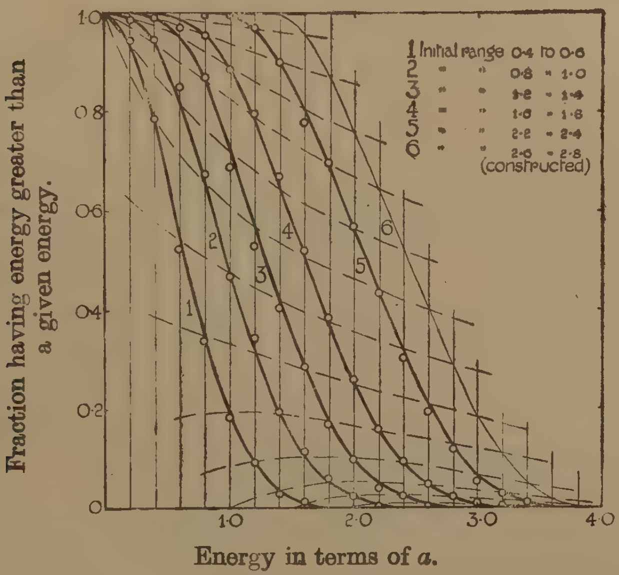

The Equilibrium Distribution.

Consider now a group of n particles occupying a particular volume V in the electric field, and having initial energies lying in a particular energy range. After an interval of time of ten units, the energies of the particles are distributed among adjacent energy ranges as shown in Table B. The energy changes which take place in this interval of time, however, involve the motion of some of the particles comprising the group to other adjacent regions of the gas, so that the group no longer occupies the specified volume V. But, if conditions are steady, the number of particles of a given energy which leave the volume V in a given time is exactly equal to the number of particles of the same energy

TABLE B.

Showing the energy distributions of various groups of particles after a time of ten units.
(Interpolated from fig. 3.)

Range after 10 units of time.	Initial Energy of Group (in terms of a).														
	0 to 0·2.	0·2 to 0·4.	0·4 to 0·6.	0·6 to 0·8.	0·8 to 1·0.	1·0 to 1·2.	1·2 to 1·4.	1·4 to 1·6	1·6 to 1·8	1·8 to 2·0	2·0 to 2·2	2·2 to 2·4	2·4 to 2·6	2·6 to 2·8	2·8 to 3·0
0 to 0·2	0·375	0·125	0·065	0·030	0·010	0·005									
0·2 ,, 0·4	0·235	0·295	0·150	0·095	0·055	0·025	0·010	0·005							
0·4 ,, 0·6	0·205	0·210	0·240	0·160	0·120	0·070	0·040	0·025	0·015						
0·6 ,, 0·8	0·110	0·180	0·195	0·205	0·155	0·135	0·090	0·050	0·030	0·020					
0·8 ,, 1·0	0·075	0·105	0·155	0·175	0·185	0·155	0·140	0·095	0·065	0·045	0·025	0·005			
1·0 ,, 1·2		0·065	0·100	0·140	0·160	0·165	0·150	0·145	0·100	0·075	0·060	0·030	0·005		
1·2 ,, 1·4		0·020	0·060	0·095	0·125	0·145	0·150	0·145	0·145	0·105	0·085	0·065	0·035	0·005	
1·4 ,, 1·6			0·025	0·055	0·085	0·120	0·140	0·140	0·140	0·140	0·110	0·095	0·075	0·045	0·005
1·6 ,, 1·8			0·010	0·025	0·055	0·075	0·105	0·130	0·130	0·135	0·135	0·110	0·105	0·085	0·045
1·8 ,, 2·0				0·015	0·025	0·050	0·075	0·100	0·125	0·125	0·125	0·130	0·110	0·105	0·095
2·0 ,, 2·2				0·005	0·020	0·030	0·050	0·065	0·095	0·120	0·125	0·125	0·130	0·115	0·115
2·2 ,, 2·4					0·005	0·015	0·025	0·050	0·065	0·085	0·110	0·120	0·120	0·125	0·115
2·4 ,, 2·6						0·010	0·015	0·025	0·045	0·065	0·085	0·110	0·115	0·120	0·125
2·6 ,, 2·8							0·010	0·015	0·025	0·045	0·065	0·080	0·110	0·110	0·120
2·8 ,, 3·0								0·010	0·015	0·020	0·040	0·065	0·075	0·105	0·105
3·0 ,, 3·2									0·005	0·015	0·020	0·035	0·060	0·075	0·105
3·2 ,, 3·4										0·005	0·010	0·020	0·035	0·060	0·070
3·4 ,, 3·6											0·005	0·010	0·015	0·030	0·060
3·6 ,, 3·8													0·010	0·015	0·030
3·8 ,, 4·0														0·005	0·010

which enter the volume V from adjacent regions of the gas during the same time. Thus, after an interval of time of ten units, the n particles can be thought of as remaining within the specified volume V and as having energies distributed among the different ranges in accordance with the probabilities given in Table B.

After a further interval of time of ten units, the energies of the n particles are still more widely distributed; the distribution being readily determined from the distribution at the end of the first interval together with a knowledge of the appropriate probabilities, as given in Table B. If the distribution of the energies is followed through successive intervals of time, each of ten units, the final equilibrium distribution is eventually obtained. Thus, Table C shows the approach to equilibrium of a group of particles, whose initial energies lie in the range $a=1{\cdot}2$ to $a=1{\cdot}4$. It will be observed that after seventy units of time, no appreciable change in the distribution takes place in a further ten units of time. In other words, the distribution shown in the last column is stable, the rate of interchange of particles between any two energy ranges being the same in either direction. Clearly, the same final distribution is obtained no matter what the initial energy of the group of particles considered.

TABLE C.

Showing the approach of a group of particles to the equilibrium distribution of energies.

Energy range in terms of a.	Time interval (arbitrary units).								
	0	10	20	30	40	50	60	70	80
0 –0·2			0·009	0·016	0·020	0·022	0·023	0·024	0·024
0·2–0·4		0·010	0·031	0·041	0·046	0·048	0·049	0·050	0·050
0·4–0·6		0·040	0·064	0·071	0·074	0·074	0·075	0·075	0·075
0·6–0·8		0·090	0·095	0·095	0·094	0·093	0·092	0·092	0·092
0·8–1·0		0·140	0·118	0·110	0·106	0·104	0·103	0·102	0·101
1·0–1·2		0·150	0·127	0·115	0·109	0·106	0·104	0·103	0·102
1·2–1·4	1·000	0·150	0·123	0·110	0·104	0·101	0·099	0·097	0·096
1·4–1·6		0·140	0·111	0·100	0·095	0·092	0·090	0·089	0·089
1·6–1·8		0·105	0·091	0·085	0·082	0·079	0·078	0·077	0·077
1·8–2·0		0·075	0·072	0·070	0·068	0·067	0·066	0·066	0·066
2·0–2·2		0·050	0·056	0·057	0·057	0·057	0·057	0·056	0·056
2·2–2·4		0·025	0·039	0·042	0·043	0·044	0·044	0·045	0·045
2·4–2·6		0·015	0·027	0·031	0·034	0·035	0·036	0·036	0·037
2·6–2·8		0·010	0·018	0·022	0·025	0·027	0·028	0·029	0·029
2·8–3·0			0·010	0·015	0·017	0·019	0·020	0·021	0·022
over 3·0			0·009	0·020	0·026	0·032	0·036	0·038	0·039
over 4·0						0·002	0·003	0·003	0·003

It follows, however, from equation (9) that the form of the distribution of the energies about the mean energy is independent of the value assigned to λ, the mean loss of energy in a collision, provided λ is small. Thus, the distribution which has been derived, on the assumption that $\lambda=0{\cdot}01$, holds equally well for values of λ of the order 10^{-3} or 10^{-4}. It is, therefore, the energy distribution for electrons moving through an ideal gas, in obedience to the classical laws of impact, which have been assumed. The energy ranges of Table C are not, however, expressed in terms of the mean energy $\overline{E}$, but in terms of $E_1=Xe\bar{l}/2\sqrt{\lambda}$ (equation (10)). Summing the energies associated with the various ranges, we obtain for the mean energy of electrons moving in an electric field X,

$$\overline{E}=1{\cdot}42E_1=0{\cdot}71\frac{Xe\bar{l}}{\sqrt{\lambda}}. \qquad \dots\dots \quad (14)$$

Thus, the numerical factor of equation (9) is now determined, *i. e.* $\bar{a}=1{\cdot}42$.

Discussion.

The distribution formulæ derived by Druyvesteyn and Townsend respectively may now be compared with that obtained by direct computation of the energies of a thousand particles. Writing $\gamma=Xe/m$ in equation (2), and expressing the velocity u of an electron in terms of the parameter a, Druyvesteyn's distribution formula becomes

Fig. 4.

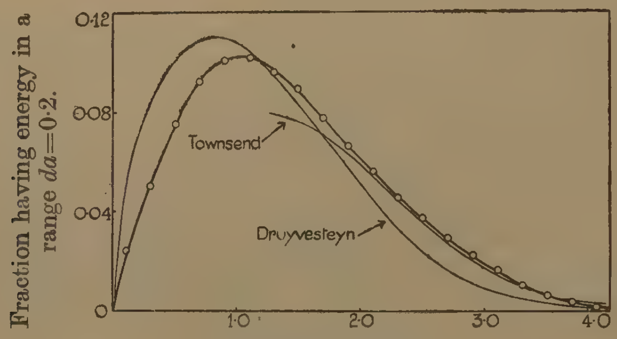

Energy in terms of *a*.

$$\frac{dn}{n}=D\,.\,\sqrt{a}\,.\,\epsilon^{-\frac{3}{8}a^2}da,$$

where D is a constant involving the quantity E_1.

Similarly, Townsend's distribution formula reduces to

$$\frac{dn}{n}=\frac{1}{\sqrt{\pi}}\,.\,\epsilon^{-\left[\frac{a}{1\cdot42}-0\cdot85\right]^2}\frac{da}{1{\cdot}42}.$$

These two distributions are exhibited graphically in fig. 4, where they may be compared with the distribution obtained by direct computation.

It will be observed that Townsend's distribution, though incomplete, since it applies only to energies in excess of the mean, agrees fairly closely with the computed distribution over the range where they may be compared. It may be remarked, however, that Townsend's formula does not give actual energies, but only expresses the energies in terms of the mean energy $\overline{E}$. Druyvesteyn's formula is not in such close agreement with the computed distribution, giving many more electrons of low energy and less of high energy than the computed distribution, which is, by comparison, more nearly symmetrical. The reason for this will be discussed later. Moreover, the mean energy, as calculated from Druyvesteyn's formula is correspondingly lower, being $1{\cdot}21\ E_1$, as compared with $1{\cdot}42\ E_1$ (equation 14). Llewellyn Jones' distribution is not shown in fig. 4, since it is not strictly comparable with the other distributions, being an empirical modification of the Druyvesteyn formula designed to allow for the variation of the effective cross-section of the molecules of a specific, non-ideal gas.

The lack of agreement between the Druyvesteyn distribution and that obtained here by direct computation calls for some explanation. One factor of importance, which is left out of account in Druyvesteyn's derivation, is the variation of the loss of energy in a collision with the angle of impact of the electron upon the molecule. The energy loss is equated to the mean energy loss, whatever the conditions of impact. Now it is clear that, if two successive free paths are inclined to the direction of the electric field at comparatively small angles, the intervening collision is made at a large angle of impact α, and the loss of energy suffered in the collision is consequently small. It follows that, in a succession of free paths where an electron is moving more or less in the negative direction of the field, and the energy, therefore, is increasing rapidly, the energy losses are less than those assumed in Druyvesteyn's derivation, *i. e.*, the energy increases more rapidly than he has supposed. On the other hand, where an electron is moving more or less in the positive direction of the field, and the energy, therefore, is decreasing rapidly, the energy losses in collision are again less than the mean, *i. e.*, the energy decreases less rapidly than Druyesteyn's derivation supposes.

It seems likely that these considerations may account for the comparatively large number of electrons of low energy and the smaller number of electrons of high energy given by the Druyvesteyn formula. There is little doubt that the distribution derived in this paper, as a result of the direct computation of the energy changes of a thousand particles, involving rather more than twelve thousand free paths and the same number of collisions, is the correct solution of the classical form of the problem, within the energy range considered.

In conclusion, my best thanks are due to my wife, who not only took a most active part in the selection of the parameters b, θ and ϕ required for the calculations, but also made herself entirely responsible for the calculation of the energy changes of one of the groups of two hundred particles.

References.

Townsend, J. S., Phil. Mag. ix. p. 1145 (1930).
Druyvesteyn, M. J., *Physica*, x. p. 69 (1930).
Druyvesteyn, M. J., *Physica*, iii. p. 65 (1936).

Smit, J. A., *Physica*, iii. p. 543 (1937).
Emeléus, K. G., Lunt, R. W., and Meek, C. A., Proc. Roy. Soc. A, clvi. p. 394 (1936).
Llewellyn Jones, F., Proc. Phys. Soc. xlviii. p. 513 (1936).
Llewellyn Jones, F., Proc. Phys. Soc. lvi. p. 239 (1944).

XXIII. *Notes on the Evaluation of Zeros and Turning Values of Bessel Functions.—IV. A New Expansion.*

By J. C. P. Miller, Ph.D. and C. W. Jones, B.Sc., University of Liverpool *.

[Received July 25, 1944.]

1. *Introduction.*

The method of computation of zeros of Bessel functions to be described in this note makes use of a pair of mutually checking series, involving the values of two Bessel functions only. These series are applied either directly to tabulated values or to interpolated values, nearer the zero, found as described in § 4. A typical computation is given in § 5.

The following standard results are quoted for easy reference.

$$J_{n+1}(x)+J_{n-1}(x)=\frac{2n}{x}J_n(x). \qquad (1.1)$$

$$J_{n-1}(x)-\frac{n}{x}J_n(x)=J_n'(x), \qquad (1.2)$$

$$-J_{n+1}(x)+\frac{n}{x}J_n(x)=J_n'(x). \qquad (1.3)$$

In these relations, and in subsequent sections of this note, $J_n(x)$ may be replaced by the general solution $\mathscr{C}_n(x)=aJ_n(x)+bY_n(x)$ of Bessel's differential equation of order n, where a and b are constants independent both of n and of x. The example in § 5 refers, in fact, to $Y_4(x)$.

2. *The Formulæ.*

2.1. Suppose that we have an approximation $x=x_1$ to a zero of $J_n(x)$, and that the exact value of the zero is $x_0(\neq 0)$. Write

$$p=p(x)=\frac{1}{2n}\left\{1+\frac{J_{n+1}(x)}{J_{n-1}(x)}\right\}=\frac{1}{x}\frac{J_n(x)}{J_{n-1}(x)}, \qquad (2.11)$$

$$q=q(x)=\frac{1}{2n}\left\{1+\frac{J_{n-1}(x)}{J_{n+1}(x)}\right\}=\frac{1}{x}\frac{J_n(x)}{J_{n+1}(x)}, \qquad (2.12)$$

$$h=x_0-x, \quad r=h/x. \qquad (2.13)$$

Clearly p, q and r all vanish at the zero $x=x_0$ of $J_n(x)$.

---

* Communicated by the Authors.

The method consists in developing r as a power-series in either p or q, with coefficients that are functions of x. Thus r involves x both explicitly and also implicitly through p or q. Provided that x_0 does not occur explicitly, the substitution $x=x_1$ in either series then leads to a direct calculation of the zero.

From (2.13)

$$x(1+r)=x_0, \quad \ldots \quad (2.14)$$

where x_0 is a constant. Differentiating this totally with respect to x:

$$1+r+x\frac{\partial r}{\partial x}+x\frac{\partial r}{\partial p}\frac{dp}{dx}=0. \quad \ldots \quad (2.15)$$

Now, by logarithmic differentiation of (2.11), and by use of (1.2) and (1.3),

$$\frac{1}{x}+\frac{1}{p}\frac{dp}{dx}=\frac{J_n'(x)}{J_n(x)}-\frac{J'_{n-1}(x)}{J_{n=1}(x)}=\frac{1}{xp}-\frac{n}{x}+xp-\frac{n-1}{x}. \quad . \quad (2.16)$$

Hence

$$x\frac{dp}{dx}=1-2np+x^2p^2, \quad \ldots \quad (2.17)$$

so that, if (2.15) and (2.17) are to be consistent,

$$(1-2np+x^2p^2)\frac{\partial r}{\partial p}+1+r+x\frac{\partial r}{\partial x}=0. \quad \ldots \quad (2.18)$$

2.2. Assuming that

$$r=-a_1p-a_2p^2-a_3p^3-\ldots \quad \ldots \quad (2.21)$$

(in which the absence of a term independent of p identifies the constant x_0 of (2.14) with a zero of $J_n(x)$, and where the coefficients a_m may be functions of x) we find, on substituting in (2.18) and equating to zero the coefficients of successive powers of p,

$$a_1=1,$$

$$2a_2=(2n-1)a_1,$$

and generally

$$(m+1)a_{m+1}=(2mn-1)a_m-(m-1)x^2a_{m-1}-x\frac{da_m}{dx}. \quad . \quad . \quad (2.22)$$

The coefficients are, successively,

$$\left.\begin{aligned}
a_1&=1\\
a_2&=\frac{1}{2!}(2n-1)\\
a_3&=\frac{1}{3!}(2n-1)(4n-1)-\frac{1}{3}x^2\\
a_4&=\frac{1}{4!}(2n-1)(4n-1)(6n-1)-\frac{1}{2}(2n-1)x^2\\
a_5&=\frac{1}{5!}(2n-1)(4n-1)(6n-1)(8n-1)-\frac{2}{5}(2n-1)(3n-1)x^2+\frac{1}{5}x^4\\
a_6&=\frac{1}{6!}(2n-1)(4n-1)(6n-1)(8n-1)(10n-1)\\
&\qquad-\frac{1}{180}(2n-1)(480n^2-278n+41)x^2+\frac{1}{2}(2n-1)x^4
\end{aligned}\right\}, \quad (2.23)$$

and generally,

$$a_m = \sum_{k=0}^{[\frac{1}{2}(m-1)]} (-1)^k C_{m,k} x^{2k}, \qquad (2.24)$$

where $$(m+1)C_{m+1,k} = (m-1)C_{m-1,k-1} + (2mn-2k-1)C_{m,k}, \qquad (2.25)$$

and $$C_{1,0}=1\,;\; C_{1,k}=0,\; k>0\,;\; C_{m,k}=0,\; k<0. \qquad (2.26)$$

The coefficients $C_{m,k}$ depend, of course, on n also.

Since a corresponding pair of values x_1 and $p=p(x_1)$ are known, r is given in a form suitable for computation by

$$r=-p\left[1+\frac{1}{2}(2n-1)p+\frac{1}{6}\{(2n-1)(4n-1)-2x_1^2\}p^2+\ldots\right]. \qquad (2.27)$$

Similarly, or by putting $-n$ for n and $-q$ for p throughout,

$$r=q\left[1+\frac{1}{2}(2n+1)q+\frac{1}{6}\{(2n+1)(4n+1)-2x_1^2\}q^2+\ldots\right]. \qquad (2.28)$$

The zero may then be calculated from (2.14).

2.3. *Remarks.*—(i.) The double calculation, using (2.27) and (2.28), checks only stages following the determination of $J_{n-1}(x)$ and $J_{n+1}(x)$. Since, as stated in § 1, the difference equation (1.1) has the general solution $\mathscr{C}_n(x)=aJ_n(x)+bY_n(x)$, it follows that a function $\mathscr{C}_n(x)$ corresponding to assigned values of $\mathscr{C}_{n-1}(x)$ and $\mathscr{C}_{n+1}(x)$ at a particular value of x can always be found by suitable choice of a and b. It is thus evident that the values of the Bessel functions used must be independently checked.

(ii.) The relations (2.23) suggest—as can be independently verified—that when $n=\frac{1}{2}$, $r=(1/x)\tan^{-1}xp$.

2.4. *The McMahon Series for $n=3/2$ and $n=5/2$.*

Combining (2.21) and (2.24), we have

$$r=-\sum_{m=1}^{\infty} p^m \sum_{k=0}^{[\frac{1}{2}(m-1)]} (-1)^k C_{m,k} x^{2k}. \qquad (2.41)$$

Now $$\left.\begin{aligned} J_{1/2}(x)&=(\tfrac{1}{2}\pi x)^{-1/2}\sin x \\ J_{3/2}(x)&=(\tfrac{1}{2}\pi x)^{-1/2}\left(\frac{\sin x}{x}-\cos x\right) \end{aligned}\right\}, \qquad (2.42)$$

so that, when s is large (*cf.* II. (1.1)) * we may take as an approximation to the sth positive zero of $J_{3/2}(x)$

$$x_1=\beta=(4s+2)\pi/4=(s+\tfrac{1}{2})\pi. \qquad (2.43)$$

---

* References in this style are to earlier notes in this series, Phil. Mag. (7) vol. xxxvi. p. 124 (1945).

[*To face* p. 203.

n	a_2	a_3		
-10	-21	$+861 \; -2x^2$	-5252	$+7560x^4$
-9	-19	$+703 \; -2x^2$	-3866	$+6840x^4$
-8	-17	$+561 \; -2x^2$	-2748	$+6120x^4$
-7	-15	$+435 \; -2x^2$	-1870	$+5400x^4$
-6	-13	$+325 \; -2x^2$	-1202	$+4680x^4$
-5	-11	$+231 \; -2x^2$	-716	$+3960x^4$
-4	-9	$+153 \; -2x^2$	-382	$+3240x^4$
-3	-7	$+91 \; -2x^2$	-172	$+2520x^4$
-2	-5	$+45 \; -2x^2$	-58	$+1800x^4$
-1	-3	$+15 \; -2x^2$	-10	$+1080x^4$
0	-1	$+1 \; -2x^2$	$-$	$+360x^4$
$+1$	$+1$	$+3 \; -2x^2$	$+1$	$+360x^4$
$+2$	$+3$	$+21 \; -2x^2$	$+23$	$+1080x^4$
$+3$	$+5$	$+55 \; -2x^2$	$+93$	$+1800x^4$
$+4$	$+7$	$+105 \; -2x^2$	$+241$	$+2520x^4$
$+5$	$+9$	$+171 \; -2x^2$	$+495$	$+3240x^4$
$+6$	$+11$	$+253 \; -2x^2$	$+885$	$+3960x^4$
$+7$	$+13$	$+351 \; -2x^2$	$+1439$	$+4680x^4$
$+8$	$+15$	$+465 \; -2x^2$	$+2185$	$+5400x^4$
$+9$	$+17$	$+595 \; -2x^2$	$+3153$	$+6120x^4$
$+10$	$+19$	$+741 \; -2x^2$	$+4371$	$+6840x^4$
$-5/2$	-6	$+66 \; -2x^2$	-105	$+2160x^4$
$-3/2$	-4	$+28 \; -2x^2$	-28	$+1440x^4$
$-1/2$	-2	$+6 \; -2x^2$	-24	$+720x^4$
$+1/2$	0	$-2x^2$		0
$+3/2$	$+2$	$+10 \; -2x^2$	$+8$	$+720x^4$
$+5/2$	$+4$	$+36 \; -2x^2$	$+504$	$+1440x^4$
$-2/3$	$-7/3$	$+77/9 \; -2x^2$	$-385/9$	$+840x^4$
$-1/3$	$-5/3$	$+35/9 \; -2x^2$	$-35/3$	$+600x^4$
$+1/3$	$-1/3$	$-1/9 \; -2x^2$	$-1/9$	$+120x^4$
$+2/3$	$+1/3$	$+5/9 \; -2x^2$	$+5/3$	$+120x^4$
$-3/4$	$-5/2$	$+10 \; -2x^2$	-55	$+900x^4$
$-1/4$	$-3/2$	$+3 \; -2x^2$	$-15/2$	$+540x^4$
$+1/4$	$-1/2$	$-2x^2$		$+180x^4$
$+3/4$	$+1/2$	$+1 \; -2x^2$	$+7/2$	$+180x^4$

Then
$$p=\frac{J_{3/2}(\beta)}{\beta J_{1/2}(\beta)}=\frac{1}{\beta^2},$$

so that
$$r=-\sum_{m=1}^{\infty}\beta^{-2m}\sum_{k=0}^{[\frac{1}{2}(m-1)]}(-1)^k C_{m,k}\beta^{2k}$$
$$=-\sum_{m=1}\beta^{-2m}\sum_{k=0}^{m-1}(-1)^k C_{m+k,k}, \quad . \quad . \quad . \quad . \quad . \qquad (2.44)$$

where
$$(m+1)C_{m+1,k}=(m-1)C_{m-1,k-1}+(3m-2k-1)C_{m,k} \quad . \qquad (2.45)$$

and the initial conditions (2.26) still apply. Then $x_0=\beta(1+r)$ gives precisely the McMahon series for $n=3/2$.

Similarly, since
$$J_{5/2}(x)=(\tfrac{1}{2}\pi x)^{-1/2}\left\{\left(\frac{3}{x^2}-1\right)\sin x-\frac{3}{x}\cos x\right\}, \quad . \quad . \quad . \qquad (2.46)$$

we may take as an approximation to the sth positive zero of $J_{5/2}(x)$
$$x_1=\beta=(4s+4)\pi/4=(s+1)\pi, \quad . \quad . \quad . \quad . \quad . \quad . \quad . \qquad (2.47)$$

giving
$$p=\frac{J_{5/2}(\beta)}{\beta J_{3/2}(\beta)}=\frac{3}{\beta^2}$$

so that
$$r=-\sum_{m=1}^{\infty}3^m\beta^{-2m}\sum_{k=0}^{[\frac{1}{2}(m-1)]}(-1)^k C_{m,k}\beta^{2k}$$
$$=-\sum_{m=1}^{\infty}3^m\beta^{-2m}\sum_{k=0}^{m-1}(-3)^k C_{m+k,k}, \quad . \quad . \quad . \quad . \qquad (2.48)$$

where
$$(m+1)C_{m+1,k}=(m-1)C_{m-1,k-1}+(5m-2k-1)C_{m,k}, \quad . \qquad (2.49)$$

again with the initial conditions (2.26); this gives the McMahon series for $n=5/2$.

These two series are given in II. (3.5 and 3.8), with numerical coefficients as far as the terms in β^{-19}.

3. *The Coefficients.*

The series being written in the form
$$r=-p-\frac{1}{2!}\alpha_2p^2-\frac{1}{3!}\alpha_3p^3-\frac{1}{4!}\alpha_4p^4-\frac{1}{5!}\alpha_5p^5-\frac{1}{6!}\alpha_6p^6-\ldots, \qquad (3.1)$$
$$r=+q+\frac{1}{2!}\beta_2q^2+\frac{1}{3!}\beta_3q^3+\frac{1}{4!}\beta_4q^4+\frac{1}{5!}\beta_5q^5+\frac{1}{6!}\beta_6q^6+\ldots, \qquad (3.2)$$

where
$$\beta_s(n)=(-1)^{s-1}\alpha_s(-n), \quad . \quad . \quad . \quad . \quad . \quad . \quad . \qquad (3.3)$$

the table opposite gives the coefficients α_2 to α_6 as polynomials in x^2 for $n=-10(1)+10$, and for some commonly needed non-integral values of n,

4. *Initial Approach to a Zero.*

Sometimes we cannot obtain directly from tables of Bessel functions a value of x_1 sufficiently near to the zero for the convergence of the series (2.27, 2.28) to be rapid enough. This is often the case if the tabular interval of x is unity and zeros are required to 10 decimals. In such cases it is often quicker first to use the following method of approach, based on the Bessel-Lommel expansions (W 140)

$$J_n(x+\xi)=\left(\frac{x+\xi}{x}\right)^n\left\{J_n(x)-\eta J_{n+1}(x)+\frac{\eta^2}{2!}J_{n+2}(x)-\ldots\right\}$$

$$=\left(\frac{x+\xi}{x}\right)^n A_n(x+\xi), \quad (4.1)$$

$$J_n(x+\xi)=\left(\frac{x}{x+\xi}\right)^n\left\{J_n(x)+\eta J_{n-1}(x)+\frac{\eta^2}{2!}J_{n-2}(x)+\ldots\right\}$$

$$=\left(\frac{x}{x+\xi}\right)^n B_n(x+\xi), \quad (4.2)$$

where $\eta=\xi(1+\xi/2x)$ and A_n, B_n are defined by these relations. In the following we shall write $x'=x+\xi=\sqrt{x^2+2\eta x}$.

Some points of detail which simplify the application of (4.1) and (4.2) in the present case should be noted :

(i.) To bring the argument near the zero, we choose a convenient value of η (and not of ξ).

(ii.) If the value of η is taken as a multiple of 0·03 the coefficients $\eta^m/m!$, which are readily tabulated, are short terminating decimals when $m<7$; a certain saving of labour is thus effected. The corresponding value of x' is obtained, usually without interpolation, from a suitable table of square roots.

(iii.) If η is positive, we use (4.2), if negative (4.1)—for the various terms making up $A_n(x')$ or $B_n(x')$ then retain the signs of the corresponding $J_{n\pm m}(x)$, so that the chance of error is reduced.

In this way, either $A_{n+1}(x')$, $A_n(x')$, $A_{n-1}(x')$ or $B_{n+1}(x')$, $B_n(x')$, $B_{n-1}(x')$ are calculated. The results are checked by the modified recurrence formulæ corresponding to (1.1), namely,

$$x'^2A_{n+1}(x')+x^2A_{n-1}(x')=2nxA_n(x'), \quad . \quad . \quad . \quad . \quad (4.3)$$

$$x^2B_{n+1}(x')+x'^2B_{n-1}(x')=2nxB_n(x'). \quad . \quad . \quad . \quad . \quad (4.4)$$

It is worth remarking that n, x, x^2 and x'^2 are usually integers or short terminating decimals, and are therefore easy to handle. On the other hand, x' will not in general terminate.

Finally, using $x_1=x'$, we evaluate

$$p=\frac{A_n(x')}{xA_{n-1}(x')}=\frac{xB_n(x')}{x'^2B_{n-1}(x')}, \quad . \quad . \quad . \quad . \quad . \quad (4.5)$$

$$q=\frac{xA_n(x')}{x'^2A_{n+1}(x')}=\frac{B_n(x')}{xB_{n+1}(x')}, \quad . \quad . \quad . \quad . \quad . \quad (4.6)$$

whence x_0 is derived by the method previously described.

5. *Example of the Use of the Formulæ.*

We shall consider the fifth zero of $Y_4(x)$, near $x=19{\cdot}224$, and derive it from the values of $Y_n(19)$ that are given below to 10 decimals. We take $\eta=+0{\cdot}24$ and use (4.2) since $\eta>0$, thus deriving the values of $B_3(x')$, $B_4(x')$, $B_5(x')$ as shown in the table. We also find

$$x'=x+\xi=\sqrt{x^2+2\eta x}=\sqrt{370{\cdot}12}=19{\cdot}23850\ 30602\ 7$$

n	$Y_n(19)$
± 5	$\mp 0{\cdot}18627\ 62496$
± 4	$-0{\cdot}04031\ 25617$
± 3	$\pm 0{\cdot}16930\ 25394$
± 2	$+0{\cdot}09377\ 65215$
± 1	$\mp 0{\cdot}14956\ 01139$
0	$-0{\cdot}10951\ 96914$

m	$\eta^m/m!$	B_3	B_4	B_5
0	1	+0·16930 25394	−0·04031 25617	−0·18627 62496
1	0·24	+ 2250 63652	+ 4063 26095	− 967 50148
2	0·0288	− 430 73313	+ 270 07638	+ 487 59131
3	230 4	− 25 23334	− 34 45865	+ 21 60611
4	13 824	+ 2 06752	− 1 51400	− 2 06752
5	66355	+ 6223	+ 9924	− 7267
6	2654	− 449	+ 249	+ 397
7	91	− 4	− 15	+ 9
8	3	+ 1		− 1
	Sums	+0·18727 04922	+0·00266 21009	−0·19088 06516

Checking by (4.4), we obtain

$$x^2B_5(x')+x'^2B_3(x')-8xB_4(x')=8{\cdot}7\times 10^{-9},$$

which is satisfactory. Next, remembering that x', not x, is our approximation to the zero, we derive:

$$p=\frac{xB_4(x')}{x'^2B_3(x')}=+\frac{0{\cdot}05057\ 99171}{69{\cdot}31255\ 457}=+0{\cdot}00072\ 97367\ 3.$$

Coefficients	Terms in Series (3.1)
$-\ 1$	$r_p=-0{\cdot}00072\ 97367\ 3$
$-7/2=-\ 3{\cdot}5$	$-\ 18638\ 0$
$-(105-2x'^2)/6=+\ 105{\cdot}87\dot{3}$	$+\ 411\ 4$
$-(2415-84x'^2)/24=+1194{\cdot}795$	$+\ 3\ 4$
	$=-0{\cdot}00073\ 15590\ 5$

Similarly,

$$q=\frac{B_4(x')}{xB_5(x')}=-\frac{0\cdot00266\ 21009}{3\cdot62673\ 2380}=-0\cdot00073\ 40218\ 7.$$

Coefficients	Terms in Series (3.2)
$+\quad 1$	$r_q=-0\cdot00073\ 40218\ 7$
$+9/2=+\quad 4\cdot5$	$+\quad 24245\ 5$
$+(153-2x'^2)/6=-\quad 97\cdot87\dot{3}$	$+\quad 387\ 1$
$+(3825-108x'^2)/24=-1506\cdot165$	$-\quad 4\ 4$
	$=-0\cdot00073\ 15590\ 5$

Thus we obtain for the zero of $Y_4(x)$

$$x'(1+r)=19\cdot22442\ 89592\ (5),$$

which may be compared with the more accurate value

$$19\cdot22442\ 89593\ 16\ldots\ldots$$

XXIV. *Notes on the Evaluation of Zeros and Turning Values of Bessel Functions.—V. Checks.*

By W. G. Bickley, D.Sc., Imperial College, London,
and
J. C. P. Miller, Ph.D., University of Liverpool*.

[Received July 25, 1944.]

1. In table making, the checking of the computations is of paramount importance, and upon occasion may be more troublesome than the original calculations. Mere repetition—even by different computers—is the worst check, involving as it does use of the same data and formulæ; *independent* checks are highly desirable. The search for, and the description of, independent methods of calculation applicable to the same ranges and to the same data, such as have been given in Notes III. and IV., is thus justified.

2.1. The check by differences is—with modern machine facilities—the simplest and most efficient general method, but it is not universally applicable, and in any case ceases to be sufficiently discriminating near the end of a sequence. With an infinite sequence the latter difficulty may be overcome if it is possible to attach values beyond those actually being checked, so that all important values are removed from near the end of the sequence differenced. Such a device is, however, not available when a sequence has a "natural" end, as in the present case when s (the serial number of the zero) is of necessity a positive integer. Moreover, it usually happens that approach to such a natural end is accompanied by increase in magnitude, and consequent rapid variation, of the differences.

---

* Communicated by the Authors.

For fixed n, each of the sequences $j_{n,s}$ and $y_{n,s}$ may be checked at the upper end (*i. e.* for large s) by differencing. First differences tend to π as s tends to infinity in both sequences. It is possible, however, to combine them into a single sequence, as may be inferred from the fact that the McMahon expansions have common coefficients (*cf.* Note III.).

Table I.

Early zeros of Bessel functions.

Y_0	J_0	Y_1	J_1	Y_2	J_2	Y_3	J_3
0·89358							
	2·40483	2·19714					
3·95768			3·83171	3·38424			
	5·52008	5·42968			5·13562	4·52702	
7·08605			7·01559	6·79381			6·38016
	8·65373	8·59601			8·41724	8·09755	
10·22235			10·17347	10·02348			9·76102
	11·79153	11·74915			11·61984	11·39647	
13·36110			13·32369	13·20999			13·01520
	14·93092	14·89744			14·79595	14·62308	
16·50092			16·47063	16·37897			16·22347
	18·07106	18·04340			17·95982	17·81846	
19·64131			19·61586	19·53904			19·40942

Combination has an effect equivalent to halving the tabular interval, and so differences become an adequate check for smaller values of s. The way in which the sequences do dovetail together can be seen from the pairs of columns devoted to the same order in Table I.

The existence of the double sequence, ordered as regards both n and s, renders possible a number of cross-checks, but before describing these it is convenient to enlarge the effective range of Table I. by considering negative values of n.

2.2. When n is an integer,

$$J_{-n}(x)=(-)^n J_n(x), \quad Y_{-n}(x)=(-)^n Y_n(x), \quad . \quad . \quad . \quad (2.21)$$

so that functions of equal and opposite order have the same zeros. Thus Table I. can be continued, by reflection in the zero vertical, to include negative orders. In the table so continued, however, a sequence characterized in the right-hand half by constant s is continued on the left by proceeding along the same diagonal line—but the entries are no longer characterized by constant s. The necessary correspondences come at once by consideration of the McMahon expansion. The coefficients are functions of n^2, and so are the same for negative as for positive n. Consequently we have

$$c_{-n,\,a}=c_{n,\,a}, \qquad (2.22)$$

and if s' is to be associated with $-n$ to give the same zero as s with n,

$$-2n+4s'=2n+4s,$$

or

$$s'=n+s \qquad (2.23)$$

Otherwise stated, the sequence with constant s becomes, on reflection in $n=0$, the sequence with constant $(n+s)$.

In this manner the sequence consisting of the fourth zeros of $J_n(x)$ for positive n would be continued using the entries of Table I. as follows :—

n	$j_{n,\,4}$	δ	δ^2	^{3}
+3	16·22347			
		−1·42752		
+2	14·79595		− 4474	
		−1·47226		− 1516
+1	13·32369		− 5990	
		−1·53216		− 2600
0	11·79153		− 8590	
		−1·61806		− 5227
−1	10·17347		−13817	
		−1·75623		−14268
−2	8·41724		−28085	
		−2·03708		
−3	6·38016			

The differences given exhibit the success of the continuation rule (2.23). The range of the difference method has been extended—but we still encounter a natural end to the available sequence.

2.3. Since

$$y_{n,\,s}\sim(s+\tfrac{1}{2}n-\tfrac{3}{4})\pi, \quad j_{n,\,s}\sim(s+\tfrac{1}{2}n-\tfrac{1}{4})\pi, \qquad (2.31)$$

we see that

$$j_{n+2,\,s-1}\sim j_{n,\,s}, \quad y_{n+2,\,s-1}\sim y_{n,\,s}, \qquad (2.32)$$

$$y_{n+1,\,s}\sim j_{n,\,s}, \quad j_{n+1,\,s}\sim y_{n,\,s+1}. \qquad (2.33)$$

These approximate equalities are visible in Table I.

Moreover, the differences between the corresponding pairs will show regular variation as n, s, or any combination of these is systematically varied. Thus the differences between the corresponding members of the last row in Table I., continued backwards by the rule (2.23), along with their successive differences, are

$j_{3,5} - y_{2,6}$	−0·12962			
		5280		
$y_{2,6} - j_{1,6}$	−0·07682		−143	
		5137		96
$j_{1,6} - y_{0,7}$	−0·02545		− 47	
		5090		94
$y_{0,7} - j_{-1,7}$	+0·02545		+ 47	
		5137		96
$j_{-1,7} - y_{-2,8}$	+0·07682		+143	
		5280		
$y_{-2,8} - j_{-3,8}$	+0·12962			

The differences show the expected regularity, and once more the rule (2.23) has extended the sequence, so that the values for small n are adequately checked. The sequence has, however, natural ends at $n = \pm 12$.

Again, using the differences between the last two rows of the combined *jyjyj*... sequences,

$j_{3,5} - y_{3,5}$	1·59096				
		−1174			
$y_{2,6} - j_{2,5}$	1·57922		498		
		− 676		−43	
$j_{1,6} - y_{1,6}$	1·57246		455		30
		− 221		−13	
$y_{0,7} - j_{0,6}$	1·57025		442		26
		+ 221		+13	
$y_{-1,7} - y_{-1,7}$	1·57246		455		30
		+ 676		+43	
$y_{-2,8} - j_{-2,7}$	1·57922		498		
		+1174			
$j_{-3,8} - y_{-3,8}$	1·59096				

We encounter the expected regularity, and again the rule (2.23) has extended the sequence, and consequently the number of values for which the check is adequate.

2.4. The sequences of the last two paragraphs are instances of the innumerable sets which could be selected from the zeros of the Bessel functions.

Sequences such as that of (2.2) will be obtained by choosing a set of $c_{n,a}$ in which there is a relation between n and a, and n (or a) is systematically varied. If the first differences are to be asymptotically equal, the relation must be linear, of the form

$$Aa+Nn=K, \qquad (2.41)$$

in which A, N and K are constants such that the equation has solutions in positive integers. The precise relation which characterizes the actual sequence in (2.2) is

$$a-2n=15. \qquad (2.42)$$

For sequences such as those of (2.3) we take

$$c_{n,a}-c_{n',a'}$$

with relations between n, a, n', a'. The sequences actually exhibited are characterized by

$$n'=n-1, \quad a'=a=25 \qquad (2.43)$$

and

$$n'=n, \quad a'=a-2=23 \qquad (2.44)$$

respectively.

3.1. In the case of the zeros of any function an obvious check is to calculate the value of the function at the calculated zero, and thus to verify that it is—to an adequate approximation—zero. This will, however, seldom be independent of the interpolation which will usually be part (if not the whole) of the process by which the zero has been calculated. (*Cf.* Note III.) In the case of the larger zeros, calculated from the McMahon expansion, computation of the function would be independent—but laborious when outside the range for which the function had been calculated at a reasonably small interval.

3.2. For any cylinder function,

$$\mathscr{C}_n(x)=aJ_n(x)+bY_n(x), \qquad (3.21)$$

where a and b are constants independent both of x and of n,

$$2n\mathscr{C}_n(x)=x\{\mathscr{C}_{n-1}(x)+\mathscr{C}_{n+1}(x)\}, \qquad (3.22)$$

so that if $x=c$ is a zero of $\mathscr{C}_n(x)$,

$$\mathscr{C}_{n-1}(c)=-\mathscr{C}_{n+1}(c). \qquad (3.23)$$

Thus the numerical equality of $\mathscr{C}_{n-1}(c)$ and $\mathscr{C}_{n+1}(c)$ is a check upon the accuracy of (c). (*Cf.* Note III., and also § 2.1 of Note IV.) In most cases this check will be independent of the calculation of c, but it assumes that the initial values of $\mathscr{C}_{n-1}$, $\mathscr{C}_n$, and $\mathscr{C}_{n+1}$ are correct.

It may here be remarked that in virtue of the formula

$$\mathscr{C}_n'(x)=\tfrac{1}{2}\{\mathscr{C}_{n-1}(x)-\mathscr{C}_{n+1}(x)\} \qquad (3.24)$$

combined with (3.23),

$$\mathscr{C}_{n-1}(c)=\mathscr{C}_n'(c)=-\mathscr{C}_{n+1}(c), \qquad (3.25)$$

so that the computation of $\mathscr{C}_{n+1}(c)$ provides more than a check on the value of c by giving also the derivative of $\mathscr{C}_n(x)$ at its zero. In addition to its intrinsic interest, this is of importance inasmuch as it enters the formula for determining the Fourier-Bessel coefficients associated with the equation

$$\mathscr{C}_n(x)=0.$$

XXV. *Stresses in an Infinite Plate due to Isolated Forces and Couples acting near a Circular Hole.*

By BIBHUTIBHUSAN SEN *.

[Received January 31, 1944.]

Introduction.

THE distribution of stresses in an infinite plate due to forces in the plane of the plate applied to the internal boundary of a circular hole has been obtained by Bickley (1928). The object of this paper is to solve a different type of problem, namely, that of finding the stresses in an infinite plate, when either a force in the plane of the plate or a couple with its axis perpendicular to it, acts at a point *outside* a circular hole, not far away from the centre. In a recent paper † which will be referred to as paper I., the stresses in a thin circular disk due to isolated forces and couples acting at points *inside* the disk have been investigated by the author. The method used in this paper, which is the same as that of paper I., is as follows :

We assume that the plate is in a state of generalized plane stress and that its middle surface is given by the plane $z=0$. Taking the origin at the centre of the circular hole of radius a, we first write down the average stresses $\breve{xx}$ $\breve{xy}_1$, $\breve{yy}_1$, due to the force or the couple, as the case may be, acting at a point (outside the hole) on the *hypothesis* that the plate is infinite in extent and that there is no hole.

Putting

$$\left.\begin{aligned} r\breve{rx}_1&=x\breve{xx}_1+y\breve{xy}_1,\\ r\breve{ry}_1&=x\breve{xy}_1+y\breve{yy}_1,\end{aligned}\right\} \quad . \quad . \quad . \quad . \quad . \quad . \quad . \quad . \quad (A)$$

where $r=\sqrt{x^2+y^2}$,

we can calculate the values of $r\breve{rx}_1$ and $r\breve{ry}_1$ on the edge $r=a$. To annul these stresses on the boundary of the hole we must superimpose a stress system $r\breve{rx}_2$, $r\breve{ry}_2$, given by

$$\left.\begin{aligned} r\breve{rx}_2&=x\breve{xx}_2+y\breve{xy}_2,\\ r\breve{ry}_2&=x\breve{xy}_2+y\breve{yy}_2,\end{aligned}\right\} \quad . \quad . \quad . \quad . \quad . \quad . \quad . \quad . \quad (B)$$

where xx_2, $\breve{xy}_2$ and $\breve{yy}_2$ are sets of average stresses possible in a thin elastic plate, such that they vanish at infinity and satisfy the conditions

$$\left.\begin{aligned} [\breve{rx}_2]_{r=a}&=-[\breve{rx}_1]_{r=a},\\ [\breve{ry}_1]_{r=a}&=-[\breve{ry}_1]_{r=a}.\end{aligned}\right\} \quad . \quad . \quad . \quad . \quad . \quad . \quad . \quad . \quad (C)$$

---

* Communicated by the Author.

† Accepted for publication elsewhere.

Expressions for $r\overset{\smile}{rx}_2$ and $r\overset{\smile}{ry}_2$ in terms of the boundary values have been given in paper I and also in a different form previously (Sen, 1938). These results are :—

$$\left.\begin{aligned} r\overset{\smile}{rx}_2&=\mathrm{R}_e\left[\frac{r^2-a^2}{4}\left\{\frac{f(z)-zf'(z)}{z}\right\}+a\mathscr{L}(z)\right],\\ r\overset{\smile}{ry}_2&=\mathrm{R}_e\left[\frac{r^2-a^2}{4}i\left\{\frac{f(z)-zf'(z)}{z}\right\}+a\mathscr{M}(z)\right],\end{aligned}\right\}\quad .\ .\ .\ .\quad (\mathrm{D})$$

where $z=x+iy$, $i=\sqrt{-1}$, R_e denotes the real part, $\mathscr{L}(z)$ and $\mathscr{M}(z)$ are functions of z, such that

$$\left.\begin{aligned} &[\overset{\smile}{rx}_2]_{r=a}=[\mathrm{R}_e\mathscr{L}(z)]_{r=a},\quad [\overset{\smile}{ry}_2]_{r=a}=[\mathrm{R}_e\mathscr{M}(z)]_{r=a},\\ &\overset{\smile}{xx}_2+\overset{\smile}{yy}_2=\mathrm{R}_e f(z),\quad f(z)=2az^{-1}[\mathscr{L}(z)+i\mathscr{M}(z)],\end{aligned}\right\}\quad .\ .\ .\quad (\mathrm{E})$$

except when $f(z)\propto z^{-1}$. [*Cf.* art. 3 (*b*), Sen, 1938.]

In these problems, $r\overset{\smile}{rx}_1$ and $r\overset{\smile}{ry}_1$ will be already known. Hence, from (C) the values of $r\overset{\smile}{rx}_2$ and $r\overset{\smile}{ry}_2$ on the edge $r=a$ can be evaluated. Then we obtain the functions $\mathscr{L}(z)$ and $\mathscr{M}(z)$ which vanish at infinity and satisfy the relations

$$[\mathrm{R}_e\mathscr{L}(z)]_{r=a}=[\overset{\smile}{rx}_2]_{r=a},\quad [\mathrm{R}_e\mathscr{M}(z)]_{r=a}=[\overset{\smile}{ry}_2]_{r=a}.$$

Knowing the values of $\mathscr{L}(z)$ and $\mathscr{M}(z)$, we can get $f(z)$ from (E), and hence from (D), the values of $r\overset{\smile}{rx}_2$ and $r\overset{\smile}{ry}_2$ can be completely determined. The resultant expressions $r\overset{\smile}{rx}$, $r\overset{\smile}{ry}$, at any point are then given by

$$\left.\begin{aligned} r\overset{\smile}{rx}&=r\overset{\smile}{rx}_1+r\overset{\smile}{rx}_2,\\ r\overset{\smile}{ry}&=r\overset{\smile}{ry}_1+r\overset{\smile}{ry}_2.\end{aligned}\right\}\quad .\ .\ .\ .\ .\ .\ .\ .\ .\quad (\mathrm{F})$$

1. *Solution for a Force acting at a point near a Circular Hole.*

Let an isolated force T act at the point A$(c, 0)$, $(c>a)$, in the direction of the x axis, that is, in the direction of the line joining the centre O to the point A. If there had been no hole in this infinite plate, we would have the corresponding average stresses (*vide* Coker and Filon, 1931, p. 327) given by

$$\left.\begin{aligned} \overset{\smile}{xx}_1&=\frac{\mathrm{T}}{4\pi}\left[-\frac{(3+\sigma)(x-c)}{r_1^{\,2}}+\frac{2(1+\sigma)(x-c)y^2}{r_1^{\,4}}\right],\\ \overset{\smile}{xy}_1&=-\frac{\mathrm{T}}{4\pi}\left[\frac{(3+\sigma)y}{r_1^{\,2}}-\frac{2(1+\sigma)y3}{r_1^{\,4}}\right],\\ \overset{\smile}{yy}_1&=\frac{\mathrm{T}}{4\pi}\left[\frac{(1-\sigma)(x-c)}{r_1^{\,2}}-\frac{2(1+\sigma)y^2(x-c)}{r_1^{\,4}}\right],\end{aligned}\right\}\quad .\ .\quad (1.1)$$

where σ is Poisson's ratio and $r_1^{\,2}=(x-c)^2+y^2$.

Hence from (A) we have

$$\left.\begin{aligned} r\overset{\smile}{rx}_1&=\frac{\mathrm{T}}{4\pi}\left[\frac{(3+\sigma)(x-r^2/c)c}{r_1^{\,2}}+\frac{(1+\sigma)y^2}{r_1^{\,2}}+\frac{(1+\sigma)y^2(r^2-c^2)}{r_1^{\,4}}\right],\\ r\overset{\smile}{ry}_1&=\frac{\mathrm{T}}{4\pi}\left[-\frac{(1-\sigma)cy}{r_1^{\,2}}-\frac{2(1+\sigma)xy}{r_1^{\,2}}+\frac{2(1+\sigma)cy^3}{r_1^{\,4}}\right].\end{aligned}\right\}\ .\quad (1.2)$$

At a point $P(x, y)$ on the circular edge we have

$$\left.\begin{aligned} [r\breve{rx}_1]_{r=a} &= \frac{T}{4\pi}\left[\frac{(3+\sigma)(x-a^2/c)c}{AP^2}+\frac{(1+\sigma)y^2}{AP^2}+\frac{(1+\sigma)y^2(a^2-c^2)}{AP^4}\right], \\ [r\breve{ry}_1]_{r=a} &= \frac{T}{4\pi}\left[-\frac{(1-\sigma)cy}{AP^2}-\frac{2(1+\sigma)xy}{AP^2}+\frac{2(1+\sigma)cy^3}{AP^4}\right]. \end{aligned}\right\} \quad (1.3)$$

If B be the inverse point of A with respect to the circle, we know that $\dfrac{1}{AP}=\dfrac{a}{c\,.\,BP}$.

Hence, expressing AP in terms of BP we find from (C) that the expressions $r\breve{rx}_2$, $r\breve{ry}_2$ to be determined, must be such that

$$\left.\begin{aligned} [r\breve{rx}_2]_{r=a} &= -\frac{T}{4\pi}\left[\frac{(3+\sigma)a^2(x-a^2/c)}{c\,.\,BP^2}+\frac{(1+\sigma)a^2y^2}{c^2\,.\,BP^2}+\frac{(1+\sigma)a^4(a^2-c^2)y^2}{c^4\,.\,BP^4}\right], \\ [r\breve{ry}_2]_{r=a} &= -\frac{T}{4\pi}\left[-\frac{(1-\sigma)a^2y}{c\,.\,BP^2}-\frac{2(1+\sigma)a^2xy}{c^2\,.\,BP^2}+\frac{2(1+\sigma)a^4y^3}{c^3\,.\,BP^4}\right]. \end{aligned}\right\} \quad (1.4)$$

Fig. 1.

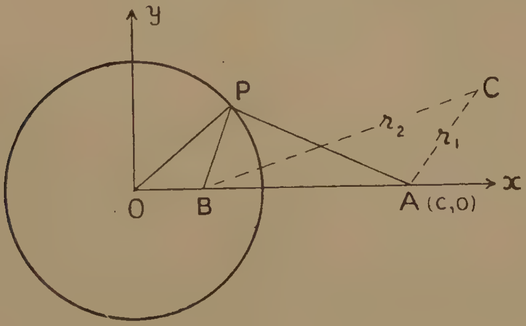

In terms of z we have the above results as

$$\left.\begin{aligned} [r\breve{rx}_2]_{r=a} &= -\frac{T}{4\pi}R_e\left[\frac{(3+\sigma)a^2}{z-a^2/c}+\frac{(1+\sigma)(z^2-a^2)}{2c(z-a^2/c)}\right. \\ &\qquad \left.-\frac{(1+\sigma)a^2(z^2-a^2)}{2c^2(z-a^2/c)^2}-\frac{(1+\sigma)(z^2-a^2)}{2cz}\right]_{r=a}, \\ [r\breve{ry}_2]_{r=a} &= -\frac{T}{4\pi}R_e\left[\frac{-(1-\sigma)ia^2}{c(z-a^2/c)}-\frac{(1+\sigma)iz^2}{z-a^2/c}\right. \\ &\qquad \left.+\frac{(1+\sigma)iz(z^2-a^2)}{2c(z-a^2/c)^2}+\frac{(1+\sigma)}{2c}\,\frac{i(z^2+a^2)}{z}\right]_{r=a}. \end{aligned}\right\} \quad (1.5)$$

The last term in each bracket on the right-hand sides of the above expressions, which gives zero values on $r=a$, has been added to secure the vanishing of stresses $\breve{xx}_2$, $\breve{xy}_2$, $\breve{yy}_2$ at an infinite distance.

We find from (E) that we can put

$$\left.\begin{aligned} a\mathscr{L}(z) &= -\frac{\mathrm{T}}{4\pi}\left[\frac{2a^2}{c(z-a^2/c)}+\frac{(1+\sigma)z^2}{c(z-a^2/c)}-\frac{(1+\sigma)z(z^2-a^2)}{2c(z-a^2/c)^2}\right. \\ &\qquad\left.-\frac{(1+\sigma)(z^2-a^2)}{2cz}\right], \\ a\mathscr{M}(z) &= -\frac{\mathrm{T}}{4\pi}\left[-\frac{(1-\sigma)ia^2}{c(z-a^2/c)}-\frac{(1+\sigma)iz^2}{z-\alpha^2/c}+\frac{(1+\sigma)iz(z^2-a^2)}{2c(z-a^2/c)^2}\right. \\ &\qquad\left.+\frac{(1+\sigma)i(z^2+a^2)}{2cz}\right], \end{aligned}\right\} \quad . \quad (1.6)$$

which give

$$\begin{aligned} f(z) &= 2a\frac{\mathscr{L}(z)+i\mathscr{M}(z)}{z} \\ &= -\frac{\mathrm{T}}{2\pi}\left[(3-\sigma)\left\{\frac{1}{z-a^2/c}-\frac{1}{z}\right\}+\frac{2(1+\sigma)z}{c(z-a^2/c)}-\frac{(1+\sigma)(z^2-a^2)}{c(z-a^2/c)^2}-\frac{(1+\sigma)}{c}\right]. \end{aligned} \quad . \quad . \quad . \quad (1.7)$$

Substituting the above values of $\mathscr{L}(z)$, $\mathscr{M}(z)$ and $f(z)$ in (D), we can obtain the values of $\breve{rx}_2$ and $\breve{ry}_2$ at any point.

The hoop stress at the point P (a, θ) on the edge of the hole

$$=[\breve{\theta\theta}]_{r=a}=[\breve{rr}+\breve{\theta\theta}]_{r=a}, \text{ since } \breve{rr}=0 \text{ on } r=a.$$

Hence, this stress

$$\begin{aligned} [\breve{\theta\theta}]_{r=a} &= [\breve{xx}_1+\breve{yy}_1+\mathrm{R}_e f(z)]_{r=a} \\ &= -\frac{\mathrm{T}}{2\pi}\left[\frac{(1+\sigma)(x-c)}{\mathrm{AP}^2}+\frac{(3-\sigma)(x-a^2/c)}{\mathrm{BP}^2}-\frac{(3-\sigma)x}{a^2}+\frac{1+\sigma}{c}\right. \\ &\qquad\left.+\frac{2(1+\sigma)a^2(x-a^2/c)}{c^2.\mathrm{BP}^2}-\frac{2(1+\sigma)a^2(c^2-a^2)y^2}{c^3.\mathrm{BP}^4}\right]. \end{aligned} \quad . \quad . \quad . \quad (1.8)$$

When the force acts at the point $(a, 0)$, $c=a$, and hence

$$\mathrm{AP}^2=\mathrm{BP}^2=2a^2(1-\cos\theta).$$

In this case

$$[\theta\theta]_{r=a}=\frac{\mathrm{T}}{2\pi a}[2+(3-\sigma)\cos\theta]. \quad . \quad . \quad . \quad . \quad . \quad (1.9)$$

This result tallies with that deduced from art. 9 of Bickley's paper.

2. *Solution for a Couple.*

Let a couple of moment Q with its axis perpendicular to the plate act at the point A$(c, 0)$. Had there been no hole, the average stresses in the infinite plate due to this couple would have been given by (*vide* Coker and Filon, 1931, p. 362) :—

$$\left.\begin{aligned}\overset{\smile}{xx}_1&=\frac{Q}{\pi}\frac{(x-c)y}{r_1^{\,4}},\\ \overset{\smile}{xy}_1&=\frac{Q}{2\pi}\frac{[y^2-(x-c)^2]}{r_1^{\,4}},\\ \overset{\smile}{yy}_1&=-\frac{Q}{\pi}\frac{(x-c)y}{r_1^{\,4}},\end{aligned}\right\}\quad . \; . \; . \; . \; . \; . \; . \; . \quad (2.1)$$

where, as before,

$$r_1^{\,2}=(x-c)^2+y^2.$$

Hence, from (A), we have

$$\left.\begin{aligned}r\overset{\smile}{rx}_1&=\frac{Qy(r^2-c^2)}{2\pi r_1^{\,4}},\\ r\overset{\smile}{ry}_1&=\frac{Q[2cr^2-x(r^2+c^2)]}{2\pi r_1^{\,4}},\end{aligned}\right\}\quad . \; . \; . \; , \; , \; . \; . \quad (4.2)$$

B being the inverse point of A with respect to the circle, we have at any point P(x y) on the edge $r=a$.

$$\left.\begin{aligned}[r\overset{\smile}{rx}_1]_{r=a}&=\frac{Qy(a^2-c^2)}{2\pi\mathrm{AP}^4}=\frac{Qya^4(a^2-c^2)}{2\pi c^4.\mathrm{BP}^4},\\ [r\overset{\smile}{ry}_1]_{r=a}&=\frac{Q[2ca^2-x(a^2+c^2)[}{2\pi\mathrm{AP}^4}=\frac{Qa^4[2ca^2-x(a^2+c^2)]}{2\pi c^4.\mathrm{BP}^4}.\end{aligned}\right\}\quad . \quad (2.3)$$

From (C) we then have

$$\left.\begin{aligned}[r\overset{\smile}{rx}_2]_{r=a}&=\frac{Qy(c^2-a^2)a^4}{2\pi c^4.\mathrm{BP}^4}=\frac{Qa^2}{2\pi c^2}\left[\mathrm{R}_e\left\{\frac{iz}{(z-a^2/c)^2}\right\}\right]_{r=a},\\ [r\overset{\smile}{ry}_2]_{r=a}&=\frac{Qa^4[x(a^2+c^2)-2ca^2]}{2\pi c^4.\mathrm{BP}^4}=\frac{Qa^2}{2\pi c^2}\left[\mathrm{R}_e\left\{\frac{z}{(z-a^2/c)^2}\right\}\right]_{r=a}.\end{aligned}\right\}\quad . \quad (2.4)$$

These results allow us to choose $a\mathscr{L}(z)$ and $a\mathscr{M}(z)$, as indicated in (E), in the forms

$$\left.\begin{aligned}a\mathscr{L}(z)&=\frac{Qa^2}{2\pi c^2}\frac{iz}{(z-a^2/c)^2},\\ a\mathscr{M}(z)&=\frac{Qa^2}{2\pi c^2}\frac{z}{(z-a^2/c)^2},\end{aligned}\right\}\quad . \; . \; . \; . \; . \; . \; . \; . \; . \; . \quad (2.5)$$

$$f(z)=2a\frac{\mathscr{L}(z)+i\mathscr{M}(z)}{z}=\frac{2Qa^2i}{\pi c^2(z-a^2/c)^2}.\quad . \; . \; . \quad (2.6)$$

Substituting the above values of $a\mathscr{L}(z)$, $a\mathscr{M}(z)$ and $f(z)$ in (D), we find the values of $r\overset{\smile}{rx}_2$ and $r\overset{\smile}{ry}_2$. The hoop stress $\overset{\smile}{\theta\theta}$ at any point P(a, θ) on the circular hole where $\overset{\smile}{rr}=0$.

$$\begin{aligned}&=[\overset{\smile}{rr}+\overset{\smile}{\theta\theta}]_{r=a}\\ &=[\overset{\smile}{xx}_1+\overset{\smile}{yy}_1+\overset{\smile}{xx}_2+\overset{\smile}{yy}_2]_{r=a}\\ &=[0+\mathrm{R}_e f)z)]_{r=a}\end{aligned}$$

$$=\frac{2Qa^2}{\pi c^2 BP^4}\times 2a\sin\theta(a\cos\theta-a^2/c)$$

$$=\frac{4Q}{\pi}\cdot\frac{c\sin\theta(c\cos\theta-a)}{(c^2+a^2-2ca\cos\theta)^2}. \qquad (2.7)$$

Taking a particular case in which $c=2a$, we get

$$[\breve{\theta\theta}]_{r=a}=\frac{32Q}{\pi c^2}I(\theta), \qquad (2.8)$$

where

$$I(\theta)=\frac{\sin\theta(2\cos\theta-1)}{(5-4\cos\theta)^2}. \qquad (2.9)$$

Values of $I(\theta)$.

θ	0°	30°	60°	90°	120°	150°	180°
$I(\theta)$	0	0·155	0	−0·040	−0·035	−0·019	0

References.

Bickley, W. G., Phil. Trans. Roy. Soc. A, ccxxvii. pp. 383–415 (1928).
Coker, E. G., and Filon, L. N. G., ‘Treatise on Photo-elasticity’ (1931).
Sen, B., Phil. Mag. xxvi. p. 108 (1938).

Bengal Engineering College,
Sibpore, Bengal.

XXVI. *Coefficients for Mid-Interval Numerical Integration with Central Differences.*

By Herbert E. Salzer *†.

[Received July 5, 1944.]

The following table lists the coefficients in the formula for numerical integration from mid-interval to mid-interval, employing central differences through the forty-ninth order. Previous calculations have gone only as far as coefficients of the seventh central difference. The coefficients K_{2s} occur in the following formula:

$$\frac{1}{h}\int_{a-h/2}^{a+(n-\frac{1}{2})h} f(x)\,dx=[f(a)+f(a+h)+\ldots+f(a+\overline{n-2}h)$$
$$+f(a+\overline{n-1}h)]+\sum_{s=1}^{m-1}K_{2s}[\delta^{2s-1}f(a+\overline{n-\tfrac{1}{2}}h)-\delta^{2s-1}f(a-\tfrac{1}{2}h)]$$
$$+nh^{2m}K_{2m}f^{(2m)}(\xi). \qquad (1)$$

Equation (1) is known as the first Gaussian summation-formula. Due to the extreme rapidity with which the coefficients K_{2s} decrease with increasing s, the table given below can be employed to obtain high accuracy in either integration or summation even though successive differences might not show the slightest tendency to decrease. Steffensen has demonstrated the following properties of these coefficients, given in equations (2) to (4):

---

* Communicated by the Author.

† Mathematical Tables Project, National Bureau of Standards, U.S.A.

Table of Coefficients.

K_2	$+\frac{1}{24}$
K_4	$-\frac{17}{5760}$
K_6	$+\frac{367}{967680}$
K_8	$-\frac{27859}{46448\ 6400}$
K_{10}	$+\frac{12958\ 03}{12262\ 44096\ 00}$
K_{12}	$-\frac{53292\ 42827}{26781\ 17105\ 664000}$
K_{14}	$+\frac{25198\ 85712\ 7}{64274\ 81053\ 59360\ 00}$
K_{16}	$-\frac{11959\ 71216\ 6949}{14985\ 21297\ 06639\ 360000}$
K_{18}	$+\frac{11153\ 23977\ 34199\ 41}{66965\ 91972\ 33029\ 97196\ 8000}$
K_{20}	$-\frac{31326\ 45059\ 69545\ 10807}{88395\ 01403\ 47599\ 56299\ 77600\ 000}$
K_{22}	+·00000 00007 65988 013
K_{24}	—·00000 00001 67709 061
K_{26}	+·00000 00000 37117 252
K_{28}	—·00000 00000 08290 382
K_{30}	+·00000 00000 01866 361
K_{32}	—·00000 00000 00423 050
K_{34}	+·00000 00000 00096 471
K_{36}	—·00000 00000 00022 116
K_{38}	+·00000 00000 00005 094
K_{40}	—·00000 00000 00001 178
K_{42}	+·00000 00000 00000 274
K_{44}	—·00000 00000 00000 064
K_{46}	+·00000 00000 00000 015
K_{48}	—·00000 00000 00000 004
K_{50}	+·00000 00000 00000 001

$$K_{2s} = \frac{1}{(2s)!} \sum_{r=1}^{r=s} \frac{D^{2r}0^{[2s]}}{2^{2r}(2r+1)!}, \quad . \quad . \quad . \quad . \quad . \quad . \quad (2)$$

where $D^{2r}x^{[2s]}$ is the $(2r)$th derivative of the central factorial polynomial

$$x^{[2s]} \equiv x^2(x^2-1)(x^2-4)\ldots(x^2-\overline{s-1}^2) \text{ for } x=0.$$

$$K_{2s} \sim \frac{(-1)^{s-1}}{2^{2s-1}s^{3/2}\pi^{5/2}}, \text{ for large } s. \quad \ldots \ldots \ldots \quad (3)$$

$$K_{2s} = \frac{1^2}{3!\,2^2}K_{2s-2} - \frac{(1.3)^2}{5!\,2^4}K_{2s-4} + \ldots + (-1)^s \frac{[1.3\ldots(2s-3)]^2}{(2s-1)!\,2^{2s-2}}K_2 + (-1)^{s+1}\frac{[1.3\ldots(2s-1)]^2}{(2s+1)!\,2^{2s}}. \quad (4)$$

(For other interesting relations among the quantities K_{2s}, see the paper by Sen.)

The coefficients from K_2 to K_{20} were checked, using their exact values, in the cumulative recursion formula (4). For $s \geqslant 8$, the successive ratios K_{2s}/K_{2s+2} were found to difference very well, affording a check on the values beyond K_{20}. All values were simultaneously checked by integrating 2 from $x=24\frac{1}{2}$ to $25\frac{1}{2}$ and by the formula due to Sen, $\frac{3}{\pi} = 1 - \sum_{s=1}^{\infty} |K_{2s}|$. The coefficients that are given in decimal form are correct to about 0·6 of a unit in the 18th decimal place.

References.

J. F. Steffensen, "On Laplace's and Gauss' Summation-Formulas," *Skandinavisk Aktuarietidskrift*, pp. 1–15 (1924).

J. F. Steffensen, 'Interpolation.' Baltimore: Williams & Wilkins Co., 1927, pp. 107–109, 190–191.

D. K. Sen, "Interpolation and Summation Formulas and the Properties of Factorials," Journ. Univ. Bombay, vol. xi. pt. 5, Section A, especially pp. 13–20 (Mar. 1943).

XXVII. *A Note on the Charge produced by Spraying Liquids with a Jet of Air.*

By Dr. Gao Chih-En, Physics Dept.,
Fukien Union University, Shaown, China *.

[Received August 2, 1944.]

Generally, the charges produced by spraying a liquid are regarded as due to friction or impact. Now in view of the change of surface tension that comes from the charge on the surface, as, for example, is produced in the capillary electrometer, the writer proposes an alternative interpretation. Namely, that the charges produced by spraying arise from the change in surface tension. It is an "inverse effect."

---

* Communicated by Dr. J. Needham, F.R.S.

If a stream of air is projected vertically upwards, and a drop of liquid (of radius R and surface tension T) is falling freely from a height to meet the stream, the drop will break into n drops each of radius r. From the law of conservation of mass, we have,

$$\frac{4}{3}\pi R^3\rho = n \,.\, \frac{4}{3}\pi r^3 \,.\, \rho \quad \text{or} \quad r = R/\sqrt[3]{n}. \quad \ldots \ldots \quad (1)$$

When the drops collect together to form again a big drop (or spread over the bottom of a container), the loss of surface energy is

$$4\pi n r^2 T - 4\pi R^2 T = 4\pi T (n^{1/3} - 1) R^2. \quad \ldots \ldots \quad (2)$$

Since there is a change of potential energy in the surface, we may expect a rearrangement of electrons causing an exchange of electrons between the two media. Each drop will thus acquire a charge q causing gain in electrical energy of

$$\frac{1}{2}\frac{q^2}{\text{capacity}} = \frac{q^2}{2r} = \frac{q^2 \,.\, n^{1/3}}{2R}. \quad \ldots \ldots \quad (3)$$

Consider that a fraction k_1 of the lost energy given in expression (2) is spent in producing the charge, we get, on equating k_1 of expression (2) to expression (3),

$$8\pi T k_1 \left(1 - \frac{1}{n^{1/3}}\right) R^3 = q^2. \quad \ldots \ldots \quad (4)$$

This relation between q and R can be tested experimentally; and calculation will give the value of k_1 showing the contribution to electric charge arising from surface energy. This equation explains the effect of the surface condition of the container, for T against an oiled container is quite different from that against a cleaned one. It also explains the slight increase of charge when some salt is dissolved in water, as T of salt solution is slightly larger than that of distilled water.

n might be calculated. The impact of a stream of air on the drop causes the surface to oscillate like the oscillation of a struck membrane. n would be given by the number of regions divided by the nodal lines of the overtone which has the largest amplitude. But such tedious calculations may be avoided by using a bigger impact, and hence a larger n. In this case, $\frac{1}{n^{1/3}}$ may be neglected, and eqn. (4) becomes

$$8\pi T k_1 R^3 = q^2. \quad \ldots \ldots \quad (5)$$

If friction or impact is chosen as the basis of calculation, $q^2 \propto R^4$ instead of R^3.

XXVIII. *Heat Conduction in Semi-Infinite Cylinders.*

By J. W. Craggs, B.Sc.*

[Received June 12, 1944.]

In a recent paper † Mr. J. C. Jaeger considered the problem of heat conduction in an infinite wedge or cylinder, using the Laplace transform method. It may be of interest to note that his results can be extended to semi-infinite regions by the use of a second integral transform. It is thus possible to find the effect of end-conditions on his results.

1. *Heat conduction in a wedge* $0<\theta<\theta_0$, $r>0$, $z>0$. *The surfaces* $\theta=0$, $z=0$ *kept at zero and* $\theta=\theta_0$ *at unity for* $t>0$. *Initial temperature zero.*

We have to solve

$$\frac{\partial^2 v}{\partial r^2}+\frac{1}{r}\frac{\partial v}{\partial r}+\frac{1}{r^2}\frac{\partial^2 v}{\partial \theta^2}+\frac{\partial^2 v}{\partial z^2}-\frac{1}{\kappa}\frac{\partial v}{\partial t}=0;$$

$$0<\theta<\theta_0,\quad r>0,\quad z>0,\quad t>0; \quad \ldots \ldots \quad (1)$$

with

$$v=0; \qquad \theta=0, \quad r>0, \quad z>0, \quad t>0, \quad \ldots \quad (2)$$

$$v=1; \qquad \theta=\theta_0, \quad r>0, \quad z>0, \quad t>0, \quad \ldots \quad (3)$$

$$v=0; \quad 0<\theta<\theta_0, \quad r>0, \quad z=0, \quad t>0, \quad \ldots \quad (4)$$

$$v=0; \quad 0<\theta<\theta_0, \quad r>0, \quad z>0, \quad t=0. \quad \ldots \quad (5)$$

Multiplying (1) and its boundary conditions (2), (3), (4) by e^{-pt}, integrating with respect to t from $0\to\infty$ and writing

$$\bar{v}(p)=\int_0^\infty e^{-pt}\, v(t)\, dt$$

for the Laplace transform of v, we get

$$\frac{\partial^2 \bar{v}}{\partial r^2}+\frac{1}{r}\frac{\partial \bar{v}}{\partial r}+\frac{1}{r^2}\frac{\partial^2 \bar{v}}{\partial \theta^2}+\frac{\partial^2 \bar{v}}{\partial z^2}-q^2\bar{v}=0; \quad 0<\theta<\theta_0,$$

$$r>0, \quad z>0, \quad \ldots \ldots \quad (6)$$

where

$$q^2=p/\kappa, \quad \ldots \ldots \quad (7)$$

---

* Communicated by the Author.

† "Heat Conduction in a Wedge, or an Infinite Cylinder whose Cross-section is a Circle or Sector of a Circle," Phil. Mag. vol. xxxiii. No. 222, p. 527 (July, 1942).

with boundary conditions

$$\bar{v}=0\,; \qquad \theta=0, \quad r>0, \quad z>0, \quad \ldots \ldots \quad (8)$$

$$\bar{v}=\frac{1}{p}\,; \qquad \theta=\theta_0, \quad r>0, \quad z>0, \quad \ldots \ldots \quad (9)$$

$$\bar{v}=0\,; \quad 0<\theta<\theta_0, \quad r>0, \quad z=0. \quad \ldots \ldots \quad (10)$$

Now multiply (6) and the boundary conditions (8) and (9) by $\sin \alpha z$ and integrate with respect to z from 0 to ∞, taking the Césaro sum (C, 1) of the integrals where this is necessary to ensure convergence *.

Write

$$\bar{v}_s(\alpha)=\int_0^\infty \bar{v}(z)\sin \alpha z\,dz \quad \ldots \ldots \quad (11)$$

for the Fourier sine transform † of $\bar{v}(z)$.

We thus obtain

$$\frac{\partial^2 \bar{v}_s}{\partial r^2}+\frac{1}{r}\frac{\partial \bar{v}_s}{\partial r}+\frac{1}{r^2}\frac{\partial^2 \bar{v}_s}{\partial \theta^2}-m^2\bar{v}_s=0, \quad \ldots \ldots \quad (12)$$

where

$$m^2=q^2+\alpha^2, \quad \ldots \ldots \quad (13)$$

with

$$\bar{v}_s=0\,; \quad \theta=0, \quad r>0 \quad \ldots \ldots \quad (14)$$

and

$$\bar{v}_s=\lim_{\lambda\to\infty}\int_0^\lambda \left(1-\frac{z}{\lambda}\right)\frac{\sin \alpha z}{p}\,dz$$

$$=\frac{1}{p\alpha}\,; \quad \theta=\theta_0\,, \quad r>0. \quad \ldots \ldots \quad (15)$$

Following Jaeger (*loc. cit.*), we seek a solution of (12) of the form

$$\bar{v}_s=\frac{\theta}{p\alpha\theta_0}+\sum_{n=1}^{\infty}\sin s\theta\int_0^\infty f_n(u)\mathrm{J}_s(ur)\,du, \quad \ldots \ldots \quad (16)$$

where ‡

$$s=n\pi/\theta_0. \quad \ldots \ldots \quad (17)$$

This form satisfies the boundary conditions, and in order that it may satisfy (12) we must have

$$\frac{m^2\theta}{p\alpha\theta_0}+\sum_{s=1}^{\infty}\sin s\theta\int_0^\infty (m^2+u^2)\mathrm{J}_s(ur)f_n(u)\,du=0,$$

or

$$\int_0^\infty (m^2+u^2)\mathrm{J}_s(ur)f_n(u)\,du=\frac{2m^2}{\pi p\alpha}\frac{(-)^n}{n}. \quad \ldots \ldots \quad (18)$$

Now

$$\int_0^\infty \frac{\mathrm{J}_s(ur)}{u}\,du=\frac{1}{s},$$

so that (18) is satisfied if we take

$$f_n(u)=\frac{2(-)^n m^2}{up\alpha\theta_0(m^2+u^2)}$$

---

* See E. C. Titchmarsh, 'Theory of Fourier Integrals,' O.U.P. 1937, Ch. I.

† We use this form—omitting a factor $\sqrt{2/\pi}$—for convenience of notation.

‡ No confusion need arise with the suffix for the sine transform.

and $$\bar{v}_s = \frac{\theta}{p\alpha\theta_0} + \sum_{n=1}^{\infty} \frac{2(-)^n m^2 \sin s\theta}{p\alpha\theta_0} \int_0^\infty \frac{J_s(ur)\,du}{u(m^2+u^2)}. \quad . \quad . \quad . \quad (19)$$

Inverting (11) by *

$$\bar{v}(z) = \frac{2}{\pi} \int_0^\infty \bar{v}_s(\alpha) \sin \alpha z \, d\alpha, \quad . \quad . \quad . \quad . \quad . \quad . \quad (20)$$

we get

$$\bar{v} = \frac{\theta}{p\theta_0} + \sum_{n=1}^{\infty} \frac{2(-)^n \sin s\theta}{p\theta_0} \int_0^\infty \frac{J_s(ur)}{u} \left\{ \frac{q^2}{q^2+u^2} + \frac{u^2}{q^2+u^2} e^{-\sqrt{(q^2+u^2)}z} \right\} du. \quad (21)$$

Inverting (21) by

$$v = \frac{1}{2\pi i} \int_{k-i\infty}^{k+i\infty} \bar{v} e^{pt} \, dp,$$

we get

$$v = \frac{\theta}{\theta_0} + 2 \sum_{n=1}^{\infty} \frac{(-)^n \sin s\theta}{\theta_0} \int_0^\infty \frac{J_s(ur)}{u} \left(1 - u^2 \int_0^{\kappa t} e^{-u^2 t} \operatorname{erf} \frac{z}{2\sqrt{t}} \, dt \right) du, \quad (22)$$

which reduces to Jaeger's result when $z \to +\infty$.

2. *A wedge as before but all surfaces kept at unity, initial temperature zero.*

A similar method gives

$$v = 1 - \frac{4}{\theta_0} \sum_{n=0}^{\infty} \sin \frac{(2n+1)\pi\theta}{\theta_0} \operatorname{erf} \frac{z}{2\sqrt{\kappa t}} \int_0^\infty e^{-\kappa t u^2} \frac{J_s(ur)}{u} \, du. \quad . \quad (23)$$

In this simple case the result may be obtained from the result for an infinite wedge by multiplying the series by $\operatorname{erf} \frac{z}{2\sqrt{\kappa t}}$. This clearly leaves the boundary conditions in θ unaltered and is a solution of the main equation.

3. Similarly the solution for the region $0 < r < a$, $0 < \theta < \theta_0$, $z > 0$, with surface kept at unity for $t > 0$ and initial temperature zero, may be obtained as

$$v = 1 - \frac{8}{\pi} \operatorname{erf} \frac{z}{2\sqrt{\kappa t}} \sum_{n=0}^{\infty} \frac{1}{2n+1} \sin \frac{(2n+1)\pi\theta}{\theta_0} \sum_{m=1}^{\infty} e^{-b\alpha^2_{s,m}} \frac{J_s(\alpha_{s,m} r/a)}{[J_s'(\alpha_{s,m})]^2}$$
$$\times \int_0^1 t J_s(\alpha_{s,m} t) \, dt, \quad (24)$$

where $b = \frac{\kappa t}{a^2}$, $s = \frac{(2n+1)\pi}{\theta_0}$ and $\alpha_{s,m} (m = 1, 2, 3 \ldots)$

are the positive roots of $J_s(\alpha) = 0$.

Military College of Science,
Stoke-on-Trent.

---

* Titchmarsh, *loc. cit.*

XXIX. *Gyroscopic Coupling Terms.*

To the Editors of the Philosophical Magazine.

Gentlemen,—

Certain difficulties which appear in paragraph 11 of Dr. Bloch's paper (1) can be avoided by an electrical analogy of gyroscopic coupling which is adequate for analytical purposes and is more convenient than thermionic valve circuits.

If the mechanical system is converted into an electrical analogue by reference to the general circuit matrices of the elements in the way described in reference (2), the gyroscopic coupling term must, according to Dr. Bloch, act as a "reciprocal network producer." The general circuit matrix of such a device is $\begin{pmatrix} 0 & 1 \\ 1 & 0 \end{pmatrix}$, and this is a special case of the matrix $\begin{pmatrix} \cos\theta & \sin\theta \\ \sin\theta & -\cos\theta \end{pmatrix}$, with $\theta=\pi/2$. This matrix characterizes a change of axes obtained by rotation through an angle θ, followed by reversal of the axis of y' (3). In fact, just as the flow of torque through the gyroscopic coupling is turned through $\pi/2$, so the general circuit matrix corresponding to the coupling characterizes a rotation through $\pi/2$. Examination of the senses of ω_1 and ω_2 in Dr. Bloch's paper, fig. 2, shows that the sense of ω_2 is the reverse of that used in reference (2), and accounts for the term corresponding to the reversal of y'. The electrical analogue of fig. 13 then becomes fig. A, where the gyroscopic coupling is replaced by a "reciprocating ideal transformer," which is conveniently represented as having a ratio of $1 : \sqrt{-1}$.

Fig. A.

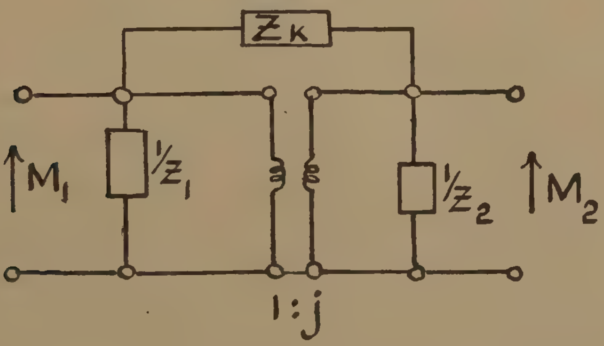

A physical non-ideal form which such a device can take can be found. An electromagnetic driver, such as a moving-coil loudspeaker mechanism, is coupled to an electrostatic receiver, such as a crystal microphone.

This device is reversible, and has, as its electrical analogue, a real transformer in tandem with a "reciprocating transformer." The overall analogue is a "reciprocating transformer" in either direct or inverse analogy.

References.

(1) "A new approach to the dynamics of systems with gyroscopic coupling terms," by A. Bloch, Dr.Ing., M.Sc., Phil. Mag. ser. 7, vol. xxxv. p. 315 (May 1944).
(2) "Notes on Electromechanical Equivalence," by H. Jefferson, 'Wireless Engineer,' vol. xxi. p. 563 (December 1944).
(3) 'Theory of Determinants, Matrices and Invariants,' by H. W. Turnbull. (Blackie: London), p. 155 (1928).

Yours faithfully,
H. JEFFERSON.

111, Ebury Street,
London, S.W. 1
22nd May, 1945.

XXX. *A Certain Multiple Integral.*

To the Editors of the Philosophical Magazine.

GENTLEMEN,—

THE theorem on a multiple integral given by A. S. Gladwin on p. 657 of Phil. Mag. ser. 7, vol. xxxv. is almost obvious.

For consider $f(t)$ as the probability function of a statistical variate t, so that when h is small $hf(\mathrm{T})$ is the chance that t lies between T and $\mathrm{T}+h$. Then Gladwin's theorem states that, when in turn n values of t are taken at random, the chance that these values all lie between x and y and are in ascending order of magnitude is $p^n/n\,!$, where p is the chance that a single random value of t lies between x and y. But p^n is the chance that all the n values of t lie between x and y, and $1/n\,!$ is the chance that n quantities arranged at random should be in ascending order of magnitude.

Gladwin's theorem can also be proved at once by putting $f(t)\equiv\phi'(t)$ and integrating with respect to u_n, u_{n-1}, u_{n-2}, ... in turn.

Yours faithfully,
HAROLD SIMPSON.

1 Bevington Road, Oxford.

[*The Editors do not hold themselves responsible for the views expressed by their correspondents.*]

XXXI *New Contributions to Interferometry.* Part V.—*New Multiple Beam White Light Interference Fringes and their Applications.*

By S. Tolansky, Ph.D., D.I.C., The University, Manchester *.

[Received November 8, 1944.]

[Plate V.]

Abstract.

A description is given of some new thin film multiple beam *white light* fringes. Both the theory and properties of these multicoloured fringes are discussed in detail and some of their many possible applications to precision interferometry are considered. It is proposed, on theoretical grounds, to call them "*fringes of equal chromatic order.*" They afford an extremely powerful new method for examining thin film interference phenomena. For example, surface defects can be measured if even only of the order of $\lambda/200$. New topographical features are revealed on the cleavage faces of mica crystals, with the same degree of precision. New properties of thin mica films can be demonstrated, with a precision some 60 per cent. better than in the case of air films. The fringes have wider application and are much more powerful analytically than even highly sharpened multiple beam monochromatic Fizeau fringes. Extremely small surface angles can be measured over very small areas, the resolution available being 100 times better than that of the Rayleigh limit.

Introduction.

It is the purpose of this paper to describe some new *white light* fringes of very great power produced by multiple beam interference. An essential feature is the employment of *many* beams, a fact which is here strongly emphasized. For in two earlier publications (1), (2) descriptions have been given of two new types of *monochromatic* interference phenomena involving multiple beams, and in both cases this fundamental distinguishing feature has been missed by subsequent commentators. The author therefore finds it necessary to emphasize at the outset that the whole characteristic high power and wide application of the new white light fringes described here depend entirely upon the employment of *many* multiple beams. With these new fringes, which are here called "*fringes of equal chromatic order*" for reasons developed later, a precision and variety in range of application has been attained which probably surpasses that shown by any other existing low-order interference fringes in the whole of optics.

---

* Communicated by the Author.

A striking feature is the optical simplicity, particularly the fact that such high precision can be attained without the use of special monochromatic sources. Although white light is used, the fringes are highly sharpened in the same sense as the monochromatic Fabry–Perot fringes, *i. e.* the fringe-width occupies only a small fraction of the distance between successive orders. This sharpness is due only to the employment of a large number of multiple beams.

The interference arises initially within a thin film, the two opposing surfaces being coated with a highly reflecting thin transmitting silver film, the reflecting coefficient being no less than 0·87 in the green, preferably as high as can be tolerated with reference to the light source. Since very bright light sources are readily available, *higher reflecting coefficients can be adopted than those in use with the usual monochromatic source methods of study,* for example, Fizeau fringe arrangements. In general, the method is applicable to any thin film between highly reflecting faces. We shall consider here initially some of the characteristic properties of the fringes produced by using the silver-modified Newton's Rings apparatus described in Part II.(3). More extensive applications, together with details of theory, will be discussed later. In the section which follows, the interference film is then that between a piece of plate glass and a convex lens, the two surfaces in juxtaposition having been first suitably silvered.

Fig. 1.

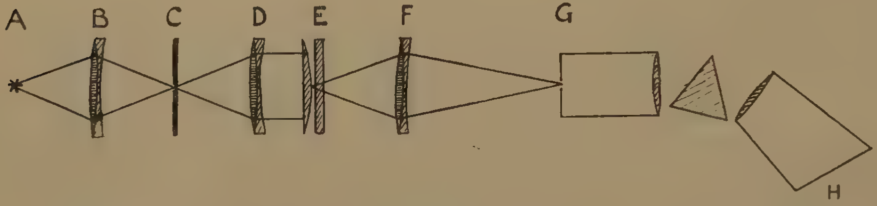

Fringes of Equal Chromatic Order. Optical Arrangement.

The optical arrangement is shown in fig. 1.

A is a white light source (a 100 watt lamp suffices), an image of which is projected by a lens B on to a circular aperture C (some 2 millimetres in diameter ; the value is not critical). C is at the focus of an achromat lens D, which projects a parallel beam of white light on to the interference system E, the incidence being normal. This is easily adjusted. (If non-normal incidence is used the phenomena are complicated by the differential polarization phase change doubling recorded in Part II. and in Part III.(3), (4).)

With the good achromat lens F an image of the interference film E is projected onto G, the slit of a prism spectrograph. In the experiments described this was a medium quartz (Hilger) spectrograph. The new fringes appear at H, where they can be observed with an eyepiece or photographed. A reproduction of the fringes is shown in Pl. V. (*b*), which covers part of the visible region from the red to the blue. A wave-length scale is superposed. Pl. V. (*a*) shows the monochromatic silver-modified Newton's Rings (green mercury line) given by the arrangement E in the manner discussed in Part II. The white light fringes in Pl. V. (*b*) correspond to the narrow section of the interference film E, which has been selected by the slit G, since an image of E is projected on to G. Pl. V. (*b*) arises when the centre of E is projected on to the slit centre.

Attention may be drawn to the following special features :—

(1) The separation between fringes, in Angstrom units, is considerable.

(2) The fringes are extremely sharp and narrow, occupying but a small fraction of the wave-length interval separating a fringe pair.

(3) Each fringe exhibits a fine detail structure.

(4) Each fringe is similar to its neighbours.

(5) Each fringe is multicoloured, and can extend over some thousands of Angstroms, according to the magnification of the lens F.

Before discussing the particular fringe-shape in Pl. V. (*b*) (which is determined by the geometry of the interference film) some general properties will first be considered, applicable to any type of thin film. (The geometrical conditions necessary for the production of *sharp* multiple beam thin-film fringes have been discussed earlier.)

In general multiple beam interference within a film (thick or thin) obeys the basic law $n\lambda = 2\mu t \cos\theta$, in which the symbols have the usual meanings. The discussion will be restricted to air films at first, taking μ unity, since this simplifies the formulæ derived. It will be convenient to classify multiple beam fringes into four groups, subdivided in pairs.

A. *Fringes with monochromatic light* (λ *constant*).

(1) When t is constant and θ varies, then, using Lummer's accepted classification, we have "fringes of equal inclination" (*e. g.* Fabry–Perot rings).

(2) When θ is constant and t varies, we get "fringes of equal thickness" (*e. g.* Newton's rings).

B. *Fringes with white light* (λ *variable*).

(3) When θ is constant and t varies we have fringes of the type shown in Pl. V. (*b*), henceforth called "fringes of equal chromatic order" (see later for reasons).

(4) When t is constant and θ varies we get "white light Fabry–Perot fringes," which fringes will be described in a succeeding paper. Edser–Butler fringes are a special case of these.

Each of the curved fringes shown in Pl. V. (*b*) belongs to the system (3) above, and each corresponds to a given value of n in the basic formula, with θ constant also. Thus for any complete fringe t/λ is constant. Each point on a fringe corresponds to a different path-thickness in the interference film, containing, however, the *same number of waves*, no matter which point is selected, for the wave-length varies continuously from point to point to compensate for the thickness change. The fringes are therefore simply "fringes of equal t/λ." If a terminology corresponding to Lummer's widely accepted descriptions is to be adopted (and since the phenomena are linked by the same basic equation, this is a desirable procedure), it is proposed here to call fringes of the type classed in (3) above as "*fringes of equal chromatic order*." This nomenclature is adopted since t/λ is the order of interference for all those points of different wave-length combining to form a single fringe. Whilst, of course, any type of fringe in optics is the locus of points having the same order of interference, these are distinctive in being *chromatic*, hence the introduction of the term "equal chromatic order." The adoption of this nomenclature will be discussed further in Part VI.

It will be seen later that the fringes of equal chromatic order can take on an infinite variety of shapes, according to the spatial form of the interference film employed, yet all are governed by the same basic formula $n\lambda=2\mu t\cos\theta$, which also controls the formation of Lummer's fringes of equal thickness and of equal inclination. It is this intimate relationship, which justifies, indeed almost compels, the adoption of a nomenclature resembling that of Lummer.

The expression $n\lambda=2\mu t\cos\theta$ is simplified here by writing $\mu=1$ and $\cos\theta=1$, for the incidence is restricted to the normal. It can be rewritten

$$n=2\nu t,$$

where ν is the wave-number.

Differentiating gives $dn=2d\nu . t$.

For successive orders $dn=1$ and writing the wave-number separation between orders as $\varDelta\nu$ gives $t=1/2\varDelta\nu$. The fringes are thus equally spaced for any given value of t. A useful extension is to write $t=m/2\varDelta\nu_m$. where $\varDelta\nu_m$ is the wave-number interval between $(m+1)$ fringes.

This simple formula can be widely used in an extensive group of applications in a manner to be described in due course.

The Shape of the Fringes Formed with a Lens-Plate Combination.

In the lens-plate we can imagine white light Newton's rings being formed in the film, and these are projected on to the slit. The spectroscope then sorts out the mixed fringes, which are generally not visible as such on the slit, except perhaps very close to the centre, in special cases. We have $\rho_\lambda^2=2\mathrm{R}(t-\epsilon)$, in which R is the radius of curvature of the lens face, ρ_λ the radius of the Newton's ring formed at a film thickness

t for a wave-length λ, ϵ being the *optical* separation at the "point of contact" of the lens and plate. The quantity ρ must be duly corrected for any enlargement introduced by the projecting lens.

Let λ_0 be the wave-length on a given fringe at a point on the slit which is the image of a point on the film at which the thickness is t_0. Let λ_a be the wave-length position of the same fringe at a further position on the slit image away from the centre, corresponding to a film thickness t_a.

Then

$$n_0\lambda_0=2t_0$$

$$n_a\lambda_a=2t_a$$

$$n_a\lambda_a-n_0\lambda_0=2(t_a-t_0)$$

$$=(\rho_a^2-\rho_0^2)/\mathrm{R},$$

where ρ_a, ρ_0 are the Newton's ring radii at the film thicknesses t_a and t_0.

At the centre of the fringe system the film thickness is ϵ, and if we suppose t_0 in the above refers to the centre then $n_0\lambda_0=2\epsilon$, giving

$$n_a\lambda_a=(\rho_a^2/\mathrm{R})+2\epsilon.$$

Since a fringe is the locus of points having all the same value of n then n_a is constant within a fringe. Since ρ_a is the distance from the fringe centre of the point of wave-length it follows that each fringe has a truly parabolic shape, providing the dispersion of the spectrograph is normal. With a prism instrument the parabola is distorted because of variable dispersion, in particular there is a gradual change in shape on moving from the red to the blue.

It is clear that the shape is independent of the value of n (variable dispersion being disregarded), hence each fringe resembles its neighbours, even as to fine detail.

Some of the applications of the approximately parabolic fringes will now be reviewed, and this reveals but only one aspect of the multi-applications of fringes of equal chromatic order. The following features can all be calculated from a single photographic plate.

(1) *Optical Separation at the "Point of Contact."*

The optical separation of the two silvered components at the "point of contact" is obtained with very high precision. It is $1/2\Delta\nu$, where $\Delta\nu$ is the wave-number separation between a pair of fringes at the *centre* of the pattern. This quantity can be evaluated with certainty to within 25 Angstrom units, *i. e.* 1/200th of a light wave (λ 5000 A.). In Pl. V. (*b*), for example, the separation is 37,040 A.U., *i. e.* some 6·78 light waves (green mercury). This optical value includes phase change at reflection. The precision far exceeds that attainable by other methods. The extrapolation procedure generally adopted is unsound for this degree of precision owing to the quite unreliable assumption of true sphericity of the lens surface.

(2) *Variation of Phase Change with Wave-length on Reflection.*

According to the simple theory given above, the value of $\Delta\nu$ should be constant for any pair of fringes. Measurement shows the existence of a quite small but regular increase in $\Delta\nu$ with diminishing wave-length. This can be attributed only to the small increase in phase change at reflection at the metal surface. A new method is thus available for the determination of this variation of phase change with wave-length.

(3) *The Radius of Curvature of the Lens.*

The curvature of the lens face can be obtained from the fringes by at least four independent methods of measurement.

(*a*) From the horizontal and vertical co-ordinates of any two points on a single fringe. This requires also a knowledge of the dispersion of the spectrograph.

(*b*) By measuring at two horizontal levels, a known distance apart, the number of fringes (including fractions) between two specific wave-lengths.

(*c*) By the evaluating of $\Delta\nu$ at different horizontal levels (two suffice) from one pair of fringes. Both this method and the preceding give the thickness of the air gaps at two points. The effect of phase change at reflection is eliminated.

(*d*) A more general procedure, which further reveals any departures from true sphericity, is to measure the positions of the intersections of the fringes by any vertical line. This gives the effective Newton's ring diameters for the particular wave-length selected by the vertical section.

The Irregularities in the Fringes.

A feature of the utmost value is revealed by the irregular fine detail structure of the fringes. These details have their origin in the small scale irregularities on the glass surfaces of the lens and plate. The plate employed was not an optical flat, but the irregularities do not entirely vanish if a very high grade optical flat is used. The residual features are then clearly the small scale surface errors on the lens face. These errors are shown variously either by the wrinkles in the circular monochromatic fringes of Pl. V. (*a*) or by the short zig-zag irregularities in the fringes of equal chromatic order in Pl. V. (*b*).

The actual dimensions of these small scale features can be calculated in a very simple manner. Since $n\lambda=2t$ then $dt=dn\,.\,\lambda/2$. It is therefore necessary only to determine, at any selected wave-length, the fraction of an order by which the small feature is displaced from neighbouring positions, to arrive at the actual change in thickness dt responsible for the production of the irregularity. Since the order separation is linear, in terms of wave-numbers, and practically linear in terms of wave-lengths, if $\Delta\nu$ is not large, the fraction is obtained very readily. Computation is simplified by adopting the well-known method of McNair and of Schrammen for measuring fractions of an order in Fabry–Perot or Lummer plate interferometer pictures.

So sharp are the fringes that a dn value of 1/100th of an order can usually be easily measured. This means that surface irregularities no greater than $\lambda/200$ can be measured, *a matter of only 25 Angstrom units at λ 5000.* Even this can be improved upon in special cases, and in mica, as will be shown later, displacements of only 12 A.U. have been detected, a quantity smaller even than the crystal lattice distance in the molecular crystal structure of mica (20 A.U.).

This is a remarkable achievement optically, and it is with respect to this power of revealing such small changes in thickness that the most valuable applications of the fringes of equal chromatic order have so far been made. Related to this is the ability to detect and measure extremely small angles.

When examining the limits of precision to which the procedure can be pushed, it will appear later that the magnification of the projecting lens F has an important bearing practically on the fringe definition and on the resolving power attainable. This aspect will for the moment be disregarded, but will be brought up later.

In a later section the relation of fringes of equal chromatic order to other types of fringes will be discussed in more detail than has been done so far.

Application of the Fringes to the Study of Surface Contours.

The fringes of equal chromatic order have proved of great value for the study of surface topography problems. In earlier work (5), (6) on the topographical features of cleavage surfaces of mica a number of unsolved problems arose, but these can now be settled. In the earlier work, multiple beam interferometry with monochromatic light was applied to the examination of crystal face topography. A typical case studied was that of a cleavage face of mica. The mica was suitably silvered with a high reflecting silver film (one face only), and this was then pressed close to a similarly coated high grade optical flat. When illuminated at normal incidence with parallel monochromatic light, localized fringes of equal thickness could be seen, and these gave contours of the topographical features of the crystal surface with very high precision. Two characteristic features appear on mica surfaces : (*a*) they are covered with hills and dales, (*b*) discontinuous cleavage steps occur and these were found to vary in height from less than 40 Angstroms upwards to many thousands of Angstroms.

It was not possible with monochromatic light to decide whether any particular group of concentric ring-type fringes represented a hill or a pit, since it was necessary to press the mica between glass plates to stop air-shock vibrations. Nor was it at all possible to decide whether a cleavage step was up or down. The *relative* directions of adjacent steps could always be determined with certainty, but in general there remained ambiguity about the true step direction and it could not be decided whether a given pattern or its mirror image was the correct picture.

Both problems are solved at one stroke by the employment of fringes of equal chromatic order, which in addition immediately reveal in a very clear and distinct manner surface features which can only be derived by laborious computation from Fizeau fringes. Experimentally it is only necessary to replace the silvered lens-plate in fig. 1 by the silvered mica-flat combination. The spectroscope slit then selects a very narrow section of the mica surface and reveals its topographical features. To cover any appreciable area of the mica it is necessary to traverse the slit with the mica image by simple scanning, moving the mica horizontally across the field. Whilst this is of necessity a laborious procedure photographically, visually it is very rapid, and a quick survey of considerable mica areas can rapidly be made.

Fig. 2.

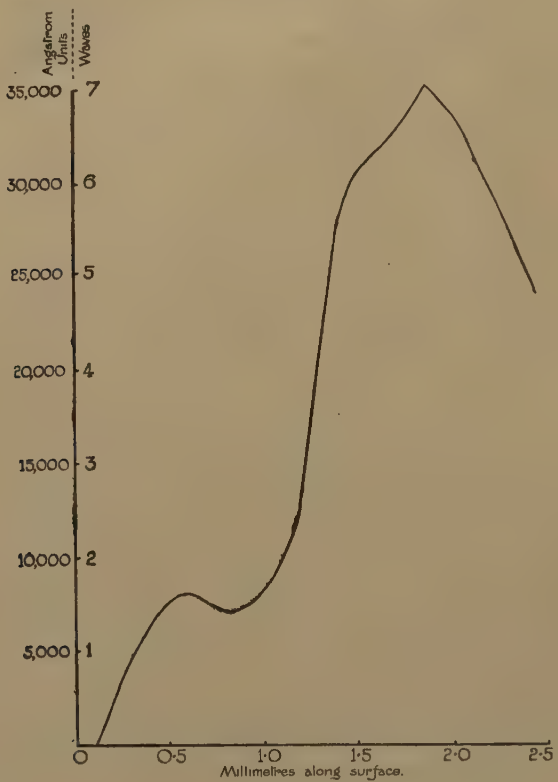

A typical fringe pattern is that shown in Pl. V. (*c*). Reference back to the fringes given by the plate-lens show at once which regions of the mica represent hills and which valleys. For fringes convex to the violet clearly represent a hill, and those convex to the red a valley. Alternatively, when the number of fringes in the field is small, this represents a high spot, and so the contour can readily be visualized. Not only is the direction of incline shown, but by measuring the $\Delta\nu$ values at the peaks, planes and valleys, the exact values of the heights and depths are obtained with the highest precision ($\lambda/200$).

From the consideration of any vertical section the rate of change of height, *i. e.* the steepness of the incline, is rendered obvious. The number of fringes intersected per unit of length of the vertical section is a measure of the slope in terms of half-waves. The more close packed the fringes the steeper the slope. The detailed analysis of the pattern is shown in fig. 2.

A beautiful effect is shown on Pl. V. (*d*). In this a mica specimen has been placed such that a cleavage step crosses the slit image. A sharp discontinuity thus appears. Two separate conclusions can be drawn from this record. From the difference in the number of fringes, in a given wave-length range, on either side of the discontinuity, the *height* of the step can be calculated. Further, the side containing the larger number of fringes is furthest from the optical flat, hence the *direction* of the step (up or down) is at once determined even by simple visual inspection. The result of detailed measurement is given in fig. 3.

Fig. 3.

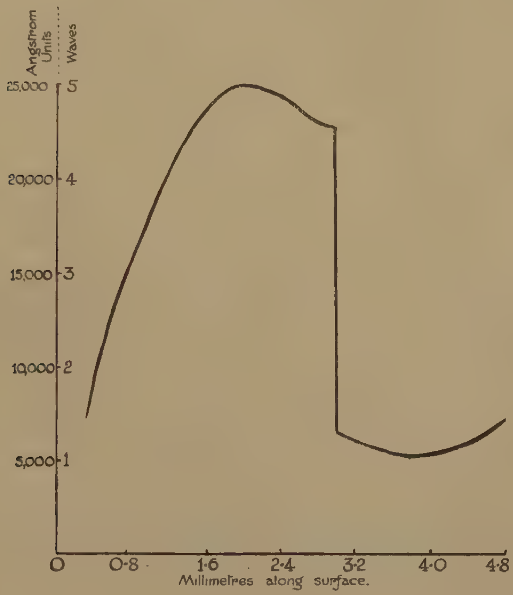

The following treatment can be employed for the evaluation of a step. The procedure will be called the method of coincidences.

Coincidence Method for Evaluation of Cleavage Steps.

It will be seen clearly that the fringes in Pl. V. (*d*) exhibit either perfect or imperfect coincidences exactly as in the case of a typical vernier scale. The exact step can be calculated either from perfect or imperfect coincidences in a very simple way. Consider first a perfect coincidence.

Let there be $m+1$ fringes in one part of the field and suppose these exactly coincide with $m+2$ fringes in the other part. Let $\Delta\nu$ be the frequency wave-number difference between the two coincidence points. Then

$$t_1=m/2\Delta\nu$$
$$t_2=(m+1)/2\Delta\nu,$$

where t_1, t_2 are the distances between the two mica surfaces and the optical flat. Thus

$$\Delta t=t_2-t_1=1/2\Delta\nu,$$

where Δt is the step. It will be noticed that this is independent of the actual value of t_1 and t_2.

It is only necessary then to evaluate the wave-number separation between the coincidence points to obtain the step.

However, the method is not restricted to perfect coincidence, and is generally applicable thus. Let two wave-lengths be selected, with wave-number separation $\Delta\nu$. (For ease in computation round numbers, say 4000 and 5000 A.U., can be selected.) Let there be $m+1$ fringes on one side of the dividing line and $n+1$ fringes on the other. In general m and n are not integers but contain fractional parts. We then have

$$t_1=m/2\Delta\nu$$
$$t_2=n/2\Delta\nu$$
$$\Delta t=t_2-t_1=(n-m)/2\Delta\nu.$$

If it happens that Δt is a fraction of a half-wave, then for convenience $\Delta\nu$ can be chosen so that n and m both contain the same integer and can thus be written $n+x$, $n+y$ respectively, where x and y are fractions of an order. From this we get $\Delta t=(x-y)/2\Delta\nu$. It is thus only necessary to measure the fractional parts x, y at the ends of the selected wave-length range.

There is, however, a much simpler procedure if Δt is a small fraction of a half-wave. For then the relation $\Delta t=dn\,.\,\lambda/2$ can be used. It is only necessary in this case to measure the fraction of an order displacement dn at *one* wave-length λ. A displacement to the violet corresponds to a step up towards the optical flat.

Applications to the Detection and Measurement of Small Angles.

The fringes of equal chromatic order can be used as a particularly sensitive device for the measurement of small surface angles. For example, ridges on surfaces which depart only very slightly from a true plane can be studied. A characteristic example is shown in Pl. V. (*c*) and in fig. 2, which refers to mica. In particular, slightly inclined vicinal faces on crystals, that is faces with very large Millerian indices, can be detected. The sharp acute angle between the almost straight fringes represents a surface wedge.

A simple wedge between planes, placed with the edge perpendicular to the spectroscope slit, leads to the formation of straight line fringes sloping across the field of view. From the measured fringe slope the wedge angle can be calculated quite simply. Let the horizontal distance between two orders be x centimetres on the photographic plate and let y be the vertical distance between two fringes (the fringes are parallel). The measured fringe slope is x/y. But the true wedge angle is $\lambda/2y$. The magnification is then $2x/\lambda$. With the spectrograph used the dispersion at 5000 A. is some 200 A./cm. Taking $x=5$ millimetres between orders, as is the case in Pl. V., leads to a value of 20,000 for the magnification of the angle. This argument implies unit magnification by the lens F.

The angles which are measurable are very much smaller than the Rayleigh limit. According to the accepted Rayleigh procedure the smallest angle measurable by a goniometer is λ/y, where y is the length of the wedge. But with these highly sharpened fringes a displacement of $\lambda/200$ is readily measured at a discontinuity, and in the case of a continuous sloping line $\lambda/50y$ can certainly be evaluated, and under suitable conditions $\lambda/100y$. Angles 100 times smaller than the Rayleigh limit can therefore be measured.

The Influence of the Magnification Produced by the Projecting Lens.

The magnification produced by the projecting lens F in fig. 1 has an important bearing on the experimental attainment of the maximum resolution.

In the case of the lens-plate combination (Newton's rings) the projection of an enlarged image (say by a factor of 5), leads to a considerable sharpening in the fringe definition. The reason is clear. For, by enlarging, the spectroscope slit is in effect selecting a still narrower portion of the interference film, reduced in width by the magnification ratio. So sensitive is the experimental procedure to small changes in thickness, that the minute variations introduced across the very narrow slit width lead to a considerable reduction in ultimate sharpness, unless magnification is employed to counteract this.

We have here the paradoxical optical situation in which the enlargement of a projected image leads to an ultimate improvement in definition. More strictly, of course, the result of enlarging is geometrically equivalent to the reduction of a stop.

When the fringes are formed by a parallel-sided film, then magnification has no appreciable effect. The step values are quite independent of this and fringe definition is not effectively improved.

If, however, sloping fringes are involved due to a wedge, as, for example, in Pl. V. (*c*), then a *diminution* in the image projected leads to an *increase* in the slope of the recorded fringes, and *vice versa* on enlargement.

The effects which occur are perhaps clearly summarized by considering a wedge between two planes as the interference film. When the wedge is set with its edge parallel to the slit, magnification improves definition of the vertical fringes which form. When the wedge is rotated through 90°, being set with its edge perpendicular to the slit, magnification has no influence on the definition but reduces the effective slope of the fringes.

If a slope is suspected, the true wedge value is only obtained if the film is rotated to give the maximum fringe slope, for a wedge set at an angle other than with its edge perpendicular to the slit gives an apparent wedge which is only a resolved component of the true wedge value. It is clear that a judicious employment of magnification must be adopted according to the problem in hand. The guiding criterion is that only the surface dimensions and not the film thickness are affected by the magnifying lens.

In Part VI. the relation between fringes of equal chromatic order and other fringe types will be discussed in further detail.

References.

(1) Tolansky, ' Nature,' clii. p. 722 (1943).
(2) Tolansky, Phil. Mag. xxxiv. p. 555 (1943).
(3) Tolansky, Phil. Mag. xxxv. p. 120 (1944).
(4) Tolansky, Phil. Mag. xxxv. p. 179 (1944).
(5) Tolansky, ' Nature,' clii. p. 722 (1043) ; cliii. p. 195 (1944).
(6) Tolansky, Proc. Roy. Soc. A. In print.

XXXII. *New Contributions to Interferometry.* Part VI.—*White Light Fabry–Perot Fringes.*

By S. Tolansky, Ph.D., D.I.C., The University, Manchester *.

[Received November 8, 1944.]

[Plate VI.]

Abstract.

It is shown how white light Fabry–Perot fringes are very easy to produce experimentally if correct attention is given to optical detail. Only low resolving power instruments are needed. The fringes appear as a large number of strongly curved narrow fringes extending across the whole spectrum. The relationship between these fringes and the fringes of equal chromatic order described in Part V. is discussed. The fringes described here have little practical application, but complete the systems possible from variations of the constituent terms in the formula $n\lambda = 2t \cos \theta$.

White Light Fabry–Perot Fringes.

In Part V.$^{(1)}$ the properties of some new multiple beam white light fringes have been discussed. It was pointed out there that from the

---

* Communicated by the Author.

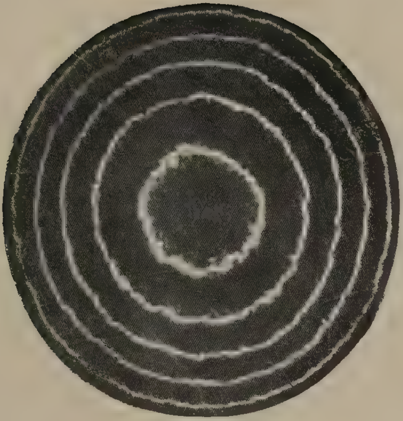

(a)

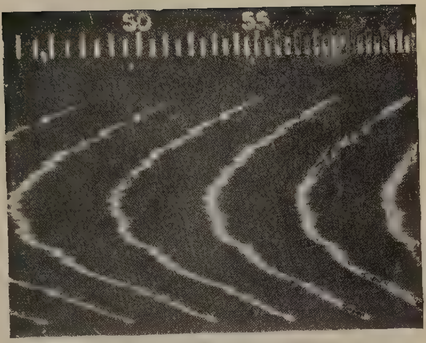

(b)

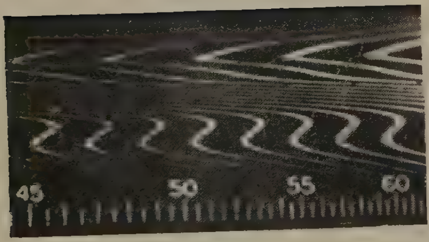

(c)

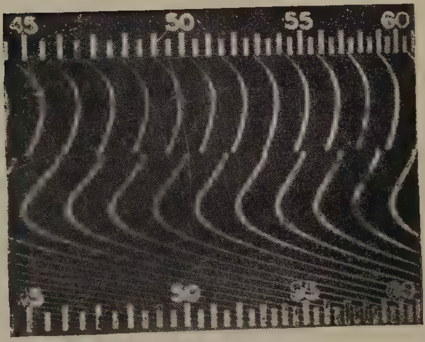
45
50
55
60
50

(d)

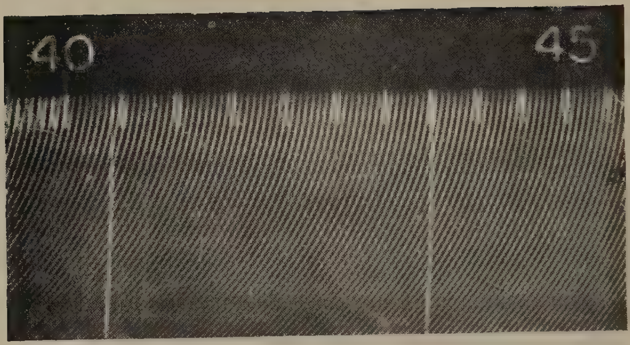

(*a*)

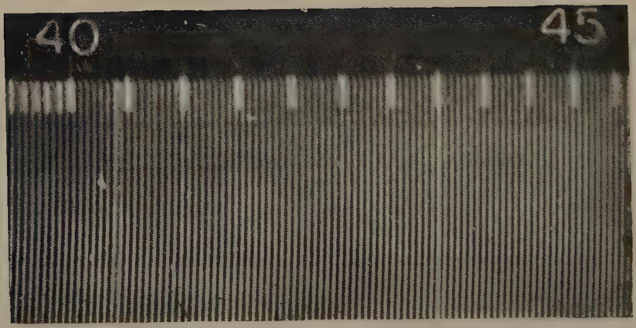

(*b*)

basic formula $n\lambda = 2t \cos \theta$ two types of multiple beam interference fringe could be expected when λ is variable (white light). In the first of these, described in Part V. as " fringes of equal chromatic order," t/λ is constant ($\cos \theta = 1$) and the fringes which form are " fringes of equal t/λ." It is the purpose of this short note to discuss the remaining case, in which t is constant and both θ and λ simultaneously vary. The fringes which result are nothing more than white light Fabry–Perot fringes, as will appear evident in the discussion which follows.

Fringes which arise when t is constant and λ and θ vary are clearly intimately related to the fringes of equal chromatic order in which θ is constant and t and λ vary. For we can consider a special case of the latter in which t is constant as a starting point for the resemblance. In this case the fringes of equal chromatic order are straight lines parallel to the slit of the spectrograph. As t increases the $\Delta\nu$ separation between the fringes diminishes (see Part V.), and clearly a point will be reached at which the prism spectrograph fails to resolve the fringes and the field appears covered with a white light continuum.

Consider now the fringes which will arise in general if both λ and θ vary. Since we are restricting the discussion to multiple beam interferometry, it is necessary for the multiple beams to be integrated for sharp fringes to be produced. If then θ varies, the only way in which this can be brought about is to bring the rays of the same inclination to a focus by means of a lens. In other words, any multiple beam fringes formed under such conditions will be *at infinity*, like Fabry–Perot rings, and will therefore require projection on a spectroscope slit, the slit being at the principal focus. This is of course distinctly different to the case of the fringes of equal chromatic order, in which *an image of the interference film* is projected on to the slit.

To produce these fringes, therefore, the experimental conditions are as follows :—An extended white light source (to give a range of θ values) is employed. A parallel-sided air film, produced by two glass flats suitably silvered, is used for the interference. The fringes are projected on to the slit of a spectroscope with an achromat, the slit being at the principal focus. But there is an overriding restriction which limits the arrangement. For the value of t, the separation in the interferometer, must be such that the $\Delta\nu$ can be resolved by the spectrograph (see Part V.). For clearly at the centre of this system of fringes, where $\cos \theta = 1$, we have the same condition as that discussed above, in which we considered the fringes of equal chromatic order as a special case when t is constant.

With the Hilger medium quartz spectrograph available, a convenient value for t is about 1/7th millimetre. Now a simple calculation shows that a Fabry–Perot interferometer with such a small value of t produces rings with very large angular diameter, thus if a number of orders are to be projected on to the slit, it is necessary to employ a projecting lens with very *small* focal length. The only suitable lens available was a 1-inch microscope objective. But even this focal length is not enough to bring an appreciable number of orders on to the slit. To do this, higher orders are brought into the field by tilting the interferometer with reference to the incident light beam.

By using these somewhat exacting optical arrangements the fringes, which strictly are fringes representing $t \cos \theta/\lambda$ constant, were obtained and are shown in Pl. VI. (*a*). It may be pointed out that the employment of a microscope objective for the projection of Fabry–Perot fringes is an unusual departure from general practice, for as a rule, with the gaps of say 1 millimetre to 10 centimetres which are in general use, the emphasis is on the use of as *long* a focal length as is available, a 1 metre lens being typical.

It is further to be noted (and this will be discussed later) that these white light Fabry–Perot fringes can, as demonstrated, readily be produced with low power prism spectrographs, providing the value of t is kept low, requiring therefore short focal length projection. It is *not* necessary, as had been thought earlier, to employ a powerful grating.

To prove that the curved white light fringes in Pl. VI. (*a*) are indeed simply Fabry–Perot fringes with continuously variable wave-length, a mercury source was simultaneously projected on to the interferometer with the white light source. The Fabry–Perot fringes of the mercury lines duly appear in their correct positions on the continua. It can be clearly seen that as one moves progressively to higher orders across the mercury line fringes, each successive monochromatic fringe falls on a successive curved continuous fringe. These curved fringes are of course fringes of equal chromatic order in the sense used in Part V., for each represents $t (\cos \theta)/\lambda$ constant. But to use this terminology would only lead to confusion, and it is clearly much more convenient to describe these fringes as "*white light Fabry–Perot fringes*," which indeed they are.

On removal of the projecting lens then, the fringe pattern obtained is that shown in Pl. II. (*b*). These fringes are simply the well-known Edser–Butler (2) fringes (improved considerably by the high reflecting coefficient of the silver). These fringes are exactly parallel to the slit, as proved by the superposed mercury lines, and do *not* require the projection lens. Clearly the Edser–Butler fringes are only the centre of the Fabry–Perot white light system. So great is the angular diameter of the latter rings that the angular variations entering the slit are much less than the diameter of the first ring. Only a small fraction of this ring appears and the fringes are therefore effectively straight line fringes, parallel to the slit.

Thus to summarize, whilst the fringes described in Part V. are produced by θ constant and t, λ variable, the fringes in Pl. VI. (*a*) are formed with t constant and λ, θ variable. This can therefore be considered to complete the separate systems of *sharp* multiple beam fringes which it is possible to obtain for the variables in the formula $n\lambda = 2t \cos \theta$. If more variables are introduced in any particular case fringe broadening can result. Strictly speaking the formula should include μ, for the complete expression is $n\lambda = 2 \mu t \cos \theta$. The effect of variations in μ will be treated in a later work, for it can lead to complexity.

Relationship to Other Fringes.

It is to be noted that the fringes described in Part V., and those described here, can be formed either by *two* interfering beams or by *multiple* beams. So very different are the two types, in sensitivity, power, application and usefulness, that they must be considered distinct. There is, as an analogy, simply no justification for identifying the original two-beam fringes of Haidinger with the immensely powerful multiple beam fringes of Fabry–Perot. To claim that the latter are merely a sharpened improvement of the former is to postulate that there is no practical difference between a grating consisting of two lines with one consisting of some forty lines. The employment of multiple beams is just that very factor which has led to so many advances in optics and is entitled to be considered as an individual procedure, involving as it does do many special techniques and requirements not existing in two-beam interferometry.

Thus a crude version of the fringes of equal chromatic order described in Part V. can be formed by projecting either simple two-beam Newton's rings, Jamin fringes, or Michelson fringes, or even Young's fringes, on to the slit of a spectrograph, using white light. But in *every* case the intensity distribution of the continuous fringes is of the cos type, *for only two interfering beams are involved* and such procedures simply cannot compare with a correct multiple beam set-up.

Whilst a number of valuable studies have been made with the fringes of equal chromatic order, so far the fringes shown in Pl. VI. (*a*), which represent $(t \cos \theta)/\lambda$ constant, appear as yet to have little practical use. They are described here for the sake of completion of the types in the formula.

This is not the first time such fringes have been described. A closely similar type of fringe was first described as long ago as in 1906 by Gehrcke and Reichenheim (3). These they called *k* fringes. These investigators employed as the interferometer either a 1-centimetre or a 1-millimetre glass Lummer plate, crossed with either a powerful multi-prism spectrograph or a powerful grating. From the above discussion, it will be realized that the optical arrangements employed (normal focal lengths were used too) are very unsuitable. As a result extremely close fringes form, and these can only be resolved with a powerful spectrograph. Further, only a very small θ range is covered, with the result that the fringes are only very slightly curved. Added to this is the complexity introduced by the variation in μ, for the interference takes place within a dispersive medium.

It will be seen, therefore, that these investigators did not fully realize the essential conditions for the simple production of the white light fringes, easy indeed to observe if the conditions are correct.

There is one further mention of these white light fringes in the literature. Meggers and Burns (4), in their well-known determination of the wave-lengths of the Fraunhofer lines in the sun's spectrum, crossed a large gap Fabry–Perot interferometer (gap of the order of 1 centimetre) with a powerful grating. They noticed that the continuous regions were crossed by a very large number of close fine parallel lines. No curvature was effectively detected. They pointed out that the fringes were indeed the white light Fabry–Perot fringes, but these were only revealed because of the high dispersion and resolution of the crossed grating spectrograph. Again the optimum conditions for facile production and study were not realized experimentally, nor discussed. It is re-emphasized that the simplest of apparatus suffices.

Finally, the relationship between the fringes described here, those in Part V., and those described by Roschdestwensky ⁽⁵⁾ will be considered briefly. The fringes described by Roschdestwensky, which he calls "hook" fringes, have been widely used for the study of dispersion in gases, particularly in the neighbourhood of absorption regions. In this arrangement white light fringes from a Jamin or Mach interferometer are projected onto the slit of a spectrograph. *There are of course, only two interfering beams* and the fringes have only a cos intensity distribution. In the one light path is a plate of glass and in the other the dispersing gas. Over most of the field straight line fringes appear, slightly inclined, but in the neighbourhood of an absorption line these twist up into a hook shape.

There are several differences between the hook fringes and the fringes of equal chromatic order. First regarding sensitivity. The multiple beams lead to so great a sharpening that sensitivity is of an altogether higher order than that possible with cos fringes. According to Jentzsch ⁽⁶⁾ "it is much easier to photograph the fringes than to measure them," for they are very broad in the very regions where measurements are to be made. A second difference concerns the type of fringe involved. Over the non-sensitive part of the field, the region of *no* absorption, the interferometer fringes in Roschdestwensky's arrangement are fringes of equal inclination, originating *at infinity*. When these are projected on to the slit, which is at the principal focus of the projecting lens, then the observed field is covered with straight line fringes converging to the violet, and these are clearly the counterpart of the white light Fabry–Perot fringes described in Pl. VI. (a), but for the case of a Jamin instead of a Fabry–Perot interferometer.

But these straight portions are not employed. In the neighbourhood of the hook these straight line fringes are modified in shape by the variation in optical path introduced by a rapid variation in μ. The fringes here, therefore, are comparable to having t constant but λ, θ, μ varying, and are thus correspondingly more complex.

In conclusion, it may be noted that it is easy to prove that the shape of the white light Fabry–Perot fringes is given by the formula $d\lambda/d\theta=\tan\theta$, so that this depends upon the dispersion curve of the spectrograph, since this affects $d\lambda$. The *increase* in curvature on approaching the blue end is very clearly marked in Pl. VI. (a), the increase in *spectrograph* dispersion being the cause.

References.

(1) Tolansky, Phil. Mag. xxxvi. p. 225 (1945).
(2) Edser and Butler, Phil. Mag. xliv. p. 207 (1898).
(3) Gehrcke and Reichenheim, *Verhand. d. Deutsch. Phys. Ges.* viii. p. 209 (1906).
(4) Megger and Burns, Public Allegheny Observ. vol. vi. no. 7, p. 105 (1929).
(5) Roschdestwensky, *Ann. der Physik*, xxxix. p. 307 (1912).
(6) Jentzsch, Gehrcke's Handbuch d. Phys. Optik. p. 185.

XXXIII. *The Stress Distribution in a Long Circular Cylinder when Discontinuous Pressure is Applied to the Curved Surface.*

By C. J. Tranter, M.A., and J. W. Craggs, B.Sc.*

[Received June 2, 1944.]

1. A formal solution giving the stresses set up in a long cylinder when an axially symmetrical static pressure involving discontinuities is applied to the curved surface is obtained by the use of the complex form of the Fourier integral transform. The case of a bar of finite length in which the curved surface and ends are subjected to various systems of applied stress involving discontinuities has been investigated by Prof. L. N. G. Filon †, and he has applied his results to cylindrical bars in testing machines. Prof. Filon has expanded the applied stresses in Fourier series and retained only a few terms, so that his results can only be regarded as approximations to the true solutions. In the present paper no such approximation is made, the solution for a real discontinuity in a boundary condition being given. Numerical results have been computed for the particular case in which the applied stress is a uniform pressure over half the length of the cylinder, the other half being unloaded, and Poisson's ratio for the material being taken as 1/4.

Similar methods apply to other problems of this type, and work on these lines is now in progress.

2. *The Equations for Solution.*—The axis of the cylinder is taken as the z-axis, the origin being at the central cross-section, and the usual cylindrical coordinates r, θ, z are employed. The radius of the cylinder is denoted by a. In the particular problem here treated, for $z>0$, unit pressure is applied to the surface $r=a$, while, for $z<0$, the boundary is unloaded and the shear stress over the curved surface is taken as zero for the whole length of the cylinder. With trifling modifications the

---

* Communicated by the Authors.

† L. N. G. Filon, "On the Elastic Equilibrium of Circular Cylinders under certain Practical Systems of Load," Phil. Trans. Roy. Soc. ser. A, vol. cxcviii. pp. 147–233 (1902).

method can be used for applied stresses under fairly wide restrictions, *e. g.* that they be of exponential type.

For symmetrical strain in a cylinder, the radial, shear, hoop and longitudinal stresses and the radial and longitudinal displacements are given in terms of a stress function χ by the equations *

$$\widehat{rr}=\frac{\partial}{\partial z}\left\{\sigma\nabla^2-\frac{\partial^2}{\partial r^2}\right\}\chi, \quad \ldots \quad (1)$$

$$\widehat{rz}=\frac{\partial}{\partial r}\left\{(1-\sigma)\nabla^2-\frac{\partial^2}{\partial z^2}\right\}\chi, \quad \ldots \quad (2)$$

$$\widehat{\theta\theta}=\frac{\partial}{\partial z}\left\{\sigma\nabla^2-\frac{1}{r}\frac{\partial}{\partial r}\right\}\chi, \quad \ldots \quad (3)$$

$$\widehat{zz}=\frac{\partial}{\partial z}\left\{(2-\sigma)\nabla^2-\frac{\partial^2}{\partial z^2}\right\}\chi, \quad \ldots \quad (4)$$

$$\mathrm{U}=-\frac{1+\sigma}{\mathrm{E}}\cdot\frac{\partial^2\chi}{\partial r\,\partial z}, \quad \ldots \quad (5)$$

$$w=\frac{1+\sigma}{\mathrm{E}}\left\{(1-2\sigma)\nabla^2+\frac{\partial^2}{\partial r^2}+\frac{1}{r}\frac{\partial}{\partial r}\right\}\chi, \quad \ldots \quad (6)$$

where σ, E are Poisson's ratio and Young's modulus of the material, ∇^2 denotes $\frac{\partial^2}{\partial r^2}+\frac{1}{r}\frac{\partial}{\partial r}+\frac{\partial^2}{\partial z^2}$ and χ satisfies

$$\nabla^4\chi=0, \quad -\infty<z<\infty, \quad r<a \quad \ldots \quad (7)$$

with the boundary conditions

$$\left.\begin{aligned}\widehat{rr}=\frac{\partial}{\partial z}\left\{\sigma\nabla^2-\frac{\partial^2}{\partial r^2}\right\}\chi&=-1, \qquad 0<z<\infty,\\ &=0, \qquad -\infty<z<0,\end{aligned}\right\} \quad r=a, \quad \ldots \quad (8)$$

$$\widehat{rz}=\frac{\partial}{\partial r}\left\{(1-\sigma)\nabla^2-\frac{\partial^2}{\partial z^2}\right\}\chi=0, \quad -\infty<z<\infty, \quad r=a. \quad \ldots \quad (9)$$

3. *The Transformed Equations and their Solution.*—Writing

$$\bar{\chi}=\int_{-\infty}^{\infty}\chi e^{i\zeta z}\,dz, \quad \ldots \quad (10)$$

where ζ has a positive imaginary part, and integrating by parts, we have †

$$\int_{-\infty}^{\infty}\frac{\partial^n\chi}{\partial z^n}e^{i\zeta z}\,dz=(-i\zeta)^n\bar{\chi} \quad (n=1, 2, 3, 4).$$

Multiplying equations (7), (8) and (9) by $e^{i\zeta z}$ and integrating with respect to z from $-\infty$ to ∞, we have, if we denote $\frac{d^2}{dr^2}+\frac{1}{r}\frac{d}{dr}-\zeta^2$ by $\overline{\nabla}^2$,

$$\overline{\nabla}^4\bar{\chi}=0 \quad \ldots \quad (11)$$

---

* A. E. H. Love, 'Treatise on the Mathematical Theory of Elasticity,' Camb. Univ. Press, 1920, p. 278.

† We assume, in the present problem, that as $z\rightarrow\pm\infty$, the limits of $\chi e^{i\zeta z}$ and $\frac{\partial^n\chi}{\partial z^n}e^{i\zeta z}$ $(n=1, 2, 3)$ are all zero.

and
$$-i\zeta\left\{\sigma\bar{\nabla}^2-\frac{d^2}{dr^2}\right\}\bar{\chi}=-\int_0^\infty e^{i\zeta z}\,dz,$$

giving
$$\left\{\sigma\bar{\nabla}^2-\frac{d^2}{dr^2}\right\}\bar{\chi}=\frac{1}{\zeta^2},\quad r=a \qquad (12)$$

and
$$\frac{d}{dr}\{(1-\sigma)\bar{\nabla}^2+\zeta^2\}\bar{\chi}=0,\quad r=a. \qquad (13)$$

The solution of (11), finite at $r=0$, is
$$\chi=\mathrm{A}\mathrm{I}_0(\rho)+\mathrm{B}\rho\mathrm{I}_1(\rho), \qquad (14)$$

where, for brevity,
$$\rho=\zeta r. \qquad (15)$$

Using the recurrence formulæ for the Bessel functions *, we find
$$\bar{\nabla}^2\bar{\chi}=2\mathrm{B}\zeta^2\mathrm{I}_0(\rho), \qquad (16)$$

and substitution in (12) and (13) yields
$$\mathrm{A}\left\{\mathrm{I}_0(\alpha)-\frac{1}{\alpha}\mathrm{I}_1(\alpha)\right\}+\mathrm{B}\{(1-2\sigma)\mathrm{I}_0(\alpha)+\alpha\mathrm{I}_1(\alpha)\}=-\frac{1}{\zeta^4}, \qquad (17)$$
$$\mathrm{A}\mathrm{I}_1(\alpha)+\mathrm{B}\{2(1-\sigma)\mathrm{I}_1(\alpha)+\alpha\mathrm{I}_0(\alpha)\}=0, \qquad (18)$$

where
$$\alpha=\zeta a. \qquad (19)$$

Hence,
$$\left.\begin{aligned}\mathrm{A}&=\frac{\alpha}{\zeta^4\mathrm{D}(\alpha)}\{2(1-\sigma)\mathrm{I}_1(\alpha)+\alpha\mathrm{I}_0(\alpha)\},\\ \mathrm{B}&=\frac{-\alpha}{\zeta^4\mathrm{D}(\alpha)}\,.\,\mathrm{I}_1(\alpha),\end{aligned}\right\} \qquad (20)$$

where
$$\mathrm{D}(\alpha)=\{\alpha^2+2(1-\sigma)\}\mathrm{I}_1^2(\alpha)-\alpha^2\mathrm{I}_0^2(\alpha). \qquad (21)$$

Substitution in (14) then gives $\bar{\chi}$ completely.

Denoting the transform of a stress or displacement by a "bar," so that
$$\overline{rr}=\int_{-\infty}^{\infty}\widehat{rr}\,e^{i\zeta z}\,dz,\text{ etc.},$$

multiplication of equations (1) . . . ., (6) by $e^{i\zeta z}$, and integration with respect to z from $-\infty$ to ∞, gives
$$\overline{rr}=-i\zeta\left\{\sigma\bar{\nabla}^2-\frac{d^2}{dr^2}\right\}\bar{\chi},\qquad \overline{zz}=-i\zeta\{(2-\sigma)\bar{\nabla}^2+\zeta^2\}\bar{\chi},$$
$$\overline{rz}=\frac{d}{dr}\{(1-\sigma)\bar{\nabla}^2+\zeta^2\}\bar{\chi},\qquad \bar{\mathrm{U}}=-\frac{1+\sigma}{\mathrm{E}}\,.\,i\zeta\frac{d\bar{\chi}}{dr},$$
$$\overline{\theta\theta}=-i\zeta\left\{\sigma\bar{\nabla}^2-\frac{1}{r}\frac{d}{dr}\right\}\bar{\chi}.\qquad \bar{w}=\frac{1+\sigma}{\mathrm{E}}\left\{(1-2\sigma)\bar{\nabla}^2+\frac{d^2}{dr^2}+\frac{1}{r}\frac{d}{dr}\right\}\bar{\chi}.$$

Using (14), (16) and (20), we find
$$\begin{aligned}rr=-\frac{1}{i\zeta}\frac{\alpha}{\rho}\frac{1}{\mathrm{D}(\alpha)}[\alpha\rho\mathrm{I}_0(\alpha)\mathrm{I}_0(\rho)+\rho\mathrm{I}_0(\rho)\mathrm{I}_1(\alpha)-\alpha\mathrm{I}_0(\alpha)\mathrm{I}_1(\rho)\\ -\{\rho^2+2(1-\sigma)\}\mathrm{I}_1(\alpha)\mathrm{I}_1(\rho)]. \qquad (22)\end{aligned}$$

---

* G .N. Watson, 'Theory of Bessel Functions,' Camb. Univ. Press, 1922, p. 79.

$$\overline{rz}=\frac{1}{\zeta}\frac{\alpha}{D(\alpha)}[\alpha I_1(\rho)I_0(\alpha)-\rho I_1(\alpha)I_0(\rho)], \quad . \quad . \quad . \quad . \quad . \quad . \quad . \quad . \quad . \quad . \tag{23}$$

$$\overline{\theta\theta}=-\frac{1}{i\zeta}\frac{\alpha}{\rho}\frac{1}{D(\alpha)}[\alpha I_0(\alpha)I_1(\rho)+2(1-\sigma)I_1(\alpha)I_1(\rho)+(2\sigma-1)\rho I_1(\alpha)I_0(\rho)], \tag{24}$$

$$\overline{zz}=\frac{1}{i\zeta}\frac{\alpha}{D(\alpha)}[\alpha I_0(\alpha)I_0(\rho)-\rho I_1(\alpha)I_1(\rho)-2I_0(\rho)I_1(\alpha)], \quad . \quad . \quad . \quad . \quad . \quad . \tag{25}$$

$$\frac{\overline{U}}{a}=-\frac{1}{i\zeta}\frac{1+\sigma}{E}\frac{1}{D(\alpha)}[\alpha I_0(\alpha)I_1(\rho)-\rho I_0(\rho)I_1(\alpha)+2(1-\sigma)I_1(\alpha)I_1(\rho)], \quad . \tag{26}$$

$$\frac{\overline{w}}{a}=\frac{1}{\zeta}\frac{1+\sigma}{E}\frac{1}{D(\alpha)}[\alpha I_0(\alpha)I_0(\rho)-\rho I_1(\alpha)I_1(\rho)-2(1-\sigma)I_0(\rho)I_1(\alpha)]. \quad . \quad . \tag{27}$$

4. *The Inversion.*—The inverse relation to (10) is *

$$\chi=\frac{1}{2\pi}\int_{i\gamma-\infty}^{i\gamma+\infty}\overline{\chi}e^{-iz\zeta}\,d\zeta \quad (\gamma>0),$$

and similar relations hold for inverting the transforms of the stresses and displacements, *e. g.*,

$$\widehat{rr}=\frac{1}{2\pi}\int_{i\gamma-\infty}^{i\gamma+\infty}\overline{rr}e^{-iz\zeta}\,d\zeta.$$

In each case the integral has no poles on the real axis, apart from the origin. The contour of the integral may therefore be deformed into the real axis from $-\infty$ to $+\infty$ with a clockwise semicircle round the origin. The integral may therefore be evaluated as the sum of the integrals along the real axis from $-\infty$ to $+\infty$ less πi times the residue of the integrand at $\zeta=0$. The residues at $\zeta=0$ for the various stresses may be found by using the power series for the Bessel functions, and are as follows:—

Quantity.	Residue at =0.	Quantity.	Residue at $\zeta=0$.
$\widehat{rr}$	$-i$	$\widehat{zz}$	0
$\widehat{rz}$	0	U/a	$-\frac{1-\sigma}{E}\frac{r}{a}i$
$\widehat{\theta\theta}$	$-i$	e_{zz}†	$2i\sigma/E$

Combining the integrals along the negative and positive parts of the real axis and writing ‡ $a\zeta=x$, we find

---

* E. C. Titchmarsh, 'Introduction to the Theory of Fourier Integrals,' Oxford Univ. Press, 1937, p. 5.

† The longitudinal strain seems of more interest than the longitudinal displacement: it is given by $e_{zz}=\frac{\partial w}{\partial z}$, so that $\overline{e_{zz}}=-i\zeta\overline{w}$.

‡ No confusion need arise with the substitution $\alpha=\zeta a$ made in (19).

$$\widehat{rr}=-\frac{1}{2}+\frac{a}{\pi r}\int_0^\infty\left[\frac{r}{a}x^2\mathrm{I}_0(x)\mathrm{I}_0\left(\frac{r}{a}x\right)+\frac{r}{a}x\mathrm{I}_0\left(\frac{r}{a}x\right)\mathrm{I}_1(x)-x\mathrm{I}_0(x)\mathrm{I}_1\left(\frac{r}{a}x\right)\right.$$

$$\left.-\left\{\frac{r^2}{a^2}x^2+2(1-\sigma)\right\}\mathrm{I}_1(x)\mathrm{I}_1\left(\frac{r}{a}x\right)\right]\frac{\sin\frac{z}{a}x}{\mathrm{D}(x)}\frac{dx}{x}. \quad (28)$$

$$\widehat{rz}=\frac{1}{\pi}\int_0^\infty\left[x\mathrm{I}_1\left(\frac{r}{a}x\right)\mathrm{I}_0(x)-\frac{r}{a}x\mathrm{I}_1(x)\mathrm{I}_0\left(\frac{r}{a}x\right)\right]\frac{\cos\frac{z}{a}x}{\mathrm{D}(x)}\,dx. \quad . \quad . \quad . \quad . \quad (29)$$

$$\widehat{\theta\theta}=-\frac{1}{2}+\frac{a}{\pi r}\int_0^\infty\left[x\mathrm{I}_0(x)\mathrm{I}_1\left(\frac{r}{a}x\right)+2(1-\sigma)\mathrm{I}_1(x)\mathrm{I}_1\left(\frac{r}{a}x\right)\right.$$

$$\left.+(2\sigma-1)\frac{r}{a}x\mathrm{I}_1(x)\mathrm{I}_0\left(\frac{r}{a}x\right)\right]\frac{\sin\frac{z}{a}x}{\mathrm{D}(x)}\frac{dx}{x}. \quad . \quad (30)$$

$$\widehat{zz}=\frac{1}{\pi}\int_0^\infty\left[2\mathrm{I}_0\left(\frac{r}{a}x\right)\mathrm{I}_1(x)+\frac{r}{a}x\mathrm{I}_1(x)\mathrm{I}_1\left(\frac{r}{a}x\right)-x\mathrm{I}_0(x)\mathrm{I}_0\left(\frac{r}{a}x\right)\right]\frac{\sin\frac{z}{a}x}{\mathrm{D}(x)}\,dx.$$

$$. \quad . \quad . \quad (31)$$

$$\frac{\mathrm{EU}}{a}=\frac{-(1-\sigma)}{2}\frac{r}{a}+\frac{(1+\sigma)}{\pi}\int_0^\infty\left[x\mathrm{I}_0(x)\mathrm{I}_1\left(\frac{r}{a}x\right)-\frac{r}{a}x\mathrm{I}_0\left(\frac{r}{a}x\right)\mathrm{I}_1(x)\right.$$

$$\left.+2(1-\sigma)\mathrm{I}_1(x)\mathrm{I}_1\left(\frac{r}{a}x\right)\right]\frac{\sin\frac{z}{a}x}{\mathrm{D}(x)}\frac{dx}{x}. \quad (32)$$

$$\mathrm{E}e_{zz}=\sigma-\frac{(1+\sigma)}{\pi}\int_0^\infty\left[x\mathrm{I}_0(x)\mathrm{I}_0\left(\frac{r}{a}x\right)-\frac{r}{a}x\mathrm{I}_1(x)\mathrm{I}_1\left(\frac{r}{a}x\right)\right.$$

$$\left.-2(1-\sigma)\mathrm{I}_0\left(\frac{r}{a}x\right)\mathrm{I}_1(x)\right]\frac{\sin\frac{z}{a}x}{\mathrm{D}(x)}\,dx, \quad (33)$$

where $$\mathrm{D}(x)=\{x^2+2(1-\sigma)\}\mathrm{I}_1^2(x)-x^2\mathrm{I}_0^2(x). \quad . \quad . \quad . \quad . \quad (34)$$

5. *Numerical Example.*—The stresses have been computed for the case in which $\sigma=1/4$, an outline of the method used being given below for the stress $\widehat{\theta\theta}$ at $r=a$.

When $r=a$, $\sigma=1/4$, equation (30) gives

$$\left.\begin{aligned}\widehat{\theta\theta}&=-\frac{1}{2}-\frac{1}{2\pi}\int_0^\infty\psi(x)\,.\sin\frac{z}{a}x\,dx,\\ \text{where}\quad \psi(x)&=\frac{\dfrac{x\mathrm{I}_0(x)}{\mathrm{I}_1(x)}+3}{x\left[\left\{\dfrac{x\mathrm{I}_0(x)}{\mathrm{I}_1(x)}\right\}^2-x^2-1\cdot5\right]}.\end{aligned}\right\} \quad . \quad . \quad . \quad . \quad (35)$$

Above $x=12$, $\psi(x)$ can be represented with sufficient accuracy for the purpose in view by using the asymptotic expansions for the Bessel functions as far as the term in x^{-4}, and we find

$$-(\widehat{\theta\theta})=\frac{1}{2}+\frac{1}{2\pi}\int_0^{12}\psi(x)\sin\frac{z}{a}x\,dx+\frac{1}{2\pi}\int_{12}^{\infty}\left\{\frac{1}{x}+\frac{4}{x^2}+\frac{5}{4x^3}-\frac{5}{x^4}\right\}\sin\frac{z}{a}x\,dx. \quad . \; . \; . \quad (36)$$

By successive integration by parts we can evaluate the second integral as

$$\left\{1-\frac{5}{8}\left(\frac{z}{a}\right)^2\right\}\left\{\frac{\pi}{2}-\mathrm{Si}\left(\frac{12z}{a}\right)\right\}-\frac{z}{a}\left\{4+\frac{5}{6}\left(\frac{z}{a}\right)^2\right\}\mathrm{Ci}\left(\frac{12z}{a}\right)$$
$$+\left\{\frac{3491}{10368}+\frac{5}{72}\left(\frac{z}{a}\right)^2\right\}\sin\left(\frac{12z}{a}\right)+\frac{5}{108}\frac{z}{a}\cos\left(\frac{12z}{a}\right),$$

where $$\mathrm{Si}(x)=\int_0^x\frac{\sin x}{x}dx,\quad \mathrm{Ci}(x)=-\int_x^{\infty}\frac{\cos x}{x}dx.$$

$Si(x), Ci(x)$ have been extensively tabulated *, and the second integral can therefore be computed for a given value of z/a.

The first integral in (36) can be evaluated by a method due to Filon †: in this method, Simpson's rule is replaced by the formula

$$\int_A^B\phi(x)\sin\frac{z}{a}x\,dx=h\left[\alpha\left\{\phi(\mathrm{A})\cos\left(\frac{z}{a}\mathrm{A}\right)-\phi(\mathrm{B})\cos\left(\frac{z}{a}\mathrm{B}\right)\right\}+\beta\mathrm{S}_{2n}+\gamma\mathrm{S}_{2n-1}\right], \quad . \; . \; . \quad (37)$$

where the range of integration is divided into equal intervals of length h, S_{2n} is the sum of all the even ordinates of the curve $y=\phi(x)\sin\left(\frac{z}{a}x\right)$ between A and B inclusive less half the first and last ordinates, S_{2n-1} is the sum of all the odd ordinates and α, β, γ are given in terms of $\theta=hz/a$ by ‡

$$\left.\begin{aligned}\alpha=\frac{1}{\theta}+\frac{\sin\theta\cos\theta}{\theta^2}-\frac{2\sin^2\theta}{\theta^3},\quad \beta=2\left[\frac{1+\cos^2\theta}{\theta^2}-\frac{2\sin\theta\cos\theta}{\theta^3}\right],\\ \gamma=4\left[\frac{\sin\theta}{\theta^3}-\frac{\cos\theta}{\theta^2}\right].\end{aligned}\right\} \quad . \quad (38)$$

This formula holds even when z/a is large, provided that the function $\phi(x)$ can be fitted with reasonable accuracy over the range $2h$ by parabolic arcs.

To evaluate the first integral in (36) the following integral,

$$\mathrm{I}=\int_0^{12}\left\{\psi(x)-\frac{2}{x}\right\}\sin\frac{z}{a}x\,dx, \quad . \; . \; . \; . \; . \; . \; . \quad (39)$$

was chosen for computation by this method, the interval selected being $h=\frac{1}{2}$. The function $\{\psi(x)-2/x\}$ vanishes when $x=0$, and can be better fitted by parabolic arcs than $\psi(x)$, which is infinite at the origin. The first integral in (36) is then given by $I+2\,Si\,(12z/a)$, and $\widehat{\theta\theta}$ at $r=a$ can thus be completely found for given values of z/a.

---

* See, for instance, B.A. Mathematical Tables, vol. i., Camb. Univ. Press, pp. 34–39.

† L. N. G. Filon, "On a Quadrature Formula for Trigonometric Integrals," Proc. Roy. Soc. Edin, vol. xlix. pp. 38–47 (1928–29).

‡ No confusion need arise with the meaning of a used in (19).

As a check that the substitution of the asymptotic expansion for $\psi(x)$ in the second integral of (36) did not lead to unacceptable errors,

Fig. 1.

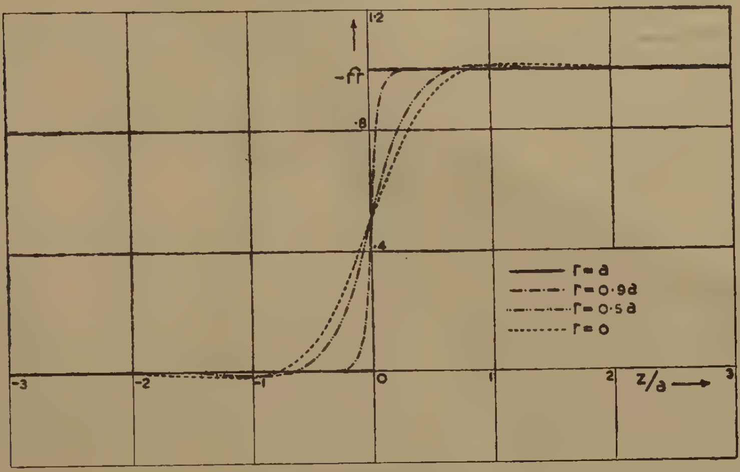

The radial stress.

Fig. 2.

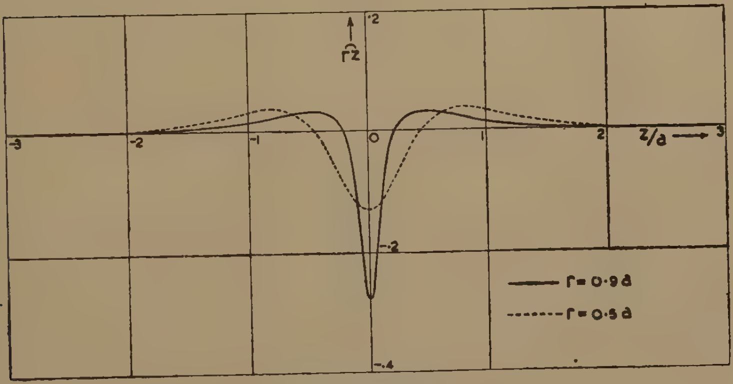

The shear stress.

the range of integration was also divided into 0 to 10, 10 to infinity, and $\widehat{\theta\theta}$ was similarly computed on this basis. Little extra work was involved, and excellent agreement was obtained in the two values of $\widehat{\theta\theta}$ so calculated.

The stresses were also calculated for $r=0{\cdot}9a$, $r=0{\cdot}5a$ and $r=0$. The method used was essentially the same as that outlined above, the only differences being :—

(i.) For $r=0{\cdot}9a$ and $r=0{\cdot}5a$, the asymptotic expansions for the integrands less the trigonometric term now involve $e^{-(1-r/a)x}$ as well as powers of $1/x$. The integrals over the range 12 to ∞ now depend on

$$\int_x^\infty e^{-kx}\frac{\sin x}{x}\,dx,\quad \int_x^\infty e^{-kx}\frac{\cos x}{x}\,dx\quad (k=0\cdot1,\ 0\cdot5).$$

Fig. 3.

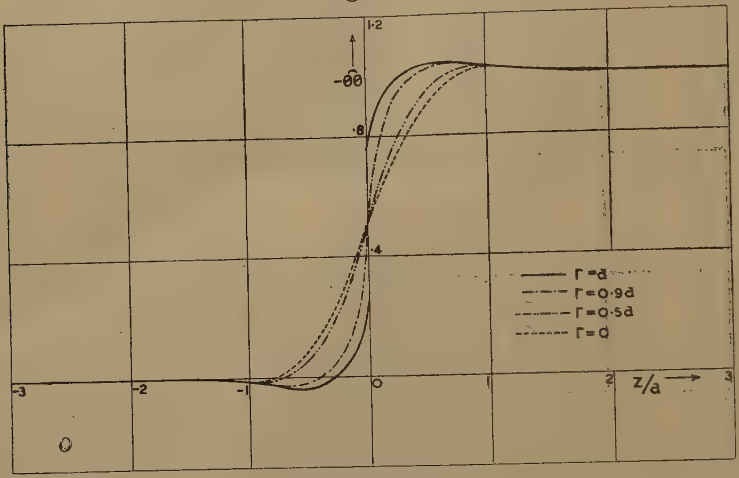

The hoop stress.

Fig. 4.

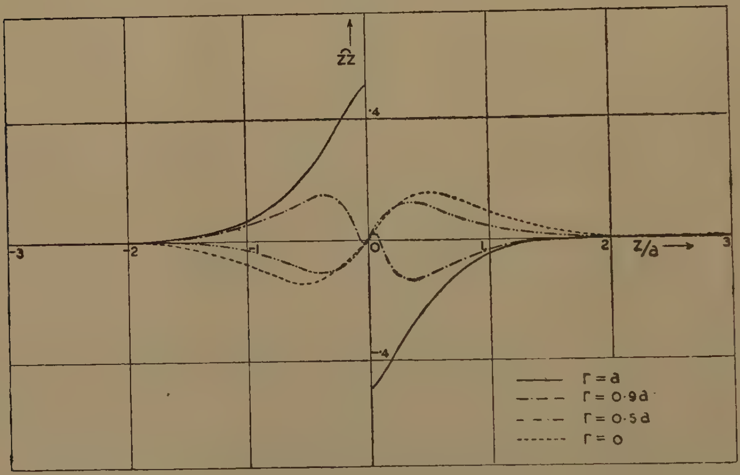

The longitudinal stress.

These integrals are easily related to

$$\int_0^x e^{-kx}\frac{\sin x}{x}\,dx,\quad \int_0^x e^{-kx}\frac{(1-\cos x)}{x}\,dx,$$

and the latter integrals had to be computed for selected values of k and x by numerical methods.

To face p. 249.]

TABLE I.

z/a.	$-\widehat{rr}$.				$\widehat{rz}$.				$-\widehat{\theta\theta}$.				$\widehat{zz}$.				$-\mathrm{EU}/r$.			
	$r=a$.	$r=0{\cdot}9a$.	$r=0{\cdot}5a$.	$r=0$.	$r=a$.	$r=0{\cdot}9a$.	$r=0{\cdot}5a$.	$r=0$.	$r=a$.	$r=0{\cdot}9a$.	$r=0{\cdot}5a$.	$r=0$.	$r=a$.	$r=0{\cdot}9a$.	$r=0{\cdot}5a$.	$r=0$.	$r=a$.	$r=0{\cdot}9a$.	$r=0{\cdot}5a$.	$r=0$.
0·0	1·000	0·500	0·500	0·500	0·000	−0·278	−0·131	0·000	0·750	0·500	0·500	0·500	−0·500	0·000	0·000	0·000	0·375	0·375	0·375	0·375
0·05	1·000	0·783	0·573	0·551	0·000	0·210	−0·128	0·000	0·849	0·647	0·562	0·551	−0·479	0·015	0·028	0·024	0·479	0·455	0·426	0·420
0·1	1·000	0·920	0·643	0·602	0·000	−0·108	−0·118	0·000	0·904	0·758	0·622	0·602	−0·449	−0·026	0·053	0·048	0·542	0·522	0·475	0·464
0·2	1·000	0·987	0·765	0·698	0·000	−0·007	−0·085	0·000	0·970	0·890	0·732	0·698	−0·384	−0·110	0·092	0·090	0·624	0·615	0·564	0·546
0·3	1·000	0·997	0·855	0·782	0·000	0·023	−0·045	0·000	1·006	0·958	0·823	0·782	−0·322	−0·139	0·110	0·121	0·676	0·674	0·637	0·617
0·4	1·000	0·999	0·916	0·852	0·000	0·032	−0·011	0·000	1·026	0·995	0·892	0·852	−0·264	−0·138	0·112	0·140	0·709	0·711	0·691	0·674
0·5	1·000	0·999	0·956	0·907	0·000	0·033	0·014	0·000	1·034	1·015	0·941	0·907	−0·214	0·125	0·103	0·147	0·731	0·734	0·728	0·717
0·6	1·000	0·999	0·980	0·948	0·000	0·031	0·030	0·000	1·037	1·025	0·975	0·948	−0·170	−0·108	0·089	0·143	0·744	0·749	0·752	0·747
0·8	1·000	0·999	1·003	0·995	0·000	0·023	0·039	0·000	1·033	1·029	1·009	0·995	−0·103	−0·073	0·060	0·118	0·757	0·761	0·773	0·776
1·0	1·000	0·999	1·009	1·014	0·000	0·016	0·033	0·000	1·024	1·024	1·019	1·014	−0·059	−0·045	0·036	0·084	0·760	0·763	0·776	0·781
1·5	1·000	1·000	1·006	1·012	0·000	0·0 4	0·012	0·000	1·008	1·009	1·011	1·012	−0·010	−0·010	0·007	0·024	0·755	0·756	0·762	0·765
2·0	1·000	1·000	1·002	1·004	0·000	0·001	0·003	0·000	1·001	1·002	1·003	1·004	0·000	−0·001	0·001	0·004	0·751	0·752	0·753	0·754
3·0	1·000	1·000	1·000	1·000	0·000	0·000	0·000	0·000	1·000	1·000	1·000	1·000	0·000	0·000	0·000	0·000	0·750	0·750	0·750	0·750
∞	1·000	1·000	1·000	1·000	0·000	0·000	0·000	0·000	1·000	1·000	1·000	1·000	0·000	0·000	0·000	0·000	0·750	0·750	0·750	0·750

N.B. $(-\widehat{rr})_{r,\,-z}=1-(-\widehat{rr})_{r,\,z}$, $(-\widehat{\theta\theta})_{r,\,-z}=1-(-\widehat{\theta\theta})_{r,\,z}$, $(-\mathrm{EU}/r)_{r,\,-z}=0{\cdot}750-(-\mathrm{EU}/r)_{r,\,z}$.
$(\widehat{rz})_{r,\,-z}=(\widehat{rz})_{r,\,z}$, $(\widehat{zz})_{r,\,-z}=-(\widehat{zz})_{r,\,z}$.

(ii.) For $r=0$ the integrand decreased so quickly with x that it was sufficient to evaluate the integral from 0 to 14 by Filon's method and to neglect entirely the integral from 14 to ∞.

The results for $\widehat{rr}$, $\widehat{rz}$, $\widehat{\theta\theta}$, $\widehat{zz}$ are given in Table I. for the values of r/a, z/a shown there. The radial displacement U was similarly computed from equation (32). A check on the somewhat extensive arithmetical work was provided by comparing the values of U computed from (32) with the values given by

$$\text{Circumferential strain}=\frac{\mathrm{U}}{r}=\frac{1}{\mathrm{E}}\{\widehat{\theta\theta}-\sigma(\widehat{rr}+\widehat{zz})\}.$$

At $z/a=0$, $r=a$, some of the quantities are discontinuous. The values here can be found from the result :—

If $f(x)$ be a bounded function, monotonic for sufficiently large x, and having the limit F as $x\rightarrow\infty$, then

$$\underset{z/a\rightarrow\pm0}{\mathrm{Lt.}}\left[\int_0^\infty f(x)\sin\frac{z}{a}x\frac{dx}{x}\right]=\pm\frac{\pi}{2}\mathrm{F}.$$

Fig. 5.

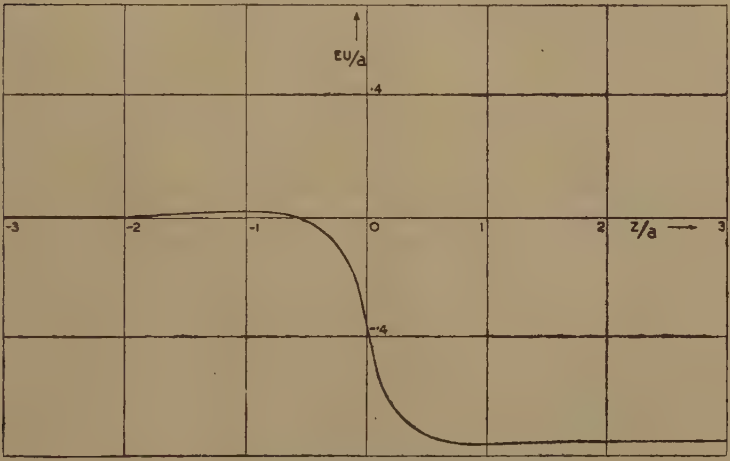

The radial displacement at $r=a$.

F can be found from the asymptotic expansions of the integrands in (28), . . ., (34), and the values so found for the stresses and displacements are quoted in Table I.

As $z/a\rightarrow\infty$, the values of the stresses are immediately given by using the results

$$\underset{z/a\rightarrow\infty}{\mathrm{Lt.}}\left[\int_0^\infty f(x)\sin\frac{z}{a}x\frac{dx}{x}\right]=\frac{\pi}{2}f(0),$$

$$\underset{z/a\rightarrow\infty}{\mathrm{Lt.}}\left[\int_0^\infty f(x)\cos\frac{z}{a}x\,dx\right]=0.$$

The stresses and the displacement of the external surface are shown graphically in figs. 1–5.

It will be noted that the maximum value of each stress exceeds that of the corresponding stress for the case of uniform loading over the whole curved surface (*i. e.*, the value as $z \to \infty$). The effect of the discontinuity dies away rapidly, so that at a distance of about three radii from the central cross-section the results reduce to the case of uniform loading.

In conclusion we wish to thank Miss G. A. Hudson for assistance with the arithmetical work.

XXXIV. *Entropy and Irreversible Processes.*

By Dr. W. Ehrenberg *.

[Received October 16, 1944.]

I HAVE recently † proposed an approach to the Second Law of Thermodynamics by which Clausius' principle is expressed as a system of differential equations. The solution of these equations leads to an expression for the entropy of a composite system ; the contribution of each body is given by dQ/T in such a way that no general condition of reversibility is imposed on the path along which dQ is taken.

Professor Wilson, in his paper "The Principles of Carnot and Clausius"‡, has criticized this approach to the second law. As a result of Professor Wilson's paper and an interesting correspondence I have had with him, I realize that the discussion of the system of differential equations (5) set out in the preceding paper was incomplete. It is the main object of this note to supplement the discussion of these differential equations. I shall give here the complete solution and show that it leads to substantially the same result as the particular solution used in E.I.P. This discussion is also intended to refute Professor Wilson's suggestion of a circularity in my approach.

But before entering this discussion I wish to review two other points raised by Prof. Wilson. There are a number of applications of the second law for which neither the existence of the entropy function of composite systems of bodies nor its maximum property is of interest. But if, *e. g.*, it is stated that a closed system of bodies is in equilibrium if its entropy is a maximum, then two ideas are implied :—(1) The entropy is defined for an assembly of bodies ; (2) The entropy of this assembly is defined for states other than the equilibrium state, viz., states such that the single bodies are internally in equilibrium, the whole system, however, is not. If entropy is introduced as the entropy of single bodies "in equilibrium," its definition must be extended to an assembly of bodies. I cannot see that this extension is obvious, though, of course, it can be postulated. It must suffice here to quote a passage from Fowler's 'Statistical Mechanics': "The addition of entropies can usually only be realized by some form of thermal contact, and is then true in general only when the temperatures are equal. . . . For example, it is argued that $S_{12}=S_1+S_2$ follows directly from the second law. It is hard to see how this can be derived except from the equation $dQ_{12}=dQ_1+dQ_2$, which is true neglecting surface interactions. This then leads to $dS=dS_1+dS_2$ . . . only if the temperatures are equal."—(Second Edition, 1936, p. 202.) In E.I.P. this difficulty was avoided by introducing entropy from the start as entropy of a system of bodies. For a single body, there can be no doubt that the version preferred by Prof. Wilson, viz. $TdS=dU+pdV$, and his discussion of the principles related to it, is most satisfactory, and I very much agree with his elucidation of the equation. Prof. Wilson rejects the restriction of reversibility, but he wishes to maintain a condition of equilibrium. I have suggested that the equilibrium condition necessary is, in fact, included in the notion of a thermodynamical body; for, when this equation is written down, the existence of T and p is implied, and more is not required for the validity of the equation. Consequently, when $dV=0$, $dS=dU/T$ quite generally. Professor Wilson states: "Even for this to be valid there must be no more than an infinitesimal variation from equilibrium." Professor Wilson does not state whether he refers to equilibrium between the bodies participating or to the internal equilibrium of the body under test. It would seem unnecessary to state the second alternative, and the first one would impose an unnecessary restriction.

---

* Communicated by the Author.

† Phil. Mag. xxxiv. p. 396 (1943) (referred to later in this paper as E.I.P.).

‡ Phil. Mag. xxxiv. p. 828 (1943). See also W. Wilson, "Thermodynamical Notes," Phil. Mag. xxxiii. p. 831 (1942).

It is probably a matter of taste, in the last resort, what should be considered as a fundamental principle, and I cannot make a case against stating the second law as $TdS=dU+pdV$, except that it is a statement incomplete with regard to an assembly of bodies and the maximum condition. I cannot, however, agree to Professor Wilson's claim that Clausius' version "Heat cannot, of itself, pass from a colder body to a hotter body" is particularly unsuitable as a basis, though I agree that it is not the only way of stating the idea. It requires a somewhat lengthy interpretation, but it is not ambiguous. Prof. Wilson actually does not indicate any particular ambiguity, but suggests alternative versions, some of which predicate less than Clausius' principle and consequently lead to a restricted interpretation of the second law, in which, *e. g.*, no mention is made of the direction of the passage of heat or the existence of irreversible processes. I fully appreciate the interest and the validity of Prof. Wilson's analysis: but I do not see that it invalidates any attempt of finding the widest possible scope of the second law.

Professor Wilson suggests that "we can only deduce

$$\frac{\partial F}{\partial \sigma_1}=\frac{\partial F}{\partial \sigma_2}=\ldots \qquad (6)$$

if the form of F is given in advance. The function F might conceivably be $F=\sigma_1.\sigma_2.\sigma_3\ldots$, for example, in which case (6) would be untrue. We do not know in advance that it is a function of $\Sigma\sigma_\nu$, since this is one of the consequences Dr. Ehrenberg sets out to deduce. There appears to me a circularity in the deduction. . . ."

Let us examine in detail the consequencies of putting $F=\sigma_1.\sigma_2\ldots$: The leading equations are

$$N_\nu dQ_\nu=d\sigma_\nu\ldots, \qquad (3)$$

$$\frac{\partial F}{\partial \sigma_1}N_1(t_1, V_1)\underset{\neq}{=}\frac{\partial F}{\partial \sigma_2}N_2(t_2, V_2)\begin{cases}t_1=t_2\\ t_1\neq t_2\end{cases} \qquad (5), (5')$$

As explained in detail in E.I.P., equ. (3) expresses that dQ_ν, the heat added to the body ν of the composite system, has an integrating factor N_ν; functions σ_ν are thus defined which are constant for $dQ_\nu=0$. The function F, the existence of which follows from Clausius' principle, depends on the σ_ν of all the bodies of the system and has the property of remaining constant for reversible processes and changing its value for irreversible processes. These properties are expressed in equations (5), (5′). The function F and the integrating factors N_ν must satisfy these equations, which are used to determine the form of the functions F and N_ν.

The inequality here called (5′) is not explicitly written down in E.I.P., but was implied and actually used in that paper (equ. 12). For the sake of simplicity, let us restrict ourselves to the two-body problem. With

$$F=\sigma_1.\sigma_2 \qquad (a)$$

equation (5) becomes

$$\sigma_2.N_1(t, V_1)=\sigma_1 N_2(t, V_2), \qquad (b)$$

where V_1 and V_2 depend on t, σ_1 and t, σ_2. From (*b*)

$$N_1/\sigma_1=N_2/\sigma_2=N(t),$$

as N_1/σ_1 does not depend on σ_2 and N_2/σ_2 does not depend on σ_1. Therefore

$$\left.\begin{aligned}N_1=\sigma_1 N(t)=\sigma_1/T,\\ N_2=\sigma_2 N(t)=\sigma_2/T.\end{aligned}\right\} \qquad (c)$$

This means: If the solution $F=\sigma_1.\sigma_2$ is adopted, it is impossible at the same time to adopt $N(t)$ as an integrating factor. The physical significance of this integrating factor σ_1/T is easily seen. Let σ_1^x be the numbering system for adiabatics traditionally adopted, so that

$$d\sigma_1^x=dQ_1/T, \qquad (d)$$

and let us introduce an alternative numbering system

$$\sigma_1=\exp.\{\sigma_1^x\}. \qquad (e)$$

Then $$d\sigma_1 = \exp.\{\sigma_1{}^x\}d\sigma_1{}^x = \sigma_1 d\sigma_1{}^x = \sigma_1 \frac{dQ_1}{T}. \quad \ldots \ldots \quad (f)$$

Thus σ_1/T is indeed an integrating factor which produces a numbering system for the adiabatics of the single bodies related to the traditional ones by (*e*), *i. e.* in the same manner as Boltzmann's probabilities are related to the entropies.

This is certainly a permissible way of measuring adiabatics. Similarly, the entropy of the composite system is given by

$$F = \sigma_1 . \sigma_2 = \exp. \{\sigma_1{}^x + \sigma_2{}^x\} = \exp.\left\{\Sigma \int \frac{dQ_\nu}{T_\nu}\right\},$$

which is a special case of

$$F = \phi\left(\int \frac{dQ_1}{T_1} + \int \frac{dQ_2}{T_2} + \ldots\right). \quad \ldots \ldots \ldots \quad (8)$$

It is thus clear that the solution

$$\frac{\partial F}{\partial \sigma_1} = \frac{\partial F}{\partial \sigma_2} = \ldots ; \quad F = F(\sigma_1 + \sigma_2 + \ldots)$$

is not a general solution of the equations (5). It holds only if $N(t)$ are chosen as the integrating factors, a permissible but not unique choice; but it is also clear that the solution $F = \sigma_1 . \sigma_2 \ldots$ does in the end lead to the essential relation (8).

The set of equations

$$\frac{\partial F}{\partial \sigma_1} = \frac{\partial F}{\partial \sigma_2} = \ldots ; \quad N_1(t_1, V_1) = N_2(t_2, V_2) = \ldots \quad \ldots \quad (6)$$

given in E.I.P. would be the general solution of (3), (5) (except for an uninteresting constant factor) if the variables on which $\partial F/\partial \sigma$ and N depend would be independent; they are not, in fact, independent. It will be shown now that equ. (8) is obtained as the general solution of (3) and (5), taking into account the interdependence of the variables.

Let us restrict ourselves again to two bodies and remember that $V_1 = V_1(t_1, \sigma_1)$ and $V_2 = V_2(t_2, \sigma_2)$. Then (5) and (5′) become

$$\frac{\partial F}{\partial \sigma_1} N_1{}^x(t_1, \sigma_1) \overset{=}{\underset{\neq}{}} \frac{\partial F}{\partial \sigma_2} N_2{}^x(t_2, \sigma_2) \begin{cases} t_1 = t_2 \\ t_1 \neq t_2 \end{cases} \quad \ldots \quad (g)\ (g')$$

or $$N_1{}^x = \left(\frac{\partial F}{\partial \sigma_2} \Big/ \frac{\partial F}{\partial \sigma_1}\right) N_2{}^x.$$

As $N_1{}^x$ is independent of σ_2, the right side must factorize

$$\frac{\partial F}{\partial \sigma_2} \Big/ \frac{\partial F}{\partial \sigma_1} = \psi_1(\sigma_1)/\psi_2(\sigma_2), \quad \ldots \ldots \quad (h')$$

$$N_2{}^x = \psi_2(\sigma_2) N_2{}'(t_2) \quad \text{and also} \quad N_1{}^x = \psi_1(\sigma_1) N_1{}'(t_1), \quad \ldots \quad (h'')$$

so that with (*g*)

$$N_1{}'(t) = N_2{}'(t) = N(t) = 1/T.$$

The result so far obtained can be enunciated: The integrating factor for dQ is given by

$$N_\nu = \psi_\nu(\sigma_\nu)/T, \quad . \quad . \quad . \quad . \quad . \quad . \quad . \quad . \quad . \quad . \quad (i)$$

so that

$$d\sigma_\nu = dQ_\nu . \psi_\nu(\sigma_\nu)/T. \quad . \quad . \quad . \quad . \quad . \quad . \quad . \quad . \quad . \quad . \quad (k)$$

The ψ are arbitrary functions, but they must not vanish on account of (g').

Equ. (h') is solved by the introduction of the new variables

$$x = \int \frac{d\sigma_1}{\psi_1} + \int \frac{d\sigma_2}{\psi_2},$$

$$y = \int \frac{d\sigma_1}{\psi_1} - \int \frac{d\sigma_2}{\psi_2},$$

so that

$$\frac{1}{\psi_1} \frac{\partial F}{\partial \sigma_2} = \frac{1}{\psi_1}\left(\frac{\partial F}{\partial x}\frac{1}{\psi_2} - \frac{\partial F}{\partial y}\frac{1}{\psi_2}\right),$$

$$\frac{1}{\psi_2} \frac{\partial F}{\partial \sigma_1} = \frac{1}{\psi_2}\left(\frac{\partial F}{\partial x}\frac{1}{\psi_1} + \frac{\partial F}{\partial y}\frac{1}{\psi_1}\right).$$

The difference between these two expressions vanishes on account of (h'), so that $\partial F/\partial y = 0$. F depends therefore on x only

$$F = F(x) = F\left(\int \frac{d\sigma_1}{\psi_1} + \int \frac{d\sigma_2}{\psi_2}\right). \quad . \quad . \quad . \quad . \quad . \quad . \quad . \quad (l)$$

$F(x)$ is an arbitrary function of its variable. The solutions $F = \sigma_1 + \sigma_2$ and $F = \sigma_1 . \sigma_2 = \exp.\{\log \sigma_1 + \log \sigma_2\}$ are included in (l).

Finally, with (k)

$$x = \int \frac{dQ_1}{T_1} + \int \frac{dQ_2}{T_2}, \quad . \quad . \quad . \quad . \quad . \quad . \quad . \quad . \quad . \quad . \quad (m)$$

$$F = F\left\{\int \frac{dQ_1}{T_1} + \int \frac{dQ_2}{T_2}\right\}. \quad . \quad . \quad . \quad . \quad . \quad . \quad . \quad . \quad . \quad (8)$$

The relation (8) holds generally. The relation $F = F(\Sigma\sigma_\nu)$ does, however, hold only if, as usual, all the ψ are chosen unity.

It is readily checked from equ. (k)

$$d\sigma = \frac{\psi(\sigma)}{T} dQ = \frac{\psi(\sigma)}{T}(X\,dt + Y\,dV) \quad . \quad . \quad . \quad . \quad . \quad . \quad . \quad (k)$$

that ψ is an arbitrary function and T an essentially unique function. Equ. (k) defines a σ by dQ and the integrating factor ψ/T, so that the form of the function σ will depend on ψ and T. Let now σ, ψ, T be particular functions for which (k) holds. (It is known from (i), (l), (k) that at least one such set exists.)

As ψ/T is an integrating factor

$$\frac{\partial}{\partial V}\left(X\frac{\psi}{T}\right) = \frac{\partial}{\partial t}\left(Y\frac{\psi}{T}\right). \quad . \quad . \quad . \quad . \quad . \quad . \quad . \quad . \quad . \quad (n)$$

from which after expanding and noting that $\partial T/\partial V = 0$

$$TY\frac{\partial'/T}{\partial t} + \frac{\partial Y}{\partial t} - \frac{\partial X}{\partial V} = \frac{1}{\psi}\frac{d\psi}{\sigma}\left(X\frac{\partial \sigma}{\partial V} - Y\frac{\partial \sigma}{\partial t}\right) = 0, \quad . \quad . \quad . \quad (p)$$

since from (k)

$$\frac{\partial\sigma}{\partial t}=\frac{\psi}{\mathrm{T}}\mathrm{X}; \quad \frac{\partial\sigma}{\partial\mathrm{V}}=\frac{\psi}{\mathrm{T}}\mathrm{Y}.$$

It is easily seen that the vanishing of the left side of (p) is the condition for $1/\mathrm{T}$ alone to be an integrating factor. It follows that T is essentially an unique function of t; for when the condition used in (n) is applied to $d\mathrm{Q}/f(t)$, it is found that $f(t)$ can only be an integrating factor as well as $1/\mathrm{T}$ if $f(t)=\text{const. } 1/\mathrm{T}$.

Finally, it will be shown that an equation

$$d\sigma''=\psi(\sigma'')/\mathrm{T}\,.\,d\mathrm{Q} \qquad (q)$$

can be satisfied for an arbitrary function $\psi(\sigma'')$. The integrating factor $1/\mathrm{T}$ defines a σ' by

$$d\sigma'=\frac{d\mathrm{Q}}{\mathrm{T}}. \qquad (r)$$

Dividing (q) by (r),

$$\frac{d\sigma''}{d\sigma'}=\psi(\sigma''),$$

so that for any ψ a σ'' can be found as a function of σ' by integration.

I wish to thank Mr. L. S. Goddard for discussions of the mathematical aspect of the problem.

XXXV. *The Application of the Characteristic Equation of a Matrix to the Evaluation of the Range of Frequencies for which Currents are passed through networks with four or more terminals without attenuation.*

By H. V. Lowry *.

[Received February 20, 1944.]

Theory of the Characteristic Equation.

If λ is a scalar and x a column matrix, which satisfy the equation $ux=\lambda x$, where u is a square matrix, then λ satisfies the equation $|u-\lambda\mathrm{I}|=0$, called the characteristic equation of u. If the roots of this equation are $\lambda_1, \lambda_2, \ldots \lambda_r$, then, when $\lambda=\lambda_1$, $x=k_1p_1$, where k_1 is a certain column matrix and p_1 is an arbitrary constant. Similarly, $x=k_2p_2$, $k_3p_3, \ldots$, k_rp_r when $\lambda=\lambda_2$, $\lambda_3 \ldots \lambda_r$. Let us suppose that $k_1, k_2, \ldots k_r$ are the columns of a square matrix k. Then any column matrix v can be put in the form

$$v=k_1p_1+k_2p_2+\ldots+k_rp_r=kp, \qquad (1)$$

---

* Communicated by the Author.

where p is the column matrix $\{p_1, p_2, \ldots p_r\}$. To find p we have merely to pre-multiply (1) by k^{-1}, which gives $p=k^{-1}v$. Now, since $uk_1=\lambda_1k_1$, $uk_2=\lambda_2k_2 \ldots$, $uk_r=\lambda_rk_r$, the effect of multiplying k by u is to multiply the first column by λ_1, the second by λ_2 and so on; this means that $uk=k\Lambda$, where Λ is the diagonal matrix, whose elements are $\lambda_1, \lambda_2, \ldots \lambda_r$. Hence

$$u^nv=u^nkp=k\Lambda^nk^{-1}v. \qquad (2)$$

Since Λ is a diagonal matrix Λ^n is the diagonal matrix with elements $\lambda_1^n, \lambda_2^n, \ldots \lambda_r^n$.

It is worth noting the resemblance of this equation to the matrix solution of r linear simultaneous differential equations of the first order. These can be written in the form $a\mathrm{D}x=bx$, where a and b are square matrices and D is the diagonal matrix in which each element is $\mathrm{D}=\frac{d}{dt}$. Pre-multiplying by a^{-1} this can be written $\mathrm{D}x=ux$. This equation has a solution $x=e^{mt}\mathrm{X}$, where X is a column matrix, if $(u-m\mathrm{I})\mathrm{X}=0$. Therefore the general solution is

$$x=k_1e^{m_1t}p_1+k_2e^{m_2t}p_2+\ldots+k\cdot e^{m_rt}p_r, \qquad (3)$$

where the k's and p's have the same meaning as in (1).

This solution can be written

$$x=k\mu p, \qquad (3\text{ A})$$

where μ is the diagonal matrix with elements e^{m_1t}, e^{m_2t}, etc.

Suppose that at $t=t_1$, $x=x_0$ (a column of elements $x_{10}, \ldots x_{r0}$, say). Then

$$x_0=k\mu_1p,$$

where μ_1 is the diagonal matrix with elements $e^{m_1t_1}$, $e^{m_2t_1}$, etc.

Hence $\qquad p=\mu_1^{-1}k^{-1}x_0$

and $\qquad x=k\mu\mu_1^{-1}k^{-1}x_0=k\mu'.k^{-1}x_0, \qquad (4)$

where μ' is the diagonal matrix with elements $e^{m_1(t-t_1)}$, $e^{m_2(t-t_2)}$, etc.

In the special case where $t_1=0$, $u'=\mu$, and

$$x=k\mu k^{-1}x_0, \qquad (4\text{ A})$$

which is of the same form as (2). The explanation of the resemblance is as follows.

Let the increase from x_0 to x take place in n successive increments, each taking a time $\frac{t}{n}$, and as t increases $\delta t=\frac{t}{n}$, let x increase to λx, so that $\delta x=(\lambda-1)x$. The equation $ux=\mathrm{D}x$ can then be written in the approximate form

$$ux \doteq (\lambda-1)\frac{n}{t}x=mx, \text{ say}. \qquad (5)$$

Hence the possible values of λ are given by

$$(\lambda-1)\frac{n}{t}=m \quad \text{or} \quad \lambda=1+\frac{mt}{n},$$

where $m=m_1, m_2$, etc.

But (5) can be written $Ux=\lambda x$, where $U=\left(1+\frac{t}{n}\right)u$, and so each new value of x starting from x_0 is got by multiplying by U. Hence the approximate value of x at time t is got by multiplying by U^n and therefore the exact value is the limit of $U^n x_0$ as $n\rightarrow\infty$. But by (2)

$$U^n x_0=k\Lambda^n k^{-1}x_0,$$

where Λ^n has elements $\lambda_1{}^n=\left(1+\frac{m_1t}{n}\right)^n$, etc. As $n\rightarrow\infty$ these elements tend to e^{m_1t}, e^{m_2t}, ..., e^{m_rt}, and so $\Lambda^n\rightarrow\mu$. Therefore in the limit

$$x=\lim_{n\rightarrow\infty} U^n x_0=k\mu k^{-1}x_0,$$

which is equation (4 A).

Networks with Four Terminals.

Let the relationship between the input and the output values of a section of a transmission system be

$$\begin{bmatrix} E_0 \\ I_0 \end{bmatrix}=\begin{bmatrix} a & b \\ c & d \end{bmatrix}\begin{bmatrix} E_1 \\ I_1 \end{bmatrix}.$$

This equation will be written $v_0=uv_1$, where

$$v_0=\begin{bmatrix} E_0 \\ I_0 \end{bmatrix},\quad v_1=\begin{bmatrix} E_1 \\ I_1 \end{bmatrix}\quad\text{and}\quad u=\begin{bmatrix} a & b \\ c & d \end{bmatrix}.$$

It is well known that $|u|=ad-bc=1$. A general proof of this result for networks with any number of terminals will be given later.

If n equal sections are put in cascade

$$v_0=uv_1=u^2v_2=u^3v_3=\ldots=u^nv_n.$$

But by

$$u^nv_n=k\Lambda^nk^{-1}v_n, \quad \ldots \quad (6)$$

where

$$\Lambda^n=\begin{bmatrix} \lambda_1^n & 0 \\ 0 & \lambda_2^n \end{bmatrix}\quad\text{and}\quad \lambda_1,\ \lambda_2$$

are the roots of the equation $\begin{vmatrix} a-\lambda & b \\ c & d-\lambda \end{vmatrix}=0.$

Expanded, this equation becomes, after putting $ad-bc=1$,

$$\lambda^2-(a+d)\lambda+1=0 \quad \ldots \quad (7)$$

It follows that $\lambda_1\lambda_2=1$, and hence either the modulus of one of λ_1, λ_2 is greater than unity and the modulus of the other is less than unity or the modulus of each is unity. Now, if in (6) the modulus of λ_1, say, is greater than unity, then $|\lambda_1|^n\rightarrow\infty$ as $n\rightarrow\infty$, and so if v_n is given $v_0\rightarrow\infty$ as $n\rightarrow\infty$, or, if v_0 is given, $v_n\rightarrow 0$ as $n\rightarrow\infty$. Thus there is attenuation in all cases except those in which $|\lambda_1|=|\lambda_2|=1$. Suppose that then $\lambda_1=e^{j\theta}$ and $\lambda_2=e^{-j\theta}$, then

$$a+d=\lambda_1+\lambda_2=2\cos\theta,$$

where θ is real. Thus the condition for λ_1 and λ_2 to have modulus unity is that $a+d$ shall be a real number between -2 and $+2$. When the values of a and d are substituted in this condition it tells us the range of frequencies for which the system will transmit currents without attenuation.

To calculate u^n we have to find k_1 and k_2. The adjugate of $[u-\lambda I]$ is

$$\begin{bmatrix} d-\lambda & -b \\ -c & a-\lambda \end{bmatrix},$$

and hence $\qquad k_1=\{d-\lambda_1, -c\}, \quad k_2=\{d-\lambda_2, -c\},$

and

$$k=\begin{bmatrix} d-\lambda_1 & d-\lambda_2 \\ -c & -c \end{bmatrix}$$

$$\therefore \qquad k^{-1}=\begin{bmatrix} -c & -(d-\lambda_2) \\ +c & d-\lambda_1 \end{bmatrix} \div c(\lambda_1-\lambda).$$

Substituting these values in

$$v_0=u^n v_1=\begin{bmatrix} d-\lambda_1 & d-\lambda_2 \\ -c & -c \end{bmatrix}\begin{bmatrix} \lambda_1^n & 0 \\ 0 & \lambda_2^n \end{bmatrix}\left\{\begin{bmatrix} -c & -(d-\lambda_2) \\ c & d-\lambda_1 \end{bmatrix} v \div c(\lambda_1-\lambda_2)\right\} v_n$$

$$=\frac{1}{c(\lambda_1-\lambda_2)}\begin{bmatrix} c(\lambda_1^{n+1}-\lambda_2^{n+1})-cd(\lambda_1^n-\lambda_2^n) & -(d-\lambda_1)(d-\lambda_2)(\lambda_1^n-\lambda_2^n) \\ c^2(\lambda_1^n-\lambda_2^n) & cd(\lambda_1^n-\lambda_2^n)-c\lambda_1\lambda_2(\lambda_1^{n+1}-\lambda_2^{n+1}) \end{bmatrix} v_n$$

$$=\frac{1}{\lambda_1-\lambda_2}\begin{bmatrix} \lambda_1^{n+1}-\lambda_2^{n+1}-d(\lambda_1^n-\lambda_2^n) & b(\lambda_1^n-\lambda_2^n) \\ c(\lambda_1^n-\lambda_2^n) & d(\lambda_1^n-\lambda_2^n)-(\lambda_1^{n-1}-\lambda_2^{n-1}) \end{bmatrix} v_n, \quad . \quad (8)$$

in which we have used the simplification

$$-(d-\lambda_1)(d-\lambda_2)=-d^2+d(a+d)-1=ad-1=bc.$$

When λ_1, λ_2 have been found (8) gives v_0 in terms of v_n, or by taking the reciprocal matrix u^{-n} it gives v_n in terms of v_0. In the case where there is no attenuation we may put $\lambda_1=e^{j\theta}$ and $\lambda_2=e^{-j\theta}$, and then (8) becomes

$$v_0=\frac{1}{\sin\theta}\begin{bmatrix} \sin(n+1)\theta-d\sin n\theta & b\sin n\theta \\ c\sin n\theta & d\sin n\theta-\sin(n-1)\theta \end{bmatrix} v_n.$$

Similarly, if λ_1 and λ_2 are real numbers they may conveniently be written e^{θ} and $e^{-\theta}$, when the trigonometrical functions in the above equation become hyperbolic functions, but if λ_1 and λ_2 are complex numbers with modulus not equal to unity there is no great advantage in any such substitutions.

Networks with more than Four Terminals.

Suppose a network has r input terminals and r output ones, and that the input voltages and currents are $E_{10}, E_{20}, \ldots E_{r0}, I_{10}, I_{20}, \ldots I_{r0}$ and the output voltages and currents are $E_{11}, E_{21}, \ldots E_{r1}, I_{11}, I_{21}, \ldots I_{r1}$, then the relationship between the input and output values may still be put in the form $v_0=uv_1$, where now v_0 is a column matrix of the r input voltages and r input currents, and v_1 a column matrix of the r output voltages and r output currents, and u is a square matrix of order $2r$. If we partition the matrices in this equation so that it can be written in the form

$$\begin{bmatrix} E_0 \\ I_0 \end{bmatrix}=\begin{bmatrix} A & B \\ C & D \end{bmatrix}\begin{bmatrix} E_1 \\ I_1 \end{bmatrix},$$

where A, B, C, D are square matrices of order r and $E_0=\{E_{10}, E_{20}, \ldots E_{r0}\}$, then

$$E_0=AE_1+BI_1,$$
$$I_0=CE_1+DI_1.$$

From which, when $E_0=V,\quad E_1=0,\quad I_1=B^{-1}V,$

and when $E_1=V,\quad E_0=0,\quad I_0=(C-DB^{-1}A)V.$

Since a network system produces the same current at whichever end the voltage is applied, these currents must be equal and opposite, I_0 being reckoned positive with the network and I_1 out of the network. Hence

$$B^{-1}=DB^{-1}A-C. \quad . \; . \; . \; . \; . \; . \; . \; . \; . \quad (9)$$

This equation is the matrix equivalent of $ad-bc=1$ for four terminal networks. We will now show that $|u|=1$.

Since

$$\begin{bmatrix} B^{-1} & -D^{-1} \\ 0 & D^{-1} \end{bmatrix}\begin{bmatrix} A & B \\ C & D \end{bmatrix}=\begin{bmatrix} B^{-1}A-D^{-1}C & 0 \\ D^{-1}C & I \end{bmatrix}, \quad . \; . \; . \quad (10)$$

and the determinant of a matrix like $\begin{bmatrix} B^{-1} & -D^{-1} \\ 0 & D^{-1} \end{bmatrix}$ is the determinant of the product of the matrices in the leading diagonal, namely, $|B^{-1}D^{-1}|$. Hence taking the determinants of each matrix in ( ) we get

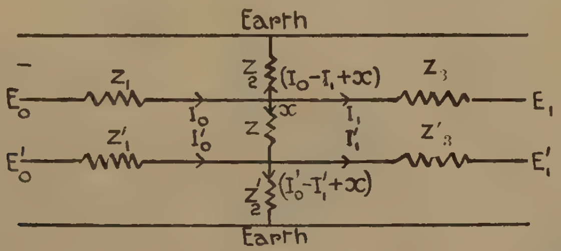

$$|B^{-1}D^{-1}|\;|u| = |B^{-1}A-D^{-1}C|. \quad . \; . \; . \; . \; . \; . \quad (11)$$

But, from (9), $B^{-1}A-D^{-1}C=D^{-1}B^{-1}$,

$$\therefore \qquad |B^{-1}A-D^{-1}C| = |D^{-1}B^{-1}| = |B^{-1}D^{-1}|.$$

Substituting in (11) it follows that $|u|=1$.

The converse, that, if $|u|=1$, then (9) follows, is not true. In fact (9) implies far more than $|u|=1$. It implies r relationships between the elements of the matrix u.

In the same way as in a four terminal network $v_0=u^n v_n$, where u^n has to be found by (2). If the $2r$ roots of $|u-\lambda I|=0$ are $\lambda_1, \lambda_2, \ldots \lambda_{2r}$, then

$$v_0=k\Lambda^n k^{-1}v_n,$$

where Λ^n is now a diagonal matrix with elements $\lambda_1{}^n, \ldots \lambda_{2r}{}^n$, and the currents are transmitted without attenuation if $|\lambda_1|=|\lambda_2| \ldots =1$.

As an example we will consider the case of a transmission system in which the elements have three input and three output terminals, one of each of which is earthed, as in the figure above.

Here we have the equations

$$\begin{gathered}
I_0Z_1+(I_0-I_1-x)Z_2=E_0,\\
I_0'Z_1'+(I_0'-I_1'+x)Z_2'=E_0',\\
-I_1Z_3+(I_0-I_1-x)Z_2=E_1,\\
-I_1'Z_3'+(I_0'-I_1'+x)Z_2'=E_1',\\
I_0Z_1+I_0'Z_1'+xZ=E_0-E_0'.
\end{gathered}$$

Hence

$$\begin{bmatrix} Z_1+Z_2 & 0 & -Z_2 & 0 & -Z_2 \\ 0 & Z_1'Z_2' & 0 & -Z_2' & Z_2' \\ Z_2 & 0 & -(Z_2+Z_3) & 0 & -Z_2 \\ 0 & Z_2' & 0 & -(Z_2'+Z_3') & Z_2' \\ Z_1 & -Z_1' & 0 & 0 & Z \end{bmatrix}\begin{bmatrix} I_0 \\ I_0' \\ I_1' \\ I_1' \\ x \end{bmatrix}=\begin{bmatrix} E_0 \\ E_0' \\ E_1 \\ E_1' \\ E_0-E_0' \end{bmatrix}.$$

Pre-multiplying both sides by

$$\begin{bmatrix} 1 & 0 & 0 & 0 & Z_2/Z \\ 0 & 1 & 0 & 0 & -Z_2'/Z \\ 0 & 0 & 1 & 0 & -Z_2/Z \\ 0 & 0 & 0 & 1 & -Z_2'/Z \\ 0 & 0 & 0 & 0 & 1 \end{bmatrix}$$

and omitting the last row, which contains x only, we get

$$\begin{bmatrix} Z_1+Z_2+(Z_1Z_2)/Z & -(Z_1'Z_2')/Z & -Z_2 & 0 \\ -(Z_1'Z_2')/Z & Z_1'+Z_2'+(Z_1'Z_2')/Z & 0 & -Z_2' \\ Z_2+(Z_1Z_2)/Z & -(Z_1'Z_2')/Z & -(Z_2+Z_3) & 0 \\ -(Z_1'Z_2')/Z & Z_2'+(Z_1'Z_2')/Z & 0 & -(Z_2'+Z_3') \end{bmatrix}\begin{bmatrix} I_0 \\ I_0' \\ I_1 \\ I_1' \end{bmatrix}$$

$$=\begin{bmatrix} 1+Z_2/Z & -Z_2/Z & 0 & 0 \\ -Z_2'/Z & 1+Z_2'/Z & 0 & 0 \\ Z_2/Z & -Z_2/Z & 1 & 0 \\ -Z_2'/Z & Z_2'/Z & 0 & 1 \end{bmatrix}\begin{bmatrix} E_0 \\ E_0' \\ E_1 \\ E_1' \end{bmatrix}.$$

From this equation, by partitioning the matrices and then taking all the terms with output voltages and currents to the right and those with input voltages and currents to the left, we get

$$\begin{bmatrix} -(1+Z_2/Z) & Z_2/Z & Z_1+Z_2+(Z_1Z_2)/Z & -(Z_1'Z_2)/Z \\ Z_2'/Z & -(1+Z_2'/Z) & -(Z_1Z_2')/Z & Z_1'+Z_2'+(Z_1'Z_2')/Z \\ -Z_2/Z & Z_2/Z & Z_2+(Z_1Z_2)/Z & -(Z_1'Z_2)/Z \\ Z_2'/Z & -Z_2'/Z & -(Z_1Z_2')/Z & Z_2'+(Z_1'Z_2')/Z \end{bmatrix}v_0$$

$$=\begin{bmatrix} 0 & 0 & Z_2 & 0 \\ 0 & 0 & 0 & Z_2' \\ 1 & 0 & Z_2+Z_3 & 0 \\ 0 & 1 & 0 & Z_2'+Z_3' \end{bmatrix}v_1.$$

If this equation is written $av_0 = bv_1$,

then $$v_0 = a^{-1}bv_1 = uv_1, \text{ say.}$$

The characteristic equation of u is $|u-\lambda\mathrm{I}|=0$, but from

$$u-\lambda\mathrm{I} = a^{-1}b-\lambda\mathrm{I},$$

pre-multiplying by a we get

$$b-\lambda a = a[u-\lambda\mathrm{I}].$$

Therefore, when $|u-\lambda\mathrm{I}|=0$, $|b-\lambda a|=0$, or, if $\mu=1/\lambda$, $|b\mu-a|=0$.

Writing out this determinant from the matrices given above and expanding it, we get

$$(1-\mu)^4\mathrm{Z}_2\mathrm{Z}_2' - \mu(1-\mu)^2\{\mathrm{Z}_2'(\mathrm{Z}_1+\mathrm{Z}_3)(1+\mathrm{Z}_2/\mathrm{Z}) + \mathrm{Z}_2(\mathrm{Z}_1'+\mathrm{Z}_3')$$
$$(1+\mathrm{Z}_2'/\mathrm{Z})\} + \mu^2(\mathrm{Z}_1+\mathrm{Z}_3)(\mathrm{Z}_1'+\mathrm{Z}_3')(1+(\mathrm{Z}_2+\mathrm{Z}_2')/\mathrm{Z}) = 0,$$

which is a quadratic in $(1-\mu)^2/\mu$.

If we write $(1-\mu)^2 = -\mu x$, the above equation becomes

$$x^2 - \left\{\frac{\mathrm{Z}_1+\mathrm{Z}_3}{\mathrm{Z}_2}\,\frac{\mathrm{Z}_2+\mathrm{Z}}{\mathrm{Z}} + \frac{\mathrm{Z}_1'+\mathrm{Z}_3'}{\mathrm{Z}_2'}\,\frac{\mathrm{Z}_2'+\mathrm{Z}}{\mathrm{Z}}\right\}x$$
$$+\frac{\mathrm{Z}_1+\mathrm{Z}_3}{\mathrm{Z}_2}\cdot\frac{\mathrm{Z}_1'+\mathrm{Z}_3'}{\mathrm{Z}_2'}\cdot\frac{\mathrm{Z}_2+\mathrm{Z}_2'+\mathrm{Z}}{\mathrm{Z}} = 0. \quad . \quad . \quad . \quad (12)$$

The equation for λ is then

$$\lambda^2 - (2+x)\lambda + 1 = 0.$$

where x is either root of (12) and hence the condition for transmission without attenuation is that x shall be real and

$$-2 < 2+x < 2 \quad \text{or} \quad -4 < x < 0.$$

Now, if in (12) the coefficients are both real positive numbers as for instance if all the impedances are resistances the roots are both real and positive and the condition is not satisfied as we should expect from physical considerations. Again, if the coefficients of (12) are complex then its roots are complex and the condition is not satisfied.

It follows that for transmission without attenuation the coefficient of x must be real and negative, the constant term must be real and positive and then the condition $-4<x<0$ is satisfied if the coefficient of x lies between -4 and 0. Thus the required conditions are

$$-4 < \frac{\mathrm{Z}_1+\mathrm{Z}_3}{\mathrm{Z}_2}\,\frac{\mathrm{Z}_2+\mathrm{Z}}{\mathrm{Z}} + \frac{\mathrm{Z}_1'+\mathrm{Z}_3'}{\mathrm{Z}_2'}\,\frac{\mathrm{Z}_2'+\mathrm{Z}}{\mathrm{Z}} < 0, \quad . \quad . \quad . \quad (13)$$

and $$\frac{\mathrm{Z}_1+\mathrm{Z}_3}{\mathrm{Z}_2}\cdot\frac{\mathrm{Z}_1'+\mathrm{Z}_3'}{\mathrm{Z}_2'}\,\frac{\mathrm{Z}_2+\mathrm{Z}_2'+\mathrm{Z}}{\mathrm{Z}} > 0. \quad . \quad . \quad . \quad . \quad (14)$$

We will now consider some special cases.

I. $$\mathrm{Z}_1=\mathrm{Z}_1'=\mathrm{Z}_3=\mathrm{Z}_3'=j\omega\mathrm{L}\,; \quad \mathrm{Z}_2=\mathrm{Z}=\frac{1}{j\omega\mathrm{C}}, \quad \mathrm{Z}_2'=\frac{1}{j\omega\mathrm{C}'}.$$

In this case (14) is satisfied for all ω and (13) becomes

$$-4 < -8\omega^2\mathrm{LC} - 4\omega^2\mathrm{LC}'\{(\mathrm{C}+\mathrm{C}')//\mathrm{C}'\} < 0,$$

or
$$\omega^2 < \frac{C}{C+3C'}\,\frac{1}{LC}.$$

The system therefore acts as a low pass filter.

II. $Z_1 = Z_1' = Z_3 = Z_3' = j\omega L$; $Z_2 = \frac{1}{j\omega C}$, $Z_2' = \frac{1}{j\omega C'}$ and $Z = j\omega l$.

In this case (14) becomes
$$\omega^2 > \frac{C+C'}{CC'l}, \quad \dots\dots\dots \quad (15)$$

and (13) becomes
$$-4 < -2\omega^2 LC\left(1-\frac{1}{\omega^2 lC}\right) - 2\omega^2 LC'\left(1-\frac{1}{\omega^2 lC'}\right) < 0,$$

or
$$2 > \omega^2(LC+LC') - \frac{2L}{l} > 0. \quad \dots\dots\dots \quad (16)$$

$$\therefore \quad \frac{2(L+l)}{Ll(C+C')} > \omega^2 > \frac{2}{l(C+C')}.$$

Since $(C+C')^2 > 2CC'$, the lower bound given by (15) is greater than the lower bound given by (15).

$$\therefore \quad \frac{C+C'}{lCC'} < \omega^2 < \frac{2(L+l)}{Ll(C+C')}.$$

But
$$\frac{C+C'}{lCC'} > \frac{2(L+l)}{Ll(C+C')}, \text{ if } \frac{l}{L} > 1,$$

so transmission without attenuation is only possible when $l < L$ when the system acts as a band pass filter. Moreover, by choosing $L-l$ small enough we can make the range of frequencies as small as we please in a way that is probably easier than that of the four terminal band pass filter.

III. $Z_1 = Z_1' = Z_3 = Z_3' = \frac{1}{j\omega C}$, $Z_2 = Z = j\omega L$, $Z_2' = j\omega L'$.

In this case (14) is satisfied for all ω and (13) becomes
$$-4 < -\frac{4}{\omega^2 LC} - \frac{2}{\omega^2 L'C}\left(\frac{L+L'}{L'}\right) < 0,$$

or
$$\omega^2 > \frac{L+3L'}{LL'C}.$$

So that the system acts as a high pass filter.

IV. $Z_1 = Z_1' = Z_3 = Z_3' = \frac{1}{j\omega C}$, $Z_2 = j\omega L$, $Z_2' = j\omega L'$, $Z = \frac{1}{j\omega c}$.

In this case (14) is satisfied if
$$\omega^2 < \frac{1}{(L+L')c},$$

and (13) becomes
$$-4 < -\frac{2}{\omega^2 LC}(1-\omega^2 Lc) - \frac{2}{\omega^2 L'C}(1-\omega^2 L'c) < 0,$$

or
$$\left(\frac{1}{L}+\frac{1}{L'}\right)\frac{1}{2(C+c)}<\omega^2<\left(\frac{1}{L}+\frac{1}{L'}\right)\frac{1}{2C}.$$

But
$$\frac{1}{L+L'}<\frac{1}{2}\left(\frac{1}{L}+\frac{1}{L'}\right)$$

so these inequalities together give

$$\left(\frac{1}{L}+\frac{1}{L'}\right)\frac{1}{2(C+c)}<\omega^2<\frac{1}{(L+L')c}.$$

This is only possible if $C<c$; then we get a band pass filter which passes only a very narrow band if $c-C$ is small.

V. $$Z_1=Z_1'=Z_3=Z_3'=j\left(L\omega-\frac{1}{C\omega}\right),$$
$$Z_2=Z=\frac{1}{(1/jL'\omega)+jC'\omega},$$
$$Z_2'=\frac{1}{(1/jL''\omega)+jC''\omega}.$$

In this case (14) becomes, after simplification,

$$(1-\omega^2L'C')(1-\omega^2L''C'')\{2L'+L''-\omega^2L'L''(C'+2C'')\}>0.$$

We will suppose that $LC\geqslant L'C''\geqslant L''C''$, then

$$\frac{L'L''(C'+2C'')}{2L'+L''}$$

lies between $L'C'$ and $L''C''$.

Hence the condition is satisfied if

$$\omega^2<\frac{1}{L'C'}\quad\text{or}\quad\frac{2L'+L''}{L'L''(C'+2C'')}<\omega^2<\frac{1}{L''C''}.$$

Equation (13) becomes

$$-4<-4\frac{(1-\omega^2LC)(1-\omega^2L'C')}{\omega^2L'C}$$
$$-2\frac{(1-\omega^2LC)(1-\omega^2L''C'')}{\omega^2L''C}\left\{1+\frac{L''}{L'}\left(\frac{1-\omega^2L'C'}{1-\omega^2L''C''}\right)\right\}<0,$$

which simplifies to

$$\frac{2\omega^2}{L(3C'+C'')}>\left(\omega^2-\frac{1}{LC}\right)\left(\omega^2-\left(\frac{3}{L'}+\frac{1}{L''}\right)\Big/(3C'+C'')\right)>0. \tag{17}$$

This condition is satisfied if

$$\omega_1^2<\omega^2<\frac{1}{LC}\quad\text{and}\quad\left(\frac{3}{L'}+\frac{1}{L''}\right)\Big/(3C'+C'')<\omega^2<\omega_2^2, \tag{18}$$

where $\omega_1{}^2$ and $\omega_2{}^2$ are the roots of (17) when the first $>$ sign is replaced by $=$.

Now
$$\frac{2L'+L''}{L'L''(C+2C'')}>\left(\frac{3}{L'}+\frac{1}{L''}\right)\Big/(3C'+C'')$$

under the assumed conditions. Therefore both inequalities in (18) are satisfied if

$$\omega_1^2 < \omega^2 < \frac{1}{LC} \quad \text{and} \quad \frac{2L'+L''}{L'L''(C'+2C'')} < \omega^2 < \omega_2^2,$$

provided

$$\omega_2^2 > \frac{2L'+L''}{L'L''(C'+2C'')}.$$

If this is so, the system passes two separate bands. It is, perhaps, worth while in this case to work out a numerical example. Suppose $L=0{\cdot}3$, $L'=0{\cdot}2$, $L''=0{\cdot}1$, $C=C'=10^{-10}$, $C''=1{\cdot}5\times10^{-10}$. Then

$$\frac{1}{LC}=\frac{10}{3}\times10^{10}, \quad \frac{1}{L'C'}=5\times10^{10}, \quad \frac{1}{L''C''}=\frac{20}{3}\times10^{10},$$

$$\frac{2L'+L''}{L'L''(C+2C'')}=\frac{25}{4}\times10^{10}, \quad \text{and} \quad \omega_1^2,\ \omega_2^2$$

are given by

$$\left(\omega^2-\frac{10}{3}\times10^{10}\right)\left(\omega^2-\frac{50}{9}\times10^{10}\right)=\frac{40}{27}\times10^{10}\omega^2,$$

whence

$$\omega^2 \simeq 2{\cdot}29\times10^{10} \quad \text{or} \quad 8{\cdot}0\times10^{10}.$$

The system therefore transmits frequencies for which

$$2{\cdot}29\times10^{10}<\omega^2<3{\cdot}33\times10^{10} \quad \text{and} \quad 6{\cdot}25\times10^{10}<\omega^2<8{\cdot}03\times10^{10}.$$

In conclusion I must acknowledge the help I have got on the introductory theory from 'Elementary Matrices,' by Frazer, Duncan and Collar, and from a lecture given before the London Mathematical Society by Dr. A. C. Aitken.

Woolwich Polytechnic.

XXXVI. *Spectrum of Radium* (B+C) *Gamma-Rays.*

By J. E. Roberts, D.Sc., F.Inst.P.*,
Barnato Joel Laboratories, Middlesex Hospital.

[Received October 6, 1944.]

Summary.

Using the experimental results of Skobelzyn and of Ellis and Aston, the energy distribution in the gamma-ray spectrum of radium (B+C) with varying degrees of filtration has been calculated. From the energy distributions, the scattering absorption coefficients of the heterogeneous radiations have been calculated and compared with recent measurements by the author of absorption in aluminium and carbon.

---

* Communicated by the Author.

GAMMA-RAY SPECTRUM ANALYSIS.

THE distribution of intensities in the gamma-ray spectrum of radium (B+C) has been investigated, using different methods, by Skobelzyn (1927, 1929) and Ellis and Aston (1930). From these results it is possible to estimate the scattering absorption coefficients of the heterogeneous radiation. In the present work, these predicted coefficients are compared with those obtained in recent experiments on the absorption of gamma-rays in carbon and aluminium.

Distribution of Quanta.

The method of Skobelzyn (1927, 1929) consists essentially in passing a narrow pencil of gamma-rays through a cloud chamber across which a magnetic field is maintained. From an examination of the curvatures and scattering angles of the recoil electron tracks it is possible in each case to determine the wave-length of the primary quantum producing the electron. Skobelzyn has made a statistical analysis of the frequency of occurrence of these different tracks. On the assumption that the scattering in air is in accordance with the Klein–Nishina formula, it is possible to draw a distribution curve of the number of emitted quanta against gamma-ray wave-length. This curve shows a series of peaks, most of which agree well in position with the gamma-ray wave-lengths deduced from the natural β-ray spectrum. Assuming that the peaks are symmetrical, they have been separated, and the relative number of quanta (ΔN) corresponding to each spectrum line deduced. This method is particularly suitable for the investigation of any very short wave-lengths present in the spectrum.

Ellis and Aston (1930) have used the photoelectric emission from platinum to reach a similar result. Radon is enclosed in a thin platinum sheath and the emitted photo-electrons analysed by the magnetic spectrum method. For each wave-length observed, this gives a value of $\Delta N.\tau_K$, where ΔN is the relative number of quanta, and τ_K is the corresponding K level photo-electric absorption coefficient of platinum. To obtain values of ΔN it is necessary to make some assumption as to the variation of τ with wave-length. For the present purpose values based on the theory of Hulme, McDougall, Buckingham and Fowler (1935) have been used. Only the eleven strongest lines in the spectrum could be measured by this method, but they cover the greater part of the total gamma-ray energy.

Energy Distribution.

Having obtained the values of ΔN, it is only necessary to multiply each one by the corresponding quantum energy $h\nu$ to obtain the relative distribution of energy among the spectral lines. The results for the two methods are shown in fig. 1. The individual energies (ΔE) are given as percentages of the total emitted energy. These figures are given so far as is possible for the condition of zero filtration. Owing to the straggling of the photo-electrons in the platinum, there is some doubt in the case of Ellis and Aston's results as to the exact filtration to which the energies correspond. As, however, the total thickness of platinum was only 0·4 mm. and the effective filtration is considerably less than this, it has been assumed that the figures correspond to zero filtration. Skobelzyn used a filter of 3·5 mm. lead and 2 mm. glass. This has been taken as equivalent to 4 mm. lead, and the energies converted to zero filtration by the method described below.

Although the two spectra are similar in general outline, there are some differences which may be significant. The line at 8·98 X.U. is much stronger in the Skobelzyn spectrum than in that of Ellis and Aston, and *vice versa* in the case of the lines at 10·92 and 20·2 X.U. Skobelzyn gives indications of a number of weak lines of very short wave-length, which do not appear in the other spectrum. The difference in the three long wave (radium B) lines cannot be regarded as significant owing to the uncertainties in the conversion of their energies to zero filtration. In practice a 4 mm. lead filter reduces the radium B contribution to something less than 5 per cent. of the whole. It is interesting to note that, considering only the radium C lines, the Ellis and Aston spectrum gives 48 per cent. of the energy in wave-lengths below 10 X.U., whilst Skobelzyn gives 65 per cent.

Fig. 1.

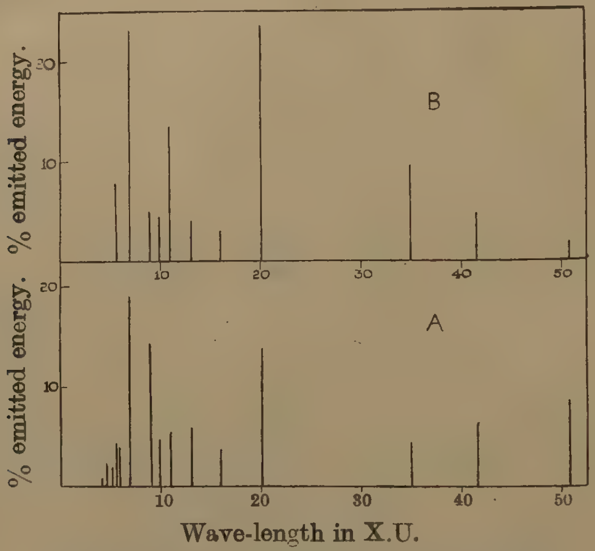

Energy distribution in radium (B+C) gamma-ray spectrum.

A. From measurements of Skobelzyn.
B. From measurements of Ellis and Aston.

Filtered Radiation.

The spectral energy distribution for lead-filtered radiations can now be derived if the absorption coefficient in lead for each component is known. These coefficients have been obtained by using the formula of Klein and Nishina (1928) for absorption by scattering, the formula of Hulme *et al* (1935) for photo-electric absorption, and the results of Bethe and Heitler (1934) for absorption by electron pair formation. In this way distributions similar to those shown in fig. 1 have been obtained for a number of filtrations up to 5 cm. of lead. Details of this calculation are given in a previous paper by the writer (Roberts, 1945).

Absorption Coefficients.

When the proportions of energy in the various wave-lengths of a heterogeneous beam are known, it is possible to predict some of its characteristics. In particular the mean absorption coefficients of the mixed radiation can be calculated. Considering only absorption by scattering, the electronic absorption coefficient (${}_e\sigma$) for any wave-length is given by the Klein–Nishina formula. This formula is well established as being in accord with experimental facts over a wide range of wave-lengths. For a heterogeneous beam then, the mean energy absorption per electron is given by

Fig. 2.

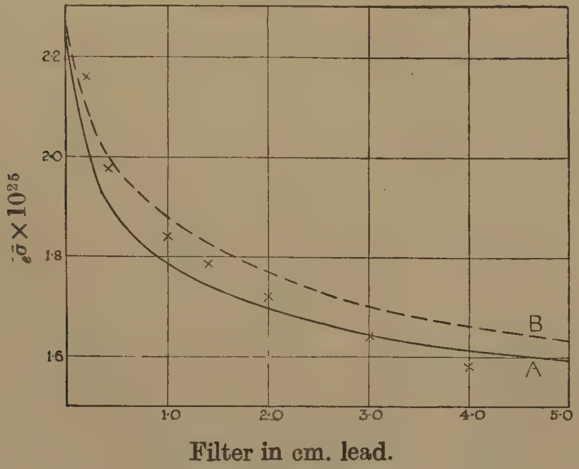

Scattering absorption coefficients for filtered gamma-rays.

Curve A. From Skobelzyn spectrum.
Curve B. From Ellis and Aston spectrum.
× Experimental points.

$$\overline{{}_e\sigma}=\frac{\Sigma\,{}_e\sigma\,.\,\Delta \mathrm{E}}{\Sigma\Delta \mathrm{E}},$$

the summation being taken over all the lines in the spectrum. Using the spectral distributions described above, the mean electronic absorption coefficients for radium (B+C) gamma-rays with filtrations from 0 to 5 cm. lead have been calculated. The results are shown in fig. 2, where curve A is obtained using the Skobelzyn spectrum, and curve B the Ellis and Aston spectrum. The difference in the two spectra is immediately evident, the Skobelzyn spectrum, which indicates a preponderance of energy in the shorter wave-lengths, giving lower values for $\overline{{}_e\sigma}$ over the whole range.

Comparison with Experiment.

In a recent paper (Roberts, 1945), the writer has described new measurements of the absorption of filtered radium (B+C) gamma-rays in aluminium and graphite, the results being given in terms of true energy absorption. Over the wave-length range concerned, for these elements, photo-electric absorption is negligible, and so the experimental values of ${}_e\mu$ are identical with ${}_e\sigma$. The electronic coefficients have been calculated from the experimental results, and a number of points are shown in fig. 2 for filters up to 4 cm. lead. The figures given are mean values for aluminium and carbon. It will be seen that there is general agreement between the predicted values of $\overline{{}_e\sigma}$ and the experimental values, but no tendency towards one or the other of the predicted curves. Except at high filtrations the $\overline{{}_e\sigma}$ curve from Skobelzyn's spectrum is lower than the experimental points. There is some evidence (Roberts, 1945) that the absorption coefficient of gamma-rays in lead, used to determine the filtered spectral distributions, rises more rapidly with increasing wave-length than is suggested by the theories mentioned earlier. No precise allowance for this can be made at present, but it can be seen qualitatively that the effect on the calculated energy distributions would be to shift more energy into the shorter wave-lengths. This would result in rather lower calculated mean values of $\overline{{}_e\sigma}$ for filtered radiations, thus lowering the high filtration end of curve A in fig. 2. The evidence seems to indicate that the Skobelzyn method of obtaining the spectral distribution tends to over-estimate the energy in the short wave components.

At nearly all filtrations the curve of $\overline{{}_e\sigma}$ against filter obtained from the Ellis and Aston spectrum is higher than the experimental points. This may indicate that the method over-estimates the relative proportion of energy in the long wave components of the spectrum. On the other hand, the effect of using theoretical values of μ and τ for lead and platinum in determining the spectral distributions is here more complex. In estimating the unfiltered energy distribution from the figures of Ellis and Aston, the theoretically predicted variation of τ with wave-length was used. If τ actually rises more rapidly with wave-length than this prediction, the calculated energies will be more concentrated in the shorter wave-lengths. This will result in lower predicted values for $\overline{{}_e\sigma}$, and so curve B in fig. 2 will be lowered. Furthermore, as with the other curve, the higher filtration points will be depressed rather more than the lower. The net result would be to bring the predicted curve of $c^{\bar{\sigma}}$ against filtration nearer to the experimental figures.

References.

Bethe and Heitler, Proc. Roy. Soc. A, cxlvi. p. 83 (1934).
Ellis and Aston, Proc. Roy. Soc. A, cxxix. p. 180 (1930).
Hulme, McDougall, Buckingham and Fowler, Proc. Roy. Soc. A, cxlix. p. 131 (1935).
Klein and Nishina, *Zeits. f. Phys.* lii. p. 853 (1928).
Roberts, Proc. Roy. Soc. A, clxxxiii. p. 338 (1945).
Skobelzyn, *Zeits. f. Phys.* xliii. p. 354 (1927); lviii. p. 595 (1929).

XXXVII. *Phase Space in Eddington's Theory* [*].

By A. J. Coleman [†].

[Received February 19, 1945.]

1. *Introduction.*

The daring speculations of Sir A. S. Eddington with regard to the theoretical calculation of the fundamental constants of nature have attracted wide interest, although they are often viewed with incredulity. The earlier stages of these investigations, in which he has been almost alone, are collected in his book 'The Relativity Theory of Protons and Electrons' (Cambridge, 1936), which we shall henceforth refer to as "P. and E." His methods arose from an effort to effect a unification of the theories of relativity and quantum mechanics. The importance of such a unification and the possibility of a theoretical determination of the fundamental constants of nature are argued most cogently by L. L. Whyte (1). In a recent paper (2) Sir Arthur amasses experimental evidence which confirms his theories at every point to well within experimental error. No other theory known to the author, except the electro-magnetic theory, achieves such accuracy of prediction for such a varied range of phenomena.

Central to the whole mathematical development of P. and E. is *phase space*, which we define in section 3 below. The numbers 10 and 136 which occur in Eddington's equation for the ratio of the masses of proton and electron are, respectively, the dimensions of the phase space of a single and a double wave tensor. Since phase space is the domain of the probability distribution of a particle, it is through phase space that physical interpretation is given to his theory. In P. and E., Eddington states "... it is an essential characteristic of space that it is occupied or has finite *à priori* probability of being occupied" (p. 5); "... phase space should be closed" (p. 97); and "... it is important for our theory that the whole volume of phase space is finite" (p. 99).

---

[*] This paper is a condensation of part of a thesis accepted by the University of Toronto in partial fulfilment of the requirements for the degree of Doctor of Philosophy.

[†] Communicated by the Author.

We shall show that *phase space as defined by Eddington has infinite volume.*

2. *Some Properties of E-numbers.*

2. In this section we recall the definition and relevant properties of E-numbers. Following Temple's paper (3), we define our fundamental E-numbers so that they differ from Eddington's by multiplication by i.

We have five distinct operators E_r (in hilbert space), which satisfy the conditions

$$E_rE_s+E_sE_r=2\delta_{rs}E_0, \qquad (2.1)$$

$$E_r^\dagger=E_r, \qquad (2.2)$$

where δ_{rs} is the kronecker delta symbol, E_0 is the identity operator and the dagger stands for hermitian conjugation. It follows from (2.1) that $E_r^2=E_0$, and if we define new symbols E_{rs} by setting

$$E_{rs}=iE_rE_s \quad (r\neq s) \qquad (2.3)$$

we shall also have $E_{rs}^2=E_0$. Any product of the above symbols is linearly dependent, over the field of complex numbers, on the sixteen symbols E_0, E_r, E_{rs} $(r<s)$, which we call a *fundamental set* of E-numbers. A *pentad* consists of five mutually anti-commuting members of a fundamental set. There are six distinct pentads in any fundamental set.

We shall allow latin indices to take on the values 1, 2, 3, 4, 5, and greek indices the sixteen values of 0, r, rs $(r<s)$. Then, adopting the summation convention, the set of operators of the form

$$A=a^\mu E_\mu, \qquad (2.4)$$

where the a^μ are arbitrary complex numbers constitute a linear algebra of dimension sixteen over the complex numbers. This is the *sixteen-fold frame* of reference of Chapter II. of P. and E. We shall refer to any operator of the form (2.4) as *an E-number.* Any sixteen linearly independent E-numbers will form a *basis* for the algebra. In general, a basis will not have the structure of a fundamental set which is specified by (2.1), (2.2), and (2.3). The failure to distinguish clearly between a basis and a fundamental set leaves Eddington's discussion of "Duality" in considerable confusion. Thus, in section (10.4) of P. and E., he seems to regard $L\sigma$, which *is* a basis, as a fundamental set which it is *not.*

We define

$$\exp(itE_\mu)=\cos tE_0+i\sin t\,E_\mu, \qquad (2.5)$$

and following Eddington replace $\prod_\mu \exp(it^\mu E_\mu)$ by $\exp(it^\mu E_\mu)$, where, in the latter expression, the summation convention holds, and since the E_μ do not all mutually commute account must be taken of the order of the terms in the sum $t^\mu E_\mu$. From the definition (2.5) it immediately follows that if $E_\mu E_\nu+E_\nu E_\mu=0$, then

$$E_\nu \exp(it\,E_\mu)=\exp(-it\,E_\mu)E_\nu. \qquad (2.6)$$

If we represent a vector in the (x^1, x^2) plane by $x^1E_1+x^2E_2$ and set

$$y^1E_1+y^2E_2=\exp(-\tfrac{1}{2}itE_{12}) \, . \, (x^1E_1+x^2E_2) \exp(\tfrac{1}{2}itE_{12}),$$

then (2.5) leads to

$$y^1=\cos tx^1+\sin tx^2,$$

$$y^2=\sin tx^1+\cos tx^2,$$

which are the equations for a rotation in the (x^1, x^2) plane.

The algebra of E-numbers can be represented by four-fold matrices, and throughout his book Eddington employs such a representation and makes essential use of the symmetry properties of the particular matrices employed. I have shown in my thesis(4) that a definition of transposition can be given for E-numbers as abstractedly defined above, which allows those parts of Eddington's theory which depend on symmetry conditions to be developed in a manner independent of the particular representation chosen. However, this is not an essential point for the present purpose; so that the reader may think of our E-numbers as four-fold matrices without any loss of rigour. Eddington chooses his E_μ so that ten of them are symmetric and six are anti-symmetric matrices. This can always be done, and throughout the remainder of this paper we shall assume that

$$E_0, E_1, E_2, E_3, E_{14}, E_{15}, E_{24}, E_{25}, E_{34}, E_{35} \quad \ldots \quad (2.7)$$

are *symmetric*, and

$$E_4, E_5, E_{45}, E_{23}, E_{13}, E_{12} \quad \ldots\ldots\ldots \quad (2.8)$$

are *anti-symmetric*.

Following Eddington we define $qs(A)$, the *quarterspur* of any E-number $A=a^\mu E_\mu$, by setting

$$qs(A)=a^0. \quad \ldots\ldots\ldots\ldots \quad (2.9)$$

It is easy to verify that with this definition,

(i.) $qs(aA+bB)=aqs(A)+bqs(B)$; (ii.) $qs(AB)=qs(BA)$; (iii.) $qs(E_0)=1$.

It follows immediately from the definition that the $qs(E_\mu)=0$, if $\mu \neq 0$.

If U is an arbitrary E-number we shall denote by U′ an E-number satisfying $UU'=U'U=E_0$, and by $\overline{U}$, the *transpose* of U. We shall say that U is *unitary* if $U^\dagger U=UU^\dagger=E_0$.

3. *Natural Co-ordinates and Volume in Phase Space.*

In this section we recall Eddington's definition of phase space as given in section (7.2) of P. and E., expand on a remark of his that phase space is equivalent to a set, $\mathscr{P}$, defined below, and prove a new result about $\mathscr{P}$—admissible transformations which will be required subsequently.

If the E-number T represents the state of a physical system, then for Eddington the E-number UTU' represents the system in the same state only viewed from a new frame of reference. We had an example of such a transformation in the preceding section when U had the particular value $\exp(itE_{12})$. Such transformations are the analogue in E-number calculus of the transformations of an ordinary mixed double tensor.

Eddington defines a *strain vector*, on the analogy of a double covariant tensor, as a set of E-numbers such that any two of them, S and T, are connected as follows :

$$T = US\bar{U},$$

where $\bar{U}$ is the matrix obtained by transposition of U. He defines phase space, $\mathscr{P}_S$, as the set of all E-numbers P of the form

$$P = US\bar{U} - USU', \quad . \quad . \quad . \quad . \quad . \quad . \quad . \quad . \quad . \qquad (3.1)$$

where U is subject only to the condition that it is unitary. In my opinion, *Eddington's most important assumption* is that the internal configurations of an elementary particle are represented by the points of $\mathscr{P}_S$. (We shall refer to the E-numbers of $\mathscr{P}_S$ as " points ".) The restriction that U is unitary is required in order to ensure that $\mathscr{P}_S$ is closed. In P. and E., Eddington does not require that U be unitary but that it be of the form exp $(it^\mu E_\mu)$, where the t^μ are real. On account of our condition (2.2) this is equivalent to requiring that U be unitary. A passing reference in a later paper(5) suggests that Eddington recognized this equivalence subsequently to writing P. and E.

We establish a one-to-one mapping of $\mathscr{P}_S$ on the set $\mathscr{P}$, consisting of the E-numbers $U\bar{U}$, by mapping P on to P_0, where

$$\begin{aligned} P_0 &= US'U'P + E_0 \\ &= US'U'(US\bar{U} - USU') + E_0 \\ &= U\bar{U}. \end{aligned}$$

The phase space $\mathscr{P}_S$, for non-singular S, is thus in one-to-one correspondence with the set $\mathscr{P}$ of all $U\bar{U}$ where U is an arbitrary unitary E-number.

The above method was suggested by a remark at the bottom of page 97 of P. and E. Since, as we shall see, $\mathscr{P}$ is in all respects equivalent to $\mathscr{P}_S$, it would seem preferable to the author to define the former as *phase space*, rather than making phase space depend on S as Eddington does.

If U is unitary, so is $U\bar{U}$. Also, $U\bar{U}$ is symmetric, since $\overline{U\bar{U}} = U\bar{U}$. Now, if A is an E-number such that $E_0 - A$ is non-singular then, solving $B = (E_0 - A)(E_0 + A)'$ for A, we obtain

$$A = (E_0 - B)(E_0 + B)'.$$

If we set A equal to $U\bar{U}$, we see from the fact that A is symmetric that $\bar{B} = B$, and from the fact that A is unitary we see that $B^\dagger = -B$. If $B = b^\mu E_\mu$ this first condition requires that b^4, b^5, b^{45}, b^{12}, b^{13}, b^{23}, be zero on account of (2.8). The second condition, coupled with (2.2), requires that the remaining ten b^μ be pure imaginaries. Thus, $\mathscr{P}$, *and therefore* $\mathscr{P}_S$, *depend on ten real parameters.*

Throughout the remainder of this paper we shall restrict μ and ν to the " symmetric " values of (2.7).

We now give Eddington's definition of *locally orthogonal co-ordinates* (*l. o. c.*). We set

$$T = \exp(\tfrac{1}{2} i dX),$$

where $dX=dx^\mu E_\mu$; so that T differs from the identity by a quantity of the first order in dx^μ. If Q is the point $Q=US\bar{U}-USU'$, then, since $T=\bar{T}$, if we replace U by TU, which differs from U only by a quantity of the first order in dx^μ, we obtain the point Q* in the neighbourhood of Q given by $Q^*=TUS\bar{U}T-TUSU'T'$. The ten quantities (dx^μ) are *locally orthogonal co-ordinates of the point Q* from the pole Q*. Now if we establish the correspondence discussed above, which maps Q on $P=U\bar{U}$ and Q* on $P^*=TU\bar{U}T=TPT$, and *define* (dx^μ) *as locally orthogonal co-ordinates of* P* *from* P, then not only is the mapping topological but it preserves the metric. Thus for non-singular S, $\mathscr{P}$ and $\mathscr{P}_S$ are completely equivalent; so, henceforth, we shall work in $\mathscr{P}$.

If locally orthogonal co-ordinates are definable from P as pole, that is, give a (1, 1) representation of a 10-dimensional neighbourhood of P, *then* $\exp(\frac{1}{2}idX)P\exp(\frac{1}{2}idX)=\exp(\frac{1}{2}idY)P\exp(\frac{1}{2}idY)$, where $dY=dy^\mu E_\mu$ must imply that $dX=dY$. That there are points at which this is not true, and therefore l.o.c. are undefinable, is an unfortunate fact which vitiates much of Eddington's argument, as we shall see in the next section.

At a point P at which l.o.c. are defined, the distance ds from P to a point whose l.o.c. are dx^μ is given by

$$ds^2=\Sigma(dx^\mu)^2=qs(dX\,dX). \quad . \quad . \quad . \quad . \quad . \quad . \quad . \qquad (3.3)$$

To justify the above definition of l.o.c. we must note an interesting invariant property of (3.3). It is known that if F_r are E-numbers satisfying our "structural equations" (2.1), then the E-number $U=F^\rho E_\rho$ is such that $F_r=UE_rU'$. Conversely, if $F_r=UE_rU'$, then F_r satisfy (2.1). If $U\bar{U}=E_0$ then it may be seen fairly easily that F_r are symmetric. Thus our definition of ds should not depend on whether we take E_r or F_r, obtained from E_r by such a U, as our fundamental set. This property follows immediately from the second expression above for ds^2, and the fact that if $dX=dx^\mu E_\mu$, and $dY=dy^\mu F_\mu$ are l.o.c. of P from the pole P, *then* $dX=dY$.

We have, thus, a Riemannian geometry defined in the ten-dimensional phase space. The geometry of this space has not been studied much, if at all, but should provide a manageable problem of considerable interest. We are here concerned only with the volume of the space. Its volume element dv is defined in the usual way, so that if (y^ν) is any system of co-ordinates in $\mathscr{P}$, then at a point P where dx^μ are l.o.c.

$$dv=|\partial x^\mu/\partial y^\nu|\,dy^0.dy^1\,\ldots\,dy^{35}. \quad . \quad . \quad . \quad . \quad . \quad . \qquad (3.4)$$

It is not difficult to see that transformations U which take any point P of $\mathscr{P}$ into a point UPU' also belonging to $\mathscr{P}$, satisfy the conditions

$$U\bar{U}=UU^\dagger=E_0. \quad . \quad . \quad . \quad . \quad . \quad . \quad . \quad . \qquad (3.5)$$

Transformations satisfying these conditions will be called *$\mathscr{P}$-admissible transformations*. By the same method as we used in proving the ten-dimensionality of $\mathscr{P}$ we can show that there is a *six-fold infinity* of $\mathscr{P}$-admissible transformations.

It is clear that if P and P* undergo a $\mathscr{P}$-admissible transformation U then the l.o.c. dX becomes UdXU′. Therefore, the distance ds_0 between the transformed points is given by

$$ds_0{}^2=qs(\mathrm{U}d\mathrm{X}\mathrm{U}'\,.\,\mathrm{U}d\mathrm{X}\mathrm{U}')=qs(d\mathrm{X}\,.\,d\mathrm{X})=ds^2.$$

Thus the metric, and, *à fortiori, the volume element is unchanged by a $\mathscr{P}$-admissible transformation* which might therefore be called a *rotation* of $\mathscr{P}$. This result will be of considerable importance in section 6.

4. *Eddington's Discussion of the Finitude of Phase Space.*

Eddington concludes section (7.4) of P. and E. with these words, " I have little doubt that a geometer could furnish a more elegant proof. Probably he could evaluate the volume. But I think the above investigation satisfies us that the volume of phase space is finite." It was the challenge contained in the second sentence which led me after a vain attempt to prove the finitude of phase space to the present proof that it is infinite. In this section we point out an error in Eddington's reasoning.

If we set U=exp $(\frac{1}{2}ix^\mu\mathrm{E}_\mu)$ where the E_μ are symmetric and x^μ are real, then U is unitary. Thus $\mathrm{U}\overline{\mathrm{U}}$ belongs to $\mathscr{P}$ and, following Eddington, we take the ten x^μ as co-ordinates for the points of $\mathscr{P}$. If x^μ is increased by 2π, U is unchanged ; so that the whole space is covered at least once, and indeed several times, when the co-ordinates vary over the range

$$0\leqslant x^\mu\leqslant 2\pi.$$

Eddington attempts to prove the finitude of phase space by showing that $|\partial y^\mu/\partial x^\nu|$, where dy^μ are l.o.c., is finite everywhere. His argument on p. 100 of P. and E. is vitiated by his assumption that the l.o.c. at $q\bar{q}$ are given by the symmetric terms of the expression $d\Theta$ which he defines in equation (7.45). This assumption is only valid if the antisymmetric terms in $d\Theta$ commute with his q, which is not the case in general.

Indeed, we shall show that in our notation the above jacobian is infinite at the point E_3. Now $\mathrm{E}_3^\dagger=\mathrm{E}_3$, and $\mathrm{E}_3^2=\mathrm{E}_0$; so E_3 is unitary. It is also symmetric and therefore lies in $\mathscr{P}$. Consider the point P_0 whose l.o.c. from E_3 as pole are such that all dy^μ are zero except dy^{34} and dy^{35}. Then

$$\mathrm{P}_0=\exp\tfrac{1}{2}i(dy^{34}\mathrm{E}_{34}+dy^{35}\mathrm{E}_{35})\mathrm{E}_3\exp\tfrac{1}{2}i(dy^{35}\mathrm{E}_{35}+dy^{34}\mathrm{E}_{34}).$$

Since E_3 anti-commutes with E_{34} and E_{35}, we have by (2.6),

$$\mathrm{P}_0=\mathrm{E}_3$$

for all dy^{34} and dy^{35}. Variations in these two parameters therefore effect no change in P_0 and thus $|\partial x^\nu/\partial y^\mu|$ is zero at E_3. Hence $|\partial y^\mu/\partial x^\nu|$ is infinite. Thus Eddington's proof fails at E_3.

However, even though there are points at which the jacobian is infinite it might well happen that the integral of the jacobian over the space is finite. To show that this is not the case we shall evaluate the jacobian explicitly in one co-ordinate system and be forced to the conclusion that the volume of phase space is infinite.

5. *Phase Space is Infinite.*

To evaluate the jacobian we introduce a system of co-ordinates x^ρ different from those used in the previous section. Since any P in $\mathscr{P}$ is unitary we have, by a well known theorem, that

$$\mathrm{P}=\mathrm{A}\,.\,\mathrm{DA}', \quad \dots\dots\dots \quad (5.1)$$

where A and D are unitary and D is a diagonal matrix. By a proper identification of the E_μ with matrices we may express D in the form

$$\mathrm{D}=\exp i(x^0\mathrm{E}_0+x^2\mathrm{E}_2+x^{14}\mathrm{E}_{14}+x^{35}\mathrm{E}_{35}), \quad \dots\dots \quad (5.2)$$

where the order in the summand does not matter since the four matrices mutually commute. Using the fact that P is symmetric we can show that A may be chosen to satisfy $\mathrm{A}\overline{\mathrm{A}}=\mathrm{E}_0$. This, together with the fact that A is unitary, suggests that we take

$$\mathrm{A}=\exp \tfrac{1}{2}i(x^4\mathrm{E}_4+x^5\mathrm{E}_5+x^{45}\mathrm{E}_{45}+x^{12}\mathrm{E}_{12}+x^{13}\mathrm{E}_{13}+x^{23}\mathrm{E}_{23}), \qquad (5.3)$$

where the summand contains the six anti-symmetric symbols of (2.8). Since these symbols do not commute we must carefully observe the order in the summand. A, as defined in (5.3), is unitary and satisfies the condition $\mathrm{A}\overline{\mathrm{A}}=\mathrm{E}_0$.

We shall henceforth restrict the Greek letters α, β to the values 4, 5, 45, 12, 13, 23 occurring in (5.3). It is worth while noticing that E_α divide into the two groups E_4, E_5, E_{45}, and E_{32}, E_{13}, E_{23}. The symbols of each group mutually anti-commute while each symbol commutes with the symbols of the other group. This remark reduces one's work by almost one-half when the calculations of the next section are carried through in detail.

We take the ten x^ρ occurring in (5.2) and (5.3) as co-ordinates in $\mathscr{P}$. It is clear that for any real x^ρ, A and D and, therefore, P is unitary. Further $\overline{\mathrm{P}}=\overline{\mathrm{A}}'\overline{\mathrm{D}}\overline{\mathrm{A}}=\mathrm{ADA}'=\mathrm{P}$, since $\overline{\mathrm{A}}=\mathrm{A}'$ and $\mathrm{D}=\overline{\mathrm{D}}$. Thus, for any real x^ρ, P belongs to $\mathscr{P}$, and therefore all P so defined form a sub-set $\mathscr{R}$ of $\mathscr{P}$. Actually $\mathscr{R}$ is identical with $\mathscr{P}$, but we do not need to prove this here in order to show that $\mathscr{P}$ has infinite volume. It will be sufficient to show that the set $\mathscr{R}$ is infinite.

In the next section we shall show that if dy^μ are l.o.c. then the jacobian

$$|\partial y^\mu/\partial x^\rho|=\pm\cos x^5\,.\cos x^{13}\,.\tan(x^{14}+x^2)\,.\tan(x^{35}+x^{14})$$
$$.\tan(x^2+x^{35})\,.\tan(x^{14}-x^2)\,.\tan(x^{35}-x^{14}),\ \tan(x^2-x^{35}). \quad (5.4)$$

This is infinite along the nine dimensional hypersurfaces of $\mathscr{R}$ for which the argument of any of the tangent factors is an odd multiple of $\pi/2$. On such surfaces the jacobian has a pole of order one which gives rise to a logarithmic infinity in the integral of the jacobian over the range of x^ρ. Q.E.D.

6. *Calculation of the Jacobian.*

We find it convenient to restrict the range of specific Greek letters as follows :—

σ : 0, 2, 14, 35

τ : 1, 3, 15, 24, 25, 34

ν, μ : 0, 2, 14, 35, 1, 3, 15, 24, 25, 34.

α, β : 4, 5, 45, 12, 13, 23

ρ, λ : 0, 2, 14, 35, 4, 5, 45, 12, 13, 23.

Whenever the order of the terms in a sum or product is important subsequently we shall assume that the indices take on values in the order in which they are written above.

We wish to calculate $|\partial y^{\mu}/\partial x^{\rho}|$ where

$$\mathrm{P}(x^{\rho}+dx^{\rho})=\exp(\tfrac{1}{2}id\mathrm{Y})\mathrm{P}(x^{\rho})\exp(\tfrac{1}{2}id\mathrm{Y}). \quad . \quad . \quad . \quad (6.1)$$

$d\mathrm{Y}=dy^{\mu}\mathrm{E}_{\mu}$, and P is expressed in terms of x^{ρ} by (5.1). If we subject $\mathscr{P}$ to a $\mathscr{P}$-admissible transformation arising from $\mathrm{A}'(x^{\rho})$ the volume element remains unchanged, that is $|\partial y^{\mu}/\partial x^{\rho}|=|\partial z^{\lambda}/\partial x^{\rho}|$ where

$$\begin{aligned}\mathrm{A}'(x^{\alpha})\mathrm{A}(x^{\alpha}+dx^{\alpha})\mathrm{D}(x^{\sigma}+dx^{\sigma})\mathrm{A}'(x^{\alpha}+dx^{\alpha})\mathrm{A}(x^{\alpha})&\\ =\mathrm{A}'(x^{\alpha})\exp(\tfrac{1}{2}id\mathrm{Y})\mathrm{A}(x^{\alpha})\mathrm{D}(x^{\sigma})\mathrm{A}'(x^{\alpha})\exp(\tfrac{1}{2}id\mathrm{Y})\mathrm{A}(x^{\alpha})&\\ =\exp(\tfrac{1}{2}id\mathrm{Z})\mathrm{D}(x^{\sigma})\exp(\tfrac{1}{2}id\mathrm{Z}), \quad . \quad . \quad . \quad . \quad . \quad . \quad . \quad . \quad . \quad (6.2)&\end{aligned}$$

and $d\mathrm{Z}=\mathrm{A}'(x^{\alpha})d\mathrm{Y}\mathrm{A}(x^{\alpha})$. Since $\mathrm{A}'(x^{\alpha})\mathrm{A}(x^{\alpha}+dx^{\alpha})$ differs from the identity by quantities of the first order in dx^{ρ}, we set

$$\mathrm{A}'(x^{\alpha})\mathrm{A}(x^{\alpha}+dx^{\alpha})=\exp(\tfrac{1}{2}id\mathrm{F}), \quad . \quad . \quad . \quad . \quad . \quad . \quad (6.3)$$

where $d\mathrm{F}=df^{\alpha}\mathrm{E}_{\alpha}$. As so defined, df^{α} will depend only on the six x^{α}, and to find $\partial f^{\alpha}/\partial x^{\beta}$ we set all $dx^{\alpha}=0$ except dx^{β}.

Thus, if only $dx^{4}\neq 0$, (6.3) becomes

$$\exp(\tfrac{1}{2}id\mathrm{F})=\exp-\tfrac{1}{2}i(x^{45}\mathrm{E}_{45}+x^{5}\mathrm{E}_{5})\exp(\tfrac{1}{2}idx^{4}\mathrm{E}_{4})\exp\tfrac{1}{2}i(x^{5}\mathrm{E}_{5}+x^{45}\mathrm{E})_{45}, \quad . \quad . \quad . \quad (6.4)$$

after all the factors on the left side of (6.3) which cancel are eliminated. Now, to the first order,

$$\exp(\tfrac{1}{2}id\mathrm{F})=\mathrm{E}_{0}+\tfrac{1}{2}idf^{\alpha}\mathrm{E}_{\alpha}$$

and

$$\exp(\tfrac{1}{2}idx^{4}\mathrm{E}_{4})=\mathrm{E}_{0}+\tfrac{1}{2}idx^{4}\mathrm{E}_{4}\,;$$

so, (6.4) becomes

$$\begin{aligned}df^{\alpha}\mathrm{E}_{\alpha}&=dx^{4}\exp-\tfrac{1}{2}i(x^{45}\mathrm{E}_{45}+x^{5}\mathrm{E}_{5})\mathrm{E}_{4}\exp\tfrac{1}{2}i(x^{5}\mathrm{E}_{5}+x^{45}\mathrm{E}_{45})\\ &=dx^{4}\mathrm{E}_{4}\exp(\tfrac{1}{2}ix^{45}\mathrm{E}_{45}\exp(ix^{5}\mathrm{E}_{5}\exp(\tfrac{1}{2}ix^{45}\mathrm{E}_{45}),\text{ by }(2.6)\\ &=dx^{4}\mathrm{E}_{4}(\cos x^{5}\exp(ix^{45}\mathrm{E}_{45})+i\sin x^{5}\mathrm{E}_{5})\\ &=dx^{4}(\cos x^{45}\cos x^{5}\mathrm{E}_{4}-\sin x^{45}\cos x^{5}\mathrm{E}_{5}+\sin x^{5}\mathrm{E}_{45}).\end{aligned}$$

Thus, $\quad \partial f^{4}/\partial x^{4}=c_{45}c_{5}, \quad \partial f^{5}/\partial x^{4}=-c_{5}s_{45}, \quad \partial f^{45}/\partial x^{4}=s_{5},$

where $s_\alpha = \sin x^\alpha$ and $c_\alpha = \cos x^\alpha$. Proceeding in this way we obtain the following matrix for $\partial f^\alpha / \partial x^\beta$:—

$$\begin{array}{lcccccc}
\beta/\alpha. & 4. & 5. & 45. & 12. & 13. & 23. \\
4\ldots\ldots\ldots & c_5 s_{45} & s_{45} & & & & \\
5\ldots\ldots\ldots & -c_5 s_{45} & c_{45} & & & & \\
45\ldots\ldots\ldots & s_5 & & 1 & & & \\
12\ldots\ldots\ldots & & & & c_{13} c_{23} & s_{23} & \\
13\ldots\ldots\ldots & & & & -c_{13} s_{23} & c_{23} & \\
23\ldots\ldots\ldots & & & & s_{13} & & 1
\end{array}$$

Unless otherwise indicated the elements of the above matrix are zero. Setting $df^\sigma = dx^\sigma$ for the four remaining co-ordinates we obtain the ten-way jacobian

$$|\partial f^\rho / \partial x^\lambda| = \cos x^5 . \cos x^{13}. \quad . \quad . \quad . \quad . \quad . \quad . \quad . \quad (6.5)$$

All that remains is to calculate $|\partial z^\lambda / \partial f^\rho|$, which is done by means of equations (6.2) and (6.3) which together give

$$\exp(\tfrac{1}{2} i d\mathrm{Z}) \mathrm{D}(x^\sigma) \exp(\tfrac{1}{2} i d\mathrm{Z}) = \exp(\tfrac{1}{2} i d\mathrm{F}) \mathrm{D}(x^\sigma + dx^\sigma) \exp(\tfrac{1}{2} i d\mathrm{F}). \quad (6.6)$$

This immediately gives, correct to the first order,

$$dz^\lambda \mathrm{A}_\lambda = df^\sigma \mathrm{A}_\sigma + df^\alpha \mathrm{B}_\alpha, \quad . \quad . \quad . \quad . \quad . \quad . \quad . \quad . \quad (6.7)$$

where
$$\mathrm{A}_\lambda = \mathrm{E}_\lambda \mathrm{D}(x^\sigma) + \mathrm{D}(x^\sigma) \mathrm{E}_\lambda \quad . \quad . \quad . \quad . \quad . \quad . \quad (6.8)$$

and
$$\mathrm{B}_\alpha = \mathrm{E}_\alpha \mathrm{D}(x^\sigma) - \mathrm{D}(x^\sigma) \mathrm{E}_\alpha . \quad . \quad . \quad . \quad . \quad . \quad . \quad (6.9)$$

Since the E_σ mutually commute they commute with $\mathrm{D}(x^\sigma)$ and with A_σ. On the other hand, each A_α and B_α commutes with two and anticommute with two E_σ. Thus, by multiplying, (6·7) simultaneously on the right and left by each E_σ and adding the four resulting equations we obtain, since $\mathrm{A}_\sigma = 2\mathrm{E}_\sigma \mathrm{D}$,

$$dz^\sigma \mathrm{E}_\sigma \mathrm{D} = df^\sigma \mathrm{E}_\sigma \mathrm{D}.$$

The D cancels and since the E_σ are linearly independent we have

$$dz^\sigma df^\sigma. \quad . \quad . \quad . \quad . \quad . \quad . \quad . \quad . \quad . \quad . \quad . \quad (6.10)$$

Multiplying (6.7) on the right and left by E_{35} and adding the resulting equation to (6.7) gives us

$$dz^1 \mathrm{A}_1 + dz^{24} \mathrm{A}_{24} = df^4 \mathrm{B}_4 + df^{12} \mathrm{B}_{12}. \quad . \quad . \quad . \quad . \quad (6.11)$$

We deduce from this after a rather lengthy but simple calculation that

$$\frac{\partial z^1}{\partial f^4} \cdot \frac{\partial z^{24}}{\partial f^{12}} - \frac{\partial z^1}{\partial f^{12}} \cdot \frac{\partial z^{24}}{\partial f^4} = \tan(x^{14} + x^2) . \tan(x^{14} - x^2).$$

There is an equation similar to (6.11) involving dz^{15}, dz^{34}, df^{45}, df^{13}, and one involving dz^3, dz^{25}, df^5, df^{23}.

Combining the results of these with (6.10) we have

$$\left| \frac{\partial z^\lambda}{\partial f^\rho} \right| = \tan(x^{14} + x^2) \tan(x^{35} + x^{14}) \tan(x^2 + x^{35}) \tan(x^{14} - x^2)$$
$$\times \tan(x^{35} - x^{14}) \tan(x^2 - x^{35}). \quad (6.12)$$

Now $$\left|\frac{\partial y^{\mu}}{\partial x^{\rho}}\right| = \left|\frac{\partial z^{\lambda}}{\partial x^{\rho}}\right| = \left|\frac{\partial z^{\lambda}}{\partial f^{\rho}}\right| \left|\frac{\partial f^{\lambda}}{\partial x^{\rho}}\right|.$$

Thus, by (6.5) and (6.12), we have formula (5.4) for the required jacobian.

7. *Conclusion.*

Eddington asserts in several places in P. and E. that the finitude of phase space is most essential for his theory ; however, it does not enter directly as a condition in the proof of any of his central results. His proof of the quadratic equation for the ratio of the masses of the proton and electron, however, depends on certain properties of " stereographic co-ordinates " discussed on page 102 of P. and E. In the derivation of equation (7.58) from (7.57) the same error is made as was discussed in section 4 above, and this certainly vitiates his proof of the quadratic equation.

Two means of avoiding the difficulty suggest themselves. We might adopt a different definition of volume (such as that used in the theory of integration on unitary groups) which leads to finite space. Alternatively we might abandon the assumption that all points of phase space are equally likely of occupation by the particles under consideration and arrange that the contribution of the singular loci is insignificant in the total probability distribution. In a letter to the author, in September 1944, Sir Arthur indicated that at that time he favoured the second method.

After writing P. and E., Sir Arthur pursued a statistical approach to his main problems which avoided the necessity of using the above type of argument about the detailed geometry of phase space. He published an account of these investigations in 1943 (6).

References.

(1) Whyte, L. L., ' Critique of Physics.' (Kegan and Paul, London, 1930.)
(2) Eddington, Sir A. S., " The Theoretical Values of the Physical Constants," Proceedings of the Physical Society, liv. p. 491 (1942).
(3) Temple, G. F., Proceedings of the Royal Society, London, series A, cxxvii. p. 339 (1930).
(4) Coleman, A. J., ' A Study in Relativistic Quantum Mechanics,' a thesis submitted to the University of Toronto in 1943 in conformity with the requirements for the degree of Doctor of Philosophy.
(5) Eddington, Sir A. S., " A New Derivation of the Quadratic Equation for the Masses of the Proton and Electron," Proceedings of the Royal Society, London, series A, clxxiv. p. 16 (1940), in the first paragraph of section eight.
(6) Eddington, Sir A. S., " The Combination of Relativity Theory and Quantum Theory," Dublin Institute of Advanced Studies, series A, no. 2.

Queen's University,
Kingston, Ont.
January, 1944.

XXXVIII. *The Electromotive Force of the Selenium Barrier-Layer Photo-Cell.*

By R. A. Houstoun, D.Sc., and A. F. Howatson, M.A.,
University of Glasgow *.

[Received November 3, 1944.]

In a former communication, R. A. Houstoun † described a theory of the selenium barrier-layer photo-cell which gave a better agreement with facts than the previously accepted theory. According to his view the cell has a constant electromotive force E, which sends a current through a resistance r', inversely proportional to the intensity of illumination; thus $r'=k/L$, where k is a constant of proportionality. This current returns partly as a current I through the external resistance R and partly as a current i through an internal resistance r, as shown in fig. 1. An application of Kirchhoff's laws gives

Fig. 1.

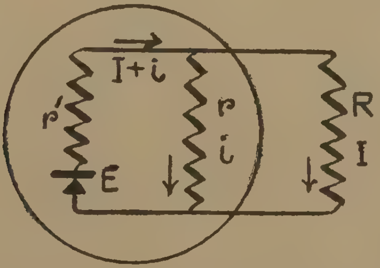

$$\frac{1}{I}=\frac{k}{E}\left(1+\frac{R}{r}\right)\frac{1}{L}+\frac{R}{E}.$$

When 1/I is graphed in terms of 1/L, the intercept on the 1/I axis is given by $1/I_0=R/E$, whence

$$E=RI_0.$$

Thus E can be calculated, and in the paper referred to results were given for five different cells.

The source of light in these determinations was an electric lamp and the current I was varied by changing its distance from the photo-cell. It is necessary that the intensity of this lamp should be constant during the process. In the former determinations the lamp was run off the lighting circuit and changes in the voltage removed by a variable resistance. The purpose of the present investigation was to measure E with greater accuracy in order to find whether it varied with the colour of the light, and to make a further study of the properties of the cells generally. In the present investigation the variation of the intensity of the lamp with the voltage of the lighting circuit was first determined; afterwards, during the measurements, this voltage was continually measured by an accurate electrometer and the effect of any variation removed by means of the preliminary results. This procedure was more satisfactory than the former one.

---

* Communicated by the Authors.
† Phil. Mag. xxxiii. p. 226 (1942).

Fig. 2

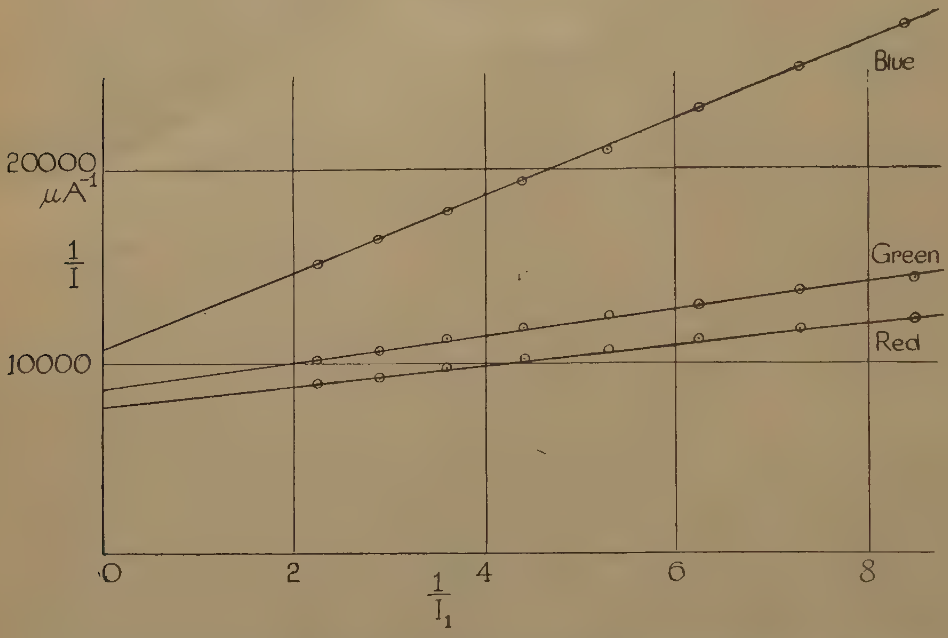

The photo-cells were those used in the former investigation with one addition. They are as follows:—

A. A Weston photronic which has been in use ten years.

B. A Weston photronic obtained three years ago. The sensitive area of these cells is circular, 37 mm. in diameter, and it is protected by glass.

C. A cell supplied by Renny and Wender. Area circular, 38 mm. in diameter. No glass cover.

D. Cell supplied by Evans Electro-selenium, Ltd. Rectangular, 30 × 13 mm.^{2}. No glass cover.

E. Cell of unknown origin. Rectangular, 30 × 15 mm.^{2}. No glass cover.

F. Cell supplied by Evans Electro-selenium, Ltd. Rectangular, 34 × 15 mm.^{2}. No glass cover.

The source of light was a 500 watt Osram projector lamp, the area of the filament being approximately 3 cm.^{2}. The photo-cell was attached to a carrier which moved along a photometer bench. The three filters of a Wratten tricolour set were placed in turn immediately in front of the photo-cell and readings of the photoelectric current taken at distances between 15 and 29 cm. from the source. Some of the cells were subject to fatigue, and to minimise this effect they were exposed to the light only when readings were being taken. The variation in mains voltage during a series of observations was usually about one per cent., and the correction to the current readings of the same magnitude.

The type of result obtained is shown in fig. 2, which is for cell E and external resistance 2000 ohms. The reciprocal of the current is plotted against the reciprocal of the intensity of illumination, expressed in arbitrary units. The graph is in every case a straight line which cuts the ordinate above the origin, the intercept being R/E.

The e.m.f.'s obtained for cells A to E are shown in the following table :

Cell.	Colour.	R (in ohms).	Number of determinations.	E (in volts).
A	Red	2000, 3000	6	0·235±·002
	Green	2000, 3000	6	0·189±·001
	Blue........	1000, 1500	6	0·160±·002
B	Red	2000, 3000	6	0·258±·001
	Green	2000, 3000	6	0·219±·001
	Blue........	1500, 2000	6	0·192±·002
C	Red	500, 1000	6	0·058±·002
	Green	500, 1000	6	0·054±·002
	Blue........	500, 1000	6	0·044±·002
D	Red	2000, 3000, 5000	8	0·424±·002
	Green	2000, 5000	6	0·475±·003
	Blue........	500, 1000, 2000	7	0·528±·016
E	Red	2000, 3000	6	0·260±·001
	Green	2000, 3000	6	0·240±·001
	Blue........	1000, 2000	6	0·201±·002

The third column gives the external resistances used, the fourth the number of independent determinations and the fifth the mean result in volts, together with its probable error. In the case of the four cells A, B, C, E, the e.m.f. increases from the blue to the red end of the spectrum, but for cell D the increase is in the opposite direction. It should be noted, that owing to an error in calculation the e.m.f. for cell C for white light is incorrectly given as 0·73 volt in the former paper. This should be 0·073 volt.

Why E varies with the colour it is impossible to say. We expected that there would be in all cases an increase from red to blue owing to the increase in the value of the quantum in this direction. But the change recorded is the other way, except for cell D. It is clear that in

Fig. 3.

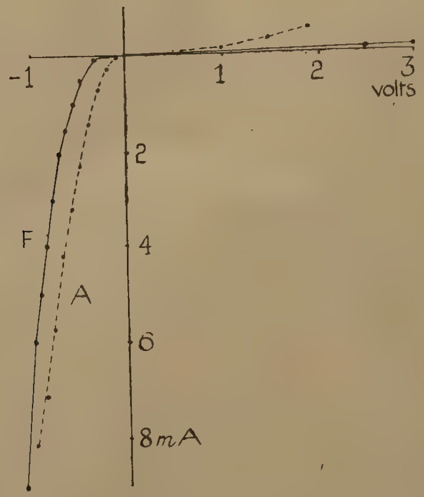

Fig. 4.

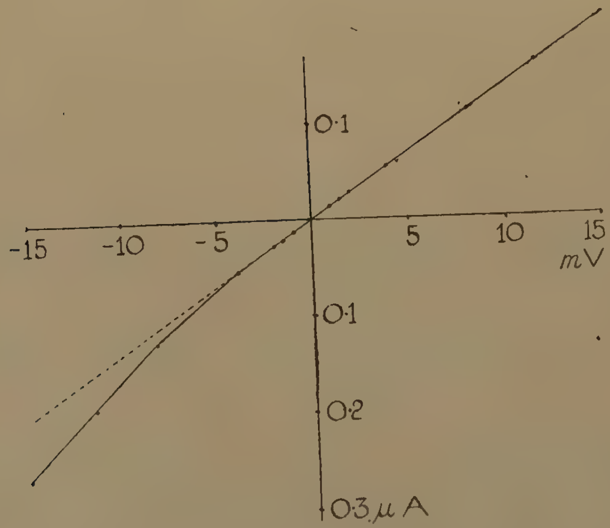

some cases this variation of E with colour will be a source of error, when the cell is used for heterochromatic photometry.

The effect of applying an e.m.f. to a photo-cell was next investigated. Cells A and F were used and they were kept in the dark. The results are shown in fig. 3, and it is obvious from this figure that the cell F is a first class rectifier. Observations were continued with this cell on the left to —2·45 volts ; then the current was 60 milliamperes, but beyond —1·5 volts the readings became irregular. A is not so good a rectifier as F.

The shape of the curve for F was then investigated with greater accuracy in the neighbourhood of the origin, the current being measured by a moving-coil galvanometer. The results are given in fig. 4. On the right the curve is a straight line ; on the left a deviation from linearity is first definitely shown at —2 millivolts.

Light was then applied to cell F simultaneously with the e.m.f. Fig. 5 shows the arrangement used : S is a battery, K a key, W a 500 ohm resistance, which was used as potentiometer, R a variable resistance, V a voltmeter, M a microammeter, P the photo-cell and G a pearl lamp. First of all K was kept open and the distance of G from P adjusted, so that the reading on M was 20 microamperes. Then K was closed and different voltages applied to the photo-cell by moving the contact at W, readings being taken at each voltage with the light on and off. The results are shown in fig. 6 for the case of R=0, the upper curve being for light on and the lower for light off.

Fig. 5.

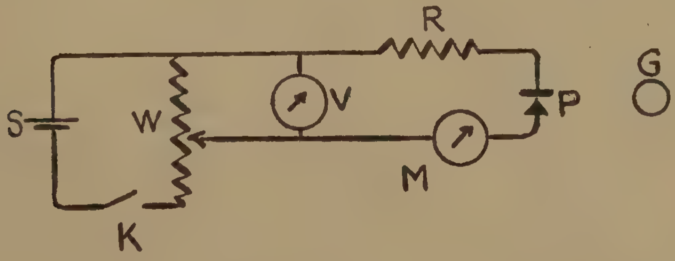

It should be noted that the scale of volts is different on the two sides of the origin. It should also be noted that the photoelectric current flows through the cell in the direction in which the conductivity is low, so that if the rectifier sign in figs. 1 and 10 is to have its usual meaning, the arrow should be reversed.

On the right the applied e.m.f. and the light are in the same direction. The difference in current increases all the way from 0 to 3 volts being 36·5 μ A. at 3 volts, so that the sensitivity of the cell is increased by the applied e.m.f. On the left the applied e.m.f. opposes the action of the light, completely neutralizing it at A ; beyond A the two curves intersect, light having then no action on the cell whatever. Readings were taken on the right up to 6·9 volts ; at this voltage the current for light off was about 750 μ A. and the readings were becoming irregular. But at about 5 volts the difference between the ordinates of the two curves becomes constant at twice the initial value, so that the gain in sensitivity obtained by using an applied e.m.f. is not worth the extra trouble entailed. On the left the curves were followed to −1 volt; after crossing they keep close and parallel to each other up to this point.

Fig. 6.

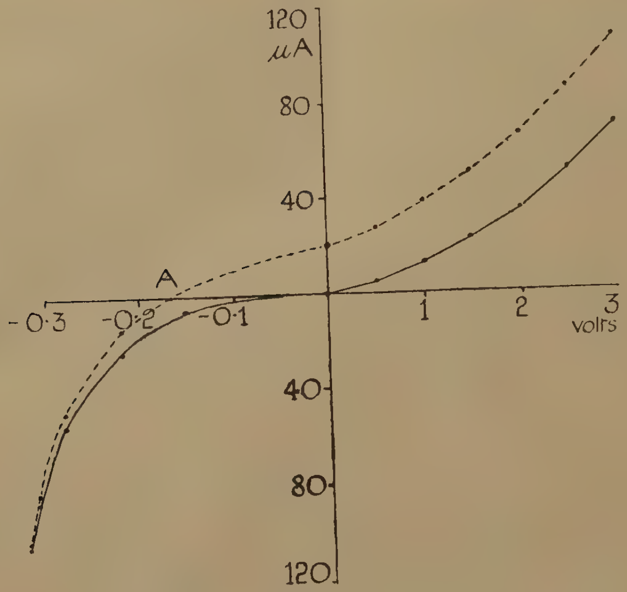

Fig. 7.

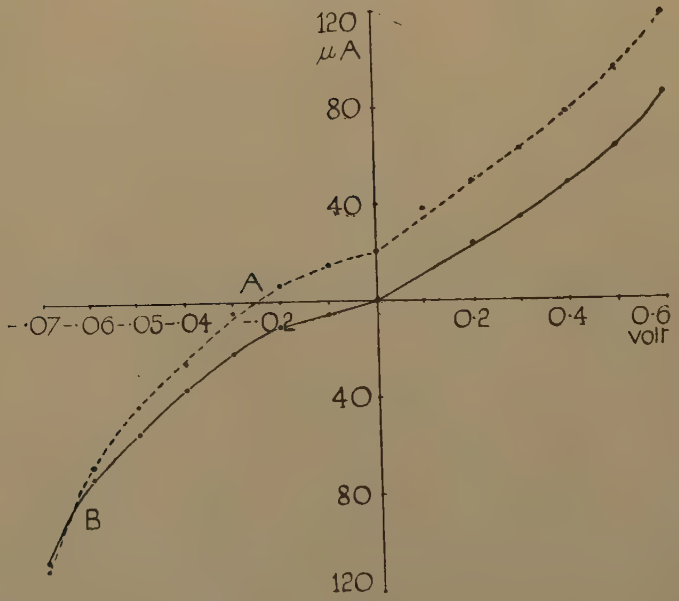

Fig. 7 is fig. 6 repeated for cell A. It shows that there is no essential difference between the two cells. It should again be noted that the scale of volts is different on the two sides of the origin.

It is obvious that the position of the zero point A must vary with the intensity of the light, as it is at the origin for zero intensity. This variation was investigated for cells A and F and the results are shown in fig. 8. Here the abscissæ give the deflection in μ A. produced by the light alone and the ordinates the e.m.f. required to annul it.

The variation of the intersection point with change in intensity was also investigated for cells A and F, and is shown in fig. 9.

Fig. 8.

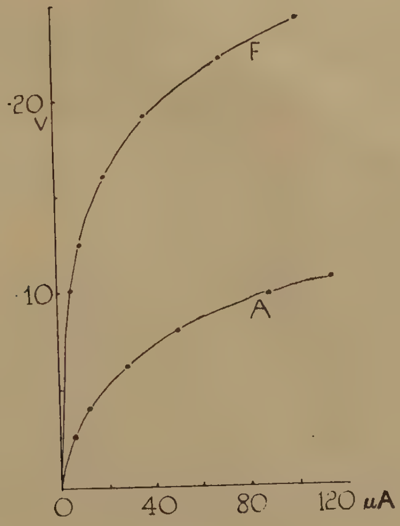

Fig. 9.

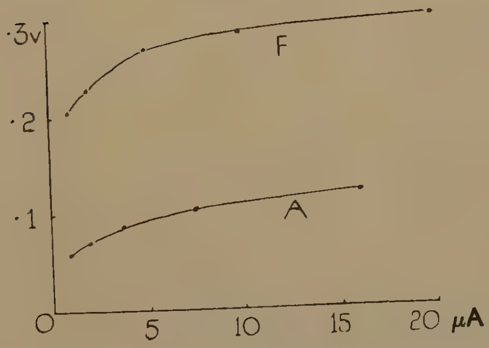

After investigating the combined effect of light and applied e.m.f. qualitatively we attempted to represent it mathematically. Fig. 10 explains itself and leads to the formula

$$E' - RI = \frac{\frac{kI}{L} - \mathbf{E}}{1 + \frac{k}{Lr}},$$

where E′ is the applied e.m.f. and the other symbols have their previous meanings. This formula is the obvious extension of the previous empirical one.

It can be given a theoretical justification. For, suppose the cell forms a condenser discharging externally through R and internally through r. The rate of discharge

$$I+i=I-\frac{E'-RI}{r}.$$

The potential difference between the plates of the condenser is RI—E′. Electrons are emitted between the plates with varying degrees of energy and we assume that the number liberated per second is proportional to the intensity of illumination L, and that the law of distribution of energy is

$$ce^{-cV}\,dV,$$

Fig. 10.

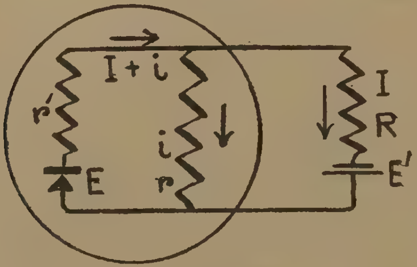

where V is the voltage required to stop an electron. V varies from 0 to E, where E is the e.m.f. of the photo-cell. The fraction of the electrons available to charge the condenser is

$$\frac{\int_{RI-E'}^{E} ce^{-cV}\,dV}{\int_{0}^{E} ce^{-cV}\,dV}=\frac{e^{-c(RI-E')}-e^{-cE}}{1-e^{-cE}}.$$

The rate of charge is the above multiplied by aL, where a is a constant of proportionality. It becomes, on taking the first two terms of the expansions and writing $k=(1-e^{-cE})/ac$,

$$\frac{L}{R}(E+E'-RI),$$

and on equating this to the rate of discharge we obtain the same formula as before.

Putting the matter in words: On the right-hand side of figs. 6 and 7 the applied e.m.f. lowers the potential of the plate and enables more of the electrons to reach it. On the left-hand side it raises the potential and may stop the current altogether. But the theory is not applicable beyond the point A; there is nothing in it to explain why the current should flow the other way.

If we put R=0 in the formula,

$$\frac{kI}{L}=E'\left(1+\frac{k}{Lr}\right)+E,$$

and the increase in the difference of the ordinates on the right-hand side of figs. 6 and 7 should be proportional to E′. This is approximately true.

A more exacting test of the truth of the formula was made with the arrangement depicted in fig. 5. The cell was first kept in the dark, R set in succession at values from 1000 to 10,000 ohms, and E′ adjusted so that in each case the reading of M was 80 μ A. E′ was then graphed against R. This was repeated with the photo-cell illuminated at different intensities. The results are shown in fig. 11; the graphs are as they should be, straight lines, the gradient of which is I. The first four are for cell A, the last for cell F. A set of readings was also obtained for F, which agreed with the third set for A within the error of observation. The last two lines are for very large values of L. The intercept on the E′ axis is then −E; the values given by the graph are 0·2 volt and 0·34 volt, which is what we should expect.

Fig. 11.

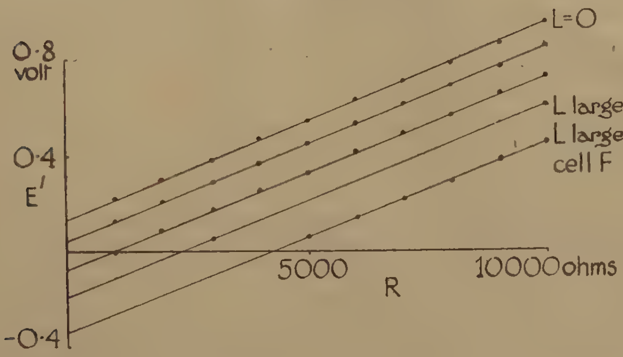

As the investigation has shown that there is no advantage in using an applied e.m.f., it does not seem desirable to pursue the verification of the formula further.

XXXIX. *The Surface Tension of Molecular Solutions.*

By HENRY MCCORMICK *.

[Received October 2, 1944.]

Abstract.

A method for determining the molecular weight is given, as it was verified that molecular solutions produce the same increase in the surface tension of the solute. The measurements were made with an improved apparatus based on the falling drop method. It was found that for a certain diameter of the dropping surface (5 mm.), the surface tension in dynes/cm. had the same numerical value as the mass of one drop in milligrams.

Description of Apparatus and Method.

This article gives a complete account of some experiments which were carried out in Rumania in 1939, the results of which were published jointly with Mr. C. Salceanu †.

The apparatus to be described is shown in fig. 1. It is surrounded by a thermostat which has the outside part (*k*) full of kieselguhr and the inner part (*e*) contains water, the temperature of which is measured by the thermometer (*t*). It has also two windows (*m*), through which the drop can be seen, one in front and the other at the back—the latter being lighted by a lamp. The apparatus is placed in a glass cylinder (f.d.f.) which is fixed with screws to the tripod. It has a reservoir (*b*) which contains the liquid whose surface tension is to be measured, and a thermometer (*t′*) graduated in 1/10° C.

The drops are formed at C, which is removable, and fall into the vessel (*h*) fixed at the other end of the cylinder (f.d.f.).

The dropping surface (C) has the form shown in fig. 2, and is made of platinum, but trials with other materials show that the nature of the surface has no influence when no chemical reactions occur between the liquid and the surface.

When the measurements are taken, the vessel (*h*) is pushed up by the spring (*g*) and the fall of the drops is regulated by the tap (*r*) at a rate of about one every 12 seconds. (It was found that the weight of the drops became constant after 8–9 secs.)

---

* Communicated by the Author.

† C. Salceanu et Henry McCormick. C. R. Paris, ccviii. pp. 1278 and 1989 (1939). C. R. Inst. Sc. Rumania, iii. no. 3, pp. 249 and 416 (1939).

To determine the constant of the apparatus, use is made of the simple formula of Tate,

$$K=\frac{M.g}{\gamma},$$

and selecting a few liquids with known surface tension.

Because of the inaccurate results obtained when determining the value of K, it was decided to study its variation for different diameters and liquids.

Fig. 1.

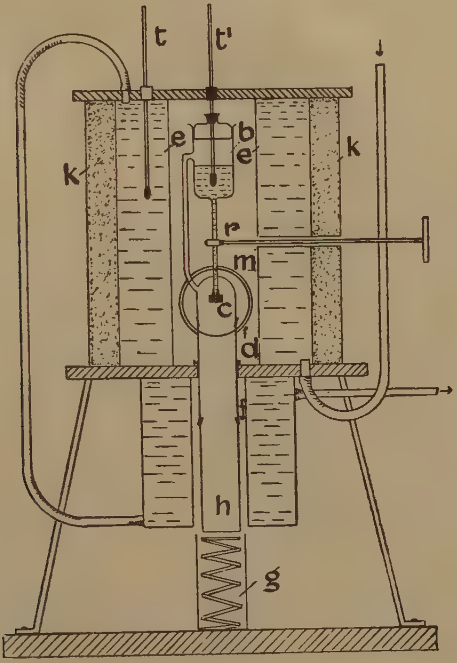

Fig. 2.

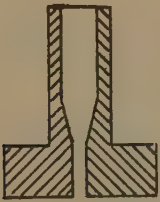

These variations can be seen in fig. 3, which shows the results for the diameters 4–5–6 mm., where the phenomenon occurs.

The following values for (20° C.) were taken from tables of constants :—

Water .... =72·8 dynes/cm.
CS_2 .... =31·4 ,,
CCl_4 .... =26·66 ,,
Acetone .... =23·0 ,,

Drawing the curves of the constants given by the above liquids, it will be seen that the variation with the diameter is almost linear, but the factor of proportionality, K, is not the same for all liquids. The curves, however, have a point of intersection corresponding to the diameter of 5 mm.

It is interesting to note that the value of the constant for that particular diameter is 0·980, the same numerical value as the acceleration of gravity.

Hence it follows that *the surface tension in dyne/cm. has the same numerical value as the mass of one drop in milligrams*, when a surface of 5 mm. is used.

Fig. 3.

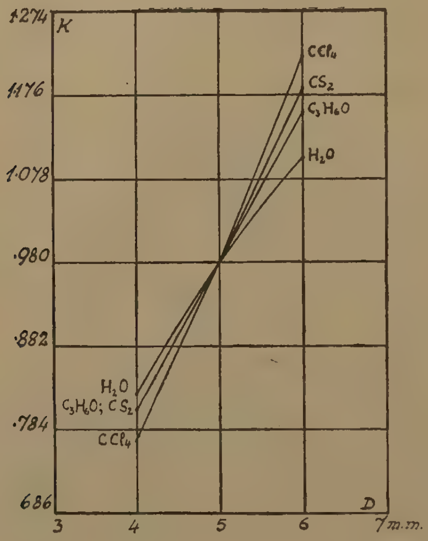

A very small variation from this diameter, as little as 2/100 mm.. gives an appreciable difference to the constant.

For each measurement a number of 50 drops were collected in the weighed vessel and the measurements were repeated several times, but it was observed that all the results were in agreement. The experiment was carried out with 29 liquids and the values obtained by this method were in agreement with the latest values given in the tables of constants.

Table I. shows the results obtained at 20° C. The first column shows the surface tension measured by this method, the second the surface tension taken from the International Critical Table (I.C.T.), and the third Ducleux.

The liquids indicated by (*x*) are taken from the Organic Chem. Lab., Bucharest, and the others from the firms " Merk " and " Kalbaum," labelled " For Analysis " :—

TABLE I.

Substance.	γ at 20° C. in dyne/cm.	γ at 20° C. I.C.T.	γ given by D 20° C.
Water	72·8	72·8	72·8
Benzene	28·3	28·86	28·5
Carbon bisulphide	31·5	31·38	33
Carbon tetrachloride	26·8	26·66	26
Chloroform	27·0	27·13	27
Acetone	23·2	23·7	23
Cyclo hexane	24·5	25·3	26·5
Ether (x)	16·8	17·1	16·5
Methyl alcohol	21·85	22·61	23
Ethyl alcohol	22·1	22·3	23
Propyl alcohol	23·04	23·8	23·5
Butyl alcohol	23·6	24·6	—
Octyl alcohol (x)	26·3	27·53	—
Formic acid	37·68	37·6	37
Acetic acid	27·9	27·63	23·5
Propionic acid	25·2	26·7	—
Butyric acid	25·88	26·8	—
Capronic acid (x)	26·96	—	—
Caprylic acid (x)	28·00	28·82	—
Heptane	19·84	—	—
Aniline	42·56	42·58	42
Nitrobenzene (x)	42·00	43·38	42
Glycerine	62·00	63·4	63
Pyridine (x)	38·3	38	37
Quinoline (x)	44·65	45	45
Methyl napthalene (a)	38·76	—	—
Ethyl acetate	23·2	23·75	24
Amyl acetate	23·5	—	24
Izo octane (trimetil pentane, 2, 2, 3).	18·32	—	—

To sum up, it was found that:

For accurate measurements of the surface tension by the drop method a diameter of 5 mm. must be used, measured accurately to within 1/100 mm., in which case the surface tension in dyne/cm. has the same numerical value as the mass of one drop in milligrams.

* * *

Some interesting results were found when we measured the surface tension of molecular solutions.

They are shown in Table II. The columns show: the solute, the solvent, concentration (grams of substance, in 10 c.c. solvent), the normality of the solution, and the difference between the surface tension of the pure solvent and that of the solution.

The measurements were taken at 20° C. The surface tension of the pure solvent was measured before every determination :—

TABLE II.

Substance.	Solvent.	Conc. gr. 10 c.c.	Normality.	Diff. in dyne/cm.
		Gr.		
Glucose	Water	0·90	½ normal	0·40
,, ...	,,	1·80	normal	0·82
,, ...	,,	2·70	$\frac{3}{2}$ normal	1·20
,, ...	,,	3·60	2 normal	1·63
Ammon. sulphocyanide	,,	0·38	½ normal	0·40
,, acetate......	,,	0·385	½ normal	0·41
Naphthalene	Benzene	0·64	½ normal	0·40
Phenanthrene	,,	0·89	½ normal	0·44
Triphenyl methane ...	Carbon bisulphide	1·22	½ normal	0·40
,, amine	,, ,,	1·225	½ normal	0·42
Acenaphthene........	,, ,,	1·54	normal	0·81
Phenanthrene	,, ,,	1·78	normal	0·84
Naphthalene	,, ,,	1·28	normal	0·78
Diphenylamine	,, ,,	1·69	normal	0·80
Iodine (I_2)...........	,, ,,	1·27	½ normal	0·42
Naphthalene	Acetone.........	1·28	normal	0·80
Phenanthrene	,,	1·78	normal	0·82
Triphenyl methane ...	,,	1·22	½ normal	0·40
Iodine (I_2)	,,	0·635	¼ normal	0·21
Mercuric chloride	,,	2·716	normal	0·82
Menthol	Ethyl alcohol ...	1·56	normal	0·78
Camphor	,, ,,	1·52	normal	0·80
Naphthalene	Carbon tetrachloride	1·28	normal	0·77
Phenanthrene	,, ,,	1·78	normal	0·80

From this table it will be seen that when phenomena such as chemical reaction, molecular association or dissociation do not occur.

1. The equimolecular solutions cause the same increase in the surface tension of the pure solvent, namely : 0·80 dyne/cm.

2. The increase is proportional to the number of gram-molecules dissolved in the solvent.

3. The increase is independent of the nature of the solvent.

These results can be expressed in the following formula :

$$\Delta\gamma = K\frac{1000.W}{v.M} \quad . \; . \; . \; . \; . \; . \; . \; . \; . \quad (1)$$

in which

$\Delta\gamma$=the increase in the surface tension of the solvent.

K=a constant and represents the increase in the surface tension corresponding to one gram-molecule of solute, numerically 0·8 dyne/cm.

W=the weight in grams of dissolved solute.

M=the molecular weight of the solute.

v=the volume in c.c. of the solvent.

(When, for example, we dissolve a gram-molecule of any substance in a litre (1000 c.c.'s) of any solvent,

v=1000 c.c.

W=M

The formula is reduced to

$\Delta\gamma = K = 0{\cdot}8$ dyne/cm.)

From the first formula we can find the molecular weight of the solute by the increase in the surface tension of the solvent produced by the solute.

$$M = K\frac{1000 . W}{v . \Delta\gamma} \quad \ldots\ldots\ldots\ldots \quad (2)$$

Weighing a quantity W of substance and dissolving it in a volume v of any liquid we can find M, the molecular weight, by measuring the increase in the surface tension produced by this solute.

The molecular weight of Iodine measured by this method corresponds to the molecule I_2. This is in perfect agreement with measurements given by other methods.

During these experiments deviations have been obtained from this law, especially in the case of water as a solvent. In this case some solutes cause an increase in the surface tension, because of their dissociation.

Below are given some of the results obtained :—

TABLE III.

Substance.	Solvent.	Solution.	$\Delta\gamma$.
NH_4Cl	Water.	normal	1·61
KCl	,,	,,	1·53
NaCl..............	,,	,,	1·64
CuSO4 (7.H_2O)	,,	½ normal	0·83
$CaCl_2$ (6 H_2O)......	,,	normal	2·50

This table shows that in the case of electrolytes the increase in the surface tension is greater than in the case of non-electrolytes shown in Table II. The increase is approximately double for the first four solutions and treble in the case of $CaCl_2$.

XL. *On the Accumulation of Chance Effects and the Gaussian Frequency Distribution.*

To the Editors of the Philosophical Magazine.

GENTLEMEN,—

I WISH to draw attention to the following points with reference to the article by Dr. L. Silberstein on "The Accumulation of Chance Effects and the Gaussian Frequency Distribution," appearing in your June, 1944, issue.

The first small point refers to a misprint on page 403 of $\Phi\left(\sqrt{\frac{3\pi}{2}}\right)$ for what should obviously read $\Phi\left(\sqrt{\frac{3n}{2}}\right)$.

A more important point refers to the evaluation of the integral of equation (9) on the previous page, namely

$$P_n=\frac{2}{\pi}\int_0^\infty\left\{\frac{\sin v}{v}\right\}^n dv.$$

Dr. Silberstein gives in his paper the values of P_n for $n=1$, 2, 3, 4, 5 and 6, stating "so far as we know, these integrals have not been previously determined," and suggesting that mechanical quadrature would give the values for larger n.

It would appear that the author is unfamiliar with Edwards' book on the Integral Calculus *; this is less surprising when one fully realizes what a great store of results there is in these two volumes.

But in Volume II., Arts. 1023–1034 are devoted to the evaluation of integrals of the form

$$u_{m,n}=\int_0^\infty\frac{\sin^m x}{x^n}dx \quad (\text{with } m\geqslant n),$$

including a recurrence formula and culminating in a general expression given in Art. 1033. These are equivalent to the following :—

$$(n-1)(n-2)P_n+n^2U_{n-2}-n(n-1)P_{n-2}=0$$

and

$$P_n=\frac{1}{2^{n-1}(n-1)!}\left\{n^{n-1}-n(n-2)^{n-1}+\frac{n(n-1)}{1.2}(n=4)^{n-1}\right.$$
$$\left.-\frac{n(n-1)(n-2)}{1.2.3}.(n-6)^{n-1}+\ldots\right\}$$

to $\frac{n}{2}$ or $\frac{n+1}{2}$ terms, as n is even or odd

where $$U_{n-2}=\frac{2}{\pi}\int_0^\infty\frac{\sin^n x}{x^{n-2}}x.$$

---

* 'A Treatise on the Integral Calculus,' by Joseph Edwards (Macmillan).

In the same reference is given the values of P_n for $n=1$ to 7, including $P_6=\frac{11}{20}$ or $\frac{88}{160}$ in place of $\frac{83}{160}$ as given by Dr. Silberstein on page 399.

The following table gives the values of P_n for $n=1$ to 12 in both rational and decimal form, with values of U_n (with which these P_n were checked, using the above recurrence relation) and of $Q_n=\sqrt{\frac{6}{\pi n}}$ to which P_n approximates. The use of Q_n as an approximation to P_n may not be regarded as good for some purposes, since there is nearly 1·3 per cent. error even for $n=12$.

n.	P_n.		Q_n.	U_n.
1		1·0000 0000	1·3819 7660	·5000 0000
2		1·0000 0000	·9772 0502	·5000 0000
3	3/4	·7500 0000	·7978 8456	·3125 0000
4	2/3	·6666 6667	·6909 8830	·2500 0000
5	115/192	·5989 5833	·6180 3872	·2005 2083
6	11/20	·5500 0000	·5641 8958	·1666 6667
7	5887/11520	·5110 2431	·5223 3806	·1411 1328
8	151/315	·4793 6508	·4886 0251	·1215 2778
9	259723/573440	·4529 2097	·4606 5887	·1060 7164
10	15619/36288	·4304 1777	·4370 1937	·0936 3426
11	381, 773, 117/928, 972, 800	·4109 6264	·4166 8162	·0834 4824
12	655177/1663200	·3939 2557	·3989 4228	·0749 8264

A final detail, one perhaps not worth mentioning, is that the direct comparison of equation (10)

$$p_n(\xi)=\sqrt{\frac{6}{\pi n}}\,e^{-\frac{6}{n}\xi^2}$$

with the Gaussian law

$$z=\frac{1}{\sigma\sqrt{2\pi}}\,e^{-\frac{\xi^2}{2\sigma^2}}$$

shows directly that $\sigma=\sqrt{\frac{n}{12}}$.

These simple remarks are submitted as details relating to this important original paper, which initiates new ideas on the aggregate effect of a number of random errors.

Yours faithfully,
A. H. R. Grimsey.

Military College of Science,
Blurton, Longton,
Stoke-on-Trent.
May 7th, 1945.

XLI. *Notices respecting New Books.*

Tables of Elementary Functions. By Fritz Emde. [Pp. lxii+181.] (Leipzig; B. G. Teubner. Reproduced by authority of the Alien Property Custodian by Edwards Bros. Inc., Michigan, U.S.A. English Agent, Scientific Computing Service, Bedford Sq.) $3.20.

A generation has passed since Jahnke and Emde first collected from a wide variety of sources the tables which they thought likely to be of value to physicists and engineers, other than the familiar logarithmic and trigonometric ones. Their belief was justified, and a second edition was published some time ago. When a third edition was called for, it was decided to break it into two parts, the earlier of which was reviewed here when it appeared. It contained all the more " advanced " tables, such as Elliptic and Bessel functions, from the older editions with much additional matter. The second part appeared in Germany in 1940 but has only now become available here. It contains a vast extension of that part of the collection which deals with elementary functions. Thus there are powers of integers up to the fifteenth, fractional powers and powers of the smaller primes up to the twenty-seventh or higher. A number of tables are provided to simplify numerical work with complex numbers, and others for solving quadratics and cubics. The trigonometrical functions which are given are tabulated in degrees, fractions of a right angle, and in radians. Similarly, there are tables of hyperbolic and exponential functions, and (particularly valuable) tables of the inverses of these functions.

So many miscellaneous functions—Planck's, Langevin's, Tschebysheff's polynomials among others—are given, that each potential reader should browse in the volume for a time so that, when he needs a particular function he may know whether it is likely to be there or not. The changes which have passed since the first edition, in particular the great use now made of calculating machines, have been kept well in mind, and the tables are arranged with this in view. In general, linear interpolation is possible to the accuracy given, and first differences are given where needed. J. H. A.

Sechsstellige trigonometrische Tafel. By Hermann Brandenburg. [Pp. xxiv +304]. (Leipzig: Alfred Lorentz. Reproduced by authority of the Alien Property Custodian by Edwards Bros. Inc., of Michigan, U.S.A.) Price $5.00.

Eight-figure and seven-figure tables of the natural trigonometric functions are already available, but a well arranged set of six-figure tables is a desideratum for many kinds of work. Brandenburg's tables give the sine, cosine, tangent and cotangent of angles in the first quadrant at intervals of 10″, with proportional parts. For the ratios less than unity, the accuracy is to six decimal figures; for their reciprocals it is to six or more significant figures, and this does not always reach six decimal places. There is a supplementary table giving cotangents to the same accuracy as the main table, but at intervals of 1″ for the first three degrees. Another supplementary table gives the sine and tangent to six significant figures (and therefore to more than six decimal places) for the first degree. There are minor tables for the conversion of mean to sidereal time, and for the conversion of time to arc. A valuable addition is a list of errata discovered by Dr. L. J. Comrie. J. H. A

[*The Editors do not hold themselves responsible for the views expressed by their correspondents.*]

XLII. *The Magnetic Potentiometer Study of Permanent Magnets.*

By Professor L. F. Bates, University College, Nottingham *.

[Received December 5, 1944.]

Abstract.

The use of the magnetic potentiometer in a suitable form for the measurement of the B, H curves of modern permanent magnets of different shapes is described, and details are given of its use for an experimental investigation of the circuit relations of permanent magnets. The measurements are discussed in the light of recent theoretical work.

§ 1. *Introduction.*

Considerable advances have recently been made in the production of new alloys for the manufacture of permanent magnets, and it is proposed to describe in this paper some experiments which show how the magnetic properties of these alloys may be investigated in a physical laboratory with ordinary university equipment. Manufacturers of such alloys usually employ the magnetic testing gear described in B.S.I. 406. This consists of a soft iron disk, mounted in ball-bearings between a pair of pole-pieces adapted to receive the magnet under test, and driven at a constant speed by a small electric motor. Collecting brushes make contact with the spindle and edge of the disk, and the magnet under test thus provides the field of a simple dynamo whose E.M.F. measures the flux produced by the magnet. The magnetic state of the latter is varied by a magnetizing coil of a specified number of turns, which encircles the magnet and which can be supplied with direct current; in the case of horseshoe magnets two magnetizing coils, one on each limb, can be used.

Another method for dealing with bars of these alloys has recently been described by Jellinghaus (1942). The remanent induction in the permanent bar magnet is measured by placing it between the poles of an electromagnet whose base contains a kind of well-made barrelled iron stopper which extends almost across the whole section of the base. In the hollow of the stopper are the windings of a coil which is connected to a fluxmeter. On placing the stopper with the plane of the windings perpendicular to the lines of induction in the iron and then rotating it quickly through 180 degrees, the fluxmeter gives a deflection directly proportional to the flux through the iron, and this is assumed to be the same as the flux through the bar.

---

* Communicated by the Author.

A complete (B, H) curve can be found ballistically by using a form of double electromagnet consisting virtually of two electromagnets of normal shape placed back to back so as to share a common base in which the stopper is located. The electromagnets are excited in opposite senses so that a flux passes through the stopper only when the gap of one electromagnet contains a permanent magnet under test. The flux through the magnet is measured by rotating the stopper, and the applied field is measured ballistically by means of a search coil placed near the bar.

An account is given below of the way in which the magnetic potentiometer may be used in such measurements. It appears to have been used previously (by Lacoste-Tayan, 1938) only for the determination of the demagnetization factors of permanent bar magnets.

§2. *Manufacture of Magnetic Potentiometers.*

The magnetic potentiometer (Chattock, 1887) used in the present experiments was of the small type used by Wolman (1928) and by Bates and Lloyd Evans (1933). The most convenient method of manufacture was as follows:—A piece of ebonite rod, of circular cross-section for large models and of rectangular cross-section for small models, was used as a former and wound from the centre towards one end with No. 40 S.W.G. d.s.c. copper wire. The winding was lightly coated with shellac and then wound back towards the other end to an equal distance from the centre. It was again lightly coated with shellac and wound back to the centre again, so that the two ends of the winding emerged from the middle of the former. The length of the former so wound with two layers of wire was next heated over a flame while it was bent round a metal tube of chosen diameter, an adequate length of bare former material being available, and the uncovered portions were then tied together until the whole was cold. The excess portions were removed and the feet of the former were filed flat until the ebonite was almost down to the wire; the final removal of ebonite was done by careful rubbing on sand-paper until bare wire was just visible. The number of turns in each half layer of the potentiometer was carefully controlled and care taken to make the windings completely symmetrical.

The whole was finally given a heavy coat of shellac. The fine end wires or leads were twisted together and wrapped twice round the middle of the potentiometer to provide material for repairs, which were necessary when the potentiometer was frequently used. The ends of the thin leads were subsequently joined to thicker copper wires and then to copper flex leads. It was found advisable to fix the two ends or feet of the potentiometer to prevent them from opening, as the ebonite tended to straighten. This was best done in the case of larger potentiometers by inserting the ends through two holes in a flat ebonite plate and cementing them in position. In the case of small potentiometers a thread binding was sufficient. The potentiometer was always calibrated during a set of measurements either in a standard solenoid (*cf.* Bates, 1939) or in a uniform field of an electromagnet with plane pole-pieces. The former method is the more reliable.

In the above description of the making of a magnetic potentiometer it has been emphasized that the ends or feet surfaces of the potentiometer were made flat. It was equally important that the surface of any magnetic specimen upon which it was placed should be reasonably plane. When these conditions were satisfied, the deflection of a sensitive galvanometer joined to the leads, which resulted on removal of the small potentiometer from the surface of the specimen, was a direct measure of the field acting upon the specimen in that region in which the potentiometer was placed. Consequently, the complete (B, H) curve for the material of a magnet could be found by the method of the following section.

§3. B, H *Measurements.*

The magnet, when in the form of a straight bar, was placed between the plane pole pieces of an electromagnet, the one used in the present work being that designed by Bates and Lloyd Evans; although a considerably less powerful magnet would normally serve, and it is relatively easy to make a simple apparatus with adjustable gap for the purpose. The middle of the test magnet was covered with a thin layer of (music roll) insulating paper and wound with 40 to 80 turns of thin d.s.c. copper wire, preferably in a single layer, whose ends were connected to a fluxmeter, so that changes in B could be measured directly.

The corresponding values of H were obtained from magnetic potentiometer readings placed first with its feet astride the B coil and clear of insulating material and then removed quickly. The potentiometer consisted of 240 turns wound on a former of $0{\cdot}95 \times 0{\cdot}30$ cm.^{2} cross-section, bent into a semi-circular arch with a distance of 1·25 cm. between the mid-points of the feet. With no other resistance in series with the galvanometer this gave a galvanometer deflection of 10 cm. at 1 metre scale distance when removed from a uniform field of about 400 oersteds.

In the case of horseshoe magnets each test magnet was placed to bridge the gap of the electromagnet, its feet resting on the upper portions of the electromagnet pole-pieces, which were flattened for this purpose over a reasonable area parallel to the line of electromagnet pole-centres. Of course, the maximum fields which could be applied were considerably weaker than those available for straight specimens. The B coil was wound on the arch of the magnet.

It was important to ensure that straight specimens were not exposed to stresses arising from slight movement of the pole-surfaces of the electromagnet. It was always possible to slide the bar without difficulty from between the electromagnet pole-pieces when the current was switched off. There was a tendency for horseshoe magnets to turn quickly through 180 degrees when H slightly exceeded H_c, the coercive field, and such movement was prevented by loose wooden stops.

Prior to recording a set of (B, H) data the test magnet was taken through the full magnetization cycle several times to get the material into a cyclic state. For most purposes, only the demagnetization portion of the (B, H) curve from $H=0$ to $H=-H_c$ is required. Hence, at the start of each measurement the electromagnet current was adjusted to its maximum value and the potentiometer reading taken. The magnet current was then switched off (usually in two steps), and the change of flux recorded. Theoretically, the permanent magnet should now have been in the state $B=B_r$ and $H=0$. This was, however, rarely found to be the case; for, on taking potentiometer readings, small values of H, sometimes positive and sometimes negative, were obtained. These were undoubtedly caused to some extent by imperfections of surface and by the way the magnet rested upon the electromagnet pole-pieces. The main point was, however, that the electromagnet current was zero and the condition was reproducible, and in what follows the corresponding induction is denoted by B_r'.

The electromagnet reversing switch was now turned, the circuit resistances fixed at chosen values and the current again switched on. The permanent magnet then suffered partial demagnetization, the change of flux being recorded by the fluxmeter; the new value of the demagnetizing field was found by the potentiometer. It was generally found unsatisfactory to continue from this stage and observe further successive changes in B and H. There was always a danger of current fluctuation while H was being measured, and serious errors in the measurement of B could result. Consequently, after each individual B, H reading the magnetization cycle was completed and the electromagnet current again adjusted to its maximum positive value. It was again switched off, the reversing key turned, the resistance adjusted to a new value and the current switched on. Another change of induction from B_r' to a new value on the demagnetization curve was thus obtained. This procedure is described in detail here in order to emphasize the danger of the less lengthy method of obtaining successive changes in flux.

It will be seen that the maximum induction, B_m, and the apparent remanent induction, B_r', had to be found separately. The former was half the sum of all the changes in B recorded as one proceeded from B_m to $-B_m$ without pausing to measure fields. The latter was obtained from the change in induction, B_m to B_r' which occurred when the current was reduced from its maximum value to zero. All fluxmeter deflections were calibrated by means of a standard mutual inductance whose secondary was permanently in series with the coil on the magnet.

Examples of (B, H) curves so obtained are reproduced in fig. 1. Curve (*a*) was obtained with an alloy of 23·3 per cent. cobalt and 76·7 per cent. platinum, prepared by Messrs Johnson and Matthey; it was in the form of a polished bar 2·02 cm. long and 1 cm. sq. in cross-section. It was made ferromagnetic by keeping it at 650° C. for three hours. With materials of such high coercivity and comparatively low induction it is necessary to correct for the lines of the applied field which are collected in the space between the B coil and the specimen on which it is wound.

Curve (*b*) was obtained with a bar of sintered " alnico " 3·73 cm. long and 0·90 cm.×0·85 cm. in cross-section. The same specimen was measured on a B.S.I. 406 equipment, and the results so obtained agreed fairly well with those of curve (*b*) at the upper end of the curve but fell away a little at the B=0 end, where the value for H_c was 490 instead of 510 oersteds, as given in fig. 1. Two reasons may be advanced to explain discrepancies of this kind. In the first place the specimen is not investigated with as completely closed a magnetic circuit as in the potentiometer method, and, secondly, it is more rigidly clamped between the mu-metal blocks of the B.S.I. 406 apparatus than between the poles of the electromagnet.

Fig. 1.

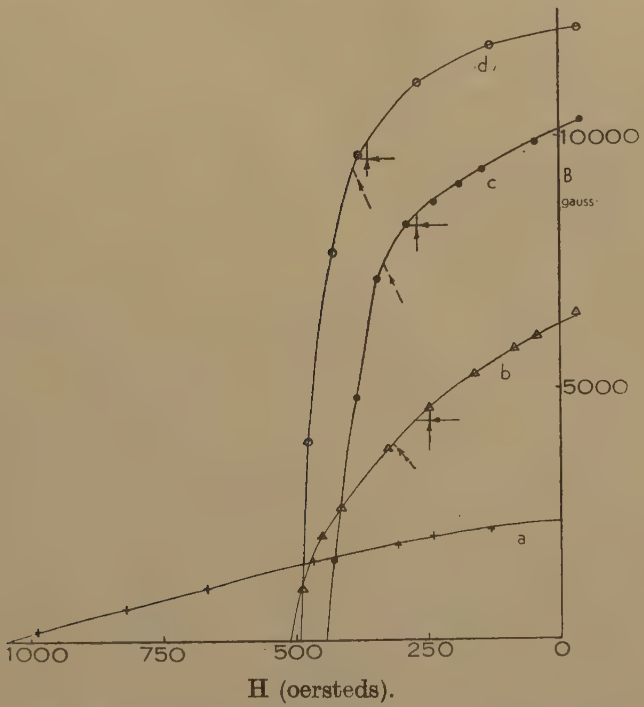

Demagnetization curves of permanent magnet materials.

⊙ " Alnico " V (" Ticonal "). △ Sintered " Alnico."
● " Alcomax." + Co-Pt.

Curves (*c*) and (*d*) were obtained respectively for " alcomax " and " alnico v " (" ticonal ") magnets of the dimensions shown in fig. 4. The difficulties which arise with horseshoe magnets were well brought out in measurements on the magnet of curve (*d*). From that curve, the values of B_r, H_c and $(BH)_{max}$ for the material of the arch of the magnet were 12,200 gauss, 500 oersteds and $3{\cdot}3\times10^6$ gauss-oersteds respectively. Two sections of this magnet were cut from the straight portions or legs of the horseshoe and tested on B.S.I. apparatus. One gave $B_r=11{,}400$ gauss, $H_c=538$ oersteds and $(BH)_{max}=3{\cdot}1\times10^6$ gauss-oersteds; the corresponding figures for the other were 11,300, 575 and $3{\cdot}2\times10^6$. The latter section was also measured by the potentiometer method, but, as it was only 1·60 cm. long and 2·39 cm. × 1·21 cm. in cross-section, it was rather too short for the size of potentiometer available. However, the corresponding figures obtained with the latter method were 10,650, 515 and $2{\cdot}75\times10^6$. The most interesting feature lay in the difference between the preceding figures and those which were expected from measurements made on a straight specimen taken during the casting of the above magnet, namely, 12,300, 575 and $4{\cdot}7\times10^6$. It should be noted that the potentiometer enabled measurements to be made in the arch region where it was impossible to cut a section.

Evershed (1920, 1925) first showed that the maximum value of the product of B and H, $(BH)_{max}$, provided a criterion of the magnetic quality of a permanent magnet material. Now, there is much experimental and theoretical evidence that the $(BH)_{max}$ point on the demagnetization curve is situated at the point of intersection with this curve of the diagonal of the rectangle bounded by the axes and the lines $B=B_r$ and $H=-H_c$. Relevant portions of such diagonals have been drawn for the curves of fig. 1. In addition, short horizontal and vertical lines have been drawn to cut the curves respectively at points $B=B_0$, the induction when the magnet is on open circuit, *i. e.* removed from the electromagnet, and at $H=-H_0$, the corresponding demagnetizing field due to the free poles of the magnet. B_0 was found by noting the fluxmeter deflection when the magnet was removed from between the poles of the electromagnet immediately after the current has been switched off; it was also measured directly by a search coil as well. H_0 was measured directly. Each pair of lines should, theoretically, intersect on the appropriate curve. They do not, although they cut as near as could be expected, because while B_0 was measured for the whole area of cross-section of the magnet, H_0 was found by measurements confined to a part of its surface. It is clear that if one desires a magnet which will work at maximum efficiency when on a partly closed circuit, it must be so designed that the point, or small region, B_0, H_0, lies below the $(BH)_{max}$ point.

§4. *The First Circuit Equation of Permanent Magnets.*

The magnetic potentiometer was also used to investigate the theoretical relations which permanent magnets obey. Suppose we place two unmagnetized horseshoe magnets in contact to form a closed ring and subject them to a very strong magnetizing field for a short time, either by means of a coil or a surge transformer arrangement. Assuming that the magnet faces are in intimate contact, we may imagine that on removal of the magnetizing field the magnetic state of the whole of the material is represented by the point B_r on the demagnetization curve (fig. 2).

On separating the magnets to a great distance from one another we assume that the magnetic state of the material of each is represented by the point P corresponding to an induction B_0 and a demagnetizing field H_0. On causing the magnets to approach until they are separated by a gap l_g between each pair of opposite poles the *recoil line* PR is followed as far as X, and we assume that the magnetic state of the whole of the magnetic material is now represented by B, H, an assumption which will be modified later. The positions of the two magnets are then as shown in figs. 3 and 3*a*, and we may apply the well-known equations of the magnetic circuit.

Fig. 2.

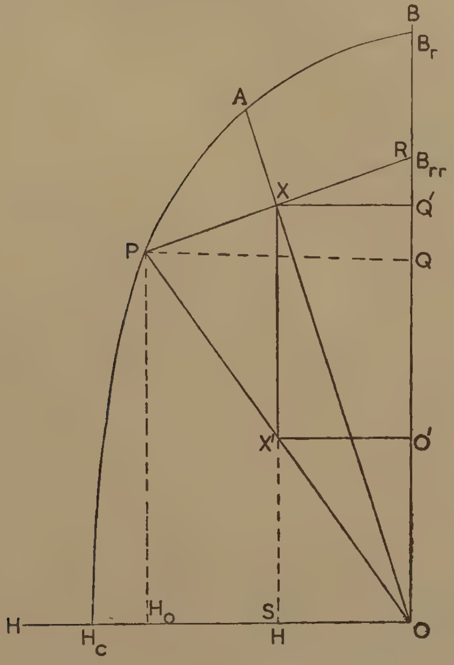

Theoretical demagnetization curve.

The first of these is

$$\int H.dl = -\int H_a \, dl_g, \quad . \quad . \quad . \quad . \quad . \quad . \quad . \quad . \quad (1)$$

where H and l refer to the steel and H_a and l_g to the gap. The correctness of equation (1) may be proved by means of a magnetic potentiometer of suitable dimensions. For example, a pair of "alcomax" magnets with "turned in toes" had their upper and lower surfaces polished and each magnet was marked out in seven regions as shown in figs. 3 and 3 *a*. The pair was placed together with 0·5 in. ebonite separators between the opposite poles. The small magnetic potentiometer was placed with the mid-points of its feet on neighbouring lines on the magnet surfaces, and when it was removed quickly the galvanometer reading measured the magnetic potential difference between points on the neighbouring lines shown in figs. 3 and 3 *a*. The edge of each magnet

Fig. 3.

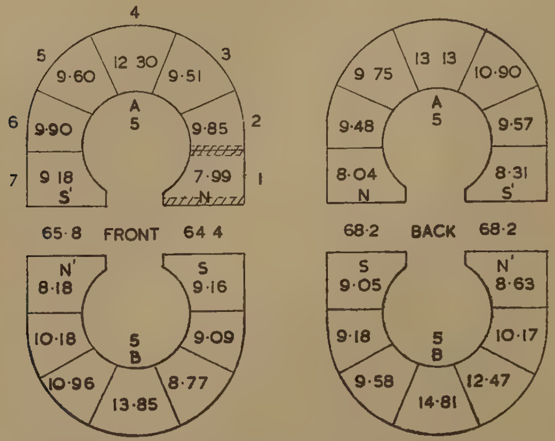
4
5
3
12 30
9·60
9·51
6
9·90
A
5
9·85
2
7
9 18
S'
7·99
1
N
65·8 FRONT 64 4
N'
8·18
S
9·16
10·18
5
B
9·09
10·96
8·77
13·85
13 13
9 75
10·90
9·48
A
5
9·57
8·04
N
8·31
S'
68·2 BACK 68·2
S
9·05
N'
8·63
9·18
5
B
10·17
9·58
14·81
12·47

Experimental proof of first circuit equation.

$\int H\,dl$ (corrected) $= 133{\cdot}5$. $\int H\,dl$ (corrected) $= 134{\cdot}9$.

$\int H_a\,dl_g \quad = -130{\cdot}2$. $\int H_a\,dl_g \quad = -136{\cdot}4$.

Mean $\int H\,dl = 134{\cdot}2$. Mean $\int H_a\,dl_g = -133{\cdot}3$.

Fig. 3 *a*.

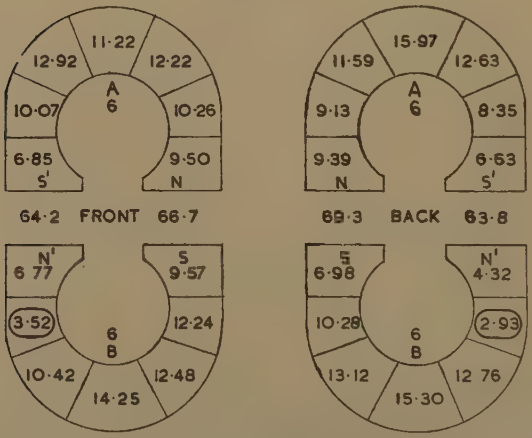
11·22
12·92
12·22
10·07
A
6
10·26
6·85
S'
9·50
N
64·2 FRONT 66·7
N'
6 77
S
9·57
3·52
12·24
6
B
10·42
12·48
14·25
15·97
11·59
12·63
9·13
A
6
8·35
9·39
N
6·63
S'
69·3 BACK 63·8
S
6·98
N'
4·32
10·28
2·93
6
B
13·12
12 76
15·30

Experimental proof of first circuit equation.

$\int H\,dl$ (corrected) $= 134{\cdot}0$. $\int H\,dl$ (corrected) $= 129{\cdot}7$.

$\int H_a\,dl_g \quad = -130{\cdot}9$. $\int H_a\,dl \quad = -133{\cdot}1$.

Mean $\int H\,dl = 131{\cdot}9$. Mean $\int H_a\,dl_g = -132{\cdot}0$.

was not treated as one such line, as it was convenient to start and end with the outer edge of a potentiometer foot exactly above the edge of the magnet material, as indicated by a shaded region in fig. 3. The sum of all the readings taken around the two magnets gave the value of $\int H\,dl$, except for the small pieces of material as under the shaded regions in fig. 3.

When the potentiometer was placed to bridge the gaps in turn with each of the mid-points of its feet on one edge of the material bordering the gaps, the sum of galvanometer readings gave the true value of $\int H_a dl_g$. To obtain the corrections for the potential differences in the small lengths of steel near the pole-edges it was necessary to take readings with the potentiometer bridging each gap (*a*) with the outer edge of one of its feet coincident with the edge of say the N pole and the other foot resting on the opposite S pole-surface, and (*b*) with the outer edge of one of its feet coincident with the edge of the S pole and the other foot resting on the opposite N pole-surface, and to obtain the mean potential difference between two points in the main body of the steel a distance apart equal to the average width of the potentiometer foot. The corrections were assumed equal for both sides of the gap and the results for a fairly uniform pair of magnets are shown in fig. 3, and for a markedly dissimilar pair in fig. 3 *a*, where the anomalous region whose potentiometer readings are encircled should be noted. It is clear that for experiments confined to paths on the surfaces equation (1) is well satisfied. It is fashionable to write it in the form $H.l = -H_a l_g$, although this is obviously incorrect. It is obvious from figs. 3 and 3*a* that the magnets had not been magnetized as strongly as possible.

Fig. 3 *b*.

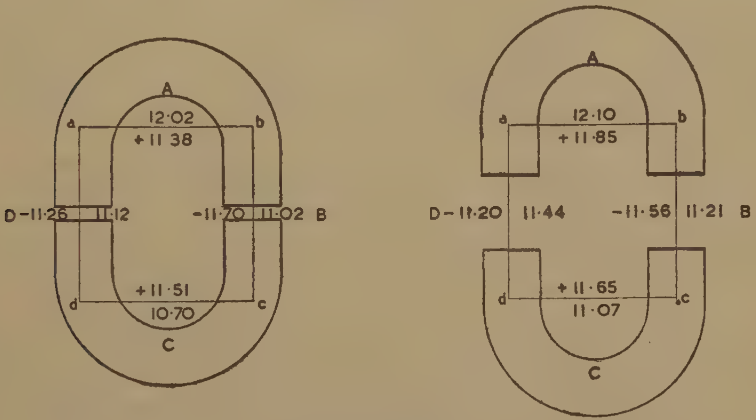

Experimental proof of first circuit equation, using larger potentiometer.

The same equation may be checked by using a potentiometer of larger dimensions. On the left side of fig. 3 *b* are depicted a pair of " alcomax " magnets which were strongly magnetized and separated by a gap of 0·32 cm. A magnetic potentiometer of 542 turns, wound in two layers on an ebonite former of 0·32 cm. radius of cross-section and bent into a semicircle of 2·20 cm. radius, was placed upon the magnets so that the mid-points of its ends successively covered the points *ab*, *bc*, *cd* and *da*. On removal of the potentiometer the corresponding scale readings given by the outermost set of figures were respectively recorded from one surface of the magnets, and the innermost set was recorded when readings were taken from the other surface. If we add the four sets of figures, with the appropriate signs, the result should theoretically be zero ; a small remainder, which is somewhat less than 0·6 per cent. of the readings added without reference to signs, is actually found. Hence, equation (1) is again satisfied within the limits of experimental error.

On the right side of fig. 3*b* are shown the same two magnets separated by a gap of 1·25 cm. The remainder is now about 1·4 per cent., and this brings into prominence the main defect of the magnetic potentiometer, namely, that it cannot be used with safety for measurements in very non-uniform fields. In the last measurements the feet of the potentiometer were bound to be very close to the "poles" of the magnets, and any slight irregularities in its windings would have important results.

§ 5. *The Second Circuit Equation of Permanent Magnets.*

We get a second equation for the circuit by considering that the normal magnetic flux through any cross-section is constant, whence

$$\mathrm{BA}_s=\mathrm{H}_a\mathrm{A}_a, \quad . \quad . \quad . \quad . \quad . \quad . \quad . \quad . \quad (2)$$

where B is the normal induction through any section of the magnet of area A_s, and H_a and A_a are respectively the field and area of cross-section of the air-gap, provided that there is no leakage parallel to the gap. We may take account of parallel leakage in two different ways. The older way is to introduce a leakage factor q and rewrite equation (2) as

$$\mathrm{BA}_s=q\mathrm{H}_a\mathrm{A}_a. \quad . \quad . \quad . \quad . \quad . \quad . \quad . \quad . \quad . \quad . \quad (3)$$

By elementary reasoning we may now deduce that the force of attraction between the two separated magnets is given by

$$\mathrm{P}=\frac{2\mathrm{H}_a{}^2\mathrm{A}_a}{8\pi}=\frac{1}{4\pi\mathrm{A}_a}\left(\frac{\mathrm{BA}_s}{q}\right)^2=\frac{1}{4\pi}\,\frac{(\mathrm{BH})\mathrm{A}_s l}{q l_g} \quad . \quad . \quad . \quad . \quad . \quad (4)$$

Hence, by measuring P, B, H, l_g and the volume of the magnet we may determine q. Values so found for "alcomax" and "ticonal" magnets of the shape shown in fig. 3 with a 1/16 in. gap between each pair of poles lie between 4·20 and 5·05.

§ 6. *New Extensions of Circuit Theory.*

The newer way of allowing for leakage is to employ the concepts of useful flux and useful energy. (I understand that a comprehensive account of these concepts will be found in a forthcoming paper to be read by D. J. Desmond before the Institution of Electrical Engineers.) Fig. 2 shows that the induction B consists of two parts, the useful part measured by XX′ and the leakage measured by X′S. It follows from the properties of similar triangles that, if B_{rr} represents the *maximum recoil induction* of the material when the gaps are completely closed on recoil, the useful induction B_u is given by $B_{rr}\left(\frac{(H_0-H)}{H_0}\right)$.

Equation (3) may now be rewritten as $B'_u A'_s = B''_u A''_s = \ldots = H_a A_a$, where B'_u, A'_s refer to region 1, B''_u, A''_s to region 2, etc., in figs. 3 and 3 *a*, so that we have finally

$$B'_{rr} A'_s \frac{H'_0 - H'}{H'_0} = B''_{rr} A''_s \frac{H''_0 - H''}{H''_0} = \ldots = \text{const.} \quad . \quad . \quad . \quad (5)$$

H'_0 and H' referring to region 1, H''_0 and H'' to region 2, and so on. We may therefore rewrite equation (4) as

$$P = \frac{1}{4\pi}\left\{\frac{\text{Useful energy per c.c. of one magnet) (Volume of one magnet)}}{\text{Thickness of one gap}}\right\},$$

or, more generally, as

$$P = \frac{1}{8\pi l_g}\left\{\begin{matrix}\text{(Total useful energy of magnet A)+(Total useful energy of} \\ \text{magnet B)}\end{matrix}\right\}$$

$$= \frac{1}{8\pi l_g}\left\{\sum_{A}\left(B'_{rr}\frac{(H'_0-H')}{H'_0}.H'A'_s l\right) + \sum_{B}\left(\qquad\qquad \right)\right\},$$

which in the case of two identical magnets reduces to

$$P = \frac{1}{4\pi l_g} B'_{rr} \frac{(H'_0-H')}{H'_0} A'_s \Sigma H' l'.$$

Now, $$\Sigma H' l' = \int H\, dl = \int H_a\, dl_g = H_a l_g,$$

and, by definition,

$$H_a A_a = B'_{rr} \frac{(H'_0-H')^2}{H'_0} A'_s,$$

whence $$P = \frac{A'_s}{4\pi} B'^2 \frac{(H'_0-H')^2}{H'^2_0} \frac{A'_s}{A_a},$$

which in the case of magnets of uniform cross-section A reduces to

$$P = \frac{B'^2_{rr}}{4\pi}\left(\frac{H'_0-H'}{H'_0}\right)^2 A, \quad . \quad . \quad . \quad . \quad . \quad . \quad . \quad (6)$$

so that for very wide gaps, for which $H'=H'_0$, $P=0$, while for very narrow gaps where $H'=0$, P takes the limiting value $\frac{B'^2_{rr}A}{4\pi}$ dynes.

For an accurate experimental test of equation (6) we need two approximately equal magnets of reasonably uniform cross-section. If a closely fitting search coil connected to a fluxmeter, placed around one of them when it is remote from its partner, is suddenly removed, the fluxmeter records A.OQ—see fig. 2—for the region originally within the coil. If, with the coil replaced over the magnet, we now quickly place the latter in contact with its partner to form a completely closed ring, the fluxmeter records the corresponding value of $A.QR$. The sum of the two fluxmeter readings thus gives us the quantity $A.B_{rr}$, say $A.B'_{rr}$, for the chosen magnet region.

H'_0 can be obtained by means of the magnetic potentiometer as used earlier in this paper, and H' can be found in the same way by repeating the potentiometer measurements with the magnet poles separated by suitable spacers, as in fig. 3, to give required values of l_g. The pull between the two magnets is now measured by a simple direct method. Different values of l_g from 2·5 cm. to 0 cm. are chosen and readings of H' and P found for them. For ease in measurement, and in order to avoid deterioration of the magnetization by repeated mechanical impacts of the two magnets upon one another, the sets of potentiometer readings are first taken, then the value of P and, finally, the fluxmeter readings for B'_{rr}.

It is often more convenient to use a single magnet placed near a thick iron plate or block of mild steel, when the preceding equations become

$$\int H\,dl + \int H_i\,dl_i = -\int H_a\,dl_g \quad \ldots\ldots\ldots \quad (7)$$

and

$$P = \frac{1}{8\pi l_g}\{(\text{Total useful energy of magnet}) + (\text{Total useful energy of iron})\}$$

$$= \frac{1}{8\pi l_g}\left\{\sum_{\text{Magnet}} B'_{rr}\frac{H'_0 - H'}{H'_0}H'A_s l' + \sum_{\text{Iron}} B'_{rr}\frac{H'_0 - H'}{H'_0}A'_i H'_i l'_i\right\}, \quad \ldots \quad (7\,a)$$

where H'_i is the field in the iron acting on a region of area A'_i and path length l'_i. Equation (7 *a*) may be simplified by taking a magnet of uniform area of cross-section A, when

$$P = \frac{A}{8\pi l_g}B'_{rr}\frac{H'_0 - H'}{H'_0}\left\{\int H\,dl + \sum_{\text{Iron}} H'_i l'_i \frac{A'_i}{A}\right\} \quad \ldots\ldots\ldots \quad (7\,b)$$

$$= \frac{A}{8\pi l_g}B'_{rr}\frac{H'_0 - H'}{H'_0}\left\{-\int H_a\,dl_g - \int H_i\,dl_i + \int H_i\,dl_i\frac{A_i}{A}\right\}$$

$$= \frac{A}{8\pi l_g}B'_{rr}\frac{H'_0 - H'}{H'_0}\left\{-2B_{rr}\frac{H'_0 - H'}{H'_0}l_g + \int H_i\,dl_i\frac{(A_i - A)}{A}\right\}$$

$$= -\frac{A}{4\pi}B'^2_{rr}\frac{H'_0 - H'}{H'_0}\left\{1 - \frac{H'_0}{2(H'_0 - H')}\,\frac{A_i - A}{A}\,\frac{\int H_i\,dl_i}{B'_{rr}l_g}\right\}. \quad \ldots \quad (7\,c)$$

The negative sign preceding the last expression for P need not disturb us, as it arises merely because the potential energy of magnetization is negative, and, to be strictly consistent, we ought also to use a negative sign in equation (6). For extremely small gaps equation (7 *c*) reduces to

$$P = \frac{A}{4\pi}B'^2_{rr}\left\{1 - \frac{1}{2l_g B'_{rr}}\,\frac{A_i - A}{A}\int H_i\,dl_i\right\},$$

whence, assuming that $A_i = A$, we have $P = \frac{A}{4\pi}B'^2_{rr}$, which means that the pull between a permanent magnet and a mild steel block should be approximately equal to and somewhat less than the pull between two similar magnets when in direct contact.

§ 7. *Experimental Results.*

The magnets used in tests of the preceding theory were usually magnetized by placing each upon the jaws of a vice, the body of the magnet being encircled by a compact coil of 80 turns of thick copper wire which could be supplied with a current of the order of 100 amperes from heavy accumulators. A similar coil could be used to magnetize a pair of magnets in contact. Experiments were made with magnets of different types and materials, and representative data are given in figs. 4 to 8. A few measurements, specially made to obtain evidence in support of the statement made at the end of the final paragraph in the last section, are given in Table II., although such evidence is clear in all the graphs, with one exception which can readily be explained. Potentiometer measurements were made in at least two regions of each magnet, usually those labelled 4 and 1 in fig. 3; these are respectively designated arch and N pole regions. Both the anterior and the posterior surfaces of the magnet as depicted in fig. 3 were polished, and potentiometer measurements were taken on both surfaces.

TABLE I.

Two "Alcomax" magnets (N) with double gap.

A_s 2·40 cm. × 1·22 cm.

Gap. cm.	Pull. gm.	Potentiometer Readings.				Calculated Pull. gm.	
		Arch.		N Pole.			
		$H_0=13·92$		$H_0=12·54$			
		H	$(H_0-H)^2$	H	$(H_0-H)^2$	Arch.	N Pole.
0·78	1982	9·78	17·1	5·56	48·8	2950	5670
0·45	3483	8·59	28·5	2·20	107·0	4820	12400
0·32	4444	8·02	34·8	0·70	140·2	6000	16300
0·17	6216	6·78	51·0	−2·13	216·0	8800	20400
0·085	8432	5·87	64·8	−3·44	256·0	12500	21800
0·00	16500	4·42	90·0	−6·98	381·0	17400	26000 limit

To obtain fields in oersteds multiply by 21·2.

Fluxmeter readings.

Arch.	*N. Pole.*
OQ $=9930$ gauss	OQ $=5770$ gauss
$QB'_{rr}=1750$ gauss	$QB'_{rr}=4780$ gauss
$B'_{rr}=11680$ gauss	$B'_{rr}=10550$ gauss

The data given in Tables I. and I.A and in figs. 4 and 4*a* refer to "alcomax" magnets of the shape shown, the depth of the pole-faces being 2·4 cm. Figs. 4 and 4*a* show the results for measurements made on the arch and N pole regions respectively. The encircled points were obtained with the two magnets placed with chosen gaps between opposite poles. The data represented by crosses were obtained with the same chosen gaps between one of the magnets and a dead mild steel block, actually the large pole-piece from a Rutherford β-ray magnet. The noteworthy feature is that H for the N pole position changes sign as we pass from the larger gaps to smaller gaps. This is not envisaged in the theory, where perfect contact between the magnet surfaces at zero gap is assumed. It was noted that the higher the initial saturation intensity of magnetization of the magnets the less pronounced were the negative values of H, and the latter were also less pronounced when one magnet was replaced by a steel block. Fig. 4*b* shows how H_0, B_0 and H, B varied from place to place when one of these magnets was used on open circuit and when on closed circuit against a steel block.

TABLE I A.

"Alcomax" magnet No. 3 (N) working with double gap against steel block.

A_s 2·40 × 1·22 cm.

Gap. cm.	Pull. gm.	Potentiometer Readings.				Calculated Pull. gm.	
		Arch.		N Pole.			
		H_0=13·21		H_0=13·88			
		H	$(H_0-H)^2$	H	$(H_0-H)^2$	Arch.	Pole.
1·23	323	11·74	2·2	11·96	3·7	388	295
0·78	781	11·17	4·2	10·55	11·1	740	885
0·45	1740	9·57	13·3	7·53	40·2	2340	3210
0·32	2350	8·88	18·8	6·13	60·0	3280	4780
0·17	3660	7·51	32·5	2·83	122·0	5720	9750
0·085	5310	6·39	46·4	+0·17	187·0	8800	15300
0	15300	3·95	85·8	−5·35	370·0	16500	(20000) limit

To obtain fields in oersteds multiply by 21·2.

Fluxmeter readings.

Arch.	*N Pole.*
OQ =9450 gauss	OQ =5490 gauss
QB'_{rr}=1420 gauss	QB'_{rr}=3760 gauss
B'_{rr}=10870 gauss	B'_{rr}=9250 gauss

Fig. 4.

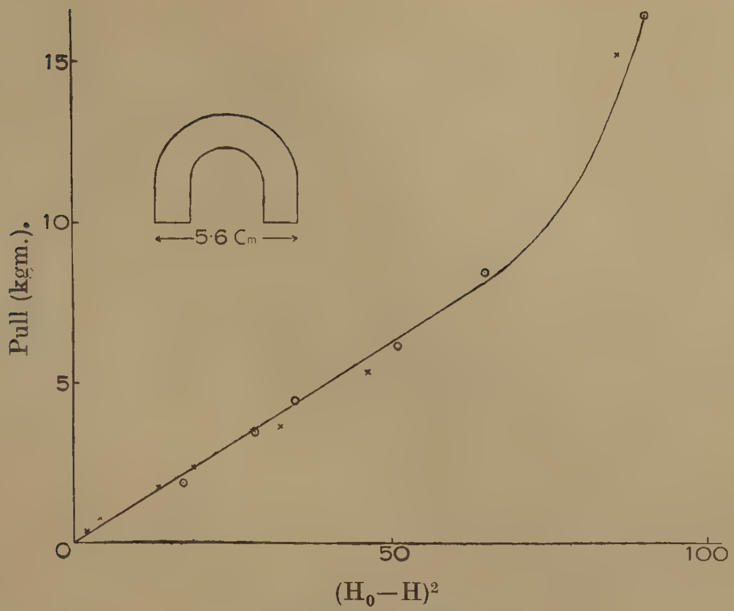

"Alcomax" magnets (N).

Potentiometer measurements on arch.

⊙ Two magnets. × Magnet and steel block.

Fig. 4 *a*.

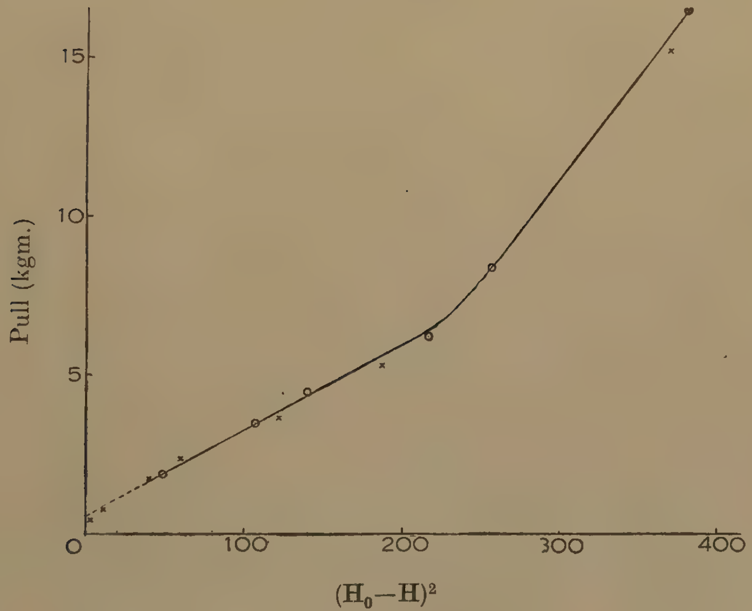

"Alcomax" magnets (N).

Potentiometer measurements on N pole.

⊙ Two magnets, × Magnet and steel block.

In the penultimate sub-column of Table I. are given the values of the pulls calculated on the basis of equation (6), with data from potentiometer measurements in the arch region, modified to take account of the existence of an appreciable demagnetizing field even when there is direct contact. For example, in Table I. it is seen that a demagnetizing field of over 90 oersteds was effective even when the two magnets were actually in contact. This meant that the value of QB'_{rr}, needed in equation (6) and measured as described in a preceding section, was too low, and had to be increased to $QB'_{rr}\left[\frac{H_0}{(H_0-H_d)}\right]$, where H_d is the value for direct contact. In Tables I. and I. A the corrected values of B'_{rr} from the arch measurements were 12,490 and 11,480 gauss respectively. The calculated and measured values of the pulls do not agree very closely, but perhaps the agreement is as good as one could expect; especially as the measured value of QB'_{rr} is always too low, because of mechanical disturbance when the magnets are brought together.

Fig. 4 *b*.

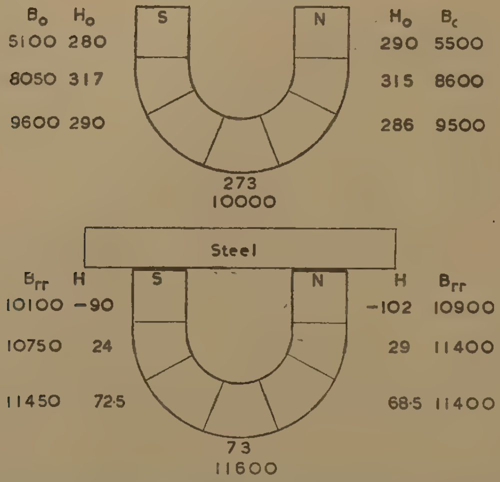

Variation of H_0, B_0 and H, B from place to place on "Alcomax" magnet.

In the case of calculations based on the N pole measurements account had to be taken of the change of sign of the field observed when the gaps were decreased. This meant that the measured values of QB'_{rr} were too large and had to be decreased to $QB'_{rr}\left[\frac{H_0}{(H_0-H_d)}\right]$, where H_d was the value of H for direct contact, and is to be treated as negative, in order to avoid change of sign throughout this paper. The corrected values of B'_{rr} so obtained from the data given in Table I. and I. A were 8,840 and 8,100 gauss respectively. Of course, the values of B′ used in the simplified form of equation (6) for the cases of direct contact were the measured values given in the tables. The results of calculations for the pulls based on these considerations are given in the final sub-columns of the tables. They are much too large, particularly in the case of two magnets working together. It thus appears that it is unreasonable to expect quantitative agreement between experiment and calculations based on potentiometer measurements in the region of the poles. We obtain reasonable values for the calculated pulls, in fact of much the same magnitude as those in the penultimate sub-column, if we assume B'_{rr} to be 8840 gauss and calculate the pulls from the expression $\frac{1}{4\pi}B'^2_{rr}A\left(\frac{H_0-H}{H_0-H_d}\right)^2$. While this is consistent with the occurrence of the linear portions of the graph, the precise significance of and justification for this method of calculation are not clear.

Turning again to figs. 4 and 4*a* it is seen that over a wide range the relation between measured pull and $(H_0-H)^2$ is approximately linear.

Fig. 5.

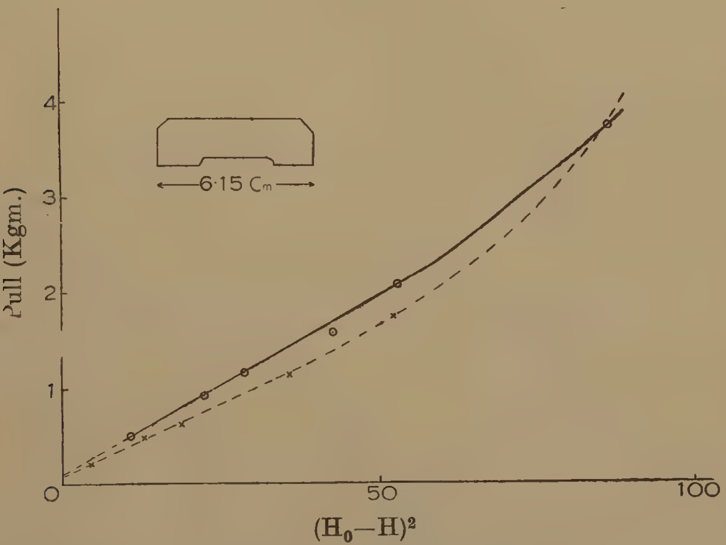

Short " Alnico " magnets.
Potentiometer measurements on outer surface of arch.
⊙ Two magnets. × Magnet and steel block.
(Pole-surfaces were in poor register.)

Generally, the linear relation holds for gaps of 1 to 8 mm. The pull between the two magnets in direct contact is seen to be a little greater than that between one magnet and a steel block for the same gap, as predicted by the theory. The magnitude of the change in $(H_0-H)^2$ as we pass from a gap of 0·085 cm. to direct contact is much greater for the single magnet and block than for a magnet pair.

In fig. 5 are given results for a pair of " alnico " magnets of the type shown, the depth of pole being 1·5 cm. The pole faces were polished, but they did not register at all well because the opposing surfaces were of unequal areas. However, a substantial portion of the graph is linear. The imperfect register accounts for the slight discrepancy in Table II.

TABLE II.

Summation of magnet pulls.

Type.	Direct Contact.		0·16 cm. Gap.	
	With steel block.	Magnets together.	With steel block.	Magnets together.
	gm.	gm.	gm.	gm.
“Alnico,” fig. 6.				
9 A	10750	11860	3470	5630
9 B	10310		3210	
“Alnico,” fig. 5.				
A	4645	4580	1150	1590
B	3815		935	
“Alcomax,” fig. 7				
5 A	15350	17990	5140	8180
5 B	14600		4880	
“Alcomax,” fig. 4				
A	16870	19730	3955	7480
B	17400		4025	

Each result was the mean of three determinations and the magnets were freshly magnetized before each set.

Fig. 6.

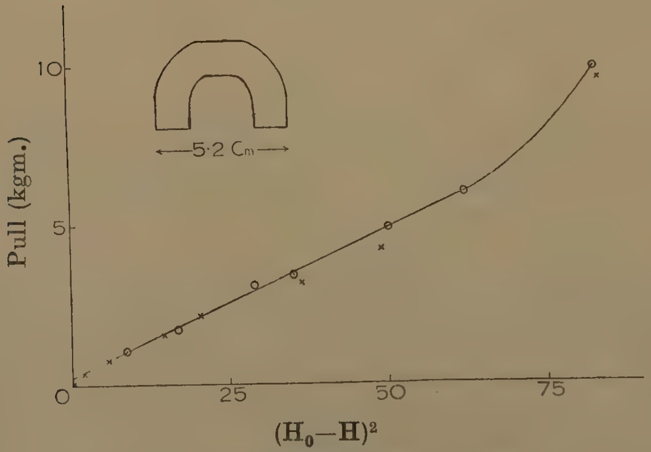

“ Alnico ” magnets (telephone type).
Potentiometer measurements on arch.
⊙ Two magnets. × Magnet with steel block.

In fig. 6 are given results obtained with a pair of "alnico" magnets of the shape shown, with a depth of pole-surface of 4·0 cm., such as are used in telephone work. It is interesting to compare the results with those of fig. 4. Negative values of H were observed only for direct contact between the two magnets or between one magnet and a steel plate, and the linear portion of the graph is remarkably definite. There was also very good agreement between the measured pulls for direct contact and the calculated values. Fig. 6*a* shows how H_0, B_0 and H, B varied from place to place when one such magnet was on open circuit and when against a steel block respectively.

The "alcomax" magnets used to obtain fig. 3*a* were of considerable interest because of the anomaly in magnet 6 B, and data were obtained both for the arch and the anomalous region. However, the anomaly was present only in earlier experiments, when it was possible that the magnetizing fields used to energize the magnet had not been great enough to change appreciably the magnetization in this exceptional region. The fact remained that after repeated magnetization with the vice and coil method and using heavy currents, the anomaly was not found. The results taken when the anomaly was present are plotted as filled circles in figs. 7 and 7*a*. The data were noteworthy for the negative values of H and the very low value of H_0 in the anomalous region and the high values of H and H_0 on the arch, when the magnet was working against a steel block, even when there was no gap. In spite of these features, B and B_0 were surprisingly high in the region of anomaly, and this leads to the conclusion that here there was a patch of material with both high remanence and very high coercivity. At the same time, we conclude that the strongest possible magnetizing fields must be used with modern magnet alloys, in order to avoid the evil effects of such patches. The writer prefers to use the coil and vice method or an electromagnet for magnetizing purposes.

Fig. 6*a*.

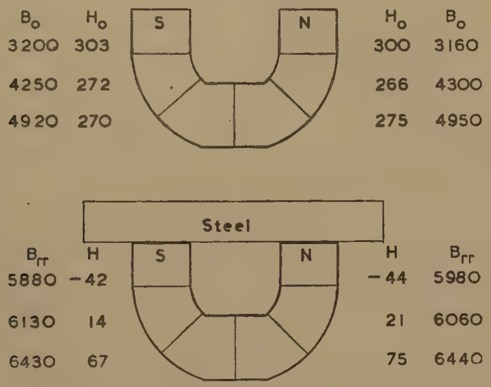

Variation of H_0, B_0 and H, B from place to place on "Alnico" magnet.

The graphs of pull against $(H_0-H)^2$ for the strongly magnetized magnets 6A and 6B are approximately linear over a wide range, although the theory could hardly be expected to hold so well for magnets of non-uniform cross-section. The calculated values of the pull based upon the arch measurements were rather low, as would be expected when B'_{rr} could not be regarded as uniform over the whole cross-section of the magnet; the value of QB'_{rr} for the arch was unusually small.

Results for a pair of " ticonal " magnets are plotted in fig. 8. Experiments were also made with a permanent magnet taken from an old form of moving-coil galvanometer. Its pole-surfaces were 1·8 cm. × 0·75 cm. and its mean overall length was 23·0 cm. An approximate analysis showed that it was a 6 per cent. tungsten steel containing about 0·7 per cent. carbon. Although the fields involved were some ten times smaller than those found with modern magnets, the same linear relation between pull and $(H_0-H)^2$ held over a wide range.

Fig. 7.

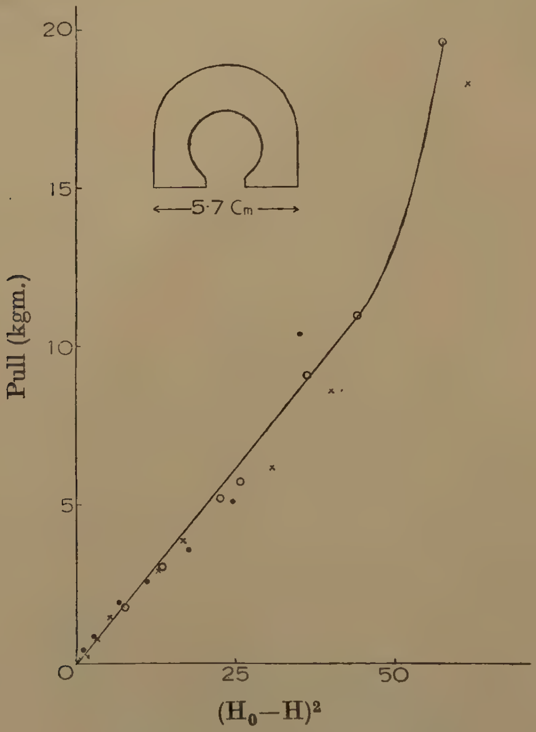

" Alcomax " magnets 6 A and 6 B.
All potentiometer readings on arch of 6 B.
⊙ Two magnets. × Magnet against steel block, with anomaly absent.
● Magnet against steel block, with anomaly present.

Certain general conclusions may be drawn from these experiments. If the theory is valid then there should be a linear relation between pull and $(H_0-H)^2$, the line passing through the origin. A linear relation was always found to hold over a wide range, and the line passed through the origin with magnets used under satisfactory experimental conditions, *e.g.* good magnet surfaces in proper register and strongly magnetized magnets with no anomalous regions of magnetization, but the experimental values of the pull for direct contact of two magnets or for very narrow gaps were always greater than would be expected from a prolongation of the linear part of the graph. This is understandable, because the material is not saturated, and as one magnet approaches another the flux distribution becomes more non-uniform; consequently, as the pull depends upon B^2A, the pull is correspondingly increased. Non-uniformity of the magnetization and slight unevenness of the pole-faces would accentuate the effect.

Fig. 7 *a*.

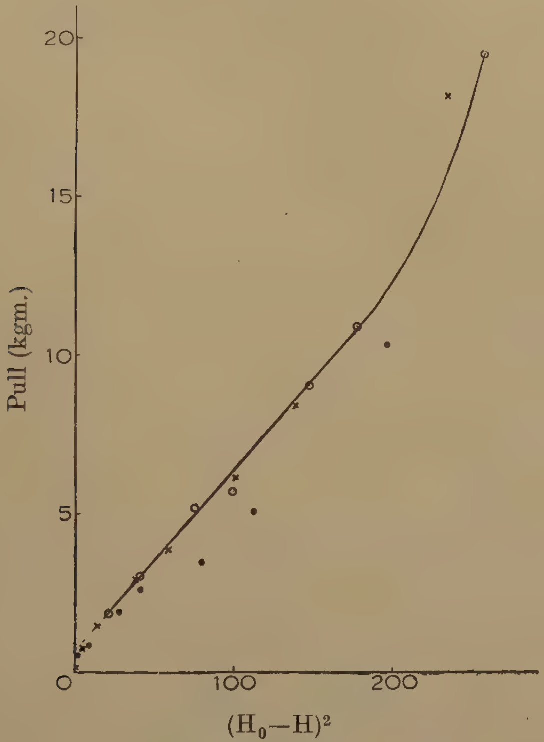

" Alcomax " magnets 6 A and 6 B.

All potentiometer readings on anomalous region.

○ Two magnets.

× Magnet against steel block, with anomaly absent.

● Magnet against steel block, with anomaly present.

Finally, there are indications that for very narrow gaps H readings on the arch and N pole regions are the smaller the more efficient the magnet, which means, in effect, the more pronounced its directional properties. The most effective magnets for tractive purposes are therefore those which give high values of H_0 and low but not negative values of H. Negative values of H mean that the recoil curve must extend beyond B_{rr} into the positive quadrant of the B, H curve, or, alternatively, that a strange kind of pole distortion takes place.

Fig. 8.

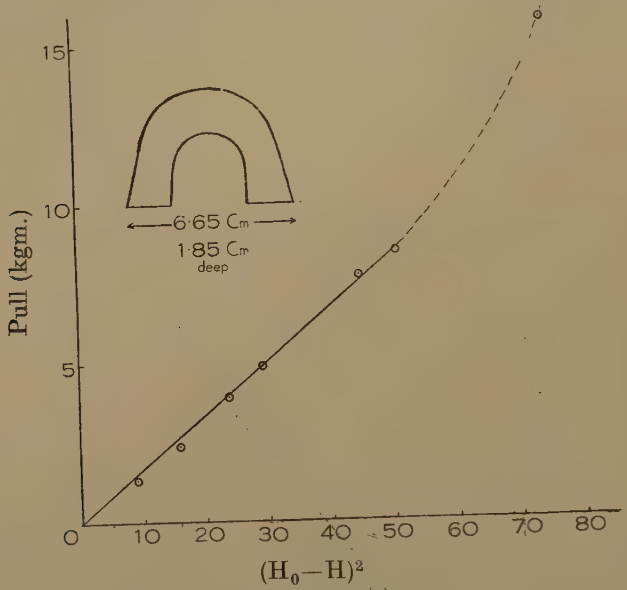

"Ticonal" magnet (M7).
Potentiometer measurements on arch.
⊙ Two magnets.

§8. *Acknowledgments.*

The electromagnet used in this work was built with a grant from the Government Grant Committee of the Royal Society. I am indebted to Mr. D. J. Desmond for the B.S.I. measurements on a sintered "alnico" rod, and to Mr. D. Hadfield for similar measurements on an "alcomax" specimen.

References.

Bates, L. F., 'Modern Magnetism' (Cambridge), p. 64 (1939).
Bates, L. F., and Lloyd Evans, B., Proc. Phys. Soc. xlv. p. 425 (1933).
Chattock, A. P., Phil Mag. **xxiv**. p. 94 (1887).
Evershed, S., Journ. Inst. Elect. Eng. lviii. p. 780 (1920).
Evershed, S., Journ. Inst. Elect. Eng. lxiii. p. 725 (1925).
Jellinghaus, W., *Zeit. für tech. Phys.* xii. p. 312 (1942).
Lacoste-Tayan, H., *Compt. Rendu.* ccvi. p. 103 (1938).
Wolman, W., *Arch. für Elektrotechnik*, xix. p. 385 (1928).

XLIII. *The Probable Number of Aggregates in Random Distributions of Points**.

By Ludwik Silberstein, Ph.D.

[Received October 10, 1944.]

Consider n points placed haphazardly within a linear segment of length L, all positions of a point on the segment being assumed to be equally likely. Let k of these points be said to form an *aggregate*, *e. g.* a doublet ($k=2$), a triplet ($k=3$), and so on, if they are all contained within a sub-interval λ of L, no matter how placed in L. Thus, two points will form a doublet if their distance apart does not exceed λ.

The probability P of any aggregates will be some function of n, L, and λ. It is easily seen that P can depend on λ and L only through their ratio. It will appear presently that P is always a polynomial in $\frac{\lambda}{L}$, viz., of degree n, with numerical coefficients dependent on n and on the complexity (k) and the number of aggregates in question.

Such being the case, we may take L for our unit length, so that henceforth λ will be a pure number, the fraction of that length. If x be the co-ordinate of a point, counted from one end of L, the total range of equiprobable co-ordinates will be 0 to 1, and the probability that the point shall fall between x and $x+dx$ will be simply dx. If y be the co-ordinate of some other point, the pair will form a doublet if $|y-x|\leqslant\lambda$, and similarly for triplets, and so on. The totality of such conditions, however, will become rapidly more complicated with increasing number of points.

The rigorous determination of the probability P of any given number of aggregates, k-ets, among n points is exceedingly complicated and becomes, to all purposes, impracticable, when n exceeds a few units, while the experimentalist is chiefly, or even exclusively, interested in great numbers n, running into thousands or millions, though in comparatively small aggregates, such as doublets, triplets, or quadruplets, and rather small values of λ. Now the main purpose of this paper is the determination, not of the probability P of any constellation (that is, of a desired number of aggregates of given complexity), but of the so-called expectation or *the probable number*, Q_k, of k-aggregates among any number n of points, which is a much easier problem. Actually, even the experimentalist is not interested in the particular probabilities of just two, or three, or four doublets, say, but in the number of doublets he can reasonably expect in a given situation, and this kind of information is precisely supplied by the probable number Q_2 of doublets; similarly, for triplets and higher aggregates.

---

* Communication No. 969 from the Kodak Research Laboratories, Rochester, New York.

Our main purpose, then, is to determine these probable numbers Q_k, first, for a linear or one-dimensional, and next for a two-dimensional haphazard distribution of points.

Before doing so, however, it will be well to evaluate the probability P itself in a few simple cases, especially as some of the results thus obtainable will be indispensable for our main purpose.

To form a good idea of the nature of the method * of rigorously determining any of these probabilities, consider the simplest case of just *two* points, $n=2$. What is the probability, $P_2(2)$, that they shall form a doublet?

Let x and y be their co-ordinates. If they are to form a doublet, x and y must satisfy the condition $|y-x| \leqslant \lambda$, where the bars indicate the absolute value. Since the *two* cases $x \leqslant y$ and $y \leqslant x$ are equally likely, we may replace this condition by $y-x \leqslant \lambda$ and then multiply the corresponding probability by 2. Thus, to begin with, we have

$$\frac{1}{2}P_2(2)=\int_0 dx\int_x^{x+\lambda} dy.$$

Now, $x+\lambda$, as the upper limit of the second integral, is possible only for $x \leqslant 1-\lambda$. If $x>1-\lambda$, then the upper limit of this integral is just 1, the condition $y-x \leqslant \lambda$ being then satisfied automatically. Hence, the formula becomes

$$\frac{1}{2}P_2(2)=\int_0^{1-\lambda} dx\int_x^{x+\lambda} dy+\int_{1-\lambda}^1 dx\int_x^1 dy.$$

The first integral is $\int_0^{1-\lambda}\lambda dx=\lambda(1-\lambda)$ and the second integral expresses the probability that both points shall lie within the localized interval λ (between $1-\lambda$ and 1) and follow each other in the order stated ($x \leqslant y$). But this is just one of two possible and equally probable orders. Hence, the integral must be equal to $\frac{1}{2}\lambda^2$. Such in fact is the case, as the reader can easily verify †. Thus, $\frac{1}{2}P_2(2)=\lambda(1-\lambda)+\frac{1}{2}\lambda^2$, and the required probability becomes

$$P_2(2)=2\lambda-\lambda^2, \quad \ldots \ldots \ldots \quad (1)$$

a quadratic function of λ, as mentioned before. It vanishes for $\lambda=0$ and becomes, of course, a certainty for $\lambda=1$. The probability of *no doublet*, or of *two singlets*, is $N(2)=1-P_2(2)$ or

$$N(2)=(1-\lambda)^2. \quad \ldots \ldots \ldots \quad (1')$$

---

* So far as the author can see, at present, the only possible method.

† The same reasoning gives, for an n-uple integral,

$$\int_{1-\lambda}^1 dx\int_x^1 dy\int_y^1 dz\ldots=\frac{\lambda^n}{n!},$$

since the order $x \leqslant y \leqslant z \ldots.$ is one of $n!$ equally probable errors.

Needless to say, the probable number of doublets is just

$$Q_2(2)=1P_2(2)=P_2(2),$$

and the probable number of singlets,

$$Q_1(2)=2(1-\lambda)^2.$$

In order to form an idea of the rapid growth of complication with increasing n, consider, briefly, the case of *three* points. Their co-ordinates, x, y, z, can be arranged as to the order of magnitude in $2\times3=6$ ways, all equally likely. If we take one of them, $x\leqslant y\leqslant z$, the probability of any event thus computed is $\frac{1}{6}$ of the complete probability. There are now four possibilities: all singlets, one doublet (and one singlet), two doublets, and a triplet. The sum of the corresponding probabilities, $N(3)$, $P_2(3)$, $P_{2,\,2}(3)$, $P_3(3)$, being 1, it is enough to evaluate any three of them. The easiest to find are the first and the last.

Consider $N(3)$, the probability of all singlets, no aggregates. If $\lambda\geqslant\frac{1}{2}$, this is manifestly impossible, so that

$$N(3)=0, \text{ for } \lambda\geqslant\tfrac{1}{2}. \quad \ldots\ldots\ldots \quad (2')$$

It remains to find $N(3)$ for any $\lambda<\frac{1}{2}$. A moment's reflection will show that

$$\frac{1}{6}N(3)=\int_0^{1-2\lambda}dx\int_{x+\lambda}^{1-\lambda}dy\int_{y+\lambda}^{1}dz;$$

or, with the substitution $y'=y-\lambda$, $z'=z-2\lambda$,

$$\frac{1}{6}N(3)=\int_0^{1-2\lambda}dx\int_{x}^{1-2\lambda}dy'\int_{y'}^{1-2\lambda}dz'.$$

This triple integral expresses the probability that x, y', z' are all contained within an interval of length $1-2\lambda$ and follow each other in the order stated (one of six equally probable), and is thus equal to $\frac{1}{6}(1-2\lambda)^3$. Hence, the required probability,

$$N(3)=(1-2\lambda)^3, \text{ for } \lambda<\tfrac{1}{2}, \quad \ldots\ldots\ldots \quad (2)$$

a cubic function of λ. It vanishes for $\lambda=\frac{1}{2}$, attaching itself continuously to the branch (2′) which holds for $\lambda\geqslant\frac{1}{2}$.

In much the same way, the probability of a triplet is found to be

$$P_3(3)=3\lambda^2-2\lambda^3, \quad \ldots\ldots\ldots \quad (3)$$

which holds for any $\lambda\leqslant1$.

The determination of $P_2(3)$, the probability of just one doublet, is more intricate. The integration process offers no difficulties, but the fixing of the limits of the integrals requires some care. In this case the probability function has two different forms according to the value of λ, namely,

$$\left.\begin{aligned} P_2(3)&=2(1-\lambda)^3, && \lambda\geqslant\tfrac{1}{2}, \\ P_2(3)&=6\lambda[(1-\lambda)(1-2\lambda)+\tfrac{1}{3}\lambda^2], && \lambda<\tfrac{1}{2}. \end{aligned}\right\} \quad \ldots\ldots \quad (4)$$

The function is continuous at $\lambda=\frac{1}{2}$, where both branches give $\frac{1}{4}$.

Lastly, subtracting the sum of the three probabilities from 1, we have the probability of two doublets:

$$P_{2,\,2}(3)=(1-\lambda)^2(4\lambda-1) \quad \text{and} \quad \lambda^2(3-4\lambda), \; \lambda \gtrless \tfrac{1}{2}. \quad . \quad . \quad (5)$$

The function is continuous at $\lambda=\frac{1}{2}$, where it amounts to $\frac{1}{4}$. This, also, is its maximum. For $\lambda=\frac{1}{2}$, two doublets are just as probable as one, but for very small λ the probability of two doublets is $3\lambda^2$, that is, small, of a higher order than the probability 6λ of one doublet. This exhausts the problem offered by three points.

The case of four or more points can be treated in exactly the same way, but with ever-increasing complication in the fixing of the integration limits and the discrimination between different λ-values. It will now be manifest that, as stated before, the rigorous probability P(n) of any desired number of aggregates of given complexity cannot be covered by a single formula valid for any number n of points and any value of λ.

Any probability $P(n)$ is, clearly, a polynomial of degree n in λ, but the values of the coefficients of this polynomial cannot be covered by a general formula, with the only exception of the two extreme cases, namely, $N(n)$, the probability of no aggregates, and $P_n(n)$, the probability of the highest aggregate, consisting of all n points. These two probabilities are easily determined for any λ and any number of points. The integrals are instantly evaluated in just the same way as in the preceding two simple cases, so that it may suffice to quote the results. These are:

$$N(n)=[1-(n-1)\lambda]^n, \text{ for } \lambda<\frac{1}{n-1}, \quad . \quad . \quad . \quad . \quad . \quad . \quad (6)$$

$$N(n)=0 \text{ for } \lambda \geqslant \frac{1}{n-1},$$

and

$$P_n(n)=n\lambda^{n-1}-(n-1)\lambda^n, \quad . \quad . \quad . \quad . \quad . \quad . \quad . \quad . \quad . \quad . \quad (7)$$

valid for any $\lambda \leqslant 1$. The probable number $Q_k(k)$ of full aggregates ($k=n$) is, of course, identical with $P_k(k)$, since but one such aggregate is possible. Thus, rigorously, for any k and any $\lambda \leqslant 1$,

$$Q_k(k)=k\lambda^{k-1}-(k-1)\lambda^k. \quad . \quad . \quad . \quad . \quad . \quad . \quad . \quad . \quad . \quad (8)$$

This probable number will be constantly required in the sequel.

We shall now turn to our main subject, the probable number of any aggregates in a random distribution of points.

One Dimension.

Let us begin with a one-dimensional distribution of points (on a line of unit length, or of events in a haphazard succession in time). We shall leave their number n unrestricted and assume only, at a later stage, that λ is a small fraction of the whole domain, briefly $\lambda \ll 1$, such values of this parameter being of main or exclusive interest in most applications.

Let $Q_k(n)$ be the unknown probable number of k-aggregates or k-ets among the n points. Add, haphazardly, one more point. If it happens to fall upon or near enough a $(k-1)$-et, it will give us one more k-et, and if it "hits" a k-et, it will convert it into a higher aggregate, depriving us of one k-et, each time with a certain probability. If the point falls elsewhere, the original number $Q_k(n)$ remains unchanged. Thus we have the recurrence formula or functional equation

$$Q_k(n+1)=(1-\pi_k)Q_k(n)+\pi_{k-1}Q_{k-1}(n), \quad \ldots \ldots \quad (9)$$

where π_k is the average probability of "hitting" a k-et, that is, of converting it into a $(k+1)$-et, in a single haphazard trial. Similarly for π_{k-1}. If, therefore, we can determine the probabilities π_k, the equation will enable us to pass from Q_1 to Q_2, thence to Q_3, and so on. Now, all these probabilities are readily found from the equation (9) itself. Put $n=k-1$. Since it is impossible to build a k-et out of $k-1$ points, $Q_k(k-1)=0$, and the equation gives

$$\pi_{k-1}=Q_k(k):Q_{k-1}(k-1), \quad \ldots \ldots \quad (10)$$

which holds for $k-1=1$, 2, 3, and so on. Thus, explicitly, by the rigorous formula (8),

$$\pi_k=\lambda\frac{k+1-k\lambda}{k-(k-1)\lambda}, \quad \ldots \ldots \quad (11)$$

a function of λ and k, independent of n. For example, $\pi_1=\lambda(2-\lambda)$ or $\pi_2=\lambda\dfrac{3-2\lambda}{2-\lambda}$ are the average probabilities of converting a singlet or a doublet, placed among no matter how many points, into a doublet and a triplet, respectively, in a single trial. From (11) we see that every probability π_k is just of the order of λ or, as we shall say, of *the first order*, regardless of the value of k, that is, for singlets, as well as for doublets, triplets, and so on.

If we introduce the *relative* probable numbers through

$$f_k(n)=Q_k(n):Q_k(k), \quad \ldots \ldots \quad (12)$$

then, with the usual notation $\Delta f(n)=f(n+1-f(n)$, equation (9) becomes

$$\Delta f_k(n)=f_{k-1}(n)-\pi_k f_k(n), \quad \ldots \ldots \quad (9')$$

a finite-difference equation for $f_k(n)$ with the "initial" value $f_k(k)=1$, and a known coefficient π_k, independent of n.

Henceforth, let $\lambda\ll 1$. We propose to retain, in the presence of 1, terms of the first, but not of the second order.

While Q_k is of the order of λ^{k-1}, all relative numbers $f_k(n)$ are of *zero-th* order; their main term, that is, does not contain λ at all, and we propose to determine this term and the next, of the first order in λ, as a refinement. Higher terms would be of no practical interest. Now, by (11), π_k is of the first order, so that it is enough to retain its leading term, $\dfrac{k+1}{k}\lambda$, and the last equation becomes

$$\Delta f_k(n)=f_{k-1}(n)-\frac{(k+1)\lambda}{k}f_k(n).$$

Since the last term contains already the small factor λ, we have to use in it only the main term of f_k. Call it f_k'. Ultimately, therefore, our equation is

$$\Delta f_k(n)=f_{k-1}(n)-\frac{(k+1)\lambda}{k}f_k'(n), \quad \ldots \ldots \quad (13)$$

with the condition $f_k(k)=1$. In order to integrate it, up to λ^2-terms, it is most convenient to determine first the main term $f_k'(n)$ of the function, as required for the last term in (13), that is, to solve the reduced equation, or rather chain of equations ($k=2$, 3, etc.),

$$\Delta f_k(n)=f_{k-1}(n), \quad \ldots \ldots \ldots \quad (13')$$

with the condition $f_k(k)=1$, where we have dropped, for the moment, the dashes.

Manifestly, $Q_1(1)=1$, so that, by the definition (12), $f_1(n)=Q_1(n)$. Thus, for doublets or $k=2$, our equation is

$$\Delta f_2(n)=Q_1(n), \text{ with } f_2(2)=1,$$

where $Q_1(n)$ is the probable number of singlets among n points. Its main term $Q_1'(n)$ which we now require is, of course, n itself, but we may as well determine its next term, in λ, needed for the sequel. This is easily accomplished.

The probability that P, one of the n points, shall be a singlet is the probability that each of the remaining points shall fail to fall within an interval 2λ centred at P, that is, $(1-2\lambda)^{n-1}$. This is based only on the assumption that λ is small enough to permit a disregard of the case that P approaches one of the extremities of the whole unit segment to within less than λ. Hence, the probable number of singlets among n points,

$$Q_1(n)=n(1-2\lambda)^{n-1} \quad \ldots \ldots \ldots \quad (14)$$

or, up to λ^2-terms,

$$Q_1(n)=n[1-2\lambda(n-1)]. \quad \ldots \ldots \ldots \quad (14\,a)$$

The leading term of this number being simply n, our last equation for doublets is

$$\Delta f_2(n)=n,$$

with the initial value $f_2(2)=1$. Since $\Delta^2 f_3(n)=1$, the solution is

$$f_2(n)=1+2(n-2)+\tfrac{1}{2}(n-2)(n-3)=\tfrac{1}{2}n(n-1)=\binom{n}{2}.$$

Thus the equation (13′) becomes, for triplets,

$$\Delta f_3(n)=\binom{n}{2}, \text{ with } f_3(3)=1,$$

whence, in like manner, $f_3(n)=\binom{n}{3}$. This suggests, for any aggregate, $f_k(n)=\binom{n}{k}$, which is actually the case. A well-known property of binomial coefficients is

$$\binom{n+1}{k}-\binom{n}{k}=\binom{n}{k-1} \quad \text{or} \quad \Delta\binom{n}{k}=\binom{n}{k-1};$$

moreover, $\binom{k}{k}=1$, so that $\binom{n}{k}$ satisfies the equation (13′) as well as the condition $f_k(k)=1$. Thus the main term of the relative probable number of any aggregates is

$$f_k'(n)=\binom{n}{k},$$

just the number of combinations of n into groups of k points.

The complete equation (13), correct up to λ^2-terms, now becomes

$$\Delta f_k(n)=f_{k-1}(n)-\frac{(k+1)\lambda}{k}\binom{n}{k}, \quad . \quad . \quad . \quad . \quad . \quad . \quad (15)$$

with the condition $f_k(k)=1$, as before. The last term, small of the first order, is a known function of the variable n with k as parameter. Since, by (14 *a*), $f_1(n)=n-4\lambda\binom{n}{2}$, the equation for doublets is

$$\Delta f_2(n)=\binom{n}{1}-\frac{11}{2}\lambda\binom{n}{2},$$

whence, by the stated property of binomial coefficients,

$$f_2(n)=\binom{n}{2}-\left(4+\frac{3}{2}\right)\lambda\binom{n}{3},$$

which satisfies also the condition $f_2(2)=1$, since $\binom{2}{3}=0$. Substituting in (15), we have, for triplets,

$$\Delta f_3(n)=\binom{n}{2}-\left(4+\frac{3}{2}+\frac{4}{3}\right)\lambda\binom{n}{3}, \quad f_3(3)=1,$$

whence, as before,

$$f_3(n)=\binom{n}{3}-\left(4+\frac{3}{2}+\frac{4}{3}\right)\lambda\binom{n}{4},$$

and so on.

For any value of k,

$$f_k(n)=\binom{n}{k}-(4+K)\lambda\binom{n}{k+1},$$

where
$$K=\frac{3}{2}+\frac{4}{3}+\frac{5}{4}+\ldots+\frac{k+1}{k}$$

or
$$K=k-1+\left(\frac{1}{2}+\frac{1}{3}+\frac{1}{4}+\ldots+\frac{1}{k}\right). \quad . \quad . \quad . \quad . \quad . \quad (16)$$

Notice that K, the contribution of the last small term in (15), is by no means negligible in comparison with 4, which is contributed by the small term of $f_1=Q_1$. In fact, for doublets, $K=\frac{3}{2}$; for triplets, $K=\frac{17}{6}$ or nearly 3; for great k,

$$K=k-2+\log k+0{\cdot}577,$$

and thus of the order of k itself.

With this meaning of the pure number K, we now have, for any aggregates,

$$f_k(n)=\binom{n}{k}\left\{1-\frac{4+K}{k+1}\lambda(n-k)\right\}.$$

This is their *relative* probable number. To find the number $Q_k(n)$ itself, we have only to multiply it by

$$Q_k(k)=k\lambda^{k-1}\left(1-\frac{k-1}{k}\lambda\right).$$

Thus, ultimately, the *probable number* of k-aggregates among n points becomes, up to higher powers of λ,

$$Q_k(n)=k\lambda^{k-1}\binom{n}{k}\left\{1-\frac{4+K}{k+1}\lambda(n-k)-\frac{k-1}{k}\lambda\right\}, \quad . \quad . \quad (17)$$

where K is the pure number given by (16). This solves our problem for any k and for any values of n unrestricted downwards, but not approaching too closely the huge number $\frac{1}{2\lambda}$. In fact, if $2\lambda n$ approaches unity, then the first order approximation (14 *a*), of the number of singlets $Q_1(n)$ begins to fail * and has to be replaced by (14), which implies higher powers of λ, beyond our present limitation. In fine, the product λn, which is the probable number of points within an interval λ, is now assumed not to approach $\frac{1}{2}$ very closely. It need not, however, be a very small fraction, such as λ. If, say, $\lambda=10^{-6}$, the formula is still applicable to 100,000 points or so, giving $\lambda n=0\cdot1$. The conditions of validity of (17) may be stated concisely by writing

$$\lambda \ll 1, \quad \lambda n<\tfrac{1}{2}. \quad . \quad . \quad . \quad . \quad . \quad . \quad . \quad . \quad (ad\ 17)$$

The case of congested distributions, or λn as great as we please, is treated in a later section of this paper.

The formula (17) includes, of course, the case of singlets, giving $Q_1(n)=n-2\lambda n(n-1)$, wherefrom it has been derived by repeated integrations. For doublets, up to higher terms, we have

$$Q_2(n)=2\lambda\binom{n}{2}=\lambda n(n-1),$$

while $Q_3(n)$, etc., are of the second and higher orders. Each doublet consists of two points, so that the total probable number of points is, up to λ^2-terms,

$$1Q_1(n)+2Q_2(n)=n,$$

as it should be. Had we pushed the approximation up to λ^3-terms, then the test would be $1Q_1(n)+2Q_2(n)+3Q_3(n)=n$, and so forth.

---

* It vanishes for $n-1=\frac{1}{2\lambda}$ and becomes, absurdly, negative for yet greater n, while the expectation of singlets should, manifestly, tend to zero asymptotically, with evergrowing congestion or $n\rightarrow\infty$, as in (14).

For great numbers n, that is to say, $n \gg k$, but always moderately small λn, the formula reduces to

$$Q_k(n) = \frac{(\lambda n)^{k-1} n}{(k-1)\,!}\left\{1 - \frac{(4+K)\lambda n}{k+1}\right\}. \quad . \quad . \quad . \quad . \quad (17\,a)$$

Thus, for instance, the probable number of doublets is

$$(\lambda n)n\left(1 - \frac{11}{6}\lambda n\right),$$

and that of triplets,

$$\frac{1}{2}(\lambda n)^2 n\left(1 - \frac{41}{24}\lambda n\right),$$

and so on. Notice that λ appears only through its product into the huge number n, and this product need not be a negligible fraction of unity.

It may be mentioned that the expression derived by Dr. W. F. Berg * for the probable number of k-aggregates (in his notation, TF_k), through a very brief reasoning just coincides with the main term of our formula (17 *a*), $\frac{n(\lambda n)^{k-1}}{(k-1)\,!}$. Dr. Berg's higher term, in λ or λn, which he ultimately disregards altogether, differs substantially from that in (17 *a*). It is, of course, without any importance in his experimental applications, where even λn is a very small fraction.

The general formula (17), applicable also to k comparable with n, answers all relevant questions concerning the expectation of aggregates in a one-dimensional random distribution of points (apart from the P. E. of this " expectation " which will be supplied later on). Before closing this part of our subject, it may be well to illustrate that formula and its special case, (17 *a*), by one or two numerical examples.

In order to make n comparable even with the first few values of k, suppose that

$$n = 20 \quad \text{and} \quad \lambda = 0{\cdot}01,$$

so that $\lambda n = 0{\cdot}2$, not violating our conditions. Then, by (17), we have, to two decimals, the expectation of

12·40 singlets,
2·53 doublets,
$0{\cdot}25_5$ triplets,
0·01 quadruplets,

and a practically evanescent expectation of quintuplets or higher aggregates. This gives a total of $\Sigma k Q_k = 18{\cdot}26$ points, with 1·74 " missing," to be accounted for (to a negligible extent by the higher aggregates and mainly) by the neglected λ^2— and higher terms, especially in our approximate expression $Q_1 = n[1 - 2\lambda(n-1)]$ for the singlets. In fact, if we replace this by the closer approximation (14), then $Q_1=20\ (0{\cdot}98)^{19}=13{\cdot}34$, so that the defect is reduced from 1·74 to 0·80 only.

---

* To whom the author is indebted for the original suggestion of this problem and whose paper on aggregates appears in this issue of the Magazine.

To illustrate the formula (17 *a*), consider the case of

$$n=1000 \quad \text{and} \quad \lambda=10^{-4},$$

so that $\lambda n=0{\cdot}1$, twice smaller than in the first example. Then, by (17 *a*), the expectation of singlets, doublets, and triplets is

$$Q_1=800, \quad Q_2=81{\cdot}7, \quad Q_3=4{\cdot}27,$$

while quadruplets would, to all purposes, be expected in vain. We now have $Q_1+2Q_2+3Q_3=976{\cdot}2$, short of 1000 by 23·8 or 2·4 per cent. only. (Of course, the smaller λn the smaller the proportionate error of the formula in accounting for the actual totality of points.) The bulk of even this small defect may again be accounted for by the coarseness of the expression for singlets, implied in (17 *a*). In fact, replacing it by (14), we have $Q_1=n(1-2\lambda)^{n-1}\doteqdot 1000.e^{-0{\cdot}20}=818{\cdot}8$, which reduces the list of missing points to 5 only *.

These two examples may suffice to illustrate our formulæ for moderate or great numbers of points, so far, for rather low values of λn. Congested distributions will be treated later on.

Two Dimensions.

It must be said forthwith that the problem in two dimensions is by far more complicated than the linear one. As will be seen presently, the main term of the *relative* number $f_k(n)$ is $\binom{n}{k}$, exactly as before, and would remain so even in three dimensions, but the determination of its next higher term and the passage from f_k to the probable number Q_k itself is much more intricate.

Let n points or particles be distributed haphazardly over a two-dimensional *field* whose area may again be taken as our unit area. All positions of a particle within the field being equally likely, the probability that a particle shall fall within a localized element of area da (henceforth a pure number) will be just da, and na will be the probable number of particles in any portion a of the field. Two or more, generally k, points or particles will be said to form an aggregate, if no two are at a distance exceeding a certain limit ρ and can, therefore, be surrounded by a circle of diameter ρ or area

$$\sigma=\tfrac{1}{4}\pi\rho^2. \quad . \quad . \quad . \quad . \quad . \quad . \quad . \quad . \quad . \quad . \quad (18)$$

It will be assumed, henceforth, that σ, a pure number, is a very small fraction, $\sigma\ll 1$, such as 10^{-3} and less, and that the distance ρ is a very small fraction of any diameter of the field, if this be central or nearly so. These assumptions are unavoidable, since a rigorous solution of any probability problem, even that of a doublet among two or a triplet among just three points (in a circular field only), would now be much more complicated than in a linear distribution. A rigorous evaluation of the probability $P_k(k)$ of a full aggregate, for any k, so easily found in the linear case, is now wholly impracticable, and since these probabilities, identical with $Q_k(k)$, are indispensable, we shall have to be content with their approximate values, up to σ^2-terms. The small area σ will now take the place of our previous λ, and terms in σ will be said to be small of the first order.

---

* This residual defect is due to the neglect of one or two doublets and a fraction of triplets. In fact, we shall see later that the aforementioned correction of Q_1 in the functional (or differential) equation affects also the probable number of doublets and higher aggregates.

As before, $Q_k(n)$ will stand for the probable number of k-ets among a total of n points, and $f_k(n)=Q_k(n):Q_k(k)$ will be the relative value of this number. For singlets, $Q_1(n)=f_1(n)$, since $Q_1(1)=1$.

If π_k be again the average conversion probability of a k-et into a $(k+1)$-et, our previous equation

$$Q_k(n+1)=(1-\pi_k)Q_k(n)+\pi_{k-1}Q_{k-1}(n)$$

will remain in force. It has, in fact, nothing to do with dimensionality and would hold as well in three dimensions. Only the integration constants $Q_k(k)$ will now have different values. As before, the equation implies $\pi_{k-1}=Q_k(k):Q_{k-1}(k-1)$, so that

$$\Delta f_k(n)=f_{k-1}(n)-\pi_k f_k(n),$$

and since π_k is, obviously, of the first order, we have to retain, in the last term, only the main parts of the two factors, to be marked by dashes. Hence, the equation for the relative probable numbers of aggregates becomes

$$\Delta f_k(n)=f_{k-1}(n)-\pi_k' f_k'(n), \quad . \quad . \quad . \quad . \quad . \quad . \quad . \quad (19)$$

with the condition $f_k(k)=1$.

Thus the problem of determining the numbers $f_k(n)$ is reduced to that of finding the coefficients π_k' and the probable number of *singlets*, $f_1(n)=Q_1(n)$.

Now, a particle P, one of n scattered over the field, will be a singlet if the remaining $n-1$ particles fail to fall within a circle about P, of radius ρ or area $\pi\rho^2=4\sigma$. For, by our assumption about σ and ρ, the impossibility of drawing a full circle about P when it is too close to the boundary may be disregarded. In other words, the area of a *border zone* of width ρ may be neglected when compared with 1, the total area of the field. Thus, the probability that P shall remain unattached is

$$(1-4\sigma)^{n-1} \doteq 1-4\sigma(n-1)$$

and the probable number of singlets, up to σ^2,

$$f_1(n)=n[1-4\sigma(n-1)]. \quad . \quad . \quad . \quad . \quad . \quad . \quad . \quad (20)$$

Our previous 2λ is now replaced by 4σ. The validity of the approximation (20) is conditioned by $\sigma(n-1)<\frac{1}{4}$ or σn not exceeding a moderate fraction. Briefly, $\sigma \ll 1$, $\sigma n<\frac{1}{4}$.

Since the main term of $f_1(n)$ is just n, equation (19) gives, for the main term of any relative number, $\Delta f_k'(n)=f_{k-1}'(n)$, with $f_1'(n)=n$ and $f_k(k)=1$. Hence, exactly as in the linear case,

$$f_k'(n)=\binom{n}{k},$$

so that the equation for the complete relative numbers becomes

$$\Delta f_k(n)=f_{k-1}(n)-\pi_k'\binom{n}{k}.$$

This is exactly of the form of (15), only with $\frac{(k+1)\lambda}{k}$ replaced by the coefficient π_k', so far unknown, but independent of n and with

$$f_1(n)=n-4\lambda\binom{n}{2}$$

replaced by (20) or

$$f_1(n)=n-8\sigma\binom{n}{2}.$$

Hence, integrating as before, we have, for the relative probable number of k-aggregates,

$$f_k(n)=\binom{n}{k}\left\{1-\frac{8+\mu_k}{k+1}\sigma(n-k)\right\}, \quad . \quad . \quad . \quad . \quad . \quad . \quad (21)$$

where $\mu_1=0$ and

$$\mu_k\sigma=\pi_2'+\pi_3'+\ldots+\pi_k', \quad . \quad . \quad . \quad . \quad . \quad . \quad . \quad (22)$$

for $k=2$, 3, etc. The previous K is now replaced by μ_k. Since π_k' is proportional to σ', all μ_k will be *pure numbers*.

It remains to find their values, through those of the main terms of π_2, π_3, and so on. This is actually the only difficult or arduous part of the two-dimensional problem.

In fact, $\pi_2=Q_3(3)/Q_2(2)=P_3(3)/P_2(2)$, $\pi_3=P_4(4)/P_3(3)$, etc., and the probabilities $P_2(2)$, $P_3(3)$, etc., required also for the passage from the relative numbers (21) to the ultimate numbers $Q_k(n)$ are (unlike the linear case) not easy to determine. Apart from the first, $P_2(2)$, even their main terms offer considerable difficulties.

The main term of $P_2(2)$, the probability of a doublet among just two particles in the field, offers no difficulty. One particle being placed anywhere, except the border zone, this term is the probability that the other particle shall fall within a circle about the first of radius ρ or area $\pi\rho^2=4\sigma$. Hence, up to higher terms,

$$P_2(2)=4\sigma=2(2\sigma);$$

this replaces the leading term in the "linear" formula, $P_2(2)=2\lambda-\lambda^2$, the rôle of λ being taken over by 2σ. If the border zone is taken into account, we find with comparative ease, assuming, *e. g.* a circular field of radius $R\gg\rho$, and $\pi R^2=1$, as a second approximation:

$$P_2(2)=4\sigma(1-\tfrac{2}{3}\sqrt{\sigma}). \quad . \quad . \quad . \quad . \quad . \quad . \quad . \quad . \quad (23)$$

Notice that the second term is here in $\sigma^{3/2}$, not σ^2.

The case of a triplet, even with a complete neglect of the border zone, is not so simple. Particle 1 may be placed anywhere (except the border zone). The probability that particle 2 shall fall within a distance r to $r+dr$ from 1 is $2\pi r\,dr$. Draw a circle about 2 with radius ρ. Let $S(r)$ be the area bounded by this circle and an equal circle about 1. This is the place for the third particle (shaded in the figure). Thus,

$$P_3(3)=2\pi\int_0^\rho rS(r)\,dr.$$

Now, the area in question is

$$S(r)=2\rho^2\left(\theta-\frac{1}{2}\frac{r}{\rho}\sin\theta\right), \text{ with } \cos\theta=\frac{1}{2}\frac{r}{\rho},$$

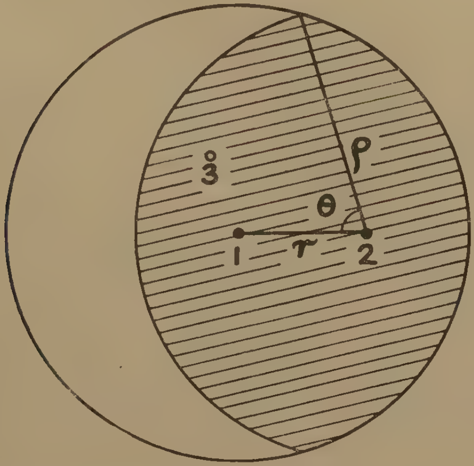

so that, with θ as integration variable and, after some trigonometrical reductions, with $x=2\theta$,

$$\frac{1}{2\pi\rho^4}P_3(3)=\int_\pi^{2\pi/3}[\sin^2 x-x\sin x]\,dx=\frac{\pi}{2}-\frac{3\sqrt{3}}{8},$$

and since $\rho^2=4\sigma/\pi$, the probability of a triplet, up to higher powers of σ, becomes

$$P_3(3)=16\sigma^2\left(1-\frac{3\sqrt{3}}{4\pi}\right)\doteqdot 6{\cdot}616\sigma^2, \quad . \quad . \quad . \quad . \quad . \quad (24)$$

or $$P_3(3)=1{\cdot}654(2\sigma)^2.$$

Compare this main term of the probability with that of the one-dimensional $P_3(3)=3\lambda^2-2\lambda^3$. The numerical factor 3 is now replaced by 1·654, which is almost twice as small *.

---

* In fine, the relations between doublets, triplets, etc., even apart from higher order niceties, are by no means the same in one and two dimensions, as was supposed by Dr. Berg. In passing from one to two dimensions it is not enough simply to replace λ by σ or 2σ. This would lead to an overestimate of the probable number of doublets by 90 per cent.

By (23) and (24),

$$\pi_2 \simeq 1{\cdot}654\sigma,$$

which, in absence of higher terms, is also our π_2', so that, by (22), the number required for the small term in (21) is

$$\mu_2 = 1{\cdot}654. \quad . \quad . \quad . \quad . \quad . \quad . \quad . \quad . \quad . \quad . \quad (25)$$

This replaces the one-dimensional $K_2 = \frac{3}{2}$ which is not much smaller, but it would be a rash extrapolation to say that $\mu_3 = \frac{1}{\sigma}(\pi_2' + \pi_3')$ will differ but little from $K_3 = \frac{3}{2} + \frac{4}{3} = 2{\cdot}83$, and so on. To find μ_3, we would have to determine $\pi_3 = P_4(4) : P_3(3)$, and thus the probability $P_4(4)$ of a quartet or, at least, its main term. From our determination of $P_3(3)$ we can see that this would be a hard task, namely: The particle 3 being placed anywhere in the domain of area $S(r)$, draw a circle of radius ρ about it, find the part S' of that area cut out by this circle, integrate S' over all positions of 3 in S, which will give some complicated function of r, say $F(r)$; lastly, evaluate the integral $P_4(4) = 2\pi \int_0^\rho F(r) r\, dr$. And the determination, even of the main term only, of $P_5(5)$, $P_6(6)$, and so on, would certainly imply prohibitive difficulties. For the present, therefore, we must be content with the couple of results found above and with the obvious property that the main term of any $P_k(k)$ is of the form $c_k \sigma^{k-1}$, where c_k are some pure numbers, starting with $c_1 = 1$, $c_2 = 4$, $c_3 = 6{\cdot}62$. If the border zone of the field is taken into account, we shall have a negative correction term of order $\sigma^{k-\frac{1}{2}}$, so that

$$P_k(k) = c_k \sigma^{k-1}(1 - \alpha_k \sqrt{\sigma}), \quad . \quad . \quad . \quad . \quad . \quad . \quad . \quad (26)$$

where $\alpha_1 = 0$, $\alpha_2 = \frac{2}{3}$, as in (23), while the higher α_k, so far unknown, will be some moderate numbers, not differing much from 1. At any rate, the correction term $\alpha_k \sqrt{\sigma}$ which, in the final formula, has not the factor n, will be a very small fraction.

Thus, by (21), the probable number of k-aggregates among n points becomes

$$Q_k(n) = c_k \sigma^{k-1} \binom{n}{k} \left\{ 1 - \frac{8 + \mu_k}{k+1} \sigma(n-k) - \alpha_k \sqrt{\sigma} \right\}, \quad . \quad . \quad (27)$$

where, to the extent of our present knowledge, $c_1 = 1$, $c_2 = 4$, $c_3 = 6{\cdot}616$; $\mu_1 = 0$, $\mu_2 = 1{\cdot}654$; $\alpha_1 = 0$, $\alpha_2 = \frac{2}{3}$. This holds for $\sigma \ll 1$ and any number n of points satisfying amply the condition $\sigma n < \frac{1}{4}$. For small n, comparable with k, the last term in (27) outweighs the preceding one (since $\sqrt{\sigma} > \sigma$) and a knowledge of α_k is necessary.

For great n, exceeding k considerably, and $\sigma n \gg \sqrt{\sigma}$ the reverse is the case, and the coefficients α_k can be dispensed with. The last formula is then reduced to

$$Q_k(n) = c_k \frac{(\sigma n)^{k-1} n}{k!} \left\{ 1 - \frac{8 + \mu_k}{k+1} \sigma n \right\}, \quad . \quad . \quad . \quad . \quad (27\,a)$$

which holds for $k \ll n$.

It gives, of course, for the number of singlets the first-order approximation $n(1-4\sigma n)$, upon which it was based, which we may, however, replace by the closer approximation, $ne^{-4\sigma n}$.

Thus we have, for singlets and doublets

$$Q_1(n)=ne^{-4\sigma n} \quad . \quad . \quad . \quad . \quad . \quad . \quad . \quad . \quad . \quad . \quad . \quad (\text{I.})$$

$$Q_2(n)=2(\sigma n)n[1-3{\cdot}22\sigma n]. \quad . \quad . \quad . \quad . \quad . \quad . \quad . \quad (\text{II.})$$

For triplets, $\frac{c_3}{3!}=1{\cdot}103$, and

$$Q_3(n)=1{\cdot}103(\sigma n)^2 n\left[1-\left(2+\frac{\mu_3}{4}\right)\sigma n\right], \quad . \quad . \quad . \quad . \quad . \quad (\text{III.})$$

where μ_3, so far unknown, cannot differ very much from 3. For quartets,

$$Q_4(n)=\frac{c_4}{24}(\sigma n)^3 n\left[1-\frac{8+\mu_4}{5}\sigma n\right], \quad . \quad . \quad . \quad . \quad . \quad (\text{IV.})$$

where c_4 is some number comparable with 8 or 10 yet to be determined, through the intricate integral just described, and μ_4, which is reducible to the knowledge of c_5/c_4, will hardly be much greater than 4. If σn, the probable number of particles within a circle of diameter ρ, is of the order of 0·01 or so, the accurate knowledge of μ_3, μ_4, etc., is wholly unimportant.

To form an idea of the numerical implications of these formulæ, suppose, *e. g.*, that

$$\sigma=10^{-8} \quad \text{and} \quad n=10^6,$$

which would suit, roughly, the circumstances of Reinders and Hamburger's experiments (1932) with silver atoms, discussed in detail by Dr. Berg. Then $\sigma n=0{\cdot}01$ and, by (I.) and (II.), we can expect, first of all,

960,800 singlets and 19,356 doublets.

Next, by (III.), $Q_3=110{\cdot}3\left[0{\cdot}98-\frac{\mu_3}{400}\right]$, so that it is immaterial whether our unknown μ_3 is just about 3 or amounts even to full four units. With the latter value, the bracketed factor is 0·97, so that we can expect

107 triplets.

The singlets, doublets, and triplets have already taken up 999,833 of the million particles. Yet, 167 particles are " missing " or left over, sufficient it might be thought, for forming some quartets and higher aggregates. The bulk, however, of that defect, 167, is accounted for by the neglected higher terms, mainly in our expression $Q_2(n)$ for doublets, and we would expect in vain a quartet or a quintet. In fact, $Q_4=\frac{c_4}{24}\left(1-\frac{8+\mu_4}{500}\right)$, so that the accurate value of μ_4 is yet less important than that of μ_3 before, and since c_4 is hardly much greater than 8, we may take, without much ado, $Q_4=\frac{1}{3}$ If the experiment were made three times, each time with a million particles, we could reasonably expect just one quartet. As for quintets, $Q_5=c_5/12{,}000$, and since c_5 is comparable with 12, one such aggregate only could be expected in a thousand experiments. The scarcity of higher aggregates is, of course, due to the thin distribution ($\sigma n=0{\cdot}01$) of particles.

This numerical example may suffice to explain the handling of our formulæ under given experimental conditions.

Dense Distributions.

We have dealt, so far, with sparse or thin distributions of particles, for which, that is, σn (or λn) did not exceed some moderate fraction. To complete our inquiry, let us now consider the case of a dense or congested distribution, with σn approaching or even exceeding unity to any extent.

The simplified, first-order approximation, $n\,[1-4\sigma(n-1)]$, for singlets must now be replaced by the full expression $n(1-4\sigma)^{n-1}$ or, since $\sigma \ll 1$ and we are henceforth interested only in great numbers n, by

$$Q_1(n)=ne^{-4\sigma n}. \quad . \quad . \quad . \quad . \quad . \quad . \quad . \quad . \quad . \quad (28)$$

Such being the probable number of singlets, let us derive from it that of doublets. If we write, as before, $Q_2(n)=4\sigma f_2(n)$, the complete equation (9′) for the relative number of doublets is

$$\Delta f_2(n)=ne^{-4\sigma n}-\pi_2 f_2(n),$$

where, as above,

$$\pi_2=a\sigma, \quad a=1{\cdot}654,$$

and $f_2(2)=1$. With this initial value we might solve the equation rigorously, passing from $f_2(2)$ to $f_2(3)$, and so on, but this would never disclose the structure of f_2 as a function of n. Since we are concerned only with great numbers n, we may replace Δ by the differentiator $\dfrac{d}{dn}$. Thus, and dropping the subscript 2, we have the linear differential equation

$$\frac{df}{dn}+a\sigma f=ne^{-4\sigma n}. \quad . \quad . \quad . \quad . \quad . \quad . \quad . \quad . \quad . \quad (29)$$

Its general integral is, with $c=4-a=2{\cdot}346$,

$$f(n)=\left\{Ae^{c\sigma n}-\frac{1+c\sigma n}{c^2\sigma^2}\right\}e^{-4\sigma n},$$

where A is an arbitrary constant. Although we are interested in great n (and the differential equation holds for such n only), we may determine A so as to give, formally, $f(2)=1$. Then

$$f(n)=\frac{1}{c^2\sigma^2}\left\{(1-c^2\sigma^2)e^{c\sigma n}-(1+c\sigma n)\right\}e^{-4\sigma n},$$

Needless to say, $c^2\sigma^2$ is wholly negligible in presence of 1, but for low n the whole bracket is of the order of σ^2. For $n=2$ it is just $c^2\sigma^2$, giving $f(2)\doteqdot 1$, as desired. Without the small term $c^2\sigma^2$ we should have $f(2)\doteqdot 2$. For considerable values of n, however, this nicety is of no importance.

Thus, after multiplication of f by 4σ, the probable number of doublets becomes

$$Q_2(n)=\frac{4}{c^2\sigma^2}\{e^{c\sigma n}-(1+c\sigma n)\}e^{-4\sigma n}, \quad . \quad . \quad . \quad . \quad . \quad (30)$$

where $c=2{\cdot}346$. This holds for any considerable number of particles and, what now is the main point, for as great σn or as high congestion as we please.

The ratio of the probable number of doublets to that of singlets, (30)/(28), is

$$R(x)=\frac{Q_2(n)}{Q_1(n)}=\frac{4}{cx}[e^x-(1+x)], \quad x=c\sigma n, \quad . \quad . \quad . \quad . \quad (31)$$

a simple function of the *congestion index* σn or $x=2{\cdot}346\ (\sigma n)$ alone, no matter what the total number of particles.

In a thin distribution, as we saw, the singlets were vastly predominant, leaving but scanty material for doublets and some crumbs only for triplets and higher aggregates, as could be expected beforehand. With growing congestion the reverse will soon tend to be the case. The doublets will be more numerous than the singlets. Manifestly, in a dense crowd it is hard to remain single. Presently, the triplets will outnumber the doublets, and so on. This can be seen without the aid of mathematics, qualitatively, that is.

Numerically, the case of doublets and singlets deserves some attention. For small x, the bracket in (31) is $\frac{1}{2}x^2+\frac{1}{6}x^3+\ldots$, and the ratio becomes

$$R(x)=\frac{2x}{c}=2\sigma n.$$

Since, at the same time, $Q_1=n$, we have $Q_2=2\sigma n^2$, in agreement with our previous finding for a thin distribution. The singlets are here by far more numerous than the doublets.

Let us now consider a somewhat dense distribution, say, $x=1$ or $\sigma n=0{\cdot}426$. Then $R=\frac{4}{c}(e-2)=1{\cdot}22$ or

$$Q_2=1{\cdot}22Q_1, \quad (Q_1=ne^{-1{\cdot}70}),$$

22 per cent. more doublets than singlets. At twice that congestion or $x=2$, $\sigma n=0{\cdot}95$, we have $R=\frac{2}{c}(e^2-3)$ and

$$Q_2=3{\cdot}74Q_1,$$

almost four times as many doublets as singlets. For $x=3$, or $\sigma n=1{\cdot}28$,

$$Q_2=9{\cdot}65Q_1,$$

and so on. If σn, the probable number of particles per σ, exceeds only a very few units, we may as well write

$$Q_2:Q_1=\frac{4e^x}{cx}=1{\cdot}70\frac{e^x}{x}.$$

For $x=5$ ($\sigma n=2{\cdot}13$), Q_2 is almost thirty times Q_1, and at twice that density the singlets would dwindle to a negligible minority.

Meanwhile, the probable number of doublets, after reaching some maximum, will, in its turn, begin to diminish, yielding its primacy to triplets, and so on.

The maximum of $Q_2(n)$ is instantly located. It is attained when $df/dn=0$ and thus, by (29), when $f=Q_1/a\sigma$ or

$$Q_2=\frac{4}{a}Q_1=2{\cdot}42Q_1,$$

that is, somewhere between $x=1$ and $x=2$. Its precise position is the root of $R(x)=\frac{4}{a}$ or $e^x=1+\frac{4}{a}x$, which is, nearly enough, $x=1{\cdot}53$, corresponding to $\sigma n=0{\cdot}65$. In other words, the doublets culminate when the mean number of particles in an area σ is 0·65, and then their probable number is 2·42 times that of singlets. Beyond this density, which would seem rather moderate, the number of doublets decreases. No such rise and fall is known to the class of singlets; with growing congestion their number decreases monotonously from totality (n) to nought.

The expectation of triplets can be found with equal ease by solving the differential equation

$$\frac{df_3}{dn}+\pi_3 f_3=f_2,$$

which is exactly of the same form as (29), with π_3 independent of n and with the function $f_2(n)$, just determined, as its second member. The number of triplets will culminate when $\pi_3 f_3=f_2$. Since $f_2(n)$, like $f_1(n)=Q_1(n)$, contains only simple exponentials of n and n itself as factor, the integration offers no difficulty. Likewise, we could pass from triplets to quartets, and so on. The explicit results, however, found above for doublets and singlets should suffice to show the effect of increasing density upon the expectation of various aggregates. The relations for dense distributions in one dimension can be worked out in exactly the same way, starting from $Q_1(n)=ne^{-2\lambda n}$, with the additional advantage that all probabilities $P_k(k)$, as in (7), and therefore also all coefficients π_k appearing in the differential equations are, in this case, completely determined.

Eastman Kodak Co.,
Rochester, New York.
February 9, 1944.

XLIV. *Aggregates in One- and Two-Dimensional Random Distributions. (Developability of Silver Specks of Known Dimensions and the Size of Photographic Sensitivity Specks.)* *

By W. F. Berg †.

[Received October 10, 1944.]

Summary.

A " burst " of k random events occurs if, and only if, an event is found immediately next to an interval Δ containing exactly $k-1$ of the random events. The frequency of the bursts is

$$F_k = P_k \frac{k}{\Delta},$$

where P_k is the Poisson probability of k events being found in a fixed Δ. Sufficiently rare bursts are assumed to be themselves randomly distributed. Similar considerations are applied to the aggregate formation of particles scattered at random on to a plane. For a " k-occurrence " in an area a the above formula applies, Δ being replaced by a. A k-occurrence will always be found as part of a $(k+1)$-occurrence. The frequency of k aggregates is therefore $\phi_k = F_k - F_{k+1}$. These formulæ are applied to the work of Reinders and Hamburger on the developability of small specks of silver. A developable speck is found to contain three atoms, as against four calculated by these authors. Similar considerations applied to the formation of sensitivity specks indicate these to contain approximately 10 silver sulphide molecules.

1. *Introduction.*

When particles, as for example silver atoms, are allowed to fall at random on to a smooth surface, aggregates will be formed if two or more particles fall sufficiently close to each other. Reinders and Hamburger (1) have investigated layers of silver on glass by means of a physical developer which deposits additional silver on any aggregates, which are sufficiently large to serve as nuclei, and thus makes these nuclei visible. The number of nuclei made visible per unit area was determined and compared with the number of aggregates of various sizes obtained by calculation. The formula derived by these authors is not rigid and it was felt desirable to repeat the calculation on a new basis. The formula is derived for the limiting case of infrequent aggregates. The results presented here have given rise to the much more thorough investigation of the mathematical problems involved given by Dr. L. Silberstein in a paper in the same issue of this journal. It seems worth while, however, to present the method of derivation of the approximate formulæ used here, if only because it appears impracticable to obtain a strict formula for the case of aggregates containing numbers of particles larger than 4, which forms the second application of our considerations.

---

* Communication No. H 991 from the Kodak Research Laboratories, Wealdstone, Harrow, Middlesex.

† Communicated by the Author.

This second case deals with the formation of photographic sensitivity specks during the process of emulsion making. Sheppard (2) has shown that photographic sensitivity depends to a considerable extent on the presence or absence of silver sulphide specks on the surface of the silver halide grains in a photographic emulsion. If it is assumed that the process of formation of these specks is one of random conglomeration of silver sulphide molecules on the grain surfaces, the size distribution of specks can be worked out from data (3) on the amount of silver sulphide formed. In the body of the paper below, we shall first treat the one-dimensional, then the two-dimensional case, and finally give the applications to the problems outlined above.

In order to avoid misunderstandings it should perhaps be made clear that in presenting the formation of silver specks by vacuum deposition, and of sensitivity specks, as a purely random process, no justification is implied as to the correctness or otherwise of these basic assumptions. This is not the place to discuss the validity of the assumptions. It is of interest, however, to see what the result will be if these assumptions are made. For the formation of any aggregate, the consideration of random scattering of particles yields a lower limit; if the mechanism bears auto-catalytic features, the resulting particles must be larger.

2. *One-Dimensional Case: "Bursts" in a Time Series of Events.*

The one-dimensional case has intrinsic interest of its own. We may, for example, have to deal with a piece of counting apparatus which has limited resolving power in time. A burst of events may be recorded as a single event only; we may be interested to know how many events are likely to be missed. Another case arises when, in order to trigger off a mechanism, a burst, *i. e.* a certain minimum number of events, may have to occur within a certain time interval. We should then want to know how often the mechanism will act when the average incidence of the events is known. Our problem is then concerned with counting the number of bursts.

Definition of Bursts.

We first require a criterion, which allows us to state in mathematical language, whether and when a burst has occurred in a time series of events. Let us plot these events as dots alone a line (fig. 1). In order to see whether any bursts have occurred within a certain length of time, we take a sub-interval of time Δ, represented by a length, and move it along the time axis, noting the number of dots in the sub-interval as we go along. We can represent the fluctuating number of events in the sub-interval in a fluctuation diagram, as in fig. 1. We shall then say that a burst of k events in a time interval Δ occurs at a time t, if one event occurs at t, and $k-1$ in the time interval preceding t. In the fluctuation diagram, a burst is characterized by the line reaching the level $n=k$, coming from $n=k-1$.

If bursts are sufficiently rare, they can themselves be regarded as randomly distributed. The general case where the bursts are not so distributed and are dependent one upon the other is much more difficult to treat and will not be considered. It will be profitable to consider under which conditions bursts are to be regarded as interdependent. This is obviously the case if events participating in one burst have an appreciable chance of also participating in a subsequent one. In that case, the fact that we know a burst has occurred at a certain time influences the probability of finding a burst in the period immediately subsequent to that time. An illustration of two interdependent bursts is also given in fig. 1. The test interval Δ is shown in two positions, in both of which the burst condition, here to find four events in Δ, is fulfilled. Three of the primary events, however, are common to both bursts, which are therefore interdependent. In this case, apparently, the " intensity " of primary events is so great that interdependent bursts have a considerable chance of occurrence. If we wish to consider the bursts as randomly distributed, we must make sure that bursts are sufficiently rare so that the chance of finding two bursts close together can be neglected when compared with the already small chance of finding one burst at all in the time interval considered ; in one of the examples below, approximately one burst occurs among 10^5 events.

Fig. 1.

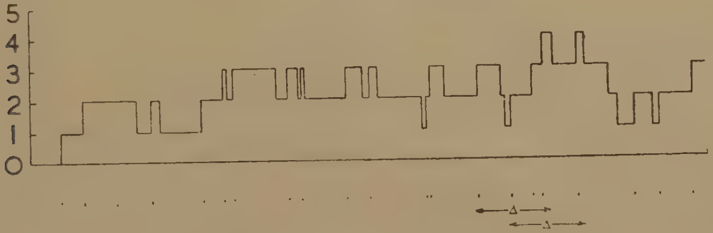

Mathematical.

If random events occur at an average rate of F per unit time, the probability that N events occur within any fixed interval of time T is given by Poisson's well-known equation :—

$$\Pi_N(T)=\frac{(FT)^N e^{-FT}}{N\,!}. \qquad (1)$$

This equation we assume to apply to our rare bursts ; it is solved, if we can work out the average burst intensity F, from the known intensity of primary events I making up the burst. The probability of finding k primary events in the "burst interval" of time Δ is again given by a Poisson distribution:

$$P_k(\Delta)=\frac{(I\Delta)^k e^{-I\Delta}}{k!}. \qquad \text{(1 } a\text{)}$$

The probability of finding a burst in dt at t can be written down as the frequency of bursts F_k multiplied by dt, and also as the compound probability of finding $k-1$ events in Δ and one in dt at t, which is $I\,dt$, thus,

$$\left.\begin{aligned} F\,dt&=P_{k-1}(\Delta)I\,dt,\\ F_k&=\frac{(I\Delta)^{k-1}e^{-I\Delta}}{(k-1)!}.\end{aligned}\right\} \qquad (2)$$

It is easily seen that this can be transformed into

$$F_k=P_k\frac{k}{\Delta}. \qquad (3)$$

Sometimes we are only interested in the question whether or no a mechanism has been triggered off by a burst during a certain time interval T; in other words, we want to know the probability of one or more bursts occurring during T. This is given by

$$\sum_{N=1}^{\infty}\Pi_N\equiv\Pi_{1+}=1-\Pi_0=1-e^{-F_kT}. \qquad (4)$$

If T is so short that the probable number of bursts F_kT is small, this, of course, reduces to

$$\Pi_{1+}\simeq\Pi_1=F_kTe^{-F_kT}\simeq F_kT=P_k\frac{k}{\Delta}T. \qquad (5)$$

3. *Two-Dimensional Case: Chance Aggregates.*

The treatment of the two-dimensional case follows closely that of the one-dimensional case. In order to see this, we have first of all to consider the distribution of randomly scattered particles in two dimensions. We shall then again perform a hypothetical "scanning experiment" in the two dimensions, moving an imaginary area about the distribution of dots and noting whenever a certain number of dots falls within the scanning area. If and when it does an aggregate is assumed to be formed.

(A) *Two-dimensional Poisson Distribution.*

For our further considerations we need the equivalent of the Poisson distribution in two dimensions; the calculation is not given in the more commonly used text-books, and is here given following the method used by Bateman (4) for the one-dimensional case. Here we ask for the probability that n particles fall into an area XY which for convenience we make rectangular (fig. 2), if the probability of finding one particle in the infinitesimally small areas $X\,dy$ and $Y\,dx$ is $f_Y X\,dy$ and $f_X Y\,dx$ respectively. For a completely random distribution $f_X=f_Y=f$. The probability that two particles fall into the areas $X\,dy$ and $Y\,dx$ or $X\,dy+Y\,dx$ * is so small compared with that for one particle that it can be neglected. We can now argue :—

The probability that $n+1$ particles fall into the area $XY+Y\,dx+X\,dy$ is made up of two alternatives :

(1) that we find n in XY and 1 in $X\,dy+Y\,dx$;

(2) ,, $n+1$ in XY and 0 in $X\,dy+Y\,dx$.

Thus, the probability of finding $n+1$ in the area $XY+X\,dy+Y\,dx$ is

$$P_{n+1}(XY,\ X dy+Y dx)=P_n(XY).f(X\,dy+Y\,dx)$$
$$+P_{n+1}(XY).\{1-f(X\,dy+Y\,dx)\}.$$

This transforms into

$$P_{n+1}(XY,\ Y\,dx+X\,dy)-P_{n+1}(XY)$$
$$=f(X\,dy+Y\,dx)\{P_n(XY)-P_{n+1}(XY)\}$$

Fig. 2.

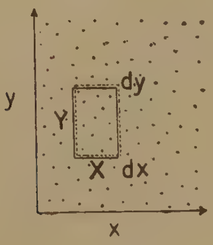

or, dropping the arguments,

$$dP_{n+1}=d(XY)f(P_n-P_{n+1}).$$

For $d(XY)$ we can put δa, the amount by which the test area has been shifted. The last equation corresponds exactly to the one-dimensional case and the integration leads to

$$P_n=\frac{(fa)^n e^{-fa}}{n!}. \quad \ldots\ldots\ldots \quad (6)$$

(B) *Aggregates.*

We are here interested in the number of particles which are likely to fall into a test area of size a, which may be situated anywhere in the field under consideration. We may imagine that we move the test area over the field, thus " scanning " the distribution. In analogy to the one-dimensional case treated in Section 2, we can represent the number of particles in an area $a=XY$ in a fluctuation diagram, in which that number is plotted against the ordinates x and y of, say, the positive sides of the test area. We shall then say that an aggregate of k particles is found at the co-ordinates x and y, if there are $k-1$ particles in a, and one particle in $X\,dy$ at y or $Y\,dx$ at x provided that on further movement of the test area the number of particles in that area drops again. If the number rises to $k+1$, then we are clearly dealing with a $(k+1)$—or an even larger—aggregate. The frequency of occurrence of aggregates can be worked out in strict analogy to the one-dimensional case, since the probabilities in the x- and y-directions are independent of each other. We shall first calculate the frequency of what we may term a " k-occurrence " of finding $k-1$ particles in XY and one in $X\,dy+Y\,dx$ at xy, without considering whether the k-occurrence signifies the occurrence of a k- or a bigger aggregate. In order to find the probability of a k-occurrence, all we need to do is to project all the particles on to the x-axis and treat the one-dimensional case thus ensuing. We can thus write, following equations (2) and (3),

---

* The area $dy\,dx$ is infinitesimally small of the second order and may be neglected.

$$F_k Y\,dx=P_k\frac{k}{X}\,dx, \qquad (7\,a)$$

and similarly

$$F_k X\,dy=P_k\frac{k}{Y}\,dy. \qquad (7\,b)$$

The probability of finding k particles in XY at x, y is the sum of (7 *a*) and (7 *b*),

$$F_k(Y\,dx+X\,dy)=P_k k\left(\frac{dx}{X}+\frac{dy}{Y}\right)=P_k\frac{k}{XY}(Y\,dx+X\,dy),$$

$$F_k\delta a=P_k\frac{k}{a}\delta a. \qquad (8)$$

δa denotes the infinitesimal amount of area by which the test area a was shifted. It is important to note that the result depends on the size of the test area only, not on its shape. We are therefore free to choose an area of any shape we like for our considerations of aggregate formation. The probability of finding N k-occurrences within an area A is thus given by an equation like (1) :

$$\Pi_N(A)=\frac{(F_kA)^N e^{-F_kA}}{N\,!}, \qquad (9)$$

in which F_k, the average frequency of a k-occurrence, is given by (8) and P_k in (8) by (6). The probable number of k-occurrences in A is then given by F_kA.

To obtain ϕ_kA, the probable number of k-aggregates from F_kA, we have to subtract from F_kA the probable number of all m-occurrences, where $m>k$. The probable number of m-occurrences is, by the same argument which led to equation (8), F_{k+1}. We have, therefore,

$$\phi_kA=A(F_k-F_{k+1}). \qquad (10)$$

For the rare occurrences in which we are interested F_{k+1} may be neglected against F_k, as can be seen from the numerical examples treated below.

4. *The Developability of Small Aggregates of Silver.*

(A) *Reinders and Hamburger's Formula.*

Reinders and Hamburger derive the following formula:

$$L=p\frac{B^k e^{-B}}{k!}, \quad \ldots\ldots\ldots \quad (11)$$

where

L=fraction of surface covered by aggregates.

k=number of atoms in the aggregate.

B=" coverage " of the surface=number of atoms deposited divided by total number depositable in a mono-atomic layer.

p is a correction factor, which is =1 for isolated atoms,
7 for di-atomic aggregates,
7 × 10 for triple aggregates,
7 × 10 × 12 for quadruple aggregates.

The derivation of (11) need not be reported here in detail. In the derivation it is considered that for mono-atomic coverage there is room for a certain number of m atoms on the surface. The surface was divided into m cells, and the probability of obtaining a k-aggregate in any one cell is represented by (11). This formula does not take into account that the particles may fall anywhere and that an actual aggregate may thus be formed by particles which, by the artificial sub-division used, fall into neighbouring cells. After the formula was derived the correction factor p was introduced to allow for the fact that the probability of a larger aggregate being hit by an additional atom is bigger than that for a small aggregate. It was felt originally that formula (11) does not meet the case of aggregate formation with sufficiently rigidity.

(11) can be transformed into the units used in the present calculation quite readily. If a is the area occupied by one k-aggregate, then

$$L=F_k a,$$

and similarly $B=fa.$

We have thus $L=F_k a=\frac{p(fa)^k e^{-fa}}{k},$

which is equivalent to $F_k=P_k\frac{1}{a}. \quad \ldots\ldots\ldots \quad (12)$

(12) differs from (8) by the factor p and the missing factor k. Another difference from the evaluation of (8) given below is that we shall allow different areas a_k for aggregates of different sizes, whereas a fixed value for a was used by Reinders and Hamburger.

There are no data in literature which would allow us to give at least an estimate of the radius of action of silver atoms as far as the process of aggregation is concerned. In the calculation below, we have assumed, following Reinders and Hamburger, that this radius is comparable with the dimensions of the atom. We shall give figures obtained on the following assumptions :—

A double aggregate is formed if two atoms—here regarded as points—fall into an area as large as one atom.

A triple aggregate is formed if three atoms fall into an area twice as large as that occupied by one atom.

A k-aggregate is formed if k atoms fall into an area $(k-1)$ times that occupied by one atom.

The other units used in the calculation are :—

A, our unit area considered $=10\mu^2$ (following Reinders and Hamburger).

An area occupied by a k-aggregate $=(k-1)\times 6{\cdot}47\times 10^{-9}$ A*. This value is obtained from the metallic structure of silver, the atomic distance being $2{\cdot}86\times 10^{-8}$ cm.

TABLE I.

k. Number of atoms in aggregate.	i.		ii.		iii.	
	a. Area of aggregate. Unit=A. $=10\mu^2$.	F_k. Probable No. of aggregates in A.	a.	F_k.	a.	F_k.
2	$6{\cdot}47\times 10^{-9}$ A	2368	$6{\cdot}47\times 10^{-9}$	8289	$6{\cdot}25\times 10^{-9}$	14,000
3	$12{\cdot}94\times 10^{-9}$	18·5	,,	107·9	,,	235
4	$19{\cdot}41\times 10^{-9}$	0·16	,,	1·27	,,	3·5
	Formula (8) $f=6{\cdot}05\times 10^5$.		Formula (12) $f=6{\cdot}05\times 10^5$.		Formula (12) $f_R=8\times 10^5$.	

$f=6{\cdot}05\times 10^5$ molecules in A. This is obtained from Reinders and Hamburger's value for the coverage $B=0{\cdot}005$, allowing for the fact that in close face-centred packing one silver atom occupies $8{\cdot}24\times 10^{-9}$ A. Reinders and Hamburger appear to have made a mistake on this point. They state that about 8×10^5 atoms in $10\mu^2$ corresponds to a coverage $B=0{\cdot}005$; this allows only $6{\cdot}25\times 10^{-9}$ A. for one atom. In order to obtain Reinders and Hamburger's values using formula (12), it was necessary to use the faulty value of $f_R=8\times 10^5$, which corresponds to $\mathrm{B}>0{\cdot}005$.

In Table I. are given the values for the probable number of aggregates of size k in an area $A=10\mu^2$, together with the values of a and f used.

---

* The value $8{\cdot}24\times 10^{-9}$ might equally well be used ; the choice is clearly an arbitrary one.

In comparing the values with Reinders and Hamburger's experiments, which show 3 to 4 developable aggregates in $10\mu^2$, we note that our calculation would give an aggregate of 3 atoms as a developable speck (column i.), whereas Reinders and Hamburger's calculation yielded an aggregate of 4 (columns ii. and iii.). The order of magnitude is the same, and there is thus no significant difference between Reinders and Hamburgers' (12) and the present, formula (8), with respect to the formation of small aggregates.

5. *Size of Sensitivity Specks.*

Principle of Calculation.

The basic consideration which allows one to calculate the dimensions of a sensitivity speck closely follows the calculations on silver aggregates. The formation of silver sulphide on the grain surfaces in a photographic emulsion is here * regarded as a random process. The amount of silver sulphide which gives optimum speed with an emulsion has been variously estimated and the evidence carefully sifted by Sheppard (3). A representative average of his figures is a concentration of 5×10^{-4} grams of silver sulphide per gram of silver bromide. This figure should perhaps be regarded as an upper limit, since it is possible that not all of the amount measured actually played a part in the sensitization process. From this figure we can work out the average number f of silver sulphide molecules on an average emulsion grain. Random distribution of these molecules means that there will be a population of silver sulphide specks of various sizes over the grain surface. For optimum sensitization a grain will carry just one optimum size speck ; specks smaller than this hypothetical size will not act at all or very inefficiently ; larger specks will be "fog specks," *i. e.* grains carrying these will be spontaneously developable. When we work out our statistics on the number of specks of different sizes, we shall find that a certain size occurs once on every one or perhaps every tenth grain in an emulsion. We shall then assume that this size is that of the most efficient sensitivity speck.

Data Used.

In the reference quoted (3), the emulsions in which the optimum amounts of silver sulphide were determined have not been sufficiently closely specified to allow us to work out our statistics. Since, however, the order of magnitude only can be of interest here, grain-size data on a fast emulsion obtained in this laboratory † have been assumed to apply. This emulsion had an average grain-size of $4\cdot8\times10^{-4}$ mm., and the number of grains was $2\cdot4\times10^{9}$ per cubic mm. The surface of an average grain, assumed to be spherical, is $2\cdot9\times10^{-6}$ square mm. Sheppard's data [3] correspond to a concentration of $5{\cdot}4\times10^{11}$ molecules of silver sulphide per square mm., which can be seen to correspond to a roughly mono-molecular coverage of our grain surfaces.

---

* It has already been mentioned that objections may be raised to this view because of some known auto-catalytic features of the chemical reactions involved.

† The writer is indebted to Miss M. Gauntlett of these laboratories for the data used.

Calculation.

The area into which molecules have to fall must depend, as it did in the case of silver aggregates, on the dimensions of the molecules. We shall assume the radius of action of a molecule to be of the order of its own dimensions. The silver sulphide molecule consists, of course, of two silver ions and one sulphur ion, the valency angle being about 90° [5]. The ionic radii are $Ag^+\simeq1{\cdot}2\times10^{-7}$ mm., $S^{--}\simeq1{\cdot}8\times10^{-7}$ mm.[6]. The area occupied by a molecule of these dimensions is approximately 10×10^{-14} square mm. The area into which k molecules have to fall to form a k-aggregate is therefore $A_k=(k-1)10^{-13}$ square mm. The results are shown in Table II. and indicate that the optimum size sensitivity speck is of the order of 9 to 10 molecules, assuming that, say, every 10th grain carries an optimum size speck. This would seem to be a satisfactory result, since the number of silver atoms which collect on the speck to form a latent image is of the same order of magnitude.

TABLE II.

k. Number of molecules in aggregate.	F_kA. Number of aggregates per grain of area A.	
7	8·5	
8	2·06	$A=2{\cdot}9\times10^{-6}$ mm.².
9	0·19	$a=(k-1)\times10^{-13}$ mm.².
10	0·032	$f=5{\cdot}4\times10^{11}$ mm.².
11	0·0054	
12	0·001	

Bibliography.

(1) Reinders and Hamburger, *Z. wiss. Phot.* xxxi. p. 32 (1932); *Recueil Trav. Chim. Pays-Bas*, l. p. 475 (1931); also Reinders and De Vries, *ibid.* lvi. p. 985 (1937).
(2) Sheppard, Trivelli and Loveland, J. Franklin Inst. cc. p. 51 (1925).
(3) Sheppard, Phot. J. lxxi. p. 331 (1931).
(4) Bateman, Phil. Mag. 6th ser. xx. p. 704 (1910).
(5) Sidgwick and Powell, Proc. Roy. Soc. A, clxxvi. p. 153 (1940).
(6) Mott and Gurney, 'Electronic Processes in Crystals,' p. 268. (Oxford, 1940.)

XLV. *The Effect of Grain or Particle Size on X-ray Reflections from Mixed Powders and Alloys, considered in relation to the Quantitative Determination of Crystalline Substances by X-ray Methods.*

By G. W. Brindley, M.Sc., Ph.D., Physics Laboratories, University of Leeds †.

[Received November 8, 1944.]

I. *Introduction.*

The question of the effect of grain or particle size on the relative intensities of X-ray reflections from powders consisting of a mixture of two or more substances is of fundamental importance in several different connections. It arises, for example, when mixtures of known composition are used for the purpose of making an accurate comparison of the intensities reflected by the individual components. The question is equally important in connection with the converse problem of determining quantitatively the composition of a mixture from the reflected X-ray intensities ; the mixture may be a simple mechanical mixture or it may be a heterogeneous solid such as an alloy or a slag or a rock specimen containing two or more phases. To see how the particle size of a mixture affects the reflected intensities it is necessary to focus attention on the steps involved in extending the generally accepted theory of reflection by a single powder to the case of mixed powders.

The theoretical calculation of the intensity of X-ray reflection by crystalline powders is usually based on the assumption that the intensity reflected by any small volume element δV of the powder is proportional to δV, which is true provided there is negligible absorption within the volume element ; see, for example, Compton and Allison, ‘X-rays in Theory and Experiment,’ ch. vi. p. 415. The total reflected intensity is then obtained by integration over the volume of the powder specimen, with due allowance for absorption and for the random orientation of the crystallites. The theory is equally applicable to fine-grained single phase solids, such as alloys and slags, provided the grains are randomly orientated. With only slight modification the theory is applicable to reflection by mixed powders and by solids containing more than one phase provided the mixture, either powdered or solid, can be regarded as homogeneous from the standpoint of X-ray absorption. The condition to be satisfied is that the volume element δV, which must be sufficiently small to have negligible absorption, must at the same time be sufficiently large to be representative of the powder or solid as a whole. δV cannot therefore be smaller than the individual particles or grains of the mixture, and if these are so coarse in relation to the radiation employed that they absorb appreciably, then the basic assumption requires modification; the powder cannot then be treated as essentially homogeneous and the theory must be developed in a manner which takes account explicitly of the heterogeneity of the mixture.

---

† Communicated by the Author.

If the particles of a mixture are sufficiently fine, the reflected intensities from different components may be regarded as equally influenced by the mean macroscopic absorption of the mixture, but with coarser particles this equalization of absorption may not occur. In a mixture ABC, consisting of such particles, whenever a crystal A reflects radiation, the reflected intensity is diminished by absorption in the particle of A to which the crystal belongs and by the large scale absorption of the radiation entering and leaving the powder specimen, and likewise for B, C, . . Equalization of the large scale absorptions can, in many cases, be assumed, but not of the absorptions in the particles to which the reflecting crystals belong. The latter will therefore act differentially on the reflections from the different substances.

This problem has already been considered by a number of writers. Rusterholz (1931) was the first to stress its importance when mixed powders are used. The theory was developed considerably by Schäfer (1933), especially the statistical aspect. It has also been discussed mainly from an experimental standpoint in connection with the "mixture method" of standardizing X-ray reflections from powders by Brentano (1935, 1938) and by Brindley and Spiers (1938). Taylor (1944 *a*, *b*) has studied the problem independently, for he appears to have been largely unaware of previous papers on the subject; he has discussed in particular the bearing of the problem on the quantitative analysis of heterogeneous alloys. Gross and Martin (1944) have considered the "quantitative determination of crystalline materials by X-ray diffraction" without any consideration of the important part played by particle size.

From a survey of the literature it is evident that there is a lack of agreement on several points. In the first place the question arises whether the crystal size or the particle size should be taken into account when correcting the intensity formula for the coarseness of the powder. Without explicit consideration of the point, most writers have taken the particle size as being the more important, but Taylor concludes that the crystal size is the more important. The present paper shows that it is essentially the particle size of which account must be taken †.

Difference of opinion also exists as to the *form* of the correction factor to be inserted in the expression for the reflected intensity. Schäfer and Taylor have given correction factors of the form

$$\frac{1}{V_a}\int_0^{V_a} e^{-\mu_a x}\, dV_a,$$

---

† If the individual crystals are of such a size that extinction effects occur, then crystal size is also important but for a quite different reason.

where V_a is the volume of a particle (or crystal) of substance A, μ_a its linear absorption coefficient, and x the path of the radiation in the particle of A when reflected by the volume element dV_a. In the present paper it will be shown that for powders which are not too coarse (such as Schäfer and Taylor considered) the correction factor takes the form

$$\frac{1}{V_a}\int_0^{V_a} e^{-(\mu_a-\bar{\mu})x}\,dV_a.$$

where V_a is the particle volume and $\bar{\mu}$ is the mean linear absorption coefficient of the solid material of the powder. Rusterholz also indicated that an expression of this kind should be used, but in place of $\bar{\mu}$ he gave μ', the mean linear absorption coefficient of the powder specimen. The change in the form of the correction factor, though apparently small, has important practical consequences, as will be shown in section IX.

A further question requiring consideration is whether a correction factor is required for single powders or only for powders consisting of a mixture of substances or phases. This is not explicitly considered by Schäfer, but Taylor definitely concludes that such a factor is required even for single powders. He develops this point more fully in his second paper, where he discusses *inter alia* certain experimental results for X-ray intensities reflected by filed metal powders by Brindley and Spiers (1935), and suggests an alternative interpretation of their results based on the idea of a *crystal* absorption factor developed in his first paper. The present analysis shows that such a correction factor is *not* required by single powders and Taylor's re-interpretation of the results is therefore wholly invalid. Brindley and Spiers were in fact well aware of the difficulties arising from coarse mixed powders and purposely developed a method which did not necessitate the use of mixtures.

With a view to resolving the differences between the writer's point of view and that of Dr. Taylor, the subject has been discussed at length privately; the results of the discussion are indicated in the two letters which have recently appeared in this journal, from which it will be seen that Dr. Taylor is now largely in agreement with the writer's point of view (see Phil. Mag. xxxv. pp. 638–641, 1944.—Note added in proof Sept. 6, 1945).

In what follows, reference will be made mainly to the particle size of powders, but it will be evident that in general the statements apply equally well to the grain size of heterogeneous solids; certain differences between powders and solids are discussed separately in section X.

II. *The Effect of Particle Size on X-ray Reflection from Mixed Powders.*

It will be found convenient to classify powders as regards their degree of coarseness in relation to X-ray absorption in the following way:—Let D be a measure of the linear size of a particle and μ the linear absorption coefficient. Then powders may be graded as fine, medium, coarse or very coarse, depending on the value of μD.

(i) *Fine Powders.* $\mu D < 0{\cdot}01$.—The individual particles have negligible absorption and the generally accepted theory of X-ray reflection by powders is applicable in this case.

(ii) *Medium Powders.* $0{\cdot}01 < \mu D < 0{\cdot}1$.—Particle absorption, though appreciable, is such that the radiation penetrates a considerable number of particles ; reflection from such a powder is essentially a "volume" process. The correction factor for particle absorption takes the form

$$\frac{1}{V_a}\int_0^{V_a} e^{-(\mu_a-\bar{\mu})x}\,dV_a.$$

(iii) *Coarse Powders.* $0{\cdot}1 < \mu D < 1$.—The statistical theory developed by Schäfer is applicable to such powders. Provided μD tends to the lower rather than to the upper limit, the particle absorption factor in the above form may be used to *estimate* the effect of the coarseness of the powder on the reflected intensities.

(iv) *Very Coarse Powders.* $\mu D > 1$.—Particle absorption is large and the reflection process is confined mainly to a surface layer of particles. No real distinction can now be drawn between particle absorption and powder absorption, and the concept of a particle absorption factor loses its meaning.

Although detailed numerical considerations of particle sizes and absorption coefficients will be given later (see section IX.), it will be of interest at this stage to indicate briefly the order of magnitude of the number of particles penetrated by the radiation in the different grades of powders. If the reflected intensity is reduced owing to absorption by a factor of (say) 1/10, then the number of particles traversed by the radiation is as follows :—case (i), more than 230 ; case (ii), between 23 and 230 ; case (iii), less than 23 ; and case (iv), 2 or 3. With very coarse powders the greater part of the reflected radiation clearly comes from the surface layer. With coarse powders, the radiation penetrates a few layers but not a sufficient number for the process properly to be regarded as a "volume" one.

III. *X-ray Reflection by Fine Powders.*

The current theory is valid in this case and it is unnecessary to do more than write down certain expressions which will be required in connection with coarser powders.

The intensity, δI, reflected by a small single crystal of volume δV having negligible absorption, is given by the expression

$$\delta I = I_0 Q \delta V,$$

where

$$Q = \frac{\epsilon^4\lambda^3}{m^2c^4} N^2F^2 \left(\frac{1+\cos^2 2\theta}{2\sin 2\theta}\right), \quad . \quad . \quad . \quad . \quad . \quad . \quad . \quad (1)$$

the symbols having their usual significance (see, for example, Compton and Allison, *loc. cit.* p. 414). When this is applied to the case of reflection by a fine powder of randomly orientated crystallites, the corresponding expression is

$$\delta I = \frac{ps}{8\pi r \sin\theta} I_0 Q \delta V,$$

$$= I_0 Q' \delta V, \quad \ldots \ldots \ldots \quad (2)$$

where
$$Q' = \frac{ps}{8\pi r}\left(\frac{e^4\lambda^3}{m^2c^4}\right) N^2F^2 \left(\frac{1+\cos^2 2\theta}{2\sin\theta\sin 2\theta}\right).$$

δI is now the intensity reflected into a line of length s on a film distant r from the powder, p is the number of planes in the crystal having the same spacing, and δV is an element of volume of the *solid* material of the powder (*cf.* Compton and Allison, *l. c.* p. 417, eq. 6·81). The total reflected intensity is obtained by integrating eq. (2) through the volume of the powder irradiated by X-rays with allowance for absorption and for the spacing of the solid material in the powder specimen.

The following cases may be briefly considered :—

(a) *Reflection from a Powder Block : Single Substance.*

An X-ray beam, of area S, is incident at a glancing angle ψ on a flat powder block (see fig. 1 *a*). The volume of the powder specimen irradiated between depths x and $(x+dx)$ is $S\,dx/\sin\psi$. If ρ and ρ' are the densities of the solid substance and powder respectively, then the volume of solid substance irradiated is

$$\delta V = \frac{S\,dx}{\sin\psi} \cdot \frac{\rho'}{\rho}.$$

The path of the radiation in the powder is

$$l = x\left\{\frac{1}{\sin\psi} + \frac{1}{\sin(2\theta-\psi)}\right\}.$$

If μ' is the absorption coefficient of the powder specimen, then from eq. (2) the total reflected intensity is given by

$$I_r = \int dI = \frac{I_0 Q' S \rho'}{\rho \sin\psi} \int_0^\infty e^{-\mu' x\{1/\sin\psi + 1/\sin(2\theta-\psi)\}} . dx$$

$$= I_0 Q' S \left[\frac{\sin(2\theta-\psi)}{\sin(2\theta-\psi)+\sin\psi}\right] \frac{\rho'}{\mu'\rho}.$$

Fig. 1.

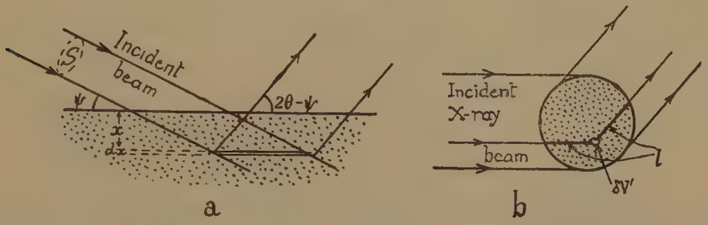

X-ray reflection from fine crystalline powders ($\mu D < 0{\cdot}01$).

For a fine powder $\mu'/\rho'=\mu/\rho$, where μ is the linear absorption coefficient of the solid substance. Writing $A(\theta, \psi)$ for the angular factor in square brackets, we have

$$I_r=I_0 Q' S A(\theta, \psi)/\mu.$$

(b) *Reflection from a Cylindrical Rod of Powder : Single Substance.*

The volume of solid substance in the volume $\delta V'$ of powder is $\delta V'\rho'/\rho$. If l is the corresponding path of the radiation in the cylinder (see fig. 1 *b*), the total reflected intensity is given by

$$I_r=I_0 Q' (\rho'/\rho)\int_0^{V'} e^{-\mu' l}\cdot dV',$$

$$=I_0 Q' V' \alpha\rho'/\rho,$$

where $$\alpha=\frac{1}{V'}\int_0^{V'} e^{-\mu' l} dV',$$

and V' is the volume of the powder cylinder irradiated by *X*-rays. In general this integral can be evaluated only by numerical methods, as Bradley (1935) in particular has shown.

(c) *Reflections from Mixed Powders.*

Let ρ'=mean density of powder specimen,
$\bar{\rho}$=mean density of solid substances,
g_a=proportion by weight of substance A in the mixture,
and ρ_a=density of solid substance A.

Then in a volume $\delta V'$ of the powder specimen, the volume of solid substance A is

$$V'(\rho'/\bar{\rho})(g_a\rho/\rho_a), \text{ i. e. } \delta V'\rho' g_a/\rho_a.$$

The intensity reflected by substance A of the mixture is therefore given by the following expressions :—

$$I_a=I_0 Q_a' S A(\theta, \psi)_a \rho' g_a/\mu'\rho_a \quad \ldots\ldots \quad (3\,a)$$

for a powder block, and

$$I_a=I_0 Q_a' V' \alpha_a \rho' g_a/\rho_a \quad \ldots\ldots \quad (3\,b)$$

for a cylindrical rod.

The ratio of the intensities, I_a and I_b, reflected by two components A and B of a mixture, is therefore given by

$$\frac{I_a}{I_b}=\frac{Q_a' A(\theta, \psi)_a g_a \rho_b}{Q_b' A(\theta, \psi)_b g_b \rho_a} \quad \ldots\ldots \quad (4\,a)$$

for a powder block, and

$$\frac{I_a}{I_b}=\frac{Q_a' \alpha_a g_a \rho_b}{Q_b' \alpha_b g_b \rho_a} \quad \ldots\ldots \quad (4\,b)$$

for a cylindrical rod.

The advantage of using a powder block is that A is more easily and probably more accurately determinable than α because A depends only on θ and ψ and does not involve absorption coefficients. The cylindrical rod has the advantage that the reflections can be more satisfactorily recorded over a wide range of angles.

IV. *X-ray Reflection by Medium Grade, Mixed Powders.*

We proceed now to consider powders the particles of which satisfy the condition $0{\cdot}01<\mu D<0{\cdot}1$. The particles will be assumed to be polycrystalline and the powder to be a mixture of two or more substances. If the adhesive used to bind the particles together has appreciable absorption it must be treated as one of the components of the powder. Reflection by such a powder is illustrated in fig. 2.

Let δv_a=volume element of a crystal of A correctly orientated to reflect radiation,
g_a=weight proportion of substance A in the mixture,
μ_a=linear absorption coefficient of substance A,
μ' and ρ'=mean absorption coefficient and mean density of the powder specimen,
$\bar{\mu}$ and $\bar{\rho}$=mean absorption coefficient and mean density of the solid material forming the powder,
l=total path of the radiation in the powder specimen,
x=path of the radiation in the particle to which δv_a belongs.

Fig. 2.

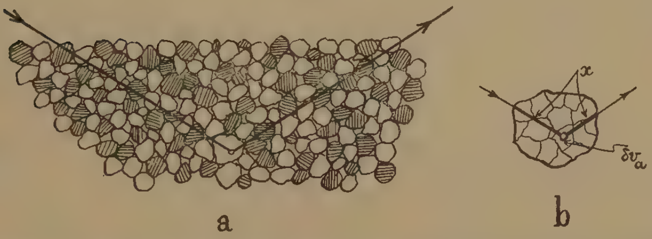

X-ray reflection from mixed medium grade powders ($0{\cdot}01<\mu D<0{\cdot}1$). (*a*) shows a two-component powder. (*b*) shows reflection from a volume-element δv_a of a crystal in a polycrystalline particle; x is the path of the radiation in the particle.

Since ρ' is less than ρ, owing to air spaces between the particles, absorption of the radiation will occur along only a fraction of the path l. Consider a thin pencil of radiation of length l, cross-section da and volume $l\,da$. Now the fraction of any volume of powder occupied by solid matter will be $(\rho'/\bar{\rho})$, provided the volume under consideration involves a sufficient number of particles; this condition, to which further reference will be made later (see section VI.), is sufficiently well satisfied by the powders now under consideration. The volume of the thin pencil occupied by particles will be $l\,da\,(\rho'/\bar{\rho})$, and therefore the length of the path occupied by particles will be $l(\rho'/\bar{\rho})$.

Along the path $\{(\rho'/\bar{\rho})l-x\}$ of the radiation in the powder we may assume the mean absorption coefficient $\bar{\mu}$ to be operative, and along the path x in the particle the absorption coefficient μ_a. The reflected intensity from the element δv_a is therefore given by

$$\delta \mathrm{I} = \mathrm{I}_0 \mathrm{Q}\, \delta v_a e^{-\bar{\mu}\{(\rho'/\bar{\rho})l - x\} - \mu_a x}.$$

Provided the radiation passes through a sufficient number of particles, we may write

$$\mu'/\bar{\mu} = \rho'/\bar{\rho}, \qquad \qquad (5)$$

where μ' is the mean absorption coefficient of the powder specimen. The justification for this step is provided by Schäfer's statistical treatment and will be considered again later (see section VI.). The reflected intensity can therefore be written

$$\delta \mathrm{I} = \mathrm{I}_0 \mathrm{Q}\, \delta v_a e^{-\mu' l} . e^{-(\mu_a - \bar{\mu})x}.$$

In the corresponding expression for reflection by fine powders the second exponential factor is omitted, for the particles are then so fine that x and consequently $(\mu_a - \bar{\mu})x$ approaches zero and the exponential is practically unity. Now for any given path length l, the reflecting crystals will occupy all possible positions equally within the particles. Since the second exponential depends only on the path of the radiation in the particle and therefore on its size and shape, while the first exponential depends only on the path in the powder specimen and not on the individual particle, we may, before integrating the expression for $\delta \mathrm{I}$ over the total volume of powder, take the mean value of the second exponential averaged over the volume of a particle, namely,

$$\tau_a = \frac{1}{\mathrm{V}_a} \int_0^{\mathrm{V}_a} e^{-(\mu_a - \bar{\mu})x}\, dv_a, \qquad \qquad (6)$$

where V_a is the particle volume. The mean reflected intensity per particle is therefore

$$\mathrm{I}_0 \mathrm{Q}' \tau_a \mathrm{V}_a e^{-\mu' l}.$$

The factor τ_a will be called the "particle absorption factor." The use of Q' rather than Q in this expression implies that allowance has been made for the random orientation of the crystallites.

Considering now an element of volume $\Delta \mathrm{V}'$ of the powder specimen, we have already seen that the volume of substance A contained in it is $\Delta \mathrm{V}' \rho' g_a/\rho_a$, and therefore the number of particles of A in this volume of powder is $\Delta \mathrm{V}' \rho' g_a/\rho_a \mathrm{V}_a$. The reflected intensity from substance A contained in $\Delta \mathrm{V}'$ is therefore given by

$$\Delta \mathrm{I}_a = \mathrm{I}_0 \mathrm{Q}' \tau_a (\rho' g_a/\rho_a)\, e^{-\mu' l} \Delta \mathrm{V}'.$$

The calculation of the total reflected intensity now follows along the same lines as for a fine powder, and the final result takes the form

$$\mathrm{I}_a = \mathrm{I}_0 \mathrm{Q}'_a \mathrm{S}\, \mathrm{A}(\theta, \psi)_a \rho' g_a \tau_a/\mu' \rho_a \qquad \qquad (7\,a)$$

for a powder block, and

$$\mathrm{I}_a = \mathrm{I}_0 \mathrm{Q}'_a \mathrm{V}' \alpha_a \rho' g_a \tau_a/\rho_a \qquad \qquad (7\,b)$$

for a cylindrical rod.

The only change introduced is therefore the inclusion of the particle absorption factor, τ_a. Similarly, if we are comparing the intensities of two reflections I_a and I_b from a mixture of medium grade particles, the factor τ_a/τ_b must be included in the expressions previously given for a mixture of fine particles:

$$\frac{I_a}{I_b}=\frac{Q'_a A(\theta,\psi)_a g_a \rho_b}{Q'_b A(\theta,\psi)_b g_b \rho_a}\left(\frac{\tau_a}{\tau_b}\right) \quad . \quad . \quad . \quad . \quad . \quad . \quad . \quad (8a)$$

for a powder block,

$$\frac{I_a}{I_b}=\frac{Q'_a \alpha_a g_a \rho_b}{Q'_b \alpha_b g_b \rho_a}\left(\frac{\tau_a}{\tau_b}\right) \quad . \quad . \quad . \quad . \quad . \quad . \quad . \quad . \quad (8\,b)$$

for a cylindrical rod.

The form which the particle absorption factor takes, namely a dependence on $(\mu_a-\bar{\mu})$, shows that for single powders, where there is no distinction between μ_a and $\bar{\mu}$, a particle absorption factor is not involved. This is an important point of difference between the theory as developed in this paper and as developed by Taylor (1944 *a*).

V. *Discussion of the Particle Absorption Factor, τ.*

The conclusions arising from the present treatment of the problem differ from those of Schäfer and of Taylor as follows:—

(i) When reflection occurs from a mixture of substances, the particles or grains of which satisfy the condition $0{\cdot}01<\mu D<0{\cdot}1$, the expression for the intensity reflected by a component of the mixture must include the particle absorption factor. This factor is concerned essentially with *particle* size and not, as Taylor shows, *crystal* size.

(ii) The factor depends on the difference $(\mu_a-\bar{\mu})$ and not on μ_a alone, as the analyses of Schäfer and Taylor indicate.

(iii) The factor applies only to mixed powders and not, as Taylor considers, to single powders.

The differences between the present results and those of Taylor arise largely through a difference of approach to the problem. Taylor begins by considering single crystal particles and shows that the absorption in the crystal reduces the reflected intensity by the factor

$$\tau_c=\frac{1}{v_c}\int_0^{v_c} e^{-\mu_a x}\,dv,$$

where v_c is the *crystal* volume. Subsequent integration over the entire powder then introduces the mean absorption coefficient of the powder in the usual way. But this treatment is tantamount to allowing twice over for absorption in the reflecting substance, first in calculating the factor τ_c and secondly in applying the mean absorption to the whole powder. What is required is a correction factor to allow for the reflecting crystal not having the same absorption coefficient as the mean absorption of the powder, or, in other words, to allow for the " absorption contrast " between the reflecting substance and the powder as a whole.

Whereas $(\mu_a - \bar{\mu})$ is zero and $\tau = 1$ for a single powder, the form of the factor given by Taylor does not become unity for a single powder. He therefore proceeds in his second paper to apply this factor to the measurements of Brindley and Spiers (1935) on filed metal powders which were made using single powders; this procedure, in the writer's opinion, is fundamentally invalid.

As regards polycrystalline particles, Taylor considers that the bulk of any such particle at any instant will be non-reflecting, and therefore that the absorption of the rest of the particle is part of the mean absorption of the powder as a whole. The present argument emphasizes that the differential absorption which operates in a mixed powder is due to the fact that whenever a crystal reflects radiation there is associated with it a particle of its own kind having an absorption characteristic of the particular substance and not of the powder as a whole, and therefore the correction factor must be related to the particle rather than to the crystal.

VI. *X-ray Reflection by Coarse Mixed Powders.*

In powders for which $0{\cdot}1 < \mu D < 1$, the depth of penetration of the radiation is such that the reflection process cannot properly be regarded as either a volume or a purely surface effect. The basic idea underlying the treatment of medium grade powders was that sufficient particles were involved for mean values, such as μ' in eq. (5), to be employed. When too few particles are involved to justify this procedure, a statistical treatment is necessary along the lines developed by Schäfer (1933).

The following is a somewhat more general exposition than was given by Schäfer. Consider a mixture composed of particles of A, B and air in the proportions p, q and r, so that $p+q+r=1$, and let the particles be all of the same size D. Consider the absorption of radiation passing through N particles. It is only when N is large that the particles will be present along the path of the radiation in the ratio $p : q : r$. The chance that there will be a particles of A, b of B, and c of air is

$$\frac{N!}{a!\,b!\,c!}\,p^a q^b r^c,$$

and $a+b+c=N$. The absorption for this distribution is

$$e^{-(\mu_a a D + \mu_b b D + \mu_c c D)}.$$

The mean absorption is therefore

$$\Sigma \frac{N!}{a!\,b!\,c!}\,(pe^{-\mu_a D})^a (qe^{-\mu_b D})^b (re^{-\mu_c D})^c,$$

which by the polynomial summation law is

$$(pe^{-\mu_a D} + qe^{-\mu_b D} + r)^N,$$

since μ_c for air can be taken as zero. If μ^* is the mean absorption coefficient when the number of particles involved is N, then the absorption is $e^{-\mu^* N D}$.

Taking logarithms of the two expressions for the absorption and expanding the exponentials, we see that

$$-\mu^{*}D=\log\{1-(p\mu_a+q\mu_b)D+\tfrac{1}{2}(p\mu_a^2+q\mu_b^2)D^2\ldots\},$$

which is of the form log $(1-x)$ where

$$x=(p\mu_a+q\mu_b)D-\tfrac{1}{2}(p\mu_a^2+q\mu_b^2)D^2\ldots.$$

Expanding log $(1-x)$ as far as terms in D^2, we obtain

$$\mu^{*}=(p\mu_a+q\mu_b)\left[1+\tfrac{1}{2}(p\mu_a+q\mu_b)D\left\{1-\frac{p\mu_a^2+q\mu_b^2}{(p\mu_a+q\mu_b)^2}\right\}\ldots\right].$$

But $(p\mu_a+q\mu_b)$ is the average value of the absorption coefficient of the powder specimen, μ', calculated on the assumption that a large number of particles are involved. We see that μ^{*} tends to μ' when

$$\left|\tfrac{1}{2}(p\mu_a+q\mu_b)D\left\{1-\frac{p\mu_a^2+q\mu_b^2}{(p\mu_a+q\mu_b)^2}\right\}\right|\ll 1.$$

Table I.

Adsorption Data for Mixtures of Two Powders for which

$\mu_a=150$, $\mu_b=500$, $D=10^{-3}$ cm.

p=proportion of particles of A,

q=proportion of particles of B.

p	0·1	0·2	0·3	0·4	0·5	0·6	0·7	0·8	0·9
q	0·9	0·8	0·7	0·6	0·5	0·4	0·3	0·2	0·1
μ^{*}/μ'	0·99	0·98	0·97	0·96	0·95	0·95	0·95	0·96	0·97

This, then, provides the upper limit for the size of the medium grade powders considered in section IV. A somewhat similar argument justifies the statement that the length of path occupied by particles is the geometrical length multiplied by the factor $(\rho'/\bar{\rho})$ (see sect. IV.).

Hitherto we have taken $\mu D=0{\cdot}1$ as an approximate upper limit for the size of medium grade particles, but as the following example will show, this limit may be exceeded without μ^{*} differing very considerably from μ'. In Table I. numerical results are given for a series of mixtures for which $\mu_a=150$, $\mu_b=500$, and $D=10^{-3}$ cm. These figures correspond approximately with the reflection of CuKα radiation from aluminium and copper powders prepared by filing. We see that $\mu_aD=0{\cdot}15$ and $\mu_bD=0{\cdot}50$, so that both components lie outside the medium grade. Calculation shows that μ^{*} differs from μ' by not more than 5 per cent.; the results are set out in Table I.

It is evident that for coarse powders defined by the conditions $0{\cdot}1<\mu D<1$, the particle absorption factor may be used to *estimate* the magnitude of the effect of the coarseness on the reflected intensities provided μD tends to the lower limit 0·1 rather than to the upper limit of unity.

VII. *X-ray Reflection by Very Coarse Powders.*

Very coarse powders are defined as those for which $\mu D > 1$. Reflection now takes place for the most part only from the surface layer of particles, as indicated in fig. 3. As in section IV., the particles will be assumed polycrystalline and the powder a mixture of two or more substances. The reflected intensity from a volume element δv_a of a crystal of A is given by

$$I_0 Q \, \delta v_a e^{-\mu_a x},$$

where x is the path of the radiation in the particle. The volume element may occur in any position in a particle, and therefore the mean reflected energy for a volume δv_a will be given by

$$I_0 Q \, \delta v_a \tau'_a,$$

where

$$\tau'_a = \frac{1}{V_a} \int_0^{V_a} e^{-\mu_a x} \, dv$$

Fig. 3.

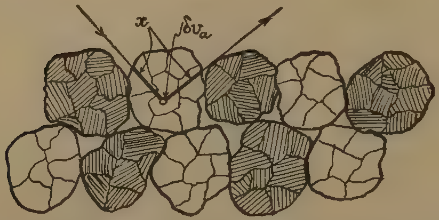

X-ray reflection from a very coarse mixed powder ($\mu D > 1$), composed of polycrystalline particles; δv_a is a volume-element of a reflecting crystal and x the path of the radiation in the particle.

and V_a is the particle volume. The mean reflected intensity per particle with allowance for random orientation of the crystals is therefore

$$I_0 Q' V_a \tau'_a .$$

If $g_a, g_b \ldots$ are the weight proportions of A, B, ... in the mixture, then the relative numbers of particles are respectively $(g_a/\rho_a V_a), (g_b/\rho_b V_b) \ldots$ Therefore the reflected intensity from substance A, I_a, is given by

$$I_a \propto I_0 Q'_a \tau'_a g_a/\rho_a,$$

and the ratio of the intensities reflected by A and B is given by

$$\frac{I_a}{I_b} = \frac{Q'_a \tau'_a g_a \rho_b}{Q'_b \tau'_b g_b \rho_a} . \quad \ldots \ldots \ldots \quad (9)$$

This expression resembles those given for medium grade powders (see eqns. 8 *a* and 8 *b*), but the angular factor $A(\theta, \psi)$ for the powder block and the absorption factor α for the cylindrical specimen do not appear. Absorption is now taken into account by τ'. To some extent it is rather artificial to regard τ' as a particle absorption factor in the same sense as τ is for medium grade powders, because the essential idea underlying the use of the factor τ is that it takes account of the *difference* between the particle absorption coefficient and the mean powder absorption coefficient. Now with very coarse powders the concept of a mean absorption coefficient disappears, and with it goes the concept of the factor τ as previously understood. It is probably better to regard τ' as the special form which $\frac{1}{\mu}A(\theta, \psi)$ or α assumes when a single layer only participates in reflection.

In the derivation of equation (9) some rather sweeping assumptions have been made; in particular it is assumed that the radiation is absorbed only in the particle where reflection occurs. This will only be partially true and will be more nearly satisfied when the radiation enters and leaves the powder surface at large than at small glancing angles. The conditions of the problem, however, are such that a rigorous treatment is not possible.

VIII. *The Effect of Particle Size on the Relative Intensities from Mixed Powders.*

This question, previously considered by the writer and Spiers (1938) from the standpoint of Schäfer's theory, requires reconsideration in the light of the new particle absorption factor. Under certain circumstances the results from the new theory are entirely different from those predicted by the older theory; under other circumstances the new results are not greatly different from the old. Let I_A/I_B be the ratio of the intensities of two reflections from the components A and B of a fine powder and I'_A/I'_B the corresponding ratio when the particles are coarse. Then the effect of the coarseness on the relative intensities may be measured by K defined as follows:

$$K = \frac{\text{Intensity ratio with coarse particles}}{\text{Intensity ratio with fine particles}} = \frac{I'_A/I'_B}{I_A/I_B}.$$

Then
$$K = \frac{I'_A/I_A}{I'_B/I_B} = \frac{\tau_A}{\tau_B} = \frac{V_B\int_0^{V_A} e^{-\mu_a-\bar{\mu})x}\,dv}{V_A\int_0^{V_B} e^{-(\mu_b-\bar{\mu})x}\,dv}.$$

The integrals can be solved explicitly only in special cases; Schäfer gave the results for cubical particles for angles $2\theta=0°$, 90° and 180°. Taylor (1944 *a*) has shown how a numerical solution may be obtained for spherical particles. His solution was worked out for his crystal absorption factor, but can be used to calculate particles absorption factors if for "crystal volume" we read "particle volume" and for μ_a we read $(\mu_a-\bar{\mu})$. The calculations were made, however, only for *positive* values of μ_a, and therefore are applicable only when $(\mu_a-\bar{\mu})$ is positive. For a mixture AB, $\bar{\mu}$ lies between μ_a and μ_b, and therefore of the two terms $(\mu_a-\bar{\mu})$ and $(\mu_b-\bar{\mu})$ one is positive and the other is negative. It is possible, however, as will be shown in the appendix to this paper, to derive the particle absorption factors for negative values of $(\mu_a-\bar{\mu})$ directly from the corresponding values for $(\mu_a-\bar{\mu})$ positive without going through the long numerical integrations involved in a direct calculation. The results are set out in Table V. at the end of the paper.

For cubical particles of sizes D_a and D_b and for angles $2\theta=0^\circ$, 90° and 180°, the modified forms of Schäfer's expressions are as follows :

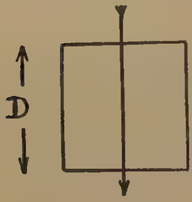

$$2\theta=0^\circ \qquad K_0=e^{-(\mu_a-\bar{\mu})D_a}/e^{-(\mu_b-\bar{\mu})D_b}. \quad \ldots \ldots \quad (a)$$

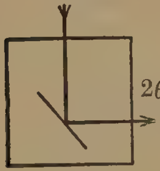

$$2\theta=90^\circ \qquad K_{90}=\left\{\frac{1-e^{-(\mu_a-\bar{\mu})D_a}}{(\mu_a-\bar{\mu})D_a}\right\}^2\Bigg/\left\{\frac{1-e^{-(\mu_b-\bar{\mu})D_b}}{(\mu_b-\bar{\mu})D_b}\right\}^2, \quad (b)$$

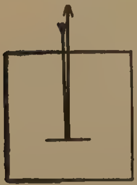

$$2\theta=180^\circ \qquad K_{180}=\left\{\frac{1-e^{-2(\mu_a-\bar{\mu})D_a}}{2(\mu_a-\bar{\mu})D_a}\right\}\Bigg/\left\{\frac{1-e^{-2(\mu_b-\bar{\mu})D_b}}{2(\mu_b-\bar{\mu})D_b}\right\}. \quad (c)$$

. . . (10)

If $(\mu_a-\bar{\mu})D_a$ and $(\mu_b-\bar{\mu})D_b$ are small, so that their squares can be neglected compared with unity, then K_0, K_{90} and K_{180} are equal to this degree of approximation and may be denoted by K, namely

$$\begin{aligned} K&=1-(\mu_a-\bar{\mu})D_a+(\mu_b-\bar{\mu})D_b \\ &=1-\mu_aD_a+\mu_bD_b+\bar{\mu}(D_a-D_b). \quad \ldots \ldots \quad (11) \end{aligned}$$

If the particles are of equal sizes, the last term disappears and the expression for K takes a particularly simple form. When this condition holds, the expression for K given by the present analysis is the same as that given by Schäfer's original treatment † ; furthermore K does not depend on $\bar{\mu}$, *i. e.* on the composition of the mixture. With particles of different sizes, K depends on the relative amounts of the components present.

---

† This has a fortunate bearing on the previous discussion by Brindley and Spiers (1938) of experimental measurements on mixed powders from the standpoint of Schäfer's theory. The powders they considered were for the most part of equal particle sizes and therefore no reconsideration of the results is required by the new analysis. In the one case where unequal sized particles were considered, it will be shown that the new analysis gives better agreement with the experimental results than does Schäfer's theory.

For purposes of calculation, the following relations are useful :—

$$\bar{\mu}/\bar{\rho} = \Sigma\,(\mu_a/\rho_a)g_a,$$
$$1/\bar{\rho} = \Sigma(g_a/\rho_a).$$

IX. *Numerical and Practical Considerations.*

In order to assess the bearing of the foregoing considerations on the interpretation of X-ray intensity measurements from mixed powders and heterogeneous solids, it will be useful to examine a list of linear absorption coefficients for CuKα radiation, the radiation most commonly used. In Table II., values of μ are given for a range of metallic elements derived from their mass absorption coefficients, μ/ρ, as listed by W. L. Bragg (see ' The Crystalline State,' vol. i, p. 325), and their densities. Table III. shows the range of absorption coefficients corresponding to fine, medium, coarse and very coarse powders for particles of various sizes.

TABLE II.

Linear Absorption Coefficients for some Metallic Elements for CuKα radiation.

Be	2·48	Mo	1678	Rh	2460	Co	3115
Mg	70·5	Cr	1838	Bi	2480	W	3290
Al	131	Sb	1900	Pd	2490	Au	4130
Si	140	Sn	1930	Fe	2545	Pt	4400
Zn	421	Cd	2020	Ta	2720	Ir	4400
Ni	438	Mn	2070	Pb	2730		
Cu	470	Ag	2340	Hg	3030		

TABLE III.

Coarseness of Powders in relation to Particle Size and X-ray Absorption Coefficient.

Size of particles.	Linear Absorption Coefficient, μ ; log. scale.				
	1	10	100	1000	10,000
10^{-3} cm.	←Fine→	←Medium→	←Coarse→	Very ←Coarse→	
10^{-4} cm.	←Fine→		←Medium→	←Coarse→	
10^{-5} cm.	←Fine→			←Medium→	
10^{-6} cm.	←Fine→				

(i) *Particles* 10^{-3} *cm. in Size.*

It is unnecessary to consider particles larger than 10^{-3} cm. for, although in alloys the crystal grains frequently exceed this size, they are generally examined in the form of fine filings. The finest filings which can be obtained by sieving through a 350 mesh gauze are of the order of 10^{-3} cm. or a little larger. The first horizontal row of Table III. therefore corresponds to filed particles.

Comparing the information in Table III. with that in Table II., we see that Be is the only metal which, with particles as large as 10^{-3} cm., can be regarded as a fine powder. Mg is the only medium powder; Al, Si, Zn, Ni and Cu give coarse powders, while all the remaining metals come in the very coarse category. We are primarily interested in mixtures rather than single powders and should therefore consider mean absorption coefficients; these, however, will depend on the composition of the mixture. Nevertheless, the general conclusion will not be materially changed. The majority of mixtures or alloys with particles as large as 10^{-3} cm. will come in the very coarse group. Mixtures or alloys of Be, Mg, Al, Si, Zn, Ni and Cu will come mainly in the first part of the coarse group, and to these we have seen the particle absorption factor may be applied. The effect of a particle size of 10^{-3} cm. on the relative reflected intensities in these cases is so large that we cannot hope to do more than *estimate* its order of magnitude. Such mixtures are wholly unsuitable for investigations which entail a precise interpretation of accurately measured intensities, *e. g.*, any attempt at a quantitative chemical analysis of a high order of accuracy by means of X-rays or any investigations necessitating the measurement of atomic scattering factors.

Various avenues of escape from this difficulty may exist depending on the nature of the problem :—(*a*) Finer particles may be used if the investigation permits this. (*b*) If coarse particles must be used, then, provided the components can be examined separately, a method using single powders such as that described by Brindley and Spiers (1938) is preferable to the use of a coarse grained mixture. (*c*) If a particular mixture must be used, then a more satisfactory radiation may be employed, either a harder radiation, such as MoKα, or a radiation on the long wave side of an absorption edge, such as FeKα instead of CuKα for any substance containing iron. (*d*) Finally, when all these possibilities fail, the effect of the coarse grain may be estimated by means of the particle absorption factor.

As a numerical illustration of the order of magnitude of the effect of a particle size as large as 10^{-3} cm. on the reflected intensities, let us consider a Cu/Al mixture. Assuming *cubical* particles and using the approximate formula (11), which is scarcely valid in this case, we find that $K = 1 - 0{\cdot}470 + 0{\cdot}131 = \overline{0{\cdot}66}$. Using the more exact expressions (10), we find for a 1 : 1 mixture by weight, $K_0 = 0{\cdot}71$, $K_{90} = 0{\cdot}72$ and $K_{110} = 0{\cdot}72_5$. Evaluation of the K's for compositions ranging from 10 per cent. to 90 per cent. Cu shows that in this particular case K_0 and K_{180} vary with composition by less than 2 per cent., while K_{90} shows a variation of about 5 per cent. For *spherical* particles, using Table V. in the appendix to the paper, we find $K = 0{\cdot}78$ for $2\theta = 0$, and the value is practically independent of the composition of the mixture and the angle of reflection. The significance of these results is that in any comparison of Cu and Al reflections using such a mixture, the copper intensities will appear to be about 25 per cent. too small compared with the Al intensities.

This illustration was previously considered by Taylor (1944 *a*, see p. 224) who gave essentially the same result as that obtained here, a coincidence which arises because with *equal sized* particles the term $\mu(D_a-D_b)$ in eq. (11) disappears.

(ii) *Mixtures Containing Partices of Different Sizes.*

Let us extend our consideration of Cu/Al mixtures to the case of (say) chemically precipitated copper with a particle size of 10^{-4} cm. and filed aluminium with a particle size of 10^{-3} cm. Reference to Tables II. and III. shows that the copper is of medium grade and the aluminium is on the border line between the medium and the coarse grade. Taking first the case of cubical particles and using the approximate formula (11), we have

Table IV.

Values of K for Cu/Al Mixtures.

$$K=\left(\frac{I_{Cu}/I_{Al}\text{ for actual powder}}{I_{Cu}/I_{Al}\text{ for fine powder}}\right).$$

$D_{Cu}=10^{-4}$ cm. ; $D_{Al}=10^{-3}$ cm.

Percentage of copper by weight.	μ.	Values of K.		
		Cubical particles.		Spherical particles. Exactly for $\theta=0$.
		Approximately, eq. (11).	Exactly, eq. (10 *a*).	
10	142	0·95	0·95	0·97
20	155	0·94	0·94	0·96
30	170	0·93	0·93	0·95
40	188	0·91	0·92	0·94
50	210	0·89	0·90	0·93
60	237	0·87	0·88	0·91
70	272	0·84	0·85	0·89
80	317	0·80	0·82	0·86
90	380	0·74	0·77	0·84

$$K=1-0{\cdot}047+0{\cdot}131+\bar{\mu}(10^{-4}-10^{-3})=1{\cdot}084-9\times10^{-4}\bar{\mu}.$$

The variation of K with the composition of the mixture is clearly important owing to the $\bar{\mu}$ term.

The numerical results for Cu/Al mixtures of different compositions are set out in Table IV. For a mixture containing only 10 per cent. copper, the copper intensities will be about 4 per cent. low compared with the aluminium intensities, but for a mixture with 90 per cent. copper, the copper intensities will be about 20 per cent. too low. Let us see in a general way how this comes about. A mixture containing only 10 per cent. Cu has a mean absorption coefficient of 142, which is not very different from that of pure aluminium, 131. In this mixture the copper particles are small and individually absorb little radiation ; the aluminium particles, though large, have about the same absorption coefficient as the mixture as a whole. Therefore in such a case we do not expect to find a large correction factor for particle size. In the mixture with 90 per cent. copper, the aluminium particles are comparatively large and have a much smaller absorption coefficient than the mixture as a whole. In consequence the Al reflections by comparison with the Cu reflections are too little absorbed ; the Al reflections are therefore enhanced and by comparison the Cu reflections appear too small.

Let us see now what the previous theories of Schäfer and of Taylor would give for these mixtures. Schäfer's expressions give $K=1{\cdot}08$ and Taylor's theory (if we apply it to particles) gives $K=1{\cdot}06$. These results indicate not only a non-dependence of K on composition, but also a relative enhancement of the Cu intensities by about 7 per cent., whereas the present analysis indicates a decrease of a few per cent. or as much as about 20 per cent., depending on the composition of the mixture. We see, therefore, that where the particle sizes of the two components differ the predictions of the present theory can be quite different from those of the former theories of Schäfer and of Taylor.

(iii) *Comparison between Experiment and Theory for a* Cu/KCl *Mixture.*

This example is worth considering because it was the one case previously examined experimentally by the writer and Spiers (1938) in which particles of unequal sizes were involved. Taking the particle sizes as $5{\cdot}10^{-4}$ cm. for KCl and $2{\cdot}10^{-3}$ cm. for Cu, the calculated value of K_0 from Schäfer's original expressions is 2·27. Experimentally the writer and Spiers obtained 1·73 and 1·56 for two different Cu powders. The experiments consisted in comparing Cu and KCl reflections (*a*) by the mixture method in which the coarseness of the powders is important, and (*b*) using separate powders where their coarseness does not affect the results. A re-calculation of K_0 using the present theory gives the following :—The composition of the mixtures used was 2 parts KCl and 1 part Cu by weight. The absorption coefficients involved are $\mu_{\mathrm{Cu}}=470$, $\mu_{\mathrm{KCl}}=247$, μ for the mixture $=269$. The re-calculated value of K_0 is 1·51 for cubical particles and 1·36 for spherical particles. These values are in somewhat better agreement with the measured K's than the value 2·27 derived from Schäfer's theory. The agreement is still not very close, but is perhaps as good as can be expected having regard to the necessarily rough estimates of the particle sizes. Again we see that where the particles sizes of the two components are different the present theory indicates different results from those given by the former theories.

X. *X-ray Reflection by Heterogeneous Solids (Alloys, Slags, etc.).*

It is evident that the intensity of X-ray reflections from solids in which two or more phases co-exist will be governed by essentially the same considerations as the intensity reflected by mixed powders. In the present paper we cannot do more than indicate briefly one or two aspects of the problem in which heterogeneous solids may differ from mixed powders.

In the first place, since the atoms forming the different phases will be the same, the absorption coefficients of the phases will tend to be less dissimilar than those of two substances containing perhaps widely different atoms which may form a mixed powder. The absorption coefficients of co-existing phases are likely to differ most when the atoms involved have very different absorption coefficients and when the single phase regions of the phase diagram are widely separated along the composition axis. In alloys of systems such as the Cu-Zn or Fe-Co-Ni system, in which the atoms have very similar absorption coefficients for the radiations normally employed, differential absorption effects are likely to be important only if the grain-sizes of the separate constituents are very different.

Another point of difference between solids and powders is that in solids one phase may crystallize in a dendritic form within grains of a different phase. Simple considerations based on particles in a mixed powder can scarcely be directly applicable to such a case. The problem is easier to handle if one constituent crystallizes in a rod-like or plate-like form ; an expression for the particle absorption factor can easily be derived for grains of these simple shapes.

When a two-phase alloy is reduced to a fine powder for X-ray examination by filing and sieving, the two phases may be differently affected by the filing process ; a coarse-grained phase will be drastically broken up in the process but a fine-grained constituent may be less affected. The effect of the subsequent heat treatment on grain growth will probably be different for the two phases. We cannot, therefore, foresee what the relative grain-sizes in the powder will be from an examination of the alloy before powdering. Some information may be obtainable from an X-ray examination of a stationary powder specimen, when grains larger than 10^{-3} cm. would be revealed by the formation of discrete spots instead of continuous lines while grains smaller than 10^{-5} cm. would be indicated by broadened reflections.

It will be evident from these brief considerations that the effect of grain-size in solids containing more than one phase on the intensity of X-ray reflections is a more complex problem than the effect of particle size in mixed powders.

XI. *Summary and Conclusions.*

It is shown to be necessary to introduce into the general expression for the intensity of X-ray reflection by a constituent of a mixed powder a factor to allow for the absorption in the individual particles as distinct from the mean absorption in the powder as a whole. Powders are classified as fine, medium, coarse and very coarse, depending on the value of μD (μ=linear absorption coefficient; D=particle size). Particles of a fine powder have negligible absorption and the usual theory is applicable in this case. Particles of a medium grade powder have appreciable absorption but reflection from the powder is essentially a "volume" process. In this case a particle absorption factor

$$\tau=\frac{1}{V_a}\int_0^{V_a} e^{-(\mu_a-\bar{\mu})x}\,dV$$

is required in the full expression for the reflected intensity. The form of this factor shows that it is unity in the case of single powders and therefore in this case it does not appear in the formula for the reflected intensity. With very coarse powders, reflection is a surface effect confined mainly to a single layer of particles; the general theory of reflection, which is essentially concerned with volume effects, is not applicable. With coarse powders, reflection is not strictly either a surface or a volume effect, but in so far as such powders tend to the medium grade rather than to the very coarse grade, the particle absorption factor may be used to estimate the effect of particle size on the reflected intensities.

The points of difference between the present theory and that given by Taylor (1944 *a*) are discussed, and it is shown that the suggestions made by Taylor (1944 *b*) regarding previous work by the writer and Spiers (1935) are invalid.

The effect of particle size on the relative intensities from mixed powders is considered and some typical numerical examples are given.

The application of the theory to solids, such as alloys and slags containing two or more co-existing phases, is discussed and it is shown that more complicated problems may arise with mixed phase solids than with mixed powders.

In an appendix it is shown how the particle absorption factor τ for spherical particles may be calculated when $(\mu_a-\bar{\mu})$ is negative from corresponding values previously given by Taylor for $(\mu_a-\bar{\mu})$ positive. A table of values of τ for $\theta=0°$, $45°$ and $90°$ is given for $(\mu_a-\bar{\mu})R$ extending to $\pm 0{\cdot}5$; R is the particle radius.

Acknowledgements.

Finally, I wish to thank Professor Stoner, F.R.S., for reading the manuscript of this paper and for making several useful suggestions, and Dr. S. R. Tibbs for discussing points which arose in connection with the calculations given in the Appendix.

I would like also to acknowledge that in discussing with Dr. A. Taylor the various points of difference between this paper and his recent work, my own ideas on the subject have been much clarified.

APPENDIX.

The Numerical Calculation of Particle Absorption Factors for Spherical Particles.

In section VIII. we have seen that the effect of particle size on the relative intensities reflected from the components of a mixed powder or a two-phase solid may be measured by the quantity K defined as follows :—

$$K=\frac{\tau_A}{\tau_B}=\frac{V_B}{V_A}\frac{\int_0^{V_A} e^{-(\mu_a-\bar{\mu})x}\,dv}{\int_0^{V_B} e^{-(\mu_b-\bar{\mu})x}\,dv}.$$

Since $\bar{\mu}$ necessarily lies between μ_a and μ_b, the exponent of e is positive in one integral and negative in the other. We therefore require to evaluate integrals of the form $\frac{1}{V}\int_0^V e^{-kx}\,dv$ and $\frac{1}{V}\int_0^V e^{+kx}\,dv$. For spherical particles the integrations can be carried out only by numerical methods. This has been done by Taylor (1944 *a*) for the case when $(\mu_a-\bar{\mu})$ is *positive* for values of $(\mu_a-\bar{\mu})R$, where R is the particle radius, from 0 to 5 and for angles of reflection $\theta=0°$, $22\frac{1}{2}°$, $45°$, $67\frac{1}{2}°$ and $90°$. The numerical work was greatly simplied by utilizing Bradley's tables for the absorption in cylindrical specimens. At first sight it appears that the corresponding calculations when $(\mu_a-\bar{\mu})$ is *negative* have to be made entirely *de novo*, for Bradley's tables are not applicable to this case. It has been shown, however, that the concept of a particle absorption factor may be validly used only when μD for the particles does not greatly exceed 0·1. This limitation makes it possible to evaluate the integral when $(\mu_a-\bar{\mu})$ is negative with sufficient accuracy from its value when $(\mu_a-\bar{\mu})$ is positive for all values of $(\mu_a-\bar{\mu})R$ which are of practical importance.

Writing $\Delta\mu$ for the positive difference between μ_a and $\bar{\mu}$, and expanding the exponentials, we have

$$\frac{1}{V}\int_0^V e^{\Delta\mu.x}\,dv+\frac{1}{V}\int_0^V e^{-\Delta\mu.x}\,dv=\frac{2}{V}\int_0^V\left[1+\frac{1}{2}(\Delta\mu.x)^2+\frac{1}{24}(\Delta\mu.x)^4\ldots\right]dv.$$

The integration of the x^2 and x^4 terms over the volume of a sphere can be carried out for $\theta=0°$, $45°$ and $90°$. With cylindrical co-ordinates the required integrals are of the form

$$\frac{3(\Delta\mu)^n}{4\pi R^3}\int_{-R}^{+R}\int_0^{R'}\int_0^{2\pi} x^n\,r\,d\phi\,dr\,dz,$$

where n is 2 or 4, $R'=\sqrt{R^2-z^2}$, and x has the following expressions :—

$\theta=0°$, $x=2\sqrt{R'^2-r^2\sin^2\phi}$.

$\theta=45°$, $x=\sqrt{R'^2-r^2\sin^2\phi}+\sqrt{R^2-r^2\cos^2\phi}+r(\sin\phi+\cos\phi)$.

$\theta=90°$, $x=2\sqrt{R'^2-r^2\sin^2\phi}+2r\cos\phi$.

TABLE V.

Numerical Values of the Particle Absorption Factor, τ, for Spherical Crystals.

$$\tau = \frac{1}{V_a}\int_0^{V_a} e^{-(\mu_a-\bar{\mu})x}\,dV.$$

$(\mu_a-\bar{\mu})$R.	$\tau(\theta=0°)$.	$\tau(\theta=45°)$.	$\tau(\theta=90°)$.	$(\mu_a-\bar{\mu})$R.	$\tau(\theta=0°)$.	$\tau(\theta=45°)$.	$\tau(\theta=90°)$.
0	1·000	1·000	1·000	0	1·000	1·000	1·000
+·01	0·986	0·986	0·986	—·01	·014	·014	·014
·02	·972	·973	·973	·02	·028	·027	·027
·03	·959	·960	·960	·03	·043	·042	·042
·04	·945	·946	·947	·04	·059	·058	·059
·05	·932	·933	·934	·05	·074	·073	·074
·06	0·918	0·919	0·921	—·06	1·090	1·091	1·091
·07	·905	·906	·908	·07	·107	·108	·108
·08	·892	·893	·895	·08	·124	·125	·125
·09	·878	·879	·882	·09	·142	·143	·144
·10	·865	·866	·870	·10	·159	·162	·163
·2	0·742	0·753	0·760	—·2	1·352	1·353	1·362
·3	·640	·653	·671	·3	·508	·573	·585
·4	·545	·569	·587	·4	·813	·807	·827
·5	·468	·496	·529	·5	2·068	2·036	2·029

The results of the integration are

$$\frac{1}{V}\int_0^V e^{\Delta\mu.x}\,dv+\frac{1}{V}\int_0^V e^{-\Delta\mu.x}\,dv$$

$$=2[1+1{\cdot}20(\varDelta\mu)^2R^2-0{\cdot}52(\varDelta\mu)^4R^4\ldots]\quad\text{for } \theta=\ 0^\circ.$$

$$=2[1+1{\cdot}37(\varDelta\mu)^2R^2-1{\cdot}22(\varDelta\mu)^4R^4\ldots]\quad\text{for } \theta=45^\circ.$$

$$=2[1+1{\cdot}60(\varDelta\mu)^2R^2-1{\cdot}93(\varDelta\mu)^4R^4\ldots]\quad\text{for } \theta=90^\circ.$$

These series can be used to obtain the particle absorption factor when $(\mu_a-\bar{\mu})$ is negative for values of $(\mu_a-\bar{\mu})R$ not exceeding $-0{\cdot}5$; for higher values it would be necessary to evaluate the next term in the power series.

The results are set out in Table V.; the values for $(\mu_a-\bar{\mu})R$ positive are taken from Taylor's paper while the values for $(\mu_a-\bar{\mu})R$ negative are calculated from the expressions given above.

References.

Bradley, A. J., Proc. Phys. Soc. xlvii. p. 879 (1935).

Brentano, J. C. M., Proc. Phys. Soc. xlvii. p. 932 (1935); l. p. 247 (1938).

Brindley, G. W., and Spiers, F. W., Phil. Mag. xx. p. 882 (1935); Proc. Phys. Soc. l. p. 17 (1938).

Gross, S. T., and Martin, D. E., Ind. and Eng. Chem. (Anal. Ed.) xvi. p. 95 (1944).

Rusterholz, A., *Helv. Phys. Acta*, iv. p. 68 (1931); Thesis, "Die Streuung von Röntgenstrahlen an Metallen" (Zurich) (1931).

Schäfer, K., *Zeit. f. Phys.* lxxxvi. p. 738 (1933).

Taylor, A., Phil. Mag. xxxv. p. 215 (1944 *a*); xxxv. p. 404 (1944 *b*).

XLVI. *Notices respecting New Books.*

Semi-Micro Quantitative Organic Analysis. By R. Belcher and A. L. Godbert. [Pp. vii+168.] (London: Longmans, Green and Co., 1945. Price 10*s.* 6*d.*)

Following a brief introduction giving an account of the principles of the analytical methods described later, a detailed account is given of the use of an ordinary analytical balance for semi-micro work requiring an accuracy of 0·01 to 0·02 mg. The use of counterpoises is advocated to minimise errors resulting from the buoyancy effect. An account is then given of the general apparatus required, and of the apparatus and technique for small-scale filtration. Most of the apparatus required is said to be on the market; where this is not the case, directions are given for its construction.

Most of the book deals with the semi-micro methods for the determination, in organic compounds, of the commoner elements (including phosphorus and arsenic). The quantities required vary from 20 to 50 mg., and it is stated that the accuracy obtainable by a practised analyst is 0·2 per cent. (0·1 per cent. for phosphorus and arsenic). The mode of presentation is admirable. In each determination described, a detailed account of the apparatus and experimental method is preceded by a summary of the principle of the method, making the introduction to the book almost superfluous.

In addition, methods are described for the determination of carboxyl, alkoxyl and acetyl groups to an accuracy of about 0·5 per cent. using 20 mg. of material. No methods are given for the determination of C.Me or N.Me groups.

The measurement on a semi-micro scale of densities, melting points, boiling points and molecular weights is described, and there is an appendix on the purification of small amounts of material as well as one on the preparation and standardisation of volumetric solutions.

Whether an experienced analyst would wish to employ semi-micro methods is doubtful, and it seems improbable that a student would have either time or inclination to carry out organic analyses for himself. However, the content, presentation and authoritativeness of the work are such that it is strongly recommended for inclusion in all chemical libraries, whether large or small.

J. R. P.

Recent Advances in Physical and Inorganic Chemistry. By A. W. STEWART and C. L. WILSON. Pp. xii—512, with 5 plates, 76 diagrams and a chart. (London : Longmans, Green and Co., 1944. Price 28*s.* net.)

LESS than half a century ago, the distinction between the physicist and the chemist was clear-cut, and physical chemistry, though a rapidly growing subject, moved within fairly well-defined limits. One knew what to expect when one opened an advanced treatise such as *Nernst* or a more elementary manual such as *Walker.* But with the coming of the electron, herald of an unexampled change in our scientific outlook, the distinction between the fields of work of the physicist and the chemist tended to disappear. There is still a difference in their outlooks, more easily recognised than defined ; but in their mathematical and technical equipments they possess more and more in common. And so it comes to pass that a manual such as the one under review may be read with profit either by physicist or chemist.

The twenty-seven chapters of which the book is composed deal with line spectra, emission band spectra and continuous emission spectra, Tesla luminescence spectra, X-ray spectra, electron diffraction, X-rays and crystal structure, the structure of solids, isotopes and their segregation, radio-activity new and old, the disintegration of the atom, the outer sphere of the atom, the structure of the nucleus, hydrides, deuterium, and electrolysis. This is a far cry from the classic topics of the older treatises—the phase rule, chemical kinetics, the relation between physical properties and chemical constitution . . ., plus a few applications of the second law of thermodynamics ; but it is to be remembered that the work deals with *Recent Advances*, and must in the nature of the case be selective.

And the authors have selected their topics well and wisely, and the result is no *omnium gatherum*, but a well developed and carefully documented treatise marked by a pronounced unity of outlook not always possessed by works of this type. It is accurate, scholarly and up-to-date, and is admirably suited to the needs of a First or Second Year Honours university student. Some measure of its up-to-date qualities may be gained from the fact that a short section of the book deals with the possible applications of atomic energy.

But what a long road have the chemists travelled since the days when John Dalton remarked to a pupil, " Thou knowest, thou canst not split an atom " !

A. F.

[*The Editors do not hold themselves responsible for the views expressed by their correspondents.*]

XLVII. *A new Type of Electrical Resonance* *.

By Erich E. Schneider, Dr.phil.nat., A.Inst.P.†

[Received September 25, 1944.]

Abstract.

Utilization of the phase inversion of a thermionic valve leads to a method of obtaining resonance with circuits containing only resistance and capacitance or only resistance and inductance. The distinctive features of these stable "valve resonant circuits" against known RC oscillating circuits and reactance valve networks are discussed and their resonance and impedance properties analyzed in detail. The usefulness of the capacitive form as selective filter and amplifier for very low frequencies is demonstrated experimentally.

§ 1. *Introduction.*

The effect of electrical resonance is usually associated with circuits built up of inductance and capacitance. The essential cause of the resonant action of such "LC" circuits lies in the phase opposition of the two reactance types. Resonance occurs at the frequency at which inductive and capacitive reactance are equal in magnitude, and since they are opposite in sign, the LC combination has zero phase angle at resonance, *i. e.* acts as a pure resistance. This resistance at resonance represents in a "parallel LC" circuit a maximum and in a "series LC" circuit a minimum of the magnitude of the impedance of the combination. The isolated or "free" LC circuit acts as oscillatory circuit, *i. e.* an initial disturbance gives rise to exponentially damped oscillations.

The object of this paper is to show a way of producing resonance with reactance of only one type. This is possible through the inherent phase inversion of a thermionic valve, viz. the 180° phase shift between input- (grid-cathode) and output- (anode-cathode) voltage. The valve converts a reactance into one of the complementary type, and this converted reactance is combined with another of the original type. Expressed in an over-simplified way this would mean the $(+90^\circ)$ versus (-90°) correspondence of the LC circuits is replaced by a relation $({}^{-}_{(+)}90^\circ+180^\circ)$ versus $({}^{-}_{(+)}90^\circ)$. Actually two resistances have to be introduced which are essential and make the phase-shifts different from 90°.

Fig. 1 shows the circuits exhibiting the resonance phenomena, the "capacitive valve resonant circuit" (fig. 1 *a*), and the "inductive valve resonant circuit" (fig. 1 *b*). The capacitive circuit is of greater interest since it allows one to extend resonance effects to frequencies of a few cycles per sec. or lower, a range not accessible to LC resonance.

---

* A paper under the same title was read before the University of Durham Philosophical Society at a meeting held at King's College, Newcastle-upon-Tyne, on February 18, 1943.

† Communicated by Professor George W. Todd.

The general analysis of both circuits and discussion of their resonant properties (§ 3) will be preceded by a consideration of related work elsewhere (§ 2). In § 4 experimental work verifying the theory is described.

Fig. 1.

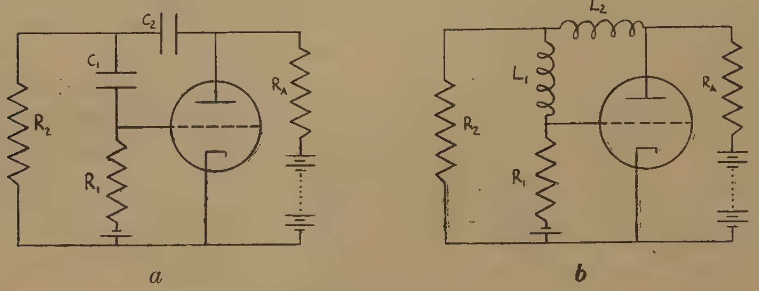

a *b*

§ 2. *Related Work.*

2.1. *Undamped RC and RL Networks.*

If the valve is removed from the circuits (fig. 1), they become simple two-mesh resistance reactance networks. Networks of this kind, containing reactance of one type only, were discussed in a general way by Tank and Graf⁽¹⁾ in 1928. They showed that such networks form always an aperiodically damped system whatever the special arrangement of the resistance and reactance elements in the loops and the linking between the loops. That means in the differential equation for the mesh circulating currents :

$$(A\mathbf{D}^2+B\mathbf{D}+C)i=0 \quad . \; . \; . \; . \; . \; . \; . \; . \quad (1)$$

$$A \text{ and } C>0\,; \; \mathbf{D}\equiv\frac{d}{dt},$$

the damping term ("**D**-term") is always related to the two other terms ("**D**^{2}-term" and "D^0-term") by

$$B^2>4AC, \quad . \; . \; . \; . \; . \; . \; . \; . \; . \quad (2)$$

so that the solution is aperiodic ($i=k_1e^{-\lambda_1 t}+k_2e^{-\lambda_2 t}$; λ_1, λ_2 real and positive) *.

---

* These results can be extended to a *n*-mesh resistance-reactance network : The coefficients of the *n*th order equation corresponding to (1)

$$\sum_0^n A_l\mathbf{D}^l i=0$$

are such that in the general solution

$$i=\sum_1^n k_l e^{-\lambda_l t}$$

all λ_l are real and positive, *i. e.* no oscillatory current can occur in any mesh. (See also a recent paper by Whitehead⁽²⁾.)

The system can only become oscillating or periodically damped if the inherent "over-critical" damping is balanced by a negative resistance, *i. e.* if through valves or other apparatus external energy is supplied to the system continuously and in the correct phase. Then we get, similarly to the exchange between electric energy of the condenser and magnetic energy of the inductance, an energy exchange between two condensers (or two groups of condensers) in the network, the energy loss in the resistances being made up by the energy supplied from the valves.

The valves make the system less than critically damped. Or expressed in terms of the above differential equation :—The valve circuit or other negative resistance introduces a negative part into the **D**-term, the system becomes either self-oscillatory (resulting $B=0$) or periodically damped $i=ke^{-\lambda t}\cos(\omega t+\phi)$. In this latter state it acts similarly to a resonant circuit.

Fig. 2.

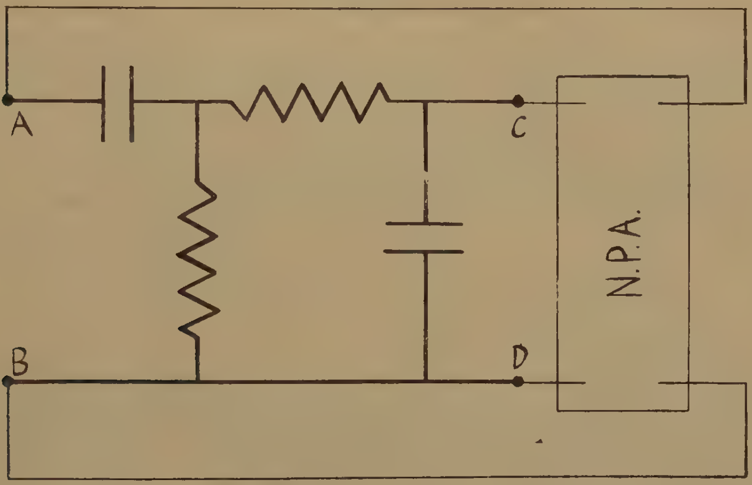

Tank and Graf applied this result to the study of the multivibrator, which gives under certain conditions sinusoidal oscillations. The same principle is inherent in all "RC oscillators" described in the literature$^{(3)-(19)}$. As an illustration, one simple form of RC oscillator, the "no-phase shift oscillator" first described by Yates-Fish$^{(5)}$, is shown in fig. 2. The "no-phase shift" amplifier N.P.A. can either consist of two valves in cascade or one valve with cathode or suppressor grid$^{(14), (17)}$ input. It acts as negative resistance, which makes the aperiodically damped resistance capacity network ABCD oscillatory. A non-oscillating filter circuit is obtained (similar to other selective circuits referred to in the literature$^{(8), (17) (20)}$) if the amplification is so adjusted that the negative resistance is just smaller than required for self-oscillation but great enough to reduce the damping below the critical value. It is obvious, however, that this adjustment is rather critical, the circuit remains capable of oscillations and is unstable. It is not a proper resonant circuit corresponding to the LC circuit, which is stable under all circumstances.

In the circuits described here the situation is quite different. Here the phase inversion by the valve is the essential point, and accordingly the circuit is not capable of self-oscillation and is stable under all conditions. As will be seen below, the effect of the valve shows itself not by a negative contribution to the damping term of the differential equation (1), but by a large positive addition to the $\mathbf{D}^2$ or $\mathbf{D}^0$ term, making in this way $4AC > B^2$, the system becomes periodic with a resonant frequency depending on the valve amplification (a useful property particularly at low frequencies). The damping term is not affected at all by the valve, so that the circuit is stable whatever the valve amplification.

A detailed study of the energy situation in LC circuits, undamped RC and RL circuits, valve resonant circuits and in resonant systems in general, including mechanical resonance, will be published elsewhere.

Fig. 3.

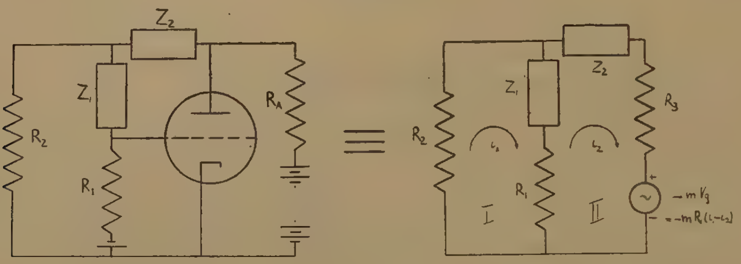

a *b*

2.2. *Reactance Valves.*

There is a certain resemblance between the circuits of fig. 1 and reactance valve circuits used for frequency modulation (see recent surveys by Reich ⁽²¹⁾ and Hund ⁽²²⁾, and a general analysis by Williams ⁽²³⁾). In some of these circuits there is also a conversion of the type of reactance through the valve circuit. But it seems that there the phase inversion is not absolutely essential. Replacement of the valve by a no-phase-shift valve or valve combination would change the reactance type produced but would hardly affect its use in frequency modulators. All the same it would be possible to develop the circuits described here, and another kind where resistance and reactance are interchanged, starting from reactance valve circuits, and preferably using Williams' method of analysis. The reason why this resonant aspect has so far not been followed up is probably that the emphasis in reactance valve development lies on their combination with LC circuits and their application to very high frequencies.

§ 3. *General Analysis.*

3.1. *Fundamental and Equivalent Circuit.*

The general scheme of the circuits is given in fig. 3 *a*, where the **Z**'s represent mainly reactive impedances consisting of pure reactance **H** (capacitive for circuit fig. 1 *a*, inductive for circuit fig. 1 *b*) and equivalent series loss resistance r. The actual analysis is carried out with the equivalent circuit (fig. 3 *b*). Here the action of the valve is represented by a generator of EMF$-m.\mathrm{V}_g$ and internal resistance R_3, where R_3 is the parallel combination of the valve impedance ρ and the load resistance $\mathrm{R_A}$ ($\mathrm{R}_3=\mathrm{R_A}\rho/\mathrm{R_A}+\rho$) and m the voltage amplification ratio of the valve, given in terms of the mutual conductance g_m by $m=g_m\mathrm{R}_3$. (For a pentode valve $\rho\gg\mathrm{R_A}$, $\mathrm{R}_3\approx\mathrm{R_A}$, $m\approx g_m\mathrm{R}_3$*.)

3.2. *Oscillatory Discharge.*

For the "free" circuit, *i. e.* without external voltage, we obtain on analysis using the loops I and I+II :

$$\left.\begin{array}{lll} \mathrm{I} & (\mathrm{R}_2+\mathrm{R}_1+\mathbf{Z}_1).i_1 & -(\mathrm{R}_1+\mathbf{Z}_1).i_2=0 \\ \mathrm{I+II} & (\mathrm{R}_2-m\mathrm{R}_1).i_1 & (\mathrm{R}_3+\mathbf{Z}_2+m\mathrm{R}_1).i_2=0 \end{array}\right\} \quad . \quad . \quad (3\,a)$$

Or

$$\boldsymbol{\varphi}.\mathbf{I}_{12}=0, \quad . \quad . \quad . \quad . \quad . \quad . \quad . \quad . \quad . \quad . \quad (3\,b)$$

where $\boldsymbol{\varphi}$ is the matrix of the coefficients and $\mathbf{I}_{12}$ that of the system of currents i_1 and i_2.

For a non-trivial solution we have

$$|\phi|\equiv m\mathrm{R}_1\mathrm{R}_2+\mathrm{R}_1\mathrm{R}_2+\mathrm{R}_1\mathrm{R}_3+\mathrm{R}_2\mathrm{R}_3$$
$$+\mathbf{Z}_1(\mathrm{R}_2+\mathrm{R}_3)+\mathbf{Z}_2(\mathrm{R}_1+\mathrm{R}_2)+\mathbf{Z}_1\mathbf{Z}_2=0. \quad . \quad (4)$$

Substituting for Z the reactance operators **H** and loss resistances r and defining two constants, the "resonant gain"

$$m'=m+1+\frac{\mathrm{R}_3}{\mathrm{R}_1}+\frac{\mathrm{R}_3}{\mathrm{R}_2}+\frac{r_1}{\mathrm{R}_1}+\frac{r_1\mathrm{R}_3}{\mathrm{R}_1\mathrm{R}_2}+\frac{r_2}{\mathrm{R}_2}+\frac{r_2}{\mathrm{R}_1}+\frac{r_1r_2}{\mathrm{R}_1\mathrm{R}_2}$$
$$(m'\simeq m \text{ if } m\gg 1 \text{ and } \mathrm{R}_1,\ \mathrm{R}_2\gg r_1,\ r_2,\ \mathrm{R}_3) \quad . \quad (5)$$

and the "damping factor"

$$g=1+\frac{\mathrm{R}_2}{\mathrm{R}_1}+\frac{r_1}{\mathrm{R}_1}+\frac{\mathrm{H}_1}{\mathrm{H}_2}\left(\frac{\mathrm{R}_2}{\mathrm{R}_1}+\frac{\mathrm{R}_3}{\mathrm{R}_1}+\frac{r_2}{\mathrm{R}_1}\right), \quad . \quad . \quad . \quad . \quad (6)$$

(4) simplifies to

$$|\boldsymbol{\varphi}|\equiv m'\mathrm{R}_1\mathrm{R}_2+g\mathbf{H}_2+\mathbf{H}_1\mathbf{H}_2=0. \quad . \quad . \quad . \quad . \quad . \quad . \quad . \quad (7)$$

We have now to distinguish the two types of circuits :—

For the *Capacitive* circuit the reactance operators are given by

$$\mathbf{H}=\mathrm{C}^{-1}\mathbf{D}^{-1},$$

and we obtain from (7)

$$|\boldsymbol{\varphi}|=m'\mathrm{R}_1\mathrm{R}_2+g\mathrm{R}_1\mathrm{C}_2^{-1}\mathbf{D}^{-1}+\mathrm{C}_1^{-1}\mathrm{C}_2^{-1}\mathbf{D}^{-2}=0. \quad . \quad . \quad . \quad . \quad (8)$$

Successive differentiation leads to the final differential equation obeyed by both branch currents

$$(m'\mathrm{R}_1\mathrm{R}_2\mathbf{D}^2+g\mathrm{R}_1\mathrm{C}_2^{-1}\mathbf{D}+\mathrm{C}_1^{-1}\mathrm{C}_2^{-1}).\mathbf{I}_{12}=0, \quad . \quad . \quad . \quad . \quad (9)$$

---

* All circuits are shown here with a single valve. A combination of valves can be used instead if the phase-shift between input and output is 180° and the overall gain is constant in the frequency range in question. Then the above analysis is strictly applicable taking for m the overall gain and for R_3 the equivalent output resistance of the valve combination.

which has a periodic and damped oscillatory solution

$$i=ke^{-\frac{\omega_0}{2Q}t}\cos(\omega_0't+\phi)\,^{*} \quad . \quad . \quad . \quad . \quad . \quad . \qquad (10)$$

$$\omega_0'=\omega_0\sqrt{1-\tfrac{1}{4}Q^2} \quad . \quad . \quad . \quad . \quad . \quad . \quad . \quad . \quad . \qquad (10\,a)$$

provided

$$g^2R_1^2C_2^{-1}<4m'R_1R_2C_1^{-1}C_2^{-1}, \quad . \quad . \quad . \quad . \quad . \quad . \qquad (11)$$

i. e.

$$g^2\frac{R_1C_1}{R_2C_2}<4m'.$$

That means we get an oscillatory discharge of, say, an initial charge on the condenser C_1 with a frequency

$$\omega_0=\frac{1}{\sqrt{m'R_1R_2C_1C_2}} \quad . \quad . \quad . \quad . \quad . \quad . \quad . \quad . \qquad (12)$$

depending on the valve constants, and a damping depending on the Q of the circuit

$$Q=\frac{\sqrt{m'}}{g}\sqrt{\frac{R_2C_2}{R_1C_1}}. \quad . \quad . \quad . \quad . \quad . \quad . \quad . \quad . \qquad (13)$$

It is clearly seen that the damping term in the differential equation is unaffected by the valve and the $\mathbf{D}^2$-term is greatly increased, in fact mainly given by the valve stage gain. If the valve is removed from the circuit, $m=0$ and the value of the resonant gain, m', is such that the inequality (11) is not fulfilled †. Then as in (2), $B^2>4AC$ and the circuit is aperiodic.

In the inductive circuit the reactance operators are given by

$$H=L\mathbf{D},$$

so that we obtain directly from (7) the final differential equation

$$(L_1L_2\mathbf{D}^2+gR_1L_2\mathbf{D}+m'R_1R_2)\mathbf{I}_{12}=0. \quad . \quad . \quad . \quad . \quad . \qquad (14)$$

Here the $\mathbf{D}^0$ term is increased by the valve but the damping term is

---

[*] The more usual notation for the exponential damping is

$$i=ke^{-2\delta\frac{t}{T}}\cos\left(2\pi\frac{t}{T}+\phi\right),$$

where δ is the "logarithmic decrement." Comparing (10) and (10 *a*) we have

$$\delta=\frac{\pi}{2Q}. \quad . \quad . \quad . \quad . \quad . \quad . \quad . \quad . \quad . \quad . \qquad (10\,b)$$

[†] This follows easily from (6)

$$g^2\frac{R_1C_1}{R_2C_2}>4\left(1+\frac{R_3}{R_2}+\frac{R_2}{R_1}+\frac{R_3}{R_1}+\frac{r_1}{R_1}+\frac{R_3r_1}{R_1R_2}+\frac{r_1r_2}{R_1R_2}+\frac{r_2}{R_1}+\frac{r_2}{R_2}\right)$$

$$=4\left(m'-m+\frac{R_2}{R_1}\right),$$

using the inequality relation

$$(1+a+b+c+\ldots)^2>4(a+b+c+\ldots).$$

again unaffected. For the frequency and damping of the oscillatory discharge we obtain

$$\omega_0 = \sqrt{\frac{m' R_1 R_2}{L_1 L_2}}, \quad \ldots\ldots\ldots \quad (15)$$

$$Q = \frac{\sqrt{m'}}{g} \sqrt{\frac{R_2 L_1}{R_1 L_2}}, \quad \ldots\ldots\ldots \quad (16)$$

i. e. the frequency increases with increasing stage gain.

3.3. *Resonant and Filter Properties of the Circuits.*

Resonant properties can be observed with the circuit (fig. 3 *a*) if a source of alternating voltage is connected to it. This can be done in various ways.

Fig. 4.

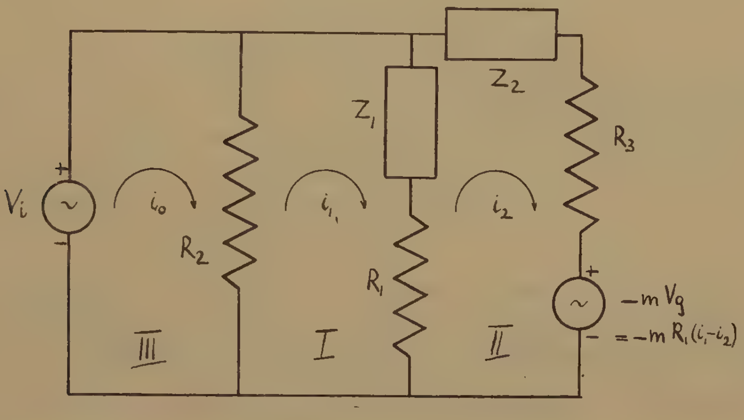

3.3.1. *Parallel Resonance.*—With a generator connected in parallel with the resistance R_2 of fig. 3 *a* we observe the effect of parallel resonance, which means that the impedance presented to the generator is equivalent to the impedance of a parallel LC circuit.

We have the scheme of fig. 4 and obtain from the loops III, I, I+II (the loops I and II being identical with fig. 3 *b*)

$$\begin{array}{ll} \text{III} & \\ \text{I} & \psi . I_{012} \equiv \\ \text{I+II} & \end{array} \begin{bmatrix} R_2 & -R_2 & 0 \\ -R_2 & \cdot & \cdot \\ -R_2 & \cdot & \cdot \end{bmatrix}_{\varphi} \cdot \begin{bmatrix} i_0 \\ i_1 \\ i_2 \end{bmatrix} = \begin{bmatrix} V_i \\ 0 \\ 0 \end{bmatrix}, \quad (17)$$

hence

$$i_0 = \frac{|\varphi|}{|\psi|} V_i. \quad \ldots\ldots\ldots \quad (18)$$

Calling the impedance presented to the generator " parallel impedance " $\mathbf{Z}_p$ we have

$$\mathbf{Z}_p=\frac{V_i}{i_0}=\frac{|\psi|}{|\varphi|}. \quad . \quad . \quad . \quad . \quad . \quad . \quad . \quad . \quad . \quad (19)$$

Expanding the numerator of (19) in terms of the reactance operators and simplifying

$$|\psi|=R_2(\mathbf{H}_1\mathbf{H}_2+R_1\mathbf{H}_2)\,^*, \quad . \quad . \quad . \quad . \quad . \quad . \quad . \quad (20)$$

so that with (7) we get the following general expression for the parallel impedance

$$\mathbf{Z}_p=R_2\frac{\mathbf{H}_1\mathbf{H}_2+R_1\mathbf{H}_2}{mR_1R_2+gR_1\mathbf{H}_2+\mathbf{H}_1\mathbf{H}_2}. \quad . \quad . \quad . \quad . \quad . \quad (21)$$

For the capacitive circuit we put now for the reactance operator $\mathbf{H}=\frac{-j}{\omega C}$ (it is to be noted that the r's represent the equivalent series loss resistances given in terms of the condenser leakage resistance R_L by $=(\omega C)^{-2}R_L^{-1}/n$). So we obtain from (21) for the complex impedance

$$\mathbf{Z}_p=R_2\frac{-1-j\omega R_1C_1}{\omega^2mR_1R_2C_1C_2-1-j\omega gR_1C_1}, \quad . \quad . \quad . \quad . \quad (22)$$

which with (12) and (13) becomes

$$\mathbf{Z}_p=R_2Q\frac{1+j\frac{\omega}{\omega_0}\frac{1}{gQ}}{Q\left(1-\frac{\omega^2}{\omega_0^2}\right)+j\frac{\omega}{\omega_0}}, \quad . \quad . \quad . \quad . \quad . \quad . \quad . \quad (23)$$

i. e. there is resonance at the oscillation frequency of the free circuit, and the selectivity factor Q determining the sharpness of resonance is the same as the Q determining the damping of the free circuit.

Writing γ for the relative frequency $\frac{\omega}{\omega_0}$, and representing the typical resonance function by

$$\mathbf{Res}\,(\gamma, Q)\equiv(1-\gamma^2)^2Q^2+\gamma^2,$$

we obtain for the effective impedance $|\mathbf{Z}_p|$, the phase angle ϕ_p, and for the resistive and reactive components, R_p and X_p, of $\mathbf{Z}_p$ compared with the corresponding expressions for a conventional LC circuit :—

---

* Equation (20) represents the practical form of the solution. In the exact solution an additional " real " term occurs which, for all practical values of the circuit components, is negligible against the first terms in the relevant frequency range ; furthermore, the exact value of the coefficient of the second term in (20) is different from unity, by an amount which is negligible in practice. As a further simplification the distinction between m and m' will be dropped from now on. Corresponding approximations will be made in the following sections so that the main argument is not obscured by practically irrelevant factors.

RC circuit.

$$|\mathbf{Z}_p|=R_2Q\left(1+\frac{1}{g^2Q^2}\right)^{\frac{1}{2}}\mathbf{Res}^{-\frac{1}{2}}(\gamma, Q). \quad (24)$$

$$\phi_p=\tan^{-1}\left[-\frac{\gamma\left(1-\frac{1}{g}\right)+\gamma^3\frac{1}{g}}{Q(1-\gamma^2)+\gamma^2}\right]. \quad (25)$$

$$R_p=R_2Q\left[Q(1-\gamma^2)+\gamma^2\frac{1}{gQ}\right] \times\mathbf{Res}^{-1}(\gamma, Q). \quad (26)$$

$$X_r=-R_2Q\left[\gamma\left(1-\frac{1}{g}\right)+\gamma^3\frac{1}{g}\right] \times\mathbf{Res}^{-1}(\gamma, Q). \quad (27)$$

LC circuit.

$$|Z_p|=\omega_0LQ\left(\gamma^2+\frac{1}{Q^2}\right)^{\frac{1}{2}}\mathbf{Res}^{-\frac{1}{2}}(\gamma, Q). \quad (24a)$$

$$\phi_p=\tan^{-1}\left[\gamma(1-\gamma^2)-\frac{1}{Q}\gamma\right]. \quad (25\,a)$$

$$R_p=\omega_0LQ\,\mathbf{Res}^{-1}(\gamma, Q). \quad (26\,a)$$

$$X_p=\omega_0LQ\left[\gamma(1-\gamma^2)-\frac{1}{Q}\gamma\right] \times\mathbf{Res}^{-1}(\gamma, Q). \quad (27\,a)$$

In the *inductive* circuit we have $H=jwL$, and the complex impedance becomes

$$\mathbf{Z}_p=R_2\frac{-1+j\frac{R_1}{\omega L_1}}{\frac{mR_1R_2}{\omega^2L_1L_2}-1+jg\frac{R_1}{\omega L_1}} \quad . \quad . \quad . \quad . \quad . \quad . \quad . \quad . \quad (28)$$

Considering (15) and (16) we see that here again resonance occurs at the oscillation frequency of the free circuit. The corresponding expressions for $|\mathbf{Z}_p|$, etc., have, apart from differences in sign, exactly the same appearance as those for the capacitive circuit if written in terms of the reciprocal relative frequency $\epsilon=\frac{\omega_0}{\omega}$.

RL circuit.

$$|\mathbf{Z}_p|=R_2Q\left(1+\epsilon^2\frac{1}{g^2Q^2}\right)^{\frac{1}{2}}\mathbf{Res}^{-\frac{1}{2}}(\epsilon, Q). \quad . \quad . \quad . \quad . \quad . \quad . \quad (29)$$

$$\phi_p=\tan^{-1}\left[\frac{\epsilon\left(1-\frac{1}{g}\right)+\epsilon^3\frac{1}{g}}{Q(1-\epsilon^2)+\epsilon^2\frac{1}{gQ}}\right]. \quad . \quad . \quad . \quad . \quad . \quad . \quad . \quad (30)$$

$$R_p=R_2Q\left[Q(1-\epsilon^2)+\epsilon^2\frac{1}{gQ}\right]\mathbf{Res}^{-1}(\epsilon, Q). \quad . \quad . \quad . \quad . \quad . \quad (31)$$

$$X_p=R_2Q\left[\epsilon\left(1-\frac{1}{g}\right)+\epsilon^3\frac{1}{g}\right]\mathbf{Res}^{-1}(\epsilon, Q). \quad . \quad . \quad . \quad . \quad . \quad (32)$$

It is interesting to compare the results obtained with those for LC circuits in graphical representation. (For properties of LC circuits see a recent survey by Sherman (24). Fig. 5 shows the comparison of a parallel LC circuit with a capacitive valve resonant circuit of the same resonance frequency and Q. In fig. 5 *a* the modulus and phase angle of $\mathbf{Z}_p$ are shown. It is seen that the modulus has the same appearance in both cases. The phase-angle curves are, however, quite different. In the LC circuit we have, at resonance zero phase-angle, purely resistive impedance ; in the valve circuit the resonance phase-angle is $-90°$, the phase-angle of a pure capacitance (and this obtained across a resistance !).

Fig. 5 *b* shows the resistive and reactive components of $\mathbf{Z}_p$ separately. LC resonance is characterized by a maximum of the always positive resistive component and an S-shaped curve of the reactance against frequency with two maxima, one positive and one negative. In the valve circuit it is the reactive component which does not change sign and which has the maximum, whereas the resistive component changes sign at resonance, the resistance becoming negative at frequencies above resonance. This fact will be of importance for coupled resonant circuits to be considered below.

Fig. 5*a*.

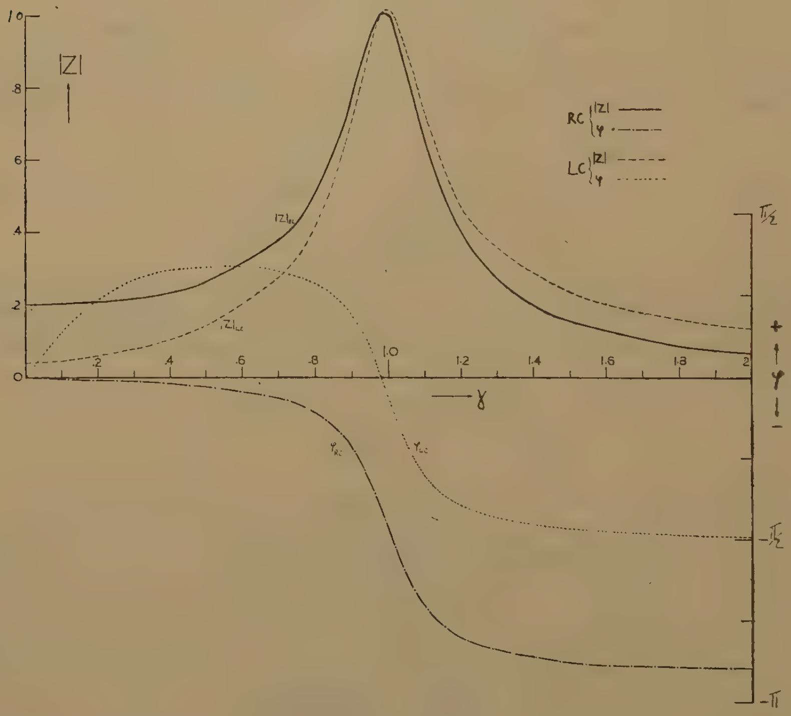

For the inductive circuit we get very similar pictures when plotted against ϵ, but with the signs reversed, the resonance phase-angle being $+90°$ and the reactive component always positive.

3.3.2. *Series Resonance.*—If in the circuit of fig. 3 a generator is connected in series with R_2, the impedance presented to the generator is of the series resonance type and will be called " series impedance " $\mathbf{Z}_s$. Is

We have the scheme (fig. 6) from which we obtain, using the loop and I+II (as in the nearly identical scheme (fig. 3 *b*))

$$\varphi . I_{12} = \begin{pmatrix} V_i \\ V_i \end{pmatrix}, \quad \ldots \ldots \ldots \tag{33}$$

hence for the series impedance

$$\mathbf{Z}_s = \frac{V_i}{i_1} = \frac{|\boldsymbol{\varphi}|}{\phi_{22} - \phi_{12}}, \quad . \quad . \quad . \quad . \quad . \quad . \quad . \quad . \quad (34)$$

which, on comparison with (7), shows directly the resonance character.

Fig. 5*b*.

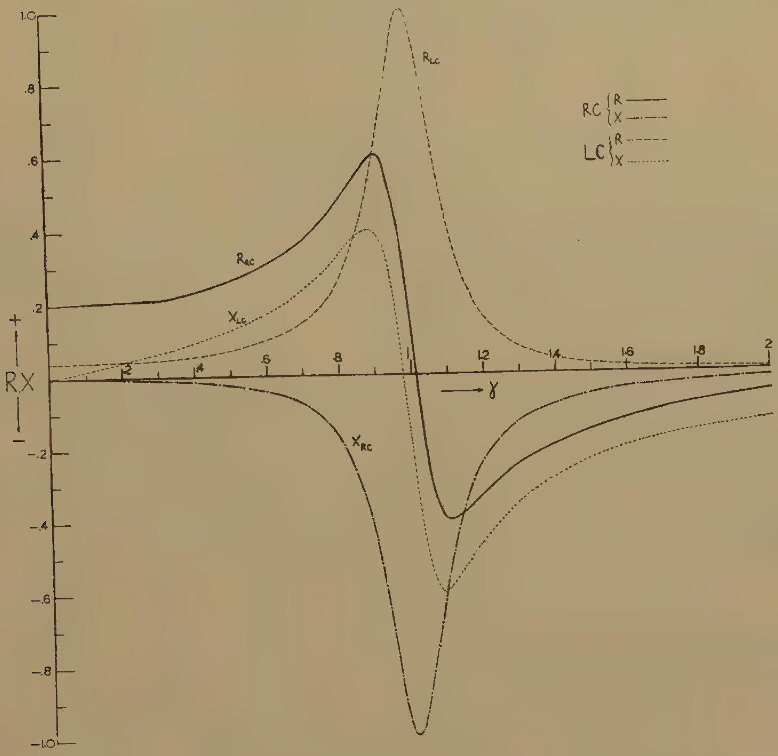

Fig. 6.

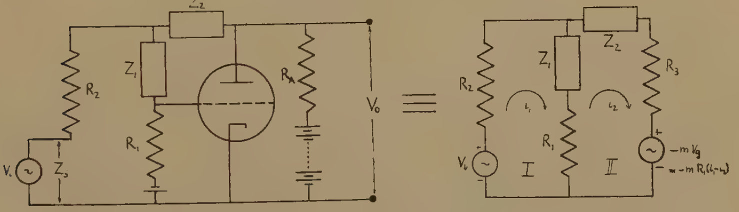
Z2
Z1
R2
R1
Rₐ
V0
V1
Zs
≡
Z1
Z2
R2
R3
i1
i2
R1
V1
I
II
-m Vg
-m R1(i1-i2)

a *b*

Evaluation of (34) leads, with (12) and (13) for the *Capacitive Circuit*, to a complex series impedance

$$\mathbf{Z}_s = -\frac{R_2}{Q\gamma^2}[(1-\gamma^2)Q + j\gamma], \quad . \quad . \quad . \quad . \quad . \quad . \quad . \quad (35)$$

and hence the modulus $|Z_s|$ and phase-angle ϕ_s

$$|\mathbf{Z}_s|=\frac{R_2}{Q\gamma^2}\,\mathbf{Res}^{\frac{1}{2}}(\gamma, Q). \quad \ldots \ldots \quad (36)$$

$$\phi_s=\tan^{-1}\left[\frac{-\gamma}{-Q(1-\gamma^2)}\right], \quad \ldots \ldots \quad (37)$$

and with (15) and (16) for the *Inductive Circuit* to

$$|\mathbf{Z}_s|=\frac{R_2}{Q\epsilon^2}\,\mathbf{Res}^{\frac{1}{2}}(\epsilon, Q), \quad \ldots \ldots \quad (38)$$

$$\phi_s=\tan^{-1}\left[\frac{\epsilon}{-\epsilon Q(1-\gamma^2)}\right]. \quad \ldots \ldots \quad (39)$$

The expressions are seen to correspond to those holding in the case of LC series resonance, R_2 taking the place of $\omega_0 L$. But we get the same difference in the phase-angle as in parallel resonance, the resonant phase-angle being $-90°$ and $+90°$ respectively for the capacitive and inductive circuits.

3.3.3. *Selective Amplification.*—Of greater practical importance than the pure resonance effects is the action of the valve circuits as selective and amplifying filters or " tuned amplifiers," using the output voltage between anode and earth of the valve produced by an alternating input connected as in fig. 6. The selective amplification is expressed by the ratio of output voltage V_0 to input voltage V_i in magnitude and phase-angle.

Since the output voltage is given by

$$V_0=R_3 i_2-mV_g=R_3 i_2-mR_1(i_1-i_2), \quad \ldots \ldots \quad (40)$$

we obtain, with (33) for the selective amplification,

$$\frac{V_0}{V_i}=\frac{1}{|\boldsymbol{\varphi}|}[(R_3+mR_1)(\phi_{11}-\phi_{21})-mR_1(\phi_{22}-\phi_{12})] \quad \ldots \quad (41)$$

which, evaluated, gives

$$\frac{V_0}{V_i}=\frac{m}{g}\,\frac{-gR_1\mathbf{H}_2}{mR_1R_2+gR_1\mathbf{H}_2+\mathbf{H}_1\mathbf{H}_2}, \quad \ldots \ldots \quad (42)$$

hence for the *Capacitive Circuit*

$$\frac{V_0}{V_i}=\frac{m}{g}\gamma\,\frac{-j}{(1-\gamma^2)Q+j\gamma}, \quad \ldots \ldots \quad (43)$$

$$\left|\frac{V_0}{V_i}\right|=\frac{m}{g}\gamma\,\mathbf{Res}^{-1}(\gamma, Q), \quad \ldots \ldots \quad (44)$$

$$\phi=\tan^{-1}\left[\frac{-Q(1-\gamma^2)}{-\gamma}\right], \quad \ldots \ldots \quad (45)$$

and for the *Inductive Circuit*

$$\frac{V_0}{V_i}=\frac{m}{g}\gamma\,\frac{-j}{(1-\epsilon^2)Q+j\gamma}, \quad \ldots \ldots \quad (46)$$

$$\left|\frac{V_0}{V_i}\right| = \frac{m}{g}\epsilon\,\mathbf{Res}^{-\frac{1}{2}}(\epsilon, Q), \quad \ldots \ldots \ldots \quad (47)$$

$$\phi = \tan^{-1}\left[\frac{Q(1-\epsilon^2)}{-\epsilon}\right]. \quad \ldots \ldots \ldots \quad (48)$$

The amplification is a maximum at resonance $\left(\left|\frac{V_0}{V_i}\right|_{\text{res}} \text{ given by } \frac{m}{g}\right)$ nearly equal to the valve stage gain, the phase-angle here being 180° as in an ordinary amplifier or in an LC tuned amplifier at resonance.

3.4. *Resonance Frequency.*

The resonance or tuning frequency in all treated cases is given by the expressions (12) and (15). The appearance of the valve stage gain m in these expressions is useful in so far as it allows low frequency resonance to be obtained, using not excessively low condensers, and high frequency resonance using not excessively low inductances. The drawback of the appearance of the valve constants in the frequency expressions with regard to frequency stability can be overcome by using valve combinations (see footnote, p. 375) and stabilizing the overall gain by negative feedback.

3.5. *The Selectivity Q.*

The sharpness of resonance or tuning is in all cases given by the equations for Q (13) and (16), increasing as one would expect with the valve stage gain. The Q of LC circuits depends directly on the ratio of reactance to resistance in the reactor. A change in resonance frequency in a given circuit by variation of the capacitance is therefore accompanied by a change in Q, and low resonance frequencies cannot be obtained as outlined above. In the present circuits the loss resistances enter the expression for Q only very indirectly (through g, and are negligible in the capacitive circuit) and the Q depends mainly on resistance and reactance *ratios*. The resonance frequency can therefore be varied and the Q kept at the same high value.

For the capacitive circuit we find in particular that there is no limitation to the obtainable resonance frequency on the low frequency side. As long as the ratio $g^2\frac{R_1C_1}{R_2C_2}$ is kept small, the individual values of the resistances can be made very high and the resonance frequency extremely low. Resonance of sufficient sharpness, *i. e.* a Q of the order of 5 to 10, can be obtained with ease at frequencies round 1 cps. or even smaller.

At radio frequencies where the inductive circuit is feasible, a Q of this order is rather low. It will, however, be possible to increase the high selectivity of LC circuits in this frequency range by *combining* them with the new inductive valve resonant circuits.

3.6. *Optimum Selectivity.*

The Q depends in a rather involved way on the various resistance and reactance ratios. It is of interest to determine for one practical case the optimum value for these ratios, *i. e.* the value which gives maximum Q.

For a given valve or valve arrangement the valve amplification m and effective resistance R_3 are given. The grid resistance R_1 should be as high as is compatible with the conditions to make g small and Q high. It will be limited by grid cathode leakage and input capacity. Assuming R_1 to be fixed we have to determine the optimum values of the ratios $a=\frac{H_1}{H_2}$ and $b=\frac{R_2}{R_1}$ in terms of the ratio $c=\frac{R_3}{R_1}$ and of the loss ratios $\alpha_1=\frac{r_1}{R_1}$; $\alpha_2=\frac{r_2}{R_1}$, *i. e.* the values of a and b which make Q a maximum or $\frac{m}{Q^2}$ a minimum.

We obtain from (13), (16) and (6)

$$\frac{m}{Q^2}=\frac{R_1}{R_2}\frac{H_2}{H_1}g^2=\eta(a,b)=\frac{1}{ab}[1+b+\alpha_1+a(b+c+\alpha_2)], \quad . \quad . \quad (49)$$

and the optimum values from

$$\frac{\partial\eta}{\partial a}=0, \quad \frac{\partial\eta}{\partial b}=0,$$

$$a_{\text{opt}}=\sqrt{\frac{1+\alpha_1}{c+\alpha_2}}, \quad b_{\text{opt}}=\sqrt{(1+\alpha_1)(c+\alpha_2)}. \quad . \quad . \quad . \quad . \quad (50)$$

The maximum value of Q under these conditions is

$$Q_{\max}=\tfrac{1}{2}\sqrt{m}(\sqrt{1+\alpha_1}+\sqrt{c+\alpha_2})^{-\frac{1}{2}}. \quad . \quad . \quad . \quad . \quad . \quad . \quad (51)$$

If the losses are negligible, we have

$$a_{\text{opt}}=\frac{1}{\sqrt{c}}, \quad b_{\text{opt}}=\sqrt{c}, \quad Q_{\max}=\tfrac{1}{2}\sqrt{m}(1+\sqrt{c})^{-\frac{1}{2}}. \quad . \quad . \quad (52)$$

And the absolute maximum of Q is obtained if $c\to 0$:

$$Q_{\max}\to\tfrac{1}{2}\sqrt{m}.$$

3.7. *Coupled Valve Resonant Circuits.*

The resonant character of the circuits described here extends also to coupling phenomena. The peculiar form of the input part of the circuits with its input resistance R_2 is most suitable for coupling the circuits together (or to ordinary non-selective amplifiers if a high input impedance for a voltage to be analyzed is required). The coupling can be effected through resistances only, no additional capacitances being required to separate d.c. and a.c. paths, a very useful feature for low frequency purposes. Fig. 7 gives the coupling element between two valve resonant circuits. The resistance R_7 is part of the load of circuit 1 as well as part of the input resistance of circuit 2. The ratio $k=\frac{R_7}{R_7+R_8}$ determines the closeness of coupling.

The case where two resonant circuits tuned to the same frequency are closely coupled is of particular interest. Typical coupling phenomena result. A quantitative analysis of the overall response, *i. e.* the dependence of the ratio of output from second circuit to input to first circuit, would be very complicated and would hardly serve a useful purpose. A qualitatative understanding, however, why the close coupling leads to the typical splitting up of the single peak response corresponding to the individual or loosely coupled circuits into two peaks on both sides of it, is obtained if it is realized that part of the parallel impedance $\mathbf{Z}_p$ of circuit 2 forms part of the load impedance of circuit 1. Consequently, since $\mathbf{Z}_p$ depends on frequency and has a reactive component, the stage gain m of circuit 1 depends on frequency and has a reactive component. The "coupled" resonant frequency and selectivity vary therefore with frequency. In particular at the resonant frequency of the individual circuits $\mathbf{Z}_p$ is purely reactive, and hence the reactive component of m will there be a maximum. This reactive part leads to an increase in the damping factor g_1*, hence producing a reduction in the amplification of circuit 1 corresponding to the depression in the coupling curve. At frequencies above and below the individual resonance the resistive component of $\mathbf{Z}_p$ will be of influence. Below resonance the resistive component of $\mathbf{Z}_p$ is positive, the resistive component of the load of valve 1

Fig. 7.

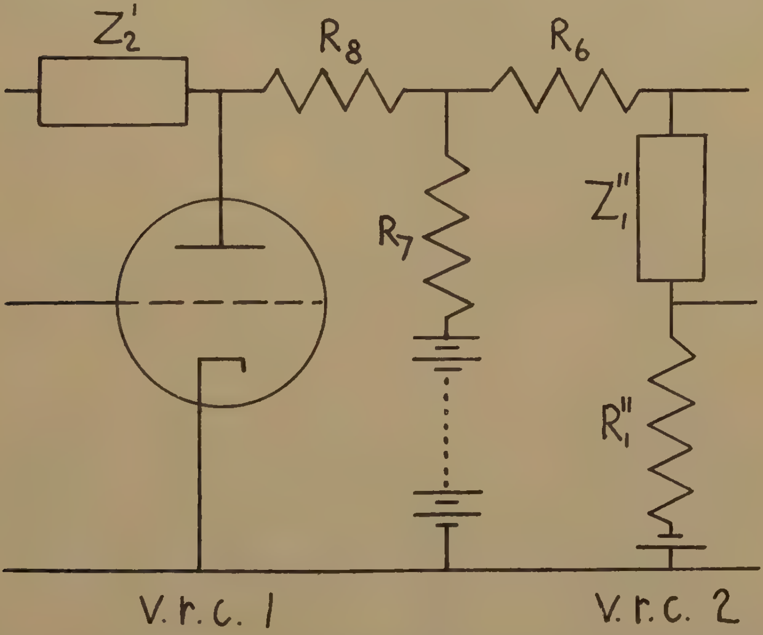

---

* This is easily seen from equations (4) and (6). p. 375: the reactive component $\mathbf{H}_m$ of m_1 leads to an additional term $\mathbf{H}_m\mathrm{R}_1\mathrm{R}_2$ in (4) and hence $\frac{\mathrm{H}_m}{\mathrm{H}_2}$ in (6). Since $\mathbf{H}_m$ is of the same reactive type as $\mathbf{H}_2$ this additional term in g_1 is positive.

is therefore increased, producing an increase in m and shifting the "coupled" resonance frequency of circuit 1 to lower frequencies. The low frequency peak of the coupling curve will therefore lie somewhere near the frequency of the positive maximum of the resistive component of $\mathbf{Z}_p$. Similarly for the high frequency peak of the coupling curve. Here the resistive component of $\mathbf{Z}_p$ is negative, m is reduced and the "coupled" resonance of circuit 1 shifted to higher frequencies.

These coupling effects can be used to obtain with closely coupled capacitive circuits tuned to the same or slightly different frequencies band pass filters for very low frequencies which may have applications in sound reproduction and in the television field.

On the other hand, using two capacitive circuits loosely coupled in succession and coupling the output of the second loosely back to the input of the first an oscillator is obtained. This is the basis of the oscillator used in the experiments described below.

§ 4. *Experimental Work.*

In order to illustrate the theoretical results of the preceding section some experimental curves are reproduced.

4.1. *Apparatus.*

The curves were obtained with the arrangement shown in fig. 8. L.F.O. is a variable low frequency oscillator of special design (consisting of two back-coupled valve resonant circuits). Its output was checked by the vertical deflection of the cathode ray oscilloscope C.R.O. 1 ("Ultrascope"). Short pulses, periodic at a rate of one per second, derived from an electric clock * and fed to the X-plates of the oscilloscope, served to check the frequency of the oscillations by counting the coincidences (a very convenient and speedy method of frequency measurement). The oscillator output is connected through a potentiometer arrangement, R_4R_5, in "series" with the capacitive valve resonant circuit $R_1R_2C_1C_2V$. The valve V used is a Mullard SP4 pentode. The biassing arrangement produces some negative feedback ensuring a certain

Fig. 8.

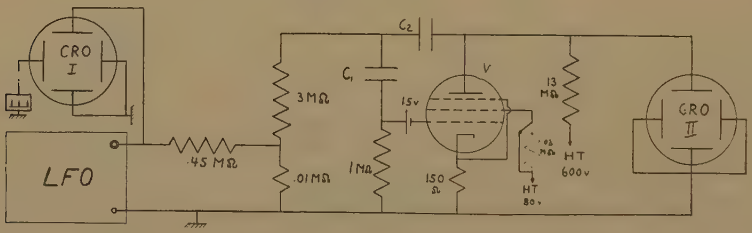

---

* "Gent's" electrically maintained pendulum clock in the Electrical Engineering Department of this College. I am indebted to Professor J. C. Prescott for permission to use the clock and to make the necessary electric connections to the Physics Department.

amount of stabilization. The output from the valve was measured with a second calibrated oscilloscope C.R.O. 2, the vertical deflection being measured with a ruler. This was found to be the most satisfactory method for the frequencies used, since ordinary valve voltmeters are not suitable for very low frequencies and d.c. (moving coil) voltmeters are only suitable for frequencies far removed from their natural mechanical vibration frequency. The stage gain m of the valve was measured by disconnecting the control grid from the circuit, connecting it to a known fraction of the mains alternating voltage and observing the output deflection. The resistance R_6 (0·03 MΩ) could be inserted in series with the screen grid to reduce the stage gain without appreciably changing the effective output resistance R_3. The latter is mainly determined by the anode load R_A (0·13 MΩ) slightly reduced by the internal valve resistance and input resistance of the Ultrascope (0·9 MΩ).

Fig. 9.

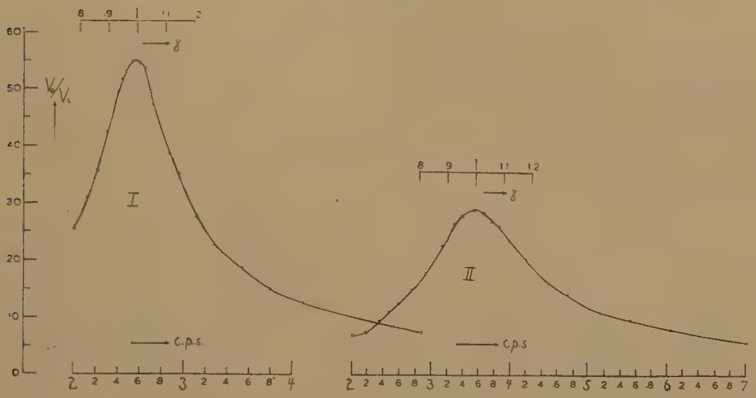

The values of the circuit components in all experiments shown here were as follows :—

$$R_1=1{\cdot}0\ \text{M}\Omega, \qquad R_3=0{\cdot}095\ \text{M}\Omega,$$
$$R_2=0{\cdot}31\ \text{M}\Omega, \qquad C_2/C_1=3,$$

so that from (6) we have for the damping factor $g=2{\cdot}5_4$ (neglecting condenser losses).

4.2. *Selective Amplification Curves.*

Measuring the output as a function of the oscillator frequency gives selective amplification curves. Fig. 9 shows curves with the same capacitances, $C_2=3C_1={\cdot}015\mu\text{F}$, for two different values of the stage gain m to demonstrate its influence on the resonant frequency and selectivity Q. For curve I : $m=145$. From the experimental curve we find $f_0=2{\cdot}5_8$ cps., $Q=4.3_7$ and $\left|\dfrac{V_0}{V_i}\right|_{\text{res}}=54{\cdot}7$. This agrees satisfactorily with the values calculated from (12), (13), (44) : $f_0=2{\cdot}6_2$ cps., $Q=4{\cdot}6_1$ and

$\left|\frac{V_0}{V_i}\right|_{res}=57{\cdot}_0$. For curve II: $m=77{\cdot}_6$, the resonant frequency is higher the selectivity * and maximum amplification smaller; we find experimentally:

$$f_0=3{\cdot}5_6 \text{ cps.}, \quad Q=3.3_0, \quad \left|\frac{V_0}{V_i}\right|_{res}=29{\cdot}_4,$$

and by calculation:

$$f_0=3{\cdot}5_8 \text{ cps.}, \quad Q=3{\cdot}3_8, \quad \left|\frac{V_0}{V_i}\right|_{res}=30{\cdot}_5.$$

In fig. 10 curves for three different pairs of capacitances are reproduced to show the possibilities of the new circuit at fixed stage gain $m=145$. Curve I was the lowest resonance curve obtainable with the available oscillator, but it is far from the low frequency limit of the circuit; the capacitances could easily be increased by a factor 100 giving resonance at ·02 cps. (1 vibration per 50 secs.!). For curve I (identical with curve I, fig. 9),

Fig. 10.

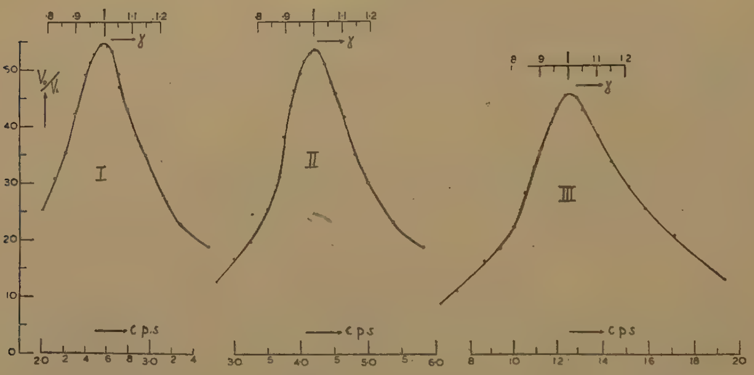

$$C_2=3C_1={\cdot}015\mu F, \quad f_0=2{\cdot}5_8, \quad Q=4{\cdot}3_7, \quad \left|\frac{V_0}{V_i}\right|_{res}=54{\cdot}7.$$

For curve II

$$C_2=3C_1={\cdot}009\mu F, \quad f_{0\text{exp.}}=4{\cdot}2_1 \text{ cps.}, \quad f_{0\text{calc.}}=4{\cdot}3_6 \text{ cps.},$$

and we see that the experimental values for Q and $\left|\frac{V_0}{V_i}\right|_{res}$, $4{\cdot}3_4$ and $54{\cdot}_0$ respectively, are near enough the same as for the lower frequency and the calculated values, confirming that the resonant frequency can be changed without affecting the selectivity. This change can cover a very wide range provided the capacitances are loss free. In the arrangement here this is not quite the case, for curve III $C_2=3C_1={\cdot}003\mu F$, $f_{0\text{exp.}}=12{\cdot}_5$ cps., $f_{0\text{calc.}}=13{\cdot}1$ cps. in satisfactory agreement, but both the $Q=3{\cdot}6_0$ and

---

* In all graphs the frequencies are plotted in such a way that the relative frequency scale is the same for all curves.

$\left|\frac{V_0}{V_i}\right|=46\cdot5$ are found to be smaller than the previous values, indicating an increased damping factor g due to the loss resistances r_1, r_2 being no longer negligible. The capacitances used are decade mica condenser boxes which, particularly for the low capacity values, are bound to have some losses. For higher frequency resonance, therefore, either more nearly perfect condensers would have to be used or alternatively lower values of the resistances R_1, R_2 $\left(\text{as far as is compatible with a small ratio } \frac{R_3}{R_1}\right)$ requiring greater capacitances for the same frequencies and so reducing the condenser losses.

It is to be noted that in the arrangement with the high resistance values the capacities required for resonance below 10 cps. are very small.

Fig. 11.

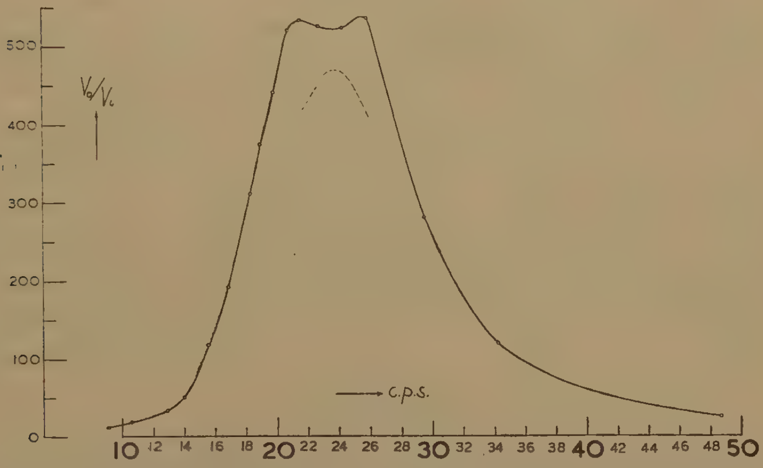

Ordinary continuously variable rotating condensers could be used with only a few steps of fixed condensers to cover a wide range of frequencies down to 2 cps. or lower. This fact, due to the appearance of the stage gain in the frequency expression, will be useful for low frequency analyzers, *e. g.* for biological purposes (encephalography ⁽²⁵⁾, ⁽²⁶⁾, etc.). The advantage gained by increasing m through the use of valve combinations in place of a single valve is therefore twofold : higher selectivity and lower capacity.

4.3. *Response of Coupled Circuits.*

Coupling effects were investigated experimentally with pentode resonant circuits of relatively high Q, and the qualitative results of section 3·7 were confirmed. Fig. 11 shows, as an example, the overall response of two identical coupled capacitive circuits having individual selectivities $Q=5$. The value of the coupling resistances was $R_7=\cdot15\ M\Omega$,

R_8=·46 MΩ, R_6=·5 MΩ, so that k=2·4$_6$. The dotted line gives the relative response curve of the individual circuits.

4.4 *Frequency Analysis.*

In order to demonstrate the usefulness and limitations of the simple experimental circuit for the purpose of analysing a complex wave the response to a periodic voltage of saw-tooth form was investigated.

Fig. 12.

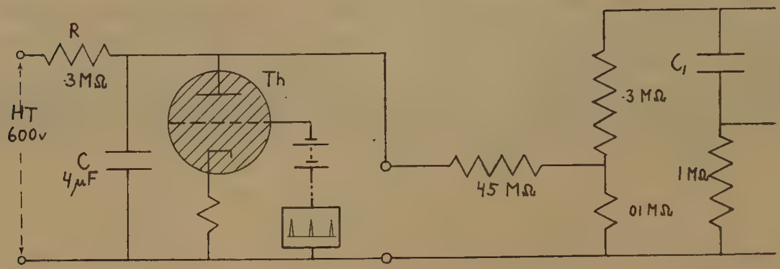

Fig. 13.

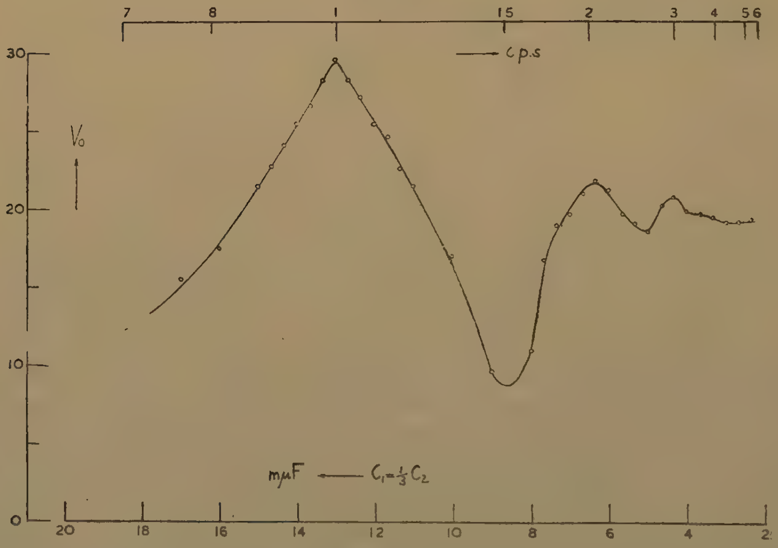

The periodic pulses from the clock were used to trigger a simple saw-tooth generator consisting of the resistance-capacitance combination RC and the thyratron valve Th (see fig. 12). The saw-tooth wave obtained, of frequency exactly 1 sec., formed the input to the valve resonant circuit. Measuring the output of the latter for varying values of the capacitances determining the tuning frequency $\left(\text{keeping always } \frac{C_2}{C_1}=3\right)$ gave a curve, reproduced in fig. 13, which represents the analysis of the complex input. The fundamental, second, and third harmonic can be recognized. There is a faint indication of the fourth harmonic, but it is almost completely drowned in the background produced by the contribution of all harmonics, particularly all the higher ones to the output.

This drowning effect shows the limitation of the circuit; it is clearly the more marked the lower the Q. It follows from equation (44) that for frequencies far above resonance the output is approximately $\frac{1}{\gamma Q}$ of the resonance output. Since the amplitude of the nth harmonic of a saw-tooth voltage of tooth height H is given by $A_n = \frac{H}{n\pi}$, it is easily seen that with a Q of only 4·5 the background must be an appreciable fraction of even the fundamental output. For periodic pulses of short duration the situation would be still worse, the fundamental and all the early harmonics being equal and small $\left(A_n \simeq \frac{H}{\pi}\frac{\tau}{T} \text{ if T is period and } \tau \text{ pulse duration}\right)$, so that hardly anything would emerge from the background. However, for the analysis of waves containing a small number of low- or non-multiple frequencies, the selectivity obtainable with the simple circuits should be sufficient.

Selectivities of a much higher order can be reached by applying Scott's (27) method of amplification with selective negative feedback, using in place of a bridge network a capacitive valve resonant circuit in the feedback path. The theory and description of a frequency analsyer of this type, with which a Q of 150 at 1–15 cps. has been reached, will form the subject of another paper.

Acknowledgement.

I am greatly indebted to the Research Committee of King's College, Newcastle-upon-Tyne, for a generous grant made in support of a wider research programme of which the work presented in this paper forms one part.

References.

(1) F. Tank and K. Graf, Helv. Phys. Act. i. p. 508 (1928).
(2) S. Whitehead, Journ. Sci. Instr. xxi. p. 73 (1944).
(3) H. W. Nichols, U.S. Patent 1,442,781 (1923).
(4) J. van d. Mack and B. van d. Pol, *Physica*, i. p. 437 (1934).
(5) N. L. Yates-Fish, Proc. Phys. Soc. xlviii. p. 125 (1936).
(6) A. Monnier and J. Bazin, *Compt. Rend.* ccii. p. 828 (1936).
(7) H. Morin, *Compt. Rend.* ccvi. p. 1560 (1938).
(8) E. W. Herold, Proc. I. R. E. xxiii. p. 1201 (1935); xxv. p. 1399 (1937).
(9) F. E. Terman, 'Fundamentals of Radio,' p. 95 (1938).
(10) P. W. Willans and N. L. Yates-Fish, British Patent 489,849 (1938).
(11) P. W. Willans, British Patent 497,148 (December, 1938).
(12) F. E. Terman, R. R. Buss, W. R. Hewlett and F. C. Cahill, Proc. I. R. E. xxvii. (October, 1939).
(13) C. Brunetti, Proc. I. R. E. xxvii. p. 88 (1939).

(14) P. S. Delaup, 'Electronics,' p. 34 (Jan. 1941).
(15) E. L. Ginzton and L. M. Hollingsworth, Proc. I. R. E. xxix. p. 43 (1941).
(16) "A New Frequency Generator," Electronic Eng. xii. p. 246 (1941).
(17) S. R. Jordan, 'Electronics,' xv. p. 42 (July, 1942).
(18) W. B. Nottingham, 'Electronics,' xv. p. 109 (July, 1942).
(19) J. A. B. Davidson, Electronic Eng. xv. pp. 316, 361 (1944).
(20) British Patent 499, 760 (1940).
(21) Reich, H. J., Proc. I. R. E. xxx. p. 288 (1942).
(22) A. Hund, 'Electronics,' p. 68 (October, 1942).
(23) E. Williams, Wireless Eng. xx. p. 369 (August, 1943).
(24) J. B. Sherman, Proc. I. R. E. xxx. p. 505 (November, 1942).
(25) G. Parr and A. Walter, Electronic Eng. xv. pp. 456, 519 (1943).
(26) A. Walter, Electronic Eng. xvi. p. 9 (1943).
(27) H. H. Scott, Proc. I. R. E. xxvi. p. 226 (1938).

XLVIII. *Derivation of the Lorentz Transformations.*

By Herbert E. Ives *.

[Received October 16, 1944.]

(1) *Introduction.*

The Lorentz transformations were obtained by Lorentz as a succession of *ad hoc* inventions, to reconcile Maxwell's theory with the results of experiments on moving bodies. By Einstein they were derived after a discussion of the nature of simultaneity, and the adoption of a *definition* of simultaneity which violates the intuitive and common-sense meaning of that term. It is proposed here to show that these transformations can be derived by imposing the laws of conservation of energy and of momentum on radiation processes as developed by Maxwell's methods.

To do this we shall study the interaction of radiation and matter, specifically the impact of a train of radiation on a perfectly reflecting particle. The energy and momentum of the radiation will be obtained from electromagnetic wave theory: the resultant momentum and energy of the particle will be obtained by requiring the conservation of momentum and energy. It will be found that there is an apparent discrepancy in the equations; the resolution of this discrepancy demands that the *mass* of the particle vary with velocity. Next, the same impact experiment will be considered with the system in uniform motion. Again a discrepancy will be encountered, and the resolution of this demands that the *lengths* and *time intervals* also vary with velocity. The exact expressions for these variations of mass, length and time interval are developed. From these variations of dimensions the Lorentz transformations can be derived. *The space and time concepts of Newton and Maxwell are retained without alteration.*

---

* Communicated by the Author.

(2) *Impact of a Wave Train and a Reflecting Particle Initially Stationary.*

We start with a parallel wave train of unit cross-section of density E, emitted in the time Δt; the total energy which strikes a particle with a reflecting surface normal to the wave direction is $E(c\Delta t)$. The result of such an impact will be the reflection of the wave train, with a change of energy content, and the recoil of the particle with a velocity dependent on its mass.

We attack the solution of the problem by finding the energy content of the reflected wave train, and the pressure which causes the recoil of the particle. Calling v the final velocity acquired, we designate the average velocity during the impact by $f(v)$, whose value will be between 0 and v. By a well-known derivation (1) (for the case of a uniformly moving reflector) we obtain, for the average pressure $\overline{P}$,

$$\overline{P}=2E\left[\frac{c-f(v)}{c+f(v)}\right], \quad . \quad . \quad . \quad . \quad . \quad . \quad . \quad . \quad (1)$$

and for the energy content of the reflected wave train (which differs in frequency and length from the incident)

$$\overline{E}=E(c\Delta t)\left[\frac{c-f(v)}{c+f(v)}\right]. \quad . \quad . \quad . \quad . \quad . \quad . \quad . \quad (2)$$

Using the definition of pressure in terms of mass and velocity

$$\text{Pressure}=\frac{\text{change of (mass} \times \text{velocity)}}{\text{time}}.$$

we can obtain a *mass equivalent*, for the incident and reflected wave trains, as follows, noting that the duration of the impact is $\dfrac{c\Delta t}{c-f(v)}$,

$$2E\left(\frac{c-f(v)}{c+f(v)}\right)\frac{c\Delta t}{c-f(v)}=mE(c\Delta t)c+mE(c\Delta t)\left(\frac{c-f(v)}{c+f(v)}\right)c, \quad . \quad (3)$$

from which m, the mass equivalent of a section of the wave train of unit normal area, is

$$m=\frac{1}{c^2}. \quad . \quad . \quad . \quad . \quad . \quad . \quad . \quad . \quad . \quad . \quad . \quad (4)$$

The mass equivalent of the incident section of the wave train is thus

$$m_i=E\frac{(c\Delta t)}{c^2} \quad . \quad . \quad . \quad . \quad . \quad . \quad . \quad . \quad . \quad . \quad (5)$$

and of the reflected wave train

$$m_r=E\frac{(c\Delta t)}{c^2}\left[\frac{c-f(v)}{c+f(v)}\right], \quad . \quad . \quad . \quad . \quad . \quad . \quad . \quad (6)$$

Since the velocities of both these wave trains are c, we write down the momenta before and after impact as

$$m_i=E\frac{(c\Delta t)}{c} \quad . \quad . \quad . \quad . \quad . \quad . \quad . \quad . \quad . \quad . \quad (7)$$

and $$m_r = \mathrm{E}\frac{(c\Delta t)}{c}\left[\frac{c-f(v)}{c+f(v)}\right]. \quad \ldots\ldots\ldots \quad (8)$$

Leaving until later the significance of the assumption, we now assume that the principle of the conservation of mass is applicable to all the masses and mass equivalents involved in the impact of wave train and particle.

For the conservation of mass we then have, equating masses and mass equivalents before and after the impact

$$\mathrm{E}\frac{(c\Delta t)}{c^2}+\mathrm{M}=\mathrm{E}\frac{(c\Delta t)}{c^2}\left[\frac{c-f(v)}{c+f(v)}\right]+\mathrm{M}, \quad \ldots\ldots \quad (9)$$

where M is the mass of the particle.

Since $$\mathrm{E}\frac{(c\Delta t)}{c^2} \quad \text{and} \quad \mathrm{E}\frac{(c\Delta t)}{c^2}\left[\frac{c-f(v)}{c+f(v)}\right]$$

are clearly not equal, expression (9) is obviously not an equality. We meet here with a *discrepancy* which, since the reflected mass equivalent is less than the incident, *demands that the mass of the particle must be greater after the impact.*

Calling the new mass of the particle after the impact Mg, we set up the equations for conservation of mass and momentum as follows :

$$\mathrm{E}\frac{(c\Delta t)}{c^2}+\mathrm{M}=\mathrm{E}\frac{(c\Delta t)}{c^2}\left[\frac{c-f(v)}{c+f(v)}\right]+\mathrm{M}g, \quad \ldots\ldots \quad (10)$$

$$\mathrm{E}\frac{(c\Delta t)}{c}=-\mathrm{E}\frac{(c\Delta t)}{c}\left[\frac{c-f(v)}{c+f(v)}\right]+\mathrm{M}gv. \quad \ldots\ldots \quad (11)$$

Solving for $f(v)$ we find

$$f(v)=\frac{(g-1)}{gv}c^2. \quad \ldots\ldots\ldots \quad (12)$$

Noting that for a very short wave train $f(v)$ will approximate to $\frac{v}{2}$ we have the approximate solution

$$g=\frac{1}{1-\frac{v^2}{2c^2}}. \quad \ldots\ldots\ldots \quad (13)$$

To obtain the exact value of g we can proceed as follows :—Suppose the impact of wave train and particle to take place after the particle is already in motion with velocity v due to a preceding portion of the wave train, then in place of (10) and (11) we have

$$\mathrm{E}\frac{(c\Delta t)}{c^2}+\mathrm{M}g_1=\mathrm{E}\frac{(c\Delta t)}{c^2}\left[\frac{c-(v+f'(v))}{c+(v+f'(v))}\right]+\mathrm{M}g_2, \quad \ldots\ldots \quad (14)$$

$$\mathrm{E}\frac{(c\Delta t)}{c}+\mathrm{M}g_1v=-\mathrm{E}\frac{(c\Delta t)}{c}\left[\frac{c-(v+f'(v))}{c+(v+f'(v))}\right]+\mathrm{M}g_2[v+\Delta v], \quad . \quad (15)$$

where $f'(v)$ approaches for a very short wave train the value $\frac{\Delta v}{2}$.

Solving as before for $v+f'(v) \simeq v+\frac{\Delta v}{2}$ we get

$$v+\frac{\Delta v}{2}=\frac{c^2(g_2-g_1)}{(v+\Delta v)g_2-vg_1}=\frac{c^2\Delta g}{(v+\Delta v)(g_1+\Delta g)-vg_1}, \quad . \; . \; (16)$$

or upon discarding the products of $\Delta v\Delta g$ as of the second order of small quantities

$$c^2\Delta g\left(1-\frac{v^2}{c^2}\right)=gv\Delta v,$$

proceeding to differentials and rearranging

$$\frac{dg}{g}=\frac{v\,dv}{c^2\left(1-\frac{v^2}{c^2}\right)},$$

which gives by integration

$$\log g=\log\frac{k}{\sqrt{1-\frac{v^2}{c^2}}},$$

$$g=\frac{k'}{\sqrt{1-\frac{v^2}{c^2}}}.$$

Since when $v=0$ $g=1$, the value of k' is unity,

$$g=\frac{1}{\sqrt{1-\frac{v^2}{c^2}}}. \quad . \; . \; . \; . \; . \; . \; . \; . \; . \; . \; (17)$$

We have, therefore, that the mass of a particle in motion with velocity v is

$$M=\frac{M_0}{\sqrt{1-\frac{v^2}{c^2}}}, \quad . \; . \; . \; . \; . \; . \; . \; . \; . \; (18)$$

where M_0 is the mass when the particle is stationary with respect to the wave transmitting medium.

We can now examine our assumption as to the conservation of mass and mass equivalent. Putting the momentum as

$$\frac{M_0v}{\sqrt{1-\frac{v^2}{c^2}}},$$

we have by a well-known process of differentiation and integration (2) that the kinetic energy of the particle is

$$M_0c^2\left[\frac{1}{\sqrt{1-\frac{v^2}{c^2}}}-1\right].$$

This kinetic energy is to be equated to the net flow of radiant energy toward the particle, or

$$Mc^2\left[\frac{1}{\sqrt{1-\frac{v^2}{c^2}}}-1\right]=E(c\Delta t)\left[1-\frac{c-f(v)}{c+f(v)}\right]. \quad . \quad . \quad . \quad (19)$$

This is precisely our equation (10), showing that the assumption made is in fact that of *the conservation of energy. The equation* (18) *for the variation of mass with velocity is thus a consequence of the conservation of energy and momentum in the impact process* (3).

(3) *Impact of a Wave Train and a Reflecting Particle; System in Uniform Motion.*

If the laws of conservation of energy and momentum are universally applicable they, of course, apply if the impact experiment described in (2) is carried out on a platform moving with respect to the wave transmitting medium. It becomes of immediate interest to investigate whether the variation of mass above deduced insures the adherence to these laws.

For this purpose we assume the source of radiation, and the reflecting particle before impact, to be moving with uniform velocity V in the direction of the wave normal. We know that the energy in the wave train will be altered by the compression of the waves, and by the shortening of the train, and perhaps other factors which, however, will be functions of V, the only factor varied. For the present we group all these changes together by expressing the incident energy in the form

$$[E(c\Delta t)]'.$$

We then set up as before the expressions for conservation of energy and momentum, using the symbol w for the velocity of the particle after the impact:

$$\frac{[E(c\Delta t)]'}{c^2}\left[1-\frac{c-f(w)}{c+f(w)}\right]=M_0\left[\frac{1}{\sqrt{1-\frac{w^2}{c^2}}}-\frac{1}{\sqrt{1-\frac{V^2}{c^2}}}\right]. \quad . \quad (20)$$

$$\frac{[E(c\Delta t)]'}{c}\left[1+\frac{c-f(w)}{c+f(w)}\right]=M_0\left[\frac{w}{\sqrt{1-\frac{w^2}{c^2}}}-\frac{V}{\sqrt{1-\frac{V^2}{c^2}}}\right]. \quad . \quad (21)$$

By addition we get

$$\frac{2[E(c\Delta t)]'}{c^2}=M_0\left[\sqrt{\frac{1+\frac{w}{c}}{1-\frac{w}{c}}}-\sqrt{\frac{1+\frac{V}{c}}{1-\frac{V}{c}}}\right]$$

$$=M_0\left[\sqrt{\frac{1+\frac{w}{c}}{1-\frac{w}{c}}}\sqrt{\frac{1-\frac{V}{c}}{1+\frac{V}{c}}}-1\right]\sqrt{\frac{1+\frac{V}{c}}{1-\frac{V}{c}}}. \quad . \quad . \quad (22)$$

By comparing this with the corresponding equation when $V=0$ we should get the value of $[E(c\Delta t)]'$ in terms of $E(c\Delta t)$, as follows:

$$\frac{[E(c\Delta t)]'}{E(c\Delta t)}=\left[\frac{\left(\sqrt{\frac{1+\frac{w}{c}}{1-\frac{w}{c}}}\sqrt{\frac{1-\frac{V}{c}}{1+\frac{V}{c}}}-1\right)}{\left(\sqrt{\frac{1+\frac{V}{c}}{1-\frac{V}{c}}}-1\right)}\right]\sqrt{\frac{1+\frac{V}{c}}{1-\frac{V}{c}}}. \quad . \quad (23)$$

Now since $[E(c\Delta t]'$ differs from $E(c\Delta t)]$ only by a function of V alone, it follows that the right-hand side of this equation must be a function of V alone, which becomes unity when $V=0$. Since the term outside the bracket is already of this form it follows that the expression within the bracket must be either unity or unity plus a function of V alone. Upon performing the division we get, for the expression in the brackets

$$1+\frac{\sqrt{\frac{1+\frac{v}{c}}{1-\frac{v}{c}}}-\sqrt{\frac{1+\frac{w}{c}}{1-\frac{w}{c}}}\sqrt{\frac{1-\frac{V}{c}}{1+\frac{V}{c}}}}{1-\sqrt{\frac{1-\frac{v}{c}}{1-\frac{v}{c}}}}.$$

The second term is not a function of V alone, and must accordingly drop out, *i. e.* must have the value zero (4). We are therefore left with the equation

$$\frac{[E(c\Delta t)]'}{E(c\Delta t)}=\sqrt{\frac{1+\frac{V}{c}}{1-\frac{V}{c}}}. \quad . \quad . \quad . \quad . \quad . \quad . \quad (24)$$

In order to proceed further it is now necessary to be more specific as to the factors composing $E(c\Delta t)$ and $[E(c\Delta t)]'$. This can be done by taking a definite radiator and mirror system, the elements entering into whose performance are capable of specification and analysis. As will be seen later there is no loss of generality in the final results occasioned by this procedure.

As radiator we take an electric charge vibrating harmonically at right angles to the direction of the wave train, with amplitude a and frequency V. Let the mirror, of area b, be at the distance r from the source. The mean value of the energy density is (5)

$$E=K\frac{a^2}{r^2}v^4, \quad . \quad . \quad . \quad . \quad . \quad . \quad . \quad (25)$$

where K is a constant involving the strength of the charge, π and c. Now the length of the train emitted in any time interval τ is proportional to τ or inversely as v, and the amount of energy striking the mirror is proportional to its area b, hence

$$E(c\Delta t)=K'\frac{a^2v^3b}{r^2}. \quad \ldots\ldots\ldots \quad (26)$$

When the system is in motion, the energy density at the same distance from the source is proportional to the frequency in space, squared, or to $\frac{1}{\left(1-\frac{V}{c}\right)^2}$ while the length of the train emitted in the given time interval is inversely as the frequency. Consequently we have

$$[E(c\Delta t)]'=K'\frac{a^2v^3b}{r^2\left(1-\frac{V}{c}\right)}. \quad \ldots\ldots\ldots \quad (27)$$

We then have

$$\sqrt{\frac{1+\frac{V}{c}}{1-\frac{V}{c}}}=\frac{[E(c\Delta t)]'}{E(c\Delta t)}=\frac{\dfrac{a^2v^3b}{r^2\left(1-\frac{V}{c}\right)}}{\dfrac{a^2v^3b}{r^2}}=\frac{1}{1-\frac{V}{c}}. \quad \ldots \quad (28)$$

Now $\sqrt{\frac{1+\frac{V}{c}}{1-\frac{V}{c}}}$ is *not* equal to $\frac{1}{1-\frac{V}{c}}$, which means that *the variation of mass with velocity is not adequate to insure that the impact process conforms to the conservation of energy and momentum.*

We have here a second discrepancy to resolve. Having discovered the alteration with velocity of mass, one of the fundamental factors of length, mass and time, we have clearly indicated the possibility of alterations of the other two, namely linear dimensions and time unit. We accordingly try the modification of these by functions of V. For the time unit, namely the period of the oscillator, we put

$$\tau'=\frac{\tau}{D_1} \quad \text{or} \quad v'=vD_1,$$

where D_1 is a function of v which becomes unity when $V=0$.

For the length dimension we have two cases to recognize. First when the length in question is moved in the direction of the wave motion. For this we put

$$r'=rD_2.$$

The second case is when the length is at right angles to the direction of motion. This figures in equation (27) in connection with the amplitude a, which we suppose measured (in a macroscopic experiment, which is not excluded, and which does not detract from the generality of the analysis) both for the stationary and moving cases, by a measuring rod at right angles to the direction of the wave train as the check on performing the "same" experiment. It also figures in connection with the reflector; which, of area b when stationary will assume a new area proportional to the square of the dimension factor (which must be the same for any orientation in an isotropic medium). Caling this dimension factor D_3, we re-write (28) as

$$\sqrt{\frac{1+\frac{V}{c}}{1-\frac{V}{c}}}=\frac{\dfrac{a^2 D_3^2 v^3 D_1^3 b D_3^2}{r^2 D_2^2\left(1-\frac{V}{c}\right)}}{\dfrac{a^2 v^3 b}{r^2}} \quad \ldots\ldots\ldots \quad (29)$$

obtaining
$$\frac{D_3^4 D_1^3}{D_2^2}=\sqrt{1-\frac{V^2}{c^2}} \quad \ldots\ldots\ldots\ldots \quad (30)$$

This equation contains three unknowns, D_1, D_2 and D_3, so that two other independent equations are required. Such equations could be obtained by considering the impact of a wave train on a reflecting particle where the angle of incidence of the radiation for the stationary condition is at right angles to the direction of motion, and at some other angle, whereby D_2 and D_3 are involved in different relations. However, the algebraic difficulties of solving the resultant equations are formidable. We can attain the answer much more simply by studying the behaviour of the clock used to measure the frequency v.

We note first that the function D_1—the variation of clock rate with motion—must, if conservation of energy and momentum are to be valid, be characteristic of *any* clock, because D_2 and D_3 express changes of lengths. These latter—functions of the velocity of the system—obviously *cannot be dependent on the clock used.* Once their values are found for *any* available clock the search is closed. This observation applies also to the type of radiator and particular arrangement of source and reflector selected above for study, and makes our results general, as was stated previously. We can accordingly select any clock whose performance with velocity of translation can be put in terms of D_2 and D_3.

We select for study the simple clock consisting of a rod with a light source at one end and a mirror at the other. The time taken for a light signal to go to the mirror and return is the period of the clock. We have at our disposal two orientations of the clock, one when the motion of the rod is parallel to its length, the other when the motion is transverse to its length. From these we derive relations between the period and the lengths in motion from which relations between D_1, D_2 and D_3 are obtained.

Taking the first case, if L is the length of the rod when stationary, and τ_1 the period, we have

$$\tau_1=\frac{2L}{c}.$$

Let the clock be put in motion with velocity V; the length will become $L'=LD_2$, the period $\tau_1'=\frac{\tau_1}{D_1}$. We have

$$\tau_1'=\frac{\tau_1}{D_1}=\frac{LD_2}{C-V}+\frac{LD_2}{C+V}=\frac{2LD_2}{C\left(\sqrt{1-\frac{V^2}{c^2}}\right)^2}=\frac{\tau_1 D_2}{\left(\sqrt{1-\frac{V^2}{c^2}}\right)^2},$$

from which $$D_1D_2=\left(\sqrt{1-\frac{V^2}{c^2}}\right)^2 . \quad . \quad . \quad . \quad . \quad . \quad . \quad . \quad . \qquad (31)$$

For the second case, which constitutes another possible clock, which, however, behaves in the same manner in motion from the considerations given above, we have

$$\tau_2'=\frac{\tau_2}{D_1}=\frac{2LD_3}{\sqrt{1-\frac{V^2}{c^2}}}=\frac{\tau_2 D_3}{\sqrt{1-\frac{V^2}{c^2}}},$$

from which $$D_1D_3=\sqrt{1-\frac{V^2}{c^2}} . \quad . \quad . \quad . \quad . \quad . \quad . \quad . \quad . \quad . \qquad (32)$$

These equations (31) and (32) constitute with (30) the three necessary to obtain D_1, D_2 and D_3. Their solution gives us

$$\left.\begin{aligned} D_1&=\sqrt{1-\frac{V^2}{c^2}},\\ D_2&=\sqrt{1-\frac{V^2}{c^2}},\\ D_3&=1. \end{aligned}\right\} \quad . \quad . \quad . \quad . \quad . \quad . \quad . \quad . \qquad (33)$$

These values of D_1, D_2 and D_3 tell us that the conservation of energy and momentum demand, in the interaction of radiation and matter in the manner prescribed by Maxwell's equations, and in the space and time of Newton, that:

In a system in uniform motion with velocity V, with respect to the wave transmitting medium,

(1) Frequencies are decreased in the ratio $\sqrt{1-\frac{V^2}{c^2}}:1$.

(2) Lengths in the direction of motion are reduced in the ratio $\sqrt{1-\frac{V^2}{c^2}}:1$.

(3) Lengths transverse to the direction of motion are unaltered.

From these behaviours of rods and clocks we can derive, by steps described elsewhere (6), the Lorentz transformations

$$x'=\frac{x-vt}{\sqrt{1-\frac{v^2}{c^2}}},$$

$$y'=y, \quad z'=z,$$

$$t'=\frac{t-\frac{vx}{c^2}}{\sqrt{1-\frac{v^2}{c^2}}},$$

which, together with the variation of mass with velocity

$$M=\frac{M_0}{\sqrt{1-\frac{v^2}{c^2}}},$$

constitute the relations which describe the *observed* behaviours of matter and radiation in interaction.

Discussion.

The derivation of the Lorentz transformations here given has for its central feature the confronting of the Maxwell electromagnetic picture of radiation with the laws of conservation of energy and momentum. The solution of apparent conflicts demands first the variation of mass with velocity, and then in turn the variation of linear dimensions and clock rate. While we have had as our goal the Lorentz transformations, it develops that the variations of mass, length, and frequency with motion are the primary physical phenomena, the Lorentz transformations are consequences. This reverses the common presentation, in which the dimensional changes are derived as consequences of the transformations, which latter are imported into the discussion from extraneous speculation.

The derivation of the Lorentz transformations here given is strictly according to the tenets of classical physics. The space and time used are absolute, the co-ordinate system is fixed in the wave transmitting medium. The momenta and energies whose conservation demand the consequences found are in terms of absolute velocities in the transmitting medium. No hybrid " space-time " is invoked (7). It is the dimensions of the material instruments for measuring space and time that change, not space and time that are distorted (8). No hypothetical " stationary " and " moving " observers are introduced, discouraged in advance by dicta of impotence, or required to accept the statement that non-simultaneous events can be made simultaneous by mere definition (9).

The indeterminancies and impotences by which the " Restricted Theory of Relativity " has been widely publicized—such as the impossibility of detecting uniform motion with respect to the ether, the constancy of the *measured* value of the velocity of light (10), the elusiveness of the establishment of exact simultaneity at different points, the indeterminancy of relative velocities except when they are equal—all follow (11) as consequences of our resolution of the apparent conflict between the laws of the conservation of energy and momentum on the one hand and the laws of light propagation on the other, our resolution being in favour of the conservation laws.

The justification for the choice would lie, had there been no experimental knowledge available, on crucial experiments made to decide whether masses, lengths and frequencies do vary with motion according to the functions D_1, D_2, D_3. Experiments which would have been indicated were the experiments of Kaufmann on masses in motion, of Michelson and Morley on lengths in motion, of Ives and Stillwell (12) on atomic clocks in motion. These experiments, having been already performed under the stimulus of other approaches to the problem, uniformly support the conclusion that these changes of dimensions are real, and according to the present analysis say that the laws of conservation of energy and momentum dominate in interactions between radiation and matter in the co-ordinate system of Newton and Maxwell.

An important feature of the development here given is that there is no suggestion of a *new* principle, co-ordinate with or superior to previously existing principles. The laws of conservation of energy and momentum; and the laws of transmission of radiant energy here shown adequate to meet the problems popularized by " Relativity," were formulated and considered generally valid fifty years ago. The fact that the Lorentz transformations with all their consequences are deducible from these classes the " Special Principle of Relativity " as a superfluous hypothesis.

Notes.

(1) The development which follows is given in more detail in a paper " Impact of a Wave-Packet and a Reflecting Particle," Journal Optical Society of America, vol. xxxiii. no. 2, pp. 163–66 (Mar. 1943).

(2) See F. K. Richtmyer ' Introduction to Modern Physics,' 2nd ed. p. 723 (McGraw-Hill, New York, 1934).

(3) As Lorentz has pointed out (' Theory of Electrons,' Stechert, N. Y., p. 40, 1923), change of mass with velocity occurs also in the hydrodynamical case of a body moving in a perfect fluid.

(4) The condition

$$\sqrt{\frac{1+\frac{v}{c}}{1-\frac{v}{c}}}-\sqrt{\frac{1+\frac{w}{c}}{1-\frac{w}{c}}}\sqrt{\frac{1-\frac{V}{c}}{1+\frac{V}{c}}}=0$$

gives the value of w, the velocity acquired by the particle. It is

$$w=\frac{V+v}{1+\frac{vV}{c^2}},$$

which will be recognized as the value commonly derived from the Lorentz transformations. It is imposed here by the conservation of energy and momentum in the interaction of radiation and matter.

(5) H. A. Lorentz, Collected Papers, vol. v. p. 169 (Hague, Nyhoff, 1937).

(6) " Experimental Proof of the Relativity of Time." Kennedy and Thorndyke, Phys. Rev. xlii. p. 400 (1932).

" Derivation of the so-called ' Chronotopic Interval.' " Ives, Journ. Optical Soc. America, 29, vii. p. 294 (1939).

(7) If " space-time " is admitted as a concept, our derivation of the variation of all three elementary dimensions from a common hypothesis should admit as equally valid " space-mass " and " mass-time."

(8) In a series of papers appearing in the 'Journal of the Optical Society of America,' 1937–44, and in 'Science' (Jan. 26th, p. 79, 1940), I have discussed a number of the problems of the optics of moving bodies, using throughout the viewpoint here expressed. The present paper, although the last in point of time, is logically the first of the series, since it establishes the premises of the others.

(9) "The notions of space and time that have always been familiar to us, and which I, for my part, consider as perfectly clear, and moreover, as distinct from one another. My notion of time is so definite that I clearly distinguish in my picture what is simultaneous and what is not." H. A. Lorentz in 'Problems of Modern Physics,' p. 221, Ginn & Co., New York, 1927.

(10) The "constancy" of the velocity of light has been much confused, and given a mystical character, in the literature of Relativity. The non-dependence of the velocity of wave-motion on the velocity of the source, which is a fundamental attribute of wave-motion, is *not* the constancy which actually figures in relativistic discussions. The latter constancy is of the velocity as *measured* by contracting rods and clocks. According to the development here given the latter is a consequence of the conservation of energy and momentum. It is on these conservation principles rather than on velocity that stress should be laid. Problems in the optics of moving bodies can indeed be expeditiously solved by the device of calling the velocity of light relative to moving matter the same as its velocity relative to the light transmitting medium. This paradox is a useful tool; why it can be used is clear when the behaviour of our measuring rods and clocks is investigated; but a paradox, while a provocative to investigation, is, if unresolved, an unsatisfactory foundation for a theoretical structure.

(11) But leaving the phenomena of aberration, the Michelson-Gale and Sagnac experiments, untouched as direct proofs of the motion of matter with respect to the light transmitting medium.

(12) Journal Optical Society of America, xxviii. pp. 215–26 (July 1938); xxxi. pp. 369–74 (May 1941).

Bell Telephone Laboratories, Inc.
New York, N.Y.
September 28th, 1944.

XLIX. *Computation of the Solution of Mathieu's Equation.*

By N. W. McLachlan, D.Sc.*

[Received November 8, 1944.]

1. *Introduction.*

The purpose of this paper is to describe a method of computing the solution of the equation

$$\frac{d^2y}{dz^2}+(a-2q\cos 2z)y=0, \quad . \quad . \quad . \quad . \quad . \quad . \quad . \quad . \quad (1)$$

a, q being real parameters. The procedure to be given applies to equations whose parametric points (a, q) lie in any region of the (a, q)

---

* Communicated by the Author.

plane. The tabular values for the (a, q) curves, pertaining to the Mathieu functions of integral order, bounding various regions, must be available. These well-known curves may be plotted from data given by Goldstein* and by Ince†, and are shown in the stability chart, fig. 1. For any point (a, q) in an unshaded area, the solution of (1) is stable, being either periodic or non-periodic, but bounded. If (a, q) lies in a

Fig. 1.

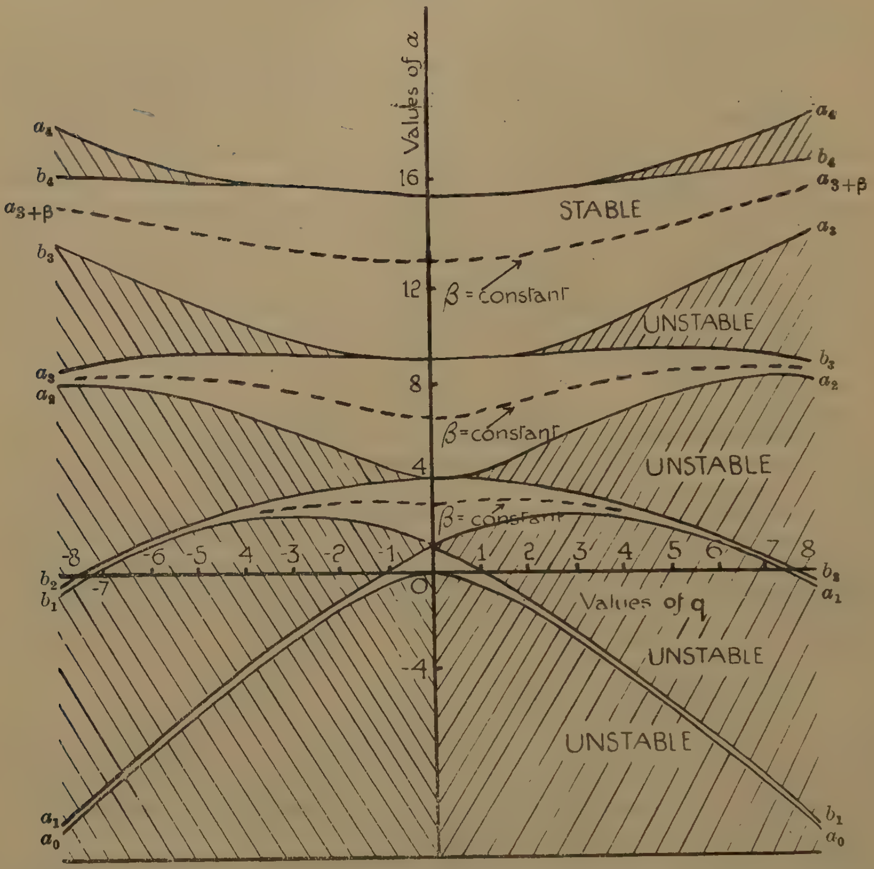

Stability chart for $y''+(a-2q\cos 2z)y=0$. The unbroken curves are the (a, q) characteristics for the Mathieu functions of integral order, having period π or 2π. The broken or *iso*-β curves are for the functions of fractional order. If $\beta=p/s$ is a proper fraction, $o<p/s<1$, the period is $2\pi s$. When (a, q) lies in an unshaded area, the solution is either periodic or non-periodic, but bounded. In the latter case β is irrational. Note that the odd order characteristics are asymmetrical about the a axis, although the chart is symmetrical.

---

* Trans. Camb. Phil. Soc. xxiii. p. 303 (1927).

† Proc. Roy. Soc. Ed. xlvi. p. 316 (1926); lii. p. 355 (1932).

shaded area, the complete solution is unstable and in general $\to \pm\infty$ as $z \to +\infty$. A single infinity of solutions exist, however, which $\to 0$ as $z \to +\infty$.

2. *Mathieu Functions of Fractional Order.*

We deal first with the region in fig. 1 bounded by the characteristic curves $[a_1, b_2]$ for the integral order functions, $q > 0$,

(characteristic number)

$$ce_1(z, q) = \sum_{r=0}^{\infty} A^{(1)}_{2r+1} \cos(2r+1)z, \qquad (a_1) \qquad . \; . \; . \quad (1)$$

$$se_2(z, q) = \sum_{r=0}^{\infty} B^{(2)}_{2r+2} \sin(2r+2)z. \qquad (b_2) \qquad . \; . \; . \quad (2)$$

Choose any point P not lying on either a_1, b_2. By Floquet's theory, the solution corresponding to (a, q) at P takes the form

$$e^{i\beta z} \sum_{r=-\infty}^{\infty} c_r e^{(2r+1)zi}, \quad . \; . \; . \; . \; . \; . \; . \; . \; . \quad (3)$$

β being a real number.

Moreover, it can be shown that if K is a normalizing constant (defined later), the coexistent * independent solutions of (1) § 1 are

$$ce_{1+\beta}(z, q) = \mathrm{K} \sum_{-\infty}^{\infty} c_r \cos(2r+1+\beta)z, \quad . \; . \; . \; . \; . \quad (4)$$

and

$$se_{1+\beta}(z, q) = \mathrm{K} \sum_{-\infty}^{\infty} c_r \sin(2r+1+\beta)z, \quad . \; . \; . \; . \; . \quad (5)$$

the c being identical in (4), (5). β is a function of (a, q), and for a stable region it is real and continuous.

To obtain the solutions of (1) § 1 in the forms (4), (5), the problem is to determine β and the c. The latter are real continuous functions of q, when (a, q) lies in a stable region.

Referring to fig. 2, in passing from N to M (in the direction of a increasing), but excluding these points, $0 < \beta < 1$. Accordingly we *define* (4), (5)—the two linearly independent solutions of (1) § 1 which correspond to any parametric point within the region—to be Mathieu functions of fractional order $(1+\beta)$. If $\beta = p/s$, a rational fraction, $0 < p/s < 1$, the functions have period $2s\pi$, but when β is irrational they are non-periodic yet bounded.

In general, when the parametric point (a, q) lies in a stable region, we define Mathieu functions of real fractional order $(2n+\beta)$, $(2n+1+\beta)$, $0 < \beta < 1$, $q > 0$, as follows :

$$\left.\begin{matrix} ce \\ se \end{matrix}\right\}_{2n+\beta}(z, q) = \sum_{r=-\infty}^{\infty} A^{(2n+\beta)}_{2r} \begin{matrix} \cos \\ \sin \end{matrix} (2r+\beta)z, \qquad (a_{2n+\beta}) \quad . \; . \quad (6)$$

$$\left.\begin{matrix} ce \\ se \end{matrix}\right\}_{2n+1+\beta}(z, q) = \sum_{r=-\infty}^{\infty} A^{(2n+1+\beta)}_{2r+1} \begin{matrix} \cos \\ \sin \end{matrix} (2r+1+\beta)z, \quad (a_{2n+1+\beta}), \quad . \quad (7)$$

---

* For the same value of a.

with $A_{2r}^{(2n+\beta)}=Kc_r$, $A_{2r+1}^{(2n+1+\beta)}=K'c_{r+1}$. In (6) the common a for the two independent solutions is written $a_{2n+\beta}$, whilst in (7) it is $a_{2n+1+\beta}$. The former is used when the parametric point lies between a_{2n}, b_{2n+1} and the latter for the region between a_{2n+1}, b_{2n+2} $(q>0)$. In this way we keep β in the range $0<\beta<1$, in any stable region.

Corresponding to any β in $0<\beta<1$, there is a continuous curve $\beta=$constant, common to both solutions, symmetrical about the a axis and lying between the bounding characteristics for the region. This feature is illustrated in fig. 1.

Fig. 2.

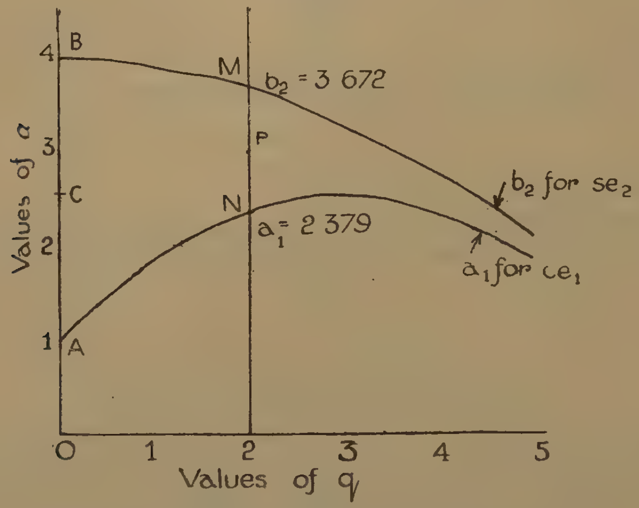

Diagram illustrating method of calculating "trial" value of β, when (1) § 3 cannot be used.

3. *Evaluation of β for a given (a, q).*

When (a, q) lies between the characteristics a_m, b_{m+1}, the formula

$$\beta\simeq\left[a-\frac{(a-1)q^2}{2[(a_1-1)^2-q^2]}-\frac{(5a+7)q^4}{32(a-1)^3(a-4)}\right]^{\frac{1}{2}}-m \quad . \quad . \quad (1)^*$$

may be used, provided the ratio of each term in [ ] to its predecessor is small enough †, and neither of the two denominators vanishes. From (1) we find, *e. g.*, that

$$\beta=0{\cdot}4873 \quad \text{for} \quad a=6{\cdot}25, \quad q=0{\cdot}8\,;$$

$$\beta=0{\cdot}4098 \quad \text{for} \quad a=2, \quad q=0{\cdot}16.$$

---

* This formula was deduced from

$$a=\nu^2+\frac{q^2}{2(\nu^2-1)}+\frac{(5\nu^2+7)q^4}{32(\nu^2-1)^3(\nu^2-4)}+\ldots,$$

where $\nu=m+\beta$, $0<\beta<1$, m integral.

† Broadly this entails $q/a\ll 1$.

When (1) does not give sufficiently accurate results or a denominator vanishes, we have a choice of methods. The first is a modification of that used by Ince*, and involves continued fractions. The second (new) is given in § 7 and is simpler than the first†. To exemplify, we shall calculate β for the equation solved by Ince‡, using the modified procedure. Ince's equation was

$$y''+(3-4\cos 2z)y=0. \quad . \quad . \quad . \quad . \quad . \quad . \quad . \quad (2)§$$

The parametric point (3, 2) is shown at P in fig. 2. Using tabular values ‖ we have

$$\frac{\mathrm{PN}}{\mathrm{MN}}=\frac{3-2{\cdot}379}{3{\cdot}672-2{\cdot}379}=0{\cdot}48 \text{ approx.} \quad . \quad . \quad . \quad . \quad . \quad (3)$$

Dividing BA in this ratio gives AC=1·44, so OC=2·44, which is the value when $q=0$. Then β at C is $\sqrt{2{\cdot}44}-1=0{\cdot}56$, this being a rough approximation to its value at P. We regard 0·56 as a *trial* value of β, and it is this method of predetermination which constitutes the modification and effects time saving. Greater accuracy is obtained by taking the square root of each number in (3). The ratio is then 0·51, and the trial $\beta=0{\cdot}59$ (see formula (3) in Appendix).

We now follow Ince and use the continued fractions

$$\frac{c_1}{c_0}=v_0=\frac{-q/(\beta+3)^2}{1-a/(\beta+3)^2-}\;\frac{q^2/(\beta+3)^2(\beta+5)^2}{1-a/(\beta+5)^2}\;-\;\frac{q^2/(\beta+5)^2(\beta+7)^2}{1-a/(\beta+7)^2}\;-\dots \quad (4)$$

$$v_0'=\frac{a-(\beta+1)^2}{q}+\frac{q/(\beta-1)^2}{1-a/(\beta-1)^2-}\;\frac{q^2/(\beta-1)^2(\beta-3)^2}{1-a/(\beta-3)^2}\;-\dots, \quad . \quad . \quad (5)$$

when (a, q) lies between a_{2n+1}, b_{2n+2}. If (a, q) is between a_{2n}, b_{2n+1} write $(\beta-1)$ for β in (4), (5) ¶. The appropriate value of β makes $v_0=v_0'$. Taking $\beta=0{\cdot}56$ in (4), (5) the working is as shown below:

$$\left.\begin{aligned}\frac{q^2/(\beta+5)^2(\beta+7)^2}{1-a/(\beta+7)^2}&=0{\cdot}0024,\\ \frac{q^2/(\beta+3)^2(\beta+5)^2}{1-a/(\beta+5)^2-0{\cdot}0024}&=0{\cdot}0114,\\ \frac{-q/(\beta+3)^2}{1-a/(\beta+3)^2-0{\cdot}0114}&=-0{\cdot}209=v_0\end{aligned}\right| \quad . \quad . \quad . \quad . \quad . \quad . \quad (6)$$

---

* Phil. Mag. vi. p. 547 (1928).

† From the viewpoint of the professional computer making a series of calculations, this may not be so.

‡ *Loc. cit. supra.*

§ The first denominator in (1) vanishes here, so it cannot be used to calculate β.

‖ Ince, *loc. cit. supra.*

¶ By so doing we preserve our convention that $0<\beta<1$, whereas Ince did not do so.

$$\left.\begin{aligned}
\frac{q^2/(\beta-3)^2(\beta-5)^2}{1-a/(\beta-5)^2}&=0\cdot0402,\\
\frac{q^2/(\beta-1)^2(\beta-3)^2}{1-a/(\beta-3)^2-0\cdot0402}&=7\cdot64,\\
\frac{q/(\beta-1)^2}{1-a/(\beta-1)^2-7\cdot64}&=-0\cdot466,\\
\frac{a-(\beta+1)^2}{q}&=0\cdot285
\end{aligned}\right\}, \quad . \quad . \quad . \quad . \quad (7)$$

so $v_0'=0\cdot285-0\cdot466=-0\cdot181$,

Examination of the fractions in (6), (7) shows that the inequality of v_0, v_0' arises from β being too small. Accordingly we now try $\beta=0\cdot58$ and find that $v_0=-0\cdot207$, $v_0'=-0\cdot208$. For the present we shall accept this result. The second calculation of v_0, v_0' will not usually show such good agreement !

4. *Calculation of c_r in* (7) § 2.

The linearly independent formal solutions of $y''+(3-4\cos 2z)y=0$ are

$$y_1=\sum_{r=-\infty}^{\infty} c_r \cos(1\cdot58+2r)z, \quad . \quad . \quad . \quad . \quad . \quad . \quad . \quad (1)$$

and

$$y_2=\sum_{r=-\infty}^{\infty} c_r \sin(1\cdot58+2r)z. \quad . \quad . \quad . \quad . \quad . \quad . \quad . \quad (2)$$

If either member of (7) § 2 be substituted in (1) § 1, and the coefficient of $\begin{smallmatrix}\cos\\ \sin\end{smallmatrix}(2r+1+\beta)z$ equated to zero, $r=-\infty$ to $+\infty$, we obtain the recurrence formula

$$[a-(2r+1+\beta)^2]c_r-q(c_{r+1}+c_{r-1})=0. \quad . \quad . \quad . \quad . \quad . \quad (3)$$

If (6) § 2 were used, the term in β would be $(2r+\beta)^2$. Now $\beta\simeq0\cdot58$, $a=3$, $q=2$, so (3) gives

$$[3-(2r+1\cdot58)^2]c_r-2(c_{r+1}+c_{r-1})=0. \quad . \quad . \quad . \quad . \quad . \quad (4)$$

When r is large enough, it may be shown that c_{r+1} is negligible in comparison with c_r, c_{r-1}, *i. e.* when c_{r+1}/c_r is small enough. This is the basis upon which calculation of the c rests. The procedure differs from the more elaborate one used by Ince.

We commence by neglecting c_6 and all the c of higher order. The accuracy resulting can be gauged when the c have been computed. Thus we take $r=5$ in (4), and get (using a 10-inch slide rule)

$$\left.\begin{aligned}
c_4&=\left(\frac{3-11\cdot58^2}{2}\right)c_5=-65\cdot5c_5,\\
c_3&=\left(\frac{3-9\cdot58^2}{2}\right)c_4-c_5=2\cdot899\times10^3c_5,\\
c_2&=\left(\frac{3-7\cdot58^2}{2}\right)c_3-c_4=-7\cdot893\times10^4c_5,\\
c_1&=\left(\frac{3-5\cdot58^2}{2}\right)c_2-c_3=1\cdot102\times10^6c_5,\\
c_0&=\left(\frac{3-3\cdot58^2}{2}\right)c_1-c_2=-5\cdot331\times10^6c_5.
\end{aligned}\right\} \quad . \quad . \quad . \quad . \quad . \quad (5)$$

These results lead to	Ince's values by machine.
$c_1=-2{\cdot}068\times10^{-1}c_0,$	$-2{\cdot}0683\times10^{-1}c_0,$
$c_2=\ \ 1{\cdot}478\times10^{-2}c_0,$	$1{\cdot}4744\times10^{-2}c_0,$
$c_3=-5{\cdot}430\times10^{-4}c_0,$	$-5{\cdot}420\ \ \times10^{-4}c_0,$
$c_4=\ \ 1{\cdot}228\times10^{-5}c_0,$	$1{\cdot}20\ \ \ \times10^{-5}c_0,$
$c_5=-1{\cdot}875\times10^{-7}c_0.$	not obtained.

. . (6)

To calculate c_{-r}, neglect c_{-7} and higher negative orders, then with $r=-6$,

$$\left.\begin{aligned}
c_{-5}&=\left(\frac{3-10{\cdot}42^2}{2}\right)c_{-6}=-52{\cdot}7c_{-6}.\\
\text{Also}\qquad c_{-4}&=\left(\frac{3-8{\cdot}42^2}{2}\right)c_{-5}-c_{-6}=1{\cdot}78\times10^3c_{-6},\\
c_{-3}&=\left(\frac{3-6{\cdot}42^2}{2}\right)c_{-4}-c_{-5}=-3{\cdot}405\times10^4c_{-6},\\
c_{-2}&=\left(\frac{3-4{\cdot}42^2}{2}\right)c_{-3}-c_{-4}=2{\cdot}807\times10^5c_{-6},\\
c_{-1}&=\left(\frac{3-2{\cdot}42^2}{2}\right)c_{\ 2}-c_{-3}=-3{\cdot}674\times10^5c_{-6},\\
c_0&=\left(\frac{3-0{\cdot}42^2}{2}\right)c_{-1}-c_{-2}=-8{\cdot}000\times10^5c_{-6}.
\end{aligned}\right\}\quad . \ . \ . \ (7)$$

These results lead to	Ince's values by machine.
$c_{-1}=\ \ 4{\cdot}592\times10^{-1}c_0,$	$4{\cdot}59527\times10^{-1}c_0,$
$c_{-2}=-3{\cdot}509\times10^{-1}c_0,$	$-3{\cdot}51349\times10^{-1}c_0,$
$c_{-3}=\ \ 4{\cdot}256\times10^{-2}c_0,$	$4{\cdot}27520\times10^{-2}c_0,$
$c_{-4}=-2{\cdot}225\times10^{-3}c_0,$	$-2{\cdot}2240\ \ \times10^{-3}c_0,$
$c_{-5}=\ \ 6{\cdot}590\times10^{-5}c_0,$	$6{\cdot}60\ \ \ \times10^{-5}c_0,$
$c_{-6}=-1{\cdot}250\times10^{-6}c_0.$	not obtained.

. . (8)

Checks on Computation.—The first is that we should have $c_1/c_0=v_0=v_0'$. The results obtained are $c_1/c_0=-0{\cdot}2068$, $v_0=-0{\cdot}2070$, $v_0'=-0{\cdot}2080$. The second check is given by putting $r=0$ in (4), which yields

$$c_{-1}=\left(\frac{3-1{\cdot}58^2}{2}\right)c_0-c_1$$

or

$$c_{-1}/c_0=0{\cdot}4588, \quad . \ . \ . \ . \ . \ . \ . \ . \ . \ . \ . \ (9)$$

which differs from the value in (8) by $0{\cdot}004$. The discrepancies in c_1/c_0, c_{-1}/c_0 arise from β being taken as $0{\cdot}58$. By the Appendix, a better value is $0{\cdot}579$, whilst to eight significant figures Ince obtained

$$\beta=0{\cdot}579{,}432{,}24.$$

Accuracy.—All calculations were done with a 10-inch slide rule, and are sufficiently accurate to *demonstrate* the method of procedure. The accuracy can, of course, be enhanced to any desired degree by using additional continued fractions in (4), (5), and repeated interpolation to get a better value of β, as shown in the Appendix. Ince's results are given in (6), (8), and, for technical purposes, the additional accuracy he got may be waived. It is evident, from the smallness of c_5, c_{-6}, that neglect of the c of higher orders is justifiable. The above procedure enables the solution to be computed in a fraction of the time needed when that of Ince is used.

5. *Solution of the Equation.*

If we take $c_0=1$ in (6), (8) § 4 the two linearly independent solutions of $y''+(3-4\cos 2z)y=0$ are, to an approximation adequate for technical work,

$$y_1(z)=\sum_{r=-6}^{5} c_r \cos(1{\cdot}58+2r)z, \quad \ldots \ldots \quad (1)$$

and

$$y_2(z)=\sum_{r=-6}^{5} c_r \sin(1{\cdot}58+2r)z. \quad \ldots \ldots \quad (2)$$

The complete solution with two arbitrary constants A, B, these being determinable from the conditions at $z=0$, is

$$y=\mathrm{A}y_1+\mathrm{B}y_2. \quad \ldots \ldots \quad (3)$$

The solution of $y''+(3+4\cos 2z)y=0$ can be obtained from (1), (2) on writing $(\frac{1}{2}\pi-z)$ for z.

Check on Solution.

The differential equation may be written in the form

$$y=y''/(4\cos 2z-3). \quad \ldots \ldots \quad (4)$$

Taking $z=0$ (or any other convenient value), we get $(z=0)$

$$y(0)=y''(0). \quad \ldots \ldots \quad (5)$$

Consequently if (1) is differentiated twice, the sum of the coefficients in the respective series for $y(0)$ and $y''(0)$ should be equal. More generally we have the relationship

$$\sum_{r=-\infty}^{\infty} c_r=-\sum_{r=-\infty}^{\infty} (1{\cdot}58+2r)^2 c_r. \quad \ldots \ldots \quad (6)$$

The term by term differentiation is permissible, since the series for $ce_{n+\beta}(z, q)$ is absolutely and *uniformly* convergent.

6. *Normalization.*

If it is desired to obtain the Mathieu functions $ce_{1{\cdot}58}(z, q)$, $se_{1{\cdot}58}(z, q)$ in (4), (5) § 2, we must define and then compute K. To fall in line with the convention adopted by Goldstein and Ince, we take

$$\mathrm{K}^2 \sum_{r=-\infty}^{\infty} c_r^2=1, \text{ i. e. } \mathrm{K}=1/\sqrt{\Sigma c_r^2}. \quad \ldots \ldots \quad (1)$$

Then from (1), and (1), (2) § 5, we obtain

$$ce_{1\cdot 58}(z,\,q)=\mathrm{K}y_1(z), \quad \ldots\ldots\ldots \quad (2)$$

and

$$se_{1\cdot 58}(z,\,q)=\mathrm{K}y_2(z). \quad \ldots\ldots\ldots \quad (3)$$

7. *Alternative Procedure for Calculating* β.

We commence, as in § 3, by computing a trial value of β, *e. g.* $\beta=0\cdot 56$. Using (4) § 4, with $\beta=0\cdot 56$, we proceed as shown at (5) § 4 *et seq.*, thereby departing from Ince's use of C.F. Put $r=3$, neglect c_4, and we get

$$\left.\begin{aligned} c_2&=\left(\frac{3-7\cdot 56^2}{2}\right)c_3 &&= -27c_3,\\ c_1&=\left(\frac{3-5\cdot 56^2}{2}\right)c_2-c_3 &&= 375c_3,\\ c_0&=\left(\frac{3-3\cdot 56^2}{2}\right)c_1-c_2 &&=-1789c_3 \end{aligned}\right\} \quad \ldots\ldots \quad (1)$$

Put $r=-4$, neglect c_{-5}, and we get

$$\left.\begin{aligned} c_{-3}&=\left(\frac{3-6\cdot 44^2}{2}\right)c_{-4} &&=-19\cdot 3c_{-4},\\ c_{-2}&=\left(\frac{3-4\cdot 44^2}{2}\right)c_{-3}-c_{-4} &&= 160c_{-4},\\ c_{-1}&=\left(\frac{3-2\cdot 44^2}{2}\right)c_{-2}-c_{-3} &&=-218c_{-4},\\ c_0&=\left(\frac{3-0\cdot 44^2}{2}\right)c_{-1}-c_{-2} &&=-466c_{-4} \end{aligned}\right\} \quad \ldots\ldots \quad (2)$$

Also

$$\begin{aligned}[3-(1+\beta)^2]c_0&=2(c_1+c_{-1})=2(375c_3-218c_{-4}),\\ &=2\left[\frac{-375}{1789}+\frac{218}{466}\right]c_0=0\cdot 517c_0. \quad \ldots \quad (3)\end{aligned}$$

Now $3-1\cdot 56^2=0\cdot 5664$, so by (3) the trial β is too small. Then a better value of β will be found by solving (3). Since $c_0\neq 0$, we obtain

$$3-(1+\beta)^2=0\cdot 517,$$

so taking the positive root

$$\beta=0\cdot 576\,*. \quad \ldots\ldots\ldots\ldots \quad (4)$$

The process is now repeated using this improved β, and a still better value obtained; and so on until the desired accuracy is attained. In this respect it will—on repeating the calculation—be necessary to increase r to include an adequate number of c. When β has been found, the c may be recalculated in terms of c_0, and the solution is complete—apart from normalization.

---

* When the difference between this and the trial β is not a small fraction of the former, the procedure outlined below must be adopted. For instance, if the trial β for $y''+(6-4\cos 2z)y=0$ were $0\cdot 24$, the β corresponding to (4) would be $1\cdot 66$. Hence the trial β is proportionately much too small, and the next step is to repeat the procedure above (4) using $\beta=0\cdot 32$, say. This also is too small, so the calculation is repeated with $\beta=0\cdot 35$, which is just too large. Interpolation then leads to a better value. The actual trial β is given in Table I., Appendix.

As an alternative to a repetition of the above process, using $\beta=0{\cdot}576$, we may take

$$[3-(1+\beta)^2]c_0+2(c_1+c_{-1})=\mathrm{L}c_0, \quad . \quad . \quad . \quad . \quad . \quad . \quad . \qquad (5)$$

and calculate L with $\beta=0{\cdot}56$. Let $\mathrm{L}_0>0$, being $\simeq 0{\cdot}0494$ in the present instance. Now use $\beta=0{\cdot}58$ and repeat the procedure at (1)–(3), thereby obtaining $\mathrm{L}_0'<0\simeq-0{\cdot}0012$. Then for L=0, interpolation as in the appendix fig. 3, gives

$$x=\frac{(0{\cdot}58-0{\cdot}56)\times 0{\cdot}0012}{0{\cdot}0494+0{\cdot}0012}$$

$$\simeq 0{\cdot}00047,$$

so

$$\beta \simeq 0{\cdot}58-0{\cdot}00047$$

$$=0{\cdot}57953, \quad . \quad . \quad . \quad . \quad . \quad . \quad . \quad . \quad . \quad . \quad . \quad . \qquad (6)$$

whereas after several interpolations Ince got 0·57943. . . .

The methods used above are applicable even if the point (a, q) lies in an unstable region of fig. 1, where μ, the characteristic exponent of the Mathieu equation, is either real or complex. For $q>0$, and (a, q) between the characteristics for se_{2n}, ce_{2n} (fig. 1), if the solution takes the form

$$e^{\mu z}\sum_{-\infty}^{\infty} c_r e^{2rzi}, \quad . \quad . \quad . \quad . \quad . \quad . \quad . \quad . \quad . \qquad (7)$$

μ is real. If $2n$ be replaced by $2n+1$, μ is real if $2r+1$ be written for $2r$. This procedure is expedient in solving equations. It corresponds to (6), (7) § 2.

Also, if β or μ be assigned for a given q, the value of a may be calculated in a similar way. This should facilitate evaluation of the characteristic numbers for functions of any order.

8. *Unstable solutions.*

μ (real) is calculated as suggested in § 7. The recurrence formula found by substituting (7) § 7 into (1) § 1 is

$$[a+(\mu+2ri)^2]c_r-q(c_{r+1}+c_{r-1}), \quad . \quad . \quad . \quad . \quad . \quad . \qquad (1)$$

which applies when (a, q) lies between b_{2n}, a_{2n} in fig. 1. If (a, q) lies between b_{2n+1} and a_{2n+1}, write $(2r+1)$ for $2r$ in (1). The c (complex by virtue of μ being real) are now calculated by the method of § 4. Iso-μ curves lying within the unstable region bounded by b_m, a_m in fig. 1 may be plotted. For $q>0$, any line $q=a$ constant intersects each iso-μ curve twice. When $q\to\infty$, the iso-μ curves are mutually asymptotic to the b_m, a_m curves bounding the region.

APPENDIX.

Linear Interpolation to find β.

v_0 and v_0' in § 3 are computed for two values of β to obtain a crossing point, as shown in fig. 3 *. The value of $\Delta\beta$ must be such that the v_0, v_0' β-curves are sensibly linear in the interval. The data already obtained are

β.	0·56.	0·58.
v_0	$-0{\cdot}209$	$-0{\cdot}207$
v_0'	$-0{\cdot}181$	$-0{\cdot}208$

as shown in fig. 3.

Fig. 3.

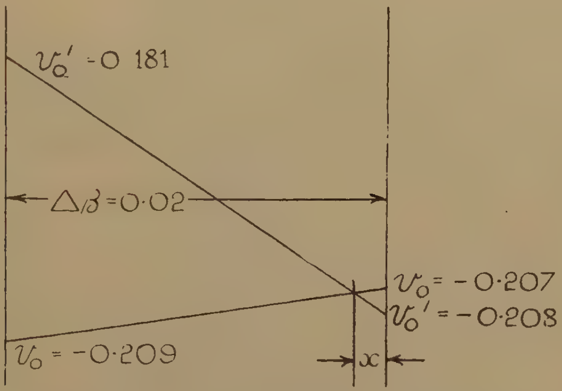

Diagram illustrating linear interpolation.

With adequate approximation for a first interpolation, we have

$$\frac{x}{(v_0-v_0')_{\beta=0\cdot58}}=\frac{0\cdot02}{(v_0'-v_0)_{\beta=0\cdot56}}, \quad . \quad . \quad . \quad . \quad . \quad . \quad (1)$$

so

$$\frac{x}{0\cdot001}=\frac{0\cdot02}{0\cdot028},$$

giving

$$x=0\cdot0007. \quad . \quad . \quad . \quad . \quad . \quad . \quad . \quad . \quad . \quad . \quad (2)$$

Hence $0{\cdot}58-0{\cdot}0007=0{\cdot}5793$ is a more accurate value of β than 0·58. Recalculation of v_0, v_0', using additional components in the C.F. and $\beta=0{\cdot}5793$ would lead to a second interpolation and a better value of β. The procedure is given in Ince's paper.

Trial values of β.

We now compare trial values of β found by (1) § 3, and also by the procedure following that formula. Such *empirical* procedure may be crystallized in the relationship

$$\beta=m\left\{\left[1+\left(\frac{2m+1}{m^2}\right)\phi\right]^{\frac{1}{2}}-1\right\}, \quad . \quad . \quad . \quad . \quad . \quad . \quad (3)$$

---

* Ince, *loc. cit.*

where $\phi=(a^{\frac{1}{2}}-a_m^{\frac{1}{2}})/(b_{m+1}^{\frac{1}{2}}-a_m^{\frac{1}{2}})<1$, the values of a_m, b_{m+1} corresponding to q in the differential equation. The point (a, q) lies between a_m, b_{m+1}. If $\left(\frac{2m+1}{m^2}\right)\phi$ is small enough, $\beta\simeq\left(1+\frac{1}{2m}\right)\phi$. Trial values are given in the Table.

TABLE.

a.	q.	Formula used:		More accurate value of β.
		(1) §3.	(3) above.	
8(m=2) ...	4	0·57	0·55	0·59
6(m=2) ...	2	0·33	0·27	0·34
36(m=5) ...	16	0·56	0·51	0·57

In the cases chosen, although q/a is not $\ll 1$, the formula (1) §3 gives better results than (3) above. If in the third row of the table q were 3, $q/a=1/12$, and the accuracy of (1) §3 would be much improved. This formula should be used wherever *possible*.

L. *Second Note on Condensation in the Form of Clouds and Dew.*

By J. W. ARCHBOLD, M.A., University College, London *.

[Received February 5, 1945.]

THIS note is written as a continuation of one with a similar title which appeared in Phil. Mag., ser. 7, vol. xxxiv. p. 632.

Corrections to the first paper are given in an appendix below. Being overseas at the time, I had not the opportunity to inspect the proof-sheets; thus two minor but regrettable slips and several misprints appeared in the published paper. Fortunately these do not affect the conclusions reached. It is assumed in what follows that the necessary alterations have been made.

10. In order to simplify the theory, the assumption was made, in section 2, that the interaction effect of the remaining drops on the potential energy of any one drop is negligible.

Such an effect appears, however, to be significant. It may be separated into two parts, one a local effect due to the influence of the near neighbours of the particular drop, and the other a smoothed effect due to the influence of the cloud as a whole. We are concerned here with this second effect.

---

* Communicated by N. K. Johnson.

It seems clear that a significant interaction effect on the part of the whole cloud must be electrical in character, and that it must appear in relation to the influence of the cloud on the strength of the electrical field normally present in the atmosphere.

11. We assume, still with a view to simplicity, that each drop carries a charge of nq e.s.u., n being the number of molecules in the drop. The atmospheric electrical field is assumed to act vertically and is reckoned as positive when it is directed downwards, as it is in fine weather. Between the levels z_0 and z_1, let the field be supposed uniform and of strength v e.s.u./cm.

The contribution of the smoothed interaction effect to the potential energy η_n is then $+nqvz$; and in addition there is a term $+(nq)^2/(2r)$ due to the acquisition of the charge by the drop. Accordingly formula (16) becomes

$$\mathrm{N}_n=\alpha\nu^n n^{3/2}e^{-\beta n^{2/3}-\gamma n^{5/3}}\psi_n, \quad . \quad . \quad . \quad . \quad . \quad . \quad (38)$$

where

$$\alpha=\frac{\mathrm{V}(2\pi mk\mathrm{T})^{3/2}}{h^3},$$

$$\beta=\frac{\sigma}{k\mathrm{T}}\left(\frac{36\pi m^2}{\rho^2}\right)^{1/3},$$

$$\gamma=\frac{q^2}{2k\mathrm{T}}\left(\frac{4\pi\rho}{3m}\right)^{1/3},$$

$$\nu=\frac{\mathrm{N}_1 h^3 e^{\frac{m(\lambda\rho-\mathrm{P})}{\rho k\mathrm{T}}}}{\mathrm{V}(2\pi mk\mathrm{T})^{3/2}};$$

$$\psi_n=\left(\frac{\vartheta}{1-e^{-\vartheta}}\right)^n\cdot\frac{1-e^{-n\vartheta'}}{n\vartheta'},$$

and

$$\vartheta=(z_1-z_0)(mg(1-\rho_0/\rho)+qv)/(k\mathrm{T}),$$

$$\vartheta'=(z_1-z_0)(mg(1-2\rho_0/\rho)+qv)/(k\mathrm{T}).$$

12. The numbers ϑ, ϑ' are practically equal since ρ_0 is very much smaller than ρ. Taking $qv=0$, these numbers are both about $3{\cdot}8\times10^{-3}$ for the layer of 50 metres considered in section 3. In practice the term qv, or rather the actual combination of charge and electrical field, is generally smaller than the term $mg(1-\rho_0/\rho)$, but the two may be comparable in magnitude and of opposite signs in the severe electrical conditions which accompany thunderstorms. Thus, still as in section 3, $\psi_n\approx1$ for small values of n and, for large values of n ($>10^4$ or 10^5 effectively when $qv>0$ but larger than this when $qv<0$), $\psi_n\approx1/(n\vartheta')$.

The value of γ for the same layer is approximately $6\times10^{-25+2u}$, assuming a drop charge of $\pm10^u$ e.s.u./c.c. It is uncommon for u to exceed 2, though this may happen in thunderstorms. Thus, in the range of observed drop sizes, for which $n<10^{21}$ approximately, the term $\gamma n^{5/3}$ is completely dominated by the term $\beta n^{2/3}$. Actually $\gamma n^{5/3}$ begins to dominate $\beta n^{2/3}$ after n exceeds about 10^{25} in the case $u=0$ and about 10^{21} in the case $u=2$.

Further, $\nu^n e^{-\gamma n^{5/3}}$ begins to tend to zero when $n > (\gamma^{-1} \log \nu)^{3/2}$; taking $\nu = 1{\cdot}01$, this occurs when n exceeds about $6 \times 10^{23-2u}$.

Thus it appears that the factor $e^{-\gamma n^{5/3}}$ in the expression for N_n is essentially related to the process which limits the sizes of drops to those actually observed.

It is easily verified that γ is too small to affect the value n_c of n at which N_n is a minimum.

The criterion for saturation remains $\nu = 1$ as before and is not affected by gravitational or electrical influences. (It is in this sense that the conclusion (i) of section 1 was intended.)

Fig. 11.

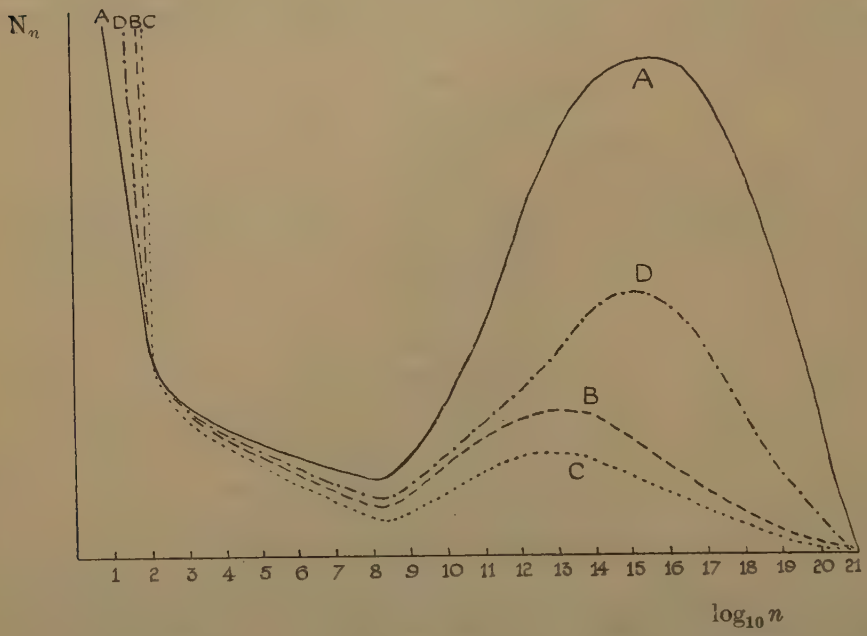

13. Remembering that ν is proportional to N_1 and observing that variations in the ratio $N_n : (N_1)^n$ give some indication of variations in the ratio $N_n : N_1$, we now see that the influences of gravity and of the smoothed interaction both affect the ratio of the number of large drops to the number of free molecules but have little influence on the ratio of the number of small drops to the number of free molecules.

These influences may perhaps most clearly be shown in a qualitative manner by the sketches of distribution curves in fig. 11. Curve A shows a meta-stable distribution in the absence of gravity (except in so far as this affects the pressure P) and of smoothed interaction. Curve B shows the modification when gravity alone is introduced ; the ordinates of curve B are smaller fractions of the ordinates of curve A when n is large than when n is small ; and the crest of curve B is to the left of the crest of curve A. Curves C and D show the further effect of introducing the smoothed interaction, C corresponding to qv positive and D to qv negative. Curve C diverges more from curve B for lower values of n than does curve D, but the ultimate divergence is greater in the case of curve D, $|qv|$ being the same for C and D. The crest of C is slightly to the left of the crest of B; the crest of D is further to the right of the crest of B and is to the left of the crest of A. Other factors being equal, qv being negative produces more and larger drops than does qv being positive.

14. The variation of the distribution curves with temperature should be noticed. Using formula (38), we find that $N_n/(N_1)^n$, regarded as a function of T, is proportional to

$$T^{-\frac{3n}{2}+\frac{5}{2}} e^{\frac{mn(\lambda\rho-P)}{\rho kT}-\beta n^{2/3}-\gamma n^{5/3}},$$

β and γ both being proportional to $1/T$; for present purposes σ, λ, *tecetera* may be treated as constants. Since $\lambda\rho$ dominates P and since also $mn(\lambda\rho-P)/(\rho kT)$ dominates $\beta n^{2/3}+\gamma n^{5/3}$ for values of n in the observed range which are large compared with $n^{2/3}$, which in general covers the range $n_c<n<10^{21}$, it follows that $N_n/(N_1)^n$ is a decreasing function of T for large n.

Thus, for a given total number of water molecules in the volume V, the crest of the distribution curve sinks as temperature increases and rises as temperature falls. This agrees with experience: warm air is capable of holding more free molecules than is cold air.

15. Let us now consider an electrified cloud whose negatively charged drops collect in the lower part and whose positively charged drops collect in the upper part.

If the charges are weak, the atmospheric field tends to be weakly positive at all heights except in the middle of the cloud, where it is stronger than usual. By considering layers in the upper and lower parts we should expect, allowing for the colder temperature aloft, about as many large drops of any given size in each part, though the most probable size in the lower part would be slightly larger than the most probable size in the upper part.

If the electrification becomes sufficiently strong, the atmospheric field becomes negative from the ground into the lower part of the cloud, remains positive in the middle, and becomes negative in the upper part. There is now a definite tendency, which increases with further electrification, for more and larger drops in the upper part of the cloud than in the lower part.

It may be considered that these ideas have some bearing on observed phenomena. With the approach of a cloud of the kind described, we should find that at the earth's surface the potential gradient would fall and both positive and negative light rain might occur through disequilibrium. Increased electrification would produce a further fall or reversal of the potential gradient; and with reversal there would be a definite tendency for heavier rain, bearing a predominantly positive charge.

These remarks are of course intended to apply only to clouds of water drops; the theory has yet to be developed for clouds containing ice-crystals.

Appendix.

Corrections to the first paper.

(The author wishes to express his thanks to Mr. S. A. Scott, who very kindly checked the first paper after it had been published.)

P. 633. Line 17 down. *For* " vertical " *read* " virtual."

Formulæ (10), (15), (22), (23), (26). *Delete* the term " $+g\rho_0 z_0$."

Formula (12). The left hand side is " θ."

P. 635. Line 14 up. The expression for ν should *read* " $2{\cdot}98\times10^{-18}N_1/V$."

Formulæ (29), (30); figures (6), (7). *For* " $\frac{2\beta}{n^{1/3}}$ " *read* " $\frac{2\beta}{3n^{1/3}}$ ".

P. 640. Line 4 down. *For* " value of n " *read* " value of N_n."

P. 640. Lines 4, 10 down; figures (6), (7), (8). *For* " $\left(\frac{c}{2\beta}\right)^{1/3}$ " *read* " $\frac{c}{2\beta}$ ".

P. 640. Lines 11–13 down. *Read* " For example, with $q=0{\cdot}001$ e.s.u. we have $n=4{\cdot}4\times10^{13}$ or $r=6{\cdot}8\times10^{-4}$; and with $q=0{\cdot}01$ e.s.u. we have $n=4{\cdot}4\times10^{15}$ or $r=3{\cdot}2\times10^{-3}$." And add " These radii are of sizes commonly attributed to country fogs, but according to Findeisen the corresponding values for q would be impossibly high."

P. 641. Line 14 down. *Read* the formula as " $q^2=\frac{27\pi\sigma^4}{2}\left(\frac{m}{\rho kT\log\nu}\right)^3$ ".

P. 641. Line 7 down. *For* " 0·054 " *read* " 0.27."

P. 641. Line 10 down. The expression at the end of the line should *read* $(4\pi r^2 q)^2/(2r)$.

Edlesborough,
January 26, 1945.

LI. *On Thermal Stresses in Circular Cylinders.*

By J. C. Jaeger *.

[Received May 5, 1944.]

I. *Introduction.*

Although there is a large literature † on thermal stresses, particularly in circular cylinders, none of these works gives adequate numerical results for practical use *. The object of this paper is primarily to give fairly complete results for the solid cylinder, initially at constant temperature V, and with, subsequently, either its surface maintained at temperature zero, or radiation at its surface into a medium at zero temperature: these problems are considered in §§ 2, 3. Formulæ for the stresses for small values of the time, when the usual expressions as series of Bessel functions converge very slowly, are given in § 4. A general result for the hollow cylinder, with zero initial temperature, and either radiation, no flow of heat, or constant temperature, at either surface, is given in § 5, and is used to indicate how rapidly the results for the hollow cylinder diverge from those for the solid cylinder. Finally, in § 6, the application of these results to the case of periodic surface temperature is discussed. The condition of plane stress is assumed to hold in all cases.

---

* Communicated by the Author.

† For a bibliography see Gatewood, Phil. Mag. (7) xxxii. p. 282 (1941). The most important works in the present connection are Lees, Proc. Roy. Soc. A, ci. p. 411 (1922), and Dahl, Trans. American Soc. Mech. Eng. xlvi. p. 161 (1924).

2. *The thermal stresses in the cylinder $0 \leqslant r < a$, initially at constant temperature V, whose surface is kept at zero temperature for $t > 0$.*

If E is Young's Modulus, ν Poisson's ratio, α the coefficient of linear expansion of the solid, and v its temperature at radius r, the results for the radial and tangential stresses are well known to be †

$$\sigma_r = \frac{\mathrm{E}\alpha}{1-\nu}\left\{\frac{1}{a^2}\int_0^a rv\,dr - \frac{1}{r^2}\int_0^r rv\,dr\right\}, \quad . \quad . \quad . \quad . \quad . \quad . \quad . \quad (1)$$

$$\sigma_\theta = \frac{\mathrm{E}\alpha}{1-\nu}\left\{\frac{1}{a^2}\int_0^a rv\,dr + \frac{1}{r^2}\int_0^r rv\,dr - v\right\}, \quad . \quad . \quad . \quad . \quad . \quad (2)$$

and, if the resultant of the normal forces over the cross-section of the cylinder is zero,

$$\sigma_z = \sigma_r + \sigma_\theta. \quad . \quad . \quad . \quad . \quad . \quad . \quad . \quad . \quad . \quad . \quad . \quad (3)$$

If K, ρ, c are the thermal conductivity, density, and specific heat of the material of the cylinder, and $\kappa = \mathrm{K}/\rho c$, introducing the well-known formulæ ‡ for the temperature v in this case, we obtain

$$\frac{(1-\nu)\sigma_r}{\mathrm{E}\alpha\mathrm{V}} = 2\sum_{s=1}^{\infty}\frac{e^{-\kappa\beta_s^2 t/a^2}}{\beta_s^2\mathrm{J}_1(\beta_s)}\left\{\mathrm{J}_1(\beta_s) - \frac{a}{r}\mathrm{J}_1\left(\frac{r\beta_s}{a}\right)\right\}, \quad . \quad . \quad . \quad . \quad . \quad . \quad (4)$$

$$\frac{(1-\nu)\sigma_\theta}{\mathrm{E}\alpha\mathrm{V}} = 2\sum_{s=1}^{\infty}\frac{e^{-\kappa\beta_s^2 t/a^2}}{\beta_s^2\mathrm{J}_1(\beta_s)}\left\{\mathrm{J}_1(\beta_s) + \frac{a}{r}\mathrm{J}_1\left(\frac{r\beta_s}{a}\right) - \beta_s\mathrm{J}_0\left(\frac{r\beta_s}{a}\right)\right\}, \quad . \quad (5)$$

where $\pm\beta_s$, $s=1, 2, \ldots$ are the roots of

$$\mathrm{J}_0(\beta) = 0. \quad . \quad . \quad . \quad . \quad . \quad . \quad . \quad . \quad . \quad . \quad . \quad (6)$$

In Tables I. and II. values of $(1-\nu)\sigma_r/\mathrm{E}\alpha\mathrm{V}$ and $(1-\nu)\sigma_\theta/\mathrm{E}\alpha\mathrm{V}$ calculated from these formulæ are given for various values of the parameters (r/a) and $(\kappa t/a^2)$. The case of small values of $\kappa t/a^2$, for which (4) and (5) are not well suited, is considered in § 4.

---

* The author encountered this problem in a study of thermal stresses in the sandstone cylinders used in the mechanical process of wood pulping; almost all the problems studied here have appeared in that connection.

† Timoshenko, 'Theory of Elasticity,' § 114.

‡ Carslaw, 'Conduction of Heat,' Ed. 2 (1921), § 57.

TABLE I.

Radial Stresses in Circular Cylinders.

$(1-\nu)\sigma_r/E\alpha V$.

$\kappa t/a^2$ \ r/a	0.	0·1.	0·2.	0·3.	0·4.	0·5.	0·6.	0·7.	0·75.	0·8.	0·85.	0·9.	0·95.
0·005	—·0773	—·0773	—·0773	—·0773	—·0773	—·0773	—·0772	—·0771	—·0766	—·0749	—·0699	—·0582	—·0357
0·01	—·1077	—·1077	—·1077	—·1077	—·1077	—·1077	—·1073	—·1049	—·1012	—·0942	—·0820	—·0628	—·0355
0·015	—·1305	—·1305	—·1305	—·1305	—·1304	—·1300	—·1280	—·1209	—·1135	—·1021	—·0855	—·0630	—·0344
0·02	—·1493	—·1493	—·1493	—·1492	—·1487	—·1471	—·1424	—·1303	—·1198	—·1053	—·0861	—·0621	—·0332
0·03	—·1797	—·1796	—·1792	—·1782	—·1757	—·1701	—·1589	—·1385	—·1238	—·1057	—·0841	—·0591	—·0309
0·04	—·2029	—·2026	—·2012	—·1983	—·1926	—·1824	—·1654	—·1394	—·1225	—·1029	—·0806	—·0558	—·0288
0·05	—·2196	—·2188	—·2161	—·2108	—·2018	—·1875	—·1663	—·1370	—·1190	—·0988	—·0766	·0526	—·0269
0·06	—·2300	—·2287	—·2246	—·2172	—·2053	—·1879	—·1640	—·1328	—·1145	—·0943	—·0726	—·0495	—·0252
0·07	—·2349	—·2332	—·2280	—·2187	—·2048	—·1853	—·1597	—·1277	—·1094	—·0897	—·0687	—·0466	—·0236
0·08	—·2353	—·2333	—·2273	—·2168	—·2014	—·1806	—·1542	—·1222	·1043	—·0851	—·0650	—·0439	—·0222
0·09	—·2324	—·2302	—·2236	—·2123	—·1960	—·1747	—·1481	—·1166	—·0991	—·0807	—·0614	—·0414	—·0209
0·1	—·2271	—·2248	—·2178	—·2061	—·1895	—·1679	—·1416	—·1109	—·0940	—·0764	—·0580	—·0390	—·0196
0·15	—·1850	—·1828	—·1761	—·1652	—·1503	—·1316	—·1095	—·0846	—·0713	—·0576	—·0435	—·0291	—·0146
0·2	—·1418	—·1400	—·1348	—·1261	—·1144	—·0998	—·0827	—·0637	—·0536	—·0432	—·0326	—·0218	—·0109
0·3	—·0802	—·0792	—·0762	—·0713	—·0645	—·0562	—·0466	—·0358	—·0301	—·0243	—·0183	—·0122	—·0061
0·4	—·0450	—·0445	—·0428	—·0400	—·0362	—·0315	—·0261	—·0201	—·0169	—·0136	—·0103	—·0069	—·0034
0·5	—·0253	·0249	—·0240	—·0224	—·0203	—·0177	—·0146	—·0113	—·0095	—·0076	—·0058	—·0038	—·0019
0·6	—·0142	—·0140	—·0134	—·0126	—·0114	—·0099	—·0082	—·0063	—·0053	—·0043	—·0032	—·0022	—·0011
0·7	—·0079	—·0078	—·0075	—·0071	—·0064	—·0056	—·0046	—·0035	—·0030	—·0024	—·0018	—·0012	—·0006
0·8	—·0045	—·0044	—·0042	—·0040	—·0036	—·0031	—·0026	—·0020	—·0017	—·0013	—·0010	—·0007	—·0003
0·9	—·0025	—·0025	—·0024	—·0022	—·0020	—·0018	—·0014	—·0011	—·0009	—·0008	—·0006	—·0004	—·0002
1·0	—·0014	—·0014	—·0013	—·0012	—·0011	—·0010	—·0008	—·0006	—·0005	—·0004	—·0003	—·0002	—·0001

TABLE II.

Tangential Stresses in Circular Cylinders.

$(1-\nu)\sigma_\theta/\mathrm{E}\alpha\mathrm{V}$.

$\kappa t/a^2$ \ r/a	0.	0·1.	0·2.	0·3.	0·4.	0·5.	0·6.	0·7.	0·75.	0·8.	0·85.	0·9.	0·95.	1·0.
0·005	—·0773	—·0773	—·0773	—·0773	—·0773	·0773	—·0772	·0742	·0635	—·0286	·0605	·2384	·5146	·8455
0·01	—·1077	—·1077	—·1077	—·1077	—·1077	—·1072	—·1021	·0700	·0250	·0549	·1803	·3534	·5630	·7845
0·015	—·1305	—·1305	—·1305	—·1304	—·1298	—·1255	—·1059	—·0402	·0251	·1194	·2447	·3972	·5670	·7390
0·02	—·1493	—·1493	—·1492	—·1486	—·1455	—·1337	—·0971	—·0077	·0663	·1628	·2806	·4153	·5589	·7014
0·03	—·1797	—·1794	—·1780	—·1736	—·1610	—·1306	—·0673	·0444	·1212	·2114	·3127	·4213	·5323	·6402
0·04	—·2029	—·2018	—·1973	—·1861	—·1621	—·1163	—·0385	·0783	·1513	·2328	·3204	·4115	·5027	·5904
0·05	—·2196	—·2171	—·2084	—·1900	—·1562	—·1002	—·0158	·0992	·1671	·2404	·3175	·3960	·4736	·5479
0·06	—·2300	—·2261	—·2134	—·1887	—·1476	—·0855	·0010	·1114	·1742	·2406	·3092	·3783	·4460	·5106
0·07	—·2349	—·2298	·2137	—·1843	·1384	—·0730	·0129	·1179	·1760	·2365	·2983	·3599	·4201	·4772
0·08	—·2353	—·2293	—·2108	—·1782	—·1294	—·0629	·0211	·1204	·1743	·2298	·2859	·3416	·3957	·4471
0·09	—·2324	—·2258	—·2057	—·1711	·1209	—·0547	·0266	·1203	·1704	·2216	·2730	·3238	·3729	·4195
0·1	—·2271	—·2202	—·1991	—·1636	—·1132	—·0481	·0300	·1184	·1651	·2125	·2599	·3065	·3515	·3942
0·15	—·1850	—·1783	·1586	—·1263	—·0827	·0292	·0319	·0978	·1316	·1654	·1988	·2313	·2624	·2919
0·2	—·1418	—·1365	—·1208	—·0954	—·0614	—·0203	·0259	·0752	·1003	·1252	·1498	·1735	·1963	·2179
0·3	—·0802	—·0772	—·0682	—·0537	—·0343	—·0111	·0150	·0426	·0566	·0705	·0842	·0974	·1101	·1220
0·4	—·0450	—·0433	—·0383	—·0301	—·0193	—·0062	·0084	·0239	·0318	·0396	·0472	·0546	·0617	·0684
0·5	—·0253	—·0243	—·0215	—·0169	—·0108	—·0035	·0047	·0134	·0178	·0222	·0265	·0306	·0346	·0384
0·6	—·0142	—·0136	—·0120	—·0095	—·0061	—·0020	·0026	·0075	·0100	·0124	·0149	·0172	·0194	·0215
0·7	—·0079	—·0076	—·0068	—·0053	—·0034	—·0011	·0015	·0042	·0056	·0070	·0083	·0096	·0109	·0121
0·8	—·0045	—·0043	—·0038	—·0030	—·0019	—·0006	·0008	·0024	·0031	·0039	·0047	·0054	·0061	·0068
0·9	—·0025	—·0024	—·0021	—·0017	—·0011	—·0003	·0005	·0013	·0018	·0022	·0026	·0030	·0034	·0038
1·0	—·0014	—·0013	—·0012	—·0009	—·0006	—·0002	·0003	·0007	·0010	·0012	·0015	·0017	·0019	·0021

3. *The thermal stresses in the cylinder* $0 \leqslant r < a$, *initially at constant temperature* V, *which for* $t > 0$ *loses heat by radiation into a medium at zero temperature, the boundary condition at* $r = a$ *being*

$$\frac{\partial v}{\partial r} + hv = 0. \quad \ldots\ldots\ldots\ldots \quad (7)$$

In this case the temperature v is given by (Carslaw, *loc. cit.* § 57)

$$v = 2ah\mathrm{V} \sum_{s=1}^{\infty} e^{-\kappa\beta_s^2 t/a^2} \frac{\mathrm{J}_0(r\beta_s/a)}{(a^2h^2+\beta_s^2)\mathrm{J}_0(\beta_s)}, \quad \ldots\ldots \quad (8)$$

where the β_s are the roots of

$$\beta \mathrm{J}_1(\beta) - ah\mathrm{J}_0(\beta) = 0. \quad \ldots\ldots\ldots \quad (9)$$

Using this result in (1) and (2) we obtain for the thermal stresses

$$\frac{(1-\nu)\sigma_r}{\mathrm{E}\alpha\mathrm{V}} = \sum_{s=1}^{\infty} \frac{2ah\, e^{-\kappa\beta_s^2 t/a^2}}{\beta_s(a^2h^2+\beta_s^2)\mathrm{J}_0(\beta_s)} \left\{ \mathrm{J}_1(\beta_s) - \frac{a}{r}\mathrm{J}_1\left(\frac{r\beta_s}{a}\right) \right\}, \quad \ldots \quad (10)$$

$$\frac{(1-\nu)\sigma_\theta}{\mathrm{E}\alpha\mathrm{V}} = \sum_{s=1}^{\infty} \frac{2ah\, e^{-\kappa\beta_s^2 t/a^2}}{\beta_s(a^2h^2+\beta_s^2)\mathrm{J}_0(\beta_s)} \left\{ \mathrm{J}_1(\beta_s) + \frac{a}{r}\mathrm{J}_1\left(\frac{r\beta_s}{a}\right) - \mathrm{J}_0\left(\frac{r\beta_s}{a}\right) \right\}. \quad (11)$$

The results thus involve the three dimensionless parameters $\kappa t/a^2$, r/a, and ah. In figs. 1 and 2 respectively the values of $(1-\nu)\sigma_r/\mathrm{E}\alpha\mathrm{V}$ and $(1-\nu)\sigma_\theta/\mathrm{E}\alpha\mathrm{V}$ as functions of $\kappa t/a^2$ are shown for the case $ah = 5$ and values of r/a ranging from 0 to 1·0.

To illustrate the way in which the stresses vary with ah, the variation with $\kappa t/a^2$ of the surface tangential stress, σ_θ for $r/a = 1$, is shown in fig. 3 for the values 0·2, 0·5, 1, 2, 5, 10, 20, ∞ of ah.

4. *The values of the stresses for small values of the time.*

The convergence of the series (4), (5), (10), (11) is unpleasantly slow if $\kappa t/a^2 < 0{\cdot}01$, and, since the tangential stresses near the surface change very rapidly for small values of the time, it is important to have approximate formulæ well suited to this region. An attempt was made by Lees, *loc. cit.*, using an empirical method, to calculate the stresses for small values of the time, but rigorous formulæ are very simply obtained by using the method developed by Goldstein * for similar problems; this method is greatly improved by the use of the repeated integrals of the error function defined and tabulated by Hartree †.

To find the radial stress, σ_r, in the constant temperature case of § 2, let $\bar{\sigma}_r$ be the Laplace transform of σ_r, *i. e.*

$$\bar{\sigma}_r = \int_0^\infty e^{-pt}\sigma_r dt, \quad \mathrm{R}(p) > 0.$$

---

* Goldstein, Proc. London Math. Soc. (2) xxxiv. p. 51 (1932).

† Hartree, Mem. and Proc. Manchester Lit. and Phil. Soc. lxxx. p. 85 (1936).

Fig. 1.

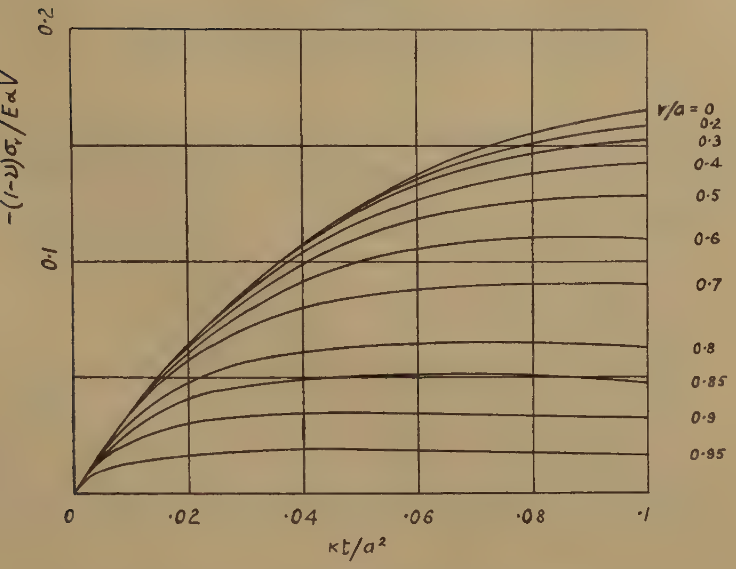
0·2
$-(1-\nu)\sigma_r/E\alpha V$
0·1
0
·02
·04
·06
·08
·1
$\kappa t/a^2$
$r/a = 0$
0·2
0·3
0·4
0·5
0·6
0·7
0·8
0·85
0·9
0·95

Fig. 2.

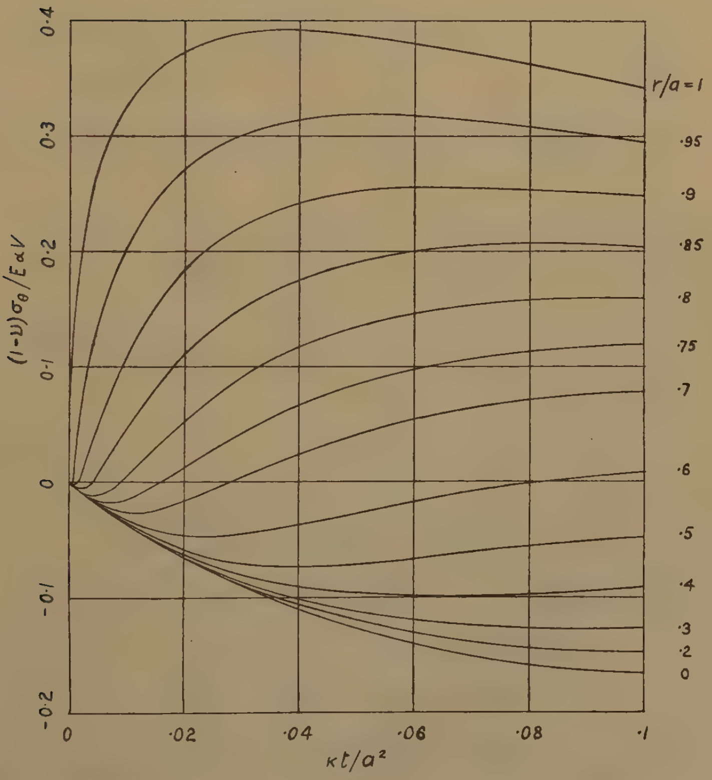
0·4
0·3
0·2
$(1-\nu)\sigma_\theta/E\alpha V$
0·1
0
-0·1
-0·2
0
·02
·04
·06
·08
·1
$\kappa t/a^2$
$r/a = 1$
·95
·9
·85
·8
·75
·7
·6
·5
·4
·3
·2
0

Then, using the standard procedure of the Laplace transformation method (see, *e. g.*, *) we easily obtain

$$\frac{(1-\nu)}{\mathrm{E}\alpha \mathrm{V}}\bar{\sigma}_r = \frac{1}{p\mathrm{I}_0(qa)}\left\{\frac{1}{aq}\mathrm{I}_1(qa)-\frac{1}{rq}\mathrm{I}_1(qr)\right\}, \quad . \quad . \quad . \quad . \qquad (12)$$

where $q=\sqrt{(p/\kappa)}$.

We consider only the important case in which r/a is not small, and, following Goldstein, *loc. cit.*, we use the asymptotic expansions of the Bessel functions and expand (12) in ascending powers of $1/q$, thus obtaining

Fig. 3.

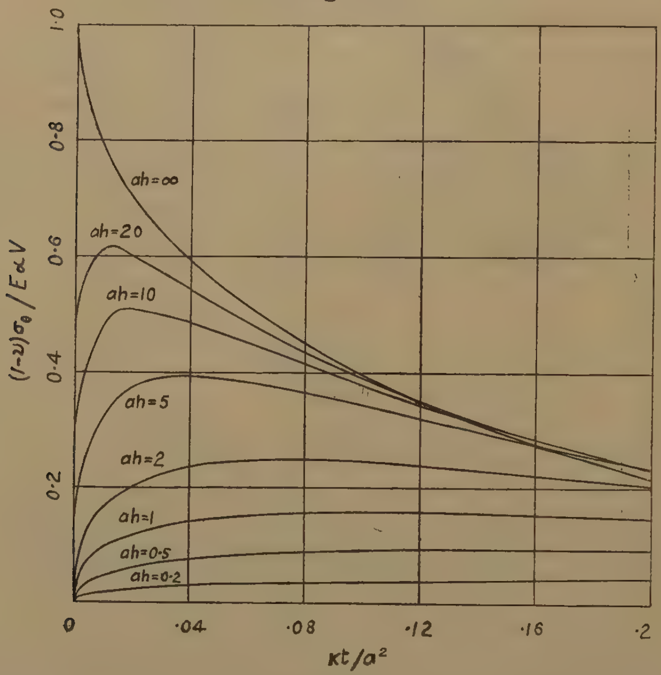

$$\frac{(1-\nu)\bar{\sigma}_r}{\mathrm{E}\alpha\mathrm{V}} = -\frac{\kappa^{\frac{1}{2}}}{ap^{3/2}}+\frac{\kappa^{\frac{1}{2}}a^{\frac{1}{2}}}{r^{3/2}p^{3/2}}e^{-(a-r)p^{\frac{1}{2}}/\kappa^{\frac{1}{2}}}+\frac{\kappa}{2a^2p^2}-\frac{\kappa(3a+r)}{8a^{\frac{1}{2}}r^{5/2}}e^{-(a-r)p^{\frac{1}{2}}/\kappa^{\frac{1}{2}}}+\ldots .$$

Then, using the results

$$\int_0^\infty e^{-pt}t^n\,dt=\Gamma(n+1)p^{-n-1}$$

$$\int_0^\infty e^{-pt}(4t)^{\frac{1}{2}n}i^n\operatorname{erfc}\left(\frac{x}{2t^{\frac{1}{2}}}\right)dt=p^{-1-\frac{1}{2}n}e^{-xp^{\frac{1}{2}}},$$

where [Hartree, *loc. cit.*]

$$i^n\operatorname{erfc}w=\int_w^\infty i^{n-1}\operatorname{erfc}\xi\,d\xi,$$

$$i^0\operatorname{erfc}w=\operatorname{erfc}w=\frac{2}{\sqrt{\pi}}\int_w^\infty e^{-\xi^2}\,d\xi,$$

---

* Carslaw and Jaeger, Proc. London Math. Soc. (2) xlvi. p. 361 (1940).

it follows that

$$\frac{(1-\nu)\sigma_r}{\mathrm{E}\alpha\mathrm{V}}=-2\pi^{-\frac{1}{2}}\mathrm{T}^{\frac{1}{2}}+2\xi^{-3/2}\mathrm{T}^{\frac{1}{2}}\,i\,\mathrm{erfc}\,\mathrm{T}'+\tfrac{1}{2}\mathrm{T}-\tfrac{1}{2}\mathrm{T}\xi^{-5/2}(\xi+3)i^2\,\mathrm{erfc}\,\mathrm{T}'+\ldots, \quad . \quad . \quad . \quad (13)$$

where $\xi=r/a$, $\mathrm{T}=\kappa t/a^2$, $\mathrm{T}'=\frac{1}{2}(1-\xi)\mathrm{T}^{-\frac{1}{2}}$. . . . . . (14)

Similarly the tangential stress is given by

$$\frac{(1-\nu)\sigma_\theta}{\mathrm{E}\alpha\mathrm{V}}=\xi^{-\frac{1}{2}}\,\mathrm{erfc}\,\mathrm{T}'-2\pi^{-\frac{1}{2}}\mathrm{T}^{\frac{1}{2}}-\frac{1}{4}\mathrm{T}^{\frac{1}{2}}\xi^{-3/2}(\xi+7)\,i\,\mathrm{erfc}\,\mathrm{T}'$$
$$+\frac{1}{2}\mathrm{T}-\frac{1}{32}\mathrm{T}\xi^{-5/2}(7\xi^2-14\xi-57)\,i^2\,\mathrm{erfc}\,\mathrm{T}'+\ldots. \quad (15)$$

For the radiation case of § 3 the results are

$$\frac{(1-\nu)\sigma_r}{\mathrm{E}\alpha\mathrm{V}}=-k\mathrm{T}+4k\xi^{-3/2}\mathrm{T}\,i^2\,\mathrm{erfc}\,\mathrm{T}'+\ldots, \quad . \quad . \quad . \quad . \quad . \quad . \quad . \quad . \quad (16)$$

$$\frac{(1-\nu)\sigma_\theta}{\mathrm{E}\alpha\mathrm{V}}=2k\xi^{-\frac{1}{2}}\mathrm{T}^{\frac{1}{2}}i\,\mathrm{erfc}\,\mathrm{T}'-k\mathrm{T}-\frac{1}{2}k\xi^{-3/2}\mathrm{T}(8\xi k-3\xi+7)\,i^2\,\mathrm{erfc}\,\mathrm{T}'+\ldots. \quad . \quad . \quad . \quad (17)$$

The surface tangential stresses take specially simple forms: for the constant temperature case

$$\frac{(1-\nu)\sigma_\theta}{\mathrm{E}\alpha\mathrm{V}}=1-4\pi^{-\frac{1}{2}}\mathrm{T}^{\frac{1}{2}}+\mathrm{T}+\frac{1}{3}\pi^{-\frac{1}{2}}\mathrm{T}^{3/2}+\frac{1}{8}\mathrm{T}^2+\ldots; \quad . \quad . \quad (18)$$

and for the radiation case

$$\frac{(1-\nu)\sigma_\theta}{\mathrm{E}\alpha\mathrm{V}}=2k\pi^{-\frac{1}{2}}\mathrm{T}^{\frac{1}{2}}-k\left(k+\frac{3}{2}\right)\mathrm{T}+\frac{4}{3}k\left(k^2+k+\frac{3}{8}\right)\pi^{\;\frac{1}{2}}\mathrm{T}^{3/2}+\ldots. \quad (19)$$

5. *The temperature and the thermal stresses in the hollow cylinder* $a<r<b$, *with zero initial temperature and with boundary conditions*

$$k_1\frac{\partial v}{\partial r}-h_1(v-v_1)=0, \quad r=a, \quad . \quad . \quad . \quad . \quad . \quad . \quad . \quad (20)$$

$$k_2\frac{\partial v}{\partial r}+h_2(v-v_2)=0, \quad r=b, \quad . \quad . \quad . \quad . \quad . \quad . \quad . \quad (21)$$

where k_1, k_2, h_1, h_2, v_1, v_2 *are constants, all of* k_1, k_2, h_1, h_2 *are positive or zero, and* h_1 *and* h_2, k_1 *and* h_1, *or* k_2 *and* h_2 *are not both to be zero.*

By suitable choice of these constants the cases of constant temperature, radiation, or no flow of heat at either surface may be obtained. The result for the temperature v is a generalization of others given elsewhere * and is easily established by the same method (Laplace transformation). Numerous special cases are given in Dahl, *loc. cit.*, and elsewhere in the literature.

---

* Carslaw and Jaeger, *loc. cit.*

The results are

$$v=\frac{ah_1v_1(k_2+bh_2\log b/r)+bh_2v_2(k_1+ah_1\log r/a)}{bh_2k_1+ah_1k_2+abh_1h_2\log b/a}$$
$$-\sum_{s=1}^{\infty}e^{+\kappa\beta_s^2t}\mathrm{F}(\beta_s)\mathrm{C}_0(r\beta_s)\,; \quad . \quad (22)$$

$$\frac{(1-\nu)\sigma_r}{\mathrm{E}\alpha}=\frac{abh_1h_2(v_2-v_1)}{2(bh_2k_1+ah_1k_2)+2abh_1h_2\log(b/a)}\left\{\frac{b^2(r^2-a^2)}{r^2(b^2-a^2)}\log\frac{b}{a}-\log\frac{r}{a}\right\}$$
$$-\sum_{s=1}^{\infty}e^{-\kappa\beta_s^2t}\mathrm{F}(\beta_s)\left\{\frac{b(r^2-a^2)\mathrm{C}_1(b\beta_s)}{r^2(b^2-a^2)\beta_s}-\frac{1}{r\beta_s}\mathrm{C}_1(r\beta_s)+\frac{2h_1(b^2-r^2)}{\pi\beta_s^2(b^2-a^2)r^2}\right\}; \quad . \quad . \quad . \quad (23)$$

$$\frac{(1-\nu)\sigma_\theta}{\mathrm{E}\alpha}=\frac{abh_1h_2(v_2-v_1)}{2bh_2k_1+2ah_1k_2+2abh_1h_2\log(b/a)}\left\{\frac{b^2(r^2+a^2)}{r^2(b^2-a^2)}\log\frac{b}{a}-1-\log\frac{r}{a}\right\}$$
$$-\sum_{s=1}^{\infty}e^{-\kappa\beta_s^2t}\mathrm{F}(\beta_s)\left\{\frac{b(r^2+a^2)\mathrm{C}_1(b\beta_s)}{r^2(b^2-a^2)\beta_s}+\frac{\mathrm{C}_1(r\beta_s)}{r\beta_s}-\mathrm{C}_0(r\beta_s)-\frac{2h_1(b^2+r^2)}{\pi r^2(b^2-a^2)\beta_s^2}\right\}; \quad . \quad . \quad . \quad (24)$$

where

$$\mathrm{C}_0(x)=\mathrm{J}_0(x)[k_1\beta_s\mathrm{Y}_1(a\beta_s)+h_1\mathrm{Y}_0(a\beta_s)]-\mathrm{Y}_0(x)[k_1\beta_s\mathrm{J}_1(a\beta_s)+h_1\mathrm{J}_0(a\beta_s)]. \quad . \quad . \quad . \quad (25)$$

$$\mathrm{C}_1(x)=\mathrm{J}_1(x)[k_1\beta_s\mathrm{Y}_1(a\beta_s)+h_1\mathrm{Y}_0(a\beta_s)]-\mathrm{Y}_1(x)[k_1\beta_s\mathrm{J}_1(a\beta_s)+h_1\mathrm{J}_0(a\beta_s)], \quad . \quad . \quad . \quad (26)$$

$$\mathrm{F}(\beta_s)=\frac{\pi[k_2\beta_s\mathrm{J}_1(b\beta_s)-h_2\mathrm{J}_0(b\beta_s)]\{h_1v_1[k_2\beta_s\mathrm{J}_1(b\beta_s)-h_2\mathrm{J}_0(b\beta_s)]+h_2v_2[k_1\beta_s\mathrm{J}_1(a\beta_s)+h_1\mathrm{J}_0(a\beta_s)]\}}{(h_1^2+k_1^2\beta_s^2)[k_2\beta_s\mathrm{J}_1(b\beta_s)-h_2\mathrm{J}_0(b\beta_s)]^2-(h_2^2+k_2^2\beta_s^2)[k_1\beta_s\mathrm{J}_1(a\beta_s)+h_1\mathrm{J}_0(a\beta_s)]^2}, \quad . \quad . \quad . \quad (27)$$

and $\pm\beta_s$, $s=1, 2, \ldots$, are the roots (all real and simple) of

$$[k_1\beta\mathrm{J}_1(a\beta)+h_1\mathrm{J}_0(a\beta)][k_2\beta\mathrm{Y}_1(b\beta)-h_2\mathrm{Y}_0(b\beta)]$$
$$-[k_2\beta\mathrm{J}_1(b\beta)-h_2\mathrm{J}_0(b\beta)][k_1\beta\mathrm{Y}_1(a\beta)+h_1\mathrm{Y}_0(a\beta)]=0. \quad (28)$$

As an example, we consider the way in which the tangential surface stress varies with a for the case in which the surface $r=b$ is kept at temperature V for $t>0$ and there is no loss of heat from the surface $r=a$, *i. e.*, $h_1=k_2=0$, $v_2=\mathrm{V}$ in (20) and (21). In fig. 4 the value of $(1-\nu)\sigma_\theta/\mathrm{E}\alpha\mathrm{V}$ for $r=b$ is plotted against $\kappa t/a^2$ for the values 0, 0·25, 0·5, 0·75 of the ratio a/b. It appears that the values for the solid cylinder are a reasonable approximation to those for the hollow cylinder only in the case of quite thick cylinders.

6. *The Case of Periodic Surface Temperature.*

In this case the solution for the temperature contains transient terms involving the roots of (6) or (28), and periodic steady state terms which may be expressed in terms of ber and bei functions. These latter expressions are cumbersome and will not be given here, but it seems worth while emphasizing that if the transient parts of the temperature or stresses are required as well (so that the roots of (6) or (28) and various functions involving them have in any case to be calculated), it is in some cases simpler to use the results which can be obtained from those given above by the application of Duhamel's theorem *. In this way we find that if $f(t)$ is the result (temperature or stress) at time t at a point of the solid for the case in which the initial temperature is zero and the surface is kept at constant temperature V for $t>0$, then the solution for the same point of the solid with zero initial temperature and its surface kept at V $\sin(\omega t+\phi)$ for $t>0$ is

$$f(t)\sin\phi+\omega\int_0^t f(\gamma)\cos[\omega(t-\gamma)+\phi]\,d\gamma. \quad . \quad . \quad . \quad . \quad (29)$$

Fig. 4.

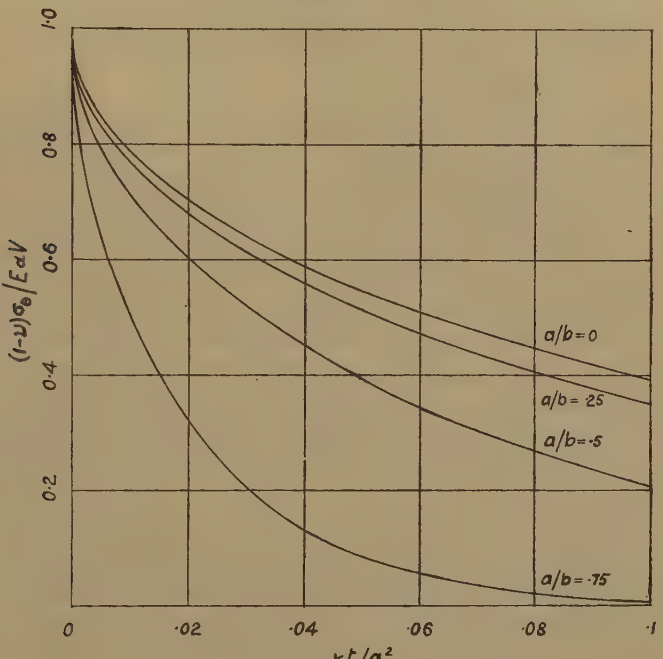

It follows that if, in the problem of § 5, in place of the constant temperature v_1 we have $V_1\sin(\omega t+\phi)$, the solutions are obtained from 22), (23), (24) by replacing v_1 by $V_1\sin(\omega t+\phi)$ in the constant first term, and in the terms of the series by replacing $v_1 e^{-\kappa\beta_s^2 t}$ by

$$e^{-\kappa\beta_s^2 t}\left\{\sin\phi-\frac{\omega\sin(\phi+\delta_s)}{(\omega^2+\kappa^2\beta_s^4)^{\frac{1}{2}}}\right\}+\frac{\omega\sin(\omega t+\phi+\delta_s)}{(\omega^2+\kappa^2\beta_s^4)^{\frac{1}{2}}}, \quad . \quad . \quad (30)$$

where $\tan\delta_s=\kappa\beta_s^2/\omega$.

If v_2, or V in § 2, varies in a similar way, the same modifications are to be made in terms involving them. The solutions obtained in this way contain the same transient terms as those obtained directly, but the steady state parts, instead of being expressed in terms of ber and bei functions, appear as infinite series, which are useful provided $a\sqrt{(\omega/\kappa)}$ and $b\sqrt{(\omega/\kappa)}$ are not too large.

---

* Carslaw, *loc. cit.*, § 9.

In conclusion, I wish to thank Miss M. E. Clarke for much assistance with the numerical work.

The University of Tasmania.

LII. *The Accumulation of Chance Effects and the Gaussian Frequency Distribution.*

By L. S. Goddard, St. John's College, Cambridge *.

[Received December 5, 1944.]

1. In a recent paper ⁽¹⁾, of the same title, Silberstein investigated a process in which the effect of the process, in a single trial, is equally likely to have any value between 0 and 1. He set out to find the probability, $p_n(x)\,dx$, that the resultant effect of an n-fold repetition of the process shall have a value between x and $x+dx$. The problem is of importance in showing how the Gaussian frequency distribution is produced in a natural manner by a sequence of events of the type described, and it also arises in certain physical problems. Fränz, for example, has recently studied an electrical problem where the function $p_n(x)$ plays an important part in some calculations relating to the signal-to-noise ratio ⁽²⁾ and the transmission of noise voltages through a linear rectifier ⁽³⁾.

Silberstein's aim was to determine *rigorously* the function $p_n(x)$ and its limiting form as $n\to\infty$, and it is a pity that his mathematical technique collapsed at the point where rigour is most needed. After determining $p_n(x)$ (a series of polynomials in x with coefficients which are functions of n) for the first few values of n, he remarks that for increasing n "the coefficients vary in an intricate manner," and no attempt is made to determine these coefficients. The maximum value of $p_n(x)$ is given by

$$P_n=\frac{2}{\pi}\int_0^\infty\left(\frac{\sin x}{x}\right)^n dx. \qquad (1)$$

and Silberstein writes "so far as we know, these integrals have not been previously determined."

The first purpose of the present paper is to give the form of the polynomials $p_n(x)$ for all n (this was derived in the paper ⁽²⁾ by Fränz referred to above), and to state that the integral P_n has been evaluated †, and the formula is easily obtained by contour integration, as we shall show presently. We have, in fact,

---

* Communicated by the Author.

† See ⁽⁴⁾, p. 123, or ⁽⁵⁾, p. 406.

$$P_n = \frac{1}{2^{n-1}(n-1)!}\Sigma(-)^r\binom{n}{r}(n-2r)^{n-1},$$

where the summation extends over integral r such that $0 \leqslant 2r \leqslant n-1$. The second purpose of the paper is to examine, in finer detail than Silberstein did, the asymptotic forms for P_n and $p_n(x)$ as $n \to \infty$. The polynomial $p_n(x)$ is represented by the Fourier integral

$$p_n(x) = \frac{2}{\pi}\int_0^\infty \left(\frac{\sin v}{v}\right)^n \cos 2\left(x-\frac{n}{2}\right)v\,dv, \quad . \quad . \quad . \quad . \quad (2)$$

and the asymptotic form for $p_n(\xi)$, the deviation from the mean $\xi = x-\frac{n}{2}$, is derived from the formula

$$p_n(\xi) = \frac{2}{\pi}\int_0^\infty \left(\frac{\sin v}{v}\right)^n \cos(2\xi v)\,dv \quad . \quad . \quad . \quad . \quad . \quad . \quad (3)$$

by replacing $\left(\frac{\sin v}{v}\right)^n$ by its asymptotic expansion.

2. As Silberstein shows, the function $p_n(x)$ is defined by the equation

$$p_{n+1}(x) = \int_{x-1}^{x} p_n(u)du,$$

with the initial conditions

$$\begin{aligned} p_1(u) &= 0 \quad (u<0), \\ &= 1 \quad (0<u<1), \\ &= 0 \quad (u>1). \end{aligned}$$

By applying the general formula * for differentiation of integrals containing a parameter α,

$$\frac{d}{d\alpha}\int_{a(\alpha)}^{b(\alpha)} f(x,\alpha)\,dx = f(b,\alpha)\frac{db}{d\alpha} - f(a,\alpha)\frac{da}{d\alpha} + \int_{a(\alpha)}^{b(\alpha)} \frac{\partial f}{\partial\alpha}dx,$$

we derive immediately the differential-difference equation †

$$\frac{d}{dx}p_{n+1}(x) = p_n(x) - p_n(x-1),$$

and, by repeated differentiation, we obtain

$$\frac{d^r}{dx^r}p_{n+1}(x) = \sum_{t=0}^{r}(-)^t\binom{r}{t}p_{n-r+1}(x-t) \quad (r=1,\ldots,n). \quad . \quad . \quad (4)$$

Fränz now proceeds as follows (we only outline the process and refer to (2) for details). We denote by $p_{i,n+1}(x)$ $(0 \leqslant i \leqslant n)$ the polynomial which represents $p_n(x)$ in the range $(i, i+1)$ of x and form the differences

$$F_{i,i-1}(x) = p_{i,n+1}(x) - p_{i-1,n+1}(x), \qquad p_{-1,n+1}(x) \equiv 0,$$

---

* See (4), p. 67.

† Such equations arise in numerous physical problems and a good discussion is given in a recent paper by Bateman (6). An example, relating to a problem in radioactivity, occurs in a paper by Sedgwick (7), and the equations arising there have recently been generalized by Ruark (8).

which, upon reversion, yield the result

$$p_{i,\,n+1}(x)=\sum_{j=0}^{i}\mathrm{F}_{j,\,j-1}(x). \qquad (5)$$

The polynomials $\mathrm{F}_{i,\,i-1}(x)$, which are all of degree n, are of a particularly simple form, since all their derivatives, except the nth, vanish at the point $x=i$. Consequently

$$\mathrm{F}_{i,\,i-1}(x)=\mathrm{F}^{(n)}_{i,\,i-1}\frac{(i-x)^n}{n\,!},$$

where $\mathrm{F}^{(n)}_{i,\,i-1}$ is the nth derivative of $\mathrm{F}_{i,\,i-1}(x)$ at the point $x=i$. This is obtained from equation (4), and Fränz shows that

$$\mathrm{F}^{(n)}_{i,\,i-1}=(-)^{n-1}\binom{n+1}{i}.$$

It follows from (5) that

$$p_{i,\,n+1}(x)=\sum_{\mu=0}^{i}(-)^{\mu}\binom{n+1}{\mu}\frac{(x-\mu)^n}{n\,!} \quad (i=0,\,1,\,\ldots,\,n), \qquad (6)$$

and this is the general expression for the polynomials that Silberstein found for small values of n.

3. The formulæ (6) are not convenient for the study of $p_n(x)$ for large values of n. For this purpose the Fourier integral form (2) is much better, and the integral may be evaluated, for any n, by contour integration. The method is described by Stewart [(5), pp. 392–394], and we give in detail the application to the integral given by equation (1).

Since $$\sin z=\frac{e^{iz}-e^{-iz}}{2i},$$

we easily derive the expansion

$$\left(\frac{\sin z}{z}\right)^n=\frac{1}{(2iz)^n}\sum_{r=0}^{n}(-)^r\binom{n}{r}e^{(n-2r)iz}.$$

Now write $$f(z)=\frac{1}{(2iz)^n}\,\Sigma\,(-)^r\binom{n}{r}e^{(n-2r)iz},$$

where the summation extends over integral values of r such that $0\leqslant 2r\leqslant n-1$. If we define $\mathrm{F}(z)$ by

$$\begin{aligned}\mathrm{F}(z)&=f(z) \quad (n\text{ odd}),\\ &=f(z)+\frac{1}{2(2iz)^n}\binom{n}{\frac{1}{2}n} \quad (n\text{ even}),\end{aligned}$$

we have for all n,

$$\mathrm{F}(z)+\mathrm{F}(-z)=\left(\frac{\sin z}{z}\right)^n. \qquad (7)$$

It is to be noted from (7) that since $\dfrac{\sin z}{z}$ is a power series in z the Laurent series for $\mathrm{F}(z)$ contains no even negative power of z. We now consider

$\int_C \mathrm{F}(z)\,dz$ taken around the contour shown, consisting of the semi-circle Γ, of radius λ, and the real axis from $x=-\lambda$ to $x=\lambda$, indented at the origin by means of a small circle γ, of radius ϵ. It is easy to show that

$$\lim_{\lambda\to\infty}\int_\Gamma \mathrm{F}(z)\,dz=0,$$

and on the real axis we have

$$\int_{-\epsilon}^{-\lambda}\mathrm{F}(x)\,dx+\int_\epsilon^\lambda \mathrm{F}(x)\,dx=\int_\epsilon^\lambda\{\mathrm{F}(x)+\mathrm{F}(-x)\}\,dx=\int_\epsilon^\lambda\left(\frac{\sin x}{x}\right)^n dx.$$

Now $\mathrm{F}(z)$ has a pole at the origin, but there are no even negative powers of z in the Laurent series for $\mathrm{F}(z)$. Hence [see (5), p. 392]

$$\lim_{\varepsilon\to 0}\int_\gamma \mathrm{F}(z)\,dz=-\pi i\mathrm{R},$$

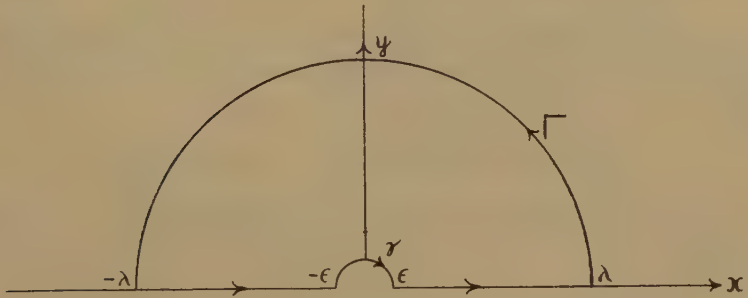

where R is the residue of $\mathrm{F}(z)$ at the origin. By making $\lambda\to\infty$ and $\epsilon\to 0$ it follows that

$$\int_0^\infty\left(\frac{\sin x}{x}\right)^n dx=\pi i\mathrm{R}.$$

The value of R may easily be obtained from the definition of $\mathrm{F}(z)$, so that we finally obtain

$$\mathrm{P}_n=\frac{2}{\pi}\int_0^\infty\left(\frac{\sin x}{x}\right)^n dx=\frac{1}{2^{n-1}(n-1)!}\Sigma(-)^r\binom{n}{r}(n-2r)^{n-1},$$

where r takes integral values such that $0\leqslant 2r\leqslant n-1$. This is the general formula for P_n, whose value Silberstein found for small values of n.

4. We now study the asymptotic forms for P_n and $p_n(\xi)$. These may be found from the asymptotic expansion of $\left(\dfrac{\sin x}{x}\right)^n$. Since

$$\log\left(\frac{\sin x}{x}\right)=\log\sin x-\log x$$
$$=\int\left(\cot x-\frac{1}{x}\right)dx,$$

we see, upon using the expansion [see (9), p. 208]

$$\cot x-\frac{1}{x}=\sum_{\kappa=1}^{\infty}\frac{(-)^\kappa 2^{2\kappa}\mathrm{B}_{2\kappa}}{(2\kappa)!}x^{2\kappa-1},$$

and performing the integration, that

$$\log\left(\frac{\sin x}{x}\right)=\sum_{\kappa=1}^{\infty}\frac{(-)^{\kappa}\mathrm{B}_{2\kappa}}{2\kappa(2\kappa)!}(2x)^{2\kappa},$$

so that the desired asymptotic form is

$$\left(\frac{\sin x}{x}\right)^{n}\sim\exp\left(n\,\Sigma\frac{(-)^{\kappa}\mathrm{B}_{2\kappa}}{2\kappa(2\kappa)!}(2x)^{2\kappa}\right)$$

$$=e^{-\frac{nx^2}{6}}.e^{-\alpha x^4-\beta x^6-\gamma x^8-\cdots},$$

where $\alpha=n/180,\quad \beta=n/2835\quad$ and $\quad\gamma=n/37800.$

We now have

$$\int_0^{\infty}\left(\frac{\sin x}{x}\right)^{n}\sim\int_0^{\infty}e^{-\frac{nx^2}{6}}.e^{-\alpha x^4-\beta x^6-\gamma x^8}\cdots dx,$$

and we apply the Laplace method [see (10), p. 431] for deriving asymptotic forms. This is permissible since the function $e^{-\frac{nx^2}{6}}$ has a strong maximum at $x=0$. Expanding the second exponential and using the known integrals

$$\int_0^{\infty}e^{-\lambda x^2}dx=\frac{1}{2}\left(\frac{\pi}{\lambda}\right)^{\frac{1}{2}},$$

$$\int_0^{\infty}x^{2\kappa}e^{-\lambda x^2}dx=\frac{1.3.5.\ \ldots\ (2\kappa-1)}{2^{\kappa+1}\lambda^{\kappa}}\left(\frac{\pi}{\lambda}\right)^{\frac{1}{2}},$$

we obtain

$$\mathrm{P}_n=\frac{2}{\pi}\int_0^{\infty}\left(\frac{\sin x}{x}\right)^{n}dx\sim\frac{2}{\pi}\int_0^{\infty}e^{-\frac{nx^2}{6}}\left\{1-\alpha x^4-\beta x^6-\left(\gamma-\frac{\alpha^2}{2}\right)x^8\right\}dx$$

$$=\sqrt{\left(\frac{6}{\pi n}\right)}\left\{1-\frac{3}{20n}-\frac{13}{1120n^2}-\frac{9}{40n^3}-\ \ldots\right\}.$$

The asymptotic series for $p_n(\xi)$ is obtained in a similar manner. We firstly evaluate some necessary integrals. The known integral

$$\int_0^{\infty}e^{-x^2}\cos 2ax\,dx=\frac{1}{2}\sqrt{\pi}e^{-a^2}$$

may, by a change of variable, be written in the form

$$\int_0^{\infty}e^{-\xi^2/\alpha}\cos 2u\xi\,d\xi=\frac{1}{2}\sqrt{(\pi\alpha)}e^{-u^2\alpha}.$$

Successive differentiation (under the integral sign) with respect to α leads to the formulæ

$$\int_0^{\infty}\xi^2e^{-\xi^2/\alpha}\cos 2u\xi\,d\xi=\frac{1}{2}\sqrt{(\pi\alpha)}e^{-u^2\alpha}\left(\frac{1}{2}\alpha-u^2\alpha^2\right),$$

$$\int_0^{\infty}\xi^4e^{-\xi^2/\alpha}\cos 2u\xi\,d\xi=\frac{1}{2}\sqrt{(\pi\alpha)}e^{-u^2\alpha}\left(\frac{3}{4}\alpha^2-3u^2\alpha^3+u^4\alpha^4\right),$$

$$\int_0^{\infty}\xi^6e^{-\xi^2/\alpha}\cos 2u\xi\,d\xi=\frac{1}{2}\sqrt{(\pi\alpha)}e^{-u^2\alpha}\left(\frac{15}{8}\alpha^3-\frac{45}{4}u^2\alpha^4+\frac{15}{2}u^4\alpha^5-u^6\alpha^6\right),$$

. . . . , the general member of this series being of the form

$$\int_0^\infty \xi^{2n} e^{-\xi^2/\alpha} \cos 2u\xi \, d\xi = \frac{1}{2}\sqrt{(\pi\alpha)}\, e^{-u^2\alpha}$$
$$\times \left(a_{0n}\alpha^n - a_{1n}u^2\alpha^{n+1} + \ldots + (-)^n a_{nn} u^{2n}\alpha^{2n}\right), \quad . \quad (1)$$

where $a_{0n}, \ldots, a_{nn}$ are numerical constants *.

Using the Laplace method we now have

$$\int_0^\infty \left(\frac{\sin x}{x}\right)^n \cos 2ux\,dx \sim \int_0^\infty e^{-\frac{nx^2}{6}}\left\{1 - \alpha x^4 - \beta x^6 - \left(\gamma - \frac{\alpha^2}{2}\right)x^8 - \ldots\right\}\cos 2ux\,dx$$

$$= \int_0^\infty e^{-\frac{nx^2}{6}} \cos 2ux\,dx - \alpha\int_0^\infty x^4 e^{-\frac{nx^2}{6}} \cos 2ux\,dx$$
$$-\beta\int_0^\infty x^6 e^{-\frac{nx^2}{6}} \cos 2ux\,dx - \left(\gamma - \frac{\alpha^2}{2}\right)\int_0^\infty x^8 e^{-\frac{nx^2}{6}} \cos 2ux\,dx - \ldots$$
$$= \frac{1}{2}\sqrt{\left(\frac{6\pi}{n}\right)}\, e^{-\frac{6u^2}{n}}\left\{1 - \frac{3}{20n} + \left(\frac{18u^2}{5} - \frac{13}{1120}\right)\frac{1}{n^2} - \ldots\right\},$$

so that the asymptotic formula for $p_n(\xi)$ follows from (3).

I would like to thank Mr. W. K. Hayman, of St. John's College, for reading the manuscript prior to publication.

References.

(1) Silberstein, L. Phil. Mag. xxxv. p. 395 (1944).
(2) Fränz, K., *Elekt. Nachr.-Tech.* xvii. p. 215 (1940).
(3) Fränz, K., *Hochfrequenztech. u. Elektroakust*, lvii. p. 146 (1941).
(4) Whittaker, E. T., and Watson, G. N., 'Modern Analysis,' 4th edn. (Cambridge, 1927.)
(5) Stewart, C. A., 'Advanced Calculus.' (London, 1940.)
(6) Bateman, H., Bull. Amer. Math. Soc. xlix. p. 494 (1943).
(7) Sedgwick, W. F., Proc. Camb. Phil. Soc. xxxviii. p. 280 (1942).
(8) Ruark, A. E., Phys. Rev. lxv. p. 88 (1944).
(9) Knopp, K., 'Theorie und Anwendung der Unendlichen Reihen.' (Berlin, 1931.)
(10) Courant, R., and Hilbert, D., 'Methoden der Mathematischen Physik,' vol. 1, 1st Edition. (Berlin, 1924.)

---

* These constants may be obained as the solutions of the difference equations

$$a_{0,\,n+1} = \left(n + \frac{1}{2}\right)a_{0n}\,; \quad a_{1,\,n+1} = a_{0n} + \left(n + \frac{3}{2}\right)a_{1n}\,; \ldots;$$
$$a_{i,\,n+1} = a_{i-1,\,n} + \left(n + \frac{2i+1}{2}\right)a_{in}\,; \ldots; \quad a_{n+1} = a_n,$$

subject to the initial conditions $a_{01} = \frac{1}{2}$, $a_{11} = 1$. These result from (1) upon differentiating with regard to α and equating like terms.

LIII. *The Primary and Secondary Scattering of Sunlight in a Plane-stratified Atmosphere of Uniform Composition.*—Part II. *Numerical Tables and Discussion of the Directional Distribution of the Primary Scattered Light.*

By A. Hammad, Ph.D., Department of Applied Mathematics,
The Egyptian University, Cairo [*].

[Received September 1, 1944.]

Introduction and Notation.

1. In a paper [†] (here referred to as Part I.) with the same (main) title as this, exact formulæ were given for the primary and secondary scattered light of any wave-length λ, emitted and received in any direction, at any point in a plane-stratified [‡] atmosphere of uniform composition, extending to infinity in all horizontal directions. No account was taken of refraction, polarization, or transformations of energy from one wave-length to another; each monochromatic component of the light was supposed independent of all others. The light scattered or reflected upwards from the ground was not considered.

Full account was taken of the Rayleigh law of scattering.

The zenith angle of the sun will be denoted by z. Relative to the vertical, and the vertical half-plane through the sun, any other direction may be specified by the polar angles θ, ϕ. For downward travelling light θ will be measured from the upward vertical, while for upward travelling light it will be measured from the downward vertical. Hence for the solar beam $\theta=z$ and $\phi=0$, and for light travelling in the opposite direction $\theta=z$ and $\phi=\pi$.

The fraction of the total mass of the atmosphere that lies *below* the horizontal plane through P is denoted by m; the remaining fraction *above* that plane is $1-m$, also denoted by $\overline{m}$. We refer to m as the *level*, and $\overline{m}$ as the depth, of P in the atmosphere.

The absorption and scattering coefficients of the air, per unit mass, for light of wave-length λ, are denoted by $\alpha(\lambda)$ and $\sigma(\lambda)$; we define $a(\lambda)$, $s(\lambda)$, $c(\lambda)$ by

$$a(\lambda)/\alpha(\lambda)=s(\lambda)/\sigma(\lambda)=\mathrm{M}, \quad c(\lambda)=a(\lambda)+s(\lambda),$$

where M denotes the total mass of air in a vertical column of unit cross-section (1 sq. cm.) extending from the ground throughout the atmosphere;

---

[*] Communicated by Prof. S. Chapman, F.R.S.

[†] A. Hammad and S. Chapman, Phil. Mag. (7) xxviii. pp. 99–110 (July, 1939). The following corrigenda may be noted:—p. 102, last line of § 10, for z read Z; line -4 (*i. e.*, fourth line from bottom), for **k** read **k**′; p. 103, line 6, for cones read cone; p. 105, line -3, for $e^{-\mathrm{Z}}$ read $e^{-\mathrm{Z}\overline{m}}$; line -2, for r read τ.

[‡] On this account the formulæ need correction for low solar altitudes or low altitudes of emission or reception of light, in order to be applicable to an atmosphere on a spherical earth.

a, s and c are called the coefficients of *total* absorption, scattering and extinction for *vertically* incident light (of wave-length λ) descending through the whole atmosphere down to ground-level.

The Direct Solar Beam.

2. The direct sunlight comes from directions confined within a cone of so small an angle (corresponding to the apparent angular diameter of the sun) that this light is here treated as *unidirectional.* If I_∞ is its intensity outside the atmosphere, its intensity at the level m is

$$I_\infty e^{-c\bar{m}\sec z},$$

which decreases steadily as the depth $\bar{m}$ increases, and the faster the lower the altitude of the sun.

The Emission of Primary Scattered Sunlight.

3. At each level in the atmosphere part of the direct sunlight received is scattered in all directions. Its directional distribution, which is not uniform, is given by Rayleigh's law of scattering; it is symmetrical about the direction of the incident sunlight. In any direction inclined to this at the angle ψ, the intensity of emission, E_1, per unit mass of air, is

$$\frac{3\sigma}{16\pi} I_\infty e^{-c\bar{m}\sec z}(1+\cos^2\psi).$$

Thus the directional distribution of the primary scattered sunlight is the same at all levels, though its amount steadily decreases as the depth $\bar{m}$ increases.

The directional distribution of E_1 is represented by the "primary emission" surface $r=E_1$, where r is the radius in the direction θ, ϕ; this is a surface of revolution, about the direction of the incident sunlight, and its polar equation relative to this direction is

$$r=K(1+\cos^2\psi).$$

This surface is far from spherical; its major radius, along the axis $\psi=0$, is 2K, twice as great as its minimum (equatorial) radius K, for $\psi=90°$. The radius of a section transverse to the axis is $r\sin\psi$; this has a maximum which exceeds the equatorial radius K, and is, in fact, $K\sqrt{(32/27)}$ or 1·089 K, corresponding to $\sin\psi=\sqrt{(2/3)}$ or $\psi=54{\cdot}7°$; the maximum cross-sections are at the distances $r\cos\psi$ or $4\,K/3\sqrt{3}$ or 0·77 K on either side of the centre. The existence of these maximum sections implies that the above surface is slightly dumb-bell shaped.

The mean value of r is 4K/3, so that the maximum and minimum values of r (namely 2K and K) are 50 per cent. greater and 25 per cent. smaller than the mean. A better representation of the departure from isotropy of the directional distribution of emission of primary scattered light is the root mean square departure of r from its mean value; its value is $10\sqrt{5}$ or 22·4 per cent. of the mean.

The Reception of Primary Scattered Sunlight.

4. The whole atmosphere is luminous with primary scattered sunlight, *emitted* in different degrees in different directions and at different levels. Such light is *received* at any point P from the whole atmosphere, from all directions (except when P is at the top or bottom of the atmosphere), and from all distances, though the light reaching P is attenuated by absorption and scattering on its journey to P from the point of its origin by primary scattering. It is shown in Part I., § 12, that the intensity of reception, R_1, at the level m, of primary scattered light from the direction θ, ϕ, falling per unit area on a surface normal to this direction, is

$$f(\lambda, z, \theta, \phi)e^{-Z}\frac{e^{mZ}-e^{-m\Theta}}{Z+\Theta} \quad . \quad . \quad . \quad . \quad . \quad . \quad . \quad (1)$$

for upward travelling light, or

$$f(\lambda, z, \theta, \phi)\frac{e^{-\bar{m}\Theta}-e^{-\bar{m}Z}}{Z-\Theta} \quad . \quad . \quad . \quad . \quad . \quad . \quad . \quad . \quad (2)$$

for downward travelling light, where

$$Z=c \sec z, \quad \Theta=c \sec \theta, \quad . \quad . \quad . \quad . \quad . \quad . \quad . \quad . \quad (3)$$

and $$f(\lambda, z, \theta, \phi)=\frac{3s}{16\pi}I_{\infty} \sec \theta\,(1+\cos^2 \psi), \quad . \quad . \quad . \quad . \quad . \quad . \quad . \quad (4)$$

$$\cos^2 \psi=\{\cos z \cos \theta+\sin z \sin \theta \cos \phi\}^2. \quad . \quad . \quad . \quad (5)\ *$$

When $\theta=z(<90°)$, the last factor in (2) is of the form 0/0, and must be replaced by $\bar{m}\, e^{-\bar{m}Z}$.

The directional distribution of the primary scattered light *received* at any point is represented by the "primary reception" surface $r=R_1$, where r is the radius in the direction θ, ϕ.

This surface differs from the surface $r=E_1$ for the primary *emitted* light (§ 3), in that it is not a surface of revolution (except when $z=0$). The two surfaces are alike in one respect, however, namely, that their conical sections θ=constant, for the same value of θ, have the same *form*; this is because both E_1 and R_1 depend on ϕ in the same way, namely, only through the factor $1+\cos^2 \psi$. The *scales* of such sections, however, vary differently with θ.

At the top of the atmosphere ($m=1$), scattered light is received solely from below, and the surface $r=R_1$ therefore consists of a curved portion lying below the horizontal and a horizontal plane "cover"; at the base of the atmosphere ($m=0$) the scattered light is received solely from above, and the surface consists of a curved portion above a horizontal plane base. At intermediate levels the surface lies both above and below the origin.

When the sun is in the zenith ($z=0$) the primary reception surface is one of revolution about the vertical. For this case Table I. illustrates the form of the surface at different levels in the atmosphere, for a particular value of c, namely 0·5 *, by giving the value of r' defined by

---

* In fact, $\cos \psi$ is positive for downward-travelling light and negative for upward-travelling light,

$$r/r' = \mathrm{R}_1/r' = 3s\,\mathrm{I}_\infty/16\pi,$$

for different directions specified by sec θ.

TABLE I.

Primary reception surface: values of r'.

Zenith sun: $c=0{\cdot}5$.

Level in atmosphere.	Direction of radiation.	sec θ.					
		1 ($\theta=0$)	1·1	1·2	2	3	∞ ($\theta=90°$).
$m=1$ (top)	Upgoing	1·2642	1·2945	1·2332	1·2948	1·4411	2
$m=0{\cdot}8$	Upgoing	0·9965	1·0240	0·9788	1·0539	1·2036	1·8097
	Downgoing	0·3619	0·3620	0·3644	0·4306	0·5469	
$m=0{\cdot}7$	Upgoing	0·8666	0·8922	0·8544	0·9325	1·0808	1·7214
	Downgoing	0·5164	0·5151	0·5173	0·5995	0·7436	
$m=0{\cdot}6$	Upgoing	0·7388	0·7620	0·7312	0·8098	0·9536	1·6375
	Downgoing	0·6550	0·6514	0·6527	0·7421	0·8997	
$m=0{\cdot}5$	Upgoing	0·6129	0·6334	0·6090	0·6849	0·8205	1·5576
	Downgoing	0·7788	0·7727	0·7723	0·8614	1·0214	
$m=0$ (ground) .	Downgoing	1·2130	1·1886	1·1736	1·1933	1·2780	1·2130

This table shows that at the top of the atmosphere more primary scattered radiation is received than at the ground; this is natural because the intensity of primary emission steadily decreases downwards owing to the downward diminishing of the intensity of the solar beam. The difference would be greater for greater values of c, and less for smaller values, corresponding (in the visible-spectrum) to longer wave-lengths.

---

* This corresponds to light of wave-length slightly less than 3700 Å, according to the Mount Wilson observations (adjusted to sea-level).

The horizontal radiation (last column) steadily decreases downwards, at the same rate as the incident solar beam; the upgoing radiation decreases downwards at a greater rate; the downgoing radiation steadily *increases* downwards.

In the upper half of the atmosphere the most intense received radiation is from the horizontal; but nearer the ground the direction of maximum received radiation rises somewhat, presumably because of the greater absorption in the lowermost layer.

Fig. 1 shows, by continuous lines, the vertical section of the surfaces r' for zenith sun, $c=0{\cdot}5$, at the top, middle and base of the atmosphere ($m=1, \frac{1}{2}, 0$).

When the sun is not in the zenith, the primary reception surface is not one of revolution about the vertical. Table II. gives values of r' for $z=60°$, $c=\frac{1}{2}$, at several levels in the atmosphere; the values of r' refer to the vertical plane ($\phi=0$ and $\phi=\pi$) through the sun.

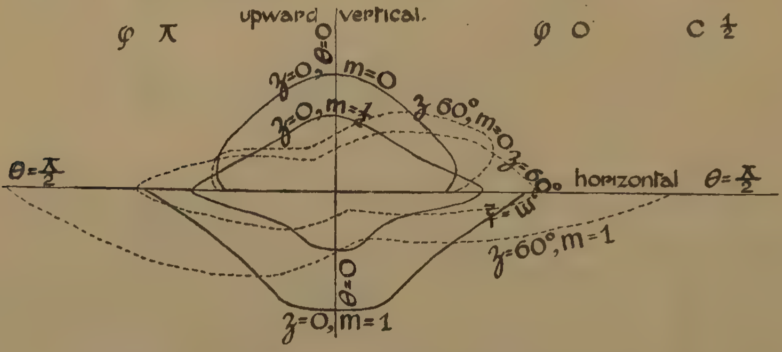

Fig. 1 shows by broken lines the form of these meridianal vertical sections of the surface for $z=60°$, for $c=\frac{1}{2}$, and for the same atmospheric levels as before ($m=1, \frac{1}{2}, 0$). The most notable changes in the primary reception surface from that for zenith sun to that for the sun at 60° zenith distance are: (*a*) the greater reduction of R_1 from the top of the atmosphere to the ground (corresponding to the greater attenuation of the incident sunlight at the ground), and (*b*) the increased preponderance of radiation from the horizontal and neighbouring directions. This is due to the infinite horizontal extension of mass in the atmosphere and the limited vertical distribution. This influence of greater horizontal extension of mass outweighs the influence of the preferential primary scattering along the direction of the solar beam, though the vertical section of the R_1 surface has a larger area in the two opposite quadrants containing the solar beam than in the intervening quadrants.

The sum of the primary radiations received from two given opposite directions varies with height, and may be shown to have its maximum value when the amounts from the two directions are equal.

TABLE II.

Primary reception surface : values of r'.

Sun's zenith distance 60° ; $c=\frac{1}{2}$.

Level in atmosphere.	Direction of radiation.	$\phi=0$ sec θ.					$\phi=\pi$ sec θ.			
		∞	3	2	1·2	1	1·2	2	3	∞
$m=1$ (top) . .	Upgoing	3·5	2·166	1·729	1·078	0·648	0·601	1·081	1·556	3·5
$m=0·8$	Upgoing	2·864	1·671	1·307	0·799	0·476	0·445	0·817	1·209	2·864
	Downgoing		0·919	0·655	0·369	0·215	0·205	0·409	0·664	
$m=0·6$	Upgoing	2·346	1·209	0·937	0·559	0·331	0·311	0·586	0·889	2·346
	Downgoing		1·428	1·072	0·628	0·371	0·350	0·670	1·032	
$m=0·5$	Upgoing	2·123	1·019	0·766	0·451	0·267	0·251	0·479	0·736	2·123
	Downgoing		1·570	1·213	0·725	0·431	0·404	0·758	1·146	
$m=0$	Downgoing	1·285	1·710	1·470	0·977	0·597	0·544	0·920	1·235	1·285

The Total Primary Scattered Radiation Received at the Ground.

5. The total primary scattered radiation received per unit time per unit *horizontal* area on the ground is obtained by integrating $R_1 \cos\theta$ at $m=0$ over all directions of downcoming radiation. The integration is in some respects similar to that of § 13 of Part I. and gives as the result

$$\frac{3s}{16} I_{\infty} \{(2+\sin^2 z) L_2(c, z, m)+(2-3 \sin^2 z) L_4(c, z. m)\},$$

where at the ground $m=0$. For $z=60°$, $c=\frac{1}{2}$, $L_2=0{\cdot}3222$ and $L_4=0{\cdot}1420$, so that the above "curly bracket" factor is 0·8505.

The above expression when $m=1$ gives the rate at which primary scattered radiation per unit horizontal area is lost to free space at the top of the atmosphere.

When tables of the functions L_2 and L_4 become available they will make possible the detailed study of how the ground-received or sky-lost primary scattered radiation varies with c and z, that is, for different wave-lengths and different altitudes of the sun.

Acknowledgement.

I wish to acknowledge the great help I got from Professor S. Chapman in putting this paper in its present form.

LIV. *Systems with Gyroscopic Coupling Terms* (1).

To the Editors of the Philosophical Magazine.

Gentlemen,—

I notice that in the circuit of fig. 14 of my paper the source of primary excitation is shown as a voltage source, whereas to be consistent with equ. (36) it should have been shown as a current source. This slip—for which I duly apologize—may have been one of the causes of the difficulties which Mr. Jefferson encountered (2) in the last section of my paper. Perhaps, however, another cause was what I believe to be a fundamental difficulty in his own approach to the direct type of electromechanical analogy, which he has since brought out clearly by an application contained in the enlarged version of his original paper (3) in the 'Marconi Review' (4).

The example given there (figs. 21 and 22) shows that in certain circumstances, which are also fulfilled in the present case, Mr. Jefferson's method will result in an electrical analogue with a parallel connection of elements where a series connection is required. (It also shows that this method will on occasion result in an open-circuited electric chain where there should be a short-circuited one.)

These difficulties do not affect the alternative suggestion put forward in his letter, and I agree that it will sometimes be sufficient to draw a representative circuit using only the inverse analogy but including the electrical counterpart of the gyrostatic coupler. I would like, however, to make it clear that by doing so he merely restates in electrical terms.the problem from which the developments of Section 11 of my paper start, He does not explain the effect of such a mixed coupling in terms of the action of simpler elements—as is done in that section.

As a gyrostatic coupler converts a mechanical impedance into its inverse, so must its electrical counterpart. Your correspondent would therefore have been entitled without further analysis to assert that the electrical counterpart of such a coupler would have to be an inverting transformer (still meaning thereby a device which converts "Z" into "1/Z"). I cannot share his preference for the designation "inverting transformer of ratio 1 : j (or, in the general case 1 : jn). We expect the square of a transformer ratio to appear as multiplier in the impedance transformation effected by the transformer; hence we are here liable to be misled into thinking that a resistance is transformed into a negative resistance. This consideration seems to be more relevant than an allusion to a certain 90 degrees spatial relation in the original gyrostatic coupler or to an interpretation of one of the various matrix forms describing the behaviour of such a device. I also think that the diagrammatic symbol shown in the letter is apt to be read as signifying an ordinary transformer of ratio 1 : j. The bridging link should evidently be labelled $1/Z_k$ instead of Z_k.

I agree again with your correspondent's observation that a tandem combination of an electro-static and an electro-magnetic converter would act as such an inverting transformer. He may be interested to know that a remark to that effect was contained in the first (1939) and second version of my paper on "Electro-Mechanical Analogies" (5), but that it was omitted together with a considerable amount of other material from the shortened version finally published.

References.

(1) 'Philosophical Magazine,' May 1944.
(2) Letter, 'Philosophical Magazine,' March 1945.
(3) 'Wireless Engineer,' December 1944.
(4) 'Marconi Review,' April/June 1945.
(5) "Electro-Mechancial Analogies and their use for the Analysis of Mechanical and Electro-Mechanical Systems," 'Journal of the Institution of Electrical Engineers,' xcii. part 1, no. 52 (April, 1945).

Yours faithfully,
A. Bloch.

Research Laboratories,
General Electric Company, Ltd.,
Wembley.
29th August, 1945.

LV. *Notices respecting New Books.*

The Lighting of Buildings. By the Lighting Committee of the Building Research Board. (H.M. Stationery Office.) Price 2*s.* 6*d.*

In 1942 the Committee was requested to review present practice at home and abroad in the lighting of buildings, and to make recommendations for post-war practice and research. A systematic collection of data, such as the report contains, was therefore only to be expected; but the Report does, in fact, accomplish a great deal more. Considering the wide variety of probable readers, the Committee has devoted much space to explanation and illustration, thus greatly improving the readability, while enhancing the practical value of the detailed analyses, and tables of design data.

The main part of the Report deals with lighting in dwelling-houses and schools only ; this limitation having been made to ensure early publication of the Report ; while much of the statistical part of the work is contained in a series of appendices. Among these are to be found details of investigations by Wartime Social Survey, the Committee having spared no pains to check experimental conclusions against the actual experiences of householders.

From so comprehensive a study it is especially unsatisfactory to particularise ; but the layman cannot fail to be impressed by the striking exposition of the principles of estate lay-out considered as a problem in daylight illumination of interiors : while the professional student will find a rich store of design data, and working instructions of a distinctively practical kind. The final standards of artificial illumination are more moderate than those of the Illuminating Engineering Society ; nevertheless, as an appendix makes clear, the average cost of installation to the Committee's specifications would exceed that of the usual installation by some 50 per cent., while the running costs would be about 100 per cent. greater. The Committee has discovered that under the Housing Act of 1936, Local Authorities may make and enforce lighting regulations. After reading the Report, one returns to this announcement with a regret that such an opportune revelation was not brought to the notice of local authorities more urgently and more emphatically ; for it seems very doubtful whether the originators of the present re-housing schemes have, after all, paid much attention to the reasonable and balanced recommendations of the Report. J. P. A.

Synthetic Rubber from Alcohol. A survey based on the Russian Literature, by Anselm Talalay and Michel Magat. (Interscience Publishers, Inc., New York, 1945.)

The synthetic rubber which has been made in Germany, the United States and Russia during the war is a co-polymer of butadiene, a compound which is mainly produced from alcohol. The authors have written up the subject from the Russian literature but they include many references to German, British and American publications and patents. The Russians favour the Lebedev process in which alcohol is passed over a combined catalyst which splits off hydrogen and water in one operation to form butadiene—and many by-products which reduce the yield. Better yields can be obtained by separate processes, but the choice of a low efficiency process is justified because the plant is simple and can be constructed quickly for war production. The survey covers not only chemical investigations of the process but also laboratory, pilot and industrial installations. More than half the book is devoted to the physical chemistry of polymerisation and of the polymers of butadiene. Russian chemists who are devising processes and building plants for the manufacture of new products—such as synthetic rubber—are using much the same methods of attack as are their fellow scientists in the U.S.A. and Britain, and they publish in their own literature no more about the processes than we do. They are very much alive to adopting processes which, while not being the most efficient, are best suited to the conditions existing in Russia. It is to be hoped that some day the whole story of a research and its application to the building up of a large industry will be written.

[*The Editors do not hold themselves responsible for the views expressed by their correspondents.*]

LVI. *Compatibility of Stress and Strain in Yielded Metals.*

By K. H. Swainger, Ph.D., B.Sc.(Eng.)*.

[Received April 12, 1945.]

Abstract.

A general theory of strain and stress compatibility in yielded metals is evolved from well-known experimental results and the Energy of Deformation Theory of Yield due to Huber, von Mises, and more recently Hencky.

Consideration of simple tension and compression tests indicates that the inelastic deformation may be regarded as built up by the superposition of an elastic component and a plastic component of strain. These strain components are regarded separately for extension to a 3-dimensional field of strain. Each component has an appropriate transverse contraction ratio.

The metal is not a continuum so the action of its constituent crystals is considered. Experimental evidence gives the anisotropic stress-strain relationships for the crystals. The crystals are more or less at random orientation and small compared with the metal specimen. Hence, we suggest the hypothesis that all effects will be statistically isotropic in an analysis.

Isotropy of strain-hardening introduces the writer's function of strain P. P is the slope of the simple tensile stress-strain curve after yield has begun. At any point in a yielded field P has the same value in all directions to satisfy isotropy.

The strain in direction 01 for the normal stresses $(S_1S_2S_3)$ is

$$e_1=\frac{1}{P}[S_1-p(S_2+S_3)-S_{01}+p(S_{02}+S_{03})]$$

$$+\frac{1}{E}[(p-q)(S_2+S_3)+S_{01}-p(S_{02}+S_{03})],$$

with similar expressions for directions 02 03 when

p is the plastic transverse contraction ratio ;

q is the elastic transverse contraction ratio ;

S_{01} S_{02} S_{03} are the stresses in the three orthogonal directions when the element yielded.

Non-linear equations result in the theory if the complete stress-strain curve is expressed in closed form. However, if P is taken as constant the expressions are greatly simplified. If P=0 as used in most of Nadai's

---

* Communicated by Prof. G. Temple, F.R.S.

analyses then the first term of strain becomes meaningless. It is seen that, in general, P must be positive and greater than zero for a stable field.

Shear stress T in plane 01, 02 gives shear strain

$$e_{12}=\frac{2(1+p)}{P}\left\{\left[1-\frac{P}{E}\left(\frac{p-q}{1+p}\right)\right]T-\left(1-\frac{P}{E}\right)T_0\right\},$$

where T_0 is the shear stress acting on the element when it began to yield. (The strain expressions show that the body suffers irreversible changes of shape in these directions.)

The strain equations may be combined with the equilibrium equations in the usual way by using stress function K and with P constant. Plane stress for cartesian axes ox, oy then gives, when body forces are zero,

$$\nabla^4 K=\left(1-\frac{P}{E}\right)\left[\begin{array}{l}\dfrac{\partial^2}{\partial x^2}(S_{0y}-p.S_{0x})\\ \qquad+\dfrac{\partial^2}{\partial y^2}(S_{0x}-p.S_{0y})\\ \qquad-2(1+p)\dfrac{\partial^2 T_0}{\partial x\,\partial y}\end{array}\right].$$

Professor Temple has pointed out that by stating $S_{0x}\,S_{0y}\,T_0$ as partial differential coefficients of a function Y_0 we call the Yield Function then the plane stress equation becomes

$$\nabla^4 K=\left(1-\frac{P}{E}\right)\nabla^4 Y_0.$$

The equation is thus seen to be invariant with rotation of the axes. When $P=E$ the right-hand side becomes zero to give the usual statement of elasticity. Our more general forms include those of elasticity as particular cases.

Plane stress due to pressure in a circular hole in a large plate is considered fully. P is justified as constant for this problem by comparing a solution found by step-by-step when P is not constant with a solution when P is constant. The stress values are not very different in the two solutions.

Superposition of stresses in yielded metals can cause either elastic or inelastic strains. Hence, Huber's yield test must be used to show if strains are elastic or inelastic when compatibility is sought in any particular problem.

The plane stress problem already solved is now freed of its boundary pressure to demonstrate superposition. The hole boundary tangential stresses are now seen as large values of compression.

Introduction.

The mathematical theory of elasticity has been evolved from the stress-strain relationships found in a simple tensile test of any given metal over a range of loading limited to the "elastic" state. It is then hypothesized that these simple tensile test results may be superimposed to represent a complex distribution of normal stresses. The deformations due to shear tractions are likewise related to the simple tensile test after stating suitable hypotheses. Hence we conclude that the mathematical theory of elasticity is entirely dependent on the simple tensile test.

It is now proposed to evolve generalized stress-strain relationships that apply beyond the elastic range of metals. The simple tensile test will be used to give the new theory. These new stress-strain relationships may form the basis for a mathematical theory of inelasticity.

1. *Strain in a Metal Specimen under Simple Tension or Compression.*

Engineering metals are usually tested for their simple tensile properties. Consider a typical stress-strain curve from such a test. There is a range of stress from O to S_0 in which the specimen behaves in an elastic manner. In this range the strain disappears when the load is released. It is understood that the temperatures at the time of test are normal and that any loading or unloading does not take too long, *e. g.* 10 mins. to load up or down so that creep does not occur appreciably. Further, the accuracy of measurement is of the usual engineering laboratory values of 10^{-4} to 10^{-5} inch. Very refined measurements have shown that the true elastic range of stress is small (Appendix B, Ref. 1.) In the present paper such refined measurements will not be discussed, so that within the limits of our imposed conditions an appreciable elastic range will be observed. Load is applied and the specimen remains elastic up to stress S_0, but beyond this stress the strain increases more rapidly than it did in the elastic range. Stress S_0 is defined as the yield stress of the

Fig. 1.1.

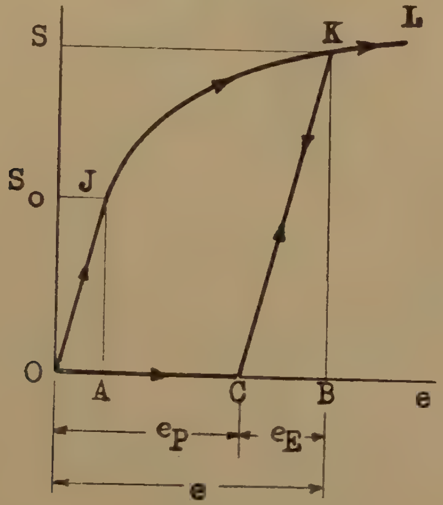

metal under the particular conditions of the test. We shall refer to the strains as " inelastic " beyond the yield point. The stress will be S and the strain e at the general point K in the inelastic part of the curve.

Releasing the load gives an approximately straight line curve parallel o OJ in fig. 1.1.

Observation 1.1.—*During unloading the specimen suffers the elastic strain* BC, *and when the load is zero there remains a permanent or " plastic " strain* CO.

Measurement shows that the specimen has suffered a permanent decrease in cross-section in sympathy with the permanent increase in length.

Fig. 1.2.

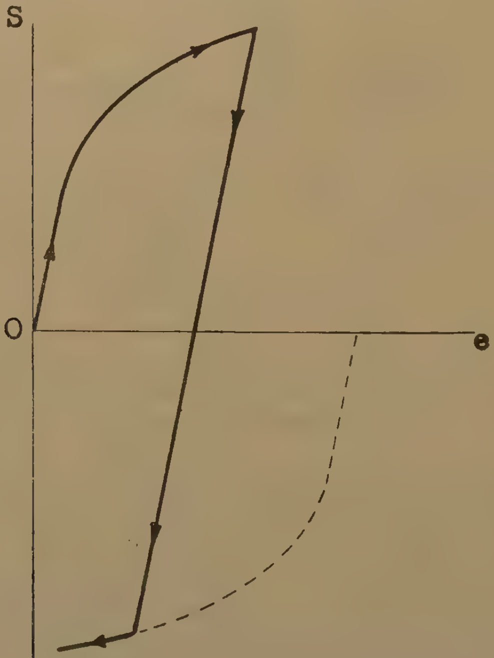

Observation 1.2.—*The stress-free specimen has now regained its initial volume, although the shape is slightly different.*

The specimen is again an elastic one of slightly different shape and with a higher yield stress.

Reloading the specimen gives the curve CKL. KL is as though it is a continuation of the curve OJK. Hence the yield stress for the curve CKL is approximately that stress from which the specimen was unloaded.

Observation 1.3.—*If, after loading up* OJK *to point* K, *a compression stress less than* S *is applied the specimen will respond elastically. If,* *after reaching* K, *the stress* S *is increased then the specimen responds inelastically.*

The increase of yield from S_0 to S is usually explained as " work-hardening " due to the inelastic strain.

Observation 1.4.—*If, after yield under simple tension, the load is reversed to simple compression then the specimen has approximately the same value of yield as it did under the tension.* (Appendix B, Ref. 2.1.) (See fig. 1.2.)

An effort towards a rational explanation and hence ultimately an analysis of inelastic strains in an aggregate of crystals such as occurs in engineering metals, has forced experimenters to study single crystals of metal as the simplest element of the problem. It has been found that under simple tension a metal crystal develops " glide planes," with a particular orientation for the metal concerned.

Fig. 1.3.

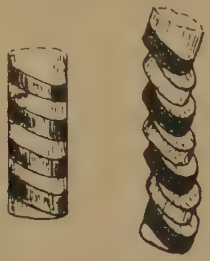

Fig. 1.4.

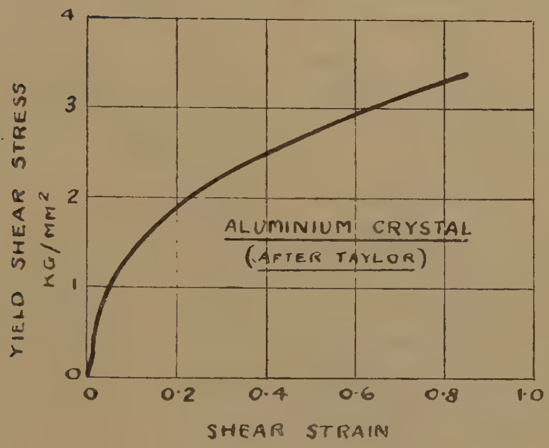

Similar glide planes develop in a simple compression specimen. (See fig. 1.3.) (Appendix B, Ref. 3.1.)

Further, a definite shear yield increase occurs in the crystal shear planes. (Fig. 1.4.) (Appendix B, Ref. 3.2.)

However, a specimen of metal is composed of many crystals and crystallites more or less at random orientation. Hence,

Observation 1.5.—*If all the crystals in a particular neighbourhood develop glide planes then that particular region is inelastically deformed in all directions.*

Evidently, the behaviour of the specimen aggregate of crystals is different from that of the single crystal in general. The behaviour of the specimen bears a statistical relationship to the behaviour of the single crystal. (Appendix B, Ref. 4.1.) Hence it is likely we shall have to explain the behaviour of the metal specimen by some law related to the law of behaviour of the crystal but different in quality.

We now have sufficient data to construct a theory of strain allowing great analytical generalization, with the help of a little more experimental evidence discussed subsequently.

2. *Strain in a Yielded Metal Element under Complex Principal Stresses.*

Elasticity problems are usually solved by using the hypothesis that the elastic material properties are isotropic in the deformed body. It is well known that this a not the exact condition prevailing, but it is sufficient as a good approximation. As a result of Observation 1.5 we now state a similar hypothesis for inelastic strains.

Hypothesis 2.1.—*In an inelastically deformed body the elastic and plastic strain effects are isotropic.*

Consider the orthogonal directions 01, 02, 03 at a point in an inelastically strained metal. A complex stress system acts on the element. Direction 01 isolated from the other two would evidently give stress-strain similar to the simple tensile of fig. 1.1. Strain will again be of two parts *,

$$\epsilon_{E1} \text{ elastic}, \quad \epsilon_{P1} \text{ plastic}.$$

The same reasoning applies to the other two directions considered separately.

Hence with Hypothesis 2.1 the elastic strain in the direction 01 when the complex system operates is

$$e_{E1}=\epsilon_{E1}-q(\epsilon_{E2}+\epsilon_{E3}), \quad \ldots \ldots \quad (2.1)$$

and the plastic strain in the direction 01 is

$$e_{P1}=\epsilon_{P1}-p(\epsilon_{P2}+\epsilon_{P3}), \quad \ldots \ldots \quad (2.2)$$

where p is the transverse contraction ratio for plastic strain.

In Observation 1.2 we saw that the simple tensile specimen regained its original volume although its shape was a little different when it was stress-free after yielding. Similarly, for the element of fig. 2.1 we may state for the plastic part of the strain

---

* Notice the change of notation. Epsilon ϵ is used for "partial" strains in the appropriate directions. The partial strains in a complex strain distribution give the total strain in any given direction after the introduction of the transverse contraction ratio. In a simple tensile test the ϵ becomes e.

$$\epsilon_{P1}+\epsilon_{P2}+\epsilon_{P3}=0, \quad . \quad . \quad . \quad . \quad . \quad . \quad . \quad (2.3)$$

or, what amounts to the same thing, suppose that we are dealing with an incompressible substance so that the plastic transverse contraction ratio may be taken as

$$p=\tfrac{1}{2}. \quad . \quad . \quad . \quad . \quad . \quad . \quad . \quad . \quad . \quad (2.4)$$

Fig. 2.1.

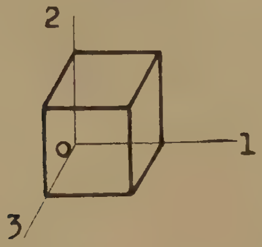

Fig. 2.2.

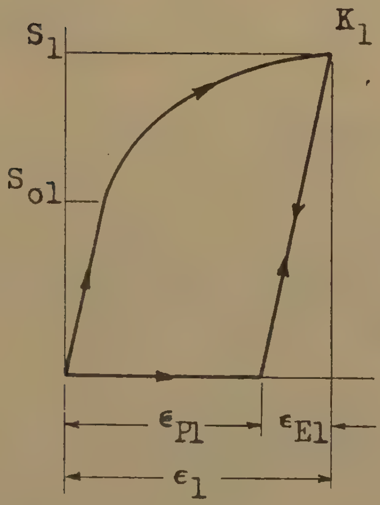

The total strain in the direction 01 is

$$e_1=e_{E1}+e_{P1} \quad . \quad . \quad . \quad . \quad . \quad . \quad . \quad . \quad (2.5)$$

with similar expressions for directions 02, 03.

But,

$$\epsilon_{P1}=\epsilon_1-\epsilon_{E1}, \quad . \quad . \quad . \quad . \quad . \quad . \quad . \quad . \quad . \quad (2.6)$$

with similar expressions for directions 02, 03.

Substitute (2.6) in (2.2) and (2.5) gives

$$e_1 = \begin{bmatrix} \epsilon_1 - p(\epsilon_2 + \epsilon_3) \\ +(p-q)(\epsilon_{E2} + \epsilon_{E3}) \end{bmatrix}, \quad . \quad . \quad . \quad . \quad (2.7)$$

with similar expressions for directions 02, 03.

3. *Stress in a Yielded Metal Element under Complex Principal Stresses.*

An element is acted upon by the three components of principal stress. The behaviour of the element is well known when it is still elastic. Now suppose the stresses are increased to S_{01}, S_{02}, S_{03} when the element is just about to yield. Now increase the stresses to S_1, S_2, S_3 so that the element suffers inelastic deformations. The problem is to relate these stresses to the strains they induce.

We now state a stress hypothesis analogous to Hypothesis 2.1 for isotropy of strain.

Fig. 3.1.

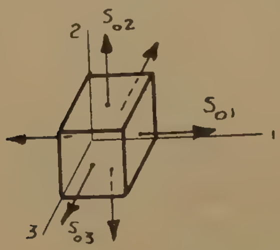

Fig. 3.2.

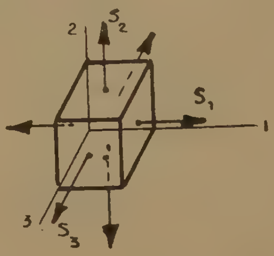

Hypothesis 3.1.—*Work hardening or rate of increase of yield stress with strain is isotropic and is a function of the stresses or the corresponding strains present.*

Suppose stress system S_1, S_2, S_3, of which S_1 is shown in fig. 2.2, is equivalent to stress S in fig. 1.1. Hypothesis 3.1 then states that the slope P at K in fig. 1.1 is the same as the slope P_1 at K_1 in fig. 2.2. Similarly for the other two directions, so that

$$P = P_1 = P_2 = P_3. \quad . \quad . \quad . \quad . \quad . \quad . \quad . \quad . \quad (3.1)$$

The values S_{01}, S_{02}, S_{03} at which yield occurs have been suggested by a number of theories. (Appendix B, Ref. 2.2.)

The *Energy of Deformation* Theory of Yield, due to Huber, von Mises, and more recently Hencky, was found to fit the experimental evidence best. (Appendix B, Refs. 2.3 and 5 respectively.) This theory divides the potential energy of an *elastic element* into two parts (Appendix B, Ref. 2.4):—

(i) due to change in volume,
(ii) due to change in shape.

Experimental evidence showed that an element behaved elastically under pure tension or compression values many times greater than those at which the material yielded under complex stresses. Hence it was suggested that the energy to change the volume of the element had a negligible effect on its yield. Therefore, Huber suggested that the energy due to *change in shape* governed the yielding of a material.

Further, we may note that the discontinuities, etc. (of various writers) in the finite body will tend to be statistically isotropic. This is in agreement with Observation 1.5. Hence we state,

Hypothesis 3.2.—*An elastic element yields when the stresses are such that the energy of change of shape reaches a value which is independent of the arrangement of the stress components.*

State the change of shape energy under a complex principal stress system S_{01}, S_{02}, S_{03}, and again under simple tension or compression S_0. Equate these two energies to satisfy Hypothesis 3.2 and we have

$$(S_{01}-S_{02})^2+(S_{02}-S_{03})^2+(S_{03}-S_{01})^2=2S_0^2. \quad . \quad . \quad . \quad (3.2)$$

Further, at any point in the yielded field where the complex principal stresses are S_1, S_2, S_3 they will satisfy the relationship

$$(S_1-S_2)^2+(S_2-S_3)^2+(S_3-S_1)^2=2S^2, \quad . \quad . \quad . \quad . \quad (3.3)$$

where S is the "Equivalent Stress" on the simple tensile stress-strain curve. S is seen in fig. 1.1 to be the new yield stress for the material at the point where S_1, S_2, S_3 operate. Corresponding to the equivalent stress S is the equivalent strain *e*.

Expression (3.2) is reasonably useful because S_0 is easily determined. In general, analytical difficulty occurs because of the squares and products of stresses. Non-linear expressions are often difficult to manipulate.

4. *Stress-Strain in a Yielded Metal Element under Complex Principal Stresses.*

The shape of the stress-strain curve beyond the yield is such that an analytical expression fitting it leads to non-linear expressions in general. Because these non-linear expressions are difficult to manipulate we consider immediately finite differences giving linear equations allowing good approximations to the true conditions. Consider the simple tensile test in fig. 1.1.

Suppose S is not very different from the yield stress S_0. Between S_0 and S draw the chord shown in fig. 4.1 at slope P, which we shall call the slope of the inelastic curve at S_0. Hypothesis 3.1 states that P will have the same value in the directions 01, 02, 03 in which the stresses S_1, S_2, S_3 operate for a complex distribution. Hence in an actual solution we calculate the upper limit stresses S_1, S_2, S_3 equivalent to S for which the value P is justified.

Partial strains from the stress-strain curve for direction 01 are

$$\epsilon_{E1}=\frac{S_1}{E}$$

$$\epsilon_1=\frac{S_{01}}{E}+\frac{S_1-S_{01}}{P}, \quad . \quad . \quad . \quad . \quad . \quad . \quad . \quad . \quad (4.1)$$

so that

$$\begin{aligned}\epsilon_{P1}&=\epsilon_1-\epsilon_{E1}\\&=\left(\frac{1}{P}-\frac{1}{E}\right)(S_1-S_{01}),\qquad\qquad(4.2)\end{aligned}$$

Fig. 4.1.

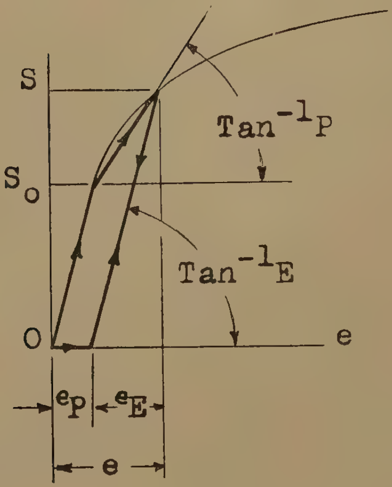
S
S_o
Tan^-1P
Tan^-1E
O
e
e_P
e_E
e

Fig. 4.2.

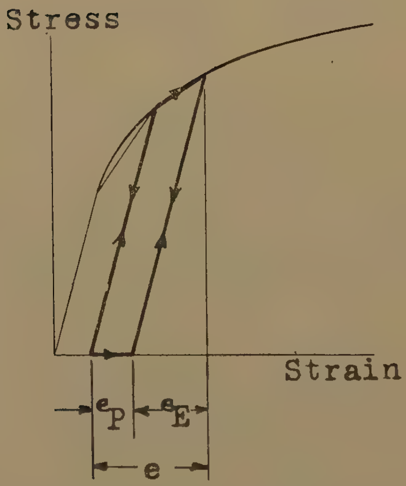
Stress
Strain
e_P
e_E
e

with two similar expressions for directions 02 and 03. Substitution in (2.7) gives

$$\begin{aligned}e_1=&\frac{1}{P}[S_1-p(S_2+S_3)-S_{01}+p(S_{02}+S_{03})]\\&+\frac{1}{E}[(p-q)(S_2+S_3)+S_{01}-p(S_{02}+S_{03})],\qquad(4.3)\end{aligned}$$

with two similar expressions for directions 02 and 03.

In the second step is used the slope of the simple tensile test inelastic curve at the upper limit equivalent stress S of the first step. The upper limit equivalent stress for the second zone with a constant P is found as for the first zone.

The procedure is repeated along the curve as far as is required. P very quickly assumes a value independent of stress or strain approximately. This paper considers only small strains such that their squares and products are negligible compared with their first order. Hence yield in the complex field cannot be considered for strains greater than a few per cent.

The strain expression (4.3) is seen to be divided into two components. Factor P^{-1} appears in one and E^{-1} in the other. Near the yield boundary P has a value of the same order of magnitude as E, so that the two components are equally important. Away from the yield boundary P decreases rapidly but cannot become zero or the strain becomes indeterminate *. Zero slope would mean physically that once yield occurs the displacements are independent of stress and so naturally lead to anomalies.

Professor Southwell remarks that the more simple relationship for elastic strains is only a working hypothesis allowing a rational theory of elasticity to be evolved, but is " more than can be verified by direct experiment." (Appendix B, Ref. 8.1.)

We must apply the statement to our inelastic strains (4.3), but shall consider it an experimental justification if the strains predicted by theory are found in some particular cases.

5. *Partial Yielding of Metal under Principal Stresses.*

Consider the adjacent elastic and inelastic elements each side of the surface, across which yield occurs for the system shown in fig. 5.1. Since the metal is continuous across the common boundary, it is obvious that as the elements decrease in size the $(S_1)_E$ and $(S_1)_P$ approach closer and finally become indistinguishable from each other. That is, that stress must be continuous across the common boundary. The same reasoning applies to directions 02 and 03. Physically this means that the elastic element is only just elastic while the inelastic element is just inelastic. We now state a working hypothesis.

---

* A Nadai, ' Plasticity,' 1932, uses the inelastic curve of zero slope beginning abruptly at the yield point. Again, in " The theory of the expanding of boiler and condenser tubes joints through rolling," A. S. M. E., November, 1943, he uses the same arbitrary assumption.

The writer used the same assumption in a discussion of plane strain yielding in his doctoral thesis. Better stress-strain compatibility was secured than in the available published work at that time. However, there appeared, as in Nadai's analyses, anomalous stress discontinuities at the yield surface.

It was concluded that the existing analyses were insufficient. The present paper is the result of a fresh attempt to secure complete stress-strain compatibility.

Hypothesis 5.1.—*Yield is continuous across the common boundary between elastic and inelastic zones in partially yielded metals.* (Appendix B, Ref. 6.1.)

Further, for continuity of the body across the common boundary the displacements must be the same. Strain expressions (4.3) show that strain is also continuous at the yield surface. Hence we state another working hypothesis.

Hypothesis 5.2.—*Strains and displacements are continuous across the common boundary between elastic and inelastic zones in partially yielded metals.*

Fig. 5.1.

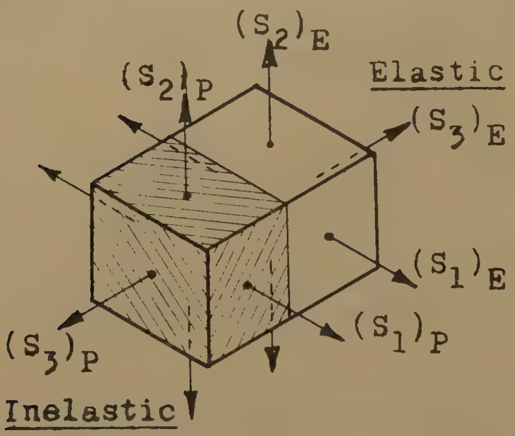

6. *Yield under Plane Stress due to Pressure in a Circular Hole in a Large Plate.*

This problem will be considered in detail as it lends itself to fairly easy experimental check.

The transverse stress S_z is zero. From symmetry there is no shear on a polar element, so that the stresses are principal stresses. The formulæ are as evolved previously when the directions are

$$01=Or,$$

$$02=\theta,$$

$$03=Oz,$$

Tensions are positive.

Yield has progressed to $r=c$ under the pressure S_R acting on the boundary of the hole.

Geometrical considerations allow the strains to be stated in terms of the radial displacement u. (Appendix B, Refs. 7.1, 8.2 or 9.1.) These expressions, together with (4.3), give

Fig. 6.1.

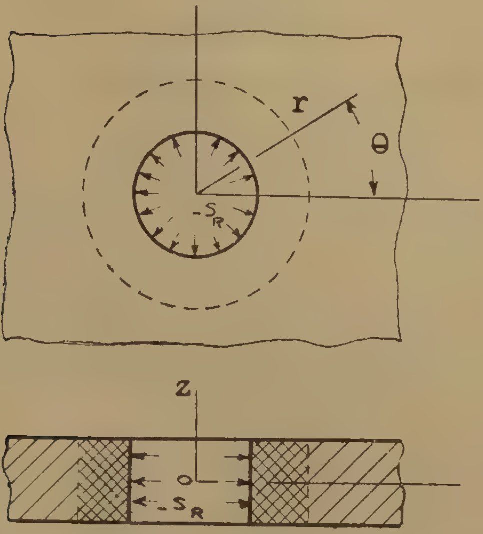

Fig. 6.2.

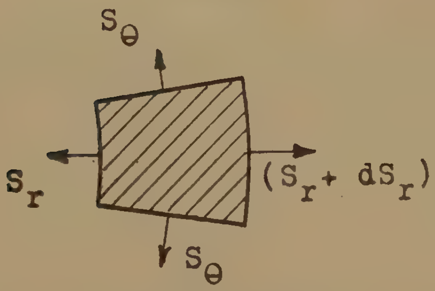

Inelastic Strains.

$$\left.\begin{aligned}
e_r = \frac{du}{dr} &= \frac{1}{\mathrm{P}}[\mathrm{S}_r - p\,.\,\mathrm{S}_\theta - \mathrm{S}_{0r} + p\,.\,\mathrm{S}_{0\theta}] \\
&\quad + \frac{1}{\mathrm{E}}[(p-q)\mathrm{S}_\theta + \mathrm{S}_{0r} - p\,.\,\mathrm{S}_{0\theta}], \\
e_\theta = \frac{u}{r} &= \frac{1}{\mathrm{P}}[\mathrm{S}_\theta - p\,.\,\mathrm{S}_r - \mathrm{S}_{0\theta} + p\,.\,\mathrm{S}_{0r}] \\
&\quad + \frac{1}{\mathrm{E}}[(p-q)\mathrm{S}_r + \mathrm{S}_{0\theta} - p\,.\,\mathrm{S}_{0r}], \\
e_z = \frac{dw}{dz} &= \frac{1}{\mathrm{P}}[-p(\mathrm{S}_r + \mathrm{S}_\theta) + p(\mathrm{S}_{0r} + \mathrm{S}_{0\theta})] \\
&\quad \frac{1}{\mathrm{E}}[(p-q)(\mathrm{S}_r + \mathrm{S}_\theta) - p(\mathrm{S}_{0r} + \mathrm{S}_{0\theta})]
\end{aligned}\right\} \quad . \; . \; . \quad (6.1)$$

It must be emphasized that these expressions will be applied across a narrow annulus in the first instance, since P will be treated as a constant.

The equilibrium of the element leads to (Appendix B, Refs. 7.2, 8.2).

$$r\,.\,\frac{dS_r}{dr}+S_r-S_\theta=0. \qquad (6.2)$$

The boundary conditions for the inelastic zone are,

$$\left.\begin{array}{lll} r=R, & S_r=-S_R. & \\ r=c, & (u)_E=(u)_P. & \text{Satisfies Hypothesis 5.2.} \\ r=c, & \left.\begin{array}{l}(S_r)_E=(S_r)_P=S_{0r},\\ (S_\theta)_E=(S_\theta)_P=S_{0\theta}.\end{array}\right\} & \text{Satisfies Hypothesis 5.1.} \end{array}\right\} \quad . \qquad (6.3)$$

The solution of (6.1) and (6.2), together with boundary conditions (6.3), is a solution of the problem for the inelastic stresses. Eliminate S_θ between (6.2) and the first two equations of (6.1). Differentiate the second equation of (6.1) and equate to the first to give the differential equation for S_r.

$$r^2\frac{d^2S_r}{dr^2}+3r\frac{dS_r}{dr}=\frac{S_0}{\sqrt{3}}\,.A, \qquad (6.4)$$

where

$$A=2(1+p)\left(1-\frac{P}{E}\right).$$

The term $\frac{S_0}{\sqrt{3}}$ comes from a consideration of the values for the initial yield stresses at each point through the yielded field.

The solution for the *elastic* plate with a circular hole containing pressure is well known. (Appendix B, Ref. 7.3.) Elastic stresses in the plate round the yielded zone

$$\left.\begin{array}{l} S_r=-S_{0r}\frac{c^2}{r^2}, \\ S_\theta=S_{0r}\frac{c^2}{r^2}. \end{array}\right\} \qquad (6.5)$$

Substituting (6.5) in the yield condition (3.2), written appropriately for this problem,

$$S_{0r}^2-S_{0r}\,.\,S_{0\theta}+S_{0\theta}^2=S_0^2 \qquad (6.6)$$

gives

$$\left.\begin{array}{l} S_{0r}=-\frac{S_0}{\sqrt{3}}, \\ S_{0\theta}=\frac{S_0}{\sqrt{3}}. \end{array}\right\} \qquad (6.7)$$

These values are independent of radius and were used to derive (6.4).

The solution of (6.4) with (6.3).3 and (6.7) is

$$\left.\begin{array}{l} \frac{\sqrt{3}S_r}{S_0}=\left(\frac{A}{4}-1\right)\frac{c^2}{r^2}+\frac{A}{2}\left(\log_e.\frac{r}{c}-\frac{1}{2}\right), \\ \frac{\sqrt{3}S_\theta}{S_0}=-\left(\frac{A}{4}-1\right)\frac{c^2}{r^2}+\frac{A}{2}\left(\log_e.\frac{r}{c}+\frac{1}{2}\right). \end{array}\right\} \qquad (6.8)$$

Consider the elastic zone displacements from the well-known solution when the plate is infinitely large.

Elastic Zone Radial Displacement

$$u=\frac{S_0}{\sqrt{3}}\frac{c}{2G}\frac{c}{r}, \qquad (6.9)$$

and hence at the yield boundary

$$r=c, \qquad u=\frac{S_0}{\sqrt{3}}\frac{c}{2G}. \qquad (6.10)$$

Substitution of stresses (6.8) in (6.1).1 gives,

Inelastic Zone Radial Strain

$$\begin{aligned}\frac{4}{(1+p)}\frac{\sqrt{3}}{S_0}e_r&=\frac{4}{(1+p)}\frac{\sqrt{3}}{S_0}\frac{du}{dr}\\&=\frac{1}{P}\left\{(A-4)\left(\frac{c^2}{r^2}-1\right)+2A\frac{(1-p)}{(1+p)}\log\frac{r}{c}\right\}\\&\quad+\frac{1}{E}\left\{\frac{(p-q)}{(1+p)}\left[-(A-4)\frac{c^2}{r^2}+2A.\log\frac{r}{c}+A\right]-4\right\}. \qquad (6.11)\end{aligned}$$

Integration and the substitution of boundary conditions (6.10) satisfying Hypothesis 5.2 gives the inelastic zone radial displacement.

Inelastic Zone Radial Displacement

$$\begin{aligned}\frac{4}{(1+p)}\frac{\sqrt{3}}{S_0}\frac{u}{r}=\frac{1}{P}\Bigg\{&-(A-4)\frac{c^2}{r^2}+2A\frac{(1-p)}{(1+p)}\log\frac{r}{c}\\&+4\left[\frac{A}{(1+p)}-2\right]\frac{c}{r}+4-\frac{(3-p)}{(1+p)}A\Bigg\}\\&+\frac{1}{E}\left\{\frac{(p-q)}{(1+p)}\left[(A-4)\frac{c^2}{r^2}+A\left(2\log\frac{r}{c}-1\right)\right]\right.\\&\left.-4\left(1-2\frac{c}{r}\right)\right\}. \qquad (6.12)\end{aligned}$$

But we have seen in (6.1).2 that the tangential strain

$$e_\theta=\frac{u}{r},$$

and hence this is given directly by (6.12).

The expressions for stress and strain and displacement (6.8), (6.11) and (6.12) are true when the yielded zone is narrow enough to allow P to be regarded as approximately constant through it.

The general case when the field is wide may be considered step-by-step over narrow annuluses working away from the yield boundary deeper into the yielded field.

Consider a narrow annulus of width d_m in the yielded zone. Hence,

$$d_m=r_{m+1}-r_m.$$

Higher powers than the first of d_m may be neglected. Put

$$\frac{d_m}{r_m}=D_m. \qquad (6.13)$$

Fig. 6.3.

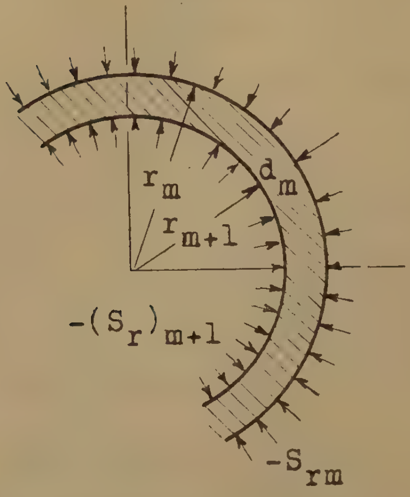

Put $p=\frac{1}{2}$ as suggested in equation (2.4) in para. 2.

Substitution for p and (6.13) in (6.8), (6.11), (6.12), after expanding in series and retaining only first orders, gives

$$\left.\begin{aligned} &S_{r(m+1)}=-(1+D_m)S_{rm}-D_m\,.\,S_{\theta m},\\ &S_{\theta(m+1)}=-\frac{S_0}{\sqrt{3}}D_m\,.\,A_m+D_m\,.\,S_{rm}+(1+D_m)S_{\theta m},\\ &\text{where, from (6.4),}\\ &A_m=3\left(1-\frac{P_m}{E}\right),\end{aligned}\right\}\quad . \quad . \quad (6.14)$$

and P_m is the slope of the simple tensile inelastic curve chord starting at S_m, the equivalent stress of system S_{rm}, $S_{\theta m}$ and finishing at S_{m+1}, the equivalent stress of $S_{r(m+1)}$, $S_{\theta(m+1)}$.

Fig. 6.4.

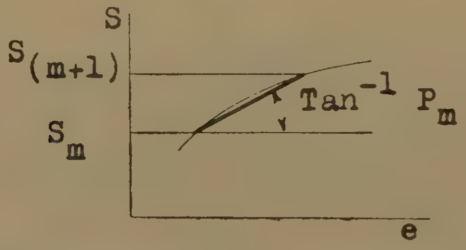

Similarly the displacements are

$$\left.\begin{aligned}\left(1+\frac{1}{D_m}\right)\frac{(u_{m+1}-u_m)}{r_m}=\frac{1}{P_m}\left[S_{rm}+\frac{1}{2}S_{\theta m}-\frac{3}{2}\,.\,\frac{S_0}{\sqrt{3}}\right]&\\ +\frac{1}{E}\left[-\frac{1}{2}(1-2q)S_{\theta m}+\frac{3}{2}\,.\,\frac{S_0}{\sqrt{3}}\right].&\end{aligned}\right\}\quad . \quad (6.15)$$

However, in general we shall choose P_m when S_m is known, and so we need to find the value of D_m that will allow the chord of slope P_m to end at S_{m+1} in fig. 6.4. This is found from the hypothesis of yield,

$$S^2_{r(m+1)} - S_{r(m+1)} \cdot S_{\theta(m+1)} + S^2_{\theta(m+1)} = S^2_{(m+1)} . \quad . \quad . \quad . \quad (6.16)$$

Substitution of (6.14) in (6.16) gives

$$D_m = \frac{S^2_{(m+1)} - S_{rm} \cdot S_{\theta m} - S^2_{rm} - S^2_{\theta m}}{3(S_{rm}+S_{\theta m})^2 - A_m(S_{rm}+2S_{\theta m})\dfrac{S_0}{\sqrt{3}}}, \quad . \quad . \quad . \quad . \quad (6.17)$$

and so determines the width of the narrow annulus.

6.1. *Example : Circular Hole in Large Duralumin Plate.* (Fig. 6.1.)

This example will be computed in sufficient detail to allow experimental check of the theoretical results.

Fig. 6.5

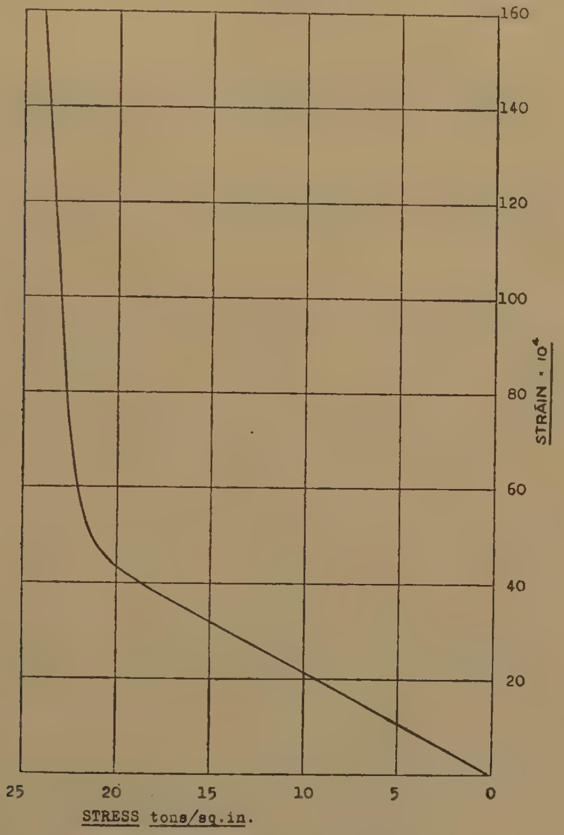

Duralumin—Tensile Test.

Ultimate stress 33·64 tons/sq. in. on original cross-section.
Elongation 10 per cent. on 2-in. gauge length.
Reduction of area 14 per cent.
Test piece 0·564-in. diameter from bar.

This case is important in the expanding of boiler and condenser tubes in end plates when the materials are other than duralumin. (Appendix B, Ref. 10.)

TABLE 6.1.

Inelastic zone.

c=2R, extent of yield.

m.	0	1	2	3	4	5	6	7
P_m/E	0·791	0·456	0·095	0·095	0·095	0·095	0·095	0·095
S_m/S_0	1·00	1·08	1·15	1·22	1·47	1·61	1·81	1·96
r_m/R	2·00	1·92	1·79	1·68	1·50	1·35	1·20	1·00
d_m/R	0·082	0·126	0·117	0·117	0·175	0·150	0·150	0·200
$S_{rm}.\sqrt{3}/S_0$	−1·00	−1·08	−1·22	−1·38	−1·63	−1·90	−2·22	−2·76
$S_{\theta m}.\sqrt{3}/S_c$	1·00	1·06	1·09	1·07	1·02	0·991	0·990	1·04
$u_m.10^3/R$	5·73	5·96	6·36	7·38	11·1	17·3	25·7	40·0
$e_{\theta m}.10^3$	2·87	3·11	3·55	4·41	7·39	12·8	21·4	40·0
$e_{rm}.10^3$	−2·75	−2·46	−8·74	−21·2	−41·3	−56·0	−71·7	−82·8
$e_{zm}.10^3$	0·105	0·153	2·55	15·1	24·8	34·9	48·2	54·3

The simple tensile curve for the duralumin plate considered is shown in fig. 6.5. Stress is calculated on the original cross-section of the test

TABLE 6.2.

Elastic zone.

$c=2R$, extent of yield.

r/R.	2·00	2·50	3·00	4·00	5·00
$S_r.\sqrt{3}/S_0$	—1·00	—0·640	—0·448	—0·252	—0·151
$S_\theta.\sqrt{3}/S_0$	1·00	0·640	0·448	0·252	0·151
$e_\theta.10^3$..........	2·87	1·83	1·27	0·715	0·458
$e_r.10^3$..........	—2·87	—1·83	—1·27	—0·715	—0·458
$u.10^3/R$........	5·73	4·58	3·82	2·86	2·29

Fig. 6.6.

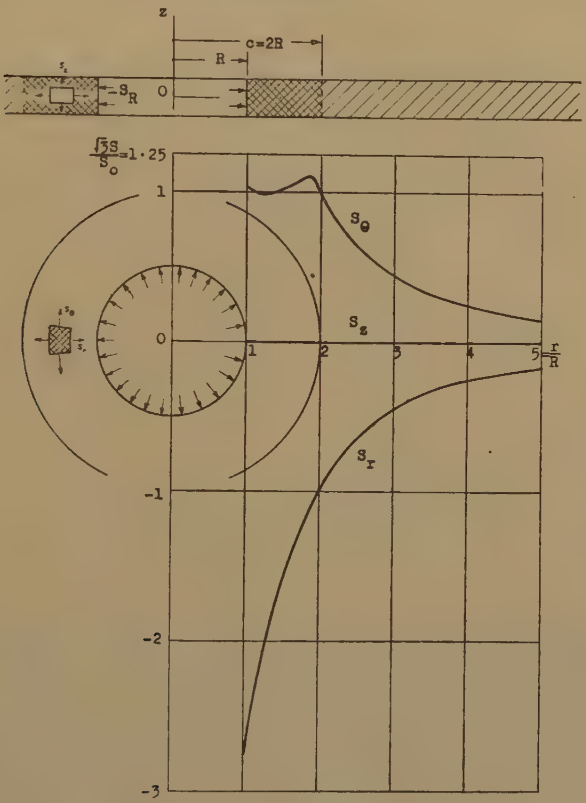

Partial yield to radius $c=2R$.
Plane stress.

piece in this curve. Correction of this curve for change of section increases the slope slightly. Correction is more important towards the ultimate stress, whereas we shall work down close to yield so no correction has been made to the curve.

Values of P_m and S_m from the curve and other values computed from equations (6.13) to (6.17) give Table 6.1. The table results are plotted in figs. 6.6 and 6.7. Constants were,

$$E = 10{\cdot}5\ 10^6 \text{ lbs./sq. in.},$$
$$q = 0{\cdot}25,$$
$$S_0 = 18{\cdot}6 \text{ tons/sq. in.}$$

Fig. 6.7.

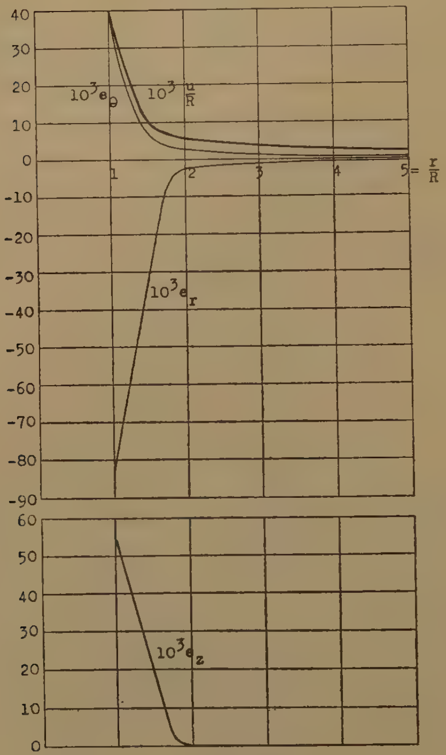

The greatest value of strain $e_r = 0{\cdot}0828$ occurs at the boundary of the hole. As mentioned in paragraph 4, the analysis applies strictly to small strains. It may be questioned that 0·0828 is small enough to neglect its square and higher powers However, the present analysis will be retained because the displacement $u = 0{\cdot}0400$ R is found in practice. (In a slightly different connection see Appendix B, Ref. 6.2.) Such high strains are recognized as the upper limit to which such an analysis can apply. Further straining would require a new analysis considering finite strains.

Notice in fig. 6.6 how the radial stresses increase at much the same rate as if the plate were elastic. The tangential stresses do not change greatly through the yielded field*. In fig. 6.7 the transverse thickening of the sheet shown by e_z increases rapidly in the yielded zone away from the yield boundary.

Step-by-step calculations are usually tedious if there are many steps. Hence, the same problem has been solved with P constant in equations (6.8), (6.11), (6.12) applied to the duralumin plate. $P=0{\cdot}583\ 10^6$ lbs./sq. in. was the value for well-established yield. In fig. 6.5 backward projection gives the simple yield stress $S_0=21{\cdot}1$ tons/sq. in.

The results of computation for various stages of yield progress $c/R=1{\cdot}1$, 1·5, 2·0 are shown in fig. 6.8. The radial stresses are negligibly different from those in fig. 6.6, but as might have been expected the rate of change of tangential stresses differ considerably near the yield boundary. The difference between the solutions is small when actual stress values are inserted, as may be seen in fig. 6.9.

Fig. 6.8.

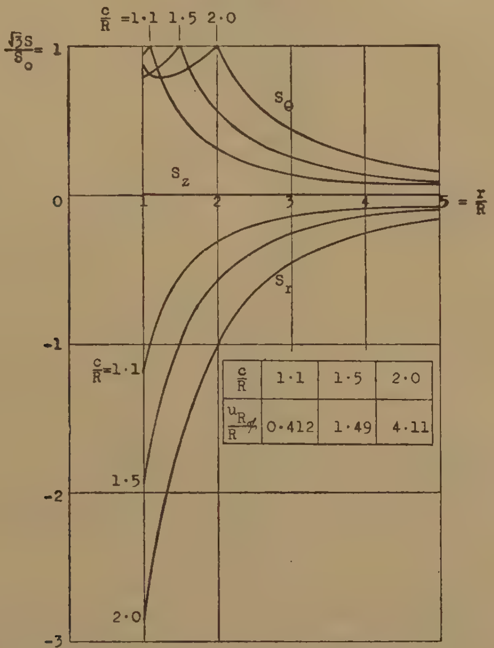

Duralumin—Partial yield to radius *c*.
Plane stress.

---

* This curve of tangential stress should be compared with similar analyses by Nadai, 'Plasticity,' p. 198, and again in "Theory of the Expanding of Boiler and Condenser Joints through Rolling," A. S. M. E., November, 1943. In these references a change of sign occurs, so that S_θ becomes a compression at the boundary of the hole. In the present analysis it remains a tension. It is not clear in Nadai's analyses if stress-strain compatibility has been achieved.

7. *Criterion of Rupture.—Tentative Suggestion.*

Experimental evidence has shown that pure compression or pure tension can reach *very high* values without rupture. Hence, change of shape rather than change of volume may be thought to cause rupture. Hence as for yield hypothesis 3.2,

Hypothesis 7.1.—*The energy of change of shape at rupture of a metal is constant for any arrangement of stresses.*

Hence, if the simple tensile rupture stress of a metal is known as "equivalent" to a given complex stress system, then the material should rupture under such a system. If the strains are not too great for such a system, then the analysis of the preceding paragraphs may be used to determine rupture. In the example of sub-para. 6.1 the ultimate strength of the duralumin is 33·64 tons/sq. in. The equivalent stress at the boundary of the hole for $c=2R$ is 36·5 tons/sq. in. Therefore, in a test small cracks should appear near the hole as the yield zone increases to about this value.

Fig. 6.9.

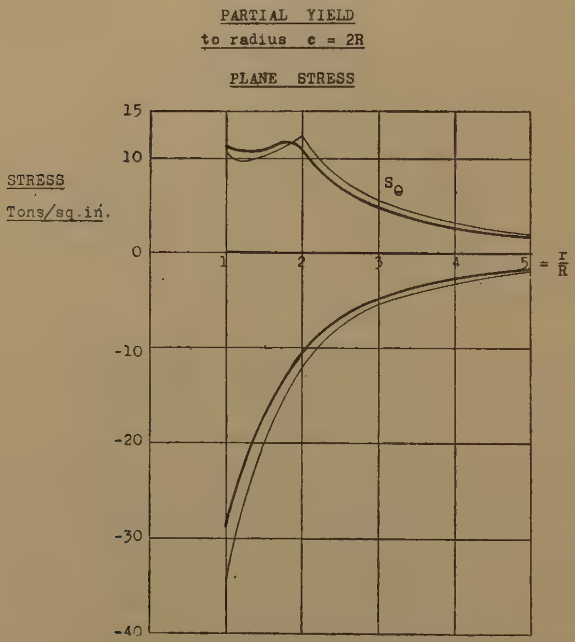

Duralumin—Heavy curve, step-by-step calculation,
with $P \neq$ constant,
$S_0=18{\cdot}6$ tons/sq. in.
Light curve, with $P=$ constant,
$=0{\cdot}583\times10^6$ lbs/sq. in.
$S_0=21{\cdot}1$ tons/sq. in.

8. *Superposition of Stresses in Yielded Zone.*

A simple tensile test piece has yielded to position K on the S–*e* curve. It has reached this position appropriate to the energy of change of shape. If further energy is put into it by increasing the load then the new appropriate position L is attained by inelastic deformation. However, if the energy is decreased by decreasing the load or superimposing a compression stress, then the position M is reached by elastic deformation.

Similarly if the stress system is complex we state,

Fig. 8.1.

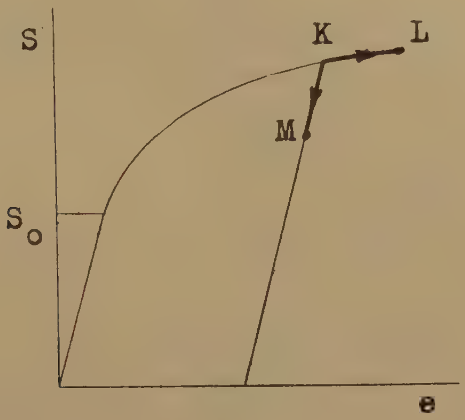

Hypothesis 8.1.—*If an element in a yielded field is at the inelastic potential* * (*i. e.* equivalent to position K), *then an increase in the potential will induce inelastic strains, but if the potential is decreased then the strains are elastic.*

Hence if systems of stress are superimposed in a yielded field a test must be made to ascertain if the strains are elastic or inelastic at any given point when compatibility is being sought.

9. *Stress Free Circular Hole after Yielding.*

An example of the superposition of stresses is the freeing from load of the hole boundary in the large duralumin plate of sub-para. 6.1.

The pressure $-S_R$ in the hole is cancelled by applying an equal and opposite stress to the hole.

A solution satisfying Hypothesis 8.1 for this stress system superimposed on the already yielded field is approached by supposing that the strains are elastic. Hence we may use the well-known solution for an elastic plate,

---

* The term "potential" was used by Hencky. (Appendix B, Ref. 5.) Love uses the term "strain energy" in the same sense.

$$\left.\begin{aligned}(S_r)^{ii}&=S_R\frac{R^2}{r^2},\\(S_\theta)^{ii}&=-S_R\frac{R^2}{r^2},\end{aligned}\right\}, \quad \ldots\ldots\ldots \quad (9.1)$$

Fig. 9.1.

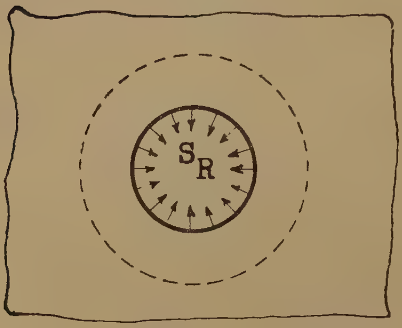

Fig. 9.2

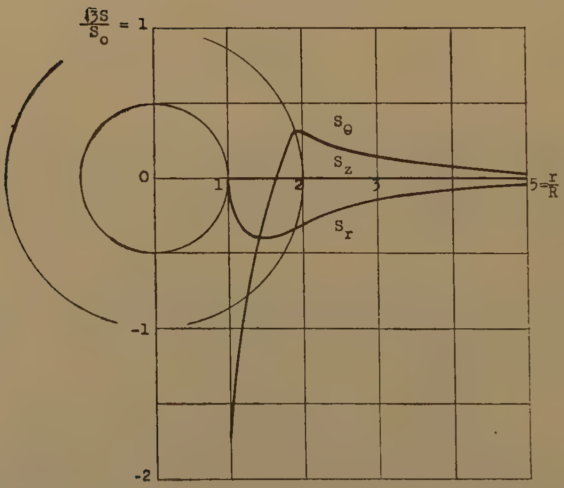

Duralumin—Partial yield to radius $c=2R$ and then hole free of stress. Plane stress.

where *ii* denotes that the stresses are a second system superimposed upon a first system *i* already existing. Hence

$$\left.\begin{aligned}S_r&=(S_r)^i+(S_r)^{ii},\\S_\theta&=(S_\theta)^i+(S_\theta)^{ii},\end{aligned}\right\} \quad \ldots\ldots\ldots \quad (9.2)$$

where $(S_r)^i$ and $(S_\theta)^i$ are given by equations (6.8).

To justify the assumption that the strains induced by the *ii* system are elastic or zero substitutes S_r and S_θ from (9.2) in the yield test,

$$S_r^2 - S_rS_\theta + S_\theta^2 \gtreqless S^2, \quad . \quad . \quad . \quad . \quad . \quad . \quad . \quad . \quad (9.3)$$

where S is the "equivalent" stress for the *i* system under which the metal yielded. (See Table 6.1.) This criterion is satisfied, so we may superimpose the stresses (9.1) on (6.8) to give the stress-free hole after yield. (See fig. 9.2.) The strains and displacements induced by system *ii* are small and are shown in Table 9.1.

TABLE 9.1.

Strains and displacements due to cancelling stress *ii*.

r/R.	1·00	1·50	2·00	3·00	4·00	5·00
$e_r . 10^3$	7·91	3·51	1·98	0·878	0·494	0·316
$e_\theta . 10^5$	−7·91	−3·51	−1·98	−0·878	−0·494	−0·316
$u . 10^3/\mathrm{R}$....	7·91	5·27	3·96	2·64	1·98	1·58

10. *Shear Strain in a Yielded Element.*

The shear stress-strain relationships for small strains in the three orthogonal directions are independent of one another until geometrical considerations introduce displacements.

Fig. 10.1.

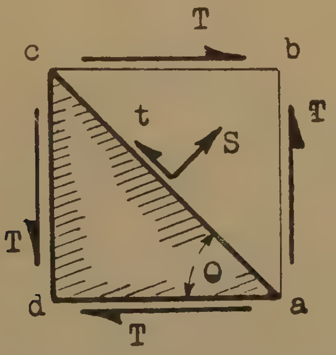

Fig. 10.1 shows a rectangular element viewed from one of the orthogonal directions.

Subscripts may be given to T to denote the plane in which it acts.

Consider the equilibrium of triangle *abc* of unit thickness. The horizontal and vertical translational equilibrium equations give that

$$t=0, \qquad \theta=45^\circ, 135^\circ, \quad . \quad . \quad . \quad . \quad . \quad . \quad . \quad . \quad (10.1)$$

and these values of θ in the rotational equilibrium equation found by taking moments about a give

$$\left.\begin{array}{ll} \theta=45^\circ & S=S_1=T \\ \theta=135^\circ & S=S_2=-T \end{array}\right\} . \quad . \quad . \quad . \quad . \qquad (10.2)$$

The rectangular element is now square with sides of unit length say. Shear strain e_{12} occurs under shear stress T. Diagonal db stretches to db', where $bb'=1 \cdot e_{12}$.

The geometry of triangle $a'b'd$ gives

$$(db')^2=(ad+bb')^2+(ab)^2. \quad . \quad . \quad . \quad . \quad . \quad . \qquad (10.3)$$

Fig. 10.2

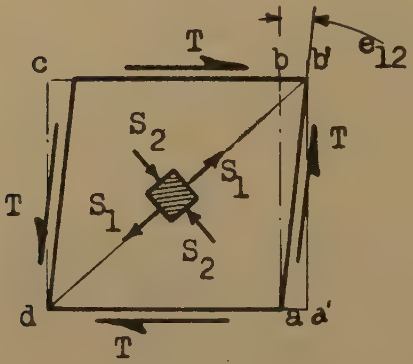

When e_1 is the strain in db' then

$$e_{12}=2e_1. \quad . \quad . \quad . \quad . \quad . \quad . \quad . \quad . \quad . \quad . \qquad (10.4)$$

Substitute (10.2) in equation (4.3) when $S_3=0$ gives, with equation (10.4),

$$e_{12}=\frac{2(1+p)}{P}\left\{\left[1-\frac{(p-q)P}{(1+p)E}\right]T-\left[1-\frac{P}{E}\right]T_0\right\}, \quad . \quad . \qquad (10.5)$$

when T_0 is the value of shear stress when the element began to yield. Subscript 12 may be given to T and T_0 and then two similar expressions obtained for the other two orthogonal directions by the cyclic interchange of 1, 2, 3.

Notice that when $T=T_0$ we have the usual expression for the *elastic* shear strain of the element under T_0 when yield is just about to begin.

11. *Plane Stress in a Yielded Field Cartesian Co-ordinates.*

Collect the strain equations (4.3) and (10.5) modified for plane stress. Geometrical considerations give the usual relationships of strain and displacements for *small strains*,

$$\left.\begin{aligned} e_x &= \frac{\partial u}{\partial x} = \frac{1}{\mathrm{P}}[\mathrm{S}_x - p\mathrm{S}_y - (\mathrm{S}_{0x} - p\mathrm{S}_{0y})], \\ &\qquad + \frac{1}{\mathrm{E}}[(p-q)\mathrm{S}_y + (\mathrm{S}_{0x} - p\mathrm{S}_{0y})], \\ e_y &= \frac{\partial v}{\partial y} = \frac{1}{\mathrm{P}}[\mathrm{S}_y - p\mathrm{S}_x - (\mathrm{S}_{0y} - p\mathrm{S}_{0x})], \\ &\qquad + \frac{1}{\mathrm{E}}[(p-q)\mathrm{S}_x + (\mathrm{S}_{0y} - p\mathrm{S}_{0x})], \\ e_{xy} &= \frac{\partial u}{\partial y} + \frac{\partial v}{\partial x}, \\ &= \frac{2(1+p)}{\mathrm{P}}\left\{\left[1 - \frac{\mathrm{P}}{\mathrm{E}}\left(\frac{p-q}{1+p}\right)\right]\mathrm{T} - \left(1 - \frac{\mathrm{P}}{\mathrm{E}}\right)\mathrm{T}_0\right\}, \end{aligned}\right\} \quad \ldots \quad (11.1)$$

Fig. 11.1.

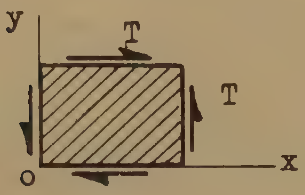

where tensions are positive and shear T positive as in fig. 11.1. Equilibrium of an element when there are no body forces gives

$$\left.\begin{aligned} \frac{\partial \mathrm{S}_x}{\partial x} + \frac{\partial \mathrm{T}}{\partial y} &= 0, \\ \frac{\partial \mathrm{S}_y}{\partial y} + \frac{\partial \mathrm{T}}{\partial x} &= 0 \end{aligned}\right\} \quad \ldots \ldots \quad (11.2)$$

The solution of (11.1) and (11.2) together with the particular boundary conditions will solve the problem.

(11.2) may be solved by using the Airey Stress Function K by putting

$$\mathrm{S}_x = \frac{\partial^2 \mathrm{K}}{\partial y^2}, \qquad \mathrm{S}_y = \frac{\partial^2 \mathrm{K}}{\partial x^2}, \qquad \mathrm{T} = -\frac{\partial^2 \mathrm{K}}{\partial x\,\partial y}. \quad \ldots \quad (11.3)$$

Substitution of (11.3) in (11.1) and reduction by differentiation leads to an expression analogous to that usually derived for the elastic field,

$$\nabla^4 \mathrm{K} = \left(1 - \frac{\mathrm{P}}{\mathrm{E}}\right) \cdot \left[\begin{aligned} &\frac{\partial^2}{\partial x^2}(\mathrm{S}_{0y} - p\mathrm{S}_{0x}) \\ &+ \frac{\partial^2}{\partial y^2}(\mathrm{S}_{0x} - p\mathrm{S}_{0y}) \\ &- 2(1+p)\frac{\partial^2 \mathrm{T}_0}{\partial x \partial y}, \end{aligned}\right] \quad \ldots \ldots \quad (11.4)$$

where
$$\nabla^4 = \frac{\partial^4}{\partial x^4} + 2\frac{\partial^4}{\partial x^2 \partial y^2} + \frac{\partial^4}{\partial y^4}. \quad . \quad . \quad . \quad . \quad . \quad . \quad (11.5)$$

Notice that if the strains are elastic then $P=E$, so that the right-hand side of (11.4) vanishes to leave the usual expression of elasticity.

For the general plane stress distribution (S_x, S_y, T) considered here the criterion of yield similar to (3.2) and (3.3) is (see Appendix B, Ref. 5),

$$S_{0x}^2 - S_{0x} . S_{0y} + S_{0y}^2 + 3T_0^2 = S_0^2. \quad . \quad . \quad . \quad . \quad . \quad (11.6)$$

Professor Temple has pointed out that (11.4) may be written more conveniently and generally as

$$\nabla^4 K = \left(1 - \frac{P}{E}\right) \nabla^4 Y_0, \quad . \quad . \quad . \quad . \quad . \quad . \quad (11.7)$$

where function Y_0, which we may call the "Yield Function," is defined as

$$S_{0x} = \frac{\partial^2 Y_0}{\partial y^2}, \qquad S_{0y} = \frac{\partial^2 Y_0}{\partial x^2}, \qquad T_0 = -\frac{\partial^2 Y_0}{\partial x \partial y}. \quad . \quad . \quad (11.8)$$

The form (11.7) shows clearly the invariance of (11.4) with respect to rotation of axes.

12. 3-*Dimensional Inelastic Stress and Strain Relationships.*

The 3-dimensional stress and strain expressions will be collected for future reference. Co-ordinate systems are orthogonal.

Fig 12.1.

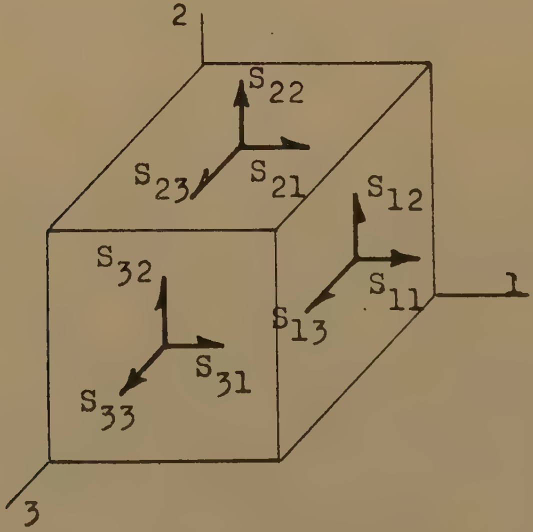

Stresses are S_{ii} S_{ij}, where

$i=1, 2, 3,$
$j=2, 3, 1,$
$k=3, 1, 2.$

Strains are e_{ii}, e_{ij}.
Displacements are u_i.
Elemental lengths in the directions of co-ordinates are δx_i.

12.1. *Yield Criterion.*

As load increases in the complex distribution the material reaches its elastic limit under three normal stresses S_{0ii} and three shear stresses S_{0ij}. Huber's hypothesis as stated in para. 3, Hypothesis 3.2, gives the single expression

$$\sum_{i,j}[(S_{0ii}-S_{0jj})^2+6\,S_{0ij}^2]=S_0^2, \quad \ldots\ldots \quad (12.1)$$

where S_0 is the primary yield stress of the metal in simple tension. This relationship must be satisfied at the successive positions of the yield surface as the yield progresses into the elastic matrix.

Observation 1.3 in para. 1 gives the single expression

$$\sum_{i,j}[(S_{ii}-S_{jj})^2+6\,S_{ij}^2]=2S^2, \quad \ldots\ldots \quad (12.2)$$

where S is the simple tensile stress "equivalent" to the six stresses S_{ii}, S_{ij}.

12.2. *Inelastic Stress-Strain Relationships.*

The three normal strains from (4.3) are

$$\left.\begin{aligned} e_{ii}&=\frac{1}{P}S_{ii}-p(S_{jj}+S_{kk})-S_{0ii}+p(S_{0jj}+S_{0kk})],\\ &\frac{1}{E}[(p-q)(S_{jj}+S_{kk})+S_{0ii}-p(S_{0jj}+S_{0kk})]\end{aligned}\right\} \quad \ldots \quad (12.3)$$

The three shear strains from (10.3) are

$$e_{ij}=\frac{2(1+p)}{P}\left\{\left[1-\frac{P}{E}\cdot\frac{(p-q)}{(1+p)}\right]S_{ij}-\left(1-\frac{P}{E}\right)S_{0ij}\right\}. \quad \ldots \quad (12.4)$$

12.3. *Strains in Terms of Displacements.*

We use the usual expressions for strains in terms of displacements. The strains are small. If the x_i are a Cartesian system then the three normal strains are

$$e_{ii}=\frac{\partial u_i}{\partial x_i}, \quad \ldots\ldots\ldots \quad (12.5)$$

and the three shear strains are

$$e_{ij}=\frac{\partial u_i}{\partial x_j}+\frac{\partial u_j}{\partial x_i}. \quad \ldots\ldots\ldots \quad (12.6)$$

12.4. *Equilibrium Equations.*

Through the yielded field we must satisfy the three equilibrium equations. When body forces are zero and the co-ordinates are Cartesian,

$$\frac{\partial S_{i1}}{\partial x_1}+\frac{\partial S_{i2}}{\partial x_2}+\frac{\partial S_{i3}}{\partial x_3}=0. \quad \ldots\ldots\ldots \quad (12.7)$$

12.5. *Boundary Conditions.*

Inspection of strain equations (12.3) and (12.4) for the *yielded* field shows that when $S_{ii}=S_{0ii}$ and $S_{ij}=S_{0ij}$ they reduce to the strains in an *elastic* element operated on by primary yield stresses S_{0ii}, S_{0ij} at the yield surface. To solve a particular problem it is necessary to find the position of the yield surface in the elastic matrix. The stresses S_{0ii}, S_{0ij} are continuous across the yield surface and so constitute one boundary condition for the yielded field. Displacements u_i must be the same on each side of the yield surface to ensure body continuity.

If the yielded zone has a surface where the metal body terminates then the usual three boundary conditions must be satisfied,

$$X_i=S_{i1}l_1+S_{i2}l_2+S_{i3}l_3, \quad \ldots\ldots\ldots \quad (12.8)$$

where X_i are the components in the directions *oi* of the forces per unit area at the point considered on the surface, and l_j are the direction cosines of the outward normal to the surface at the point considered.

APPENDIX A.

NOTATION.

x, y, z	Cartesian co-ordinates.
r, θ, z	Cylindrical co-ordinates.
01, 02, 03	Orthogonal directions at a point.
S	Normal stress with appropriate subscript for direction, *e. g.* S_x is the normal stress on an element in the direction $0x$. Note that in para. 12 it is convenient to use S with mixed subscripts to denote shear on the various planes.
T	Shear stress. No subscripts used for plane stress.
S_0	Simple tensile yield stress. A direction subscript denotes that it is a normal stress on the element in that direction when yield occurred at the element, *e. g.* S_{0x} is the normal stress in the direction $0x$ when yield occurred.
T_0	Shear on the element when it yielded under a complex system. No subscripts for plane stress.
e	Strain with appropriate direction subscript(s).
ϵ	Partial strain with direction subscripts appropriate.
E	Young's Modulus for an elastic metal.
P	The writer's modulus denoting the slope of the inelastic stress-stain curve. It is a function of strain.
q	Poisson's transverse contraction ratio for an elastic metal.
p	Transverse contraction ratio for the *plastic* strains. $p=\frac{1}{2}$ if a plastic metal is incompressible.

$A=2(1+p)\left(1-\frac{P}{E}\right)$ is a convenient constant first used in equation (6.4).

K Airey Stress Function used in para. 11.

Y_0 "Yield Function" defined in equations (11.8) for plane stress. The second differentials of this function give the primary yield stresses through the yielded zone.

APPENDIX B.

References.

(1) A. C. Phillips and A. F. C. Pollard, "Experimental investigations on the safe limit of static pressure between spherical and plane surfaces," 'Engineering,' vol. cxliii. 1937, pp. 223, 281, 339, 398.

(2) S. Timoshenko, 'Strength of Materials' (Macmillan), vol. i. 1940, vol. ii. 1941. (2.1) vol. ii. p. 410. (2.2) vol. ii. p. 477. (2.3) vol. ii. p. 478. (2.4) vol. ii. p. 479.

(3) Houwink, 'Elasticity, plasticity and the structure of matter' (Cambridge Univ. Press), 1940. (3.1) p. 85. (3.2) p. 91.

(4) H. Levy, 'A philosophy for a modern man' (Gollancz), 1938. (4.1) Chapter II., Professor Levy develops an interesting philosophical discussion of the behaviour of units in an aggregate compared with the behaviour of the aggregate as a result of the behaviour of the units.

(5) H. Hencky, "On the nature of plastic deformation," Z. V. D. I., vol. lxix. no. 20, 16–5–1925, pp. 695–6; no. 39, 26–9–1925, pp. 1253–4. Translation by Ministry of Aircraft Production, R. T. P., no. 2127, by M. Flint, 1944.

(6) K. H. Swainger, "The stresses in and round rivets in thin plating" (Ph.D. Thesis, University of London, 1944). (6.1) Appendix H, para. 2, p. 79. (6.2) Appendix J and Appendix L.

(7) Timoshenko, 'Theory of Elasticity' (Engineering Monograph, McGraw Hill), 1934. (7.1) p. 7. (7.2) p. 53. (7.3) p. 57. (7.4) p. 9.

(8) Southwell, 'Theory of Elasticity' (Oxford Press), 1936. (8.1) pp. 117–118. (8.2) pp. 285–289. (8.3) p. 280.

(9) A. E. H. Love, 'Mathematical theory of elasticity' (Cambridge Univ. Press), 1934. (9.1) p. 38.

(10) A Nadai, "Theory of the expanding of boiler and condenser tubes joints through rolling," Trans. A. S. M. E., Nov. 1943.

(11) A. Nadai, 'Plasticity' (Engineering Monograph, McGraw Hill), 1932.

LVII. *The Application of the Helmholtz Resonator to the Measurement of Sound Absorption.*

By W. S. Tucker, D.Sc., A.R.C.Sc.*

[Received May 28, 1945.]

Summary.

The excellence of the resonance curves obtained from a Helmholtz resonator equipped with a hot-wire microphone suggests the possibility of measuring the energy losses due to the absorption of sound in the

---

* Communicated by the Author.

interior walls of that resonator. The damping coefficient K_1, due to radiation and viscous losses concerned with the neck of the resonator, is increased by that due to this absorption K_2, which is taken as a function of viscosity.

The method described derives the value of K_1 from a resonator of perfectly reflecting walls and similarly that of K_1+K_2 from one having porous walls.

Losses due to the resonator neck are equalized in the two cases by using the same neck-fitting, and the two resonators to be strictly comparable are tuned by volume adjustment to approximately the same frequency.

The assumption made is that the hot-wire microphone measures the radiating power of the two resonators regarded as secondary sources when subjected to the same external source, and that the absorbing power α of the material of the walls of the second resonator is expressed by the ratio of loss of its radiating power to the radiating power of the resonator with non-absorbent walls, and is expressed by the simple relation $K_2/(K_1+K_2)$.

Values of α are derived from the resonance curves for six frequencies ranging from 150 to about 600 cycles per second, the material chosen being porous earthenware.

OF all acoustical resonators the Helmholtz resonator is best adapted for acoustical measurements. When its dimensions are small compared with the wave-length it gives single frequency maximum response and a resonance curve in very close agreement with the relation

$$A=f/\{(n^2-p^2)^2+4K^2p^2\}^{\frac{1}{2}},$$

where f is the external periodic force of frequency $p/2\pi$ producing resonant vibration in the resonator of amplitude A, the natural frequency of the resonator being $n/2\pi$, and the damping factor K which deals with the dissipation of energy through radiation and viscous losses.

A is the value of x derived from the equation of motion of a particle in the neck of the resonator

$$\frac{d^2x}{dt^2}+2K\frac{dx}{dt}+n^2x=f\cos pt.$$

If the resonator has rigid and perfectly reflecting walls, the motion of the air particle in the neck is subject to two resisting forces: (1) due to radiation loss, and (2) due to viscous losses in the neck of the resonator. Both of these forces can be proved to be proportional to the particle velocity.

If now, the walls of the resonator are absorbent owing to their porous character, further damping is imposed on the vibrations—resulting in the flattening of the resonance curve. The nature of this resisting force is that of an additional viscosity and is the sum of the resistances to the flow of air into the capillaries of the porous walls. This resistance is also, therefore, proportional to the velocity. Hence the factor K can include all the damping forces, which are purely additive.

In the neighbourhood of resonance the power required to maintain vibrations against viscosity and radiation losses as compared with the maximum power at resonance is given by

$$\frac{\mathrm{P}}{\mathrm{P}_{\text{max.}}}=\frac{4\mathrm{K}^2p^2}{(n^2-p^2)^2+4\mathrm{K}^2p^2},$$

and when $$(n^2-p^2)^2=4\mathrm{K}^2p^2,\quad \frac{\mathrm{P}}{\mathrm{P}_{\text{max.}}}=\frac{1}{2}.$$

It can be shown that if K * is small compared with n, $\mathrm{K}=p-n$ or $n-p$, according as the imposed frequency $p/2\pi$ is $\gtrless n/2\pi$. As will be shown later, such a condition is realized with all Helmholtz resonators where the viscosity and radiation losses, determined by the dimensions of the orifice, are small.

The adoption of the resistance term $2\mathrm{K}\,\frac{dx}{dt}$ in the equation of motion and the subsequent application of the above conclusions are justified if the resonance curves obtained show the requisite symmetry, *i. e.* when developing half the power the differences between the imposed and natural frequencies are equal.

Experimental Verification.

The resonance of the Helmholtz resonator can be investigated in the simplest way by the hot-wire microphone, the full description of which was given in a paper produced by the author and Paris †. It was shown that the resistance changes produced by the vibrations in the neck of the Helmholtz resonator were to a close approximation proportional to the square of the velocity, *i. e.* to the power of the resonator, if the amplitudes of the vibrations were small. Owing to the extreme sensitivity of the hot wire to vibrations from the lowest to those of frequency 500 cycles, this condition was easily realized. With the microphone as an accessory, the first step in the development of a method for obtaining a measure of viscous losses due to porosity of the resonator walls, was to establish the truth of the assumption that resonance curves were obtainable which were in accord with the above theory with a high degree of accuracy. The following conditions were imposed before this accuracy could be realized : —

(1) The source of sound, a moving-coil loud-speaker, must be actuated by an acoustic oscillator of guaranteed steady output throughout the range of frequencies employed.

(2) the oscillator must have an accurate scale of frequencies.

(3) the resonator with its microphone must be so disposed with the loud-speaker as to be in a uniform acoustic field free of standing waves.

---

* For the accurate value of K see Appendix.

† Phil. Trans. of Roy. Society, series A, vol. ccxxi. pp. 389–430 (1921).

(4) the microphone must be actuated by a constant electric current.

(5) the conditions of temperature, both in the neck of the resonator and the air surrounding the resonator, must be constant.

(6) the galvanometer must be sufficiently sensitive to deal with the small current changes which are produced by the microphone in order that they may record the energy of the oscillatory current of air in the neck of the resonator.

These conditions were all realized. (3) and (5) were ensured by enclosing loud-speaker and resonator in a closed heavily lagged box in which all draughts were excluded, the temperature of the laboratory constant, and the grid current of the microphone maintained until the galvanometer recorded that, for the requisite period, no change in resistance occurred when the loud-speaker was silent.

In the first instance a microphone and resonator with perfectly reflecting brass walls was employed having a frequency of 232·2 cycles per second. A large number of tests was made with different sources of sound of constant intensity output over the range of frequencies employed.

Resonance curves are shown for this resonator illustrating their close proximity to the symmetrical condition when the deflection is plotted against $p/2\pi$. Any lack of symmetry would be partially due to the increase of K with frequency. The value of K, derived from the mean of $(n-p)$ when frequency $p/2\pi$ is below $n/2\pi$ and $(p-n)$ when p is above n, should give a good value of K at frequency $n/2\pi$. The shape of the curves is submitted as good evidence in favour of the steadiness of the output of the source of sound, and the capacity of the microphone to respond accurately to the resonant vibrations set up in the resonator. There would of course be a reduction of sensitivity of the hot wire to the higher frequency sounds which would also contribute to a smaller response on the higher frequency side of the resonance curve. Both of these departures from the lack of symmetry in resonance curves are regarded as of second-order effects.

The above experiments serve to show that the technique of resonance curve production justifies a further development.

The microphone is mounted in a fitting which includes the resonator neck and a heavy brass flange. This can be bolted to a similar flange which forms the means of attachment to the cylindrical brass resonator and alternatively to a flange fitted to a cylindrical porous pot (diagram 8). The volumes of the porous pot and the brass resonator are adjusted to equality, as far as possible, by adjustment of a sliding tube on the latter, the tube being tight fitting. In this way the frequencies of the resulting resonators are tuned so that they are approximately equal.

The use of the same resonator orifice and the same adjustment of microphone grid within it ensures that the radiation loss and that due to viscous forces in the neck are the same in both cases, and therefore that the damping factor due to these losses K_1 would be the same. Additional loss due to the absorbent wall of the porous pot would make the damping factor for the latter K_1+K_2 as derived from its resonance curve. Thus K_2 can be found.

In order to vary the frequency of the resonators, two methods can be employed. If n_1 is the frequency required, the volume of the resonator S can be altered, or the conductivity (c) of the neck, a function of its dimensions, can be changed in accordance with the relation

$$n_1=\frac{V}{2\pi}\sqrt{\frac{c}{S}}.$$

The variation of S in the brass resonator can be made by adjustment of the sliding tube within limits, or the use of a shorter cylinder of the same diameter—thus a frequency rising to about 600 cycles could be obtained. The volume within the porous pot was adjusted by introducing the desired quantity of mercury.

The variation of the neck, by insertion of tight-fitting hollow cylinders of different internal diameters enabled tuning to be carried into the lower frequencies. Owing to increased viscous losses in the neck there was a limit to this adjustment, as it was not desirable to increase them unduly, as compared with the losses by absorption of sound in the porous walls. Nevertheless, good results could be obtained working down to a frequency of 150 cycles.

By adjustment of the volume, using a sliding tube for the brass resonator, and by adding mercury to the porous pot, the volumes can be equally reduced, thereby raising the frequency. The highest frequency employed was nearly 600 cycles, beyond which the sensitivity of the hot-wire microphone and the lessening amplitude of the resonance curves for a given output of the loud-speaker introduced inaccuracies in the reading of deflections.

Theory of the Method.

The absorbing power of a reflecting surface for sound "α" is generally expressed by the ratio of the energy of sound absorbed by the surface to that incident upon it. The relation between α and the damping factor K is arrived at by regarding the resonator as a secondary source of sound stimulated by sound generated by a controlled primary source exerting a periodic force $f\cos pt$. The mean power of this secondary source is a maximum at resonance and expressed by $P_{\text{max.}}=f^2/4K$. This power can be measured by the deflection of the galvanometer in the microphone circuit. If P_1 and P_2 are the powers of the resonators composed respectively of the perfectly reflecting brass and the absorbent earthenware, and K_1 and K_1+K_2 their respective damping coefficients, then under the same stimulus

$$P_1=f^2/4K_1,\quad P_2=f^2/4(K_1+K_2),$$

where K_2 is the extra damping due to the absorbent walls.

The difference of these powers measures the loss of energy due to the absorbent walls, *i. e.*

$$P_1-P_2=\frac{f^2}{4}\left\{\frac{1}{K_1}-\frac{1}{K_1+K_2}\right\}=\frac{f^2}{4}\frac{K_2}{K_1(K_1+K_2)}.$$

By definition, therefore, the coefficient of absorption

$$\alpha=\frac{P_1-P_2}{P_1}=\frac{f^2}{4}\left\{\frac{K_2}{K_1(K_1+K_2)}\right\}\Big/\left(\frac{f^2}{4K_1}\right)=\frac{K_2}{K_1+K_2}.$$

The quantities K_1 and K_1+K_2 can be measured directly from the resonance curves as indicated above, and the values, depending only on the sharpness of the curves, can be accurately obtained, independent of the intensity output of the stimulating source. This important fact makes it possible to use the two resonators in succession without the necessity of ensuring equal outputs from the source. Nevertheless, if such constancy in output is assured, the value of α can be obtained directly from observation of maximum galvanometer deflections only. If these are δ_1 and δ_2 respectively,

$$\alpha=\frac{P_1-P_2}{P_1}=\frac{\delta_1-\delta_2}{\delta_1}.$$

An example of this method is quoted in the following results. Owing to the care necessary in placing the microphones in the same positions relative to the loud-speaker, the method is not so reliable as that in which the values of K are derived.

The above theory assumes that the rigid brass surface of the interior of the brass resonator gives 100 per cent. reflection, and that the porous material of the second resonator presents the same internal area. In none of the porous resonators, adapted to give different resonance frequencies, is this correct, and the value of α produced on this assumption must be corrected by a factor. Thus the upper end of the resonator is brass in all cases, and the lower end of the porous resonator, where mercury is introduced for tuning purposes, also reduces the area of the porous surface. It is assumed that, as in the case of brass, the mercury is 100 per cent. reflecting.

If β is the value of the absorption coefficient derived from experiment on the assumption that the whole internal area A is absorbent, β must be multiplied by the factor A/A', where A' is the actual exposed area of the porous material, so that $\alpha=\beta A/A'$.

For the higher frequencies A/A' in these determinations becomes relatively larger.

The following table gives observations and results derived from resonance curves for the different frequencies as reproduced in the diagrams 1 to 6. The values of K are doubled, being the difference of frequencies, both corresponding to the half-maximum deflections, one above and the other below the maximum resonance frequency. In this way a mean value is derived from the two branches of the resonance curves.

Observations and Results.

Nature of resonator.	Resonance frequency. c/sec.	Mean frequency. c/sec.	Frequency readings at $\frac{1}{2}$ max. deflection.		$2K_1$ $=p_2-p_1$.	$2(K_1+K_2)$ $=p_2-p_1$.	$\beta = \frac{K_2}{K_1+K_2}$.	Areas of surface. sq. cm.	Ratio of areas A/A′.	Coefficient of absorption. $\alpha=\beta A/A'$.
			Below "n" (p_1).	Above "n" (p_2).						
Brass	158·6	156·6	152·5	163·8	11·3		0·062	159·1	0·98	0·061
Earthenware .	154·7		148·76	160·8		12·04		162·0		
Brass	226·7	230·0	221·76	231·35	9·59		0·106	159·1	0·98	0·104
Earthenware .	233·3		227·90	238·62		10·72		162·0		
Brass	357·8	358·6	349·25	365·3	16·05		0·146	77·1	1·35	0·197
Earthenware .	359·4		350·20	369·0		18·8		57·17		
Brass	439·6	437·0	430·8	448·2	17·4		0·187	60·52	1·46	0·273
Earthenware .	434·4		424·6	446·0		21·4		41·44		
Brass	562·0	561·2	551·1	571·6	20·5		0·429	43·6	1·77	0·759
Earthenware .	560·5		542·6	578·5		35·9		24·5		
Brass	588·6	586·5	578·9	598·4	19·5		0·501	42·2	1·83	0·917
Earthenware .	584·5		564·6	603·7		39·1		23·15		

Diagram 1.

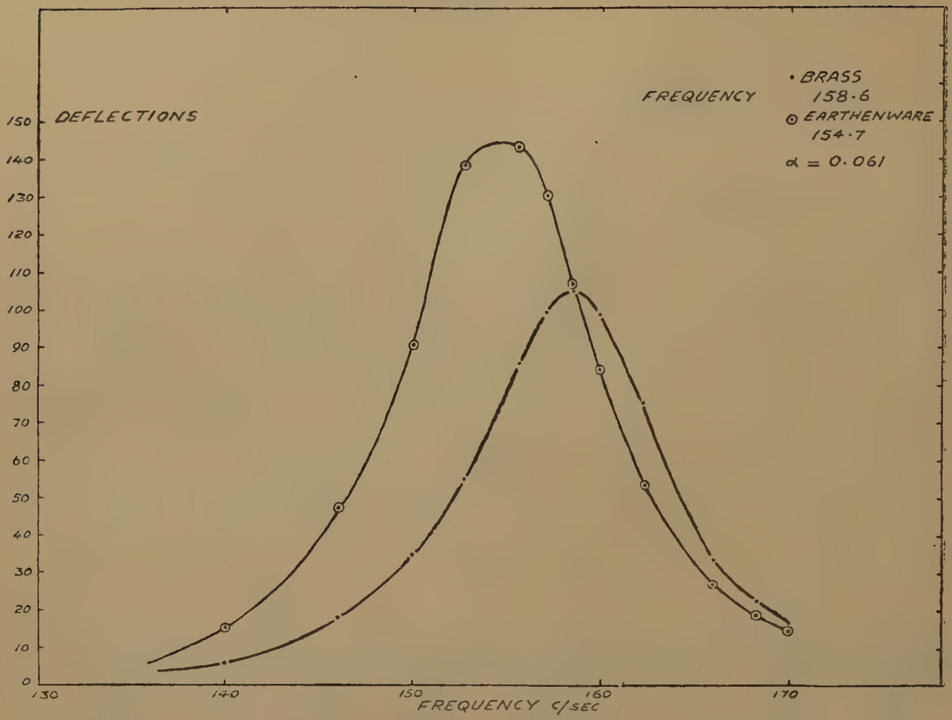

Diagram 2.

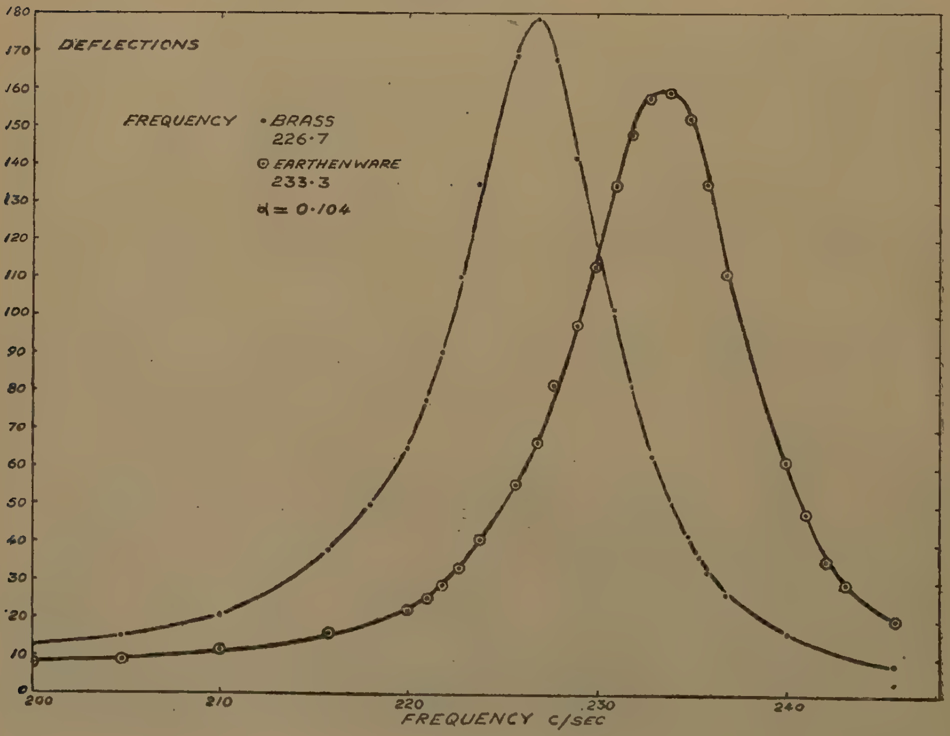

Diagram 3.

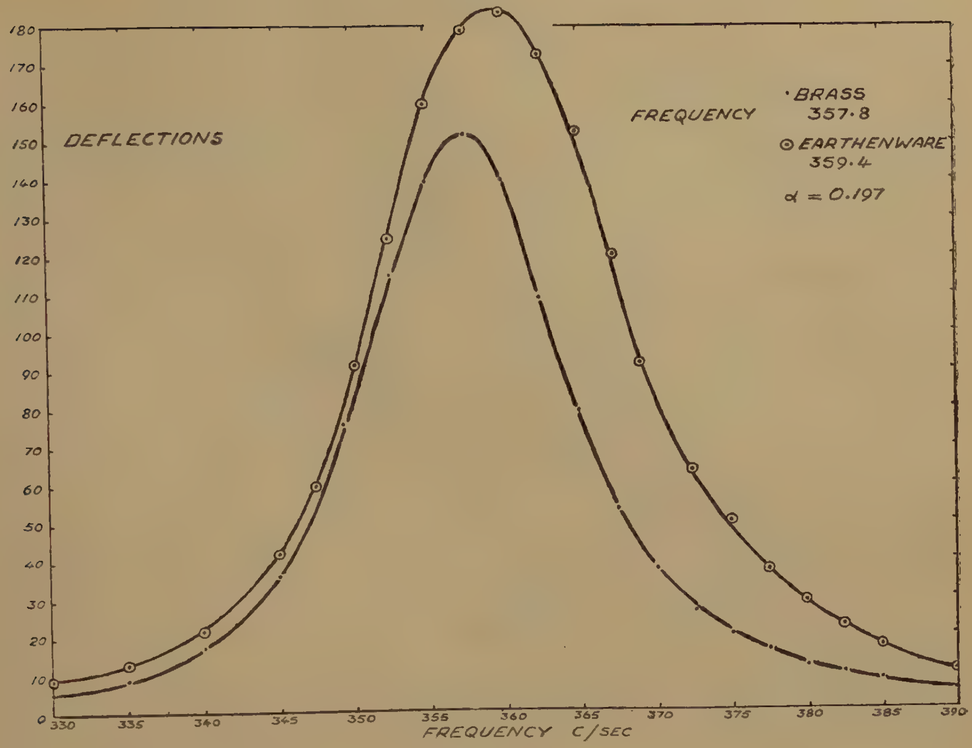

Diagram 4.

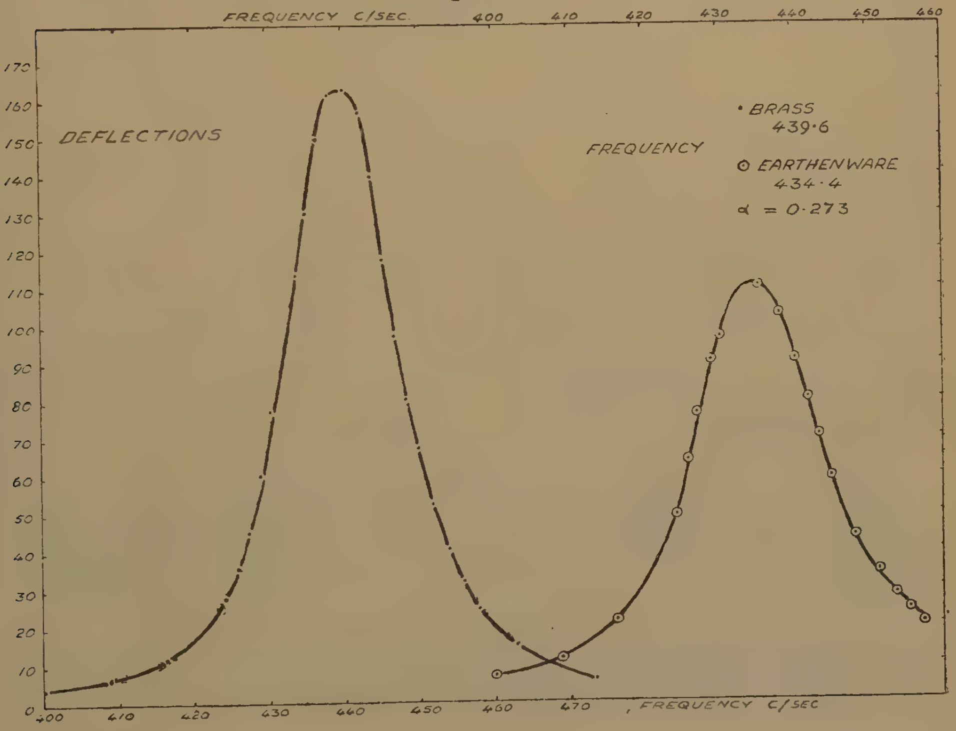

Diagram 5.

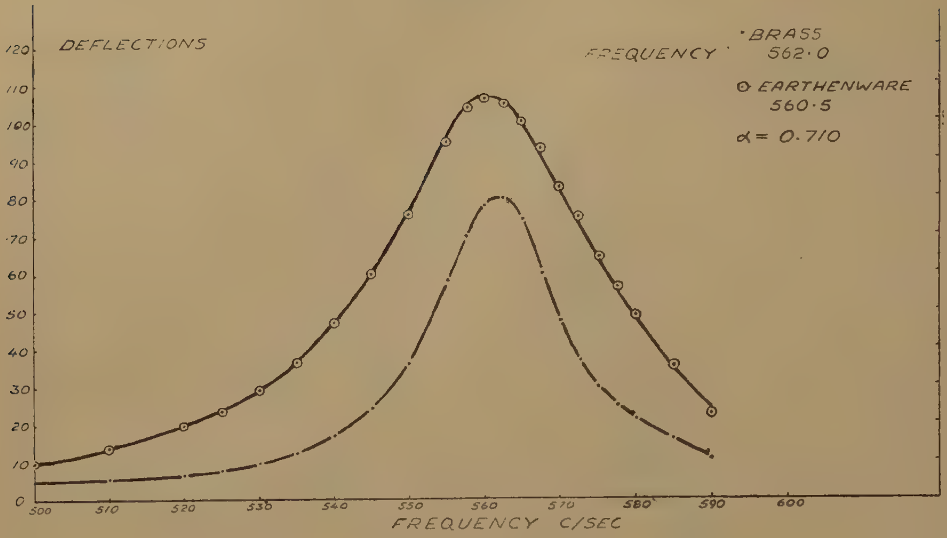

Diagram 6.

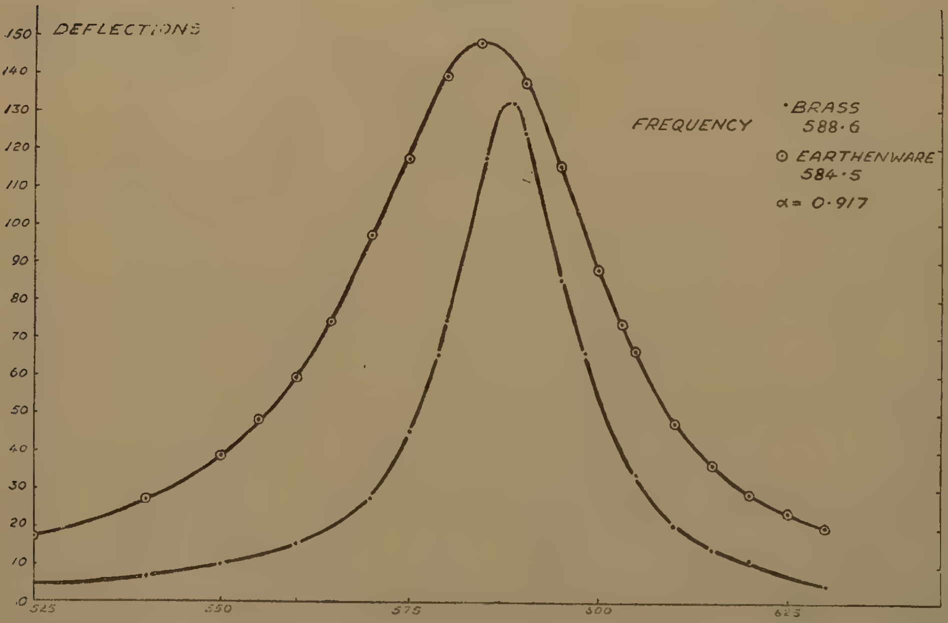

With specially careful adjustment of output of the acoustic oscillator, microphone sensitivity, and equal exposure of the two resonators, conditions fulfilled for a mean frequency of 230 cycles/sec. as illustrated by diagram 2.

$$\beta = \frac{P_1 - P_2}{P_1} = \frac{\delta_1 - \delta_2}{\delta_1} = \frac{179 - 160}{179} = 0{\cdot}107,$$

from which a corrected value $\alpha = 0{\cdot}105$ is obtained.

A curve (diagram 7) shows the relation between absorbing power and frequency and exhibits the rapid increase of α as the frequency rises in the region of the higher frequencies. It is interesting to note that the curve appears to pass through the origin, indicating total lack of absorption as the wave-length of the sound becomes very large. The high degree of absorption at 600 cycles would be more pronounced when recorded instrumentally than when observed aurally, owing to the greater sensitivity of the ear to the higher frequency sounds.

The curve shows a steep increase from 400 cycles upwards, indicating that total absorption will occur well within audible limits. Obviously the curve must bend over and become asymptotic to the line $\alpha=100$.

The hot wire microphone cannot explore regions of higher frequency owing to its insensitivity. Earthenware was chosen for this investigation on account of its highly absorbent nature and because of the uniformity of its texture and the fineness of its pores. Some indication of its nature was revealed by special preliminary experiments to find its rate of leak when filled with air under pressures varying from 2 atmospheres to $\frac{1}{2}$ atmosphere. It was found to be that of a capillary tube $\frac{1}{2}$ millimetre bore and 23 cm. long under the same conditions of pressure and temperature. The areas of surface effective for sound absorption are indicated in the table. Diagram 8 is a sectional diagram showing the build-up of the resonator and its dimensions. While it might be desirable to employ larger resonators with a bigger absorbing surface, greater difficulty would be experienced in obtaining good resonance curves. With more elaborate equipment, not at present available, such difficulties would be overcome.

Diagram 7.

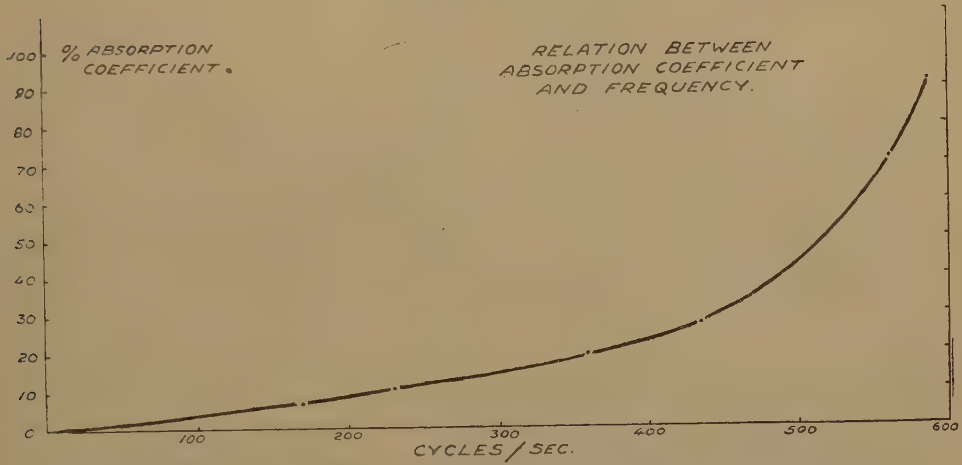

The method is not open to the objection that the surface is exposed to directive sound-waves as in the stationary wave method. Reverberation methods also involve the use of large surfaces in specially constructed rooms. The judgment of the ear in assessing reverberation times is also eliminated, although for practical purposes aural assessments must be made. The method here described can, however, afford information on the relative acoustical properties of various absorbent surfaces. While the values obtained above are in reasonable agreement with tabulated values derived by other methods, the aural assessment makes it impossible to check those results owing to the variation of sensitivity of the ear to sounds of different frequencies.

Diagram 8.

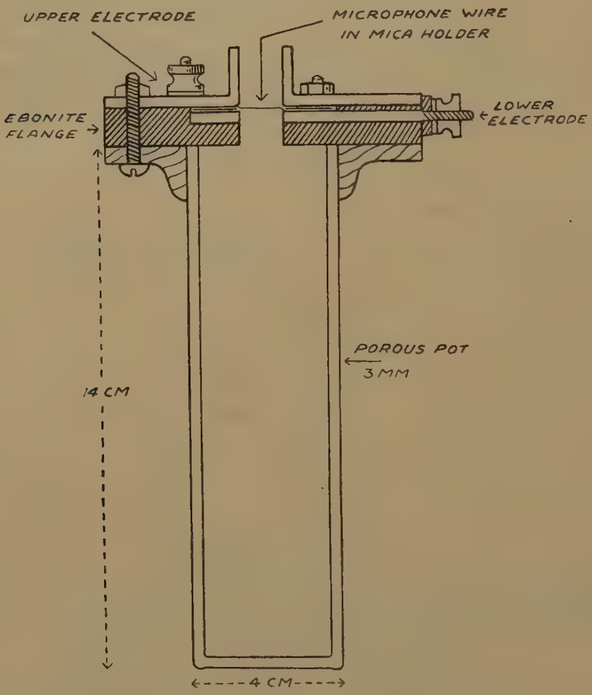

In conclusion the author wishes to acknowledge his indebtedness to the Research Committee of King's College, Newcastle-upon-Tyne, for the grant of funds for the acquirement of apparatus, and to Professors G. W. Todd and G. R. Goldsbrough of King's College for their interest and advice.

Appendix.

For a reduction of 50 per cent. of the amplitude

$$(n^2-p^2)^2=4k^2p^2,$$

from which $k=\frac{(n+p)\,(n-p)}{2p}$.

If n is nearly equal to p to a first approximation, $k=n-p$ or $p-n$.

according as we take the ascending or descending portions of the resonance curve.

If p has alternatively values $n-\delta n$ and $n+\delta n$, the resulting two values of k, k' and k'' are respectively higher and lower than the true value of k, but if the mean value of k' and k'' be taken it can be shown that

$$k=\frac{k'+k''}{2}=\delta n+\frac{(\delta n)^3}{2n^2}-\frac{(\delta n)^5}{2n^4}.$$

The error produced in the final results quoted, due to the second term, wolud not be more than 0·3 per cent. The effect of the third term is negligible.

LVIII. *A Summary Statement of the Principles of Measurement.*

By D. P. Dalzell *.

[Received August 17, 1944.]

In view of the attribution by Professor Dingle † of certain strange features to what I described ‡ as the existing system of electrical measurement, an account of what this phrase was intended to mean may not be out of place. The vocabulary used is in some respects different from that of Campbell § and Jeffreys ‖ because their use of the term fundamental is not here adopted, some new descriptive phrases are introduced and some older ones are retained.

Although the brief exposition which follows has some appearance of novelty, the introduction of new ideas into the subject under discussion is not intended. The aim is by progressive exposition and by the application of a systematic nomenclature to detach certain aberrations from the existing system. This process of clarification is necessary in order to avoid finding oneself in the position of defending several incompatible schemes. To avoid complications some difficult matters are entirely omitted; real numbers are presumed to be relevant to measurement, corrections and errors are not mentioned.

A physical quantity conceived as capable of having magnitudes which possess the serial properties of real numbers, may be called measurable. By the use of these serial properties a real number may be attached to each magnitude of a measurable quantity, a process which may be called serial comparison. This process is discussed by Campbell * in connection with density and hardness.

---

* Communicated by the Author.

† Phil. Mag. xxxv. p. 296 (1944).

‡ Phil. Mag. xxxv. p. 188 (1944).

§ Campbell, N. R., ‘ Physics : The Elements ’ (Cambridge, 1920).

‖ Jeffreys, H. ‘ Scientific Inference ’ (Cambridge, 1931).

Thermometric temperature, mentioned by Professor Dingle, is also measured by a process similar to serial comparison; at the same time I trust that, by his example of "sonority" Professor Dingle does not mean to express contempt for the measurement of times of reverberation, which is of interest in acoustics and to which his example has a slight resemblance.

When a physical quantity has an additive property †, real numbers may be so assigned that the addition of two real numbers corresponds to the additive process appropriate to the physical quantity. Given any two magnitudes of an additive physical quantity, the construction of a series of inequalities between integral multiples of them determines a series of rational numbers approximating by excess and defect to the ratio of their magnitudes. This, or any other similar process which yields the same numerical value for the ratio of two magnitudes of an additive physical quantity, may be called conjunctive comparison, and is substantially what Campbell ‡ and Jeffreys § call fundamental measurement. Euclid's application of comparison to length, angle and area is discussed and criticized by Jeffreys ‖. In using the word comparison we here follow Maxwell ¶.

Some physical quantities are such that their magnitudes must be compared indirectly by arranging matters in such a way that the ratio of two magnitudes of that physical quantity is equal to the ratio of two magnitudes of an additive physical quantity. The reasons for regarding such a method of comparison as appropriate will depend on the nature of the physical quantity to which it is applied. For example, the densities, supposed uniform, of two bodies are compared by comparison of the masses of equivoluminal parts of those two bodies. This process may be called indirect conjunctive comparison. The additive property is clearly associated, by the methods of comparison we have described, with uniformity of scale in measurement, for which no other satisfactory criterion is known.

Physical quantities, whereof the magnitudes are comparable by conjunctive comparison or by appropriate indirect conjunctive comparison, may be called uniformly measurable.

Given a collection of uniformly measurable physical quantities mutually related by physical laws, a particular magnitude of each such quantity, called the unit magnitude, may be selected and given a name. In that case the ratio of a magnitude of one of these physical quantities

---

* *Op. cit.* pp. 270–277.

† Campbell, *op. cit.* pp. 277–290.

‡ *Op. cit.* pp. 267–294.

§ *Op. cit.* pp. 84–106.

‖ *Op. cit.* pp. 107–130.

¶ Maxwell, J. C., "A Treatise on Electricity and Magnetism,' 3rd Edn. (Oxford, 1904), i. pp. 350, 471, ii. p. 392.

to the corresponding unit magnitude is called the numerical measure of that magnitude relative to the unit. Maxwell* speaks of a measure as consisting of a numerical part and a denominational part, the latter being the name of the unit.

A system of units is constructed by selecting from the original collection of physical quantities a subset of additive physical quantities which are called fundamental, and whereof the unit magnitudes are regarded as capable of arbitrary choice ; at the same time definitions of the units, called derived units, of the other physical quantities are framed by means of conventions in such a manner that while the conventions remain fixed the magnitudes of the derived units are determinate functions of the magnitudes of the fundamental units, when both the conventions and the physical laws are taken into account.

Thus a system of units is determined by fixed conventions and by the choice of fundamental quantities, the unit magnitudes of the fundamental quantities being regarded as variables. Clearly the choice and definition of the units is an essential feature of the existing system, and there is no reason for surprise that in a discussion of it units appear to be vital.

The dependence of the magnitudes of the derived units upon those of the fundamental units is called dimensionality. When the magnitude of a derived unit varies as the power k of the magnitude of a fundamental unit, the derived unit or the corresponding physical quantity is said to be of k dimensions in the fundamental unit or the corresponding physical quantity †.

When the conventions have been fixed all the uniformly measurable physical quantities in the system have definite dimensions, and there is no place in the system for measurable physical quantities of unknown dimensions.

The fundamental quantities should be as few as conveniently possible and are usually desired to be adapted to standardization, that is preferably to the production of a material configuration which embodies a chosen unit magnitude or a physical magnitude with a definite numerical relation to the unit, or alternatively to the production or adoption of a standard device or process which is capable of reproducing a chosen unit magnitude or a physical magnitude with a definite numerical relation to the unit. Additionally, or alternatively, some derived units may be standardized. Such material configurations or processes are called standards. Thus standardization is the selection of unit magnitudes and the construction of suitable standards. It is convenient here to refer to the choice of fundamental unit magnitudes as standardization and to omit consideration of the construction of standards.

The statement that a combination of numerical measures is independent of our artificial standards is presumably the same thing as to say that in a given system, that is, with fixed conventions, the number in question is independent of the standardization. It is, of course, impossible to say that anything is independent of convention because of the possible vagaries in the choice of conventions ; for instance, one man may think that to count a flock of sheep one must count the heads and another man may think that one should count the legs. Probably no amount of argument could persuade the latter, if he were both a butcher and a disciple of Professor Dingle, to agree with the former.

---

* ‘Theory of Heat’ (London, 1908), p. 75.

† Maxwell, ‘Treatise,’ i. p. 2 ; Campbell, *op. cit.* p. 372.

In the above description, a system of units is, as far as I am aware, identical with what is meant by Maxwell [*] in his discussion of the term which is applicable to the two systems of dynamical units in electricity and magnetism. and commonly called the electrostatic and electromagnetic systems. The dimensions of the various physical quantities in these two systems are given by Maxwell [†] and Jeans [‡], and these authors are in agreement. There seems to be no reason to doubt the accuracy of their results, which are obtained by tracing out the implications of two sets of conventions. Those who speak of the dimensions of K and μ as unknown are not, therefore, discussing the existing system in which dimensionality is a consequence jointly of prearranged conventions and physical law. Similarly those who say that the dimensions of charge must be the same in all systems of units [§] are not referring to the existing system.

Professor Dingle summarizes the problem of measurement of charge by the exhortation " Here is a charge ; state the operation of measuring it." The answer to this is quite simple : we may assign to the charge any numerical measure we please, and doubtless most of us would choose unity. In other words, when we have at our disposal one and only one charge, that charge is unit charge. Alternatively we might not think in terms of numbers, but give the charge a name, say Archibald. The problem of measurement arises only when we have to consider at least two charges, and we then say " Here we have two charges, how can we compare them ? " If we know that there are many other charges in the world, we may well refrain from assigning unit magnitude to one of the two charges of which we were at first aware.

Professor Dingle's description of the status of measurement in physics at any moment is, in my opinion, too simple. Measurements do not become, as it were, recognized until they are associated with interesting or important phenomena which may or may not be easily described in terms of equations. The possibility of usefully framing definitions of units, measures or methods of measurement, as if one were ignorant of their implications is, paradoxically, only possible when the nature of at least some of those implications is in fact well known. I do not quite appreciate how one is genuinely to select a list of recognized measurements without having or assuming some foreknowledge of the nature of the appropriate equations if that selection has to be such as to facilitate the discovery of those equations. The process which occurs in the development of physics is rather an interaction between measurement, the observation of phenomena and the determination of equations, and unless exceptional powers of intuition are exercised readjustments may from time to time have to be made and some rubbish may have to be discarded. When a branch of physics has reached a certain stage of systematization, definitions of units or of measures can be framed in such a way as to conceal the experimental achievements which have made them possible. If, as in the accepted system, the unit is defined separately and the comparison of a given physical magnitude with the unit is regarded as a distinct process, the definition of the unit can be made such as to be independent of the acquisition of further knowledge in certain directions. For instance, the definition of unit electrostatic charge assumes neither the proportionality of force to charge nor the law of inverse square, but depends only on the notion of isolated charges of similar magnitude. The definition therefore need not be changed to accommodate variations in the technique of measurement, and the procedure adopted for comparison of a given charge with the unit will depend on the particular purpose and circumstances of the measurement and the experimental resources available at the time.

---

[*] 'Heat,' p. 81.

[†] 'Treatise,' ii. pp. 263–269.

[‡] Jeans, Sir James, 'The Mathematical Theory of Electricity and Magnetism,' 5th Edn. (Cambridge, 1943), p. 531.

[§] Kaye, G. W. C., and Laby, T. H., 'Tables of Physical and Chemical Constants,' 9th Edn. (London, 1941), p. 12.

The use of the term equivalence adopted by Professor Dingle seems to be somewhat strange. I would suggest that the relation between the systems commonly called electrostatic and electromagnetic could better be described by some such phrase as coextensive and dimensionally incompatible: coextensive because they apply to the same collection of physical quantities and dimensionally incompatible in the sense that measures of at least one physical magnitude in the two systems with the same choice of fundamental units differ by a conversion factor which depends on the magnitudes of the chosen fundamental units. Apparently Professor Dingle would regard any two coextensive systems as equivalent.

Evidently in the scheme described above great emphasis is placed on additivity, not only for the reason already mentioned, but also because additivity may be regarded as one of the clues to physical reality in the sense of suggesting laws of conservation, whether in the form of invariability of totals or of the equation of continuity. A law of conservation may then also indicate atomicity. I believe that these remarks are in accordance with past experience and that contemplation of the possibility of conservation does suggest that, as it were, nature might have some difficulty in conserving a continuous quantity.

A system of units, in the Maxwellian sense of the term, is a function of the variable magnitudes of the fundamental units, the conventions whereby the derived units are defined remaining fixed. A particular value of this function is obtained by standardization. The magnitudes of the fundamental units may be regarded as analogous to the variables in a polynomial, the conventions as analogous to the coefficients. When the conventions which define the derived units in terms of the fundamental units are varied a trajectory of systems of units is generated. This trajectory may be multidimensional in the geometrical sense of that word. When the conventions depend on certain real variables we may call these the systemic parameters. The systems of units used in electricity and magnetism are discussed in this manner by Thomson *, who employs two trajectories of systems of units and shows how the electrostatic and electromagnetic systems are obtained by assigning the systemic parameters.

If, when two electric charges of similar magnitude are separated in a vacuum by unit distance and exert unit force upon each other the numerical measure to be assigned to each is stated to be $\sqrt{\kappa}$, where κ is a variable of unspecified value, the meaning conveyed is that κ is a systemic parameter, and this is only another way of saying that no decision has yet been made as to whether or how the unit of charge is to be defined in terms of the units of the selected fundamental quantities.

LIX. *The Behaviour of Liquids in Shear.*

By E. G. Richardson, B.A., Ph.D., D.Sc. (King's College, University of Durham, Newcastle-upon-Tyne) *.

[Received September 10, 1945.]

Introduction.

In 1933 the writer described some qualitative experiments on gelatine and similar solutions during setting, which consisted mainly of observations on the time-period and damping of a disk set in oscillation in the fluid ‡. From these observations it was possible to exhibit the acquirement of elasticity and the change in the viscosity of the liquid as it passed from sol to gel.

In 1939 the apparatus described below, which it was hoped would give quantitative data, was set up in the Physical Laboratory of the South-East Essex Technical College, of which Dr. E. Tyler was then in charge. It was intended to make this a joint research with Dr. Tyler, but the seconding of the writer to the Civil Service Scientific Pool and the subsequent promotion of Dr. Tyler elsewhere prevented this project from being carried out. The apparatus was transferred to Newcastle on the writer's return there in 1945, and the work continued in the Physics Department of King's College. The writer wishes to express his gratitude to Dr. Tyler and the authorities of the Technical College for their collaboration in the early stages of the investigation.

---

* Thomson, Sir J. J., ' Elements of the Mathematical Theory of Electricity and Magnetism,' 5th Edn. (Cambridge, 1921), pp. 343–347.

† Communicated by the Author.

‡ Trans. Faraday Soc. xxix. p. 494 (1933).

Scope of Work.

It is well-known that certain liquids show elastic as well as viscous effects when sheared. Merrington [*] has recently drawn attention to a remarkable display of this double property in rubber solution. When this liquid is forced through a capillary tube it contracts on entering and swells out again on leaving the tube. Such relaxation is also a property of certain solids such as rubber [†] and dough [‡], and is usually shown by applying to a specimen a sudden stress and observing the rate at which the body recovers equilibrium. Since time is an essential factor in this behaviour, the application of an oscillatory stress suggests itself. In the experiments about to be described the liquid is contained in a cylindrical vessel which is given simple harmonic motion about a central vertical axis so that an alternating torque is applied to the liquid and the modulus of rigidity as well as the viscosity comes into play.

Two cases will be considered.

Case A.—The liquid in the form of a column extending along the y axis is given an oscillatory torque $\theta=\theta_0 e^{ipt}$ over the face $y=0$. If N is the appropriate modulus of shear (rigidity), η the coefficient of viscosity and ρ the density, the equation of motion for an annulus δr wide and δy thick at radius r and depth y is

$$2\pi r^3\,\delta r\,\delta y\,\rho\frac{\partial^2\theta}{\partial t^2}=2\pi r^3\,\delta r\,\delta y\left(\mathrm{N}\frac{\partial^2\theta}{\partial y^2}+\eta\frac{\partial^3\theta}{\partial^2 y\,.\,\partial t}\right)$$

or

$$\frac{\partial^2\theta}{\partial t^2}=\frac{\mathrm{N}}{\rho}\cdot\frac{\partial^2\theta}{\partial y^2}+\frac{\eta}{\rho}\,\frac{\partial^3\theta}{\partial^2 y\,.\,\partial t}=c^2\frac{\partial^2\theta}{\partial y^2}+\nu\frac{\partial^3\theta}{\partial^2 y\,.\,\partial t}, \quad . \quad . \quad . \quad (1)$$

and the solution for waves travelling up and down the column

$$\theta=\mathrm{C}e^{(\alpha+i\beta)l}[e^{(\alpha+i\beta)(y-l)}-e^{-(\alpha+i\beta)(y-l)}]e^{ipt}, \quad . \quad . \quad . \quad . \quad (2)$$

when a rigid barrier prevents movement at $y=l$. The amplitude at any level y in terms of that at the base is given by

$$\theta_y{}^2=2\theta_0{}^2[\cosh\{2\alpha(y-l)\}-\cos\{2\beta(y-l)\}]. \quad . \quad . \quad . \quad . \quad (3)$$

(If the upper surface is perfectly free, *plus sine* replaces *minus cosine* in this expression.) Substituting (2) in (1), we find

$$\begin{cases}(\alpha^2-\beta^2)(c^4+\nu^2p^2)=-p^2c^2,\\ \quad 2\alpha\beta(c^4+\nu^2p^2)=-\nu p^3,\end{cases}$$

---

[*] 'Nature,' clii. p. 663 (1943).

[†] *Cf.* Barus, Amer. J. Sci., xlv. p. 87 (1893).

[‡] *Cf.* Schofield and Scott-Blair, Proc. Roy. Soc. cxxxviii. A, p. 707 (1932); cxxxix. A, p. 557 (1933); cxli. A, p. 72 (1933).

or $$\alpha^2=p^2\left[\frac{\sqrt{(c^4+\nu^2p^2)}-c^2}{2(c^4+\nu^2p^2)}\right];\quad \beta^2=p^2\left[\frac{\sqrt{(c^4+\nu^2p^2)}+c^2}{2(c^4+\nu^2p^2)}\right].$$

$$\left(\text{If } \nu=0,\quad \alpha=0,\quad \beta=\frac{p}{c};\quad \text{if } c=0,\quad \alpha=\beta=\sqrt{\frac{p}{2\nu}}.\right)$$

The function $\frac{\theta_0}{\theta}$ is plotted on fig. 1 for $l=24$, $\beta=\frac{\pi}{24}$ and values of α equal to 0, $0{\cdot}1\beta$, $0{\cdot}25\beta$, $0{\cdot}5\beta$. The first case gives the usual stationary wave distribution of amplitude. The others show pseudo-nodes whose position begins to deviate from the first and at which the minimum amplitude gets greater with α/β.

Fig. 1.

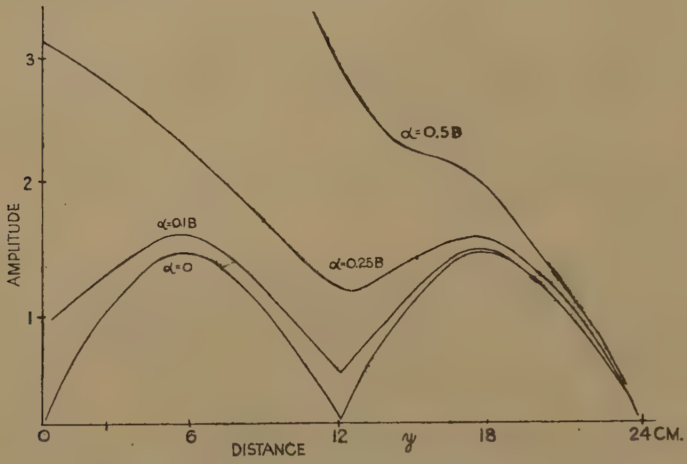

Theoretical distribution of amplitude (axial case).

Case B.—The sides of the column are given an oscillatory torque—the same throughout the column—and waves are propagated radially. The equation of motion is now

$$2\pi r^3\,\delta r\,\delta y\,\rho\frac{\partial^2\theta}{\partial t^2}=\mathrm{N}\left(2\pi r^3\frac{\partial\theta}{\partial r}\right)\delta r\,.\,\delta y+\eta\frac{\partial}{\partial r}\left(2\pi r^3\frac{\partial^2\theta}{\partial t\,.\,\partial r}\right)\delta r\,.\,\delta y,$$

or $$\frac{\partial^2\theta}{\partial t^2}=c^2\left(\frac{\partial^2\theta}{\partial r^2}+\frac{3}{r}\frac{\partial\theta}{\partial r}\right)+\nu\left(\frac{\partial^3\theta}{\partial r^2\,.\,\partial t}+\frac{3}{r}\frac{\partial^2\theta}{\partial r\,.\,\partial t}\right). \quad . \quad . \quad (4)$$

If we substitute $\theta=\phi e^{ipt}$, ϕ being a function of r alone,

$$\frac{\partial^2\phi}{\partial r^2}+\frac{3}{r}\frac{\partial\phi}{\partial r}+\left(\frac{p^2}{c^2+ip\nu}\right)\phi=0,$$

or $$\frac{\partial^2\phi}{\partial r^2}+\frac{3}{r}\frac{\partial\phi}{\partial r}+(\alpha-i\beta)^2\phi=0. \quad . \quad . \quad . \quad . \quad . \quad . \quad . \quad . \quad (5)$$

The solution of this may be obtained in terms of Bessel functions of complex argument*, as $\phi=\frac{J_1 r(\alpha-i\beta)}{r(\alpha-i\beta)}$. The function $J_1(\alpha-i\beta)$ is plotted on fig. 2 for values corresponding to those of fig. 1. Those for $\alpha=0$ and β are available in the tables of the Bessel and the ber and bei functions; the others have been calculated as series from the formula *:

$$J_1(\alpha+i\beta)=\sum_{m=0}^{m=\infty} J_{(1+m)}\alpha \, . \, J_m(i\beta).$$

In the experiments about to be described, it is the modulus of the linear displacement amplitude at each radial distance in the liquid which is actually measured. This is related to the angular amplitude at the same place by $\omega=\theta r$. Thus the curves of fig. 2 give the theoretical distribution of amplitude through the liquid, measuring from the centre outwards, when $p/c=1$.

Fig. 2.

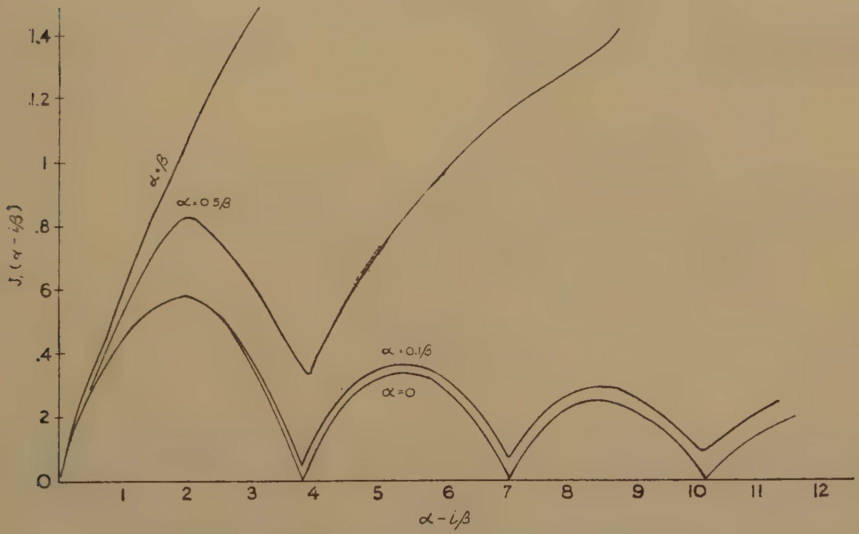

Theoretical distribution of amplitude (radial case).

The purely elastic fluid therefore shows nodal circles at the appropriate resonant frequencies of oscillation. A liquid having elasticity and viscosity exhibits pesudonodes and antinodes as in Case A. When the liquid has an overwhelming viscosity, the amplitude at any radial distance falls off steadily from the edge towards the centre, there are no pseudonodal circles, but this does not mean to say that the liquid moves *en bloc* as there is a progressive phase change with radial distance, so that different parts of the fluid may be moving in opposition of phase.

---

* See, for example, McLachlan, 'Bessel Functions for Engineers'; Lamb, 'Hydrodynamics,' § 357.

Experimental Work.

In the experiments a metal bowl 22 cm. diameter with upright sides 10 cm. deep formed the container of the liquids, which were: diesel oil, cellulose acetate in acetone sols and gelatine in water sols of small concentration (up to 6 per cent.). The container was mounted on a table which through connecting rods to an electric motor could be oscillated through various small angles and at constant frequency. In order to simulate the condition A a fixed guard-ring was held just inside the container so that disturbances could not be propagated inwards from the moving walls, only upwards from the base. To simulate condition B a guard-disk was fixed just above the base of the vessel. It will be noted that neither of these experiments corresponds exactly to the two-dimensional motion assumed in the analysis. In the first case the guard-ring causes a diminution of amplitude in its vicinity, but it was noticed that the angular amplitude was constant over the main portion of the surface where the measurements were made. In the second type of experiment the guard-disk imposed an overall zero amplitude at the base, but did not affect measurements made in the vicinity of the free surface. It did not, in fact, prevent a distribution closely resembling that of fig. 2 in the body of the liquid being set up, the disturbing effect being confined to a centimetre above the guard-disk. These regions were avoided in placing the anemometer about to be described.

Fig. 3.

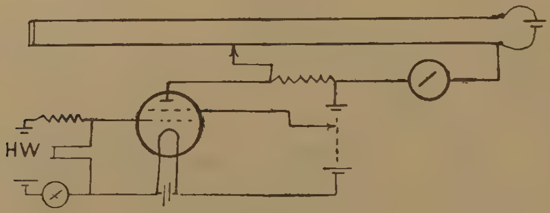

Hot-wire circuit.

Plotting of Velocity Fields.

As the introduction of recording devices having bulk and inertia was undesirable, it was decided to use a hot wire anemometer. A nickel wire 1 mil. diameter and 1 cm. long was soldered to a fork formed of two steel needles which could be located at any position in the liquid, being mounted as it was on a micrometer for traverse either along a radius of the tank (the wire itself being vertical) or parallel to the axis of the tank (the wire then lying along a radius) for the B and A cases respectively.

The wire heated by a current of 0·1 to 0·15 amp. was connected in the grid circuit of a variable μ valve (WR. 2), as the plate current is then more nearly related in a linear fashion to the velocity changes which accompany the motion of the liquid; further, the valve acts as a rectifier, so that the *steady* change in the value of the plate current caused by an oscillating fluid current may be used as a measure of its amplitude. Actually, the change in potential drop across a fixed resistance in the plate circuit was used as measure of the velocity amplitude at the wire. The circuit is shown in fig. 3.

Fig. 4.

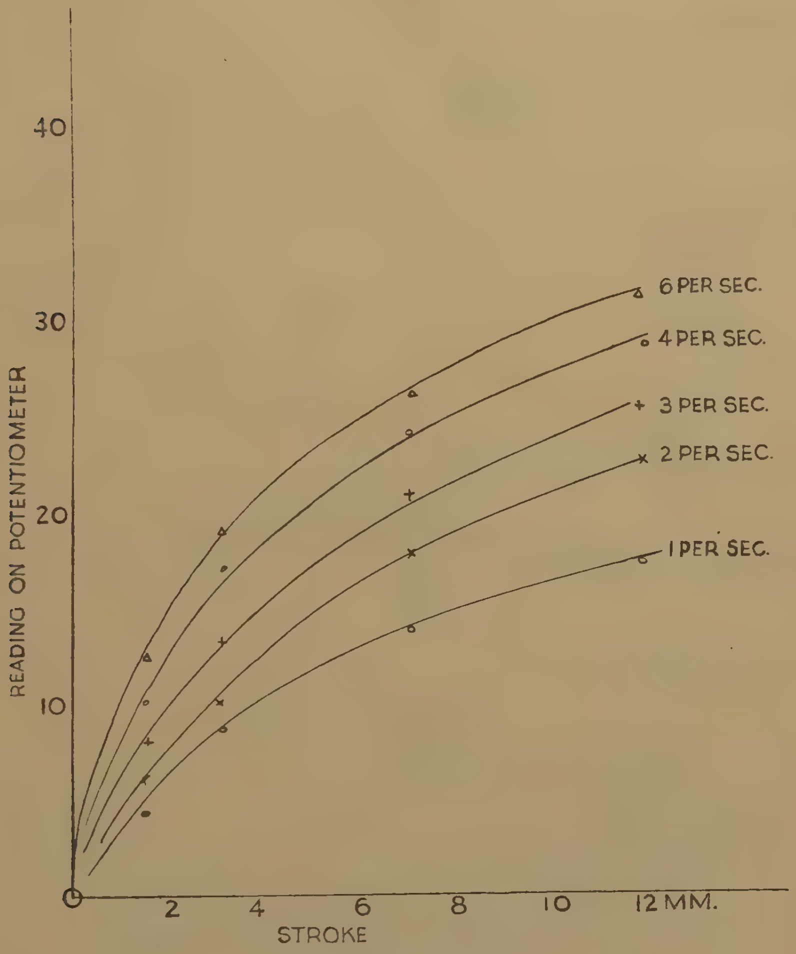

Hot-wire calibration.

An alternative method of studying the elastic constants of the liquid is to measure the pseudo wave-length by employing two hot wires at a distance along a radius (B) or vertically over each other (A), and recording the phase difference between the oscillations in potential (at double the applied frequency) across them. For this purpose, tappings from each wire were led to the X and Y plates of a cathode-ray oscillograph, and the relative positions of the wires adjusted until an easily recognizable

Lissajons figure—straight line or ellipse—was drawn by the electron spot on the screen.

As the thermal lag of the hot-wire varies with frequency it was necessary to calibrate the indications of the hot-wire recorder over a range of frequency and amplitude, covering that to be used in the experiments.

Fig. 5.

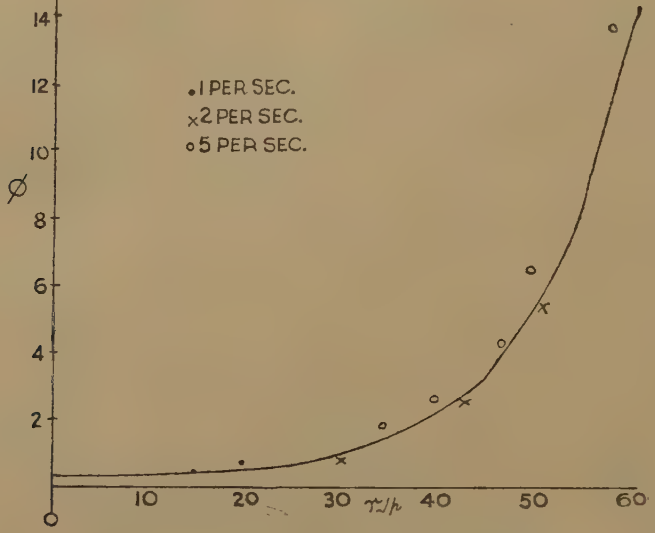

Amplitudes in Diesel oil (ν=1·8) ; Case B.

Fig. 6.

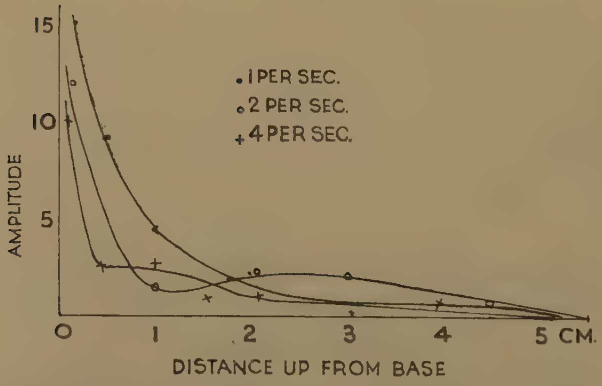

Amplitudes in 6 per cent. cellulose acetate sol (N=225, ν=20, c.g.s.) ; Case A.

This was done for each liquid by mounting the hot-wire fork on the connecting rod of a reciprocating motor which carried it to and fro in simple harmonic motion in the liquid. A typical set of calibration curves, potential *v.* amplitude for various frequencies in oil, is given in fig. 4.

The measured potentials are nearly proportional to the square roots of the amplitudes.

Results.

Experimental plots of displacement amplitude and of places in and out of phase are given in figs. 5 to 9, for diesel oil having no elasticity, for cellulose acetate in acetone with viscous and elastic properties of the same order of magnitude, and for gelatine solutions in which the elastic structure overrides the viscosity. (The arrows on figs. 8 and 9 indicate sections moving in opposition of phase.)

Fig. 7.

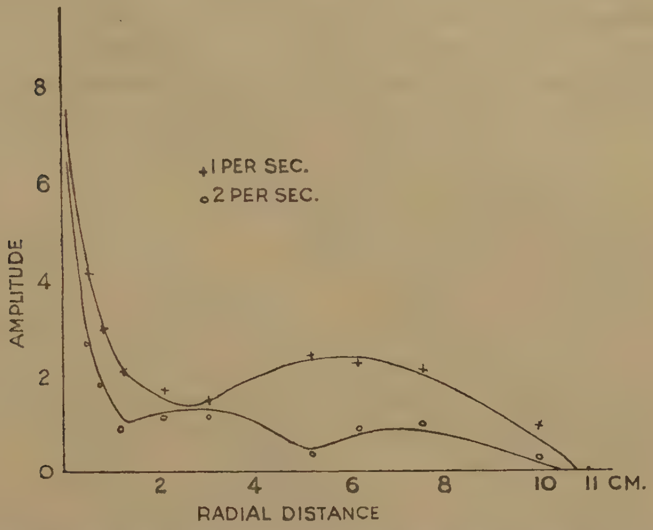

Amplitudes in 6 per cent. cellulose acetate sol (N=225, ν=20 c.g.s.); Case B.

Fig. 8.

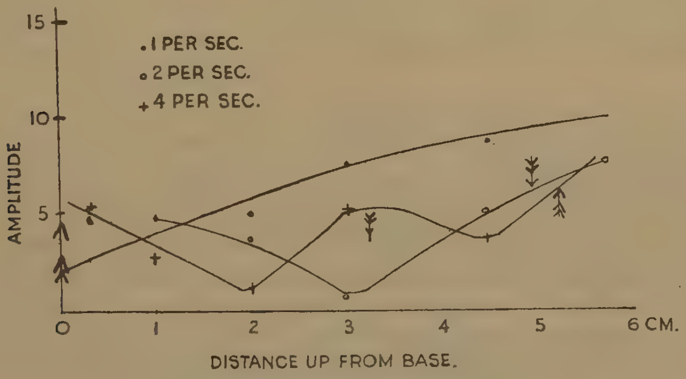

Amplitudes in 2 per cent. gelatine sol (N=625, ν=10 c.g.s.); Case A.

On comparing these with figs. 1 and 2, we observe a general agreement in the shape of the curves. Some discrepancy may be ascribed to experimental inaccuracy but a major difficulty in all work with sols and gels is that the effective viscosity varies with the rate of shear. Since it is impossible to maintain the rate of shear constant throughout the fluid we should expect such variations, the deduced value of the coefficient of viscosity being greater when the amplitude and frequency are small. On the other hand, a greater consistency in the deduced values of the elastic moduli with frequency and amplitude are apparent, though another difficulty arises herein since continued agitation of a gel tends to break down the structure to which the elasticity is due. These physical considerations must limit the accuracy and consistency attainable in any work on fluids exhibiting either anomalous viscosity or structural elasticity.

Fig. 9.

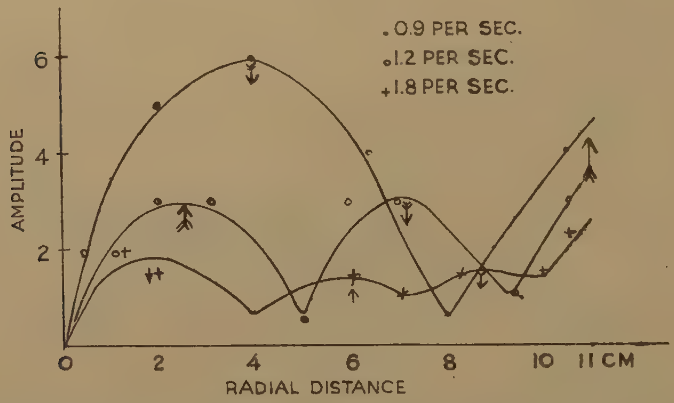

Amplitudes in 3 per cent. gelatine sol ($N=2500$, $\nu=100$ c.g.s.) ; Case B.

To calculate the physical properties of the fluid from an overall comparison of theoretical and experimental curves would be a laborious task. They may, however, be derived by an inspection of the amplitudes at judicious points. If the system exhibits resonance and is not highly viscous, the elastic constants may be obtained from a knowledge of the natural frequencies in either the axial or radial modes. When to the elasticity a moderate amount of damping is added, quasi-resonances can be set up and the amplitudes at the quasi-nodes measured and compared with the corresponding ones read off figs. 1 or 2. In the axial case the nodal amplitude can be readily obtained from equation (3), since this expression has minimum values of 2 sinh $\alpha(y-l)$ (providing α is not too large) at the nodes.

When the liquid is merely viscous, the logarithm of the amplitude may be plotted against distance and the approximate value of $\log_{10} \sinh \alpha(y-l)$ used to deduce the value of α. The liquid of large viscosity and small elasticity presents the greatest difficulty to attempts to separate its elastic and viscous constants, since the nodes become ill-defined and are considerably displaced from the positions they would occupy in purely elastic systems. The shortest road to their elucidation in such a case is probably to plot a set of curves such as those of figs. 1 or 2 for a number of values of α, expressed as multiples of β, and to compare the theoretical and practical distributions of amplitude, noting in particular the values at the best approximations to resonance, *i. e.* segmental delineation, that one can attain.

The deduced values of N and η are shown beneath the figures.

It may be objected that the physical characteristics of sols and gels should not be separated into rigidity and viscosity in the manner adopted in these experiments, that, in fact, " jelliness " is an indivisible property. Maxwell, however, regarded such systems as characterized in this way, the ratio of viscosity to elasticity being a dependent variable τ characterizing the rate at which the system recovers equilibrium when displaced. When the liquid is subjected to simple harmonic forcing, the effective viscosity $\bar{\eta}$ should decrease from the " rest-value " η_0 according to the formula $\bar{\eta}=\frac{\eta_0}{1+p^2\tau^2}$, so that the viscosity will effectively experience a rapid drop as p approaches $1/\tau$. Evidence for these ideas cannot be derived from the present experiments, since in the systems used $1/\tau$ is a quantity probably much larger than the maximum frequency attainable.

Summary.

By subjecting a liquid having elasticity and viscosity to shearing forces of simple harmonic nature, it is shown how values of the two coefficients (of elasticity and viscosity) may be deduced by plotting the distribution of amplitude of oscillation throughout the system. The amplitude and the relative phase of motion are measured by means of hot-wire anemometers. Results are presented for oil, and for sols of cellulose acetate and gelatine of small concentration.

LX. *Expansion in Series of the Exact Solution for Compressible Flow Past a Circular or an Elliptic Cylinder.*

By A. R. Manwell, now at Department of Mathematical Physics, Queen's University, Belfast *.

[Received October 19, 1944.]

SUMMARY.

This problem has been treated by various writers by successive approximation from the potential flow solution. The following method is practically just as laborious as previous methods but has the theoretical advantages of (*a*) using the exact hodograph equations of flow, and

---

* Communicated by the Author.

(*b*) giving a sequence of equations for the coefficients in the expansion in powers of "q" ("q" is the local stream velocity with the velocity of sound at infinity taken as unity). From these equations each coefficient may be determined in terms of those preceding. The two series giving the distribution of q along the boundary of the cylinder and along the axis of x, together with the two hodograph expressions for the rectangular co-ordinates, are all expansions of the true analytic solution, but unfortunately a parameter "b_1," which may be expanded in powers of "u" the Mach number, is involved. Unless, which is in fact so up to the term q^5 for the circular boundary, b_1 occurs only as a linear factor in the second of these series, the expansion used for finding $b_1(u)$, and hence the critical Mach number, is not the analytic expansion but merely an approximation formed by neglecting higher powers of q and so the coefficients of these powers. This is not at first sight apparent. Convergence is fair but, judging by the numerical results, at least one more term in q^7 is needed to get an accurate value of the critical Mach number.

---

1. *Introduction.—Hodograph Solutions.*

THE known hodograph solutions for compressible flow may be written

$$x'=\sum_{1}^{\infty} a_n \cos n\phi \, X_n, \qquad \text{(A)}$$

$$y'=\sum_{1}^{\infty} a_n \sin n\phi \, Y_n, \qquad \text{(B)}$$

where

$$x'=x\cos\phi+y\sin\phi,$$

$$y'=x\sin\phi-y\cos\phi,$$

$$X_n=\frac{1}{n}F_n'(q),$$

$$Y_n=\frac{F_n}{q},$$

and

$$q^2F_n''+q(1-q^2)F_n'-n^2F_n(1-q^2)=0$$

for isothermal flow.

More generally

$$F_n''+\left\{\frac{d}{dq}\log\rho q\right\}\left\{\frac{dF_n}{dq}-n^2\frac{F}{q}\right\}=0,$$

where

$$\int\frac{dp}{\rho}+\tfrac{1}{2}q^2=\text{a constant}.$$

In the case of isothermal flow F_n is a polynomial of $n(n-1)/2+1$ terms, viz.:

$$F_n(q)=\sum_{p=0}^{p=\infty} a_{2p}q^{2p+n},$$

where

$$a_{2p}=(-1)^p\frac{[n(n-1)][n(n-1)-2]\ldots[n(n-1)-2p-2]}{(4n+4)(8n+16)\ldots[4p(n+p)]}.$$

$F_n(q)$ may also be expressed as a definite integral similar to that for the hypergeometric function.

2. *Expansion for Circular Cylinder in Isothermal Flow.*

The potential flow solution is with the usual notation

$$w = u(z + 1/z),$$

$$\frac{dw}{dz} = u\left(1 - \frac{1}{z^2}\right),$$

whence

$$x' = \cos\phi + \frac{1}{2} q/u \cos 2\phi + \frac{3}{8}(q/u)^2 \cos 3\phi + \frac{5}{16}(q/u)^3 \cos 4\phi$$

$$+ \frac{35}{128}(q/u)^4 \cos 5\phi + \frac{63}{256}(q/u)^5 \cos 6\phi + \frac{231}{1024}(q/u)^6 \cos 7\phi$$

and $$y' = \sin\phi + \tfrac{1}{2} q/u \sin 2\phi, \text{ etc.}$$

The boundary conditions are that $x' = 0$ and and $y' = 1$ on the circular boundary defining the relation $\lambda = 2\cos\phi = q/u$, and that as $q \to u$ along the x axis $x \to \infty$. in fact $(1 - q/u)^{-\frac{1}{2}} = R$. Assume then that in the compressible flow solution

$$\lambda = 2\cos\phi = A_1 q + A_3 q^3 + A_5 q^5 \ldots$$

and that $$R = [1 - f(q)]^{-\frac{1}{2}}, \quad \ldots\ldots\ldots\ldots \quad (C)$$

where $$f(q) = b_1 q + b_3 q^3 + b_5 q^5 \ldots$$

We have now the following identities:

$$R \equiv [1 - f(q)]^{-\frac{1}{2}} \equiv \sum_{1}^{\infty} a_n X_n(q),$$

where $f(u) = 1$ from the condition at infinity. Expanding by the binomial theorem and equating coefficients of q^n we find the following relations for $a_1 \ldots a_7$ in terms of b_1, b_3 and b_5. The speed of sound has been taken as unity.

$$a_1 = 1,$$

$$a_2 = \frac{1}{2} b_1.$$

$$a_3 = \frac{3}{8} b_1^2,$$

$$a_4 = \frac{5}{16} b_1^3 + \frac{1}{2} b_3 + \frac{a_2}{3},$$

$$a_5 = \frac{35}{128} b_1^4 + \frac{3}{4} b_1 b_3 + \frac{5}{8} a_3,$$

$$a_6 = \frac{63}{256} b_1^5 + \frac{15}{16} b_1^2 b_3 + \frac{1}{2} b_3 + \frac{9}{10} a_4,$$

$$a_7 = \frac{231}{1024} 4 b_1^6 + \frac{35}{32} b_1^3 b_3 + \frac{3}{8} b_3^2 + \frac{3}{4} b_1 b_5 + \frac{7}{6} a_5 - \frac{7}{80} a_3.$$

Again by expanding $\cos n\phi$ in powers of $\lambda = 2\cos\phi$

$$\cos\phi = \lambda/2,$$
$$\cos 2\phi = \lambda^2/2 - 1,$$
$$\cos 3\phi = (\lambda^3 - 3\lambda)/2,$$
$$\cdot\quad\cdot\quad\cdot\quad\cdot\quad\cdot\quad\cdot\quad\cdot\quad\cdot$$
$$\cos 7\phi = (\lambda^7 - 7\lambda^5 + 14\lambda^3 - 7\lambda)/2.$$

The boundary condition (A) $x' = 0$ becomes

$$0 \equiv a_1\frac{\lambda}{2} + a_2\left(\frac{\lambda^2}{2} - 1\right)\left(\frac{q - q^3}{3}\right) + a_3\frac{(\lambda^3 - 3\lambda)}{2}\left(q^2 - \frac{5}{8}q^4 \dots\right)$$
$$+ a_4\frac{(\lambda^4 - 4\lambda^2 + 2)}{2}\left(q^3 - \frac{9}{10}q^5 \dots\right) + a_5\frac{(\lambda^5 - 5\lambda^3 + 5\lambda)}{2}(q^4 \dots)$$
$$+ a_6\frac{(\lambda^6 - 6\lambda^4 + 9\lambda^2 - 2)}{2}(q^5 \dots),$$

where $\lambda = A_1q + A_3q^3 + A_5q^5 \dots.$

Substituting for λ and arranging in powers of q gives the following three relations :—

$$0 = a_1\frac{A_1}{2} - a_2, \quad \cdot\;\cdot\;\cdot\;\cdot\;\cdot\;\cdot\;\cdot\;\cdot\;\cdot\;\cdot\;\cdot\;\cdot\;\cdot\;\cdot\;\cdot \quad \text{(A)}$$
$$0 = a_1\frac{A_3}{2} + \frac{A_1{}^2a_3}{2} + \frac{a_2}{3} - \frac{3A_1a_3}{2} + a_4,$$
$$0 = a_1\frac{A_5}{2} + a_2(A_1A_3 - A_1{}^2/6) + a_3\left\{\frac{(A_1{}^3 - 3A_3)}{2} + \frac{15}{16}A_1\right\}$$
$$- a_4\left(\frac{9}{10} + 2A_1{}^2\right) + \frac{5}{2}A_1a_5 - a_6.$$

Similarly, since $\sin n\phi/\sin\phi$ may be expanded in powers of λ, viz. :

$$\sin\phi/\sin\phi = 1,$$
$$\sin 2\phi/\sin\phi = \lambda,$$
$$\sin 3\phi/\sin\phi = \lambda^2 - 1,$$
$$\cdot\quad\cdot\quad\cdot\quad\cdot\quad\cdot\quad\cdot\quad\cdot\quad\cdot\quad\cdot\quad\cdot\quad\cdot$$
$$\sin 7\phi/\sin\phi = \lambda^6 - 5\lambda^4 + 6\lambda^2 - 1.$$

We have, after expanding $(\sin\phi)^{-1} = (1 - \lambda^2/4)^{-\frac{1}{2}}$, the following identity :—

$$1 + \frac{\lambda^2}{8} + \frac{3}{128}\lambda^4 + \frac{5}{1024}\lambda^6 \equiv a_1 + a_2\lambda Y_2 + a_3(\lambda^2 - 1)Y_3 + a_4(\lambda^3 - 2\lambda)Y_4$$
$$+ a_5(-3\lambda^2 + 1)Y_5 + a_6 3\lambda Y_6 + a_7(\dots - 1)Y_7,$$

where

$$Y_1 = 1,$$
$$Y_2 = q - \frac{1}{6}q^3,$$
$$Y_3 = q^2 - \frac{3}{8}q^4 + \frac{3}{80}q^6 \dots,$$

$$\mathrm{Y}_4=q^3-\frac{3}{5}q^5\ldots,$$

$$\mathrm{Y}_5=q^4-\frac{5}{6}q^6\ldots,$$

$$\mathrm{Y}_6=q^5\ldots,$$

$$\mathrm{Y}_7=q^6\ldots.$$

Substituting for λ and equating coefficients of q^n we find the following relations :—

$$a_1=1, \quad \ldots\ldots\ldots\ldots\ldots \quad \text{(B)}$$

$$\frac{1}{8}\mathrm{A}_1{}^2=a_2\mathrm{A}_1-a_3,$$

$$\frac{1}{4}\mathrm{A}_1\mathrm{A}_3+\frac{3}{128}\mathrm{A}_1{}^4=a_2\left(\mathrm{A}_3-\frac{\mathrm{A}_1}{6}\right)+a_3\left(\frac{3}{8}+\mathrm{A}_1{}^2\right)-2\mathrm{A}_1a_4+a_5,$$

$$\frac{1}{4}\mathrm{A}_1\mathrm{A}_5+\frac{1}{8}\mathrm{A}_3{}^2+\frac{3}{32}\mathrm{A}_1{}^3\mathrm{A}_3+\frac{5}{1024}\mathrm{A}_1{}^6$$
$$=a_2\left(\mathrm{A}_5-\frac{\mathrm{A}_3}{6}\right)+a_3\left(-\frac{3}{80}-\frac{3}{8}\mathrm{A}_1{}^2+2\mathrm{A}_1\mathrm{A}_3\right)$$
$$+a_4\left(\frac{6}{5}\mathrm{A}_1-2\mathrm{A}_3+\mathrm{A}_1{}^3\right)+a_5\left(-3\mathrm{A}_1{}^2-\frac{5}{6}\right)+3\mathrm{A}_1a_6-a_7.$$

Substituting for the a's in terms of the b's and reducing, we find

$$\frac{\mathrm{A}_3}{2}+\frac{b_3}{2}+\frac{2}{3}b_1=0,$$

$$\frac{\mathrm{A}_3}{4}-\frac{b_3}{4}-\frac{b_1}{24}=0,$$

$$\mathrm{A}_3=-\frac{1}{4}b_1,$$

$$b_3=-\frac{5}{12}b_1,$$

and using these values the next pair of equations derived from the coefficients of q^5 and q^6 are found to simplify to

$$\frac{(\mathrm{A}_5-b_5)}{2}+(0)b_1{}^3+(0)b_1{}^5+\frac{3}{40}b_1=0,$$

$$\frac{b_1\mathrm{A}_5}{4}+\frac{3b_1b_5}{4}-\frac{29}{480}b_1{}^2=0.$$

The vanishing of the coefficient of $b_1{}^5$ follows from the known potential flow solution and that of $b_1{}^3$ is, it seems, only a coincidence in the case of the circle.

Therefore $$\mathrm{A}_5=-\frac{5}{96}b_1,$$

$$b_5=+\frac{47}{480}b_1,$$

$$f(q)=b_1\left(q-\frac{5}{12}q^3+\frac{47}{480}q^5\ldots\right),$$

and since $$f(u)=1,$$

$$\lambda(q)=\frac{q-\frac{1}{4}q^3-\frac{5}{96}q^5\ldots}{u-\frac{5}{12}u^3+\frac{47}{480}u^5\ldots}.$$

As explained above, both $f(q)$ and $\lambda(q)$ have been expanded in powers of q with no approximation. It is only because b_1 has so far only occurred as a linear factor that $1/b_1$ is equal to $f(u)$.

The linearity of $f(q)$ in b_1 may be used to give a simple check by expanding both $f(q)$ and $\lambda(q)$ in a series of X_n.

Thus $$[1-f(q)]^{-\frac{1}{2}}=1+a_2X_2+a_3X_3\ldots a_nX_n.$$

Therefore $$\tfrac{1}{2}f(q)=\overline{a}_2X_2+\overline{a}_4X_4+\overline{a}_6X_6,$$

and again from the condition $x'\equiv0$

$$\tfrac{1}{2}\lambda(q)=\overline{a}_2X_2-\overline{a}_4X_4+a_6X_6,$$

where the notation $\overline{a_n}$ means that part of a_n linear in b_1. Using the values of a in terms of b_n, etc., we find

$$\overline{a}_2=\frac{1}{2},$$

$$\overline{a}_4=-\frac{1}{24},$$

$$\overline{a}_6=-\frac{3}{80}+\frac{1}{2}\overline{b}_5,$$

where also $$X_2=q-\frac{q^3}{3},$$

$$X_4=q^3-\frac{9}{10}q^5\ldots,$$

$$X_6=\left(-\frac{3}{40}+b_5\right)q^5\ldots.$$

Therefore $$f(q)=q-\frac{5}{12}q^3+b_5q^5,$$

$$\lambda(q)=q-q^3/4-\frac{5}{96}q^5,$$

as was found directly. This provides a check on the working but could not be used to find the coefficients because it needs to be shown that $f(q)$ is linear in b_1.

3. *Expansion for Circular Cylinder in Adiabatic Flow.*

$$\int\frac{dp}{\rho}+\tfrac{1}{2}q^2=\text{a constant},$$

$$k\frac{\gamma}{\gamma-1}(\rho^{\gamma-1}-\rho_0^{\gamma-1})+\tfrac{1}{2}(q^2-u^2)=0,$$

$$a^2=\left(\frac{dp}{d\rho}\right)_0=k\gamma\rho_0^{\gamma-1},$$

$$\left(\frac{\rho}{\rho_0}\right)^{\gamma-1}=1-\frac{(\gamma-1)}{2}\frac{(q^2-u^2)}{a^2}.$$

The equation for $F_n(q)$ is, when a is taken as unity,

$$F_n''+\left(F_n'-n^2\frac{F_n}{q}\right)\frac{1}{q}\left(1-q^2\Big/\left[1-\frac{\gamma-1}{2}(q^2-u^2)\right]\right)=0.$$

Solving by the method of Frobenius

$$F_n=q^n[1+p_2q^2+p_4q^4\ldots\infty],$$

where

$$p_2=-\frac{n(n-1)}{4n+4}\cdot\frac{1}{a'^2},$$

$$p_4=\frac{n(n-1)\{n(n-1)-2\}}{(4n+4)(8n+16)}\cdot\frac{1}{\left(1+\frac{\gamma-1}{2}u^2\right)^2}$$

$$-\frac{n(n-1)}{16(n+2)}\cdot\frac{\gamma-1}{\left(1+\frac{\gamma-1}{2}u^2\right)^2}.$$

The equation corresponding to (C) in the isothermal case is as follows:—

$$R\equiv a_1+a_2\left\{q-\frac{q^3}{3a'^2}+3\,{}_2\beta_4\frac{q^5}{a'^4}\right\}$$

$$+a_3q^2\left[1-\frac{5}{8}\frac{q^2}{a'^2}+\frac{7}{80}\frac{q^4}{a'^4}+\frac{7}{3}\,{}_3\beta_4\frac{q^4}{a'^4}\right]$$

$$+a_4q^3\left[1-\frac{q^2}{a'^2}\frac{9}{10}\right]+a_5q^4\left(1-\frac{7}{6}\frac{q^4}{a'^2}\right)$$

$$+a_6q^5\left(1-\frac{10}{7}\frac{q^2}{a'^2}\right)+a_7q^6.$$

Apart from a factor $a'^2=1+\frac{\gamma-1}{2}u^2$, the only fresh terms are those designated ${}_n\beta_4$, and

$${}_n\beta_4=-\frac{n(n-1)(\gamma-1)}{16(n+2)}.$$

The boundary condition (A) is

$$0\equiv a_1\frac{\lambda}{2}+a_2\left(\frac{\lambda^2}{2}-1\right)\left\{q\left(1-\frac{q^2}{3a'^2}\right)+3\,{}_2\beta_4\frac{q^5}{a'^4}\right\}$$

$$+a_3\frac{(\lambda^3-3\lambda)}{2}q^2\left(1-\frac{5}{8}\frac{q^2}{a'^2}\right)+a_4\left(\frac{\lambda^4}{2}-2\lambda^2-1\right)q^3\left(1-\frac{9}{10}\frac{q^2}{a'^2}\right)$$

$$+a_5\frac{5}{2}\lambda q^4-a_6q^5.$$

Therefore $A_3=-\frac{1}{4a'^2}b_1,$

$$b_3 = -\frac{5}{12a'^2}b_1,$$

and
$$A_5 - b_5 + \frac{3}{20}\frac{b_1}{a'^4} = 0$$

from (A), whilst

$$A_5 + 3b_5 - \frac{29}{120}\frac{b_1}{a'^4} + [-16\,{}_2\beta_4 + 2\,{}_3\beta_4]\frac{b_1}{a'^4} = 0$$

from (B).

The final result is

$$\lambda \equiv 2\cos\phi = \frac{\dfrac{q}{a'} - \dfrac{1}{4}\left(\dfrac{q}{a'}\right)^3 - \left\{\dfrac{5}{96} + \dfrac{7}{80}(\gamma-1)\right\}\left(\dfrac{q}{a'}\right)^5}{\dfrac{u}{a'} - \dfrac{5}{12}\left(\dfrac{u}{a'}\right)^3 + \left\{\dfrac{47}{480} - \dfrac{7}{80}(\gamma-1)\right\}\left(\dfrac{q}{a'}\right)^5}.$$

The same check as in the case of isothermal flow may be applied by equating to zero the coefficient of b_1 in relations (A) and (C), given $\lambda(q)$ and $f(q)$ as series in $X_n(q)$.

4. *Expansion for Flow Past an Elliptic Cylinder.*

Take as the potential flow solution

$$w = \zeta + 1/\zeta,$$

$$\zeta = Re^{i\Theta},$$

$$z = re^{i\theta},$$

and
$$z = \zeta + \epsilon^2/\zeta.$$

The boundary is an ellipse $\left(\dfrac{x}{1+\epsilon^2}\right)^2 + \left(\dfrac{y}{1-\epsilon^2}\right)^2 = 1$ in the plane of z, and a circle radius unity in the plane of ζ

$$\frac{dw}{dz} = qe^{-i\phi} = (\zeta - 1/\zeta)/(\zeta - \epsilon^2/\zeta),$$

and on the boundary ellipse

$$qe^{-i\phi} = \frac{2i\sin\theta}{(1-\epsilon^2)\cos\theta + i(1+\epsilon^2)\sin\theta}.$$

Therefore
$$q = 2\sin\theta/\sqrt{(1-\epsilon^2)^2\cos^2\theta + (1+\epsilon^2)^2\sin^2\theta}$$

and
$$\tan\phi = \frac{1-\epsilon^2}{1+\epsilon^2}\cot\theta.$$

The boundary relation between q and ϕ is $q = 2\cos\phi/1+\epsilon^2$ or $\lambda = (1+\epsilon^2)q$.

Corresponding to $x' = 0$ $y' = 1$ in the case of the circle, we have for the ellipse

$$x' = 4\epsilon^2\sin\phi\cos\phi/\sqrt{(1+\epsilon^2)^2\sin^2\phi + (1-\epsilon^2)^2\cos^2\phi},$$

$$y' = \sqrt{(1+\epsilon^2)^2\sin^2\phi + (1-\epsilon^2)^2\cos^2\phi}.$$

Again on the x axis $\phi = 0$ and

$$R = (1-\epsilon^2 q)^{\frac{1}{2}}(1-q)^{-\frac{1}{2}} + \epsilon^2/1-q)^{\frac{1}{2}}(1-\epsilon^2 q)^{-\frac{1}{2}}.$$

Expanding R by the binomial theorem we find

$$\mathrm{R}=l+(l^2-4m)\left[\frac{1}{2}q+\frac{3}{8}lq^2+\frac{1}{16}(5l^2-4m)q^3\right.$$
$$+\frac{5l}{128}(7l^2-12m)q^4+\frac{3}{256}(21l^4-56l^2m+16m^2)q^5$$
$$\left.+\frac{l}{1024}(231l^4-84l^2m+560m^2)q^6.\right], \quad \ldots\ldots \quad \text{(C}$$

where $$l=1+\epsilon^2, \quad m=\epsilon^2.$$

For compressible flow we suppose that q is replaced by

$$f(q)=b_1q+b_3q^3+b_5q^5.\;.$$

and that the coefficients in the expansion of x' and y' are $a_1, a_2 \ldots a_n$. Then the a's may be determined in terms of the b's using the generalized form of (C).

Again the boundary condition (A) is now replaced by

$$x'=\frac{2m}{l}\lambda\left[1+\left(\frac{4m}{l^2}-1\right)\frac{\lambda^2}{8}+\left(\frac{48m^2}{l^4}-\frac{8m}{l^2}-1\right)\frac{\lambda^4}{128}\right],$$

whilst (B) is now

$$y'(\sin\phi)^{-1}=l\left[1+\{1-(4m/l^2)\}\frac{\lambda^2}{8}+\left(\{3-(8m/l^2)\}-\frac{16m^2}{l^4}\right)\frac{\lambda^4}{128}\right.$$
$$\left.+\left(\{5-(12m/l^2)\}-\frac{16m^2}{l^4}-\frac{64m^3}{l^6}\right)\frac{\lambda^6}{1024}\right].$$

Again we assume $$\lambda=\mathrm{A}_1q+\mathrm{A}_3q^3+\mathrm{A}_5q^5.$$

The work of reduction proceeds very much as in the case of the circle from this point onwards and the result is very similar, viz. :

$$\lambda\equiv 2\cos\phi=(1+\epsilon^2)\frac{q-\frac{1}{4}q^3-\left(\frac{5}{96}+\frac{b_1{}^2\epsilon^2}{20}\right)q^5}{u-\frac{5}{12}u^3+\left(\frac{47}{480}-\frac{b_1{}^2\epsilon^2}{20}\right)u^5},$$

whilst $$f(u)=1=b_1u-\frac{5}{12}b_1u^3+\left(\frac{47}{480}b_1-\frac{1}{20}b_1{}^3\epsilon^2)\right)u^5$$

is the equation for finding b_1 in terms of u, the Mach number. It will be seen that in this case $f(u)$ involves a term in $b_1{}^3$ so that the next approximation involves a change in the u^2 term in $b_1(u)$. By inspecting the working it was found that the adiabatic relation is derived by making the same change in the coefficient of q^5 as in the case of the circle.

The result is

$$2\cos\phi=(1+\epsilon^2)\frac{q-\frac{1}{4}q^3-\left(\frac{5}{96}+\frac{b_1{}^2\epsilon^2}{20}+\frac{7}{80}\overline{\gamma-1}\right)q^5}{u-\frac{5}{12}u^3+\left\{\frac{47}{480}-\frac{b_1{}^2\epsilon^2}{20}-\frac{7}{80}(\gamma-1)\right\}u^5},$$

where

$$f(u)=1=b_1u-\frac{5}{12}b_1u^3+b_1\left(\frac{47}{480}-\frac{b_1^2\epsilon^3}{20}-\frac{7}{80}\overline{\gamma-1}\right)u^5$$

is the equation determining b_1 for a given value of u.

5. *Convergence of $f(q)$ and $\lambda(q)$.*

The only check on the convergence is numerical in view of the complications which quickly arise in finding higher coefficients A_n and b_n. The following facts are, however, interesting.

$$[1-f(q)]^{-\frac{1}{2}}=\sum_1^\infty a_nX_n(q),$$

$$\tfrac{1}{2}f'(q)/[1-f(q)]^{3/2}=\sum_1^\infty a_nX_n'(q).$$

If $u>1$ then $f(1)<1$ and the expansion is legitimate for $q=1$. In this case, since $X_n'(1)=0$ for all n, as can be easily seen from the differential equation or verified in the expansions of $X_n'(q)$, $f'(1)$ must vanish. We have only proved this for supersonic flow but from the principle of continuity, since the terms in $f(q)$ are obviously diminishing fairly rapidly, it is at least very probably true in the subsonic case.

Assume then

$$f(q)=q-\frac{5}{12}q^3+\frac{47}{480}q^5+b_7q^7,$$

$$f'(q)=1-\frac{5}{4}q^2+\frac{47}{96}q^4+7b_7,$$

$$f'(1)=1-\frac{5}{4}+\frac{47}{96}+7b_7,$$

$$b_7=-\frac{23}{96}\times 7.$$

In the calculation of the critical Mach number $q<0{\cdot}5$ and so b_7q^7 is negligible according to this estimate.

Again, if the ellipse became very flat and in the limit a straight line, it is to be expected that the solution would reduce to $q=u=1$. Putting $\epsilon=1$ and $\phi=0$

$$2\sim 2\frac{\left[1-\frac{1}{4}-\left\{\frac{5}{96}+\frac{b_1^2}{20}+\frac{7}{80}(\gamma-1)\right\}\right]}{1-\frac{5}{12}+\frac{47}{480}-\frac{b_1^2}{20}-\frac{7}{80}(\gamma-1)}.$$

The discrepancy is therefore

$$-\frac{1}{4}-\frac{5}{96}+\frac{5}{12}-\frac{47}{480}=\frac{1}{60}.$$

This result suggests an error of a few per cent. in the calculation of the Mach number, and renders the result for an ellipse of aerofoil shape practically useless since the change due to compressibility is of this order,

6. *Critical Mach Numbers for the Circular Cylinder.*

Isothermal Flow.

$$\lambda=2\cos\phi=\frac{q-\frac{1}{4}q^3-\frac{5}{96}q^5}{u-\frac{5}{12}u^3+\frac{47}{480}u^5}.$$

Put $q=1$ and $\phi=0$.

The first approximation is $u=0{\cdot}398$ and the second $u=0{\cdot}369$, obtained by neglecting q^5 and q^7 respectively. If we neglect q^3 the result is $u=0{\cdot}5$, *i. e.* the incompressible case.

Adiabatic Flow.

$$a^2-a_0^2+\frac{\gamma-1}{2}(q^2-u^2)=0,$$

where local velocity of sound is .... a
velocity of sound at infinity .... a_0
local velocity at a point .... u
velocity at infinity .... u_0

Therefore at a shock wave $q=a$ and

$$a^2\left(\frac{\gamma+1}{2}\right)=a_0^2+\frac{\gamma-1}{2}u^2$$

$$a=\sqrt{\frac{2}{\gamma+1}}\,a'$$

of the previous notation.

The equation for calculating u is therefore, with $\gamma=1{\cdot}4$,

$$2=\frac{\frac{1}{\sqrt{1{\cdot}2}}-\frac{1}{4(\sqrt{1{\cdot}2})^3}-\left(\frac{5}{96}+\frac{7}{200}\right)\frac{1}{(1{\cdot}2)}^{5/2}}{\frac{u}{a'}-\frac{5}{12}\left(\frac{u}{a'}\right)^3+\left(\frac{47}{480}-\frac{7}{200}\right)\left(\frac{u}{a'}\right)^5}.$$

The result is to a first approximation

$$u=0{\cdot}400$$

and the second approximation

$$u=0{\cdot}361.$$

Acknowledgement.

I wish to express my gratitude to Professor Bates and Mr. Davy of Nottingham University for their helpful encouragement in connection with this work, and to Professor Havelock for his kindness in going through the paper and pointing out various errors and omissions. I am indebted to the latter for the list of references below.

I am indebted to Dr. R. Cooper, of the Mathematics Department, Queen's University, Belfast, for pointing out the following relation for the case of isothermal flow :—

$$\int_0^\infty e^{-q^2/} X_n(q) X_m(q)\, q\, dq = \delta_{mn} k_n,$$

the X_n being in fact degenerate Laguerre polynomials. This relation follows readily from the differential equation. More generally for any pressure density relation

$$\int_0^{q_\infty} \rho(q) X_m(q) X_n(q)\, d\, dq = \delta_{mn} k_n',$$

where $\rho(q_\infty)=0$.

In the case of isothermal flow the Kn are quite simple and various formal results similar to those known for classical orthogonal polynomials can be deduced. Since, however, the main labour is required in satisfying the boundary conditions their expansion theorems do not lead to a great practical simplification of the working.

References.

(i) Rayleigh (Phil. Mag., 1916) : first approximation.

(ii) G. I. Taylor (Journ. L.M.S. v. 1930) : general review and an experimental method of solution, which gave an estimated critical mach number of 0·45.

(iii) Imai (Phys. Math. Soc. Japan, xx. 1938) : extended Rayleigh's method to the second approximation, with in particular the result

$$\frac{q}{u} = 2 + \frac{7}{6} M^2 + \left\{ \frac{281}{120} + \frac{71}{120} (\gamma - 1) \right\} M^4$$

with q=velocity at the boundary at the point $\phi=0$ and $M=u/a$. This result gives a critical value of $M=0·409$.

(iv) Tamada and Saito (Phys. Math. Soc. Japan, xxi. 1939) carried out second approximation by Poggi's Method and confirmed Imai's expression.

(v) Kaplan (N.A.C.A. reports) : work on circular and elliptic cylinders by similar methods.

LXI. *On the Theory of Light-Scattering—A Note.*

By S. Parthasarathy, D.Sc., F.Inst.P., F.I.C.*

[Received October 31, 1943.]

The note [1] published by R. S. Krishnan in this Journal, arising out of my paper [(2)], does not contain any new facts or material to warrant change of conclusion arrived at. On the contrary, my arguments that his results have been vitiated by grave errors are now strengthened, as will be evident from this note.

---

* Communicated by the Author.

There are many defects in his arguments, but it is necessary to explain the following facts before one can follow them :—

Arguments.

1. At the outset we should recognize that the factors measured are are ρ_u, ρ_v, ρ_h, and that the results have to be interpreted on the basis that these measurements are correct. If they are not, then there is no further basis for argument.

2. If the measured ρ_u, ρ_v, ρ_h differ very much from those to be expected from theory, then the variation could be attributed to either the scattering medium or to the error due to convergence of the beam.

3. Before one attributes such variation to the scattering medium, one should be certain that there was no correction to be made for convergence.

4. The error due to the convergence of the beam can be easily and directly calculated in simple cases, as in the case of a beam of light brought to a focus at a point and which passes wholly through a homogenious medium. If the beam passes through different media contained in differently shaped vessels, then the convergence to be determined is not so simple. In any case, one cannot assume from the dimensions of the lens alone what the error would be, as there are other factors besides. If, through a rectangular tank of water in which is immersed a bulb containing a highly refractive liquid, a paralled beam is allowed to pass, it remains no longer parallel inside the bulb ; for the bulb of liquid acts as a lens and the beam converges.

5. The error due to convergence in all cases where aperture of the lens is varied can be easily overlooked by wrong argument. Let us suppose that for an angle of convergence of 3° the correction for ρ_v is 0·03 per cent., then for 0·75 per cent. (one fourth) or 12° (four times) the correction is 0·002 per cent. or 0·48 per cent., *i. e.* in one case we cannot detect, the difference being much below the powers of observation, while in the other we can, easily, for it is as high as 0·48 per cent.

But the argument does not stop here, for the most important point for consideration, which has been missed by R. S. Krishnan, is whether we are justified in neglecting the convergence error for ρ_h *for all values of* ρ_v. The answer is definitely NO. It can be easily seen from the graphs of my paper in Phil. Mag. that for low values of ρ_v, namely 0·4 per cent. and of this order, even a difference of 0·1 per cent. in ρ_v will show a difference of 200 per cent. in ρ_h, for the curve ρ_h—ρ_v is very steep for small values of ρ_v. In other words, even though convergence error for ρ_v itself can be neglected, *that for* ρ_h, *which is the crucial point here, cannot be neglected.*

6. If, in spite of our taking all the precautions enumerated above, we still get $\rho_h > 1$, we observe that it can be so in the following cases :—

(*a*) in liquids containing impurities ;

(*b*) in colloidal solutions : emulsions and suspensions ;

(*c*) in liquids where there are supposed to be molecular aggregates.

(*a*) and (*b*) are not pure liquids, while for (*c*), even according to R. Gans, there is a limit for ρ_h which is 1·2. I have, in another paper (3), clearly shown that this is so. But R. S. Krishnan obtains values well over 3·5, and therefore Gans's theory is not the one applicable to his liquid mixtures.

For cases coming under (*b*), Mie's theory is, in general, applicable.

7. Finally, the factor ρ_h can be greater than 1 in suspensions, such as protein solutions, etc. But as suspensions and critical solution mixtures are widely different in composition, in phases and quality, one should not confuse the issues and apply the same theory to both. Consequently the laws of scattering applicable to each are different (please see point 6 above also).

After the foregoing analysis it is easy to show that the points raised by R. S. Krishnan have really no basis.

Point 1 *in his Note.*

Put briefly, he says, that the calculated value of ρ_h when $\rho_v=0{\cdot}4$ per cent. for semi-angle of convergence, 1/18 of a radian comes to only 1·25. while he obtains a value of about 3·2, which is therefore much above the corrected value. But this is on the assumption that 1/18 of a radian as set by him remains so throughout. That this is not the case is explained in the next paragraph. (Please see also argument 4 above.) The question to be answered here is whether for $\rho_v=0{\cdot}4$ per cent. and $\rho_h=3{\cdot}2$ [measured quantities (argument 1 above)] semi-angle of convergence has remained at 1/18 of a radian, or has it changed ? The answer is it has, and is provided in the next paragraph. (Please see the latter portion of argument 5 above also.)

Point 2 *in his Note.*

Krishnan appears surprised at the suggestions made in my paper that his results were vitiated by high values for the angle of convergence, and also at the fact that I had suggested different values of apertures for different mixtures. For he wonders how they could be when he had used the same " long focus short aperture lens." I quote from his paper published in Proc. Ind. Acad. Sci. 1. p. 917 (1935). wherein he had described the disposition of the experiment.

> " The bulb was kept immersed in dust free distilled water contained in a rectangular brass vessel provided with three glass windows. . . ."

My suggestions are now confirmed for the following reasons :—

Firstly, the bulb contained a more highly refractive liquid than the surrounding water, and naturally acted as a lens in converging the beam. This evidently gave rise to high values for the angle of convergence—higher than what the lens by itself would give.

Secondly, different mixtures gave different values because the various mixtures had different refractive indices.

And thirdly, the various mixtures were contained, not in the same bulb, but in bulbs of different sizes ; hence this fact gave different values for the aperture.

Point 3 *in his Note.*

The point raised in this paragraph is answered in our argument 5 above.

Point 4 *in his Note.*

This has been answered in argument 6 above. In the case of scattering by molecular aggregates, Gans's theory definitely shows, as pointed out by me in the paper in Phil. Mag. and the other in which I had given results of earlier experiments, that ρ_h cannot be greater than 1·2. But Krishnan gets 3·7 and above. Since convergence correction can easily account for 3·7 and over for ρ_h, it is not necessary to invoke any new hypothesis.

Point 5 *in his Note.*

The point raised therein has been answered by arguments 6 and 7 above.

Summing up, it would appear that Krishnan had apparently tried to eliminate, though partially, the error due to convergence of the beam by working at portions of the curve $\rho_h-\rho_v$ (given in my paper in the Phil. Mag.), which are more or less flat ; but due to various causes explained in this note (see especially answers to his points 1 and 2) the portion investigated shifted to a steeper part of the curve, with the result that unintentionally and unknowingly greater convergence of the beam was introduced.

I shall, with others, be only too glad if any new discovery is made which further reveals Nature. Such a discovery should be above criticism and be capable of being repeated elsewhere. My feeling here is that the method used by Krishnan is neither free from error nor decisive to prove the existence, if they do, of clusters of molecules in liquids, and his method has failed to stand the test of fair criticism. And, apart from it, the following points are worth considering in this connection :—

1. One could explain small values of ρ_h up to 1·2 on the basis of Gans's theory. But why has no theory been put forward so far, even after a lapse of eight years, to account for such high values of ρ_h, namely 3·7 and above ?

2. It has been conclusively shown in my earlier paper in Phil. Mag., and also in this note, that the chief mistake was due to the neglect of the convergence error. When this fact satisfactorily explains Krishnan's anomalous results there is no need to postulate any new theory. This is the answer to the question asked above.

3. Krishnan's results have not, so far, been confirmed either by himself or by any other. This is again significant.

I do hope, however, that this reply will not act as a damper to further efforts of R. S. Krishnan in other directions.

References.

(1) R. S. Krishnan, Phil. Mag. xxix. p. 515 (1940).
(2) S. Parthasarathy, Phil. Mag. xxix. p. 148 (1940).
(3) S. Parthasathy, Journal of the Bombay University, vol. v. pt. 2, p. 16 (1936).

Board of Scientific and Industrial Research,
University Buildings, Delhi.

LXII. *Notice respecting New Book.*

The Advancement of Science.—Vol. III. No. 10 (May, 1945). [Pp. 128.] (Published by the British Association for the Advancement of Science, Burlington House, London, W. 1. Price 5*s.* 0*d.*)

THE British Association began with the efforts of a group of men of science who were desirous of carrying their new gospel to the heathen who knew not the nature of scientific method nor anything of its results. It developed at one time, or at least showed a danger of developing, into an unwieldy collection of specialist scientific societies, each holding an annual meeting at which the papers read in one room were quite unintelligible, not only to the layman, but even to the professional scientists who were debating their own recondite problems in a neighbouring room.

In recent years, it has consciously resolved to revert to the earlier conception of its task, and has devoted far more of its energies to the discussion of such problems as the impact of science on ordinary life, and the place of the scientist in Society. Consequentl , it has had to change the nature of its chief publications ; in place of a collection of Reports, issued after the Annual meeting, it now issues a quarterly Journal, which should, and does, make an appeal to the cultured man interested in the structure and behaviour of that world, animate and inanimate, in which he finds himself.

The number for May, 1945, is of great interest ; it appeared before the world knew that an atomic bomb was in preparation, to be dropped later in the year, and for that reason it has an old-fashioned air when compared with the flood of informed and uninformed discussion about the place of science in society which has drenched us since that bomb was dropped. We are reminded that one topic occupying the minds of thinking people then, as it will do again, was that of India. The Indian Scientific Delegation had just been visiting this country and we have here the reprinted addresses given by Professor Saha, Sir Jnan Ghosh, Professor Mitra, Sir Shanti Bhatnagar, Dr. Ahmad and Professor Mukherjee. They have obviously thought out some of the difficulties of their great country in a most thorough manner—its energy supplies and production, population problems, agriculture and the avoidance of famine, possibilities of increasing the fertility of the soil. A great part of the issue is devoted to a report of the Conference on the Place of Science in Industry, a conference far too big in its scope to attempt to summarize here. Suffice it to note that great leaders both in science and in industry contributed and that a lively discussion was evoked.

The work being done in this way by the British Association is of obvious value, and its quarterly journal, 'The Advancement of Science,' is an integral part of the work, for without it the work would be unknown to some of those whom it is essential to reach. J. H. A.

[*The Editors do not hold themselves responsible for the views expressed by their correspondents.*]

LXIII. *The Precision of Measurement of Broad Spectrum Lines, with Special Reference to Electron-Diffraction Photographs.*

By T. B. Rymer, Ph.D., and C. C. Butler, B.Sc.,
The University, Reading *.

[Received February 24, 1945.]

Abstract.

The factors affecting the precision of measurement of the position of spectrum lines by visual and microphotometric methods are discussed. A statistical study of an extensive set of data shows that as a useful working rule the standard deviation of a single reading of the position of a line by means of a measuring microscope may be taken as 0·3 times the square root of the line width, if all lengths are measured in microns, whereas the standard deviation of a micro-photometer reading is about half this. The systematic errors of such measurements and methods for their determination are also discussed. The validity of these estimates of systematic and random error has been confirmed by a comparison of the radii of electron-diffraction circles with theory.

Introduction.

In the course of a study of the lattice constants of certain crystals by electron diffraction, we have had occasion to make accurate measurements of the radii of Debye–Scherrer circles. This problem—the determination of the position of the centre of a fairly broad line—is one which is common to spectroscopy, X-ray and electron diffraction analysis, and it might well be supposed that the best technique and the precision attainable would be well established. This does not appear to be the case. Spectroscopists often make visual measurements of line position with whatever measuring microscope is immediately available, and one looks in vain for information as to the most suitable magnification and other conditions to employ. The precision of setting on a spectrum line is seldom stated explicitly, but appears for lines with a width of about 100μ † to lie between 1 and 10μ, most measurements tending towards the upper limit. As one example of a paper which *does* give a clear indication of the precision of measurement, Petrie (9) publishes a

---

* Communicated by Professor J. A. Crowther, M.A., Sc.D.

† Throughout this paper, we understand by the width of a line the distance between the two points at which the intensity is half that at the peak.

table of results from which it may be calculated that the *mean deviation* of a single observation of the *distance between two spectrum lines* is 5·7 μ. This corresponds to a *standard deviation* of a *setting on a single line* of 5·1 μ. The width of the lines is not clearly stated, but appears to be rather less than 100 μ. The results to be given in the present paper indicate that the ×8 magnification of the projection microscope used by Petrie is distinctly less than the optimum value, and this may account for the fact that we are able to obtain practically the same precision as Petrie with much wider lines.

The present results show that, provided the optimum microscope magnification is used, the standard deviation of setting on a line is closely proportional to the square root of the line width, being almost exactly 0·3 of this if all lengths are measured in microns. The precision of most spectroscopic measurements is less than this, probably due to the use of an incorrect microscope magnification.

Measuring microscopes have sometimes been replaced by microphotometers in an attempt to improve the precision of measurement, but published data about the actual precision are very sparse. An investigation has been made using a microphotometer already described(10), and the results show that, as with visual measurements, the standard deviation of a reading of a line position is proportional to the square root of the line width. The precision is about twice that obtainable with the best visual methods.

In the following discussion, the particular numbers are naturally relevant only to our electron-diffraction photographs, but the general conclusions regarding the best technique and the orders of magnitude involved are likely to be of wider interest. The *systematic* errors to which measurements of the distance between spectrum lines are liable have also been considered. The success of these investigations can be judged by comparing the experimental results with those of theory. This has been done in the case of Debye–Scherrer electron-diffraction photographs.

Part I.—*Visual Measurements.*

In this part, the random errors found when a measuring microscope is used are discussed. The main considerations are

(*a*) the colour of the light used and method of illumination ;

(*b*) the most suitable magnification and arrangement of cross-wires.

(*a*) In order to reduce fatigue, metrologists usually employ green light, which can be varied in intensity to give maximum comfort during a lengthy set of observations. The degree of convergence and diffuseness of the light falling on the plate is unimportant, since a high resolving power is not required ; on the contrary, we seek a fairly high magnification without undue graininess. For the same reason, the N.A. of the microscope objective is not critical, but only its focal length. It is, however, important to ensure that the conditions of illumination remain perfectly constant whatever part of the plate is in the field of view. If this is not so, the same zones of the objective are not used at all settings of the microscope, and aberrations in the objective may introduce errors (6). Of the possible methods of securing the necessary constancy in the conditions of illumination, the simplest is to use a fixed optical system and to traverse the plate in its own plane and at right angles to the axis of the microscope. Alternatively, an accurately parallel beam of light may be directed parallel to the slide of the instrument and reflected through the fixed plate into the movable microscope by a mirror rigidly fixed to the latter (5). Having tried both methods, we prefer the first on account of its simplicity.

(*b*) There is some advantage in using a cross-wire consisting of two parallel vertical lines intersected centrally by a horizontal one. The setting is made by arranging the spectrum line to lie symmetrically between the two vertical lines. In electron-diffraction plates, the lines are circles with a radius of the order of 1 cm., and the setting is made on the portion of the line intersected by the horizontal cross-wire. The separation of the vertical lines should be such that, on looking through the microscope, they appear to straddle the width of the line.

The most suitable objective may be selected by a method which can be best illustrated by an actual test made on three objectives, A, B and C, of focal lengths 3 in., $1\frac{1}{2}$ in. and $\frac{2}{3}$ in. respectively, each used in conjunction with a ×7 eye-piece fitted with the type of cross-wire described above. Sixteen settings were made on a spectrum line having a width of 250μ. These were repeated, using each objective in turn in the following sequence :—

1	2	3	4	5	6
A	B	C	C	B	A

This completes one set of observations, 96 in all. The plate was displaced between each group of 16 readings. During a run, the skill of the observer may change (due to improved practice or onset of fatigue) so that the *variance* (defined below) of the readings for any particular objective may depend on the time. We assume that the variation is linear, and that the time taken for each group of 16 observations is the same. Now, if for group 1 the settings are $r_1, r_2 \ldots . r_{16}$, the unit being the micron, the variance for this group is

$$V_1 = \Sigma (r^2) - \frac{1}{16} (\Sigma r)^2.$$

In the same way, the variances $V_2 - V_6$ of the other groups are calculated. Suppose that

$$V_1 = M_A + \tfrac{1}{2} kT,$$

where M_A is a constant depending on the skill of the observer and the objective A, k is a constant depending on the rate of change of skill with time, and T is the time taken for the 16 readings of group 1. Similarly,

$$V_2 = M_B + \frac{3}{2} kT,$$

$$V_3 = M_C + \frac{5}{2}kT,$$

$$V_4 = M_C + \frac{7}{2}kT,$$

$$V_5 = M_B + \frac{9}{2}kT$$

$$V_6 = M_A + \frac{11}{2}kT.$$

Hence,

$$V_1 + V_6 = 2M_A + 6kT,$$

$$V_2 + V_5 = 2M_B + 6kT,$$

$$V_3 + V_4 = 2M_C + 6kT.$$

By taking differences between these equations, the temporal factors are eliminated.

Three sets of observations were made. A sufficient interval was allowed between each set of readings to prevent fatigue. Table I. gives the variances ($2M + 6kT$ of the above equations) observed.

TABLE I.

Objective	(1)	(2)	(3)	Total	S.D. (μ)
A	912	757	617	2286	5·04
B	472	380	595	1447	4·01
C	912	917	911	2740	5·52
Total variance for 270 degrees of freedom				5473	

The sum of any row gives a measure of the suitability of the corresponding objective. Comparing the A and B objectives, the total variances are 2286 and 1447 respectively. Now the standard deviation (S.D.) of a variance V is

$$\sqrt{2V^2 \div \text{number of degrees of freedom}},$$

the number of degrees of freedom being the number of readings less the number of fitted constants. In the present case, there are 96 readings in the three sets for any one objective and six fitted constants (the mean settings for each group of 16), giving 90 degrees of freedom. The S.D. of the *difference between the variances* for the A and B lenses is therefore

$$\sqrt{\frac{2286^2 + 1447^2}{45}} = 403.$$

Since the observed difference of the two variances (839) is 2·1 times its S.D., we conclude that the B objective is significantly better than the A one. In the same way, it may be shown that the B lens is significantly better than the C one, and that there is no significant difference between the A and C lenses. The actual figures are

Difference of variances of B and C lenses = 1293
S.D. of this difference = 462
Difference of variances of A and C lenses = 454
S. D. of this difference = 532

The S.D. of a single setting, using any particular objective, may be calculated from the corresponding variance using the formula

$$\text{S.D.} = \sqrt{\text{variance} \div \text{number of degrees of freedom}},$$

the results being given in the extreme right-hand column of the table. Using the most suitable objective, the S.D. of a single setting is $4{\cdot}01\,\mu$ for a line of width $250\,\mu$. The over-all magnification of the microscope using this objective is 35.

To study the influence of the type of graticule used, the above experiment was repeated using a simple cross-wire set (*a*) horizontally and vertically, (*b*) at 45 degrees to the horizontal, and the variances were analyzed as described above. In each case, the $1\frac{1}{2}$-in. or B objective was found to be the best, and the graticule consisting of two parallel vertical lines was found to be slightly superior to either of the simpler arrangements, but the differences were barely significant. It is possible that the separation of the vertical wires was not quite the optimum.

To get an indication of the effect of training, tests were made on a number of observers. There was no significant difference between the authors themselves, who had both had about equal experience in using the microscope, the total variances for 270 degrees of freedom being 7531 (T. B. R.) and 6473 (C. C. B.). It can at once be shown that there is no significant difference between these figures. In each case, the $1\frac{1}{2}$-in. objective was appreciably better than the others. Since one of us had acquired his experience mainly by the use of the 3-in. lens and the other with the $1\frac{1}{2}$-in. one, it would seem that the preference for a particular objective is not due to familiarity. Further sets of readings were provided by two other observers, A. C. M. and R. H. K., neither of whom had had any previous experience of this type of measurement. The S.D.'s of a single setting were $6{\cdot}9\,\mu$ (A. C. M) and $10{\cdot}9\,\mu$ (R. H. K.). Presumably owing to the lower accuracy, it was impossible to distinguish between the different objectives in the case of the untrained observers.

The effect of line width was studied by making similar sets of readings on a line $700\,\mu$ wide. In this case, both the authors found that there was nothing to choose between the 3-in. and $1\frac{1}{2}$-in. objectives, which were both much better than the $\frac{2}{3}$-in. one. It is not surprising that the broader line appears to require a somewhat lower magnification. The S.D. of a single setting, using either the 3 in. or the $1\frac{1}{2}$-in. objectives, was practically the same for both authors, and its average value was $8{\cdot}65\,\mu$. The striking fact is that the S.D. does not increase anything like in proportion to the width of the line, but instead appears to depend rather closely on the *square root* of the latter. In fact, the results for both narrow and wide lines are given within the limits of error by the law

$$\text{S.D. of setting on a line} = 0{\cdot}3\ \sqrt{\text{width of line}},$$

the unit of length being the micron. This may be taken as a useful guide indicating the precision to be expected under given circumstances. The constant will naturally vary slightly from one person to another, but for experienced observers will not be far from the value given. For example, the rule indicates that for lines $10\,\mu$ wide, the S.D. should be $1\,\mu$. In fact, Bäcklin (1), in a precision measurement of X-ray wavelength, claims a *mean error* of $\frac{1}{2}\,\mu$ in setting on lines rather less than $10\,\mu$ wide.

In applying this rule, it is assumed (*a*) that the optimum magnification is used, (*b*) that the line is moderately intense, the peak density relative to the background being of the order of 0·5. It is well known that weak lines become invisible under high magnification ; for these the optimum magnification cannot be employed.

It might be objected that the method we have described for determining the optimum conditions is unreliable, because in repetition readings there is a tendency to set on the same feature of the line (for example, a small group of developed grains) and the S.D.'s obtained are therefore misleading. That this has not occurred is shown by the following. An electron-diffraction photograph showing Debye–Scherrer circles of etched gold foil was taken and the radius of each ring measured at 36 equally spaced points, using the rotating plate-holder on a microphotometer (10) which can be simply adapted for visual work. The earlier statistical work has shown that the correct objective to use is the 1½-in. type. We find that the pattern is not exactly a set of concentric circles, but the significance of this does not here concern us. Four rings were measured, four traverses along each of 18 diameters being made, thus giving for each ring four determinations of each of 36 radii. It will be seen that seven settings on other rings intervene between two successive settings on the same part of any ring ; this would appear to eliminate the difficulty just referred to. In all, the mean errors of 144 radii were found. These, when averaged and converted to a standard deviation, gave for the S.D. of any radius $4{\cdot}5\,\mu$. As the circles had a width of $250\,\mu$, the figure found here for the S.D. is in good agreement with the value given earlier for lines of this width ($4{\cdot}0\,\mu$). The error of setting on the central spot of the pattern is included in this figure, but this is very small owing to its smallness and clearness.

PART II.—*Microphotometer Measurements.*

A microphotometer can be used for determining the position of a spectrum line, and it is reasonable to suppose that it will introduce smaller random errors than the best visual methods. The use of a microphotometer introduces certain systematic errors, which are discussed in Part III.*

Visual and microphotometric measurements require rather different types of photograph. For the former, lines of moderate density (say 0·8) are best, and a moderate graininess can be tolerated, but the microphotometer demands the finest grain plates for the best results and operates best with lower densities (say 0·3). For electron-diffraction work, we find Ilford Thin Film Half-Tone plates processed with a borax fine-grain developer to be very suitable. Plates such as Ilford Special Rapid or ordinary X-ray film are far too grainy for accurate work. Before using any type of plate, it is well to verify that the characteristic is suitable over the range of densities required, for it is shown in Part III. that otherwise large sysematic errors may occur in the determination of the line position. In the case of the Thin Film Half-Tone plates, it is found that the density is proportional to the exposure time up to densities of at least unity ; since the reciprocity law holds for electrons (2), a similar relation exists between density and intensity. For densities greater than unity, the density increases more slowly than the intensity. For some other types of emulsion, the relation between density and exposure is irregular and not reproducible.

Fig. 1

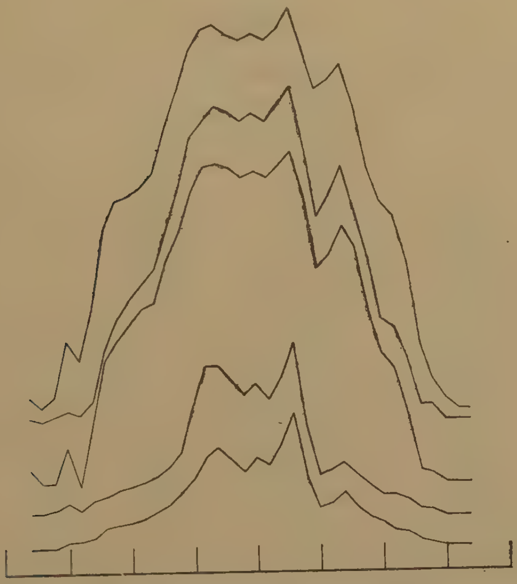

One division represents 50 μ.

The microphotometer used for this type of work need not have a linear response, provided the non-linearity does not result in a flattening of the line peaks. On the contrary, if the non-linearity is such as to accentuate the peaks, there is a marked gain in sensitivity. Such a microphotometer has been described by the authors (10). The fact that a non-linear microphotometer characteristic does not introduce errors can easily be shown by taking a set of contours of a spectrum line using a grainy plate ; the grains introduce subsidiary maxima into the line contour and these can be checked for position. The five curves of fig. 1 were taken with different microphotometer characteristics. Although the general shape of the line contour is very different, the positions of all the maxima are exactly the same in all the curves, showing that a non-linear microphotometer is not dangerous ; the gain in sensitivity may be judged from the fact that the lowest curve was made using a substantially linear circuit, and is reproduced in the figure with its vertical scale exaggerated twofold in relation to the other four curves.

---

* Similar errors may well occur in visual measurements, but their magnitude cannot then be easily estimated.

Fig. 2

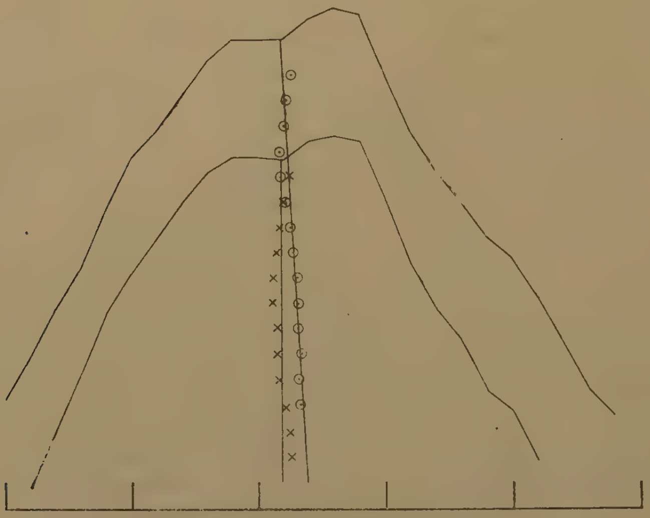

One division represents 50 μ.

When line contours have been determined, two different methods can be employed to establish the position. Jay (7) and Bradley and Jay (3) bisect lines joining pairs of points at which the intensity is the same. The points of bisection are found to lie on a median line, and the intersection of this with the line contour is taken as the peak of the line (see fig. 2). On the other hand, Bradley and Jay also determine the position of the centre of area of the region below the line contour. It is evident that both methods give the same result only if the line contour is perfectly symmetrical. This is not always the case for spectroscopic and X-ray lines, and in electron-diffraction photographs a slight asymmetry is usually found. In these cases, the centre of area method will give a definite result only if the extent of the area is specified ; for example, the whole area lying between the line contour and the curve of background intensity. Any such specification appears somewhat artificial, and it is necessary to correct the microphotometer record for non-linearity of the characteristics of the photographic emulsion and microphotometer before applying the method. For electron-diffraction plates the centre of area method was found to be unsuitable, but the median method is capable of giving very consistent results even with lines of very irregular contour. Owing to the asymmetry of the line contour and the non-linear response of the microphotometer, the median line is theoretically curved; in practice, however, it is found that the curvature is negligible and so the best straight line is fitted. Measurements on a given line, using different microphotometer characteristics, always give the same position to within 1 μ. This is illustrated in fig. 2, which shows two measurements on the same line, using different microphotometer characteristics.

Table II.

Microphotometer readings for (200) ring,
11770 μ + following amounts.

Deg.	I	II	D.	Deg.	I	II	D.	Deg.	I	II	D.
0	36	40	−4	120	62	70	−8	240	98	95	+3
10	8	34	−26	130	68	63	+5	250	110	107	+3
20	40	39	+1	140	76	75	+1	260	113	110	+3
30	44	50	−6	150	73	86	−13	270	115	111	+4
40	68	72	−4	160	102	105	−3	280	108	106	+2
50	72	77	−5	170	109	110	−1	290	108	100	+8
60	65	73	−8	180	118	116	+2	300	104	95	+9
70	56	65	−9	190	126	119	+7	310	94	91	+3
80	65	69	−4	200	124	124	0	320	81	76	+5
90	63	66	−3	210	123	119	+4	330	85	83	+2
100	56	63	−7	220	114	110	+4	340	62	57	+5
110	65	67	−2	230	88	83	+5	350	49	43	+6

To test the precision of measurement, an electron-diffraction plate of etched gold-leaf has been exhaustively measured. The plate was set up on the rotatable plate-holder of the microphotometer with the centre of the pattern as near as possible to the axis of rotation, so that the radii of the rings could be measured at every 10 degrees round their circumference.

Readings of the position of the (200) ring were made with the plate-holder set at 0, 10, . . . 350 degrees. Some days later, after a number of other measurements had been made on the plate, these readings were repeated. These two sets of readings are designated I and II and are listed, together with their differences D, in Table II.

The average value of the differences is of the order of 7 μ, but closer examination reveals that they are not distributed as would be expected if they were due merely to random errors, for almost all the negative values occur in the range 0 to 120 degrees, whereas the positive values occur in the remainder of the table. The probability of this grouping occurring by chance is infinitesimal, and so there must be a systematic difference between the two sets of readings. The obvious explanation is that a slight shift of the plate on the plate-holder occurred between the two sets of readings owing to the different thermal expansions of the glass plate and the brass plate-holder causing the former to slip slightly under the clamping springs. We have very frequently noticed such slight displacements when a plate is left on the microphotometer for some days. It can easily be shown that the effect of such a movement is to create a difference between I and II values which is related to the angular setting θ by the equation

$$D'=A_1 \cos\theta+B_1 \sin\theta, \qquad \ldots\ldots\ (1)$$

A_1 and B_1 being constants. A movement of the rotating plate-holder relative to its mount on the microphotometer would introduce a constant term A_0 into this expression ; this is unlikely, but the possibility cannot be entirely ruled out. Analyzing the values of D to determine the values of A_0, A_1 and B_1 gives

$$A_0=-0{\cdot}58 \qquad A_1=-1{\cdot}50 \qquad B_1=-5{\cdot}74.$$

The variance of the D can now be calculated with due regard to the systematic difference.

$$\text{Variance of } D=\Sigma(D^2)-36\,A_0^2-18\,A_1^2-18\,B_1^2$$
$$=1018.$$

Three constants have been fitted, so there are 33 degrees of freedom. Hence the S.D. of any one value of $D=\sqrt{1018/33}=5{\cdot}56$. *Two* settings on the line are involved in the determination of this quantity, and therefore the S.D. of a single setting is $5{\cdot}56/\sqrt{2}=3{\cdot}51\,\mu$.

Unfortunately, the value of D at the 10-degree setting differs from that calculated from (1) by $23\,\mu$, or more than four times the S.D. The probability of such a large error occurring by chance in a group of 36 observations is only 0·02 per cent. Clearly this observation is a " rogue " arising from a misreading of the microphotometer or some such cause, and the value of the S.D. calculated will be misleading. There is no well-established statistical procedure for dealing with such a situation, and the following method is the best that can be devised. The value of D at the 10-degree setting calculated from (1) is -3. Using this value instead of the observed -26, we can calculate a second approximation to the constants :

$$A_0=0{\cdot}06, \qquad A_1=-0{\cdot}24, \qquad B_1=-5{\cdot}52.$$

Using the new values of A_1 and B_1, we find the variance of D to be 446· As before, there are 33 degrees of freedom : the A_0 has been rejected as insignificant, but so has the 10-degree reading, thus giving the same total number of degrees of freedom. The S.D. of a single value of D is $3{\cdot}67\,\mu$ and that of a single reading is $2{\cdot}60\,\mu$.

A check on this value is obtained from a similar group of two sets of readings of the ring position at angular settings 5, 15 . . . 355 degrees. An analysis of these data by the method described gives for the S.D. of a single reading of the line position $2{\cdot}65\,\mu$.

The width of the line to which the above measurements relate is $250\,\mu$. To see the effect of line width on the accuracy of measurement, a similar set of readings has been made on a plate of a diffraction pattern of gold evaporated *in vacuo* on to cellulose. The rings on this plate had a width of $700\,\mu$ and the S.D. of a reading was found to be $3{\cdot}8\,\mu$. As with visual measurements, the S.D. is not proportional to the line width but to the square root of this quantity. Within the limits of error we find

$$\text{S.D. of a single reading} = 0{\cdot}15\ \sqrt{\text{line width}}$$

if all measurements are made in microns.

The precision obtainable using the non-linear microphotometer is at least as high as that obtained with other instruments. Bradley and Jay (3) claim to find the position of a line of width $300\,\mu$ to 1 or $2\,\mu$, butthe data published are meagre, and they state that most of their measurements were made to much lower precision.

For the determination of actual radii of electron-diffraction circles, it is necessary to make settings on the centre spot of the pattern. This is best accomplished visually by removing the photo-cell from the microphotometer and replacing by an eye-piece. The plate is moved until the image of the slit, which is only 25μ wide, is set across the centre of the solarized region, readings being taken at every 10 degrees. If the plate is not perfectly centred on the rotating plate-holder, the settings will vary with angle according to the equation

$$C = A_0 + A_1 \cos\theta + B_1 \sin\theta. \quad . \quad . \quad . \quad . \quad . \quad . \quad . \quad (2)$$

The observed values of C are analysed to find the constants of (2). On re-synthesizing, smoothed values of C are obtained which are a closer approximation to the true values. The average difference between observed and smoothed values of C is usually just under $1\,\mu$.

It has been verified that the median method of determining line position gives the same result as visual observation. An electron-diffraction pattern of gold foil was set up on the microphotometer and settings were made on the four rings on both sides of the centre spot. The photo-cell was then replaced by an eye-piece and the microscope was adjusted so that the cross-wires coincided with the image of the slit formed by the condensing objective. The latter was then removed and four traverses made of the plate diameter. The optical results were then compared with those of the microphotometer. Only one systematic correction, that due to the finite length of the slit, need be applied to the microphotometer readings as the other systematic errors are common to both types of measurement. The results show that there is no statistically significant difference between the diameters found by two methods of measurement.

Part III.—*Systematic Errors.*

By taking the mean of a sufficient number of observations, the effect of the *random* errors discussed in Parts I. and II. can be reduced to negligible proportions. *Systematic* errors will affect all the readings of a given line to the same extent, and can be eliminated only by determining their magnitude and applying the appropriate correction to the readings. The chief errors are those due to

(*a*) the microphotometer screw ;
(*b*) the photographic emulsion ;
(*c*) the presence of a diffuse background ;
(*d*) over-exposure or non-linearity of the microphotometer response, resulting in a marked flattening of the peaks of the lines ;
(*e*) displacement of the peak of a curved line towards the concave side due to a concentration of the radiation on that side ;
(*f*) a further displacement of the peak of a curved line due to the finite length of the microphotometer slit.

The first four of these occur in all types of spectra. The last two are appreciable only with the small radius rings encountered in electron-diffraction patterns.

(*a*) Measuring microscopes can be obtained which are direct reading to 1μ or even $\frac{1}{2}\mu$, and whose screws are guaranteed accurate to these limits, but the more common type is graduated in 10μ divisions. It is easy to fit the simpler instrument with a vernier enabling it to be read to 1μ. Usually the screw errors of a good quality instrument of this type will nowhere exceed 5 to 10μ, and it is possible, without the use of special apparatus, to determine their magnitude and hence to construct a table of corrections enabling measurements to be made to better than 1μ.

Screw errors are of two kinds : periodic and pitch errors. The former are errors which recur regularly at intervals, usually of one complete turn, while the latter arise through successive turns of the screw not advancing the nut by exactly the same amount.

The most precise method of determining the periodic error is due to Bessel ⁽⁴⁾, and consists in expressing the error in the form

$$\text{Periodic error} = \Sigma \mathrm{A}_n \cos \frac{2\pi n x}{p} + \Sigma \mathrm{B}_n \sin \frac{2\pi n x}{p} .$$

where p is the pitch of the screw (or recurrence period of the error) and x is the screw reading. The constants A_n and B_n are determined by measuring the same length (which need not be known) using different parts of the screw. The reference given should be consulted for further details. A simpler method is to make use of a stage micrometer scale. Such scales are usually 1 or 2 mm. long and are divided into 10μ-divisions. If prepared *photographically*, the divisions can be assumed to be exactly equal, but their absolute magnitude may be in error by about 1 per cent. Such a scale is placed on the measuring microscope so that its zero graduation coincides with the cross-wire when the microscope reads a whole number of mm. Microscope readings are taken for the position of each graduation of the scale over a range of 1 mm., and a curve is drawn of the difference between the scale and microscope readings against the microscope reading. The first and last points are then joined by a straight line. The correction to be applied for the periodic error is then given, as a function of the microscope reading, by the vertical distance between the straight line and the curve.

The pitch error of a screw is essentially similar to the internal errors of an ordinary scale of millimetres, and is determined by an adaptation of the methods used for testing such scales. The Thiesen–Leman method (11) is the most convenient and makes use of an auxiliary scale of millimetres, which need not be particularly accurate. For an account of this method the reference given should be consulted. When the pitch and periodic errors have been determined, appropriate corrections can be applied to the microscope readings. These are then *relatively* but not necessarily *absolutely* correct; this is usually all that is required.

(*b*) The position of the peak of a line may be displaced during the processing of the plate. Such effects are not exactly reproducible, and therefore cannot usually be allowed for. Fortunately, the errors they introduce seldom exceed 1 μ, and attain this value only in regions where the density exceeds unity. There are at least three distinct phenomena involved, and for a general account of them an article by Junkes (8) should be consulted. The effects are most pronounced when two strong lines lie close together, in which case the separation of the peaks may be changed.

We verified that our own plates were substantially free from these effects by making a negative contact print of the plate whose measurements were discussed in Part II. A positive copy was made from the negative and measured up. The distribution of density was very different on the original plate and the copy, so any emulsion errors should produce systematic differences between them. It was found that the mean radius of the (200) ring on the copy differed from that on the original by only 0·6 μ. As 18 observations of the radius were made on the copy (one reading every 20 degrees) and each has a S.D. of 2·6 μ (*cf.* Part II.), the S.D. of the mean radius is 0·6 μ. To this limit of accuracy there is no evidence of emulsion errors.

(*c*) The intensity of the radiation falling on the photographic plate is the sum of the line and background intensities. It follows that if the background intensity varies from point to point, the maximum of the total intensity curve will not coincide with the maximum of the line intensity. The maximum of the former occurs when the gradient of the line intensity is equal and opposite to that of the background intensity, and is therefore displaced in the direction of greater background intensities. The most precise method of eliminating this error is to plot the line contours with a *linear* microphotometer and to convert the resulting curve to a curve of intensities by making use of the known emulsion characteristic. The background intensity curve is then sketched in by interpolation from the parts of the total intensity curve remote from the centre of the line. The line intensity curve is then obtained by taking the difference between the total and background intensity curves, and its maximum found in the usual way.

If the error due to this cause is small, it may be estimated by making use of the result

$$\text{Background error} = \frac{k}{I_l} \Delta I_b W,$$

where

I_l is the peak intensity of the line,

ΔI_b is the change in background intensity across the width of the line,

k is a constant depending on the form of the line contour.

For lines with Gaussian contour, $k=0{\cdot}18$, while for lines of the form $I=(\sin x/x)^2$, $k=0{\cdot}19$. For almost all contours, k lies within 0·02 of this.

(*d*) If the line profile is distorted owing to over-exposure or other factors, so that the peak is flattened, it is evident that the median line method of determining the line position from the microphotometer trace will give a false result if the median line is inclined to the vertical. There is no easy way of estimating this error, but it can always be avoided by a correct choice of exposure and attention to the microphotometer characteristics. In the case of the photographic copy, the measurement of which was discussed in the section on emulsion errors, it was found that the mean radius of the (111) ring differed from that on the original plate by $1{\cdot}3\mu$ owing to over-exposure. The magnitude of this difference warns us to look with suspicion on measurements made on regions of the plate where the density much exceeds unity.

(*e*) If a spectrum line is highly curved, the radiation falling on the concave side is compressed into a shorter arc than that falling on the convex side. This results in an enhancement of the intensity and a displacement of the peak towards the concave side. The magnitude of the effect may be calculated as follows. Suppose that the spectrum line in the absence of this effect, is a circle of radius r_0 and that the intensity near the peak ($r=r_0$) is given by

$$I=1-a\Delta^2+\ldots, \qquad \ldots\ldots\ldots \quad (3)$$

where $\Delta=r-r_0$.

The effect of the concentration is to introduce an additional factor r_0/r, so that the observed intensity distribution is not I but I′, where

$$I'=\frac{r_0}{r}I=(1-a\Delta^2+\ldots)\left(1-\frac{\Delta}{r_0}+\frac{\Delta^2}{r_0^2}+\ldots\right)$$

$$=1-\frac{\Delta}{r_0}-\Delta^2\left(a-\frac{1}{r_0^2}\right)+\ldots.$$

The maximum intensity occurs when

$$\frac{dI'}{d\Delta}=-\frac{1}{r_0}-2\Delta\left(a-\frac{1}{r_0^2}\right)\ldots=0$$

or

$$\Delta\approx-\frac{1}{2ar_0}.$$

We can express this in terms of the width of the line if we assume a certain shape for the line profile. For lines with a Gaussian profile, the width W is related to the constant of (3) by

$$a=\frac{2{\cdot}772}{W^2},$$

so that the displacement of the peak is given by

$$\Delta=-0{\cdot}18W^2/r_0. \quad . \quad . \quad . \quad . \quad . \quad . \quad . \quad . \quad . \quad . \quad (4)$$

For lines with a profile of the form $(\sin x/x)^2$, the constant 0·18 of equation (4) is replaced by 0·19; for almost all other line shapes, the constant lies within 0·02 of this. In the case of lines $250\,\mu$ wide and 1 cm. in radius, this correction amounts to just over $1\,\mu$, so it is clear that the higher terms in the above expressions are negligible.

(*f*) When a curved line is scanned by a straight slit, the different parts of the slit do not lie on the same part of the line profile. This results in a distortion of the microphotometer trace and an apparent shift of the peak towards the concave side of the line.

Let the line be a circle of radius r_0, so that the light flux transmitted through unit area of the plate on to the photo-cell of the microphotometer is proportional to

$$I(r)=a_0+a(r-r_0)^2+\ldots$$

This represents a maximum opacity at $r=r_0$. The centre of curvature $(r=0)$ of the line is taken as the origin of co-ordinates.

If the centre of the image of the slit on the plate is distant R from the origin, a portion of the image distant s from its centre is at a distance

$$(R^2+s^2)^{\frac{1}{2}}=R+\frac{s^2}{2R}+\ldots$$

from the origin. If L be the length of the image of the slit on the plate, the total light flux through it is

$$F=\int_{-L/}^{+L/} I(r)\,ds$$

$$F=\int_{-L/2}^{+L/2}\left\{a_0+a\left(R-r_0+\frac{s^2}{2R}+\ldots\right)^2+\ldots\right\}ds.$$

This is a minimum when $dF/dR=0$, *i. e.* when

$$\frac{dF}{dR}=\int_{-L/2}^{+L/2}\left\{2a\left(R-r_0+\frac{s^2}{2R}+\ldots\right)\left(1-\frac{s^2}{2R^2}\right)+\ldots\right\}ds=0$$

or

$$R\approx r_0-L^2/24R$$

$$\approx r_0-L^2/24r_0.$$

The peak of the line is therefore apparently displaced a distance $L^2/24r_c$ towards the concave side.

Part IV.—*The Application of Bragg's Law to the Radii of Electron-Diffraction Patterns.*

Microphotometer measurements.—A transmission specimen was prepared from gold leaf, etched and then annealed. Eighteen determinations of the radii of four rings were made and the average radius of each found. The line width is $200\,\mu$ and the standard error of each observation is thus $2{\cdot}1\,\mu$ (*cf.* Part II.) and that of the mean is $0{\cdot}5\,\mu$. The eighteen measurements cannot be regarded as separate attempts to measure the same quantity and so the standard error of their mean cannot be calculated from their scatter, for we have been able to show that there is a systematic variation of radius round each ring the nature of which will be discussed elsewhere. The factors causing this variation do not, however, affect the *average* radius. Up to the present, only the first four rings of the gold pattern have been measured owing to the small aperture of the rotating plate-holder on the microphotometer.

Corrections must be applied for systematic errors of types (*a*), (*c*), (*e*) and (*f*) of Part III. The line widths W were found, using a linear microphotometer ; as the corrections are small, four determination of W for each ring suffice.

Using the relation (12)

$$\lambda L = \frac{aR}{\sqrt{h^2+k^2+l^2}}, \qquad \dots \dots \dots \quad (5)$$

where
λ is the wave-length of the electrons,
L is the camera length,
a is the lattice constant of the specimen,
R is the radius of the diffraction ring,
h, k, l are the indices of the diffraction ring,

values of λL corresponding to each ring are found. This assumes that $\tan\theta=\theta$, where θ is the angle of diffraction. To a higher order of accuracy, the values λL will depend on R^2 according to the relation

$$\lambda L = (\lambda L)_0 + kR^2, \qquad \dots \dots \dots \quad (6)$$

where $k = 3(\lambda L)_0/8L^2$.

As k is small, an approximate value of $(\lambda L)_0$, the value of λL corresponding to zero radius, may be used. For our camera, $L = 47 \pm 1$ cm.

The values of $(\lambda L)_0$ calculated from (5) and (6) for the different rings are not equal but vary systematically according to the relation

$$(\lambda L)_0 = A + B/R^2, \qquad \dots \dots \dots \quad (7)$$

where A and B are constants. The origin of this decrease in magnitude of $(\lambda L)_0$ with radius, which has not been previously recognized, will be discussed elsewhere ; at the moment, we are concerned only with the goodness of fit of this equation.

The (111) ring has a large background correction as it is faint owing to orientation of the crystallites in the specimen. The standard error of the mean for this correction is approximately 0·3 μ for the first ring and very much smaller for the others. The screw error has a S.E. of 0·3 μ. We may take 1·0 μ as the S.D. of each of the total corrections.

PLATE D/117. Systematic Corrections (microns).

h, k, l.	Background *.	Curvature *.	Slit length †.	Screw.	Total.
111	+1·7	+0·8	+2·6	−0·2	+4·9
200	+0·2	+0·5	+2·3	−0·8	+2·2
220	+0·1	+0·4	+1·6	−1·1	+1·0
311	+0·2	+0·4	+1·4	+0·4	+2·4

PLATE D/118.

h, k, l	Radii + systematic corrections.	$\lambda L \times 10^{12}$ cm.^{2}	A	$(\lambda L)_0$	$(\lambda L)_0$ calc.
111	10114·0	23766·0	4·1	23761·9	23764·3
200	11681·0	23770·8	5·5	23765·3	23758·5
220	16512·6	23761·0	11·0	23750·0	23749·8
311	19360·2	23757·9	15·1	23742·8	23747·4

Column A gives the correction kR^2 of equation (6).

Applying the method of least squares to the numbers of the last column but one,

$$(\lambda L)_0 = 23738{\cdot}4 \pm 3{\cdot}0 + \frac{28{\cdot}3 \pm 10{\cdot}6}{R^2}.$$

The values of $(\lambda L)_0$ given by this equation are listed under $(\lambda L)_0$ calc. The S.D. of a single $(\lambda L)_0$ is 6·05, corresponding to an accuracy of one part in 4000. The expected error in any radius arises from the measurements themselves (0·5) and the systematic corrections (1·0) and therefore amounts to $\sqrt{0{\cdot}5^2 + 1{\cdot}0^2} = 1{\cdot}12\,\mu$, corresponding to an accuracy of one part in 13000 on the average radius. These estimates of internal and external error are in poor agreement. Most of the discrepancy between them arises from the measurement of the first ring. We have independent evidence of anomalies in the radii of the diffraction rings of gold foil; it is probable that there is a real anomaly in the radius of the (111) ring, which we hope to discuss elsewhere.

---

* This assumes a Gaussian contour of the line.

† This corresponds to a slit length of 800 μ.

Visual measurements.—An ammonium chloride photograph was measured at every 20 degrees, three settings being made at each position, thus giving 54 determinations of each radius. The line width is 100μ, and the S.D. of a single setting is found by repetition settings to be $2{\cdot}2\mu$. The procedure for determining the systematic errors is as before.

PLATE D/119.

h, k, l	Mean radius.	Systematic corrections.	Corrected radius.	λL	A	$(\lambda L)_0$	$(\lambda L)_0$ calc.
110	8928·0	+0·8	8928·8	24364·2	3·3	24360·9	24361·0
111	10931·6	−0·4	10931·2	24354·7	5·0	24349·7	24349·0
200	12619·1	−0·3	12618·8	24348·0	6·6	24341·4	24343·1
210	14108·9	−1·1	14107·8	24347·2	8·3	24338·9	24339·5
211	15455·2	−0·9	15454·3	24347·2	9·9	24337·3	24337·1
310	19953·3	+0·7	19954·0	24350·3	16·5	24333·8	24332·3

$$(\lambda L)_0 = 24325{\cdot}2 \pm 0{\cdot}4 + \frac{28{\cdot}6 \pm 1{\cdot}1}{R^2}.$$

The S.D. of a single $(\lambda L)_0$ is 0·90, corresponding to an accuracy of one part in 27000. The S.D. of a single radius is 0·3, while that of the systematic corrections is also 0·3. These combine to give an overall S.D. of 0·45, corresponding to an accuracy of one part in 30000. These estimates of internal and external accuracy are in very good agreement.

As a final example, the results for a sodium chloride photograph are given, the measurements being made in the same way as before. The line width is 200μ, and the S.D. of a single setting is $3{\cdot}5\mu$.

PLATE D/137.

h, k, l	Mean radius.	Systematic corrections.	Corrected radius.	λL	A	$(\lambda L)_0$	$(\lambda L)_0$ calc.
111	7641·7	+3·9	7645·6	24843·1	2·5	24840·6	24841·9
200	8825·2	+1·9	8827·1	24839·5	3·3	24836·2	24833·8
220	12476·9	+0·1	12477·0	24826·7	6·6	24820·1	24821·5
420	19730·3	+1·0	19731·3	24831·0	16·5	24814·5	24814·2

$$(\lambda L)_0 = 24809{\cdot}3 \pm 1{\cdot}1 + \frac{19{\cdot}1 \pm 1{\cdot}9}{R^2}.$$

The S.D. of a single $(\lambda L)_0$ is 2·2, corresponding to an accuracy of one part in 11300. The S.D. of a radius is 0·48, that of the background error

0·5, that of the curvature error also 0·5 and that of the pitch error 0·3. These amount to a total S.D. of 0·9 μ, corresponding to an accuracy of one part in 14,000. The agreement of the internal and external errors is very close.

The final conclusion from this section is that the relative positions of the rings fit the given relations to within the expected accuracy, confirming the investigations of Parts I.–III.

Acknowledgments.

It is with pleasure that we thank Professor J. A. Crowther for the facilities placed at our disposal, and for much help and encouragement with the work. Our thanks are also due to Dr. P. White for advice on statistical work, and to Mr. R. H. Kidd who plotted many of the microphotometer results.

References.

(1) E. Bäcklin, *Zeit. f. Phys.* xciii. 1935, pp. 450–463.
(2) A. Becker and E. Kipphan, *Ann. d. Phys.* x. 1931, pp. 15–51.
(3) A. J. Bradley and A. H. Jay, Phys. Soc. Proc. xlv. 1933, pp. 507–522.
(4) H. Geiger and K. Scheel, *Handbuch der Physik*, Bd. ii. p. 86. (Springer, 1926.)
(5) R. Glazebrook, 'Dictionary of Applied Physics,' iii. p. 234. (Macmillan, 1923.)
(6) J. Guild, Phys. Soc. Proc. xxix. 1916, pp. 311–335.
(7) A. H. Jay, Phys. Soc. Proc. xlvi. 1934, pp. 713–720.
(8) J. Junkes, *Zeit. f. wiss. Photogr.* xxxvi. 1937, pp. 217–234.
(9) D. P. R. Petrie, Phys. Soc. Proc. xlvii. 1935, p. 637.
(10) T. B. Rymer and C. C. Butler, Phil. Mag. xxxv. 1944, pp. 202–209.
(11) K. Scheel, 'Grundlagen der praktischen Metronomie.' (Braunschweig, 1912.)
(12) G. P. Thomson and W. Cochrane, 'Theory and Practice of Electron Diffraction.' (Macmillan, 1939.)

LXIV. *Some Criticisms of the Theory of Point Electrons.*

By T. Lewis [*].

[Received April 17, 1945.]

§1. In a number of papers Dirac has examined afresh the behaviour of point electrons in an electromagnetic field from the standpoint of Classical Theory. From considerations of conservation of energy and momentum, including field energy and momentum, he arrives at well-defined equations of motion after first of all discarding awkward infinite quantities. These equations contain terms representing the reaction of the electron to its own field, or radiation damping, and are invariant with respect to Lorentz transformations. They are not new equations, but the well-known first approximations based on the electromagnetic theory of mass. Dirac, however, maintains that they are the correct equations of motion and not approximations. This may be the case, though the validity of the method of their derivation is extremely doubtful. Though they are not universally accepted as the correct equations of motion for an electron (Synge, 1940), we shall accept them for the purpose of the following paragraphs.

---

[*] Communicated by the Author.

Dirac makes the further claim (1938) that these equations of motion follow from a certain *variational principle*. We are able to show that they certainly don't follow from this particular form of the *variation principle*. In his Bakerian Lecture (1942) Dirac gives his derivation, but we shall show in §3 that this derivation involves a serious mathematical error which invalidates all his subsequent results. Later, in his lecture at the Dublin Institute for Advanced Studies (1943), he expresses the equations of motion in terms of Poisson brackets, but it can be shown that he is guilty of the same mathematical error here too. It follows that all his quantum mechanical results based on this Hamiltonian formulation are invalid in so far as they are supposed to contain a term corresponding to radiation damping.

In § 6 of the present paper we draw attention to a differential coefficient of the electromagnetic potential with respect to the proper time of an electron which is widely used by Dirac, and show that it leads to fantastic results, strongly reminiscent of J. W. Dunne's theory of serial time. Dirac, of course, states that he is not concerned with making a model of the world in the classical sense, but with setting up a mathematical scheme from which the results of experiments can be predicted. But such a mathematical scheme must be above reproach from a mathematical point of view, and lead to unique values of field quantities at a given point of space-time. Dirac's scheme satisfies neither condition.

The co-ordinates of a field point will be denoted by the four vector $\mathbf{x}=(x^\mu)$ $(\mu=0, 1, 2, 3)$, $x_0=ct$. When $\mathbf{x}$ refers to a point on the world-line of an electron it will be denoted by $\mathbf{z}=\mathbf{z}(s)$, where, as usual

$$s=\int\sqrt{dx_0^2-dx_1^2-dx_2^2-dx_3^2}.$$

The velocity vector of an electron will be denoted by $\mathbf{v}=\dot{\mathbf{z}}\equiv\frac{d\mathbf{z}}{ds}$.

The scalar product of two four vectors **A** and **B** is defined by

$$(\mathbf{AB})=\mathrm{A}_\mu\mathrm{B}^\mu=\mathrm{A}_0\mathrm{B}_0-\mathrm{A}_1\mathrm{B}_1-\mathrm{A}_2\mathrm{B}_2-\mathrm{A}_3\mathrm{B}_3.$$

The retarded and advanced potentials of an electron are given by

$$\mathrm{A}(\mathbf{x})=\frac{e\dot{\mathbf{z}}}{(\dot{\mathbf{z}},\,\mathbf{x}-\mathbf{z})}\text{ with }(\mathbf{x}-\mathbf{z})^2=0, \quad . \quad . \quad . \quad . \quad . \quad (1.1)$$

$x_0>z_0$ in the case of retarded potentials and $x_0<z_0$ for advanced potentials.

From expansions given by Dirac (1938) we easily verify that near the world-line of an electron

$$A_{\mu\,\mathrm{ret}}(\mathbf{x})=e\epsilon^{-1}[1-(\boldsymbol{\gamma},\dot{\mathbf{v}})]^{-\frac{1}{2}}\{v_\mu-\epsilon\dot{v}_\mu+\ldots\}, \quad . \quad . \quad . \quad (1.2)$$

where ϵ is a small number which vanishes when $\mathbf{x}$ is actually on the world-line, and $\boldsymbol{\gamma}$ is a small space-like vector, whose magnitude is of order ϵ.

To the same order,

$$A_{\mu\,\mathrm{adv}}(\mathbf{x})=e\epsilon^{-1}[1-(\boldsymbol{\gamma},\dot{\mathbf{v}})]^{-\frac{1}{2}}\{v_\mu+\epsilon\dot{v}_\mu+\ldots\}. \quad . \quad . \quad . \quad (1.3)$$

It follows that the difference of the two is finite on the world-line of the electron and equal to

$$A_{\mu\,\mathrm{ret}}-A_{\mu\,\mathrm{adv}}=-2e\dot{v}_\mu. \quad . \quad . \quad . \quad . \quad . \quad . \quad . \quad (1.4)$$

This result will be used in the next paragraph.

§2. In his *Classical Theory of Radiating Electrons* (1938) Dirac deduces the equations of motion of a single electron in an external radiation field, which he calls F_{in}. In order to place advanced potentials on the same footing as retarded potentials he defines another field, F_{out}, by means of the equation

$$F_{\mathrm{act}}=F_{\mathrm{in}}+F_{\mathrm{ret}}=F_{\mathrm{out}}+F_{\mathrm{adv}}, \quad . \quad . \quad . \quad . \quad . \quad . \quad (2.1)$$

where F_{act} is the actual field at any point $\mathbf{x}$.

We see that

$$F_{\mathrm{out}}=F_{\mathrm{in}}+(F_{\mathrm{ret}}-F_{\mathrm{adv}}). \quad . \quad . \quad . \quad . \quad . \quad . \quad . \quad (2.2)$$

Dirac identifies the term in brackets with the radiation field of the electron and he shows that it is finite on the world-line of the electron. In fact

$$F_{\mu\nu\,\mathrm{rad}}=F_{\mu\nu\,\mathrm{ret}}-F_{\mu\nu\,\mathrm{adv}}=\frac{4e}{3}(\dot{v}_\mu v_\nu-\ddot{v}_\nu v_\mu). \quad . \quad . \quad . \quad . \quad (2.3)$$

He eventually arrives at the equations of motion of the electron in the form

$$m\dot{v}_\mu=\tfrac{2}{3}e^2\{\ddot{v}_\mu-(\mathbf{v}\ddot{\mathbf{v}})v_\mu\}+ev^\nu F_{\mu\nu\,\mathrm{in}}. \quad . \quad . \quad . \quad . \quad . \quad . \quad (2.4)$$

But in virtue of the equation (1.3) these equations may be written

$$m\dot{v}_\mu=ev^\nu\{\tfrac{1}{2}(F_{\mu\nu\,\mathrm{ret}}-F_{\mu\nu\,\mathrm{adv}})+F_{\mu\nu\,\mathrm{in}}\}. \quad . \quad . \quad . \quad . \quad (2.5)$$

These equations are Lorentz-invariant, and Dirac further claims that they can be derived from a certain *variation principle*. For a number of electrons the integral to be varied consists of the sum of two integrals, I_1 and I_2, where

$$I_1=\Sigma_n\int m\,ds_n+\tfrac{1}{2}\sum_n\sum_{m\neq n}\int\frac{e^2(\,_m\mathbf{v}_n)\,ds_n}{(\mathbf{z}_n-\mathbf{z}_m,\,\mathbf{v}_m)}\bigg|_{\mathrm{ret}}+\tfrac{1}{2}\sum_n\sum_{m\neq n}\int\frac{e^2(\mathbf{v}_m\mathbf{v}_n)\,ds_n}{(\mathbf{z}_n-\mathbf{z}_m,\,\mathbf{v}_m)}\bigg|_{\mathrm{adv}} \quad . \quad . \quad . \quad (2.6)$$

and m and n are labels for electrons at the points $\mathbf{z}_m$, $\mathbf{z}_n$, respectively, and

$$I_2=\sum_n e\int\tfrac{1}{2}(A_{\mu\,\mathrm{in}}+A_{\mu\,\mathrm{out}})v_n^\mu\,ds_n. \quad . \quad . \quad . \quad . \quad . \quad . \quad (2.7)$$

Variation of I by itself gives the equations of motion of electrons in one another's presence but without the reaction of an electron to its own field, which is represented by the first term in the right-hand side of equation (2.5). Dirac maintains that the addition of I_2 to I_1 remedies this deficiency. In order to obtain the contribution of I_2 let us consider the case of a single electron in a radiation field F_{in}. The sum of I_1 and I_2 in this case is

$$I=\int m\,ds+\tfrac{1}{2}e\int(A_{\mu\,\text{in}}+A_{\mu\,\text{out}})v^{\mu}\,ds.$$

According to (2.2)

$$A_{\mu\,\text{out}}=A_{\mu\,\text{in}}+(A_{\mu\,\text{ret}}-A_{\mu\,\text{adv}}), \quad \ldots\ldots \quad (2.8)$$

so that

$$I=\int m\,ds+e\int A_{\mu\,\text{in}}v^{\mu}\,ds+\frac{e}{2}\int(A_{\mu\,\text{ret}}-A_{\mu\,\text{adv}})v^{\mu}\,ds. \quad \ldots \quad (2.9)$$

Without the last term, variation of I leads to the equations of motion without damping. But we have shown in § 1 above that on the world-line of the electron

$$\tfrac{1}{2}(A_{\mu\,\text{ret}}-A_{\mu\,\text{adv}})=-e\dot{v}_{\mu}. \quad \ldots\ldots \quad (2.10)$$

It follows that

$$\tfrac{1}{2}(A_{\mu\,\text{ret}}-A_{\mu\,\text{adv}})v^{\mu}=-e\dot{v}_{\mu}v^{\mu}\equiv 0, \quad \ldots\ldots \quad (2.11)$$

so that the inclusion of this term makes no difference to I in the case of a single electron. In the case of several electrons, however, the addition of I_2 to I_1 is equivalent to omitting the last term in I_1, so that retarded potentials only are effective. But there are reasons for preferring I_1 as it stands (Lewis, 1940).

§3. In his *Bakerian Lecture* (1941) Dirac gives details of the derivation of the equations (2.5) from a *variational principle.* In order to show that it involves a serious mathematical error one need not go into the details of his method of variation. For the sake of argument let us accept *his* equations (1.14), which, according to him, are a consequence of varying a certain integral. These equations are

$$\begin{aligned} m_i\frac{dv_i^{\mu}}{ds_i}&=e_i\left[\left(\frac{\partial A_i^{\nu}}{\partial x_{\mu}}\right)_{z_i}v_{\nu i}-\frac{dA^{\mu}(z_i)}{ds_i}\right]\\ &=e_i\left[\frac{\partial A_i^{\nu}}{\partial x_{\mu}}-\frac{\partial A_i^{\mu}}{\partial x_{\nu}}\right]_{z_i}v_{\nu i}, \quad \ldots\ldots \quad (3.1)\end{aligned}$$

where

$$A_i^{\nu}=\tfrac{1}{2}[A_{\text{in}}^{\nu}+A_{\text{out}}^{\nu}]+\tfrac{1}{2}\sum_{j\neq i}[A_{j\,\text{ret}}^{\nu}+A_{j\,\text{adv}}^{\nu}], \quad \ldots \quad (3.2)$$

i, j being mere labels for the different electrons.

In order not to confuse the issue, let us again take the case of a single electron, so that

$$A^{\nu}=\tfrac{1}{2}[A_{\text{in}}^{\nu}+A_{\text{out}}^{\nu}]=A_{\text{in}}^{\nu}+\tfrac{1}{2}(A_{\text{ret}}^{\nu}-A_{\text{adv}}^{\nu}). \quad \ldots \quad (3.3)$$

Now in passing from the first to the second of equations (3.1) [Dirac's 1.14], he has assumed that

$$\frac{dA^{\mu}(z)}{ds}=\left[\frac{\partial A^{\mu}}{\partial x_{\nu}}\right]_{z}v_{\nu}, \quad \ldots\ldots \quad (3.4)$$

which is correct only provided A^μ does not involve s explicitly. But $\frac{1}{2}(A^\nu_{\mathrm{ret}}-A^\nu_{\mathrm{adv}})$ is a function of $\mathbf{x}$, $\mathbf{z}$ and $\dot{\mathbf{z}}$, the last two being functions of s. And on the world-line of the electron this term reduces to a function of s only. However one looks at it, the relation (3.4) simply does not hold in this case.

We accepted (3.1) for the sake of argument only. It will be obvious to anyone who takes the trouble to go through Dirac's work in detail that the variational principle will not yield (3.1) when A^ν_i is defined as in (3.2). Dirac deceives himself, and others, obviously, by assuming in the first place that A^ν is a given function of co-ordinates and deriving the results appropriate to such an assumption. It is only when he has obtained the form of equations which he wants that he specifies the exact nature of his potentials, but he does not seem to have inquired whether his derivation is valid for these potentials.

§4. The same error is perpetuated in the lecture on *Quantum Electrodynamics* (1943). In §6 of this lecture Dirac takes as his starting point a Hamiltonian for a single electron in a given field of potential $\mathbf{A}(\mathbf{x})$. This Hamiltonian is

$$\mathrm{F}=-\frac{1}{2m}\{(\mathrm{p}-e\mathbf{A}(\mathbf{z}))^2-m^2\}=0. \qquad (4.1)$$

After deriving the equations of motion in the form he wants Dirac specifies his $\mathrm{A}(\mathrm{x})$ (his eqn. 6.16). He writes

$$\mathbf{A}=\mathbf{A}_{\mathrm{in}}+\sum_{j\neq i}\mathbf{A}_{j\,\mathrm{ret}}+\tfrac{1}{2}(\mathbf{A}_{i\,\mathrm{ret}}-\mathbf{A}_{i\,\mathrm{adv}}), \qquad (4.2)$$

which, for a single electron, reduces to

$$\mathbf{A}=\mathbf{A}_{\mathrm{in}}+\tfrac{1}{2}(\mathbf{A}_{\mathrm{ret}}-\mathbf{A}_{\mathrm{adv}}). \qquad (4.3)$$

Dirac here expresses equations of motion in terms of Poisson brackets. For example

$$\frac{d\xi}{ds}=[\xi,\mathrm{F}]. \qquad (4.4)$$

When $\mathrm{A}(\mathbf{x})$ is a given function of x and parameters under control we get for the motion of an electron:

$$\frac{dz_\mu}{ds}=-\frac{\partial \mathrm{F}}{\partial p^\mu}=\frac{1}{m}(p_\mu-e\mathrm{A}_\mu(\mathbf{z})) \qquad (4.5)$$

$$\frac{dp_\mu}{\partial s}=\frac{\partial \mathrm{F}}{\partial z^\mu}=\frac{e}{m}(p_\nu-e\mathrm{A}_\nu(\mathbf{z}))\frac{\partial \mathrm{A}^\nu(\mathbf{z})}{\partial z^\mu}. \qquad (4.6)$$

Differentiation of (4.5) gives

$$m\frac{d^2z_\mu}{ds^2}=\frac{dp_\mu}{ds}-e\frac{d\mathrm{A}_\mu}{ds}=\frac{e}{m}(p_\nu-e\mathrm{A}_\nu)\frac{\partial \mathrm{A}_\nu}{\partial z^\mu}-e\frac{d\mathrm{A}_\mu}{ds}. \qquad (4.7)$$

Now when $\mathbf{A}$ is a function of x only,

$$\frac{d\mathrm{A}_\mu}{ds}=\frac{\partial \mathrm{A}_\mu}{\partial x^\nu}v_\nu\Big|_{\mathbf{x}=\mathbf{z}}. \qquad (4.8)$$

Substituting this expression in equation (4.7) and using (4.5) once again, we obtain

$$m\frac{d^2z_\mu}{ds^2}=ev_\nu\frac{\partial A^\nu}{\partial z^\mu}-ev^\nu\frac{\partial A_\mu}{\partial z^\nu}$$

$$=ev^\nu\left(\frac{\partial A_\nu}{\partial z^\mu}-\frac{\partial A_\mu}{\partial z^\nu}\right). \quad . \quad . \quad . \quad . \quad . \quad . \quad . \qquad (4.9)$$

This equation is the accepted equation of motion of an electron in a given field of force. But Dirac ultimately defines his potentials according to the equation (4.2) above, which for a single electron reduces to (4.3). Now the term in brackets on the right-hand side of (4.3) involves s explicitly, through the terms $\mathbf{z}$, $\dot{\mathbf{z}}$, so that (4.8) is no longer true. It follows that (4.9) is not a valid deduction from (4.7), even were that equation valid. Equation (4.7) itself is not valid because the Hamiltonian F involves the velocity of the electron as well as its momenta and co-ordinates.

§5. In this paragraph we give the form of *Hamilton's Principle* from which equations (2.4) may be derived. It is a form appropriate to non-conservative and non-holonomic dynamical systems. If for a single electron we write

$$h=m\sqrt{\dot{\mathbf{x}}^2}+eA_{\mu\,\mathrm{in}}\dot{\mathbf{x}}^\mu \quad . \quad . \quad . \quad . \quad . \quad . \quad . \qquad (5.1)$$

and

$$Q_\mu=\tfrac{2}{3}e^2\{\ddot{v}_\mu-(\mathbf{v}\mathbf{v})v_\mu\}, \quad . \quad . \quad . \quad . \quad . \quad . \quad . \qquad (5.2)$$

the equations (2.4) are embodied in the statement

$$\int(\delta h+Q_\mu\delta x^\mu)\,ds=0. \quad . \quad . \quad . \quad . \quad . \quad . \quad . \qquad (5.3)$$

But the Hamiltonian and Poisson bracket techniques employed by Dirac in his subsequent work do not apply in this case, at least, not without suitable modification.

§6. We now proceed to further criticism of Dirac's theory of *Classical Electrodynamics* as expounded by him in his lecture (1943, §6). To do this effectively his results will have to be quoted rather extensively.

He defines a *Wentzel field* by means of the equation

$$A_{\mu w}=A_{\mu\,\mathrm{in}}+\Sigma_i e_i\int_{-\infty}^{s_i} v_{\mu i}(s_i')\varDelta(\mathbf{x}-\mathbf{z}(s_i'))\,ds_i', \quad . \quad . \quad . \qquad (6.1)$$

where

$$\varDelta(\mathbf{x}-\mathbf{z})=\frac{1}{r}\{\delta(r-x_0+z_0)-\delta(r+x_0-z_0)\} \quad . \quad . \quad . \quad . \quad . \qquad (6.2)$$

and

$$r^2=(x_1-z_1)^2+(x_2-z_2)^2+(x_3-z_3)^2,$$

$\delta(x)$ being an ordinary δ-function.

The contribution of a single electron to $A_{\mu w}$ is

$$e\int_{-\infty}^{s} v_\mu'\varDelta(\mathbf{x}-\mathbf{z}')\,ds',$$

where $z'=z(s')$, etc.

This integral has the value

(1) $A_{\mu\,\mathrm{ret}}$, when $\mathbf{x}$ is a point outside the light cone of $\mathbf{z}(s)$,

(2) zero, when $\mathbf{x}$ is a point inside the future light cone of $\mathbf{z}(s)$,

(3) $A_{\mu\,\mathrm{ret}}-A_{\mu\,\mathrm{adv}}$, when $\mathbf{x}$ is a point inside the past light cone of $\mathbf{z}(s)$.

Dirac then assumes that all electron points lie outside one another's light cones, *i. e.*,

$$(\mathbf{z}_i-\mathbf{z}_j)^2<0, \quad i\neq j. \qquad (6.3)$$

It then follows without difficulty that $A_{\mu w}$ has the value

(1) $\mathbf{A}_{\mathrm{in}}+\sum_j \mathbf{A}_{j\,\mathrm{ret}}$, if one approaches the point $\mathbf{x}=\mathbf{z}_i$ along a path outside the light cone of $\mathbf{z}_i$,

(2) $\mathbf{A}_{\mathrm{in}}+\sum_{j\neq i} \mathbf{A}_{j\,\mathrm{ret}}$, if one approaches the point $\mathbf{x}=\mathbf{z}_i$ along a path inside the future light cone of $\mathbf{z}_i$,

(3) $\mathbf{A}_{\mathrm{in}}+\sum_j \mathbf{A}_{j\,\mathrm{ret}}-\mathbf{A}_{i\,\mathrm{adv}}$, if one approaches the point $\mathbf{x}=\mathbf{z}_i$ along a path inside the past light cone of $\mathbf{z}_i$.

Expression (1) is just the Maxwell field. The mean of (2) and (3) is

$$\mathbf{A}_{\mathrm{in}}+\sum_{j\neq i} \mathbf{A}_{j\,\mathrm{ret}}+\tfrac{1}{2}(\mathbf{A}_{i\,\mathrm{ret}}-\mathbf{A}_{i\,\mathrm{adv}}), \qquad (6.4)$$

which is exactly equal to the potential defined in (4.2).

In order to ensure that he gets the right value of the potential everywhere Dirac introduces what he calls the $\boldsymbol{\lambda}$ limiting process, where $\boldsymbol{\lambda}$ is a small time-like vector which is ultimately made to tend to zero. He now defines his potentials by means of the relation

$$\mathbf{A}(\mathbf{x})=\tfrac{1}{2}\{\mathbf{A}_w(\mathbf{x}+\boldsymbol{\lambda})+\mathbf{A}_w(\mathbf{x}-\boldsymbol{\lambda})\} \qquad (6.5)$$

and replaces the condition (6.3) by

$$(\mathbf{z}_i-\mathbf{z}_j\pm\boldsymbol{\lambda})^2<0, \quad i\neq j. \qquad (6.6)$$

To sum up, the field at a point on the world-line of an electron is given by (6.4), but at points not on the world-line of an electron the field is the sum of the in-field and the retarded fields of the electrons. Dirac may not agree with this summing up for his subsequent work suggests that he is groping after something strongly reminiscent of J. W. Dunne's theory of serial time. He writes down what he calls the equation of motion for $\mathbf{A}_\mu(\mathbf{x})$, namely

$$\frac{dA_{\mu w}}{ds_i}=e_i v_{\mu i}\Delta(\mathbf{x}-\mathbf{z}_i), \qquad (6.7)$$

from which it follows that

$$\frac{d\mathbf{A}_\mu(\mathbf{x})}{ds_i}=\tfrac{1}{2}e_i v_{\mu i}\{\Delta(\mathbf{x}-\mathbf{z}_i+\boldsymbol{\lambda})+\Delta(\mathbf{x}-\mathbf{z}_i-\boldsymbol{\lambda})\}. \qquad (6.8)$$

It is true that the right-hand side of (6.7) is the differential coefficient with respect to s_i of the integral on the right-hand side of (6.1). But what is its interpretation in this case? It is obviously not the same as the $\dfrac{dA}{ds_i}$ which occurs in (3.1). Dirac regards the potentials defining the fields as functions of $\mathbf{x}$ and all the s_i, which are assumed to be independent variables subject to the restrictions (6.6) only. It follows that the field at a given point $\mathbf{x}$ of space-time has different values according as the ith electron is imagined to be at a point $\mathbf{z}_i$ of its world-line inside the past light cone of $\mathbf{x}$, outside this light cone or inside its future light cone. To put it in another way: an electron contemplating a given point $\mathbf{x}$ of space-time in its future light cone assigns a certain value to the field at $\mathbf{x}$. Later in the experience of this electron the point $\mathbf{x}$ is outside its light cone, and a different value is assigned to the field. Later still in the experience of the electron the point $\mathbf{x}$ will be in its past light cone and the field assigned to it will again be different. All this is very confusing, but it follows if the s_i are regarded as independent variables. The situation is rendered still more confusing when we consider the restriction (6.6) which ensures that the field at a point $\mathbf{x}=\mathbf{z}_i$ on the world-line of an electron has a unique value, at least as far as the contribution of other electrons is concerned. We suggest that the condition (6.6) should be replaced by the more general condition

$$(\mathbf{x}-\mathbf{z}_i\pm\boldsymbol{\lambda})^2<0, \quad \mathbf{x}\neq\mathbf{z}_i. \quad \ldots \ldots \quad (6.9)$$

This means that the field at a point $\mathbf{x}$ of space-time is defined when all the electrons are outside the light cone of $\mathbf{x}$. The Wentzel field defined by the equation (6.1) then leads to the familiar retarded field, and the differential coefficient (6.8) has no meaning. The fact that it is formally correct merely proves that the δ-function, though a useful servant, is an unreliable master.

Dirac is also led to the following expression for the divergence of the electromagnetic four-vector potential

$$\frac{\partial A_\mu}{\partial x^\mu}=-\tfrac{1}{2}\sum_i e_i\{\Delta(\mathbf{x}-\mathbf{z}_i+\boldsymbol{\lambda})+\Delta(\mathbf{x}-\mathbf{z}_i-\boldsymbol{\lambda})\}. \quad \ldots \quad (6.10)$$

When the point $\mathbf{x}$ is on the light-cone of $\mathbf{z}_i$ the right-hand side of (6.10) has a singularity of the nature of an ordinary δ-function. Now every point $\mathbf{x}$ of space-time is on the light cone of the ith electron for some value of $\mathbf{z}_i$, and it follows that every point $\mathbf{x}$ is a singular point of the divergence—a state of affairs very difficult to imagine. The fact is that the divergence of A_μ vanishes identically, except at points on the world-lines of electrons (the divergences of the retarded and advanced potentials vanish separately) where it is indeterminate.

The statement (6.10) should be contrasted with the assumption that

$$\Box\mathbf{A}(\mathbf{x})\equiv 0 \quad \ldots \ldots \ldots \quad (6.11)$$

at all points of space time. It is true that $\Box\Delta(\mathbf{x})\equiv 0$ everywhere except when $r(=\sqrt{(x_1-z_1)^2+(x_2-z_2)^2+(x_3-z_3)^2})$ is zero, when each of the two terms on the right-hand side of (6.2) defining $\Delta(\mathbf{x})$ has a singularity. In ordinary potential theory $\nabla\left(\frac{1}{r}\right)$ vanishes identically except for $r=0$, where it has a singularity. It may be argued that the two singularities cancel in the case of $\Box\Delta(\mathbf{x})$, but this surely requires investigation. A case might also be made for the vanishing of the divergence of $\mathbf{A}(\mathbf{x})$ on the world-line of an electron, due to the cancelling of two singularities. Later in his lecture (1943), § 8, in the passage to quantum theory, Dirac appears to have difficulty with the divergence of $\mathbf{A}(\mathbf{x})$. The value (6.10) for it is inconsistent with the commutation relations, and he has to make a special assumption to overcome this difficulty. This making of special assumptions is a feature of Dirac's recent investigations. For example, in § 6 we find the following :—

" The equation of motion

$$\frac{d\mathrm{A}_\mu(\mathbf{x})}{ds_i}=[\mathrm{A}_\mu(\mathbf{x}),\ \mathrm{F}_i]$$

agrees with (6.21) [our (6.8)] provided we assume

$$[\mathrm{A}(\mathbf{x}),\ \mathrm{A}_\nu(\mathbf{x}')]=\tfrac{1}{2}g_{\mu\nu}\{\Delta(\mathbf{x}-\mathbf{x}'+\boldsymbol{\lambda})+\Delta(\mathbf{x}-\mathbf{x}'-\boldsymbol{\lambda}).\}"$$

He does not explain what he means by the Poisson bracket

$$[\mathrm{A}_\mu(\mathbf{x}),\ \mathrm{A}_\nu(\mathbf{x}')].$$

He is dealing with a classical system where a Poisson bracket involves differential coefficients with respect to momenta and co-ordinates. In quantum mechanics the bracket is more or less intelligible, but its interpretation from the point of view of classical mechanics deserves some explanation. But whatever Dirac means by this expression and its assumed value, it breaks down in the light of the fact that F_i is not a legitimate Hamiltonian for the ith electron, involving, as it does, velocities in addition to co-ordinates and momenta.

References.

Dirac, P. A. M., Proc. Roy. Soc. A, clxvii. pp. 148–169 (1938).
Dirac, P. A. M., Proc. Roy. Soc. A, vol. clxxx. pp. 1–40 (1941).
Dirac, P. A. M., " Quantum Electrodynamics," Dublin Inst. for Advanced Studies (1943).
Lewis, T., Phil. Mag. vol. xxix. pp. 495–507 (1940).
Synge, J. L., Proc. Roy. Soc. A, vol. clxxvii. pp. 118–139 (1940).

LXV. *Note on the Helmholtz Make-and-Break Theorem and an Application to the Wheatstone Net.*

By G. F. Freeman, M.Sc.(Eng.), M.I.E.E., A.M.I.Mech.E., of West Ham Municipal College *.

[Received July 31, 1944.]

In an earlier paper † the effect of altering the value of a component arm of a network was developed as a generalization of the Helmholtz make-and-break theorem (re-invented by, and sometimes ascribed to, Thévenin) by the substitution of one impedance for another. There is, however, some advantage on occasion in considering the *change* in impedance as the independent variable rather than the impedance itself. This extension is perhaps not so well known as it might be; possibly its very simplicity has contributed to its neglect. It has therefore been thought worth while to make brief mention of it here, together with an example illustrative of its use.

---

* Communicated by the Author.

† Phil. Mag. xxxiii. p. 679, Sept. 1942.

Fig. 1 *a*.

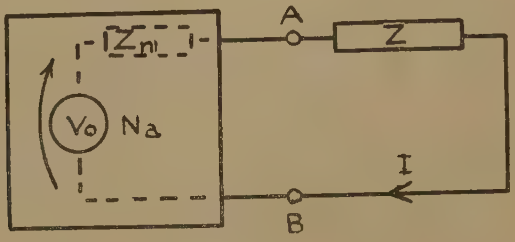

Fig. 1 *b*.

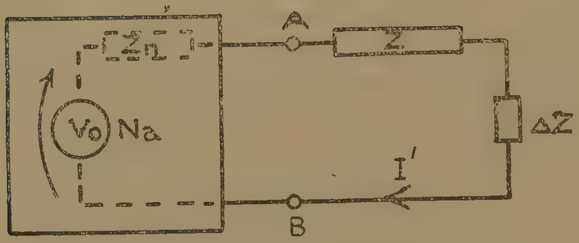

Fig. 1 *c*.

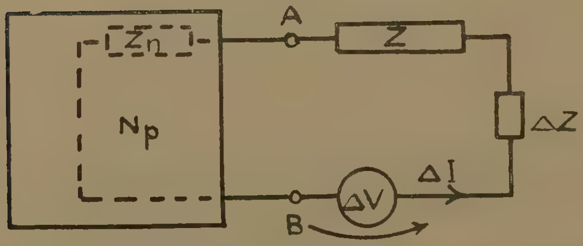

Theorem.

Consider the active network N_a. This may be represented, as in fig. 1 *a*, by a voltage source V_0 in series with a network impedance Z_n, which supplies a current I to an impedance Z connected between terminals A and B of the network. It is clear that $I=\frac{V_0}{Z_n+Z}$, and that in the corresponding fig. 1 *b*, where Z is increased by ΔZ the current has a modified value $I'=\frac{V_0}{Z_n+Z+\Delta Z}$.

Now write $I\Delta Z=\Delta V$, and apply ΔV as the sole voltage source in the circuit fig. 1*c*, where the network N_p is N_a rendered passive by the shortcircuiting of its voltage sources. The current ΔI—which flows in the opposite direction to I in fig. 1*a*—is

$$\Delta I = \frac{\Delta V}{Z_n+Z+\Delta Z}=\frac{I\Delta Z}{Z_n+Z+\Delta Z}.$$

Hence

$$I-\Delta I=\frac{V_0}{Z_n+Z}\left(1-\frac{\Delta Z}{Z_n+Z+\Delta Z}\right)$$

$$=\frac{V_0}{Z_n+Z+\Delta Z}=I'.$$

The relations are vectorial throughout. In d.c. applications the vectors are of course all co-phasal.

It is then established that the *change* in current due to the *change*

any arm of any network,

832

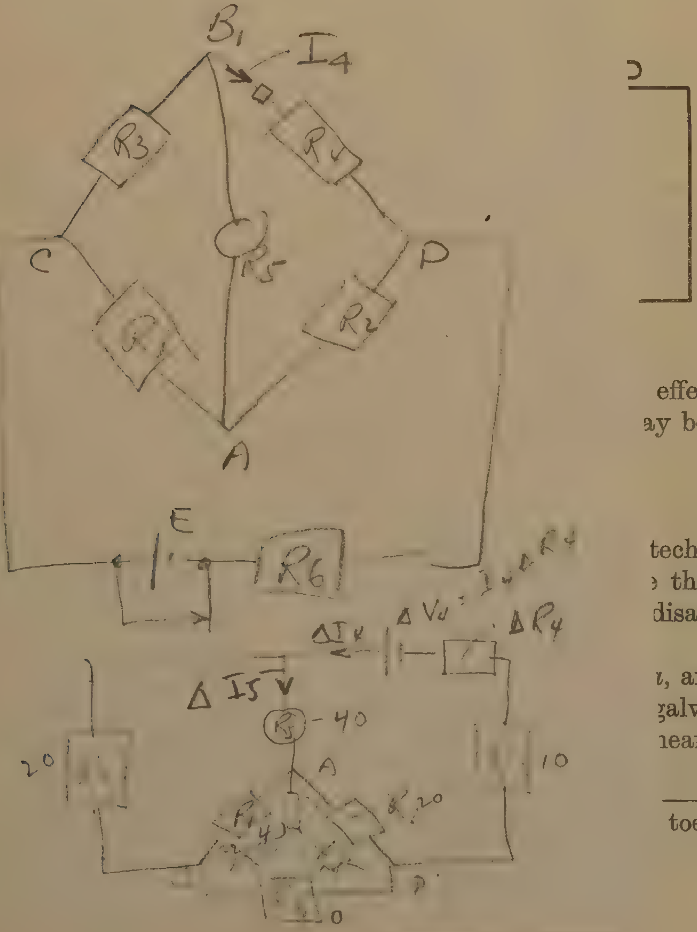

effect of the original

ay be at once deduced

technique is found in

the galvanometer is

disappearing filament

, and suppose that it

galvanometer current

neanwhile remaining

---

toeorem. (Dic. App'.

Choosing initially the value of R_4 for which the bridge is in balance, $\frac{R_1}{R_3}=\frac{R_2}{R_4}=n$ (say). The corresponding value of I_4 yields a voltage $\Delta V_4=I_4\Delta R_4$ which is applied to the circuit of fig. 2*b* (in which some rearrangement of components is made for the sake of clarity), deducing ΔI_5 from ΔI_4 by the ordinary rules. Since I_5 is initially zero it follows that $I_5=\Delta I_5$. Where R_6, the resistance of the battery link, is not negligible it is convenient to replace the ACD delta of fig. 2*b* by the equivalent

Fig. 2*b*.

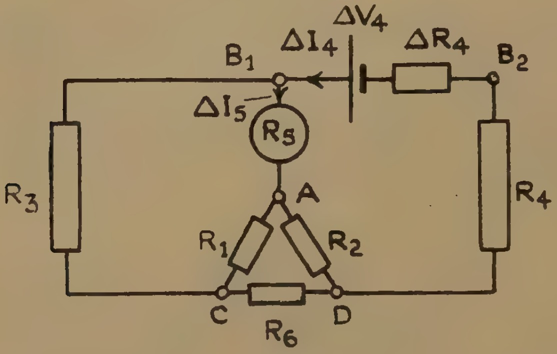

Fig. 2*c*.

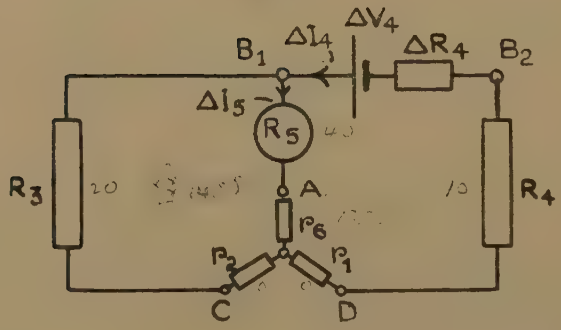

star of fig. 2*c* $\left(r_6=\frac{R_1R_2}{R_1+R_2+R_6}, \text{etc.}\right)$. Thus I_5 is resolved as a simple function of ΔR_4.

It is quite straightforward to conduct the whole operation numerically. Alternatively, substitution in a formula may be preferred. It is easy to show that

$$I_5=\frac{nER_p\Delta R_4}{(R_5+r_6)(R_4+r_1+R_p+\Delta R_4)\{(n+1)R_6+(R_1+R_2)\}}, \quad . \quad (1)$$

in which R_p is the parallel resistance of (R_5+r_6) and (R_3+r_2).

In order that the *comparative* variation shall be preserved, it is evidently necessary that $\frac{R_4+r_1+R_p}{R_4}$ shall be constant—in other words, the resistance between B_1 and B_2 in fig. 2*c* must be proportional to R_4. This entails reciprocal relations between the various resistances: *e. g.*, if R_6 goes up R_5 must come down (which may be realized by shunting the galvanometer). The requisite sensitivity may then be obtained by variation of the supply voltage.

Numerical Example.

(*a*) Suppose

$$R_1=40\,\Omega,\quad R_2=20\,\Omega,\quad R_3=20\,\Omega,\quad R_4=10\,\Omega,\quad R_5=40\,\Omega,\quad R_6=0,$$
$$E=6 \text{ volts}.$$

Then $\quad n=2,\quad r_1=r_2=0,\quad r_6=13{\cdot}33\,\Omega,\quad : \frac{R_1R_2}{R_1+R_2+R_6} = \frac{R_1R_2}{R_1+R_2}$

83.2 Y

(Fig 2a)

Δ

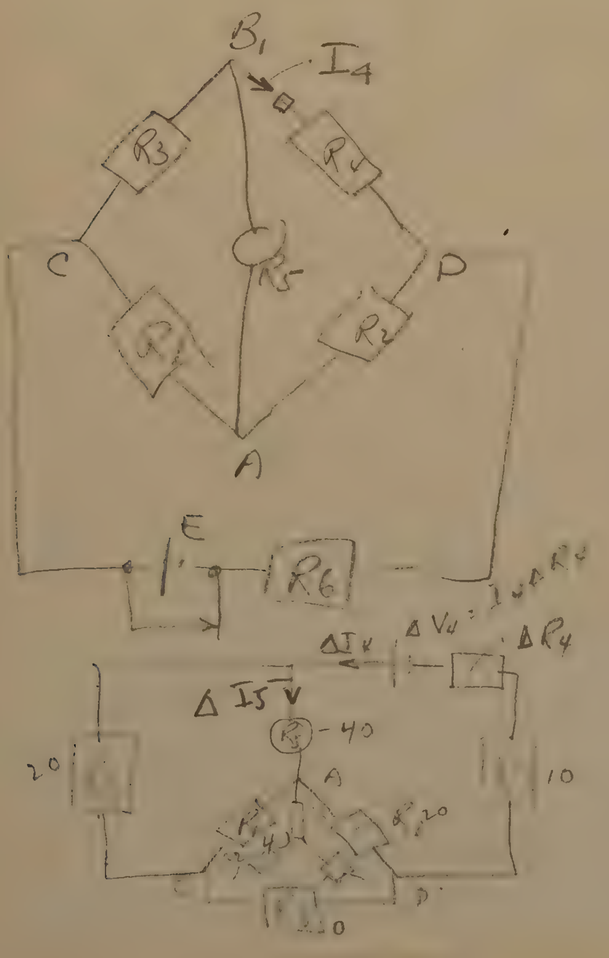

$\overline{5}$ amp. $\quad = \frac{(I_4 \Delta R_4)}{\Delta R_4 + R_4 + R}$ =

amp. $\quad = \Delta I_4 \cdot \frac{R_3}{R_5 + R_6 +}$

$\frac{546}{24{\cdot}55}$ amp./ohm

=0.)

$\frac{R_4}{{\cdot}55}$ amp.

is to be realized by

y voltage. We now

s before.

s and $R_5=4{\cdot}0$ ohms.

$\frac{\Delta R_4}{24{\cdot}55}$ amp.,

of $6\times\frac{0{\cdot}0546}{0{\cdot}6682}=4{\cdot}80$

atio of 10, however,

meter current (and

}, ... (2)

where m is the shunting ratio.

Thus $$E=6\times\frac{10\times14\cdot0}{53\cdot33}\times\frac{14\cdot55}{9\cdot55}\times\frac{60+60}{60}=48 \text{ volts}$$

as before.

Conclusion.

It will be appreciated that only one aspect of this corollary to the Helmholtz theorem has been touched upon in this short note. Too much stress should not be laid upon the formulæ developed ; although they are convenient for the immediate purpose they and others like them are very readily obtained to suit the conditions of such problems as may appear suitable for the treatment. The important thing is to recognize the occasions on which the process may profitably be applied, and it is hoped that this introduction may help towards such an end. The process is. in fact. a species of electrical " relaxation method," to which, however, no iteration is needed, since the result obtained is exact.

LXVI. *Monochromatic Lens Aberration Theory.*

By H. H. Hopkins, Ph.D., F.Inst.P.,
W. Watson and Sons, High Barnet, Herts.*.

[Received February 6, 1945.]

Abstract.

A spherical wave proceeding from (or to) an object point and traversing a lens system undergoes a series of refractions which produce changes in the curvature of the wave, this latter taking forms departing slightly from the spherical. Such departures are made the measure of aberration. and these when related to the auxiliary axes—*i. e.* the lines joining the appropriate object points and the centres of curvature of the refracting surfaces—take the form of a simple spherical aberration. Formulæ for the aberrations of the wave-front of different orders are derived on this basis. The image at any stage being, in the absence of wave-front aberration, the paraxial image along the auxiliary axis, the locus of such image points, defined here as the paraxial image surface, provides a concept of image curvature which is valid for finitely large apertures and angles of field. The Petzval surface appears to correspond with the " first order " paraxial image surface—except in a special case.

This method of viewing the problem leads to particularly simple derivations of the conditions for flatness of field, and of a "Seidel" first-order theory of wave-front aberration. The possibilities of focusing-out

---

* Communicated by the Author.

small amounts of spherical aberration, and of coma producing a small distortion are indicated, together with formulæ for treating these two problems: astigmatism and distortion are discussed on a new basis. Accurate formulæ for dealing with the aberrations of the wave-front are arrived at on the basis of the physical concepts described, and using the basic formulæ for spherical aberration.

A feature of the method is the direct correlation between the approximate and accurately calculated values of the aberrations.

---

1. *Introduction.*

THE principle of Fermat, defining the possible light ray-paths from P_1 to P_2 in terms of the stationary values of the optical path lengths, a condition generally written

$$\delta\int_{P_1}^{P_2} n\,dl=0 \quad . \; . \; . \; . \; . \; . \; . \; . \; . \; . \quad (1)$$

is readily extended to the case of the imagery of P_1 in the region of P_2 by means of a lens system. An element of a wave, originating at P_1, travels from this point through the system along a permitted ray-path defined by (1), and finally passes through or near the point P_2. If a sphere is drawn with centre P_2, which is intersected at S (in the final medium) by the ray-path emerging from the system and proceeding towards P_2, then the distribution of light in a plane through P_2 will be that due to "perfect" imagery, providing

$$\int_{P_1}^{S} n\,dl=\text{constant} \quad . \; . \; . \; . \; . \; . \; . \; . \; . \; . \quad (2)$$

for all parts of the wave. Any departure from this condition entails a "deterioration" of the image viewed in the given plane. Such departures manifest themselves in the images viewed in planes near P_2 as aberration; and, in the absence of a simple relationship between them and the resulting changed light distribution, they form the most direct physical basis for the measurement of the aberrations of lens systems.

This analysis of the question has, of course, long been recognized *, but it is a signal fact that no theory of aberrations based upon it has so far found general acceptance among optical designers. The design of systems seems generally to be accomplished using either one or both of Von Seidel's theory of first order aberrations and the tracing of suitable ray-paths, both of which in their usual form seek to express the departures from sphericity of the emergent wave-fronts in terms of the departures from homocentricity of the ranges of wave-normals associated with them.

In what follows an attempt is made to develop a theory of lens aberrations on the basis of differences in optical path, expressed in terms of the departure of the wave-front after refraction from the "paraxial" sphere.

---

* It was first put forward by Huygens ('Treatise on Light,' 1690).

2. *The Departure of an Incident Spherical Wave-Front from Sphericity,* w, *after Refraction at a Spherical Interface, the Rate of Change of* w *with Aperture being small.*

In fig. 1, O is an object point to which the incident spherical wave-front, of which AB is a portion, proceeds. After refraction at the spherical interface AP, centre C, the emergent wave-front, considered paraxially, is a sphere centred on O′, the image of O. AB′ is a section through part of this sphere projected backwards (in the second medium) to pass through A. B, B′ are corresponding points on these incident and emergent paraxial wave-fronts.

Writing r, s, s' for the radii of the refracting interface, the incident and emergent wave-fronts, $\alpha=\widehat{PCA}$, $u=\widehat{BOA}$, $u'=\widehat{B'O'A}$, it can be shown, by an approximation to be justified later, that, providing $\frac{1}{s}\frac{\partial \mathrm{w}}{\partial u}$ is small,

Fig. 1.

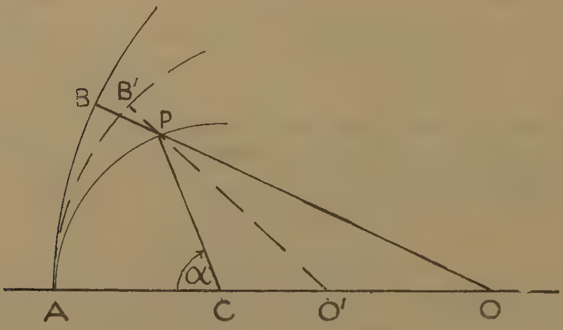

the departure of the actual emergent wave-front from the emergent paraxial sphere for the element refracted at P is given by

$$\mathrm{w}=n't'-nt, \quad . \quad . \quad . \quad . \quad . \quad . \quad . \quad . \quad . \quad . \quad (3)$$

where $t=\mathrm{BP}$, $t'=\mathrm{B'P}$; n, n' are the refractive indices of the media to the left and right of AP. w is positive when the wave-front is in advance of the paraxial sphere.

From the triangle POC

$$(s-t)^2=s^2\left\{1-\frac{Q}{ns}(2r\sin\tfrac{1}{2}\alpha)^2\right\},$$

where $$Q=n\left(\frac{1}{r}-\frac{1}{s}\right)=n'\left(\frac{1}{r}-\frac{1}{s'}\right).$$

Writing $$A=Q(2r\sin\tfrac{1}{2}\alpha)^2, \quad . \quad . \quad . \quad . \quad . \quad . \quad . \quad . \quad . \quad . \quad (4)$$
this gives

$$nt=\frac{1}{2}A+\frac{1}{8}A^2\left(\frac{1}{ns}\right)+\frac{1}{16}A^3\left(\frac{1}{ns}\right)^2+\frac{5}{128}A^4\left(\frac{1}{ns}\right)^3+\frac{7}{256}A^5\left(\frac{1}{ns}\right)^4+\dots \quad . \quad . \quad . \quad (5)$$

In an identical manner it can be shown that

$$n't'=\frac{1}{2}\mathrm{A}+\frac{1}{8}\mathrm{A}^2\left(\frac{1}{n's'}\right)+\frac{1}{16}\mathrm{A}^3\left(\frac{1}{n's'}\right)^2+\frac{5}{128}\mathrm{A}^4\left(\frac{1}{n's'}\right)^3+\frac{7}{256}\mathrm{A}^5\left(\frac{1}{n's'}\right)^4+\ldots \quad (6)$$

Subtraction gives

$$\mathrm{w}=\frac{1}{8}\mathrm{A}^2\varDelta\left(\frac{1}{ns}\right)+\frac{1}{16}\mathrm{A}^3\varDelta\left(\frac{1}{ns}\right)^2+\frac{1}{25{\cdot}6}\mathrm{A}^4\varDelta\left(\frac{1}{ns}\right)^3+\frac{1}{36{\cdot}57}\mathrm{A}^5\varDelta\left(\frac{1}{ns}\right)^4+\ldots, \quad (7)$$

and the aberrations of various orders are *

$$\left.\begin{aligned}\mathrm{w}_1&=\frac{1}{8}\mathrm{A}^2\varDelta\left(\frac{1}{ns}\right),\\ \mathrm{w}_2&=\frac{1}{16}\mathrm{A}^3\varDelta\left(\frac{1}{ns}\right)^2,\\ \mathrm{w}_3&=\frac{1}{25{\cdot}6}\mathrm{A}^4\varDelta\left(\frac{1}{ns}\right)^3,\\ \mathrm{w}_4&=\frac{1}{36{\cdot}57}\mathrm{A}^5\varDelta\left(\frac{1}{ns}\right)^4.\\ &\ldots\ldots\ldots\end{aligned}\right\} \quad (8)$$

Fig. 2.

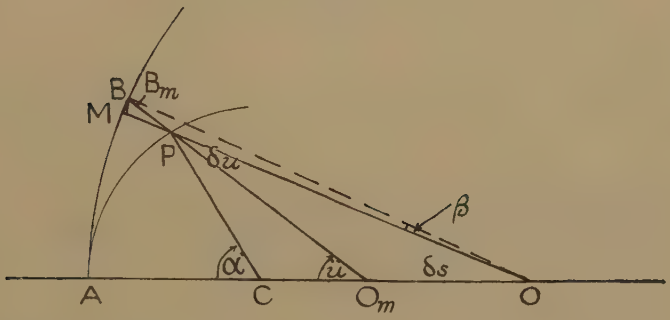

The definition of $\varDelta\left(\frac{1}{ns}\right)^k$ is

$$\varDelta\left(\frac{1}{ns}\right)^k=\left(\frac{1}{n's'}\right)^k-\left(\frac{1}{ns}\right)^k. \quad (9)$$

3. *The Wave-Advancement after Refraction,* W', *measured along the actual Ray-Path and from the Paraxial Sphere, the Incident Wave-Advancement being* W.

In fig. 2, AMB is a section through the incident paraxial sphere of centre O. AP is the refracting interface, and P the point of intersection with this of a ray-path BPO_m, which intersects the paraxial sphere in B.

---

* Whence the Aplanatic Condition for no aberration $ns=n's'$.

This latter is met by OP in M. The element of the incident wave-front associated with the ray-path through P is B_m, and $BB_m=\frac{W}{n}$.

The angular and longitudinal ray-aberrations are δu and δs, as shown. For small angles δu

$$\delta u=\frac{\delta s}{s-t}.\sin u. \quad \ldots \ldots \ldots \quad (10)$$

Let a similar notation with dashes apply to the refracted wave-front projected backwards (in the second medium) to touch the refracting surface at A.

Join BO, drop a perpendicular from B on MO; then

$$B_mP=\frac{t-s(1-\cos\beta)}{\cos\delta u}-\frac{W}{n},$$

where $\beta=\widehat{BOM}$. For small angles δu and β

$$n(B_mP)=nt+\frac{1}{2}\delta u^2.\left(\frac{s-t}{s}\right)nt-W.$$

Substituting the value of δu from (10), this gives

$$n(B_mP)=nt+\frac{1}{2}\left(\frac{\delta s\sin u}{s}\right)^2.\frac{s}{s-t}.nt-W. \quad \ldots \quad (11)$$

Using the formulæ of Section 2, it can be shown that

$$\frac{s}{s-t}.nt=\frac{1}{2}A+\frac{3}{8}A^2\left(\frac{1}{ns}\right)+\frac{5}{16}A^3\left(\frac{1}{ns}\right)^2+\ldots$$

and (11) becomes

$$n(B_mP)=nt-W+\left(\frac{\delta s.\sin u}{s}\right)^2\left\{\frac{1}{4}A+\frac{3}{16}A^2\left(\frac{1}{ns}\right)+\frac{5}{32}A^3\left(\frac{1}{ns}\right)^2+\ldots\right\}, \quad \ldots \quad (12)$$

with a similar expression for the refracted wave-front.

Since B_m, B'_m are on the incident and refracted wave-fronts respectively,

$$n(B_mP)=n'(B'_mP),$$

that is, writing $k=\left(\frac{\delta s.\sin u}{s}\right)^2$,

$$W'-W=w+\frac{1}{4}A.\Delta(k)+\frac{3}{16}A^2.\Delta\left\{k.\frac{1}{ns}\right\}+\ldots \quad \ldots \quad (13)$$

since, by definition, $w=n't'-nt$.

The change in W is thus

$$\delta W=w+S \quad \ldots \ldots \quad (14)$$

where S is the series in (13).

With some approximation, it is seen that

$$\delta u=\frac{\delta s.\sin u}{s}.$$

And again, very nearly,

$$\delta u=\frac{1}{s}\frac{\partial w}{\partial u},$$

the smallness of which is assumed in (7). Thus, with this small,

$$\delta W = w$$

and the correction term S is negligible.

The expression

$$S = \frac{1}{4} A \Delta(k) + \frac{3}{16} A^2 \Delta\left(k . \frac{1}{ns}\right) + \dots \quad . \quad . \quad . \quad . \quad . \quad (15)$$

will tend to converge rapidly, since $k = \left(\frac{\delta s \sin u}{s}\right)^2 \ll 1$. Because of this in a majority of cases either S can be neglected, or the first term of (15) suffices.

The above formulæ depend for their accuracy on the location of P, and the smallness of δu^3, $\delta u^4 \dots$, etc. A ray-trace to four figures is sufficient in many cases for the determination of both the angle α, $k = \left(\frac{\delta s . \sin u}{s}\right)^2$, and k'. When α is small it can be noted that the factor $(2r \sin \frac{1}{2}\alpha)$, which is equal to the chord AP, becomes more nearly equal to the incidence height at the surface, *i. e.*

$$2r \sin \tfrac{1}{2}\alpha \rightarrow s \tan u, \quad . \quad . \quad . \quad . \quad . \quad . \quad . \quad . \quad (16)$$

s and u referring here to the actual ray-path, not the paraxial trace.

4. *The Paraxial Image Surface.*

In the imagery of object points situated off the line of centres of a lens system, the physical event involved at each surface is the refraction of a portion of a spherical, or nearly spherical, wave at a spherical boundary. If, therefore, at any stage, an off-axis object point is joined to the centre of the appropriate refracting surface, the line so formed will constitute an auxiliary axis for the surface, with reference to which the preceding formulæ will apply, providing the two wave-fronts and the refracting sphere are considered to have a common tangent plane at the pole on the latter defined by the point of intersection with it of the auxiliary axis. The "paraxial" image of the off-axis object point is, of course, on the same auxiliary axis; and this point joined to the centre of the next refracting surface serves to define the succeeding auxiliary axis. At each refraction the contours w=constant are circles, whose centres lie on the auxiliary axis. The systems of circular contours corresponding to different refractions have different radial distributions with reference to their centres, which latter are at different distances (both positive and negative) from the axis.

This view of the problem leads to a simple physical interpretation of the curvature of the image surface. For since at each refraction the w-contribution is measured with reference to a sphere whose centre is the "paraxial image" along the auxiliary axis for the surface, then at any stage, given the w-contributions for all parts of the aperture summing to zero, the wave-front will be parallel with the reference sphere and "ideal" imagery will occur at the given "paraxial" image point, Thus, the image surface in the absence of wave-front aberration, *i. e.* the paraxial image surface, is the locus of paraxial images as formed along the auxiliary axes, and this provides a basis for a derivation of the conditions for flatness of field.

Where necessary the previous notation, when relating to that axis coinciding with the line of centres of the system, is given zero as a suffix : s, s' then relate to the auxiliary axis. In fig. 3 ACO is the auxiliary axis joining C and O, an object point off the axis. A perpendicular from O to the Gaussian object plane through O_0 meets this plane in F. $AO=S$, and $FO=\delta s$, where δs is reckoned negative or positive according as O is to the right or left of F. The basis for this convention is that a "change of focus" in the direction from O to F introduces a w-contribution whose sign is negative or positive when O is to the right or left of F. O_0F is equal to η, and a dashed notation applies to the conditions after refraction.

It is seen that

$$s=r+(s_0-r-\delta s)\frac{1}{\cos\beta}$$

$$=s_0\left\{1-\frac{\delta s}{s_0}+\frac{\eta}{s_0}\cdot\frac{1-\cos\beta}{\sin\beta}\right\}.$$

With an obvious approximation,

$$\frac{1}{s}=\frac{1}{s_0}+\frac{\delta s}{s_0^2}-\frac{\eta}{s_0^2}\cdot\frac{1-\cos\beta}{\sin\beta}.$$

Multiplying this equation by n, and using Δ, as above, to denote the difference between quantities after and before refraction,

$$\Delta\left(\frac{n}{s}\right)=\Delta\left(\frac{n}{s_0}\right)+\Delta\left(\frac{n\delta s}{s_0^2}\right)-\Delta\left(\frac{n\eta}{s_0^2}\cdot\frac{1-\cos\beta}{\sin\beta}\right).$$

The law of paraxial imagery between O, O′ and O_0, O_0' gives

$$\Delta\left(\frac{n}{s}\right)=\frac{n'-n}{r}=\Delta\left(\frac{n}{s_0}\right).$$

Thus, multiplication of the former equation by h^2, h being the paraxial intersection height appropriate to the ray-trace along A_0CO_0, gives

$$\Delta(nu^2\delta s)=\frac{1}{2}H^2\Delta\left(\frac{2}{n\eta}\cdot\frac{1-\cos\beta}{\sin\beta}\right), \quad . \quad . \quad . \quad . \quad (17)$$

where

$$n_1u_1\eta_1=n_1'u_1'\eta_1'=n_2u_2\eta_2=\ldots=n_\lambda'u_\lambda'\eta_\lambda'=H, \quad . \quad . \quad (18)$$

the suffixes referring to the refracting surfaces, of which there are λ. u is defined paraxially by $u=\frac{h}{s_0}$. Addition of equations of the type (17) gives

$$n_\lambda'u_\lambda'^2\delta s_\lambda'-n_1u_1^2\delta s_1=\tfrac{1}{2}H^2\sum_{\nu=1}^{\lambda}P_\nu, \quad . \quad . \quad . \quad . \quad . \quad (19)$$

which determines the form of the paraxial image surface as defined above,

In this expression

$$P_\nu = \Delta\left(\frac{2}{n_\nu \eta_\nu} \cdot \frac{1-\cos\beta_\nu}{\sin\beta_\nu}\right),$$

or, writing $\tan\beta = \frac{\eta}{s_0 - r}$,

$$P_\nu = \left\{1 - \left(\frac{1-\cos\beta_\nu}{\sin\beta_\nu}\right)^2\right\} \cdot \Delta\left\{\frac{1}{n(s_0 - r)}\right\}_\nu.$$

This can take a more convenient form. Thus

$$\frac{1}{n(s_0 - r)} = \frac{1}{Qrs},$$

so that

$$\Delta\left\{\frac{1}{n(s_0 - r)}\right\} = \frac{1}{Qr} \cdot \Delta\left(\frac{1}{s}\right).$$

Noting that

$$\frac{1}{s_0} = \frac{1}{r} - \frac{Q}{n}. \quad \frac{1}{s_0'} = \frac{1}{r} - \frac{Q}{n'} \quad \text{or} \quad \Delta\left(\frac{1}{s}\right) = -Q \cdot \Delta\left(\frac{1}{n}\right),$$

the expression becomes

$$P_\nu = -\left\{1 - \left(\frac{1-\cos\beta_\nu}{\sin\beta_\nu}\right)^2\right\} \cdot \frac{1}{r_\nu} \cdot \Delta\left(\frac{1}{n}\right)_\nu. \quad . \quad . \quad . \quad . \quad (20)$$

For small values of β this gives the usual Petzval term

$$P_\nu = -\frac{1}{r_\nu} \cdot \Delta\left(\frac{1}{n}\right)_\nu. \quad . \quad . \quad . \quad . \quad . \quad . \quad . \quad . \quad (21)$$

It will be seen that P is zero when $\beta \to \pi/2$; or, that is, when $Q \to 0$. In this case, as is shown later, a field curvature term due to "wavefront aberration" assumes importance. Together, the two field curvatures sum to give (very nearly) the Petzval term (21). This form is therefore used in calculating the first-order aberrations of systems. The paraxial image surface is to be preferred as an analytical concept in that it is defined in terms of a finite aperture, and relates to the condition for equal phase over the paraxial sphere rather to the limiting values of ray-intersection distances. It is useful in determining the aberrations of a system surface by surface, and in analysing the manner in which these arise.

The form of the paraxial image can be found accurately by obvious "ray-tracing" methods.

The above expressions assume η small compared with s_0, and this is generally true. The case of a field lens is, however, an exception. In this case either η and s_0 are of comparable magnitude, or s_0 is less than η; it may be zero: and an alternative analysis is demanded.

When both η and s_0 are small compared with the radius of the refracting interface, the angle β and the differences

$$\partial s = AO - A_0O_0 = s - s_0,$$
$$\partial s' = s' - s_0'$$

are all small. Differentiation of the equation relating paraxial conjugates gives

$$\frac{n'}{s_0'^2}\,.\,\partial s' - \frac{n}{s_0^2}\,.\,\partial s = 0,$$

which, multiplied by h^2, becomes

$$\Delta(nu^2\,\partial s) = 0. \qquad \qquad (22)$$

From the geometry of fig. 3,

$$\mathrm{S} = \left\{s_0 - \delta s - r(1 - \cos\beta)\right\}\frac{1}{\cos\beta},$$

that is, β being small,

$$-\partial s = \delta s - (s_0 - r)\,\frac{1 - \cos\beta}{\cos\beta},$$

Fig. 3.

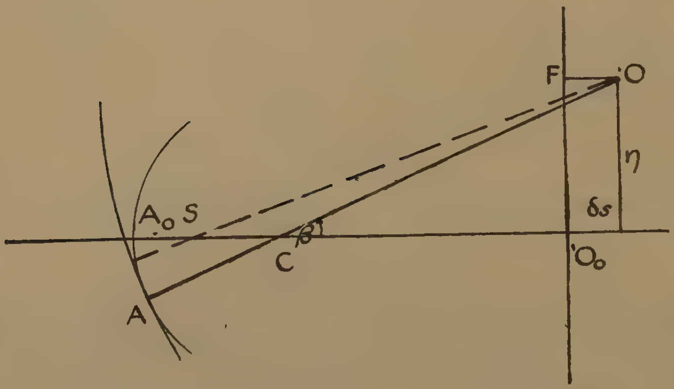

with a similar expression for $\partial s'$. Use of this in (22) gives

$$\Delta(nu^2\,\delta s) = \Delta\left\{nu^2(s_0 - r)\,\frac{1 - \cos\beta}{\cos\beta}\right\}$$

$$= \frac{1}{2}\mathrm{H}^2\Delta\left\{\frac{1}{n(s_0 - r)}\right\},$$

which, by the reduction used above, gives

$$\Delta(nu^2\,\delta\mathrm{S}) = -\frac{1}{2}\mathrm{H}^2\,.\,\frac{1}{r}\,\Delta\left(\frac{1}{n}\right), \qquad \qquad (23)$$

the usual Petzval coefficient. The approximation involved in (23) is adequate for most cases.

These expressions are sufficient to determine, with the stated conditions and accuracy, the form of the paraxial image surface. This is the surface of focus in the absence of wave-front aberration. In this case, the images viewed in the Gaussian plane of focus are not at the best focus, unless the paraxial image surface is also plane. If OS (fig. 3) is the line joining O to S, the axial point of the stop position appropriate to the object space of the given refracting surface, the object O, viewed out of focus in the Gaussian plane, will have a position determined by the point at which this plane is intersected by OS; for this line is the axis of symmetry of the wave-front proceeding to O. Let this point of intersection be at a distance $\eta-\delta\eta$ from the line of centres, where η here refers to the object size as determined by the paraxial magnification law *. Further, write $\bar{\eta}$ for the distance of O from the line of centres; and let $A_0S=x$. The component of distortion due to image curvature is then given by $\delta\eta$, and is reckoned positive when the image is nearer to the line of centres.

By similar triangles, assuming $\delta\eta$ and δs small compared with η and $(s-x)$, it can be seen that

$$\bar{\eta}=\eta\left(1-\frac{\delta\eta}{\eta}\right)\left\{1-\frac{\delta s}{s-x}\right\}$$

with a similar expression for $\bar{\eta}'$. Again, by similar triangles, C, O and O$'$ being collinear,

$$\frac{s-r-\delta s}{\bar{\eta}}=\frac{s'-r-\delta s'}{\bar{\eta}'}$$

or, noting the smallness of $\delta\eta$ and δs,

$$\frac{(s-r)+\left(\frac{x-r}{s-x}\right).\delta s}{\eta\left(1-\frac{\delta\eta}{\eta}\right)}=\frac{(s'-r)+\left(\frac{x'-r}{s'-x}\right)\delta s'}{\eta'\left(1-\frac{\delta\eta'}{\eta'}\right)}.$$

Writing $$Q_x=n\left(\frac{1}{r}-\frac{1}{x}\right)=n'\left(\frac{1}{r}-\frac{1}{x'}\right)$$

and using Q as before, the equation becomes

$$\frac{Qh^2+\frac{Q_x}{Q-Q_x}nu^2\,\delta s}{nu\eta\left(1-\frac{\delta\eta}{\eta}\right)}=\frac{Qh^2+\frac{Q_x}{Q-Q_x}n'u'^2\,\delta s'}{n'u'\eta'\left(1-\frac{\delta\eta'}{\eta'}\right)}.$$

Since $H=nu\eta=n'u'\eta'$, and $\delta\eta$, $\delta\eta'$ are small,

$$\Delta(nu\,\delta\eta)=\frac{-Q_x}{Qh^2(Q-Q_x)}\cdot\tfrac{1}{2}H^3P. \quad . \quad . \quad . \quad . \quad . \quad (24)$$

Summation of difference equations of the type (35) over λ refracting surfaces gives

$$n_\lambda'u_\lambda'\,\delta\eta_\lambda'-n_1u_1\,\delta\eta_1=\tfrac{1}{2}H^3\sum_{\nu=1}^{\lambda}D_\nu, \quad . \quad . \quad . \quad . \quad . \quad (25)$$

which determines the distortion due to image curvature in the final Gaussian plane. In (25)

$$D_\nu=\left\{\frac{1}{Qh^2}+\frac{1}{h^2(Q_x-Q)}\right\}_\nu.P_\nu,$$

---

* This law has been previously assumed. Evidently it suffices to show that $\delta\eta$ is zero for a proof of the law. This is seen later to be so for small field sizes,

or, in the notation to be introduced later,

$$D_\nu = B_\nu . P_\nu . \qquad (26)$$

5. *Longitudinal and Transverse Focal Shifts.*

The wave-front aberrations consist of departures of the wave-fronts from sphericity. They will, therefore, depend on the choice of reference sphere, particularly from the point of view of the location of its centre. A change in radius has the effect of adding (or subtracting) a constant to the W-contributions for all parts of the wave-front considered.

There are two types of focal shift to be considered: one along, and the other perpendicular to, the axis of symmetry of the finally emergent wave-front.

Suppose OX (fig. 4) to be the axis of symmetry of the emergent wave-front; and P (ρ, ϕ) a point on the paraxial reference sphere, centre O.

Fig. 4.

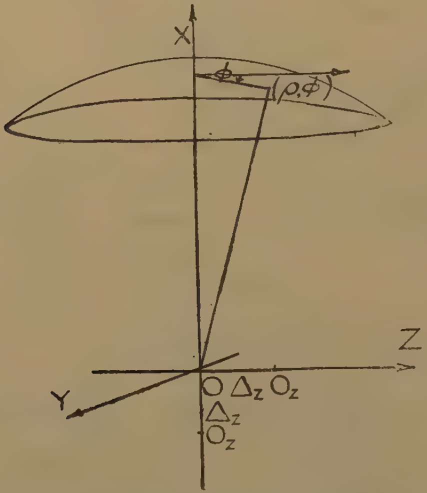

A sphere centre O_x, where $OO_x = \Delta x$, of radius $R + \Delta x$ is the reference sphere for the focus O_x. Δx is reckoned positive away from the approaching wave-front. The line O_xP meets the new sphere in P_x, and, if the medium has refractive index n, a term $n.PP_x$ is added to the W-contribution at P, if this latter is measured with reference to the new sphere, centre O_x.

The equation of the sphere centred on O is

$$X^2 + Y^2 + Z^2 = R^2,$$

where $PO = R$; P is the point (X, Y, Z). The length O_xP is given, Δx being small, by

$$O_xP = R + \frac{X}{R} . \Delta x$$

and, since

$$O_xP_x = R + \Delta x,$$

$$PP_x = \Delta x\left(1 - \frac{X}{R}\right).$$

The X-co-ordinate of P is $X=R\cos\vartheta$, where $\vartheta=\widehat{POX}$. Thus

$$PP_x=\frac{1}{2}\Delta x\left(\frac{\rho}{R}\right)^2\left\{1-\frac{1}{12}\left(\frac{\rho}{R}\right)^2+\dots\right\},$$

and the first term of the W-contribution to be added to W_λ' is

$$\delta W_{\text{long.}}=\frac{1}{2}n\,\Delta x\,.\left(\frac{h}{R}\right)^2.\left(\frac{\rho}{h}\right)^2 \quad . \quad . \quad . \quad . \quad . \quad . \quad (28)$$

in which the variable $\left(\frac{\rho}{h}\right)$ is introduced. $\delta W_{\text{long.}}$ has the same sign as Δx.

If the centre of the reference sphere is taken at O_z, where $OO_z=\Delta z$ is positive in the direction of positive z (*i. e.* away from the line of centres), a similar reasoning gives

$$\delta W_{\text{trans.}}=n\,\Delta z\,.\left(\frac{h}{R}\right):\left(\frac{\rho}{h}\right)\cos\phi. \quad . \quad . \quad . \quad . \quad . \quad (29)$$

Fig. 5.

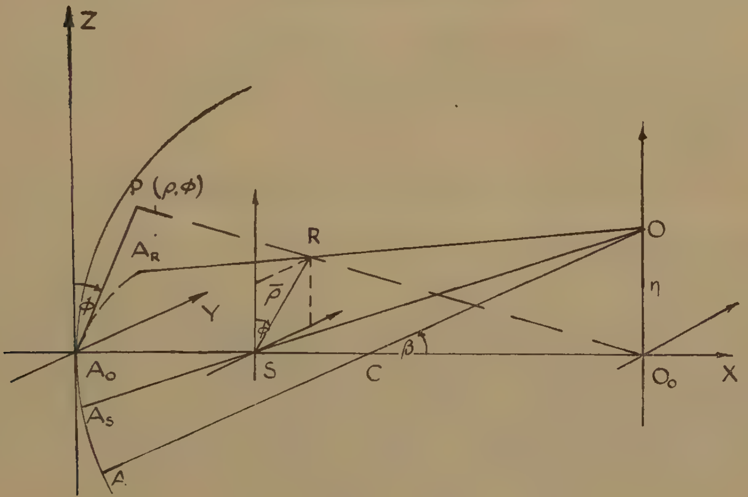

The formulæ (28) and (29) thus treat focal shifts as introducing wave-front aberrations; and by their help the W-contributions for the emergent wave-fronts can be related to foci lying on any given surface. Their use is apparent in later treatment of the wave-front aberrations.

6. *First-Order Wave-Front Aberrations.*

From the standpoint adopted here the problem is again looked upon as that of the refraction of spherical wave-fronts at spherical interfaces, the relating of which refractions to the auxiliary axes yields a simple "spherical aberration." It is assumed, both at each refraction and in the addition of aberration contributions throughout the system, that the paths of the elements of wave-front traversing the system are unaffected by the presence of aberration.

The co-ordinate axes XYZ (fig. 5), whose origin is at the pole of the refracting surface A_0, are determined by the line of centres, A_0X, and the plane XA_0Z containing the object point for the surface, O. The centre of the refracting surface is C: its radius $A_0C=r$. S, O_0 have the meanings given previously. The auxiliary axis is CO; and SO is the incident principal ray. RO is a ray proceeding to the object point, O, through R, a point having co-ordinates $(\bar{\rho}, \phi)$ in the plane of the pupil appropriate to the object space of the surface considered.

The first-order aberration contributions, δW_1, consequent on refraction at the νth surface are, for the elements of the wave-front travelling along SO and RO,

$$(\delta W_1)_S=\tfrac{1}{8}Q_\nu^2(2r \,.\, \sin \tfrac{1}{2}\alpha_S)_\nu^4 \,.\, \varDelta\left(\frac{1}{ns}\right)_\nu$$

and

$$(\delta W_1)_R=\tfrac{1}{8}Q_\nu^2(2r \,.\, \sin \tfrac{1}{2}\alpha_R)_\nu^4 \,.\, \varDelta\left(\frac{1}{ns}\right)_\nu,$$

where s and Q relate to the paraxial imagery of O along the auxiliary axis; and α_S, α_R are the angles $\widehat{A_SCA}$, $\widehat{A_RCA}$. With that for the element of wave-front travelling along SO regarded as zero, the first-order W-contribution at the νth surface for the element travelling along RO is given by

$$(\delta W_S)_\nu=\tfrac{1}{8}Q_\nu^2\{(2r \,.\, \sin \tfrac{1}{2}\alpha_R)_\nu^4-(2r \,.\, \sin \tfrac{1}{2}\alpha_S)_\nu^4\} \,.\, \varDelta\left(\frac{1}{ns}\right)_\nu, \qquad . \quad (30)$$

where δW_S is measured with reference to a sphere centred on O′, the paraxial image of O along the auxiliary axis. In using this expression the wave-front aberrations are thus related to spheres centred on the paraxial image surface. The suffix S is used because the development of (30) leads directly to aberration coefficients and aberration types analogous to the "ray-aberrations" of the Seidel first-order theory.

It will be seen that s and s_0 are of comparable magnitude, providing η is small in comparison with s_0. On the other hand,

$$\frac{s-r}{s_0-r}=\frac{1}{\cos\beta},$$

so that, to a first approximation,

$$Q^2 \,.\, \varDelta\left(\frac{1}{ns}\right)=\frac{1}{\cos^2\beta} \,.\, Q_0^2 \,.\, \varDelta\left(\frac{1}{ns_0}\right).$$

Omitting the zero suffix, (30) becomes, introducing a paraxial incidence height h,

$$(\delta W_s)_\nu=\tfrac{1}{8}A_\nu \,.\, \frac{1}{h_\nu^4\cos^2\beta_\nu}\{(AA_R)_\nu^4-(AA_S)_\nu^4\}. \qquad . \quad . \quad . \quad (31)$$

A_R, A_S being the points shown in fig. 5, and

$$A_\nu=Q_\nu^2 h_\nu^4 \,.\, \varDelta\left(\frac{1}{ns}\right). \qquad . \quad . \quad . \quad . \quad . \quad . \quad . \quad . \quad (32)$$

Let A_R have co-ordinates (X_R, Y_R, Z_R). Then those of A being

$$\{r(1-\cos\beta),\quad 0,\quad -r\sin\beta\},$$

it follows that

$$AA_R^2 = 2r^2(1-\cos\beta) + 2rX_R . \cos\beta + 2rZ_R . \sin\beta. \quad . \quad . \quad (33)$$

The co-ordinates X_R, Z_R are determined, for A_R lies on both the sphere $X^2-2rX+Y^2+Z^2=0$, and the straight line OR, *i. e.* on the line

$$\frac{X-s}{s-x} = \frac{Y}{-\bar{\rho}\sin\phi} = \frac{Z-\eta}{\eta-\bar{\rho}\cos\phi},$$

the co-ordinates of O and R being respectively (s, o, η), $(x, \bar{\rho}\sin\phi, \rho\cos\phi)$.

Elimination of Y and Z gives

$$\left\{1+\left(\frac{\rho}{s}\right)^2+\left(\frac{\eta}{s-x}\right)^2-\frac{2\eta\rho\cos\phi}{s(s-x)}\right\}X_R^2-2r\left\{1+\frac{\rho^2}{rs}+\frac{x\eta^2}{r(s-x)^2}\right.$$

$$\left.-\frac{\eta\rho\cos\phi}{r(s-x)}-\frac{x\eta\rho\cos\phi}{rs(s-x)}\right\}X_R+\left\{\rho^2+\left(\frac{x\eta}{s-x}\right)^2-\frac{2x\eta\rho\cos\phi}{(s-x)}\right\}=0,$$

use being made of the relation

$$\frac{\rho}{s} = \frac{\bar{\rho}}{s-x},$$

which follows from the similarity of the triangles PA_0O_0, RSO_0. P is the point of intersection of O_0R with the plane YA_0Z, in which it has co-ordinates (ρ, ϕ).

Solution of this equation for X_R gives, neglecting higher powers of small quantities,

$$2rX_R = \frac{H^2h^2}{h^4(Q_x-Q)^2} + 2\frac{Hh}{h^2(Q_x-Q)} . \rho\cos\phi + \rho^2, \quad . \quad . \quad . \quad (34)$$

H, Q, and Q_x being defined as before. Solution of the $X-Z$ equation relating to the line OR, with the same degree of approximation gives

$$2rZ_R . \sin\beta = \cos\beta\left\{2\frac{H^2h^2}{h^2(Q_x-Q) . Qh^2} + 2\frac{Hh}{Qh^2} . \rho\cos\phi\right\}. \quad . \quad (35)$$

Substitution of (34) and (35) in (33) yields

$$\frac{1}{\cos\beta} . AA_R^2 = H^2(B^2-C^2)h^2 + 2HBh . \rho\cos\phi + \rho^2, \quad . \quad . \quad (36)$$

where, replacing r by $\dfrac{H\cot\beta}{Qh}$,

$$C = \frac{1}{Qh^2}\left(\frac{1-\cos\beta}{\sin\beta}\right) \quad . \quad . \quad . \quad . \quad . \quad . \quad . \quad . \quad (37)$$

and

$$B = \frac{1}{Qh^2} + \frac{1}{h^2(Q_x-Q)}. \quad . \quad . \quad . \quad . \quad . \quad . \quad . \quad (38)$$

In (36), putting $\rho=0$

$$\frac{1}{\cos\beta} . AA_S^2 = H^2(B^2-C^2)h^2. \quad . \quad . \quad . \quad . \quad . \quad . \quad . \quad (39)$$

Thus

$$\frac{1}{h^4\cos^2\beta}\{(AA_R)^4-(AA_S)^4\}=4(HB)^2.\left(\frac{\rho}{h}\right)^2\cos^2\phi+\left(\frac{\rho}{h}\right)^4$$
$$+4H^3(B^2-C^2)B.\left(\frac{\rho}{h}\right)\cos\phi+2H^2(B^2-C^2).\left(\frac{\rho}{h}\right)^2$$
$$+4HB.\left(\frac{\rho}{h}\right)^3\cos\phi,$$

and (31) becomes

$$(\delta W_s)=\tfrac{1}{8}A.\left(\frac{\rho}{h}\right)^4+\tfrac{1}{2}H.AB.\left(\frac{\rho}{h}\right)^3\cos\phi+\tfrac{1}{4}H^2.AB^2.\left(\frac{\rho}{h}\right)^2[3\cos^2\phi+\sin^2\phi]$$
$$+\tfrac{1}{2}H^3.AB^3.\left(\frac{\rho}{h}\right)\cos\phi-\tfrac{1}{4}H^2.AC^2.\left(\frac{\rho}{h}\right)^2-\tfrac{1}{2}H^3.AC^2.B.\left(\frac{\rho}{h}\right)\cos\phi.$$

To the order of approximation contemplated, $\left(\frac{\rho}{h}\right)$ is constant throughout the system : h conveniently refers to the full aperture, and then $\left(\frac{\rho}{h}\right)$ denotes the zone whose radius is this fraction of the full aperture. The aberration of the finally emergent wave-front is, after λ refractions,

$$(W_s)_\lambda'=S_I.\left(\frac{\rho}{h}\right)^4+S_{II}.\left(\frac{\rho}{h}\right)^3.\cos\phi+S_{III}.\left(\frac{\rho}{h}\right)^2\{3\cos^2\phi+\sin^2\phi\}$$
$$+S_{IV}.\left(\frac{\rho}{h}\right)\cos\phi-S_V.\left(\frac{\rho}{h}\right)^2-S_{VI}.\left(\frac{\rho}{h}\right)\cos\phi, \qquad (40)$$

where

$$\left.\begin{aligned}S_I&=\tfrac{1}{8}\sum_{\nu=1}^{\lambda}A_\nu,\\ S_{II}&=\tfrac{1}{2}H\sum_{\nu=1}^{\lambda}A_\nu B_\nu,\\ S_{III}&=\tfrac{1}{4}H^2\sum_{\nu=1}^{\lambda}A_\nu B_\nu^2,\\ S_{IV}&=\tfrac{1}{2}H^3\sum_{\nu=1}^{\lambda}A_\nu B_\nu^3,\end{aligned}\right\} \qquad (41)$$

and

$$\left.\begin{aligned}S_V&=\tfrac{1}{4}H^2.\sum_{\nu=1}^{\lambda}\left(\frac{1-\cos\beta}{\sin\beta}\right)_\nu^2.\Delta\left(\frac{1}{ns}\right)_\nu,\\ S_{VI}&=\tfrac{1}{2}H^3.\sum_{\nu=1}^{\lambda}\left(\frac{1-\cos\beta}{\sin\beta}\right)_\nu^2.B_\nu.\Delta\left(\frac{1}{ns}\right)_\nu,\end{aligned}\right\} \qquad (42)$$

the first four corresponding with the Seidel sums *. For larger values of Q, S_V and S_{VI} are small ; but as Q approaches zero they assume significance, S_V introducing a field curvature, and S_{VI} a distortion. The combined field curvature coefficient is

$$\overline{P}_\nu=-\left\{1-\left(\frac{1-\cos\beta}{\sin\beta}\right)_\nu^2\right\}.\frac{1}{r_\nu}\Delta\left(\frac{1}{n}\right)_\nu-\left(\frac{1-\cos\beta}{\sin\beta}\right)^2.\Delta\left(\frac{1}{ns}\right)_\nu. \qquad (43)$$

---

[*] See Whittaker, "Theory of Optical Instruments," Camb. Math. Tracts, vii. p. 44.

and the combined distortion

$$\overline{D}_\nu = B_\nu . \overline{P}_\nu .$$

It will be seen that, for all values of β, $\overline{P}$ is nearly equal to $-\frac{1}{r}\Delta\left(\frac{1}{n}\right)$, the usual Petzval sum.

In (40) ρ and h can be related to the exit pupil of the system ; and, to the required first-order of accuracy, $\frac{\rho}{h}$ can equally express the fractional aperture in planes at right angles to the finally emergent principal rays. This is of use in considering the effects of longitudinal and transverse focal shifts.

Fig. 6 (*a*).

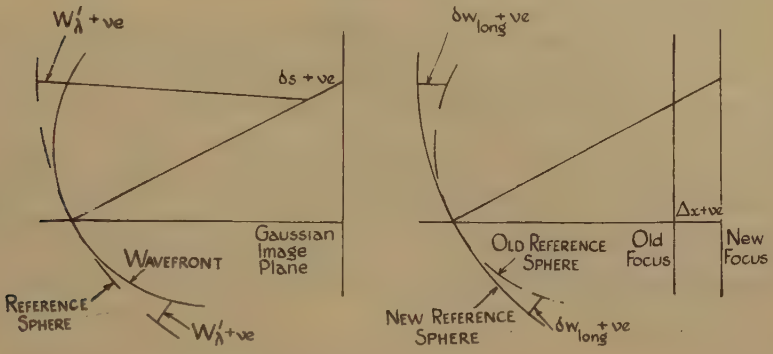

W'_λ +ve
δs +ve
Gaussian Image Plane
Wavefront
Reference Sphere
W'_λ+ve
δw_{long} +ve
Old Reference Sphere
Old Focus
Δx+ve
New Focus
New Reference Sphere
δw_{long} +ve

Forms of wave-front :—
Positive spher. aberr.
,, astigmatism.
,, field curvature.

Positive longitudinal focal shift.

Fig. 6 (*b*).

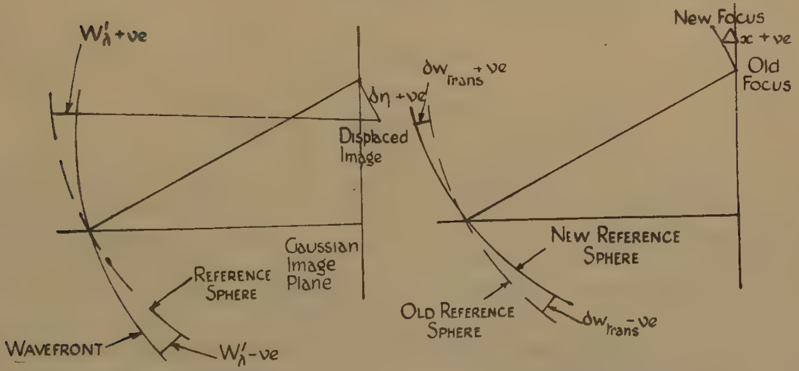

W'_λ+ve
$\delta\eta$ +ve
Displaced Image
Gaussian Image Plane
Reference Sphere
Wavefront
W'_λ-ve
New Focus
Δx +ve
Old Focus
δw_{trans} +ve
New Reference Sphere
Old Reference Sphere
δw_{trans} -ve

Forms of wave-front :—
Positive coma.
,, distortion.

Positive transverse focal shift.

The sums S_I, S_{II} are associated with the aberrations, spherical aberration and coma. The former is symmetrical about the principal ray :

it is proportional to the fourth power of the aperture, and independent of the size of field. Thus small amounts of spherical aberration can be compensated by a small longitudinal change of focus. The form of wave-front is shown in fig. 6 (*a*).

If S_{II} is positive, and the others zero, the form of wave-front in the meridian section is as shown in fig. 6 (*b*), giving inward coma. The W_λ' due to the coma term is proportional to the aperture cubed and to the size of field. Small amounts can be compensated by a small transverse change of focus, and thus amount to a distortion. Coma is regarded as positive (inward) when W_λ' is positive on the side of the principal ray removed from the line of centres.

It will be noted that the compensation of small amounts of positive spherical aberration and coma requires small negative focal shifts. This is the reason for the sign convention adopted, which is illustrated in fig. 6.

Since the S_{III} and S_V terms are proportional to the square of the aperture, a suitable longitudinal change of focus can make the W_λ' term associated with them zero in a chosen meridian. For the sagittal and tangential sections, *i. e.* $\phi=\frac{\pi}{2}$ and $\phi=0$ respectively, the focal shifts required are found by (43) to be

$$(\Delta x)_S=-\tfrac{1}{2}\eta_\lambda'^2 . n_\lambda' . \sum_{\nu=1}^{\lambda} A_\nu . B_\nu^2,$$

$$(\Delta x)_T=-\frac{3}{2} . \eta_\lambda'^2 . n_\lambda' \sum_{\nu=1}^{\lambda} A_\nu . B_\nu^2,$$

which, related to the Gaussian plane, become

$$\left.\begin{aligned}(\delta s)_S&=\tfrac{1}{2}\eta_\lambda'^2 . n_\lambda' . \left\{\sum_{\nu=1}^{\lambda}\bar{P}_\nu+\sum_{\nu=1}^{\lambda}A_\nu B_\nu^2\right\},\\(\delta s)_T&=\tfrac{1}{2}\eta_\lambda'^2 . n_\lambda' . \left\{\sum_{\nu=1}^{\lambda}\bar{P}_\nu+3\sum_{\nu=1}^{\lambda}A_\nu B_\nu^2\right\}\end{aligned}\right\}, \quad . \quad . \quad . \quad (44)$$

where the aberration intersection distance $(\delta s)_S$ has the opposite sign to the focal shift $(\Delta_x)_S$. These give the form of the surfaces containing the sagittal and tangential focal lines *. To a first approximation these surfaces are spherical. In the absence of astigmatism $\left(\sum_{\nu=1}^{\lambda} A_\nu B_\nu^2=0\right)$ and, given the other wave-front aberrations zero, the image surface is also spherical to a first approximation. Its curvature is

$$\sigma_P=n_\lambda' . \sum_{\nu=1}^{\lambda}\bar{P}_\nu .$$

---

[*] Since $\frac{d}{d\phi}\begin{pmatrix}\cos^2\phi\\ \sin^2\phi\end{pmatrix}=0$ when $\phi=\begin{pmatrix}0\\ \pi/2\end{pmatrix}$ there will be good areas of the wave-front close to the spherical form, whose centres are at the tangential and sagittal foci. The existence of focal lines corresponding to these directions, and to no other value of ϕ, would seem to depend upon this fact.

The first-order sagittal and tangential focal surfaces are symmetrically placed about the Gaussian image plane when

$$\sum_{\nu=1}^{\lambda} A_\nu B_\nu^2 = -\tfrac{1}{2} \sum_{\nu=1}^{\lambda} \bar{P}_\nu . \quad . \quad . \quad . \quad . \quad . \quad . \quad . \quad (45)$$

The terms S_{IV} and S_{VI} can be compensated by a transverse focal shift of opposite sign. If S_{IV} is positive, a displacement of the image towards the line of centres (inward) occurs, whose amount, using (29), is seen to be

$$\delta\eta_\lambda' = \tfrac{1}{2} H^2 \eta_\lambda' . \sum_{\nu=1}^{\lambda} A_\nu B_\nu^3 .$$

Combining this with (25) the total distortion is, assuming $\delta\eta_1 = 0$,

$$\delta\eta_\lambda' = \tfrac{1}{2} H^2 \eta_\lambda' . \left\{ \sum_{\nu=1}^{\lambda} \bar{P}_\nu . B_\nu + \sum_{\nu=1}^{\lambda} A_\nu . B_\nu^3 \right\} . \quad . \quad . \quad . \quad . \quad (46)$$

With the sign convention used above, distortion is reckoned positive when the image is smaller than that given by the paraxial magnification law.

The calculation of the first-order coefficients is effected by tracing a paraxial ray for an axial object point, using the " Abbe Invariant " form of the paraxial law : viz.,

$$n\left(\frac{1}{r} - \frac{1}{s}\right) = Q = n'\left(\frac{1}{r} - \frac{1}{s'}\right),$$

from which A_ν is readily obtained for each surface.

The values of B_ν can be found by the trace

$$n\left(\frac{1}{r} - \frac{1}{x}\right) = Q_x = n'\left(\frac{1}{r} - \frac{1}{x'}\right),$$

or alternatively, it can be shown that

$$B_\nu = \frac{1}{Q_\nu h_\nu^2} + C_\nu . \quad . \quad . \quad . \quad . \quad . \quad . \quad . \quad . \quad . \quad (47)$$

where

$$C_\nu = \sum_{p=\gamma+1}^{\nu} \frac{d_p}{n_p h_p h_{p-1}} .$$

Use of (47) then gives B_ν from the one paraxial trace. d_p is the axial separation between the $(p-1)$th and pth refracting surfaces : γ can be regarded as a surface of infinite radius, and across which $\Delta(n) = 0$. It is the plane containing the limiting aperture stop. This is the surface at which the principal ray crosses the axis, and $C\gamma$ is zero. In fact, C_ν is a measure (in both magnitude and sign) of the distance from the axis at which a principal ray meets the νth surface. This is shown in what follows.

From the definition of B_ν (38), the quantity C_ν in (47) is

$$C_\nu = \frac{1}{h_\nu^2 (Q_x - Q)_\nu} .$$

Let a principal ray meet the plane YA_0Z at the point $(0, 0, Z)$, then by similar triangles

$$\frac{\eta_p}{Z_p}=\frac{x_p-S_p}{x_p},$$

which can be written

$$C_p=\frac{1}{h_p^2(Q_x-Q)_p}=\frac{1}{H}\cdot\frac{Z_p}{h_p}. \qquad (48)$$

This indicates the dependence of Z_p on C_p.

By similar triangles it can be seen that

$$\frac{Z_p}{Z_{p-1}}=1-\frac{d_p}{x'_{p-1}},$$

$$\frac{h_p}{h_{p-1}}=1-\frac{d_p}{S'_{p-1}},$$

subtracting which gives

$$\frac{Z_p}{Z_{p-1}}-\frac{h_p}{h_{p-1}}=\frac{d_p}{n_p}(Q_x-Q)_{p-1}.$$

Multiplication by $\frac{Z_{p-1}}{h_p}$, and using (48)

$$\frac{Z_p}{h_p}-\frac{Z_{p-1}}{h_{p-1}}=\frac{d_p}{n_p h_p}\cdot Z_{p-1}(Q_x-Q)_{p-1}$$

$$=H.\frac{d_p}{n_p h_p h_{p-1}}.$$

Thus

$$C_p-C_{p-1}=\frac{d_p}{n_p h_p h_{p-1}},$$

and summation of such differences gives

$$C_\nu=\sum_{p=\gamma+1}^{\nu}\frac{d_p}{n_p h_p h_{p-1}}. \qquad (49)$$

where γ is the surface at which $Z_\gamma=0$.

7. *Accurate Calculation of Wave-Front Aberration in the Meridian Section.*

The calculation of the wave-front aberration by means of the formulæ of Sections 2 and 3 requires a knowledge of the values at each surface of the angle α, k and k'. What was in these Sections the common axis of symmetry of the incident paraxial sphere and the refracting surface is now, of course, the auxiliary axis appropriate to the surface considered.

The aberrations occurring at a given surface along a number of ray paths having been found, they are related to the principal ray by subtracting from each the wave-front aberration at the surface for the element of wave-front travelling along this ray. In the presence of large amounts of angular aberration the outer parts of the wave-front close up or open out. A transference formula giving $W_{\nu+1}$ from W_ν' is then required.

In fig. 7, $A_\nu B_\nu'$ and $A_{\nu+1}B_{\nu+1}$ are the emergent and incident paraxial spheres at the νth and $(\nu+1)$th refracting surfaces respectively. O_ν' $(\equiv O_{\nu+1})$ is the νth image [*i. e.* $(\nu+1)$th object] point on the paraxial image surface. The distance between the two paraxial spheres is

$$A_\nu X = A_\nu O_\nu' - A_{\nu+1} O_\nu'$$
$$= s_\nu' - s_{\nu+1}. \qquad \qquad (50)$$

Fig. 7.

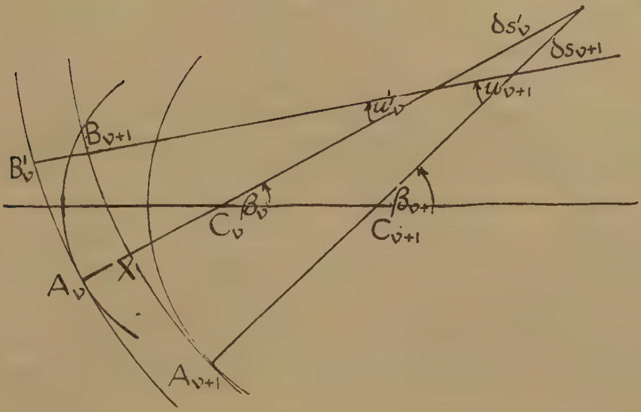

Fig. 8.

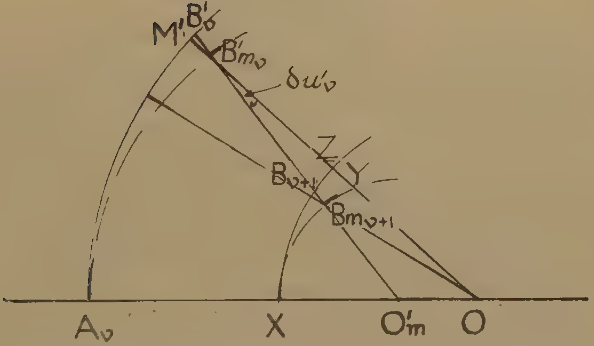

The state of affairs is represented in fig. 8. It is seen that

$$(B'B_m')_\nu = \frac{W_\nu'}{n_\nu'},$$

$$(BB_m)_{\nu+1} = \frac{W_{\nu+1}}{n_{\nu+1}}.$$

The normal to the paraxial sphere after the νth refraction is $M'Bm'YO$; it meets the wave-front incident at the $(\nu+1)$th surface in Y. The element of wave-front Bm' travels along the actual ray-path $B_\nu'O_m'$ to $B_{\nu+1}$. The two paraxial spheres and the two wave-fronts are respectively parallel surfaces. Thus

$$B_{m'_\nu} B_{m_{\nu+1}} = A_\nu X = M'Z,$$

that is,
$$\left(A_\nu X - \frac{W_{\nu+1}}{n_{\nu+1}}\right).\cos\delta u_\nu' = A_\nu X - \frac{W_\nu'}{n_\nu'}\cos\delta u_\nu',$$

where $\delta u_\nu'$ is the angular aberration. Assuming $\delta u_\nu'$ small, this reduces to
$$W_{\nu+1} = W_\nu' - \tfrac{1}{2}n_\nu'.AX.\delta u_\nu'^2,$$

or
$$W_{\nu+1} = W_\nu' - \tfrac{1}{2}n_\nu'(s_\nu' - s_{\nu+1}).k_\nu'^2. \quad . \quad . \quad . \quad . \quad . \quad (51)$$

In this $A_\nu X$ has been written from (50), and a small approximation made in putting $\delta u_\nu' = k_\nu'$. A significant conclusion from (51) is that in the presence of larger amounts of aberration the diffraction patterns associated with a wave-front proceeding to a focus are not uniquely determined by the angular aperture and the angular distribution of wave-front aberration, since this latter changes as the wave-front progresses to the region of focus: they are additionally dependent upon the radius of the reference sphere. In the absence of wave-front aberration it is, of course, true.

The correction terms that have been dealt with will apply only to systems of considerable aperture. When they do apply, it is necessary to have an analytical conception, and measure, of the manner in which, and the extent to which, they operate, in order that they may be more easily controlled or employed.

8. *Final Aberrations.*

The wave-front aberrations are related in the above formulæ to spheres centred on the final paraxial image surface. This is generally not plane, and "the final" wave-front aberrations may be of finite amount. In a given lens system it is usually a simple matter to change the coefficients of the first-order wave-front aberrations by pre-determined small amounts, introducing thereby but negligible amounts of wave-front aberration of higher order. Particularly in systems such as photographic objectives is it necessary to employ such small first-order aberrations (of opposite sign) to minimize the effects of higher order aberration. Further, the fact that the image is generally viewed with reference to a plane makes it necessary to investigate the effects of longitudinal focal shift; and finally, the distance of an image point from the axis needs to be considered by studying the effects of transverse focal shifts. These factors are frequently studied empirically in the experimental model of a new design by varying the air separations and such like. It is a simple matter to investigate them before this stage by means of the methods and formulæ which have been elaborated above. It is convenient to use for this purpose two simple diagrams which are described below.

In fig. 9 the paraxial sphere, the actual wave-front and the point O′ on the paraxial image surface are shown, all of which relate to the conditions after refraction at λ surfaces. Values of W_λ' are known for a number of ray-paths corresponding with points such as P, which are at distances, ρ, from the central axis QO of the wave-front. QO is not necessarily a ray-path: it is simply the central radius of the paraxial sphere. If ρ has a maximum value h, W_λ' is plotted graphically as ordinate in two ways (fig. 10). The first has $\left(\frac{\rho}{h}\right)^2$, and the second $\left(\frac{\rho}{h}\right)$ as abscissæ. In the first case points are plotted to the right and left of

Fig. 9.

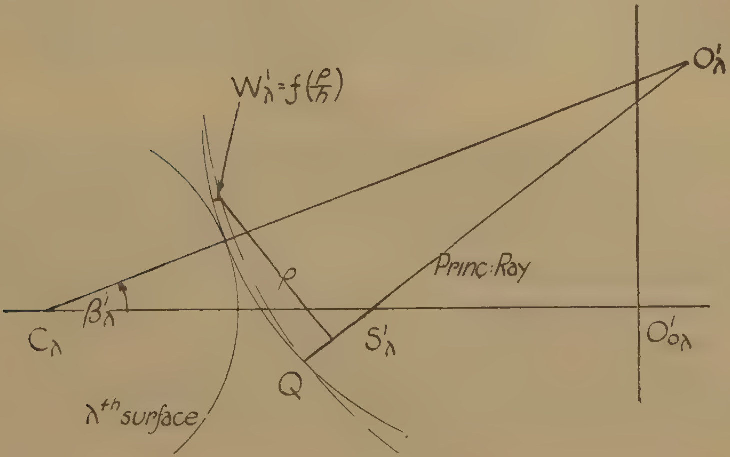
$W'_\lambda = f\left(\frac{\rho}{h}\right)$
O'_λ
ρ
Princ: Ray
β'_λ
C_λ
S'_λ
$O'_{o\lambda}$
Q
λ^{th} surface

Fig. 10.

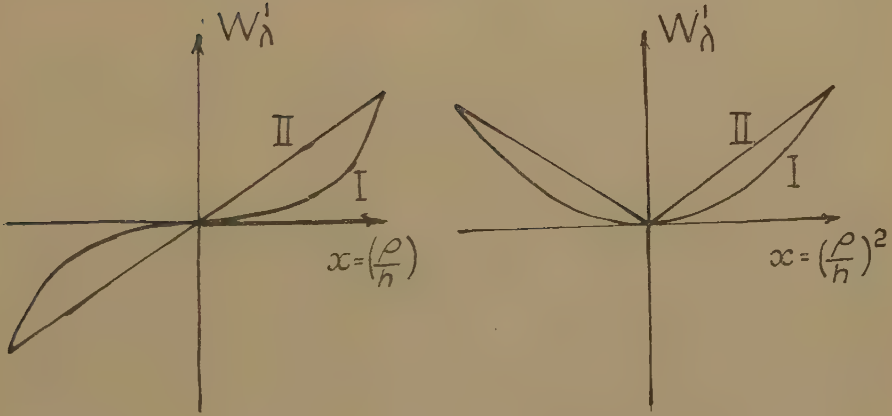

I—Spher. aberr. $\alpha \left(\frac{\rho}{h}\right)^4$.

II—Long. focal shift $\alpha \left(\frac{\rho}{h}\right)^2$.

I—Cóma $\alpha \left(\frac{\rho}{h}\right)^3$.

II—Trans. focal shift $\alpha \left(\frac{\rho}{h}\right)$.

$\left(\frac{\rho}{h}\right)^2 = 0$, according as they are above or below the axis QO, *i. e.* according to the sign of $\left(\frac{\rho}{h}\right)$ not $\left(\frac{\rho}{h}\right)^2$.

The effects of first-order spherical aberration are then studied by means of the family of parabolæ

$$y=\text{const.}\times x^2, \quad \ldots\ldots\ldots \quad (52)$$

suitable members of which can be drawn on transparent tracing-paper. The closest parabola can be interpolated, and the required change in ΣA (of opposite sign) is readily found. The vertical difference between the two curves is now plotted on the same scale, and the effects of change of focus, or of the terms ΣAB^2, ΣP, studied by noting the differences in ordinates between the new curve and the two straight lines,

$$y=\text{const.}\times x. \quad \ldots\ldots\ldots \quad (53)$$

These differences give the wave-front aberrations related to the new focus. It will be appreciated that neither the parabolæ nor the straight lines need necessarily pass through the origin, since a constant added to (or subtracted from) W_λ' is immaterial. The constants in (52) and (53) are known from (40) and (28). In this case the effects in the sagittal section must be also noted.

In the second diagram the family of cubics

$$y=\text{const.}\times x^3 \quad \ldots\ldots\ldots \quad (54)$$

and the straight line

$$y=\text{const.}\times x \quad \ldots\ldots\ldots \quad (55)$$

are used in a similar manner. The constants in (54) and (55) are found from (40)—first-order coma—and (29). The changes (55) amount to a distortion, or transverse focal shift.

These diagrams can be used with advantage in determining what amounts of (primary or secondary) chromatic aberration—of both focus and magnification—are required to minimize the effects of the chromatic variations of the monochromatic aberrations. Their general use, however, raises the question of the relationship between the departures of the wave-front from the spherical and the corresponding distributions of light in the image. For the nature of this relationship determines the criteria to be applied in deciding what distribution of remaining W_λ' will give the least impairment of the light distribution. Providing the residual W_λ' is a small fraction of a wave-length the difficulty is of no practical consequence: when larger, it is necessary to rely in the main on certain considerations of a "commonsense" nature—that is, until a more precise tool is available.

LXVII. *An Application of the Method of Finite Difference Equations to a Problem of Bending Moments.—Continuous Beam of N equal Spans under Transverse Loading and an Axial Force.*

By N. J. DURANT *.

[Received January 22, 1945.]

Summary.

In a previous paper I have shown that the moment at any support of a continuous beam could be obtained explicitly from a formula which is the solution of a Finite Difference Equation.

An application of the formula would show a great saving in time over orthodox methods.

In the present paper the problem has been generalized so that the effects of clamping the ends of the beam and applying an axial force of either sign could be considered.

This is a case in which the Principle of Superposition is not applicable.

(1) THE most general formula † for the moments at the supports of a continuous beam of N equal spans with an axial force and a uniform transverse loading is

$$f(\alpha)\mathrm{M}_{n-1}+4\phi(\alpha)\mathrm{M}_n+f(\alpha)\mathrm{M}_{n+1}=-\psi(\alpha)\tfrac{1}{2}wl^2, \quad (n=1, 2, \ldots \mathrm{N}-1), \qquad (1)$$

where N is any positive integer, and in which, for compression,

$$f(\alpha)=\frac{3}{2}\cdot\frac{2\alpha\operatorname{cosec}2\alpha-1}{\alpha^2}, \quad \ldots\ldots \quad \text{(i)}$$

$$\phi(\alpha)=\frac{3}{4}\cdot\frac{1-2\alpha\cot 2\alpha}{\alpha^2}, \quad \ldots\ldots \quad \text{(ii)}$$

$$\psi(\alpha)=3\cdot\frac{\tan\alpha-\alpha}{\alpha^3}, \quad \ldots\ldots \quad \text{(iii)}$$

and for tension,

$$\mathrm{F}(\alpha)=\frac{3}{2}\cdot\frac{1-2\alpha\operatorname{cosech}2\alpha}{\alpha^2}, \quad \ldots\ldots \quad \text{(iv)}$$

$$\phi(\alpha)=\frac{3}{4}\cdot\frac{2\alpha\coth 2\alpha-1}{\alpha^2}, \quad \ldots\ldots \quad \text{(v)}$$

$$\psi(\alpha)=3\cdot\frac{\alpha-\tanh\alpha}{\alpha^3}, \quad \ldots\ldots \quad \text{(vi)}$$

---

* Communicated by the Author.

† The derivation of equation (1), together with the tabular values of the Berry functions, are given in 'Aeroplane Structures,' by A. J. S. Pippard an J. L. Pritchard. Longmans, Green and Co.

where $\alpha = \frac{1}{2}l\sqrt{\frac{|P|}{\beta}}$, P the applied axial force, and β the flexural rigidity of the beam about an axis through the centroid and perpendicular to the plane of flexure.

If P=0 each of the functions (i) to (vi), known as Berry functions, becomes unity (this being the limiting value of each function as $\alpha \rightarrow 0$).

Equation (1) can be written

$$M_{n-1} + 4\frac{\phi(\alpha)}{f(\alpha)}M_n + M_{n+1} = -\frac{1}{2}\frac{\psi(\alpha)}{f(\alpha)}wl^2. \quad (n=1, 2, \ldots N-1). \quad (1\,a)$$

If we substitute

$$U_n = M_n + \frac{3\psi(\alpha)}{f(\alpha)+2\phi(\alpha)} \cdot \frac{wl^2}{12}. \quad (n=0, 1, 2, \ldots N), \quad . \quad . \quad . \quad (2)$$

which for brevity may be written

$$U_n = M_n + f(w). \quad (n=0, 1, 2, \ldots N), \quad . \quad . \quad . \quad . \quad (2\,a)$$

where

$$f(w) = \frac{3\psi(\alpha)}{f(\alpha)+2\phi(\alpha)} \cdot \frac{wl^2}{12}. \quad . \quad . \quad . \quad . \quad . \quad . \quad . \quad . \quad . \quad . \quad (\text{vii})$$

Then equation (1 *a*) becomes

$$U_{n-1} + 4\frac{\phi(\alpha)}{f(\alpha)}U_n + U_{n+1} = 0. \quad (n=1, 2, \ldots N-1). \quad . \quad . \quad (3)$$

If we write

$$\frac{\phi(\alpha)}{f(\alpha)} = r \quad . \quad . \quad . \quad . \quad . \quad . \quad . \quad . \quad . \quad . \quad (\text{viii})$$

and substitute $U_n = E^n$, then equation (3) becomes

$$E^{n-1}(1+4rE+E^2) = 0 \quad . \quad . \quad . \quad . \quad . \quad . \quad . \quad . \quad . \quad . \quad (4)$$

$$\therefore \quad E = -2r \pm \sqrt{4r^2-1} = E_1 \text{ and } E_2 \quad . \quad . \quad . \quad . \quad . \quad . \quad (\text{ix})$$

(the value E=0 being of no physical significance),

but
$$E_1E_2 = 1. \quad . \quad . \quad . \quad . \quad . \quad . \quad . \quad . \quad . \quad . \quad . \quad . \quad . \quad . \quad (\text{x})$$

Hence
$$U_n = AE^n + BE^{-n}, \quad . \quad . \quad . \quad . \quad . \quad . \quad . \quad (5)$$

and therefore
$$M_n = AE^n + BE^{-n} - f(w), \quad . \quad . \quad . \quad . \quad . \quad . \quad . \quad (6)$$

which is the general solution of equation (3) for the moment at any support. The arbitrary constants A and B have to be determined from the boundary conditions.

Suppose the beam is clamped at both ends, then the constants can be determined from the condition that the angular changes at $n=0$ and $n=N$ are zero.

The angles which the beam makes with the horizontal to the right and left of any support n are respectively :

$$\theta = \frac{l}{24\beta}\{\psi(\alpha)wl^2 + 8\phi(\alpha)M_n + 4f(\alpha)M_{n+1}\}, \quad . \quad . \quad . \quad . \quad (7)$$

$$\phi = \frac{l}{24\beta}\{\psi(\alpha)wl^2 + 8\phi(\alpha)M_n + 4f(\alpha)M_{n+1}\}. \quad . \quad . \quad . \quad . \quad (8)$$

For $n=0$ and $n=\mathrm{N}$, $\theta=\phi=0$.

Hence
$$\mathrm{M}_0=-\left\{\frac{1}{2}\cdot\frac{f(\alpha)}{\phi(\alpha)}\mathrm{M}+\frac{\psi(\alpha)}{\phi(\alpha)}\frac{wl^2}{8}\right\} \quad . \quad . \quad . \quad . \quad . \quad . \quad (9)$$

and
$$\mathrm{M}_\mathrm{N}=-\left\{\frac{1}{2}\cdot\frac{f(\alpha)}{\phi(\alpha)}\mathrm{M}_{\mathrm{N}-1}+\frac{\psi(\alpha)}{\phi(\alpha)}\frac{wl^2}{8}\right\}. \quad . \quad . \quad . \quad . \quad (10)$$

Substituting these values in the general solution (6) and solving for the constants A and B, we obtain

$$\mathrm{A}=(\mathrm{E}^{-\mathrm{N}}-\mathrm{E}^{\mathrm{N}})^{-1}\{\mathrm{E}^{-\mathrm{N}}(\mathrm{M}_0+f(w))-(\mathrm{M}_\mathrm{N}+f(w))\}, \quad . \quad . \quad (11)$$

$$\mathrm{B}=(\mathrm{E}^{-\mathrm{N}}-\mathrm{E}^{\mathrm{N}})^{-1}\{(\mathrm{M}_\mathrm{N}+f(w))-\mathrm{E}^{\mathrm{N}}(\mathrm{M}_0+f(w))\}. \quad . \quad . \quad . \quad (12)$$

Hence

$$\mathrm{M}_n=\frac{(\mathrm{M}_0+f(w))\{\mathrm{E}^{-(\mathrm{N}-n)}-\mathrm{E}^{(\mathrm{N}-n)}\}+(\mathrm{M}_\mathrm{N}+f(w)(\mathrm{E}^{-n}-\mathrm{E}^{n})}{\mathrm{E}^{-\mathrm{N}}-\mathrm{E}^{\mathrm{N}}}-f(w). \quad (13)$$

2. Equation (13) can be put into a more convenient form by writing $\mathrm{E}=-e^{-\gamma}$ (where $\mathrm{E}=-2r+\sqrt{4r^2-1}$ and e is the base of Napierian logarithms) from which γ can be calculated since P, and consequently r, will be known. Making this substitution, the moment at any support is

$$\begin{aligned}\mathrm{M}_n=(-1)^n \operatorname{cosech} \gamma\mathrm{N}\{(\mathrm{M}_0+f(w))\sinh\gamma(\mathrm{N}-n)&\\ +(\mathrm{M}_\mathrm{N}+f(w))\sinh\gamma n\}-f(w).& \quad . \quad . \quad . \quad (14)\end{aligned}$$

As the beam is symmetrical and symmetrically loaded about the centre of its length $\mathrm{M}_0=\mathrm{M}_\mathrm{N}$, and so equation (14) becomes

$$\mathrm{M}_n=(-1)^n(\mathrm{M}_0+f(w))\{\cosh\gamma n-\tanh\tfrac{1}{2}\gamma\mathrm{N}\sinh\gamma n\}-f(w), \quad . \quad (15)$$

which is the general equation for the moment at any support of a beam clamped at both ends and loaded in the manner specified.

3. The following particular cases are derivable from equation (14) :—

(*a*) if either end of the beam (right end for example) is hinged, then $\mathrm{M}_\mathrm{N}=0$ and so

$$\mathrm{M}_n=(-)^n \operatorname{cosech}\gamma\mathrm{N}\{(\mathrm{M}_0+f(w))\sinh\gamma(\mathrm{N}-n)+f(w)\sinh\gamma n\}-f(w). \quad (16)$$

(*b*) if both ends of the beam are hinged $\mathrm{M}_0=\mathrm{M}_\mathrm{N}=0$, then

$$\mathrm{M}_n=f(w)\{(-)^n(\cosh\gamma n-\tanh\tfrac{1}{2}\gamma\mathrm{N}\sinh\gamma n)-1\}, \quad . \quad . \quad (17)$$

(*c*) if the axial force is zero, $\alpha=0$ and $f(w)=\frac{1}{12}wl^2$.

(*d*) if in equation (9) $\alpha=0$, then

$$\mathrm{M}_0=-\{\tfrac{1}{2}\mathrm{M}_1+\tfrac{1}{8}wl^2\}. \quad . \quad . \quad . \quad . \quad . \quad . \quad . \quad . \quad (9a)$$

(*e*) If this value of M_0 is substituted in equation (15) it will be found that

$$\mathrm{M}_n=-\frac{1}{12}wl^2. \quad (n=0, 1, 2, \ldots \mathrm{N}-1). \quad . \quad . \quad . \quad . \quad (18)$$

The argument has been developed on the assumption that the axial force produces compression. If the axial force is a tensile force the appropriate functions must be used. See functions (iv) to (vi).

Acknowledgments.

I am indebted to Professor W. J. Duncan for his comments on my previous paper, and for his suggestion to generalize it, and to Dr. J. Bronowski for his comments on this paper.

LXVIII. *Struts of Variable Flexural Rigidity.*

By N. J. Durant *.

[Received June 12, 1945.]

1. The following investigation of the elastic stability of struts of variable flexural rigidities of which there are large well-defined classes, is general, so that the solution will give the answer to many strut problems.

Elastic stability is a subject of great and increasing importance, firstly because steels and alloys of great strengths are in general use, secondly, the permissible stresses in low strength steels have been increased by twenty to thirty per cent. during the last decade. These influences have a pronounced effect on the stability of members because their cross-sections are thereby reduced, and their slenderness ratios increased, so that failure may result not by reason of the normal compressive stresses exceeding the strengths of the materials but through insufficient elastic stability.

Again, in built-up struts the critical loading is always less than in struts of solid cross-section of the same moment of inertia, and failure of such struts may occur through local buckling apart from buckling as a whole.

2. The solution of the problem of the critical thrust of struts of constant moment of inertia is well known, but large classes of struts such as

(*a*) transmission towers ;
(*b*) locomotive connecting rods ;
(*c*) locomotive coupling rods ;
(*d*) crane jibs, and
(*e*) aircraft spars,

have moments of inertia which vary along their lengths, but which can be represented by equation (1) by a suitable adjustment of the parameter k.

---

* Communicated by the Author.

To find the value of k we could proceed as follows :—calculate, as ordinates, the moments of inertia at a few cross-sections along the strut, then plot (see equation (1)) the straight line $\log_e I_x/I = -kx/l$, with x/l as abscissæ. The numerical value of k will be given by the gradient of this line.

3. In the following analysis the weight of the strut has not been considered, so that it does not apply to locomotive connecting and coupling rods in which inertia forces have to be considered. Again in these two classes of struts the thrusts vary with the time.

Fig. 1.

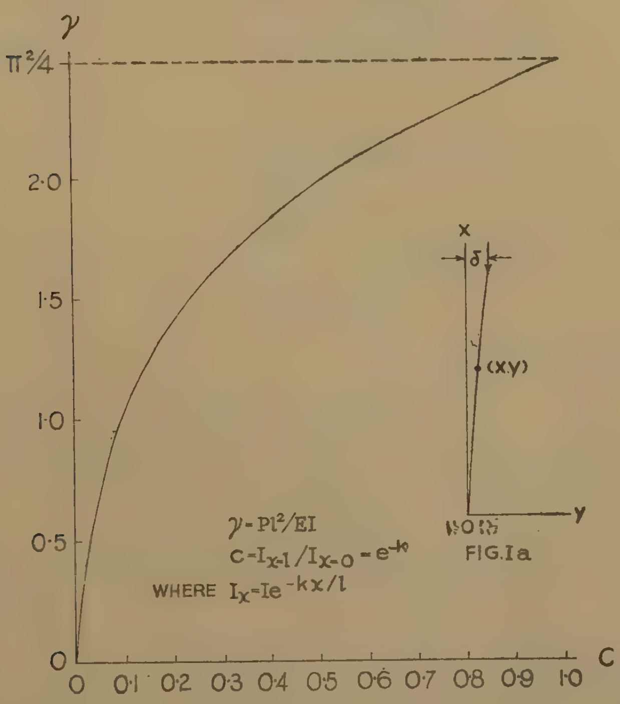

4. *Analysis.*

Suppose the moment of inertia about the axis (through the centroid) perpendicular to the plane of flexure at any cross-section at x is

$$I_x = Ie^{-kx/l}, \quad \ldots\ldots\ldots \quad (1)$$

where I is the moment of inertia at $x=0$, and l is the total length of the strut.

The moment at any point (x, y), fig. 1 a, is

$$M_x = P(\delta - y), \quad \ldots\ldots\ldots \quad (2)$$

then the differential equation of flexure is

$$\mathrm{EI}e^{-kx/l}\frac{d^2y}{dx^2}+\mathrm{P}(y-\delta)=0. \quad . \quad . \quad . \quad . \quad . \quad . \quad . \quad (3)$$

This equation can be integrated in terms of Bessel Functions for all values of k. It can be integrated in terms of elementary functions only if $k=0$.

E is the modulus of elasticity of the material in compression.

5. To solve equation (3) we first change the dependent variable by writing

$$y=\phi+\delta, \quad . \quad . \quad . \quad . \quad . \quad . \quad . \quad . \quad . \quad . \quad (4)$$

then divide the resulting equation by $\mathrm{EI}e^{-kx/l}$ and so obtain

$$\frac{d^2\phi}{dx^2}+n^2e^{kx/l}\phi=0, \quad . \quad . \quad . \quad . \quad . \quad . \quad . \quad . \quad . \quad . \quad (5)$$

where

$$n^2=\mathrm{P/EI}. \quad . \quad . \quad . \quad . \quad . \quad . \quad . \quad . \quad (6)$$

If we now change the independent variable by writing

$$\xi=ne^{\frac{1}{2}kx/l}, \quad . \quad . \quad . \quad . \quad . \quad . \quad . \quad . \quad . \quad . \quad (7)$$

then, after reduction, equation (5) becomes

$$\frac{d^2\phi}{d\xi^2}+\frac{1}{\xi}\cdot\frac{d\phi}{d\xi}+\frac{4l^2}{k^2}\phi=0. \quad . \quad . \quad . \quad . \quad . \quad . \quad . \quad . \quad (8)$$

The solution of this equation is

$$\phi=\mathrm{AJ}_0\left(\frac{2l}{k}\xi\right)+\mathrm{BY}_0\left(\frac{2l}{k}\xi\right), \quad . \quad . \quad . \quad . \quad . \quad . \quad (9)$$

where J_0 and Y_0 are Bessel Functions of the 1st and 2nd kinds respectively of zero order.

The solution of equation (3) is therefore

$$y-\delta=\mathrm{AJ}_0\left(\frac{2ln}{k}e^{\frac{1}{2}kx/l}\right)+\mathrm{BY}_0\left(\frac{2ln}{k}e^{\frac{1}{2}kx/l}\right). \quad . \quad . \quad . \quad . \quad (10)$$

6. Boundary conditions are

when $x=0$, then $\frac{dy}{dx}=0$, and when $x=l$, then $y=\delta$.

Differentiating equation (10) with respect to x we get

$$\frac{dy}{dx}=ne^{\frac{1}{2}kx/l}\left\{\mathrm{AJ}_0'\left(\frac{2ln}{k}e^{\frac{1}{2}kx/l}\right)+\mathrm{BY}_0'\left(\frac{2ln}{k}e^{\frac{1}{2}kx/l}\right)\right\}, \quad . \quad . \quad (11)$$

but and

$$\left.\begin{array}{l}\mathrm{J}_0'(z)=-\mathrm{J}_1(z)\\ \mathrm{Y}_0'(z)=-\mathrm{Y}_1(z)\end{array}\right\}, \quad . \quad . \quad . \quad . \quad . \quad . \quad . \quad . \quad (12)$$

where the primes denote differential coefficients.

Equation (11) then becomes

$$\frac{dy}{dx}=-ne^{\frac{1}{2}kx/l}\left\{\mathrm{AJ}_1\left(\frac{2ln}{k}e^{\frac{1}{2}kx/l}\right)+\mathrm{BY}_1\left(\frac{2ln}{k}e^{\frac{1}{2}kx/l}\right)\right\}. \quad . \quad . \quad (13)$$

Substituting the boundary conditions in their respective equations we get

$$\mathrm{AJ}_1\left(\frac{2ln}{k}\right)+\mathrm{BY}_1\left(\frac{2ln}{k}\right)=0, \quad . \quad . \quad . \quad . \quad . \quad . \quad (14)$$

$$\mathrm{AJ}_0\left(\frac{2ln}{k}e^{\frac{1}{2}k}\right)+\mathrm{BY}_0\left(\frac{2ln}{k}e^{\frac{1}{2}k}\right)=0. \quad . \quad . \quad . \quad . \quad . \quad . \quad (15)$$

For convenience write

$$\frac{2ln}{k}=\theta \quad \text{and} \quad e^{\frac{1}{2}k}=\beta. \quad . \quad . \quad . \quad . \quad . \quad . \quad . \quad . \quad (16)$$

In order that equations (14) and (15) shall be consistent, we must have

$$\mathrm{J}_0(\beta\theta)\mathrm{Y}_1(\theta)-\mathrm{Y}_0(\beta\theta)\mathrm{J}_1(\theta)=0. \quad . \quad . \quad . \quad . \quad . \quad . \quad . \quad (17)$$

From this equation we determine the condition of stability because, for a given β, the least value of θ which satisfies this equation determines the critical thrust.

We obtain from equation (6) and (16)

$$\frac{2l}{k}\sqrt{\frac{\mathrm{P}}{\mathrm{EI}}}=\theta. \quad . \quad . \quad . \quad . \quad . \quad . \quad . \quad . \quad (18)$$

The critical thrust is therefore

$$\mathrm{P}=\frac{\theta^2k^2}{4}\cdot\frac{\mathrm{EI}}{l^2}, \quad . \quad . \quad . \quad . \quad . \quad . \quad . \quad . \quad (19)$$

which can be written

$$\mathrm{P}=\gamma\frac{\mathrm{EI}}{l^2}, \quad . \quad . \quad . \quad . \quad . \quad . \quad . \quad . \quad . \quad . \quad (20)$$

where

$$\gamma=\left(\frac{\theta k}{2}\right)^2, \quad . \quad . \quad . \quad . \quad . \quad . \quad . \quad . \quad . \quad . \quad (21)$$

which depends only on the parameter k in the formula for the moment of inertia.

7. Table I. gives the least values of θ for various values of k which satisfy equation (17). Column 6 of the above table gives the values of γ, which, inserted in formula (20), gives the critical thrusts for a strut fixed at one end and free at the other.

8. By substituting $\frac{1}{2}l$ for l in formula (20) we obtain the critical thrust for a strut hinged at its ends, symmetrical and symmetrically loaded with respect to the centre of its length.

If we write Q for the critical thrust in this case, then

$$\mathrm{Q}=\eta\frac{\mathrm{EI}}{l^2}. \quad . \quad . \quad . \quad . \quad . \quad . \quad . \quad . \quad . \quad . \quad . \quad (22)$$

where

$$\eta=4\gamma. \quad . \quad . \quad . \quad . \quad . \quad . \quad . \quad . \quad . \quad . \quad . \quad (23)$$

9. It is assumed in the analysis that the strut is sufficiently slender, so that the stresses are within the limits of linear elasticity of the material.

To find the range of validity of formulas (20) and (22) suppose the limiting stress of the material is $\overline{xx}$, then we must have

$$\frac{P}{A_x}=\frac{\gamma EI_0}{A_x l^2}=\frac{\gamma EA_0}{A_x\left(\frac{l}{r_0}\right)^2}<\overline{xx}, \quad . \quad . \quad . \quad . \quad . \quad . \quad (24)$$

where A_x is the area of cross-section at x and A_0 its value at $x=0$; r_0 is the least radius of gyration of the cross-section at $x=0$ about an axis through its centroid.

In many cases A_x is constant and $(=A_0)$ we would then obtain from formulæ (20) and (22) the following conditions for the ratio l/r_0;

$$\frac{l}{r_0}\geqslant\sqrt{\frac{\gamma E}{\overline{xx}}} \quad \text{(strut-fixed at one end and free at the other)} \quad . \quad (25)$$

TABLE I.

$I_{x=l}/I_{x=0}$. 1. C.	2. $k=\log_e\frac{1}{c}$.	3. $\beta=e^{\frac{1}{2}k}$.	4. $\theta=\frac{2ln}{k}$.	5. $\beta\theta$.	6. γ.	7. $\eta=4\gamma$.
0·025	3·6889	6·3245	0·3973	2·5127	0·5370	2·1480
0·050	2·9957	4·4721	0·5848	2·6153	0·7674	3·0696
0·10	2·3026	3·1623	0·8947	2·8293	1·0610	4·2440
0·20	1·6094	2·2361	1·4800	3·3094	1·4183	5·6732
0·30	1·2040	1·8257	2·1374	3·9023	1·6557	6·6228
0·40	0·91630	1·5811	2·9574	4·6757	1·8359	7·3436
0·50	0·69315	1·4142	4·0618	5·7442	1·9817	7·9268
0·60	0·51083	1·2910	5·6803	7·3333	2·1049	8·4196
0·70	0·35668	1·1952	8·3401	9·9681	2·2123	8·8492
0·80	0·22314	1·1180	13·6137	15·2201	2·3070	9·2280
0·90	0·10536	1·0541	29·3426	30·9300	2·3894	9·5576
1·00	0	1·00	∞	∞	2·4674	9·8696
					$-\pi^2/4$	$=\pi^2$

$$\text{and} \quad \frac{l}{r_0}\geqslant 2\sqrt{\frac{\gamma E}{\overline{xx}}} \quad \text{(strut-hinged at both ends).} \quad . \quad . \quad . \quad . \quad . \quad . \quad . \quad (26)$$

This ratio in the case of a uniform strut is termed the slenderness ratio.

Suppose $\overline{xx}=5.10^4$ lb./in.^{2},

$E=3.10^7$ lb./in.^{2},

$C=I_{x=l}/I_{x=0}=0·8,$ } Table I.,

then $\gamma=2·3070,$ }

then $l/r\geqslant 37·2$ and $l/r\geqslant 74·4$ respectively for formulas (25) and (26).

10. It is of interest to investigate what happens as $k\to 0$. Evidently, the case $k=0$ is the familiar case of the uniform strut for which the Euler formula gives the critical thrust.

From formula (16) it follows that as $k \to 0$ $\theta \to \infty$, since the critical thrust must remain finite.

To solve the consistency equation (17) we need the principal parts of the asymptotic expansions of the Bessel Functions which are as follows :—

$$J_\nu(z) \sim \sqrt{\frac{2}{\pi z}} \cos(z - \tfrac{1}{4}\pi + \nu\pi), \qquad (27)$$

$$Y_\nu(z) \sim \sqrt{\frac{2}{\pi z}} \sin(z - \tfrac{1}{4}\pi + \nu\pi). \qquad (28)$$

Equation (17) then becomes for this limiting case :

$$\cot(\beta\theta - \tfrac{1}{4}\pi) = \cot(\theta + \tfrac{1}{4}\pi). \qquad (29)$$

$$\therefore \quad \theta(\beta - 1) = \tfrac{1}{2}\pi. \qquad (30)$$

$$\therefore \quad n = \frac{\pi k}{4l(\beta - 1)}. \qquad (31)$$

$$n^2 = \frac{P}{EI} = \frac{\pi^2}{4l^2}\left(\frac{\tfrac{1}{2}k}{e^{\frac{1}{2}k} - 1}\right)^2. \qquad (32)$$

$$\therefore \quad P = \frac{\pi^2 EI}{4l^2}, \qquad (33)$$

since

$$\lim_{k \to 0}\left(\frac{\tfrac{1}{2}k}{e^{\frac{1}{2}k} - 1}\right)^2 = 1. \qquad (34)$$

To avoid the necessity of using an interpolation formula for intermediate values, the graph (fig. 1) has been prepared from the tabular values shown in Table I.

Acknowledgments.

I am indebted to Dr. J. Bronowski and Dr. F. Garwood for valuable suggestions and to Dr. F. Garwood for the numerical work.

LXIX. *A Relation between some Natural Constants and the Lesser Particles.*

By H. D. K. Drew *.

[Received November 2, 1945.]

It is generally held that matter and energy are interchangeable, the experimental basis being the change of mass sometimes observed in disintegration reactions. An alternative view, however, is that neither energy nor mass is an entity, both being properties of matter and expressible in terms of the structure of the matter which exhibits them. In that case it would follow that all material particles have a structure, that is to say, that every kind of particle is composed of one or more kinds of lesser particles, all of which are themselves composite in the same manner. Matter would thus be endlessly, though not necessarily continuously, divisible into series of diminishing particles ('Chemistry and Industry,' 1943, p. 390). Considering one and the same particle under different influences, its structure could be conceived to vary in two ways : in the relative positions of the particles composing it, and in the nature of those particles, at any instant ; for it can be conceived that the composing particles themselves may not only vary their relative positions but may combine together or divide, thus composing or becoming new particles, in response to external conditions. The writer recently noticed a correspondence in the values of two extremely minute masses, connected with some of the fundamental constants, so close that it can hardly be fortuitous ; and this is described below, in that it leads to a fresh relationship among the constants and may have a bearing on the question of the existence of very minute particles.

---

* Communicated by the Author.

The constants involved are : Rydberg's general wave-number constant (R_∞), the velocity of light (c), Planck's constant (h), Avogadro's number (N), and the masses of the electron (m_e) and the neutron (M_N). The relation of the gram to the oxygen unit of mass or to the electron mass is required : reserving the symbol m_e to denote the mass of the electron in any unit of mass, let M=the mass of the electron in grams and let m=the same in oxygen units ; then $1/N=M/m$. The values of M and m adopted by Chernyaev (1938) and by Aston (1942) are nearly identical, and, from the foregoing relationship, the values adopted for N by these authors are seen to correspond very closely ; the mean (quoted below) of these two values for N has been taken in calculating M, using the present writer's value for m (*loc. cit.*, given below as m_e). For R_∞, the mean of the nearly identical values of Chernyaev (1938) and of Drinkwater, Richardson and Williams (1940) will be used ; for c, that of the values of Birge (1934) and Anderson (1936), which differ only by 1 part in about 30,000. The value of Planck's constant is probably not so accurately known ; the mean value given by Shiba (1938), which is very close to the mean of Millikan's value (1938) and that deduced from Chernyaev's figures, is perhaps the best yet given and will be used. For the mass of the neutron, the writer's value (*loc. cit.*, and below) is taken. The values of the constants are then :

$N = 6{\cdot}0238 \times 10^{23}$;

$R_\infty = 109737{\cdot}3$ cm.$^{-1}$;

$c = 2{\cdot}99770 \times 10^{10}$ cm. sec.$^{-1}$;

$h = 6{\cdot}625 \times 10^{-27}$ erg. sec.$^{-1}$;

$m_e = 0{\cdot}0005428835233$ oxygen units ;

$M = 9{\cdot}01231 \times 10^{-28}$ grams ;

$$\text{M}_{\text{N}}=1{\cdot}0086861363731 \text{ oxygen units}=\left(1858+\frac{1}{f}\right) \text{electron masses} \left(\text{where } f=63{\cdot}494801787, \text{ or } \frac{1}{f}=0{\cdot}015749320761\right).$$

On a basis of Bohr's theory, the energy of ionization of the ^{1}H atom is $\text{R}_\infty ch$, and this energy would become available on recapture of the electron from infinity in the innermost orbit, the greater part of it, $\text{R}_{\text{H}}ch$, being radiated at wave number R_{H}. Suppose, however, that the whole of this energy were communicated to an already existing particle of such a mass that the particle acquired the velocity of light, on a basis of the classical theory of dynamics (on a basis of the special relativity theory, the attainment of velocity c by a particle with finite rest mass would not be possible) ; then, if the rest mass of the particle is m_s,

$$m_s=2\ \text{R}_\infty h/c. \quad . \quad . \quad . \quad . \quad . \quad . \quad . \quad . \quad . \quad . \quad \text{(i)}$$

With the above values of the constants, this gives $m_s=53{\cdot}820275\times10^{-6}$ electron masses.

There is, however, a second equation, viz. :

$$m_s=m_e^2/10\text{M}_{\text{N}}, \quad . \quad . \quad . \quad . \quad . \quad . \quad . \quad . \quad . \quad . \quad \text{(ii)}$$

which is evidently practically identical with (i), since it gives $m_s=53{\cdot}820857\times10^{-6}$ electron masses, the difference between these two calculations of m_s being only 1 part in about 90,000. It seems improbable that future revision of the values of the constants will be so extensive as to render the correspondence otherwise than close. On the other hand, the simplicity of the expressions involved inclines the writer to believe that they are based upon a natural law, and that the above correspondence would, in fact, be exact if the values of the fundamental constants were known exactly. If this be assumed, then

$$\frac{2\text{R}_\infty h}{c}=\frac{m_e^2}{10\text{M}_{\text{N}}} \quad \text{and} \quad \text{R}_\infty=\frac{m_e^2 c}{20\text{M}_{\text{N}}h}. \quad . \quad . \quad . \quad . \quad . \quad \text{(iii)}$$

The energy of ionization of ^{1}H can thus be expressed in terms of c and the masses of electron and neutron, as $m_e^2c^2/20\text{M}_{\text{N}}$. From (iii) the value of h is $6{\cdot}62507\times10^{-27}$ erg. sec.$^{-1}$.

On combining (iii) with Bohr's equation, viz., $\text{R}_\infty=2\pi^2m_ee^4/h^3c$, a fresh relationship is obtained between the charge on the electron (e), h and c, together with the masses ; for example

$$h=\frac{2\pi e^2}{c}\sqrt{\frac{m_e}{m_s}}=\frac{2\pi e^2}{c}\sqrt{\frac{10\text{M}_{\text{N}}}{m_e}}; \quad \text{and} \quad e=\left(\frac{ch}{2\pi}\right)^{\frac{1}{2}}\left(\frac{m_e}{10\text{M}_{\text{N}}}\right)^{\frac{1}{4}}.$$

The last, with the value of h obtained from (iii), gives $e=4{\cdot}81545\times10^{-10}$ e.s.u., and $h/e=1{\cdot}375794\times10^{-17}$; the latter is nearer to the observed value of $1{\cdot}3765\times10^{-17}$ than is Birge's estimate of $1{\cdot}37929\times10^{-17}$; the mean of three recent estimates of e is $4{\cdot}8030\times10^{-10}$.

All of the above equations are dimensionally correct. It will be noticed that they are based on the writer's previous assumption, arrived at only by general argument, that the mass of the electron is equal to the cube root of 16×10^{-11}, when expressed in $^{16}\mathrm{O}$ units of mass, or, otherwise expressed, that the number of electron masses in the $^{16}\mathrm{O}$ atom is the cube root of $16^2\times10^{11}$. The simplicity of the relations given in the present paper appears to afford support to the previous suggestion as to the mass of the electron and also to its suggested relationship with that of the neutron. It will be noticed, also, that the cube of the mass of the electron in any unit of mass is equal to ten times the product of the masses of neutron, electron, and the very small particle here denoted as s, and that the cube of the mass of the $^{16}\mathrm{O}$ atom is consequently $16^2\times10^{12}$ times the product of these three masses.

Avogadro's number, which has been assumed in the foregoing, can be calculated from the relation: $\mathrm{N}=cm_e/20j\mathrm{R}_\infty h$, where $j=\left(1858+\frac{1}{fl}\right)$, h being expresssed in c.g.s. units, the mass of the electron being in oxygen units.

The masses of the neutron and of the electron and the hypothetical mass m_s bear a simple relationship, viz., $\mathrm{M_N}/m_e=j$, $m_e/m_s=10j$, $\mathrm{M_N}/m_s=10j^2$, suggesting that they might belong to a series of particles, one possibility of several being that alternate neutral and electrical particles occur whose masses diminish by the alternate factors 10 and j, in which case a neutral particle of mass $m_e/10$ would be missing.

The question of the existence of minute particles may also have a bearing on that of the nature of kinetic energy; for example, if any particle is struck (normally, for the sake of simplicity) by another similar particle having a greater velocity, the more peripheral minute composing particles of the latter will impinge upon and displace those of the former, so that the structures of both particles will be altered equally in opposite senses, in accordance with the laws of elastic collision. Thus it is possible to suggest that a particle which is moving in a given environment differs from a similar particle which is stationary in the same environment in having a certain actual displacement of its constituent particles, some relative to others, in the direction of the motion, as compared with the stationary particle; or, in other words, that the displacement occasions or determines the motion, which will not cease until the displacement is by some means cancelled (for example, by an opposed collision with another particle.) Since, in a particle so set in motion by collision, all of its constituent particles are eventually equally in motion, there must logically be complete internal material connection between these constituent particles, presumably through the agency of the infinite series of their subconstituents.

Queen Mary College
(University of London), E. 1.

LXX. *Drainage of a Vertical Plate.*

By George Wyllie, B.Sc., Assistant to the Professor of Applied Physics, Glasgow University *.

[Received September 18, 1944.]

The profile of a film of viscous liquid draining from a wetted surface is of interest in several applications. The simplest type of surface is the vertical plane plate. If such a plate is covered with a uniform film of infinite extent and thickness "a," which is allowed to descend under the action of gravity and of the retardation due to its own viscosity, the limiting velocity of the liquid at a distance "x" from the plate is, as shown later in this paper, given by

$$v_0=\frac{g}{\nu}(ax-\tfrac{1}{2}x^2),$$

where "g" is the acceleration due to gravity and "ν" is the kinematic viscosity of the liquid.

Goucher and Ward (1) applied this result to calculate the relation between the thickness of the coating formed by drawing a wire vertically from an enamel bath, the enamel solidifying a little distance above the surface, and the rate of motion of the wire. Their conclusion agreed well with experiment.

In the case where the material remains liquid, however, the simple theory of Goucher and Ward, who assumed almost immediate solidification, becomes inadequate, as is shown, *e. g.* by Morey (2), and it is then of interest to know the form which the profile of the film actually assumes.

If we suppose the liquid to be of uniform thickness in a horizontal plane, but to vary in thickness in a vertical direction, and to be descending at every point with the limiting velocity appropriate in an infinite uniform film of thickness equal to the actual thickness at that point, we obtain with Jeffreys (3) the following relation between the thickness of the film "x," the distance measured downwards from the top of the film "y," and the time "t":—

$$-\frac{\partial x}{\partial t}=\frac{g}{\nu}x^2\frac{\partial x}{\partial y}. \qquad \text{(A)}$$

The fundamental assumption involved in this equation is reasonable if the profile is of such slight curvature that the effects of surface tension may be neglected, and so we may expect the profile of the film to be a solution of the equation (A). Jeffreys assumed a solution of the form

---

* Communicated by Professor T. Alty.

$$x = ky^{d}t^{\mathrm{B}},$$

thus obtaining the relation

$$x = \sqrt{\frac{\nu y}{gt}}.$$

The parabola thus derived, however, has a large curvature in the region near the top of the film, and it is to be expected that surface tension effects will so modify the initial conditions as to distort the profile in this neighbourhood.

A series of experiments to test this was devised and carried out by Satterley (4) and others. They found, after taking most stringent precautions, that Jeffreys' equation held accurately for the lower portion of the film, but diverged widely from the experimental results near the top.

Green (5) suggested an explanation of this, supposing that initially the film near the top was of uniform thickness "a" and at rest. He further supposed that the profile of the film would be nearly the same as the curve of descent of the liquid in an infinite film of the same thickness, as equation (A) cannot be applicable in the first stages of the motion. Green's solution for the curve of descent was obtained by the method developed by him in several previous papers (6). In the present case, however, the limiting condition of flow is easily obtained, and, in consequence, the curve of descent can be obtained by a rather simpler method, as follows :—

The equation of motion of an element of the film is

$$\frac{\partial v}{\partial t} = g + \nu \frac{\partial^2 v}{\partial x^2},$$

and the boundary conditions are, $v=0$ when $t=0$, $v=0$ when $x=0$, $\frac{\partial v}{\partial x}=0$ when $x=a$.

To find the limiting velocity we solve

$$g + \nu \frac{d^2 v}{dx^2} = 0,$$

obtaining

$$v_0 = \frac{g}{\nu}\left(ax - \frac{x^2}{2}\right).$$

Then, if $u = v - v_0$, the equation above becomes

$$\frac{\partial u}{\partial t} = \nu \frac{\partial^2 u}{\partial x^2}.$$

Since $u=0$ when $x=0$, $\frac{\partial u}{\partial x}=0$ when $x=a$, the solution of this equation gives

$$u = \sum_{n=0}^{\infty} \mathrm{A}_n e^{-\left(\frac{2n+1}{2}\frac{\pi}{a}\right)^2 \nu t} \sin\left(\frac{2n+1}{2}\pi\frac{x}{a}\right).$$

Now when $t=0$, $v=0$, so $u=\frac{g}{\nu}(\frac{1}{2}x^2-ax)$, and evaluating the Fourier coefficients we obtain,

$$v=\frac{g}{\nu}(ax-\tfrac{1}{2}x^2)-\frac{16a^2g}{\pi^3\nu}\sum_{n=0}^{\infty}\frac{e^{-\lambda_n^2\nu t}}{(2n+1)^3}\sin(\lambda_n x),$$

where $\lambda_n=\frac{2n+1}{2}\frac{\pi}{a}$.

Accordingly the curve of descent has equation

$$y=\frac{g}{\nu}(ax-\tfrac{1}{2}x^2)t-\frac{64a^4g}{\pi^5\nu^2}\sum_{n=0}^{\infty}\frac{\sin(\lambda_n x)}{(2n+1)^5}(1-e^{-\lambda_n^2\nu t}). \quad . \quad . \quad . \quad (\mathrm{B})$$

If we apply this to the case of a finite film it requires the liquid at a distance x from the fixed surface to move with velocity $\frac{g}{\nu}(ax-\frac{1}{2}x^2)$. But a little while after the start of the motion the thickness of the film at some point in the upper region will be "l," where $x<l<a$. Then the limiting velocity appropriate in the film at that level will be

$$\frac{g}{\nu}(lx-\tfrac{1}{2}x^2)<\frac{g}{\nu}(ax-\tfrac{1}{2}x^2).$$

Thus it is evident that equation (B) requires the liquid in the upper portion of the film to move with velocity $\left(\text{ultimately}=\frac{g}{\nu}(ax-\frac{1}{2}x^2)\right)$ greater than the limiting velocity appropriate to the thickness of the film there. A better approximation to the shape of the curve may then be obtained on the following considerations :—

The general solution of the differential equation (A) is of the form

$$f\left(y-\frac{g}{\nu}x^2t,\, x\right)=0,$$

where "f" is an arbitrary function. If we put this in the form

$$y-\frac{g}{\nu}x^2t=f(x), \quad . \quad . \quad . \quad . \quad . \quad . \quad . \quad . \quad (\mathrm{C})$$

we see that Jeffreys' solution amounts to taking $f(x)\equiv 0$.

Now (A) does not hold at the start of the motion, and (B) becomes invalid after the initial stages. Thus we may approximate to the shape of the profile by assuming Green's solution for the early part of the motion and then using it to establish the form of the arbitrary function in (C) at some definite moment.

Let this moment be taken at time t_0 from the start of the motion. The equation to the profile thereafter will be

$$y-\frac{g}{\nu}x^2(t-t_0)=f(x),$$

so at $t=t_0$, $\qquad y=f(x).$

By Green's solution, at $t=t_0$,

$$y=\frac{g}{\nu}(ax-\tfrac{1}{2}x^2)t_0-\frac{64a^4g}{\pi^5\nu^2}\sum_{n=0}^{\infty}\frac{\sin(\lambda_n x)}{(2n+1)^5}(1-e^{-\lambda_n^2\nu t_0}).$$

Hence the equation to the profile will be

$$y-\frac{g}{\nu}x^2t=\frac{g}{\nu}\left(ax-\frac{3}{2}x^2\right)t_0-\frac{64a^4g}{\pi^5\nu^2}\sum_{n=0}^{\infty}\frac{\sin(\lambda_n x)}{(2n+1)^5}(1-e^{-\lambda_n^2\nu t_0}).$$

In the paper by Satterly and Givens already referred to, sufficient data are given to enable us to find the appropriate values of a, t_0 for one profile. In this case the film was of water at 0·9° C. ; it was prepared by lowering a beaker of water from a clean vertical glass plate which had been immersed for some time to ensure satisfactory wetting of the surface. A series of interference bands was formed in the plane of the film by reflection of the light from a sodium arc lamp. The resulting pattern was photographed 20 secs. after the flow had begun, the plate being referred to by Satterly and Givens as P.p. no. 56. The remaining numerical data are

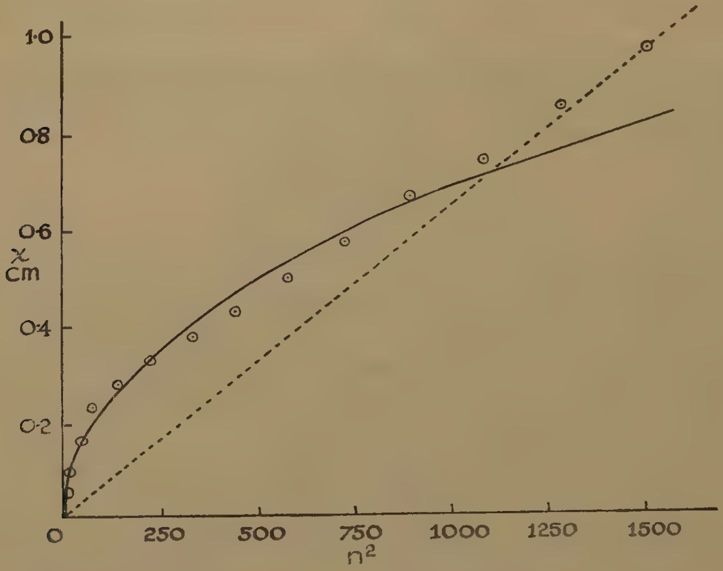

$$\nu=0{\cdot}01738 \text{ poise/gm.}$$

$$g=980 \text{ cm./sec.}^2 \text{ (at Toronto).}$$

l=increase in film thickness per interference line$=2{\cdot}23\times10^{-5}$ cm. Magnification of camera$=1{\cdot}15$.

If the nth line on the plate occurs "x" cm. from the image of the edge of the film, then according to the above equation

$$\frac{x}{1{\cdot}15}-5{\cdot}608\times10^{-4}n^2=1{\cdot}257at_0n-4{\cdot}207\times10^{-5}t_0n^2 \quad . \quad . \quad \text{(D)}$$

—trigonometrical terms.

In the figure, "x" is graphed as a function of "n^2," to emphasise the discrepancies with the profile predicted by Jeffreys. The experimental results, which are shown by the small circles in the figure, agree with Jeffreys' profile (shown as a dotted straight line) for $x > 0{\cdot}75$ cm., but for values of "x" up to 0·65 cm. they agree much more closely with the solid curve, which is given by equation (D) with $a = 0{\cdot}0011$ cm., $t_0 = 14$ secs. This gives the relation

$$x = 0{\cdot}0223n - 0{\cdot}00003225n^2.$$

The coefficient of the trigonometrical series is then

$$\frac{64a^4g}{\pi^5\nu^2} \doteqdot 10^{-6},$$

so it may be neglected in this case.

The reasonable values for a, t_0 tend to confirm the validity of the assumptions on which this theory is based. This can only be fully tested by examining a series of profiles obtained, under otherwise similar conditions, for various values of the total time of flow "t." Such experimental results do not seem to be at present available. Other curves given by Satterly and Givens without sufficient auxiliary details are of similar shape and should respond to similar treatment.

Conclusion.

The shape of the upper part of a liquid film draining on a vertical plate is predicted from simple assumptions regarding the initial conditions. It appears from examination of the only complete experimental curve available that the actual profile may be very nearly represented by the curve given in this paper as far as the point where this curve meets Jeffreys' profile, after which the latter holds.

Finally I wish to express my thanks to Professor T. Alty and to Dr. G. Green for the helpful and critical interest which they have taken in the preparation of this paper.

References.

(1) Research Staff of the General Electric Co. (Goucher and Ward), Phil. Mag. xliv. p. 1002 (1922).
(2) Morey, U.S. Bureau of Standards Journal of Research, xxv. p. 385 (1940).
(3) Jeffreys, Proc. Camb. Phil. Soc. xxvi. p. 204 (1929–30).
(4) Satterly and Givens, Trans. Roy. Soc. Can. xxvii. section iii. p. 145 (1933), which contains full references to earlier papers.
(5) Green, Phil. Mag. xxii. p. 730 (1936).
(6) Green, Phil. Mag. iii. p. 787 (Suppt. 1927), and other papers.

LXXI. *Notice respecting New Book.*

Chemical Crystallography.—An introduction to optical and X-ray methods. By C. W. Bunn. [Pp. xii+422.] (Oxford : Clarendon Press, 1945. 25*s.* net.)

This book is written by a chemist who appreciates the use which can be made in his own work of modern crystallographic techniques. It is throughout illustrated by a wealth of examples drawn from the practice of chemistry. To classify the book is a little difficult, for it is neither a usual text-book nor a monograph ; perhaps it is best described as a guide-book to the crystallographic country. The writing is lucid and the text is illustrated excellently with many figures.

The book is divided into two principal sections dealing respectively with the identification of crystals and the analysis of crystal structure. The first section includes the elements of morphological crystallography, and crystal optics (including convergent light figures). The theory of the reflection of X-rays from crystals is treated in an elementary manner and its application to powder photographs is demonstrated. The first section concludes with a chapter describing the most recent indexes which have been compiled for identifying crystals by their X-ray powder photographs. The second section opens with the methods of dealing with single crystals, which are introduced as an extension of the powder method. All the main methods of taking single crystal X-ray photographs are briefly described. Extensive use is made of the properties of the reciprocal lattice and the reflecting sphere. It may be asked whether the author is entirely justified in claiming that the reciprocal lattice is imaginary while the Bravais lattice is real. The discussion of the single crystal methods includes rotation, oscillation, Laue, various moving film methods and the ionisation spectrometer technique.

After this discussion of the experimental methods the book passes on to the symmetry properties of crystals as expressed in the space groups. The fundamentals of the subject are explained though the more difficult problems of space-group theory are omitted. The calculation of structure factors is described and the theoretical basis laid for the three chapters which give many excellent examples of the application of the theories. This part of the book will be expecially valuable to all who are studying the determination of crystal structures. With excellent feeling for the balance of the work the author has chosen examples from structures of different complexity, and from different types of materials. The description, though necessarily discursive, covers all the well known methods of Fourier, Patterson and "fly's-eye" analysis. The last chapter gives an account of line broadening, due to stress and permanent strain in the material, which forms a useful introduction to a technique requiring much further research. The appendices include information on the measurement of the refractive indices of crystals using immersion media and also a description of the modified Bjurstrom charts for the interpretation of powder photographs.

The scope of this work is much wider than that of any book so far published on the subject and can be warmly recommended to all those who require to know in a general way the principles of crystal structure analysis. In detailed techniques, such as the various methods of taking X-ray photographs of single crystals, it is not, however, a substitute for other books which deal especially with them.

There are some errors against which the reader should be warned ; figs. 43 *c* and *d* have been interchanged, the account of the relation between hexagonal and rhombohedral axes on p. 135 is misleading, and the key formula for integrated reflection on p. 208 is wrongly defined.

The author is to be warmly congratulated on producing a comprehensive, up to-date, and original account of the subject. W. A. Wooster.

[*The Editors do not hold themselves responsible for the views expressed by their correspondents.*]

LXXII. *Calculations concerning Theoretical Values of Boundary-Layer Thickness and Coefficients of Friction and of Heat Transfer for steady Two-Dimensional Laminar Flow in an incompressible Boundary-Layer with Mainstream Velocity* $U \propto x^m$ *or* $U \propto e^{\alpha x}$.

By J. G. Oldroyd, B.A., Trinity College, Cambridge*.

[Received August 28, 1944.]

Summary.

1. The boundary-layer thicknesses and coefficients of friction at the boundary, derived respectively from a numerical solution of the boundary layer equations and from Pohlhausen's adaptation of the momentum equation, are compared in the case of a steady two-dimensional laminar incompressible boundary-layer with mainstream velocity $U \propto x^m$ or $U \propto e^{\alpha x}$ ($\alpha > 0$). The results give an indication of the accuracy of Pohlhausen's method of treating the boundary-layer in those cases in which the assumption of similar velocity profiles in all sections of the boundary layer is strictly valid. Discrepancies are found to be small in the cases of negative pressure gradient.

2. The coefficient of heat transfer by forced convection through a laminar incompressible boundary-layer, when the mainstream velocity is proportional to x^m or $e^{\alpha x}$, is also considered. The heat transfer and skin-friction coefficients are compared for different values of Prandtl's number, σ. The results indicate that a law of the form $C_H/\frac{1}{2}C_f = A\sigma^n$ may be expected to give reliable results at least in the range $0{\cdot}6 \leqslant \sigma \leqslant 7{\cdot}0$. The index n is dependent on the form of the mainstream velocity and takes values between $-0{\cdot}60$ and $-0{\cdot}73$ in the cases considered. The value of A is unity only in the case of constant mainstream velocity, and, in the cases considered, is less than unity when the pressure gradient is negative.

Notation.

x, y = co-ordinates measured along and perpendicular to the wall, $y=0$ being the equation of the wall.
u, v = velocity components in the co-ordinate directions in the boundary-layer.
U, 0 = velocity components in the co-ordinate directions in the main stream.
ν = kinematic coefficient of viscosity.
m = constant when $U \propto x^m$.

---

* Communicated by Professor L. Rosenhead, Ph.D., D.Sc., Liverpool University.

α =positive constant when $U \propto e^{\alpha x}$.

β $=2m/(m+1)$ ($\beta=2$ corresponds to the case $U \propto e^{\alpha x}$).

δ =thickness of boundary-layer.

δ_1 =displacement thickness of boundary-layer.

δ_2 =momentum thickness of boundary-layer.

$\delta', \delta_1', \delta_2'$=corresponding values derived from Pohlhausen's adaptation of the momentum equation.

ϵ $=1-u/U$ at the limit, $y=\delta$, of the boundary-layer.

λ $=\dfrac{\delta'^2}{\nu}\dfrac{dU}{dx}$, Pohlhausen's parameter.

$g(\lambda), h(\lambda), k(\lambda)$=functions of λ defined by equations (13), (14), (27).

γ =constant value of $\delta\left(\dfrac{1}{\beta\nu}\dfrac{dU}{dx}\right)^{\frac{1}{2}}$.

γ_1 =constant value of $\delta_1\left(\dfrac{1}{\beta\nu}\dfrac{dU}{dx}\right)^{\frac{1}{2}}$.

γ_2 =constant value of $\delta_2\left(\dfrac{1}{\beta\nu}\dfrac{dU}{dx}\right)^{\frac{1}{2}}$.

$\gamma', \gamma_1', \gamma_2'$=corresponding values derived from Pohlhausen's adaptation of the momentum equation.

τ_0 =shearing stress at the wall.

ρ =density of fluid (constant).

C_f $=\tau_0/\frac{1}{2}\rho U^2$, the coefficient of friction at the wall.

κ =thermometric conductivity of fluid.

σ $=\nu/\kappa$, Prandtl's number.

T =temperature in the boundary-layer.

T_0 =temperature of wall.

T_1 =temperature of main stream.

C_H $=\dfrac{\kappa}{(T_1-T_0)U}\left(\dfrac{\partial T}{\partial y}\right)_{y=0}$, the heat transfer coefficient at the wall.

Y $=\left(\dfrac{1}{\beta\nu}\dfrac{dU}{dx}\right)^{\frac{1}{2}} y$, a dimensionless variable.

F(Y)=function of Y defined by equations (7) and (8).

$G(Y)=\displaystyle\int_0^Y F(Y')dY'$.

$\theta(Y)$=function of Y defined by equations (38) and (39).

a $=\theta'(0)$

n =constant index in the approximate formula $C_H/\frac{1}{2}C_f \propto \sigma^n$.

---

1. *General.*

The equation of steady two-dimensional laminar flow near the wall of a cylindrical obstacle reduces to

$$u\frac{\partial u}{\partial x}+v\frac{\partial u}{\partial y}=U\frac{\partial U}{\partial x}+\nu\frac{\partial^2 u}{\partial y^2}. \quad \text{. . . . . . .} \quad (1)$$

With this equation are associated the equation of continuity for an incompressible fluid,

$$\frac{\partial u}{\partial x}+\frac{\partial v}{\partial y}=0, \quad \ldots \ldots \ldots \ldots \quad (2)$$

and the boundary conditions

$$\left.\begin{array}{l} u=0,\ v=0 \text{ on } y=0, \\ u\to U \text{ as } y\to\infty \end{array}\right\}. \quad \ldots \ldots \ldots \quad (3)$$

It has been proved (1) that the above equations admit a solution in which there are similar velocity profiles in different sections of the boundary layer, *i. e.* in which

$$u=\theta(x)f\left\{\frac{y}{\phi(x)}\right\} \quad \ldots \ldots \ldots \quad (4)$$

for some functions θ, f, ϕ, only in the particular cases in which (a) $U\propto x^m$ and (b) $U\propto e^{\alpha x}(\alpha>0)$. Clearly $\phi(x)$ is then a measure of the boundary-layer thickness and $\theta(x)$ a measure of the mainstream velocity. In both cases it is convenient to use the dimensionless parameter

$$Y=\left(\frac{1}{\beta\nu}\frac{dU}{dx}\right)^{\frac{1}{2}}y, \quad \ldots \ldots \ldots \quad (5)$$

in terms of which the solution of equations (1) to (3) is

$$u=UF'(Y)\,; \quad v=-\left(\frac{\nu}{\beta}\frac{dU}{dx}\right)^{\frac{1}{2}}\{F(Y)+(\beta-1)YF'(Y)\}, \quad \ldots \quad (6)$$

where F(Y) satisfies the differential equation

$$F'''+FF''=\beta[(F')^2-1] \quad \ldots \ldots \ldots \quad (7)$$

and the boundary conditions

$$F(0)=0\,; \quad F'(0)=0\,; \quad F'(Y)\to 1 \text{ as } Y\to\infty. \quad \ldots \ldots \quad (8)$$

The value of β is $2m/(m+1)$ in the case (a) $U\propto x^m$ and $\beta=2$ in the case (b) $U\propto e^{\alpha x}$. The convention that $\frac{1}{\beta}\frac{dU}{dx}$ be interpreted as $\frac{1}{2}\frac{U}{x}$ in the case $\beta=0$ ($m=0$) is convenient in order to avoid treating this as a special case. In the sequel, general formulæ are written in such a form that they apply, with this convention, to cases (a)—whether or not m is zero—and (b).

The numerical integration of equation (7) with the boundary conditions (8) has been considered by Hartree (2) for particular values of β between $-0{\cdot}199$ and $2{\cdot}4$, a range which includes the cases (a), $m\geqslant -0{\cdot}090$, and (b). The results are used in the following sections as a basis for obtaining further numerical results concerning laminar boundary-layers associated with the same values of β.

Pohlhausen's approximate method of solution (3) of the boundary-layer equations depends essentially on the use of an equation of the type (4) with the further assumption that $f\{y/\phi(x)\}$ can be considered as a polynomial of the fourth degree in $y/\phi(x)$. It is therefore of interest to compare approximate results derived on the basis of these assumptions with results obtained on the basis of Hartree's figures in the cases for which equation (4) is strictly valid. Such a comparison is a test of the validity of Pohlhausen's approximate method under the most favourable circumstances.

Pohlhausen's result for the velocity distribution is

$$u=\mathrm{U}\{(2\eta-2\eta^3+\eta^4)+\tfrac{1}{6}\lambda\eta(1-\eta)^3\}, \quad \ldots \ldots \quad (9)$$

where

$$\eta=\frac{y}{\delta'}, \quad \ldots \ldots \quad (10)$$

and

$$\lambda=\frac{\delta'^2}{\nu}\frac{d\mathrm{U}}{dx}. \quad \ldots \ldots \quad (11)$$

The boundary conditions $u=0$ when $y=0$ and $u=\mathrm{U}$ when $y=\delta'$ are satisfied, so that $\delta'=\delta'(x)$ is to be regarded as the thickness of the boundary-layer. The momentum equation, which reduces to

$$\frac{d}{dx}\left(\lambda\Big/\frac{d\mathrm{U}}{dx}\right)=\frac{g(\lambda)}{\mathrm{U}}+\left(\lambda\Big/\frac{d\mathrm{U}}{dx}\right)^2\frac{d^2\mathrm{U}}{dx^2}h(\lambda) \quad \ldots \ldots \quad (12)$$

in this case, must be satisfied. The functions $g(\lambda)$ and $h(\lambda)$ are defined by

$$g(\lambda)\equiv\frac{15120-2784\lambda+79\lambda^2+\frac{5}{3}\lambda^3}{(12-\lambda)\left(37+\frac{25}{12}\lambda\right)} \quad \ldots \ldots \quad (13)$$

and

$$h(\lambda)\equiv\frac{8+\frac{5}{3}\lambda}{(12-\lambda)\left(37+\frac{25}{12}\lambda\right)}, \quad \ldots \ldots \quad (14)$$

and are tabulated (4) for values of λ between -12 and $+12$.

2. *Boundary-layer Thickness.*

The thickness $\delta(x)$ of the boundary-layer may be defined as the value of y at which u differs from $\mathrm{U}(x)$ by a fixed small fraction ϵ. Thus the curve $y=\delta(x)$ is given by

$$\mathrm{F}'(\mathrm{Y})=1-\epsilon$$

or

$$\mathrm{Y}=\gamma(\epsilon).$$

Hence

$$\delta=\gamma\left(\frac{1}{\beta\nu}\frac{d\mathrm{U}}{dx}\right)^{-\frac{1}{2}}, \quad \ldots \ldots \quad (15)$$

where γ is a constant depending on ϵ and defined by

$$\mathrm{F}'(\gamma)=1-\epsilon. \quad \ldots \ldots \quad (16)$$

The displacement thickness $\delta_1(x)$ and the momentum thickness $\delta_2(x)$ defined by

$$\delta_1(x)=\int_0^\infty\left(1-\frac{u}{\mathrm{U}}\right)dy$$

and
$$\delta_2(x)=\int_0^\infty \frac{u}{\mathrm{U}}\left(1-\frac{u}{\mathrm{U}}\right)dy,$$

give
$$\delta_1=\gamma_1\left(\frac{1}{\beta\nu}\frac{d\mathrm{U}}{dx}\right)^{-\frac{1}{2}}, \quad \ldots\ldots\ldots \quad (17)$$

and
$$\delta_2=\gamma_2\left(\frac{1}{\beta\nu}\frac{d\mathrm{U}}{dx}\right)^{-\frac{1}{2}}, \quad \ldots\ldots\ldots \quad (18)$$

where, from equations (5) and (6),

$$\gamma_1=\int_0^\infty [1-\mathrm{F}'(\mathrm{Y})]\,d\mathrm{Y} \quad \ldots\ldots\ldots \quad (19)$$

TABLE I.

Values of $\delta\left(\frac{1}{\beta\nu}\frac{d\mathrm{U}}{dx}\right)^{\frac{1}{2}}$.

β.	$\gamma(0{\cdot}1)$.	$\gamma(0{\cdot}01)$.	$\gamma(0{\cdot}001)$.	γ'.	γ_1.	γ_1'.	γ_2.	γ_2'.
—0·198$_8$	3·72	4·78$_5$	5·5$_4$	5·878	2·359	2·100	0·585	0·703
—0·19	3·35	4·42	5·2$_0$	5·680	2·007	1·994	0·577	0·680
—0·18	3·21	4·28	5·0$_5$	5·496	1·871	1·898	0·567$_5$	0·659
—0·16	3·02$_5$	4·10	4·8$_5$	5·211	1·707	1·752	0·552	0·625
—0·14	2·89	3·97	4·7$_4$	4·991	1·597	1·642	0·538	0·598
—0·10	2·70	3·78	4·5$_7$	4·658	1·443	1·482	0·515	0·555
0	2·39	3·47	4·2$_5$	4·126	1·217	1·238	0·469$_6$	0·485
+0·1	2·19	3·26	4·0$_4$	3·787	1·080	1·091	0·435	0·438
0·2	2·03	3·09	3·8$_9$	3·542	0·984	0·988$_5$	0·408	0·404
0·3	1·91	2·97	3·7$_5$	3·352	0·911	0·911	0·386	0·378
0·4	1·81	2·85	3·6$_4$	3·198	0·853	0·850$_5$	0·366$_5$	0·356
0·5	1·72	2·75	3·5	3·071	0·804$_5$	0·801	0·350	0·338
0·6	1·64	2·65	3·4	2·963	0·764	0·759	0·336	0·322$_5$
0·8	1·52	2·51	3·3	2·789	0·699	0·692	0·312	0·297
1·0	1·41$_5$	2·38	3·1	2·656	0·648	0·641	0·292	0·277$_5$
1·2	1·33	2·27	3·0	2·551	0·607	0·599	0·276	0·261
1·6	1·20	2·09	2·8	2·409	0·544	0·536	0·250	0·236
2·0	1·10	1·99	2·6	2·449$_5$	0·497	0·490	0·231	0·218

and
$$\gamma_2=\int_0^\infty \mathrm{F}'(\mathrm{Y})[1-\mathrm{F}'(\mathrm{Y})]\,d\mathrm{Y}. \quad \ldots\ldots\ldots \quad (20)$$

Values of γ for $\epsilon=0{\cdot}1$, $0{\cdot}01$, $0{\cdot}001$ and of γ_1 and γ_2 are given in Table I. Values of $\gamma(\epsilon)$ and γ_1 are easily obtained from the numerical results given by Hartree; to find γ_2 use is made of the relation

$$\mathrm{F}''(0)=(1+\beta)\int_0^\infty \mathrm{F}'(1-\mathrm{F}')\,d\mathrm{Y}+\beta\int_0^\infty (1-\mathrm{F}')\,d\mathrm{Y}, \quad \ldots \quad (21)$$

which follows either from the momentum equation in the form

$$\frac{\nu}{\mathrm{U}^2}\left(\frac{\partial u}{\partial y}\right)_{y=0}=\frac{d\delta_2}{dx}+\frac{1}{\mathrm{U}}\frac{d\mathrm{U}}{dx}(\delta_1+2\delta_2), \quad \ldots\ldots \quad (22)$$

or on integration of equation (7) with respect to Y with the assumption of the property

$$\operatorname*{Lt.}_{Y\to\infty} \{F(1-F')\}=0$$

for the function F(Y).

The boundary-layer thickness $\delta'(x)$ in the approximate solution can be written as

$$\delta'=\gamma'\left(\frac{1}{\beta\nu}\frac{dU}{dx}\right)^{-\frac{1}{2}}, \quad . \quad . \quad . \quad . \quad . \quad . \quad . \quad . \quad (23)$$

where γ' is a constant. The parameter λ then has the constant value

$$\lambda=\beta\gamma'^2 \quad . \quad . \quad . \quad . \quad . \quad . \quad . \quad . \quad . \quad . \quad (24)$$

and the equation (12) reduces to

$$2(1-\beta)[\lambda h(\lambda)+1]\gamma'^2=g(\lambda). \quad . \quad . \quad . \quad . \quad . \quad . \quad . \quad (25)$$

(The forms of the last two equations are such that they are true for the limiting cases $\beta=0$ and $\beta=2$.) Equation (25) can be written in the form

$$\frac{\beta}{1-\beta}=\frac{g(\lambda)}{2\lambda[\lambda h(\lambda)+1]},$$

and therefore

$$\beta=k(\beta\gamma'^2), \quad . \quad . \quad . \quad . \quad . \quad . \quad . \quad . \quad . \quad (26)$$

where

$$k(\lambda)\equiv\frac{888\lambda-8\lambda^2-\frac{5}{6}\lambda^3}{15120-1896\lambda+71\lambda^2+\frac{5}{6}\lambda^3}. \quad . \quad . \quad . \quad . \quad . \quad (27)$$

A graph of $k(\lambda)$ is given in fig. 1. To avoid ambiguity in values of λ (*i. e.* of γ') for a fixed $\beta\left(-\frac{2}{9}\leqslant\beta\leqslant 2\right)$, it is convenient to use only the region $-12\leqslant\lambda\leqslant+12$. When this convention is adopted, the results derived in the approximate method of solution are unique and are found to agree fairly well with the exact results deduced from Hartree's solution of equation (7).

Values of γ', essentially positive, obtained by solving equation (26) for various β, are given in Table I.

On the basis of Pohlhausen's approximation, the displacement and momentum thicknesses are given by

$$\delta_1'=\gamma_1'\left(\frac{1}{\beta\nu}\frac{dU}{dx}\right)^{-\frac{1}{2}}, \quad . \quad . \quad . \quad . \quad . \quad . \quad . \quad . \quad . \quad (28)$$

$$\delta_2'=\gamma_2'\left(\frac{1}{\beta\nu}\frac{dU}{dx}\right)^{-\frac{1}{2}}, \quad . \quad . \quad . \quad . \quad . \quad . \quad . \quad . \quad . \quad (29)$$

where

$$\gamma_1'=\frac{\gamma'}{120}(36-\lambda), \quad . \quad . \quad . \quad . \quad . \quad . \quad . \quad . \quad . \quad . \quad (30)$$

$$\gamma_2'=\frac{\gamma'}{315}\left(37-\frac{\lambda}{3}-\frac{5\lambda^2}{144}\right). \quad . \quad . \quad . \quad . \quad . \quad . \quad . \quad (31)$$

The values of γ_1', γ_2' are easily found when γ' and $\lambda(=\beta\gamma'^2)$ are known, and are included in Table I.

Comparing the columns of Table I., it is possible to assess the accuracy to which results derived on the basis of Pohlhausen's approximation can be relied upon. The displacement thickness (given by γ_1') agrees with the exact value γ_1 to within 2 per cent. for positive values of β, but the error exceeds 2 per cent. for some negative β. The momentum thickness (given by γ_2') agrees with the exact value γ_2 to within 6 per cent. for positive β, but the error becomes much larger as β decreases from zero.

It is of interest also to compare γ' with $\gamma(\epsilon)$ for different values of ϵ. It is clear that the thickness δ' which occurs in Pohlhausen's approximate solution corresponds to a limit of the boundary-layer, where u differs from U by less than 1 per cent. in all cases.

Fig. 1.

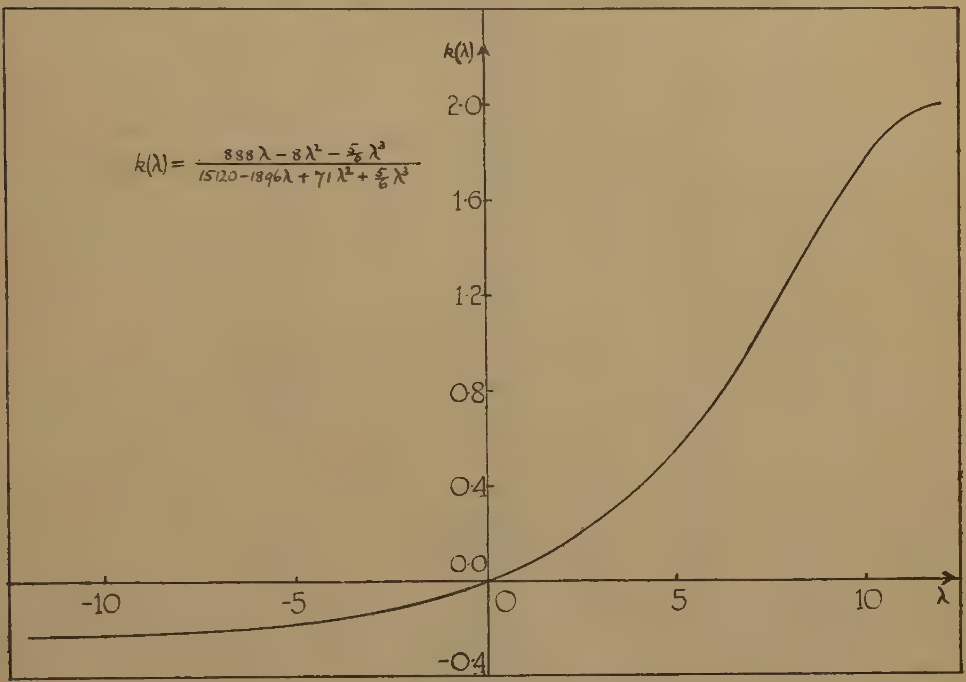

3. *Coefficient of Friction at the Wall.*

The shearing stress at the wall is given by

$$\frac{\tau_0}{\rho}=\nu\left(\frac{\partial u}{\partial y}\right)_{y=0}, \quad \ldots \ldots \ldots \quad (32)$$

and hence the coefficient of friction C_f is given by

$$\tfrac{1}{2}C_f=\frac{\tau_0}{\rho U^2}=\frac{F''(0)}{U}\left(\frac{\nu}{\beta}\frac{dU}{dx}\right)^{\frac{1}{2}}. \quad \ldots \ldots \ldots \quad (33)$$

(The formula in this form applies to the special cases $\beta=2$ and $\beta=0$, with the convention that $\dfrac{1}{\beta}\dfrac{dU}{dx}$ is to be interpreted as $\frac{1}{2}U/x$ in the case $\beta=0$.)

Pohlhausen's approximate formula for the friction coefficient is

$$\tfrac{1}{2}C_f=\frac{\nu}{U\delta'}\left(2+\frac{\lambda}{6}\right),$$

TABLE II.

Values of $\frac{1}{2}C_fU\left(\dfrac{\nu}{\beta}\dfrac{dU}{dx}\right)^{-\frac{1}{2}}$.

β.	$F''(0)$.	$\dfrac{1}{\gamma'}\left(2+\dfrac{\beta\gamma'^2}{6}\right)$.
$-0{\cdot}198_8$	0·0000	0·1455
−0·19	0·086	0·172
−0·18	$0{\cdot}128_5$	0·199
−0·16	$0{\cdot}190_5$	0·245
−0·14	$0{\cdot}239_5$	0·284
−0·10	$0{\cdot}319_1$	0·352
0	0·4696	0·485
+0·1	0·5870	0·591
0·2	$0{\cdot}686_9$	0·683
0·3	$0{\cdot}774_8$	0·764
0·4	$0{\cdot}854_2$	0·8385
0·5	$0{\cdot}927_7$	0·907
0·6	$0{\cdot}996_0$	0·971
0·8	1·120	1·089
1·0	1·2326	1·196
1·2	1·336	1·294
1·6	1·521	1·473
2·0	1·687	1·633

which can be written in terms of γ' and β as

$$\tfrac{1}{2}C_f=\frac{1}{\gamma'}\left(2+\frac{\beta\gamma'^2}{6}\right)\frac{1}{U}\left(\frac{\nu}{\beta}\frac{dU}{dx}\right)^{\frac{1}{2}}. \quad . \quad . \quad . \quad . \quad . \quad . \qquad (34)$$

Values of $\frac{1}{2}C_fU\left(\dfrac{\nu}{\beta}\dfrac{dU}{dx}\right)^{-\frac{1}{2}}$ from the exact and approximate solutions are given side by side in Table II. for values of β which are considered by Hartree (exact values are quoted from Hartree's paper).

A comparison of the columns of Table II. shows that Pohlhausen's approximation gives a value within about 3 per cent. of the exact one for $0\leqslant\beta\leqslant 2$, but that the approximate value is too large for $0>\beta\geqslant-0{\cdot}198_8$. In particular the value $C_f=0$ is not predicted for the case $\beta=-0{\cdot}198_8$ by Pohlhausen's method.

4. *Coefficient of Heat Transfer by Forced Convection to the Wall.*

The temperature equation for steady two-dimensional heat transfer by forced convection from a cylindrical wall through a laminar boundary-layer reduces to

$$u\frac{\partial \mathrm{T}}{\partial x}+v\frac{\partial \mathrm{T}}{\partial y}=\kappa\frac{\partial^2 \mathrm{T}}{\partial y^2}, \quad \dots\dots\dots \quad (35)$$

when heat generated by dissipation is neglected. This equation is to be solved with the boundary conditions

$$\left.\begin{array}{l}\mathrm{T}=\mathrm{T}_0 \text{ at } y=0,\\ \mathrm{T}\rightarrow\mathrm{T}_1 \text{ as } y\rightarrow\infty\end{array}\right\}. \quad \dots\dots\dots \quad (36)$$

T_0 and T_1 are taken as constants and the temperature differences are assumed to be so small that the velocity distribution is the same as for isothermal flow.

In the cases in which the velocity distribution is given by (6), a solution for T of the form T(Y) is possible. Writing

$$\mathrm{T}=\mathrm{T}_0+(\mathrm{T}_1-\mathrm{T}_0)\theta(\mathrm{Y}), \quad \dots\dots\dots \quad (37)$$

equation (35) becomes (in both cases (*a*) and (*b*))

$$\theta''(\mathrm{Y})+\sigma \mathrm{F}(\mathrm{Y})\theta'(\mathrm{Y})=0. \quad \dots\dots\dots \quad (38)$$

The boundary conditions are

$$\left.\begin{array}{l}\theta(0)=0,\\ \theta(\mathrm{Y})\rightarrow 1 \text{ as } \mathrm{Y}\rightarrow\infty\end{array}\right\}. \quad \dots\dots\dots \quad (39)$$

Writing $\mathrm{G}(\mathrm{Y})\equiv\int_0^{\mathrm{Y}}\mathrm{F}(\mathrm{Y})\,d\mathrm{Y}$, the solution of equations (38) and (39) is seen to be

$$\theta(\mathrm{Y})=a\int_0^{\mathrm{Y}}e^{-\sigma\mathrm{G}(\mathrm{Y})}\,d\mathrm{Y}, \quad \dots\dots\dots \quad (40)$$

where a is a function of σ and β defined by

$$\frac{1}{a}=\int_0^{\infty}e^{-\sigma\mathrm{G}(\mathrm{Y})}\,d\mathrm{Y}. \quad \dots\dots\dots \quad (41)$$

It is convenient to note also that

$$\frac{1}{a^2}\frac{\partial a}{\partial \sigma}=\int_0^{\infty}\mathrm{G}(\mathrm{Y})e^{-\sigma\mathrm{G}(\mathrm{Y})}\,d\mathrm{Y}. \quad \dots\dots\dots \quad (42)$$

The Appendix deals with the computation of the integrals involved in (41) and (42) for any chosen values of β and σ.

The heat transfer coefficient, $\mathrm{C_H}$, may be defined by

$$\mathrm{C_H}=\frac{\kappa}{(\mathrm{T}_1-\mathrm{T}_0)\mathrm{U}}\left(\frac{\partial \mathrm{T}}{\partial y}\right)_{y=0}.$$

Hence

$$\mathrm{C_H}=\frac{1}{\mathrm{U}}\left(\frac{\nu}{\beta}\frac{d\mathrm{U}}{dx}\right)^{\frac{1}{2}}\frac{\theta'(0)}{\sigma}; \quad \dots\dots\dots \quad (43)$$

and, from (33),

$$\frac{\mathrm{C_H}}{\frac{1}{2}\mathrm{C}_f}=\frac{\theta'(0)}{\sigma\mathrm{F}''(0)}. \quad \dots\dots\dots \quad (44)$$

Since $\theta'(0)=a$, the values of $C_H U\left(\frac{\nu}{\beta}\frac{dU}{dx}\right)^{-\frac{1}{2}}$ are obtainable from the Appendix, and are tabulated in Table III. for various values of β and σ. The ratios $C_H/\frac{1}{2}C_f$ are given in Table IV. Fig. 2 shows similar information graphically.

TABLE III.

Values of $C_H U\left(\frac{\nu}{\beta}\frac{dU}{dx}\right)^{-\frac{1}{2}}$.

β.	$\theta'(0)/\sigma$.				
	$(\sigma=0{\cdot}6)$.		$(\sigma\doteqdot 1{\cdot}0)$.	$(\sigma=7{\cdot}0)$.	
$-0{\cdot}198_8$	0·472	(0·473)	$0{\cdot}326\sigma^{-0{\cdot}730}$	0·077	(0·079)
0·0	0·653	(0·654)	$0{\cdot}4696\sigma^{-0{\cdot}649}$	$0{\cdot}130_5$	(0·133)
0·5	0·739	(0·741)	$0{\cdot}539\sigma^{-0{\cdot}622}$	0·156	(0·161)
1·0	0·777	$(0{\cdot}779_5)$	$0{\cdot}570_5\sigma^{-0{\cdot}611}$	0·168	(0·174)
1·6	0·805	(0·808)	$0{\cdot}594\sigma^{-0{\cdot}602}$	0·178	(0·184)
2·0	0·819	(0·821)	$0{\cdot}605\sigma^{-0{\cdot}597}$	$0{\cdot}182_5$	(0·189)

Values in brackets are those obtained by substituting $\sigma=0{\cdot}6$ or $\sigma=7{\cdot}0$ in the formula of the type $C_H \propto \sigma^n$ valid near $\sigma=1$.

TABLE IV.

Values of $C_H/\frac{1}{2}C_f$.

σ. β.	0·6.	Approx. 1·0.	7·0.
$-0{\cdot}198_8$	∞	∞	∞
0·0	1·390	$1{\cdot}000\sigma^{-0{\cdot}649}$	0·2779
0·5	0·796	$0{\cdot}581\sigma^{-0{\cdot}622}$	0·168
1·0	0·631	$0{\cdot}463\sigma^{-0{\cdot}611}$	0·137
1·6	0·529	$0{\cdot}390\sigma^{-0{\cdot}602}$	0·117
2·0	0·485	$0{\cdot}359\sigma^{-0{\cdot}597}$	0·108

The ratio $C_H/\frac{1}{2}C_f$ may conveniently be quoted as approximately of the form $A\sigma^n$ for values of σ not differing very widely from unity (3), A being independent of σ. If, for σ approximately equal to σ_1,

$$\frac{C_H}{\frac{1}{2}C_f}\propto\sigma^n,$$

then, from (44),

$$a(=\theta'(0)\propto\sigma^{n+1}.$$

Hence

$$\left(\frac{1}{a}\frac{\partial a}{\partial\sigma}\right)_{\sigma=\sigma_1}=\frac{n+1}{\sigma_1}$$

or
$$n=\sigma_1\left(\frac{1}{a}\frac{\partial a}{\partial \sigma}\right)_{\sigma=\sigma_1}-1. \quad . \quad . \quad . \quad . \quad . \quad . \quad . \quad . \qquad (45)$$

Appropriate values of n for different β are obtained in this way in the Appendix for the case $\sigma_1=1$. Tables III. and IV. include values of $C_H U\left(\frac{\nu}{\beta}\frac{dU}{dx}\right)^{-\frac{1}{2}}$ and $C_H/\frac{1}{2}C_f$ in the neighbourhood of $\sigma=1$, which involve a power of σ. It is seen (fig. 2 and Table III.) that the values of C_H corresponding to $\sigma=0\cdot6$ and $\sigma=7\cdot0$ are in agreement with the approximate formula $C_H \propto \sigma^n$ (valid near $\sigma=1$) with errors of, at most, $\frac{1}{3}$ per cent. and 4 per cent. respectively. This result indicates that the range of σ in which the formula $C_H \propto \sigma^n$ is approximately valid extends at least from $\sigma=0\cdot6$ to $\sigma=7\cdot0$ for the range of values of β included in the graphs.

Fig. 2.

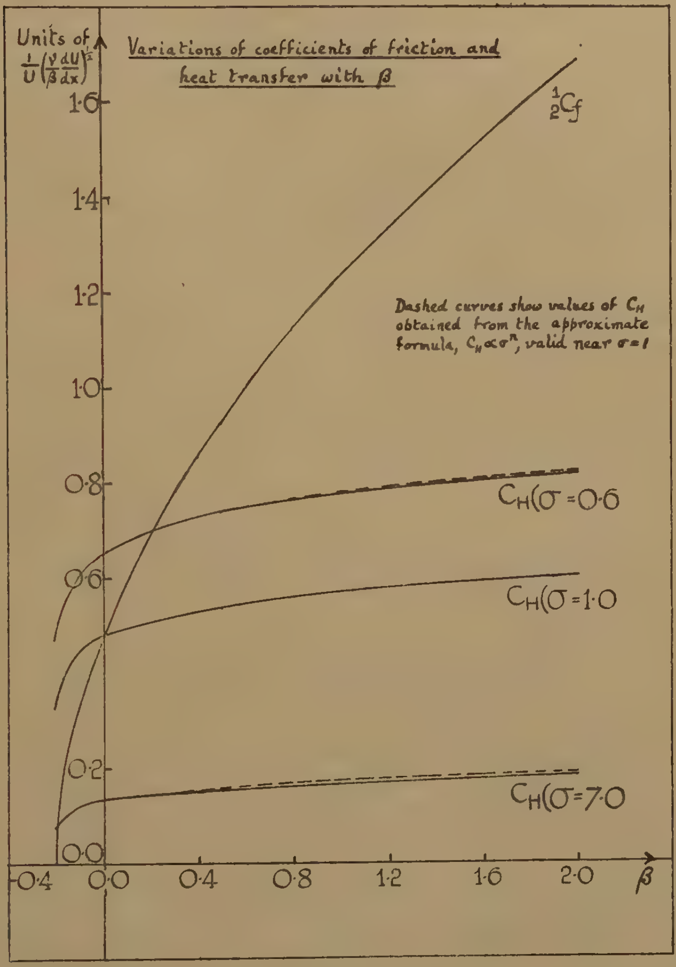

The general conclusion to be drawn from fig. 2 is that while C_H varies roughly as $\frac{1}{U}\left(\frac{\nu}{\beta}\frac{dU}{dx}\right)^{\frac{1}{2}}$ for a given σ $(\beta \geqslant 0)$, $\frac{1}{2}C_f$ increases much more rapidly with β. More precisely, if $C_H/\frac{1}{2}C_f \doteqdot A\sigma^n$, A is unity when $\beta=0$ and decreases markedly as β increases; on the other hand, n lies within the range $-0{\cdot}60 \geqslant n \geqslant -0{\cdot}73$ for all β considered.

APPENDIX.

Extension of functions tabulated in a finite range for integration from 0 *to* ∞.

(i) $F'(Y)$ is tabulated by Hartree⁽²⁾ as increasing from $F'(0)=0$ to $F'(Y_1)=1{\cdot}0000$. Since $F'(Y)\to 1$ as $Y\to\infty$ and is an increasing function, we take $F'(Y)=1$ for $Y \geqslant Y_1$ with a possible error of less than 1 in 20,000.

(ii) $F(Y)$ is obtained by integrating $F'(Y)$ numerically. It increases from $F(0)=0$ to $F(Y_1)=F_1$. We take

$$F=F_1-Y_1+Y \text{ for } Y \geqslant Y_1$$

to conform with (i).

(iii) $G(Y)$ is obtained by numerical integration of $F(Y)$ and increases from $G(0)=0$ to $G(Y_1)=G_1$. We take

$$G=G_1-\tfrac{1}{2}F_1^2+\tfrac{1}{2}(F_1-Y_1+Y)^2 \text{ for } Y \geqslant Y_1.$$

(iv) $\int_0^{Y_1} e^{-\sigma G}\,dY$ is found by numerical integration. Using (iii) we have

$$\int_{Y_1}^{\infty} e^{-\sigma G}\,dY=\sqrt{\frac{\pi}{2\sigma}}\,e^{-\sigma(G_1-\frac{1}{2}F_1^2)}\left(1-\operatorname{erf}\sqrt{\frac{\sigma}{2}}F_1\right).$$

Hence, from (41),

$$\frac{1}{a}=\int_0^{Y_1} e^{-\sigma G}\,dY+\sqrt{\frac{\pi}{2\sigma}}\,e^{-\sigma(G_1-\frac{1}{2}F_1^2)}\left(1-\operatorname{erf}\sqrt{\frac{\sigma}{2}}F_1\right). \quad . \quad . \quad (46)$$

(v) $\int_0^{Y_1} Ge^{-\sigma G}\,dY$ is found by numerical integration. Using (iii),

$$\int_{Y_1}^{\infty} Ge^{-\sigma G}\,dY=\left(G_1-\tfrac{1}{2}F_1^2+\frac{1}{2\sigma}\right)\int_{Y_1}^{\infty} e^{-\sigma G}\,dY+\frac{F_1}{2\sigma}e^{-\sigma G_1}.$$

Hence, from (42),

$$\frac{1}{a^2}\frac{\partial a}{\partial \sigma}=\int_0^{Y_1} Ge^{-\sigma G}\,dY+\left(G_1-\tfrac{1}{2}F_1^2+\frac{1}{2\sigma}\right)\int_{Y_1}^{\infty} e^{-\sigma G}\,dY+\frac{F_1}{2\sigma}e^{-\sigma G_1}. \quad (47)$$

The use of the assumption $F'(Y)=1$ (exactly) for $Y \geqslant Y_1$ in deriving the results (46) and (47) is justified if the contributions to $\frac{1}{a}$ and $\frac{1}{a^2}\frac{\partial a}{\partial \sigma}$ from integration between Y_1 and ∞ are small. This is seen to be so from the summary of the calculations in Table V.

Numerical integrations to find a and n as suggested in (iv) and (v)

TABLE V.

Summary of calculations of a (for σ=0·6, σ=0·7, σ=1·0) and of n (appropriate to the neighbourhood of σ=1·0).

β	−0·198$_8$	0·0	0·5	1·0	1·6	2·0
Y_1	6·2	5·2	4·4	4·0	3·6	3·4
F_1	3·8413	3·9833	3·5955$_5$	3·3521	3·0561	2·9025
G_1	7·9064	8·2842	6·6715$_5$	5·7679	4·7820	4·3087$_5$
(*a*) σ=0·6						
$\int_0^{Y_1} e^{-\sigma G}\,dY$	3·5280	2·5504	2·2481	2·1305	2·0424	1·9979
$\int_{Y_1}^{\infty} e^{-\sigma G}\,dY$	0·0034$_5$	0·0027	0·0076$_5$	0·0139	0·0279	0·0375
$\frac{1}{a}$	3·5314	2·5531	2·2558	2·1444	2·0703$_5$	2·0354
(*b*) σ=7·0						
$\int_0^{Y_1} e^{-\sigma G}\,dY$	1·8532$_5$	1·0947	0·9147$_5$	0·8486	0·8035	0·7826
$\int_{Y_1}^{\infty} e^{-\sigma G}\,dY$	0·0000	0·0000	0·0000	0·0000	0·0000	0·0000
$\frac{1}{a}$	1·8532$_5$	1·0947	0·9147$_5$	0·8486	0·8035	0·7826
(*c*) σ=1·0						
$\int_0^{Y_1} e^{-\sigma G}\,dY$	3·0692	—	1·8550	1·7521	1·6814	1·6481
$\int_{Y_1}^{\infty} e^{-\sigma G}\,dY$	0·0001	—	0·0003	0·0009	0·0025	0·0042
$\frac{1}{a}$	3·0693	2·129$_5$	1·8553	1·7529	1·6839	1·6523
$\int_0^{Y_1} Ge^{-\sigma G}\,dY$	0·8270	—	0·6980	0·6765	0·6561	0·6431
$\int_{Y_1}^{\infty} Ge^{-\sigma G}\,dY$	0·0008	—	0·0025	0·0058	0·0143	0·0220
$\frac{1}{a^2}\frac{\partial a}{\partial \sigma}$	0·8278	0·7475	0·7005	0·6823	0·6704	0·6652
n	−0·730	−0·649	−0·622	−0·611	−0·602	−0·597

are unnecessary in the special case $\beta=0$, $\sigma=1$, for then equation (7) reduces to

$$F'''+FF''=0,$$

giving $$G(Y)=\int_0^Y F(Y)\,dY=-\int_0^Y \frac{F'''(Y)}{F''(Y)}\,dY=\log\frac{F''(0)}{F''(Y)}$$

and $$\int_0^\infty e^{-G}\,dY=\frac{1}{F''(0)}.$$

Then $$a=\theta'(0)=F''(0).$$

Also $$a\int_0^\infty Ge^{-G}\,dY=\int_0^\infty F''(Y)G(Y)\,dY=G_1-\tfrac{1}{2}F_1^2,$$

so that $$n=G_1-\tfrac{1}{2}F_1^2-1.$$

This value is $-0{\cdot}649$, which corresponds to Pohlhausen's value (3), $n=-\frac{2}{3}$.

The values of a for the cases $\beta=0$, $\beta=1$ are in agreement with the values of $\alpha_1(\alpha)/\sqrt{2}$, $\alpha_3(\sigma)$ in ' Modern Developments in Fluid Dynamics ' (Oxford, 1938), pp. 624, 632, except for a $\frac{1}{2}$ per cent. discrepancy in the case $\beta=0$, $\sigma=0{\cdot}6$.

References.

(1) Goldstein, Proc. Camb. Phil. Soc. xxxv. (1939), p. 338.
(2) Hartree, Proc. Camb. Phil. Soc. xxxiii. (1937), pp. 223–239.
(3) Pohlhausen, *Zeitschr. f. angew. Math. u. Mech.* i. (1921), pp. 115–120, 252–268.
(4) Howarth, A. R. C. Reports and Memoranda, No. 1632 (1935), pp. 14–22.

LXXIII. *Heat Conduction in Elliptical Cylinder and an Analogous Electromagnetic Problem.*

By N. W. McLachlan, D.Sc.*

[Received November 21, 1944.]

1. *The Differential Equation.*

We treat the case where the cylinder is long enough in comparison with its major axis for end effect to be neglected. If θ is temperature, κ diffusivity, and t time, the two-dimensional equation for heat transmission, expressed in rectangular co-ordinates, is

$$\frac{\partial^2\theta}{\partial x^2}+\frac{\partial^2\theta}{\partial y^2}-\frac{1}{\kappa}\frac{\partial\theta}{\partial t}=0. \quad \text{. . . . .} \quad (1)$$

---

* Communicated by the Author.

Let $\theta-\theta_0=\theta_1=f(x, y)e^{-\kappa\nu^2 t}$, where $f(x, y)$ is a function independent of t, and ν is a parameter explained later. Then

$$\frac{\partial\theta}{\partial t}=-\kappa\nu^2\theta, \quad . \quad . \quad . \quad . \quad . \quad . \quad . \quad . \quad . \quad (2)$$

and on substituting into (1), we obtain

$$\frac{\partial^2 f}{\partial x^2}+\frac{\partial^2 f}{\partial y^2}+\nu^2 f=0. \quad . \quad . \quad . \quad . \quad . \quad . \quad . \quad . \quad (3)$$

We have now to transform (3) to elliptical co-ordinates (ξ, η), where $x=h\cosh\xi\cos\eta$, $y=h\sinh\xi\sin\eta$, $2h$ being the common interfocal distance for the family of confocal ellipses and hyperbolas. By substitution, $f=e^{i\nu x}$ is found to satisfy (3). Thus, when the latter is expressed in elliptical co-ordinates, $f_1(\xi, \eta)=e^{i\nu h\cosh\xi\cos\eta}$ will be a solution. Then

$$\frac{\partial^2 f_1}{\partial\xi^2}=(-\nu^2h^2\sinh^2\xi\cos^2\eta+i\nu h\cosh\xi\cos\eta)f_1; \quad . \quad . \quad . \quad (4)$$

$$\frac{\partial^2 f_1}{\partial\eta^2}=(-\nu^2h^2\cosh^2\xi\sin^2\eta-i\nu h\cosh\xi\cos\eta)f_1; \quad . \quad . \quad (5)$$

so
$$\frac{\partial^2 f_1}{\partial\xi^2}+\frac{\partial^2 f_1}{\partial\eta^2}+\nu^2h^2(\cosh^2\xi\sin^2\eta+\sinh^2\xi\cos^2\eta)f_1=0, \quad . \quad . \quad (6)$$

or
$$\frac{\partial^2 f_1}{\partial\xi^2}+\frac{\partial^2 f_1}{\partial\eta^2}+2k^2(\cosh 2\xi-\cos 2\eta)f_1=0, \quad . \quad . \quad . \quad . \quad . \quad . \quad . \quad (7)^*$$

with $k^2=\frac{1}{4}\nu^2h^2=q$.

2. *Solution of* (7), §1.

Write $f_1(\xi, \eta)=\chi(\xi)\psi(\eta)$, where χ is a function of ξ alone and ψ one of η alone. Dividing throughout by $\chi\,\psi$, we obtain after rearrangement,

$$-\frac{1}{\psi}\frac{d^2\psi}{d\eta^2}+2k^2\cos 2\eta=\frac{1}{\chi}\frac{d^2\chi}{d\xi^2}+2k^2\cosh 2\xi. \quad . \quad . \quad . \quad . \quad (1)$$

Now the l.h.s. is independent of ξ, and the r.h.s. of η, so each must be a constant, say, a. Thus we get the two ordinary equations

$$\frac{d^2\psi}{d\eta^2}+(a-2k^2\cos 2\eta)\psi=0, \quad . \quad . \quad . \quad . \quad . \quad . \quad . \quad (2)$$

and
$$\frac{d^2\chi}{d\xi^2}-(a-2k^2\cosh 2\xi)\chi=0. \quad . \quad . \quad . \quad . \quad . \quad . \quad . \quad (3)$$

a is called the separation constant. (2) is the canonical form of Mathieu's equation, while (3) can be derived from (2) on writing $i\xi$ for η. $\psi(\eta)$, the solutions of (2), are defined to be Mathieu functions, while those of (3) are *modified*† Mathieu functions, $\chi(\xi)$. A solution of (1), §1, in elliptical co-ordinates is, therefore,

$$\theta_1(\xi, \eta, t)=f_1(\xi, \eta)e^{-\kappa\nu^2 t}=\chi(\xi)\psi(\eta)e^{-\kappa\nu^2 t}. \quad . \quad . \quad . \quad . \quad . \quad (4)$$

---

* The method of transformation used here is not rigorous, but it is simple and effective !

‡ This is analogous to the standard nomenclature for Bessel Functions.

3. *Particular Form of Solution.*

The appropriate forms of $\chi(\xi)$, $\psi(\eta)$ in (4), § 2, are governed by physical conditions. Herein we consider a case where the temperature distribution is symmetrical about both axes of the bounding ellipse. Thus $\psi(\eta)$ must be even, single-valued and periodic in η, with period π. The only solution of (2), § 3, having these properties is the even Mathieu function of the first kind of even integral order, namely,

$$ce_{2n}(\eta, k^2)=\sum_{r=0}^{\infty} A_{2r}^{(2n)} \cos 2r\eta, \quad \ldots \ldots \quad (1)$$

where $n=0, 1, 2, \ldots$ and the coefficients $A_{2r}^{(2n)}$ are continuous functions of k^2, a and k^2 being real numbers.

Writing $i\xi$ for η in (1) yields the solution of (3), § 2, for the same values of a, k^2, as in (2), § 2, and we get a modified Mathieu function of the first kind, namely,

$$Ce_{2n}(\xi, k^2)=\sum_{r=0}^{\infty} A_{2r}^{(2n)} \cosh 2r\xi. \quad \ldots \ldots \quad (2)$$

A second solution of (3), § 2, corresponding to (2), may be expressed in the form

$$Fe_{2n}(\xi, k^2)=C_{2n}(k^2)\left[\xi Ce_{2n}(\xi, k^2)+\sum_{r=0}^{\infty} f_{2r+2}^{(2n)} \sinh(2r+2)\xi\right], \quad . \quad (3)$$

$C_{2n}(k^2)$ being a continuous function of k^2 which vanishes therewith, while the $f_{2r+2}^{(2n)}$ are also c.f. of k^2.

The conditions to be fulfilled in crossing the major axis orthogonally are—for symmetry about this axis—

(*a*) continuity of temperature at any $t>0$, *i. e.* $\chi(0)\psi(\eta)=\chi(0)\psi(-\eta)$;

(*b*) continuity of temperature gradient at any $t>0$, *i. e.*

$$\psi(\eta)\frac{\partial}{\partial\xi}[\chi(\xi)]_{\xi\to 0}=-\psi(-\eta)\frac{\partial}{\partial\xi}[\chi(\xi)]_{\xi\to 0};$$

(*c*) we also have $\theta>0$ when $t>0$, $\xi=0$.

If we take $\chi(\xi)\psi(\eta)=Ce_{2n}(\xi, k^2)ce_{2n}(\eta, k^2)$, (*a*), (*b*) and (*c*) are satisfied. With $\chi\psi=Fe_{2n}(\xi)ce_{2n}(\eta)$, although (*a*) is satisfied, (*b*), (*c*) are not. Thus if C_{2n} is an arbitrary constant *,

$$\chi_{2n}(\xi)\psi_{2n}(\eta)=C_{2n}Ce_{2n}(\xi, k^2)ce_{2n}(\eta, k^2), \quad \ldots \ldots \quad (4)$$

is an appropriate particular solution of (7), § 1. Since (4) satisfies this equation for all positive integral values of n, it follows that the formal solution of (1), § 1, expressed in elliptical co-ordinates, is

$$\theta-\theta_0=f_1(\xi, \eta)e^{-\kappa\nu^2 t}=\sum_{n=0}^{\infty} C_{2n}Ce_{2n}(\xi, k^2)ce_{2n}(\eta, k^2)e^{-\kappa\nu^2 t}. \quad . \quad . \quad (5)$$

---

* This is *not* $C_{2n}(k^2)$.

4. *Incorporation of Boundary Conditions.*

We take the simple conditions that

(*a*) $\theta=0$, $t<0$ throughout the cylinder,

(*b*) $\theta=\theta_0$, $t\geqslant 0$, at the surface, where $\xi=\xi_0$,

and (*c*) $\theta\to\theta_0$, $t\to+\infty$, $0\leqslant\xi\leqslant\xi_0$.

The problem is to determine the temperature at any internal point of the cylinder when $t>0$. At the surface $\xi=\xi_0$, and when $t\geqslant 0$, $\theta-\theta_0=\theta_1=0$ for all η, so by (5), § 3,

$$\mathrm{Ce}_{2n}(\xi_0, k^2)=0. \qquad (1)$$

Thus k^2 has those values $k^2_{2n,m}$ which make $\mathrm{Ce}_{2n}(\xi_0, k^2)$ vanish, *i. e.* the parametric zeros of the function. For each value of n, $m=1, 2, 3, \ldots.$ Now as $t\to-0$, $\theta=0$, so $\theta_1=-\theta_0$, and (5), § 3, becomes

$$-\theta_0=\sum_{n=0}^{\infty}\sum_{m=1}^{\infty} \mathrm{C}_{2n}\mathrm{Ce}_{2n}(\xi, k^2_{2n,m})\mathrm{ce}_{2n}(\eta, k^2_{2n,m}), \qquad (2)$$

so we have to determine the coefficients C_{2n}. For this purpose we employ the orthogonality theorem given in Appendix I. Accordingly we multiply each side of (2) by

$$(\cosh 2\xi-\cos 2\eta)\mathrm{Ce}_{2p}(\xi, k^2_{2p,r})\mathrm{ce}_{2p}(\eta, k^2_{2p,r}), \qquad (3)$$

and integrate with respect to η from 0 to 2π, and to ξ from 0 to ξ_0. Then, by Appendix I., the r.h.s. vanishes except when $p=n$, $r=m$, so

$$-\theta_0\int_0^{\xi_0}\int_0^{2\pi}\mathrm{Ce}_{2n}(\xi, k^2_{2n,m})\mathrm{ce}_{2n}(\eta, k^2_{2n,m})(\cosh 2\xi-\cos 2\eta)\,d\xi\,d\eta$$

$$=\mathrm{C}_{2n}\int_0^{\xi_0}\int_0^{2\pi}\mathrm{Ce}^2_{2n}(\xi, k^2_{2n,m})\mathrm{ce}^2_{2n}(\eta, k^2_{2n,m})\,(\cosh 2\xi-\cos 2\eta)\,d\xi\,d\eta. \quad (4)$$

Taking individual integrals, we have

$$\int_0^{2\pi}\mathrm{ce}_{2n}(\eta, k^2_{2n,m})\cos 2\eta\,d\eta=\pi\mathrm{A}_2^{(2n)}\,; \quad \int_0^{2\pi}\mathrm{ce}_{2n}(\eta, k^2_{2n,m})\,d\eta=2\pi\mathrm{A}_0^{(2n)}\,;$$

$$\int_0^{2\pi}\mathrm{ce}^2_{2n}(\eta, k^2_{2n,m})\cos 2\eta\,d\eta=0\,; \quad \int_0^{2\pi}\mathrm{ce}^2_{2n}(\eta, k^2_{2n,m})d\eta=\pi \text{ (by definition)}. \qquad (5)$$

Hence (4) may be written

$$\pi\theta_0\int_0^{\xi_0}\mathrm{Ce}_{2n}(\xi, k^2_{2n,m})[\mathrm{A}_2^{(2n)}-2\mathrm{A}_0^{(2n)}\cosh 2\xi]\,d\xi$$

$$=\pi\mathrm{C}_{2n}\int_0^{\xi_0}\mathrm{Ce}^2_{2n}(\xi, k^2_{2n,m})\cosh 2\xi\,d\xi, \qquad (6)$$

so

$$\mathrm{C}_{2n}=\frac{\theta_0\displaystyle\int_0^{\xi_0}\mathrm{Ce}_{2n}(\xi, k^2_{2n,m})[\mathrm{A}_2^{(2n)}-2\mathrm{A}_0^{(2n)}\cosh 2\xi]\,d\xi}{\displaystyle\int_0^{\xi_0}\mathrm{Ce}^2_{2n}(\xi, k^2_{2n,m})\cosh 2\xi\,d\xi}. \qquad (7)$$

Using (7) in (5), § 3, we obtain

$$\theta=\theta_0\left\{1-\sum_{n=0}^{\infty}\sum_{m=1}^{\infty}e^{-\kappa\nu^2_{2n,m}t}\mathrm{Ce}_{2n}(\xi,k^2_{2n,m})\mathrm{ce}_{2n}(\eta,k^2_{2n,m})\times\frac{\int_0^{\xi_0}\mathrm{Ce}_{2n}(\xi)[2\mathrm{A}_0^{(2n)}\cosh 2\xi-\mathrm{A}_2^{(2n)}]\,d\xi}{\int_0^{\xi_0}\mathrm{Ce}^2_{2n}(\xi)\cosh 2\xi\,d\xi}\right\}, \quad . \quad (8)$$

where $\nu^2_{2n,m}h^2=4k^2_{2n,m}$. Since the factor in (8), which involves integrals, is independent of ξ, η, it follows from (5), § 3, that (8) is a solution of (1), § 1, when the latter is expressed in elliptical co-ordinates. Also it satisfies the boundary conditions.

5. *Transition to Circular Cylinder.*

When the eccentricity of a confocal ellipse within a cross-section of the cylinder tends to zero, $h\rightarrow 0$, and it may be shown that

$$(a) \qquad \mathrm{ce}_{2n}(\eta,k^2)\rightarrow\cos 2n\phi,$$

ϕ being the angle any radius vector makes with the X axis,

$$(b) \qquad \mathrm{Ce}_{2n}(\xi,k^2)\rightarrow p'_{2n}\mathrm{J}_{2n}(k_1r),$$

p'_{2n} being a constant *, $k_1=\nu_{2n,m}$, and r is the radius of the circle into which the ellipse degenerates. Thus (5), § 3, becomes

$$\theta_1=\sum_{n=0}^{\infty}\mathrm{C}_{2n}p'_{2n}\mathrm{J}_{2n}(k_1r)\cos 2n\phi\,.\,e^{-\kappa k_1^2t}. \quad . \quad . \quad . \quad . \quad (1)$$

For a circular cylinder, the boundary conditions in § 4 are such that θ_1 is independent of ϕ, so all the terms of (1) vanish except for $n=0$. Thus from a physical viewpoint †, we must have

$$\theta_1=\mathrm{C}_0p'_0\mathrm{J}_0(k_1r)e^{-\kappa k_1^2t}. \quad . \quad . \quad . \quad . \quad . \quad . \quad . \quad . \quad (2)$$

At the surface when $t\geqslant 0$;

$$r=a, \quad \theta_1=0, \quad \text{so} \quad k_1a=\alpha_{0,m}, \quad m=1, 2, 3, \ldots,$$

these being the roots of $\mathrm{J}_0(k_1a)=0$. Also, as $e\rightarrow 0$,

$$\xi\rightarrow+\infty, \quad \sinh\xi\rightarrow\cosh\xi, \quad r\rightarrow h\cosh\xi \ (h\rightarrow 0),$$
$$dr\rightarrow h\sinh\xi\,d\xi, \quad \cosh 2\xi\,d\xi\rightarrow 2\cosh\xi\sinh\xi\,d\xi\simeq 2r\,dr/h^2.$$

Using the latter and $\mathrm{Ce}_0(\xi,k^2_{0,m})\rightarrow p'_0\mathrm{J}_0(\alpha_{0,m}r/a)$, $\mathrm{ce}_0(\eta,k^2_{0,m})\rightarrow 1\sqrt{2}$,

$$\mathrm{A}_0^{(0)}=1/\sqrt{2}, \quad \mathrm{A}_2^{(0)}\rightarrow 0 \ [\text{as } e\rightarrow 0, \text{ and } k^2_{0,m}\rightarrow 0], \quad \nu^2_{0,m}\rightarrow\alpha^2_{0,m}/a^2;$$

---

* See (2), Appendix 3.

† See Appendix 4 for mathematical proof.

(8), § 4, degenerates to

$$\theta=\theta_0\left\{1-\sum_{m=1}^{\infty}e^{-\kappa\alpha^2_m t/a^2}\mathrm{J}_0(\alpha_m r/a)\frac{\int_0^a r\mathrm{J}_0(\alpha_m r/a)\,dr}{\int_0^a r\mathrm{J}_0^2(\alpha_m r/a)\,dr}\right\}, \quad . \quad . \quad (3)$$

where α_m replaces $\alpha_{0,m}$. Evaluating the integrals in (3) leads to the well-known result, namely,

$$\theta=\theta_0\left\{1-2\sum_{m=1}^{\infty}\frac{\mathrm{J}_0(\alpha_m r/a)}{\alpha_m\mathrm{J}_1(\alpha_m)}e^{-\kappa\alpha^2_m t/a^2}\right\}. \quad . \quad . \quad . \quad . \quad . \quad (4)^*$$

6. *Solenoid with Metal Core of Elliptical Cross-Section.*

We shall consider a long uniformly wound solenoid of length l with n turns, having a uniform homogeneous metal core of elliptical cross-section. The metal has resistivity ρ, constant permeability μ, and H_0, the magnetizing force at the curved surface, is assumed to be uniform. At time $t=0$, a battery is connected to the solenoid through a high resistance R, such that the time taken for the current to reach a substantially constant value I_0 is small enough to be ignored. Thus for analytical purposes the current-time relationship is Heaviside's unit function. The problem is to calculate the magnetizing force at any point in a cross-section of the core, and thence to find the inductance (variable) of the solenoid due to the core flux alone, when $t>0$.

7. *Differential Equation for* H.

It can be shown that in cartesian co-ordinates, the equation for H at any point (x, y) of a cross-section of the core is

$$\frac{\partial^2\mathrm{H}}{\partial x^2}+\frac{\partial^2\mathrm{H}}{\partial y^2}-\frac{4\pi\mu}{\rho}\frac{\partial\mathrm{H}}{\partial t}=0. \quad . \quad . \quad . \quad . \quad . \quad . \quad (1)$$

If in (1), § 1, we write H for θ and $4\pi\mu/\rho$ for $1/\kappa$, the equation is identical with (1) above. Hence *mutatis mutandis*, (5), § 3, is a formal solution of the latter, so we have

$$\mathrm{H}-\mathrm{H}_0=\sum_{n=0}^{\infty}\mathrm{C}_{2n}\mathrm{Ce}_{2n}(\xi, k^2)ce_{2n}(\eta, k^2)e^{-\rho\nu^2t/4\pi\mu}. \quad . \quad . \quad . \quad (2$$

8. *Incorporation of Boundary Conditions.*

These are

$$\left.\begin{aligned}&(a)\ \mathrm{H}=0, \quad t<0;\\&(b)\ \mathrm{H}=\mathrm{H}_0=4\pi n\mathrm{I}_0/l, \quad t\geqslant 0 \text{ at the surface where } \xi=\xi_0;\\&(c)\ \mathrm{H}\to\mathrm{H}_0, \quad t\to+\infty, \quad 0\leqslant\xi\leqslant\xi_0.\end{aligned}\right\} \quad . \quad . \quad (1)$$

If we write θ for H, conditions (1) are identical with those in § 4. Hence (8), § 4, gives the solution for H, provided H be written for θ, and

---

* McLachlan, 'Complex Variable and Operational Calculus,' p. 69.

$\rho/4\pi\mu$ for κ. Accordingly the magnetizing force at any point (ξ, η) of a cross-section of the core is

$$\mathrm{H}=\frac{4\pi n\mathrm{I}_0}{l}\left\{1-\sum_{n=0}^{\infty}\sum_{m=1}^{\infty}e^{-\rho\nu^2_{2n,m}t/4\pi\mu}\mathrm{Ce}_{2n}(\xi, k^2_{2n,m})ce_{2n}(\eta, k^2_{2n,m})\right.$$
$$\left.\times\frac{\int_0^{\xi_0}\mathrm{Ce}_{2n}(\xi)[\mathrm{A}_0^{(2n)}\cosh 2\xi-\mathrm{A}_2^{(2n)}]\,d\xi}{\int_0^{\xi_0}\mathrm{Ce}^2_{2n}(\xi)\cosh 2\xi\,d\xi}\right\}. \quad (2)$$

When the ellipse tends to a circle, this expression degenerates to a known form for a metal core of circular cross-section[*].

9. *Inductance arising from Core Flux alone.*

This is defined to be the total flux interlinkage when unit current (constant) flows in the n turn winding. If Φ is the total core flux, then

$$\mathrm{L}=\frac{n\Phi}{\mathrm{I}_0}=\frac{\mu n}{\mathrm{I}_0}\iint\mathrm{H}\,ds_1\,ds_2, \quad \ldots\ldots\ldots \quad (1)$$

where $ds_1\times ds_2$ is an elemental area of cross-section. Now

$$ds_1=\frac{h}{\sqrt{2}}(\cosh 2\xi-\cos 2\eta)^{\frac{1}{2}}\,d\xi,$$

and

$$ds_2=\frac{h}{\sqrt{2}}(\cosh 2\xi-\cos 2\eta)^{\frac{1}{2}}\,d\eta,$$

so

$$\mathrm{L}=\tfrac{1}{2}\frac{h^2\mu n}{\mathrm{I}_0}\int_0^{\xi_0}\int_0^{2\pi}\mathrm{H}\,(\cosh 2\xi-\cos 2\eta)\,d\xi\,d\eta. \quad \ldots\ldots \quad (2)$$

Using (2), § 8, in (2), and employing formulæ (5), § 4, leads to

$$\mathrm{L}=\frac{4\pi^2n^2ab\mu}{l}\left\{1-\frac{h^2}{2ab}\sum_{n=0}^{\infty}\sum_{m=1}^{\infty}e^{-\rho\nu^2_{2n,m}t/4\pi\mu}\right.$$
$$\left.\times\frac{\left[\int_0^{\xi_0}\mathrm{Ce}^2_{2n}(\xi, k^2_{2n,m})[2\mathrm{A}_0^{(2n)}\cosh 2\xi-\mathrm{A}_2^{(2n)}]\,d\xi\right]^2}{\int_0^{\xi_0}\mathrm{Ce}^2_{2n}(\xi, k^2_{2n,m})\cosh 2\xi\,d\xi}\right\}. \quad (3)$$

In obtaining (3) we used the relationships $h=ae$, $b=a(1-e^2)^{\frac{1}{2}}$, $\cosh\xi_0=e^{-1}$, $\sinh\xi_0=(1-e^2)^{\frac{1}{2}}e^{-1}$, where a, b are the semi axes, and e is the eccentricity of the bounding ellipse.

When the ellipse tends to a circle, (3) degenerates to a known form[†].

The author has pleasure in acknowledging valuable suggestions by Mr. T. Lewis, M.A.

---

[*] 'Complex Variable and Operational Calculus,' p. 242.

[†] 'Complex Variable and Operational Calculus,' p. 240.

APPENDIX I.

Orthogonality Theorem.—Let $k^2_{n,m}$ be such that for n a positive integer, $m=1, 2, \ldots$, and $\xi=\xi_0$, $\chi_n(\xi_0, k^2_{n,m})=0$, where χ_n is a solution of (3), § 2. Then if a, k^2 are real, the point $(a_{n,m}, k^2_{n,m})$ lies on the characteristic or (a, k^2) curve for the function $\psi_n(\eta, k^2)$. For instance the (a, k^2) curve for $ce_n(\eta, k^2)$ is also that for $\mathrm{Ce}_n(\xi, k^2)$, the a, k^2 being identical for the same n[*]. It follows that we may write [see (2), (3), § 2]

$$\frac{d^2\psi_n}{d\eta^2}+(a_{n,m}-2k^2_{n,m}\cos 2\eta)\psi_n=0, \quad \ldots \quad (1)$$

and

$$\frac{d^2\chi_n}{d\xi^2}-(a_{n,m}-2k^2_{n,m}\cosh 2\xi)\chi_n=0. \quad \ldots \ldots \quad (2)$$

We remark that if $\psi_n=ce_{n,m}$, or $se_{n,m}$, these functions do not satisfy the usual orthogonal relations, since $ce_{n,m}$, $ce_{p,r}$ have different values of k^2, as also have $se_{n,m}$. $se_{p,r}$, $n\neq p$, $m\neq r$.

Write $\zeta_{n,m}=\psi_n\chi_n$, then for $(a_{n,m}, k^2_{n,m})$ we have

$$\frac{\partial^2\zeta_{n,m}}{\partial\xi^2}+\frac{\partial^2\zeta_{n,m}}{\partial\eta^2}+2k^2_{n,m}(\cosh 2\xi-\cos 2\eta)\zeta=0. \quad \ldots \quad (3)$$

Also for $(a_{p,r}, k^2_{p,r})$

$$\frac{\partial^2\zeta_{p,r}}{\partial\xi^2}+\frac{\partial^2\zeta_{p,r}}{\partial\eta^2}+2k^2_{n,m}(\cosh 2\xi-\cos 2\eta)\zeta_{p,r}=0. \quad \ldots \quad (4)$$

Multiplying (3) by $\zeta_{p,r}$, (4) by $\zeta_{n,m}$ and subtracting the second from the first, we obtain

$$\frac{\partial}{\partial\xi}\left[\zeta_{p,r}\frac{\partial\zeta_{n,m}}{\partial\xi}-\zeta_{n,m}\frac{\partial\zeta_{p,r}}{\partial\xi}\right]+\frac{\partial}{\partial\eta}\left[\zeta_{p,r}\frac{\partial\zeta_{n,m}}{\partial\eta}-\zeta_{n,m}\frac{\partial\zeta_{p,r}}{\partial\eta}\right]$$
$$+2(k^2_{n,m}-k^2_{p,r})(\cosh 2\xi-\cos 2\eta)\zeta_{n,m}\zeta_{p,r}=0. \quad . \quad (5)$$

Integrating with respect to ξ from 0 to ξ_0, and to η from 0 to 2π, we get

$$\int_0^{2\pi}\left[\zeta_{p,r}\frac{\partial\zeta_{n,m}}{\partial\xi}-\zeta_{n,m}\frac{\partial\zeta_{p,r}}{\partial\xi}\right]_0^{\xi_0}d\eta+\int_0^{\xi_0}\left[\zeta_{p,r}\frac{\partial\zeta_{n,m}}{\partial\eta}-\zeta_{n,m}\frac{\partial\zeta_{p,r}}{\partial\eta}\right]_0^{2\pi}d\xi$$
$$+2(k^2_{n,m}-k^2_{p,r}\int_0^{\xi_0}\int_0^{2\pi}(\cosh 2\xi-\cos 2\eta)\zeta_{n,m}\zeta_{p,r}\,d\xi\,d\eta=0. \quad (6)$$

If $\zeta_{n,m}=\mathrm{Ce}_{n,m}ce_{n,m}$ or $\mathrm{Se}_{n,m}se_{n,m}$, $\zeta_{p.r}=\mathrm{Ce}_{p,r}ce_{p,r}$ or $\mathrm{Se}_{p,r}se_{p,r}$, the first integral vanishes at $\xi=0$, ξ_0, while the second vanishes by virtue of its periodicity in η—period 2π or π according as n is odd or even. Hence it follows that the last integral is also zero if $p\neq n$, *i. e.*

$$\int_0^{\xi_0}\int_0^{2\pi}(\cosh 2\xi-\cos 2\eta)\zeta_{n,m}\zeta_{p,r}\,d\xi\,d\eta=0. \quad \ldots \ldots \quad (7)$$

This holds also if $p=n$, $r\neq m$. When $p=n$, $r=m$, the double integral does not vanish, and we get

$$\int_0^{\xi_0}\int_0^{2\pi}\left.\begin{matrix}\mathrm{Ce}^2_{n,m}(\xi)ce^2_{n,m}(\eta)\\ \mathrm{Se}^2_{n,m}(\xi)se^2_{n,m}(\eta)\end{matrix}\right\}(\cosh 2\xi-\cos 2\eta)\,d\xi\,d\eta=\pi\int_0^{\xi_0}\left.\begin{matrix}\mathrm{Ce}^2_{n,m}(\xi)\\ \mathrm{Se}^2_{n,m}(\xi)\end{matrix}\right\}\cosh 2\xi\,d\xi.$$
$$\ldots \quad (8)$$[†]

---

[*] See Phil Mag. xxxvi. p. 404, fig. 1 (1945).

[†] The evaluation of these integrals will be given in a later publication.

APPENDIX II.

Parametric zeros of $\mathrm{Ce}_{2n}(\xi, k^2)$, *i. e.* $k^2_{2n,m}$, *when* ξ *is large and positive.*

Under this condition, we have [*]

$$\mathrm{Ce}_{2n}(\xi, k^2) \sim \frac{ce_{2n}(o, k^2)ce_{2n}(\tfrac{1}{2}\pi, k^2)}{\mathrm{A}_0^{(2n)}} \sqrt{\frac{2}{\pi k e^{\xi}}} \cos(ke^{\xi} - \tfrac{1}{4}\pi), \quad . \quad . \quad (1)$$

where $k^2 > 0$. Hence the zeros occur approximately when

$$\cos(ke^{\xi} - \tfrac{1}{4}\pi) = 0, \quad . \quad . \quad . \quad . \quad . \quad . \quad . \quad . \quad . \quad . \quad . \quad (2)$$

or

$$ke^{\xi} - \tfrac{1}{4}\pi = (m + \tfrac{1}{2})\pi,$$

i. e.

$$ke^{\xi} = (m + \tfrac{3}{4})\pi, \quad . \quad . \quad . \quad . \quad . \quad . \quad . \quad . \quad . \quad (3)$$

Thus

$$k^2_{2n,m} = (m + \tfrac{3}{4})^2\pi^2 e^{-2\xi}. \quad . \quad . \quad . \quad . \quad . \quad . \quad . \quad . \quad (4)$$

It follows that as $\xi \to +\infty$, $k^2_{2n,m} \to 0$, so the parametric zeros condense in the neighbourhood of $k^2 = 0$, $n = 0, 1, 2, \ldots$.

From (3) the large zeros in ξ are given for $n = 0, 1, 2 \ldots$, by

$$\xi = \log[(m + \tfrac{3}{4})\pi/k], \quad . \quad . \quad . \quad . \quad . \quad . \quad . \quad . \quad . \quad (5)$$

where k is any real number > 0, and m is any integer such that ke^{ξ} is large enough for (1) to hold. Formula (1) shows that $\mathrm{Ce}_{2n}(\xi, k^2) \to 0$ as $\xi \to +\infty$.

APPENDIX III.

Parametric zeros of $\mathrm{Ce}_{2n}(\xi, k^2)$ *when the ellipse tends to a circle.*

Under this condition $\mathrm{Ce}_{2n}(\xi, k^2) \to p'_{2n}\mathrm{J}_{2n}(k_1 r)$, where $k_1 r \sim ke^{\xi}$, $2k = k_1 h$. When $k_1 r$ is large enough

$$\mathrm{J}_{2n}(k_1 r) \sim (-1)^n \sqrt{\frac{2}{\pi k_1 r}} \cos(k_1 r - \tfrac{1}{4}\pi), \quad . \quad . \quad . \quad . \quad . \quad . \quad (1)$$

so by (1) and (1) Appendix II., the large zeros in $k_1 r$ and ke^{ξ} are alike. If we let $\xi \to +\infty$, it follows from these two formulæ that

$$p'_{2n} = (-1)^n \frac{ce_{2n}(o)ce_{2n}(\tfrac{1}{2}\pi)}{\mathrm{A}_0^{(2n)}}. \quad . \quad . \quad . \quad . \quad . \quad . \quad . \quad . \quad (2)$$

For a circular cylinder of radius a, the zeros of $\mathrm{J}_{2n}(k_1 a)$ are $\alpha_{2n,m} = k_1 a$, $m = 1, 2, 3, \ldots$ where the subscripts $2n$, m are tacitly implied for k_1. Now $k_1 = 2k_{2n,m}/h$, so

$$\alpha_{2n,m} = k_1 a = 2k_{2n,m}a/h$$

and

$$k^2_{0,m} = \alpha^2_{0,m}h^2/4a^2. \quad . \quad . \quad . \quad . \quad . \quad . \quad . \quad . \quad . \quad (3)$$

But

$$k^2_{0,m} = \tfrac{1}{4}\nu^2_{0,m}h^2,$$

so

$$\nu^2_{0,m} = \alpha^2_{0,m}/a^2. \quad . \quad . \quad . \quad . \quad . \quad . \quad . \quad . \quad . \quad . \quad (4)$$

---

[*] S. Goldstein, Trans. Camb. Phil. Soc. xxiii. p. 303 (1927).

APPENDIX IV.

Proof that for $n>0$, $C_{2n}(\xi)C_{2n}/\theta_0 \to 0$ *as the ellipse tends to a circle.*

Then $h\to 0$, $k^2\to 0$, all the $A^{(2n)}_{\left.\begin{smallmatrix}0\\2\end{smallmatrix}\right\}}\to 0$ except for $n=\left.\right\}\begin{smallmatrix}0\\1\end{smallmatrix}$, when $A^{(2n)}_{\left.\begin{smallmatrix}0\\2\end{smallmatrix}\right\}}\to 1$. Thus we have to prove that $Ce_2(\xi)C_2\to 0$ with h. Then $Ce_2(\xi)\to p_2'J_2(k_1r)$, so by aid of the degenerate forms below (2), § 5, we get

$$\lim_{h\to 0} -Ce_2(\xi)C_2 = \lim_{h\to 0}\frac{J_2(k_1r)\int_0^a J_2(k_1r)\left[\frac{4A_0^{(2)}r}{h^2}-\frac{A_2^{(2)}}{r}\right]dr}{(2/h^2)\int_0^a J_2{}^2(k_1r)r\,dr} \quad . \quad . \quad (1)$$

$$= \lim_{h\to 0}\frac{J_2(k_1r)\int_0^a J_2(k_1r)[2A_0^{(2)}r-A_2^{(2)}h^2/2r]\,dr}{\int_0^a J_2{}^2(k_1r)r\,dr}. \quad . \quad . \quad (2)$$

As $h\to 0$, $A_0^{(2)}\to 0$, the integral in the numerator $\to 0$, but that in the denominator >0. Hence the theorem has been proved.

LXXIV. *An Expression for following the Process of Refinement in X-ray Structure Analysis using Fourier Series.*

By A. D. BOOTH *.

[Received October 15, 1945.]

IT has long been known that the expression

$$R_1 = \frac{\sum_{hkl}\big|\,|F_{\text{obs}}(hkl)|-|F_{\text{calc}}(hkl)|\,\big|}{\sum_{hkl}|F_{\text{obs}}(hkl)|} \quad . \quad . \quad . \quad . \quad . \quad . \quad (1)$$

tends to a minimum as the trial structure, whose Fourier coefficients are $F_{\text{calc}}(hkl)$, approaches the true one—defined by the observed coefficients and the possible molecular shape. This minimum varies with the type of structure investigated from 0·12 for oxalic acid(1) to 0·15 for dibenzyl(2) and 0·18 for geranylamine hydrochloride(3). It is usually accepted that a structure determination is reliable if $R_1<0{\cdot}20$.

If it were possible to calculate $F(hkl)$ from a quantum mechanical model of the molecular system, the value of R_1 would be greatly reduced, the present large values being due to the only approximate validity of the assumptions made in deducing the values of $F(hkl)$ from the atomic co-ordinates. The residual value of R_1 would be due then to experimental errors in $F_{\text{obs}}(hkl)$. An examination of the independent sets of $|F|$(obs) for dibenzyl, obtained by Jeffrey and Robertson ((2) *loc cit.*), shows that in this case R_1(residual)$=0{\cdot}05$ against the normal $R_1=0{\cdot}15$ quoted above.

---

* Communicated by Sir Lawrence Bragg, F.R.S.

The value of R_1 is still, despite these objections, a very reliable criterion of the progress of any particular structure analysis and its value would be greatly enhanced were it possible to say, for example, that when $R_1<0{\cdot}3$, none of the co-ordinates was in error by more than 0·1 A.

Unfortunately the form of R_1, involving as it does moduli, is mathematically intractable, and in the course of examining the whole question the author was led to consider the expression :

$$R_2=\frac{\sum\limits_{hkl}(|F_{\text{obs}}|-|F_{\text{calc}}|)^2}{\sum\limits_{hkl}|F_{\text{obs}}|^2}; \quad . \quad . \quad . \quad . \quad . \quad . \quad . \quad . \quad . \qquad (2)$$

the results of this examination will be given in the following treatment, in which it will be seen that R_2 can be expressed in terms of the deviations between the true and approximate co-ordinates.

Notation.

As in a previous paper (4), the following contracted notation will be adopted.

$$\sum_3=\sum\sum_{-hkl}^{+hkl}\sum,$$

$$\sum_3^{\infty}=\sum\sum_{-\infty}^{+\infty}\sum,$$

$$\theta=2\pi\left(h\frac{x}{a}+k\frac{y}{b}+l\frac{z}{c}\right),$$

$\alpha=\alpha(hkl)$—the phase angle,

$F_0=F_{\text{obs}}(hkl)$—the observed structure factor,

$F_c=F_{\text{calc}}(hkl)$—the calculated structure factor.

Treatment in Three Dimensions.

It has been shown that the electron density at any point (xyz) in the unit cell of a crystal can be represented by

$$\rho(x,y,z)=\frac{1}{V}\sum_3|F|\cos(\theta-\alpha), \quad . \quad . \quad . \quad . \quad . \quad . \quad . \qquad (3)$$

whence, for the observed and calculated density distributions—

$$\rho_0-\rho_c=\frac{1}{V}\sum_3\{|F_0|-|F_c|\}\cos(\theta-\alpha), \quad . \quad . \quad . \quad . \quad . \quad . \qquad (4)$$

since the phase angle, being derived from the trial structure, is the same for F_0 and F_c.

We thus have

$$\int_V(\rho_0-\rho_c)^2dV=\frac{1}{V^2}\int_V\Big[\sum_3\{|F_0|-|F_c|\}\cos(\theta-\alpha)\Big]^2dV, \quad . \quad . \qquad (5)$$

where the integration extends over the unit cell. Using the elementary properties of the trigonometrical integral (5) reduces to

$$\int_V(\rho_0-\rho_L)^2dV=\frac{1}{V}\sum\{|F_0|-|F_c|\}^2, \quad . \quad . \quad . \quad . \quad . \qquad (6)$$

whence
$$\sum_{3} \{|\mathrm{F}_0|-|\mathrm{F}_c|\}^2=\mathrm{V}\int_{\mathrm{V}}(\rho_0-\rho_c)^2\,d\mathrm{V}, \quad . \quad . \quad . \quad . \quad . \quad (7)$$

and similarly
$$\sum_{3} |\mathrm{F}_0|^2=\mathrm{V}\int_{\mathrm{V}}(\rho_0)^2\,d\mathrm{V}. \quad . \quad . \quad . \quad . \quad . \quad . \quad . \quad (8)$$

Now the density distribution over a unit cell can be written to a good approximation⁽⁵⁾ :—

$$\rho(x,y,z)=\sum_{r=1}^{\mathrm{M}}\left(\frac{p_r}{\pi}\right)^{3/2}\mathrm{N}_r e^{-p_r\{(x-x_r)^2+(y-y_r)^2+(z-z_r)^2\}}, \quad . \quad . \quad . \quad (9)$$

where M is the number of atoms in the unit cell and $(x_r y_r z_r)$ are the co-ordinates of a particular atom, p_r being constant. N_r is the atomic number of the rth atom.

Using (9) we obtain

$$(\rho_0-\rho_c)=\sum_{r=1}^{\mathrm{M}}\mathrm{N}_r\left\{\left(\frac{p_r}{\pi}\right)^{3/2}e^{-p_r\{(x-x_r)^2+(y-y_r)^2+(z-z_r)^2\}}\right.$$
$$\left.-\left(\frac{p_r'}{\pi}\right)^{3/2}e^{-p_r'\{(x-x_r')^2+\ldots\}}\right\}, \quad . \quad . \quad . \quad . \quad . \quad (10)$$

where it is assumed that the characteristics of true and calculated atomic peaks are different. Assuming that the real and calculated atomic positions are not very different:

$$(\rho_0-\rho_c)^2 \simeq \sum_{r=1}^{\mathrm{M}}\mathrm{N}_r^2\left\{\left(\frac{p_r}{\pi}\right)^3 e^{-2p_r\{(x-x_r)^2+\ldots\}}+\left(\frac{p_r'}{\pi}\right)^3 e^{-2p_r'\{(x-x_r')^2+\ldots\}}\right.$$
$$\left.-2\left(\frac{p_r p_r'}{\pi^2}\right)^{3/2}e^{-\{[(p_r+p_r')x^2-2(p_r x_r+p_r' x_r')x+p\,x_r^2+p_r' x_r'^2]+\ldots\}}\right\}, \quad . \quad (11)$$

since cross-products of the type $(r.s)$ will all be very small.

The true density distributions are periodic functions and this can be introduced into (11) by writing $(x-\lambda a)$ for x, $(y-\mu b)$ for y and $(z-\nu c)$ for z and summing for all integral values of (λ,μ,ν) from $-\infty$ to $+\infty$. Making this assumption (7) becomes

$$\sum_{3}\{|\mathrm{F}_0|-|\mathrm{F}_c|\}^2=\mathrm{V}\sum_{r=1}^{\mathrm{M}}\mathrm{N}_r^2\iiint_0^{abc}\sum_{\substack{3\\ \lambda,\mu,\nu}}^{\infty}\left\{\left(\frac{p_r}{\pi}\right)^3\right.$$
$$\left.\times e^{-2p_r\{(x-xr-\lambda a)^2\ldots\}}+\ldots\right\}dx\,dy\,dz$$
$$=\mathrm{V}\sum_{-1}^{\mathrm{M}}\mathrm{N}^2\iiint_{-\infty}^{+}\left\{\left(\frac{p_r}{\pi}\right)^3\right.$$
$$\left.\times e^{-2p_r\{(x-x_r)^2+(y-y_r)^2+(z-z_r)^2\}}+\ldots\right\}dx\,dy\,dz$$
$$=\mathrm{V}\sum_{r=1}^{\mathrm{M}}\mathrm{N}_r^2\left[\left(\frac{p_r}{2\pi}\right)^{3/2}+\left(\frac{p_r'}{2\pi}\right)^{3/2}-2\left(\frac{p_r p_r'}{\pi(p_r-p_r')}\right)^{3/2}\right.$$
$$\left.\times e^{-\frac{p_r p_r'}{p_r+p_r'}\{(x_r-x_r')^2+\ldots\}}\right]. \quad . \quad . \quad . \quad . \quad (12)$$

And similarly
$$\sum_{3}|\mathrm{F}_0|^2=\mathrm{V}\sum_{r=1}^{\mathrm{M}}\mathrm{N}_r^2\left(\frac{p_r}{2\pi}\right)^{3/2}, \quad . \quad . \quad . \quad . \quad . \quad . \quad (13)$$

whence

$$R_2=\frac{\sum_{r=1}^{M} N_r^2\left[p_r^{3/2}+p_r'^{3/2}-2\left(\frac{2p_rp_r'}{p_r+p_r'}\right)^{3/2}e^{-\frac{p_rp_r'}{p_r+p_r'}\{(x_r-x_r')^2+\dots\}}\right]}{\sum_{r=1}^{M} N_r^2p_r^{3/2}}. \quad . \quad (14)$$

If, as is usual, the trial structure is approximately correct so that (x_r-x_r'), etc., are small, (14) may be written

$$R_2\simeq\frac{\sum_{r=1}^{M} N_r^2\left[p_r^{3/2}-2\left(\frac{2p_rp_r'}{p_r+p_r'}\right)^{3/2}+p_r'^{3/2}+\left(\frac{2p_rp_r'}{p_r+p_r'}\right)^{5/2}\{\delta x_r^2+\delta y_r^2+\delta z_r^2\}\right]}{\sum_{r=1}^{M} N_r^2p_r^{3/2}}, \quad . \quad . \quad (15)$$

where $\delta x_r=(x_r-x_r')$, etc.

It is seen from (15) that when the trial structure becomes equivalent, as regards atomic co-ordinates, to the true structure, R_2 attains a minimum value :

$$R_2(\min)\simeq\sum_{r=1}^{M} N_r^2\left[p_r^{3/2}-2\left(\frac{2p_rp_r'}{p_r+p_r'}\right)^{3/2}+p_r'^{3/2}\right]\Big/\sum_{r=1}^{M} N_r^2p_r^{3/2}. \quad . \quad . \quad (16)$$

The author has shown (5) that p_r' is approximately constant for a large number of atoms, and assuming

$$kp_r=p_r'=p,$$

equation (16) becomes

$$R_2(\min)\simeq\left[1+k^{3/2}-2\left(\frac{2k}{1+k}\right)^{3/2}\right]; \quad . \quad . \quad . \quad . \quad (17)$$

examination of several structures gives a mean value

$$\bar{R}_2(\min)=0{\cdot}05,$$

and it is easily calculated from (17) that

$$k=1{\cdot}231,$$

or

$$k\doteq 0{\cdot}769,$$

and since, in general, the true structure will have " sharper " atomic peaks than those calculated, the value $k=0{\cdot}769$ is to be taken.

Making the same assumption as that used in obtaining (17), (15) reduces to

$$R_2\simeq 0{\cdot}05+p_r\left(\frac{2k}{1+k}\right)^{5/2}\frac{\sum_{r=1}^{M} N_r^2(\delta x_r^2+\delta y_r^2+\delta z_r^2)}{\sum_{r=1}^{M} N_r^2}, \quad . \quad . \quad . \quad (18)$$

or, using the value of k given above, and the value $p'=4{\cdot}69$ given by the author(),

$$R_2=0{\cdot}05+4{\cdot}3\frac{\sum_{r=1}^{M} N_r^2(\delta x_r^2+\delta y_r^2+\delta z_r^2)}{\sum_{r=1}^{M} N_r^2}; \quad . \quad . \quad . \quad . \quad (19)$$

this equation may be taken as defininng a form of "R.M.S." error $\bar{\delta}$, being that error which, when applied to all co-ordinates in a structure, produces a given value of R_2. Its value is tabulated below :—

R_2	$\bar{\delta}$
0·05	0·000 A
0·10	0·062
0·15	0·088
0·20	0·108
0·25	0·124
0·30	0·139

Treatment in Two Dimensions.

In the case of two dimensional synthesis an exactly similar treatment yields the result

$$ {}_2R_2 = \frac{\sum_{r=1}^{M} N_r^2 \left[p_r + p_r' - \frac{4p_r p_r'}{p_r + p_r'} e^{-\frac{p_r p_r'}{p_r + p_r'} \{(x_r - x_r')^2 + (y_r - y_r')^2\}} \right]}{\sum_{r=1}^{M} N_r^2 p_r}, \quad . \quad . \quad (20) $$

which, using the same assumption of constancy of p_r' reduces to

$$ {}_2R_2 = \left[1 + k - 2\left(\frac{2k}{1+k}\right)\right] + p_r \left(\frac{2k}{1+k}\right)^2 \frac{\sum_{r=1}^{M} N_r^2 \{\delta x_r^2 + \delta y_r^2\}}{\sum_{r=1}^{M} N_r^2}. \quad . \quad . \quad . \quad (21) $$

Using the previous values of k and p' this becomes

$$ {}_2R_2 = 0{\cdot}029 + 4{\cdot}6 \frac{\sum_{r=1}^{M} N_r^2 \{\delta x_r^2 + \delta y_r^2\}}{\sum_{r=1}^{M} N_r^2}. \quad . \quad . \quad . \quad . \quad (22) $$

An actual trial on a final structure (6) for which $R_2(\text{min}) = 0{\cdot}05$ gave ${}_2R_2(\text{min}) = 0{\cdot}027$, quite satisfactory agreement. The function $\bar{\delta}_2$ defined in the same way as before is tabulated below :—

${}_2R_2$	$\bar{\delta}_2$
0·029	0·00 A
0·079	0·07
0·129	0·10
0·179	0·13
0·229	0·15
0·279	0·17

Treatment in One Dimension.

In this case it can be shown that

$$_1\mathrm{R}_2=\left[1+\sqrt{k}-2\sqrt{\frac{2k}{1+k}}\right]+p_r\left(\frac{2k}{1+k}\right)^{3/2}\frac{\sum\limits_{r=1}^{\mathrm{M}}\mathrm{N}_r^2\delta x_r^2}{\sum\limits_{r=1}^{\mathrm{M}}\mathrm{N}_r^2}, \quad . \quad . \quad . \quad (23)$$

or

$$_1\mathrm{R}_2=0{\cdot}012+4{\cdot}95\frac{\sum\limits_{r=1}^{\mathrm{M}}\mathrm{N}_r^2\delta x_r^2}{\sum\limits_{r=1}^{\mathrm{M}}\mathrm{N}_r^2}. \quad . \quad . \quad . \quad . \quad . \quad . \quad (24)$$

Here, actual trials give widely fluctuating values of $_1\mathrm{R}_2(\min)$ owing to the very small number of terms included in the summations.

Discussion.

The criteria derived above possess the advantage over that previously adopted of giving a result which can be interpreted in terms of errors in atomic co-ordinates. The function R_2 is the most valuable as the assumptions made in its interpretation are rigorously true; $_1\mathrm{R}_2$ and $_2\mathrm{R}_2$ suffer the disadvantages that if overlapping of atoms occurs the assumption used to obtain (11) is no longer true, together with the fact that the paucity of terms used in calculating their values makes them liable to random fluctuation and undue sensitivity to extinction effects. It is interesting to note that R_2 is independent of the number of atoms when $\bar{\delta}$ is defined in the way suggested, and also that approximately

$$\mathrm{R}_2=\mathrm{R}_1^2$$

—a device useful in rough calculation.

Finally, in computing $_n\mathrm{R}_2$ there are one or two points which must be observed :—

(1) $\mathrm{F}^2(000)$ must be included in $\Sigma|\mathrm{F}_{\mathrm{obs}}|^2$.

(2) $\Sigma|\mathrm{F}_0|^2$ and $\Sigma(|\mathrm{F}_0|-|\mathrm{F}_c|)^2$ must include negative as well as positive values of (h, k, l)—or a "multiplicity" correction must be made.

(3) Extinction effects in intense reflections of low order must be taken into account and their $|\mathrm{F}|$ values possibly excluded from the summations as the squaring process gives them undue weight.

Summary.

A new criterion for the process of refinement of Fourier synthesis is suggested, and it is shown that the expression

$$\frac{\sum\limits_{hkl}(|\mathrm{F}_{\mathrm{obs}}|-|\mathrm{F}_{\mathrm{calc}}|^2)}{\sum\limits_{hkl}|\mathrm{F}_{\mathrm{obs}}|^2}=\mathrm{A}+\mathrm{B}\sum_{r=1}^{\mathrm{M}}\mathrm{N}_r^2(\delta x_r^2+\delta y_r^2+\delta z_r^2)$$

is generally true. On the basis of this expression a relation between the R.M.S. error in atomic co-ordinates and the value of R_2 is tabulated.

The new expression should be valuable in rejecting trial structures.

References.

(1) Robertson, J. C. S. p. 1817 *et seq.* (1936).
(2) Jeffrey, Proc. Roy. Soc. (In press.)
(3) Jeffrey, *ibid.*, A, clxxxiii. p. 388 (1945).
(4) Booth, Trans. Faraday Soc. (In press.)
(5) Booth, Nature, clvi. p. 51 (1945); Proc. Roy. Soc. (In press.)
(6) Booth and Llewellyn. Unpublished.

LXXV. *Factorization of a Class of Determinants and Applications to Dynamical Chains.*

By W. J. Duncan, D.Sc., M.I.Mech.E., F.R.Ae.S.,
Wakefield Professor of Aeronautics at University College, Hull*.

[Received September 29, 1944.]

Summary.

It is shown that a class of determinants of order *mn* can be factorized as the product of *n* determinants of order *m*, each of which contains one of the latent roots of a matrix of order *n*. The theorem is applicable to the determinants of motion of a large class of dynamical chains, and in such cases the latent roots are real. Detailed applications are given to segmented aircraft-wings, and comments made on the case where the number of segments tends to infinity.

CONTENTS.

		Page
1.	Introduction	2
2.	The Factorization Theorem	2
3.	Dynamical Applications	4
4.	Applications to a Segmented Wing	5
	References	8

1. *Introduction.*

Some years ago R. A. Frazer and the writer were concerned with the stability of aircraft-wings constructed of elastic material. The "exact" treatment of the motions of a continuous elastic wing when exposed to an airstream is a problem of extreme difficulty which has only been solved in a few special cases, and it is therefore in general necessary to use some approximate method of treatment. One such method consists in supposing the wing to be divided into a number of segments which are themselves rigid but provided with elastic connections. In order to get a good representation of the wing the number of segments must be large, and the determinants of motion become extremely unwieldy and

---

[*] Communicated by the Author.

laborious in use. With the object of saving labour an attempt was made to factorize the determinant, and in certain circumstances it was found possible to do this by complicated operations with rows and columns. The point of special interest was that the factors were all binary determinants of the same form containing the several roots of a numerical algebraic equation whose degree was equal to the number of segments. Moreover, the roots were independent of the speed of the air current and of the dynamical constants of the wing, so that the solution of the problem became easy once they had been calculated.

The factorization just mentioned remained an isolated curiosity until it occurred to the present writer that it was connected with the theory of partitioned matrices and the reduction of numerical matrices to the diagonal form by collineatory transformation. It is shown in the present paper that a class of determinants of order mn can be factorized as the product of n determinants of order m, each of which contains one of the latent roots of a matrix of order n. In dynamical applications these roots are real. The paper includes applications to the problems of wing motion which suggested the investigation, and comments on the limiting case where the number of segments tends to infinity.

2. *The Factorization Theorem.*

Let u be a numerical square matrix of order n which is convertible into a diagonal matrix by a collineatory transformation, so that

$$\mathrm{K}uk=\rho, \qquad (2.1)$$

where

$$\mathrm{K}k=\mathrm{I}, \qquad (2.2)$$

and ρ is the diagonal matrix of the latent roots of u. This transformation is always possible when the latent roots of u are all distinct, and k can be identified with the modal matrix of u *.

Now consider the square matrix

$$\mathrm{F}\equiv\begin{bmatrix} \mathrm{P}+u_{11}\mathrm{C} & u_{12}\mathrm{C} & \cdots \\ u_{21}\mathrm{C} & \mathrm{P}+u_{22}\mathrm{C} & \cdots \\ \cdots & \cdots & \cdots \end{bmatrix}, \qquad (2.3)$$

where P and C are arbitrary square numerical or lambda-matrices of order m, so that F is a square matrix of order mn, and u_{ij} is the typical element of u. Also let

$$j=\begin{bmatrix} k_{11}\mathrm{I}_m & k_{12}\mathrm{I}_m & \cdots \\ k_{21}\mathrm{I}_m & k_{22}\mathrm{I}_m & \cdots \\ \cdots & \cdots & \cdots \end{bmatrix} \qquad (2.4)$$

and

$$\mathrm{J}=\begin{bmatrix} \mathrm{K}_{11}\mathrm{I}_m & \mathrm{K}_{12}\mathrm{I}_m & \cdots \\ \mathrm{K}_{21}\mathrm{I}_m & \mathrm{K}_{22}\mathrm{I}_m & \cdots \\ \cdots & \cdots & \cdots \end{bmatrix}, \qquad (2.5)$$

where I_m is the unit matrix of order m. Then, on account of the relations between elements which are implicit in (2.1) and (2.2), it follows that

$$\mathrm{J}j=\mathrm{I}_{mn}, \qquad (2.6)$$

---

* See, for example, p. 66 of Ref. (1).

and

$$\mathrm{JF}j=\begin{bmatrix} \mathrm{P}+\rho_1\mathrm{C} & 0 & \dots \\ 0 & \mathrm{P}+\rho_2\mathrm{C} & \dots \\ \cdot & \cdot & \cdot \\ \dots & \dots & \mathrm{P}+\rho_n\mathrm{C} \end{bmatrix} \quad \text{. . . . . .} \quad (2.7)$$

By (2.6)

$$|\mathrm{J}|\,|j|=1, \quad \text{. . . . .} \quad (2.8)$$

so that (2.7) yields

$$|\mathrm{F}|=\prod_{s=1}^{s=n}|\mathrm{P}+\rho_s\mathrm{C}|. \quad \text{. . . . .} \quad (2.9)$$

Numerical Example.

$$u=\begin{bmatrix} 2 & 1 \\ 2 & 3 \end{bmatrix} \quad \rho=\begin{bmatrix} 1 & 0 \\ 0 & 4 \end{bmatrix} \quad k=\begin{bmatrix} 1 & 1 \\ -1 & 2 \end{bmatrix}$$

$$\mathrm{K}=k^{-1}=\frac{1}{3}\begin{bmatrix} 2 & -1 \\ 1 & 1 \end{bmatrix}$$

$$\mathrm{P}=\begin{bmatrix} \lambda^2-1 & \lambda \\ 3\lambda & 4 \end{bmatrix} \quad \mathrm{C}=\begin{bmatrix} \lambda^2 & 1 \\ \lambda & 2 \end{bmatrix}.$$

Hence

$$\mathrm{F}=\begin{bmatrix} 3\lambda^2-1 & \lambda+2 & \lambda^2 & 1 \\ 5\lambda & 8 & \lambda & 2 \\ 2\lambda^2 & 2 & 4\lambda^2-1 & \lambda+3 \\ 2\lambda & 4 & 6\lambda & 10 \end{bmatrix}$$

$$j=\begin{bmatrix} 1 & 0 & 1 & 0 \\ 0 & 1 & 0 & 1 \\ -1 & 0 & 2 & 0 \\ 0 & -1 & 0 & 2 \end{bmatrix} \quad \mathrm{J}=\frac{1}{3}\begin{bmatrix} 2 & 0 & -1 & 0 \\ 0 & 2 & 0 & -1 \\ 1 & 0 & 1 & 0 \\ 0 & 1 & 0 & 1 \end{bmatrix}$$

$$\mathrm{F}j=\begin{bmatrix} 2\lambda^2-1 & \lambda+1 & 5\lambda^2-1 & \lambda+4 \\ 4\lambda & 6 & 7\lambda & 12 \\ -2\lambda^2+1 & -\lambda-1 & 10\lambda^2-2 & 2\lambda+8 \\ -4\lambda & -6 & 14\lambda & 24 \end{bmatrix}$$

$$\mathrm{JF}j=\begin{bmatrix} 2\lambda^2-1 & \lambda+1 & 0 & 0 \\ 4\lambda & 6 & 0 & 0 \\ 0 & 0 & 5\lambda^2-1 & \lambda+4 \\ 0 & 0 & 7\lambda & 12 \end{bmatrix}.$$

This accords with (2.7) since

$$\mathrm{P}+\rho_1\mathrm{C}=\mathrm{P}+\mathrm{C}=\begin{bmatrix} 2\lambda^2-1 & \lambda+1 \\ 4\lambda & 6 \end{bmatrix}$$

and

$$\mathrm{P}+\rho_2\mathrm{C}=\mathrm{P}+4\mathrm{C}=\begin{bmatrix} 5\lambda^2-1 & \lambda+4 \\ 7\lambda & 12 \end{bmatrix}.$$

3. *Dynamical Applications.*

A dynamical chain consists of physical elements or links arranged linearly, each link being in general a dynamical system having m degrees of freedom. The links are in general coupled to each other, but typically each link is only directly coupled to one or two of its nearest neighbours on either side. It will be supposed that the rth link in the chain has the dynamical co-ordinates ϕ_r, θ_r, ψ_r . . . . . . The corresponding co-ordinates for all the elements, such as the set ϕ, will be called homologous co-ordinates.

The determinant of motion of a dynamical chain can be partitioned into square arrays of order m, and those arrays lying outside the principal diagonal contain the elements representing the couplings between the links of the chain. In general each element of the determinant will be of the form

$$a\lambda^2+b\lambda+c,$$

where the displacements in the mode of motion considered are proportional to $\exp(\lambda t)$. It is convenient to call the coefficients a, b and c the inertias, damping coefficients and stiffnesses respectively. In general, the couplings will involve all three types of coefficient.

Inspection of (2.3) shows that the factorization theorem is applicable to dynamical systems in the following circumstances :—

(i) When the sub-matrices representing the couplings between the links are all scalar multiples of a common matrix. The situation can be described by saying that the couplings must be *similar*.

(ii) When, in addition, the sub-matrices in the principal diagonal, which represent the individual links, are identical except for the addition of arbitrary numerical multiples of the common coupling matrix. By an obvious extension, they can be arbitrary numerical multiples of such sums.

In dynamical applications the matrix u will usually be real and symmetrical. The latent roots ρ are then all real, so that the factors are also real.

4. *Applications to a Segmented Wing.*

The cantilever wing considered has rigid support at the root and is of rectangular plan form. It is supposed to be divided into a number of equal segments by fore-and-aft cuts. In the example considered in detail the number of segments is six, but the method of treatment is the same whatever the number. Each segment is rigid and is connected by elastic springs to its neighbours in the following manner :—

(i) By flexural hinges lying at a constant distance aft of the leading edge at the position of the "front spar." These all have the stiffness e (moment per radian).

(ii) By flexural hinges lying at a constant distance aft of the leading edge at the position of the "rear spar." These all have the stiffness f (moment per radian).

(iii) By torsion springs which resist relative angular movements of the segments in pitch. These all have the stiffness T (moment per radian).

Let h be the distance between the spars. Then the flexural axis is situated at the distance d aft of the front spar given by

$$d=\frac{hf}{e+f}. \quad . \quad . \quad . \quad . \quad . \quad . \quad . \quad . \quad . \qquad (4.1)$$

$$(\lambda)=\begin{vmatrix}
A_1+6L & G_1 & -4L & 0 & L & 0 & 0 & 0 & 0 & 0 & 0 & 0 \\
A_3 & G_3+6M+2T & 0 & -4M-T & 0 & M & 0 & 0 & 0 & 0 & 0 & 0 \\
-4L & 0 & A_1+6L & G_1 & -4L & 0 & L & 0 & 0 & 0 & 0 & 0 \\
0 & -4M-T & A_3 & G_3+6M+2T & 0 & -4M-T & 0 & M & 0 & 0 & 0 & 0 \\
L & 0 & -4L & 0 & A_1+6L & G_1 & -4L & 0 & L & 0 & 0 & 0 \\
0 & M & 0 & -4M-T & A_3 & G_3+6M+2T & 0 & -4M-T & 0 & M & 0 & 0 \\
0 & 0 & L & 0 & -4L & 0 & A_1+6L & G_1 & -4L & 0 & L & 0 \\
0 & 0 & 0 & M & 0 & -4M-T & A_3 & G_3+6M+2T & 0 & -4M-T & 0 & M \\
0 & 0 & 0 & 0 & L & 0 & -4L & 0 & A_1+5L & G_1 & -2L & 0 \\
0 & 0 & 0 & 0 & 0 & M & 0 & -4M-T & A_3 & G_3+5M+2T & 0 & -2M-T \\
0 & 0 & 0 & 0 & 0 & 0 & L & 0 & -2L & 0 & A_1+L & G_1 \\
0 & 0 & 0 & 0 & 0 & 0 & 0 & M & 0 & -2M-T & A_3 & G_3+M+T
\end{vmatrix}. \qquad (4.2)$$

The dynamical co-ordinates for the rth segment are z_r and θ_r, where z_r is the downward normal displacement measured at the flexural axis and θ_r is the angle of pitch or twist. Then the determinant of motion * is as given in (4.2), where the symbols have the following meanings :—

$$A_1=a_1\lambda^2+b_1\lambda+c_1. \quad \dots\dots \quad (4.3)$$

$$G_1=g_1\lambda^2+j_1\lambda+k_1. \quad \dots\dots \quad (4.4)$$

$$A_3=a_3\lambda^2+b_3\lambda+c_3. \quad \dots\dots \quad (4.5)$$

$$G_3=g_3\lambda^2+j_3\lambda+k_3. \quad \dots\dots \quad (4.6)$$

The coefficients a and g represent the inertias of the segment, the b's and j's represent aerodynamic damping coefficients, while the c's and k's represent aerodynamic stiffnesses. All the aerodynamic coefficients are functions of the speed and density of the air current to which the wing is exposed.

$$L=\frac{e+f}{a^2}, \quad \dots\dots \quad (4.7)$$

where a is the span-wise width of each segment.

$$M=\frac{d^2e+(h-d)^2f}{a^2}, \quad \dots\dots \quad (4.8)$$

and T is the stiffness of the torsion springs, as already stated. The details of the method by which the determinant was obtained are omitted, since the interest lies in the factorization rather than in the equations of motion.

Inspection of (4.2) shows that the array is not in general of the form (2.3) ; thus the coupling sub-matrices are not all scalar multiples of a common matrix. If, however, T=0, then (4.2) can be factorized, for its matrix can be identified with (2.3) when

$$P=\begin{bmatrix} A_1 & G_1 \\ A_3 & G_3 \end{bmatrix}, \quad \dots\dots \quad (4.9)$$

$$C=\begin{bmatrix} L & O \\ O & M \end{bmatrix}, \quad \dots\dots \quad (4.11)$$

and

$$u=\begin{bmatrix} 6 & -4 & 1 & 0 & 0 & 0 \\ -4 & 6 & -4 & 1 & 0 & 0 \\ 1 & -4 & 6 & -4 & 1 & 0 \\ 0 & 1 & -4 & 6 & -4 & 1 \\ 0 & 0 & 1 & -4 & 5 & -2 \\ 0 & 0 & 0 & 1 & -2 & 1 \end{bmatrix}. \quad \dots\dots \quad (4.11)$$

Since u is symmetrical, its latent roots ρ are all real. By (2.9) the typical factor of (4.2) is

$$\begin{vmatrix} A_1+\rho_r L & G_1 \\ A_3 & G_3+\rho_r M \end{vmatrix}. \quad \dots\dots \quad (4.12)$$

---

* For clearness the rows and columns of the determinant are separated by dotted lines.

The wing is a dynamical system having 12 degrees of freedom, but on account of the factorization it is equivalent to 6 independent binary systems. All questions regarding the motions and stability of the wing at any wind speed can be answered by reference to (4.12) when the numerical roots ρ have been obtained once for all.

The determinant (4.2) can also be factorized when T is retained but L and M made zero. Now the matrix of (4.2) can be identified with (2.3) when

$$P=\begin{bmatrix} A_1 & G_1 \\ A_3 & G_3 \end{bmatrix},$$

$$C=\begin{bmatrix} 0 & 0 \\ 0 & T \end{bmatrix}, \quad . \quad . \quad . \quad . \quad . \quad . \quad . \quad . \quad . \quad . \quad (4.13)$$

and

$$u=\begin{bmatrix} 2 & -1 & 0 & 0 & 0 & 0 \\ -1 & 2 & -1 & 0 & 0 & 0 \\ 0 & -1 & 2 & -1 & 0 & 0 \\ 0 & 0 & -1 & 2 & -1 & 0 \\ 0 & 0 & 0 & -1 & 2 & -1 \\ 0 & 0 & 0 & 0 & -1 & 1 \end{bmatrix} \quad . \quad . \quad . \quad . \quad . \quad . \quad (4.14)$$

The latent roots ρ are again real, and the typical factor is

$$\begin{vmatrix} A_1 & G_1 \\ A_3 & G_3+\rho_r T \end{vmatrix}. \quad . \quad . \quad . \quad . \quad . \quad . \quad . \quad . \quad . \quad (4.15)$$

The determinant of motion can be factorized in the circumstances already mentioned when the wing is divided into any number of equal segments, and it is to be expected that this will remain true when the number of segments becomes infinite, so that we have to deal with a continuous elastic wing; it would then be expected that ρ would be a root of a transcendental function. Independent investigations show that this is correct $^{(2), (3)}$. When the torsion springs are absent * the characteristics of the motion are determined by

$$\begin{vmatrix} A_1'+L'\mu^4 & G_1' \\ A_3' & G_3'+M'\mu^4 \end{vmatrix}=0, \quad . \quad . \quad . \quad . \quad . \quad . \quad (4.16)$$

where μ is a root of

$$1+\cos\mu\cosh\mu=0, \quad . \quad . \quad . \quad . \quad . \quad . \quad . \quad (4.17)$$

while L′ and M′ are proportional to the total flexural rigidity of the spars and A_1', G_1', A_3' and G_3' have a similar meaning to the corresponding unaccented symbols, but refer to unit span of the wing. When the only elastic stiffness of the continuous elastic wing is torsional, the effective determinant of motion is †

$$\begin{vmatrix} A_1' & G_1' \\ A_3' & G_3'+T'\mu^2 \end{vmatrix}=0, \quad . \quad . \quad . \quad . \quad . \quad . \quad . \quad (4.18)$$

---

* That is, when the torsional stiffness of the wing is entirely attributable to the flexural stiffnesses of its two spars.

† See the Appendix of Ref. (4).

where μ is now a root of

$$\cos \mu = 0, \quad . \quad . \quad . \quad . \quad . \quad . \quad . \quad . \quad . \quad (4.19)$$

and T′ is proportional to the torsional rigidity of the wing.

It will be noted that the elements in a row in the middle or "regular" part of (4.11) are the coefficients in the expansion of $(1-x)^4$. This is related to the fact that the normal elastic reaction per unit run is proportional to d^4z/dx^4 when the distance between the hinges tends to zero. The apparent irregularity of the two lowest rows of (4.11) is the expression of the "boundary condition" at the tip of the wing. Similarly, the regular rows in (4.14) contain the coefficients in the expansion of $-(1-x)^2$, and this is related to the fact that in the limiting case of the uniform elastic beam the torsional reaction per unit run is proportional to $-\dfrac{d^2\theta}{dx^2}$.

References.

(1) Frazer, R. A., Duncan, W. J., and Collar, A. R., 'Elementary Matrices.' (Cambridge, 1938.)

(2) Frazer, R. A., and Duncan, W. J., "Conditions for the Prevention of Flexural-Torsional Flutter of an Elastic Wing." R. & M. 1217 (December, 1928).

(3) Frazer, R. A., and Duncan, W. J., "The Flutter of Monoplanes, Biplanes and Tail Units." (A.R.C. Monograph.) R. & M. 1255 (January, 1931).

(4) Duncan, W. J., Collar, A. R., and Lyon, H. M., "Oscillations of Elastic Blades and Wings in an Airstream." R. & M. 1716 (January, 1936).

LXXVI. *On the Change in the Dielectric Constants of Liquids Flowing Through Narrow Separations.*

By B. N. Singh, D.Sc., and B. D. Singh, M.Sc.*.

[Received August 14, 1944.]

Introduction.

In a preliminary note (1), it has been reported by the present authors that the dielectric constant values of certain liquids show a very small decrease when they are made to flow through narrow separations. In the present paper a detailed description of the experimental arrangement and the results has been given. The liquids were made to flow through a specially designed condenser and the changes in their dielectric constant values were obtained from the measurements of the variations in the capacity of the condenser by the heterodyne beat method, using wavelengths of the order of about 300 metres. The amounts of the changes observed in the d.c. values of liquids are of an order of magnitude much higher than those which can be expected to be due to the birefringence ⁽²⁾ produced in those liquids due to flow. It is very likely that the charges observed by the authors are caused by the production of electric changes near the interface of the liquids and the plates of the condenser.

---

* Communicated by the Authors.

Experimental Arrangement.

The section of the experimental condenser through which liquids were made to flow is shown in fig. 1. One of the plates of the condenser (made of brass) is in the form of a circular platform P and is provided with an opening O in the centre. The other plate, which is also made of brass, is in the form of a circular disk D, with a handle fixed to it. The two plates of the condenser are separated from each other by means of thin pieces of mica MM (thickness of the order of 0·005 mm. to 0·02 mm.). The disk D is sufficiently loaded with weights W, resting on a porcelain ring Q, to prevent any displacement or bulging of the disk due to hydrostatic pressure from below. In continuation with the platform P there is a circular raised rim RR and an outer annular space B with an outlet T. The opening O is connected through a tube F to a vertical glass tube of a wide diameter (about 2·5 cm.). S is a stopper which is provided with a long ebonite handle. The entire body of the apparatus is made of brass and is fitted with three legs LL provided with levelling screws. When the experimental liquid is poured in the glass tube G, it passes through the U-tube, comes out of the opening O, then fills the space between the plates and rises over the disk D. On reaching the level of the rim RR the liquid passes to the annular space B and is collected in a receiver when it comes out of the outlet T. First the liquid is allowed to fill all the spaces indicated above and when it begins to overflow over the rim RR, if the stopper S is closed, the flow of the liquid

Fig. 1.

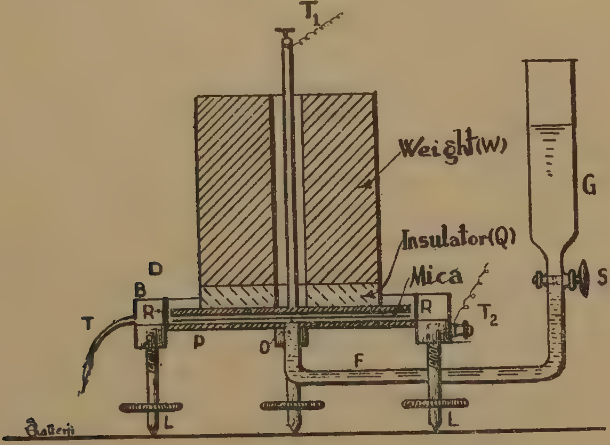

through the space between the plates stops. On opening the stopper S, the flow of liquid begins, and if the level of the liquid in the glass tube be maintained constant, it is obvious that its rate of flow through the separation between the plates will remain constant. T_1 and T_2 are two terminals fixed to the two plates of the condenser which are connected to their proper positions in the oscillatory system mentioned below. The entire apparatus described above was enclosed within a box lined with tin, which was connected to the earth. The box was provided with a glass window in front and a circular hole in the top for the vertical glass tube to come out. The stopper S was worked from outside by means of an ebonite handle.

A radio-frequency generator of Hartley type, producing waves of lengths of the order of about 300 metres was used. The experimental condenser was connected in parallel with the variable air condenser of the oscillatory circuit of the h.f. generator. Another specially designed mercury-plate condenser was also connected in parallel with the above condensers. A complete description of the mercury-plate condenser used by us is given elsewhere (3). The h.f. generator and the mercury-plate condenser were also kept in boxes lined with tin and the latter were connected to earth. The interconnections between the different condensers and generator were made by means of suitable wires passing through earth-connected pipes of lead.

The h.f. signals from the generator were received by an oscillator-detector valve circuit, followed by two stages of low-frequency amplification and a loud-speaker. When the detector circuit was nearly in tune with the oscillator, a heterodyne note was heard in the loud-speaker. The low-frequency current from an audio-frequency oscillator was fed into the same loud-speaker and the usual beat note was heard. When the experimental condenser was filled with a given liquid, the detector condenser was adjusted to get the condition of no beat. As soon as the flow of the liquid began, the beat appeared and the mercury-plate condenser was adjusted to bring back the condition of no beat. The flow was again stopped and the mercury-plate condenser was again adjusted to produce the no-beat condition. Only such readings were recorded in which the first and final positions of the mercury-plate condenser were the same. Knowing the dimensions of the experimental condenser and the dielectric constants of the liquids, the change in their dielectric constant values were easily calculated. Separate experiments were performed to find out if the conductivity of the liquids indicated any change due to flow, but no appreciable change was detected. It may be observed, however, that even if there be any increase in the conductivity (say due to the production of electric charges) of the liquids, that would cause an apparent increase in their d.c. values. In order to be sure that the decrease observed in the dielectric constant was not due to any mechanical displacement or bulging of the upper disk of the experimental condenser, produced by the hydrostatic pressure of the liquid, experiments were performed by keeping different weights over the disk D and measuring the corresponding changes in the capacity of the condenser. Finally, such weights were placed over the disc that any increase or decrease in its value, even by 1 kgm., did not produce any detectable change in the capacity of the experimental condenser. The hydrostatic pressure of the liquids were always a small fraction of that due to 1 kilogram. Further, with the help of a sensitive thermo-couple thermometer it was ascertained that there was no such appreciable rise of temperature of liquids when flowing through narrow separations so as to cause the observed changes in the dielectric values.

Experimental Results.

The experimental results for the following liquids are given in the present paper (shown graphically in figs. 2 to 6); xylene (a mixture of ortho-, para- and meta-), carbon tetrachloride, toluene, benzene and olive oil. It may be noted that some of the liquids are volatile, and hence produced a lowering of temperature at the time of flow. This, no doubt, caused considerable difficulties in the manipulation of the experiments, but it is important to remember that the fall of temperature will only tend to increase and not decrease the d.c. of the liquids. For each liquid experiments were performed several times, and the observations were distributed over sufficiently long intervals. The order of change observed in the case of a given liquid was, however, found to remain the same for a given rate of flow and for a given separation between the plates of the experimental condenser. The shape of this condenser is,

Fig. 2.

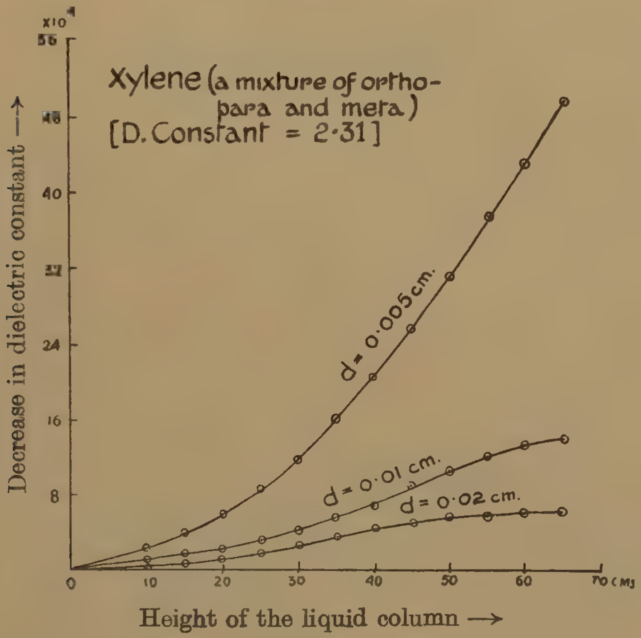

Fig. 3.

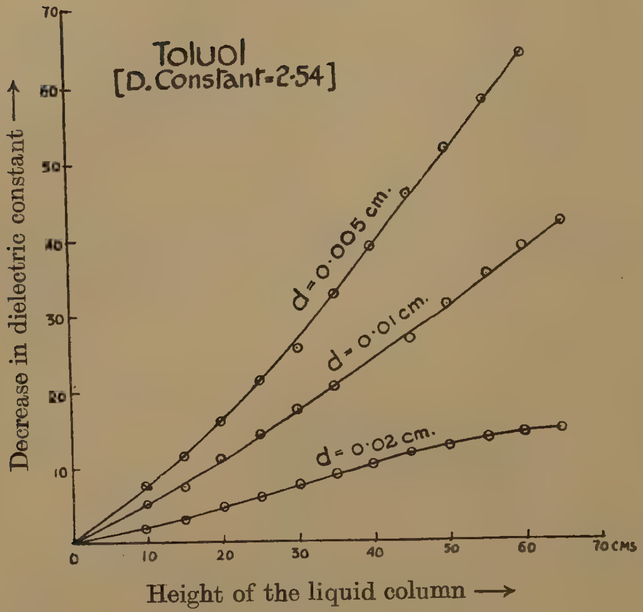
Toluol
[D. Constant=2·54]
d = 0·005 cm.
d = 0·01 cm.
d = 0·02 cm.
Decrease in dielectric constant →
Height of the liquid column →
0
10
20
30
40
50
60
70 CMS
70

Fig. 4.

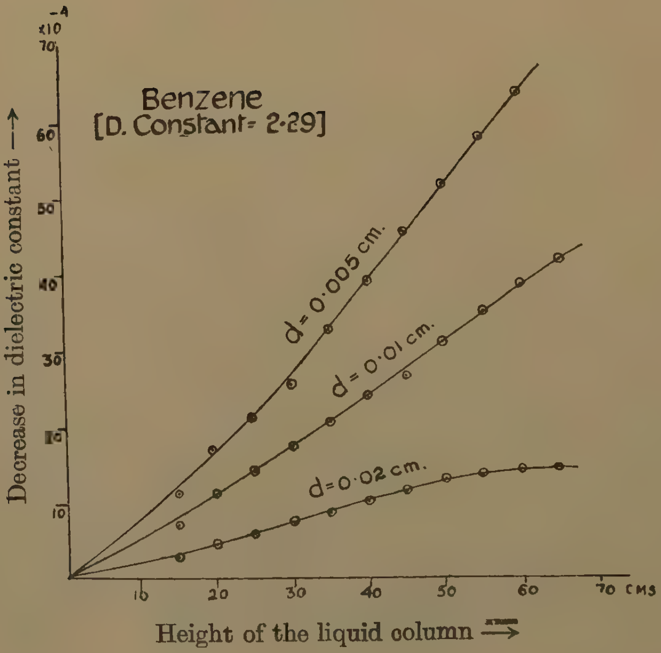
Benzene
[D. Constant= 2·29]
d = 0·005 cm.
d = 0·01 cm.
d = 0·02 cm.
×10⁻⁴
Decrease in dielectric constant →
Height of the liquid column →
10
20
30
40
50
60
70
70 CMS

however, circular and liquids spread out radially, and hence their rate of flow varies along the radius. But it is possible to calculate the average rate of flow for the given liquid if the height under which it flows and the separation between the plates of the condenser are given. The graphs shown in figs. 2 to 6 indicate the changes in the d.c. values of liquids with heights under which they flow for different separations (*d*) between condenser plates. The actual values of the d.c. of samples of liquids used were determined and are given in the corresponding figures. It will be seen that the amount and rate of change of d.c. with height (and hence with rate of flow) increase with the decrease in the separation between the plates of the condenser. Except for the difference in the order of magnitude, the nature of the changes observed in different liquids is the same and appears to be entirely unrelated to the molecular anisotropy of the liquids. As mentioned above, it is possible to calculate the average rate of flow from the knowledge of the dimensions of the condenser, the viscosity and height of liquid column. For a given liquid, however, the average rate of flow will depend only upon the dimensions of the condenser and the height under which flow takes place. The graph in fig. 7 has been drawn to show the variation in the change of dielectric constant of carbon tetrachloride with separation for a given rate of flow.

Fig. 5.

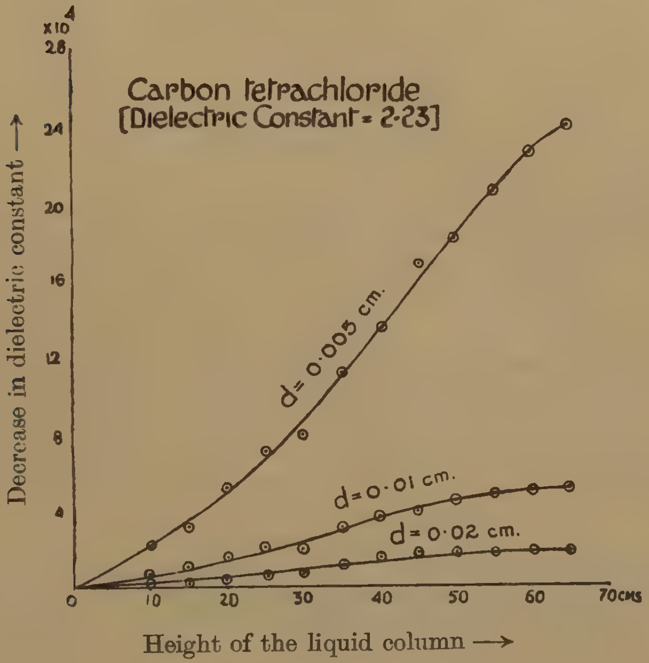

Fig. 6.

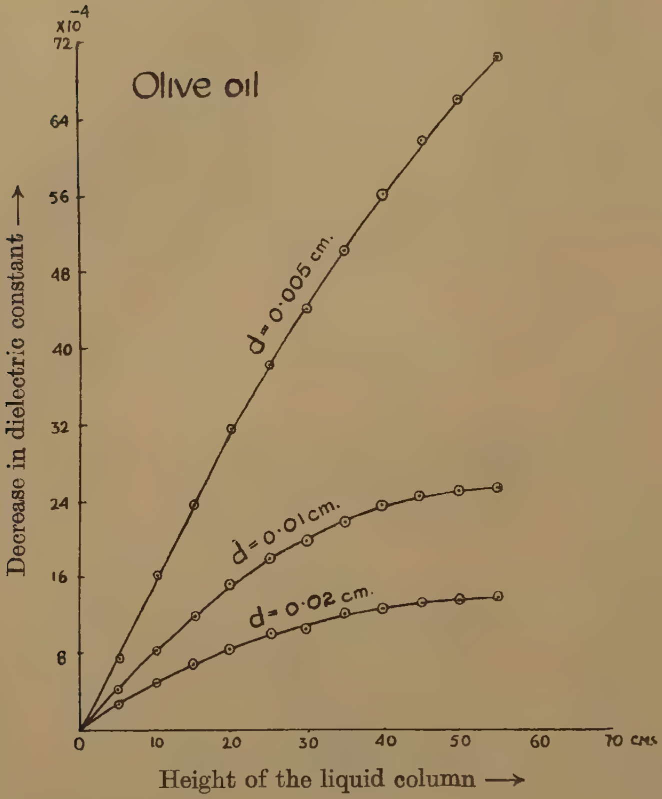
×10⁻⁴
72
64
56
48
40
32
24
16
8
0
Olive oil
d = 0·005 cm.
d = 0·01 cm.
d = 0·02 cm.
10
20
30
40
50
60
70 CMS
Decrease in dielectric constant →
Height of the liquid column →

Fig. 7.

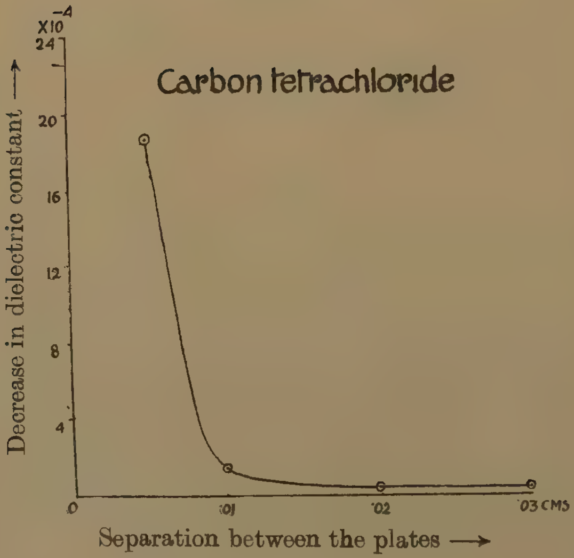
×10⁻⁴
24
20
16
12
8
4
0
Carbon tetrachloride
·01
·02
·03 CMS
Decrease in dielectric constant →
Separation between the plates →

References.

(1) Prasad, S. P., Singh, B. N., and Singh, B. D., 'Nature,' cxlvii. p. 712 (1941).
(2) Raman, C. V., and Krishnan, K. S., Phil. Mag. v. p. 769 (1928)
(3) Prasad, S. P., and Verma, M. N., *Zeit. für Physik*, xcix. p. 552 (1936).

Physics Laboratory,
Science College,
Patna, India.
T. N. J. College,
Bhagalpur, India.

LXXVII. *A Note on the Equations of Plane Plastic Flow.*

By Ian N. Sneddon *.

[Received September 1, 1944.]

1. Recently, A. C. Stevenson (1) has succeeded in applying the methods of the complex variable in a very elegant manner to a wide variety of problems in two-dimensional elasticity. This is effected by observing that the use of the combinations $\widehat{xx}+\widehat{yy}$, $\widehat{xx}-\widehat{yy}+2i\,\widehat{xy}$ enables the equations of equilibrium to be put into a simple form. Equivalent results have been derived subsequently by Milne-Thomson (2), who approached the problem in a more general (if less direct) fashion.

The purpose of this note is to suggest a possible approach to two-dimensional problems of plastic flow by the methods employed by Stevenson. The use of the method is illustrated by finding the solutions of a few well-known problems of plane plastic flow.

2. A two-dimensional problem in the theory of plasticity can arise, as in elasticity, in either of two ways—as a problem of plane strain or as one of plane stress. In both cases the equations of equilibrium reduce to the simplified form

$$\left.\begin{aligned}\frac{\partial\widehat{xx}}{\partial x}+\frac{\partial\widehat{xy}}{\partial y}&=0,\\ \frac{\partial\widehat{xy}}{\partial x}+\frac{\partial\widehat{yy}}{\partial y}&=0\end{aligned}\right\} \quad . \quad . \quad . \qquad (1)$$

If we introduce the complex variable

$$z=x+iy \quad . \quad . \quad . \quad . \quad . \quad . \quad . \quad . \quad . \qquad (2)$$

and write

$$\widehat{xx}+\widehat{yy}=\phi\ ;\quad \widehat{xx}-\widehat{yy}+2i\,\widehat{xy}=\psi, \quad . \quad . \quad . \quad . \quad . \quad . \qquad (3)$$

---

* Communicated by the Author.

then multiplying the second of equations (1) by i, adding to the first and making use of the relations

$$\frac{\partial}{\partial x}=\frac{\partial}{\partial z}+\frac{\partial}{\partial \bar{z}}, \quad \frac{\partial}{\partial y}=i\left(\frac{\partial}{\partial z}-\frac{\partial}{\partial \bar{z}}\right),$$

we obtain the equation

$$\frac{\partial\psi}{\partial z}+\frac{\partial\phi}{\partial \bar{z}}=0, \quad . \quad . \quad . \quad . \quad . \quad . \quad . \quad . \quad . \quad (4)$$

where $\bar{z}$ denotes the complex conjugate of z. Thus the equations of equilibrium (1) are satisfied by the introduction of a new function $F(z\,;\,\bar{z})$ of the variables z and $\bar{z}$ in terms of which

$$\phi=\frac{\partial F}{\partial z}; \quad \psi=-\frac{\partial F}{\partial \bar{z}}. \quad . \quad . \quad . \quad . \quad . \quad . \quad . \quad . \quad (5)$$

There will, of course, be further restrictions on the nature of the function F. In the first place it is obvious on physical grounds that ϕ must be purely real, that is, that

$$\mathscr{I}(\phi)=0 \quad . \quad . \quad . \quad . \quad . \quad . \quad . \quad . \quad . \quad . \quad (6)$$

(where $\mathscr{I}$ denotes " the imaginary part of ").

To the set of equations (4) and (6) we add a fourth equation—the " plasticity condition " in one of its forms. Confining our attention to the case of plane strain, we find that the condition of constant energy of distortion gives (3)

$$(\widehat{xx}-\widehat{yy})^2+4\widehat{xy}^2=4k^2, \quad . \quad . \quad . \quad . \quad . \quad . \quad . \quad . \quad (7)$$

where the constant k is related to s_0, the yield point in tension of the material, by the equation

$$3k^2=s_0{}^2.$$

The maximum shear theory gives precisely the same condition, except that now the relation between k and s_0 is $2k=s_0$. Thus, in both cases, the plasticity condition can be expressed in the form

$$|\psi|=2k. \quad . \quad . \quad . \quad . \quad . \quad . \quad . \quad . \quad . \quad . \quad (8)$$

If we write

$$\psi=2ke^{i\left(\frac{\pi}{2}+2\vartheta\right)}; \quad \phi=2p,$$

where ϑ, p are real, then equations (6) and (8) are satisfied and

$$\tan 2\vartheta=\frac{\widehat{yy}-\widehat{xx}}{2\widehat{xy}}. \quad . \quad . \quad . \quad . \quad . \quad . \quad . \quad . \quad . \quad (9)$$

Substituting in equation (4) we have

$$\frac{\partial p}{\partial \bar{z}}+2kie^{i\left(\frac{\pi}{2}+2\vartheta\right)}\frac{\partial\vartheta}{\partial z}=0,$$

and on separating real and imaginary parts, we obtain

$$\left.\begin{aligned}\frac{\partial p}{\partial x}&=2k\left(\cos 2\vartheta\frac{\partial\vartheta}{\partial x}+\sin 2\vartheta\frac{\partial\vartheta}{\partial y}\right),\\ \frac{\partial p}{\partial y}&=2k\left(\sin 2\vartheta\frac{\partial\vartheta}{\partial x}-\cos 2\vartheta\frac{\partial\vartheta}{\partial y}\right)\end{aligned}\right\}, \quad . \quad . \quad . \quad . \quad (10)$$

—equations which, with (9), form the basis of the important Hencky slip-line theorems in two-dimensional plastic flow⁽⁴⁾.

3. If in equation (5) we take

$$F=4\frac{\partial\chi}{\partial\bar{z}},$$

where χ is a real function of z, $\bar{z}$, then

$$\phi=4\frac{\partial^2\chi}{\partial z\,\partial\bar{z}};\quad \psi=-4\frac{\partial^2\chi}{\partial\bar{z}^2}. \qquad \qquad (11)$$

Thus ϕ is real and equation (8) gives

$$\left|4\frac{\partial^2\chi}{\partial\bar{z}^2}\right|=2k. \qquad \qquad (12)$$

But
$$4\frac{\partial^2}{\partial\bar{z}^2}=\left(\frac{\partial}{\partial x}+i\frac{\partial}{\partial y}\right)^2=\left(\frac{\partial^2}{\partial x^2}-\frac{\partial^2}{\partial y^2}\right)+2i\frac{\partial^2}{\partial x\,\partial y}.$$

Hence (12) becomes

$$\left(\frac{\partial^2\chi}{\partial x^2}-\frac{\partial^2\chi}{\partial y}\right)^2+4\left(\frac{\partial^2\chi}{\partial x\,\partial y}\right)^2=4k^2, \qquad \qquad (13)$$

and from (11) it follows that if χ is a solution of (13) then the complete solution of the problem is given by

$$\widehat{xx}=\frac{\partial^2\chi}{\partial y^2};\quad \widehat{yy}=\frac{\partial^2\chi}{\partial x^2};\quad \widehat{xy}=-\frac{\partial^2\chi}{\partial x\,\partial y}. \qquad \qquad (14)$$

This is the "Airy stress-function" method of solution of the plane plastic problem⁽³⁾.

4. Let us now consider some special solutions of the set of equations (4), (6) and (8). Condition (8) is automatically satisfied if we write

$$\psi=2k\{\sqrt{1-f^2}+if\}, \qquad \qquad (15)$$

where f is a *real* function of z and $\bar{z}$. Thus, if we take

$$f=\frac{z+\bar{z}}{2a},$$

f is real, equation (8) is satisfied, and we have from (4)

$$\frac{\partial\phi}{\partial\bar{z}}=-\frac{\partial\psi}{\partial z}=-2k\left[-\frac{z+\bar{z}}{2a}\left\{1-\left(\frac{z+\bar{z}}{2a}\right)^2\right\}^{-\frac{1}{2}}+\frac{i}{2a}\right].$$

Integrating, we have

$$\phi=-2k\left[\left\{1-\left(\frac{z+\bar{z}}{2a}\right)^2\right\}^{\frac{1}{2}}+\frac{i\bar{z}}{2a}\right]+g(z),$$

where the function $g(z)$ must be chosen to make ϕ real. This is achieved if we take

$$g(z)=-ki\,.\,(z/a)+2C,$$

where C is an arbitrary (real) constant. Thus

$$\phi=2C-2k\left[\sqrt{1-\left(\frac{z-\bar{z}}{2a}\right)^2}+i\frac{z-\bar{z}}{2a}\right]. \qquad \qquad (16)$$

Replacing z by $x+iy$, $\bar{z}$ by $x-iy$, and separating real and imaginary parts, we have finally

$$\widehat{xx}=\mathrm{C}-ky/a\,;\quad \widehat{yy}=\mathrm{C}-ky/a-2k\sqrt{1-x^2/a^2}\,;\quad \widehat{xy}=kx/a. \quad \cdot\cdot \quad (17)$$

It is obvious from (7) that the numerical value of the stress $\widehat{xy}$ cannot exceed k. Hence the two straight lines

$$x=\pm a$$

form natural limits for the plastic mass, and (17) is the solution of the problem of a plastic mass pressed between two rough parallel plates (5).

5. If we choose

$$\phi=f(z)+\bar{f}(\bar{z})\pm 2\mathrm{C}, \quad . \quad . \quad . \quad . \quad . \quad . \quad . \quad . \quad (18)$$

where C is an arbitrary real constant and $f(z)$ is a function of z alone, then equation (6) is automatically satisfied, and it follows as an immediate consequence of equation (4) that

$$\psi=g(\bar{z})-z\bar{f}'(\bar{z}), \quad . \quad . \quad . \quad . \quad . \quad . \quad . \quad . \quad (19)$$

where $g(\bar{z})$ is arbitrary as far as the integration goes ; however g must be so chosen that ψ satisfies equation (8).

As an example of this type of solution we may take

$$\mathrm{C}=0\,;\quad g(\bar{z})=0\,;\quad f(z)=-2k.\log(z/a)\,;$$

then

$$\phi=-2k\log(z\bar{z}/a^2)\,;\quad \psi=2k(z/\bar{z}). \quad . \quad . \quad . \quad . \quad . \quad . \quad (20)$$

Thus writing $z=re^{i\theta}$ and separating real and imaginary parts we have

$$\left.\begin{aligned}\widehat{xx}&=k(\cos 2\theta+\log a^2/r^2,\\ \widehat{yy}&=k(-\cos 2\theta+\log a^2/r^2,\\ \widehat{xy}&=k\sin 2\theta.\end{aligned}\right\} \quad . \quad . \quad . \quad . \quad . \quad . \quad (21)$$

To interpret these results physically we make use of the formulæ for the transformation of the components of stress to polar co-ordinates (6). In the usual notation

$$\widehat{rr}-\widehat{\theta\theta}+2i\widehat{r\theta}=\frac{\bar{z}}{z}(\widehat{xx}-\widehat{yy}+2i\,\widehat{xy})=\frac{\bar{z}\psi}{z}. \quad . \quad . \quad . \quad . \quad (22)$$

Substituting from (20) into (22) we have, on equating real and imaginary parts,

$$\widehat{rr}-\widehat{\theta\theta}=2k\,;\quad \widehat{r\theta}=0, \quad . \quad . \quad . \quad . \quad . \quad . \quad . \quad . \quad (23)$$

showing that $\widehat{rr}$ and $\widehat{\theta\theta}$ are the principal stresses. Making use of the fact that

$$\widehat{rr}+\widehat{\theta\theta}=\widehat{xx}+\widehat{yy}, \quad . \quad . \quad . \quad . \quad . \quad . \quad . \quad . \quad . \quad (24)$$

we have from (21) that

$$\widehat{rr}=2k.\log\frac{a}{r}\,;\quad \widehat{\theta\theta}=2k\left(\log\frac{a}{r}-1\right), \quad . \quad . \quad . \quad . \quad . \quad . \quad (25)$$

showing that the functions $\widehat{rr}$, and $\widehat{\theta\theta}$ are functions of r alone.

The slip-lines corresponding to this system of stress form two orthogonal systems of logarithmic spirals of the form commonly observed in wrought-iron plates whose material has been stressed beyond the yield-point by the identation of a cylindrical punch (7).

A second solution of this type is obtained by taking

$$g(\bar{z})=0\,;\quad f(z)=2ki\,.\log(z/a), \qquad (26)$$

then
$$\phi=2ki\,.\log(z/\bar{z})+2\mathrm{C}\,;\quad \psi=2ki\,.(z/\bar{z}). \qquad (27)$$

Using (22), (24), and equating real and imaginary parts, we obtain the solution

$$\widehat{rr}=\widehat{\theta\theta}=\mathrm{C}-2k\theta\,;\quad \widehat{r\theta}=k. \qquad (28)$$

6. As a final example of the use of these equations let us consider the so-called "*vortical flow*" in a plastic mass. If we take

$$f=-\frac{a^2}{z\bar{z}} \qquad (29)$$

in (15) then ψ satisfies equation (8). If we multiply (15) throughout by $z/\bar{z}$ the modulus of ψ is unaltered. Hence we may take

$$\psi=2k\frac{z}{\bar{z}}\left[\left\{1-\frac{a^4}{(z\bar{z})^2}\right\}^{\frac{1}{2}}-i\frac{a^2}{z\bar{z}}\right]. \qquad (30)$$

Also from equation (4)

$$\frac{\partial\phi}{\partial\bar{z}}=-\frac{\partial\psi}{\partial z}=-\frac{2k}{\bar{z}}\left[\left\{1-\frac{a^4}{(z\bar{z})^2}\right\}^{\frac{1}{2}}-i\frac{a^2}{z\bar{z}}\right]-2kz\left[\frac{-ff'}{\sqrt{1-f^2}}+if'\right].$$

Integrating

$$\phi=-2k\int\frac{\sqrt{1-f^2}+if}{\bar{z}}d\bar{z}-2k[\sqrt{1-f^2}+if]+g(z), \qquad (31)$$

where the function $g(z)$ is chosen so as to make ϕ real.

Now
$$\int(f/\bar{z})d\bar{z}=-f.$$

To evaluate
$$\mathrm{I}=\int\frac{\sqrt{1-f^2}}{\bar{z}}d\bar{z},$$

let $a^2/z\bar{z}=\cos 2\beta$, then

$$\mathrm{I}=\tfrac{1}{2}\log\frac{1+\sin 2\beta}{1-\sin 2\beta}-\sin 2\beta=\log\tan(\beta+\pi/4)-\sin 2\beta.$$

Substituting in (31) we have

$$\phi=-2k\log\tan\,(\beta+\pi/4), \qquad (32)$$

$g(z)$ being taken as *zero*.

Using (22) and (24) we have from (30) and (32) that the stresses $\widehat{rr}$, $\widehat{\theta\theta}$, $\widehat{r\theta}$ are determined as functions of the parameter β by the equations

$$\left.\begin{aligned}\widehat{rr}&=-k[\log\tan(\beta+\pi/4)-\sin 2\beta],\\ \widehat{\theta\theta}&=-k[\log\tan(\beta+\pi/4)+\sin 2\beta],\\ \widehat{r\theta}&=-k\cos 2\beta\end{aligned}\right\}, \qquad (33)$$

as have been obtained otherwise (7).

7. If we assume that the material of the plastic body is incompressible we can also determine expressions for the components of the rate of displacement. If we denote these components by v_x and v_y, then the equation of continuity for the medium is

$$\frac{\partial \rho}{\partial t}+\frac{\partial}{\partial x}(\rho v_x)+\frac{\partial}{\partial y}(\rho v_y)=0,$$

and in the case of incompressibility ρ is constant, so that this equation reduces to

$$\frac{\partial v_x}{\partial x}+\frac{\partial v_y}{\partial y}=0. \quad \ldots \ldots \quad (34)$$

Introducing the complex function

$$w=v_x+iv_y,$$

we can write equation (34) in the form

$$\frac{\partial w}{\partial z}+\frac{\partial \bar{w}}{\partial \bar{z}}=0. \quad \ldots \ldots \quad (35)$$

Furthermore, for an incompressible medium we can write

$$\left.\begin{aligned} \widehat{xx}&=-\tfrac{1}{2}\phi+2\mu\frac{\partial v_x}{\partial x}, \\ \widehat{yy}&=-\tfrac{1}{2}\phi+2\mu\frac{\partial v_y}{\partial y}, \\ \widehat{xy}&=\mu\left(\frac{\partial v_x}{\partial y}+\frac{\partial v_y}{\partial x}\right) \end{aligned}\right\}, \quad \ldots \ldots \quad (36)$$

where μ is a real function of x and y. Thus we have

$$\widehat{xx}-\widehat{yy}+2i\widehat{xy}=4\mu\frac{\partial w}{\partial \bar{z}},$$

giving

$$4\frac{\partial w}{\partial \bar{z}}=\frac{\psi}{\mu}.$$

Taking the complex conjugate of both sides we obtain

$$4\frac{\partial \bar{w}}{\partial z}=\frac{\bar{\psi}}{\mu},$$

since $\bar{\mu}=\mu$. Hence

$$\frac{\partial^2}{\partial z^2}\left(\frac{\psi}{\mu}\right)+\frac{\partial^2}{\partial \bar{z}^2}\left(\frac{\bar{\psi}}{\mu}\right)=4\frac{\partial^2}{\partial z\,\partial \bar{z}}\left(\frac{\partial w}{\partial z}+\frac{\partial \bar{w}}{\partial \bar{z}}\right)=0, \quad \ldots \quad (37)$$

by equation (35).

Thus in any problem in which the functions ϕ and ψ are known, μ can be determined from equation (37) and the rates of displacement from the relations (36).

I am indebted to the Director-General of Scientific Research and Development, Ministry of Supply, for permission to publish this note.

References.

(1) A. C. Stevenson, Phil. Mag. Series 7, xxxiv. p. 766 (1943).
(2) L. M. Milne-Thomson, Journ. Lond. Math. Soc. xvii. p. 115 (1942).
(3) A. Nadai, 'Plasticity' (New York, 1931), p. 184.
(4) H. Geiringer and W. Prager, *Ergebnisse der Exacten Naturwissenschaften*, xiii. p. 335 (1934).
(5) L. Prandtl, *Zeits. f. ang. Math. u. Mech.* iii. p. 401 (1923).
(6) A. C. Stevenson, *op. cit.* p. 772.
(7) A. Nadai, *op. cit.* ch. 34.

The Department of Natural Philosophy,
The University of Glasgow.

LXXVIII. *Quantum Equations and Nuclear Field Theories.*

By H. T. Flint, Professor of Physics, Bedford College, University of London*.

[Received December 5, 1945.]

Introduction.

The idea that the equations of the quantum theory are gauging equations in a geometrical and metrical system suited to the world of physics enables their relation to the rest of physics to be appreciated and gives a clue to their generalization in nuclear theories.

The system in which this idea finds its best expression is that of matrix geometry and metrics(1).

The starting point is found in the work of Kaluza(2), who undertook the unification of the theories of gravitation and electromagnetism by giving a new degree of freedom to an electrically charged particle and by using the notation of Riemannian geometry in five dimensions.

With this system a metrical scheme is incorporated after the manner of Weyl.

Five four-rowed matrices play a fundamental role in this geometry. They are denoted typically by (γ_μ) and are related to the coefficients $(\gamma_{\mu\nu})$ of the line element

$$d\sigma^2=\gamma_{\mu\nu}\,dx^\mu\,dx^\nu \qquad (\mu, \nu=1, 2, 3, 4, 5), \quad . \quad . \quad . \quad . \quad . \quad (1)$$

by Tetrode's relations

$$\gamma_\mu\gamma_\nu+\gamma_\nu\gamma_\mu=2\gamma_{\mu\nu}. \quad . \quad . \quad . \quad . \quad . \quad . \quad . \quad (2)$$

The metrics associated with this geometry are characterized by a single column matrix ψ.

If the components of an ordinary vector of this space are (C^μ), the matrix length of the vector is defined to be

$$L=\gamma_\mu C^\mu\psi. \quad . \quad . \quad . \quad . \quad . \quad . \quad . \quad . \quad (3)$$

---

* Communicated by the Author.

Significance is attached to the change of length of this quantity when (C^μ) undergoes a parallel displacement defined by

$$dC^\mu = -\Delta^\mu_{\nu\lambda} C^\nu dx^\lambda, \quad \ldots \ldots \quad (4)$$

where $\Delta^\mu_{\nu\lambda}$ is a Christoffel bracket expression for the continuum. In the case considered by Weyl there was no change of length in a parallel displacement of this kind in the absence of an electromagnetic field. In the present five-dimensional case the gravitational and electromagnetic field together are analogous to the gravitational field alone in Weyl's theory. Thus the analogy leads naturally to the investigation of the condition to be satisfied by ψ in order that L may remain unchanged when (C^μ) changes in accordance with equation (4).

The condition⁽³⁾ is

$$\gamma^\mu \frac{\partial \psi}{\partial x^\mu} = 0. \quad \ldots \ldots \quad (5)$$

which is Dirac's equation for the case of a charged particle in a gravitational and electromagnetic field.

The Influence of Nuclear Fields.

Equation (5) determines ψ for the particular case in which there are no fields except those of gravitation and electromagnetism. It is now supposed that ψ is modified by other fields, such as are considered in nuclear theories. The effect of these is supposed to be that a change in matrix length is produced when the displacement defined by equation (4) occurs⁽¹⁾.

The change is defined by

$$dL = H_\lambda L dx^\lambda. \quad \ldots \ldots \quad (6)$$

In its form this is like the assumption made by Weyl when he introduced a system of metrics in attempting a unitary theory of gravitation and electromagnetism.

This leads to the following relation for ψ :

$$\gamma^\mu \frac{\partial \psi}{\partial x^\lambda} + \kappa^\mu_\lambda \psi = H_\lambda \gamma^\mu \psi, \quad \ldots \ldots \quad (7)$$

where

$$K^\mu_\lambda = \frac{\partial \gamma^\mu}{\partial x^\lambda} + \gamma^\rho \Delta^\mu_{\rho\lambda}. \quad \ldots \ldots \quad (8)$$

In Riemannian geometry the relation

$$\frac{\partial \gamma^{\mu\nu}}{\partial x^\lambda} + \Delta^\mu_{\alpha\lambda} \gamma^{\alpha\nu} + \Delta^\nu_{\alpha\lambda} \gamma^{\mu\alpha} \equiv 0. \quad \ldots \ldots \quad (9)$$

Equation (8) can be interpreted as the corresponding identity in matrix geometry satisfied by the matrices (γ^μ).

The identity⁽³⁾

$$\kappa^\mu_\mu = 0 \quad \ldots \ldots \quad (10)$$

then leads to

$$\gamma^{\mu}\frac{\partial\psi}{\partial x^{\mu}}=\mathrm{H}_{\mu}\gamma^{\mu}\psi, \qquad . \ . \ . \ . \ . \ . \ . \ . \quad (11)$$

which can be interpreted as a metrical law or a law of gauging. It is, on the other hand, a generalization of Dirac's equation for the nuclear particles.

The procedure is similar to that of Einstein who, in order to obtain the law of gravitation, imposed a limitation on the reduced form of the Riemannian tensor.

(H_{μ}) which is supposed to depend upon the field components may be a matrix.

In the theory of Weyl the corresponding quantity was the electromagnetic potential, but in the five-dimensional theory the corresponding potential is expressed by the components with a suffix 5 e.g. V_{m5}, so that it is natural in this theory to suppose that the field components occur in (H_{μ}).

It is possible to deduce equations similar to (7) and (9) by a procedure more in accordance with that introduced by Eddington in his generalization of Weyl's theory(4).

Let the definition of parallel displacement, in the case of the existence of a nuclear field, be

$$d\mathrm{C}_{\mu}=\Lambda^{\nu}_{\mu\lambda}\mathrm{C}_{\nu}\,dx^{\lambda}. \qquad . \ . \ . \ . \ . \ . \ . \quad (12)$$

Consider the change in the matrix length in the case of this displacement.

It follows that

$$d\mathrm{L}=\left\{\gamma^{\mu}\frac{\partial\psi}{\partial x^{\lambda}}+\gamma^{\rho}(\Lambda^{\mu}_{\rho\lambda}-\Delta^{\mu}_{\rho\lambda})\psi+\kappa^{\mu}_{\lambda}\psi\right\}\mathrm{C}_{\mu}\,dx^{\lambda}. \qquad . \ . \ . \ . \quad (13)$$

The gauging equation is deduced by postulating

$$\gamma^{\mu}\frac{\partial\psi}{\partial x^{\mu}}+\gamma^{\rho}(\Lambda^{\mu}_{\rho\mu}-\Delta^{\mu}_{\rho\mu})\psi+\kappa^{\mu}_{\mu}\psi=0. \qquad . \ . \ . \ . \ . \ . \quad (14)$$

This equation takes the form of (11) if

$$\mathrm{H}_{\mu}\gamma^{\mu}\gamma^{\rho}(\Delta^{\mu}_{\rho\mu}-\Lambda^{\mu}_{\rho\mu}). \qquad . \ . \ . \ . \ . \ . \ . \quad (15)$$

It is proposed, however, to retain the implications of the former derivation.

The Form of the Quantum Equation in Different Types of Field(5).

1. Let a field be characterized by a vector (V_{μ}) $(\mu=1, 2, 3, 4, 5)$ such that

$$\frac{\partial \mathrm{V}_{\mu}}{\partial x^{\lambda}}-\frac{\partial \mathrm{V}_{\lambda}}{\partial x^{\mu}}=0. \qquad . \ . \ . \ . \ . \ . \ . \ . \quad (16)$$

A vector (T^{μ}) also exists related to (V^{μ}) in a way similar to the relation between H and B in a magnetic field, or E and D in an electric field.

(T^{μ}) satisfies the relation

$$\operatorname{div} T_{\mu}=0, \qquad (17)$$

the term div being understood in its covariant sense.

The left-hand side of equation (11) can be expressed in terms of the four-dimensional matrices (β^{m}) and $(\beta.)$ in the usual way by writing

$$\gamma^{m}=\beta^{m}, \qquad \gamma_{5}=\beta. \qquad (18)$$

It then becomes

$$\beta^{m}\left(\frac{\partial}{\partial x^{m}}-\frac{2\pi ie}{hc}\phi_{m}\right)\psi+i\kappa\beta.\psi=H_{\mu}\gamma^{\mu}\psi, \qquad (19)$$

it being assumed that x^{5} occurs only in the factor $\exp(\iota\kappa x^{5})$.

Thus $\frac{hc}{2\pi\iota}H_{\mu}\gamma^{\mu}\psi$ represents an additional energy term.

The value of this energy is calculated from an expression of the form $\frac{hc}{2\pi i}.\theta H_{\mu}\gamma^{\mu}\psi$, where θ will take the value $\psi^{+}\iota\beta_{4}$ or $\psi^{+}\iota\beta_{4}\beta\beta.$ in the different types of field considered.

The value of this expression will be chosen so that it represents a real quantity.

The type of field now considered can be described as of the vector and scalar type, since the vector (V_{μ}) can be replaced by a four-dimensional vector (A_{m}) and a scalar A. by means of the relations $V^{m}=A^{m}$, $V_{5}=A$.

The simplest assumption which can be made about (H_{μ}) in the present case is that it takes the form $(g_{1}V_{\mu})$ where g_{1} is a constant and (V_{μ}) is the field vector.

Thus the energy term in this case is

$$\frac{hc}{2\pi i}.g_{1}V_{\mu}\theta\gamma^{\mu}\psi+\text{complex conjugate}. \qquad (20)$$

It is necessary to take account of nuclear transitions in this formula by introducing the operators $\tau=\begin{pmatrix}0 & 0\\ 1 & 0\end{pmatrix}$ and $\tau^{*}=\begin{pmatrix}0 & 1\\ 0 & 0\end{pmatrix}$ to denote the changes from neutron to proton and proton to neutron respectively. Thus the expression (20) becomes

$$\frac{hc}{2\pi i}.g_{1}V_{\mu}\theta\gamma^{\mu}\tau\psi \qquad (21)$$

and the conjugate complex term will be omitted for simplicity but will be understood.

In the four-dimensional form the expression is :

$$\frac{hc}{2\pi i}.g_{1}A_{m}\theta\beta^{m}\tau\psi+\frac{hc}{2\pi i}.g_{1}A.\theta\beta.\tau\psi. \qquad (22)$$

It is unnecessary to take account of the gravitational field in these theories so that $\beta^{m}=\beta_{m}$.

Writing $\theta=\psi^{+}\iota\beta_4$ and introducing the Dirac matrices

$$\alpha_k=-\iota\beta_4\beta_k, \qquad \beta=-\iota\beta_4\beta. \qquad (k=1,\,2,\,3), \quad . \quad . \quad . \quad (23)$$

the expression (22) takes the form :

$$\frac{hc}{2\pi}g_1 i\mathrm{A}_k\psi^{+}\alpha_k\tau\psi-\frac{hc}{2\pi}g_1 i\mathrm{A}_0\psi^{+}\tau\psi+\frac{hc}{2\pi}g_1 i\mathrm{A}\,.\,\psi^{+}\beta\tau\psi, \quad . \quad . \quad . \quad (24)$$

where $\mathrm{A}_4=-i\mathrm{A}_0$.

It should also be noted that on account of the fact that x^4 is imaginary $\mathrm{A}_4{}^{*}=-\iota\mathrm{A}_4{}^{*}$. Thus, in spite of the notation $\mathrm{A}_4{}^{*}$ is not the complex conjugate of A_4 although $\mathrm{A}_0{}^{*}$ is of A_0. A similar remark applies to other quantities containing the suffix 4.

2. Let the field be characterized by antisymmetric tensors of the second rank $(\mathrm{V}_{\mu\nu})$ and $(\mathrm{T}_{\mu\nu})$.

The field equations in this case are

$$\frac{\partial \mathrm{V}_{\mu\nu}}{\partial x^{\lambda}}+\frac{\partial \mathrm{V}_{\mu\lambda}}{\partial x^{\mu}}+\frac{\partial \mathrm{V}_{\lambda\mu}}{\partial x}=0, \quad . \quad . \quad . \quad . \quad . \quad . \quad . \quad (25)$$

$$\operatorname{div}(\mathrm{T}^{\mu\nu})=0,$$

and the latter can be reduced to the form

$$\frac{\partial \mathrm{T}^{\mu\nu}}{\partial x^{\nu}}=0. \quad . \quad . \quad . \quad . \quad . \quad . \quad . \quad . \quad (26)$$

In this case the form adopted for H_{μ} is

$$\mathrm{H}_{\mu}=g_2\gamma^{\nu}\mathrm{V}_{\nu\mu}{}^{(6)} \quad . \quad . \quad . \quad . \quad . \quad . \quad . \quad . \quad (27)$$

and the energy expression from the quantum equation is in this case

$$\frac{hc}{2\pi i}g_2\mathrm{V}_{\nu\mu}\theta\gamma^{\nu}\gamma^{\mu}\tau\phi. \quad . \quad . \quad . \quad . \quad . \quad . \quad . \quad (28)$$

The four-dimensional form of this is

$$\frac{hc}{2\pi i}g_2(\mathrm{A}_{mn}\theta\beta^{m}\beta^{n}\tau\psi+2\mathrm{A}_{m}\,.\,\theta\beta^{m}\beta\,.\,\tau\psi). \quad . \quad . \quad . \quad . \quad (29)$$

Writing $\theta=\psi^{+}\iota\beta_4\beta$. and introducing the Dirac matrices this expression becomes

$$\frac{hc}{2\pi}g_2\mathrm{A}_{kl}\psi^{+}\iota\beta\alpha_k\alpha_l\tau\psi-\frac{hc}{2\pi}2g_2\mathrm{A}_{k0}\psi^{+}\iota\beta\alpha_k\tau\psi$$
$$-\frac{hc}{2\pi}2g_2\iota\mathrm{A}_k\,.\,\psi^{+}\alpha_k\tau\psi-\frac{hc}{2\pi}2g_2\mathrm{A}_4\,.\,\psi^{+}\tau\phi. \quad . \quad . \quad . \quad . \quad (30)$$

3. Let the field characterized by tensors of the third rank $(\mathrm{V}_{\lambda\mu\nu})$ and $(\mathrm{T}_{\lambda\mu\nu})$ antisymmetric in (λ,μ) and (μ,ν). The field equations are

$$\frac{\partial \mathrm{V}_{\mu\nu\rho}}{\partial x^{\lambda}}-\frac{\partial \mathrm{V}_{\nu\rho\lambda}}{\partial x^{\mu}}+\frac{\partial \mathrm{V}_{\rho\lambda\mu}}{\partial x^{\nu}}-\frac{\partial \mathrm{V}_{\lambda\mu\nu}}{\partial x^{\rho}}=0, \quad . \quad . \quad . \quad . \quad (31)$$

$$\frac{\partial \mathrm{T}^{\lambda\mu\nu}}{\partial x^{\lambda}}=0. \quad . \quad . \quad . \quad . \quad . \quad . \quad . \quad . \quad (32)$$

In this case the form chosen for H_μ is

$$H_\mu = g_3 \gamma^\nu \gamma^\rho \gamma^\mu V_{\nu\rho\mu}. \qquad (33)$$

A similar procedure shows the appearance of a new term containing $\psi^+ \iota \alpha_1 \alpha_2 \alpha_3 \psi$ and $\psi^+ \iota \alpha_2 \alpha_3 \psi$ in the energy expression which have been described as representing a pseudo-vector field.

4. Finally when the field tensors are $(V_{\lambda\mu\nu\rho})$ and $(T^{\lambda\mu\nu\rho})$ the equations are

$$\frac{\partial V_{\mu\nu\rho\sigma}}{\partial x^\lambda} + \frac{\partial V_{\nu\rho\sigma\lambda}}{\partial x^\mu} + \frac{\partial V_{\rho\sigma\lambda\mu}}{\partial x^\nu} + \frac{\partial V_{\sigma\lambda\mu\nu}}{\partial x^\rho} + \frac{\partial V_{\lambda\mu\nu\rho}}{\partial x^\sigma} = 0 \qquad (34)$$

and

$$\frac{\partial T^{\lambda\mu\nu\rho}}{\partial x^\lambda} = 0. \qquad (35)$$

These tensors are antisymmetric in neighbouring suffixes.

The expression for H_μ is

$$H_\mu = g_4 \gamma^\sigma \gamma^\nu \gamma^\rho \gamma^\mu V_{\sigma\nu\rho\mu}. \qquad (36)$$

In this case $\theta = \psi^+ \iota \beta_4 \beta$. and a new term $\psi^+ \iota \beta \alpha_1 \alpha_2 \alpha_3 \psi$, described as a pseudoscalar term, appears in the energy expression.

Interaction Terms.

These additional terms have been described as arising from the interaction between the field and the sources. Thus in the expression (30) $(A_{mn}, A_m.)$ are descriptive of the meson field while $\psi^+ \iota \beta \alpha_k \alpha_l \tau \psi$, etc., are said to arise from the nuclear particles.

In the derivation of the quantum equations given here the matrix terms occur in the same way as the coefficients (g_{mn}) in the theory of gravitation. They represent a particular kind of geometry and metrics which may be described as matrix geometry.

Nuclear Field Theories. Analogy with the Electromagnetic Theory of a Polarizable Medium.

The quantum equations can be described as the particle representation of the phenomenon to which they refer. But the form of the interaction terms which they contain gives the clue to another aspect of the phenomenon. They suggest the interaction which occurs between the field and polarization in the electromagnetic theory of polarizable media. If the suggestion is followed up, the analogy is revealed as very close.

This can be studied by means of the second example of the nuclear field theories in which the field is represented by a tensor. But it will appear that the same significance exists in the other cases.

Maxwell's equations for the electromagnetic field are:

$$\left.\begin{aligned} \operatorname{curl} H - \dot{E}/c &= 4\pi s, & \operatorname{curl} E + \dot{H}/c &= 0, \\ \operatorname{div} E &= 4\pi\rho, & \operatorname{div} H &= 0. \end{aligned}\right\} \qquad (37)$$

In the relativistic form these equations are written as follows:

$$\frac{\partial F_{kl}}{\partial x^j}+\frac{\partial F_{lj}}{\partial x^k}+\frac{\partial F_{jk}}{\partial x^l}=0, \qquad \text{(38)}$$

$$\frac{\partial F^{jk}}{\partial x^k}=P^j. \qquad \text{(39)}$$

The characteristic feature is the occurrence of a single tensor (F^{jk}) or (F_{jk}) of the form

$$F_{jk}=\frac{\partial \phi_k}{\partial x^j}-\frac{\partial \phi_j}{\partial x^k}, \qquad \text{(40)}$$

$$(F_{jk})=\begin{pmatrix} 0 & H_z & -H_y & -\iota E_x \\ -H_z & 0 & H_x & -\iota E_y \\ H_y & -H_x & 0 & -\iota E_y \\ \iota E_x & \iota E_y & \iota E_z & 0 \end{pmatrix}. \qquad \text{(41)}$$

The case in which $(P^j)=0$ is that of a pure radiation field.

The corresponding case in nuclear field theory is that of the pure meson field described by the equations

$$\frac{\partial V_{\mu\nu}}{\partial x^\lambda}+\frac{\partial V_{\nu\lambda}}{\partial x^\mu}+\frac{\partial V_{\lambda\mu}}{\partial x^\nu}=0, \qquad \text{(42)}$$

$$\frac{\partial V^{\mu\nu}}{\partial x^\nu}=0, \qquad \text{(43)}$$

$$V_{\mu\nu}=\frac{\partial f_\nu}{\partial x^\mu}-\frac{\partial f_\mu}{\partial x^\nu}. \qquad \text{(44)}$$

$(\lambda, \mu, v)=1, 2, 3, 4, 5)$ and x^5 occurs only in the factor exp.$(\iota\kappa x^5)$, where $\kappa=2\pi m_0 c/h$ and m_0 is the mass of the particle associated with the field. In this case m_0 is the mass of the meson.

It has become customary to write $\kappa f_m=U_m$.

The characteristic feature is that only one field tensor occurs. In the electromagnetic theory the presence of ponderable matter is represented by the introduction of the vectors B and D related to the polarization by the familiar relations

$$B=H+4\pi I, \qquad D=E+4\pi P. \qquad \text{(45)}$$

In their relativistic form the field equations now become

$$\frac{\partial B_{kl}}{\partial x^j}+\frac{\partial B_{lj}}{\partial x^k}+\frac{\partial B_{jk}}{\partial x^l}=0, \qquad \text{(46)}$$

$$\frac{\partial F^{jk}}{\partial x^k}=P^j, \qquad \text{(47)}$$

$$B_{jk}=\frac{\partial \phi_k}{\partial x^j}-\frac{\partial \phi_j}{\partial x^k}, \qquad \text{(48)}$$

$$(F^{jk})=\begin{pmatrix} 0 & H_z & -H_y & -\iota D_x \\ -H_z & 0 & H_x & -\iota D_y \\ H_y & -H_x & 0 & -\iota D_z \\ \iota D_x & \iota D_y & D_z & 0 \end{pmatrix}, \quad . \quad . \quad . \quad (49)$$

$$(B_{jk})=\begin{pmatrix} 0 & B_z & -B_y & -\iota E_x \\ -B_z & 0 & B_x & -\iota E_y \\ B_y & -B_x & 0 & -\iota E_z \\ \iota E_x & \iota E_y & \iota E_z & 0 \end{pmatrix}. \quad . \quad . \quad . \quad (50)$$

In contrast to the case without a polarizable medium a new tensor (F^{jk}) appears which is not identical with the contravariant tensor derived from (B_{jk}).

The relations (45) are included in

$$B_{mn}=F_{mn}+4\pi I_{mn}. \quad . \quad . \quad . \quad . \quad . \quad . \quad . \quad . \quad (51)$$

In the electromagnetic theory the polarizations P and I can be regarded as the generators of the field in the case in which the current and charge densities are zero.

The nuclear field equations (25) and (26) are analogous to this case since there is no term corresponding to (P^j). The tensor $(S_{\mu\nu})$ is introduced by means of the relation

$$V_{\mu\nu}=T_{\mu\nu}+4\pi S_{\mu\nu}, \quad . \quad . \quad . \quad . \quad . \quad . \quad . \quad . \quad (52)$$

so that it appears that the field is derivable from $(S_{\mu\nu})$. From the energy tensor of the field it is possible to find those terms which represent an interaction between the field $(V_{\mu\nu})$ and the polarization components $(S_{\mu\nu})$.

If these are compared with the interaction terms of the quantum equation, the values of the polarization components can be determined.

The Energy Tensor.

The tensor which corresponds to the momentum-energy tensor in the four-dimensional continuum now includes momentum, energy and current.

In order to derive it the tensor $(P_{\mu\nu})$ is formed.

$$P^{\mu\nu}=T^{*\mu\alpha}V^{\nu}_{\alpha}+\text{conjugate complex}. \quad . \quad . \quad . \quad . \quad (53)$$

The energy tensor is

$$R^{\mu\nu}=P^{\mu\nu}-\tfrac{1}{4}\gamma^{\mu\nu}P, \quad . \quad . \quad . \quad . \quad . \quad . \quad . \quad (54)$$

where

$$P=\gamma_{\mu\nu}P^{\mu\nu}. \quad . \quad . \quad . \quad . \quad . \quad . \quad . \quad . \quad (55)$$

The energy density term $(-R^{44})$ has the value

$$-R^{44}=-P^{44}+\tfrac{1}{4}\gamma^{44}P=-T^{*4\alpha}V^{4}_{\alpha}+\tfrac{1}{4}\gamma^{44}T^{*\alpha}_{\mu}V^{\mu}_{\alpha}, \quad . \quad . \quad (56)$$

the addition of the complex conjugate terms being understood.

If the components of the tensor $(\mathrm{T}^{\mu\tau})$ be substituted by means of equation (52), the terms containing products of the components of $(\mathrm{S}^{\mu\nu})$ and $(\mathrm{V}^{\mu\nu})$ are found to be

$$4\pi(\mathrm{S}^{*4\alpha}\mathrm{V}^{4}_{\alpha}-\tfrac{1}{4}\gamma^{44}\mathrm{S}^{*\alpha}_{\mu}\mathrm{V}^{\mu}_{\alpha}). \quad \ldots\ldots \quad (57)$$

Let the four-dimensional counterparts of the tensors $(\mathrm{S}^{\mu\nu})$ be (I^{mn}) and $(\mathrm{I}^{m}.)$. Neglecting gravitational effects the expression (57) can be expressed in the form

$$4\pi(-\tfrac{1}{4}\mathrm{I}^{*}_{kl}\mathrm{A}_{kl}+\tfrac{1}{2}\mathrm{I}^{*}_{4l}\mathrm{A}_{4l}-\tfrac{1}{2}\mathrm{I}^{*}_{l.}\mathrm{A}^{*}_{l.}+\tfrac{1}{2}\mathrm{I}^{*}_{4.}\mathrm{A}_{4.}) \quad \ldots \quad (58)$$
$$(k, l=1, 2, 3).$$

It follows by comparison with expression (30) which also represents the interaction terms that

$$\left.\begin{aligned}
\mathrm{I}^{*}_{kl}&=-\frac{hc}{2\pi^2}g_2\psi^{+}\iota\beta\alpha_k\alpha_l\tau\psi=-\frac{hc}{2\pi^2}g_2\psi^{+}\beta_4\beta\,.\,\beta_k\beta_l\tau\psi,\\
\mathrm{I}^{*}_{ol}=\iota\mathrm{I}^{*}_{4l}&=-\frac{hc}{2\pi^2}g_2\psi^{+}\iota\beta\alpha_l\tau\psi=-\frac{hc}{2\pi^2}g_2\psi^{+}\iota\beta\,.\,\beta_l\tau\psi,\\
\mathrm{I}^{*}_{l.}&=\frac{hc}{2\pi^2}g_2\psi^{+}\alpha_l\tau\psi=-\frac{hc}{2\pi^2}g_2\psi^{+}\iota\beta_4\beta_l\tau\psi,\\
\mathrm{I}^{*}_{4.}&=-\frac{hc}{2\pi^2}g_2\psi^{+}\tau\psi.
\end{aligned}\right\} \quad \ldots \quad (59)$$

From these results the values of I_{kl}, etc., can be determined, e.g.

$$\mathrm{I}_{kl}=-\frac{hc}{2\pi^2}g_2{}^{*}\psi^{+}\beta_4\beta\,.\,\beta_k\beta_l\psi. \quad \ldots\ldots \quad (60)$$

Conclusion.

These components of the polarization tensor (I_{mn}) and of the vector $(\mathrm{I}_{m.})$ are thus all derived from the fundamental matrices and the matrix ψ, which, according to the present approach to the proble m, can be described as a metrical factor. It is evident that the field components are determined by the polarization tensors and vectors. Thus the field finds its origin in the system of matrix geometry and metrics.

This gives to nuclear phenomena an interpretation like that given to gravitational phenomena by an appeal to the form of Riemannian geometry. Thus it may be said of matrix geometry, as has been said of four-dimensional geometry, that it is both the framework and the events of the physical world.

References.

(1) Flint, Proc. Roy. Soc. A. 150, p. 428, 1935.
(2) Kaluza, S.B. Akad. Wiss. p. 966, 1921.
(3) Flint, Phil. Mag. Ser. 7, xxix. p. 417, 1940.
(4) Eddington, Math. Theory Rel. 1st ed. § 93.
(5) Kemmer, Proc. Roy. Soc. A, 167, p. 125, 1938. (Summary on Quantum Fields.)
(6) Chirgwin and Flint, Nature, 155, p. 724, June 16, 1945.

LXXIX. *Switching Problems and Instantaneous Impulses.*

By J. C. JAEGER[*].

[Received July 18, 1944.]

1. PROBLEMS on transients in electric circuits caused by switching operations are of considerable practical importance, but their theory does not seem to be fully discussed in works on circuit theory. Such problems involve an electrical system started at time $t=0$ with arbitrarily given initial conditions, which may or may not be compatible with the equations to be satisfied by the currents and charges for $t>0$; a simple example of the latter case is that of two inductances, with different initial currents, connected in series at $t=0$. The operational, or Laplace transformation methods, applied formally in the usual way to such problems with their given initial conditions, lead to a solution, but clearly this procedure needs justification; this point was raised by Brown[†], but he does not give a complete discussion of it. The latter has been studied by Ghizzetti[‡], whose discussion of the case in which the given initial conditions are incompatible with the system of equations does not seem to be adequate. The point of view of the present note is that in this case there is a rapid readjustment of conditions in a very short time following $t=0$, similar to that of a moving dynamical system when additional constraints are imposed, and that Ghizzetti's algebra can be used to show that, under sufficiently general conditions, the solutions obtained by the formal Laplace transformation procedure tend to the readjusted conditions as $t\rightarrow 0$. The question is bound up with the theory of impulsive currents, and the related one of impulsive E.M.F.'s, and it is shown that the use of these, regarded as purely symbolical, leads to correct results.

2. The Laplace transformation method for solving [§] a system of simultaneous ordinary linear differential equations with constant coefficients (dashes are used for differentiation with respect to t)

$$\sum_{s=1}^{n} a_{rs}Q_s''+b_{rs}Q_s'c_{rs}Q_s=E_r(t), \quad r=1, \ldots, n,\ t>0, \quad . \quad . \quad . \quad (1)$$

---

[*] Communicated by the Author.

[†] Math. Gazette, xxvi. p. 157 (1942).

[‡] *Rendiconti Circ. Math. di Palermo,* lxi. p. 339 (1937).

[§] Carslaw and Jaeger, 'Operational Methods in Applied Mathematics' (Oxford, 1941); Doetsch, 'Theorie und Anwendung der Laplace Transformation' (Springer, 1937).

with initial values

$$\overset{\circ}{Q}_s \text{ of } Q_s \text{ and } \overset{\circ}{Q}{}'_s \text{ of } Q'_s, \quad s=1, \ldots, n, \qquad . \quad . \quad . \quad . \quad (2)$$

consists of writing down the system of "subsidiary equations,"

$$\sum_{s=1}^{n} (a_{rs}p^2+b_{rs}p+c_{rs})\overline{Q}_s=\overline{E}_r+\sum_{s=1}^{n} \{a_{rs}(p\overset{\circ}{Q}_s+\overset{\circ}{Q}{}'_s)+b_{rs}\overset{\circ}{Q}_s\}, \quad r=1, \ldots, n, \quad (3)$$

for the Laplace transforms $\overline{Q}_s$ defined by

$$\overline{Q}_s(p)=\int_0^\infty e^{-pt}Q_s(t)\,dt \qquad . \quad . \quad . \quad . \quad . \quad . \quad (4)$$

(where p is a number whose real part is positive and sufficiently large to make the integrals convergent), solving (3) for the $\overline{Q}_s$, and deriving the solutions $Q_s(t)$ from the $\overline{Q}_s$. Strictly this procedure is merely formal, but for the system (1) it can be made rigorous by a general verification * that the solutions Q_s obtained in this way do satisfy the differential equations (1) and initial conditions (2), provided the determinant of the a_{rs} is not zero.

If a problem in dynamics or circuit theory can be formulated as a system of equations of type (1), to be solved with initial conditions (2), we can thus assert immediately that the solution obtained by the usual Laplace transformation or operational procedure does satisfy the differential equations and initial conditions. Usually, however, problems in circuit theory do not lead to systems of type (1) but to some algebraic, some first-order and some second-order differential equations; the general system may be taken to be †

$$\sum_{k=1}^{n} (a_{ik}Q''_k+b_{ik}Q'_k+c_{ik}Q_k)=E_i(t), \quad i=1, \ldots, \alpha, t>0, \quad . \quad . \quad (5)$$

$$\sum_{k=1} (b_{jk}Q'_k+c_{jk}Q_k)=E_j(t), \quad j=\alpha+1, \ldots, \alpha+\beta, t>0, \quad (6)$$

$$\sum_{k=1}^{n} c_{lk}Q_k=E_l(t), \quad l=\alpha+\beta+1, \ldots, n, t>0. \quad (7)$$

Here Q_k is the charge on the condenser in the kth circuit element at time t, if there is a condenser in this element; if not, it is defined as the charge which has passed a point of that element at time t. In either case

$$Q'_k=I_k, \quad t>0, \qquad . \quad . \quad . \quad . \quad . \quad . \quad . \quad . \quad . \quad (8)$$

where I_k is the current in the k-th element. The applied E.M.F.'s, E_i, E_j, E_l are supposed to have continuous differential coefficients for $t>0$, though this restriction can be partially removed.

Equations of types (5), (6), (7) will arise as follows:—(5) is the result of applying Kirchhoff's second law to closed circuits containing some

---

* A verification by elementary methods is given by Doetsch, *loc. cit.* Kap. 18. A shorter discussion can be given using complex variable, see, *e. g.* Carslaw and Jaeger, *loc. cit.* §§34, 45.

† The notation is that of Ghizzetti's paper, *loc. cit.*

inductance ; we assume that the rank of the matrix (a_{ik}) is α, that is that no algebraic or first-order equations can be formed by linear combinations of equations (5)—if this were possible with a given set of equations, such equations of lower order would be formed and included in (6) or (7). Equations of type (6) may arise in three ways : (i) first-order equations derived as above by linear combinations of second-order equations *, (ii) Kirchhoff's second law for closed circuits containing resistance and capacity only, (iii) linear connections between currents arising from Kirchhoff's first law at the junctions †. We assume that the rank of the matrix (b_{jk}) is β, *i. e.* that the equations have been so reduced that no algebraic equations may be formed by linear combinations of them. Finally, equations of type (7) arise either as linear combinations as above or first- or second-order equations, or from the application of Kirchhoff's second law to closed circuits containing condensers only. The rank of the matrix (c_{lk}) must be $n-\alpha-\beta$, or the number of algebraic equations could be reduced.

Following Ghizzetti we assume that Δ, the n-rowed determinant of the quantities a_{ik}, b_{jk}, c_{lk} does not vanish. This includes the statements made above about the ranks of the matrices (a_{ik}), (b_{jk}), (c_{lk}), and also excludes the possibility of forming equations of lower order by combining some of (5), (6), (7) with the derivatives of others, for example, some of (6) with the differential coefficients of some of (7), namely

$$\sum_{k=1}^{n} c_{lk}Q'_k = E'_l(t), \quad l=\alpha+\beta+1, \ldots, n,\ t>0. \quad . \quad . \quad . \quad (9)$$

We have to solve (5), (6), (7) with given initial values ‡

$$\overset{\circ}{Q}_k \text{ of } Q_k \text{ and } \overset{\circ}{Q}'_k \text{ of } Q'_k, \quad . \quad . \quad . \quad . \quad . \quad . \quad . \quad (10)$$

and, proceeding in the usual way, we write down the formal subsidiary equations corresponding to (5), (6), (7), (10), namely

$$\sum_{k=1}^{n} (a_{ik}p^2+b_{ik}p+c_{ik})\bar{Q}_k = \bar{E}_i + \sum_{k=1}^{n} a_{ik}(p\overset{\circ}{Q}_k+\overset{\circ}{Q}'_k)+b_{ik}\overset{\circ}{Q}_k, \quad i=1, \ldots, \alpha, \quad (11)$$

---

* An example of this occurs in the case of " perfect " coupling.

† Ghizzetti does not mention this point and gives the impression that his currents are chosen throughout to satisfy Kirchhoff's first law automatically, but his analysis holds for the more general case above. It is important that the currents need not be specified so as to satisfy Kirchhoff's first law automatically (for example, by the use of mesh currents), as this greatly restricts the possible choices of initial conditions : for example, we may have several inductances in series and wish to give each of them its own initial current ; this case is provided for in the specification (5), (6), (7).

‡ It is desirable to be precise about this point. $\overset{\circ}{Q}_k$ and $\overset{\circ}{Q}'_k$ are thought of as the given values *at* the instant $t=0$ when the system is started. If the $Q_k(t)$ were discontinuous at $t=0$, it would not be these $\overset{\circ}{Q}_k$ but the (unknown) values $\lim\limits_{t\to+0} Q_k(t)$ which would appear in the subsidiary equation as derived by the usual arguments. Thus, if there is any suspicion of this (11), (12), (13), which include the $\overset{\circ}{Q}_k$, are purely tentative, and the whole burden of proof rests on the verification process.

$$\sum_{k=1}^{n}(b_{jk}p+c_{jk})\overline{Q}_k=\overline{E}_j+\sum_{k=1}^{n}b_{jk}\mathring{Q}_k,\quad j=\alpha+1,\ldots,\alpha+\beta, \tag{12}$$

$$\sum_{k=1}^{n}c_{lk}\overline{Q}_k=\overline{E}_l,\quad l=\alpha+\beta+1,\ldots,n. \tag{13}$$

Since $\varDelta\neq 0$ we can solve these for the $\overline{Q}_k$ and from them find the solutions $Q_k(t)$. Then it is necessary to verify that the $Q_k(t)$ calculated in this way do satisfy (5), (6), (7), (10). Ghizzetti extends the procedure of Doetsch (*loc. cit.*) to show that they do satisfy the equations (5), (6), (7) whatever the values of $\mathring{Q}_k$ and $\mathring{Q}'_k$, so this point need not be referred to again. With the initial conditions (10) there is clearly a difficulty: if the arbitrary initial values $\mathring{Q}_k$ and $\mathring{Q}'_k$ of Q_k and Q'_k do not satisfy (6), (7), (9) (that is to say are incompatible with the system of equations proposed), there is, strictly, no solution. Ghizzetti shows that if they do satisfy these equations, the Q_k and Q'_k obtained by the Laplace transformation procedure do satisfy the initial conditions (10).

It remains to discuss the question, which is of importance in connection with switching operations, of what happens when the $\mathring{Q}_k$ and $\mathring{Q}'_k$ prescribed are incompatible with (6), (7) or (9). Ghizzetti attempts to argue that the solutions obtained by the Laplace transformation procedure should still be regarded as the solution of the problem, but his arguments do not seem to be conclusive. Physically the problem is analogous to that of a dynamical system in motion, on which additional constraints are imposed at $t=0$. In dynamics it would be said that there was an impulsive readjustment at $t=0$ due to the imposition of the new constraints, and new initial values would be calculated from the laws of impulsive motion, and used with the equations of motion of the constrained system for $t>0$. What is needed here, then, is a theory of impulsive motion in an electric circuit, analogous to the theory of impulses in dynamics *. In the present problem we suppose that there is an "impulsive" readjustment of conditions in an extremely short time, starting at $t=0$, and that in this time the Q_k and Q'_k vary continuously but extremely rapidly from the values $\mathring{Q}_k$, $\mathring{Q}'_k$ to new values $Q_k(+0)$ and $Q'_k(+0)$. To find these new values, we proceed as in the dynamical case and integrate the equations of motion over this very small time, neglecting the integrals of finite quantities. In this way (5) and (6) give

$$\sum_{k=1}^{n}\{a_{ik}[Q'_k(+0)-\mathring{Q}'_k]+b_{ik}[Q_k(+0)-\mathring{Q}_k]\}=0,\quad i=1,\ldots,\alpha, \tag{14}$$

$$\sum_{k=1}^{n}b_{jk}[Q_k(+0)-\mathring{Q}_k]=0,\quad j=\alpha+1,\ldots,\alpha+\beta. \tag{15}$$

---

* In the final analysis both come down to Lagrange's equations, but familiarity with an elementary theory of impulses would be as useful in electricity as it is in dynamics.

Also integrating (5) twice gives

$$\sum_{k=1}^{n} a_{ik}[Q_k(+0)-\overset{\circ}{Q}_k]=0, \quad i=1,\ldots,\alpha. \quad . \quad . \quad . \quad . \quad (16)$$

In addition to these we know that the new values $Q_k(+0)$ and $Q'_k(+0)$ will satisfy (6), (7) and (9); that is

$$\sum_{k=1}^{n} [b_{jk}Q'_k(+0)+c_{jk}Q_k(+0)]=E_j(+0), \quad j=\alpha+1,\ldots,\alpha+\beta, \quad . \quad (17)$$

$$\sum_{k=1}^{n} c_{lk}Q_k(+0)=E_l(+0), \quad l=\alpha+\beta+1,\ldots,n, \quad . \quad (18)$$

$$\sum_{k=1}^{n} c_{lk}Q'_k(+0)=E'_l(+0), \quad l=\alpha+\beta+1,\ldots,n. \quad . \quad (19)$$

Equations (14) . . . (19) are the equations of impulsive readjustment for the system (5), (6), (7), and have determinant $\Delta^2\neq 0$. Of these (15), (16), (18) are a system of n equations with determinant $\Delta\neq 0$ for the n unknowns $Q_k(+0)$. When these have been found (14), (17), (19) are a system of n equations with determinant $\Delta\neq 0$ for the n unknowns $Q'_k(+0)$. Thus these equations determine new initial conditions $Q_k(+0)$ and $Q'_k(+0)$ which are compatible with (6), (7), (9), and we could proceed to solve (5), (6), (7) with these new initial conditions. However, there is no need to do this as we shall show that *the solutions* $Q_k(t)$ *and* $Q'_k(t)$ *derived by the Laplace transformation procedure from the formal subsidiary equations* (11), (12), (13), *which use the given initial values* $\overset{\circ}{Q}_k$ *and* $\overset{\circ}{Q}'_k$ *take, when* $t=0$, *the values* $Q_k(+0)$ *and* $Q'_k(+0)$, *which are the solutions of the impulsive equations* (14) . . (19). *That is, that the solutions obtained by the Laplace transformation method using arbitrary initial values of the* Q_k *amd* Q'_k *tend as* $t\rightarrow 0$ *to the values existing in the circuit after impulsive readjustment, if this takes place.*

This follows immediately from Ghizzetti's equations (34) and (38), though, as remarked above, he interprets these in a different connection.

3. *Impulsive functions and impulsive currents.*

In the analysis above no mention of impulsive currents has been made. It has been verified that in some circumstances a finite alteration in charge can take place in a vanishingly short time; there will in this case be a very great current for a very short time, and the time-integral of this current will be finite—that is, what is usually called an impulsive current. The symbolic discussion of such impulsive currents by the use of the δ function * is a very important and easy way of following what is going on in a circuit, but it must be regarded as a symbolic method only, the results obtained by it being justified by an argument, such as that of § 2, which does not involve the explicit use of the δ function.

---

* For fuller discussion see Carslaw and Jaeger, *loc. cit.* Appendix III. Also van der Pol, Journ. Inst. Elect. Eng. lxxxi. p 381 (1937). The function is defined as a limit, so that it is extremely difficult to justify any limiting operations on it.

We define $\delta(t)$ to be zero for $t \leqslant 0$, very great in a vanishingly small neighbourhood to the right of $t=0$, and zero elsewhere, and such that

$$\int_0^\infty \delta(t)\,dt=1. \quad . \quad . \quad . \quad . \quad . \quad . \quad . \quad . \quad (20)$$

It has the property that if $f(t)$ is continuous

$$\int_0^\infty f(t)\,\delta(t-a)\,dt=f(a),$$

and, in particular,

$$\int_0^\infty e^{-pt}\,\delta(t)\,dt=1. \quad . \quad . \quad . \quad . \quad . \quad . \quad . \quad . \quad (21)$$

Thus the Laplace transform of the δ function is unity, and a function whose Laplace transform is unity may be interpreted as a δ function.

If we had sought the Laplace transforms of the currents in the problem of § 2 we should, in general, have found such terms. From (8), with the given initial values $\mathring{Q}_k$ of the Q_k, we obtain the formal subsidiary equation

$$\bar{I}_k=p\bar{Q}_k-\mathring{Q}_k. \quad . \quad . \quad . \quad . \quad . \quad . \quad . \quad . \quad (22)$$

Now, if $Q_k(t)$ is the solution of the problem derived from (11), (12), (13) we have shown above that $Q_k \to Q_k(+0)$ as $t \to 0$. Thus

$$\bar{Q}'_k=p\bar{Q}_k-Q_k(+0). \quad . \quad . \quad . \quad . \quad . \quad . \quad . \quad . \quad (23)$$

It follows that

$$\bar{I}_k=\bar{Q}'_k+Q_k(+0)-\mathring{Q}_k,$$

and, using (21), this may be interpreted as

$$I_k=Q'_k+[Q_k(+0)-\mathring{Q}_k]\,\delta(t). \quad . \quad . \quad . \quad . \quad . \quad . \quad . \quad . \quad (24)$$

If we had worked with I_k in the subsidiary equations instead of Q_k, we would thus have found the value Q'_k (which has been verified in § 2 to be the correct one) together with the term $[Q_k(+0)-\mathring{Q}_k]\delta(t)$, which we interpret as expressing the current flowing when the charge readjusts itself impulsively from $\mathring{Q}_k$ to $Q_k(+0)$, and, again from the work of § 2, the amount of this readjustment is the correct one. Thus the use of impulsive currents in problems of this type is completely justified.

4. *Impulsive E.M.F. applied to a circuit.*

It is often of interest to determine the behaviour of a circuit when an impulsive E.M.F., typifying a very large potential for a very small time, is applied to it, just as in dynamics motion caused by blows is studied. In dynamics the new velocities due to the blows are first calculated, and then the equations of motion solved with these initial conditions *. In circuit theory the same procedure could be used, but we shall show that *if formal subsidiary equations are written down using* (21) *for the transform of the impulsive E.M.F., the solutions obtained from these satisfy the differential equations, and as $t\to 0$ tend to the solutions of the impulsive equations for the impulsive E.M.F.'s applied to the circuit.*

---

* The discussion below applies to the dynamical as well as the electrical case: that is, the Laplace transformation solution, using $Pd(t)$ as a force corresponding to a blow of impulse P, gives the correct solution without the necessity of calculating these new initial conditions.

Here, again, the δ function is only used symbolically, the proof rests on the verification process, which involves only the classical treatment of impulses and no properties of the δ function. We consider only the case of impulsive E.M.F's applied to the circuit system with zero initial conditions and with no other applied E.M.F's; there is no difficulty in including these cases. We also suppose impulsive E.M.F.'s are not applied in circuits containing condensers only (a further extension is needed to handle this case, which is not of much practical interest). Then, as in (5), (6), (7) we have to solve

$$\sum_{k=1}^{n}(a_{ik}Q_k''+b_{ik}Q_k'+c_{ik}Q_k)=P_i\delta(t),\quad i=1,\ldots,\alpha,\ t>0, \qquad (25)$$

$$\sum_{k=1}^{n}(b_{jk}Q_k'+c_{jk}Q_k)=P_j\delta(t),\quad j=\alpha+1,\ldots,\alpha+\beta,\ t>0, \qquad (26)$$

$$\sum_{k=1}^{n}c_{lk}Q_k=0,\qquad l=\alpha+\beta+1,\ldots,n, \qquad (27)$$

where the P_i, P_j are constants. The formal subsidiary equations are

$$\sum_{k=1}^{n}(a_{ik}p^2+b_{ik}p+c_{ik})\bar{Q}_k=P_i, \qquad (28)$$

$$\sum_{k=1}^{n}(b_{jk}p+c_{jk})\bar{Q}_k=P_j, \qquad (29)$$

$$\sum_{k=1}^{n}c_{lk}\bar{Q}_k=0. \qquad (30)$$

We have to show that the values of $Q_k(t)$ derived from (28), (29), (30) satisfy (25), (26), (27), and as $t\to 0$ tend to the solutions of the impulsive equations. These are

$$\sum_{k=1}^{n}a_{ik}Q_k'(+0)+b_{ik}Q_k(+0)=P_i, \qquad (31)$$

$$\sum_{k=1}^{n}b_{jk}Q_k(+0)=P_j, \qquad (32)$$

obtained by integration of (25) and (26) over a very short time.

Also, by integrating (25) twice,

$$\sum_{k=1}^{n}a_{ik}Q_k(+0)=0. \qquad (33)$$

Finally there are the equations obtained from (26) and (27) at very small times

$$\sum_{k=1}^{n}b_{jk}Q_k'(+0)+c_{jk}Q_k(+0)=0, \qquad (34)$$

$$\sum_{k=1}^{n} c_{lk} Q_x(+0) = 0, \qquad . \quad . \quad . \quad . \quad . \quad . \qquad (35)$$

$$\sum_{k=1}^{n} c_{lk} Q'_k(+0) = 0. \qquad . \quad . \quad . \quad . \quad . \quad . \qquad (36)$$

As in § 2 it follows that (31) to (36) give the $Q_k(+0)$ and $Q'_k(+0)$. The verification that the $Q_k(t)$ and $Q'_k(t)$ derived from (28) to (30) tend to these values as $t \to 0$ is precisely the same as the earlier one with some of the symbols renamed.

The University of Tasmania.

LXXX. *Theory of Ground-Water Accumulation* *.

By H. Löwy, Dr.Phil.†

[Received July 26, 1944.]

The pessimism concerning the water question in deserts depends upon a meteorologic calculus : The quantity of rain being very small, the evaporation very great, there is left only an extremely small quantity of water for infiltration into the soil.

Fig. 1.

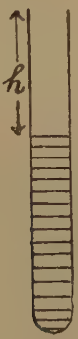

This balance, generally admitted, is not correct. According to my opinion, one has not sufficiently specified the quantities of evaporation during and after soil infiltration. I will show how one can improve the meteorologic balance by applying Stefan's theory of evaporation ‡.

---

* First published in French, in 1941, in '*L'Egypte Contemporaine*,' xxxii. p. 702, as chapter xxii. of my paper " Quelques considerations sur l'exploration et l'utilisation des déserts."

† Communicated by the Author.

‡ J. Stefan, *Sitzungsber. d. Akad. d. Wiss., Math.-Naturwiss. Classe*, Abt. II. lxviii. p. 385, Wien, 1874.

In 1874, J. Stefan established the law that the evaporation velocity of a liquid contained in a tube (fig. 1) is inversely proportional to the depth h and independent of the tube section. I suppose that the soil constitutes a system of tubes and that one can apply the theory of Stefan to the water contained in the soil.

We consider a vertical soil column of 1 cm.^{2} section (fig. 2). We suppose that the infiltration, originating from a certain shower, is contained at the time t in a layer between the depths h and H. The thickness of this water column is D$=$H$-h$. The variation with time of the level h is caused by two phenomena: (1) the evaporation, and (2) the infiltration. I put:

$$\frac{dh}{dt}=\frac{dh_1}{dt}+\frac{dh_2}{dt}. \quad \dots\dots\dots \quad (1)$$

Fig. 2

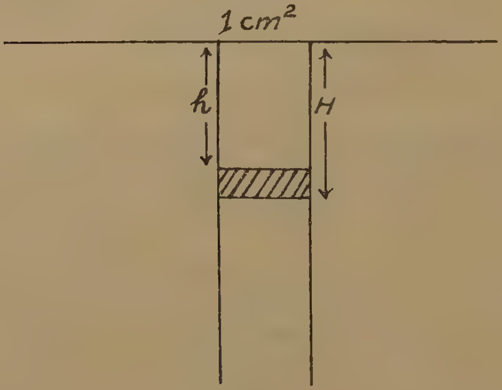

This equation expresses the *addition of velocities*: The evaporation velocity $\frac{dh_1}{dt}$ must be added to the infiltration velocity $\frac{dh_2}{dt}$.

The velocity of evaporation is, according to Stefan,

$$\frac{dh_1}{dt}=\frac{C}{h}, \quad \dots\dots\dots \quad (2)$$

C being a constant characteristic of the liquid.

The infiltration velocity being independent of the depth h, we put

$$\frac{dh_2}{dt}=K, \quad \dots\dots\dots \quad (3)$$

K being a constant.

In substituting (3) and (2) in (1), we obtain as integral of this differential equation

$$t=\frac{h}{K}-\frac{C}{K^2}\log\left(1+\frac{Kh}{C}\right), \quad \dots\dots\dots \quad (4)$$

if we suppose that $h=0$ for $t=0$.

On the lower surface of the water column the evaporation is negligible ; therefore

$$\frac{d\mathrm{H}}{dt}=\mathrm{K}. \quad . \quad . \quad . \quad . \quad . \quad . \quad . \quad . \quad . \quad (5)$$

If D_0 signifies the initial height of the column, we have

$$\mathrm{H}=\mathrm{K}t+\mathrm{D}_0. \quad . \quad . \quad . \quad . \quad . \quad . \quad . \quad . \quad . \quad (6)$$

In eliminating t from (4) and (6) we obtain the height of the column at the time t:

$$\mathrm{D}=\mathrm{H}-h=\mathrm{D}_0-\frac{\mathrm{C}}{\mathrm{K}}\log\left(1+\frac{\mathrm{K}h}{\mathrm{C}}\right). \quad . \quad . \quad . \quad . \quad . \quad (7)$$

Equation (7) *determines the diminution* $\mathrm{D}_0-\mathrm{D}$ *with the depth* h *of a water column, infiltrating in the soil with the velocity* K.

If the infiltration is blocked by an impermeable layer, a variation of the water-level can be caused by evaporation and a new infiltration. The variation caused by ulterior rain is

$$\frac{dh_3}{dt}=-\mathrm{J}, \quad . \quad . \quad . \quad . \quad . \quad . \quad . \quad . \quad . \quad (8)$$

where J signifies the annual precipitation (in cm.), divided by $3{\cdot}10^7$ (the corresponding number of seconds).

The *addition of velocities* gives

$$\frac{dh}{dt}=\frac{\mathrm{C}}{h}-\mathrm{J}. \quad . \quad . \quad . \quad . \quad . \quad . \quad . \quad . \quad . \quad (9)$$

The solution is

$$t=\frac{h_0-h}{\mathrm{J}}-\frac{\mathrm{C}}{\mathrm{J}^2}\log\frac{\mathrm{C}-h\mathrm{J}}{\mathrm{C}-h_0\mathrm{J}}, \quad . \quad . \quad . \quad . \quad . \quad . \quad (10)$$

h_0 signifies the depth of the upper level of the infiltration at the time $t=0$, when the water is blocked by an impermeable layer. *From this moment, one can use formula* (10) *for calculating the time t, necessary for an elevation* h_0-h *of the water-level.*

We will now determine the quantity of water W, which corresponds to a certain time of accumulation t. Denoting by P the porosity of the soil, by F its surface, the relation between W and h is

$$\mathrm{W}=(h_0-h)\mathrm{PF}. \quad . \quad . \quad . \quad . \quad . \quad . \quad . \quad . \quad . \quad (11)$$

For applying the results, contained in the formulas (7) and (10), one must know the values of the three constants J, K, C.

The mean annual precipitation in a desert is about 3 cm., or

$$\mathrm{J}=10^{-7}\ \mathrm{cm./sec.}$$

The value of K is in permeable soils of the order

$$\mathrm{K}=10^{-1}\ \mathrm{cm./sec.}$$

The evaporation constant C is, according to Stefan,

$$\mathrm{C}=\lambda\frac{d_1}{s_1}\log\frac{p}{p-p_1}. \quad . \quad . \quad . \quad . \quad . \quad . \quad . \quad (12)$$

λ signifies the constant of diffusion of the water vapour through air, d_1 the density of the water vapour at 0° C. and 760 mm. Hg., s_1 the density of the liquid, p the atmospheric pressure and p_1 the saturation pressure of the vapour.

The density of the water vapour in its normal state is, relatively to air, equal to 0·6218. Relatively to water, which is 773 times more dense than air, it is $d_1=0{\cdot}6218/773=8{\cdot}10^{-4}$. We put

$$\frac{d_1}{s_1}=8{\cdot}10^{-4},$$

$$\lambda=0{\cdot}282 \text{ cm.}^2/\text{sec. at } 15^\circ \text{ C.},$$

$$p_1=13 \text{ mm. at } 15^\circ \text{ C.},$$

$$p=760 \text{ mm.}$$

Therefore $$C=4{\cdot}10^{-6} \text{ cm.}^2/\text{sec.}$$

Using these values of C, K, J, one can deduce from the equations (7) and (10) the following results :—

I. *The diminution of the quantity of water during the infiltration is negligible.*

II. *The increase of the quantity of water, after being blocked by an impermeable layer, can be very considerable.*

For proving the result I. we chose for h in formula (7) an extremely great value, that is, a value greater than the depths which could be of interest from the practical point of view, for instance, $h=3000$ m. In this case, the diminution of the water column is

$$D_0-D=9{\cdot}10^{-4} \text{ cm.}$$

The diminution, therefore, is negligible in every case ($h \leqslant 3000$ m.).

Equation (7) is the quantitative expression of Georges Rolland's observation that the rain, falling on the dunes, is altogether absorbed and no more subject to evaporation *.

Concerning equation (10), we distinguish two cases : (1) the case that the evaporation is very great relatively to the precipitation ($C \gg J$) and (2) the case inverse ($J \gg C$).

If $C \gg J$, we develop $\log\dfrac{C-hJ}{C-h_0J}$ in series according to the powers of hJ/C and h_0J/C. We find, thus, that t is negative for $h<h_0$: an accumulation of water is therefore impossible in this case.

If $J \gg C$, equation (10) reduces to

$$t=\frac{h_0-h}{J}. \qquad (13)$$

In deserts, C and J are nearly of the same order of magnitude. A simple consideration, however, shows that also in this case equation (10) reduces to (13) for all values of h and h_0, which may have a practical interest. From the fact that the argument of the logarithm must be positive, it follows that h and h_0 are both either greater or smaller than C/J. In the case ($h<\mathrm{C/J}$, $h_0<\mathrm{C/J}$), the impermeable layer is situated in a depth smaller than 40 cm. This case, therefore, concerns thin æquifers near the surface. In the other case ($h>\mathrm{C/J}$, $h_0>\mathrm{C/J}$), the logarithm

---

* Georges Rolland, 'Géologie du Sahara Algérien' (Paris, 1890), p. 226.

$$\log\frac{\mathrm{C}-\mathrm{J}h}{\mathrm{C}-\mathrm{J}h_0}=\log\frac{h-\mathrm{C/J}}{h_0-\mathrm{C/J}}=f(h,\,h_0). \quad \ldots\ldots \quad (14)$$

is a monotonic increasing function f in h, and monotonic decreasing in h_0. The expression

$$\frac{h_0-h}{\mathrm{J}}=\mathrm{F}(h,\,h_0) \quad \ldots\ldots\ldots \quad (15)$$

is a monotonic decreasing function in h, and monotonic increasing in h_0.

We suppose that in the beginning the height of the water column is zero, that is : $h_0=\mathrm{H}_0$. The value of h_0 therefore represents the depth of the impermeable layer.

In sandy deserts, the depth of the impermeable layer is equal to or greater than the mean height A of the dunes :

$$h_0 \geqslant \mathrm{A}. \quad \ldots\ldots\ldots \quad (16)$$

This height is about A=30 m.=3000 cm., whereas C/J=40 cm. The condition $h_0>\mathrm{C/J}$, therefore, is satisfied.

The depth of the level h is contained in the interval

$$\mathrm{C/J}<h\leqslant \mathrm{B}, \quad \ldots\ldots\ldots \quad (17)$$

if B represents the maximum value of h.

For proving that equation (10) reduces to (13) in the intervals (16) and (17), we demonstrate that, *in these intervals, the absolute maximum value of* $f(h,\,h_0)$ *multiplied with* $\mathrm{C/J}^2$, *is negligible relatively to the absolute minimum value of* $\mathrm{F}(h,\,h_0)$.

From the inequality

$$\left|\frac{\mathrm{C}}{\mathrm{J}^2}f_{\max}(h,\,h_0)\right| \ll |\mathrm{F}_{\min}(h,\,h_0)|, \quad \ldots\ldots \quad (18)$$

we conclude that, in the whole range

$$\left|\frac{\mathrm{C}}{\mathrm{J}^2}f(h,\,h_0)\right| \ll |\mathrm{F}(h,\,h_0)|. \quad \ldots\ldots\ldots \quad (19)$$

The functions $f(h, h_0)$ and $\mathrm{F}(h, h_0)$ being monotonic, their extreme values are situated on the borders of the intervals (16) and (17).

Thus, we obtain

$$\mathrm{F}(h,\,h_0)=\text{minimum for}\begin{Bmatrix}h_0=\mathrm{A}\\ h\ =\mathrm{B}\end{Bmatrix}, \quad \ldots\ldots \quad (20)$$

and

$$f(h,\,h_0)=\text{maximum for}\begin{Bmatrix}h_0=\mathrm{A}\\ h\ =\mathrm{B}\end{Bmatrix}. \quad \ldots\ldots \quad (21)$$

$\mathrm{F}_{\min}$ is situated on the same place as $f_{\max}$.

The value of A being given, we will choose for B a value such that our intervals contain the great water accumulations. We suppose that the thickness of the water layer may be not smaller than a :

$$h_0-h \geqslant a. \qquad (22)$$

This condition is satisfied, according to (16) and (17), if

$$\mathrm{A}-\mathrm{B}=a. \qquad (23)$$

For a minimum thickness of the water-bearing layer equal to $a=1$ m., we obtain

$$\left.\begin{aligned}\mathrm{A}&=3.10^3 \text{ cm.}\\ \mathrm{B}&=2{\cdot}9.10^3 \text{ cm.}\end{aligned}\right\} \qquad (24)$$

and

$$\left.\begin{aligned}\mathrm{F}_{\min}&=10^9 \text{ sec.}\\ \frac{\mathrm{C}}{\mathrm{J}^2}f_{\max}&=1{\cdot}4.10^7 \text{ sec.}\end{aligned}\right\} \qquad (25)$$

One can therefore reduce equation (10) to (13) and one obtains, in combining this last equation with (11), a formula by means of which one can evaluate *the increase per second of the total ground-water volume of deserts* :

$$\frac{\mathrm{W}}{t}=\mathrm{JPF}. \qquad (26)$$

In expressing F in m^2 and J in m per year, one obtains the *annual increase in* m^3.

According to A. v. Tillo, the dunes occupy 6·2 per cent. of the continental surface * (*l. c.* p. 819). This surface being equal to 134·8 million km.^{2}, the dunes cover a surface of 8·4 million km.^{2}. In subtracting from this number the total surface of beaches, equal to 1·6 million km.^{2} (*l. c.* p. 266), we obtain for this total surface of sandy deserts a value of 6·8 million km.^{2}, which is somewhat too small, since in the subtracted number (1·6 million km.^{2}) there are contained the coastal parts of the sandy deserts. We will use this somewhat too small value $\mathrm{F}=6{\cdot}8$ million km.$^2=6{\cdot}8.10^{12}$ m.^{2}. By reason of caution, we choose also a too small value of the porosity : $\mathrm{P}=0{\cdot}15$. The annual precipitation in m. is $\mathrm{J}=3{\cdot}10^{-2}$ m. In substituting these values in formula (26), we obtain an *annual increase of ground water equal to* $3{\cdot}10^{10}$ m.^{3} *in the sandy deserts.*

This result is in accordance with the observation of Georges Rolland that the dunes in the Sahara—and not only in the Sahara—represent " de véritables réservoirs d'eau " (Rolland, *l. c.*, p. 226).

Equation (10) explains how it is possible that such great quantities of underground water have not been discovered till now. The level of the thick water layers is, according to this equation, deeper than C/J. *Even during a geologic time of infiltration the water of the great accumulations never can ascend to the surface.*

---

* A. Supan, 'Grundzüge der physischen Erdkunde' (6 Aufl., Berlin und Leipzig, 1921).

Equation (10) also explains the fact that deep-rooted plants represent indicators of ground water *. The necessary condition is: $l > C/J$, if l signifies the root length. In an Appendix to Meinzer's book (*l. c.*, p. 89), Walter N. White communicates his observations concerning *alfalfa* as a ground-water plant. The soil is penetrated by the root system to a depth $l = 8{\cdot}5$ feet $= 255$ cm. The climate of Escalante Valley, Utah, being arid, we may put, as before: $C/J = 40$ cm. The condition $l > C/J$ is satisfied.

The arithmetical fact concerning the logarithm of $(C-hJ)/(C-h_0J)$ represents a " selection rule " which, combined with the electrodynamic prospection method, could spare many unproductive borings. If the electrodynamic determination of the ground-water depth h gives a value

$$h < \frac{C}{J},$$

we must consider this as an indication that the thickness D of the water accumulation at this place is

$$D < \frac{C}{J} - h, \qquad \qquad (27)$$

the depth of the lower surface being $H = H_0 = h_0$.

By means of this simple rule, one can distinguish the large and small water accumulations.

Cairo, May 1944.

LXXXI. *Notices respecting New Books.*

Table of Arcsin x. Prepared by the Mathematical Tables Project. [Pp. xix +121.] (New York: Columbia University Press, 1945.) Price $3.50.

THE function arcsin x is much more than the inverse of the trigonometric function sin x; it is one of the more fundamental functions of analysis, for it represents the integral of $(1-x^2)^{-\frac{1}{2}}$, and thus, with $(1+x^2)^{-\frac{1}{2}}$, it is necessary and sufficient for the integration of any algebraic function involving only one square root of a quadratic expression.

For arcsin x to be real x must lie in the range $(-1, 1)$, so that a table need cover only the range $(0, 1)$ and different tables differ only in the interval of sub-division of this range and in the accuracy with which the function is given. In the present case the interval is 0·0001 up to 0·9890 and 0·00001 thereafter; the function is given to 12 decimals throughout, and for interpolation the second differences (modified in the later part of the table, though this does not affect the user) are tabulated. At the highest values of x, fourth differences are given. In either case the formulæ for interpolation are given on pp. xii and xiii, and the functions required in them are tabulated on pp. 114 and 116.

---

* O. E. Meinzer, " Plants as Indicators of Ground-Water," U.S. Geological Survey, Water-Supply Paper 577 (Washington, 1927).

As the function becomes "irregular" when x tends to 1, further help is given in this region by tabulating an auxiliary function $f(v)$, which is such that, for small v, $\arcsin(1-v)=\pi/2-(2v)^{\frac{1}{2}}f(v)$. This function is much better for interpolation and thus enables the accuracy in arc sin x to be maintained even when x is in the neighbourhood of 1. J. H. A.

Physical Methods of Organic Chemistry. Edited by A. WEISSBERGER. Pp. 736. (Interscience Publishers, Inc.: New York, 1945. Vol. I. Price $8.50).

THE principal aim of the organic chemist may perhaps be regarded as the preparation in a state of purity and the elucidation of the structure of compounds of carbon. In both directions, physics and physical chemistry can play a helpful part. The assistance of physics depends on the use of its methods in characterising the substances and ensuring their purity by their so-called physical properties, and of these the determination of melting point, boiling point, and refractive index have long been familiar to organic chemists. These are included in the present volume, together with a number of other properties not so familiar but also important in the elucidation of structure in the newer methods of organic chemistry. The sixteen sections are contributed by recognised specialists, and the contents of the second volume, early publication of which is promised, are announced. This second volume will contain an index, the absence of which is a defect of the first volume.

The articles deal with melting and freezing temperatures, boiling and condensation temperatures, density, solubility, viscosity, surface and interfacial tension (with a section on the parachor), monolayers and duplex films, osmotic pressure, diffusivity, calorimetry, microscopy, determination of crystal form, crystallographic analysis, X-ray diffraction, electron diffraction, and refractometry. All of them are capably written, contain much valuable information (including not a little which cannot be found elsewhere), and are provided with adequate bibliographies. It is perhaps unfair to single out any of these sections for special mention, but the reviewer was particularly struck by the articles on surface tension and calorimetry, which are really comprehensive monographs on the subjects, the interest of which is by no means confined to organic chemistry. The most modern developments seem to be covered in all the articles; particular attention is paid to units in such cases as density, heat capacity, and surface tension, and there are some useful tables of constants. The treatment throughout is critical and practical. Some of the articles, such as those on osmotic pressure and diffusivity, deal mostly with the parts of particular interest to organic chemistry, but others are of a general character, so that the book will be useful to physicists and physical chemists, as well as to organic chemists and biologists. The section on crystal form, occupying about thirty pages, seems too short to make the subject intelligible, and the optical theory in the section on microscopy is also so brief as to be, in some cases, very hard to follow. One drawback in having each article contributed by a specialist is that the latter is often unaware of the slender knowledge which some of his readers may have of the subject he deals with, and in the opinion of the reviewer the editor might well have asked for a little more detail in some places and a little less in others. All the contributers seem to have taken great pains to make their subjects intelligible and useful, and their efforts have been richly rewarded. The volume is one which every chemist, physicist, and biologist will wish to have, and one on which he may rely to give him help and instruction in his work. The production is excellent, and the price reasonable in view of the abundance of good material which the book contains. J. R. P.

[*The Editors do not hold themselves responsible for the views expressed by their correspondents.*]

LXXXII. *The Buckling of Flat Rectangular Plywood Plates.*

By A. E. Green and R. F. S. Hearmon *.

[Received February 26, 1945.]

Introduction.

1. General equations are established for the buckling of a thin rectangular plate of any æolotropic material under the action of stresses along its edges. The application of the analysis to plywood plates, cut at any angle to the grain, is discussed by deriving approximate formulæ which are fairly simple to use for calculations. The main numerical results are given for plates of mahogany 5-ply, with all the plies of equal thickness †, and the edges either all simply supported or all clamped. The influence of plywood structure, of wood species, and of other edge conditions is, however, briefly discussed.

Many of the results given in the present paper are new, but other writers have previously considered the problem of the buckling of plywood plates under edge forces for certain special cases, although their results are obtained by different methods from those used here. Unfortunately, it is not possible to give detailed references to much of this work, nor to quote from it, since it has been issued in restricted or confidential report form ‡. It can be said, however, that where comparison is possible, the present results do not differ by more than a few per cent. from those of previous workers.

The stability of isotropic rectangular plates under various edge forces has received considerable attention by many writers. In particular, approximate and exact values for the critical stress have been found for a clamped isotropic rectangular plate under compression over two opposite edges, and although the results are fairly complete, they are usually obtained after considerable calculation. A simple approximate formula for this problem is obtained as a special case of the present work on æolotropic plates, and results found from it are compared with those given by previous writers.

The Stability Equations.

2. Consider a flat rectangular plywood plate bounded by the lines $\xi=0$, $\xi=a$; $\eta=0$, $\eta=b$, where (ξ, η) are ordinary rectangular axes.

---

* Communicated by the Authors.

† Plywood construction will be denoted by a series of figures giving the relative thicknesses of the successive plies, e. g. 3-ply 1 : 2 : 1 denotes a plywood having the centre ply twice the thickness of the face plies.

‡ See note added in proof, p. 688.

The plate is acted on by a system of stress-resultants (forces per unit length) P_1, P_2, S on the edges of the plate, as shown in fig. 1, and θ is the angle between the face grain of the outer plies and the side a of the plate. If $w\,(\xi, \eta)$ is the displacement of a point in the middle plane of the plate, the stress-couples and the differential equation governing the stability of the plate can be expressed in the known forms

$$\left.\begin{aligned} -G_1&=D_{11}\frac{\partial^2 w}{\partial \xi^2}+D_{12}\frac{\partial^2 w}{\partial \eta^2}+2D_{16}\frac{\partial^2 w}{\partial \xi\,\partial \eta},\\ -G_2&=D_{12}\frac{\partial^2 w}{\partial \xi^2}+D_{22}\frac{\partial^2 w}{\partial \eta^2}+2D_{26}\frac{\partial^2 w}{\partial \xi\,\partial \eta},\\ -H_2=H_1&=D_{16}\frac{\partial^2 w}{\partial \xi^2}+D_{26}\frac{\partial^2 w}{\partial \eta^2}+2D_{66}\frac{\partial^2 w}{\partial \xi\,\partial \eta},\end{aligned}\right\} \quad . \quad . \quad . \quad (2.1)$$

Fig. 1.

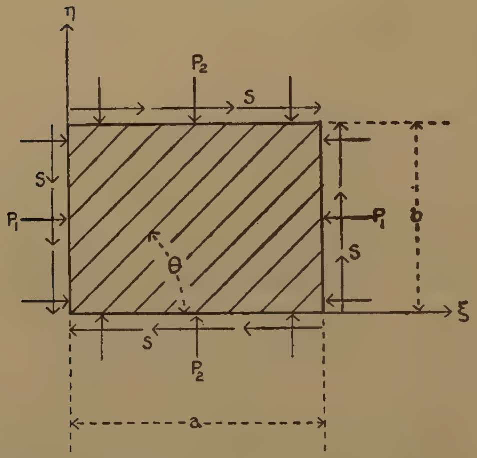

where G_1, G_2 are the bending moments per unit length, and H_1 and H_2 are the twisting moments per unit length, and

$$D_{11}\frac{\partial^4 w}{\partial \xi^4}+4D_{16}\frac{\partial^4 w}{\partial \xi^3\,\partial \eta}+2(D_{12}+2D_{66})\frac{\partial^4 w}{\partial \xi^2\,\partial \eta^2}+4D_{26}\frac{\partial^4 w}{\partial \xi\,\partial \eta^3}+D_{22}\frac{\partial^4 w}{\partial \eta^4}$$
$$+P_1\frac{\partial^2 w}{\partial \xi^2}+P_2\frac{\partial^2 w}{\partial \eta^2}+2S\frac{\partial^2 w}{\partial \xi\,\partial \eta}=0, \quad . \quad . \quad . \quad . \quad (2.2)$$

where $$D_{ij}=\int_{-h}^{h} c_{ij} z^2\,dz, \quad . \quad . \quad . \quad . \quad . \quad . \quad . \quad . \quad (2.3)$$

z being the co-ordinate measured from the middle plane of the plate. The thickness of the plate is $2h$ and c_{ij} are the elastic constants of the individual plies defined in the usual way (Love ⁽⁹⁾, p. 99). For convenience, the co-ordinate axes (ξ, η) are changed to non-dimensional axes (x, y) by the relations

$$\xi=ax/\pi, \quad \eta=by/\pi, \quad p=a/b, \quad . \quad . \quad . \quad . \quad . \quad . \quad (2.4)$$

and the equations (2.1) and (2.2) may then be written in the forms

$$\left.\begin{aligned} -a^2\mathrm{G}_1/\pi^2&=\mathrm{D}_{11}\frac{\partial^2 w}{\partial x^2}+\rho^2\mathrm{D}_{12}\frac{\partial^2 w}{\partial y^2}+2\rho\mathrm{D}_{16}\frac{\partial^2 w}{\partial x\,\partial y},\\ -a^2\mathrm{G}_2/\pi^2&=\mathrm{D}_{12}\frac{\partial^2 w}{\partial x^2}+\rho^2\mathrm{D}_{22}\frac{\partial^2 w}{\partial y^2}+2\rho\mathrm{D}_{26}\frac{\partial^2 w}{\partial x\,\partial y},\\ -a^2\mathrm{H}_2/\pi^2=a^2\mathrm{H}_1/\pi^2&=\mathrm{D}_{16}\frac{\partial^2 w}{\partial x^2}+\rho^2\mathrm{D}_{26}\frac{\partial^2 w}{\partial y^2}+2\rho\mathrm{D}_{66}\frac{\partial^2 w}{\partial x\,\partial y}, \end{aligned}\right\} \quad . \quad (2.5)$$

and

$$\mathrm{D}_{11}\frac{\partial^4 w}{\partial x^4}+4\rho\mathrm{D}_{16}\frac{\partial^4 w}{\partial x^3\,\partial y}+2\rho^2(\mathrm{D}_{12}+2\mathrm{D}_{66})\frac{\partial^4 w}{\partial x^2\,\partial y^2}+4\rho^3\mathrm{D}_{26}\frac{\partial^4 w}{\partial x\,\partial y^3}$$
$$+\rho^4\mathrm{D}_{22}\frac{\partial^4 w}{\partial y^4}+\rho^2\mathrm{X}\frac{\partial^2 w}{\partial x^2}+\rho^4\mathrm{Y}\frac{\partial^2 w}{\partial y^2}+2\rho^3\mathrm{Z}\frac{\partial^2 w}{\partial x\,\partial y}=0, \quad . \quad . \quad . \quad (2.6)$$

where $\mathrm{X}=b^2\mathrm{P}_1/\pi^2,\quad \mathrm{Y}=b^2\mathrm{P}_2/\pi^2,\quad \mathrm{Z}=b^2\mathrm{S}/\pi^2.$ . . . . . (2.7)

The potential energy of bending will also be needed and is given by

$$\mathrm{V}_b=\frac{\pi^2}{2\rho a^2}\int_0^\pi\int_0^\pi\left\{\mathrm{D}_{11}\left(\frac{\partial^2 w}{\partial x^2}\right)^2+2\rho^2\mathrm{D}_{12}\frac{\partial^2 w}{\partial x^2}\frac{\partial^2 w}{\partial y^2}+\rho^4\mathrm{D}_{22}\left(\frac{\partial^2 w}{\partial y^2}\right)^2\right.$$
$$\left.+4\rho\frac{\partial^2 w}{\partial x\,\partial y}\left[\mathrm{D}_{16}\frac{\partial^2 w}{\partial x^2}+\rho^2\mathrm{D}_{26}\frac{\partial^2 w}{\partial y^2}+\rho\mathrm{D}_{66}\frac{\partial^2 w}{\partial x\,\partial y}\right]\right\}dx\,dy. \quad (2.8)$$

The above equations apply to an isotropic material, for which

$$\mathrm{D}_{16}=\mathrm{D}_{26}=0,\quad \mathrm{D}_{11}=\mathrm{D}_{22}=\mathrm{D}_{12}+2\mathrm{D}_{66}=2\mathrm{E}h^3/3(1-\sigma^2), \quad . \quad (2.9)$$

where E is Young's modulus and σ is Poisson's ratio.

Solution by Fourier Series : Simply Supported Edges.

3. In this section a solution of the general stability equation (2.6) is given for the case when all the edges of the plate are simply supported. The boundary conditions which correspond to simply supported edges are

$$w=0,\quad \mathrm{G}_1=0,\quad \text{for}\quad x=0,\pi, \quad . \quad . \quad . \quad . \quad . \quad . \quad (3.1)$$
$$w=0,\quad \mathrm{G}_2=0,\quad \text{for}\quad y=0,\pi, \quad . \quad . \quad . \quad . \quad . \quad . \quad (3.2)$$

and using (2.5) these become

$$w=0,\quad \mathrm{D}_{11}\frac{\partial^2 w}{\partial x^2}+2\rho\mathrm{D}_{16}\frac{\partial^2 w}{\partial x\,\partial y}=0,\quad \text{for}\quad x=0,\pi. \quad . \quad . \quad (3.3)$$

$$w=0,\quad \rho\mathrm{D}_{22}\frac{\partial^2 w}{\partial y^2}+2\mathrm{D}_{26}\frac{\partial^2 w}{\partial x\,\partial y}=0,\quad \text{for}\quad y=0,\pi. \quad . \quad . \quad (3.4)$$

The problem is to find values of X, Y, Z for which a non-zero solution of (2.6) exists which satisfies the boundary conditions (3.3) and (3.4). It is assumed that the displacement $w(x, y)$ is a function such that w and all its partial derivatives up to the fourth order may be expanded as double Fourier series in the region $0<x<\pi$, $0<y<\pi$. Then, since w vanishes at the edge of the region, it is possible to write (see Green ⁽⁴⁾)

$$w(x, y)=\sum_{r=1}^{\infty}\sum_{s=1}^{\infty} \mathrm{A}_{rs} \sin rx \sin sy \quad (0 \leqslant x \leqslant \pi,\ 0 \leqslant y \leqslant \pi), \quad . \quad . \quad . \quad (3.5)$$

$$\frac{\partial w(x, y)}{\partial x}=\sum_{r=1}^{\infty}\sum_{s=1}^{\infty} r\mathrm{A}_{rs} \cos rx \sin sy \quad (0 \leqslant x \leqslant \pi,\ 0 \leqslant y \leqslant \pi), \quad . \quad . \quad . \quad (3.6)$$

$$\frac{\partial^2 w(x, y)}{\partial x^2}=-\sum_{r=1}^{\infty}\sum_{s=1}^{\infty} r^2\mathrm{A}_{rs} \sin rx \sin sy \quad (0<x<\pi,\ 0 \leqslant y \leqslant \pi), \quad . \quad . \quad (3.7)$$

$$\begin{aligned}\frac{\partial^3 w(x, y)}{\partial x^3}=\frac{1}{2}\sum_{s=1}^{\infty} a_s \sin sy+\sum_{r=2,\, r\text{ even}}^{\infty}\ \sum_{s=1}^{\infty} (-r^3\mathrm{A}_{rs}+a_s) \cos rx \sin sy \\ +\sum_{r=1,\, r\text{ odd}}^{\infty}\ \sum_{s=1}^{\infty} (-r^3\mathrm{A}_{rs}+b_s) \cos rx \sin sy, \quad (3.8)\end{aligned}$$

$$\begin{aligned}\frac{\partial^4 w(x, y)}{\partial x^4}=\sum_{r=2,\, r\text{ even}}^{\infty}\ \sum_{s=1}^{\infty} (r^4\mathrm{A}_{rs}-ra_s) \sin rx \sin sy \\ +\sum_{r=1,\, r\text{ odd}}^{\infty}\ \sum_{s=1} (r^4\mathrm{A}_{rs}-rb_s) \sin rx \sin sy, \quad (3.9)\end{aligned}$$

$$\frac{\partial w(x, y)}{\partial y}=\sum_{r=1}^{\infty}\sum_{s=1}^{\infty} s\mathrm{A}_{rs} \sin rx \cos sy \quad (0 \leqslant x \leqslant \pi,\ 0 \leqslant y \leqslant \pi), \quad . \quad . \quad (3.10)$$

$$\frac{\partial^2 w(x, y)}{\partial y^2}=-\sum_{r=1}^{\infty}\sum_{s=1}^{\infty} s^2\mathrm{A}_{rs} \sin rx \sin sy \quad (0 \leqslant x \leqslant \pi,\ 0<y<\pi), \quad . \quad (3.11)$$

$$\begin{aligned}\frac{\partial^3 w(x, y)}{\partial y^3}=\frac{1}{2}\sum_{r=1}^{\infty} c_r \sin rx+\sum_{r=1}^{\infty}\ \sum_{s=2,\, s\text{ even}}^{\infty} (-s^3\mathrm{A}_{rs}+c_r) \sin rx \cos sy \\ +\sum_{r=1}^{\infty}\ \sum_{s=1,\, s\text{ odd}}^{\infty} (-s^3\mathrm{A}_{rs}+d_r) \sin rx \cos sy, \quad (3.12)\end{aligned}$$

$$\begin{aligned}\frac{\partial^4 w(x, y)}{\partial y^4}=\sum_{r=1}^{\infty}\ \sum_{s=2,\, s\text{ even}}^{\infty} (s^4\mathrm{A}_{rs}-sc_r) \sin rx \sin sy \\ +\sum_{r=1}^{\infty}\ \sum_{s=1,\, s\text{ odd}}^{\infty} (s^4\mathrm{A}_{rs}-sd_r) \sin rx \sin sy, \quad . \quad (3.13)\end{aligned}$$

$$\begin{aligned}\frac{\partial^4 w(x, y)}{\partial x^3\, \partial y}=\frac{1}{2}\sum_{s=1}^{\infty} sa_s \cos sy+\sum_{r=2,\, r\text{ even}}^{\infty}\ \sum_{s=1}^{\infty} (-r^3s\mathrm{A}_{rs}+sa_s) \cos rx \cos sy \\ +\sum_{r=1,\, r\text{ odd}}^{\infty}\ \sum_{s=1}^{\infty} (-r^3s\mathrm{A}_{rs}+sb_s) \cos rx \cos sy, \quad (3.14)\end{aligned}$$

$$\begin{aligned}\frac{\partial^4 w(x, y)}{\partial x\, \partial y^3}=\frac{1}{2}\sum_{r=1}^{\infty} rc_r \cos rx+\sum_{r=1}^{\infty}\ \sum_{s=2,\, s\text{ even}}^{\infty} (-rs^3\mathrm{A}_{rs}+rc_r) \cos rx \cos sy \\ +\sum_{r=1}^{\infty}\ \sum_{s=1,\, s\text{ odd}}^{\infty} (-rs^3\mathrm{A}_{rs}+rd_r) \cos rx \cos sy, \quad (3.15)\end{aligned}$$

$$\frac{\partial^4 w(x, y)}{\partial x^2\, \partial y^2}=\sum_{r=1}^{\infty}\sum_{s=1}^{\infty} r^2s^2\mathrm{A}_{rs} \sin rx \sin sy, \quad . \quad . \quad . \quad . \quad . \quad . \quad . \quad . \quad . \quad . \quad (3.16)$$

where $A_{rs}=0(r^{-3}s^{-3})$ and where the constants a_s, b_s, c_r, d_r are defined by the equations

$$a_s=\frac{4}{\pi^2}\int_0^\pi\left\{\frac{\partial^2 w(\pi, y)}{\partial x^2}-\frac{\partial^2 w(0, y)}{\partial x^2}\right\}\sin sy\, dy, \quad . \quad . \quad . \quad (3.17)$$

$$-b_s=\frac{4}{\pi^2}\int_0^\pi\left\{\frac{\partial^2 w(\pi, y)}{\partial x^2}+\frac{\partial^2 w(0, y)}{\partial x^2}\right\}\sin sy\, dy, \quad . \quad . \quad . \quad (3.18)$$

$$c_r=\frac{4}{\pi^2}\int_0^\pi\left\{\frac{\partial^2 w(x, \pi)}{\partial y^2}-\frac{\partial^2 w(x, 0)}{\partial y^2}\right\}\sin rx\, dx, \quad . \quad . \quad . \quad (3.19)$$

$$-d_r=\frac{4}{\pi^2}\int_0^\pi\left\{\frac{\partial^2 w(x, \pi)}{\partial y^2}+\frac{\partial^2 w(x, 0)}{\partial y^2}\right\}\sin rx\, dx. \quad . \quad . \quad . \quad (3.20)$$

The boundary condition $w=0$ is satisfied by the above Fourier expansions, and in order to satisfy the remaining boundary conditions in (3.3) and (3.4) it is necessary to know the values of $\partial^2 w/\partial x^2$ on the edges $x=0, \pi$ and $\partial^2 w/\partial y^2$ on the edges $y=0, \pi$ respectively. Fourier expansions for these quantities can, however, be found by using (3.17) to (3.20). Thus

$$\frac{\partial^2 w(0, y)}{\partial x^2}=-\frac{\pi}{4}\sum_{s=1}^{\infty}(a_s+b_s)\sin sy, \quad . \quad . \quad . \quad . \quad (3.21)$$

$$\frac{\partial^2 w(\pi, y)}{\partial x^2}=\frac{\pi}{4}\sum_{s=1}^{\infty}(a_s-b_s)\sin sy, \quad . \quad . \quad . \quad . \quad (3.22)$$

$$\frac{\partial^2 w(x, 0)}{\partial y^2}=-\frac{\pi}{4}\sum_{r=1}^{\infty}(c_r+d_r)\sin rx, \quad . \quad . \quad . \quad . \quad (3.23)$$

$$\frac{\partial^2 w(x, \pi)}{\partial y^2}=\frac{\pi}{4}\sum_{r=1}^{\infty}(c_r-d_r)\sin rx. \quad . \quad . \quad . \quad . \quad . \quad (3.24)$$

With the help of (3.21), (3.22) and the Fourier expansion for $\frac{\partial^2 w}{\partial x\, \partial y}$, the second boundary condition in (3.3) now gives the equations

$$\left.\begin{aligned}&\pi D_{11}\sum_{s=1}^{\infty}(a_s+b_s)\sin sy-8\rho D_{16}\sum_{s=1}^{\infty}\sum_{r=1}^{\infty} rsA_{rs}\cos sy=0,\\ &\pi D_{11}\sum_{s=1}^{\infty}(a_s-b_s)\sin sy+8\rho D_{16}\sum_{s=1}^{\infty}\sum_{r=1}^{\infty}(-)^r rsA_{rs}\cos sy=0,\end{aligned}\right\} \quad . \quad (3.25)$$

for all values of y in the range $(0, \pi)$. To satisfy these equations $\cos sy$ must be expanded as a sine series:

$$\left.\begin{aligned}&\cos sy=\sum_{r=1}^{\infty} h_{sr}\sin ry \quad (0<y<\pi),\\ \text{where} \quad &h_{sr}=\frac{4r}{\pi(r^2-s^2)} \quad (r+s \text{ odd}),\\ &\quad\;=\;0 \quad (r+s \text{ even}),\end{aligned}\right\} \quad . \quad . \quad . \quad (3.26)$$

Substituting these series in (3.25) and equating to zero the coefficients of sin ry then gives, after a slight rearrangement,

$$\left.\begin{aligned} \pi D_{11}a_r &= 8\rho D_{16} \sum_{s=1}^{\infty} \sum_{m=1,\, m\text{ odd}}^{\infty} ms\, h_{sr} A_{ms}, \\ \pi D_{11}b_r &= 8\rho D_{16} \sum_{s=1}^{\infty} \sum_{m=2,\, m\text{ even}}^{\infty} ms\, h_{sr} A_{ms}, \end{aligned}\right\} \quad . \quad . \quad . \quad . \quad (3.27)$$

for $r=1, 2, \ldots$ Similarly, the second boundary condition in (3.4) can be satisfied if

$$\left.\begin{aligned} \pi\rho D_{22}c_r &= 8D_{26} \sum_{s=1}^{\infty} \sum_{m=1,\, m\text{ odd}}^{\infty} ms\, h_{sr} A_{sm}, \\ \pi\rho D_{22}d_r &= 8D_{26} \sum_{s=1}^{\infty} \sum_{m=2,\, m\text{ even}}^{\infty} ms\, h_{sr} A_{sm}, \end{aligned}\right\} \quad . \quad . \quad . \quad (3.28)$$

for $r=1, 2, \ldots$

It is now necessary to satisfy the differential equation (2.6). To do this it is convenient to express cos mx cos ny as a double Fourier sine-sine series,

$$\left.\begin{aligned} \cos mx \cos ny &= \sum_{r=1}^{\infty} \sum_{s=1}^{\infty} h_{rs}^{mn} \sin rx \sin sy \quad \begin{pmatrix} 0<x<\pi \\ 0<y<\pi \end{pmatrix}, \\ \text{where} \qquad h_{rs}^{mn} &= \frac{16rs}{\pi^2(m^2-r^2)(n^2-s^2)} \quad \begin{pmatrix} m+r \text{ odd} \\ n+s \text{ odd} \end{pmatrix}, \\ &= \quad 0 \qquad\qquad \begin{pmatrix} m+r \text{ even} \\ n+s \text{ even} \end{pmatrix}. \end{aligned}\right\} \quad . \quad (3.29)$$

If the expressions (3.5) to (3.16) are substituted in (2.6) and if, with the help of (3.29), it is assumed that the resulting series can be rearranged as a double Fourier sine-sine series, then the equation (2.6) is satisfied if the coefficient of each term is zero. This gives the set of equations

$$\left.\begin{aligned} &\{f(r, s)-\rho^2r^2X-\rho^4s^2Y\}A_{rs} \\ &\quad + \sum_{m=1}^{\infty} \sum_{n=1}^{\infty} \{2\rho^3mnZ-4\rho mn(D_{16}m^2+\rho^2D_{26}n^2)\}\, h_{rs}^{mn}A_{mn} \\ &\quad + 4\rho D_{16} \sum_{n=1}^{\infty} \left\{\tfrac{1}{2}na_n h_{rs}^{0n} + \sum_{m=2,\, m\text{ even}}^{\infty} na_n h_{rs}^{mn} + \sum_{m=1,\, m\text{ odd}}^{\infty} nb_n h_{rs}^{mn}\right\} \\ &\quad + 4\rho^3 D_{26} \sum_{m=1}^{\infty} \left\{\tfrac{1}{2}mc_m h_{rs}^{m0} + \sum_{n=2,\, n\text{ even}}^{\infty} mc_m h_{rs}^{mn} + \sum_{n=1,\, n\text{ odd}}^{\infty} md_m h_{rs}^{mn}\right\} \\ &\qquad\qquad = rD_{11}a_s + \rho^4 sD_{22}c_r \quad (r \text{ even}, s \text{ even}), \\ &\qquad\qquad = rD_{11}a_s + \rho^4 sD_{22}d_r \quad (r \text{ even}, s \text{ odd}), \\ &\qquad\qquad = rD_{11}b_s + \rho^4 sD_{22}c_r \quad (r \text{ odd}, s \text{ even}), \\ &\qquad\qquad = rD_{11}b_s + \rho^4 sD_{22}d_r \quad (r \text{ odd}, s \text{ odd}), \end{aligned}\right\} \quad . \quad (3.30)$$

where $$f(r, s)=D_{11}r^4+2(D_{12}+2D_{66})\rho^2r^2s^2+D_{22}\rho^4s^4. \quad . \quad . \quad (3.31)$$

Using the summations

$$\left.\begin{aligned} \frac{1}{2n^2}+\sum_{m=2,\, m\text{ even}}^{\infty}\frac{1}{n^2-m^2}&=0 \quad (n\text{ odd}),\\ \sum_{m=1,\, m\text{ odd}}^{\infty}\frac{1}{n^2-m^2}&=0 \quad (n\text{ even}), \end{aligned}\right\} \quad . \quad . \quad . \quad . \quad (3.32)$$

equations (3.30) can be simplified, and then the constants a_s, b_s, c_r, d_r can be eliminated from (3.27), (3.28), and (3.30), giving

$$\{f(r,s)-\rho^2r^2\mathrm{X}-\rho^4s^2\mathrm{Y}\}\mathrm{A}_{rs}$$
$$+2\rho\sum_{m=1}^{\infty}\sum_{n=1}^{\infty}\{\rho^2\mathrm{Z}-\mathrm{D}_{16}(r^2+m^2)-\mathrm{D}_{26}\rho^2(s^2+n^2)\}mnh_{rs}^{mn}\mathrm{A}_{mn}=0, \quad (3.33)$$

for all integral values of r and s.

These equations for A_{rs} divide into two groups, one containing constants A_{rs} for which $r+s$ are even numbers and the other for which $r+s$ are odd numbers, and for a non-zero solution of each group, two corresponding infinite determinants, D_1 and D_2 respectively, must vanish. If $\mathrm{X}=k\mathrm{Z}$, $\mathrm{Y}=k'\mathrm{Z}$, where k, k' are given constants, the minimum value of Z which will cause buckling can be obtained from one or other of the infinite determinants D_1 and D_2. The convergence of these determinants will not be considered here.

4. Suppose now that the side a of the plate is infinitely long, so that the boundary conditions over the ends of the plate may be ignored. If

$$w=\mathrm{W}(y)e^{i\mu\pi\xi/b}, \quad . \quad . \quad . \quad . \quad . \quad . \quad . \quad . \quad (4.1)$$

where μ is a real constant, then, from (2.2), it is found that W satisfies the equation

$$\mathrm{D}_{22}\frac{d^4\mathrm{W}}{dy^4}+4i\mu\mathrm{D}_{26}\frac{d^3\mathrm{W}}{dy^3}-2(\mathrm{D}_{12}+2\mathrm{D}_{66})\mu^2\frac{d^2\mathrm{W}}{dy^2}-4i\mu^3\mathrm{D}_{16}\frac{d\mathrm{W}}{dy}+\mu^4\mathrm{D}_{11}\mathrm{W}$$
$$-\mu^2\mathrm{X}\mathrm{W}+\mathrm{Y}\frac{d^2\mathrm{W}}{dy^2}+2i\mu\mathrm{Z}\frac{d\mathrm{W}}{dy}=0, \quad . \quad . \quad . \quad . \quad . \quad . \quad (4.2)$$

where X, Y, Z are still given by (2.7). From (2.5), (3.2) and (4.1) it is found that the boundary conditions take the form

$$\mathrm{W}=0, \quad \mathrm{D}_{22}\frac{d^2\mathrm{W}}{dy^2}+2i\mu\mathrm{D}_{26}\frac{d\mathrm{W}}{dy}=0 \quad (y=0,\pi). \quad . \quad . \quad (4.3)$$

If it is assumed that W and its first four derivatives can be expanded as Fourier series in the range $(0,\pi)$, then, since W vanishes at the end points of the interval, it is possible to write

$$\mathrm{W}(y)=\sum_{r=1}^{\infty}\mathrm{A}_r\sin ry \qquad (0\leqslant y\leqslant\pi), \quad . \quad . \quad . \quad . \quad (4.4)$$

$$\frac{d\mathrm{W}(y)}{dy}=\sum_{r=1}^{\infty}r\mathrm{A}_r\cos ry \qquad (0\leqslant y\leqslant\pi), \quad . \quad . \quad . \quad . \quad (4.5)$$

$$\frac{d^2\mathrm{W}(y)}{dy^2}=-\sum_{r=}^{\infty}r^2\mathrm{A}_r\sin ry \quad (0<y<\pi), \quad . \quad . \quad . \quad . \quad (4.6)$$

$$\frac{d^3\mathrm{W}(y)}{dy^3}=\tfrac{1}{2}k_2+\sum_{r=2,\ r\ \mathrm{even}}^{\infty}(-r^3\mathrm{A}_r+k_2)\cos ry+\sum_{r=1,\ r\ \mathrm{odd}}^{\infty}(-r^3\mathrm{A}_r+k_1)\cos ry, \quad . \quad . \quad . \quad (4.7)$$

$$\frac{d^4\mathrm{W}(y)}{dy^4}=\sum_{r=2,\ r\ \mathrm{even}}^{\infty}(r^4\mathrm{A}_r-rk_2)\sin ry+\sum_{r=1,\ r\ \mathrm{odd}}^{\infty}(r^4\mathrm{A}_r-rk_1)\sin ry, \quad . \quad (4.8)$$

where $\mathrm{A}_r=0(r^{-3})$ and where

$$\left.\begin{aligned}\frac{\pi k_2}{2}&=\frac{d^2\mathrm{W}(\pi)}{dy^2}-\frac{d^2\mathrm{W}(0)}{dy^2},\\ \frac{\pi k_1}{2}&=-\frac{d^2\mathrm{W}(\pi)}{dy^2}-\frac{d^2\mathrm{W}(0)}{dy^2}.\end{aligned}\right\} \quad . \quad . \quad . \quad . \quad . \quad . \quad (4.9)$$

With the help of (4.5) and (4.9) the second boundary condition in (4.3) then gives, after some rearrangement,

$$\left.\begin{aligned}\pi\mathrm{D}_{22}k_2&=8i\mu\mathrm{D}_{26}\sum_{m=1,\ m\ \mathrm{odd}}^{\infty}m\mathrm{A}_m,\\ \pi\mathrm{D}_{22}k_1&=8i\mu\mathrm{D}_{26}\sum_{m=2,\ m\ \mathrm{even}}^{\infty}m\mathrm{A}_m.\end{aligned}\right\} \quad . \quad . \quad . \quad . \quad . \quad (4.10)$$

If the expressions (4.4) to (4.8) are substituted in (4.2) and if, with the help of the expansions (3.26), the resulting series is expressed as a Fourier sine series, then the differential equation (4.2) is satisfied if the coefficient of each term is zero. After some simplification the constants k_1 and k_2 may be eliminated from the resulting equations and equations (4.10), giving

$$\{f(r)-\mu^2\mathrm{X}-r^2\mathrm{Y}\}\mathrm{A}_r+2i\mu\sum_{s=1}^{\infty}\{\mathrm{Z}-2\mu^2\mathrm{D}_{16}-(r^2+s^2)\mathrm{D}_{26}\}sh_{sr}\mathrm{A}_s=0 \quad (4.11)$$

for all integral values of r, where

$$f(r)=\mathrm{D}_{22}r^4+2(\mathrm{D}_{12}+2\mathrm{D}_{66})\mu^2r^2+\mathrm{D}_{11}\mu^4. \quad . \quad . \quad . \quad (4.12)$$

For a non-zero solution of (4.11) an infinite determinant D_3 must vanish. To prove that the determinant converges divide the rth row by r^2 and the rth column by r^2 for all integral values of r. This is equivalent to dividing (4.11) by r^2 and replacing A_r by B_r/r^2, which is possible, since A_r is $0(r^{-3})$. Then, if a typical diagonal term is $1+a_{rr}$ an a typical non-diagonal term is a_{rs}, it can be shown that the series

$$\sum_r|a_{rr}| \quad \text{and} \quad \sum_{r,s}|a_{rs}|^2$$

converge and so the determinant converges by Von Koch's test (12).

Numerical Discussion : Pure Compression : Simply Supported Edges.

5. If an accurate and exhaustive numerical discussion is needed it is necessary to consider a fairly large number of terms of the determinants D_1, D_2, D_3 for each problem. Such a discussion is not attempted here, but some information has been obtained from approximate formulæ which are derived from the above theory. These formulæ are not too

complicated for the necessary numerical calculations and, with some exceptions, they probably give results which are reasonably accurate for practical purposes.

If the equations (3.33) are arranged so that the first two coefficients are A_{r1}, A_{m2}, $(m=r\pm1)$, then a first approximation to the critical stress (when $Y=Z=0$) is obtained by equating to zero the determinant consisting of the first four elements of either of the two infinite determinants D_1 or D_2. This gives the critical stress in the form

$$2\rho^2 DEX = AE + DC - \{(AE-DC)^2 + DEB^2\}^{\frac{1}{2}}, \quad . \quad . \quad (5.1)$$

where

$$\left.\begin{aligned} A &= D_{11}m^4 + 8(D_{12}+2D_{66})\rho^2 m^2 + 16D_{22}\rho^4, \\ C &= D_{11}r^4 + 2(D_{12}+2D_{66})\rho^2 r^2 + D_{22}\rho^4, \\ 3\pi^2(r^2-m^2)B &= 128\rho rm\{D_{16}(m^2+r^2) + 5D_{26}\rho^2\}, \\ D &= m^2, \quad E = r^2, \quad m = r\pm1, \end{aligned}\right\} \quad . \quad . \quad . \quad (5.2)$$

and where the minimum value of X is required corresponding to integral values of r. If the right-hand side of (5.1) is expanded in powers of $DEB^2/(AE-DC)^2$, and if the expansion is limited to three terms, then (5.1) takes the simpler approximate form

$$\rho^2 X = \frac{C}{E} - \frac{B^2}{4(AE-DC)}. \quad . \quad . \quad . \quad . \quad . \quad . \quad (5.3)$$

This equation is very convenient for calculations, and it is found to give results which are very little different from those found from (5.1), and (5.3) is used for some, though not all, of the calculations recorded below. For grain angles of 0° and 90° both (5.1) and (5.3) reduce to the known accurate result (Timoshenko (11), p. 381)

$$\rho^2 X = D_{11}r^2 + 2(D_{12}+2D_{66})\rho^2 + D_{22}\rho^4/r^2. \quad . \quad . \quad . \quad . \quad (5.4)$$

Results found from (5.1) or (5.3) are probably satisfactory for plates which are square, or nearly square, but as ρ increases the accuracy will be less reliable *. For an infinitely long plate ($\rho\to\infty$) the formulæ (5.1) and (5.3) have limiting forms which, for some grain angles other than 0° or 90°, are not very satisfactory. Better results may be obtained by using the determinant D_3. Here again approximations are made to avoid excessive labour in computation. Taking only the first nine elements in the determinant gives the following equation for the critical stress X as a function of the variable μ,

$$\{f(1)-\mu^2X\}\left\{[f(2)-\mu^2X][f(3)-\mu^2X] - \left(\frac{48\mu}{5\pi}\right)^2[2\mu^2D_{16}+13D_{26}]^2\right\}$$
$$= \left(\frac{16\mu}{3\pi}\right)^2\{f(3)-\mu^2X\}\{2\mu^2D_{16}+5D_{26}\}^2, \quad . \quad . \quad . \quad (5.5)$$

where $f(1)$, $f(2)$ and $f(3)$ are given by (4.12). This equation may be further simplified, probably without much sacrifice in accuracy. The minimum stress occurs approximately at the minimum value of $\mu^{-2}f(1)$ for varying

---

* The accuracy may also be less reliable for large values of D_{16} or D_{26}.

μ, *i. e.* when $\mu^4 = D_{22}/D_{11}$. Using this value of μ and replacing X by its approximate value $\mu^{-2}f(1)$, except in the first bracket, gives

$$X = 2\{D_{12} + 2D_{66} + (D_{11}D_{22})^{\frac{1}{2}}\} - \left(\frac{16}{3\pi}\right)^2 \left(\frac{D_{22}}{D_{11}}\right)^{\frac{1}{2}} \left\{2D_{16} + 5D_{26}\left(\frac{D_{11}}{D_{22}}\right)^{\frac{1}{2}}\right\}^2 \times \left\{ 6(D_{12} + 2D_{66}) + 15(D_{11}D_{22})^{\frac{1}{2}} - \frac{\left(\frac{12}{5\pi}\right)^2 \left(\frac{D_{22}}{D_{11}}\right)^{\frac{1}{2}} \left[2D_{16} + 13D_{26}\left(\frac{D_{11}}{D_{22}}\right)^{\frac{1}{2}}\right]^2}{D_{12} + 2D_{66} + 5(D_{11}D_{22})^{\frac{1}{2}}} \right\}^{-1} . \quad (5.6)$$

Table I.

Values of $a_{ij} = \frac{3D_{ij}}{2Mh^3}$ for mahogany, where $M = 0{\cdot}586(10^6)$ lb. per sq. in.

(*a*) Solid wood (parallel plies).

θ (deg.).	0	15	30	45	60	75	90
a_{11}	2·319	2·053	1·416	0·756	0·340	0·191	0·169
$a_{12} + 2a_{66}$.	0·268	0·634	1·366	1·732	1·366	0·634	0·268
$-a_{16}$	0	0·480	0·677	0·538	0·255	0·058	0
a_{22}	0·169	0·191	0·340	0·756	1·416	2·053	2·319
$-a_{26}$	0	0·058	0·255	0·538	0·677	0·480	0

(*b*) Plywood (5 perpendicular plies, all of equal thickness).

θ (deg.).	0	15	30	45	60	75	90
a_{11}	1·861	1·666	1·192	0·756	0·564	0·578	0·617
$a_{12} + 2a_{66}$.	0·268	0·634	1·366	1·732	1·366	0·634	0·268
$-a_{16}$	0	0·368	0·482	0·314	0·060	−0·054	0
a_{22}	0·617	0·578	0·564	0·756	1·192	1·666	1·861
$-a_{26}$	0	−0·054	0·060	0·314	0·482	0·368	0

At 0° and 90°, $D_{16} = D_{26} = 0$, and equation (5.6) reduces to the known form

$$X = 2\{D_{12} + 2D_{66} + (D_{11}D_{22})^{\frac{1}{2}}\} . \quad . \quad . \quad . \quad . \quad . \quad (5.7)$$

At 45°, $D_{11} = D_{22}$ and $D_{16} = D_{26}$, so that (5.6) becomes

$$X = 2\{D_{12} + 2D_{66} + D_{11}\} - 141{\cdot}2D_{16}^2\left\{6(D_{12} + 2D_{66}) + 15D_{11} - \frac{131{\cdot}3D_{16}^2}{D_{12} + 2D_{66} + 5D_{11}}\right\}^{-1} . \quad (5.8)$$

Calculations have been carried out for a specimen of 5-ply mahogany (1 : 1 : 1 : 1 : 1) using values given by Goland and Aleck (3). These values do not check accurately among themselves, nor with other data given by Goland and Aleck, but the discrepancies are small, so their figures are quoted without modification in Table I.

The results of calculations are expressed in terms of a buckling stress coefficient k_c defined by

$$p_{cr}=k_c\mathrm{E_L}(2h/b)^2, \qquad (5.9)$$

where p_{cr} is the critical stress acting on the sides b of the plate and $\mathrm{E_L}$ is the longitudinal Young's modulus of the solid wood composing the plywood. A similar equation is, of course, frequently used for isotropic plates. The equation has been used for plywood by previous writers and has the advantage that once k_c has been calculated, the only quantities involved are the dimensions of the plate, and $\mathrm{E_L}$, the elastic constant of wood about which most is known. It has been suggested that although the values of k_c will depend on the structure of the plywood, they will be approximately independent of the elastic constants of the solid wood. Numerical results given in § 14 show, however, that variations in the elastic constants may, in extreme cases, affect the values of k_c by as much as ±20 per cent.

Fig. 2.

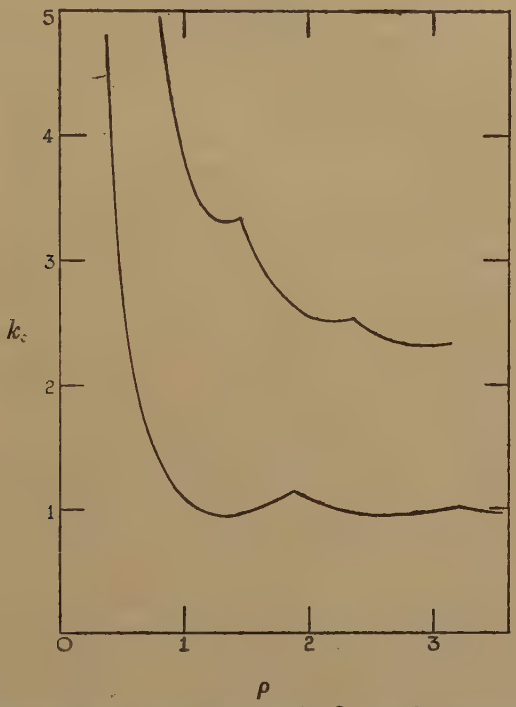

Upper curve—all edges clamped. } $\theta=0°$ mahogany.
Lower curve—all edges supported. } 5-ply 1 : 1 : 1 : 1 : 1.

From equations (2.7) and (5.9) it is found that

$$k_c=\frac{\pi^2\mathrm{X}}{8h^3\mathrm{E_L}}, \qquad (5.10)$$

and, for the specimen of mahogany used here, $E_L=1\cdot35\times10^6$ lb./sq. in., so that $k_c=0\cdot914X/10^6h^3$.

Values of k_c for square plates of solid wood and for plywood (*i. e.* perpendicular plies), which have been found from (5.2) and (5.3), are recorded in the first two lines of Table II., where, for convenience, the main supported edge results, including those for shear (§ 6), are collected together. Calculations have also been made, for other values of ρ at grain angles of 0°, 45° and 90°, and these results are shown graphically in figs. 2–4. For grain angles of 0° and 90°, the supported edge results are accurate and well known. At 45° the results are probably rather high at the larger values of ρ.

Fig. 3.

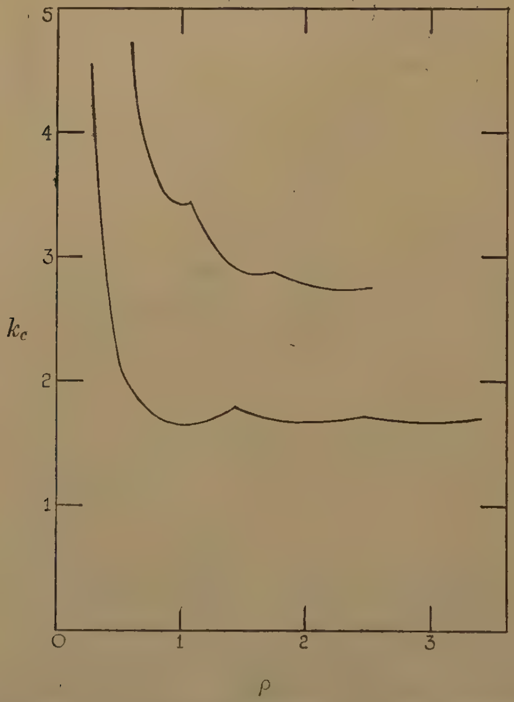

Upper curve—all edges clamped. } $\theta=45°$ mahogany
Lower curve—all edges supported. } 5-ply 1 : 1 : 1 : 1 : 1.

When the plate is infinitely long, calculations have been made for various angles, using the approximate formula (5.6), and the results are shown in the third line of Table II. Values of k_c have been found previously by other writers for an infinitely long plate under compression, but their results were obtained by a different method.

Pure Shear : Simply Supported Edges.

6. In this section the forces on the edge of the plate consist of a uniform shearing resultant S. Except for grain angles of 0° and 90°, S will have

different values according as it is a positive or negative shear, a positive shear being defined in fig. 1. In order to find the value of the critical shear to a reasonable degree of accuracy it is necessary to take a fairly large number of terms of the infinite determinants D_1 and D_2 corresponding to the equations (3.33). By arranging the coefficients A_{rs} in (3.33) in the order A_{11}, A_{22}, A_{13}, A_{31}, A_{33} when $r+s$ is even, a quadratic equation is obtained for Z by taking the first 25 terms in D_1. A quadratic form is still obtained if other terms are added which are the coefficients of A_{rs} for r, s both odd, thus

$$\rho^4 Z^2 \sum_{r\text{ odd}} \sum_{s\text{ odd}} G_{rs} - 2\rho^2 Z \sum_{r\text{ odd}} \sum_{s\text{ odd}} H_{rs} + \sum_{r\text{ odd}} \sum_{s\text{ odd}} K_{rs} = \frac{\pi^4 f(2, 2)}{(128\rho)^2}, \qquad (6.1)$$

Fig. 4.

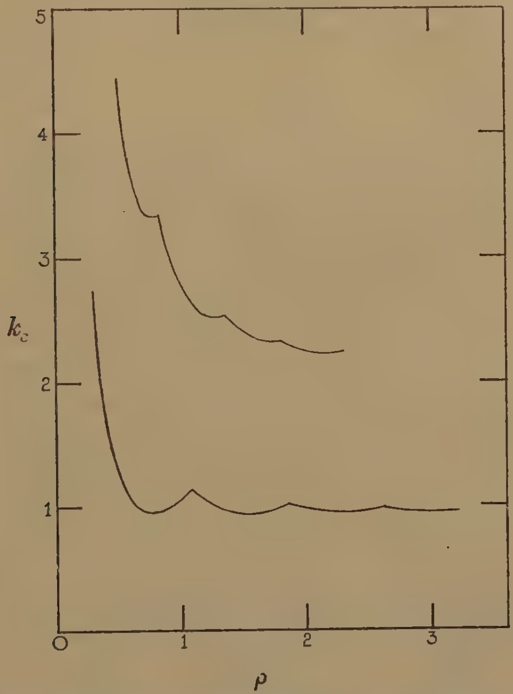

Upper curve—all edges clamped. } $\theta=90°$ mahogany
Lower curve—all edges supported. } 5-ply 1 : 1 : 1 : 1 : 1.

where

$$\left.\begin{aligned} G_{rs} &= \frac{r^2 s^2}{(r^2-4)^2(s^2-4)^2 f(r, s)}, \\ H_{rs} &= \frac{r^2 s^2\{D_{16}(r^2+4)+\rho^2 D_{26}(s^2+4)\}}{(r^2-4)^2(s^2-4)^2 f(r, s)}, \\ K_{rs} &= \frac{r^2 s^2\{D_{16}(r^2+4)+\rho^2 D_{26}(s^2+4)\}^2}{(r^2-4)^2(s^2-4)^2 f(r, s)}, \end{aligned}\right\} \quad . \quad . \quad . \quad . \quad (6.2)$$

and $f(r, s)$ is given by (3.31).

Table II.

Values of k_c and k_s for 5-ply mahogany plates with simply supported edges.
(Square plate, $\rho=1$; infinite plate, $\rho=\infty$.)

Stress.	ρ.	Equations.	θ (degrees).						
			0	15	30	45	60	75	90
(1) Solid wood.									
Compression (k_c)	1	(5.2) and (5.3)	1·08	1·13	1·32	1·44	1·32	0·87	0·64
(2) Plywood (5-plies, all of equal thickness).									
Compression (k_c)	1	(5.2) and (5.3)	1·08	1·21	1·50	1·65	1·50	1·21	1·08
Compression (k_c)	∞	(5.6)	0·96	1·13	1·49	1·52	1·29	1·06	0·96
Shear (k_s)	1	(6.1) and (6.2) 4 terms	2·56 —2·56	2·24 —3·61	2·41 —4·89	2·53 —5·50	2·41 —4·89	2·24 —3·61	2·56 —2·56
Shear (k_s)	1	(6.1) and (6.2) 8 terms	2·54 —2·54	2·21 —3·59	2·34 —4·88	2·44 —5·50	2·34 —4·88	2·21 —3·59	2·54 —2·54

If the remaining coefficients of A_{rs} (r, s both even) are also included in D_1, it is not possible to express Z as the root of a quadratic, but the above approximation is probably satisfactory when ρ is not too large or small. The other determinant, D_2, must also be considered, since the minimum value of the critical shear may be a root of D_2, and not D_1, for plywood. A similar form of approximation can be found for D_2, but experience shows that important terms would then be omitted, so D_2 is left in the determinant form in which the terms correspond to the order A_{12}, A_{21}, A_{23}, A_{32}, A_{52}, A_{41} of the constants A_{rs} in (3.33). In the calculations which are made here, only one result is found from the determinant D_2.

The numerical results are expressed in terms of a buckling shear stress coefficient k_s defined by

$$q_{cr}=k_s E_L(2h/b)^2,$$

where q_{cr} is the critical shear stress. Thus

$$k_s=\frac{\pi^2 Z}{8E_L h^3},$$

and for the specimen of mahogany used here $k_s=0{\cdot}914Z/10^6h^3$. Using the values of D_{ij} given in Table I., the buckling shear stress coefficients for a square mahogany plywood plate have been found with the help of equation (6.1) by including in the series the eight terms corresponding to $r, s=1, 1$; $1, 3$; $3, 1$; $3, 3$; $3, 5$; $5, 3$; $1, 5$; $5, 1$. These results are shown in the last two lines of Table II., which also contains the values found from only four terms of the series. Positive values of k_s correspond to shear as in fig. 1, while negative values correspond to shear of the opposite sense. If more terms are included in the summations in (6.1), little change is found in the negative shear, but the positive value of k_s reduces to 2·39 for $\theta=45°$ and to 2·30 for $\theta=30°$.

When $\rho=1{\cdot}5$, eight terms of the series (6.1) give

$$\theta=0,\qquad k_s=\pm 1{\cdot}57,$$
$$\theta=45°,\quad k_s=1{\cdot}59 \text{ or } -3{\cdot}74,$$

but for $\theta=90°$ the minimum value of k_s is obtained from the determinant D_2. Using 36 elements of D_2 gives k_s approximately 2·32 for this case.

When the plate is infinitely long, the determinant D_3 corresponding to equations (4.11) must be used. Calculations for this case have been limited to grain angles of 0° and 90°, and only the first nine elements in the determinant were considered. Thus

$$k_s=\pm 1{\cdot}12 \text{ for } \theta=0°,\quad k_s=\pm 1{\cdot}95 \text{ for } \theta=90°.$$

Clamped Edges.

7. All the edges of the plate are now supposed to be clamped, so that the boundary conditions are

$$w=\frac{\partial w}{\partial x}=0 \text{ for } x=0,\pi;\quad w=\frac{\partial w}{\partial y}=0 \text{ for } y=0,\pi. \quad . \quad . \quad (7.1)$$

It is possible to obtain a formal solution of the general stability problem with these edge conditions in a number of different forms. Using the Fourier series given in § 3, the boundary conditions (7.1) and the differential equation (2.6) may be satisfied, but the form of the result only seems to be convenient for numerical work for a plywood plate, under compression, cut at grain angles of 0° or 90°. This method of solution was given by Green (4) for an isotropic plate, the final result being in a form which was obtained previously by other writers using different methods.

Iguchi (5) gave a solution for the stability of a clamped isotropic plate under shear by using a displacement function of the form

$$w=\sum_{r=1}^{\infty}\sum_{s=1}^{\infty}X_r(x)Y_s(y), \qquad . \quad . \quad . \quad . \quad . \quad . \quad . \qquad (7.2)$$

where

$$\left.\begin{aligned}X_r(x)&=(r/\pi^2)\{x^3-2x^2\pi+x\pi^2+(-)^r(x^3-\pi x^2)\}-\sin rx,\\ Y_s(y)&=(s/\pi^2)\{y^3-2y^2\pi+y\pi^2+(-)^s(y^3-\pi y^2)\}-\sin sy,\end{aligned}\right\} \quad . \qquad (7.3)$$

and the differential equation for stability. This method could be used in the present general problem, or the displacement function (7.2) could be used with a strain energy method. It has been found, however, that the displacement function

$$w=\sin x\sin y\sum_{r=1}^{\infty}\sum_{s=1}^{\infty}A_{rs}\sin rx\sin sy, \qquad . \quad . \quad . \quad . \qquad (7.4)$$

used in the strain energy equation gives better results in many cases, and this method is adopted here. A slight modification is made in the strain energy method which considerably reduces the amount of algebra and gives the same results.

Let $w'(x, y)$ be a function which satisfies the same conditions (7.1) as $w(x, y)$ on the edge of the plate. If equation (2.6) is multiplied by w' and integrated throughout the rectangle, and if the boundary conditions for w, w' are used, then it is found that

$$\begin{aligned}\int_0^\pi\int_0^\pi\Big\{&D_{11}\frac{\partial^2 w}{\partial x^2}\frac{\partial^2 w'}{\partial x^2}+4\rho\frac{\partial^2 w}{\partial x\,\partial y}\left(D_{16}\frac{\partial^2 w'}{\partial x^2}+\rho^2 D_{26}\frac{\partial^2 w'}{\partial y^2}\right)\\ &+2\rho^2(D_{12}+2D_{66})\frac{\partial^2 w}{\partial x\,\partial y}\frac{\partial^2 w'}{\partial x\,\partial y}+\rho^4 D_{22}\frac{\partial^2 w}{\partial y^2}\frac{\partial^2 w'}{\partial y^2}-\rho^2 X\frac{\partial w}{\partial x}\frac{\partial w'}{\partial x}\\ &-\rho^4 Y\frac{\partial w}{\partial y}\frac{\partial w'}{\partial y}-2\rho^3 Z\frac{\partial w}{\partial x}\frac{\partial w'}{\partial y}\Big\}dx\,dy=0. \qquad . \quad . \quad . \quad . \quad . \qquad (7.5)\end{aligned}$$

Since $\sum_{r=1}^{\infty}\sum_{s=1}^{\infty}A_{rs}\sin rx\sin sy$ is valid in the closed region $0\leqslant x\leqslant\pi$, $0\leqslant y\leqslant\pi$, it may be differentiated at least twice with respect to x or y, if it is assumed that the derivatives can be expanded as double Fourier series, the second derivatives, in general, being valid in the open region. If

$$w'=\sin x\sin mx\sin y\sin ny, \qquad . \quad . \quad . \quad . \quad . \qquad (7.6)$$

and if w is given by (7.4), then term-by-term integration of the series in (7.5) may be justified, giving

$$\sum_{r=1}^{\infty}\sum_{s=1}^{\infty}\alpha_{rsmn}A_{rs}=0 \quad . \quad . \quad . \quad . \quad . \quad . \quad . \qquad (7.7)$$

for all integral values of m, n where

$$\alpha_{1111}=12D_{11}+8\rho^2(D_{12}+2D_{66})+12\rho^4D_{22}-3\rho^2X-3\rho^4Y, \quad . \quad . \quad . \qquad (7.8)$$

$$\begin{aligned}\alpha_{1s1s}=8D_{11}+4\rho^2(D_{12}+2D_{66})(s^2+1)+\tfrac{3}{2}\rho^4D_{22}(s^4+6s^2+1)&\\ -2\rho^2X-\tfrac{3}{2}\rho^4(s^2+1)Y \quad (s\neq1),& \quad . \qquad (7.9)\end{aligned}$$

$$\begin{aligned}\alpha_{r1r1}=\tfrac{3}{2}D_{11}(r^4+6r^2+1)+4\rho^2(D_{12}+2D_{66})(r^2+1)+8\rho^4D_{22}&\\ -\tfrac{3}{2}\rho^2(r^2+1)X-2\rho^4Y \quad (r\neq1),& \quad . \qquad (7.10)\end{aligned}$$

$$\begin{aligned}\alpha_{rsrs}=D_{11}(r^4+6r^2+1)+2\rho^2(D_{12}+2D_{66})(r^2+1)(s^2+1)+\rho^4D_{22}(s^4+6s^2+1)&\\ -\rho^2(r^2+1)X-\rho^4(s^2+1)Y \quad (r\neq1,\ s\neq1),& \qquad (7.11)\end{aligned}$$

$$\begin{aligned}\alpha_{rsmn}&=-\tfrac{1}{2}D_{11}(r+1)^4-\rho^2(D_{12}+2D_{66})(r+1)^2(s^2+1)-\tfrac{1}{2}\rho^4D_{22}(s^4+6s^2+1)\\ &\quad+\tfrac{1}{2}\rho^2(r+1)^2X+\tfrac{1}{2}\rho^4(s^2+1)Y \quad (m=r+2,\ n=s\neq1), \quad . \quad . \qquad (7.12)\\ &=-\tfrac{3}{4}D_{11}(r+1)^4-2\rho^2(D_{12}+2D_{66})(r+1)^2-4\rho^4D_{22}\\ &\quad+\tfrac{3}{4}\rho^2(r+1)^2X+\rho^4Y \quad (m=r+2,\ n=s=1), \quad . \quad . \qquad (7.13)\\ &=-\tfrac{1}{2}D_{11}(r^4+6r^2+1)-\rho^2(D_{12}+2D_{66})(r^2+1)(s+1)^2-\tfrac{1}{2}\rho^4D_{22}(s+1)^4\\ &\quad+\tfrac{1}{2}\rho^2(r^2+1)X+\tfrac{1}{2}\rho^4(s+1)^2Y \quad (m=r\neq1,\ n=s+2), \quad . \quad . \qquad (7.14)\\ &=-4D_{11}-2\rho^2(D_{12}+2D_{66})(s+1)^2-\tfrac{3}{4}\rho^4D_{22}(s+1)^4\\ &\quad+\rho^2X+\tfrac{3}{4}\rho^4(s+1)^2Y \quad (m=r=1,\ n=s+2), \quad . \quad . \qquad (7.15)\\ &=\tfrac{1}{4}D_{11}(r+1)^4+\tfrac{1}{2}\rho^2(D_{12}+2D_{66})(r+1)^2(s+1)^2+\tfrac{1}{4}\rho^4D_{22}(s+1)^4\\ &\quad-\tfrac{1}{4}\rho^2(r+1)^2X-\tfrac{1}{4}\rho^4(s+1)^2Y \quad (m=r+2,\ n=s+2), \qquad (7.16)\\ &=\tfrac{1}{4}D_{11}(r+1)^4+\tfrac{1}{2}\rho^2(D_{12}+2D_{66})(r+1)^2(n+1)^2+\tfrac{1}{4}\rho^4D_{22}(n+1)^4\\ &\quad-\tfrac{1}{4}\rho^2(r+1)^2X-\tfrac{1}{4}\rho^4(n+1)^2Y \quad (m=r+2,\ s=n+2),. \qquad (7.17)\end{aligned}$$

$$\begin{aligned}2\pi^2(r^2-m^2)(s^2-n^2)\{(r-2)^2-m^2\}\{(r+2)^2-m^2\}\{(s-2)^2-n^2\}&\\ \times\{(s+2)^2-n^2\}\,\alpha_{rsmn}&\\ =(16)^3\rho rsmn\{\rho^2Z(r^2+m^2-2)(s^2+n^2-2)&\\ -4D_{16}(r^2+m^2+r^2m^2-3)(s^2+n^2-2)&\\ -4\rho^2D_{26}(r^2+m^2-2)(s^2+n^2+s^2n^2-3)\}&\\ \begin{pmatrix}r+m \text{ odd}\\ s+n \text{ odd}\end{pmatrix}, \quad . \qquad (7.18)&\end{aligned}$$

and $\alpha_{mnrs}=\alpha_{rsmn}$.

The equations (7.7) for A_{rs} divide into two groups, one containing constants A_{rs} for which $r+s$ are even numbers and the other for which $r+s$ are odd numbers, and for a non-zero solution of each group two corresponding infinite determinants, D_4 and D_5 respectively, must vanish. If $X=kZ$, $Y=k'Z$, where k, k' are given constants, the minimum value of Z which will cause buckling can be obtained from one or other of the infinite determinants D_4 and D_5. The convergence of these determinants will not be discussed. This solution is suitable for finite plates. The corresponding problem for a plate which is infinitely long in one direction is considered in the next section.

8. Using the notation of § 4, the boundary conditions for clamped edges can be written in the form

$$W=\frac{dW}{dy}=0 \quad (y=0, \pi). \qquad (8.1)$$

As for a finite plate, a number of methods of solution are possible. The most natural extension of the method of the previous section would be to use the expansion

$$W=\sin y \sum_{r=1}^{\infty} A_r \sin ry \qquad (8.2)$$

in the energy equation, but it is found that better results are obtained in the present case by using

$$W=\sum_{r=1}^{\infty} A_r Y_r(y), \qquad (8.3)$$

where $Y_r(y)$ is given by (7.3). The energy method is again slightly modified in order to simplify the algebra by multiplying equation (4.2) by a *real* function $W'(y)$ which satisfies the same boundary conditions (8.1) as W, and integrating the equation over the range $0 \leqslant y \leqslant \pi$. Using the boundary conditions for W, W′, it is found that

$$\int_0^{\pi}\left\{D_{22}\frac{d^2W}{dy^2}\frac{d^2W'}{dy^2}-4i\mu D_{26}\frac{d^2W}{dy^2}\frac{dW'}{dy}+2\mu^2(D_{12}+2D_{66})\frac{dW}{dy}\frac{dW'}{dy}\right.$$
$$-4i\mu^3D_{16}\frac{dW}{dy}W'+\mu^4D_{11}WW'-\mu^2XWW'$$
$$\left.-Y\frac{dW}{dy}\frac{dW'}{dy}+2i\mu Z\frac{dW}{dy}W'\right\}dy=0. \qquad (8.4)$$

Since W vanishes at $y=0, \pi$, it is possible to justify two differentiations of the series (8.3) for W, and if

$$W'=Y_m(y), \qquad (8.5)$$

the series in (8.4) may be integrated term by term, giving

$$\sum_{r=1}^{\infty} \alpha_{rm}A_r=0 \qquad (8.6)$$

for all integral values of m, where

$$\alpha_{rr}=D_{22}\left(r^4-\frac{8r^2}{\pi^2}\right)+\{2\mu^2(D_{12}+2D_{66})-Y\}\left(\frac{5r^2}{3}-\frac{16}{\pi^2}\right)$$
$$+(\mu^4D_{11}-\mu^2X)\left(1+\frac{\pi^2r^2}{15}-\frac{16}{\pi^2r^2}\right) \quad (r \text{ odd}), \qquad (8.7)$$
$$=D_{22}\left(r^4-\frac{24r^2}{\pi^2}\right)+\{2\mu^2(D_{12}+2D_{66})-Y\}\left(\frac{7r^2}{5}-\frac{48}{\pi^2}\right)$$
$$+(\mu^4D_{11}-\mu^2X)\left(1+\frac{\pi^2r^2}{105}-\frac{48}{\pi^2r^2}\right) \quad (r \text{ even}), \qquad (8.8)$$

$$\alpha_{rm} = -\frac{8rm\mathrm{D}_{22}}{\pi^2} + \{2\mu^2(\mathrm{D}_{12}+2\mathrm{D}_{66}) - \mathrm{Y}\}\left\{\frac{2rm}{3} - \frac{8(r^2+m^2)}{\pi^2 rm}\right\}$$

$$+(\mu^4\mathrm{D}_{11}-\mu^2\mathrm{X})\left\{\frac{\pi^2 rm}{15} - \frac{8(r^4+m^4)}{\pi^2 r^3 m^3}\right\} \quad \begin{pmatrix} r \text{ odd, } m \text{ odd} \\ r \neq m \end{pmatrix}, \quad . \quad . \quad . \quad (8.9)$$

$$= -\frac{24rm\mathrm{D}_{22}}{\pi^2} + \{2\mu^2(\mathrm{D}_{12}+2\mathrm{D}_{66}) - \mathrm{Y}\}\left\{\frac{2rm}{5} - \frac{24(r^2+m^2)}{\pi^2 rm}\right\}$$

$$+(\mu^4\mathrm{D}_{11}-\mu^2\mathrm{X})\left\{\frac{\pi^2 rm}{105} - \frac{24(r^4+m^4)}{\pi^2 r^3 m^3}\right\} \quad \begin{pmatrix} r \text{ even, } m \text{ even} \\ r \neq m \end{pmatrix}, \qquad (8.10)$$

$$\alpha_{rm} = \frac{8i\mu\mathrm{D}_{26}}{\pi}\left\{\frac{24m}{\pi^2 r} + \frac{2m^3 r}{r^2-m^2}\right\}$$

$$+\frac{4i\mu}{\pi}(\mathrm{Z}-2\mu^2\mathrm{D}_{16})\left\{\frac{\pi^2 rm}{30} - \frac{24m}{\pi^2 r^3} - \frac{2(r^4+m^4-r^2m^2)}{rm(r^2-m^2)}\right\} \quad \begin{pmatrix} r \text{ odd,} \\ m \text{ even} \end{pmatrix}, \quad . \quad . \quad . \quad (8.11)$$

$$= -\frac{8i\mu\mathrm{D}_{26}}{\pi}\left\{\frac{24r}{\pi^2 m} + \frac{2mr^3}{m^2-r^2}\right\}$$

$$-\frac{4i\mu}{\pi}(\mathrm{Z}-2\mu^2\mathrm{D}_{16})\left\{\frac{\pi^2 rm}{30} - \frac{24r}{\pi^2 m^3} + \frac{2(r^4+m^4-r^2m^2)}{rm(r^2-m^2)}\right\} \quad \begin{pmatrix} r \text{ even,} \\ m \text{ odd} \end{pmatrix}. \quad . \quad . \quad . \quad (8.12)$$

For a non-zero solution of equations (8.6) an infinite determinant D_6 must vanish. It can be proved that the determinant converges by using Von Koch's test (12).

Numerical Discussion : Pure Compression : Clamped Edges.

9. As for simply supported edges, no attempt is made to give an exhaustive numerical discussion, but approximate formulæ are derived from the above theory which are likely to be reasonably accurate for practical purposes.

If the equations (7.7) are arranged so that the first two coefficients are A_{r1}, A_{m2} $(m=r\pm1)$, then a first approximation to the critical stress is obtained by equating to zero the determinant consisting of the first four elements of either of the two infinite determinants D_4 or D_5. This gives the critical stress in the form (5.1), or the further approximate form (5.3), where

$$\left.\begin{aligned}
&\mathrm{A}=2\mathrm{D}_{11}(m^4+6m^2+1)+20(\mathrm{D}_{12}+2\mathrm{D}_{66})\rho^2(m^2+1) \\
&\qquad\qquad +(82\mathrm{D}_{22}\rho^4 \text{ if } m\neq1, \quad \text{or} \quad 123\mathrm{D}_{22}\rho^4 \text{ if } m=1), \\
&\mathrm{C}=3\mathrm{D}_{11}(r^4+6r^2+1)+8(\mathrm{D}_{12}+2\mathrm{D}_{66})\rho^2(r^2+1) \\
&\qquad\qquad +(24\mathrm{D}_{22}\rho^4 \text{ if } r=1, \quad \text{or} \quad 16\mathrm{D}_{22}\rho^4 \text{ if } r\neq1), \\
&\mathrm{B}=\frac{(256)^2\rho rm\{\mathrm{D}_{16}(r^2+m^2+r^2m^2-3)+2\mathrm{D}_{26}\rho^2(r^2+m^2-2)\}}{15\pi^2(m^2-r^2)\{(m-2)^2-r^2\}\{(m+2)^2-r^2\}}, \\
&\mathrm{D}=2(m^2+1), \quad \mathrm{E}=3(r^2+1), \quad m=r\pm1
\end{aligned}\right\} . \qquad (9.1)$$

and where the minimum value of X is required, corresponding to integral values of r.

Results found from (5.1), 5.3) and (9.1) are probably satisfactory for plates which are square or nearly square, but as ρ increases the accuracy will be less reliable. The formulæ (5.1) and (5.3) have limiting forms for an infinitely long plate, but better results can be obtained for this case by using the determinant D_6, which was found in § 8. Taking only the first four elements in the determinant gives

$$\alpha_{11}\alpha_{22}=\alpha_{12}^2,$$

and the minimum value of X is to be found for various values of μ. The minimum value occurs approximately at the minimum value of X found from the equation $\alpha_{11}=0$, *i.e.* when $\mu^4=5{\cdot}143D_{22}/D_{11}$. Using this value of μ, and making a further approximation in the term α_{22}, then gives

$$X=2{\cdot}472(D_{12}+2D_{66})+4{\cdot}536(D_{11}D_{22})^{\frac{1}{2}} - \frac{\left(\frac{D_{22}}{D_{11}}\right)^{\frac{1}{2}}\left\{D_{16}+1{\cdot}620D_{26}\left(\frac{D_{11}}{D_{22}}\right)^{\frac{1}{2}}\right\}^2}{0{\cdot}1649(D_{12}+2D_{66})+0{\cdot}3680(D_{11}D_{22})^{\frac{1}{2}}}. \quad . \quad (9.2)$$

At grain angles of 0° and 90° equation (9.2) takes the simple form

$$X=2{\cdot}472(D_{12}+2D_{66})+4{\cdot}536(D_{11}D_{22})^{\frac{1}{2}}, \quad . \quad . \quad . \quad (9.3)$$

while at 45°

$$X=2{\cdot}472(D_{12}+2D_{66})+4{\cdot}536D_{11}-\frac{D_{16}^2}{0{\cdot}02402(D_{12}+2D_{66})+0{\cdot}05360D_{11}}. \quad . \quad . \quad . \quad (9.4)$$

Calculations have been carried out using the elastic constants from Table I., and the results are again given in terms of the buckling stress coefficient k_c. Values of k_c for square plates of solid wood and plywood have been found from (5.3) and (9.1), and are recorded in the first two lines of Table III., where the main clamped-edge results are collected together ; the values of k_s are discussed below (§ 11). Calculations have also been made for plywood plates for other values of ρ at grain angles of 0°, 45° and 90°, and the results, together with those for simply supported edges, are shown in figs. 2–4.

When the plate is infinitely long, calculations have been made for various grain angles using (9.2), and the results are shown in the third line of Table III.

10. The results for a clamped isotropic plate in compression, given by (5.1) and (9.1), reduce to the simple form

$$k_c=\frac{\pi^2G}{36\rho^2(1-\sigma^2)(r^2+1)}, \quad . \quad . \quad . \quad . \quad . \quad . \quad (10.1)$$

where

$$G=3(r^4+6r^2+1)+8\rho^2(r^2+1)+(24\rho^4 \text{ if } r=1, \quad \text{or} \quad 16\rho^4 \text{ if } r\neq 1). \quad (10.2)$$

TABLE III.

Values of k_c and k_s for 5-ply mahogany plates with clamped edges. (Square plate, $\rho=1$; infinite plate, $\rho=\infty$.)

Stress.	ρ.	Equations.	θ (degrees).						
			0	15	30	45	60	75	90
(1) Solid Wood.									
Compression (k_c) . .	1	(5.3) and (9.1)	3·81	3·41	2·91	2·71	2·48	1·85	1·63
(2) Plywood (5-plies, all of equal thickness).									
Compression (k_c) . .	1	(5.3) and (9.1)	3·81	3·67	3·48	3·40	3·26	2·89	2·77
Compression (k_c) . .	∞	(9.2)	1·97	2·13	2·35	2·32	2·18	2·03	1·97
Shear (k_s)	1	(7.7)	4·81 —4·81	3·98 —6·18	3·66 —7·53	3·58 —8·14	3·66 —7·53	3·98 —6·18	4·81 —4·81

Values of k_c calculated from (10.1) and (10.2) are given in Table IV., where σ is assumed to be 0·3. These values are compared with those found previously by Maulbetsch (7) and Levy (8). Some of the values quoted by Maulbetsch were calculated by him, while others were calculated by Faxen (2). Table IV. shows that the values given by equation (10.1) agree closely with Maulbetsch's energy method results, but compared with Levy's values, which are stated to be exact, they are consistently some 4–5 per cent. too high. It should be noted, however, that neither Maulbetsch's nor Levy's results were calculated from a general equation such as (10.1). They appear, in fact, to have been obtained on the basis of somewhat lengthy calculations which had to be repeated for each value of ρ.

TABLE IV.

Values of k_c for clamped isotropic plates ($\sigma=0·3$).

ρ.	r.	Equation (10·1).	Maulbetsch's values.		Levy's values.
			Energy method.	Taylor-Treffitz method.	Exact method.
0·5	1	17·7	18·0, 17·9	17·1, 17·5	—
1·00	1	9·63	9·68, 9·52, 9·48	8·79, 9·11	9·10
1·50	2	7·88	7·64	7·24, 7·50	7·52
1·75	2	7·77	7·39	6·78, 7·37	7·33
2·00	3	7·40	7·47, 7·32, 7·29	6·00, 6·88, 7·08	7·12
2·75	4	7·04	7·11, 7·02	6·45	6·72

Pure Shear: Clamped Edges.

11. When the edges of the plate were simply supported it was found that an approximation to the infinite determinant gave the critical shear stress as a root of a quadratic equation (6.1). Using the determinants D_4 or D_5, a similar approximation can be made for a plate with clamped edges, but the coefficients in the corresponding quadratic for Z are, in general, too complicated for practical use. For clamped edges, therefore, critical stresses are found directly from the determinants D_4 and D_5.

Calculations have been made for a square mahogany plywood plate using only 25 elements of the determinant D_4, which correspond to the equation (7.7) when the constants are arranged in the order A_{11}, A_{22}, A_{13}, A_{31}, A_{33}. (For this case the determinant D_5 gives higher values for Z.) The results, expressed in terms of the shear stress coefficient k_s, are shown in the last two lines of Table III.

It is to be expected that these values will be somewhat higher than the actual critical stress, but the percentage inaccuracy can only be found after lengthy calculations with more terms of the determinant D_4. Some estimate of the accuracy can, however, be found by finding the critical stress for an isotropic plate and comparing it with the value given by Iguchi ⁽⁵⁾, who used rather more terms of his infinite determinant for his calculations. The value for a square isotropic plate, obtained by using 25 elements of D_4, is $Z=11{\cdot}25Eh^3$ ($k_s=13{\cdot}9$), compared with $Z=10{\cdot}68Eh^3$ ($k_s=13{\cdot}2$) given by Iguchi. The present result is, therefore, about 5 per cent. too high; it is similar to the value ($k_s=14{\cdot}0$) given by Cox ⁽¹⁾.

Other Boundary Conditions.

12. When the ends $x=0, \pi$ of the plate are supported and the sides $y=0, \pi$ are clamped, a solution of the general stability problem can be obtained by the strain energy method if

$$w=\sin y \sum_{r=1}^{\infty} \sum_{s=1}^{\infty} A_{rs} \sin rx \sin sy. \quad . \quad . \quad . \quad . \quad . \quad (12.1)$$

The general results are not quoted here. When the plate is under pure compression over the edges $x=0, \pi$ an approximate equation for the critical stress can be found by a similar method to that used previously. Thus it is found that the critical stress is given by (5.1) or (5.3), where

$$\left.\begin{aligned}
&A=2D_{11}m^4+20(D_{12}+2D_{66})\rho^2m^2+82D_{22}\rho^4,\\
&C=3D_{11}r^4+8(D_{12}+2D_{66})\rho^2r^2+16D_{22}\rho^4,\\
&15\pi^2(r^2-m^2)B=2048\rho rm\{D_{16}(m^2+r^2)+8D_{26}\rho^2\},\\
&D=2m^2, \quad E=3r^2, \quad m=r\pm1.
\end{aligned}\right\} \quad . \quad . \quad (12.2)$$

When the ends $x=0, \pi$ of the plate are clamped, and the sides $y=0, \pi$ are supported, the appropriate expression for w is

$$w=\sin x \sum_{r=1}^{\infty} \sum_{s=1}^{\infty} A_{rs} \sin rx \sin sy. \quad . \quad . \quad . \quad . \quad (12.3)$$

Again, only the approximate formulæ for pure compression are given here. The critical stress is found from (5.1) or (5.3), where

$$\left.\begin{aligned}
&A=D_{11}(m^4+6m^2+1)+8(D_{12}+2D_{66})\rho^2(m^2+1)\\
&\qquad\qquad+(16D_{22}\rho^4 \text{ if } m\neq1, \quad \text{or} \quad 24D_{22}\rho^4 \text{ if } m=1),\\
&C=D_{11}(r^4+6r^2+1)+2(D_{12}+2D_{66})\rho^2(r^2+1)\\
&\qquad\qquad+(\tfrac{3}{2}D_{22}\rho^4 \text{ if } r=1, \quad \text{or} \quad D_{22}\rho^4 \text{ if } r\neq1),\\
&B=\frac{1024\rho rm\{4D_{16}(r^2+m^2+r^2m^2-3)+5D_{26}\rho^2(r^2+m^2-2)\}}{3\pi^2(m^2-r^2)\{(m-2)^2-r^2\}\{(m+2)^2-r^2\}},\\
&D=m^2+1, \quad E=r^2+1, \quad m=r\pm1.
\end{aligned}\right\} \quad (12.4)$$

Calculations for other Edge Conditions, and for Plywood of other Constructions.

13. Equation (2.3) gives the constants D_{ij} as

$$D_{ij}=\int_{-h}^{h} c_{ij}z^2\,dz. \quad . \quad . \quad . \quad . \quad . \quad . \quad . \quad . \quad (13.1)$$

Now suppose that the apparent overall c_{ij} in bending of a symmetrical $2n-1$ plywood is c, and that the c_{ij} of the qth ply from the centre is c_q. Then

$$c\int_0^{t_n} z^2\,dz = \int_0^{t_n} c_q z^2\,dz = c_1\int_0^{t_1} z^2\,dz + c_2\int_{t_1}^{t_2} z^2\,dz + \dots + c_n\int_{t_{n-1}}^{t_n} z^2\,dz.$$

Thus

$$ct_n^3 = c_1t_1^3 + c_2(t_2^3 - t_1^3) + \dots + c_n(t_n^3 - t_{n-1}^3), \quad . \quad . \quad . \quad (13.2)$$

where t_1=distance to the first glue line,
t_2=distance to the second glue line,
. . . .
$t_n = h$=distance to outer surface of plywood,

and all distances are measured in the z direction from the centre of the plywood. Equation (13.2) has been given previously by Price (10), March (6) and others.

In a normal plywood having the grain directions perpendicular in adjacent plies

$$c_1 = c_3 = c_5 = \dots; \quad c_2 = c_4 = c_6 = \dots.$$

Thus for such a plywood

$$c = Ac_n + (1-A)c_{n-1}, \quad . \quad . \quad . \quad . \quad . \quad . \quad . \quad (13.3)$$

where $At_n^3 = t_n^3 - t_{n-1}^3 + t_{n-2}^3 - t_{n-3}^3 + \dots.$

For example, in a 5-ply 1 : 1 : 1 : 1 : 1

$$t_1 = \frac{1}{5}t_n; \quad t_2 = \frac{3}{5}t_n; \quad t_3 = t_n,$$

and from (13.2)

$$c = \frac{1}{125}c_1 + \frac{26}{125}c_2 + \frac{98}{125}c_3$$

$$= 0{\cdot}793c_3 + 0{\cdot}207c_2 \text{ (since } c_1 = c_3).$$

$$\therefore \quad A = 0{\cdot}793.$$

Values of A, and of D_{ij} (lb./sq. in.)$\times 10^{-6}/h^3$, calculated from the figures in Table I., are given below (Table V.) for a number of mahogany plywoods at grain angles of 0°, 45° and 90°.

The curves of fig. 5 have been constructed for 3-ply 1 : 1 : 1, using the above values of the constants for this plywood. These curves refer to 0° and 90° plates in pure compression, and under various edge conditions. The buckling stress coefficient is plotted against $\rho(D_{22}/D_{11})^{\frac{1}{4}}$, since this procedure brings the 0° and 90° curves into coincidence. This method of plotting has been used previously in unpublished reports by other workers.

In fig. 6, k_c in pure compression for plates with simply supported edges, is plotted against A. The curves refer to grain angles of 0°, 45° and 90° and $\rho=1$ (eqn. 5.2) or $\rho=\infty$ (eqn. (5.6)). For plates of a given size and grain angle, the calculated points in general lie on a smooth curve. This suggests that the results can be extended to plywoods of a construction

TABLE V.

Construction.	A.	θ (degree).	$\frac{10^{-6}D_{11}}{h^3}$.	$\frac{10^{-6}(D_{12}+2D_{66})}{h^3}$.	$\frac{-10^{-6}D_{16}}{h^3}$.	$\frac{10^{-6}D_{22}}{h^3}$.	$\frac{-10^{-6}D_{26}}{h^3}$.
Solid wood	1·000	0	0·907	0·105	0·000	0·066	0·000
		45	0·296	0·677	0·210	0·296	0·210
		90	0·066	0·105	0·000	0·907	0·000
3-ply 1 : 1 : 1	0·963	0	0·874	0·105	0·000	0·097	0·000
		45	0·296	0·677	0·195	0·296	0·195
		90	0·097	0·105	0·000	0·874	0·000
3-ply 1 : 2 : 1	0·875	0	0·801	0·105	0·000	0·171	0·000
		45	0·296	0·677	0·158	0·296	0·158
		90	0·171	0·105	0·000	0·801	0·000
5-ply 1 : 1 : 1 : 1 : 1....	0·793	0	0·732	0·105	0·000	0·240	0·000
		45	0·296	0·677	0·123	0·296	0·123
		90	0·240	0·105	0·000	0·732	0·000
5-ply 1 : 2 : 2 : 2 : 1....	0·593	0	0·564	0·105	0·000	0·408	0·000
		45	0·296	0·677	0·039	0·296	0·039
		90	0·408	0·105	0·000	0·564	0·000

Fig. 5.

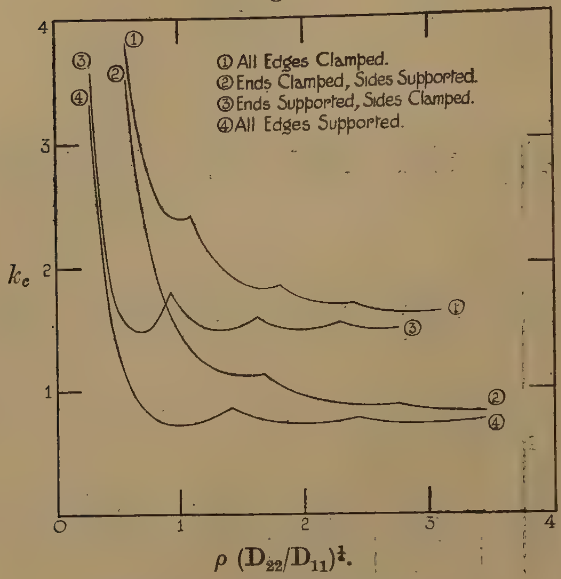

θ=0° or 90° mahogany 3-ply 1:1:1.

Fig. 6.

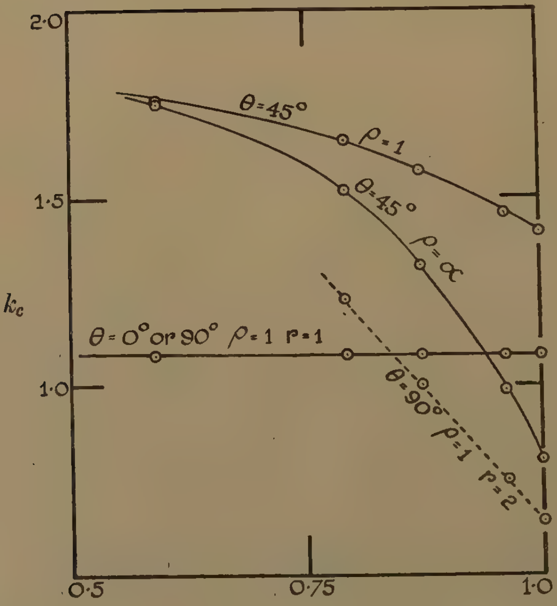

for which calculations have not been made, by finding A for this plywood and interpolating on a k_c–A curve, provided r and m do not alter over the interpolation ranges.

The necessity for the latter proviso is shown by the results for a square plate at 90°. At 0° and 90°, the only integer involved in k_c is r, which at these two angles is the number of half-waves into which the specimen buckles. Fig. 6 shows that at 0° and 90° the k_c of square plates is independent of A up to $A \gtrsim 0{\cdot}84$. Above this value k_c is still independent of A for the 0° plates, but not for the 90° plates, since minimum values of k_c are now given by $r=2$, and are shown on the dotted curve. Thus for the 90° plates interpolation should be made on the $r=1$ curve if $A<0{\cdot}84$, and on the $r=2$ curve if $A>0{\cdot}84$.

The Effect of Wood Species.

14. In the present section, the effect of variation in fundamental elastic constants of wood on the buckling stress coefficients is discussed, but for simplicity the discussion is limited to infinite plates in compression at grain angles of 0°, 45° and 90°.

The elastic constants of woods have been determined by a number of workers. Certain of these measurements have been converted to c_{ij} and are given in Table VI. (*a*).

With the exception of the mahogany, the figures in Table VI. (*a*) refer to the longitudinal-tangential plane of wood (the plane defined by the axial direction in the tree and the direction parallel with the growth rings). The figures for mahogany refer to the longitudinal-radial plane in the tree (the plane defined by the axial radial directions) and are derived from Table I. The remaining c_{ij} in Table VI. (*a*) are obtained from the familiar elastic constants, using the two dimensional equations:

$$c_{11}=E_L/\lambda\,; \quad c_{22}=E_T/\lambda\,; \quad c_{12}=E_L\sigma_{TL}/\lambda=E_T\sigma_{LT}/\lambda\,; \quad c_{66}=G_{LT},$$

where

E_L=longitudinal Young's modulus,

E_T=tangential Young's modulus,

G_{LT}=rigidity modulus corresponding to shear stresses in the L and T directions,

$$\sigma_{LT}=\frac{\text{contraction in T direction}}{\text{extension in L direction}} \text{ for a tensile stress in L direction,}$$

$\lambda=1-\sigma_{TL}\sigma_{LT}$ and can be taken approximately as 0·99.

The effective c_{ij} of the plywood at 0° are found by inserting the values from Table VI. (*a*) in equation (13.3). The constants D_{ij} (at 0°) are then given by the integrated form of equation (13.1), namely,

$$D_{ij}=\tfrac{2}{3}h^3\times\text{effective } c_{ij} \text{ of plywood.}$$

TABLE VI.

Species.			Spruce (1).	Spruce (2).	Birch.	Beech.	Hoop pine.	Douglas fir.	Mahogany.
(*a*) Elastic constants.									
c_{11}		$\times 10^{-6}$ lb./sq. in.	1·97	1·45	2·39	2·01	2·02	1·98	1·36
c_{22}		,, ,,	0·071	0·060	0·091	0·166	0·078	0·114	(0·099)
$c_{12}+2c_{66}$		,, ,,	0·182	0·209	0·317	0·382	0·269	0·309	(0·156)
(*b*) Buckling stress coefficients for infinite plates in compression.									
3-ply 1 : 1 : 1	Supported edges	$k_c(\theta=0^\circ$ or $90^\circ)$	0·59	0·69	0·66	0·87	0·66	0·75	0·72
		$k_c(\theta=45^\circ)$	0·74	0·82	0·82	1·10	0·82	0·93	0·99
	Clamped edges	$k_c(\theta=0^\circ$ or $90^\circ)$	1·18	1·32	1·28	1·67	1·27	1·45	1·44
		$k_c(\theta=45^\circ)$	1·41	1·51	1·51	1·84	1·50	1·63	1·68
5-ply 1 : 1 : 1 : 1 : 1	Supported edges	$k_c(\theta=0^\circ$ or $90^\circ)$	0·87	0·97	0·94	1·09	0·94	1·01	0·96
		$k_c(\theta=45^\circ)$	1·42	1·44	1·43	1·56	1·43	1·48	1·52
	Clamped edges	$k_c(\theta=0^\circ$ or $90^\circ)$	1·82	1·95	1·91	2·16	1·91	2·02	1·99
		$k_c(\theta=45^\circ)$	2·16	2·23	2·21	2·44	2·21	2·30	2·32

The D_{ij} at 45° are obtained from the 0° values, using the known transformation formulæ, which at 45° become

$$\begin{aligned} D'_{11}=D'_{22} &= \tfrac{1}{4}\{D_{11}+2(D_{12}+2D_{66})+D_{22}\}, \\ D'_{12}+2D'_{66} &= \tfrac{1}{4}\{3D_{11}-2(D_{12}+2D_{66})+3D_{22}\}, \\ D'_{16}=D'_{26} &= \tfrac{1}{4}(D_{22}-D_{11}), \end{aligned}$$

where the values at 45° are distinguished from those at 0° by dashes. Finally, the values of X at 0° and 90° are obtained from equations (5.7) and (9.3), and at 45° from equations (5.8) and (9.4), and converted to k_s by equation (5.10).

The results of the calculations are given in Table VI. (*b*). They do not cover a wide enough range for any general conclusions to be drawn, since they include neither plates in shear nor plates of low a/b ratios Nevertheless, if the deviations from the mean in a single line of figure. are expressed as a percentage of the mean value in that line, some results of interest are indicated.

For the 3-ply, the extreme values differ from the means by ±14–20 per cent. If the results for beech (which are invariably high) and for spruce 1 (which are invariably low) are omitted, the deviations are reduced to ±7–10 per cent. For the 5-ply, the corresponding figures are ±5–10 per cent. and ±2–4 per cent. Apparently, therefore, variations in elastic constants affect the final answer less when the factor A (§ 13) is low than when it is high. From the point of view of the practical calculation of buckling stresses, the deviations given above might not be serious, although the largest deviation (±20 per cent.) is certainly quite high. If the elastic constants of the plywood were known, the errors could be reduced by calculating the buckling stress coefficients for that particular plywood. If this were impracticable, or if the elastic constants were unknown, then errors of ±20 per cent. would, in extreme cases, have to be accepted.

Acknowledgment.

The work involved in the contributions of one of the authors (R. F. S. H.) to this paper was carried out in the Physics Section, Forest Products Research Laboratory. To this extent, publication is by permission of the Department of Scientific and Industrial Research.

References.

(1) Cox, H. L., Rep. Memor. Aero. Res. Com. Lond. no. 1553 (1933).
(2) Faxen, O. H., *Z. angew. Math. Mech.* xv. p. 268 (1935).
(3) Goland, M., and Aleck, B., Curtis Wright Res. Lab. Airplane Division, Buffalo, N.Y. Res. Rept. No. 5, S. 57 (1943).
(4) Green, A. E., Proc. Camb. Phil. Soc. xl. p. 222 (1944).
(5) Iguchi, S., Proc. Phys. Math. Soc. Japan, xx. p. 814 (1938).
(6) March, H. W., Physics, vii. p. 32 (1936).
(7) Maulbetsch, J. L., J. App. Mech. iv. A, 59 (1937).
(8) Levy, S., J. App. Mech. ix. A, 171 (1942).

(9) Love, A. E. H., 'The Mathematical Theory of Elasticity,' 4th ed. (1927), Cambridge Univ. Press.
(10) Price, A. T., Philos. Trans. A, ccxxviii. p. 1 (1928).
(11) Timoshenko, S., 'The Theory of Elastic Stability,' 1st ed. (1936), McGraw Hill Book Co., New York and London.
(12) Von Koch, H., *Rendiconti circ. Mat. Palermo*, t. xxviii. p. 225 (1909).

Note added in proof April 1946.—Owing to war-time difficulties, an unavoidably long interval has elapsed between the communication and publication of the present paper. During this period, security restrictions have been modified or removed and it is now possible to give details of reports which were frequently consulted during the preparation of the paper, but which were not included in the references of paragraph 16. They are as follows :—

H. W. March, C. B. Norris, A. W. Voss, J. Palma and P. F. McKinnon, 'The Buckling of Flat Plywood Plates in Compression, Shear, and Combined Compression and Shear,' U.S. Dept. Agric. For. Prod. Lab. Madison, Mimeo, 1316 and Supplements A–I, April 1942–March 1945.

J. P. O. Silberstein and R. C. T. Smith. 3-ply Flat Panels in End Compression at 45° to the Grain, Div. of Aeronautics, C.S.I.R. Australia Rept. S.M. 42, October 1944.

R. C. T. Smith, 'The Buckling of Flat Plywood Panels in Compression.' Australian Council of Aeronautics, Rept. A.C.A. 12, December 1944.

In addition, the following translation of what appears to be the earliest theoretical discussion of buckling stresses in plywood has recently been made available :—

L. Balabuch, 'The Stability of Plywood Plates.' Aeronautical Engineering, U.S.S.R. 11 (1937) 19 (Ministry of Aircraft Production, R.T.P. Translation No. 2199).

LXXXIII. *An Extension of Campbell's Theorem of Random Fluctuations.*

By R. S. Rivlin [*].

[Received April 19, 1945.]

1. *Introduction.*

Campbell's Theorem (1) states that if, at the instant of time t, the response y of a linear instrument to a single event occurring at any time τ is given by

$$y=s(t-\tau),$$

then the mean square deviation of the response to a large number of such events, occurring at random in time, is given by

$$\overline{(y-\bar{y})^2}=\lambda\int_0^\infty s^2(t)\,.\,dt, \qquad (1)$$

---

[*] Communicated by the Author.

where λ is the mean rate at which the events occur. Here it is assumed that the events are all of an exactly similar nature. In particular cases it may not be possible to assign the occurrence of an event to a particular instant in time. In such a case, the time τ, at which an event is assumed to occur, is the instant of occurrence of some recognizable feature of the event. In this paper we shall, however, assume that $s(t)=0$ for all values of t less than 0.

If the events are not all of an exactly similar nature, equation (1) takes the form

$$\overline{(y-\bar{y})^2}=\sum_{r=1}^{N}\lambda_r\int_0^\infty s_r{}^2(t).dt. \qquad (2)$$

Here it is considered that there are N different types of event. The events of each type occur at random in time, and events of different types occur independently of each other. A single event of the rth type occurring at the time τ is assumed to give a response $s_r(t-\tau)$ at the time t, and the mean rate of occurrence of an event of the rth type is λ_r. In this paper we shall be concerned with events of this type and shall discuss the values of $\overline{(y-\bar{y})^p}$, where p has integral values greater than 2. The formulæ for these quantities are derived by a method very similar to that adopted by J. M. Whittaker (2) in proving Campbell's Theorem.

As far as we are aware, the formula (2) has only been proved, so far, for the case when $s_r(t)=r.s(t)$ for all values of r, but the form given emerges as a particular case of the results obtained in Section 3.

2. *The Value of* $\overline{(y-\bar{y})^p}$.

Let us first assume that the events are all of the same type and occur at a mean rate λ. Let the response of the instrument to one of these events occurring at time τ be $s(t-\tau)$.

Following Whittaker (2), we divide the response characteristic of the instrument to a single event into a large number of small intervals of duration L, so that the response to a single event occurring at a time kL before the instant of observation is $s(k\mathrm{L})$. Suppose that ν_k events occur in the interval kL to $(k-1)$L before the instant of observation. Then the contribution of these events to the resultant reading of the instrument is $\nu_k.s(k\mathrm{L})$. The actual reading y of the instrument is given by

$$y=\sum_k \nu_k.s(k\mathrm{L}). \qquad (3)$$

The mean value $\bar{y}$ of y, taken over a large number of instantaneous observations of the instrument response, is given by

$$\bar{y}=\sum_k \bar{\nu}_k.s(k\mathrm{L}). \qquad (4)$$

Combining equations (3) and (4), we have

$$y-\bar{y}=\sum_k(\nu_k-\bar{\nu}_k).s(k\mathrm{L}). \qquad (5)$$

Then $$(y-\bar{y})^p=[\sum_k(\nu_k-\bar{\nu}_k).s(k\mathrm{L}].[\sum_l(\nu_l-\bar{\nu}_l).s(l\mathrm{L})]\ldots, \quad . \quad . \quad . \quad (6)$$

where the product of p terms is taken.

From equation (6), we have

$$\overline{(y-\bar{y})^p}=\overline{[\sum_k(\nu_k-\bar{\nu}_k).s(k\mathrm{L})].[\sum_l(\nu_l-\bar{\nu}_l).s(l\mathrm{L})]\ldots}$$

$$=\sum_{k,\,l,\,m\ldots}\overline{[(\nu_k-\bar{\nu}_k).(\nu_l-\bar{\nu}_l).(\nu_m-\bar{\nu}_m)\ldots s(k\mathrm{L}).s(l\mathrm{L}).s(m\mathrm{L})\ldots]}, \quad (7)$$

where the summation is carried out over all possible combinations of $k, l, m \ldots$

Before proceeding further, we must evaluate expressions of the form

$$\overline{(\nu_k-\bar{\nu}_k).(\nu_l-\bar{\nu}_l).(\nu_m-\bar{\nu}_m)\ldots}, \quad . \quad . \quad . \quad . \quad . \quad . \quad (8)$$

where there are p factors in the expression. We must bear in mind that the quantities

$$(\nu_k-\bar{\nu}_k),\ (\nu_l-\bar{\nu}_l),\ (\nu_m-\bar{\nu}_m)\ldots$$

vary in an unrelated manner. Thus, if $k, l, m \ldots$ are all unequal, the expression (8)

$$=\overline{(\nu_k-\bar{\nu}_k)}.\overline{(\nu_l-\bar{\nu}_l)}.\overline{(\nu_m-\nu_m)}\ldots=0,$$

since $$\overline{(\nu_k-\bar{\nu}_k)}=\bar{\nu}_k-\bar{\nu}_k=0.$$

However, in the right-hand side of equation (7) not all of the terms

$$\overline{(\nu_k-\bar{\nu}_k).(\nu_l-\bar{\nu}_l).(\nu_m-\bar{\nu}_m)\ldots}$$

have the values of $k, l, m \ldots$ all unequal. Such terms may be conveniently written

$$\overline{(\nu_k-\bar{\nu}_k)^\alpha.(\nu_l-\bar{\nu}_l)^\beta.(\nu_m-\nu_m)^\gamma\ldots} \quad . \quad . \quad . \quad . \quad . \quad . \quad (9)$$

where $k, l, m \ldots$ are all unequal and $\alpha, \beta, \gamma \ldots$ are positive integers such that

$$\alpha+\beta+\gamma\ldots=p. \quad . \quad . \quad . \quad . \quad . \quad . \quad . \quad . \quad (10)$$

The expression (9)

$$=\overline{(\nu_k-\bar{\nu}_k)^\alpha}.\overline{(\nu_l-\bar{\nu}_l)^\beta}.\overline{(\nu_m-\bar{\nu}_m)^\gamma}\ldots,$$

since the values of $\nu_k, \nu_l, \nu_m \ldots$ are unrelated.

This expression is zero if one or more of the integers $\alpha, \beta, \gamma \ldots$ is unity. If α is not unity,

$$\overline{(\nu_k-\bar{\nu}_k)^\alpha}=\lambda\mathrm{L}+f(\mathrm{L}, \alpha),$$

where $f(\mathrm{L}, \alpha)$ is a polynomial in L depending on α and which tends to zero more rapidly than L, as L tends to zero. This was shown for the case when $\alpha=2$ by Schrodinger (3) and later by Whittaker (2) and has been extended for higher values of α by N. R. Campbell and V. J. Francis (unpublished).

Now the term

$$\overline{(\nu_k-\bar{\nu}_k)^\alpha . (\nu_l-\bar{\nu}_l)^\beta . (\nu_m-\bar{\nu}_m)^\gamma \ldots s^\alpha(k\mathrm{L}) . s^\beta(l\mathrm{L}) . s^\gamma(m\mathrm{L})}$$

occurs in the expression (7) in $\dfrac{p\,!}{\alpha\,!\,\beta\,!\,\gamma\,!\ldots}$. ways.

Consequently,

$$\overline{(y-\bar{y})^p} = \Sigma \frac{p\,!}{\alpha\,!\,\beta\,!\,\gamma\,!\ldots}[s^\alpha(k\mathrm{L}) . \lambda\mathrm{L}] . [s^\beta(l\mathrm{L}) . \lambda\mathrm{L}] \ldots , \quad . \quad . \quad (12)$$

the summation being carried out over all sets of values of α, β, $\gamma \ldots$ for which none of the quantities is unity and equation (10) is obeyed, and over all values of $k, l \ldots$ Here we have neglected $f(\mathrm{L}, \alpha)$, $f(\mathrm{L}, \beta) \ldots$ in comparison with $\lambda\mathrm{L}$. This is justified by the fact that we shall now proceed to the limit $\mathrm{L}\rightarrow 0$.

Now in equation (12), proceeding to the limit $\mathrm{L}\rightarrow 0$, we have, writing t for $k\mathrm{L}$, $l\mathrm{L} \ldots$ and dt for L, and replacing the summation over all values of $k, l, \ldots$ by integration with respect to t,

$$\overline{(y-\bar{y})^p} = \Sigma \lambda^\mu \frac{p\,!}{\alpha\,!\,\beta\,!\,\gamma\,!\ldots}\int_0^\infty s^\alpha(t) . dt \int_0^\infty s^\beta(t) . dt \ldots , \quad . \quad . \quad (13)$$

the summation being carried out over the same range of values of α, β, $\gamma \ldots$ as in equation (12). μ is the number of integrals in each product under the summation sign.

Under certain conditions which are of particular physical importance, but which will not be discussed in detail here, the term

$$\left[\lambda \int_0^\infty s^2(t) . dt\right]^{p/2}$$

in the expression of equation (13), when p is even, and the term

$$\left[\lambda \int_0^\infty s^2(t) . dt\right]^{p-3/2} . \lambda \int_0^\infty s^3(t) . dt$$

when p is odd, are very considerably greater than the other terms. Then, the expression (13) can be re-written

$$\overline{(y-\bar{y})^p} = \left[\lambda \int_0^\infty s^2(t) . dt\right]^{p/2} \qquad \text{when } p \text{ is even,} \quad (14a)$$

or $$\overline{(y-\bar{y})^p} = \left[\lambda \int_0^\infty s^2(t) . dt\right]^{p-3/2} . \left[\lambda \int_0^\infty s^3(t) . dt\right] \quad \text{when } p \text{ is odd.} \quad (14b)$$

It can readily be seen that the necessary conditions for the validity of equations (14 *a*) and (14 *b*) obtain for sufficiently large values of λ, provided $s(t)$ does not change sign as t varies from 0 to ∞.

We see that when $p=2$, equation (13) reduces to equation (1).

3. *Generalization of the Theorem.*

Now, let us suppose that the events are not all identical, but consist of N different types. The mean rate at which the rth type occurs is λ_r.

Let us suppose, too, that an event of the rth type occurring at the instant of time τ gives a response

$$y=s_r(t-\tau),$$

at the instant of time t, on the linear instrument.

Equation (6) then becomes

$$\begin{aligned}(y-\bar{y})^p=&\left[\sum_{r=1}^{N}\sum_{k}(\bar{\nu}_{kr}-\nu_{kr}).s_r(kL)\right],\\ &\left[\sum_{r=1}^{N}\sum_{l}(\nu_{lr}-\bar{\nu}_{lr}).s_r(lL)\right],\\ &\left[\sum_{r=1}^{N}\sum_{m}(\nu_{mr}-\bar{\nu}_{mr}).s_r(mL)\right]\ldots,\end{aligned} \quad . \quad . \quad . \quad (15)$$

where ν_{kr} is the number of events of the rth type occurring in the kth interval of length L before the instant of observation.

Following the argument of the previous section, we have

$$\begin{aligned}\overline{(y-\bar{y})^p}&=\sum_{k,l,m\ldots}\overline{\left[\sum(\nu_{kr}-\bar{\nu}_{kr}).s_r(kL)\right].\left[\sum_{v=1}^{N}(\nu_{lv}-\bar{\nu}_{lv}).s_v(lL)\right]\ldots}\\ &=\sum_{k,l,m\ldots}\sum_{r=1,\,v=1,\ldots}^{r=N,\,v=N,\ldots}[\overline{(\nu_{kr}-\bar{\nu}_{kr})(\nu_{lv}-\bar{\nu}_{lv})}\ldots s_r(kL).s_v(lL)\ldots]. \end{aligned}\quad (16)$$

The general expression for a term in this sum is

$$\frac{p!}{\prod\limits_{r=1}^{N}\alpha_r!\prod\limits_{v=1}^{N}\beta_v!\ldots}\prod_{r=1}^{N}\overline{(\nu_{kr}-\bar{\nu}_{kr})^{\alpha_r}}.\prod_{v=1}^{N}\overline{(\nu_{kv}-\bar{\nu}_{kv})^{\beta_v}}\ldots\prod_{r=1}^{N}s_r^{\alpha_r}(kL).\prod_{v=1}^{N}s_v^{\beta_v}(lL)\ldots, \quad . \quad . \quad . \quad (17)$$

where $\Sigma\alpha_r+\Sigma\beta_v+\ldots=p$, provided none of the quantities α_r, $\beta_v\ldots$ is unity.

If one or more of the terms α_r, β_v, . . . is unity, then the expression (17) vanishes.

Now, $\overline{(\nu_{kr}-\bar{\nu}_{kr})^{\alpha_r}}$ may be put equal to $\lambda_r L$, as explained in the previous section. Consequently, proceeding to the limit in which L is vanishingly small and so can be replaced by dt, and kL can be replaced by t, we have

$$\overline{(y-\bar{y})^p}=\sum\frac{p!}{\prod\limits_{r=1}^{N}\alpha_r!\prod\limits_{v=1}^{N}\beta_v!\ldots}\prod_{r=1}^{N}\left[\lambda_r\int_0^{\infty}s_r^{\alpha_r}(t).dt\right].\prod_{v=1}^{N}\left[\lambda_v.\int_0^{\infty}s_v^{\beta_v}(t).dt\right]\ldots, \quad , \quad . \quad . \quad (18)$$

where the summation is carried out over all groups of positive integral values α_r, β_v, $\gamma_w\ldots$ satisfying the relation given above, in which none of the quantities α_r, β_v, . . . is unity.

The author desires to acknowledge gratefully the privilege of many helpful discussions with Dr. N. R. Campbell and V. J. Francis, Esq., relevant to this work.

Abstract.

Campbell's Theorem is extended to give explicit formulæ for the mean cubed, fourth and higher integral powers of the deviation from the mean level of a random fluctuation, due to the linear superposition of the effects of events occurring at random in time.

Two cases are considered :—

(1) All the events are identical but occur at random in time.

(2) The events are of N different types, which occur in an unrelated manner, each type of event occurring at random in time.

References.

(1) N. R. Campbell, Proc. Camb. Phil. Soc. xv. p. 117 (1909).
(2) J. M. Whittaker, Proc. Camb. Phil. Soc. xxxiii. p. 451 (1937).
(3) E. Schrodinger. Akad. Wiss. Wien, cxxviii. p. 177 (1919).

Addendum.

Since this paper was written, and while its publication has been held in abeyance from war-time security considerations, a paper has been published by Rice (Bell Syst. Tech. J. xxiii. p. 326 (1944)), in which the following relations are obtained :

$$\bar{y}=m_1=\mu_1,$$
$$\overline{y^2}=m_2=\mu_2+\mu_1 m_1,$$
$$\overline{y^3}=m_3=\mu_3+2\mu_2 m_1+\mu_1 m_2,$$
$$\cdot \quad \cdot \quad \cdot \quad \cdot \quad \cdot \quad \cdot$$
$$\cdot \quad \cdot \quad \cdot \quad \cdot \quad \cdot \quad \cdot$$

where $$\mu_n=\lambda \int^{\infty} s^n(t)\,.dt.$$

Here, we have slightly modified Rice's notation to fit in with our own and have taken $s(t)=0$ for t less than 0, as we have in our calculations.

Putting $p=3$ in equation (13) of Section 2 of our paper, we have

$$\overline{(y-\ )^3}=\lambda \int_0^{\infty} s^3(t)\,.\,dt.$$

Bearing in mind that

$$\overline{(y-\bar{y})^2}=\overline{y^2}-\bar{y}^2=\lambda \int_0^{\infty} s^2(t)\,.\,dt$$

and $$\bar{y}=\lambda \int_0^{\infty} s(t)\,.\,dt,$$

we see that

$$\overline{y^3}=\lambda \int_0^{\infty} s^3(t)\,.\,dt+3\lambda^2 \int_0^{\infty} s^2(t)\,.\,dt\,.\int_0^{\infty} s(t)\,.\,dt+\lambda^3 \left[\int_0^{\infty} s(t)\,dt\right]^3,$$

which agrees with the corresponding formula for $\overline{y^3}$, which can be obtained from Rice's equations given above.

Rice apparently only considers the case in which all the events are identical, and, moreover, does not give an explicit formula for either $\overline{y^n}$ or $\overline{(y-\bar{y})^n}$, even for this case.

LXXXIV. *The Two-Dimensional Electric Field of a Single Semi-Infinite Rectangular Conductor.*

By N. Davy, University College, Nottingham *.

[Received February 23, 1945.]

Abstract.

The electric fields of two two-dimensional conductors are investigated theoretically, and some of the conclusions are checked experimentally. The conductors are (*a*) a single semi-infinite rectangular cylinder charged externally, and (*b*) a single semi-infinite thin-walled hollow rectangular cylinder charged internally. Equipotentials and lines of force are obtained theoretically and also experimentally. Electric intensities, surface densities, total charges, capacities and mechanical forces on various objects are calculated. One or two special cases are discussed.

§ 1. *Statement of the Problem.*

It is proposed to investigate the electric field of the following two-dimensional systems :—

(*a*) A single semi-infinite rectangular conductor charged externally.

(*b*) A single hollow thin-walled semi-infinite rectangular conductor charged internally.

§ 2. *A Single Semi-Infinite Rectangular Conductor charged Externally. Transformation from z-plane to t-plane.*

In fig. 1 the line ABOCD represents a section of a single semi-infinite rectangular conductor of width $2b$, BOC being the finite end. Let this be raised to an electric potential $+V_0$ e.s.u. by a static charge on its external surface. Let it be regarded as surrounded by a cylinder of infinite radius and potential zero. To find the electric potential at any point external to the conductor, the well-known method of Schwarz-Christoffel transformations is used. Let fig. 1 represent the z-plane, O the origin, and BOC part of the x-axis. The y-axis is a straight line through O parallel to AB or DC. To transform the edge ABOCD into the real axis in the t-plane, and the external region into the upper half of the t-plane, let the point A correspond to $t=-\infty$, B to $t=-1$, C to $t=+1$, and D to $t=+\infty$. Then

$$dz=C_1(t+1)^{\frac{1}{2}}(t-1)^{\frac{1}{2}}\,dt=C_1(t^2-1)^{\frac{1}{2}}\,dt, \quad . \quad . \quad . \quad . \quad . \quad (1)$$

---

* Communicated by Professor L. F. Bates, D.Sc.

where C_1 is a constant. Put

$$t=\cosh u. \quad \ldots \ldots \quad (2)$$

Then, on integration,

$$z=\frac{C_1}{2}(\sinh u \cosh u-u)+C_2, \quad \ldots \ldots \quad (3)$$

where C_2 is a constant of integration. If at the point C, $z=b$, $t=1$, then

$$\cosh u=1, \quad \sinh u=0, \quad \text{and} \quad u=0, \quad \ldots \ldots \quad (4)$$

taking $u=0$ as the lowest value of $u=\pm i2n\pi$, the solution of (4).

Hence

$$C_2=b. \quad \ldots \ldots \quad (5)$$

Also at the point B,

$$z=-b, \quad t=-1, \quad \cosh u=-1, \quad u=i\pi, \quad \ldots \ldots \quad (6)$$

Fig. 1.

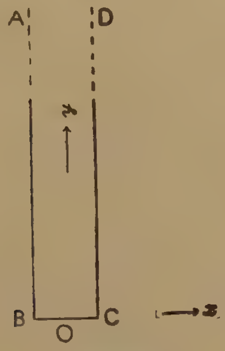

z-plane.

taking $u=i\pi$ as the lowest value of $u=\pm i(2n+1)\pi$. Then on substituting in (3) we get

$$C_1=-\frac{i4b}{\pi}. \quad \ldots \ldots \quad (7)$$

Equation (3) then becomes

$$z=-\frac{i2b}{\pi}(\sinh u \cosh u-u)+b. \quad \ldots \ldots \quad (8)$$

This also satisfies the condition that at O, $t=0$ when $z=0$.

Writing $z=x+iy$ and $u=p+iq$, where p and q are real, in (8) we get

$$x=b+\frac{b}{\pi}\cosh 2p \sin 2q-\frac{2bq}{\pi}, \quad \ldots \ldots \quad (9)$$

and

$$y=\frac{2bp}{\pi}-\frac{b}{\pi}\sinh 2p \cos 2q. \quad \ldots \ldots \quad (10)$$

These are the required equations of geometrical transformation.

§ 3. *Equipotentials and Lines of Force.*

The W-plane corresponding to the z-plane of fig. 1 is represented in fig. 2 in which the edge of ABOCD of fig. 1, or rather its complex potential, is represented by the horizontal straight line LNM whose equation is $W=U+iV_0$. The transformation required to convert this line into the real axis of the t-plane is

$$dW=+C_3dt, \quad \ldots \quad (11)$$

which integrates to

$$W=+C_3t+C_4. \quad \ldots \quad (12)$$

Let the point N, whose co-ordinates are 0, iV_0, correspond to $t=0$. Then (12) gives

$$C_4=iV_0. \quad \ldots \quad (13)$$

C_3 appears to be an indefinite constant. Writing $t=\cosh u$, equation (12) becomes

$$W=U+iV=+C_3\cosh u+iV_0, \quad \ldots \quad (14)$$

reducing to

$$U+iV=+C_3\cosh p\cos q+iC_3\sinh p\sin q+iV_0, \quad \ldots \quad (15)$$

Fig. 2.

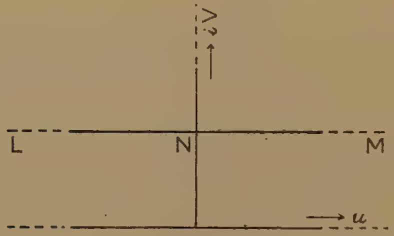

W-plane.

when we put $u=p+iq$. Hence

$$U=+C_3\cosh p\cos q. \quad \ldots \quad (16)$$

$$V=V_0+C_3\sinh p\sin q. \quad \ldots \quad (17)$$

Lines of force are given by U=const., *i. e.*,

$$\cosh p\cos q=\text{const.} \quad \ldots \quad (18)$$

Equipotentials are given by V=const., *i. e.*

$$\sinh p\sin q=\text{const.} \quad \ldots \quad (19)$$

To draw an equipotential a numerical value of q in radians and of the constant in (19) are selected arbitrarily. Then substituting these in (19) a value of p is found. These values of p and q are inserted in (9) and (10) giving values of x and y for one point only on an equipotential. Other points on the same equipotential are found by selecting arbitrarily a different value of q, keeping the same constant in (19), but otherwise proceeding as before. To draw lines of force, equation (18) is used instead of (19).

In fig. 3 a set of such equipotentials and lines of force are represented. These have been obtained by the aid of (19) and (18) combined with (9) and (10), and taking b as one cm.

§ 4. *Electric Intensity* F *and Surface Density* σ *at any Point.*

As usual in such cases $F=\left|\frac{dW}{dz}\right|$ and is evaluated by dividing dW as given by (11), by dz as given by (1), (2) and (7). Hence $F=\left|\frac{+i\pi C_3}{4b\sinh u}\right|$, and the surface density

$$\sigma=\frac{F}{4\pi}=\left|\frac{+iC_3}{16b\sinh u}\right|. \quad . \quad . \quad . \quad . \quad . \quad . \quad . \quad . \quad (20)$$

Fig. 3.

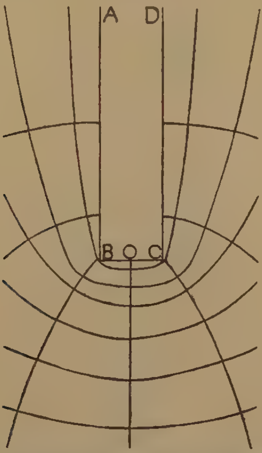

Equipotentials and lines of force of a semi-infinite rectangular conductor charged externally. Curves obtained by calculation and confirmed by experiment.

Hence at the projecting corners B and C of fig. 1, the electric intensity F and the surface density σ are found to be infinite, as expected. For at B, $u=i\pi$, $\sinh u=0$, and at C, $u=0$, $\sinh u=0$. At the midpoint O of the end, $u=\frac{i\pi}{2}$ and $\sinh\frac{i\pi}{2}=i\sin\frac{\pi}{2}=i$. Hence at B the intensity $F=\frac{\pi C_3}{4b}$ and $\sigma=\frac{C_3}{16b}$. At the point A, u is real and infinite and $\sinh u=\infty$, so that there $F=0$ and $\sigma=0$. The variation of σ along the edge ABOCD is represented in fig. 4.

§ 5. *Total Charge and Capacity.*

The total charge per cm. depth on any length of the edge ABOCD is

$$Q_1=\int_{z_1}^{z_2}\sigma dz=\frac{1}{4\pi}\int_{z_1}^{z_2}\frac{dW}{dz}dz=\frac{W_2-W_1}{4\pi}=\frac{C_3(t_2-t_1)}{4\pi}=\frac{C_3(\cosh u_2-\cosh u_1)}{4\pi}. \quad . \quad . \quad (21)$$

On the end BC the charge per cm. depth is therefore $\frac{C_3}{2\pi}$. On each lateral edge it is infinite, and hence it is infinite on the whole edge. The potential is V_0, hence the whole capacity per cm. depth is infinite. The effective capacity of the end BC is $\frac{C_3}{2\pi V_0}$ e.s.u. per cm.

§ 6. *Mechanical Forces.*

The normal mechanical force per sq. cm. acting outwards on the end BC is

$$\left|2\pi\int_{-b}^{+b}\sigma^2\,dz\right|=\left|\frac{1}{8\pi}\int_{-b}^{+b}\left(\frac{dW}{dz}\right)^2 dz\right|=\left|\frac{1}{8\pi}\int_{i\pi}^{0}\frac{dW}{dz}\cdot\frac{dW}{du}\cdot du\right|. \quad . \quad (22)$$

Using (20) and (14) this is found to be

$$\frac{\pi C_3^{\,2}}{32b}\text{ dynes.} \quad . \quad . \quad . \quad . \quad . \quad . \quad . \quad . \quad (23)$$

Fig. 4.

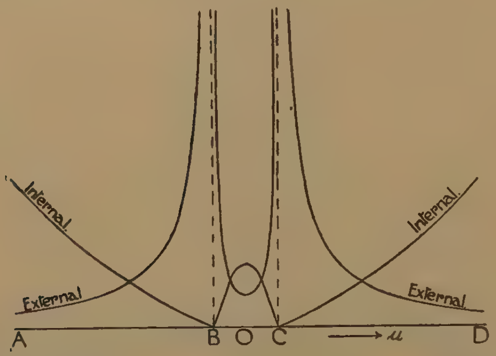

Variation of surface density along the edge of a semi-infinite rectangular conductor.
(*a*) Externally charged. (*b*) Internally charged.
Ordinates are proportional to the surface density, abscissæ to the variable *u*.

When the electric system under discussion is replaced by the corresponding magnetic one, the conductor becomes a magnetic pole-piece. The mechanical force on a small para- or diamagnetic body placed at any external point is $P=\left|\frac{(\chi_2-\chi_1)}{2}\frac{dF^2}{dz}\right|$ dynes per gram where χ_1, χ_2 are mass-susceptibilities of the medium and small body, respectively. Using (20) this is found to be

$$P=+\frac{\pi^3C_3^{\,2}(\chi_2-\chi_1)\cosh u}{64b^3\sinh^5 u}\text{ dynes per gram.} \quad . \quad . \quad . \quad (24)$$

This force is therefore zero where $\cosh u=0$, $u=\frac{i\pi}{2}$, *i. e.* near the midpoint O of the end BC in fig. 1. It is infinite where $\sinh u=0$, $u=0$ or $i\pi$, *i. e.* near either corner B or C.

§ 7. *Special Case.—Thin Plate.* $b=0$.

When the semi-infinite conductor is of negligible thickness, the corners B and C close in on the midpoint O (see fig. 5) and the differential equation of transformation is $dz=C_1t\,dt$ giving

$$z=\frac{C_1t^2}{2}+C_2. \quad . \quad . \quad . \quad . \quad . \quad . \quad . \quad . \quad . \quad (25)$$

When $z=0$, $t=0$, hence

$$C_2=0. \quad . \quad . \quad . \quad . \quad . \quad . \quad . \quad . \quad . \quad (26)$$

C_1 appears to be an indefinite constant. Write

$$t^2=\frac{2z}{C_1}=a^2z, \quad . \quad . \quad . \quad . \quad . \quad . \quad . \quad . \quad . \quad (27)$$

Fig. 5.

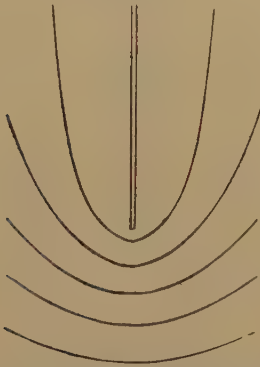

Equipotentials of a thin semi-infinite rectangular conductor obtained by experiment.

where $a^2=\frac{2}{C_1}$. Then

$$t=\pm az^{\frac{1}{2}}. \quad . \quad . \quad . \quad . \quad . \quad . \quad . \quad . \quad . \quad (28)$$

As in equation (11)

$$dW=+C_3\,dt \quad \text{and} \quad W=+C_3t+C_4. \quad . \quad . \quad . \quad . \quad . \quad (29)$$

As before

$$C_4=iV_0. \quad \text{and} \quad W=\pm C_3az^{\frac{1}{2}}+iV_0. \quad . \quad . \quad . \quad . \quad . \quad (30)$$

Using polar co-ordinates

$$W=U+iV=\pm C_3ar^{\frac{1}{2}}e^{i\frac{\theta}{2}}+iV_0=\pm C_3ar^{\frac{1}{2}}\left(\cos\frac{\theta}{2}+i\sin\frac{\theta}{2}\right)+iV_0. \quad (31)$$

Hence

$$U=\pm C_3ar^{\frac{1}{2}}\cos\frac{\theta}{2} \quad \text{and} \quad V=\pm C_3ar^{\frac{1}{2}}\sin\frac{\theta}{2}+V_0. \quad . \quad . \quad (32)$$

Lines of force are given by

$$r^{\frac{1}{2}}\cos\frac{\theta}{2}=\text{const.} \quad . \quad . \quad . \quad . \quad . \quad . \quad . \quad . \quad . \qquad (33)$$

They form a set of parabolas. Equipotentials are represented by

$$r^{\frac{1}{2}}\sin\frac{\theta}{2}=\text{const.} \quad . \quad . \quad . \quad . \quad . \quad . \quad . \quad . \quad . \qquad (34)$$

When the above electrical system is replaced by the equivalent magnetic one, the electrode becomes a polepiece. The mechanical force on a small para- or diamagnetic body placed at any point in its field is $\frac{(\chi_2-\chi_1)}{2}\cdot\frac{dF^2}{dz}$ dynes/gram, where χ_1 and χ_2 are the mass-susceptibilities of the body and medium, respectively, and F is the magnetic field strength at the point. Here $F=\left|\frac{dW}{dz}\right|=\left|\frac{C_3a}{2z^{\frac{1}{2}}}\right|$ by (30), so that the mechanical force

$$=-\frac{(\chi_2-\chi_1)C_3^2}{4C_1z^2}\text{ dynes/gm.,} \quad . \quad . \quad . \quad . \quad . \quad . \qquad (35)$$

since $a^2=\frac{2}{C_1}$. The force varies as the inverse square of z.

Reverting to the electrical system, the electric intensity at any point is also

$$F=\left|\frac{dW}{dz}\right|=\left|\frac{C_3a}{2z^{\frac{1}{2}}}\right|. \quad . \quad . \quad . \quad . \quad . \quad . \quad . \quad . \quad . \qquad (36)$$

The surface density on the conductor at any point

$$=\frac{F}{4\pi}=\left|\frac{C_3a}{8\pi z^{\frac{1}{2}}}\right|, \quad . \quad . \quad . \quad . \quad . \quad . \quad . \quad . \quad . \quad . \qquad (37)$$

and is inversely proportional to the square root of z, *i. e.* of the distance from the end. It is, of course, infinite at the end itself. The mechanical force per sq. cm. is

$$2\pi\sigma^2=\left|\frac{C_3^2a^2}{32\pi z}\right|=\left|\frac{C_3^2}{16\pi C_1z}\right|\text{dynes per sq. cm.} \quad . \quad . \quad . \qquad (38)$$

at any point of the conductor.

The total charge between any two points, per cm. depth, is

$$Q_1=\int_{z_1}^{z_2}\sigma\,dz=W_2-W_1=\frac{C_3(t_2-t_1)}{4\pi}=\frac{C_3a(z_2^{\frac{1}{2}}-z_1^{\frac{1}{2}})}{4\pi}\text{ e.s.u.} \quad . \qquad (39)$$

Thus along the total length of each edge the charge per cm. depth is infinite. Between the end and any other point on one side, the total charge is $\frac{C_3az^{\frac{1}{2}}}{4\pi}$, *i. e.* it is proportional to the $\sqrt{\text{length of edge concerned}}$. On the end the charge per cm. depth is zero, even though the surface density is infinite.

§ 8. *Experimental Confirmation.*

The systems of equipotentials obtained by calculation, and represented in figs. 3 and 5, have been confirmed experimentally using the device described in earlier papers including a beat frequency oscillator.

§ 9. *A Single Hollow Semi-Infinite Rectangular Conductor charged Internally. Transformation from z-plane to t-plane.*

In fig. 6 let ABOCD represent a hollow semi-infinite rectangular conductor, with thin walls, charged internally. Let the potential be V_0 e.s.u. We require the electric potential and intensity at any point. In his book 'Conjugate Functions for Engineers,' 1933, Prof. M. Walker has obtained the transformation we need, but in his case it was to solve the equivalent problem of the flow of electric current in a semi-infinite conductor. For the sake of continuity, the transformation will be derived here also, using the same notation as that used in the external problem just discussed. The Schwarz-Christoffel method is again used to obtain the transformation which changes the edge ABOCD into the real axis of the *t*-plane, and the region *inside* ABOCD into the upper half of the *t*-plane.

Fig. 6.

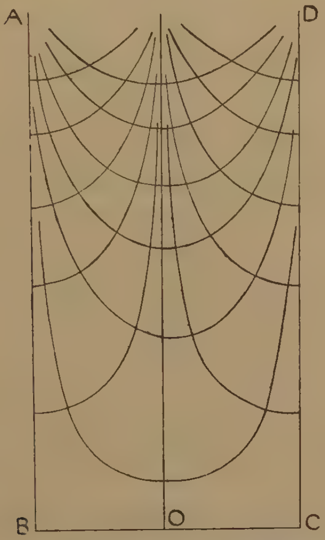

Lines of force and equipotentials of a semi-infinite rectangular conductor charged internally obtained by experiment.

Let A correspond to $t=-\infty$, B to $t=-1$, C to $t=+1$ and D to $t=+\infty$. The differential equation of transformation is

$$dz=C_1\frac{dt}{(t^2-1)^{\frac{1}{2}}} \quad . \quad . \quad . \quad . \quad . \quad . \quad . \quad . \quad (40$$

Write $t=\cosh u$, $$dt=\sinh u \, . \, du. \quad . \quad . \quad . \quad . \quad . \quad . \quad . \quad . \quad (41)$$

Then we find $$dz=C_1\,.\,du,\quad\text{and}\quad z=C_1u+C_2. \qquad (42)$$

At B, $z=-b$, $t=-1$, and the lowest value of u, whose cosh is -1, is $i\pi$.

Hence $$-b=C_1i\pi+C_2. \qquad (43)$$

Similarly, at the point C, $z=+b$, $t=+1$, and the lowest value of u, whose cosh is 1, is zero. Hence

$$+b=C_2. \qquad (44)$$

Then by (43) $$C_1=\frac{2ib}{\pi}. \qquad (45)$$

On substituting in (42) we get

$$z=x+iy=\frac{2ibu}{\pi}+b. \qquad (46)$$

Putting $u=p+iq$, where p and q are real, this gives

$$x=b-\frac{2bq}{\pi},\quad y=\frac{2bp}{\pi}. \qquad (47)$$

§ 10. *Equipotentials and Lines of Force.*

The W-plane is represented in fig. 2, in which the straight line LNM, corresponding to the edge ABOCD in fig. 6, has the equation

$$W=U+iV_0. \qquad (48)$$

LNM is transformed into the real axis of the t-plane by the equation

$$dW=C_3\,.\,dt, \qquad (49)$$

which, on integrating, becomes

$$W=C_3t+C_4. \qquad (50)$$

Let the point N correspond to $t=0$, $W=iV_0$. Then

$$C_4=iV_0. \qquad (51)$$

Equation (50) then becomes

$$W=C_3t+iV_0. \qquad (52)$$

C_3 appears to be an indefinite constant. Write

$$t=\cosh u. \qquad (53)$$

Then $$W=C_3\cosh u+iV_0. \qquad (54)$$

Put $u=p+iq$, where p and q are real. This gives

$$W=U+iV=C_3\cosh(p+iq)+iV_0 \qquad (55)$$

$$=C_3(\cosh p\cos q+i\sinh p\sin q)+iV_0. \qquad (56)$$

Lines of force are given by U=const., *i. e.*

$$\cosh p\cos q=\text{const}. \qquad (57)$$

Equipotentials are given by V=const., *i. e.*

$$\sinh p\sin q=\text{const}. \qquad (58)$$

To draw a "theoretical" exponential, a numerical value of q is selected arbitrarily, and also a constant for the right-hand side of (58). Substituting these in (58) a value of p is found. These values of p and q are then inserted in (47), giving values of x and y for one point only, on an equipotential. Other points on the same equipotential are found by repeating the process with a fresh arbitrarily selected value of q, but the same constant in (58) as before. To draw lines of force, equation (57) is used instead of (58).

On page 52 of Prof. Walker's book, fig. 41, the two systems of curves are represented. Experimental lines of force and equipotentials obtained by the present author by a method described in earlier papers are shown in fig. 6.

§ 11. *Electric Intensity* F *and Surface Density at any Point.*

The electric intensity F at any internal point is equal to $\left|\frac{d\mathrm{W}}{dz}\right|$.

Now $\mathrm{W}=\mathrm{C}_3 \cosh u+i\mathrm{V}_0$ by (54).

Hence

$$d\mathrm{W}=\mathrm{C}_3 \sinh u\,.\,du. \qquad (59)$$

Also, since by (46)

$$z=\frac{2ibu}{\pi}+b,\quad dz=\frac{2ib}{\pi}.du. \qquad (60)$$

Dividing (59) by (60) we get

$$\mathrm{F}=\left|\frac{d\mathrm{W}}{dz}\right|=\left|\frac{-i\pi\mathrm{C}_3}{2b}\sinh u\right|. \qquad (61)$$

The surface density at any point is

$$\sigma=\frac{\mathrm{F}}{4\pi}=\left|\frac{-i\mathrm{C}_3}{8b}\sinh u\right|. \qquad (62)$$

At the internal corner C, $z=+b$, $t=+1$, $u=0$, and $\sigma=0$. At the internal corner B, $z=-b$, $t=-1$, $u=+i\pi$ and $\sigma=0$. At the origin O, which is the midpoint of the end, $q=\frac{\pi}{2}$ and $p=0$, by (47).

Also at O,

$$u=\frac{i\pi}{2} \quad \text{and} \quad \sigma=\left|\frac{\mathrm{C}_3}{8b}\right|. \qquad (63)$$

Values of σ for this case are shown in fig. 4, for comparison with the values along the edge of an externally charged conductor raised to the same potential V_0.

§ 12. *Total Charge and Capacity.*

The total charge Q_1 on any portion of the edge ABOCD, per cm. depth, is

$$\int_{z_1}^{z_2}\sigma\,.\,dz=\frac{1}{4\pi}\int_{z_1}^{z_2}\left|\frac{d\mathrm{W}}{dz}\right|dz=\frac{\mathrm{W}_2-\mathrm{W}_1}{4\pi}, \qquad (64)$$

and also to

$$\frac{C_3(t_2-t_1)}{4\pi}=\frac{C_3(\cosh u_2-\cosh u_1)}{4\pi}. \quad . \quad . \quad . \quad . \quad . \quad . \quad (65)$$

On the end, therefore, the charge is

$$Q_1=\frac{C_3}{2\pi}, \quad . \quad . \quad . \quad . \quad . \quad . \quad . \quad . \quad . \quad . \quad (66)$$

since at B, $\cosh u=-1$, and at C, $\cosh u=+1$. The effective capacity of the end is

$$\frac{C_3}{2\pi V_0} \text{ e.s.u. per cm. depth.} \quad . \quad . \quad . \quad . \quad . \quad . \quad . \quad (67)$$

§ 13. *Mechanical Forces.*

The normal mechanical force per unit area on any part of the internal face is

$$2\pi\sigma^2=\frac{\pi C_3{}^2\sinh^2 u}{32b^2} \text{ by (62).} \quad . \quad . \quad . \quad . \quad . \quad . \quad . \quad (68)$$

On any length of internal edge the total force is

$$2\pi\int_{z_1}^{z_2}\sigma^2\,dz=\left|\frac{1}{8\pi}\int_{z_1}^{z_2}\left(\frac{dW}{dz}\right)^2 dz\right|=\left|\frac{1}{8\pi}\int_{u_1}^{u_2}\frac{dW}{dz}\cdot\frac{dW}{du}\cdot du\right|. \quad . \quad . \quad (69)$$

Hence, using (61) and (59), the force on the finite internal end per cm. depth is

$$\frac{C_3{}^2\pi}{32b}. \quad . \quad . \quad . \quad . \quad . \quad . \quad . \quad . \quad . \quad . \quad . \quad (70)$$

This is the same result as for the force on the external end, equation (23).

When the electrical system is replaced by the equivalent magnetic one, the inner surface becomes a magnetic equipotential. The mechanical force per gram on a small para- or diamagnetic body placed at any internal point is $P_1=\frac{(\chi_2-\chi_1)}{2}\frac{dF^2}{dz}$ in the direction of increasing z, where χ_2 and χ_1 are the mass susceptibilities of the body and medium, respectively. Substituting for F from (61) it is found that

$$P_1=\frac{(\chi_2-\chi_1)\pi^3C_3{}^2\sinh 2u}{16b^3}. \quad . \quad . \quad . \quad . \quad . \quad . \quad . \quad (71)$$

§ 14. *Special Case. Infinitely Narrow Hollow Conductor.*

When the internal width decreases to an infinitely small quantity, the points B and C close in on O, which becomes the whole of the closed end. Corresponding to the point A let $t=-\infty$, to O, $t=0$ and to the point D, $t=+\infty$. The differential equation of transformation is

$$dz=C_1\frac{dt}{t}, \quad . \quad . \quad . \quad . \quad . \quad . \quad . \quad . \quad . \quad . \quad . \quad (72)$$

giving

$$z=C_1\log t+C_2. \quad . \quad . \quad . \quad . \quad . \quad . \quad . \quad . \quad (73)$$

Since $t=0$ when $z=0$, C_2 is infinite. C_1 is again indefinite. . . (74)

We need only consider the surface density which in this case is

$$\sigma=\frac{1}{4\pi}\left|\frac{dW}{dz}\right|=\frac{C_3 t}{4\pi C_1}, \qquad (75)$$

i. e. $\sigma=0$ at the inner end, and elsewhere is proportional to t.

§ 15, *Inversion.*

Reverting to the general cases, the process of inversion about a point on the axis of symmetry solves the problems of the electric fields of two-dimensional crescent-shaped conductors, charged either internally or externally.

LXXXV. *A Power Law of the Viscosity of Liquids.*

By W. J. Jones and S. T. Bowden *.

[Received September 17, 1945.]

It is well known that for homopolar liquids the relation between surface tension and temperature can be represented by a power law of the form

$$\sigma=\sigma_0(1-T/T_c)^n,$$

where σ is the surface tension at the absolute temperature T, T_c is the critical temperature, and σ_0 and n are constants which, according to Ferguson and Kennedy (1), vary from liquid to liquid. Since viscosity, like surface tension, is a manifestation of the cohesive forces of a liquid, it is of interest to ascertain whether a viscosity function can be found which can be similarly related to the temperature by a power law of the form

$$\eta-c=a(1-T/T_c)^n,$$

where c, a and n are specific constants of the liquid. We have tested the applicability of such an equation for all the homopolar liquids whose viscosities have been determined over a wide range of temperature. The evaluation of the constants a and n in the above equation for a particular liquid was carried out in the following way. The value of η was plotted against the corresponding value of $(1-T/T_c)$ at ten-degree intervals, and the value of the differential $d\eta/d(1-T/T_c)$ corresponding to each plotted point was then determined from the slope of the curve passing through all these points. In practice it was found that, except for the sharpest curvatures, the value of this differential

---

* Communicated by the Authors.

for an absolute temperature T was given sufficiently closely by the expression $(\eta'-\eta'')T_c/20$, where η', η'' are the viscosities at the temperatures $(T-10)°$ and $(T+10)°$ respectively. The value of the differential and that of its corresponding $(1-T/T_c)$ were then substituted in the derived equation

$$\log \frac{d\eta}{d(1-T/T_c)} = \log (an) + (n-1) \log (1-T/T_c)$$

TABLE I.

Viscosity Data for Non-associated Liquids.

Temp. ° C.	Methyl acetate. $\eta_c=0{\cdot}0009584$ $\eta_0-\eta_c=0{\cdot}0260853$ $n=2{\cdot}569857$ $T_c=507{\cdot}8°$		Ethyl acetate. $\eta_c=0{\cdot}0008699$ $\eta_0-\eta_c=0{\cdot}0224353$ $n=2{\cdot}316053$ $T_c=523{\cdot}2°$		Carbon tetrachloride. $\eta_c=0{\cdot}001625$ $\eta_0-\eta_c=0{\cdot}084153$ $n=3{\cdot}24276$ $T=556{\cdot}3°$	
	$\eta_{obs.}$	η alc.	$\eta_{obs.}$	$\eta_{calc.}$	$\eta_{obs.}$	$\eta_{calc.}$
20....	0·381	0·378	—	—	—	—
30....	0·344	0·345	0·4036	0·3886	0·843	0·818
40....	0·312	0·315	0·3560	0·3581	0·739	0·738
50....	0·284	0·287	0·3242	0·3291	0·651	0·665
60....	0·258	0·261	0·2941	0·3019	0·585	0·598
70....	0·237	0·238	0·2687	0·2768	0·524	0·538
80....	0·217	0·217	0·2462	0·2532	0·468	0·484
90....	0·198	0·197	0·2261	0·2315	0·426	0·435
100....	0·182	0·180	0·2082	0·2115	0·384	0·392
110....	0·166	0·165	0·1924	0·1930	0·352	0·354
120....	0·154	0·152	0·1782	0·1763	0·323	0·320
130....	0·142	0·140	0·1652	0·1612	0·299	0·291
140....	0·130	0·130	0·1528	0·1477	0·276	0·266
150....	—	—	0·1409	0·1357	0·255	0·244
160....	—	—	0·1294	0·1251	0·234	0·226
170....	—	—	0·1189	0·1160	0·217	0·211
180....	—	—	0·1090	0·1083	0·201	0·198

for each of the plotted points, and the value of log (an) and that of $(n-1)$ best satisfying all the equations thus obtained were calculated by the method of least squares. The value of the constant c was found by taking the mean of the values given by the expression

$$c=\eta-a(1-T/T_c)^n$$

for each of the plotted points.

If no fundamental alteration in the internal structure of the liquid accompanied change of temperature, this equation might be expected to hold over the entire range of the liquid state, and could then be written in the form

$$\eta-\eta_c=(\eta_0-\eta_c)(1-T/T_c)^n,$$

where η_c and η_0 were the viscosities of the liquid at the critical temperature and absolute zero, respectively.

TABLE I. (*cont.*).

Temp. ° C.	Benzene.		Fluorobenzene.		Chlorobenzene.	
	$\eta_c=0{\cdot}0010490$ $\eta_0-\eta_c=0{\cdot}059537$ $n=3{\cdot}32498$ $T_c=561{\cdot}5°$		$\eta_c=0{\cdot}001104$ $\eta_0-\eta_c=0{\cdot}042503$ $n=2{\cdot}9620$ $T_c=559{\cdot}7°$		$\eta_c=0{\cdot}001153$ $\eta_0-\eta_c=0{\cdot}047070$ $n=3{\cdot}21352$ $T_c=632{\cdot}2°$	
	$\eta_{obs.}$	$\eta_{calc.}$	$\eta_{obs.}$	$\eta_{calc.}$	$\eta_{obs.}$	$\eta_{calc.}$
20....	0·6473	0·6163	0·598	0·583	0·799	0·751
30....	0·5592	0·5556	0·532	0·532	0·705	0·693
40....	0·4889	0·5004	0·478	0·486	0·631	0·638
50....	0·4325	0·4497	0·428	0·442	0·567	0·588
60....	0·3854	0·4039	0·389	0·402	0·515	0·540
70....	0·3464	0·3620	0·357	0·366	0·471	0·496
80....	0·3141	0·3254	0·329	0·333	0·431	0·456
90....	0·2865	0·2923	0·300	0·302	0·397	0·418
100....	0·2618	0·2626	0·275	0·275	0·367	0·383
110....	0·2392	0·2364	0·250	0·250	0·339	0·351
120....	0·2189	0·2134	0·231	0·228	0·313	0·322
130....	0·2007	0·1935	0·214	0·208	0·293	0·296
140....	0·1842	0·1762	0·198	0·191	0·274	0·272
150....	0·1696	0·1615	0·182	0·176	0·256	0·250
160....	0·1563	0·1490	0·168	0·162	0·239	0·230
170....	0·1440	0·1386	0·156	0·151	0·223	0·213
180....	0·1323	0·1300	0·144	0·142	0·209	0·197
190....	—	—	—	—	0·196	0·183
200....	—	—	—	—	0·185	0·171
210....	—	—	—	—	0·173	0·161
220....	—	—	—	—	0·163	0·152
230....	—	—	—	—	0·153	0·144
240....	—	—	—	—	0·144	0·137

Few homopolar liquids have been investigated over a wide range of temperature, and in view of the frequent lack of agreement in the results recorded by different workers, we have used the experimental values obtained in one series of investigations (2), except in the case of water (3). The values of the constants η_c, $\eta_0-\eta$ and n are given in Table I., and the values of the viscosities calculated from the last equation are compared with those observed; the values of the constants are given in terms of poises, but those of viscosity are expressed in centipoises.

The general agreement between the observed and calculated values of the viscosity shows that the equation is applicable over a very wide range of temperature, and it is remarkable that the power law is followed so closely in view of the fact that the viscosity is so much more sensitive to temperature change than is surface tension. This conformity indicates that temperature change within the range under consideration is not accompanied by any fundamental change in the internal structure of these liquids or in the nature of the intermolecular forces. It is interesting to note that these liquids conform to the Macleod relation (4) and do not exhibit a parachor anomaly (5).

According to Friend (6), the assumption that rise in temperature merely separates the molecules of a liquid, leads to the conclusion that surface tension should be proportional to the square-root of viscosity. He claims that this relation is approximately true for non-associated liquids over a considerable range of temperature below the boiling point, and that, if M is the molecular weight and D the density of the liquid, the quantity $M\eta^{1/8}/D$ is a constant endowed with additive characteristics depending on the nature of the atoms and linkages in the molecule. The premises of this argument, however, are open to question, inasmuch as the viscosity, unlike the surface tension, is essentially a dynamical quantity, and it may be shown that the quantity is not a constant even in those cases where the liquid is found to conform accurately to the Macleod equation, $\sigma^{1/4}/D=C$, where C is a constant. The results for dioxan are recorded in Table II.

TABLE II.

Viscosity and Surface Tension Data for Dioxan.

Temp. °C.	D.	η (poise).	σ.	$\sigma^{1/4}/D$.	$\eta^{1/8}/D$.	$\eta^{1/12}/D$.
20	1·0330	0·01255	35·42	2·36	0·560	0·672
30	1·0225	0·01063	33·97	2·36	0·556	0·670
40	1·0111	0·00917	32·54	2·36	0·550	0·669
50	1·0006	0·00778	30·88	2·36	0·545	0·668
60	0·9895	0·00685	29·48	2·36	0·542	0·667
70	0·9787	0·00606	28·37	2·36	0·540	0·668
80	0·9674	0·00539	27·03	2·36	0·538	0·669

It is evident that the quantity $\eta^{1/12}/D$ is more nearly constant than $\eta^{1/8}/D$.

A more precise formulation of the relation between the viscosity, surface tension and density of a liquid substance is obtainable by eliminating the factor $(1-T/T_c)$ between the following equations :—

$$\eta-\eta_c=(\eta_0-\eta_c)(1-T/T_c)^{n_1},$$

$$\sigma=\sigma_0(1-T/T_c)^{n_2},$$

$$D-d=D_0(1-T/T_c)^{n_3},$$

where d is the density of the vapour at the absolute temperature T, and n_1, n_2, and n_3 are the appropriate exponents (7). Thus for benzene the approximate values of the exponents are $n_1=10/3$, $n_2=6/5$, $n_3=3/10$, so that

$$\frac{(\eta-\eta_c)^{n_2/n_1}}{\sigma}=\frac{(\eta-\eta_c)^{9/25}}{\sigma}=k_1.$$

$$\frac{(\eta-\eta_c)^{n_3/n_1}}{\mathrm{D}-d}=\frac{(\eta-\eta_c)^{9/100}}{\mathrm{D}-d}=k_2,$$

where k_1 and k_2 are constants. In Table III. the values of these constants for benzene are compared with those of the quantities $\eta^{1/2}/\sigma$ and $\eta^{1/8}/(\mathrm{D}-d)$, both of which are seen to exhibit a pronounced drift, while the others remain steady over the entire range of temperature under consideration.

TABLE III.

Surface Tension and Viscosity Data for Benzene.

Temp. ° C.	σ.	$\mathrm{D}-d$.	$10^3\eta^{1/2}/\sigma$.	k_1.	$\eta^{1/8}/(\mathrm{D}-d)$	k_2.
20...........	29·11	0·8786	2·77	5·25	0·606	0·712
30...........	27·78	0·8679	2·69	5·16	0·603	0·709
40...........	26·46	0·8568	2·58	5·10	0·600	0·707
50...........	25·17	0·8455	2·55	5·07	0·599	0·707
60...........	23·87	0·8342	2·60	5·05	0·598	0·706
70...........	22·59	0·8228	2·61	5·06	0·599	0·707
80...........	21·31	0·8118	2·63	5·09	0·599	0·707
90...........	20·06	0·8005	2·67	5·11	0·600	0·707
100...........	18·84	0·7880	2·72	5·19	0·604	0·710
110...........	17·62	0·7749	2·78	5·25	0·607	0·712
120...........	16·42	0·7615	2·85	5·31	0·611	0·714
130...........	15·23	0·7472	2·94	5·38	0·616	0·716
140...........	14·05	0·7322	3·06	5·45	0·622	0·718
150...........	12·90	0·7166	3·19	5·51	0·629	0·721
160...........	11·76	0·7012	3·36	5·52	0·636	0·720
170...........	10·64	0·6834	3·57	5·57	0·646	0·722
180...........	9·56	0·6657	3·81	5·46	0·656	0·718

The behaviour of associated liquids is of interest inasmuch as they show a definite parachor anomaly which arises from the circumstance that the quantity $\sigma^{1/4}/(\mathrm{D}-d)$ changes in value with temperature. For ethyl alcohol and water the values of the parachor calculated from Sugden's constants are 132·2 and 54·2, respectively, but the observed values depend on the temperature as shown in Table IV. The table also includes the observed values of the viscosities and those calculated from the power law equation.

Water and ethyl alcohol are termed associated liquids in view of their abnormal surface-energy relationships and their high critical ratios and Trouton ratios. For our present purposes we need not discuss the question as to whether these criteria indicate the actual degree of association or its rate of change with temperature, and we shall use the term to cover either alternative. In general, associated liquids are characterized by a rapid change of viscosity with temperature, and since this demands a high value of n in the power law equation, the value of this exponent may be taken as indicative of the degree of association. The fact that the value of n for ethyl alcohol is only slightly higher than for non-associated liquids shows that the degree of association of the alcohol is relatively small. While water has a parachor value which is nearly normal, the high value of the exponent indicates that it is highly associated.

Table IV.

Parachor and Viscosity Data for Associated Liquids.

	Ethyl alcohol. $\eta_c=0{\cdot}001190$ $\eta_0-\eta_c=0{\cdot}20275$ $n=3{\cdot}58780$ $T_c=516{\cdot}2°$				Water. $\eta_c=0{\cdot}002145$ $\eta_0-\eta_c=4{\cdot}1237$ $n=10{\cdot}27915$ $T_c=647{\cdot}1°$		
Temp. ° C.	[P].	$\eta_{obs.}$	$\eta_{calc.}$	Temp. ° C.	[P].	$\eta_{obs.}$	$\eta_{calc.}$
30	127·0	0·991	0·967	0	53·1	1·789	1·687
40	—	0·825	0·830	10	—	1·306	1·328
50	—	0·701	0·715	20	52·7	1·005	1·050
60	—	0·591	0·611	30	—	0·802	0·838
70	—	0·503	0·521	40	52·4	0·653	0·674
80	128·8	0·435	0·444	50	—	0·550	0·551
90	—	0·376	0·378	60	52·3	0·470	0·458
100	—	0·325	0·322	70	—	0·406	0·389
110	—	0·283	0·276	80	52·2	0·356	0·338
120	—	0·248	0·237	90	—	0·315	0·301
130	—	0·217	0·206	100	52·1	0·282	0·275
140	129·7	0·191	0·182				
150	—	0·166	0·162				

It will also be noticed that the values of η_0 for water and ethyl alcohol are much greater than for the non-associated liquids.

References.

(1) Ferguson and Kennedy, Trans. Farad. Soc. xxxii. p. 1474 (1936).

(2) Titani, *Bull. C. S. Japan*, ii. p. 95 (1927).

(3) Bingham and Jackson, "Scient. Paper Bureau of Standards," no. 298 (1917).

(4) Macleod, Trans. Farad. Soc. xix. p. 38 (1923).

(5) Sugden, "The Parachor and Valency," p. 157 (1930) (Routledge).

(6) Friend, 'Nature,' cl. p. 432 (1942); Friend and Hargreaves, Phil. Mag. xxxiv. p. 643 (1943); *ibid.* xxxv. p. 136 (1944).

(7) Verschaffelt, "Commun. of Leiden," no. xxviii. (1896); Sugden, J. Chem. Soc. p. 1780 (1927).

University College,
Cardiff.

LXXXVI. *Orientation Effect in Powder Photographs of Graphite.*

By J. B. Nelson * and D. P. Riley *,
Crystallographic Laboratory, Cambridge †.

[Received February 23, 1946.]

[Plate VII.]

Abstract.

The doubling of $000l$ lines in powder photographs of graphite is shown to be due to preferred orientation of crystals in the specimen. An extrapolation procedure to obtain accurate values of the c dimension is described.

---

1. *Introduction.*

In the course of an investigation on graphite, we had occasion to take a large number of powder photographs of natural or well-crystallized artificial specimens. We were able, in addition, to examine photographs of similar specimens taken previously by Dr. A. R. Stokes. In all cases, an anomalous effect was observed in connection with the $000l$ reflections.

This was so, however the specimen was prepared (rolling the powder with gum tragacanth, sticking the powder to a hair with canada balsam, extruding a paste of the powder through a thick-walled capillary tube or filling a thin-walled capillary by tamping).

The $000l$ reflections were composite in nature, generally consisting of two well-defined separate lines. Taylor (1941) has remarked that the 0004 reflection always consists of two lines. Our observations confirmed this, and, in addition, the 0002 reflection (which is usually greatly over-exposed) could be seen to be doubled when examined by reflected light. None of the other reflections, such as $10\bar{1}0$, $10\bar{1}1$, $11\bar{2}0$, etc., showed this effect. In connection with work on the accurate determination of the unit-cell dimensions of graphite, it became necessary to examine the effect more closely.

2. *Investigation of the Effect.*

Gum tragacanth specimens of 1·32, 0·77, and 0·43 mm. diameter were prepared, and photographed with cobalt radiation in a 19-cm. diameter powder camera. The width of the camera slit was such that the 1·32 mm.

---

* Scientific Officer, British Coal Utilisation Research Association.

† Communicated by Sir Lawrence Bragg, F.R.S.

specimen was just completely bathed in the beam. Sections of the photographs are compared in fig. 1 (Pl. VII.). It will be seen that the splitting of the 0004 reflections is very pronounced in the largest specimen, less evident in the medium one, and indiscernible in the small one. This made it clear that the X-rays were being preferentially reflected from the surface layers of the specimen, as the separation of the components could be shown to be directly proportional to the diameter of the specimen. That the effect could not be wholly due to absorption was evident, as the μr value for the thick specimen was less than 1·2. This value corresponds to a "transparent" specimen. Also, the effect would not be confined to the $000l$ reflections if absorption were the cause.

The simplest explanation appears to be that there is a preferred orientation of the graphite crystals, particularly at the surface of the specimen. The disk-shaped crystals tend to arrange themselves parallel to the surface during the preparation of the specimen. The resulting state of affairs is illustrated in fig. 2. For convenience, we shall consider the 0002, 0004, and $10\bar{1}1$ reflections only. Owing to the preferred orientation, for a given reflection, the major part of the diffracted energy is contributed by those parts of the surface regions in which the lattice planes are inclined at the appropriate angle to the X-ray beam, the remainder of the diffracted energy coming from a fraction of the disoriented material present in the sample. For the $000l$ reflections, we have what is effectively a hollow specimen, and doubling occurs as shown schematically in the diagram. For the $10\bar{1}1$ reflection, however, the two components almost coincide and a single line results. There is, however, another position for the $10\bar{1}1$ planes to reflect, which gives

Fig. 2.

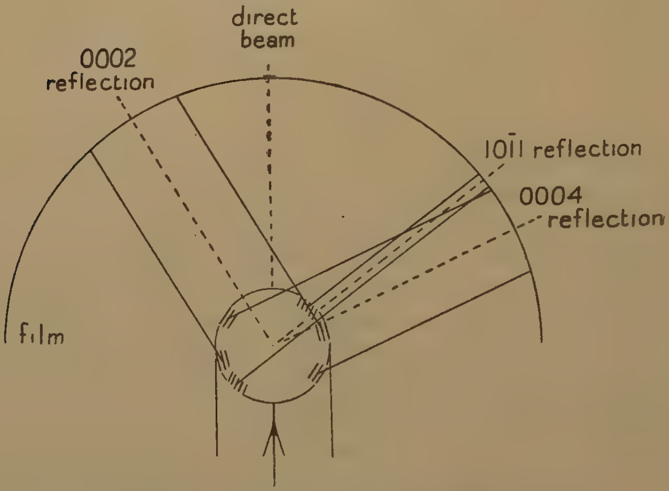

Schematic representation of orientation effect.

a wider separation than this, but the resultant effect produces only broadened rather than resolved lines. The $10\bar{1}0$ reflection is similar, but slightly broader ($10\bar{1}2$ and $10\bar{1}3$ are also slightly broadened). As is shown in fig. 2, the effect is greater for low- than for high-order reflections. The fact that the beam is in practice divergent increases this tendency. For this reason, the 0006 reflection is not affected to the same extent as the lower orders. When observed, the effect takes the form of a triplet with a strong central component, owing to the superposition of the two α-doublets.

As can be seen in fig. 1, the lower-angle component of the 0004 reflection is less intense than its companion. This would be expected from the greater length of its path in the specimen and the consequent greater absorption.

The presence of this type of preferred orientation was shown directly by taking photographs in a 6 cm.-diameter Unicam camera. The pattern given by the 0·77-mm. specimen is reproduced in fig. 3 (Pl. VII.). The 0002 and 0004 reflections show intense equatorial arcs, whereas this effect is not observed with the other lines (*e. g.* $10\bar{1}1$). The doubling of the 0004 reflection can also be seen.

3. *Effect on Determination of Unit-cell Dimensions.*

From this viewpoint the effect is similar to the case of high absorption. The more intense component of the doubled line is recorded on the film at the same position as would be the single line given by a highly absorbing specimen. It gives too high a value for the angle θ and, therefore, too low a spacing. The less intense component is symmetrically displaced from the true position by the same amount. Therefore it yields too high a spacing. The mean of these two angles approaches the correct value for θ, and should give a nearly correct spacing.

It is always advisable in the accurate determination of unit-cell dimensions to adopt an extrapolation procedure. We have shown (Nelson and Riley, 1945) that the most suitable function to eliminate absorption errors is $\frac{\cos^2\theta}{\sin\theta}+\frac{\cos^2\theta}{\theta}$. This function can also be used here. Spacings derived from the stronger components will give a steep ascending plot (towards $\theta=90°$), while those from the weaker will give a steep descending extrapolation. It should be noted that the slope of the former extrapolation will be very much greater than would have been the case if absorption only were responsible.

4. *Application to Graphite.*

The extrapolation with values of the *a*-dimension derived from the $10\bar{1}0$, $11\bar{2}0$, $20\bar{2}0$ reflections is, of course, straightforward. The extrapolation is practically horizontal owing to the low absorption. The difficulty with regard to the *c*-dimension lies in the composite nature of the weak 0006 reflection. As stated earlier, this is often a triplet, and this superposition of two α-doublets is troublesome. However, with manganese radiation, which was used for the precision photographs, the lower-angle component of the 0006 reflection is practically extinguished and only a single weak α-doublet is observed. This is probably due to the fact that there is a longer path for this component with manganese radiation than with cobalt (θ for CoKα is 53°, for MnKα it is 70°), and, moreover, the absorption is greater. The 0004 reflection remains doubled.

The procedure adopted was to derive an apparent c dimension from the stronger component of the 0004 reflection and also from the single α_1 and α_2 lines of 0006. An extrapolation against $\frac{\cos^2\theta}{\sin\theta}+\frac{\cos^2\theta}{\theta}$ to $f(\theta)=0$ ($\theta=90°$) was used to obtain the true value of c. The extrapolation for a photograph taken at 14·6° C. is shown in fig. 4. The soundness of this procedure was confirmed in the following way. The weaker component of the 0004 doubled line was also measured, and the mean angle θ derived from the values given by the two components. As stated in section 3, this mean angle should give a nearly correct value for c. This value is shown in fig. 4, and it will be seen that it is exactly the same as the extrapolated value.

Fig. 4.

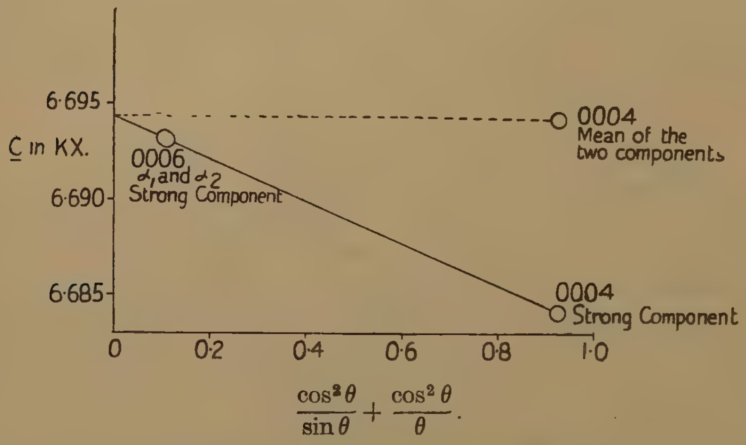

Extrapolation of c values for graphite.

References.

Taylor, A., J. Sci. Instr. xviii. p. 94 (1941).
Nelson, J. B., and Riley, D. P., Proc. Phys. Soc. lvii. p. 160 (1945).

LXXXVII. *The Principal Directions of Loading and the Principal Directions of Forced Oscillation at a Point of an Elastic Body or System.*

By Prof. W. J. Duncan, D.Sc., M.I.Mech.E.*

[Received May 4, 1945.]

SUMMARY.

A principal direction of static loading or of forced oscillation at a point is such that the displacement produced by a force acting in that direction at the point is parallel to the force. It is shown that for any point of a body or system which obeys Hooke's law and is conservative, there are three real mutually perpendicular principal directions, which depend, in general, on the frequency of the applied force. These results, although elementary, appear to be little known.

CONTENTS.

Page
1. Introduction 715
2. Assumptions 715
3. The Principal Directions of Static Loading 716
4. The Principal Directions of Forced Oscillation 717
5. Generalized Treatment of Forced Oscillations 717

1. *Introduction.*

Proofs are given here of the existence of three real and orthogonal principal directions of static loading, or of forced oscillation of stated frequency, for any point of a body or system which is conservative and obeys Hooke's law. In general, the principal directions of forced oscillation depend on the frequency.

These general theorems, although elementary, do not appear to be well known, and the present brief paper has been written to draw attention to them. The static theorem was given on p. 265 of "Elementary Matrices" † as an example of the general orthogonal property of the modal matrix of a symmetrical matrix.

2. *Assumptions.*

The body or system is such, and the applied loads are so limited, that the forces applied at the point P considered and the static displacements which they produce there are related by homogeneous linear equations. In other words, the body satisfies Hooke's law *.

---

* Communicated by the Author.

† Frazer, Duncan and Collar, 'Elementary Matrices.' (Cambridge, 1938.)

Let unit load applied at P in the direction OX produce displacements f_{11}, f_{21}, f_{31} of P in the directions OX, OY, OZ respectively. Similarly, let the displacements due to unit loads in the directions OY, OZ be f_{12}, f_{22}, f_{32} and f_{13}, f_{23}, f_{33}, respectively. Then the displacements of P due to a force at P having components X, Y, Z are

$$\left.\begin{aligned} x&=f_{11}X+f_{12}Y+f_{13}Z, \\ y&=f_{21}X+f_{22}Y+f_{23}Z, \\ z&=f_{31}X+f_{32}Y+f_{33}Z. \end{aligned}\right\} \quad . \quad . \quad . \quad . \quad . \quad . \quad . \quad (1)$$

The coefficients f are the flexibilities.

It is next assumed that the body is conservative, *i. e.* that it cannot serve as a source of energy. The consequence is that the corresponding cross-flexibilities must be equal, so that

$$f_{ij}=f_{ji}. \quad . \quad . \quad . \quad . \quad . \quad . \quad . \quad . \quad . \quad . \quad (2)$$

It is easy to show that, when (2) is not satisfied, a finite amount of work can be gained by moving P in a closed circuit. Thus the matrix of the flexibilities must be symmetrical.

Condition (2) is not universally satisfied in practice. Systems exposed to currents of fluid (*e. g.* parts of aircraft) are not conservative, and, in general, the matrix of the flexibilities is not symmetrical.

3. *The Principal Directions of Static Loading.*

Let l, m, n be the direction cosines of a principal direction, R the resultant load and r the resultant displacement. Then, since load and displacement are parallel, by hypothesis, it follows that

$$\left.\begin{matrix} x=rl, & y=rm, & z=rn, \\ X=Rl. & Y=Rm. & Z=Rn. \end{matrix}\right\} \quad . \quad . \quad . \quad . \quad . \quad . \quad (3)$$

Let

$$\lambda=\frac{r}{R}, \quad . \quad . \quad . \quad . \quad . \quad . \quad . \quad . \quad . \quad . \quad . \quad . \quad (4)$$

so that λ is the flexibility measured in the principal direction. Then equation (1) can be written

$$\left.\begin{aligned} l(\lambda-f_{11})-mf_{12}-nf_{13}&=0, \\ -lf_{21}+m(\lambda-f_{22})-nf_{23}&=0, \\ -lf_{31}-mf_{32}+n(\lambda-f_{33}&=0. \end{aligned}\right\} \quad . \quad . \quad . \quad . \quad . \quad . \quad . \quad (5)$$

Hence λ is a latent root of the flexibility matrix. Since that matrix is symmetrical, in accordance with the assumption made above, it follows from known theorems on matrices that there are three real values of λ satisfying (5), and that the three corresponding real principal directions are mutually orthogonal *. This can be seen otherwise as follows. On account of (2) the equations (5) give the direction cosines of the principal axes of the central quadric (conicoid)

---

* This is obviously a more stringent condition than a linear relation between stress and strain at all points.

$$\tfrac{1}{2}f_{11}X^2+\tfrac{1}{2}f_{22}Y^2+\tfrac{1}{2}f_{33}Z^2+f_{23}YZ+f_{31}ZX+f_{12}XY=\text{const.}, \quad . \quad (6)$$

and these principal axes are known to be real and orthogonal for all real values of the coefficients f.

The expression on the left-hand side of (6) is, from (1), equal to

$$\tfrac{1}{2}(xX+yY+zZ),$$

i. e. it is the potential energy stored in the body. When, as usual, the potential energy is essentially positive, the quadric (6) is an ellipsoid.

When P has only two degrees of freedom, *i. e.* is constrained to move on a surface, there are two perpendicular principal directions of loading for which the flexibility is not zero.

4. *The Principal Directions of Forced Oscillation.*

Let attention be confined to simple-harmonic applied loads of a given frequency and all in phase. Then equations (1) hold good when X, Y, Z are interpreted as the amplitudes of the applied forces and x, y, z as the amplitudes of the corresponding steady forced oscillations. The coefficients f are now admittances which are functions of the frequency of the applied forces. Provided that, as before, the body is conservative, the matrix of the admittances is symmetrical. Hence it follows, as before, that there are three real mutually orthogonal principal directions. These directions, in general, depend on the frequency.

5. *Generalized Treatment of Forced Oscillations.*

The same conclusion can be obtained from the equations of motion of the body or system as a whole. It will be assumed that the motions are so limited that the equations of motion can be treated as linear with constant coefficients, and that damping and gyrostatic terms are absent. The stiffnesses are assumed to be derivable from a potential. The point P at which the forces are applied has three degrees of freedom, while the body or system as a whole has $(3+m)$ degrees of freedom.

The first generalized co-ordinate for the system is taken as x, the displacement of P in the direction OX, and the displacements of other points associated with a variation of x are compatible with the connections of the system, but otherwise arbitrary.

Similarly, the second and third generalized co-ordinates are taken as y, z, the displacements of P in the directions OY, OZ, respectively. The remaining generalized coordinates q_1, q_2 . . . . q_m are such that P does not move when they vary, and they can always be chosen to satisfy this condition.

---

* See, for example, § 3.8 of 'Elementary Matrices.'

Let the symbols for force and displacement represent amplitudes. Then the dynamical equations can be written

$$\left.\begin{array}{r} r_{11}x+r_{12}y+r_{13}z+r_{14}q_1+\text{ etc.} =\mathrm{X}, \\ r_{21}x+r_{22}y+r_{23}z+r_{24}q_1+\text{ etc.} =\mathrm{Y}, \\ r_{31}x+r_{32}y+r_{33}z+r_{34}q_1+\text{ etc.} =\mathrm{Z}, \\ r_{41}x+r_{42}y+r_{43}z+r_{44}q_1+\text{ etc.} = 0, \\ \text{etc.}, \end{array}\right\} \quad . \quad . \quad . \quad . \quad . \quad (7)$$

where

$$\left.\begin{array}{l} r_{ij}=c_{ij}-\omega^2 a_{ij}=r_{ji}, \\ c_{ij}=\text{stiffness coefficient}, \\ a_{ij}=\text{inertial coefficient}, \\ \omega=2\pi \text{ times frequency}. \end{array}\right\} \quad . \quad . \quad . \quad . \quad . \quad . \quad (8)$$

On account of the manner of defining the generalized co-ordinates, the generalized forces in the first three equations are the components of applied force at P and the other generalized forces are zero. The theorem will be proved by eliminating the "internal" co-ordinates q from equations (7).

For a principal direction of forced oscillation

$$\mathrm{X}=\sigma x, \quad \mathrm{Y}=\sigma y, \quad \mathrm{Z}=\sigma z, \quad . \quad . \quad . \quad . \quad . \quad . \quad (9)$$

where σ is the effective stiffness or dynamic impedance. On account of (9) and the symmetry of the coefficients, the equations (7) can be written in the partitioned matrix form *

$$\begin{bmatrix} \mathrm{A}-\sigma\mathrm{I} & \mathrm{B} \\ \mathrm{B}' & \mathrm{C} \end{bmatrix} \begin{bmatrix} x \\ q \end{bmatrix} = 0, \quad . \quad . \quad . \quad . \quad . \quad . \quad . \quad (10)$$

where

$$x \equiv \begin{bmatrix} x \\ y \\ z \end{bmatrix}, \quad . \quad . \quad . \quad . \quad . \quad . \quad . \quad . \quad . \quad (11)$$

while A and C are square and symmetrical and of order 3 and m respectively, and I is the third order unit matrix. Equation (10) gives

$$\left.\begin{array}{l} (\mathrm{A}-\sigma\mathrm{I})x+\mathrm{B}q=0, \\ \mathrm{B}'x \quad +\mathrm{C}q=0, \end{array}\right\} \quad . \quad . \quad . \quad . \quad . \quad . \quad . \quad (12)$$

and the second of these yields

$$q=-\mathrm{C}^{-1}\mathrm{B}'x. \quad . \quad . \quad . \quad . \quad . \quad . \quad . \quad . \quad . \quad (13)$$

Hence, the first can be written

$$(\mathrm{N}-\sigma\mathrm{I})x=0, \quad . \quad . \quad . \quad . \quad . \quad . \quad . \quad . \quad . \quad (14)$$

where

$$\mathrm{N}\equiv\mathrm{A}-\mathrm{B}\mathrm{C}^{-1}\mathrm{B}'. \quad . \quad . \quad . \quad . \quad . \quad . \quad . \quad . \quad . \quad (15)$$

Since C is symmetrical, C^{-1} and N are also symmetrical. Hence, σ is a latent root of a third order symmetrical matrix. Consequently there

---

* Transposition of a matrix is indicated by an accent.

are three real principal directions, and, by the orthogonal property of the modes of a symmetrical matrix, these are mutually perpendicular.

Pre-multiply the first of equations (12) by x' and rearrange

$$\sigma x'x = x'Ax + x'Bq. \qquad (16)$$

But $x'Bq$ is a scalar and equal to its transposed. Hence,

$$\begin{aligned} x'Bq &= q'B'x \\ &= -q'Cq \qquad (17) \end{aligned}$$

by the second of equations (12). Thus (16) becomes

$$\sigma x'x = x'Ax - q'Cq, \qquad (18)$$

where $x'Ax$ and $q'Cq$ are quadratic forms in x only and q only, respectively. Since x is real, $x'x$ is a real positive number. Thus

$$\begin{aligned} x'x &= x^2+y^2+z^2 \\ &= \sigma^{-2}(X^2+Y^2+Z^2), \end{aligned}$$

by (9). Hence (18) becomes

$$\begin{aligned} \sigma(x^2+y^2+z^2) = \sigma^{-1}(X^2+Y^2+Z^2) &= x'Ax - q'Cq \qquad (19) \\ &= x'Nx, \qquad (20) \end{aligned}$$

on substitution for q from (13). Equation (20) also follows at once from (14).

It has been proved above, by elimination of the "internal" co-ordinates q, that the simple harmonic displacement at any point P of a system of any degree of complexity, induced by the application at P of a simple harmonic force, is related to the force by linear equations of the type (1), where the coefficients are admittances depending on the frequency. As a consequence, there are three real orthogonal principal directions of forced oscillation at P which, in general, vary with the frequency.

LXXXVIII. *Crystalline Sheen of Moonstones.*

By B. V. Thosar, M.Sc., A.Inst.P., College of Science, Nagpur, India.

[Received July 3, 1944.]

Introduction.

Moonstones belong to the felspar group of minerals and are a variety of monoclinic orthoclase, $KAlSi_3O_8$. They are hard, colourless bi-axial crystals and are available as flawless single crystals of fairly big size. They have a remarkable optical property, namely, they show a bluish-white sheen, often called opalescence, when a specimen is held suitably inclined to incident light, and they are, for this reason, prized as gem-stones. Writers on gems seem to have recognised that "this so-called opalescence is due to reflection of light from a particular plane within the crystal." The purpose of this study is to determine the nature of this peculiar reflection of light or sheen from the crystals and its probable cause. It is to be noted that moonstones exhibiting this sheen are apparently single crystals and differ in this respect from opals or iridescent shells. The other well-known case of crystalline reflection is that of crystals of potassium chlorate as studied by Stokes(1) and explained by Rayleigh(2), who attributed the reflection of light to the discontinuity at a twin-plane within the crystal. The vigour and intensity of reflection, which is highly coloured, was, according to him, due to regularly spaced repeated twinning inside the crystal. The sheen of moonstones is clearly due to reflection from *within* the crystal, as the results of the following experimental study reveal. Also the crystallographers have noted that among the class of crystals to which moonstones belong, numerous repititions of twinning within a crystal are an extremely common occurrence. The explanation of this peculiar optical property is therefore to be sought in this fact.

---

* Communicated by the Author.

Fig. 1.

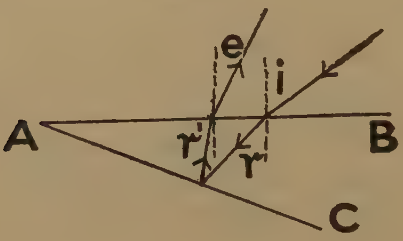

Experimental.

(1) The relationship between the angle of incidence of light on the crystal face and the angle of emergence of the sheen.—The crystal was mounted on the prism table of an ordinary spectrometer, the slit of the collimator being replaced by a small circular aperture and the telescope by an eyepiece with cross-wire A sodium lamp was used as the source of light. In many specimens it was at once obvious that ordinary reflection from the crystal face and the peculiar sheen were quite distinct and their directions were inclined at a considerable angle. The values of e, the angle of emergence of the sheen, were determined for various values of i, the angle of incidence. Then, referring to the figure, if we assume the reflection to be taking place at a definite plane AC within the crystal inclined at an angle α with the crystal face AB, then,

$$\frac{\sin i}{\sin r}=\mu \quad \text{and} \quad \frac{\sin e}{\sin r'}=\frac{\sin e}{\sin(2\alpha-r)}=\mu.$$

Taking $\mu = 1 \cdot 52$ for the material of the crystal (the three principal refractive indices (3) of this bi-axial crystal differ only in the third place of decimal) and eliminating r from the two equations, α could be calculated for each pair of values of i and e. This came out to be constant within the instrumental accuracy.

Table I. gives the values of i, e, and α for two specimens of the crystal. The angle at which the reflecting plane is inclined with the crystal face is 21° 27′ in one and 34° 58′ in the other specimen. Thus in every specimen there is a definite plane, whose inclination with the crystal face can be determined, from which the " sheen " seems to proceed by reflection.

The interesting study of the position of this reflecting plane with reference to the crystallographic axes of the crystal, and of the change in its position from specimen to specimen, will be undertaken when instrumental facilities for an accurate crystallographic study are available.

TABLE I.

i.	e.	α.	
11°·5	61°·5	21° 25′	Mean value of α= 21° 27′ for one specimen.
21°·5	47°·5	21° 29′	
33°·5	33°·5	21° 18′	
50°	20°	21° 38′	
50°	75°	34° 52′	Mean value of α =34° 58′ for second specimen.
61°	61°	35° 7′	
76°	50°	34° 56′	

(2) One of the specimens was ground so that various faces with different inclinations were formed in turn. It was found that there is no other plane within the crystal which throws out this sheen by reflection.

(3) No particular single plane is responsible for the reflected sheen, but the whole body of the crystal. For any specimen ground down to any extent on faces slightly inclined to the reflecting plane retained this property.

(4) Polarization characteristics of the reflected sheen.—(*a*) A narrow beam of unpolarized light was incident on the crystal plate and the reflected sheen was examined through a polaroid (or Nicol). On rotating the polaroid the intensity passes through a maximum and a minimum corresponding to two mutually perpendicular positions of the polaroid.

(*b*) Having examined the crystal plate between two crossed polaroids in parallel light, the two directions of extinction for the section were carefully noted and marked on the crystal face. These are the two principal axes of the elliptic section in which the crystal face cuts the biaxial indicatrix. A ray incident on the crystal face normally will give two extraordinary rays within the crystal with directions of vibrations parallel to these axes.

The crystal was mounted so that the reflected sheen emerged from it, making only a small angle with the diection of incident light. It was found that two perpendicular positions of polaroid for maximum and minimum intensity of sheen, noted in (*a*) above, corresponded to the directions of extinction of the crystal section—the vibration directions for maximum and minimum intensity being parallel to the traces of the extinction directions on the plane of polaroid. Whatever the angle of emergence of the sheen from the crystal, on rotating it about the normal to the reflecting plane, it was found that the vibration directions for maximum and minimum intensity of sheen always correspond to the two directions of extinction of the crystal section, which we shall call the A and B axes of the section respectively.

(*c*) The incident light was plane polarized with direction of vibration, say vertical, and the crystal plate was rotated until the A-axis on its face was also vertical. The reflected sheen was then completely plane-polarized with vibration direction parallel to A, *i. e.* vertical. The same could be observed when the crystal was mounted with the B-axis vertical, except that the intensity of the sheen in this case was much smaller. For any other position of the crystal plate the reflected sheen was thus made up of two portions with mutually perpendicular directions of vibration corresponding to the positions of A and B axes on the crystal face.

These polarization characters were also shown when the sheen came out of the crystal nearly in the direction of incident light *i. e.* when the light met the reflecting plane within the crystal at nearly normal incidence.

(*d*) Two narrow plane-polarized beams of monochromatic light of equal intensity were formed by means of a double-image prism with vibration directions vertical and horizontal. These were incident on the face of the crystal, which was so oriented that the A-axis on its face was vertical. Two bright patches of sheen by reflection lying side by side could be seen, each one completely plane-polarized—one with vibration direction vertical and the other horizontal. These were observed through a rotating polaroid and the position for balanced intensity, inclined at angle θ with the vertical, was determined. Then $\tan^2\theta=\frac{I_A}{I_B}$, the ratio of the intensities of the two patches. This was found to be 2·56, *i. e.* about 72 per cent. of light in the reflected sheen of the moonstone is due to vibration parallel to the A-axis on the crystal and is thus highly polarized. These observations were repeated for light from a mercury arc lamp corresponding to different lines—λ 4358, λ 5460 and λ 5790. The ratio $\frac{I_A}{I_B}$ was found to be the same.

(5) Variation of intensity of sheen with colour.—A narrow beam of light from a mercury arc lamp was passed through a double-image prism and two beams of equal intensity were formed—one due to light vibrating along the vertical and the other along the horizontal. The former fell on the face of the crystal, which was mounted with the A-axis vertical. Largest possible intensity of the sheen, plane-polarized along the vertical, was thus obtained. The other beam with horizontal light vibration fell on a good plane glass surface, the face of a prism, and the reflected spot arranged to be seen side by side with that due to the crystalline reflection. Both were viewed through a polaroid, which could be rotated to give a position of balanced intensities. With suitable Zeiss filters monochromatic light corresponding to the three lines λ 4358, λ 5460, and λ 5790 was used.

Table II.

λ in A.U.	$\rho=\frac{I_{\text{crystal}}}{I_{\text{air-glass}}}\times 100.$	Reflecting Power of Crystal.
6200	7·7	0·31
5790	28·3	1·13
5460	49·0	1·96
4471	72·2	2·89
4358	73·8	2·95

A helium lamp with filters was used to give light of λ 4471, and an electric bulb with a combination of filters gave red light within a narrow band with centre at λ 6200. The ratio of intensity of reflection from within the crystal and from air-glass surface was calculated from these observations for the different wave-lengths used. Knowing the refractive index of the glass for the wave-lengths used and the angle of incidence of the horizontally polarized light on the prism face, a correction for the variation of intensity of reflection with wave-length could be calculated. This was, however, small. The second column in Table II. gives in arbitrary units the intensity of reflected sheen for different wave-lengths. The curve gives the variation of the reflecting power of the crystal with colour. This increases rapidly as the blue end of the spectrum is approached and accounts for the marked blue tinge of the sheen of the gem in ordinary light.

The last column gives a rough estimate of the absolute reflecting power of one specimen, *i. e.* the percentage of incident light reflected as sheen, It can be shown that for the experimental arrangement described above,

$$k.a=\tan\theta.\frac{\tan(\phi-\psi)}{\tan(\phi+\psi)},$$

where 'a' is the fraction of amplitude of vibration reflected by the crystal, θ is the inclination with vertical of the polaroid when adjusted for intensity balance, and ϕ and ψ are the angles of incidence and refraction of light at the face of the glass prism. 'k' is a correction to be applied for loss of light by ordinary reflection as it enters and leaves the crystal face and is given by

$$k=\frac{4\cos i\sin r\sin e\cos r_1}{\sin(i+r)\sin(e+r_1)},$$

Fig. 2.

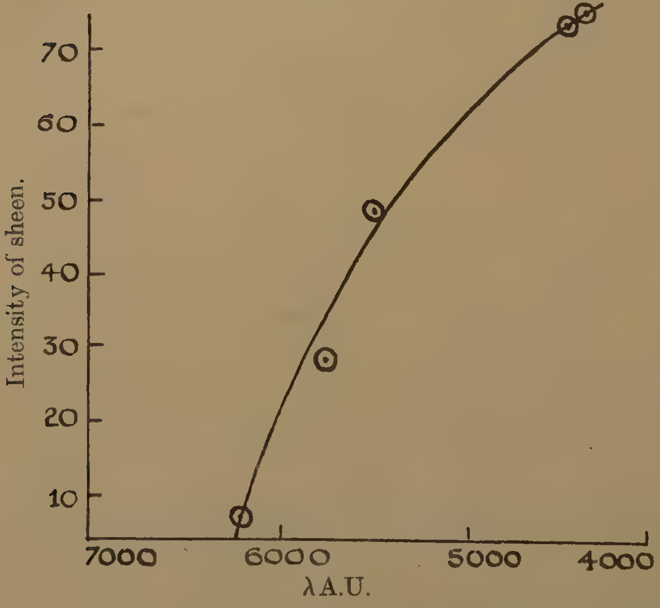

where i, r and r_1, e are the angles of incidence and refraction as light enters and leaves the face, respectively. Different specimens have different absolute reflecting powers; thus one specimen reflected nearly four times as much light as the one described above. But the variation of intensity with colour could in this case also be represented by the above graph.

(6) A wedge-shaped plate of the crystal was examined in parallel light between crossed polaroids. A quarter-wave plate of mica was interposed with its axes parallel to the extinction axes A and B of the crystal section. From the change in the interference colours it could be deduced that the A-axis of the crystal, parallel to which the crystalline reflection is more vigorous, is the direction of "slow" vibration propagated through the crystal.

(7) The reflected sheen was examined and photographed in a spectrograph, using monochromatic light of different wave-lengths. In each case the wave-length reflected was the same as in incident light, showing absence of fluorescence. When white light was incident on the crystal the sheen also gave a continuous spectrum.

(8) Examination of different crystal sections in parallel light between crossed polaroids fails to reveal under the microscope any visible discontinuity within the crystal, *e. g.* twinning.

Explanation of the Phenomenon.

All writers on crystallography (4) have made a special note of the visible multiple twinning in albite, $NaAlSi_3O_8$, which is really tri-clinic but simulates monoclinic symmetry by visible multiple twinning. Orthoclase, $KAlSi_3O_8$, of which the moonstones are a variety, is shown to be monoclinic by microscopic examination. But there exists a tri-clinic variety of orthoclase, microcline, which shows visible multiple twinning and thus simulates monoclinic symmetry. The physical properties of microcline and orthoclase are similar, and their refractive indices almost identical. The suggestion that orthoclase is really a tri-clinic substance, ultra-microscopically twinned, and thus imitates the higher symmetry, seems to have found considerable support (5).

We may therefore regard the moonstone crystal as made up of innumerable repititions of twinning, the two components of the twin being tri-clinic with a common composition plane perpendicular to the twin-axis. One component of the twin is identical with the other except that it is rotated with respect to the other through 180° about the twin-axis. In a tri-clinic crystal the principal axes of the indicatrix have no relation whatever with the crystallographic axes, to which, however, the twin-axis is definitely and usually simply related. Taking OX, OY, OZ as reference axes, we shall take the direction of OY to coincide with the twin-axis so that the plane XZ will be the common composition plane between the two components of the twin. Three mutually perpendicular axes OX_p, OY_p and OZ_p, *not* coincident with the reference axes, would then be the directions of the principal axes of the indicatrix in the upper medium. For the lower component of the twin, the indicatrix will be obtained by rotation through 180° about OY, and it is clear that the principal axes of the indicatrix will be quite differently oriented with respect to the reference axes in the lower medium. There will thus be an optical discontinuity at the XZ plane as a ray of light passes from the upper to the lower medium. If OY_p, the principal axis of the indicatrix, coincides with OY, the twin axis, rotation about OY through 180° will bring about no change in the orientation of the indicatrix, and all optical distinction between the two components of the twin will vanish. Each of the two components in that case will become monoclinic.

As light enters the apparently monoclinic crystal of moonstone crystal, two perpendicularly polarized extraordinary rays are propagated through the crystal with unequal velocities. There is, however, the finer optical discontinuity, though very minute, at each twin plane and a very small amount of light will be reflected back from it, corresponding to each of the two extraordinary rays. The reflected intensity at a single twin plane will be extremely minute, as the largest optical discontinuity due to twinning will correspond to a difference of refractive index 0·007 in a mean refractive index 1·52, the three principal indices of tri-clinic orthoclase being 1·518 (α), 1·522 (β) and 1·525 (γ). The whole body of the crystal being extremely finely twinned in innumerable repetitions, there is on the whole an appreciable reflected intensity from the crystal which forms the characteristic sheen of the gem. For a particular incident ray the two extraordinary rays are reflected back along different directions but the actual birefringence is so small that these directions are almost coincident. Corresponding to one of the rays—that due to the "slow" vibration, parallel to the extinction direction A of the crystal section—the optical discontinuity must be more pronounced, giving a large intensity.

If the numerous twin-planes within the crystal are not regularly spaced, the alternate twin lamellæ having unequal thickness, the reflection of light will not be selective and will not produce colour, but it will be a silvery white reflection. Madan and Rayleigh had prepared some crystals of potassium chlorate which gave such white reflection instead of the iridescent colours. According to Rayleigh⁽⁶⁾, "there is little doubt that these were composed of twin layers, the alternations being irregular and also more numerous."

It seems possible that between the distinctly tri-clinic microcline and the monoclinic forms of orthoclase there may be a variety of crystals of finer gradations of twinning, the optical effect of the sheen of moonstones appearing at a certain stage and vanishing when the crystal becomes truly monoclinic. The intensity of the reflected sheen will depend, besides the size of the crystal, on the "frequency" of twinned alternations.

It is well known that in bi-axial crystals of tri-clinic symmetry the blue indicatrix is not coincident with the red, due to dispersion—the principal axes of the ellipsoid for blue are not coincident with those for red light. The cause of the preponderance of blue in the crystalline sheen is explained by considering this dispersion of the indicatrix in the moonstone crystals. We have seen that when the twin-axis OY and the principal axis of the ellipsoid OY_p coincide, the optical distinction between the two components of the twin vanishes. It may be seen that as the inclination of OY_p to OY increases (while yet it is small), the optical discontinuity becomes stronger. If, now, OY_p for blue is more inclined to OY than OY_p for red, the crystal is in effect more removed from monoclinic symmetry for blue than for red light and for any particular ray travelling in the upper medium, the change in refractive index across the common plane will be more for blue light. For intermediate colours the inclination of OY_p with OY, the twin-axis, will have intermediate values, and hence the optical discontinuity between the two media and the intensity of reflection will progressively increase as we go from the red to the blue, giving the type of variation of intensity with wave-length, obtained by experiment.

In the above explanation the alternate lamellæ are supposed to have the same chemical composition and crystalline structure, the optical discontinuity being due solely to twinning. Moonstones, though mainly of orthoclase composition, $KAlSi_3O_8$, contain some percentage of sodium, sometimes up to 30 per cent., and may thus be represented by $KNaAlSi_3O_8$. Kôzu (7) and Endô have suggested that the alternate lamellæ may be two different crystalline phases, one rich in sodium atoms and the other in potassium atoms, the optical discontinuity in that case being due to the difference in crystal structure of these phases. The present experimental evidence is not enough to decide this point. The doubling of Laue spots, observed by these workers in moonstones, can be as well due to twinning —Taylor (8) has obtained similar doubling of spots due to polysynthetic twinning in microcline. As for the disappearance of the sheen of moonstones at temperatures above 1100°, this can be due to the crystal actually merging into the monoclinic form it simulates by twinning. Madan's crystals of potassium chlorate, referred to by Rayleigh, behaved in a similar manner on heating. Many cases of polysynthetic twinning (9) are known, where at higher temperatures the crystal actually passes into the more symmetrical form that it imitates by twinning at ordinary temperatures.

Summary.

The characteristic bluish white sheen of moonstone crystals has been studied. It is shown to arise due to reflection from a definite plane within the crystal, the whole body of which contributes to the effect. The polarization characteristics of the reflected sheen are studied, using unpolarized and polarized incident light in different azimuths. The intensity distribution of the sheen is determined, revealing a progressive increase in the reflecting power of the crystal as we go from the red to the blue end of the spectrum. Similar to Rayleigh's explanation of the iridescent crystals of potassium chlorate, the optical discontinuity giving rise to reflection of light from within the moonstone is attributed to twinning, the whole crystal being made up of numerous but irregular alternations of twinned lamellæ. The blue of the sheen is shown to be due to the dispersion of the bi-axial indicatrix in the tri-clinic component of the twin, *i. e.* due to the non-coincidence of the principal axes of the optical ellipsoid for blue and for red light.

The author is grateful to Nagpur University for financial help and to the authorities of the College of Science for laboratory facilities.

References.

(1) 'Physical Optics,' by R. W. Wood, p. 161.
(2) Lord Rayleigh, Phil Mag. xxvi. p. 256 (1888).
(3) Landolt-Bornstein, *Physik. Chemische Tabellen.*
(4) Tutton, 'Crystallography,' vol. i. p. 508.
(5) 'Crystals and the Polarising Microscope,' Hartshorne and Stuart, p. 49 (1934).
(6) Lord Rayleigh, *loc. cit.*
(7, 8) 'Atomic Structure of Minerals,' by Bragg, pp. 240–1 (1937).
(9) Tutton, 'Crystallography,' vol. ii. p. 1264.

LXXXIX. *Notices respecting New Books.*

Frontiers in Chemistry. Edited by R. E. Burk and O. Grummitt. (Vol. III. pp. 165, Advances in Nuclear Chemistry and Theoretical Organic Chemistry ; Vol. IV. pp. 151, Major Instruments of Science and their Applications to Chemistry.) (Interscience Publishers, Inc. : New York, 1945. Price $3.50 each).

These volumes, based on lectures given at Western Reserve University by well-known authorities in the fields which they survey, are of the character of reports on lectures delivered to students' chemical societies, and are elementary in character. The object of the volumes is stated to be to present to graduate students proceeding to research some accounts by specialists of fields of work likely to be important in research and industry. The articles are provided with short bibliographies of unequal merit. In some cases the bibliography is largely confined to one field of publication and is not representative. Some of the articles are sketchy, others contain rather too much detail, but on the whole they provide interesting and intelligible accounts of their subjects. Whilst such volumes may be of use to junior students, it is hard to see what place there is for them in a market already provided with good books, annual reports and review journals in the field they enter. The typography, paper, and illustrations are of high standard.

Volume III. has articles on isotopes and their applications in bio-chemistry (Keston), applications of isotopes in catalytic reactions at surfaces (Taylor), techniques in nuclear physics (Crane), resonance in organic chemistry (Brooker), and the hydrogen bond and its significance in chemistry (Rodebush).

Volume IV. has sections on electron diffraction and the examination of surfaces (Germer), the electron microscope and its applications (Marton), X-ray diffraction and its applications (Huggins), chemical spectroscopy (Brode), the applications of absorption spectra to chemical problems (Brode), and the infra-red spectrometer and its applications (Barnes). J. R. P.

Photosynthesis and Related Processes. By E. I. Rabinowitch. Volume I : Chemistry of Photosynthesis, Chemosynthesis and Related Processes in Vitro and in Vivo (pp. 599.) (Interscience Publishers, Inc. : New York, 1945. Price $8.50.)

Since the books by Stiles and by Spoehr, which appeared in 1925 and 1926 respectively, there has been no adequate monograph on the subject of Photosynthesis, or the production of organic matter by chlorophyll-containing plants in presence of light. In the intervening period, much new work of high significance, both in the chemical and botanical fields, has appeared, some of which has materially altered the views held as to the nature of the process. The appearance of a new book is, therefore, an event of importance, and there can be no doubt that Dr. Rabinowitch has provided both chemists and botanists with an authoritative, full, and well-documented treatise. The subject has been divided into four parts, comprising the chemistry of photo-synthesis and related processes, the structure and chemistry of the photo-synthetic apparatus, the spectroscopy and fluorescence of the pigments, and the kinetics of photosynthesis. The first two of these are dealt with in the present volume, and the other two are to form the subject of the second volume, which it is hoped will appear within a year. The first volume contains dredominantly chemical material, the second will be predominantly physical.

The volume opens with a concise survey of the total yield of photo-synthesis on the earth ; this is followed by an interesting history of the discovery of photosynthesis, from the guess by Hales in his *Vegetable Staticks* (1727) that " plants draw through their leaves some part of their nourishment from the air," and that light " may contribute much to ennobling the principles of vegetables," through the work of Priestley, Ingen-Housz, Senebier, and de Saussure, to the establishment of the fact that atmospheric carbon dioxide, water, and solar light energy provide the raw materials for the production of carbohydrates in the plant. The products of photosynthesis, the energy absorbed, and the all-important question of the stages of the reaction receive full treatment. Bacteria and algæ are dealt with as well as green plants. The pigments and the morphological apparatus receive generous treatment. Each chapter is provided with a most extensive bibliography.

Among the new discoveries dealt with in the book are the very recent proof, by the use of radioactive tracer-elements, that all the oxygen evolved in photosynthesis comes from water and not from carbon dioxide, and, on the botanical side, the proof of the existence of the heterogeneous nature of the chloroplasts as consisting of grana and stroma. The chemistry of chlorophyll is fully dealt with. The supposed proofs of photosynthesis without chlorophyll are critically discussed, and the results are considered unproved. The question of the immediate products of photosynthesis is very fully treated, and some time-honoured beliefs are shown to be without foundation. Particular emphasis is laid on the oxidation-reduction character of the reactions, and although some readers will think that too many types of reaction which cannot have any conceivable counterpart in the living plant are brought in, with some resulting loss of clarity, it cannot be denied that the author has made a good case for his view of photosynthesis as a reaction of this type sensitised by chlorophyll pigment. The new work, which makes it probable that eight, not four, light quanta are concerned with the process, is reviewed.

Dr. Rabinowitch has produced a work of the highest interest and value, and his second volume will be eagerly awaited. While there is still much that is obscure in photosynthesis, it seems as if further work on lines which he suggests will soon lead to a clarification of the subject, and the book will provide research workers with valuable information. J. R. P.

Tables of Associated Legendre Functions. Prepared by the Mathematical Tables Project. [Pp. xvli+303.] (New York : Columbia University Press, 1945.) Price $5.00.

LEGENDRE's functions arise typically in such problems as the potential due to a gravitating plate at a point off the axis, and have become familiar in applied mathematics in the 50 years or so which have elapsed since Perry set his students to calculate tables of them. The associated functions arise when the system itself is not symmetrical about its axis. Although quite familiar in analysis, they are not often used by practical men, chiefly because there have not been convenient and accessible tables. The need for the functions has been much more noticeable in recent years owing to their application to the wave mechanics of the atom.

This volume will thus fill a very definite want. It contains as the first table, the values of P_n^m (cos θ) for values of θ from 0 to 90° at 1° intervals, and for $n=1$ to 10 and $m=1$ to 4, and as the next table the derivative of this function ; the following tables give the same functions but with $x(1-0{\cdot}1-10)$ as argument. In these tables, P_n^m is the function of the first kind, which is finite at the origin ; the function of the second kind, infinite at the origin, is tabulated in the next tables, and there follow tables with imaginary argument. The volume closes with tables of the functions whose order (n) is of the form ($\frac{1}{2}$+integer), and a few miscellaneous tables.

In nearly every case the range of values of x, n and m is as stated above. The functions themselves are given to six significant figures. To make effective use of the tables it will be essential to study the introduction, where methods of interpolation are discussed. The methods used in the calculation of the tables are also explained at length, and any reader of it must feel admiration for those who carried the work through, as well as gratitude for the provision of tables which are not likely to be available in any other form.

J. H. A.

Currents in Aerials and High Frequency Networks. By F. B. Pidduck. [Pp. 97.] (Oxford University Press. Price 8*s.* 6*d.*)

This little book develops the theory of aerials on unfamiliar lines. After a brief sketch of fundamental electromagnetic theory in terms of the m.k.s. system of units, attention is called to a neglected paper by Pocklington, published in 1897. This paper, in effect, deals with the problem of the rod aerial, achieving considerable simplification by assuming the rod to be thin. The merits of the Pocklington scheme are then combined with methods originally due to Murray, in the development of a general theory of arrays of thin aerials ; advantage thus being taken of one of the chief results of Murray's work, namely the unambiguous definition of mutual impedances, even when applied to open circuits radiating into space. From the general theory a number of important extensions are made, to networks, to jointed aerials, etc., and a series of specific problems are dealt with, as, for instance, those of parallel aerials, currents in straight receiving aerials, parallel arrays, and others. The treatment of the Lecher wire problem is particularly interesting, as an illustration of a sounder approach to the theory of transmission lines. Finally, the methods of the book are successfully applied to the theory of diffraction. The work is rounded off with tables of the integral

$$\mathrm{E}i(z)=\int_0^z \frac{\exp.z}{z}\,dz,$$

and of cosine and sine x when x is in circular measure.

The book, mathematical throughout, is by no means easy reading ; in that respect not differing from the numerous and indigestible papers on aerial theory which have appeared in recent years. On the other hand, there can be no doubt that the effort demanded of the reader is better repaid in this book, which does (for the first time, perhaps) trace succintly a logical and inclusive theory of aerials and aerial systems ; and which has the striking merit of producing, not an imposing exposition of intractable integrals—which a student of aerial theory learns pessimistically to expect—but a series of results capable of translation into design. The work does perhaps await the attention of the "middleman" to exhibit the application in full detail to specific aerial systems, but no one interested in aerial theory can afford to neglect this hitherto unpublished account.

J. P. A.

[*The Editors do not hold themselves responsible for the views expressed by their correspondents.*]

Fig. 1.

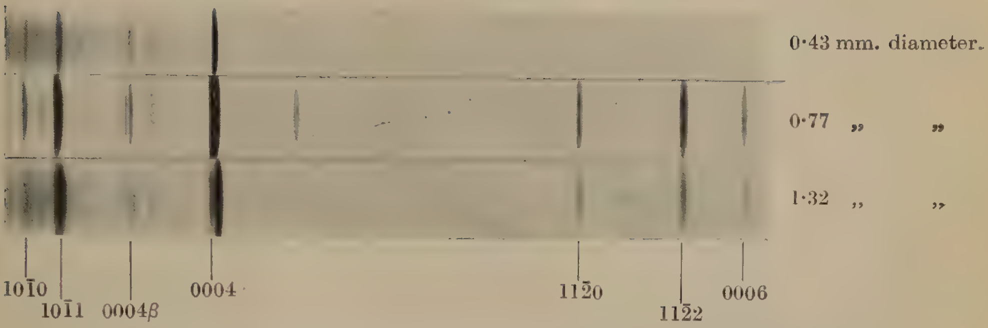
0·43 mm. diameter.
0·77 ,, ,,
1·32 ,, ,,
$10\bar{1}0$
$10\bar{1}1$
0004β
0004
$11\bar{2}0$
$11\bar{2}2$
0006

Sections of photographs from graphite specimens of different diameter.

Fig. 3.

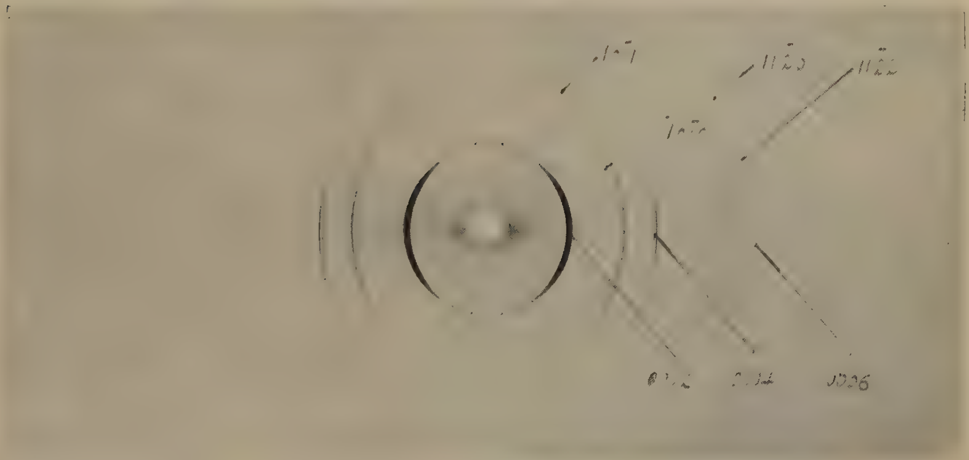
$11\bar{2}0$
$11\bar{2}2$
0006

Photograph showing preferred orientation arcs.

XC. *Viscosity and the Hydrogen Bond. Hydroxyl and Ortho Effects.*

By J. Newton Friend and William D. Hargreaves *.

[Received February 13, 1945.]

Attempts to link up viscosity and chemical constitution have not in general proved very successful. The object of the present research is to show that viscosity is closely linked up with problems involving association and the hydrogen bond.

Two important factors are found to influence the relative viscosities of isomerides, namely, intramolecular structure and intermolecular association.

As regards the former it appears to be a general rule that the more symmetrical the molecule the less are its viscosity and density. This is exemplified by the aliphatic ketones and aldehydes (1). Thus, there is a steady rise in viscosity and density on passing successively from di-ethyl ketone through methyl propyl ketone to the still less symmetrical isovaleric aldehyde :

$$C_2H_5COC_2H_5 \rightarrow CH_3COC_3H_7 \rightarrow C_4H_9CHO \text{ (iso)}.$$

On the other hand, when intermolecular association occurs, whether as the result of hydrogen bonding, dipole attraction or van der Waals' forces, the viscosity is increased. Thus the lower aliphatic alcohols, which are known to be associated, are more viscous than their isomeric unassociated ethers; similarly, free fatty acids are more viscous than their isomeric esters. It has also been observed (2) that methyl and di-methyl anilines show progressively lower viscosities than aniline itself, despite their increasing molecular weights, as the possibility of association through hydrogen bonds step-wise diminishes. In the di-alkyl anilines such association is not possible, consequently di-methyl aniline has a lower viscosity than its isomeric mono-ethyl aniline, which has one "free" hydrogen ; also in virtue of its lower molecular weight it is less viscous than unassociated di-ethyl aniline. Similar remarks apply to the toluidines.

The rheochor has already (3) been defined as $M(10^3\eta)^{\frac{1}{8}}/(D+2d)$, where M is the molar weight, D and d the density of liquid and vapour, η being the viscosity. In calculating d at any absolute temperature T, when d is not known from published data, Sugden's equation (14) has been used, namely

$$\log_{10} d/d_b = 5(T/T_b - 1),$$

---

* Communicated by the Authors.

where d_b represents the vapour density at the absolute boiling point T_b. Among the atomic group and structural rheochors, which have already been evaluated at the boiling point R(*b*), the following are used in the sequel:—C=12·8; H, 5·5; O (etheric), 10; Cl, 27·3; NO_2, 38·9; C=O, 26.

The rheochor of the C_6H_5-group attached to alkyls, as in toluene and the xylenes, is fairly constant, the mean value previously found (13) being 100·7. The present research gives an almost identical value, calculated from the following new data:—

TABLE I.

Rheochor of the Phenyl Group at the Boiling Point.

	R (*b*).	R (C_6H_5).
Chlor-toluene, *o*	151·2	100·1
m	151·7	100·6
p	151·6	100·5
Dichlor-benzene, *o*	149·7	100·6
m	150·1	101·0
p	151·0	101·9
Cresyl (tolyl) methyl ether, *o*	163·2	100·1
m	163·7	100·6
p	163·3	100·2
o-chlor-phenyl methyl ether (*o*-chlor-anisole)	162·1	101·0
o-nitro-phenyl methyl ether (*o*-nitro-anisole)	172·8	100·1
Mean	—	100·6

Certain other constituent groups have been observed to raise the rheochor by one or more units. Hence, when calculating the theoretical rheochor of an aromatic compound, the known value for C_6H_5 in a closely similar substance is chosen (4).

When the rheochors, evaluated at various temperatures, are plotted against the temperature (R–T curves, fig. 1), the curve falls as the temperature rises from the melting point; this is entirely independent of whether the substance is normally regarded as associated or as monomeric, and is attributable in the main to the breaking down of ordered liquid structure or molecular orientation such as normally occurs prior to solidification (3).

If, now, the temperature is still further raised, the rheochor tends to reach a substantially constant value. This may be attained well below the boiling point, as with benzene (3) and salicyl aldehyde, or possibly not until the boiling point has been passed. This latter is the case with water.

When the rheochor is constant it may be taken that both the symmetry and degree of association are constant; *e. g.* the chlor-anilines.

If, however, the observed rheochor is numerically equal to the sum of the constituent rheochors, the substance is essentially monomeric; *e. g.* water from 140° C. upwards (3), at which temperatures it is known from other sources to be unassociated (12).

The rheochor thus offers useful indications of the presence or absence of association.

Fig. 1.

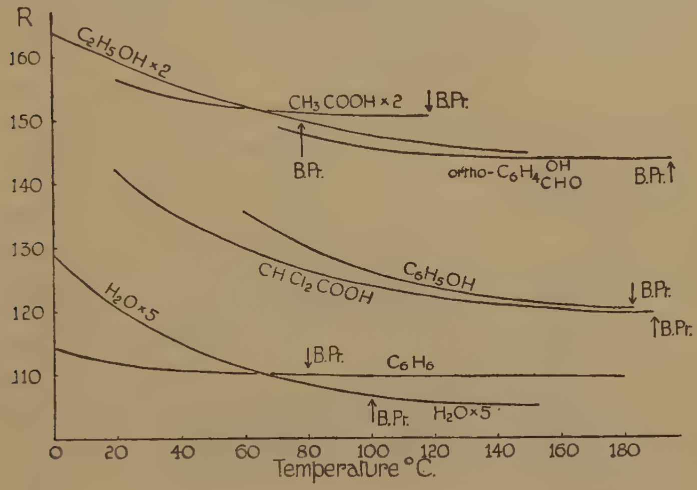

The Hydroxyl Effect.

It has long been recognized that liquids containing "free" hydroxyl are often highly associated. The earlier indications obtained by surface tension (8) and other methods have recently been amplified by studies of infra-red absorption, both in the pure liquids and in solutions (10). The mean value for the rheochor of OH at the boiling point in aliphatic alcohols and acids has been given (4) as 20, which is 4·5 units above the theoretical 15·5. The great increases in viscosity caused by introducing hydroxyl into benzene (phenol), toluene (cresol) and cyclohexane (cyclohexanol) respectively, are clearly shown in figs. 2 and 7. The R–T curve for ethyl alcohol (3) (fig. 1) continues to fall as the temperature rises and does not reach constancy even at 150° C., some 70° above its boiling point (4). Its value then is 72·3, as against the theoretical 68·6, showing that it is still appreciably associated (see Table II.).

The R–T curve for acetic acid (6) differs from that of ethyl alcohol in that its slope is less and it is almost horizontal from 80° C. upwards. Even at the boiling point it is still strongly associated, its rheochor exceeding the theoretical by 4·6 units. The greater slope of the alcohol curve indicates more rapid breaking down of association with rise of temperature. This is to be expected, since its hydrogen bond energy, 6·2 k.cals./mol., is only three-quarters of that of acetic acid, 8·2 k.cals. (7)

Dichlor-acetic acid is even more viscous than acetic acid (fig. 2), and is likewise highly associated at the boiling point, its rheochor exceeding the theoretical by 5·5 units.

The rheochor of phenol at the boiling point is 120·2, *i. e.* three units above the calculated 117·2. This shows that phenol is still associated at the boiling point, but less so than acetic acid, a conclusion that is supported by surface tension measurents (8). Replacement of phenolic H by CH_3, as in anisole, greatly reduces the viscosity (fig. 2).

Despite its greater molecular weight, benzyl alcohol is less viscous than phenol (fig. 2); it is less associated, its rheochor at the boiling point being only 0·5 unit greater than that calculated.

Fig. 2.

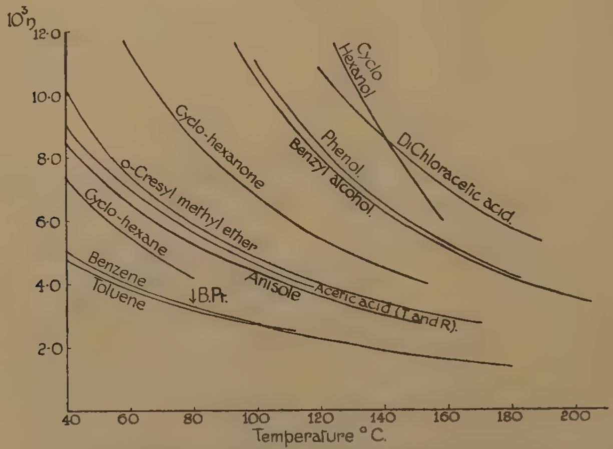

T and R=Data of Thorpe and Rodger (6).

The viscosity-temperature curve for cyclohexanol (4) is steeper even than that for phenol, indicating a rapid breakdown of association. Even so, at the boiling point its rheochor indicates considerable association. Cyclohexanone, on the other hand, has a much lower viscosity than corresponds to a mere loss of 2H-atoms, and at the boiling point its rheochor indicates little or no association. The boiling points lie so close together that the difference in the viscosities cannot be merely a temperature effect. Both compounds are more viscous than cyclohexane (4), as we should expect.

Water is particularly interesting partly owing to its complexity, and also because data are available to some 50° above the boiling point (12a). The rheochor falls to a constant value (21·0) at about 140° C., when it is equal to the sum of 2H+O, indicating virtual absence of association (3). Above this temperature thermal agitation is too great to permit clustering of the molecules (13). As the temperature falls the rheochor rises rapidly; it is known from its infra-red spectrum that the liquid is then associated through hydrogen bonds (9), quite apart from ordered structures due to local crystalline lattices, which become more pronounced and regular as the melting point is reached (11).

The foregoing numerical data are summarized in Table II., the last column of which gives the excess of the observed over the theoretical values for the rheochor, and hence a measure of the extent of association at the temperatures quoted.

The Ortho Effect.

Ring compounds with substituents in the ortho position usually differ in their properties from their meta and para isomerides, which latter may be closely similar. The differences may be of all grades from slight to very pronounced and are not all attributable to the same cause. Viscosity measurements indicate at least two important types of ortho effect, namely, those due respectively to symmetry and to hydrogen bonding.

TABLE II.

	Temp. ° C.	R theor.	R obs.	Excess R obs.
C_2H_5OH (5)	*78°	68·6	75·1	6·5
	150°	68·6	72·3	3·7
$CHCl_2COOH$	*189·5°	114·4	119·9	5·5
CH_3COOH (6)	*118·5°	70·8	75·4	4·6
C_6H_5OH	*183°	117·2 †	120·2	3·0
$C_6H_5CH_2OH$	*205°	140·2 ‡	140·7	0·5
Cyclo-Hexanol (4) ..	*158·5°	147·2	151·4	4·2
Cyclo-Hexanone ..	*153·5°	139·4	140·2	0·8
H_2O (12), (3)	*100°	21·0	21·4	0·4
	153°	21·0	21·0	0·0

1. *Symmetry.*—It has already been mentioned that among isomeric monomeric substances those possessing the greater symmetry have the lower viscosities. It is therefore to be expected that ortho derivatives will be more viscous than their meta and para isomerides, other things being equal, as the latter possess more evenly balanced molecules. This appears to be established by the results shown in figs. 3 and 4, which embody data obtained with isomerides of five different types of ortho derivatives, in which possible inteference by internal hydrogen bonding

---

* Boiling point.

† Taking R (C_6H_5)=101·7 as in anisole.

‡ Taking R (C_6H_5)=100·9 as in toluene since the OH is in the side chain (13).

is negligible. In every case the ortho derivative is more viscous than its isomerides over the whole range of comparable temperatures. On the other hand, the difference between the meta and para forms is at most relatively small, as with the xylenes, or too small to be shown in the diagram, as with the chlor-toluenes.

The data summarized in Table III. show that, in the absence of internal hydrogen bonding,

(i.) In addition to increased viscosity ortho isomerides show increased density. The two effects balance each other so that the rheochors remain constant.

Table III.

Ortho Effects due to Symmetry.

	B. Pt. ° C.	$10^3\eta$ 120° C.	D 120° C.	R (*b*).	B ∝ L.
Xylene (6), *o*	142·6°	2·94	0·7887	153·8	82·7 *
m	139°	2·50	7750	153·6	81·9 *
p	138°	2·51	7733	154·0	81·0 *
Toluidine, *o*	199°	6·57	0·9128	146·6	747
m	199°	5·97	9058	147·3	720
p	200°	6·15 †	9043 †	147·3	761
Chlor-toluene, *o*	159°	3·74	0·9795	151·2	72·6 *
m	162°	3·38	9687	151·7	—
p	162°	3·36	9673	151·6	73·1 *
Dichlor-benzene, *o*	178·6°	4·83	1·1933	149·7	517
m	172°	4·13	1·1891	150·1	487
p	172°	4·30	1·1749	151·0	498
Cresyl methyl ether *o*	170·6°	3·97	0·8924	163·2	593
m	175·5°	3·71	8831	163·7	567
p	176°	3·79	8854	163·3	598

(ii.) The latent heats of the isomerides are closely similar. In column 6 are given either the latent heats per gram, when known, or values found for B, the constant in Sheppard's equation, $\log 10^3\eta = B/T + A$, since B ∝ molar latent heat (15), L.

(iii.) The boiling points are closely similar.

2. *Hydrogen Bonds.*—The second type of ortho effect occurs when two substituent groups contain respectively an electron receptive and an electron donating atom. Ortho-substituted phenols are cases in point

---

* Observed latent heats per gram. Ref. (16).

† By extrapolation.

when the second substituent group contains an electron attractive atom, such as O in NO_2 or CHO. Sidgwick and Callow ⁽¹⁷⁾ explained this very satisfactorily on the assumption that a ring is formed between the donor

Fig. 3.

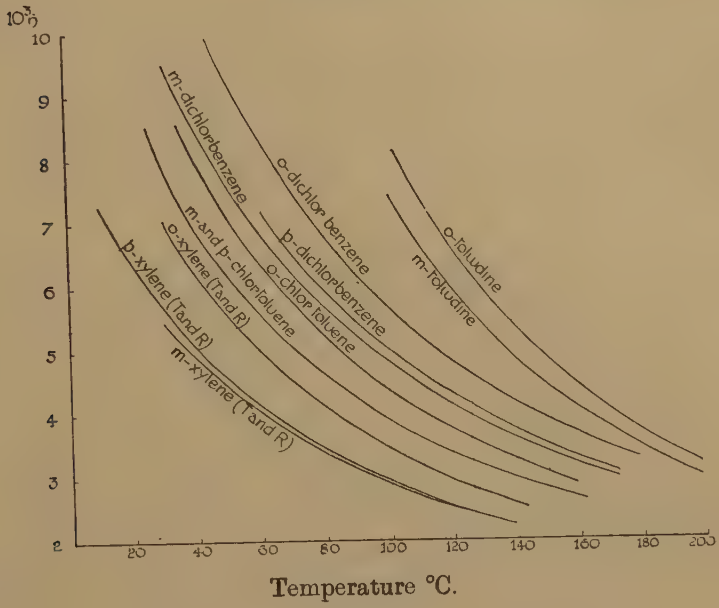

Fig. 4.

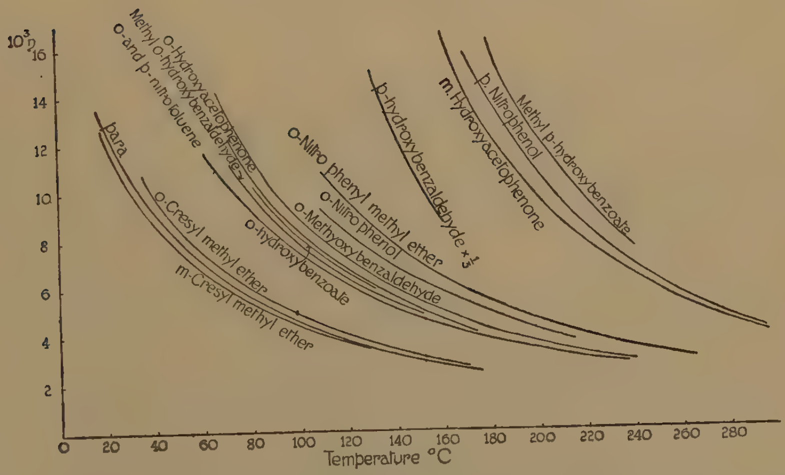

atom and the phenolic hydrogen. In these "internally associated" compounds the hydroxyl properties are more or less completely suppressed, so that less external association occurs. The meta and para isomerides cannot behave in the same way because aromatics are apparently unable to yield meta and para rings, and are thus free to associate intermolecularly.

We should thus expect the viscosities of such internally associated ortho derivatives to be reduced on two counts, namely (i.) increased symmetry caused by bridge-ring formation, and (ii.) reduced external association. This latter factor will also effect a reduction in the latent heat.

If these factors are sufficiently powerful, the viscosity of the ortho derivative may become equal to or even less than that of its meta and para isomerides.

The viscosities of a number of di-substituted benzenes have accordingly been studied, and the results most definitely support the above conclusions.

To sum up :—The ortho effect due to hydrogen bonds differs from that due to symmetry in that the viscosity, density, latent heat and rheochor of the ortho derivative are reduced, and may even be less than those of its meta and para isomerides. The boiling point of the ortho is lower also, as Sidgwick has pointed out. See Table IV.

Six-membered Resonance Rings.

The Nitro-phenols.—The ortho compound is regarded (17) as possessing the following co-planar structure :

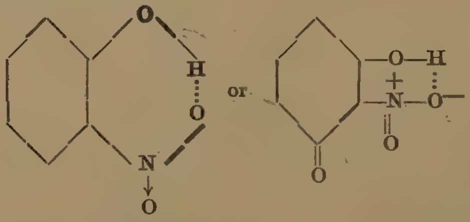

and is the first example to be chosen because the H-bond is particularly strong. It thus affords an excellent opportunity of checking the above conclusions. As Pauling points out, steric conditions are specially favourable for bridge-ring formation. The stability of the ring is so great that hydroxylic properties are completely suppressed. For example, the infra-red absorption of a dilute solution in carbon tetrachloride at room temperature shows no band in the 7000 cm.$^{-1}$ region characteristic of the presence of hydroxyl (10), although the meta isomeride shows it clearly and hence, presumably, the para isomeride would do so.

The curves in fig. 4, and the data in Table IV., show that *o*-nitrophenol has a slightly lower viscosity and molar latent heat than its ether (*o*-nitrophenyl methyl ether), which is incapable of yielding hydrogen bonds, as we should expect from its lower molecular weight if association were absent. On the other hand, the viscosity, density and latent heat of *p*-nitrophenol are much greater, indicating a high degree of association at the ordinary temperature. The steepness of the viscosity-temperature curve indicates rapid breaking down of association as the temperature rises. At the boiling point, however, the rheochor of *p*-nitrophenol is virtually theoretical *, so that association is negligible.

The difference of 1·7 units between the observed and theoretical rheochors of the ortho isomeride probably represents a shrinkage due to bridge-ring formation. A small effect is to be expected, but only a small one, because even when a benzene ring is formed there is only a shrinkage of 3·6 units.

The Hydroxy-benzaldehydes.—Spectroscopic evidence (10) supports the view (17) that, in the ortho compound, (salicyl aldehyde), hydrogen bridge formation occurs as follows :

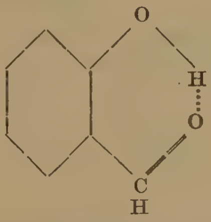

Not only is the infra-red absorption band characteristic of the presence of free hydroxyl absent from dilute solutions of salicyl aldehyde in carbon tetrachloride (10), but the Raman effect is also regarded as indicating hydrogen bonding (18).

The curves in fig. 4, and the data in Table IV., show that salicyl aldehyde has a slightly lower viscosity and molar heat than its methyl ether (ortho methoxy benzaldehyde), which is incapable of yielding hydrogen bonds. On the other hand, its para isomeride is much more viscous, more dense and possesses a much higher latent heat. At 160° C. the rheochor of the para compound suggests considerable association. Owing to decomposition occurring at about 170° C. data at higher temperatures could not be obtained. At its boiling point the ortho compound is substantially monomeric.

The Hydroxy-benzoates.—The methyl *o*-ester, *i. e.* methyl salicylate, is believed to have a similar structure to salicyl aldehyde, viz. :

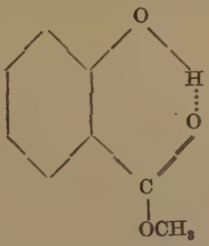

Dilute solutions in carbon tetrachloride show no absorption band characteristic of free hydroxyl. (10) The Raman effect in ethyl salicylate is regarded as indicating hydrogen bonding (18), and the same will apply, presumably, to the methyl ester.

---

* Owing to decomposition above 225°, extrapolation to the boiling point is too lengthy to give more than an approximate value for R(*b*).

The curves in figs. 1 and 4, and the data in Table IV., lend their support to the above structure. The density, latent heat, and particularly the viscosity of the para compound, are greater than those of the ortho. The latter appears to be virtually unassociated at the boiling point, whereas the para compound has a high rheochor indicating appreciable association.

The Hydroxy-acetophenones.—In dilute solution in carbon tetrachloride at room temperature the ortho derivative shows no infra-red absorption band in the 7000 cm.$^{-1}$ region, thus indicating absence of free hydroxyl (10). The structure would thus appear to be

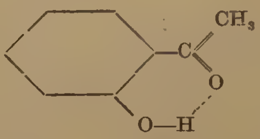

This receives support from the curves in fig. 4 and the data in Table IV. The meta compound, which cannot yield an analogous bridge-ring, is more dense, more viscous, and possesses a higher latent heat. At the boiling point its rheochor indicates considerable association, whereas the ortho compound appears to be monomeric; the small difference between the observed and calculated rheochors of the latter is possibly, as with *o*-nitrophenol, due to shrinkage caused by bridge-ring formation.

The Nitro-toluenes.—It is very difficult to loosen the hydrogen of an alkyl group sufficiently to allow bonding, but Sidgwick and Callow (17) suggest " this may be possible to some extent " when a powerful donating atom occupies an ortho position. Thus, *o*-nitro-toluene might contain some molecules of the bridge-ring type, namely :

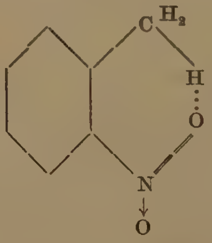

and it is suggested that this would explain the fact that its boiling point is lower than that of its meta and para isomerides.

The viscosities and densities of the ortho and para isomerides are closely similar; the latent heat of the ortho is slightly greater; on the other hand its rheochor is slightly less. These observations point to a directive tendency towards a bridge-ring structure in the ortho, even although it may not be sufficiently strong to yield an actual O—H....C bond. The small difference between the observed and theoretical rheochors of the ortho may possibly be due to shrinkage caused by this orientation; neither compound is appreciably associated at the boiling point.

Five-Membered Resonance Rings.

The tendency to form these in di-substituted ortho compounds is distinctly less than to form 6-membered rings. If actually formed they will be less stable and exert a proportionately less influence on the molecular volume (rheochor). When cis and trans forms of a molecule are possible, the cis may be expected to predominate owing to the attraction of the two electron-attractive atom for the hydrogen, thus reducing external association.

The Chlorphenols.—Three possible structures suggest themselves for the ortho isomeride, namely:

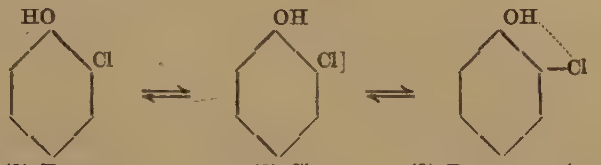

(1) Trans (2) Cis (3) Resonance ring

In dilute solution in carbon tetrachloride the compound shows, like phenol, absorption in the 7050 cm.$^{-1}$ region (10). This is attributed to the presence of "free" OH as in the trans structure (7). A second absorption peak occurs at 6910 cm.$^{-1}$, analogous to that in trichlorphenol, indicating the presence of cis molecules. As this latter band has some ten times the area of the former, it is assumed that the cis form predominates owing to the stabilizing influence of the electron-attractive Cl-atom.

A third peak has been observed (19) in the pure liquid at 6620 cm.$^{-1}$, and is taken to indicate inter-molecular association of trans molecules such as occurs in unsubstituted phenols (7).

In view of the instability of a 5-membered resonance ring, the number of molecules of the third kind cannot be great; there may be some, however, the ordinary liquid thus being an equilibrium mixture of all three forms, cis predominating. Less association will therefore occur in the ortho than in the para compound, a fact that has long been recognized from surface tension measurements (8). But the difference between the two will be less pronounced than between ortho and para nitrophenol in view of the great stability of the ortho nitro bridge-ring.

The foregoing views harmonize with, and serve to explain, our viscosity curves in fig. 5 and numerical data in Table V. Thus:

(i.) Despite its greater molecular weight, *o*-chlorphenol is less viscous than phenol, whereas the para is more viscous over the whole range of temperature studied.

(ii.) *o*-chlorphenol is more viscous than its methyl ether, which is

TABLE IV.

	B. pt. ° C.	$10^3\eta$ 150° C.	D 150° C.	B ∝ L.	R(*b*) obs.	R theor *.
Nitrophenol, ortho	215°	6·23	1·1802	702	147·3	149·0
Nitrophenol, para	295°	20·80	1·2506	1171	147·8	149·0
o-nitrophenyl methyl ether (*o*-nitro anisole)	265°	7·00	1·1235	735	(approx.) 172·8	172·8
o-hydroxy benzaldehyde (salicyl aldehyde)	195°	4·91	1·0343	638	143·8	143·5 †
p-hydroxy benzaldehyde	Decomp. at 170°	30·8	1·1190	1304 at 160°	165·2 at 160°	143·5
o-methoxy benzaldehyde	240°	5·42	1·0111	672	167·3	167·3
Methyl *o*-hydroxy benzoate (methyl salicylate)	223·5°	5·02	1·0553	643	177·1	177·3
Methyl *p*-hydroxy benzoate	C. 290° Decomp.	29·0	1·1173	1205	181·7	177·3
o-hydroxy aceto phenone	213°	5·02	1·0000	679	165·8	167·3 †
m-hydroxy aceto phenone	296° §	20·0	1·0726	1035	170·9	167·3
Nitro-toluene, ortho	221·5°	4·78	1·0365	614	161·7	163·1 ‡
Nitro-toluene, para	237·5°	4·82	1·0355	568	163·0	163·1

* Omitting any effect due to bridge-ring formation.

† R(C_6H_5) taken as 102·0 as in *o*-methyoxy-benzaldehyde.

‡ R(C_6H_5) taken as 100·4, the observed mean for chlor-toluenes (Table I.).

§ Decomposition occurred above 250°.

incapable of yielding hydrogen bonds. This is readily explained by the presence in the ortho chlorphenol of some associated trans molecules.

(iii.) The latent heat of ortho chlorphenol is less than that of the para but greater than that of the ether.

The rheochor indicates that at the boiling point the ortho compound may be very slightly associated, but less so than the para.

The Chloranilines.—The curves in fig. 6 indicate progressively increasing viscosity on passing from aniline through ortho to para chloraniline. The boiling point, density and latent heat of the para (Table V.) are also greater than those of the ortho.

Fig. 5.

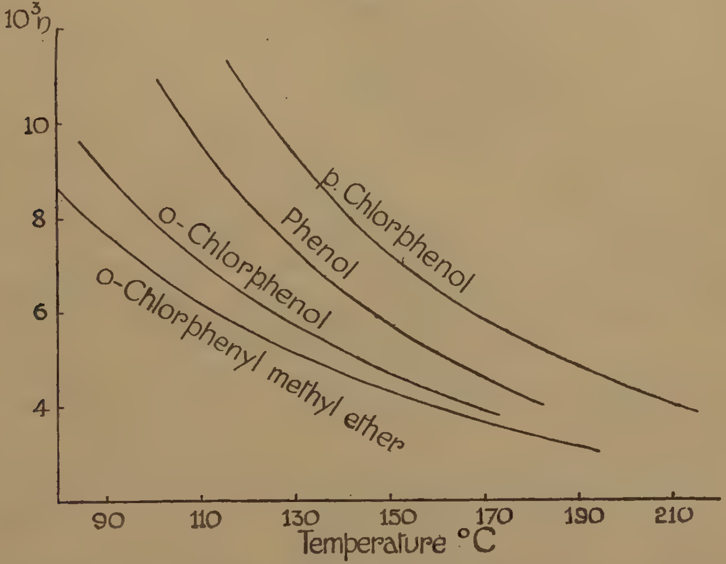

These observations suggest a directive tendency in *o*-chloraniline towards a bridge-ring structure, even though an actual Cl—H—N bond may not be formed, except possibly in a relatively few molecules. Thus :

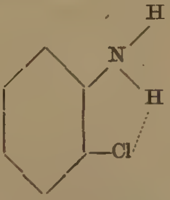

This directive tendency would reduce intermolecular association by more or less binding one H-atom ; but the other H-atom would still be free, so that differences between the ortho and para isomerides will be even less than those between the corresponding chlorphenols which possess no second hydrogen. The data in Table V. show this to be the case; the differences in boiling point, viscosity, density and latent heat are all less than between the two chlorphenols. All three anilines show appreciable association at their boiling points, their rheochors being several units above the theoretical.

Fig. 6.

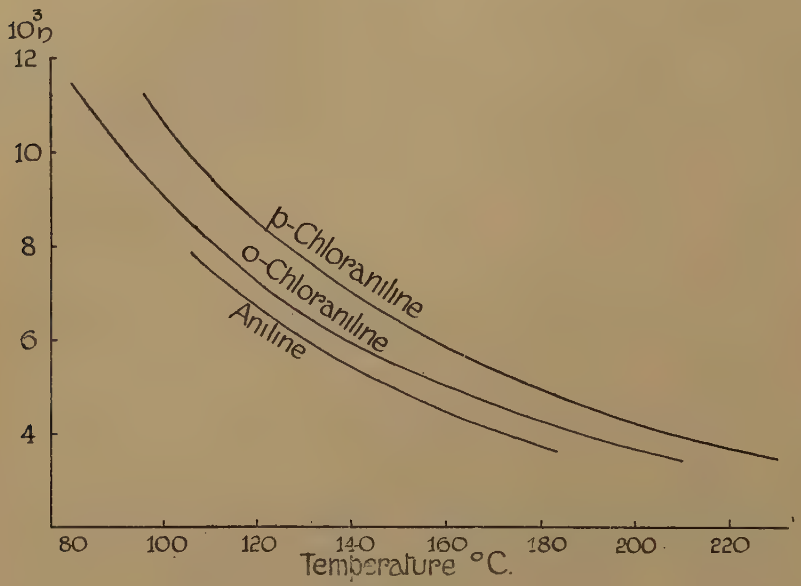

Fig. 7.

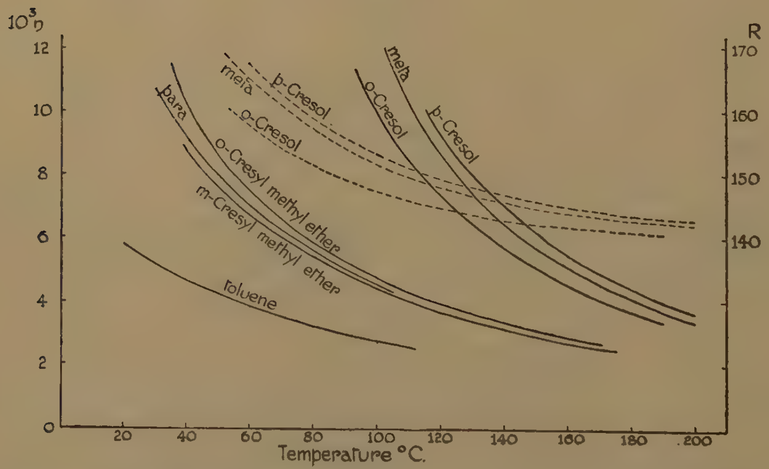

Viscosities and rheochors (broken lines) of cresols and their methyl ethers.

The Cresols.—The viscosities of the cresols are shown in fig. 7 together with those of their methyl ethers. The great increase in viscosity caused by the introduction of hydroxyl into toluene is apparent. As with the chlorphenols and chloranilines the ortho isomeride has a lower viscosity than the meta and para, whereas the reverse is the case for the cresol ethers, which differ in symmetry only, being incapable of forming hydrogen bonds.

Two forms of *o*-cresol are clearly possible, namely :

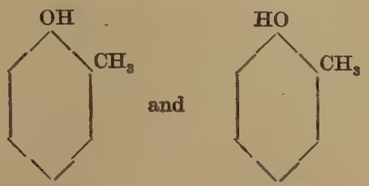

Cis Trans

Wulf and his co-workers (10) studied the infra-red absorption spectrum in dilute carbon tetrachloride solution, and interpreted the results as indicating that either equal amounts of cis and trans were present or an overwhelming predominance of trans alone. The former suggestion is probably correct and equally probably applies also to the pure liquid. It appears impossible for *o*-cresol to form a bridge-ring, owing partly to the difficulty of removing a proton from carbon and also to the fact that hydroxyl is essentially an electron acceptor (20). Even if no directive tendency towards the cis structure is present we shall still expect a roughly 50 : 50 ratio of cis to trans. The tendency to associate inter-

TABLE V.

	B. pt. ° C.	$10^3\eta$.	D.	B ∝ L.	R_b obs.	R_b calc.
		174° C.	174° C.			
Chlorphenol, *o* ...	174°	3·84	1·0881	703	138·9	138·3*
p ...	218°	5·73	1·1267	859	140·2	138·3
o-chlorphenyl methyl ether ...	196°	3·57	1·0300	635	162·1	162·1
		210° C.	210° C.			
Chloraniline, *o* (4) .	210°	3·40	1·0184	690	145·1	142·7†
p ...	230°	3·91	1·0378	713	145·5	142·7
Aniline (4)	183°	—	—	760	123·9	120·9
		150° C.	150° C.			
Cresol, *o*	190°	5·07	0·9302	882	140·6	139·7‡
m	200°	5·80	0·9277	951	142·1	139·7
p	200°	6·15	0·9293	930	142·9	139·7

---

* Taking C_6H_5 as 101·0 as in *o*-chlorphenyl methyl ether, Table I.

† Taking C_6H_5 as 103·3 as in aniline and NH_2 as 6·6+11·0, *i. e.* assuming no association. The mean observed value for NH_2, viz. 20·6, includes association.

‡ Taking C_6H_5 as 101·3, the mean value found for the cresyl methyl ethers, Table I.

molecularly will thus be reduced to about half, because the cis form, owing presumably to steric hindrance, must experience difficulty in linking up with other molecules. Hence the difference in physical properties between *o*-cresol and its isomerides will be definite but appreciably less pronounced than between the chlorphenols, since in *o*-chlorphenol the cis form predominates.

The above conclusions receive support from the curves in fig. 7 and the numerical data in Table V. Not only are the differences in the viscosities, latent heats and boiling points smaller than between the chlorphenols, but the density of *o*-cresol is greater than that of either the meta or para, whereas in all cases so far examined, where either a bridge-ring is formed, or, at least, a definite directive force exists, the density of the ortho form is less.

From surface tension measurements it has long been concluded that *o*-cresol is progressively less associated than its meta and para isomerides. This is supported by the R–T curves in fig. 7. At the boiling point the rheochor indicates only slight association, the meta and para showing progressively increasing association. As the temperature falls association steps up rapidly in all cases.

Experimental.

Many of the substances used in this research were either hygroscopic or easily oxidized at high temperatures ; also the viscosities decreased over the temperature range studied from some 50 to 3 millipoises. It was therefore necessary to modify the methods hitherto employed in determining the viscosities (3). The experiments were conducted in a new type of viscometer (21) in an atmosphere of nitrogen and, when necessary, under a constant additional applied pressure. In this latter case the usual correction has been applied for the kinetic energy of efflux.

Temperatures up to 200° C. were obtained, as previously described, save that the all-mercury temperature regulator was replaced by one containing normal butyl phthalate (with a mercury column), which gave a constancy of 0·2° near to 200° C. and 0·05° below 100° C.

Temperatures above 200° C. were obtained in an air bath constructed as follows. A " Hysil " glass cylinder, 33 cm. long and 12 cm. in diameter, was wrapped alternately with asbestos paper and copper foil—four thicknesses of each. A thicker layer of asbestos followed, on which was evenly wound a kilowatt resistance wire ; lagging was supplied by further wrapping of asbestos to a thickness of about three-quarters of an inch. Small windows were cut to allow observation of both the flow and adjustment of the capillary to the vertical from two directions at right angles. The viscometer was rigidly held by suitably bored bark corks which, after some preliminary charring, were found to withstand the high temperatures satisfactorily.

The three chlortoluenes were prepared from the corresponding toluidines by Sandmeyer's method (22), and the cresyl methyl ethers from the re-distilled cresols by methylation with dimethyl sulphate in alkaline solution (23) ; *o*-chlorphenyl methyl ether was similarly prepared from *o*-chlorphenol. To obtain *m*-dichlorbenzene, *m*-phenylene diamine was diazotized in the presence of cuprous chloride at the boiling point (24), whilst the ortho derivative was prepared by Sandmeyer's reaction using pure *o*-chloraniline. The remaining substances were obtained from the British Drug Houses.

The following general methods of obtaining pure specimens were used. Those compounds that were liquid at room temperature were dried and fractionated to constant boiling point, using a lagged or even, if necessary, a heated column. Solids were kept in a desiccator for some days, melted immediately before use and allowed to solidify, the first and last portions being rejected. This was repeated until the resulting product melted sharply. Such solid substances as distilled unchanged were first fractionated and the middle fraction of each distillate was subjected to further fractionation on freezing. By these methods very pure products were obtained.

The viscosity and density data are given below. As before, in all cases the densities refer to water at 4° C. The values for A and B refer to Sheppard's equation and apply to the linear portion of the curve obtained on plotting log $10^3 \eta$ against $1/T$. Values in parentheses have been calculated. The compounds are dealt with in the order in which they appear in the Tables.

o-Chlortoluene.—B. pt. 159·0° C. at 751·0 mm. A = −0·7203 ; B = 508·3, from 50° upwards.

Temp.	35·4	57·1	75·7	94·9	114·3
D	1·0638	1·0422	1·0120	0·9926	0·9852
1000η	8·564	6·597	5·465	4·567	3·912

Temp.	120·0	125·0	135·0	145·9	153·1	159·0
D	(0·9795)	0·9745	0·9645	0·9534	0·9461	(0·9401)
1000η	(3·743)	3·606	3·348	3·114	2·970	(2·861)

R(b) = 151·2 ; calculated 151·8.

Our extrapolated density at 19·8°, viz. 1·0790, is identical with that found by Dobrosserdow (25).

m-Chlortoluene.—B. pt. 161·7° C. at 749·9 mm. A = −0·6719 ; B = 472·2, above 48°.

Temp.	25·0	48·8	69·5	89·5	109·6
D	1·0647	1·0410	1·0204	1·0001	0·9794
1000η	8·55	6·252	5·090	4·271	3·649

Temp.	120·0	130·3	139·2	150·2	161·7
D	0·9687	0·9580	0·9489	0·9376	(0·9258)
1000η	3·384	3·155	2·977	2·780	(2·597)

R(b) = 151·7 ; calculated 151·8.

Our extrapolated densities at 18° and 19·6° lie close to those of Cohen (26) and Dobrosserdow (25) respectively.

p-Chlortoluene.—B. pt. 161·7° C. at 746·4 mm. A=−0·6583; B=465·58, above 54°.

Temp.	32·3	54·4	75·7	94·8	114·9	120·0	125·1	135·0	145·5	152·1	161·7
D	1·0553	1·0331	1·0120	0·9926	0·9722	(0·9673)	0·9623	0·9523	0·9417	0·9352	(0·9258)
1000η	7·59	5·820	4·753	4·046	3·483	(3·361)	3·242	3·043	2·845	2·733	(2·587)

R(b)=151·6; calculated 151·8.

Our density (1·0682) extrapolated to 19·5° compares favourably with 1·0686 (Dobrosserdow (25)), Jaeger's value (27) (0·928) at 160° is close to ours, 0·9273.

o-Dichlorbenzene.—B. pt. 178·6° C. at 732·7 mm. A=−0·6328; B=517·34, above 65°.

Temp.	23·3	44·5	65·95	84·5	105·0	120·0	124·8	144·2	154·0	163·1	178·6
D	1·3023	1·2782	1·2545	1·2335	1·2104	(1·1933)	1·1878	1·1652	1·1539	1·1434	(1·1255)
1000η	13·19	9·94	7·83	6·517	5·444	(4·826)	4·660	4·036	3·787	3·577	(3·257)

R(b)=149·7; calculated 149·8.

Our density (1·3057) at 20° compares (28) favourably with Narbutt's 1·3048.

m-Dichlorbenzene.—B. pt. 172·3° C. at 757·7 mm. A=−0·6240; B=486·96, above 75°.

Temp.	30·6	54·2	75·6	94·1	114·2	120·0	134·8	144·3	157·2	172·3
D	1·2788	1·2513	1·2268	1·2058	1·1823	(1·1891)	1·1580	1·1465	1·1312	(1·1134)
1000η	9·51	7·325	5·945	5·050	4·310	(4·126)	3·722	3·491	3·221	(2·948)

R(b)=150·1; calculated 149·8.

Our density extrapolated to 20° (1·2910) compares (28) with Narbutt's 1·2881.

p-Dichlorbenzene.—M. pt. 52·8 to 53·0° C. Narbutt (28) gives 52·9°; Kruyt (29), 53·0°. B. pt. 172·3° C. at 750·8 mm. A=−0·6344; B=497·56, above 80° C.

Temp.	60·7	81·7	101·3	120·0	130·0	139·9	150·2	159·8	172·3
D	1·2442	1·2195	1·1964	1·1749	1·1630	1·1513	1·1387	1·1268	(1·1113)
1000η	7·22	5·862	4·953	4·295	3·981	3·719	3·479	3·277	(3·042)

R(b)=151·0; calculated 149·8.

o-Cresyl methyl ether.—B. pt. 170·6° C. at 739·8 mm. A=−0·9090; B=592·6, above 75°.

Temp.	15·0	34·9	45·0	55·1	75·1	85·1	95·2	105·4	115·0	120	125·0	135·0	145·2	154·4	165·0	170·6
D	0·9903	0·9723	(0·9628)	0·9533	0·9360	0·9256	0·9159	0·9063	0·8971	(0·8924)	0·8877	0·8776	0·8671	0·8572	0·8456	(0·8395)
1000η	15·69	10·81	(9·25)	7·965	6·226	5·580	5·019	4·534	4·146	(3·971)	3·808	3·493	3·214	2·986	2·780	(2·672)

R(b)=163·2; calculated 163·8.

Our interpolated density and viscosity at 45° are appreciably higher than those of Thole (30), viz. 0·9589 and 8·49 respectively.

m-Cresyl methyl ether.—B. pt. 175·5° C. at 738·9 mm. A=−0·8724; B=566·67.

Temp.	18·3	39·4	45·0	60·0	79·8	89·9	99·9	110·1	120·0	130·2	139·8	150·1	158·0	167·0	175·5
D	0·9753	0·9565	(0·9514)	0·9380	0·9202	0·9111	0·9019	0·8924	0·8831	0·8735	0·8641	0·8538	0·8461	0·8370	(0·8288)
1000η	12·71	8·94	(8·25)	6·765	5·426	4·892	4·446	4·039	3·707	3·414	3·156	2·931	2·743	2·606	(2·460)

R(b)=163·7; calculated 163·8.

Thole (30) gives 8·75 for the viscosity at 45°.

p-Cresyl methyl ether.—B. pt. 176° C. at 750·2 mm. A=−0·9425; B=597·65, above 35°.

Temp.	16·75	35·6	45	55·6	65·0	74·7	85·2	94·7	105·0	114·6	120·0	124·8	135·0	144·5	155·6	165·3	176·0
D	0·9796	0·9627	(0·9543)	0·9449	0·9367	0·9278	0·9182	0·9097	0·8999	0·8908	(0·8854)	0·8807	0·8707	0·8612	0·8507	0·8408	(0·8299)
1000η	13·59	9·83	(8·64)	7·51	6·69	5·95	5·304	4·812	4·355	3·972	(3·785)	3·631	3·323	3·083	2·834	2·639	(2·446)

R(b)=163·3; calculated 163·8.

Thole's density and viscosity (30) at 45° are 0·9497 and 8·06 respectively.

o-Chlorphenyl methyl ether.—B. pt. 196·0° C. at 757·5 mm. A=−0·8685; B=635·3, above 100°.

Temp.	17·3	49·7	79·8	99·7	119·1	139·9	159·2	173·0	174·0	185·0	196·0
D	1·1975	1·1643	1·1332	1·1121	1·0912	1·0685	1·0470	1·0312	(1·0300)	1·0170	(1·0040)
1000η	24·61	13·09	8·65	6·87	5·644	4·672	3·996	3·591	(3·57)	3·296	(3·061)

R=162·1; calculated 161·8.

o-Nitrophenyl methyl ether.—B. pt. 265·0° C. at 754·1 mm. A=−0·8929; B=735·3, above 109°.

Temp.	13·25	50·6	80·3	109·3	120·0	124·0
D	1·2612	1·2234	1·1937	1·1646	(1·1538)	1·1497
1000η	74·9	26·61	15·79	10·73	(9·504)	9·115

Temp.	139·7	150·0	155·1	170·0	185·1
D	1·1337	(1·1235)	1·1185	1·1034	1·0885
1000η	7·745	(7·00)	6·674	5·821	5·152

Temp.	209·0	225·0	235·0	250·0	265·0
D	1·0644	1·0487	1·0387	1·0236	(1·0089)
1000η	4·315	3·829	3·585	3·258	(2·981)

R(*b*)=172·8 ; calculated 173·4.

Our densities lie close to those of Jaeger (27), and at 22·5° and 26° are virtually identical with those of Kauffmann (52) and Brunck (53).

Dichlor acetic acid.—B. pt. 189 to 189·5° C. at 744·4 mm. A=−1·0245 ; B=807·8.

Temp.	19·3	87·8	99·5	120·0	140·3
D	1·5568	1·4641	1·4483	1·4207	1·3912
1000η	54·8	16·72	14·13	10·83	8·53
R	142·4	125·3	124·0	122·3	121·0

Temp.	160·0	180·0	189·5
D	1·3621	1·3314	(1·3169)
1000η	7·00	5·634	(5·272)
R	120·4	119·7	

R(*b*)=119·9 ; calculated 114·4.

Phenol.—M. pt. 41·5 to 42° C. Dawson (31) gives 41°. B. pt. 183° C. at 741·7 mm. A=−1·3550 ; B=895·44, from 100° upwards.

Temp.	60·45	80·2	100·2	119·8	139·8
D	1·0417	1·0249	1·0077	0·9900	0·9709
1000η	25·77	16·08	11·08	8·34	6·426
R	135·6	129·9	126·2	123·8	122·3

Temp.	150·0	160·8	174·7	183·0
D	0·9610	0·9506	0·9367	(0·9284)
1000η	5·721	5·091	4·416	(4·06)
R	121·5	121·0	120·5	

R(*b*)=120·2 ; calculated 117·2.

Our densities differ appreciably from those of Sidgwick and Bayliss (32), but agree with those of Buehler (33) (who states that he purified his phenol by Sidgwick's method) up to 150° and of Bramley (34) up to 175°. At about 100° our viscosity data agree closely with those of Bramley, but at 175° our value is appreciably lower.

Our data do, however, obey Sheppard's equation fairly well, whereas Bramley's data do not.

Benzyl alcohol.—B. pt. 205·0° C. at 757·8 mm. A=−1·2078 ; B=827·57, above 125°.

Temp.	48·6	67·9	87·7	107·4	127·6
D	1·0237	1·0084	0·9924	0·9763	0·9592
1000η	28·36	18·45	12·84	9·46	7·223

Temp.	148·0	162·5	178·7	185·1	193·0	205·0
D	0·9418	0·9289	0·9135	0·9071	0·8995	(0·8880)
1000η	5·721	4·920	4·207	3·970	3·700	(3·34)

R(b)=140·7 ; calculated 140·0.

Cyclo-hexanone.—B. pt. 153·5° C. at 749·6 mm. A=−1·0220 ; B=689·2, from 60° upwards.

Temp.	16·3	57·75	85·5	109·65	129·0	147·0	153·5
D	0·9477	0·9111	0·8867	0·8647	0·8470	0·8308	(0·8245)
1000η	25·18	11·72	7·99	6·00	4·94	4·147	(3·91)

R(b)=140·2 ; calculated 139·4.

Our interpolated densities at 20°, 64·6° and 87·6° lie close to Vogel's values (42).

o-Nitrophenol.—M. pt. 45·0° C. Sidgwick (35) gives 44·9°. B. pt. 215·0° C. at 750·2 mm. A=−0·8648 ; B=701·89, over whole range studied.

Temp.	108·9	120·0	136·0	150·0	160·5	185·0	200·0	215·0
D	1·2254	(1·2132)	1·1957	(1·1802)	1·1687	1·1407	1·1238	(1·1072)
1000η	9·40	(8·34)	7·08	(6·23)	5·675	4·646	4·159	(3·74)

R(b)=147·3 ; calculated 149·0.

p-Nitrophenol.—M. pt. 112·8 to 113·1° C. Sidgwick (35) gives 113·8° ; Swarts (36), 114° ; Mills (37), 111·4°. B. pt. *c.* 295° C., but decomposition occurred above 225°. Above 150° until decomposition. A=−1·4497 ; B=1171·4.

Temp.	129·5	149·5	150·0	169·3	180·8
D	1·2690	1·2511	(1·2506)	1·2331	1·2227
1000η	29·41	20·96	(20·80)	15·80	13·65

Temp.	213·0	223·5	295
D	1·1932	1·1834	(1·1167)
1000η	9·14	8·113	(4·10)

R(b)=147·8 (approx.) ; calculated 149·0.

o-Hydroxy benzaldehyde (*Salicyl aldehyde*).—B. pt. 195·2 at 749·9 mm. A=−0·8172 ; B=638·29, from 120°.

Temp.	71·1	82·8	96·3	109·3	120·0	121·3	133·3
D	1·1098	1·0991	1·0865	1·0742	(1·0611)	1·0624	1·0510
1000η	11·34	9·67	8·216	7·124	(6·41)	6·324	5·675
R	149·1	147·5	146·2	145·3	—	144·8	144·2

Temp.	146·7	150·0	159·8	172·0	184·3	191·2	195·2
D	1·0378	(1·0343)	1·0242	1·0116	0·9988	0·9914	(0·9871)
1000η	5·049	(4·91)	4·550	4·140	3·789	3·611	(3·516)
R	143·8	—	143·7	143·7	143·8	143·8	143·8

R(b)=143·8 ; calculated 143·5.

p-Hydroxy benzaldehyde.—M. pt. 114 to 115° C. Reimer and Tiemann give 115 to 116° C. Decomposition occurred above 160° C.

Temp.	130·5	140·1	149·7	150·0	160·0
D	1·1341	1·1267	1·1192	(1·1190)	1·1113
1000η	45·5	36·80	30·97	(30·8)	26·19

R (160°)=165·2 ; calculated 143·5.

Our densities are slightly higher than those of Eijkman (39) and of Sidgwick (32).

o-Methoxy benzaldehyde.—M. pt. 34·5 to 35° C. Voswinckel (40) gives 35°. B. pt. 240·0° C. at 744·4 mm. A=−0·8544 : B=672·0, from 130° upwards.

Temp.	56·4	86·0	114·8	128·9	143·7	150·0	159·1	175·2	190·0	213·0	240·0
D	1·0972	1·0705	1·0441	1·0310	1·0171	(1·0111)	1·0024	0·9869	0·9720	0·9486	(0·9211)
1000η	16·85	10·72	7·58	6·57	5·73	(5·42)	5·026	4·410	3·951	3·378	(2·852)

R(*b*)=167·3.

Our densities are very slightly higher than those of Sidgwick (32).

Methyl salicylate.—B. pt. 223·5° C. at 739·5 mm. A=−0·8189 ; B=642·85, from 120° upwards.

Temp.	80·5	109·9	120·0	125·1	138·9	150·0	154·6	169·9	186·7	199·7	214·6	223·5
D	1·1237	1·0957	(1·0752)	1·0803	1·0666	(1·0553)	1·0507	1·0351	1·0174	1·0036	0·9876	(0·9774)
1000η	10·33	7·31	(6·56)	6·252	5·531	(5·02)	4·844	4·295	3·800	3·475	3·159	(2·991)

R(*b*)=177·1 ; calculated 177·3.

Our extrapolated densities below 80° agree closely with those of Jaeger (27).

Methyl p-hydroxy benzoate.—M. pt. 131° C. v. Hoessle (41) gives 131°. B. pt. 290 to 292° C. With decomposition, a thick viscid liquid remaining. A=−1·4652 ; B=1205·2, from 212° upwards.

Temp.	140·0	150	159·7	179·0	197·5	212·0	225·5	241·0	290·0
D	1·1247	(1·1173)	1·1102	1·0958	1·0813	1·0702	1·0598	1·0478	(1·0083)
1000η	35·08	(29·0)	23·06	16·36	12·57	10·47	8·99	7·59	(4·66)

R(*b*)=181·7 ; calculated 177·3.

o-Hydroxy acetophenone.—B. pt. 213° C. at 755·4 mm. A=−0·8992 ; B=679·08, above 110°.

Temp.	48·0	71·3	91·1	111·0	131·5	150·0	151·6	170·0	186·0	197·4	213·0
D	1·0985	1·0773	1·0595	1·0406	1·0212	(1·0000)	1·0017	0·9833	0·9673	0·9562	(0·9407)
1000η	18·16	12·24	9·29	7·42	6·01	(5·02)	5·007	4·303	3·805	3·502	(3·148)

R(*b*)=165·8 ; calculated 167·3.

m-Hydroxy acetophenone.—M. pt. 93° C. Biginelli (43) gives 92 to 93° ; Pfeiffer (44), 95 to 96°. B. pt. given in literature as 296° C., but decomposition occurs above 250°. The plot of log η against 1/T linear above 215°, when A=−1·2085 ; B=1035·2.

Temp.	102·0	129·7	150·0	160·0	179·3	199·2	215·0	231·0	245·2	296
D	1·1089	1·0859	(1·0726)	1·0660	1·0441	1·0272	1·0141	1·0008	0·9884	(0·9440)
1000η	58·14	29·16	(20·00)	16·69	12·54	9·783	8·194	7·000	6·155	(4·087)

R(*b*)=170·9 ; calculated 167·3.

o-Nitrotoluene.—B. pt. 221·5° C. at 757·9 mm. A=−0·7732 ; B=614·3, above 100°.

Temp.	19·7	61·0	100·6	119·9	120·0	139·4	150·0	160·5	180·8	190·9	221·5
D	1·1621	1·1225	1·0844	1·0659	(1·0658)	1·0470	(1·0365)	1·0261	1·0053	0·9950	(0·9637)
1000η	23·59	11·74	7·417	6·170	(6·164)	5·201	(4·78)	4·404	3·818	3·565	(2·944)

R(*b*)=161·7 ; calculated 163·1.

Our interpolated densities at 36°, 56·5° and 79° agree closely with those of Sugden and Wilkins (45).

p-Nitrotoluene.—M. pt. 51·8 to 52·0° C. Holleman and Vermeuten (46) give 51·4° ; Rintoul (47), 51·6 to 51·9°. B. pt. 237·5° C. at 743·7 mm. A=−0·6597 ; B=568·03, above 150°.

Temp.	99·0	120·0	124·2	138·6	150	150·3	162·2	177·5	187·7	200·5	215·5	237·5
D	1·0822	(1·0631)	1·0593	1·0463	(1·0355)	1·0350	1·0243	1·0100	1·0003	0·9878	0·9732	(0·9518)
1000η	7·534	(6·14)	5·946	5·278	(4·82)	4·807	4·424	3·992	3·737	3·465	3·184	(2·838)

R(*b*)=163·0 ; calculated 163·1.

Our interpolated densities at 100° and 125° agree closely with those of Jaeger (27).

o-Chlorphenol.—B. pt. 174·0° C. at 757·1 mm. A=−0·9871 ; B=702·7, above 100°.

Temp.	40·7	61·1	84·5	103·5	121·9	131·6	141·0	152·0	163·0	174·0
D	1·2386	1·2155	1·1890	1·1678	1·1472	1·1363	1·1254	1·1129	1·1005	(1·0881)
1000η	21·71	14·07	9·715	7·564	6·216	5·617	5·117	4·630	4·212	(3·843)

R(*b*)=138·9 ; calculated 138·3.

Above 80° our viscosity data are appreciably lower than Bramley's (34).

p-Chlorphenol.—M. pt. 37° C. Beilstein and Kurbatoff (48) give 37°. B. pt. 218° C. at 757·6 mm. A=−1·1627 ; B=859·27, above 135°.

Temp.	98·7	116·8	125·5	137·2	150·5	162·1	174·0	175·5	187·0	200·1	210·0	218·0
D	1·2042	1·1867	1·1778	1·1658	1·1519	1·1396	(1·1267)	1·1251	1·1128	1·0980	1·0871	(1·0780)
1000η	15·00	11·27	9·956	8·56	7·345	6·486	(5·73)	5·662	5·072	4·508	4·131	(3·868)

R(*b*)=140·2 ; calculated 138·3.

p-Chloraniline.—M. pt. 69 to 70° C. Mills (49) gives 69·7°. B. pt. 230·0° C. at 748·9 mm. A=−0·8828 ; B=712·75, above 112°.

Temp.	92·0	112·0	131·8	151·9	162·1	171·5
D	1·1542	1·1357	1·1171	1·0981	1·0881	1·0787
1000η	11·87	9·29	7·55	6·220	5·682	5·249

Temp.	181·5	192·0	201·0	210·0	212·0	230·0
D	1·0685	1·0575	1·0476	(1·0378)	1·0356	(1·0160)
1000η	4·834	4·467	4·174	(3·91)	3·864	(3·42)

R(b)=145·5 ; calculated 142·7.

Our interpolated densities are very slightly higher than those of Sugden (50) and Jaeger (27).

o-Cresol.—M. pt. 30·0° C. Dawson and Mountford (31) give 30·45°. B. pt. 190·0° C. at 757·8 mm. A=−1·3797 ; B=881·75, above 100°.

Temp.	53·4	72·5	91·6	106·1	120·0	135·8	150·0
D	1·0183	1·0015	0·9844	0·9714	0·9587	0·9436	(0·9302)
1000η	27·05	16·61	11·34	8·89	7·37	6·005	(5·07)
R	160·4	153·2	148·8	146·3	144·8	143·4	—

Temp.	152·8	166·8	177·5	185·0	190·0
D	0·9276	0·9137	0·9020	0·8942	(0·8891)
1000η	4·943	4·238	3·802	3·528	(3·366)
R	142·0	141·3	141·0	140·8	140·6

R(b)=140·6 ; calculated 139·7.

Our densities agree with those of Bramley (34), but our viscosities above 80° are appreciably lower.

m-Cresol.—B. pt. 199·7° C. at 750·1 mm. A=−1·4853 ; B=951·34, above 120°.

Temp.	42·05	62·0	81·95	102·3	123·5	141·6	150·0
D	1·0177	1·0023	0·9856	0·9687	0·9511	0·9354	(0·9277)
1000η	57·67	29·08	17·32	11·97	8·201	6·383	(5·80)

Temp.	161·0	172·0	182·1	192·3	199·7
D	0·9176	0·9072	0·8971	0·8872	(0·8799)
1000η	5·087	4·490	4·034	3·622	(3·362)

R(b)=142·1 ; calculated 139·7.

Our interpolated densities at 33·1° and 53·8° are almost identical with those of Schwers (51). At 60° and 110° our viscosities are virtually identical with Bramley's (34).

p-Cresol.—M. pt. 33·5 to 34·0° C. Sidgwick (35) gives 33·8° ; Dawson (31), 34·15°. B. pt. 199·7° C. at 762·5 mm. A=−1·4084 ; B=929·73, above 140°.

Temp.	59·56	80·3	100·64	114·75	130·0	144·3
D	1·0046	0·9878	0·9709	0·9597	0·9468	0·9344
1000η	34·60	19·56	12·71	10·09	8·01	6·582
R	167·6	158·8	153·0	150·4	148·1	146·5

Temp.	150·0	160·0	174·7	190·0	199·7
D	(0·9293)	0·9203	0·9070	0·8921	(0·8827)
1000η	(6·15)	5·470	4·661	3·971	(3·61)
R	—	145·0	144·0	143·2	142·9

R(b)=142·9 ; calculated 139·7.

Our interpolated densities lie close to those of Jaeger (27) and Bramley (34) ; our viscosities at 80° and 110° are virtually identical with those of Bramley.

References.

(1) Friend and Hargreaves, Phil. Mag. xxxv. p. 619 (1944).

(2) Friend, 'Chemistry and Industry,' p. 179 (1944); also ref. (1) above.

(3) Friend, 'Nature,' cl. p. 432 (1942); Friend and Hargreaves, Phil. Mag. xxxiv. p. 643 (1943).

(4) Friend and Hargreaves, Phil. Mag. xxxv. p. 57 (1944).

(5) Using the data of Titani, *Bull. C. S. Japan*, ii. p. 95 (1927).

(6) Using the data of Thorpe and Rodger, Phil. Trans. clxxxv. p. 45 (1895).

(7) Pauling, "Nature of the Chemical Bond" (Cornell U.P. 1940), p. 333, etc.; also ref. (10).

(8) Turner, "Molecular Association" (Longmans, 1915), p. 59, etc.

(9) Kinsey and Ellis, 'Physical Review,' li. p. 1074 (1937); Bosschieter and Errera, J. Phys. Radium, viii. p. 229 (1937).

(10) Various papers by Wulf and his Co-workers, 'Nature,' cxxxv. p. 137 (1935); J. Amer. Chem. Soc. lvii. p. 1464 (1935); lviii. pp. 548, 2287 (1936); Pauling's discussion, *ibid.* lviii. p. 94 (1936).

(11) See Bernal and Fowler, J. Chem. Phys. i. p. 515 (1933); Collins, 'Physical Review,' xxvi. p. 771 (1925); Williams and Millett, *ibid.* lxvi. p. 6 (1944)

(12) Compare Llewellyn, 'Chemistry and Industry,' p. 619 (1940).

(12 *a*) Data taken from "International Critical Tables," v. p. 10.

(13) Friend and Hargreaves, Phil. Mag. xxxv. p. 136 (1944).

(14) Sugden, "The Parachor and Valency" (Routledge, 1930), p. 205.

(15) Friend, Trans. Farad. Soc. xxxi. p. 542 (1935).

(16) Matthews, J. Amer. Chem. Soc. xlviii. p. 562 (1926).

(17) Sidgwick and Callow, J. Chem. Soc. cxxv. p. 527 (1924); Sidgwick, "The Electronic Theory of Valency" (1927).

(18) Kahovec and Kohlrausch, *Z. phys. Chem.* B, xxxviii. p. 119 (1937); Watson, "Modern Theories of Organic Chemistry" (Oxford U.P., 1941), p. 243.

(19) Errera and Mollet, J. Phys. Radium, vi. p. 281 (1935).

(20) See discussion by Watson, ref. (18).

(21) Hargreaves, in the press.

(22) Sandmeyer, *Berichte*, xvii. p. 1633 (1884).

(23) Ullmann, *Annalen*, cccxxvii. p. 116 (1903).

(24) Sandmeyer, *Berichte*, xvii. p. 2652 (1884).

(25) Dobrosserdow, J. Russ. Phys. Chem. Soc. xliii. pp. 73, 225, 454 (1911). The data are recalculated with reference to water at 4° C.

(26) Cohen and Co-workers, J. Chem. Soc. xcvii. p. 1627 (1910).

(27) Jaeger, *Zeits. anorg. Chem.* ci. p. 1 (1917).

(28) Narbutt, *Berichte*, lii. p. 1034 (1919).

(29) Kruyt, *Zeits. phys. Chem.* lxxix. p. 667 (1912).

(30) Thole, J. Chem. Soc. xcvii. p. 2601 (1910).

(31) Dawson and Mountford, J. Chem. Soc. cxiii. p. 937 (1918).

(32) Sidgwick and Bayliss, J. Chem. Soc. p. 2027 (1930).

(33) Buehler, Wood, Hull and Erwin, J. Amer. Chem. Soc. liv. p. 2398 (1932).

(34) Bramley, J. Chem. Soc. cix. p. 10 (1916).

(35) Sidgwick, Spurrell and Davies, J. Chem. Soc. cvii. p. 1208 (1915).

(36) Swarts, *Rec. Trav. Chim.* xxxiii. p. 281 (1914).

(37) Mills, Phil. Mag. xiv. p. 27 (1882).

(38) Reimer and Liemann, *Berichte*, ix. p. 824 (1876).

(39) Eijkman, Bergema and Henrard, *Chem. Zent.* xxix. p. 817 (1905).

(40) Voswinckel, *Berichte*, xv. p. 2024 (1882).

(41) v. Hoessle, *J. prakt. Chem.* xlix. p. 501 (1894).

(42) Vogel, J. Chem. Soc. p. 1323 (1938).

(43) Biginelli, *Gazzetta*, xxiv. p. 440 (1894).

(44) Pfeiffer, *Annalen*, ccclxxxviii. p. 141 (1912).

(45) Sugden and Wilkins, J. Chem Soc. cxxvii. p. 2517 (1925).
(46) Holleman and Vermenten, *Rec. Trav. Chim.* xxxiii. p. 10 (1914).
(47) Rintoul, J. Soc. Chem. Ind. xxxiv. p. 60 (1915).
(48) Beilstein and Kurbatoff, *Annalen*, clxxvi. p. 30 (1875).
(49) Mills, *Annalen*, clxxvi. p. 355 (1875).
(50) Sugden, J. Chem. Soc. cxxv. p. 1174 (1924).
(51) Schwers, *J. Chim. phys.* ix. p. 50 (1911).
(52) Kauffmann, *Zeits. phys. Chem.* lv. p. 554 (1906).
(53) Brunck, *Zeit. Chem.* p. 205 (1867).

The Technical College,
Birmingham.
February 12th, 1945.

XCI. *A Viscometer with Constant Working Volume suitable for Measurements over a Wide Range of Viscosities.*

By William D. Hargreaves, M.Sc.*

[Received February 13, 1945.]

The simple viscometer of the Ostwald type is very satisfactory for the determination of the viscosities of liquids over relatively small temperature ranges. It is not suitable, however, for substances which readily react with the oxygen of the air or with moisture. Neither is it convenient if the temperature range is such that the viscosity changes are very great, as for example from 2 to 100 millipoises; the time of flow is then inconveniently long at the lower temperatures if it is not to be too short for accurate measurement at the higher. Further, it is desirable, when dealing with substances whose purification depends on crystallization to constant melting point, that these should be introduced into the viscometer entirely free from dust.

The instrument shown in the figure is designed to overcome the above difficulties. It was made in Phœnix glass by Mr. L. D. V. Scorah, of Birmingham, to whom the author's thanks are tendered. Tube KG_1 lies behind FB and is additionally supported by the bracing rod L. K fits accurately into the short arm of a U-tube, the other arm of which is rigidly supported above the bath liquid. An additional holding device at the top of KG_1 allows the capillary to be adjusted accurately to the vertical. The device recently mentioned (1) might also be used.

The substance used is introduced through the sintered glass filter which has a ground joint at G_1, gentle suction being applied at N. When sufficient has been introduced, the filter tube is replaced by MG_2. Thermal equilibrium having been attained, the level in B is adjusted by forcing liquid in from K. Tap M is then closed, H opened, and pressure is applied at N. This is conveniently done by Barr's method (2). Liquid is thus forced into the bulb A, where it can be held by closing taps H and N.

---

* Communicated by the Author.

When the liquid is to flow under its own hydrostatic head, excess pressure is released by opening the taps M, N and H (in that order), the viscometer arms are connected by the three-way tap F and the flow is timed. If pressure is to be applied, the source is connected to H, F is kept closed, M, N and H are opened, and the flow is timed.

The viscosity can be calculated from the usual equation

$$\eta = K(P+xDg)\theta - CD/\theta, \quad . \quad . \quad . \quad . \quad . \quad . \quad . \quad . \quad (1)$$

where K and C are the instrument constants, P the applied pressure, x the mean hydrostatic head of liquid of density D, and θ is the time of flow. $(P+xDg)$ represents the effective pressure : C can easily be found from the measured dimensions of the viscometer.

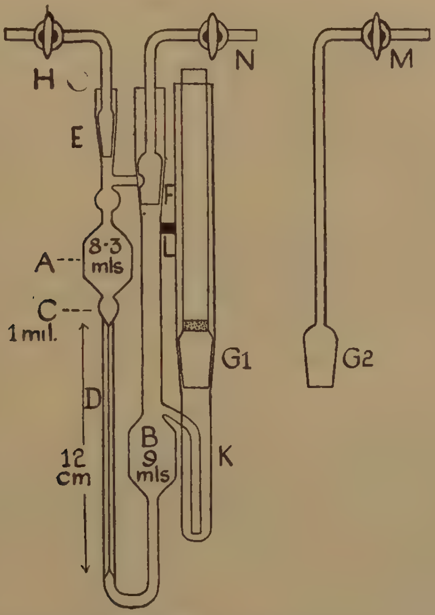

**Diameter of capillary D=0·0175 cm. (calculated from time of flow).
Bore of taps H, N, M=2 mm.**

Meissner (3) has derived an equation giving the effective pressure as a function of the applied pressure and the initial and final heads of liquid. The derivation neglects the kinetic energy correction and assumes uniformity of cross-section of the bulb ; it indicates that the mean hydrostatic head varies with the applied pressure.

Experiments carried out with the viscometer described indicate that x is independent of P, and is but little different from the mean of the initial and final heads.

Writing equation (1) in the form

$$K \,.\, P + K \,.\, xDg = (\eta\theta + CD)/\theta^2$$

for one liquid at one temperature, the plot of P against $(\eta\theta+\mathrm{CD})/\theta^2$ is linear for the pressure range over which x is constant. The slope of the curve gives K, and the intercept on the $(\eta\theta+\mathrm{CD})/\theta^2$ axis gives $\mathrm{K}\,.\,xDg$, from which x is obtained. Experiments have been carried out with water at 26·9° C. and at 89·0° C. while, in order to study the effects of surface tension, benzene at 26·9° C. was included.

The water was distilled three times, whilst the benzene was of Analar quality, redistilled. The viscosities and densities of water were taken from the International Critical Tables. The corresponding values for benzene were those of Bingham and Sarver (4). The following are some of the results obtained with water at 26·9° C. The initial and final heads of liquid were 13·6 and 5·4 cm. respectively.

P* (cm. of water)....	0	6·34	11·24	22·47	51·74	82·70	112·76
x (cm.)	9·52	9·41	9·43	9·45	9·49	9·49	9·40

The value of K obtained from the slope was $10^{-9}\times 0{\cdot}36140$; the intercept gave $x=9{\cdot}46$ cm. Benzene at 26·9° C. gave $\mathrm{K}=10^{-9}\times 0{\cdot}36179$ with $x=9{\cdot}63$ cm., while water at 89·0° C. gave $x=9{\cdot}65$ cm. In no case was any progressive deviation from linearity noticed when P was plotted against $(\eta\theta+\mathrm{CD})/\theta^2$.

The agreement between the two values of K at 26·9° C. was considered satisfactory. Surface effects appear to cause an uncertainty of about 0·2 cm. in the value of the mean head. Hence, in subsequent work with the instrument a value of 9·58 cm. was assumed, and no pressure of less than 40 cm. of water was used.

References.

(1) See 'Chemistry and Industry,' p. 39 (1945).
(2) Barr, "A Monograph of Viscometry" (Oxford University Press, 1931), p. 69.
(3) Meissner, *Chem. Rev. über die Fett. und Harz-industrie*, xvii. p. 202 (1910).
(4) Bingham and Sarver, J. Amer. Chem. Soc. xlii. p. 2011 (1920).
(5) Bingham and Jackson, "Bureau of Standards," Bull. xiv. p. 59 (1918).

The Technical College,
Birmingham.

XCII. *Determination of the Electric Intensity near an Aerial Cage.*

By J. C. Simmonds, Ph.D., M.Sc.† ‡

[Received November 22, 1945.]

Summary.

Two methods are developed which enable the charge distribution on the wires of an aerial cage to be determined. Once the charge distribution is known, the electric intensity and hence the corona voltage can be found

---

* Corrected by the method of Bingham and Jackson (5).

† Communicated by the Author.

‡ Radio Branch, Engineer-in-Chief's Office, G.P.O.

The first method is applicable to only a small number of wires, whilst the second is only applicable to a large number of wires. The first method is used to check charge distribution measurements made on a rubber sheet, and the rubber sheet is then used to confirm the second method.

1. *Introduction.*

A CAGE formed from a number of wires in the manner shown in fig. 1 is frequently used as the conductor of aerials and lead-outs, and has also been used as the conductor of an inductor of large dimensions. In some cases the potentials concerned are so high that the possibility of corona formation, which involves power loss, must be considered. Corona is due to the ionization of the air in the neighbourhood of a conductor, and the main factor to be considered in determining whether it will occur is the maximum value of the electric intensity *. In designing the cage, it is thus necessary to estimate the values of the maximum electric intensity corresponding to a given potential of the cage, relative to earth or to other conductors.

Fig. 1.

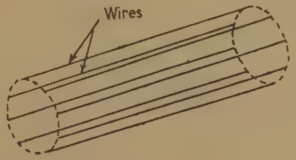

Cage of wires.

The rationalized M.K.S. system of units is used throughout.

2. *Statement of the Problem.*

The cage is assumed to be above and parallel to a conducting plane representing the earth. The section of the cage is taken to be circular, and the wires of which the cage is composed are also of circular section. All the wires forming the cage are assumed to be at the same potential relative to the earth. End effects are neglected, and the field is taken to be purely electrostatic, the dimensions of the system being assumed small compared with one wave-length of the energizing signal. With these assumptions the maximum electric intensity will occur near that wire of the cage which is nearest to the conducting plane. The problem is therefore to determine the maximum electric intensity near this wire. It will be noted that the solution of this problem includes the case of two parallel cages in space, since a conducting plane can be inserted midway between two such cages without altering the field distribution. The first step in the solution is to find the charge on each wire for a given potential of the cage above earth; when the charges are known the electric intensity at any point can be found.

---

* See " Dielectric Phenomena in High Voltage Engineering," by F. W. Peek.

3. *Determination of the Charges on the Wires by the Line-Charge Method.*

Consider a cage of n wires shown in section in fig. 2. An exact solution for the charge on each wire does not appear possible. However, an approximate solution can be obtained as shown below, but even this becomes very laborious when n is large.

Assume that the cross section of the wires shown in fig. 2 shrinks indefinitely so that the charges $q_1, q_2, \ldots q_n$, per metre length, become line-charges. The potential at any point z of the system whose coordinates are (x, y) is given by the real part of the complex potential W, where

Fig. 2.

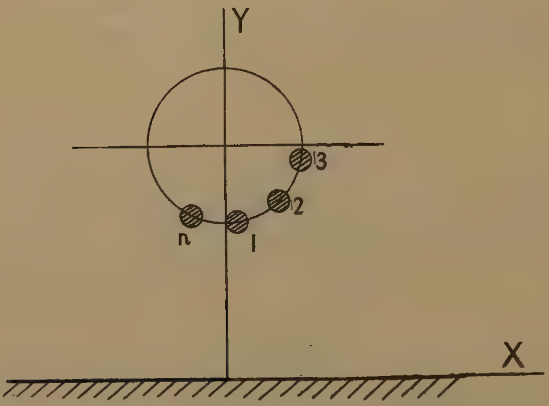

Cage of wires above earth.

$$\mathrm{W}=\mathrm{U}+j\mathrm{V}=\frac{-1}{2\pi\epsilon}\sum_{r=1}^{n} q_r \log\left\{\frac{z-z_r}{z+z_r}\right\},$$

$z=x+jy$,

$z_r=x_r+jy_r$,

x_r, y_r=coordinates of the rth line-charge,

ϵ=permittivity of the dielectric, for air

$\epsilon=\epsilon_0=8{\cdot}85\times10^{-12}$ farads per metre.

Whence,

$$\mathrm{U}=\frac{-1}{4\pi\epsilon}\sum_{r=1}^{n} q_r \log\left\{\frac{(x-x_r)^2+(y-y_r)^2}{(x+x_r)^2+(y+y_r)^2}\right\}.$$

If now z is taken near to each line-charge in turn, at the same distance δ

say from each, n equations will be obtained as below, where U'_s denotes the potential at the point (x'_s, y'_s) distant δ from the sth line-charge.

$$
\begin{aligned}
U'_1 &= \frac{-1}{4\pi\epsilon} \sum_{r=1}^{n} q_r \log\left\{\frac{(x'_1-x_r)^2+(y'_1-y_r)^2}{(x'_1+x_r)^2+(y'_1+y_r)^2}\right\} \\
&\ \ \vdots \\
U'_s &= \frac{-1}{4\pi\epsilon} \sum_{r=1}^{n} q_r \log\left\{\frac{(x'_s-x_r)^2+(y'_s-y_r)^2}{(x'_s+x_r)^2+(y'_s+y_r)^2}\right\} \\
&\ \ \vdots \\
U'_n &= \frac{-1}{4\pi\epsilon} \sum_{r=1}^{n} q_r \log\left\{\frac{(x'_n-x_r)^2+(y'_n-y_r)^2}{(x'_n+x_r)^2+(y'_n+y_r)^2}\right\}.
\end{aligned}
$$

It is now possible to find values of the line-charges such that

$U'_1=U'_2=$ - - - - - $U'_n=U$, these are :

$$
q_r = \frac{\begin{vmatrix}
P_{11} & P_{12} & \cdots & P_{1(r-1)} & 4\pi\epsilon U' & P_{1(r+1)} & \cdots & P_{1n} \\
\vdots & \vdots & & \vdots & \vdots & \vdots & & \vdots \\
P_{s1} & P_{s2} & \cdots & P_{s(r-1)} & 4\pi\epsilon U' & P_{s(r+1)} & \cdots & P_{sn} \\
\vdots & \vdots & & \vdots & \vdots & \vdots & & \vdots \\
P_{n1} & P_{n2} & \cdots & P_{n(r-1)} & 4\pi\epsilon U' & P_{n(r+1)} & \cdots & P_{nn}
\end{vmatrix}}{\begin{vmatrix}
P_{11} & P_{12} & \cdots & P_{1r} & \cdots & P_{1n} \\
\vdots & \vdots & & \vdots & & \vdots \\
P_{s1} & P_{s2} & \cdots & P_{sr} & \cdots & P_{sn} \\
\vdots & \vdots & & \vdots & & \vdots \\
P_{n1} & P_{n2} & \cdots & P_{nr} & \cdots & P_{nn}
\end{vmatrix}}
$$

where

$$
P_{sr} = \log\left\{\frac{(x'_s+x_r)^2+(y'_s+y_r)^2}{(x'_s-x_r)^2+(y'_s-y_r)^2}\right\}.
$$

The equipotential surfaces due to the system of line-charges tend to circular section cylinders concentric with the line-charge as they approach the line-charge. This is obviously true since sufficiently near to a line-charge the potential contribution due to all the other line-charges is negligible compared with the potential contribution due to the line-charge under consideration. If then the line-charges are replaced by charges on circular section cylinders, only small changes in the charges will occur providing the radii of the cylinders are small compared with the distance between them and between the cylinders and earth. The charges on the cylinders can, therefore, be calculated approximately by means of the foregoing equations, taking δ equal to the radius of each cylinder and U′ equal to the potential at the surfaces of the cylinders.

An estimate of the magnitude of error introduced by calculating the charges on the cylinders in this manner can be made by finding the charges required to give the same potential at different points at the same distance δ from the line-charges.

For example, consider the simple system shown in fig. 3. To make the potentials at points "*a*" and "*c*" equal, the charge on line 1 must be 54·8 per cent. of the total; to give equal potentials at points "*b*" and "*d*" the charge on line 1 must be 56·3 per cent. of the total; whilst to give equal potentials at "*b*" and "*c*" the charge on line 1 must be 55·2 per cent. of the total.

Fig. 3.

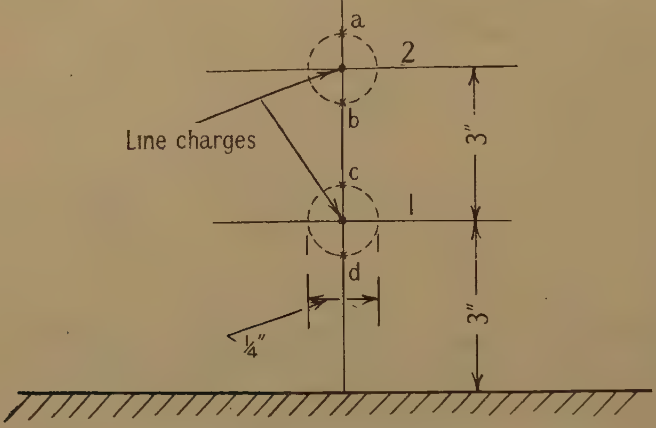

Potential near line-charges.

If the wires in the cage are symmetrically disposed relative to the "*y*" axis then the number of unknown charges will be $n/2$ for n even. Thus the charges on a six-wire cage can be easily found by this method, an eight-wire cage is rather laborious because fourth order determinants have to be evaluated. For a large number of wires the method becomes almost impracticable unless a machine for solving simultaneous equations is available.

4. *Solution of Potential Problems by Elastic Membrane.*

It can be shown that a stretched elastic membrane when displaced from the datum level obeys approximately the equation [*]

$$\frac{\partial^2 H}{\partial x^2}+\frac{\partial^2 H}{\partial y^2}=0,$$

where H is the displacment.

---

[*] P. B. Moon and M. L. Oliphant, Proc. Camb. Phil. Soc. xxv. p. 461 (1929).

This is Laplace's two-dimensional equation which is obeyed by all two-dimensional electrostatic fields. We have then a direct analogy between displacement from a datum level, loading on the membrane, and slope of the membrane on the one hand and difference of potential, charge and electric intensity on the other hand.

A suitable membrane can be made by stretching a thin sheet of elastic rubber, usually horizontally, and loading as desired. Such an arrangement has been used by several investigators—mainly for the solution of problems connected with thermionic valves *.

A suitable sheet of rubber, about $3' \times 3'$ and 0·010–0·014 inches thick, was obtained, and a length of red rubber tube about $\frac{3}{8}''$ diameter was cemented to the edge of the sheet. A frame to support the sheet was constructed from electrical conduit and the sheet suspended from it by a number of strings and battery clips. A sketch of the arrangement is shown in fig. 4.

Fig. 4.

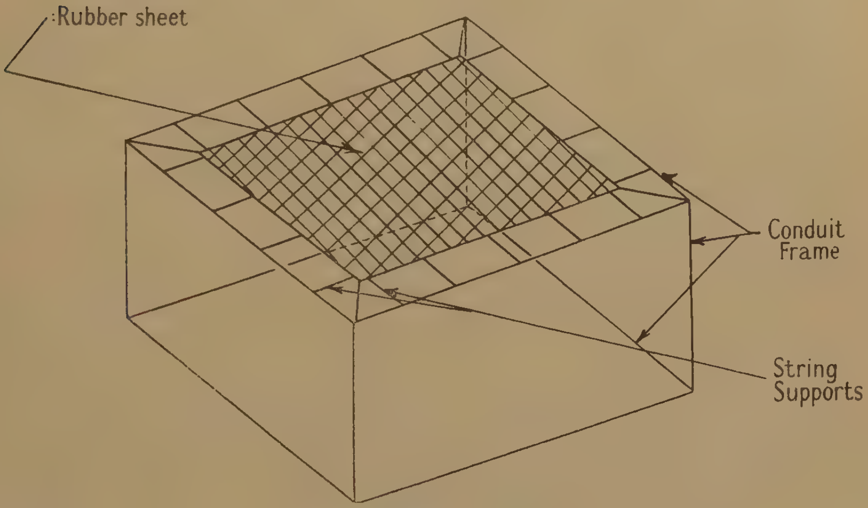

Rubber sheet and frame.

4.1. *Check Measurements on Rubber Sheet.*

To check that the rubber sheet results are reliable, measurements were made on simple configurations. First a circular lamp shade about 13·75 inches diameter was placed beneath the sheet and raised so that the rim of the shade just lifted the sheet. The flange of a reel of wire, 2·2 inches diameter, was used as another electrode, and was first placed coaxial with the outer boundary. The displacement of the rubber beneath the reel was then measured relative to the flange of the shade. This arrangement is obviously analogous to the electrostatic problem of a charged circular cylinder coaxial with an outer circular cylinder. The displacement is, therefore, inversely proportional to the capacitance of the electrostatic system. This capacitance was calculated for one metre length of the cylinders. The reel of wire was then off-set from the centre of the shade by an amount δ and the displacement again measured. From the original displacement, the new displacement and the calculated capacitance, the capacitance of the new systems follows directly. This was repeated for a number of values of δ and the capacitances plotted against δ as shown in fig. 5. The curve shown on the figure gives the theoretical capacitances of the eccentric systems.

---

* P. H. J. A. Kleynen, Phillips Techn. Rev. ii. p. 338 (1937); J. R. Pierce, Bell Labs. Record, xvi. p. 305 (1938); J. H. Fremlin, Phil. Mag. xxvii. p. 709 (1939).

Fig. 5.

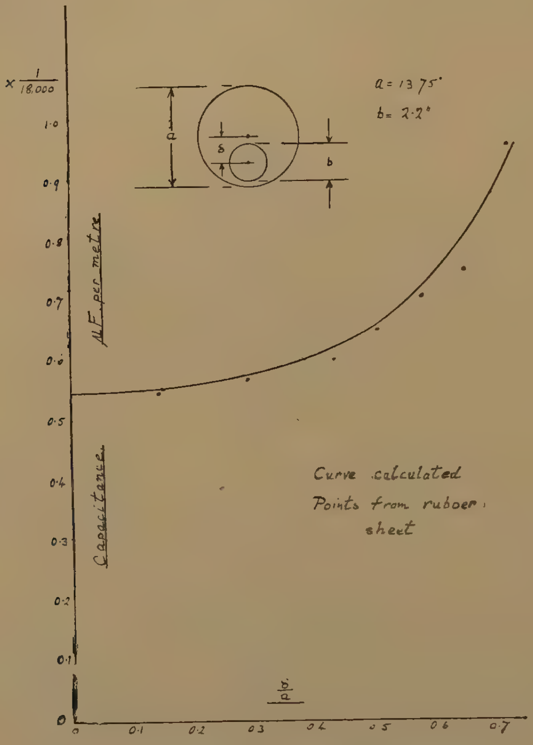

Capacitance between eccentric cylinders.

Next a straight line boundary was obtained by placing a brass bar underneath the sheet at one end and raising it just to take the weight of the sheet; a similar boundary was also erected at the other end of the sheet. A circular electrode, 3″ diameter was cut from sheet aluminium and placed on the rubber sheet with its centre distant D from one of the boundaries, D being, of course, small compared with the dimensions of the sheet. Load was placed on the electrode to give a displacement of 0·5 inch below the datum level by means of a simple lever arrangement. Care was taken to ensure that the electrode was level, this being effected by applying the load off the centre of the electrode. In this way the load required to give a displacement of 0·5 inch was found for several values of D. The analogous electrostatic problem is that of a long circular cylinder parallel to an earthed plane. Obviously the load is proportional to the capacitance of the system and, by calculating the capacitance per metre length of cylinder at one spacing, the constant of proportionality can be determined. The experimental results are shown in fig. 6, together with a theoretical curve of capacitance.

4.2. *Comparison with Line-charge Method.*

The simple system dealt with in section 3, and shown in fig. 3, was set up on the rubber sheet, but in this and subsequent experiments it was found more convenient to load the sheet from below. The load required at each electrode to give the same displacement above the datum level was measured; one electrode being made rigid in turn. Since the load is analogous to charge, the percentage of the total charge carried by either cylinder, in the electrostatic case, is equal to the percentage of the total load carried by either electrode. The actual charge carried by each cylinder may be found by calibrating the rubber sheet, using one electrode only and loading to give the same deflection. The capacitance per metre length of the corresponding electrostatic system can be calculated, and thence the charge per metre length is known in terms of the potential difference (since Q=CU). From this the relationship between charge and load follows directly.

Fig. 6.

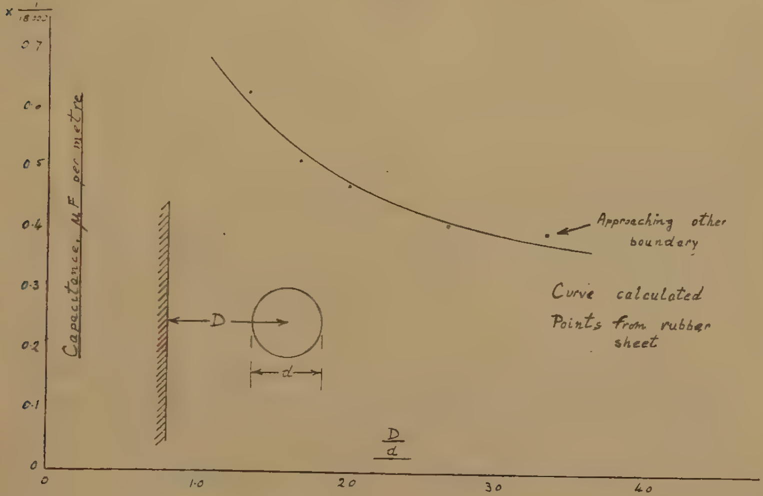

Capacitance between cylinder and plane.

Three entirely separate measurements on the sheet gave the percentage charge on cylinder 1, 55·2, 55·8, and 56 per cent. of the total. The average value is, therefore, 55·5 per cent., whilst the average of the calculated charges is 55·4 per cent. The measured and calculated total charges on the system differed by less than 3 per cent.

Measurements on other relatively simple systems have been made and compared with calculated values. The percentage distribution of charge is shown in fig. 7, whilst the agreement between the measured and calculated total charges was nearer than 5 per cent. in all cases. The results show that the charge on the wires of a cage can be determined with a fair degree of accuracy by means of the rubber sheet.

Fig. 7.

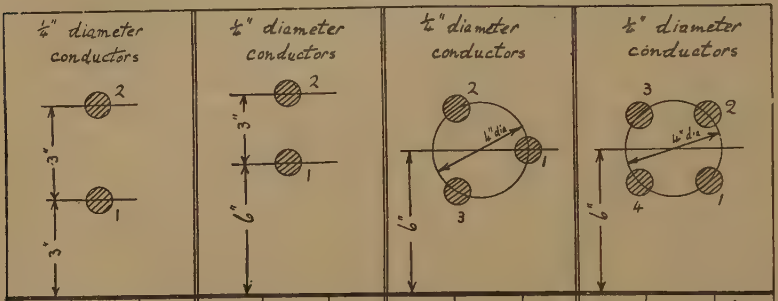

No.	%	%	No.	%	%	No.	%	%	No.	%	%
1	55·4	55·4	1	53·6	53·7	1	34·0	33·2	1	28·5	28·2
2	44·6	44·6	2	46·4	46·3	2	30·0	29·4	2	21·5	21·8
						3	36·0	37·4	3	21·5	21·8
									4	28·5	28·2

% charge given in first column measured by rubber sheet.
% charge given in second column calculated—see section 3.
Distribution of charge between parallel circular cylinders.

5. *Charge Distribution of a Cage of Wires.*

Two methods of determining the way in which the charge is shared by the wires of a cage are now available—one by measurement on the rubber sheet and the other by calculation. The first method would often be impracticable as the size of sheet is limited, and scaling down would lead to very small diameter electrodes. The second method is impracticable for cages consisting of more than eight or so wires. It is necessary, therefore, to develop a less restricted method.

Accordingly the charge distribution on a six-wire cage, see fig. 8, was measured by the rubber sheet method. The results obtained are shown in the figure.

Referring to fig. 9, it is easily shown that for a charged circular cylinder parallel to a conducting plane the percentage of the total charge on the arc $(\theta_2-\theta_1)$ is

$$\frac{(V_1-V_2)}{2\pi}\times 100, \quad \text{where} \quad \cot V=\frac{R\sec\theta+D\tan\theta}{\sqrt{D^2-R^2}}.$$

The total charge on the cylinder for any potential can be obtained from fig. 6 (the range being extended if necessary). If the section of the cylinder is split into six arcs, each centred on the wires shown in fig. 8, and the percentage charge on each arc calculated, the results shown in the figure are obtained. The charge carried by each cylinder per metre was measured by the rubber sheet method and the results are given in the figure. It is seen from these results that the percentage charge carried by each arc is a tolerably good approximation to the percentage

Fig. 8.

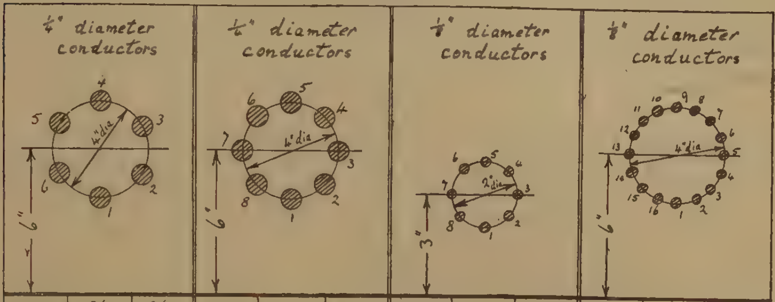
¼" diameter conductors
4" dia
6"
¼" diameter conductors
4" dia
6"
⅛" diameter conductors
2" dia
3"
⅛" diameter conductors
4" dia
6"
1
2
3
4
5
6
7
8
9
10
11
12
13
14
15
16

No.	%	%	No.	%	%	No.	%	%	No.	%	%
1	20·9	23·0	1	16·7	17·5	1	19·1	17·5	1	7·5	8·8
2	18·4	18·9	2	15·3	15·4	2	15·2	15·4	2, 16	7·5	8·5
3	14·7	13·9	3	12·3	11·8	3	12·1	11·8	3, 15	7·3	7·6
4	12·7	11·4	4	9·7	9 5	4	9·1	9·5	4, 14	6·8	6·8
5	14·7	13·9	5	9·7	9·0	5	8 2	9·0	5, 13	6·5	5·9
6	18·4	18·9	6	9·7	9·5	6	9·1	9·5	6, 12	5·3	5·1
			7	12·3	11·8	7	12·1	11·8	7, 11	5 0	4·9
			8	15·3	15·4	8	15·2	15·4	8, 10	5·3	4·5
									9	5·3	4·4

% charge given in first column measured by rubber sheet.
% charge given in second column calculated—see section 5.

Distribution of charge between parallel circular cylinders

Fig. 9.

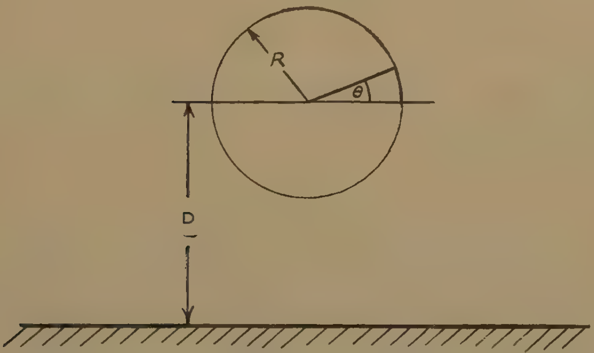

Charge distribution on cylinder.

charge carried by each wire, even in a case where relatively few wires are used and the cage is relatively near the earth *. Similar measurements were made on other similar systems and the results are shown in fig. 8. In every case the measured and calculated total charges agreed to within 20 per cent., and to within 10 per cent. when only eight and six cylinders were used. The large errors in the case of the sixteen cylinders is no doubt largely due to the small loads carried by each electrode and the consequent difficulty in determining them. Also non-uniformity of the sheet would presumably be more apparent the smaller the diameter of the electrodes.

The spacing between the cage and the earthed plane will usually be greater than that used in these experiments. In these circumstances it seems quite reasonable to believe that the charge carried by each wire would approximate even more closely to the charge carried by the corresponding arc of a cylinder.

Fig. 10.

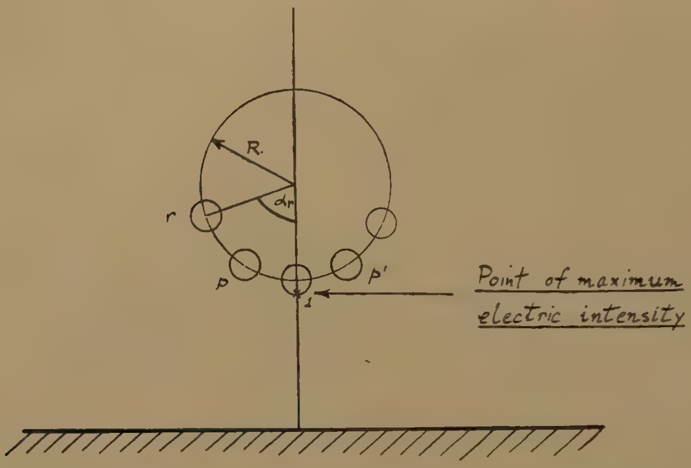

Point of maximum electric intensity near an aerial cage.

6. *Determination of the Maximum Electric Intensity.*

Methods of estimating the charge on each wire of a cage are now available. For a cage of only a few wires the method of section 3 may be used, whilst for more than six wires and reasonable cage dimensions the charge can be estimated from the distribution of charge on a cylinder of the same diameter as the cage. The maximum electric intensity will obviously occur at the point indicated in fig. 10, assuming the configuration shown in the figure. The contribution to the electric intensity in the vicinity of wire 1 from a pair of wires, one either side of the bottom wire, say p and p' in the figure is vertical and is

---

* The writer is indebted to Mr. D. E. Watt-Carter for suggesting that this would be so.

$$E_p = \frac{-q_p}{\pi\epsilon d},$$

where d=diameter of the cage.

The total electric intensity in the vicinity of wire 1 due to all charges except that on wire 1 is, therefore,

$$E_1 = \frac{-1}{\pi\epsilon d} \sum_{p=2}^{\left(\frac{n-a-1}{2}\right)} q_p - \frac{a q_{\left(\frac{n}{2}+1\right)}}{2\pi\epsilon d},$$

where $a=0$ when n is odd and $a=1$ when n is even.

It is now necessary to find the electric intensity in the vicinity of wire 1 due to the charge induced on the earth. This produces exactly the same effect as an image of the system in the earth plane. If the height above earth of the cage is large compared with the dimensions of the cage then obviously the image will produce little effect at the point under consideration. The contribution to the electric intensity, however, is given by

$$E_2 = \frac{-1}{2\pi\epsilon} \sum_{r=1}^{r=n} q_r \left\{ \frac{2D-R-R\cos\alpha_r}{(2D-R-R\operatorname{cosec}\alpha_r)^2 + R^2\sin^2\alpha_r} \right\},$$

where α_r=the angle shown in fig. 10.

The electric intensity in the vicinity of wire 1 due to all charges except that on wire 1 is, therefore,

$$E_0 = E_1 + E_2 = \frac{-1}{\pi\epsilon d} \sum_{r=2}^{\left(\frac{n-a-1}{2}\right)} q_p - \frac{a q_{\left(\frac{n}{2}+1\right)}}{2\pi\epsilon d}$$
$$- \frac{1}{2\pi\epsilon} \sum_{r=1}^{r=n} q_r \left\{ \frac{(2D-R-R\cos\alpha_r)}{(2D-R-R\cos\alpha_r)^2 + R^2\sin^2\alpha_r} \right\}.$$

We may now regard wire 1 as being situated in a uniform field E_0. In these circumstances it can be shown that the maximum electric intensity is

$$E = \frac{-q_1}{\pi\epsilon d_w} + 2E_0\,^*,$$

where d_w=diameter of wire.

7. *Conclusions.*

Methods of estimating the maximum electric intensity near a cage of circular wires have been given. One method, based upon the assumption that the wires are of small diameter compared with the distance apart, can theoretically be applied to any number of wires but in practice is restricted to only a few wires due to computational difficulties. This method should be capable of good accuracy providing the initial assumption is justified. The other method is applicable when the cage is formed from a large number of wires so that the distance apart is relatively small compared with the cage diameter. This method is simple to apply and should give the electric intensity at least to within about 20 per cent., a degree of accuracy which should be ample in view of the large factors of safety usually employed in corona problems.

---

* See 'Principles of Electricity,' by Page and Adams.

The author's thanks are due to the Engineer-in-Chief of the Post Office for permission to publish, and to Messrs. R. C. Looser, B.Sc. and W. A. Baxter for assistance with the experimental work.

XCIII. *On the Solid Solutions of Chromium and Manganese in Aluminium.*

By G. V. Raynor, M.A., D.Phil., The Department of Metallurgy,
The University of Birmingham *.

[Received June 25, 1945.]

I. *Introduction.*

In recent papers (1), (2), (3) investigations of the aluminium-rich alloys of the systems aluminium–copper–manganese, aluminium–manganese–nickel and aluminium–chromium–manganese have been described. Comparison of the constitutional diagrams of these systems shows that both atomic and electronic factors may be operative in affecting the equilibrium in this type of alloy. In the systems aluminium–copper–manganese and aluminium–manganese–nickel, well-defined ternary compounds enter into equilibrium with the primary aluminium-rich solid solution. In both cases, the ternary compound is based upon an atomic ratio of four aluminium atoms to one (Mn+X) atom, where X represents copper or nickel. The ratio Mn : Ni in the one compound is different from the ratio Mn : Cu in the other, and this difference may be interpreted in terms of the Pauling theory of transitional metals.

According to the Pauling theory of the metals from chromium to nickel in the Periodic Table (4), 5·78 of the electrons of the 4*s* and 3*d* quantum groups are in each case employed in cohesion. The remainder of the electrons build up round the atom in " atomic orbitals." On semi-empirical grounds, it is deduced that there are 2·44 of these atomic orbitals, each of which may contain two electrons of opposite spin. Each orbital, however, tends to be occupied by one electron only, until the number of electrons to be accommodated exceeds 2·44 ; above this limit, some orbitals must contain two electrons with paired spin. On this model, therefore, chromium, with six electrons in the 3*d* and 4*s* groups, has only 0·22 electrons in atomic orbitals. Manganese and iron have respectively 1.22 and 2·22 electrons in atomic orbitals. For cobalt, the number of electrons in atomic orbitals (3·22) exceeds 2·44, and, from magnetic evidence, it is suggested that there are 1·71 unpaired and 1·51 paired electrons in atomic orbitals. For nickel, the corresponding figures are 0·61 and 3·61. According to this scheme, therefore, since the atomic orbitals can accommodate 4·88 electrons in each case, there must be vacancies for electrons to the following extent :—

---

* Communicated by the Author.

Cr, 4·66 ; Mn, 3·66 ; Fe, 2·66 ; Co, 1·71 ; Ni, 0·61.

If it is now assumed that, in the alloys of transitional elements with aluminium, the transitional metal atoms act as electron acceptors by filling up their atomic orbitals to the maximum extent possible on the above theory, the two ternary compounds referred to above are found to occur at the same ratio of valency electrons per atom (1·85).

In the case of the aluminium–chromium–manganese system, since the chromium atom has more vacancies in its atomic orbitals than has the atom of manganese, it is impossible to attain an electron : atom ratio of 1·85 with a ratio of four aluminium atoms to one transitional metal atom. It is significant that in this system no ternary compound corresponding with those in the aluminium–copper–manganese and aluminium–manganese–nickel systems is obtained.

The formation of ternary compounds of this type may therefore be governed by the simultaneous satisfaction of atomic and electronic conditions, the transitional metals acting as electron acceptors, and exhibiting an effectively negative valency.

The tendency of transitional metal atoms to absorb electrons should also be recognizable in the primary aluminium-rich solid solutions. Evidence in this connection is given by an examination of the lattice-spacing-composition curves for chromium and manganese in aluminium.

II. *Solid Solutions of Chromium in Aluminium.*

The face-centred cubic metal aluminium, with three valency electrons, is characterized by a first Brillouin zone from which there is a moderate overlap of electrons across the (200) planes (5). According to the theory of H. Jones (6) an overlap of electrons across the face of a Brillouin zone leads to internal stresses in such a sense that the zone tends to contract in a direction at right angles to the overlapped plane. Any diminution of the overlap therefore allows the zone to expand, and there is a corresponding contraction of the lattice. Similarly, an increase in the number of overlapping electrons leads to a contraction of the Brillouin zone and an expansion of the lattice. Application of this theory (7) accounts satisfactorily for the variation of the apparent size of the aluminium atom in solid solution in various solvents.

The solution in aluminium of an element of lower valency, by reducing the number of valency electrons in the structure, causes a reduction in the overlap of electrons across the planes bounding the Brillouin zone for aluminium. This gives rise to a tendency for the lattice spacing of the solid solution to contract relatively to the lattice-spacing-composition curve as deduced from the atomic diameters of the components (Vegard curve). In a similar manner, the solution of a metal of higher valency in aluminium will tend to give rise to an expansion of the lattice relative to the curve deduced from Vegard's law.

As an example of the operation of this principle, the solid solution of magnesium in aluminium may be considered. The interatomic distance at room-temperature in the crystal of magnesium (close-packed hexagonal structure, co-ordination number 12) is 3·2 A., so that the lattice spacing of a hypothetical face-centred cubic structure in which the same interatomic distance was preserved would be 4·5254 A. If the relative sizes of the atoms alone controlled the lattice-spacing relationships, the lattice-spacing curve would be expected to follow the broken line in fig. 1, obtained by drawing a straight line between the values 4·0402 A. for aluminium and 4·5254 A. for magnesium. The experimental results of Schmid and Siebel (8) are plotted as a full line in fig. 1, and it is clear that there is a contraction relative to the broken curve.

Fig. 1.

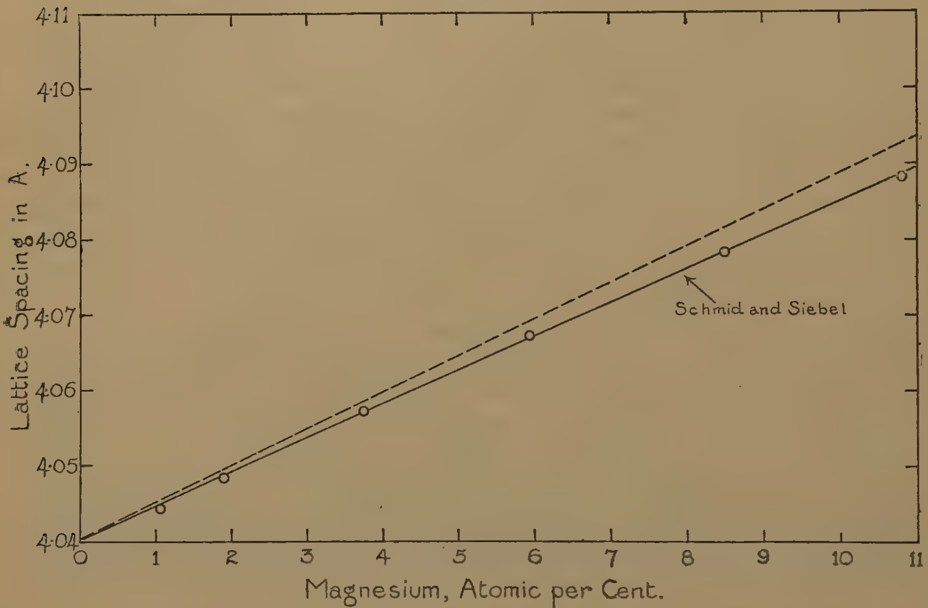

If chromium, when dissolved in aluminium, behaves as an element of effective negative valency by absorbing electrons, from the structure as a whole, into its vacant atomic orbitals, a considerable reduction in the number of overlapping electrons is to be expected. The lattice-spacing-composition curve for the primary solid solution of chromium in aluminium should therefore show a marked contraction relatively to the Vegard curve.

The interatomic distance in the crystal of chromium is 2·4929 A. ; the crystal structure is body-centred cubic with co-ordination number 8. In order to obtain the interatomic distance corresponding with a structure of co-ordination number 12, it is necessary to multiply this value by 1·03, in accordance with the work of Goldschmidt (9), who states that a change in co-ordination number from 8 to 12 is accompanied by an expansion of 3 per cent. The required interatomic distance is therefore 2·57, corresponding with a lattice spacing of 3·6345 for a hypothetical face-centred cubic structure.

In fig. 2 the broken line shows the lattice-spacing curve to be expected on size-factor principles alone, while the full curve shows the experimental results of Koch and Winterhager (10). There is a very marked additional contraction in the experimental curve in agreement with the theory.

Fig. 2.

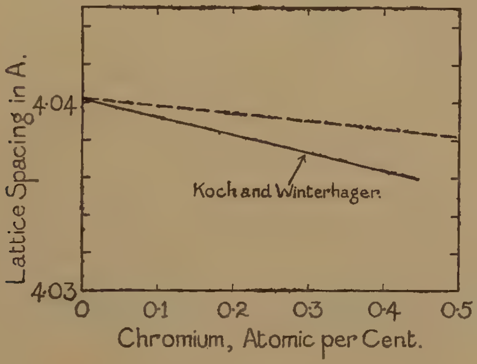

III. *Solid Solutions of Manganese in Aluminium.*

Since manganese, like chromium, has vacancies for electrons in the atomic orbitals considered by Pauling, analogous results on comparing the experimental lattice spacing curve with the Vegard curve may be expected. It is, however, difficult to obtain a satisfactory assessment of the atomic diameter of manganese.

The crystal structure of α-manganese (the form stable below 742° C.) is very complicated, and, as shown by Bradley and Thewlis (11), may be regarded as built up from atoms with four types of environment. Each atom is surrounded by from thirteen to sixteen other atoms, and the interatomic distances are given in Table I.

It will be noted that the symmetrically-distributed group of twelve atoms surrounding each X atom lies at a distance of 2·71 A. from the central atom ; this appears to be the nearest approach which can be obtained to an interatomic distance for co-ordination number 12.

It is of interest to consider the average values of the distances of the atoms from the D_1, X, D_2 and A atoms in turn. The D_1 atoms are surrounded by 13 atoms at an average distance of 2·59 A.; the X atoms are surrounded by 16 atoms at an average distance of 2·74 A.; the corresponding figures for the D_2 and A atoms are 13 neighbours at an average distance of 2·63 A. and 2·76 A. respectively. These average values are thus divided into two sets, one of the order of 2·6 A. and the other of the order 2·75 A. The overall average distance apart of atoms in the α-manganese crystal structure, corresponding to an average co-ordination number of 13·75, may be written $\frac{2\cdot59+2\cdot74+2\cdot63+2\cdot76}{4}$ or 2·68 A. This distance compares very closely with the distance (2·71 A.) of the twelve symmetrically situated atoms surrounding each X atom.

TABLE I.

D_2 atoms.		X atoms.	
1 neighbour at	2·24 A.	12 neighbours at	2·71 A.
2 neighbours at	2·38	4 neighbours at	2·82
1 neighbour at	2·45		
2 neighbours at	2·51		
2 neighbours at	2·66		
2 neighbours at	2·69		
1 neighbour at	2·71		
2 neighbours at	2·89		

D_1 atoms.		A atoms.	
1 neighbour at	2·45 A.	3 neighbours at	2·49 A.
1 neighbour at	2·49	3 neighbours at	2·69
2 neighbours at	2·51	1 neighbour at	2·82
2 neighbours at	2·66	3 neighbours at	2·89
6 neighbours at	2·67	3 neighbours at	2·96
1 neighbour at	2·96		

The value of 2·7 A. may be arbitrarily taken as the interatomic distance for manganese with a co-ordination number of 12. Although in the actual α-manganese crystal structure both larger and smaller interatomic distances are found, this value is close to the average of the observed values.

Some justification for the choice of the value 2·7 A. is given by a consideration of the crystal structure of the quenched Heusler alloy Cu_2MnAl, which has been examined by Persson (12), and by Bradley and Rodgers (13). The structure is cubic, and the unit cell may be regarded as built up from eight small body-centred cubes (fig. 3); at the cube centres characterized by the co-ordinates $(\frac{3}{4}, \frac{3}{4}, \frac{3}{4})$, $(\frac{3}{4}, \frac{1}{4}, \frac{1}{4})$, $(\frac{1}{4}, \frac{3}{4}, \frac{1}{4})$ and $(\frac{1}{4}, \frac{1}{4}, \frac{3}{4})$ manganese atoms are situated, while the other cube centres are occupied by aluminium atoms. The lattice spacing is 5·950 A. In this structure, each atom clearly has the co-ordination number 8, and the Cu–Mn. distance is $\frac{5\cdot95}{2} \times \frac{\sqrt{3}}{2}$ or 2·57 A. The atomic radius ($\frac{1}{2}$ interatomic distance) for copper, corrected to co-ordination number 8, is 1·24 A., so that the atomic diameter for manganese, at co-ordination number 8, is 2×1·33 or 2·66 A. For a co-ordination number of 12, therefore, the atomic diameter of manganese, as deduced from the alloy Cu_2MnAl, is 2·66 (1·03) or 2·74 A.

The lattice spacing of a face-centred cubic structure with an interatomic distance of 2·7 A. would be 3·8184 A., and if this value is used to calculate the lattice-spacing curve corresponding to Vegard's law, the broken curve in fig. 4 is obtained. The full curve in fig. 4 shows the experimental results obtained by Hofmann(14), and it is clear that there is again a marked contraction of the lattice relative to that calculated from the sizes of the component atoms.

Fig. 3.

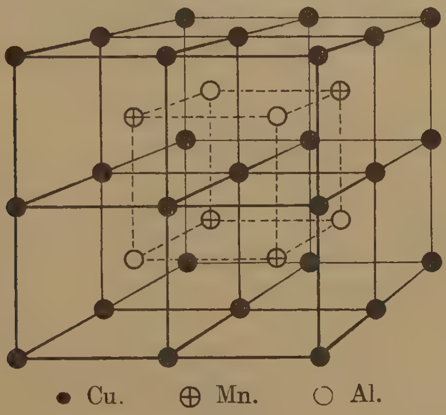

Fig. 4.

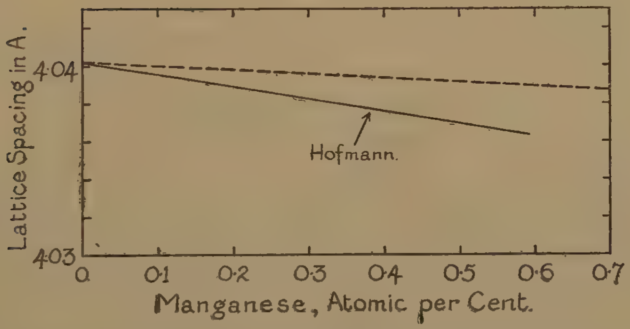

IV. *Discussion of Results.*

The lattice spacing curves for the primary solid solutions of chromium and manganese in aluminium, as shown in figs. 2 and 4, indicate that there is a pronounced contraction of the lattice relative to that to be expected from size considerations. In fig. 5 the deviation from the curve calculated from the sizes of the component atoms is plotted for the solutes magnesium, aluminium and manganese. The deviation for magnesium is very small compared with those for the transitional elements, in agreement with the hypothesis that transitional elements are much more effective in reducing the overlap from the aluminium Brillouin zone. The deviation for chromium is greater than that for manganese; this is to be expected, since, according to the suggestions made above with regard to the role of transitional elements in solid solution in aluminium, chromium may accept electrons up to a limit of 4·66 per atom, as compared with the number 3·66 for manganese. One atomic per cent. of chromium can therefore reduce the overlap from the Brillouin zone to a greater extent than can an equal amount of manganese, giving rise to a more marked contraction.

Fig. 5.

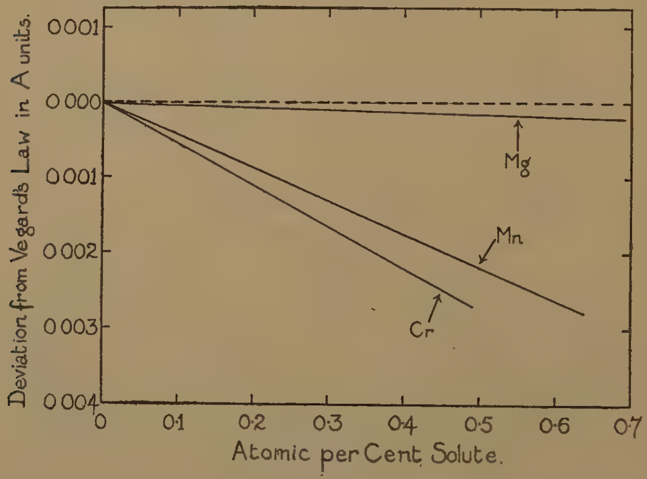

It is of interest to note than the slopes of the curves for manganese and chromium as shown in fig. 5 are in the ratio 1 : 1·26, which is almost exactly the same as the ratio of the numbers of unoccupied atomic orbitals in manganese and chromium; this ratio is 3·66 : 4·66=1 : 1·27. This exact agreement is not thought to be significant, since it depends upon the somewhat arbitrary choice of the value 2·7 A. for the atomic diameter for manganese for co-ordination number 12. Since, however, the atomic diameter for manganese in alloys with this co-ordination number probably lies between 2·65 and 2·75 A., the relative slopes of the deviation curves in fig. 5 cannot differ greatly from that quoted above. In these aluminium-rich alloys, therefore, the deviation of the lattice-spacing curve from the curve calculated assuming Vegard's law is, at equiatomic percentage of solute, approximately proportional to the number of unoccupied atomic orbitals per atom in the crystal of the solute element.

References.

(1) G. V. Raynor, J. Inst. Metals, lxx. p. 507 (1944).
(2) G. V. Raynor, J. Inst. Metals, lxx. p. 531 (1944).
(3) G. V. Raynor and K. Little, J. Inst. Metals, lxxi. p. 493 (1945).
(4) L. Pauling, Phys. Rev. (ii.) liv. p. 899 (1938).
(5) N. F. Mott and H. Jones, Proc. Roy. Soc. (A), clxii. p. 49 (1937).
(6) H. Jones, Proc. Roy. Soc. (A), cxlvii. p. 400 (1934).
(7) W. Hume-Rothery and G. V. Raynor, Proc. Roy. Soc. (A), clxxvii. p. 27 (1940).
(8) E. Schmid and G. Siebel, *Z. Metallkunde,* xxiii. p. 202 (1931).
(9) V. M. Goldschmidt, *Z. physikal Chem.* cxxxiii. p. 397 (1928).
(10) W. Koch and H. Winterhager, *Metallwirtschaft,* xvii. p. 1159 (1938).
(11) A. J. Bradley and J. Thewlis, Proc. Roy. Soc. (A), cxv. p. 456 (1927).
(12) E. Persson, *Z. Physik.* lvii. p. 115 (1929).
(13) A. J. Bradley and J. W. Rodgers, Proc. Roy. Soc. (A), cxliv. p. 340 (1934).
(14) W. Hofmann, 'Aluminium,' xx. p. 865 (1938).

XCIV. *The Behaviour of Glass under Impact and Static Loading** †.

By R. N. Haward, B.Sc., Ph.D. ‡

[Received August 28, 1944.]

[Plates VIII.–X.]

Abstract.

Numerous experiments have been performed on the strength of glass in the form of beams and plates. The beams, cut from sheet glass approximately 0·28 cm. thick, were tested by a slow loading test and by the impact of a pendulum. The squares were tested both by pressing a steel ball against the square and also by the impact of a falling ball.

It was shown that in the case of slow impact when using objects much heavier than the glass, the energy required to break the glass is greater than that needed under static conditions. The difference can be explained

---

* The following symbols used in this paper generally follow the British Standard Handbook No. 560, 1934. Where they differ from those used by Professor S. Timoshenko, to whose book several references are made, his symbols are given in brackets afterwards. V, velocity; t, the time; E, Young's modulus of elasticity; f, the modulus of rupture or bending strength; P, the aggregate normal force; δ, the deflection of a plate or beam; σ, (ν) Poisson's ratio; n, the frequency of vibration; L, the length of a beam; h, the thickness of a beam or plate; a, the side of a square plate; ρ, the specific gravity; p_m (σ max.), the maximum stress; v, the coefficient of variation $\left(\frac{\text{standard deviation}}{\text{average value}} \times 100\right)$ for a series of measurements.

† Read at the Sheffield Meeting of the Society of Glass Technology, November 24th, 1943.

‡ Communicated by Professor W. E. S. Turner, F.R.S.

if the known changes in the modulus of rupture of glass with time are taken into account. As the velocity of impact is increased, however, the energy required to shatter a glass plate generally diminishes markedly. This decrease in strength is ascribed to the operation of stresses, due to the weight of the glass, the initial value of which is given approximately by the relation $V\sqrt{E\rho}$.

When glass is broken by small balls at high velocites characteristic cone or " shell " fractures are produced, which appear to be an extension of the statically formed ring cracks along lines perpendicular to the maximum tension in the glass.

The coefficients of variation of the measured quantities are given in a number of cases. Impact tests give a larger variation in the results than static tests since the former give estimates of the energy required to break and hence contain the term $(f(1+v))^2$, where v is the coefficient of variation of the stress required to break.

INTRODUCTION.

THE course and effect of the rupture of glass, which takes place under tension, differ in many ways from those associated with the breaking of other materials. The most striking difference is that of being dependent on the size and shape of the specimen under test, a property most strikingly shown in thin fibres (1), although it must be borne in mind that a somewhat similar effect is shown by metals (2), by drawn nylon (3), and other plastics (4). What is remarkable and characteristic of glass is that this variation in very small specimens also occurs in large bulks of the material, giving a general decrease in the " bending strength " or modulus of rupture as the dimensions of the speicmen are increased (5). Experiments by A. J. Holland and W. E. S. Turner have also shown that the strength of beams is greater when they are broken with the diamond-cut edges in compression than in tension (6), and can be markedly increased by polishing (7). Similarly, sulphur, sulphur dioxide in furnace gases reacts with the glass at the surface under certain conditions, and effects the strength favourably (8).

As a result of these and other experiments, it has been generally concluded that the strength of glass is controlled by the distribution of flaws within the material, a theory which also explains the large variations obtained between similar test-pieces broken under like conditions (9). Such flaws may be widely distributed so that their spheres of influence overlap (10) and, as a consequence of them, the strength of glass is a property which has a meaning only in a statistical sense.

Values of bending strength, therefore, must also be coupled with a statement of the size and shape of the piece tested. It would appear that the fundamental property of the glass is not so much its bulk strength as the distribution of flaws within it. On the basis of such a theory an interesting attempt to correlate strength measurements has been made by J. Bailey (11).

Besides the variations mentioned, the effects of water (12) and weathering (13) have also been investigated, but indefinite results have been obtained so far as small humidity changes have been concerned (14). With large humidity changes F. W. Preston (15) has shown that very considerable alterations of strength occur, and he has estimated that the errors involved due to this source in ordinary laboratory measurements may amount to a "few per cent." It has been clearly established, however, that the statistical average bending strength is strongly influenced by the rate of loading or other factors controlling the time occupied by the tests (16); and J. B. Murgatroyd (17) has suggested that the property is due to the slow extension of small cracks *. Of these investigations two have particular interest for the purpose of the present paper. First, A. J. Holland and W. E. S. Turner give an empirical equation to relate the bending strength, or modulus of rupture (f) as a function of the time (t) *i. e.*, $f=\mathrm{K}\left(\frac{1}{t}\right)^{\frac{1}{12\cdot 8}}$. Secondly, F. W. Preston's work (18) is important because the breaking of glass was studied down to times as short as 10^{-2} second, and the curve of bending strength against time is shown to be continuous for a range of 10^7 in time. Furthermore, the relation of Holland and Turner can be applied to these results. giving calculated results in fair agreement with the observed, the error being within ± 15 per cent.

In general, significant experiments on the strength of glass should exclude, where possible, unusual shapes which are liable to give rise to regions of stress concentration (19) and may be conveniently based on rectangular pieces of glass. In these circumstances a given series of experiments will lead to a result for the bending strength or modulus of rupture (f), which may be written $f_{(abc,\,t)}$, where a, b, c are the dimensions, t is the average duration of the experiments and f is expressed in kg./sq. cm.

It follows that in the average case, the most highly stressed part of a test-piece will before breaking absorb $\frac{1}{2}\,(f_{abc,\,t})^2/\mathrm{E}$ kg. cm. work per cm.^{3}, and that for a given geometrical form of the test-piece under a given form of test (for example, a beam of given size breaking under central stress) the average total work absorption will be proportional to the same figure so long as the total deformation at the break is controlled by the elasticity. The significance of this reservation will be discussed later.

If we now extend this generalization to cover a wide range of time and, in particular, to the long and short intervals involved, respectively, in bending and impact tests, we can conclude that the work required to break a beam of glass is proportional to $(f_{abc,\,t})^2$; and if we assume that the effect of time is such that it produces the same proportional change in f

---

* This process has recently been the subject of considerable discussion, and Orowen, 'Nature,' cliv. p 341 (1944), has put forward a theory, according to which diffusion in an adsorbed layer of water or other impurities is responsible for the time factor.

for different conditions of edge treatment, it follows that for a beam of given dimensions:

$$\frac{\text{Impact strength}}{(\text{Slow bending strength})^2} \sim \text{constant } (cf. \text{ Haward}^{(20)}). \quad . \quad . \quad (1)$$

Further, if we now treat our impact experiments so as to derive the highest stress present at the time of rupture, as described by F. W. Preston (21), we may check the value of $(f_{abc,\,t})$ so obtained, with predicted values based on the application of existing empirical equations (22) to the slow breaking experiments.

One point may be noted here. Since, in any assembly of measurements of bending strength based on individual breaking experiments, there is a wide distribution of values, with a coefficient of variation v often up to 20 per cent., it follows from the above theory that the work absorption in impact experiments which contain $(f_{abc,\,t})^2$ will in the average case be proportional to

$$(f_{abc,\,t}(1\pm v))^2, \; i.\,e., \text{ approx. } (f_{abc,\,t})^2\ (1\pm 2v).$$

For this reason the results of impact tests, or of any other tests based on the work required to cause breakage, will be even more variable than ordinary measurements of bending strength, a characteristic which was noted by G. Gehlhoff and M. Thomas (23), and one which may have been responsible for the non-publication of the results of O. Graf (24). In fact, such wide variations have been found in all the impact experiments described here, and introduce a corresponding error into the results.

THE TYPE AND PREPARATION OF THE GLASS USED.

All the measurements described here were made on Pilkington's Special Selected Quality (S.S.Q.) sheet glass as used in the manufacture of laminated glass. The pieces were cut by a diamond cutter on felt tables, and different experiments must be presumed to be made on glass from different batches, except where otherwise stated. Evidence showing the reproducibility of the figures is given separately.

THE MEASUREMENT OF THE MODULUS OF ELASTICITY.

The deformation of glass at ordinary temperature is particularly simple, being entirely of the ideal Hookean or reversible elastic type (25). Hence, if the Young's modulus of elasticity is measured, the extension of the material under stress can be quantitatively described. The measurement of this modulus can be carried out in the usual way by the static bending of a beam; and in four such experiments the following results were obtained with the sheet glass :—715,000, 724,000, 717,000, 699,000 kg./cm.^{2}.

It was felt desirable, however, to check these figures by an independent method involving shorter times, and the following procedure was used.

A long glass beam of length L and thickness h was clamped between two thick glass plates and the frequency measured by counting the vibrations (n) within a time interval determined with a stop-watch, a procedure which made it impossible to measure any but the lowest frequencies. The modulus of elasticity can then be found from the formula(26) :

$$n=0{\cdot}162\sqrt{\frac{\mathrm{E}h^2}{\rho \mathrm{L}^4}},$$

where ρ the density = 2·51 for our glass. It was soon found that such methods yielded different results (Table I.) according as the beam was in the horizontal or the vertical position.

Consistent results are obtained only when the beam was in the horizontal position. When the beam was vertical high results were obtained, for then both gravity and the elasticity combined to hold the beam straight, and low results when the two forces acted in the opposite directions. These experiments show that the weight of a long beam under the influence of gravity produces accelerations comparable to those given by the elasticity. The results with the horizontal beam, together with the bending experiments, show that this glass has a modulus of elasticity not significantly different from 700,000 kg./cm.².

TABLE I.

Values of Young's Modulus determined by Vibration.

L.	n.	E.
(1) Beam hanging vertically, rigidly held at the top (h= 0·2235 cm.).		
145·5 cm.	1·035 sec.$^{-1}$	940,000 kg./cm.^{2}
131·0 ,,	1·235 ,,	880,000 ,,
122·0 ,,	1·400 ,,	840,000 ,,
(2) Beam vertical, rigidly held at the bottom (h=0·279 cm.).		
138·0 cm.	1·135 sec.$^{-1}$	580,000 kg./cm.^{2}
128·4 ,,	1·337 ,,	620,000 ,,
117·1 ,,	1·624 ,,	630,000 ,,
108·1 ,,	1·866 ,,	620,000 ,,
102·4 ,,	2·137 ,,	640,000 ,,
(3) Beam horizontal (h=0·279 cm.).		
130·5 cm.	1·378 sec.$^{-1}$	697,000 kg./cm.^{2}
112·2 ,,	1·875 ,,	694,000 ,,
94·5 ,,	2·605 ,,	693,000 ,,

THE BREAKING STRENGTH OF BEAMS BY LOADING AND BY IMPACT.

These experiments were all carried out on thin glass beams accurately cut to 13×1 in. In the slow breaking experiments by loading they were suspended between knife edges 30 cm. apart and were broken by pouring lead shot from a cylinder at a rate of 150–300 gm./sec. into a container suspended from the centre of the beam, it having been found that this rate could be readily judged and reproduced manually within these limits. The strength was calculated from the average of twenty-five tests.

A further twenty-five, exactly similar, pieces were then broken by a heavy pendulum, the weight of which at the striking end could be varied from 1·1 to 1·6 kg. It was allowed to fall from a height such that the strongest pieces were only just broken. This pendulum was similar to that described by the author in another paper (27), except that the holding arrangement was altered so that the beam could be allowed to rest on supports 31·5 cm. apart.

The results obtained may be used to test the relation given in equation (1), which should be constant for any given thickness of bar, with different edge conditions (see Table II.).

It will be seen that the values in the last column are sensibly constant at each thickness, indicating that time effects act in a similar way for different edge conditions.

Table II.

Strength determined by Pendulum Test.

Effective weight of pendulum (kg.).	Weight of glass beam (kg.).	Thickness (cm.).	Edge condition.	Kg./cm.²		$\frac{10^6 W}{f^2}$.
				(f) slow.	Impact work, W.	
1·10	0·039	0·205	Diamond edges compressed	950* *a*	2·5* *b*	2·8
,,	,,	,,	Diamond edges in tension	660* *c*	0·95* *d*	2·2
1·10	0·054	0·284	Diamond edges compressed	800	2·8	4·4
,,	,,	,,	Diamond edges in tension	720	2·2	4·2
,,	,,	,,	Edges ground	650	2·0	4·7
1·10	0·079	0·415	Diamond edges compressed	681	3·9	8·4
1·60	,,	,,	Diamond edges compressed	718	3·5	6·8
1·10	,,	,,	Diamond edges in tension	590	2·7	7·7
1·10	,,	,,	Edges ground	572	2·5	7·5

These results can be re-arranged so as to allow of the calculation of *f* for short times. This is done on the assumptions that (*a*) the bar bends as in the slow application of the load ; (*b*) the time is twice that taken by the pendulum to traverse the total bending distance at its maximum velocity ; (*c*) slow loading is at the rate of 225 gm./sec. Also, in this calculation no correction is introduced to allow for the loss of energy consequent on the division of momentum between the beam and the pendulum (*cf.* R. J. Roark (28))†, but these connections would be small (<5 per cent.), as the pendulum is in all cases much heavier than the beam. The values of *f* are thus calculated and compared with those predicted by the relation

---

* The approximate coefficients of variation were (*a*) 17 per cent., (*b*) 31 per cent., (*c*) 7 per cent.. (*d*) 24 per cent.

† In the case of a body of mass M striking a beam of mass M_1 at the centre, the available energy should be reduced by a factor

$$\frac{1+\frac{13}{35}\frac{M_1}{M}}{\left(1+\frac{1}{2}\frac{M_1}{M}\right)^2}.$$

given by A. J. Holland and W. E. S. Turner (28), which makes the *f* proportional to $\frac{1}{\text{time}}^{\frac{1}{12\cdot 8}}$. This equation does not differ appreciably from the average of the three results treated by W. Harries (29), which give a value of $\frac{1}{11\cdot 9}$ instead of $\frac{1}{12\cdot 8}$ for the index.

Table III. shows quite clearly that the increase in bending strength under impact can be fully accounted for by the time factor. The increases in bending strength are all smaller than those predicted from the Holland and Turner equation, a deviation which may possibly be accounted for by the following factors :—

Table III.

The fast and slow breaking of Glass Beams.

h (c.m.).	f (slow) (kg./cm.^{2}).	Time, slow (sec.).	f (fast) (kg./cm.^{2}).	Impact velocity (cm./sec.).	Fast, deformation (cm.).	Time, fast (sec.).	$\frac{t\text{ slow}}{t\text{ fast}}$.	$\frac{f\text{ fast}}{f\text{ slow}}$.	$\left(\frac{t\text{ slow}}{t\text{ fast}}\right)^{\frac{1}{12\cdot 8}}$.
0·205	950	9·5	1380	85	1·6	0·038	250	1.45	1·54
,,	660	6·6	850	85	1·0	0·023	290	1·29	1·56
0·284	800	12·5	1240	105	1·03	0·020	625	1·55	1·65
,,	720	14·0	1110	105	0·92	0·017	820	1·54	1·69
,,	650	15·5	1050	105	0·87	0·017	916	1·62	1·70
0·415	681	29	1220	105	0·70	0·013	2230	1·80	1·87
,,	718	28	1150	105	0·66	0·0125	2240	1·60	1·87
,,	590	24	1010	105	0·57	0·0110	2206	1·72	1·84
,,	572	23·5	970	105	0·55	0·0105	2240	1·70	1·87

1. The equation does not accurately describe the breaking of this type of glass at very short times.

2. The bending of the beam, particularly under impact, is too large to be described by the simple bending equations which assume the deformation to be small.

3. The dynamic bending of the beam differs from the slow bending, as discussed later in connection with the bending of plates, and as was found with the vibration of glass beams. This factor is reduced to a minimum by using low impact velocities.

It should be noted that the factor due to dissipation of energy during impact would operate in the opposite sense to the above. This has been shown experimentally by the work of Z. Tuzi and M. Nisida (30), who found by photo-elastic measurements, using a heavy pendulum and a relatively light plastic beam, that the dynamic stresses in the beam were somewhat less than would be expected. The velocities used by these workers were similar to those in the above experiments.

In view of these uncertainties, the agreement between theory and experiment must be regarded as satisfactory. The results are also in general agreement with those discussed by F. W. Preston (31), though his figures contain some low values, and also with those of F. Schmeer (32). They do not, however, agree with those which can be derived from the experiments of A. E. Williams (33), whose results yield ratios of fast and slow bending strength in the neighbourhood of 1·0–1·2. This difference is probably due to the fact that Williams used a 6-oz. (0·17-kg.) striker and a longer and heavier piece of glass, thus obtaining low values of the impact strength through the operation of the dynamic factors described in (3) above, which will be discussed later.

The Breaking of Squares of Glass.

1. *The Bending of Squares of Glass.*

In order to obtain a full picture of what happens when a ball falls on a pane of glass, we must first know how such a pane behaves when simply supported and subjected to slow bending under a central force. For this purpose a simple apparatus was designed (fig. 1) in which a ball-bearing could be pressed upwards against a square of glass with a known force and the deformation measured at the centre of the upper surface using a large spherometer. The radius of the ball-bearing used in these experiments was $1\frac{7}{16}$ in. unless otherwise stated. By plotting the deformation against load for several plates of the same size, an average curve was obtained which was always linear except for slight deviations with the thinnest plates. These could then be expressed by a single figure giving the deformations (cm.) for unit central load (kg.), and could be compared

Fig. 1.

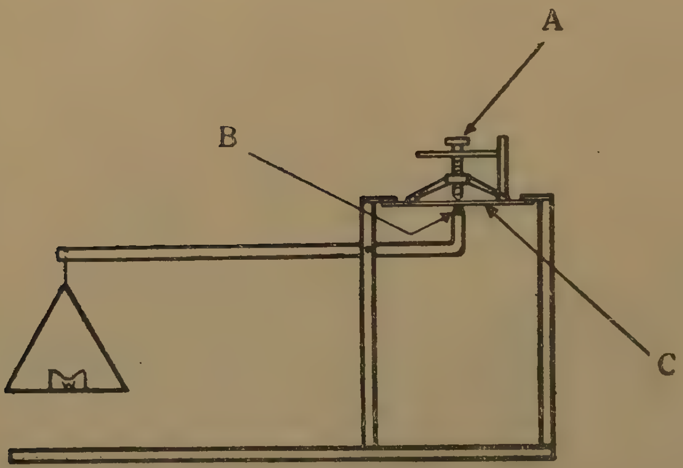

Apparatus for bending and breaking Glass.
(A) Spherometer. (B) Steel ball. (C) Glass square.

with those calculated from the theory given by S. Timoshenko (34), which states that the deformation δ is given by

$$\frac{\delta}{\mathrm{P}}=\frac{0{\cdot}1265\,a^2}{\mathrm{E}h^3},$$

where a = side of the square, h = thickness, and P = central force, and the Poisson's ratio δ does not differ very greatly from 0·3*.

The results in Table IV. all show good agreement with theory except for the thinnest plates, where the experimental values are low. This is probably due to the fact that the deflections on these occasions were too large for the theory of small deflections to apply. The thin plates probably behave in a manner intermediate between that of a stiff plate and a membrane.

TABLE IV.

Deformation of squares of Glass.

Thickness.	δ/P (found).	δ/P (calculated).
A. Squares 12×12 in.		
Spherometer with leg 5 in. long, corresponding to square 25·4 cm. side.		
0·408 cm.	0·0020	0·0018
0·273 ,,	0·0057	0·0058
0·211 ,,	0·0091	0·013
0·096 ,,	0·039	0·13
B. Squares 6×6 in.		
6×6 in. squares of glass in frame 5·3 in.=13·5 cm. Spherometer went effectively to edge of frame.		
0·416 cm.	0·00046	0·00052
0·291 ,,	0·0016	0·0013
0·209 ,,	0·0036	0·0038
0·146 ,,	0·011	0.011
0·094 ,,	0·0146	0·041

2. *The Breaking of Glass Plates under a Central Force.*

According to S. Timoshenko (35) the stress p_m at the centre of the bottom face of a plate bent by a central force is given by

$$2=\frac{\mathrm{P}_{(\mathrm{max.})}}{p^m}\left((1+\sigma)\;(0{\cdot}485\;\log_{10}\frac{2a}{\pi h}+0{\cdot}52)+0{\cdot}48\right).$$

Experiments to measure $\mathrm{P}_{(\mathrm{max.})}$ and p_m could be made either by slowly increasing the force, for example, by running lead shot into a scale pan as in the experiments with the beams, or by a discontinuous addition of weights, increasing the central force by increments of approximately 10 per cent. The latter course was adopted, since it was desired to compare the results with impact experiments in which height of fall of a ball-bearing was increased by definite increments. In order, however, to vary the rate at which the slow breaking experiments were made, it was found necessary to use a spring balance for applying the load in relatively fast experiments. In this case a small correction, equal to one-half of the average stress increase in the discontinuous experiments, was added to the results obtained with the spring balance.

---

* The formula contains $(1-\sigma^2)$ as part of the constant 0·1265, and hence a likely value of σ for our glass of 0·23–0·25 would not greatly affect the results.

All the experiments were carried out with two or more diamond-cut edges in compression. This means that any given sample will contain pieces with two, three or four diamond-cut edges in compression and that the relative results could, in theory, be varied by changes in this distribution. However, since nearly all the squares break in radial cracks starting from the centre, as in the photographs of H. E. Edgerton and F. E. Barstow (36), it seemed unlikely that edge effects would play a large part in the process. This point is confirmed by experiments described below.

TABLE V.

Thickness.	Central breaking force $P_{(\text{max.})}$ (kg.). 12×12 in.	6×6 in.	Mean.	Bending strength p_m. 9×9 in. calc.
0·096	10·3	9·2	9·7	2550 kg./cm.^{2}
0·210	25·8	28	26·9	1360 „
0·280	52	46*	49	1340 „
0·410	71	91	81	1000 „

It was also found that if the average of twenty-five results was taken, the errors of measurement arising from variation in the glass exceeded the value of the correction introduced by change in the length of the edge of the plate. In the results shown in Table V. the average of the breaking force for 12 in. × 12 in. and 6in. × 6in. glass was taken, and the value of p_m calculated as for a 9 in. × 9 in. square. The breaking time averaged 0·3–1 minute.

Even if we eliminate the first value quoted, on the ground that our bending theory is not obeyed (see Table IV.), it is still reasonable to conclude that, as with other types of test, the modulus of rupture decreases as the dimensions increase. The values obtained are also in agreement with those of O. Graf (37), but appear to be somewhat larger than those found by A. F. Dufton (38). They agree, however, with those of the latter in that the spread of the figures is very large, yielding a value of v of approximately 25 per cent.

THE EFFECT OF DIAMOND-CUT EDGE ON THE SLOW BREAKING OF GLASS.

The relatively high values of v are illustrated in the figures given below, which are primarily designed to show that the position of the diamond-cut edge has little effect on this type of break. The average breaking force is given, together with the average time and values of v for glass squares which had been specially cut with all the diamond-cut edges on the same side.

---

* Based on fifty experiments, *vida infra*.

Position of diamond edge.	Central breaking force (kg.).	v, %	Mean Time (sec.).
Upwards—tension	48·0	28	27
Downwards—compression ..	46·6	27	27

The glass used was selected in two lots of 50 from a single sample of 100 pieces of 24-oz. sheet averaging 0·280 cm. thick. The difference between the two results is assumed not to be significant.

The Variation of the Breaking Force with Time.

In order to ascertain if glass broken in this way showed the usual variations with time, experiments were made at different rates of application of stress, the fastest ones being carried out with a spring balance as described above. Glass of two thicknesses was used, and, in general, lots of twenty-five pieces were chosen at random from a larger group. In this way any variation in the glass, other than the purely statistical one, was eliminated. The time of breaking was measured for each experiment and the average taken.

Table VI.

The Bending of Glass Plates under a Central Force.

(6×6 in. glass in 13·5 cm. frame.)

No. of Tests.	Thickness (cm.).	Average breaking time (min.).	Average central force (kg.).	Average central force* (kg.).
25	0·278–0·286	6·4	38·3	38·3
50	0·278–0·286	0·56	46·1	46·1
25	0·278–0·286	0·03	50·4	52·4
25	0·408–0·417	9·8	82·5	82·5
25	0·408–0·417	0·86	91·0	91·0
25	0·408–0·417	0·03	109·2	112·2

It is clear that when glass is tested under these conditions it shows time effects generally similar to those which have been obtained by other workers in bending experiments with beams, for example, by A. J. Holland and W. E. S. Turner (39).

---

* Corrected for discontinuous application.

The Breaking of Glass Squares by Impact.

Experimental Method.

Squares of glass of different sizes and thicknesses were simply supported and broken by dropping steel ball-bearings of a wide range of sizes from gradually increasing heights. Application of the equations given by H. R. Hertz (40) shows that the energy absorbed by a ball 1 cm. radius under a force of 100 kg. is of the order of 0·1 kg.-cm., and the effect of the ball is therefore neglected in the discussion, given later, of the energy required to cause fracture. On the other hand, it is of importance, if comparable results are to be obtained at a wide range of heights, that the percentage increment of height should not vary greatly over the whole range of experiments. This was assured by standardizing the increment at 10–20 per cent.; for example, the range of heights over which a given series of experiments was carried out might be 6, 7, 8, 9, 10, 12, 14, 16, 18, 20, 24, 28, 32, 36, 40, 45, 50, 60, 70.

The lowest height could be chosen such that not more than one piece of glass was broken under this impact. Care was taken, so far as possible, to hit the glass centrally, but this was only judged by eye, and any series of results would be the average of a number of shots grouped round the centre.

In these experiments it was not possible to take all the glass from a single source. It was therefore necessary to discover what was likely to be the effect of changing batches of glass on the average breaking height. For this purpose a series of lots of fifty squares of glass of dimensions 15×15×0·284 cm. were broken at periods separated by at least a week by a 0·200-kg. ball. The average heights obtained were 34, 30, 40, 37·5, 35, 30 cm., and the corresponding coefficients of variation 53, 43, 44, 38, 46 and 49 per cent., respectively.

Taking $v = 46$ per cent., we find that for a group of fifty the standard deviation of the difference is 2·2; and therefore we should expect that most of the experiments would give an average result within 35±2 cm. (standard deviation), that is, 35±4·4 cm. The fact that three results are just outside this limit probably indicates that variations between different lots of glass are of approximately the same magnitude as those from statistical sources. In any case, the above figures illustrate the margin of error to be expected.

The Effect of Diamond-Cut Edges.

For these experiments forty-eight squares 6 in.×6 in. and average thickness 0·284 cm. were chosen at random from a sample of ninety-six which had been specially prepared with all the diamond-cut edges on one side. They were then broken by the impact of a 0·200-kg. ball. The results were:

Description	Highest impact.	Lowest impact.	Average.	v.
Diamond-cut edges compressed	(32 in.) 81 cm.	(6 in.) 15 cm.	32·2	55%
Diamond-cut edges in tension	(28 in.) 71 cm.	(6 in.) 15 cm.	31·1	35%

The standard difference of the means comes to 3·1 cm., that is, the difference found is definitely not significant. It is probable that the difference in the values of v is also not significant, since the figure of 55 per cent. actually depends on two values of 81 cm. only. The average of 46 per cent. found above is interesting, however, since it is of the order of twice the figure of 27 per cent. found for the breaking force as predicted by theory. Clearly, if the difference due to all four diamond-cut edges being on one side or the other is so small, the effect of changes in distribution of groups 2, 3 and 4 diamond-cut edges upwards are likely to be neglible compared with the experimental error.

The Variation with the Size of the Square.

The experiments were carried out using a 0·200 kg. ball and a series of plates with sides 4, 6, 9 and 12 in. simply supported in wooden frames * 3·7, 5·3, 8·3 and 11 in. wide, respectively. The results, which are based on twenty-five tests, are shown graphically in fig. 2. Cursory examination shows that the energy absorbed in breaking the plates of a given thickness does not increase proportionally with the area of the plate, though it does increase appreciably. The relative increase in energy absorption

Fig. 2.

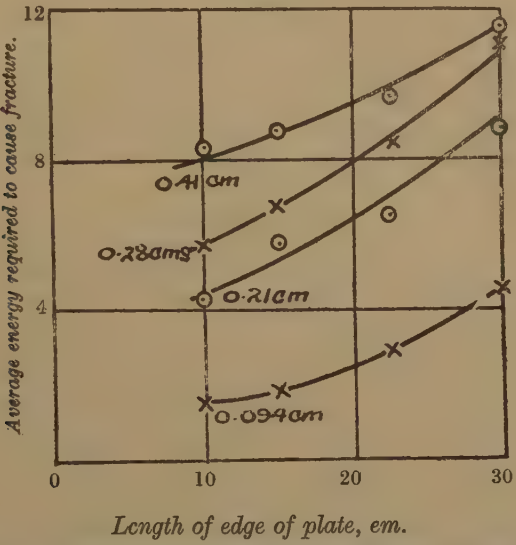

Average energy required to cause breakage of glass plates of varying length of edge (area) and thickness.

---

* A few experiments have been carried out in an iron frame, and in these cases the energy absorbed has been up to 30 per cent. below that associated with the wooden frame. The difference appears to be due to the absence of any damping of the vibrations of the plate, such as occurs in a wooden frame, with a consequent tendency of the vibrating plate to break from the edge instead of from the centre. In this way, squares that would resist impact in a wooden frame break in an iron frame, yielding a lower average.

with area is greater with thin than thick plates. Again, thick plates absorb more energy than thin ones, but the increase is by no means proportional to the thickness.

The Effect of the Size and Weight of Impacting Ball on the Energy Required to Fracture a Plate.

The plates were broken with a series of steel balls of weights 0·0015 kg. to 0·88 kg., as previously described. It must be emphasized that the accuracy of any particular figure obtained in any of these experiments, which were generally based on not more than twenty-five impacts, is not very great; but the differences between the results were so large as not to leave the general character of the variations in doubt. In some cases, particularly with the small balls at high velocities, a small proportion of the plates would break in an unusual manner. For example, the square might crack from the side, breaking off a corner. Such cases were always countered as broken, but they did not occur frequently enough (less than 15 per cent.) to affect the averages substantially, nor did they appear to occur at energies markedly higher or lower than the normal

TABLE VII. (*a*).

Average height of fall in cm. required to break Plates with Steel Balls.

Wt. of Ball (kg.): Size of square.	0·88	0·44	0·20	0·067	0·0213	0·0084	0·0034	0·0015
0·093 × 15^2 cm.	—	4·6	9·4	24·4	—	155	290	487
0·117 × 28^2 ,,	—	—	15	—	137	259	466	531
0·208 × 15^2 ,,	6·4	—	29·5	64	92	248	—	—
0·208 × 30^2 ,,	12·5	—	44	121	195	438	—	—
0·280 × 15^2 ,,	7·2	18·8	34	66	177	223	409	—
0·280 × 30^2 ,,	15·5	—	56	—	217	348	—	—
0·41 × 15^2 ,,	16	—	38	—	177	259	—	—
0·41 × 30^2 ,,	16	—	57	127	390	—	—	—

TABLE VII. (*b*).

Average energy in kg. cm. required to break Plates with Steel Balls of different sizes.

Wt. of ball (kg.): Size of square.	0·88	0·44	0·20	0·067	0·0213	0·0084	0·0034	0·0015	Breaking.
0·093 × 15^2 cm.	—	2·0	1·9	1·6	—	1·3	1·0	0·7	0·7
0·117 × 28^2 ,,	—	—	3·0	—	3·0	2·2	1·6	0·8	—
0·208 × 15^2 ,,	5·6	—	5·9	4·3	2·0	2·1	—	—	1·2
0·208 × 30^2 ,,	10·9	—	8·8	8·1	4·2	3·6	—	—	3·3
0·280 × 15^2 ,,	6·4	8·2	6·8	4·6	3·8	1·9	1·4	—	1·6
0·280 × 30^2 ,,	13·7	—	11·2	—	4·7	2·9	—	—	6·7
0·41 × 15^2 ,,	14	—	7·6	—	3·8	2·2	—	—	1·9
0·41 × 30^2 ,,	14	—	11·4	8·5	8·5	—	—	—	6·6

breaks. The results of a series of such tests are given in Table VII. (*a*) and Table VII. (*b*), together with the slow breaking work derived from the bending and breaking experiments. In the calculation of the energy required to break the glass no correction was applied for the bending of the glass during impact, but this was always very small compared with the height of fall.

The slow breaking times in Table VII. (*b*) were 0·3–1 minute and the central forces used the average ones for plates of 6 in. and 12 in. sides.

A first examination shows that the values of the slow breaking work correspond with those obtained with light to medium-sized balls. This correlation is, however, a purely chance one, as we can see when we note that the difference between the slow breaking experiments and the slowest impact experiments is in close keeping with the results obtained with the beams struck by the pendulum.

Table VIII.

The fast and slow breakage of Glass Plates.

Size of frame and thickness (cm.).	$\delta \times 10^3$ (cm./(kg.).	Slow breaking force at centre $=P^s$ (kg.).	Impact energy (kg./c.m).	Calculated central breaking force (fast) $=P^f$(kg.).	Impact velocity (cm./sec.).	Fast deformation (cm.).	$\frac{\text{Slow time}}{\text{fast time}}$.	$\frac{P^f}{P^s}$.	$\left(\frac{t\text{ slow}}{t\text{ fast}}\right)^{\frac{1}{12\cdot8}}$
13·5×0·095	14·6	9·7	2·0	16·7	95	0·24	5,900	1·7	2·0
13·5×0·21	3·6	26·9	5·6	56	106	0·20	8,100	2·1	2·0
29 ×0·21	10·4	26·9	10·9	46	155	0·27	4,900	1·7	1·9
13·5×0·28	1·6	49	6·5	90	113	0·144	14,300	1·8	2·1
29 ×0·28	6·5	49	13·7	65	164	0·42	5,900	1·3	2·0
13·5×0·41	0·46	81	14·0	247	166	0·114	21,000	3·0	2·2
29 ×0·41	2·3	81	14·0	110	166	0·25	10,000	1·4*	2·1

A Treatment of the Slow Impacts.

The breaks made with the heaviest balls (0·88 kg. and 0·44 kg.) are presented in Table VIII. in a manner similar to that used for the fast and slow breakage of beams in Table III. Deformation and breaking time are calculated from the measured energy required to cause fracture and the deformation lines for the glass squares given in Table IV. However, these lines were corrected for the fact that the spherometer did not always go to the edge of the frame used to hold the square during breaking experiments by assuming that the deformation was proportional to the square of the side. This correction was quite small.

All these experiments were made with the 0·88-kg. ball except the first one (13·5×0·095 cm.), when the 0·44-kg. ball was used. The slow time was taken as 30 seconds.

An examination of Table VIII. shows that in the case of the first four squares the increases in bending strength required to account for the energy absorption under impact are close to those which the Holland and Turner equation predicts. In all cases the dynamic stresses are larger than those required to break the glass statically, but the two largest squares at the bottom of the table appear to give lower stresses than would be expected. It is possible that this deficiency in impact strength is to be ascribed to the deviation of the plate from static type bending under the dynamic conditions of impact, as described in the next section. One further point may be noted here. In Pl. IX. some illustrations of the breaking patterns of strong and weak squares are given for slow breakage and impact. It will be seen that the forms are generally similar and that, in each case the stronger glass shows the greater amount of cracking. The theory that the two breaks are formed under the action of similar forces is therefore supported by the breaking patterns.

---

* A subsequent repetition of this experiment gave a figure of 1·8 here.

In the above table no attempt is made to apply a factor accounting for the loss of energy during impact. In the case of the 29×0·28 and 29×0·41 cm. plates it is not safe to assume that this correction is small, since the weight of the glass is comparable with that of the ball. Such corrections, however, have not been worked out in the case of impact on squares, and if they were applied here they would still further increase the difference between the last two columns of Table VIII., that is, this factor does not account for the apparent anomalies found with them.

The Decline in Impact Strength at High Velocities.

A further reference to Table VII. will show a universal feature of the results. As the weight of the ball is reduced, and the velocity of impact therefore increased, the energy required to break the plate declines. Before this point is discussed it may be noted that the same type of effect was found by the National Physical Laboratory and Department of Scientific and Industrial Research (Building Research Station)⁽⁴¹⁾. L. Longchambon ⁽⁴²⁾ also found a similar result, though in somewhat different circumstances. This decline in energy cannot be due to change in the size of the ball by itself, resulting in a smaller area of contact with the plate, since the plate bends statically in a manner consistent with the theory of a central force which is independent of the size of the ball. This applies in all cases where the glass breaks in tension from the lower surface. Further, this point was checked by slow breaking experiments, using balls of widely varying size, the results, based on sets of twenty-five from one batch of 15×0·280 cm. glass being as follows :—

Ball diameter.	Ball weight.	Breaking force.	v.
½ in.	0·0084 kg.	51·8 kg.	38%
2⅜ ,,	0·88 ,,	56·5 ,,	32%

The difference between these results is not outside the probable statistical error, and in any case could not account for the very large variations in energy absorption associated with a similar change in the size of a ball in an impact experiment.

The cause of the decline in strength is therefore to be looked for in the conditions of impact itself, and, in particular, in the dynamic aspect of the impact deformation. To illustrate the phenomenon further, a graph has been drawn for several glass plates, in which the energy required to cause fracture is plotted against the velocity of the ball for four sizes of square (see fig. 3) using some of the data quoted in Tables VII. (*a*) and (*b*). The results illustrate strikingly the general character of the effect. Further evidence that some new factor is beginning to operate is the high velocities indicated by the cracking patterns shown in Pl. VIII., which differ strikingly from those of Pl. IX.

Fig. 3.

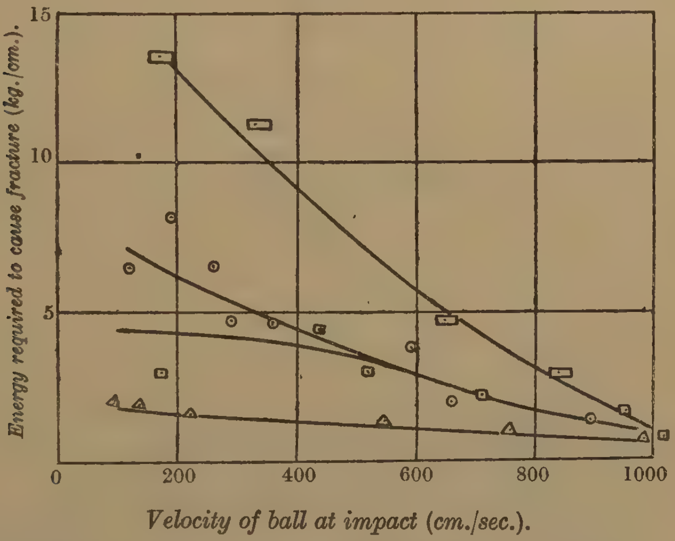

The average energy required to break glass squares of different sizes plotted against the average velocity of impact. Each point was obtained using a ball of a given size.

⊡ *Glass square* $0{\cdot}280 \times 30^2$ cm.
⊙ „ $0{\cdot}280 \times 15^2$ „
⊡ „ $0{\cdot}117 \times 28^2$ „
△ „ $0{\cdot}093 \times 15^2$ „

A Theory of the Decline in Breaking Energy at High Impact Velocities.

A simple statement of the underlying idea is that when a plate is struck at the centre by a ball falling at a high velocity, the bending differs from that characteristic of slow bending because of the inertia of the plate which it is necessary to set in motion. The plate, in consequence, is less easily deformed by a given central stress at high speeds, and therefore absorbs less energy. Alternatively, we may say that for a given deformation the central stress will be higher under impact than under static deformation. This was shown experimentally by R. N. Arnold (43) in the case of relatively slow impacts on an iron rail. He also showed that the curvature of the rail is initially reversed in the outer regions in a manner which, operating on a plate, could account (fig. 4) for the circular cracks in Pl. VIII. Arnold has also shown that the theoretical equation given by S. Timoshenko (44) leads to the result that stress under impact can be higher than under static conditions. We may therefore conclude that the decrease in deformation and energy absorption under impact can be ascribed to the inertia of the plate.

The subject may, however, be further elucidated by using a somewhat different approach. In fig. 5 the case of an ideal tension impact on a long bar is illustrated. The bar is assumed to be suddenly extended with a velocity V. In consequence, the initial stresses, before the stress wave reaches the end of the bar, will be, not zero, but equal to $V\sqrt{E\rho}$. This conclusion is not in any essential new, since S. Timoshenko (45) has given an equation which reduces to this one at zero time, and M. J. Boussinesq (46) has shown that, in the case of a transverse impact on a circular plate, there will be, on the theory of a limited elastic extension, a critical velocity above which any object, however small, will damage the plate. By putting the deformation $= p/E$, his equation becomes the same as the one above, except for a factor of 0·94 in the Boussinesq equation, which is presumably due to the transverse conditions of impact.

Fig. 4.

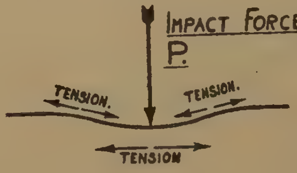

Fig. 5.

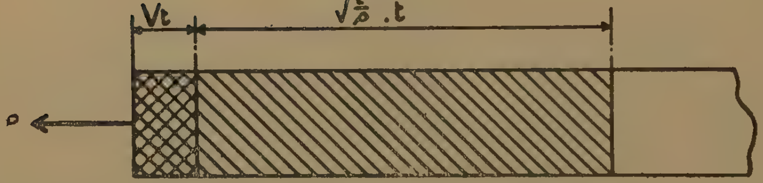

$$\textit{Stress}=P=E\times\textit{strain}=E\,\frac{Vt}{\sqrt{\frac{E}{\rho}}\,.\,t}=V\sqrt{E\rho}.$$

Diagram illustrating the initial stress produced by suddenly extending a bar with velocity V.

It follows from this factor that the initial stresses in a material near the point of impact are not zero when the bending is zero, but proportional to $V\sqrt{E\rho}$. This clearly alters the whole approach to the problem in all cases in which the velocity of the impact is sufficiently large to yield initial stresses comparable to the breaking stresses.

Indeed, in the case of an elastic material which has either a maximum tensile stress or a maximum elastic extension there will be a critical velocity above which any impact will cause damage. It is possible that this factor has a bearing on the critical impact velocities found by H. C. Mann (47) in experiments on the high velocity deformation of metals. For instance, he obtained a decline in impact strength with steels at velocities of impact of from 50 to 320 ft./sec. If these velocities are substituted in the above expression *, we obtain values of the stress of $91–580\times10^3$ lb./sq. in., which compare with a normally quoted tensile strength of $80–330\times10^3$ lb./sq. in. This agreement in magnitude between the two quantities suggests that in Mann's experiments the work absorbed was reduced because the material was broken before all parts of the test-pieces had been able to take up elastic work. At the same time the occurrence of a substantial non-Hookean deformation in his experiments introduces a complication not present in experiments made on glass.

In the case of glass, little is known about the stresses required to break it in very short times and hence there is no opportunity to check the effect of any critical velocity with the theory. We may, however, use the equation $p=V\sqrt{E\rho}$ † to show that each velocity is associated with the setting up of a stress of particular value. At a velocity of 750 cm./sec. (25 ft./sec.), corresponding to a fall of 10 ft., this stress will be of the order of 1000 kg./cm.^{2} in glass, which is approximately that required to break this material under slow conditions. It is clear, therefore, that the velocities used in the author's experiments will cause stresses high enough to be comparable with those required to cause rupture, and that the assumption of specific effects due to high velocity is reasonable. if we proceed, however, to use still smaller balls falling at higher velocities in order to investigate the possibility of a critical velocity, certain difficulties arise in addition to the experimental ones, connected with the fact that as the size of the ball is reduced, so that it is comparable with the thickness of the plate, the whole stress picture changes from one in some degree characteristic of a thin plate under a central force, to that of a massive block subjected to a point force. In the latter case the stress pattern is quite different and the glass breaks from the top surface. In this new form of crack, which is discussed below, there will be associated a different and unknown series of breaking stresses and hence a different critica velocity.

---

* Using $S=7{\cdot}7$ gm./c.c.$=480$ lb. cub. ft. $E=32\times10^3$ lb./sq. in.

† Since $\frac{1}{2}\frac{p_m^2}{E}$ and $\frac{1}{2}mV^2\rho$ are the maximum strain energy and the kinetic energy of unit volume $p_m=V\sqrt{E\rho}$ corresponds to the equality of these two energies.

The Breaking of Glass at High Velocities.

That a new type of break occurs when glass is struck by a projectile at high speeds can be simply shown by projecting a $\frac{3}{16}$-in. ball at a 0·28-cm. piece of glass either manually or by some " pea-shooter " arrangement. The same effect, however, can be brought about by more easily attainable velocities if rather more massive pieces of glass are used. Under these conditions, when the height of fall is well below that required to shatter the glass, small circular ring cracks are found in the surface similar to those reported by C. V. Raman (48), L. Longchambon and F. W. Preston (49). As the weight of the ball employed was increased, the height of fall being 20 ft. or more, a point was reached where a cone or " shell " could be knocked out of the glass, sometimes, as in Pl. X. (*a*), without forming any other cracks. Probably the conditions for getting such a clean break as that shown in Pl. X. (*a*) are critical, too little energy giving a ring crack or even a single crack across the glass, and excessive energy giving additional cracking as in Pl. X. (*b*) or (*c*). In this connection the experiments were very far from exhaustive, but the reproducibility of the general " shell " effects shown in these photographs is well established. Some generally similar effects have been reported by E. L. Hettinger (50), who used an air-gun to break the glass.

An explanation of the form of these " shell " breaks may be founded on the suggestion made by F. W. Preston (51) with regard to the small ring cracks found in a glass block under a concentrated load which grow into the larger " shells " under the special conditions of high velocity impact. Preston suggested that the rings are simply the consequence of the distribution of forces in the block and the property of the glass of breaking under tension. This opinion has been quantitatively confirmed by W. Weibull (52), who showed that consistent results were obtained on the assumption that the glass broke under tension, but not under shear. The further extension of this explanation to the larger " shells " described here presents no difficulties, since the shape of the products corresponds with the stress diagrams calculated by H. R. Hertz (53) and R. Fuchs (54). Also two " shells," one produced when the ball fell 26 ft. and the other 156 ft., showed only very slight differences in shape, a characteristic in agreement with an explanation which does not itself depend on the velocity. It is concluded, therefore, that the effect of the high velocity is simply to cause a concentration of stress around the point of impact, and that the resulting break follows the lines of compression at right angles to the lines of maximum tension in the glass.

Undoubtedly these breaks have a bearing on the behaviour of glass under high velocities of impact. Yet the speeds used in these experiments are far below those reached by bullets (of the order of 1500 ft./sec.). After a free fall of 32 ft. under gravity a steel ball will reach a velocity of 45 ft./sec. (30 m.p.h.). Whilst this speed may correspond to that of a moving vehicle or a thrown stone, a bullet would only travel so slowly when nearly spent. At these lower velocities it appears likely that the round holes will be easily formed in glass, but, as F. W. Preston (55) has shown, a bullet completely shatters a pane of glass. Clearly, between the velocities attained by falling objects and those of bullets there is another large experimental gap, akin to the one between slow breakages and those resulting from impact. Nor can this gap be overcome by extrapolating from normal velocities, since the intervention of possible critical velocities and fresh modes of cracking prohibits such a step in this case. All that can be said is that the energy required to crack glass by a bullet should be small, whilst that required to set the glass in motion and push it out of the path of the projectile may be large. In any case, the process will be very different from that which occurs at low velocity impact, when the bending of the glass is the dominant feature responsible for the absorption of energy.

ACKNOWLEDGMENTS.

The author received much help from Dr. A. Lawton of this Laboratory in the early stages of the work, and he is also indebted to Dr. H. W. Coultas of the Uuiversity of Birmingham and to Prof. R. N. Arnold, formerly of Metropolitan-Vickers Electrical Co., Ltd., Manchester, and now of the University College, Swansea, for much helpful criticism in the final preparation of the paper. He also wishes to thank the directors of Colmore Adhesives, Ltd., for permission to publish this communication.

The Laboratory,
Colmore Adhesives, Limited,
Team Valley Trading Estate,
Gateshead-on-Tyne, 11.

References.

(1) A. A. Griffith, Phil. Trans. A, cci. p. 163 (1920); E. J. Gooding, Journ. Soc. Glass Tech., Trans. xvi. p. 145 (1932).
(2) C. Karmarsch, 'Mitteilungen des gewerben Vereins für Hanover' (1858).
(3) W. C. Goggin and R. D. Lowry, Ind. Eng. Chem. xxxiv. p. 327 (1942).
(4) C. J. Warrington, Chem. and Ind. xx. p. 230 (1941).
(5) A. J. Holland and W. E. S. Turner, Journ. Soc. Glass Tech., Trans. xx. p. 72 (1936); S. Jurkov, *J. Tech. Phys. U.S.S.R.* i. p. 386 (1935); O. Graf, *Glastech. Ber.* xiii. p. 232 (1935).
(6) Journ. Soc. Glass Tech., Trans. xviii. p. 225 (1934).
(7) *Ibid.* xx. p. 279 (1936).
(8) J. Boow and W. E. S. Turner, *ibid.* xxii. p. 357 (1938).
(9) A. J. Holland and W. E. S. Turner, *ibid.* xx. p. 72 (1936); S. Jurkov, *J. Tech. Phys. U.S.S.R.* i. p. 386 (1935).
(10) A. Smekal, Journ. Soc. Glass Tech., Trans. xx. p. 432 (1936).
(11) Glass Ind. xx. pp. 21–25, 59–65, 95–99, 143–147 (1939).
(12) L. H. Milligan, Journ. Soc. Glass Tech., Trans. xiii. p. 351 (1929).
(13) J. B. Murgatroyd, *ibid.* xvi. p. 350 (1932).
(14) A. J. Holland and W. E. S. Turner, Journ. Soc. Glass Tech., Trans. xx. p. 72 (1936).
(15) J. Appl. Phys. xiii. p. 623 (1942).
(16) F. W. Preston, J. Appl. Phys. xiii. p. 623 (1942); A. J. Holland and W. E. S. Turner, Journ. Soc. Glass Tech., Trans. xxiv. p. 46 (1940); L. V. Black, Bull. Amer. Ceram. Soc. xv. p. 274 (1936); J. M. McCormick, *ibid.* xix. p. 68 (1936); G. Appelt, *Zeit. Physik.* xci. p. 336 (1934); L. Grenet, *Bull. Soc. d'encour de l'Ind.* iv. p. 839 (1899).

(17) Journ. Soc. Glass Tech., Trans. xxvi. p. 155 (1935).
(18) J. Appl. Phys. xiii. p. 623 (1942).
(19) J. Bailey, Glass Ind. xvi. p. 173 (1935).
(20) R. N. Haward, Trans. Farad. Soc. xxxix. p. 267 (1943).
(21) J. Amer. Ceram. Soc. xiv. p. 428 (1931).
(22) A. J. Holland and W. E. S. Turner, Journ. Soc. Glass Tech., Trans. xxiv. p. 46 (1940); W. Harries, *Zeit. tech. Phys.* xviii. p. 48 (1937).
(23) *Z. tech. Phys.* vii. p. 105 (1926).
(24) *Glastech. Ber.* vi. p. 582 (1929).
(25) Classification of Rheological Materials. The British Rheologist's Club, 'Nature,' cxlix. p. 702 (1942).
(26) "A Textbook of Sound," by A. B. Wood. G. Bell & Sons, Ltd., p. 113 (1932).
(27) "Formulas for Stress and Strain," McGraw-Hill Book Co., p. 288 (1938).
(28) Journ. Soc. Glass Tech., Trans. xxiv. p. 46 (1940).
(29) W. Harries, *Zeit. tech. Phys.* xviii. p. 48 (1937).
(30) Phil. Mag. xxi. p. 448 (1936).
(31) J. Amer. Ceram. Soc. xiv. p. 432 (1931).
(32) *Glastech. Ber.* ix. p. 544 (1931).
(33) J. Amer. Ceram. Soc. vi. p. 980 (1923).
(34) "The Theory of Plates and Shells." McGraw-Hill Book Co., pp. 165 and 276 (1940).
(35) "The Theory of Plates and Shells." McGraw-Hill Book Co., pp. 76 and 165 (1940).
(36) Glass. Ind. xx. p. 174 (1939).
(37) *Glastech. Ber.* xiii. p. 232 (1935).
(38) Phil. Mag. xxii. p. 1165 (1936).
(39) *Loc. cit.* 1940.
(40) "Miscellaneous Papers," English trans. by D. E. Jones and G. A. Schott. Macmillan, pp. 163–183 (1896).
(41) Journ. Soc. Glass Tech., Abs. xvii. p. 261 (1933).
(42) *Compt. rend.* cxcix. p. 1381 (1934).
(43) Proc. Inst. Mech. Eng. cxxxvii. p. 217 (1937).
(44) "Vibration Problems in Engineering." D. Van Nostrand Co., New York, pp. 279–281 (1928).
(45) "Theory of Elasticity." McGraw-Hill Book Co., p. 389 (1934).
(46) See "History of Elasticity and Strength of Materials," I. Todhunter and K. Pearson, Vol. II, Part II, p. 286 (1893).
(47) Proc. A. S. T. M. xxxvi. p. 85 (1936).
(48) 'Nature,' ciii. p. 113 (1919).
(49) Journ. Soc. Glass Tech., Trans. x. p. 236 (1936).
(50) Glass Ind. xxiii. p. 20–22 (1942).
(51) Journ. Soc. Glass Tech., Trans. x. p. 236 (1936).
(52) *Ingeniörs Vetenskabs. Akad. Handl.* p. 149 (1938).
(53) *Ibid.* p. 173, fig. 19.
(54) See A. E. H. Love, "Mathematical Theory of Elasticity," 4th Edition, p. 198, fig. 15 (1927).
(55) Journ. Soc. Glass Tech., Trans. xi. p. 283 (1927).

XCV. *The Lattice Spacings of Lithium at* 20° C. *and* —183° C.

By Kathleen Lonsdale, F.R.S., and William Hume-Rothery, F.R.S.*

[Received December 4, 1945.]

I.

The lattice spacing of lithium has been measured by Aruja and Perlitz ⁽¹⁾ who used Debye-Scherrer cameras of diameters ranging from 5·7 to 11·4 cm. A detailed examination (see page below) showed that the extrapolation lines of these investigators were not entirely convincing, and a re-determination was therefore desirable. The thermal expansion of massive lithium at low temperatures has been determined by Simon and Bergmann ⁽²⁾, whose results are of interest because they suggest that the metal shows a genuine deviation from Grüneisen's relation between specific heat and thermal expansion. A direct determination of the lattice spacing at low temperatures is thus of value as a check on the accuracy of the expansion data. Circumstances arose in which the present authors made quite independent measurements of the lattice spacing of lithium, and this paper describes some of the results obtained.

II.

The lithium used at the Royal Institution was ordinary (98·5 per cent. purity) commercial metal from Hopkins and Williams, Ltd., London, such as had been used for observation of extra X-ray reflections due to scattering by thermal waves. The specimen was prepared by cutting a thin sliver of metal of approximately square cross-section and sealing it in a very thin-walled capillary soda-glass tube. On raising this to the melting-point and cooling very slowly, a single-crystal specimen was obtained, about 2·5 cm. long by 0·5 mm. diameter. This was mounted, in its glass tube, in a setting of dental cement, as accurately as possible at the centre of a camera that could take either 29 cm. or 17·5 cm. diameter circular films with the van Arkel arrangement; the orientation of the single crystal having been previously adjusted so that the [001] axis was vertical. Using Cu Kα radiation, spots due to (400), (330) and (420) Bragg reflections were observed on the central layer line, the latter corresponding to a Bragg angle of about 80°. A device has previously been described ⁽³⁾ whereby X-ray diffraction photographs may be taken with a specimen bathed in a stream of liquid oxygen. A copper-constantan thermocouple was used to check the fact that this really did give a temperature of —183° C. The following exposures were then made on a film of the smaller size :—(*a*) 1 hour with a powdered quartz specimen diameter 1 mm. at 20° C., to give known calibration lines, (*b*) 1 hour with the lithium single crystal at 20° C., and (*c*) 35 minutes with the lithium single crystal at —183° C. The resulting lines and spots were then measured as accurately as possible, and the following values were obtained by the latest extrapolation methods $\left[a \text{ plotted against } \frac{1}{2}\left(\frac{\cos^2\theta}{\sin\theta}+\frac{\cos^2\theta}{\theta}\right)\right]$

---

* Communicated by the Authors.

—183° C. $a=3{\cdot}4762$ *k*X

20° C. $a=3{\cdot}5023$ *k*X

The main source of error in these values is a difference in the centering of the vertical quartz and inclined lithium specimens, but most of this error should be removed by the extrapolation method.

III.

The lithium used at Oxford was specially pure metal presented to one of us (W. H.-R.) by Professor R. S. Hutton. It has not been analysed in the elementary form, but magnesium-lithium alloys made from the same batch of lithium have shown no indication of impurity on a scale which could be detected by ordinary chemical analysis. A strip of this metal was cut up under xylol, and was rolled on a file under xylol to give a thin cylinder, which was slipped into a silica capillary and sealed off. The specimen was then annealed at 90° C. for a short time in order to remove any strain produced by the rolling process. The resulting specimen showed slight surface oxidation, and the diffraction film showed a few extra lines which may have been due to oxide, but the method of preparation should ensure freedom from metallic impurities and from silicon. Using cobalt radiation, a satisfactory film was obtained in a 19 cm. diameter Unicam camera. With this radiation the highest line was the strong (321) Kα doublet at approximately 73°. Experience has shown that with a 19 cm. camera accurate lattice spacings can be obtained even though the highest angle is only at 70°, and the present film gave a satisfactory extrapolation line which gave the lattice spacing as

$a=3.5023$ *k*X at 20° C.,

in exact agreement with the value obtained at the Royal Institution.

IV.

The above work suggests that the lattice spacing of lithium at room temperature is 3·5023 *k*X, and the error is not likely to exceed ±0·0002 *k*X. Aruja and Perlitz gave the lattice spacing of their lithium as 3·5019 *k*X at 20° C., and estimated the value for perfectly pure lithium as lying between 3·5015 *k*X and 3·5019 *k*X. These values are all slightly lower then those of the present work, but examination of the diagrams of Aruja and Perlitz shows that most of their results could be reconciled with the present value. Aruja and Perlitz drew their extrapolation lines so as to fit the points as whole most closely. Many investigators would prefer to give greater weight to the high angle lines, and in several cases this policy would result in the data of Aruja and Perlitz yielding a slightly higher value for the lattice spacing*.

The thermal expansion data of Simon and Bergmann can be used to calculate the lattice spacing of lithium at $-183°$ C., if the value at room temperature is assumed. Working in this way, the calculated value is 3·4771 kX at $-180°$ C., as compared with the present experimental value of 3·4762 kX at $-183°$ C. The agreement is thus satisfactory, and suggests that the expansion data for the massive metal are in agreement with those for the lattice expansion.

Acknowledgements.

The experiments at the Royal Institution were made using the 5 KW. rotating target tube, and our thanks are due to Dr. Muller for permission to use this apparatus and to Mr. H. Smith for experimental assistance.

One of us (W. H.-R.) must express his gratitude to Professor C. N. Hinshelwood, F.R.S., for laboratory accommodation and many other facilities which have greatly encouraged the present research. Acknowledgement must also be made of grants from the Royal Society, and from the British Non-Ferrous Metals Research Association.

References.

(1) E. Aruja and H. Perlitz, Phil. Mag. xxx. p. 55 (1940).
(2) F. Simon and R. Bergmann, *Z. phys. chem.* B. viii. p. 268 (1930).
(3) K. Lonsdale and H. Smith, J. Sci. Inst. xviii. p. 133 (1941).

XCVI. *Notices respecting New Books.*

Circular and Hyperbolic Functions (B. A. Mathematical Tables, Vol. 1). By the Committee for the Calculation of Mathematical Tables. [Pp. xi+72.] (Cambridge: The University Press, 1946.) Price 10*s.* 0*d.*

Fifteen years have passed since the British Association Committee on Mathematical Tables issued its first volume which contained a collection of miscellaneous tables, including the circular and hyperbolic functions, the exponential integral, the gamma function and the polygamma functions. They were all taken to high accuracy (*e.g.*, the tetragamma function $d^2/dx^2 \log (x!)$ was given to 15 decimals), but the interval of tabulation was fairly wide. The second edition, which is now published, is practically a reprint of the first, with a few last-figure errors corrected and a supplement to the gamma function, increasing its accuracy from 12 to 18 figures. On the other hand, the introductory matter has been cut down from 35 pages to 11, and whilst the excised matter may not be of great importance to the user, it was of considerable interest. The material which remains contains enough, but only just enough, to enable the user to see what methods of interpolation to adopt in the several tables.

J. H. A.

---

* This difficulty arises from the fact that Aruja and Perlitz used Fe Kα radiation, for which the highest line is from the (222) reflection and is relatively weak.

The Cavendish Laboratory. By Alexander Wood. [Pp. 59.] (Cambridge : The University Press, 1946.) Price 2*s.* 6*d.*

It was in 1846, amost exactly a century ago, that Kelvin took over a disused cellar and started in it the first class for what we should now call practical physics, and another quarter of a century elapsed before Cambridge had its Cavendish Laboratory. In 1871, Clerk Maxwell was appointed the first professor with duties "to teach and illustrate the laws of Heat, Electricity and Magnetism ; to apply himself to the advancement of the knowledge of such subjects ; and to promote their study in the University." This he undoubtedly did, though at first it must have been under difficulties, for the building of the Cavendish Laboratory went on at no great pace, and it was not opened until 1874.

After Maxwell came Rayleigh, then J. J. Thomson, Rutherford and now Sir Lawrence Bragg.

Dr. Wood has told in short compass the story of this Laboratory, its equipment, its personnel, the achievements of its leaders, the regulations which governed it at different times, and has, one imagines, drawn largely on his recollections, for he has been connected with it for a long span of years. As is natural, his memory has misled him on details in a few small points, but none the less, the story is an interesting and exciting one. Others might have selected different points for recall, as when Dr. Wood quotes from Maxwell's inaugural lecture, but omits the delightful detail that because of a difference between Scottish and English custom, those dignitaries of the University who came to do him honour at his first lecture, attended the one intended for first-year students and not the carefully prepared formal lecture-address. (But perhaps my memory has played me false ; I have not verified the reference.)

Especially in the days of Thomson and Rutherford, the laboratory was the acknowledged world headquarters of physics, and the names of many who passed through it or were connected in one way or another with its teaching appear in these pages. Even so, the list does not pretend to be complete, and among those known to the man in the street, who do not figure here, are Appleton, who was a demonstrator and lecturer soon after the 1914–1918 war, and Andrade, whose measurement of the wave-length of gamma rays was carried out there.

The book must primarily be of interest to old Cavendish men, for whom it will be something like a chat over old times, and will recall to them other incidents and events not mentioned in it ; but it is an interesting story in itself, which can, one imagines, be read by many others without boredom. One lesson it drives home—which is common to all physical laboratories and not only to the Cavendish—the change in the *scale* of physical apparatus, which has occurred since about 1925. To carry out new research on the nature of the atom calls uncompromisingly for pieces of apparatus occupying large space, with a price measured in tens of thousands of pounds and needing a small team to run it while the results are being obtained.

[*The Editors do not hold themselves responsible for the views expressed by their correspondents.*]

(*a*)

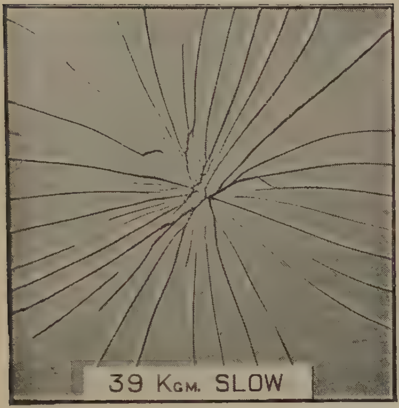

(*b*)

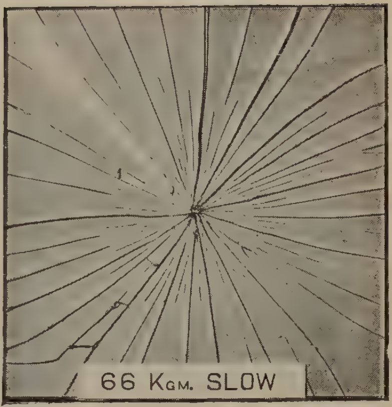

(*c*)

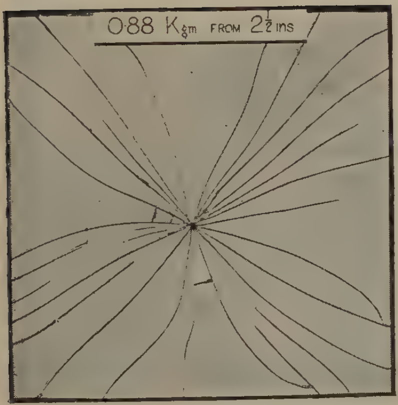
0·88 Kgm FROM 2½ ins

(*d*)

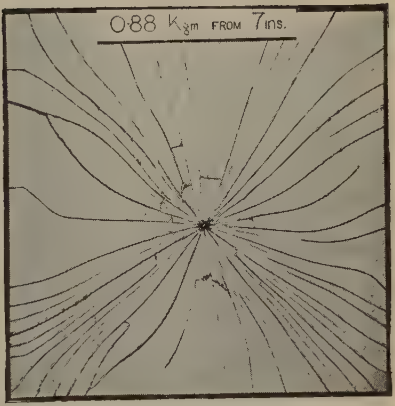
0·88 Kgm FROM 7ins.

(*a*)

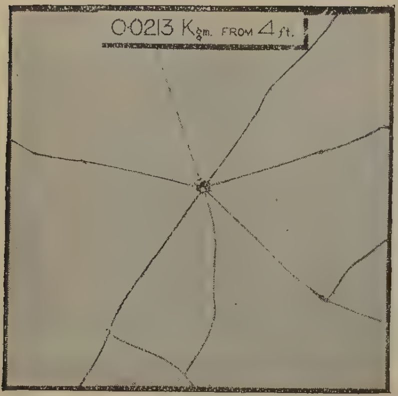
0·0213 Kgm. FROM 4 ft.

(*b*)

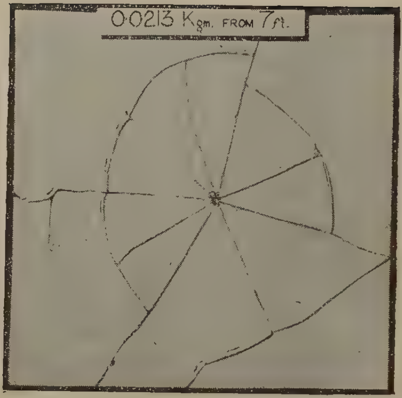
0·0213 Kgm. FROM 7 ft.

(*c*)

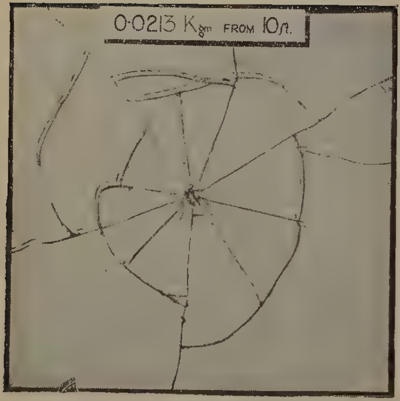
0·0213 Kgm. FROM 10 ft.

(*d*)

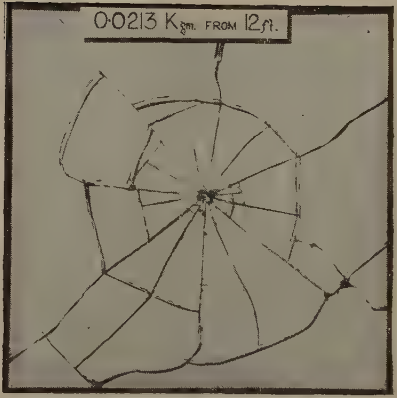
0·0213 Kgm. FROM 12 ft.

(*a*)

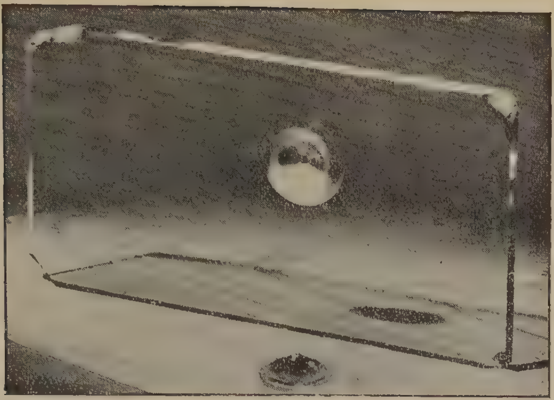

3·4 gm. ball from 26 ft. on $\frac{1}{4}$ in. thick glass.

(*b*)

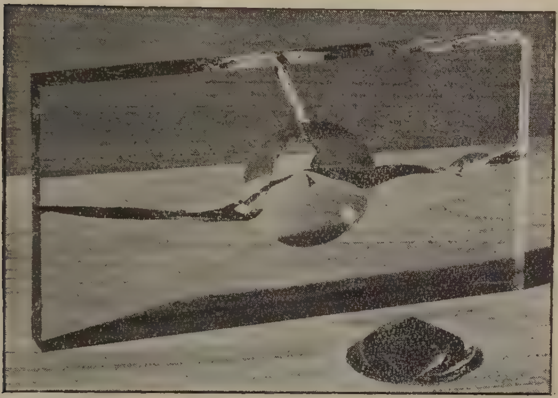

8·4 gm. ball from 26 ft. on $\frac{1}{2}$ in. glass.

(*c*)

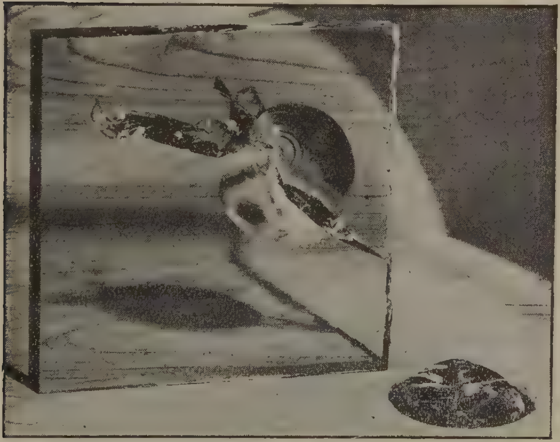

14 gm. ball from 37 ft. on $\frac{3}{4}$ in. glass.

XCVII. *The Demagnetizing Factors for Ellipsoids.*

By Edmund C. Stoner, Sc.D., F.R.S., Professor of Theoretical Physics at the University of Leeds*.

[Received August 13, 1945.]

1. *Introductory.*

Formulæ for the demagnetizing field in a uniformly magnetized ellipsoid of revolution, first derived by Maxwell, are given in many books, but the numerical evaluation of the expressions, although it presents no essential difficulty, is somewhat troublesome. No comprehensive table of values seems to have been published, and the short lists of illustrative values which are sometimes given are seldom free from significant errors. As the need for a reliable set of values of demagnetizing coefficients for ellipsoids makes itself felt in connection with a variety of magnetic problems, it was thought that a useful purpose might be served by carrying out the calculations systematically over the whole of the range of the parameters with a degree of accuracy which would ensure adequacy for any likely theoretical or practical application. The results of the calculations are embodied in the tables in this paper.

The direct practical application of the demagnetizing factors for ellipsoids, except for such special cases as the sphere and the disc, is rather limited, though these factors are required in connection with a number of methods which have been used for measurements on ferromagnetics. In spite of the difficulty of making accurately ellipsoidal test pieces, the advantages, for precision work, of uniformity of magnetization throughout the specimen, would seem to make the development of methods employing them worthy of fuller consideration. Indirectly, the exactly calculable fields in magnetized ellipsoids are of very considerable value in providing a guide in estimating the field and intensity distribution in the variously shaped pieces of magnetic material used in magnetic and electromagnetic equipment. Moreover, the range of shapes covered by the term ellipsoid of revolution is sufficiently wide to include approximations to most of the shapes of portions of ferromagnetic material which it may be desirable to consider in connection with the internal structure of ferromagnetic metals and alloys.

The form in which the general expressions for the demagnetizing factors of the ellipsoid with three unequal axes is given by Maxwell and later writers is not appropriate for direct numerical evaluation. These demagnetizing factors seldom come into use, and the labour of drawing up extensive numerical tables would be out of all proportion to their usefulness. To supplement the numerical tables for ellipsoids of revolution, however, it has seemed worth while to re-express the Maxwell formulæ in terms of elliptic integrals of standard form, so that with the aid of readily available tables, numerical values can be obtained, when required, with a minimum of difficulty. Moreover the interesting inter-relations between the general demagnetizing factors, for three unequal axes, and the special factors, for two axes equal, are not clearly or fully brought out by the expressions which have previously been given.

---

* Communicated by the Author.

For a body which is uniformly magnetized, with intensity of magnetization I, the usual demagnetizing coefficient, N, may be defined by the relation

$$H_t = H_a - NI, \quad . \quad . \quad . \quad . \quad . \quad . \quad . \quad . \quad . \quad (1.1)$$

where H_a is the applied field, and H_t the total field in the material (the "pipe" field), H_t, H_a, and I being co-directional. Except in the special case where the specimen is magnetized to saturation in very strong fields, uniformity of magnetization is possible in a uniform applied field only for an ellipsoid. (Approximate uniformity of magnetization may be obtained by the use of non-uniform fields along limited lengths of bars as in some permeameter arrangements.) The field, H, due to the magnetization alone (putting H_a in (1.1) equal to zero) is co-directional with I for magnetization along the principal axes; taking these as a, b, c along the x, y, z directions, the components of the field due to magnetization of intensity I are given by

$$H_x = -N_a I_x, \quad H_y = -N_b I_y, \quad H_z = -N_c I_z, \quad . \quad . \quad . \quad (1.2)$$

N_a, N_b and N_c being the demagnetizing coefficients. Except for the sphere, the resultant field, H, will not in general be co-directional with the intensity I. It may be noted that

$$N_a + N_b + N_c = 4\pi. \quad . \quad . \quad . \quad . \quad . \quad . \quad . \quad . \quad (1.3)$$

Although the coefficients, N, defined as above, have usually been used in the past, there are several advantages in using a modified factor, D, defined by

$$D = N/4\pi. \quad . \quad . \quad . \quad . \quad . \quad . \quad . \quad . \quad . \quad (1.4)$$

The numerical relations between the various factors then become more immediately obvious, as illustrated by the form taken by (1.3), namely,

$$D_a + D_b + D_c = 1. \quad . \quad . \quad . \quad . \quad . \quad . \quad (1.5)$$

Moreover, from a practical standpoint, the use of D is no less convenient than N. The field due to the magnetization is given, in terms of D, by

$$H = -D(4\pi I) = -D(B-H) = DB/(1-D) \quad . \quad . \quad . \quad . \quad (1.6)$$

With an applied field, H_a, the field, H_t, in the specimen (see (1.1)) is given by

$$H_t = H_a - \frac{D(B-H_a)}{1-D} \quad . \quad . \quad . \quad . \quad . \quad . \quad . \quad . \quad (1.7)$$

When, as is most usual, data are given for B rather than I, division by factors such as $4\pi - N$ is necessary if the coefficients N are used; little purpose is therefore served by multiplying the factors D, which are first evaluated, by 4π, when this, more often than not, merely renders the calculations made in applications more troublesome. In the sequel, therefore, the factors D will be used exclusively, and referred to as demagnetizing factors.

In a field which has been so long and so intensively explored as that involving the geometry of ellipsoids, fundamentally new results are not to be expected. It so happens, however, that although the physical problem of the uniformly magnetized ellipsoid was solved, in a fundamental sense, some seventy years ago, the results have remained, to a large extent, in a form which is neither readily intelligible nor readily applicable. The present paper is a contribution to the filling of a gap between fundamental theory and its practical application.

2. *Outline of Derivation of General Formulæ.*

The problem of magnetic induction in an ellipsoid is presented by Maxwell (' Treatise,' Articles 437 and 438) in a very simple manner and his treatment will be outlined in this paragraph. Following a method due to Poisson, the theoretical determination of the magnetic potential in a uniformly magnetized body is shown to be mathematically equivalent to the determination of the gravitational field in a body of the same shape and of uniform density. In Maxwell's words, " If V is the potential at a point (x, y, z), due to the gravitation of a body of any form of uniform density ρ, then $-dV/dx$ is the potential of the same body if uniformly magnetized in the direction of x with the intensity $I=\rho'$." The proof given is to the effect that $-(dV/dx)\delta x$ would be the potential due to a body of density ρ together with a body of the same shape and density $-\rho$ shifted a distance $-\delta x$ relative to the first; elements $\rho\delta v$ and $-\rho\delta v$ with the second element shifted $-\delta x$ relative to the first, are equivalent to a magnetic element of moment $\rho\delta v\delta x$, the intensity of magnetization of the element being $\rho\delta x$; hence $-(dV/dx)\delta x$ is the potential due to a body magnetized with the intensity $\rho\delta x$ in the direction of x, and $-dV/dx$ is that of a body magnetized with intensity ρ. If the magnetization is to be uniform and hence also the field due to it (the applied field is assumed to be uniform, the value zero being tacitly included), the magnetic potential, Ω, must be a linear function of the co-ordinates x, y, z within the body, and the corresponding " gravitational " potential V must be a quadratic function of the co-ordinates. To quote Maxwell again, " The only cases with which we are acquainted in which V is a quadratic function of the co-ordinates within the body are those in which the body is bounded by a complete surface of the second degree, and the only case in which such a body is of finite dimensions is when it is an ellipsoid." The standard integral expression, in a form equivalent to that given below, for the potential of an ellipsoid is then introduced, with a reference to Thomson and Tait's 'Natural Philosophy,' and the integral forms of the expressions for the demagnetizing coefficients follow immediately. The explicit expressions which may be obtained for these coefficients for ellipsoids of revolution are then given in the often quoted forms, involving the eccentricities.

The inter-relation between the magnetic potential of a uniformly magnetized body and the gravitational potential of a body of the same shape of uniform density may be shown generally and with brevity by using vector notation (*cf.* Stoner, 'Magnetism and Matter,' p. 28, 1934).

The symbol ∇ will be used, where

$$\nabla=\mathbf{i}\frac{\partial}{\partial x}+\mathbf{j}\frac{\partial}{\partial y}+\mathbf{k}\frac{\partial}{\partial z},$$

i, **j** and **k** being unit vectors in the x, y, z directions. The dot symbol is used to denote a scalar product. It may be noted that $\nabla\cdot$ applied to a vector is equivalent to div, and ∇ applied to a scalar to grad. A general expression for the magnetic potential, Ω, due to a magnetized body (obtained by simple generalization of the expression for the potential due to a dipole) is

$$\Omega=-\int \mathbf{I}\cdot\nabla\left(\frac{1}{r}\right)d\mathrm{V}, \quad . \quad . \quad . \quad . \quad . \quad . \quad . \quad (2.1)$$

which for uniform magnetization becomes

$$\Omega=-\mathbf{I}\cdot\int\nabla\left(\frac{1}{r}\right)d\mathrm{V}. \quad . \quad . \quad . \quad . \quad . \quad . \quad . \quad (2.2)$$

Since $-\int\nabla\left(\frac{1}{r}\right)d\mathrm{V}$ gives the gravitational force due to a volume of uniform unit density of mass (apart from the constant G), or the electric force due to a volume of uniform unit density of charge, the required theorem is immediately proved. It may be noticed that (2.1) may be transformed by Green's theorem to give the potential in terms of Poisson's equivalent surface and volume distributions. With $\mathbf{n}_1$ as the unit normal to the surface element dS,

$$\Omega=\int\frac{1}{r}(\mathbf{I}\cdot\mathbf{n}_1)\,d\mathrm{S}-\int\frac{1}{r}(\nabla\cdot\mathbf{I})\,d\mathrm{V}. \quad . \quad . \quad . \quad . \quad . \quad (2.3)$$

For uniform magnetization, the second term vanishes, and the distribution can be treated as a surface distribution of magnetic charge of pole strength per unit area $\mathbf{I}\cdot\mathbf{n}_1$ (equal to I cos θ, where θ is the angle between I and the outward drawn normal). The great difficulty in predetermining the fields due to magnetized materials in forms of practical interest, such as rods and bars and electromagnet pole pieces, is that the second term is usually comparable with the first, and it is only by exceedingly laborious methods that even rough approximations to the distribution and thence to the value of the integral can be obtained *. The ellipsoid is troublesome to deal with; but it is easier than anything else.

---

* A good account of work in the latter part of the last century on the general problem of demagnetizing fields is given in the book by Du Bois (1896), and in a paper by Bozorth and Chapin (1942) on the demagnetizing factors of rods references are given to more recent work.

The potential at an internal point of an ellipsoid of unit uniform density, with semi-axes a, b, c in the x, y, z directions respectively may be expressed in the following form which was first given by Dirichlet in 1839 :

$$\mathrm{V}=\pi abc\int_0^\infty\left\{1-\frac{x^2}{a^2+s}-\frac{y^2}{b^2+s}-\frac{z^2}{c^2+s}\right\}\frac{ds}{(a^2+s)^{1/2}(b^2+s)^{1/2}(c^2+s)^{1/2}}. \quad (2.4)$$

There is no short cut to this formula, and for its derivation reference must be made to treatises dealing with potential theory. A detailed treatment of this classical problem of the ellipsoid is given, for example, in Thomson and Tait's 'Natural Philosophy' (vol. i. part ii., articles 494 and 519–533) and in Webster's 'Dynamics' (articles 151–161), in both of which books an indication is given of the historical sequence of development of the theory. Certain aspects of the mathematical theory are discussed fully in Jeans's 'Electricity and Magnetism' in connection with the problem of an ellipsoid in a uniform electric field, and a more succinct treatment with reference to the present problem is given in Stratton's 'Electromagnetic Theory' (sections 3.27 and 4.18).

From the relation proved above it follows that the x component of the demagnetizing field for a uniformly magnetized ellipsoid is given by

$$\mathrm{H}_x=-\frac{\partial\Omega}{\partial x}=\frac{\partial^2\mathrm{V}}{\partial x^2}=-2\pi abc\mathrm{I}_x\int_0^\infty\frac{ds}{(a^2+s)^{3/2}(b^2+s)^{1/2}(c^2+s)^{1/2}}, \quad (2.5)$$

with similar expressions for H_y and H_z. The demagnetizing factors, as defined in (1.2) and (1.4), are therefore given by

$$\mathrm{D}_\nu=\frac{abc}{2}\int_0^\infty\frac{ds}{(\nu^2+s)\mathrm{R}_s}, \quad \ldots\ldots\ldots \quad (2.6)$$

where $\nu=a, b, c$ and $\mathrm{R}_s=\{(a^2+s)(b^2+s)(c^2+s)\}^{1/2}$.

These are the general integral expressions for the demagnetizing factors of an ellipsoid.

3. *Expression of Demagnetizing Factors in Terms of Normal Elliptic Integrals.*

The integrals in the formulæ (2.6) for the demagnetizing factors of an ellipsoid are elliptic integrals, and for their evaluation it is appropriate to express them in terms of elliptic integrals which have been tabulated. The tabulated integrals are Legendre's normal integrals of the first and second kinds, namely,

$$\mathrm{F}(k,\phi)=\int_0^\phi\frac{d\psi}{(1-k^2\sin^2\psi)^{1/2}}=\int_0^x\frac{dz}{(1-z^2)^{1/2}(1-k^2z^2)^{1/2}}, \quad . \quad (3.1)$$

and

$$\mathrm{E}(k,\phi)=\int_0^\phi(1-k^2\sin^2\psi)^{1/2}d\psi=\int_0^x\frac{(1-k^2z^2)^{1/2}dz}{(1-z^2)^{1/2}}, \quad . \; . \quad (3.2)$$

where $k^2<1$, $x=\sin\phi$.

Taking $a\geqslant b\geqslant c$, by the substitution $z^2=(a^2-c^2)/(a^2+s)$, the expressions (2.6) become

$$\mathrm{D}_\nu=\frac{abc}{(a^2-c^2)^{1/2}}\int_0^x\left[z^2\Big/\left\{\left(1-\frac{a^2-\nu^2}{a^2-c^2}z^2\right)^{1/2}(1-z^2)^{1/2}(1-k^2z^2)^{1/2}\right\}\right]dz, \quad (3.3)$$

where $k^2=(a^2-b^2)/(a^2-c^2)$, $x^2=1-c^2/a^2$.

For $\nu=a$, the required transformation is immediately effected since

$$\frac{z^2}{(1-z^2)^{1/2}(1-k^2z^2)^{1/2}}=\frac{1}{k^2}\left\{\frac{1}{(1-z^2)^{1/2}(1-k^2z^2)^{1/2}}-\frac{(1-k^2z^2)^{1/2}}{(1-z^2)^{1/2}}\right\}.$$

For $\nu=b$, an integration by parts is necessary, and the required form is most readily obtained by using the relation

$$\frac{d}{dz}\left\{\frac{z(1-z^2)^{1/2}}{(1-k^2z^2)^{1/2}}\right\}=\frac{(1-z^2)^{1/2}}{(1-k^2z^2)^{1/2}}-(1-k^2)\frac{z^2}{(1-z^2)^{1/2}(1-k^2z^2)^{3/2}}.$$

For $\nu=c$, a similar procedure may be followed, using the relation

$$\frac{d}{dz}\left\{\frac{z(1-k^2z^2)^{1/2}}{(1-z^2)^{1/2}}\right\}=\frac{(1-k^2z^2)^{1/2}}{(1-z^2)^{1/2}}+(1-k^2)\frac{z^2}{(1-z^2)^{3/2}(1-k^2z^2)^{1/2}}.$$

The formulæ finally obtained for the demagnetizing factors in terms of F and E are

$$\left.\begin{aligned}
D_a&=\frac{abc}{(a^2-c^2)^{1/2}(a^2-b^2)}\{F(k,\phi)-E(k,\phi)\},\\
D_b&=-\frac{abc}{(a^2-c^2)^{1/2}(a^2-b^2)}\{F(k,\phi)-E(k,\phi)\}\\
&\qquad+\frac{abc}{(a^2-c^2)^{1/2}(b^2-c^2)}E(k,\phi)-\frac{c^2}{b^2-c^2},\\
D_c&=-\frac{abc}{(a^2-c^2)^{1/2}(b^2-c^2)}E(k,\phi)+\frac{b^2}{b^2-c^2},
\end{aligned}\right\}\quad . \quad . \quad (3.4)$$

where $k^2=(a^2-b^2)/(a^2-c^2)$, $\sin^2\phi=x^2=1-c^2/a^2$.

Since the demagnetizing factors depend on the relative and not the absolute lengths of the semi-axes, it is convenient to express them in terms of dimensional ratios. The final formulæ are therefore set out below in this form.

For an ellipsoid of semi-axes a, b, c $(a\geqslant b\geqslant c)$, let $b/a=\beta$, $c/a=\gamma(1\geqslant\beta\geqslant\gamma)$. Then

$$\left.\begin{aligned}
D_a&=\frac{\beta\gamma}{(1-\gamma^2)^{1/2}(1-\beta^2)}\{F(k,\phi)-E(k,\phi)\},\\
D_b&=-\frac{\beta\gamma}{(1-\gamma^2)^{1/2}(1-\beta^2)}\{F(k,\phi)-E(k,\phi)\}\\
&\qquad+\frac{\beta\gamma}{(1-\gamma^2)^{1/2}(\beta^2-\gamma^2)}E(k,\phi)-\frac{\gamma^2}{\beta^2-\gamma^2},\\
D_c&=-\frac{\beta\gamma}{(1-\gamma^2)^{1/2}(\beta^2-\gamma^2)}E(k,\phi)+\frac{\beta^2}{\beta^2-\gamma^2},
\end{aligned}\right\}\quad . \quad . \quad (3.5)$$

where $k^2=(1-\beta^2)/(1-\gamma^2)$, $\sin^2\phi=x^2=1-\gamma^2$.

The arguments in tables of incomplete elliptic integrals $F(k,\phi)$ and $E(k,\phi)$ are usually ϕ and θ where $\theta=\sin^{-1}k$. Suitable tables are given in the collections of Dale (1937), Hayashi (1930) (5-place), and Jahncke-Emde (1933) (4-place). In all of these, values are given for every degree of ϕ, and every fifth degree of θ. The 9-place tables given in Legendre's treatise (1825–8) at intervals of one degree in both arguments have been reprinted (1931). The evaluation of the demagnetizing factors for given values of the dimensional ratios, using (3.5), involves a double interpolation in the tables of integrals, and, with the intervals used in the tables, higher differences must be taken into account if an accuracy corresponding to the tabular accuracy is required in the interpolates. The rapid increase of $F(k, \phi)$ as k and $\sin \phi$ approach unity would make the use of the tables in this region inappropriate, but here series developments could be obtained for each demagnetizing factor, the leading term being that corresponding to the factor for the ellipsoid of revolution to which the general ellipsoid approximates.

Fig. 1.

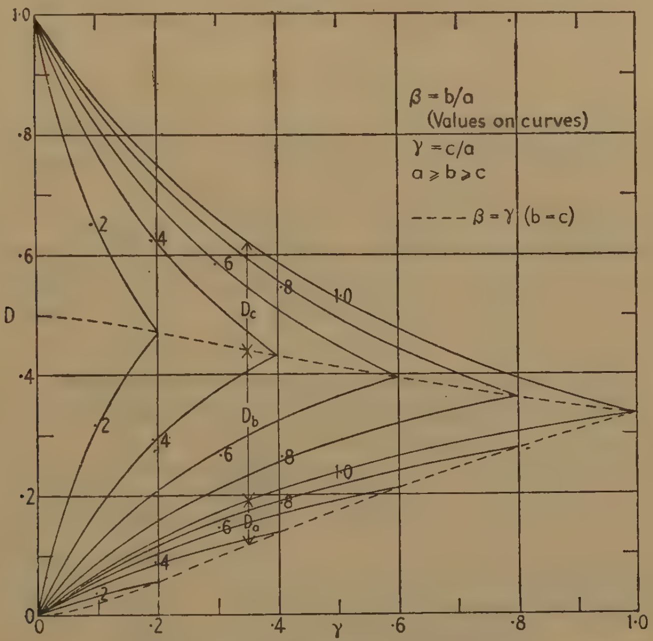

Demagnetizing factors for ellipsoids.

The demagnetizing field, H, is given by $H = -4\pi DI$. Curves are drawn for varying γ, with β constant. The broken curves do not fall in this series, but are limiting curves for $\beta=\gamma$. With $a \geqslant b \geqslant c$, $D_a \leqslant D_b \leqslant D_c$. The regions in which the values fall are indicated.

Extensive numerical tables of D_a, D_b and D_c are unlikely to be required, but a sufficient number of values have been obtained, to 3- or 4-place accuracy, to make clear the character of the dependence of the values on the dimensional ratios $\beta(=b/a)$ and $\gamma(=c/a)$. The curves obtained are shown in fig. 1.

In fig. 1 the whole range of values is covered, though at the wide interval of 0·2 in β. The two broken curves for $\beta=\gamma$ give the demagnetizing factors for prolate ellipsoids of revolution, the lower curve along the polar axis, the upper along the equatorial axis, as functions of the ratio of the shorter (equatorial) to the longer (polar) axis. The two curves for $\beta=1$ (i. e., $a=b$) give the demagnetizing factors for oblate ellipsoids of revolution, the upper along the polar axis, the lower along the equatorial axis, as functions of the ratio of the shorter (polar) to the longer (equatorial) axis. The curves all meet at the value 1/3, corresponding to a sphere. The limiting values on the left-hand side of the figure for $\gamma\rightarrow0$ depend on how that limit is approached. For $1>\beta>\gamma$, the limiting values, for $\gamma\rightarrow0$, are 1, 0 and 0 for D_c, D_b, and D_a respectively; for $\beta=\gamma$, the limiting values are 0·5, 0·5 and 0. For given values of β and γ the sum of the three demagnetizing factors, as shown by (3.4) or (3.5), is unity. This is brought out clearly in the figure, in which, it should be noticed, the lower of the $\beta=1\cdot0$ curves consists of coincident curves for D_a and D_b, and the upper broken curve of coincident curves for D_b and D_c.

4. *The Ellipsoid of Revolution.*

Derivation of Formulæ.—For ellipsoids of revolution the elliptic integrals in the general expressions (2.6) for the demagnetizing factors reduce to inverse circular or logarithmic functions. Formulæ may be obtained from (3.4) or (3.5) for the limits $b\rightarrow a$ (oblate ellipsoid) and $c\rightarrow b$ (prolate ellipsoid), the first corresqonding to $k^2\rightarrow0$, the second to $k'^2=1-k^2\rightarrow0$, by expanding the integrands of $F(k, \phi)$ and $E(k, \phi)$ as power series in k^2 or k'^2 as appropriate. It is, however, simpler to proceed directly from the basic integrals (2.6), putting $a=b$, or $b=c$, as appropriate, or, for the special case of the sphere $a=b=c$.

To avoid the use of unusual symbols, the convention $a\geqslant b\geqslant c$ used in section 3 will not be retained, and in connection with the ellipsoid of revolution, treated in this section, the following symbols will be used:

a, polar semi-axis; b, equatorial semi-axis; $m=a/b$; $\mu=1/m=b/a$.

The entire range is covered by $0\leqslant m\leqslant\infty$, or by $0\leqslant\mu\leqslant\infty$, or by $0\leqslant m\leqslant1$ together with $0\leqslant\mu\leqslant1$.

The general formulae (2.6) become

$$\left.\begin{aligned} D_a&=\frac{ab^2}{2}\int_0^\infty\frac{ds}{(a^2+s)^{3/2}(b^2+s)},\\ D_b&=\frac{ab^2}{2}\int_0^\infty\frac{ds}{(a^2+s)^{1/2}(b^2+s)^2}.\end{aligned}\right\}\quad\ldots\ldots\quad(4.1)$$

It is convenient, though not essential, in evaluating the integrals, to treat separately the cases $\mu<1$ and $m<1$.

A. *Prolate spheroid.*

$$a>b,\quad a/b=m>1,\quad b/a=\mu<1.$$

The substitution $z^2=(a^2-b^2)/(a^2+s)$ in (4.1) results in

$$D_a=\frac{\mu^2}{(1-\mu^2)^{3/2}}\int_0^{(1-\mu^2)^{1/2}}\frac{z^2\,dz}{1-z^2},$$

$$D_b=\frac{\mu^2}{(1-\mu^2)^{3/2}}\int_0^{(1-\mu^2)^{1/2}}\frac{z^2\,dz}{(1-z^2)^2}.$$

In the expression for D_a the integral may be rewritten

$$\frac{z^2}{1-z^2}=\frac{1}{2}\left(\frac{1}{1+z}+\frac{1}{1-z}\right)-1$$

and the integration immediately effected. In the expression for D_b, an integration by parts is required, using the relation

$$\frac{d}{dz}\,\frac{z}{1-z^2}=\frac{1}{1-z^2}+\frac{2z^2}{(1-z^2)^2}.$$

The final formulae may be put in the forms :

$$D_a=\frac{\mu^2}{1-\mu^2}\left[\frac{1}{(1-\mu^2)^{1/2}}\ln\left\{\frac{1+(1-\mu^2)^{1/2}}{\mu}\right\}-1\right],$$

$$=\frac{1}{(m^2-1)}\left[\frac{m}{(m^2-1)^{1/2}}\ln\{m+(m^2-1)^{1/2}\}-1\right]; \quad . \quad . \quad . \quad (4.2)$$

$$D_b=\frac{1}{2(m^2-1)}\left[m^2-\frac{m}{(m^2-1)^{1/2}}\ln\{m+(m^2-1)^{1/2}\}\right],$$

$$=\frac{1}{2}(1-D_a). \quad . \quad . \quad . \quad . \quad . \quad . \quad . \quad . \quad . \quad . \quad . \quad . \quad . \quad . \quad (4.3)$$

The form (4.2) is suitable for numerical evaluation. The simple relation (4.3), a special case of the general relation (1.5), makes separate evaluation (and tabulation) of D_b unnecessary.

For the prolate spheroid the eccentricity, ϵ, is given by

$$\epsilon^2=1-(b/a)^2=1-\mu^2=(m^2-1)/m^2.$$

In terms of the eccentricity, the demagnetizing factor is given by

$$D_a=\frac{1-\epsilon^2}{\epsilon^2}\left\{\frac{1}{2\epsilon}\ln\frac{1+\epsilon}{1-\epsilon}-1\right\}, \quad . \quad . \quad . \quad . \quad . \quad (4.4)$$

the form originally given by Maxwell.

B. *Oblate spheroid.*

$$a<b, \quad a/b=m<1, \quad b/a=\mu>1.$$

The substitution $z^2=(b^2-a^2)/(b^2+s)$ in (4.1) results in

$$D_a=\frac{m}{(1-m^2)^{3/2}}\int_0^{(1-m^2)^{1/2}}\frac{z^2\,dz}{(1-z^2)^{1/2}}.$$

Use of the relation

$$\frac{d}{dz}\,\frac{z}{(1-z^2)^{1/2}}=\frac{z^2}{(1-z^2)^{3/2}}+\frac{1}{(1-z^2)^{1/2}}$$

reduces the integral to the standard form

$$\int(1-z^2)^{-1/2}\,dz=\sin^{-1}z,$$

leading to the formula

$$D_a=\frac{1}{1-m^2}\left\{1-\frac{m}{(1-m^2)^{1/2}}\cos^{-1}m\right\}, \quad . \quad . \quad . \quad . \quad (4.5)$$

a form suitable for numerical evaluation. D_b is obtained using (4.3).

For the oblate spheroid the eccentricity, ϵ, is given by

$$\epsilon^2=1-(a/b)^2=1-m^2=(\mu^2-1)/\mu^2.$$

In terms of the eccentricity, the demagnetizing factor is given by

$$D_a=\frac{1}{\epsilon^2}\left\{1-\frac{(1-\epsilon^2)^{1/2}}{\epsilon}\sin^{-1}\epsilon\right\}, \quad . \quad . \quad . \quad . \quad . \quad (4.6)$$

the Maxwell form.

Relation between factors for $m>1$ and $m<1$.—The formula (4.2) is in a practically useful form for $m>1$ ($\mu<1$), but its formal validity is not restricted to this range, and it is of interest to obtain, from this single formula, formulae appropriate to the two ranges $m>1$ and $m<1$, and of similar character. From the equations

$$x=\cosh u=\tfrac{1}{2}(e^u+e^{-u})$$

and

$$x=\cos u=\tfrac{1}{2}(e^{iu}+e^{-iu}),$$

it is readily shown that

$$\cosh^{-1}x=\ln\{x+(x^2-1)^{1/2}\}\,;\quad \cos^{-1}x=-i\ln\{x+i(1-x^2)^{1/2}\}.$$

Using these relations the formula (4.2) can at once be put in the form

$$D_a=\frac{1}{m^2-1}\left\{\frac{m}{(m^2-1)^{1/2}}\cosh^{-1}m-1\right\}, \quad . \quad . \quad . \quad . \quad (4.7)$$

appropriate for $m>1$, and in the form

$$D_a=\frac{1}{1-m^2}\left\{1-\frac{m}{(1-m^2)^{1/2}}\cos^{-1}m\right\}, \quad . \quad . \quad . \quad . \quad (4.8)$$

appropriate for $m<1$.

C. *Sphere.*—The formula (4.1) becomes

$$D_a=\frac{a^3}{2}\int_0^\infty\frac{ds}{(a^2+s)^{5/2}}, \quad . \quad . \quad . \quad . \quad . \quad . \quad . \quad . \quad (4.9)$$

which integrates immediately to give

$$D_a=\frac{1}{3}, \quad . \quad . \quad . \quad . \quad . \quad . \quad . \quad . \quad . \quad . \quad (4.10)$$

a result usually obtained by elementary methods dependent essentially on (2.3).

Series Expansions.—Series expansions are of value in showing the limiting forms of the expressions for the demagnetizing factors, in indicating in an obvious way the character of the variation, and, for certain ranges, in facilitating numerical evaluation. They may be developed from the series for the logarithmic and inverse circular functions which are given in many books (*e. g.*, Dwight, 1934; Milne-Thomson and Comrie, 1931). Usually the general expressions for the coefficients are cumbersome, and it is probably more useful to give explicitly the coefficients for the leading terms.

Elongated Prolate Spheroid.—$m \gg 1$, $\mu = 1/m \ll 1$.

$$D_a = \mu^2 \left\{ \left(1 + \frac{3}{2}\mu^2 + \frac{15}{8}\mu^4 + \frac{35}{16}\mu^6 + \ldots\right) \ln 2m \right.$$

$$\left. - \left(1 + \frac{5}{4}\mu^2 + \frac{47}{32}\mu^4 + \frac{319}{192}\mu^6 + \ldots\right) \right\}, \quad . \quad . \quad (4.11\,a)$$

$$= \mu^2(\ln 2m - 1) + \tfrac{1}{4}\mu^4(3 \ln 2m - 5)$$

$$+ \frac{1}{32}\mu^6(15 \ln 2m - 47) + \frac{1}{192}\mu^8(420 \ln 2m - 319) + \ldots . \quad (4.11\,b)$$

Fig. 2.

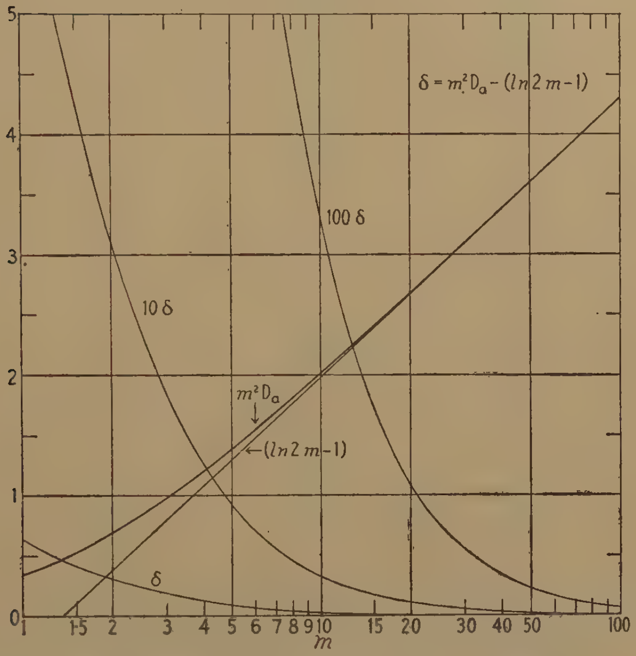

Demagnetizing factors for prolate spheroids.

$m = a/b$; a, polar semi-axis ; b, equatorial semi-axis. D_a, demagnetizing factor for polar axis. $m^2 D_a$ is plotted against m (logarithmic). For large values of m, $m^2 D_a$ approximates to $\ln 2m - 1$. The differences between $m^2 D_a$ and $\ln 2m - 1$ are shown on three scales.

This series up to the term in μ^8 gives D_a to an accuracy of 1 unit in the eighth place at $m = 10(\mu = 0{\cdot}1)$, and to 1 unit in the sixth place for $m = 5(\mu = 0{\cdot}2)$. For larger values of m (or smaller values of μ), for which the series is useful in practice, the accuracy obtainable by breaking off at any term can readily be estimated from the next term.

The first term in the series in the form (4.11 b) is well known. The character of the approximation provided by this single term is shown by the logarithmic plot in fig. 2. At $m = 10$, the error is less than 1·7 per cent., at $m = 100$ less than 0·016 per cent.

The demagnetizing factor, D_b, along the equatorial axis, cannot be conveniently represented with the form of graph used in fig. 2, but the two broken curves in fig. 1 give D as a function of μ, the lower D_a and the upper D_b, for the range $0 \leqslant \mu \leqslant 1$. A double logarithmic plot, which has been used by Bozorth and Chapin (1942), has advantages for some purposes.

Flattened Oblate Spheroid.—$m \ll 1$, $\mu = 1/m \gg 1$.

$$D_a = 1 + 2m^2 + \frac{8}{3}m^4 + \frac{16}{5}m^6 + \frac{128}{35}m^8 + \ldots$$
$$- \frac{m\pi}{2}\left(1 + \frac{3}{2}m^2 + \frac{15}{8}m^4 + \frac{35}{16}m^6 + \frac{315}{128}m^8 + \ldots\right). \quad . \quad (4.12)$$

$(\pi/2 = 1{\cdot}570\ 796.)$

Fig. 3.

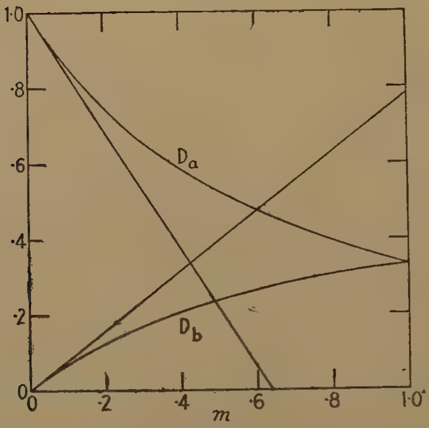

Demagnetizing factors for oblate spheroids.

$m = a/b$; a, polar semi-axis ; b, equatorial semi-axis. D_a, D_b, demagnetizing factors for polar, equatorial axis. The straight lines of slopes $-\pi/2$ and $+\pi/4$ are tangential to the curves.

This series up to the term in m^8 gives D_a to an accuracy of 1 unit in the seventh place at $m = 0{\cdot}1 (\mu = 10)$, and to 1 unit in the fifth place at $m = 0{\cdot}2 (\mu = 5)$. A graph of D_a and D_b against m is shown in fig. 3. The tangent to the D_a curve, of slope $-\pi/2$, and the tangent to the D_b curve, of slope $+\pi/4$, are also shown in the diagram.

The curves of fig. 3, it may be noted, are the same as the curves for $\beta = 1{\cdot}0$ in fig. 1.

Nearly Spherical Spheroid.—$1 - \mu^2 \ll 1$ (prolate) and $(1 - m^2) \ll 1$ (oblate). When the eccentricity, ϵ, approaches zero, series in ϵ^2, that is in $(1 - m^2)$ or $(1 - \mu^2)$, are more convenient than series in $(1 - m)$ or $(1 - \mu)$. These series are readily developed from (4.4) and (4.6).

For the prolate spheroid, with $a>b$, $\epsilon^2=1-(b/a)^2=1-\mu^2\leqslant 1$,

$$\mathrm{D}_a=\frac{1}{3}-\frac{2\epsilon^2}{15}\left(1+\frac{3}{7}\epsilon^2+\frac{5}{21}\epsilon^4+\ldots\right). \quad . \quad . \quad . \quad (4.13)$$

For the oblate spheroid, with $a<b$, $\epsilon^2=1-(a/b)^2=1-m^2\leqslant 1$,

$$\mathrm{D}_x=\frac{1}{3}+\frac{2\epsilon^2}{15}\left(1+\frac{4}{7}\epsilon^2+\frac{8}{21}\epsilon^4+\ldots\right). \quad . \quad . \quad . \quad (4.14)$$

These series, though appropriate for small eccentricities, are of limited utility with reference to the m or μ range; with (4.13), which is less slowly convergent than (4.14), it is necessary to carry the series to the term in ϵ^{10} to obtain an accuracy of 1 unit in the sixth place even for $m=1{\cdot}1$. The series are of interest, however, in giving at once for the sphere ($m=\mu=1$) the value for D_a of 1/3, which is not an immediately obvious limit to the expressions (4.2) to (4.6).

Fig. 4.

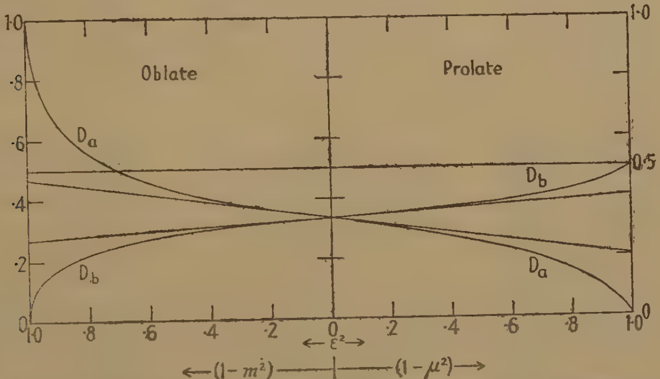

Demagnetizing factors for spheroids as functions of eccentricity.

$m=a/b$; $\mu=b/a$; a, polar semi-axis; b, equatorial semi-axis; ϵ, eccentricity. For prolate spheroid, $\epsilon^2=1-\mu^2$; for oblate spheroids, $\epsilon^2=1-m^2$. The straight lines of slopes $-2/15$ and $+1/15$ are tangential to the curves at $\epsilon^2=0$.

A graphical representation of the dependence of the demagnetizing factors on the eccentricity is given in fig. 4, the straight lines being the tangents to the curves at $\epsilon^2=0$, as given by (4.13) and (4.14); the slopes of the tangents are $-2/15$ for the D_a curve, and $+1/15$ for the D_b curve.

A consideration of the series (4.11) to (4.14) shows that their practical usefulness is limited to very restricted ranges of the values of the dimensional ratio, $m=a/b$, of an ellipsoid of revolution. Numerical evaluation of the expressions (4.2) and (4.5) is in general necessary, and even in the ranges to which the series are in practice applicable, the series expressions are comparable in convenience only for large and small values of m (say $m>10$ and $m<0{\cdot}1$) and for values in the neighbourhood of unity (say $m=1\pm 0{\cdot}05$). The series expressions do.

TABLE I.

Demagnetizing Factors for Ellipsoids of Revolution.

m-Table.

$m=a/b$; a, polar semi-axis; b, equatorial semi-axis. $m<1$, oblate spheroid; $m>1$, prolate spheroid. The demagnetizing field is given by $H=-4\pi DI$. $D_b=\frac{1}{2}(1-D_a)$. ($4\pi=12{\cdot}566\ 371$.)

m.	D_a.	m.	D_a.	m.	D_a.
0·0	1·000 000	3·5	0·089 651	20	0·006 749
0·1	0·860 804	3·6	86 477	21	6 230
0·2	750 484	3·7	83 478	22	5 771
0·3	661 350	3·8	80 641	23	5 363
0·4	588 154	3·9	77 954	24	4 998
0·5	0·527 200	4·0	0·075 407	25	0·004 671
0·6	475 826	4·1	72 990	30	3 444
0·7	432 065	4·2	70 693	35	2 655
0·8	394 440	4·3	68 509	40	2 116
0·9	361 822	4·4	66 431	45	1 730
1·0	0·333 333	4·5	0·064 450	50	0·001 443
1·1	308 285	4·6	62 562	60	1 053
1·2	286 128	4·7	60 760	70	0 805
1·3	266 420	4·8	59 039	80	0 637
1·4	248 803	4·9	57 394	90	0 518
1·5	0·232 981	5·0	0·055 821	100	0·000 430
1·6	218 713	5·5	48 890	110	363
1·7	205 794	6·0	43 230	120	311
1·8	194 056	6·5	38 541	130	270
1·9	183 353	7·0	34 609	140	236
2·0	0·173 564	7·5	0·031 275	150	0·000 209
2·1	164 585	8·0	28 421	200	125
2·2	156 326	8·5	25 958	250	083
2·3	148 710	9·0	23 816	300	060
2·4	141 669	9·5	21 939	350	045
2·5	0·135 146	10	0·020 286	400	0·000 036
2·6	129 090	11	17 515	500	24
2·7	123 455	12	15 297	600	17
2·8	118 203	13	13 490	700	13
2·9	113 298	14	11 997	800	10
3·0	0·108 709	15	0·010 749	900	0·000 008
3·1	104 410	16	09 692	1000	7
3·2	100 376	17	08 790	1100	6
3·3	096 584	18	08 013	1200	5
3·4	093 015	19	07 339	1300	4

TABLE II.

Demagnetizing Factors for Ellipsoids of Revolution.

μ-Table.

$\mu=b/a=1/m$; *a*, polar semi-axis; *b*, equatorial semi-axis. $\mu<1$, prolate spheroid; $\mu>1$, oblate spheroid. The demagnetizing field is given by $H=-4\pi DI$. $D_b=\frac{1}{2}(1-D_a)$. ($4\pi=12{\cdot}566\ 371$.)

μ.	D_a.	μ.	D_a.	μ.	D_a.
0·0	0·000 000	3·5	0·673 006	20	0·926 181
0·1	020 286	3·6	679 625	21	929 494
0·2	055 821	3·7	685 984	22	932 522
0·3	095 370	3·8	692 097	23	935 301
0·4	135 146	3·9	697 979	24	937 860
0·5	0·173 564	4·0	0·703 641	25	0·940 224
0·6	209 962	4·1	709 097	30	949 778
0·7	244 110	4·2	714 357	35	956 700
0·8	275 992	4·3	719 432	40	961 944
0·9	305 689	4·4	724 330	45	966 056
1·0	0·333 333	4·5	0·729 061	50	0·969 366
1·1	359 073	4·6	733 633	60	974 359
1·2	383 059	4·7	738 055	70	977 961
1·3	405 437	4·8	742 332	80	980 673
1·4	426 344	4·9	746 473	90	982 790
1·5	0·445 906	5·0	0·750 484	100	0·984 490
1·6	464 237	5·5	768 780	110	985 885
1·7	481 442	6·0	784 585	120	987 048
1·8	497 615	6·5	798 373	130	988 034
1·9	512 843	7·0	810 506	140	988 881
2·0	0·527 200	7·5	0·821 265	150	0·989 616
2·1	540 758	8·0	830 870	200	992 196
2·2	553 578	8·5	839 497	250	993 749
2·3	565 717	9·0	847 288	300	994 786
2·4	577 227	9·5	854 359	350	995 528
2·5	0·588 154	10	0·860 804	400	0·996 085
2·6	598 539	11	872 125	500	996 866
2·7	608 422	12	881 743	600	997 388
2·8	617 837	13	890 017	700	997 760
2·9	626 817	14	897 210	800	998 040
3·0	0·635 389	15	0·903 520	900	0·998 257
3·1	643 581	16	909 101	1000	998 431
3·2	651 417	17	914 071	1100	998 574
3·3	658 920	18	918 526	1200	998 692
3·4	666 110	19	922 542	1300	998 793

however, bring out the character of the variation, and they have value in enabling a rough estimate of the demagnetizing factors to be easily obtained.

5. *Numerical Tables.*

Numerical values of the demagnetizing factors for an ellipsoid of revolution, polar semi-axis a, equatorial semi-axis b, have been calculated from the expressions (4.2) and (4.5) which are repeated here for convenience :

$$D_a = \frac{1}{m^2-1}\left[\frac{m}{(m^2-1)^{1/2}}\ln\{m+(m^2-1)^{1/2}\}-1\right] \text{ for } a/b=m>1. \quad (5.1)$$

$$D_a = \frac{1}{1-m^2}\left[1-\frac{m}{(1-m^2)^{1/2}}\cos^{-1} m\right] \text{ for } a/b=m<1. \quad . \quad . \quad . \quad (5.2)$$

The demagnetizing factor along the equatorial axis is given by

$$D_b = \frac{1}{2}(1-D_a). \quad . \quad . \quad . \quad . \quad . \quad . \quad . \quad . \quad . \quad . \quad (5.3)$$

An accuracy higher than 1 in 10^3 or at most 1 in 10^4 will seldom be required in physical applications. For the smaller values of D_a, however, a considerably lower accuracy will be sufficient, for it is the absolute rather than the relative accuracy which is relevant. The demagnetizing field is given by

$$H = -4\pi DI, \quad . \quad . \quad . \quad . \quad . \quad . \quad . \quad . \quad . \quad . \quad (5.4)$$

and the highest values of $4\pi I$ are of the order 10^4. (For iron, for example, the saturation value of $4\pi I$ is about $2{\cdot}16\times10^4$, for 34 per cent. ferrocobalt about $2{\cdot}37\times10^4$.) Thus, even in extreme cases, a value of D_a correct to 1 in the fifth place will give H to about 0·1 oersted. Six place values of D_a will therefore adequately cover all likely requirements. To ensure accuracy to the sixth place the calculations have been carried out so as to give an accuracy to 1 unit in the seventh place, and the rounded six place values are presented in the tables.

It is believed that the most useful form of the tables is with the dimensional ratio as argument. With $m(=a/b)$ as argument, a number of changes of interval are necessary if the relevant range is to be covered with a reasonable number of entries. The smallest interval used is 0·1 over the range $0\leqslant m\leqslant 5$. This interval, however, is too large over the range $0\leqslant m\leqslant 1$, over which D_a changes from 1 to 1/3, but the character of the variation is such that the range can be covered more conveniently by a complementary table with $\mu(=1/m)$ as argument than by the use of intervals smaller than 0·1 in the m table. Two tables, complementary to each other, have therefore been drawn up, an m table (Table I.) and a μ table (Table II.), each with 105 entries, the numerical values of the arguments being the same in each. In the μ table there are 95 entries for $\mu\geqslant 1$, covering the same range as is covered by the 11 entries for $0\leqslant m\leqslant 1$ in the m table ; and conversely. In general the

m table will be appropriate for prolate spheroids ($m>1$, $\mu<1$) and the μ table for oblate spheroids ($m<1$, $\mu>1$).

In the calculations, use was made of Barlow's Tables (Comrie, 1941) for the powers and roots, and for the logarithms of Chambers's seven-place tables (ed. Pryde, 1937), supplemented in certain ranges by the Peters's ten-place tables (1922). No suitable table of the inverse circular functions being available, the inverse cosines were obtained by inverse interpolation in Gifford's eight-place table of natural sines (1914). A Brunsviga 20×12 calculating machine was used.

In each range of the two tables the numbers, usually seven- or eight-place, were checked by the method of differences. Additional checks were provided by cross interpolation between the two tables, and by the use of the series expansions (4.11) to (4.14).

Interpolation may be carried out using Bessel's formula. The necessary coefficients are given by Comrie (1936). The m table would ordinarily be used for $m>1$ and the μ table for $\mu>1$, but for values slightly less or greater than 1 the μ table will be found more convenient. For the greater part of each of the ranges in the tables, it is unnecessary to take into account differences beyond the second to obtain the tabular accuracy in the interpolates, but in the first part of each range the contribution from the fourth difference is not negligible. For the accuracy which is likely to be required in applications differences beyond the second will seldom be required.

It is a pleasure to acknowledge my indebtedness to Mr. C. W. Gilham, of the Department of Mathematics, University of Leeds, for guidance on the reduction of elliptic integrals.

Note added in proof (28 May, 1946).

Since this paper was submitted a paper has appeared, by J. A. Osborn (Phys. Rev. lxvii. p. 351, 1945), on the "Demagnetizing Factors of the General Ellipsoid." Expressions are given for the demagnetizing factors in forms essentially the same as those obtained in section 3 of the present paper, and there are three figures together equivalent to fig. 1, but on a larger scale, and with the curves at smaller intervals. In addition two numerical tables are given for ellipsoids with three unequal axes. The first of these gives the values of c/a, b/a and the associated demagnetizing factors corresponding to appropriate sets of equidistant tabular values in the elliptic integral tables. The second gives values of the demagnetizing factors for b/a at intervals of 0·1 from 0·1 to 1·0, in each case for a series of values of c/a, this set of values having been obtained by graphical interpolation from the first set. The values, it is stated, "are accurate to three decimal places and are probably in error several units in the fourth place." This accuracy seems adequate for any likely requirements in connection with the general ellipsoid, and the tables form a useful complement to those given here for the ellipsoid of revolution.

SUMMARY.

The paper deals with the demagnetizing factors, D, of ellipsoids, D, being defined by the relation $H = -4\pi DI$, where H is the demagnetizing field and I the intensity of magnetization, H and I being co-directional.

The derivation of the usual integral formulae for the demagnetizing factors for the three principal axes of an ellipsoid with three unequal axes is outlined. These integral formulae are re-expressed in terms of normal elliptic integrals of the first and second kinds, enabling the factors to be evaluated without difficulty with the aid of standard tables of these integrals. The variation of the three demagnetizing factors with the ratio of the smallest to the greatest principal axis for a series of constant values of the ratio of the intermediate to the greatest axis is shown in a figure. Particular curves in this figure correspond to an ellipsoid of revolution.

The formulae for the demagnetizing factors, D_a and D_b of an ellipsoid of revolution (a, polar semi-axis ; b, equatorial semi-axis) are derived, and the various alternative forms, and the relations between them and the expressions for an ellipsoid with three unequal axes are discussed. Series expansions are obtained in terms of the dimensional ratio, $m (m = a/b)$, or its inverse, $\mu (\mu = b/a)$, suitable for $m \gg 1$, $m \ll 1$ and $m \doteq 1$. Values of D_a are given to six places of decimals in two numerical tables, an m-table and a μ-table, each with 105 entries. Values of the argument, m or μ, range from 0 to 1300, the range being covered with the intervals shown in brackets: 0·0 (0·1) 5·0 (0·5) 10·0 (1) 25 (5) 50 (10) 150 (50) 400 (100) 1,300. The first table is most useful for prolate spheroids ($m > 1$), the second for oblate spheroids ($\mu = 1/m > 1$). The demagnetizing factor along an equatorial axis, D_b, is not tabulated, as it is easily obtained from D_a, being equal to $\frac{1}{2}(1 - D_a)$.

References.

Bozorth, R. M., and Chapin, D. M 1942 J. App. Phys. vol. xiii. p. 320.

Comrie, L. J. (ed.). 1936. "Interpolation and Allied Tables." Reprinted from the 'Nautical Almanac' for 1937. H.M. Stationery Office.

Comrie, L. J. (ed.). 1941. 'Barlow's Tables,' 4th ed. London : Spon.

Dale, J. B. 1937. 'Five-Figure Tables of Mathematical Functions.' London : Arnold.

Du Bois, H. 1896. 'The Magnetic Circuit.' London : Longmans.

Dwight, D. B. 1934. 'Tables of Integrals and other Mathematical Data.' New York : Macmillan.

Gifford, E. 1914. 'Natural Sines.' Manchester : Printed by Heywood.

Hayashi, K. 1930. 'Fünfstellige Funktionentafeln.' Berlin : Springer.

Jahncke, E., and Emde, F. 1933. 'Funktionentafeln mit Formeln und Kurven.' Leipzig : Teubner.

Jeans, J. H. 1920. 'Electricity and Magnetism,' 4th ed. Cambridge : University Press.

Legendre, A. M. 1931. "Tafeln der elliptischen Integrale." (Reprinted from Legendre's 'Traité des fonctions elliptiques,' 1825–28.) Stuttgart : Wittwer.

Maxwell, J. C. 1881. 'A Treatise on Electricity and Magnetism,' vol. ii. 2nd ed. Oxford : Clarendon Press.
Milne-Thomson, L. M., and Comrie, L. J. 1931. 'Standard Four-Figure Mathematical Tables.' London : Macmillan.
Peters, J. (ed.). 1922. 'Zehnstellige Logarithmentafeln.' Berlin : Reichsamt für Landesaufnahme.
Pryde, J. (ed.). 1937. 'Chambers's Seven-Figure Mathematical Tables.' London : Chambers.
Stoner, E. C. 1934. 'Magnetism and Matter.' London : Methuen.
Stratton, J. A. 1941. 'Electromagnetic Theory.' London : McGraw-Hill.
Thomson, W., and Tait, P. G. 1883. 'Treatise on Natural Philosophy,' 2nd ed. vol. i. pt. ii. Cambridge : University Press.
Webster, A. G. 1925. 'The Dynamics of Particles and of Rigid, Elastic and Fluid Bodies,' 3rd ed. Leipzig : Teubner.

Physics Department,
University of Leeds.

XCVIII. *The Technique of Precise Electron-Diffraction Measurements with Polycrystalline Specimens.*

By T. B. Rymer, Ph.D., and C. C. Butler, B.Sc.,
The University, Reading*.

[Received June 18, 1945.]

[Plate XI.]

Abstract.

Some factors affecting the size and shape of the electron-diffraction rings obtained with transmission specimens are considered. The most important of these are the accumulation of electric charge on the photographic plate and the presence of weak stray magnetic fields.

In an earlier paper (3) we have discussed the problem of the measurement of the radii of the Debye–Scherrer rings produced by the diffraction of electrons by polycrystalline specimens, and we have shown that it is possible to measure these radii with an accuracy of about one part in ten thousand. Measurements of this precision reveal a number of unexpected features, which are partly instrumental in origin and in part are related to the crystal structure of the specimen. These peculiarities have mostly escaped notice because the accuracy of previous measurements has seldom exceeded one part in a thousand. In the present paper some of the instrumental effects encountered in high-precision measurements are considered ; those due to crystal structure must form the subject of a subsequent communication.

---

* Communicated by Prof. J. A. Crowther, M.A., Sc.D.

The diffraction camera used in this work was of the type described by Finch, Quarrell and Wilman (1), with certain minor additions described below. Before attempting precision measurements, it is necessary to be sure that the apparatus is free from such major defects as alternating magnetic fields. When these have been remedied, the residual instrumental effects, such as the distortion of the pattern by the unavoidable presence of iron in the vicinity, must be studied.

1. *Alternating Magnetic Fields.*

Various writers have called attention to the danger that the alternating magnetic fields from the rheostats controlling the high-tension equipment may blur the pattern if they are placed too close to the camera. It is found that not only the rheostats, but also the wiring, high-tension transformers and pumps may produce alternating fields of serious magnitude. For example, the field from our high-tension transformer situated 3 metres from the axis of the camera has a peak value of 100γ * ; a uniform field of this magnitude would cause an elongation of the central spot of the order of 200 μ. One way of overcoming this trouble is to balance these fields by mounting near to the camera large coils carrying currents of suitable magnitude and phase. Since the direction and phase of the resultant field change from point to point along the axis of the camera, a single coil does not suffice for compensation ; our own equipment uses four coils each supplied with current of different magnitude and phase. The best arrangement of these coils is found by trial, using a search coil with high-gain amplifier and cathode-ray oscillograph to measure the field along the axis of the camera. It has been found possible to reduce the alternating field at all points along the camera axis to a peak value of 10 γ. Were this residual field uniform, it would cause an elongation of the central spot of about 20 μ ; the actual elongation is much less as the direction and phase of the field vary along the axis. Once installed, the compensation equipment is found to need no attention, and therefore does not add to the experimental difficulties. It is not possible to compensate the fields due to the diffusion pump heater and backing pump motor owing to the magnitude of the former and the poor wave-form of the latter. We therefore switch off the pumps before making an exposure, relying on the high thermal capacity of the diffusion pump to prevent any deterioration of the vacuum during the exposure.

The effect of the alternating fields arising from the high-tension unit (situated 3 metres from the camera) is illustrated by the four photomicrographs of fig. 5 (Pl. XI.). These show a section of the (110) ring of an ammonium chloride pattern at every 90 deg. There is a marked broadening along the E.–W. direction as the field is predominately in the N.–S. direction. For comparison, fig. 6 (Pl. XI.) shows a similar set of photomicrographs when the A.C. fields are compensated. The widths* of the lines in microns are marked below each photograph.

---

* $1\gamma = 10^{-5}$ gauss.

An alternative way of eliminating the alternating fields is to use high-frequency current for energizing the high-tension equipment (2). The brass walls of the camera constitute a perfect screen for such fields. We have not had an opportunity of trying this method, but our experience of the difficulty of eliminating low-frequency fields by compensation indicates that it merits careful consideration in future installations.

2. *High-Tension Voltage Fluctuations.*

Fluctuations of high-tension voltage will produce variations in the wave-length of the electrons with a resulting broadening of the diffraction rings. The ripple voltage on the camera discharge tube is made small by supplying it through a diode valve run at saturation (1). With this circuit, the ripple voltage is found to be about 75 V. r.m.s. when the discharge tube voltage is 40 kV. and the current is $\frac{1}{2}$ mA. This corresponds to a peak-to-peak broadening of the diffraction rings of about 30 μ. The ripple voltage has a frequency of 100 c.p.s., with no trace of 50 c.p.s. component, showing that the current through the diode is entirely thermionic, gas ionization being negligible ; the 100 c.p.s. ripple of course arises from fluctuations of the temperature of the diode cathode, which occur with double the frequency of the A.C. supply. The above data refer to a Philips K125 diode, the type used by Finch. Most of our work has had to be done using an old X-ray tube as diode. This contained a trace of helium (introduced to assist the focusing of the electron beam on to the anticathode). The ripple voltage with this tube was about double that previously found, and both 50 and 100 c.p.s. frequencies were present, showing that part of the current is being carried by gas ionization. By connecting a 0·0005 μF. condenser across the camera discharge tube, the ripple voltage is reduced to about 75 V.; the reduction occurs mainly in the 50 c.p.s. component, the other being but little changed. It therefore appears that the presence of a small condenser across the camera discharge tube is helpful if the diode contains a trace of gas, but has no effect if it is perfectly hard. It is advisable to disconnect this condenser when using the spark-gap voltmeter to prevent excessive surges.

The factors discussed in this and the preceding section might affect the measurements of the radii of the diffraction rings in two ways : by increasing the random errors of measurement owing to a broadening of the rings, and by introducing systematic errors. The first effect is unimportant, for the broadening amounts to less than 40 per cent. of the width of even the sharpest rings and hence results in less than 20 per cent. increase in the random error (3). Systematic errors might arise owing to diffuse background and the curvature of the rings. If near the peak of a line, the intensity can be expressed as a function of position by

---

* By the width of a line is understood the distance apart of the two points where the intensity is half that at the peak.

$$I=I_0(1-Ax^2+\ldots), \quad \ldots\ldots\ldots \quad (1)$$

the background and curvature errors are each proportional to 1/2A (3). The corrections for these effects are determined by measuring the line width W and calculating the quantity 1/2A from the relation

$$1/2A=0{\cdot}18W^2, \quad \ldots\ldots\ldots \quad (2)$$

derived on the assumption that the line has a Gaussian contour. If the line is broadened by the presence of A.C. magnetic fields or high-tension voltage ripple, the constant of equation (2) is increased, resulting in the corrections for the background and curvature errors being under-estimated. The magnitude of this effect can readily be calculated. The diffraction beam, which may be assumed to have an intensity variation of the form

$$I=\frac{I_0}{\sqrt{\pi}}e^{-x^2/\sigma^2}, \quad \ldots\ldots\ldots \quad (3)$$

is displaced bodily through a distance which varies harmonically with the time. The observed intensity variation is therefore given not by (3) but by

$$I=\frac{I_0}{\sqrt{\pi}}\frac{1}{2\pi}\int_{-\pi}^{+\pi} e^{-(x-a\cos\theta)^2/\sigma^2}\,d\theta, \quad \ldots\ldots\ldots \quad (4)$$

where a is the amplitude of the displacement. From this equation, we can determine W in terms of a and σ, while by expressing the integral in the form of (1), we can determine A in terms of a and σ. This enables us to set up a relation of the form

$$1/2A=kW^2$$

in place of (2), where k depends on a/σ. For $a/\sigma=0$ (no broadening), $k=0{\cdot}18$, while if $a/\sigma=0{\cdot}416$, $k=0{\cdot}20$, a 14 per cent. increase. The case $a/\sigma=0{\cdot}416$ corresponds to $a/W=0{\cdot}25$, *i. e.* a total broadening equal to half the observed line width. It will be evident from the results given above that this is a generous estimate of the broadening due to high-tension ripple and A.C. fields even for lines as narrow as 100 μ. Since, for lines of this width, the systematic corrections are always less than 2 μ, the error in their determination will be less than 14 per cent. of 2 μ, *i. e.* 0·3 μ. For wider lines the systematic corrections are larger, but on the other hand the broadening is a smaller fraction of the true line width and the constant k is nearer to its normal value of 0·18. The error in the determination of the systematic corrections is roughly independent of the line width, and is unlikely to amount to more than 0·3 μ.

The effect of a *slow steady drift* of high-tension voltage during an exposure can be examined in the same way. It is found that if the total shift of the line due to this cause is half the observed line width, the error introduced into the determination of the systematic corrections is only 10 per cent., *i. e.* that the measured position of the line is that corresponding to the time average of the high-tension voltage during the exposure to within this limit. Hence, if the rings are not obviously blurred, we may conclude that the errors in the determination of the systematic corrections will be less than 10 per cent., and therefore, except for very broad lines, will not exceed $\frac{1}{2}\,\mu$.

3. *Focusing Technique and Width of Central Electron Beam.*

The horizontal component of the Earth's magnetic field deflects a vertical electron beam accelerated by 50 kV., approximately 2 cm. in the course of a 1-metre trajectory. It is both convenient and very desirable that the beam should be as nearly vertical as possible and so along the axis of the camera. Hence the Earth's field is compensated by a series of electromagnets placed E. and W. of the camera. The compensation is such that the residual field along the axis from plate-holder to anode nowhere exceeds 10 per cent. of the horizontal Earths' field.

Magnetic focusing as described by Finch ⁽¹⁾ is employed, but to avoid small distortions of the pattern special precautions are necessary. The Earth compensator is switched on and the position of the cathode over the anode is adjusted until the beam hits the centre of the fluorescent screen. This position may not be the one giving the maximum intensity of the beam for a given discharge current ; in practice we find that it is permissible to allow deviations up to 1 cm. from the centre of the screen to achieve maximum intensity. It is very desirable to have the beam adjusted for maximum intensity, and if this is impossible within these limits, adjustment of the aluminium cathode in the discharge tube is usually effective ; if not, the cathode must be re-ground and polished. The focusing coil is adjusted in position so that the focused beam impinges on the screen at the same place as the unfocused beam. When this adjustment is completed, the spot on the screen should remain stationary, merely changing in size as the focusing coil current is varied. The plane of the coil is kept as nearly at right angles to the camera axis as possible during this lining up process.

If axial rays are not used, a single unscreened focusing coil has large aberrations, particularly coma. Coma is very undesirable as the rings on the side of the tail are seriously broadened. After the lining up described above, there is often a small and weak tail ; this can be reduced by slightly tilting the coil until the tail coils up into the central spot. The electrons are then travelling along the axis of the lens. A very small residual tail may sometimes be seen on the photograph which was imperceptible on the fluorescent screen, but is unimportant if no broadening of the rings is visible under a ×30 microscope.

The use of a second diaphragm immediately above the specimen to cut out scattered electrons ⁽¹⁾ does not render these adjustments unnecessary. The photomicrographs of fig. 7 (Pl. XI.) illustrate the effect of aberrations of the type described. No attempt was made to send the beam down the axis of the coil, but the usual diaphragm over the ammonium chloride specimen was employed. The four photomicrographs, which were printed to the same density, are of regions of the (110) ring spaced at equal intervals. A distinct broadening is seen in the direction of the tail (S.), and this extends over a wide region of the diffraction rings; E. and W. show slight broadening, the line being sharpest at N. The widths of the lines in microns are quoted below the photographs. The central solarised spot of the pattern is reproduced on the same scale in fig. 8 (Pl. XI.) and shows hardly any asymmetry, the comatic tail having been removed by the second diaphragm. The broadening in fig. 7 (Pl. XI.) cannot be ascribed to wave-length changes of the electron beam, for these would cause a bodily displacement of the pattern, resulting in equal broadening at N. and S. Fig. 6 (Pl. XI.) shows for comparison a similar set of photomicrographs of a plate when the aberrations had been reduced to a minimum, and the measurements given show that the line width is constant round the ring to better than 10 per cent. of its average value.

Considerable care is necessary in the actual focusing adjustment. On switching on the coil, a slightly diffuse image of the cathode spot is seen on the screen, and if the focusing current be raised above the optimum value, a fairly sharp circle will form round this spot. This bright ring is an image of the anode diaphragm, and we normally adjust the focusing current until this contracts almost into the image of the cathode spot. (This cathode spot is not situated at the cathode, but is a virtual image above it produced by the bending of the electron rays in the discharge.) Since the anode is nearer the screen than the cathode spot, the focus for the latter will be just above the plate; this cannot be avoided, as it is quite impossible to judge the true focus from the size of the very small and bright image on the fluorescent screen.

We have attempted to reduce the uncertainty in the focus of the cathode spot by the introduction of a low power magnetic lens just below the anode diaphragm. This reduces the magnification of the system by approximately 30 per cent. To measure the magnification, the beam width at the plate must be measured. This requires a rather elaborate technique as very short exposures are necessary to avoid solarisation and the non-linear region of the emulsion characteristic. A pair of parallel condenser plates with a separation of 3 mm. and length 4 cm. was placed 15 cm. below the anode diaphragm. A simple thyratron circuit was designed so that a potential of 200 V. was normally applied to this condenser, so deflecting the beam off the lower diaphragm. On depressing a key, this potential could be removed for periods ranging from 1/500 sec. to several seconds. This allows the beam to travel normally, uninfluenced by added electrostatic fields during the exposure. Magnetic deflection was used to draw the trace on the plate out into a line which could be microphotometered. An electromagnet was placed with one pole touching the camera wall and about 20 cm. above the photographic plate. This magnet was fed from a specially constructed low-frequency oscillator of frequency 300 c.p.s. The eddy currents set up in the brass walls of the camera produced fields which deflected the beam along an ellipse of high eccentricity and with semi-major axis about 2 cm. The exposure was adjusted so as to record just over half a cycle. The resulting trace was microphotometered, the image of the slit on the plate being $800 \times 19\,\mu$. The lines on the plate are not of uniform density along their length owing to the varying velocity of the beam round the ellipse, and the region of maximum velocity was chosen for measurement. The smallness of the length of the microphotometer slit in comparison with the length of the trace enables us to ignore the variation of density along the length of the slit. A number of photographs were taken with gradually increasing currents through the top coil. The cathode was first polished and then left untouched during a run of 14 exposures. It was found to be necessary to allow the cathode to age for about 5 minutes as at first the spot is abnormally small. After this preliminary ageing, the size remains constant for about 30 minutes running and then the beam begins to broaden and a dark region develops at the centre of the unfocused beam, indicating pitting of the cathode. Check measurements with no current through the top coil were made at the beginning and end of the run. The peak densities of these plates were different, but the widths were the same, indicating that both microphotometer and emulsion characteristics were linear ; the maximum peak densities on the plates never exceeded unity. The results shown in fig. 1 give an indication of the performance of the focussing system and indicate that the presence of the top coil produces a reduction in magnification amounting to 30 per cent. Since the anode diaphragm was $60\,\mu$ diameter, the minimum magnification obtained was 0·7. This is not necessarily the lowest possible, as the best position of the upper coil may not have been found. This estimate of the magnification is likely to be somewhat high as the A.C. field used to provide a line for microphotometry will introduce a small amount of broadening.

Fig. 1.

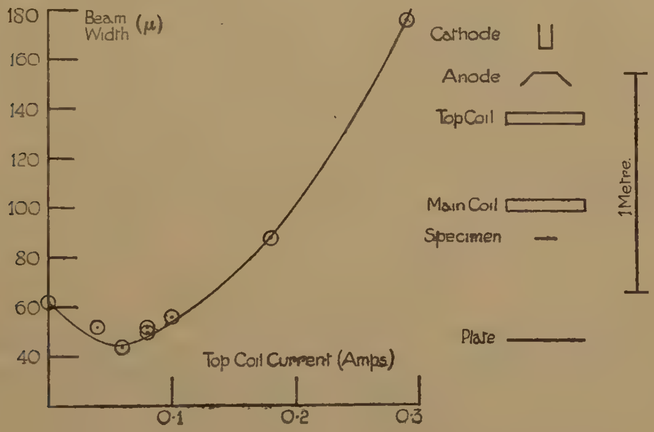

4. *Electrostatic Effects.*

To a first approximation, the radius R of a diffraction ring is related to the corresponding crystal spacing d, the wave-length λ of the electrons and the distance L of the plate from the crystal by the equation

$$\mathrm{R}d=\lambda\mathrm{L}. \quad \ldots\ldots\ldots \quad (5)$$

This equation assumes that the angle of diffraction θ is small, so that $\tan\theta \simeq \theta$. When higher powers of θ than the first are considered, (5) is replaced by

$$\mathrm{R}d=\lambda\mathrm{L}+\frac{3\lambda\mathrm{L}}{8\mathrm{L}^2}\mathrm{R}^2. \quad \ldots\ldots\ldots \quad (6)$$

If we calculate the values of λL for the different rings of a pattern according to (6), we find that they are not constant but vary systematically with the radius according to

$$(\lambda\mathrm{L})_{\mathrm{obs.}}=\mathrm{A}+\mathrm{B}/\mathrm{R}^2, \quad \ldots\ldots\ldots \quad (7)$$

Fig. 2.

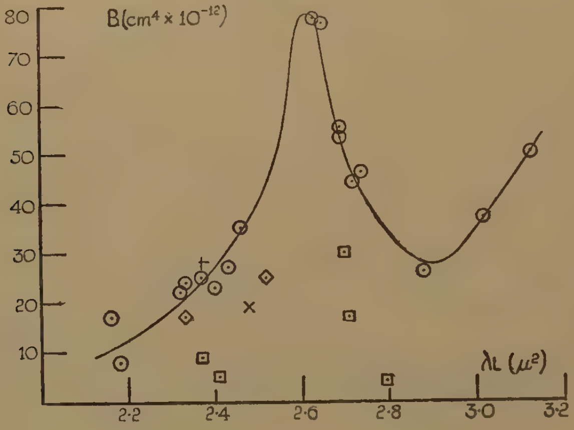

⊙ ammonium chloride.
+ gold.
× sodium chloride.
◇ ammonium chloride (no magnetic focusing).
⊡ ammonium chloride (central beam intercepted).

where A and B are constants (3). The obvious interpretation of this equation is that A is the true value of λL and that the rings are displaced from their normal positions by amounts inversely proportional to their radii. The variation of B with λL is shown in fig. 2, which gives the results of measurements on a number of ammonium chloride, sodium chloride and gold specimens. It will be seen that B increases as the wave-length of the electrons increases, *i. e.* as the *velocity decreases*. This is to be expected if the displacement of the rings from their normal position is due to a force roughly independent of the electron velocity, which acts on the electrons during part of their journey from specimen to plate. The displacement of the rings is mainly due to the *charging up of the photographic plate by the undiffracted beam.* This is demonstrated by taking photographs with the central beam intercepted just above the photographic plate by an earthed Faraday cylinder. Photographs taken at both low and high electron velocities show that the interception of the central beam reduces the constant B to less than one-fifth of its normal value. The explanation given accounts for the general form of equation (7), for it predicts an outward displacement of the electrons which is greater for the innermost rings. It also accounts for the fact that, as may be seen from fig. 2, the magnitude of the effect is independent of the nature of the specimen (type of crystal, and whether the substrate is conducting or non-conducting) and the presence or absence of magnetic focussing. It is to be expected that variations in the extent of the charging up will occur between one photograph and another, and these doubtless account for the scatter of the points in the figure, which is considerably greater than can be accounted for by errors of measurement.

It should be noted that there is a clear indication that the constant B of equation (7) is abnormally large for values of λL lying in a narrow range around $2{\cdot}6\times10^{-8}$ cm.^{2}, corresponding to high-tension voltages of about 47 kV. Similar abnormally high values of B are observed at this voltage even when the central beam is intercepted, showing that some factor other than charging up of the photographic plate comes into play at this particular voltage. We have so far been unable to form any conjecture as to the cause of this effect, and further investigation is required.

5. *Magnetic Effects.*

Distortions of the diffraction pattern can arise through magnetic fields acting on the electrons during their journey from specimen to photographic plate. These fields originate partly in the focusing coil and partly in masses of iron (such as the diffusion pump) near the camera. Before discussing the experimental evidence of these distortions, it is convenient to give the simple theory in terms of which the observed results can be interpreted.

Erect a system of right-handed rectangular axes with origin in the specimen and let the undiffracted beam be directed vertically downwards from specimen to plate along the positive z axis. Since the angle of diffraction hardly ever exceeds 0·05 radian, negligible error will be introduced in the calculation of the distortions if the z component of the velocity of a diffracted electron is identified with its total velocity, which is independent of the angle of diffraction and will be denoted by V. A diffracted electron will emerge from the specimen with velocity components of the form $v\cos\theta$, $v\sin\theta$, V and all electrons belonging to the same diffraction ring will have the same v.

For simplicity, the distortions will first be calculated on the assumption that there is no magnetic focusing ; the modifications introduced by this will be considered later. Then the equations of motion of the electrons are very approximately

$$\left.\begin{aligned} \ddot{x}-\mathrm{H}_y\frac{e}{m}\,\mathrm{V}=0 \\ \ddot{y}+\mathrm{H}_x\frac{e}{m}\,\mathrm{V}=0 \\ \ddot{z}=0 \end{aligned}\right\}, \qquad \text{(8)}$$

for, provided the components H_x, H_y, H_z of the magnetic field are of the same order, terms such as $\mathrm{H}_z\dot{x}$, $\mathrm{H}_y\dot{x}$ are negligible compared with those given. To a first approximation, the components of H may be expressed in terms of the co-ordinates by

$$\left.\begin{aligned} \mathrm{H}_x=\mathrm{H}_0+\alpha x+\beta y+\gamma z \\ \mathrm{H}_y=\mathrm{H}_0+\beta x+\alpha' y+\gamma' z \end{aligned}\right\}. \qquad \text{(9)}$$

The co-ordinate system is supposed so oriented that the magnetic field at the origin makes equal angles with the x and y axes.

Substituting from (9) in (8),

$$\left.\begin{aligned} \ddot{x}-bx-a'y-c'z-d=0 \\ \ddot{y}+ax+by+cz+d=0 \\ z=0 \end{aligned}\right\}. \qquad \text{(10)}$$

where $a=(e\mathrm{V}/m)\alpha$ and similarly for the other coefficients.

In the absence of magnetic fields we have

$$\left.\begin{aligned} x=vt\cos\theta \\ y=vt\sin\theta \\ z=\mathrm{V}t \end{aligned}\right\}. \qquad \text{(11)}$$

A good approximation to (10) is obtained by writing these values of x, y and z in the smaller terms; solving the resulting equations gives

$$x=\frac{vt^3}{6}(b\cos\theta+a'\sin\theta)+\frac{c'\mathrm{V}t^3}{6}+\frac{dt^2}{2}+vt\cos\theta,$$

$$y=-\frac{vt^3}{6}(a\cos\theta+b\sin\theta)-\frac{c\mathrm{V}t^3}{6}-\frac{dt^2}{2}+vt\sin\theta.$$

Writing $t=\mathrm{L}/\mathrm{V}=\mathrm{T}$, where L is the distance from specimen to plate, in these equations gives the co-ordinates of the point where the electron strikes the plate. Referred to parallel axes through a new origin at $(\frac{1}{6}c'\mathrm{VT}^3+\frac{1}{2}d\mathrm{T}^2,\ -\frac{1}{6}c\mathrm{VT}^3-\frac{1}{2}d\mathrm{T}^2,\ \mathrm{VT})$ in the plate, these co-ordinates become

$$\left.\begin{aligned} x=v\mathrm{T}\cos\theta+\frac{v\mathrm{T}^3}{6}(b\cos\theta+a'\sin\theta) \\ y=v\mathrm{T}\sin\theta-\frac{v\mathrm{T}^3}{6}(a\cos\theta+b\sin\theta) \end{aligned}\right\}. \qquad \text{(12)}$$

Whence

$$R=\sqrt{x^2+y^2}=vT+\frac{vT^3}{6}\sqrt{b^2+\frac{(a'-a)^2}{4}}\cos(2\theta-\psi),$$
$$+\text{higher powers of T},$$

where $\tan\psi=\frac{a'-a}{2b}$.

Thus $R=R_0+R_0q\cos(2\theta-\psi)$, ... (13)

where R_0=normal radius

$$q=\frac{L^2e}{6mV}\sqrt{\beta^2+\frac{(\alpha'-\alpha)^2}{4}}.$$

Since the second terms in (12) are only about one-thousandth of the first, we may regard (13) as the polar equation of the diffraction ring referred to the centre spot as origin. If the radii of a ring be measured at equally spaced values of θ, Fourier analysis of the results should yield a constant term, equal to the radius predicted by Bragg's law, and a second harmonic. Equation (13) predicts the following properties of the second harmonic :—

(i) its azimuth is the same for all diffraction rings, and remains constant from one photograph to another provided there is no change in the stray fields,

(ii) its amplitude is proportional to the mean radius of the ring,

(iii) the constant of proportionality is inversely proportional to the electron velocity and therefore directly proportional to the electron wave-length.

Further, the *mean* radius of the diffraction rings is that given by Bragg's law.

These general conclusions are very little modified by the presence of magnetic focusing. When the focusing coil is correctly aligned as described in § 3, the magnetic field due to it is axially symmetrical about the central undiffracted beam. The effect of such a field *in the absence of any other stray field* can be shown to be two-fold : (a) the radii of the diffraction rings are *very slightly* reduced by amounts proportional to their normal radii, and (b) the electrons are rotated about the z axis through angles independent of the horizontal component of the electron velocity. The co-ordinates of the electrons are given not by (11) but by

$$\left.\begin{aligned}x&=\frac{v}{V}f(z)\cos(\theta+g(z))\\ y&=\frac{v}{V}f(z)\sin(\theta+g(z))\\ z&=Vt\end{aligned}\right\}, \qquad (14)$$

where, to a good approximation, $f(z)=z$. By the operation of focusing, the magnetic focusing field is so related to the electron velocity V that an electron emitted in a given direction describes a certain trajectory which is independent of V. This means that $f(z)$ and $g(z)$ of (14) *do not depend on* V.

The effect of stray fields together with the focusing field is determined by carrying out the preceding calculation, using (14) instead of (11) as the equations of the unperturbed motion. This gives in place of (13)

$$R=R_0+pR_0+kR_0\cos(2\theta+\phi), \quad . \; . \; . \; . \; . \; . \quad (15)$$

where

$$p=\frac{e}{LVm}\left[\frac{\alpha'+\alpha}{2}S\right],$$

$$k=\frac{e}{LVm}\sqrt{(C^2+S^2)\left(\beta^2+\frac{(\alpha'-\alpha)^2}{4}\right)},$$

$$C=\int_0^L\int_0^L f(z)\cos g(z)\,dz\,dz,$$

$$S=\int_0^L\int_0^L f(z)\sin g(z)\,dz\,dz,$$

$$\tan\phi=\frac{(\alpha-\alpha')C+2\beta S}{2\beta C-(\alpha-\alpha')S}.$$

The term pR_0 represents merely a slight change in the scale of the diffraction pattern ; this is the only qualitative change introduced by the focusing field.

The presence of higher powers of the co-ordinates than the first in the expression for the stray fields can be shown by a similar method to result in the addition of harmonic terms to (13) or (15) proportional to higher powers of R_0.

Most of the theoretical predictions given above have been verified experimentally. This can be illustrated by measurements of a photograph taken with an ammonium chloride specimen. The diameters of five rings were measured at every 20 degs., four settings being made at each position ; by Fourier analysis, the constants R_0, (kR_0) and ϕ of equation (15) were determined for each ring. The results are given in the table, lengths being measured in microns and the east direction on the plate being taken as axis of polar co-ordinates.

Plate D/237.

R_0	(kR_0)	ϕ (degs.)
10241·2	4·9	68
12587·8	7·8	75
14483·3	10·6	62
16196·6	10·6	69
17745·1	11·3	72

Fig. 3 shows (kR_0) plotted against R_0. The line drawn has been fitted by least squares and has the equation

$$(kR_0)=(-3{\cdot}2\pm2{\cdot}5)+(8{\cdot}6\pm1{\cdot}7)\times10^{-4}R_0, \quad . \; . \; . \; . \quad (16)$$

the S.D. of a single point being $1{\cdot}0\,\mu$. The predicted linear variation of (kR_0) with R_0 is thus verified.

The theory predicts that the gradient of the $(kR_0)-R_0$ curve should be proportional to λ, the wave-length of the electrons. Fig. 4 shows a plot of gradient against λL, where L is the constant camera length, based on the results for sixteen plates. The full line has been fitted by least squares and has the equation

$$k=(-4{\cdot}0\pm4{\cdot}6)\times10^{-4}+(4{\cdot}5\pm1{\cdot}8)\times10^{-4}\lambda L$$

if all lengths are measured in microns. Clearly, the line passes through the origin within the limits of error, in agreement with the theory. The best fitting line passing through the origin is shown as a broken line in the figure, and has the equation

$$k=(2{\cdot}97\pm0{\cdot}38)\times10^{-4}\lambda L,$$

the S.D. of a single point being $1{\cdot}5\times10^{-4}$.

Fig. 3.

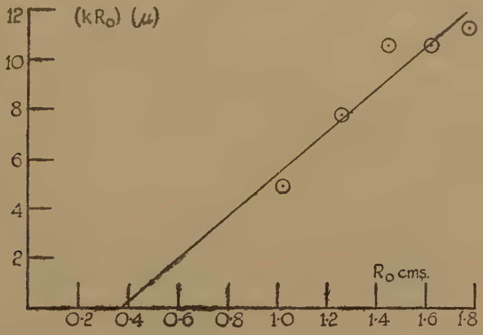

The order of magnitude of the gradient of the stray field can be obtained from this result by making use of equation (13) in conjunction with the known camera length L=47 cm. and the familiar relation $\lambda=h/mV$.

It will be found that

$$\sqrt{\beta^2+\frac{(\alpha'-\alpha)^2}{4}}=160\gamma \text{ per cm.}$$

Rough tests with a search coil and highly sensitive ballistic galvanometer show that the field gradients at points near the axis of the camera vary between zero and 500γ per cm. A more exact calculation of the field gradients would require a knowledge of the field due to the focusing coil in order that the integrals of equation (15) could be evaluated; this has not been attempted.

The constancy of the azimuth of the second harmonic in the rings on a plate is illustrated by the results quoted above, the mean ϕ for this plate being 69 degs. and the S.D. of a single ϕ 5 degs. The constancy of ϕ from one plate to another is shown by the fact that the mean ϕ's for eleven of the plates represented in fig. 4 (the orientation of the remaining plates on the microscope was not noted when they were measured) are distributed about a mean value of 64 degs., the S.D. of the mean for a single plate being 9 degs.

The reliability of the experimental data and of the conclusions drawn from it is shown by the consistency of the calculated limits of error. The width of the rings on the plates varied between 100 and 150 μ, and it is known (3) that for rings of this width the S.D. of a single reading of the radius is 3 to 4 μ. Now it can be shown that the amplitude of a harmonic calculated from N observations of the radius has a S.D. equal to $\sqrt{2/N}$ times that of a single radius measurement. In the present case, $N=72$ (4 settings at each of 18 azimuths), so that the S.D. of the second harmonic should be 0·5 to 0·7 μ. The S.D. of a single point from the line of fig. 3 is 1·0 μ, in reasonable agreement with this estimate. Further, it can be shown that the S.D. in the azimuth of a harmonic of amplitude A is d/A radian, where d is the S.D. of the amplitude. In the case of Plate D/237, the average amplitude is 9.0 μ, so that the S.D. of an azimuth should be 1·0/9·0 radian, or 6 degs., compared with the observed 5 degs. The gradient of the line in fig. 3 has a S.D. of $1{\cdot}7\times10^{-4}$, in agreement with the fact that in fig. 4 the S.D. of a single point from the broken line is $1{\cdot}5\times10^{-4}$. The S.D. of the mean azimuth of a plate (9 degs.) is rather larger than the S.D. of a single ring from the mean for the plate (5 degs.); possibly the stray fields were not quite the same for all photographs.

Fig. 4.

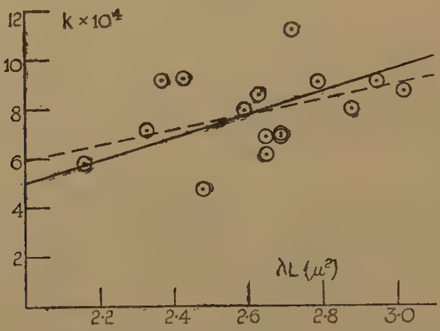

These measurements were made when the stray fields had been reduced as far as possible. In the absence of certain precautions, the second harmonic has at least three times the amplitude given. A prominent cause of stray fields is the diffusion pump, which becomes magnetized in the Earth's magnetic field. The effect of this can be reduced by surrounding the pump by a coil of wire carrying a suitable direct current. The omission of this " degaussing " roughly doubles the second harmonic. An even more serious source of trouble is the use of ferromagnetic mountings for the specimen. Many workers have used steel knife-edges or nickel gauze as mounts for their specimens. Such mounts become magnetized in the field of the focusing coil and produce second harmonics at least double those recorded here ; they are therefore completely unsuitable for precision work. It is worth noting that the shape of a gauze specimen mount introduces such a large demagnetizing factor that nickel and iron gauzes acquire roughly the same magnetic moment. We have found platinum gauze to be very satisfactory. A cheaper, but less durable, substitute is the copper gauze used for petrol filters.

ACKNOWLEDGEMENTS.

The authors' thanks are due to Professor J. A. Crowther not only for departmental facilities, but also for the continued interest and encouragement without which the work could not have been carried out. The senior author also desires to thank the Research Board of the University of Reading for a grant for the purchase of the electron camera.

REFERENCES.

(1) G. I. Finch, A. G. Quarrell and H. Wilman, Faraday Soc., Trans. xxxi. p. 1051 (1935).
(2) J. Hillier and A. W. Vance, Proc. I.R.E. xxix. p. 167 (1941).
(3) T. B. Rymer and C. C. Butler, Phil. Mag. xxxvi. p. 515 (1945).

XCIX. *The Equilibrium Diagrams of Certain Alloys of Iron.*

By W. HUME-ROTHERY, F.R.S., and J. W. CHRISTIAN *.

[Received March 25, 1946.]

THE principles underlying the form of the equilibrium diagrams of alloy systems were first discovered by a study of the alloys of copper, silver and gold as typical univalent metals, and were later confirmed by systematic examination of the alloys of different elements with magnesium as a divalent element. The effects of atomic size factor, electron concentration, and electro-chemical factor have been recognized in a general way for many alloys, but systematic examination of alloys of the transition elements does not appear to have been made, and in many cases the experimental data are too inaccurate for detailed examination. In the present paper we discuss the equilibrium diagrams of the alloys of iron with the transition elements of the same period in order to see what relations can be traced.

Table I. gives the interatomic distances in the crystals of the elements from titanium to copper in the First Long Period. With the exception of manganese, all these elements crystallize in one or more of the three typical metallic structures, body-centred cubic, face-centred cubic, and close-packed hexagonal. The closest distance of approach of two atoms in α-iron is 2·48 A., and if we take the zone of favourable size factor to be limited by a difference of 15 per cent. in the atomic diameters of solvent and solute, the limits of the favourable zone for iron are 2·11 A. and 2·85 A. It will be seen that titanium lies outside the zone of favourable size factor, but that the remaining elements in Table I. are within the favourable zone.

---

* Communicated by the Authors.

TABLE I.

Element.	Crystal Structure.	Closest Distance of Approach of Atoms.
Ti.	*c.p.*-hex.	2·92 2·91
V.	B.*c.*-cubic.	2·63
Cr.	B.*c.*-cubic.	2·49
Mn.	α Mn-Complex.	2·24 to 2·96
	β Mn-Complex.	2·37 to 2·67 The Goldschmidt Diameter for Mn is 2·75 for Co-ordination No. 12
	γ Mn. Face-centred tetragonal.	2·58
Fe.	α Fe. *b.c.*-cubic.	2·48
Co.	α Co. *c.p.*-hex.	2·50
	β Co. *f.c.*-cubic.	2·51
Ni.	α Ni. *c.p.*-hex.	2·49
	β Ni. *f.c.*-cub.	2·49
Cu.	*f.c.*-cubic.	2·55

In the above series of elements we have to distinguish between the inner electrons of the (1*s*), (2*s*) (2*p*), (3*s*), (3*p*) levels, and the outer electrons. On passing from potassium to copper the number of outer electrons increases by one for each unit increase in the atomic number, and if Pauling's hypothesis (1) is accepted, these electrons may be divided into bonding and non-bonding electrons according to the following scheme :—

TABLE II.

Element.	K.	Ca.	Sc.	Ti.	V.	Cr.	Mn.	Fe.	Co.	Ni.
No. of outer electrons ..	1	2	3	4	5	6	7	8	9	10
No. of bonding electrons ..	1	2	3	4	5	5·8	5·8	5·8	5·8 ?	5·8 ?
No. of electrons in atomic orbitals	0	0	0	0	0	0·2	1·2	2·2	3·2	4·2 ?

According to this hypothesis the number of bonding electrons increases from 1 to 5 on passing from potassium to vanadium, and these electrons exist in hybridized (4*s*, 4*p*, 3*d*) orbitals : there are 9 such orbitals, and hence the conditions for strong bonding are present. On proceeding to chromium Pauling concludes that on the average 5·8 electrons per atom exist in bonding ortibals, and the remaining 0·2 electrons per atom enter atomic *d* orbitals which are not concerned in the bonding process. From a study of the magnetic properties it is concluded that the number of bonding electrons per atom remains approximately constant on passing from chromium to nickel, and that the additional electrons enter the atomic or non-bonding orbitals, which thus begin to build up the electron cloud of the ion. This scheme is not universally accepted, but it accounts for many facts. It suggests * that in alloys with iron, the general electronic similarity of the two metals will increase on passing from Ti→V→Cr→Mn and will then diminish on proceeding to Co→Ni. We may say, therefore, that the valency or electronic factors become increasingly favourable in the order Ti<V<Cr<Mn Co>Ni.

Figs. 1–6 show the equilibrium diagram of the systems Fe–Ti, Fe–V, Fe–Cr, Fe–Mn, Fe–Co, and Fe–Ni, and the following interpretations may now be suggested. (All these diagrams are in atomic per cent.)

Fig. 1.

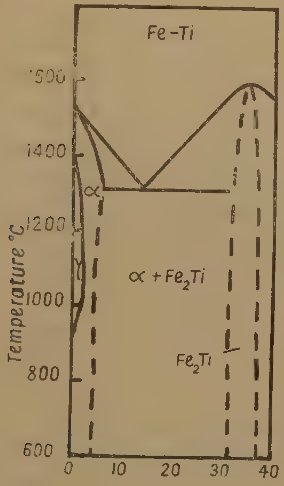

In the system Fe–Ti, the size factor is unfavourable, and the solid solution of titanium in iron is restricted, whilst the liquidus and solidus curves fall comparatively steeply. The system is one with a narrow γ-loop, and the intermetallic compound Fe_2Ti gives rise to a maximum on the liquidus curve; there is also a compound, Fe–Ti, whose crystal structure has not been determined.

In the system, Fe–V, the atomic diameters differ by 6 per cent., so that both the size factor and the electronic factor are more favourable than in the system Fe–Ti. In agreement with this, the depressions of the liquidus and solidus curves are much smaller in the system Fe–V, whilst the extent of the solid solution in both α- and γ-iron is greater. The system is still one with a γ-loop, and the α body-centred cubic phase undergoes a prominent transformation in the equiatomic region (fig. 2).

---

* This conclusion will still hold to some extent even if Pauling's hypothesis is discarded.

Fig. 2.

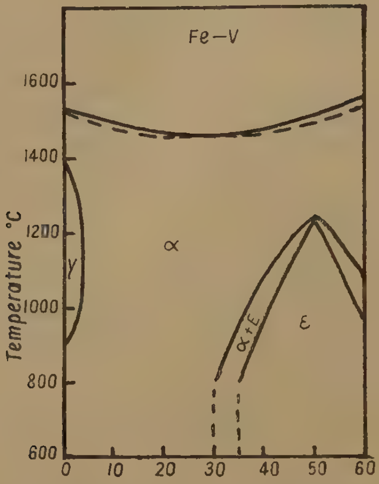

In the system Fe–Cr the size factor and electronic factors are still more favourable, and as shown in fig. 3 the depressions of the solidus and liquidus curves are very slight. The system has been investigated very accurately by Adcock and is one with a relatively wide γ-loop and a continuous solid solution in the body-centred cubic phase at high temperatures.

Fig. 3.

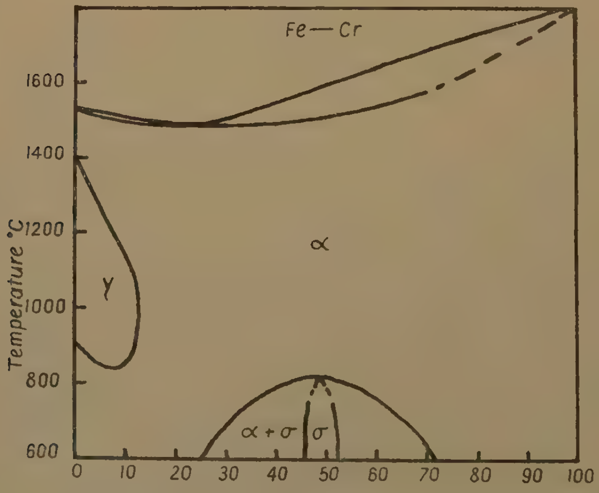

At lower temperatures there is a transformation in the equiatomic region, which results in the formation of the so-called σ phase. Comparison of figs. 2 and 3 show that for the equiatomic alloy this transformation is at a much lower temperature than that of the equiatomic transformation in the system Fe–V. This is in complete agreement with the general principle that when compared with intermediate phases, primary solid solutions become increasingly more stable as the two elements concerned become more nearly similar in size and electronic characteristics. The Fe–Cr diagram has been examined with sufficient accuracy for a critical examination to be made, and it is of interest to note that the minimum in the liquidus curve is almost exactly at the composition Fe_3Cr (25 atomic per cent. of chromium); this clearly suggests some kind of a short range order structure in the liquid and solid phases. It may be of significance that the maximum solubility of chromium in γ-iron is 12–13 atomic per cent., *i. e.*, 1 atom in 8.

Fig. 4 shows the equilibrium diagram of the system Fe–Mn. The difference in the crystal structures of the two metals prevents the formation of a continuous series of solid solutions, but there are wide solid solutions of each metal in the other in accordance with what would be expected from the favourable size factor and electronic factor. The liquidus curve falls continuously from the freezing point of iron to that of manganese, with only slight bends in the region of the peritectic horizontals, and this is in agreement with expectation. The solidus curves for the solid solutions in γ-iron and γ-manganese behave similarly, but the solidus curve for the small region of the solid solution in δ-iron (body centred cubic) falls unexpectedly steeply. Comparison of figs. 3 and 4 will show that apart from the effect of the abnormal crystal structures of manganese, a great change in the general form of the diagram occurs on passing from chromium to manganese. The effect of manganese is greatly to extend the region of the γ (face-centred cubic) solid solution, and this process is continued in the systems Fe–Co and Fe–Ni. It seems

Fig. 4.

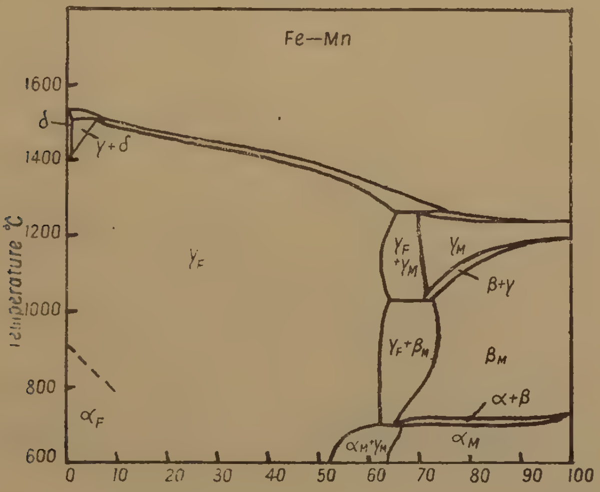

reasonable to associate this with the filling up of the atomic *d* orbitals rather than with the effect of the bonding electrons, since, if Pauling's hypothesis is accepted, the number of bonding electrons is the same for chromium and manganese. It may be noted that electron distribution N(E) curves for body-centred cubic iron and face-centred cubic iron have been calculated by Manning (2). These curves do not suggest that there is any simple relation between the relative stability of the two phases and the electron concentration such as was found by H. Jones (3) in his theory of the α/β brass equilibrium. If we adopt Pauling's hypothesis, then as the atomic *d* orbitals are filled, the electron clouds of the ions are built up, and the structures may be regarded as more and more resembling assemblies of hard spheres (ions) held in contact by the bonding electrons. In the case of copper it has been shown by Fuchs (4) that the effect of the ionic overlap is to favour a face-centred cubic structure rather than a body-centred cube, and we may suggest, therefore, that it is the filling up of the atomic *d* orbitals which is responsible for the great extension of the face-centred cubic (cubic close packed) structure in the system Fe–Mn, Fe–Co, and Fe–Ni, and also for the fact that on passing from Fe→Co→Ni, the body-centred cubic modification of the *element* disappears, and only close packed structures (face-centred cubic or *c.p.*-hexagonal) are found.

Fig. 5.

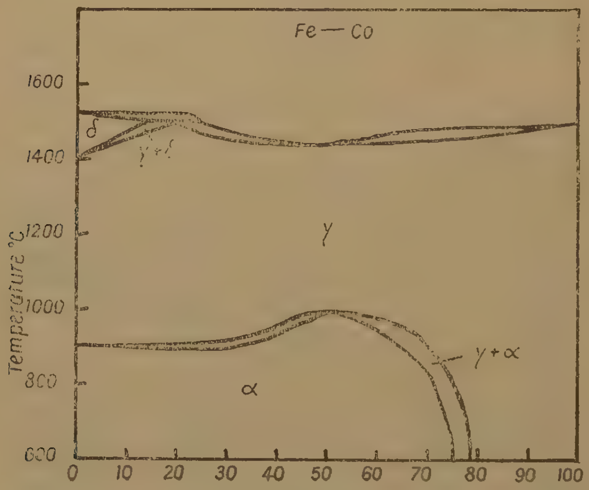

It is to be noted that if the N(E) curves calculated by Manning for body-centred cubic iron and face-centred cubic iron are assumed to hold approximately for cobalt and nickel, they indicate that for nickel the electronic factor will make the face-centred cubic structure more stable. For nickel, therefore, the face-centred cubic structure may be stabilized both by the electronic factor, and by the building up of the electron cloud of the ion.

The Fe–Mn equilibrium has been investigated in detail by Gayler (5), and some interesting points may be noted. The maximum solid solubility of manganese in γ-iron is placed at 65–66 atomic per cent. manganese. This is very nearly the simple atomic ratio 1Fe : 2Mn, and the data could probably be reconciled with the exact whole number ratio. The liquidus point on the $\gamma\text{Fe}+\text{Liq}\rightleftharpoons\gamma\text{Mn}$ peritectic horizontal lies almost at 75 atomic per cent. manganese, and hence corresponds with the simple atomic ratio 1 Fe : 3 Mn. The Fe-Co and Fe–Ni equilibrium diagrams are shown in figs. 5 and 6. The liquidus and solidus curves, and the wide ranges of solid solutions are in agreement with the favourable size factors and electronic factors. The existence of superlattices is, however, unexpected in view of the similarity between the constituent elements. We suggest that the formation of these superlattices may also be connected with the filling up of the atomic *d* orbitals. The scheme suggested by Pauling suggests that as we proceed along the series Fe→Co→Ni, the atomic *d* orbitals fill up rapidly, so that the ions become more and more like "hard spheres," and this may create the difference between the atoms which is necessary if an ordered arrangement is to be more stable than a random solid solution.

Fig. 6.

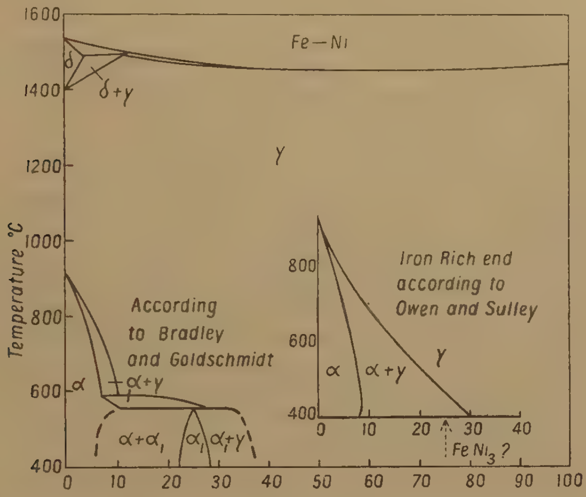

In general, therefore, it may be suggested that the form of the above equilibrium diagrams can be understood if the existing theories of alloy structure are united with the ideas of Pauling.

Acknowledgements.

The authors must express their gratitude to Professor C. N. Hinshelwood, F.R.S., for laboratory accommodation and other facilities which have greatly encouraged their investigations.

References.

(1) L. Pauling, Phys. Rev. liv. p. 899 (1938) ; also "The Nature of the Chemical Bond."
(2) M. F. Manning, Phys. Rev. lxiii. p. 190 (1943).

M. F. Manning and J. B. Green, Phys. Rev. lxiii. p. 203 (1943).
(3) H. Jones, Proc. Phys. Soc. xlix. p. 250 (1937).
(4) K. Fuchs, Proc. Roy. Soc. cli. p. 585 (1935).
(5) M. L. V. Gayler, J. Iron and Steel Inst. cxxviii. p. 293 (1933).
M. L. V. Gayler and C. J. Wainwright, J. Iron and Steel Inst. cxxxv. p. 269 (1937).

The Inorganic Chemistry Laboratory,
The University Museum,
Oxford.

C. *The Lattice Spacing of Rubidium between* −183° C. *and* +19° C.

By W. Hume-Rothery, F.R.S., and Kathleen Lonsdale, F.R.S.*

[Received May 9, 1946.]

I.

The lattice spacing of rubidium at −173° C. was measured by Simon and Vohsen (1), who gave the value 5·62 *k*X with an experimental error of the order ½ per cent. By the kindness of the General Electric Co. Ltd., the present authors were supplied with a specimen of extremely pure redistilled rubidium, and experimental work at Oxford, and at the Royal Institution, has led to a more accurate determination of the lattice spacing, together with data for the mean coefficients of linear expansion over certain ranges of temperature.

II.

The specimen of rubidium was contained in a thin-walled silica capillary, and had been prepared from the azide by thermal decomposition followed by redistillation in a high vacuum. Examination at the Royal Institution showed that the specimen consisted almost entirely of a single crystal whose orientation was such that no lines appeared on an ordinary Debye-Scherrer film taken with the specimen vertical. The specimen was then mounted on an X-ray goniometer at an angle such that on oscillation the (310) reflection occurred on the equatorial plane. Using a 29 cm. camera, and unfiltered CuK radiation, an exposure of 1 hour was given with the specimen at 17·5° C., followed by 30 minutes with the specimen bathed in liquid air by means of the device described by Lonsdale and Smith (2). The temperature was checked by thermocouple readings. These exposures were taken on the same film on which standard lines had been previously made with a separate specimen of quartz. The resulting film showed that at 17·5° C. the rubidium specimen produced two adjacent spots for each of the 310 $K\alpha_1$, 310 $K\alpha_2$, and 310 $K\beta$ reflections (*i. e.* the specimen really contained two crystals of very slightly different orientation), but that the cooling in liquid air had caused fragmentation of the crystal, with the result that the low temperature reflection consisted of short lines, and the 310 $K\alpha$ doublet was not resolved. There was no indication of any higher reflection on the film. In this experiment the film was on one side of the camera only, and consequently the data do not allow the lattice spacing to be deduced because the eccentricity and absorption* are different for the specimens of rubidium and quartz. They do, however, enable the expansion between −183° C. and +17·5° C. to be measured, and the results, which differ by about 7 per cent. for the α and β reflections, are given in Table I.

---

* Communicated by the Authors.

III.

After the above experiments the specimen was heated to slightly above the melting point, and was quenched by dipping the capillary into iced paraffin. It was then mounted in an 18 cm. low-temperature Debye-Scherrer camera (3) and a photograph at 18·5° C. with Cu radiation showed lines from the (110) α and β, (211) α and β, (220), (310), and (321) α reflections, the latter being at approximately 30°. The strength of the (211) reflection was abnormally great, and indicated that considerable preferred orientation existed. In spite of the low angles of these reflections, the measured values of the lattice spacing gave a satisfactorily linear plot against the $\frac{1}{2}\left(\frac{\cos^2\theta}{\sin\theta}+\frac{\cos^2\theta}{\theta}\right)$ extrapolation function of Nelson and Riley (4). The extrapolated value of the lattice spacing at 18·5° C. was 5·699 *k*X.

After the above exposure the specimen was cooled to −50° C., and a photograph was taken at this temperature. Owing to an accident, the film was rather under exposed, but the (211) $K\alpha$ line was clear and distinct, and its measurement enabled the mean coefficient of between −50° C. and +18·5° C. to be determined. A further experiment was made in which the specimen was cooled to −97·5° C., and an exposure was then taken. The resulting film showed the (211), (310), and (321) $K\alpha$ lines clearly, and their measurement enabled the mean coefficient of expansion between −97·5° C. and +18·5° C. to be determined. The above experiments were carried out without removing the specimen from the camera, and consequently errors due to eccentricity, absorption, etc., were constant throughout the series and do not affect the coefficients of expansion. The specimen was then transferred to a 19 cm. Unicam camera, and an exposure made at +19·4° C. The resulting film was satisfactory and showed all the Kα lines up to (321) except for the (310) line, together with the stronger Kβ lines; the disappearance of the (310) line suggests that the treatment at −100° C. produced some further change in orientation of the specimen. In the film from the 19 cm. Unicam camera, the (321) doublet was nearly resolved, and the extrapolated value for the lattice spacing was 5·698 *k*X in very good agreement with the result from the 18 cm. camera.

---

* The centering of the rubidium specimen was extremely difficult because it had to be set obliquely. Examination of this source of error in another case has shown that the lattice spacing cannot legitimately be deduced from a film from one side of the camera only.

IV.

The results obtained in the course of the above work are summarised in Table I. The exact value of the lattice spacing at room temperature depends on the value of the wave-length assumed for the lines whose α-doublets were not resolved, and for this purpose the effective wave-length was assumed to be given by a ($2\,\alpha_1 : 1\,\alpha_2$) ratio. The justification of this assumption lay in the fact that the points from α and β lines then lay on the same extrapolation curve. The α_1 and α_2 wave-lengths differ by approximately 1 part in 400, so that the difference between a ($2\alpha_1 : 1\,\alpha_2$) weighted mean, and a simple ($\alpha_1 : \alpha_2$) mean is of the order 1 part in 2,000. The extrapolation from a highest angle of 30° is of course a very long one, and it may not be justifiable to claim an accuracy of more than 1 part in 1,000, although it is satisfactory to note that the results from two different cameras agree to within 1 part in 5,000. It will be appreciated that the coefficient of expansion between room temperature and −50° C. and −97·5° C. are not affected by the above errors, since the same specimen and the same camera were used. The coefficient of expansion between −183° C. and room temperature is rather less certain because the reflection at the one temperature was an unresolved line and at the other temperature two sharp spots.

Table I.

Lattice Spacing of Rubidium at 18·5°—19·5° C.=5·698—5·699 *k*X.

Contraction $\frac{\Delta\alpha}{\alpha}$ between temperature limits stated, as estimated from different X-ray diffraction lines.

	211 Kα	310 Kα	321 Kα	Most Probable Value
+19° −50° ….	·00458			·00458
+19° −97·5° ….	·0074	·0077	·0080	·0077
+17·5° −183° ….		·0127 ·0136	310 Kα 310 Kβ	·0131

The above results show that the coefficient of linear expansion over the range of temperature +19° C. to −183° C. decreases slowly, having a mean value of $6{\cdot}6 . 10^{-5}$ over the range +19° to −97·5°. It is difficult to understand the much higher values found at room temperatures by

Hackspill ⁽⁵⁾ (coefficient cubical expansion 0° to 38° C., $27 \cdot 10^{-5}$) and Deuss ⁽⁶⁾ (coefficient cubical expansion 1·6° to 17·5° C., $26 \cdot 86 . 10^{-5}$).

The lattice constant at −183° is found to be 5·624 *k*X, in agreement with the value 5·62 *k*X given by Simon and Vohsen ⁽¹⁾.

Acknowledgements.

One of us (W. H.-R.) must express his thanks to Professor C. N. Hinshelwood, F.R.S., for laboratory accommodation and other facilities which have greatly encouraged the present research. Thanks are also due to the Council of the Royal Society, and to the British Non-Ferrous Metals Research Association for financial assistance.

We are indebted to Mr. H. Smith for his help with the experiments made at the Royal Institution, which were carried out on the 5 KW. rotating target tube designed by Dr. A. Müller, and we must also thank Dr. H. Rooksby for his kindness in connection with the preparation of the specimen.

References.

(1) F. Simon and E. Vohsen, *Zeit. phys. Chem.* cxxxiii. p. 165 (1928).
(2) K. Lonsdale and H. Smith, J. Scientific Instruments, xviii. p. 133 (1941).
(3) W. Hume-Rothery and D. J. Strawbridge ; an account of the low temperature Debye-Scherrer camera will be published shortly.
(4) J. B. Nelson and D. P. Riley, Proc. Phys. Soc. Lond. lvii. p. 160 (1945).
(5) L. Hackspill, *Comptes rend.* clii. p. 161 (1911).
(6) E. Deuss, *Vierteljahrsschr. Naturf. Ges. Zurich.* lvi. p. 15 (1911).

CI. *A New Form of Chart for Determining Temperatures in Bodies of Regular Shape during Heating or Cooling.*

By A. J. Ede.

(Low Temperature Station for Research in Biochemistry and Biophysics, University of Cambridge and Department of Scientific and Industrial Research *.)

[Received November 4th, 1945.]

It is assumed that a body, homogeneous and at a uniform temperature, is suddenly transferred to surroundings at a different (constant) temperature. Heat transfer takes place such that the heat flow at any point on the surface is proportional to the difference between the temperatures of the point and the surroundings. Charts are presented here which enable the mean- and centre-temperatures at any time to be obtained for the cases of the infinite solid bounded by two parallel planes

---

* Communicated by the Author.

(infinite slab), the infinite solid bounded by two mutually perpendicular pairs of parallel planes (infinite bar), the finite rectangular parallelepiped (brick), the infinite circular cylinder, the finite right circular cylinder, and the sphere.

Theoretical solutions to these problems have long been available (1), (2), (3), (4) (the most complete are given by Carslaw), but they are in the form of series which are laborious to evaluate. Several forms of chart (8), (9), (10), (11) have been published, from which temperatures can be read off directly, but they suffer from defects due to the difficulty of covering the wide range of variables involved. The present charts overcome this difficulty and cover the entire range of variables.

It has been shown (5), (6), (7) that, when the law governing the flow of heat at the surface is as described above, solutions for all the shapes mentioned can be obtained from solutions for the infinite slab, infinite cylinder and sphere. If the temperature at, for example, the central plane of an infinite slab of thickness $2a$ is $F(a)$ at a given time, then the centre temperature of a brick of size $2a \times 2b \times 2c$ will be $F(a).F(b).F(c)$, other things being equal; and if the temperature at the axis of an infinite cylinder of radius r is $f(r)$, then the centre-temperature for a finite cylinder of length $2a$ and radius r will be $F(a).f(r)$. Three cases only therefore need be considered.

The variables involved in the case of the infinite slab are:—θ, the temperature at the point considered; θ_1, the initial uniform temperature of the solid; θ_0, the temperature of the surroundings; h, the rate of heat transfer per unit area of surface, per unit temperature difference; k, s, ρ, the thermal conductivity, specific heat and density of the solid; $2a$, the thickness of the slab; and x, the distance of the point considered from the central plane. These variables can be collected into the four dimensionless groups $\frac{\theta-\theta_0}{\theta_1-\theta_0}, \frac{ah}{k}, \frac{kt}{s\rho a^2}, \frac{x}{a}$; it is usual to consider the variation of the first three for particular values of the last. The possible ranges of these variables are 0 to 1, 0 to ∞, 0 to ∞, and 0 to 1 respectively. In the well-known Gurney-Lurie (9) charts, $\frac{\theta-\theta_0}{\theta_1-\theta_0}$ is plotted against $\frac{kt}{s\rho a^2}$, on log-linear paper, for six values of $\frac{ah}{k}$. Not only is interpolation to other values of ah/k difficult, but the variation of $\frac{\theta-\theta_0}{\theta_1-\theta_0}$ from 1 to 0·1—usually the most interesting part of the process—is cramped into a small section of the chart, and the available accuracy suffers accordingly. Schack (10) and Newman (11) have produced charts in which $\frac{\theta-\theta_0}{\theta_1-\theta_0}$ is plotted against $\frac{ah}{k}$ for different values of $\frac{kt}{s\rho a^2}$: these are more accurate and easier to use, but a large number of curves must be drawn and the scale of ah/k is repeatedly telescoped in order to cover the range of variation, 0·1 to 50, given for $kt/s\rho a^2$.

The method suggested here is to plot $kt/s\rho a^2$ against ah/k, for various values of $\frac{\theta-\theta_0}{\theta_1-\theta_0}$, using log-log paper. A uniform degree of accuracy is obtained and a wider range of variables covered; indeed, the form of the curves makes it possible to cover the entire range of variation of ah/k and $kt/s\rho a^2$. A sketch showing the general shape of such a chart is shown below; to be of value, it should be drawn on a large scale, and Tables I.–VI. provide sufficient data for constructing charts giving centre and mean temperatures. Elementary considerations show that when ah/k tends to infinity, the curves become horizontal straight lines; when ah/k tends to zero, they become straight lines at a slope of 45°; so that extrapolation in either direction is simple and accurate.

Fig. 1.

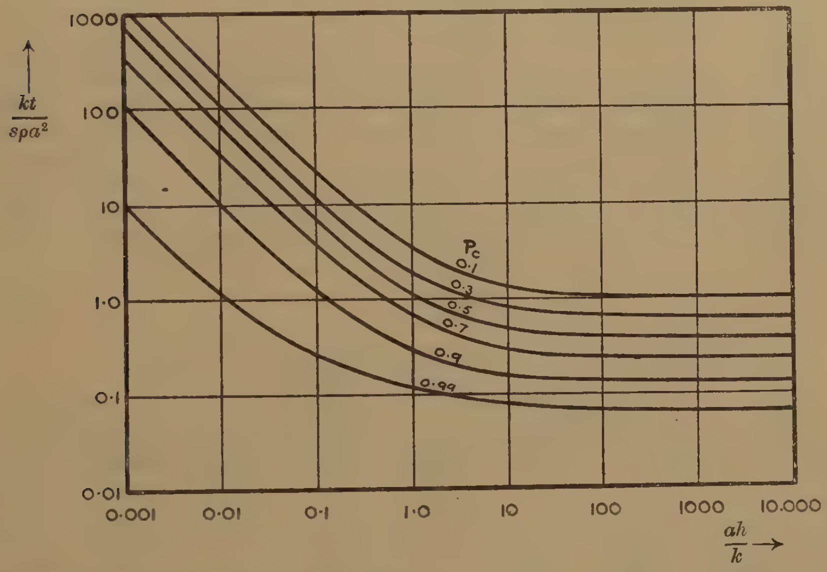

Rough sketch of chart corresponding to Table I., for temperatures at the centre of an infinite slab. (Also infinite rectangular bar, and rectangular brick.)

The value of $kt/s\rho a^2$ corresponding to particular values of $\frac{\theta-\theta_0}{\theta_1-\theta_0}$ and $\frac{ah}{k}$ must, of course, be obtained from the appropriate plot of $\frac{\theta-\theta_0}{\theta_1-\theta_0}$ against $\frac{kt}{s\rho a^2}$, so that this type of chart is of secondary accuracy only; but it will be found quite accurate enough for the great majority of cases, since it is rarely possible to define the experimental conditions with great precision.

The greater part of the charts giving the centre temperatures of slab and cylinder can be constructed from data given by Russell (13); the bulk

TABLE I.

For Constructing Chart for Determination of the Centre Temperature of an Infinite Slab. See Fig. 1.
(Also infinite rectangular bar, and rectangular brick, see text.)

$\frac{ah}{k}\rightarrow$ $P_c\downarrow$	10^{-n} $(n>2)$	0·01	0·1	0·3	1·0	3	10	100	∞
					$\frac{kt}{spa^2}$				
0·1	2·30×10^n	230	23·4	8·5	3·30	1·80	1·26	1·05	1·00
0·2	1·61	161	16·6	6·2	2·38	1·27	0·91	0·76	0·75
0·3	1·20	120	12·5	4.6	1·82	1·00	0·72	0·60	0·59
0·4	0·92	92	9·6	3·50	1·41	0·79	0·57	0·48	0·47
0·5	0·69	69	7·4	2·70	1·11	0·63	0·46	0·385	0·379
0·6	0·51	51	5·5	2·04	0·84	0·50	0·365	0·310	0·304
0·7	0·357	35·7	3·90	1·49	0·64	0·380	0·288	0·245	0·240
0·8	0·223	22·3	2·50	1·00	0·46	0·283	0·220	0·190	0·185
0·85	0·163	16·3	1·86	0·77	0·372	0·240	0·187	0·160	0·158
0·9	0·105	10·5	1·28	0·55	0·290	0·196	0·154	0·132	0·129
0·93	0·073	7·3	0·93	0·43	0·238	0·168	0·132	0·114	0·112
0·95	0·051	5·2	0·72	0·348	0·200	0·147	0·117	0·102	0·100
0·97	0·0305	3·15	0·50	0·258	0·160	0·122	0·099	0·087	0·084
0·99	0·0100	1·12	0·251	0·163	0·112	0·089	0·074	0·065	0·064

TABLE II.

For Constructing Chart for determination of the Mean Temperature of an Infinite Slab.

(Also infinite rectangular bar, and rectangular brick, see text.)

$\frac{ah}{k}\rightarrow$ $P_M\downarrow$	10^{-n} $(n>2)$	0·1	1·0	3	10	30	100	1000	∞
					$\frac{kt}{spa^2}$				
0·1	2·30×10^n	23·0	3·10	1·58	1·05	0·91	0·87	0·83	0·83
0·2	1·61	16·3	2·19	1·12	0·72	0·63	0·59	0·56	0·56
0·3	1·20	12·4	1·61	0·81	0·51	0·44	0·43	0·42	0·42
0·4	0·92	9·5	1·20	0·60	0·370	0·315	0·295	0·290	0·290
0·5	0·69	7·2	0·90	0·45	0·263	0·219	0·204	0·195	0·195
0·6	0·51	5·2	0·66	0·315	0·182	0·141	0·126	0·123	0·123
0·7	0·357	3·70	0·46	0·218	0·115	0·083	0·073	0·071	0·071
0·8	0·223	2·30	0·285	0·129	0·062	0·040	0·033	0·0320	0·0315
0·85	0·163	1·71	0·204	0·089	0·040	0·0234	0·0184	0·0182	0·0180
0·9	0·105	1·12	0·132	0·054	0·0230	0·0120	0·0085	0·0079	0·0079
0·93	0·073	0·76	0·089	0·0355	0·0145	0·0068	0·0043	0·00380	0·00380
0·95	0·051	0·54	0·061	0·0245	0·0095	0·0043	0·00225	0·00195	0·00190
0·97	0·0305	0·315	0·0355	0·0135	0·0050	0·00220	0·00090	0·00067	0·00066
0·99	0·0100	0·105	0·0109	0·0035	0·00120	—	—	—	—

TABLE III.

For Constructing Chart for Determination of the Centre Temperature of an Infinite Cylinder.

(Also finite cylinder, see text.)

$\frac{ah}{k}$ $C_c \downarrow$	10^{-n} $(n>2)$	0·01	0·1	0·3	1·0	3	10	100	∞
					$\frac{kt}{spa^2}$				
0·1	$1{\cdot}15\times10^n$	115	12·0	4·3	1·37	0·84	0·59	0·49	0·47
0·2	0·80	80·0	8·3	3·05	1·14	0·61	0·44	0·370	0·360
0·3	0·60	60·0	6·3	2·30	0·89	0·49	0·345	0·295	0·290
0·4	0·46	46·0	4·8	1·79	0·70	0·40	0·285	0·244	0·240
0·5	0·347	34·7	3·65	1·37	0·56	0·325	0·238	0·202	0·200
0·6	0·255	25·5	2·74	1·04	0·45	0·270	0·200	0·169	0·168
0·7	0·178	17·8	1·96	0·77	0·350	0·218	0·165	0·139	0·139
0·8	0·112	11·2	1·28	0·52	0·260	0·172	0·133	0·113	0·113
0·85	0·081	8·1	0·97	0·41	0·218	0·148	0·117	0·099	0·099
0·9	0·053	5·3	0·67	0·315	0·177	0·124	0·100	0·085	0·085
0·93	0·0363	3·63	0·50	0·252	0·151	0·108	0·090	0·076	0·076
0·95	0·0256	2·56	0·380	0·202	0·130	0·098	0·081	0·069	0·069
0·97	0·0152	1·56	0·270	0·160	0·110	0·083	0·069	0·060	0·060
0·99	0·0050	0·70	0·158	0·107	0·079	0·063	0·054	0·049	0·048

TABLE IV.

For Constructing Chart for Determination of the Mean Temperature of an Infinite Cylinder.

(Also finite cylinder, see text.)

$\frac{ah}{k}\rightarrow$ $\downarrow$	10^{-n} $(n>2)$	0·1	1·0	3	10	30	100	1000	∞
					$\frac{kt}{spa^2}$				
·1	$1{\cdot}15\times10^n$	11·7	1·48	0·69	0·44	0·380	0·355	0·345	0·340
·2	0·80	8·3	1·05	0·50	0·295	0·245	0·229	0·220	0·218
·3	0·60	6·2	0·78	0·365	0·204	0·170	0·155	0·150	0·148
·4	0·46	4·8	0·58	0·269	0·145	0·117	0·104	0·100	0·098
·5	0·347	3·60	0·44	0·199	0·105	0·081	0·070	0·066	0·065
·6	0·255	2·63	0·315	0·138	0·069	0·049	0·042	0·040	0·037
·7	0·178	1·86	0·214	0·091	0·042	0·0275	0·0229	0·0204	0·0200
·8	0·112	1·16	0·132	0·052	0·0224	0·0132	0·0099	0·0086	0·0081
·85	0·081	0·85	0·095	0·0355	0·0144	0·0079	0·0056	0·0048	0·0044
·9	0·053	0·56	0·062	0·0219	0·0083	0·0042	0·00265	0·00209	0·00195
·93	0·0363	0·380	0·042	0·0144	0·0052	0·0[illegible]4	0·00141	0·00102	0·00095
·95	0·0256	0·269	0·0295	0·0102	0·00345	0·00140	—	—	—
·97	0·0152	0·158	0·0162	0·0056	0·00186	—	—	—	—
·99	0·0050	0·050	0·0051	0·00178	—	—	—	—	—

TABLE V.

For Constructing Chart for Determination of the Centre Temperature of a Sphere.

$\frac{ah}{k}\rightarrow$ Sc ↓	10^{-n} $(n>2)$	0·01	0·1	0·3	1·0	3	10	100	∞
					$\frac{kt}{spa^2}$				
0·1	0·77×10^n	77·0	8·0	2·88	1·02	0·53	0·372	0·307	0·304
0·2	0·53	53·0	5·5	2·04	0·75	0·40	0·284	0·238	0·235
0·3	0·40	40·0	4·2	1·55	0·59	0·322	0·233	0·196	0·193
0·4	0·305	30·9	3·18	1·20	0·47	0·268	0·197	0·166	0·163
0·5	0·231	23·5	2·45	0·93	0·377	0·223	0·167	0·142	0·138
0·6	0·170	17·4	1·82	0·71	0·302	0·187	0·142	0·121	0·119
0·7	0·119	12·2	1·27	0·53	0·240	0·154	0·121	0·102	0·100
0·8	0·074	7·7	0·87	0·375	0·184	0·126	0·099	0·085	0·083
0·85	0·054	5·7	0·65	0·302	0·156	0·112	0·088	0·076	0·074
0·9	0·0351	3·73	0·46	0·234	0·129	0·095	0·077	0·067	0·065
0·93	0·0242	2·60	0·348	0·190	0·112	0·085	0·069	0·061	0·059
0·95	0·0171	1·86	0·275	0·158	0·100	0·077	0·063	0·056	0·054
0·97	0·0102	1·14	0·197	0·126	0·085	0·067	0·057	0·050	0·048
0·99	0·00335	0·46	0·117	0·085	0·063	0·052	0·046	0·041	0·040

TABLE VI.

For Constructing Chart for Determination of the Mean Temperature of a Sphere.

$\frac{ah}{k}\rightarrow$ $S_M\rightarrow$	10^{-n} $(n>2)$	0·1	1·0	3	10	30	100	1000	∞
					$\frac{kt}{spa^2}$				
0·1	0·77×10^n	7·7	0·93	0·44	0·251	0·214	0·195	0·186	0·186
0·2	0·53	5·3	0·66	0·295	0·170	0·135	0·123	0·115	0·112
0·3	0·40	4·0	0·49	0·215	0·118	0·089	0·079	0·072	0·071
0·4	0·305	3·05	0·372	0·157	0·083	0·060	0·053	0·048	0·046
0·5	0·231	2·31	0·278	0·116	0·059	0·040	0·0342	0·0307	0·0300
0·6	0·170	1·70	0·200	0·082	0·0391	0·0250	0·0204	0·0182	0·0178
0·7	0·119	1·19	0·138	0·056	0·0243	0·0142	0·0110	0·0097	0·0095
0·8	0·074	0·74	0·085	0·0330	0·0133	0·0071	0·0050	0·0041	0·0040
0·85	0·054	0·54	0·062	0·0234	0·0088	0·0045	0·00290	0·00229	0·00219
0·9	0·0351	0·351	0·040	0·0146	0·0052	0·00245	0·00145	0·00100	0·00094
0·93	0·0242	0·242	0·0275	0·0099	0·00331	0·00149	0·00076	—	—
0·95	0·0171	0·171	0·0192	0·0069	0·00225	0·00095	—	—	—
0·97	0·0102	0·102	0·0112	0·00398	0·00124	—	—	—	—
0·99	0·00335	0·0330	0·00347	0·00126	—	—	—	—	—

of the data necessary to construct similar charts for other values of x/a can also be obtained from the same source. A small part of the data for mean temperatures can be found in papers by Newman (12). It is believed that the remainder of the data is new.

In order to illustrate the method of using the charts, it will be assumed that the centre and mean temperatures at time t are required for a cylinder of length $2a$ and diameter $2r$, the various physical constants being as given above. The first step is to calculate the numbers $\frac{ah}{k}$, $\frac{kt}{s\rho a^2}$; these define a point on the chart corresponding to Table I., from which a value of P_c can be found. Similarly, the numbers $\frac{rh}{k}, \frac{kt}{s\rho r^2}$ are found, and the corresponding value of C_c obtained from the chart corresponding to Table III. Then the centre temperature required, θ_c, is given by

$$\frac{\theta_c-\theta_0}{\theta_1-\theta_0}=P_c . C_c .$$

In a precisely similar way the mean temperatures can be found from values of P_M and C_M obtained from charts 2 and 4. Temperatures for the infinite bar and finite brick respectively are found by multiplying together two or three values of P or P_M.

These charts were developed as part of the programme of the Food Investigation Board. They are published by permission of the Department of Scientific and Industrial Research.

References.

Theory.

(1) Fourier, 'Analytical Theory of Heat.' Paris, 1822.
(2) Carslaw, 'Introduction to the Mathematical Theory of the Conduction of Heat in Solids.' London, 1906.
(3) Ingersoll and Zobel, 'The Mathematical Theory of Heat Conduction.' Boston, 1912.
(4) Gröber and Erk, 'Die Grundgesetze der Wärmeübertragung.' Berlin, 1933.
(5) Lederer, *Zeit. Angew. Chem.* xxxvii. 750 (1924): *Kolloid-Zeit.* xliv. 108 (1928).
(6) Newman, Tr. Am. Inst. Chem. Eng. xxvii. 310, 203 (1931).
(7) Berger, *Zeit Angew. Math. u. Mech.* viii. 479 (1928); xi. 45 (1931).

Charts.

(8) Williamson and Adams, Phys. Rev. xiv. 99 (1919).
(9) Gurney and Lurie, Ind. Eng. Chem. xv. 1170 (1923).
(10) Schack, *Stahl u. Eisen,* l. 1289 (1930).
(11) Newman, Ind. Eng. Chem. xxviii. 545 (1936).

Tables.

(12) Newman (see 6).
(13) Russell, 'First Report of Alloy Steels Research Committee,' p 149 (1936).
(14) Olson and Schultz, Ind. Eng. Chem. xxxiv. 874 (1942).

CII. *A Closer Approximation to the Theory of the Field of Gerlach-Stern Magnets.*

By N. Davy, University College, Nottingham *.

[Received March 20, 1946.]

Abstract.

Since an exact theory of the field of Gerlach-Stern magnets, with a wedge-shaped polepiece facing a slotted one, does not seem possible, an approximate theory is worked out. This is the exact theory of a two-dimensional system in which the wedge is replaced by a semi-infinite thin plate with a sharp edge. This edge faces the slotted pole piece, and the slot is of finite depth as in the actual case. Intensities of magnetisation, field strengths and gradients likely to be useful in molecular beam work are calculated. Experimentally obtained diagrams exhibiting equipotentials and lines of force for magnets of (*a*) the true Gerlach-Stern type and (*b*) the type worked out in the present case, are inserted. Inspection reveals that the fields are very similar at points along the line of symmetry in front of the edge or wedge, *i. e.* in the region through which the molecular beam usually passes.

Introduction.

A formal theory giving a quantitative account of the Gerlach-Stern magnetic field between a wedge-shaped and a slotted polepiece does not seem to have been published. If we regard the problem as a two-dimensional one, and the faces of each pole as magnetic equipotentials, we still get what seems to be an unintegrable expression, when the Schwarz-Christoffel method is applied. This method is successful, however, when the wedge is replaced by a semi-infinite plane polepiece with a sharp edge facing the slot. Such a system is only degenerate in that one respect, compared with the true Gerlach-Stern arrangement. It has three sharp edges and a slot of finite depth in common with the original, to which it can therefore be regarded as a fair approximation.

§ 1. *A Plane Polepiece with a Sharp Edge facing a Slotted Polepiece. The Geometrical Transformation.*

In fig. 1 is represented a section of a pair of magnetic polepieces consisting of a thin semi-infinite plate AB facing a slotted pole LMNOPQR. B represents the sharp edge of the plane polepiece AB. This system is assumed to be two-dimensional and the faces of the poles are assumed to be equipotentials. The straight line BO will be a line of force, AO an axis of symmetry and the boundary ABONML forms a polygon to which the Schwarz-Christoffel theorem can be applied in order to transform the interior into the upper half of a t-plane, in the usual way. The theorem gives

---

* Communicated by Professor L. F. Bates, D.Sc.

$$dz = \frac{C_1(t-1)^{\frac{1}{2}}\,dt}{t^{\frac{1}{2}}(t-k^2)^{\frac{1}{2}}} \quad . \quad . \quad . \quad . \quad . \quad . \quad . \quad . \qquad (1)$$

if we select $t=1$ at M, $t=0$ at O, and $t=+k^2$ at N.

To integrate (1), write

$$t = \frac{1}{\mathrm{sn}^2(u, k)} \quad \text{and} \quad dt = \frac{-2\,\mathrm{cn}\,u\,\mathrm{dn}\,u\,du}{\mathrm{sn}^3\,u} \quad . \quad . \quad . \quad . \quad . \qquad (2)$$

Fig. 1.

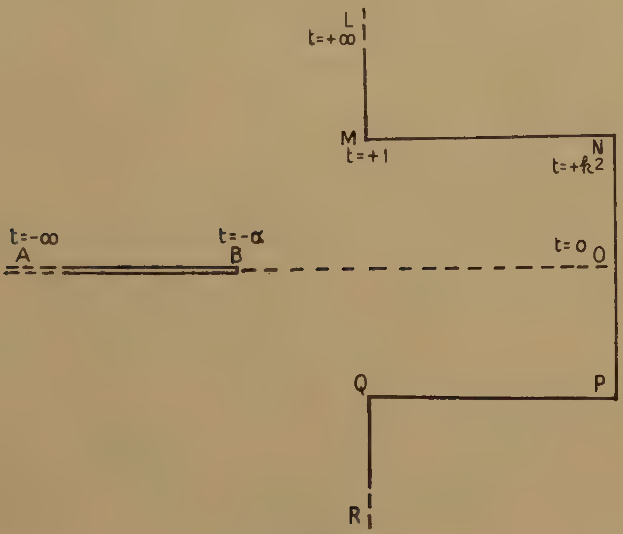

The z-plane.

This gives

$$dz = \frac{-2C_1\,\mathrm{cn}^2\,u\,.\,du}{\mathrm{sn}^2\,u}, \quad . \quad . \quad . \quad . \quad . \quad . \quad . \quad . \qquad (3)$$

whose integral is

$$z = 2C_1\left\{\frac{u\,.\,\mathrm{E}}{\mathrm{K}} + \mathrm{Z}(u) + \frac{\mathrm{cn}\,u\,.\,\mathrm{dn}\,u}{\mathrm{sn}\,u}\right\} + C_2, \quad . \quad . \quad . \quad . \quad . \qquad (4)$$

where the symbols have their usual meanings in the theory of Jacobian elliptic functions. This equation may also be written

$$z = 2C_1\left\{\frac{u\,.\,\mathrm{E}}{\mathrm{K}} + \mathrm{Z}(u+i\mathrm{K}') + \frac{i\pi}{2\mathrm{K}}\right\} + C_2, \quad . \quad . \quad . \quad . \qquad (5)$$

At the point O, where $t=0$, $\mathrm{sn}^2\,u=\infty$, so let $u=i\mathrm{K}'$ and $z=0$.

At N, where $t=k^2$, $\mathrm{sn}^2\,u=1/k^2$, so let $u=\mathrm{K}-i\mathrm{K}'$ and $z=+il$.

At M, where $t=1$, $\mathrm{sn}^2\,u=1$, so let $u=+\mathrm{K}$ and $z=-f+il$.

On inserting these values in equation (5), in turn, we find

$$C_1=\frac{il}{2E} \quad \text{and} \quad C_2=-f. \quad \text{. . . . .} \quad (6)$$

Also

$$\frac{f}{l}=\frac{2EK'-\pi}{2KE}=\frac{K'-E'}{E}. \quad \text{. . . . . . .} \quad (7)$$

Equation (7) is the one which gives us the value of the modulus k. We get the numerical value of k, by the help of, say, the Smithsonian Tables of Elliptic Functions by Adams and Hippisley. By trial, we find what value of the right-hand side of (7) is equal to the numerical value of f/l for the polepiece system we are using. Each value of the right-hand side of (7) depends on the value of k chosen, and we go on until a value of k is found which makes the two sides equal. Thus, if we take $f=2l$, as we do in the experimental part of this paper, we find k is very nearly equal to sin 4°=0·0698.

Fig. 2.

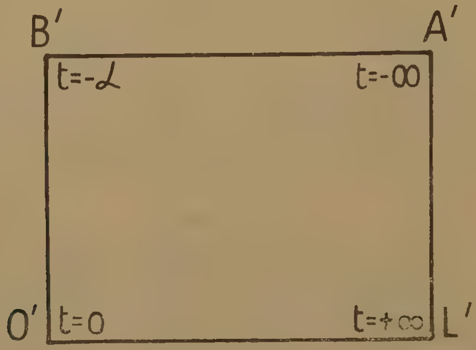

The W-plane.

§ 2. *The Electrical Transformation.*

In fig. 2 is represented the rectangle in the W-plane, which is also to be transformed into the upper half of the t-plane, and thus link the geometrical with the electrical conditions. This rectangle has its corners (1) at O′, where $t=0$ corresponding to the point O in the z-plane, (2) at B′, where $t=-\alpha$ corresponding to B, (3) at A′, where $t=-\infty$ corresponding to A, and (4) at L′, where $t=+\infty$, corresponding to L. The value of α is as yet undetermined. The differential equation of transformation is therefore, by Schwarz and Christoffel's theorem,

$$dW=\frac{C_3 . dt}{t^{\frac{1}{2}}(t+\alpha)^{\frac{1}{2}}}, \quad \text{. . . . .} \quad (8)$$

whose integral is

$$W=2C_3 \log \{t^{\frac{1}{2}}+(t+\alpha)^{\frac{1}{2}}\}+C_4. \quad \text{. . . . .} \quad (9)$$

If we let

$$W=0 \text{ when } t=0, \text{ and } W=iV_1 \text{ when } t=-\alpha, \quad \text{. .} \quad (10)$$

we soon find

$$C_3=\frac{V_1}{\pi}, \quad \text{and} \quad C_4=\frac{-2V_1}{\pi}\log\alpha^{\frac{1}{2}}=\frac{-V_1}{\pi}\,.\log\alpha. \quad . \quad . \quad (11)$$

These results then correspond to the case when the face of the wedge is at potential V, and the slotted polepiece at potential zero. Equation (9) can be written thus :—

$$W=\frac{2V_1}{\pi}\log\frac{t^{\frac{1}{2}}+(t+\alpha)^{\frac{1}{2}}}{\alpha^{\frac{1}{2}}}. \quad . \quad . \quad . \quad . \quad . \quad . \quad . \quad . \quad (12)$$

Write $t=\frac{1}{\mathrm{sn}^2 u}$ and $\alpha=\frac{1}{\mathrm{sn}^2\beta}$. Then

$$W=\frac{2V_1}{\pi}\,.\log\frac{\mathrm{sn}\,\beta+(\mathrm{sn}^2\beta+\mathrm{sn}^2 u)^{\frac{1}{2}}}{\mathrm{sn}\,u}, \quad . \quad . \quad . \quad . \quad . \quad . \quad (13)$$

α and β are as yet unknown, but if at B, where $t=-\alpha$, we let $z=-h$, then as we know k we can find β by trying various values of u in (4) or (5) by the aid of tables. That value of u which makes $z=-h$ will be the one which satisfies $\alpha=-\frac{1}{\mathrm{sn}^2 u}=\frac{1}{\mathrm{sn}^2\beta}$. This gives both β and α. The full calculation of the numerical values of β and α is carried out later in this paper, in section 7.

It seems possible to obtain equations representing equipotentials and lines of force in terms of t but not in terms of u.

Thus equation (12) can be rewritten

$$t^{\frac{1}{2}}+(t+\alpha)^{\frac{1}{2}}=\alpha^{\frac{1}{2}}e^{\frac{\pi W}{2V_1}}=\alpha^{\frac{1}{2}}e^{\frac{\pi}{2V_1}(U+iV)}. \quad . \quad . \quad . \quad . \quad . \quad (14)$$

Writing $t=re^{i\theta}$, and

$$t+\alpha=r_2e^{i\theta_2} \quad . \quad . \quad . \quad . \quad . \quad . \quad . \quad . \quad . \quad . \quad (15)$$

we get

$$r\cos\theta+r_2\cos\theta_2+i(r\sin\theta+r_2\sin\theta_2)=\alpha^{\frac{1}{2}}e^{\frac{\pi U}{2V_1}}\cos\frac{\pi V}{2V_1}+i\alpha^{\frac{1}{2}}e^{\frac{\pi U}{2V_1}}\sin\frac{\pi V}{2V_1}. \quad . \quad . \quad . \quad (16)$$

Hence

$$r\cos\theta+r_2\cos\theta_2=\alpha^{\frac{1}{2}}e^{\frac{\pi U}{2V_1}}\cos\frac{\pi V}{2V_1}, \quad . \quad . \quad . \quad . \quad . \quad . \quad (17)$$

and

$$r\sin\theta+r_2\sin\theta_2=\alpha^{\frac{1}{2}}e^{\frac{\pi U}{2V_1}}\sin\frac{\pi V}{2V_1}. \quad . \quad . \quad . \quad . \quad . \quad . \quad (18)$$

Equipotentials are obtained by dividing (17) by (18), after which, putting V=const., we get

$$\tan\frac{\pi V}{2V_1}=\frac{r\sin\theta+r_2\sin\theta_2}{r\cos\theta+r_2\cos\theta_2}=\text{const.}=A, \text{ say.} \quad . \quad . \quad . \quad (19)$$

Fig. 3 represents the t-plane and shows that

$$r_2\sin\theta_2=r\sin\theta \text{ and } r_2\cos\theta_2=r\cos\theta=r\cos\theta+\alpha. \quad . \quad . \quad (20)$$

Thus, equipotentials are given by

$$\frac{2r\sin\theta}{2r\cos\theta+\alpha}=\mathrm{A},$$

which reduces to

$$r\sin\theta=\mathrm{B}(2r\cos\theta+\alpha), \quad \ldots\ldots\ldots \quad (21)$$

if we put $\frac{\mathrm{A}}{2}=\mathrm{B}$. Also if we write $t=\mathrm{X}+i\mathrm{Y}$, then $r\sin\theta=\mathrm{Y}$, and $r\cos\theta=\mathrm{X}$ so that equation (21) becomes

$$\mathrm{Y}=\mathrm{B}(2\mathrm{X}+\alpha). \quad \ldots\ldots\ldots\ldots \quad (22)$$

This equation represents all those straight lines which pass through $t=-\frac{\alpha}{2}$. Hence the lines of force are represented by the set of concentric circles in the t-plane whose centre is $t=-\frac{\alpha}{2}$. The equations to equipotentials and lines of force in the z-plane, which are what we should really like to get, do not seem obtainable by theory, but the shapes of the curves are readily obtainable by experiment. For further details on this point see section 8 and figs. 4 and 5.

Fig. 3.

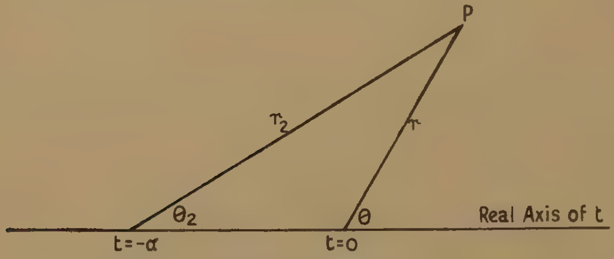

The t-plane.

§3. *Field Strength and Intensity of Magnetization.*

The field strength

$$\mathrm{H}=\left|\frac{d\mathrm{W}}{dz}\right|=\frac{\mathrm{C}_3(t-k^2)^{\frac{1}{2}}}{\mathrm{C}_1(t+\alpha)^{\frac{1}{2}}(t-1)^{\frac{1}{2}}}, \quad \ldots\ldots\ldots \quad (23)$$

which, of course, is infinite at the projecting edges B and M where $t=-\alpha$ and $+1$, respectively. It is zero at the re-entrant corner N where $t=k^2$.

At O, where $t=0$,

$$\mathrm{H}=\left|\frac{\mathrm{C}_3\,.\,k}{\mathrm{C}_1\,.\,\alpha^{\frac{1}{2}}}\right|=\frac{2\mathrm{EV}_1\,.\,k}{\pi l\alpha^{\frac{1}{2}}}. \quad \ldots\ldots\ldots \quad (24)$$

The intensity of magnetization $\mathrm{I}=\frac{\mathrm{H}}{4\pi}$. It is infinite at the projecting edges, zero at the re-entrant corner and equal to $\frac{\mathrm{EV}_1 k}{2\pi^2 l\alpha^{\frac{1}{2}}}$ at O. At any point, by (23), it is

$$\mathrm{I}=\left|\frac{\mathrm{C}_3(t-k^2)^{\frac{1}{2}}}{4\pi\mathrm{C}_1(t+\alpha)^{\frac{1}{2}}(t-1)^{\frac{1}{2}}}\right|=\frac{\mathrm{EV}_1\,\mathrm{dn}\,u\,.\,\mathrm{sn}\,u}{2\pi^2 l\,.\,\mathrm{cn}\,u(1+\alpha\,\mathrm{sn}^2\,u)}\,.\quad .\quad .\quad .\quad (25)$$

The numerical value of α is obtained in section 7.

§ 4. *The Total Pole Strength.*

The total pole strength per cm. distributed along any portion of either pole is $\mathrm{Q}=\frac{1}{4\pi}(\mathrm{W}_1-\mathrm{W}_2)$ where the suffixes refer to the limiting points. Now

$$\mathrm{Q}=\frac{1}{4\pi}(\mathrm{W}_1=\mathrm{W}_2)=\frac{\mathrm{C}_3}{2\pi}\log\frac{t_1^{\frac{1}{2}}+(t_1+\alpha)^{\frac{1}{2}}}{t_2^{\frac{1}{2}}+(t_2+\alpha)^{\frac{1}{2}}}\quad \text{by (9)}\ .\quad .\quad .\quad (26)$$

Hence from M to N, *i. e.*, from $t_1=1$ to $t_2=k^2$, noting that $\mathrm{C}_3=\frac{\mathrm{V}_1}{\pi}$ and taking $\sqrt{k^2}=-k$.

$$\mathrm{Q}=\frac{\mathrm{V}_1}{2\pi^2}\,.\log\frac{(1+\alpha)^{\frac{1}{2}}+1}{(k^2+\alpha)^{\frac{1}{2}}-k}\,.\quad .\quad .\quad .\quad .\quad .\quad .\quad .\quad (27)$$

From N to O, *i. e.*, from $t_1=k^2$ to $t_2=0$

$$\mathrm{Q}=\frac{\mathrm{V}_1}{2\pi^2}\log\frac{(k^2+\alpha)^{\frac{1}{2}}-k}{\alpha^{\frac{1}{2}}}\,.\quad .\quad .\quad .\quad .\quad .\quad .\quad .\quad (28)$$

The total pole strength on AB or LM is infinite.

§ 5. *Calculation of* $\frac{d\mathrm{H}}{dz}$ and $\frac{d\mathrm{H}^2}{dz}$.

On differentiating (23) with respect to z and writing

$$\mathrm{C}_1=\frac{il}{2\mathrm{E}}\quad\text{and}\quad\mathrm{C}_3=\frac{\mathrm{V}_1}{\pi},\quad .\quad .\quad .\quad .\quad .\quad .\quad (29)$$

we get

$$\frac{d\mathrm{H}}{dz}=\frac{2\mathrm{E}^2\mathrm{V}_1 t^{\frac{1}{2}}\{t^2-2k^2t+\alpha+k^2-\alpha k^2\}}{\pi l^2(t+\alpha)^{3/2}(t-1)^2}\,.\quad .\quad .\quad .\quad .\quad .\quad (30)$$

This quantity is important in molecular beam experiments, for the mechanical forces on molecules having a definite magnetic moment are proportional to it.

$$\frac{d\mathrm{H}^2}{dz}=\frac{8\mathrm{E}^3\mathrm{V}_1{}^2 t^{\frac{1}{2}}(t-k^2)^{\frac{1}{2}}\{t^2-2k^2t+\alpha+k^2-\alpha k^2\}}{\pi^2 l^3(t+\alpha)^2(t-1)^{5/2}}\,.\quad .\quad .\quad .\quad .\quad (31)$$

The mechanical force on a small para- or diamagnetic body is proportional to this quantity.

§ 6. *The Mechanical Force on a Pole Face.*

The mechanical force on unit area of any face is

$$2\pi\mathrm{I}^2=\frac{\mathrm{E}^2\mathrm{V}_1{}^2(t-k^2)}{2\pi^3 l^2(t+\alpha)(t-1)}\ \text{dynes per sq. cm.}\quad .\quad .\quad .\quad (32)$$

The total force on any length of face, per cm. depth, is

$$\int_{t_1}^{t_2} 2\pi \mathrm{I}^2 . dt = \frac{\mathrm{E}^2 \mathrm{V}_1^2}{2\pi^3 l^2 (1+\alpha)} \left\{ (\alpha + k^2) \log \frac{t_2+\alpha}{t_1+\alpha} + (1-k^2) \log \frac{t_2-1}{t_1-1} \right\} \text{ dynes.} \quad . \quad . \quad . \quad (33)$$

§ 7. *The Value of α.*

At the edge B in fig. 1 $t = \frac{1}{\mathrm{sn}^2 u} = -\alpha = -\frac{1}{\mathrm{sn}^2 \beta}$ and $z = -h$.

Hence at this point

$$z = -h = \frac{il}{\mathrm{E}} \left\{ \frac{u\mathrm{E}}{\mathrm{K}} + \mathrm{Z}(u) + \frac{\mathrm{cn}\, u . \mathrm{dn}\, u}{\mathrm{sn}\, u} \right\} - f. \quad . \quad . \quad . \quad . \quad . \quad (34)$$

Fig. 4.

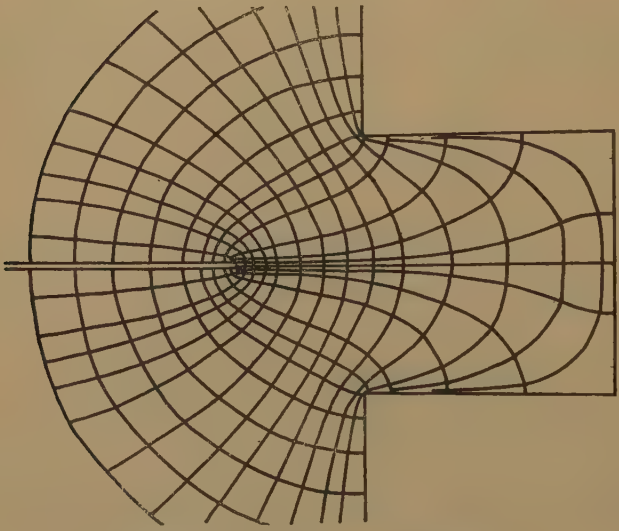

Field of force of the present system.

To find this value of u, we must fix the ratios of h and f to l. Thus let $h = 3l$, and $f = 2l$ so that (34) reduces to

$$-1 = \frac{i}{\mathrm{E}} \left\{ \frac{u\mathrm{E}}{\mathrm{K}} + \mathrm{Z}(u) + \frac{\mathrm{cn}\, u . \mathrm{dn}\, u}{\mathrm{sn}\, u} \right\} . \quad . \quad . \quad . \quad . \quad . \quad . \quad (35)$$

Since at A, $t = -\infty$, $u = 0$, and at O, $t = 0$, $u = -i\mathrm{K}'$, the value of u at B lies between zero and $-i\mathrm{K}'$. Let its value be

$$u = -iq. \quad . \quad . \quad . \quad . \quad . \quad . \quad . \quad . \quad . \quad . \quad (36)$$

Substitute this in (35) and eliminate i by expressing the elliptic functions in terms of modulus k'. (35) reduces to

$$-1 = \frac{1}{\mathrm{E}} \left\{ q \left(1 - \frac{\mathrm{E}'}{\mathrm{K}'} \right) - \mathrm{Z}(q, k') - \frac{\mathrm{dn}\,(q, k') . \mathrm{cn}\,(q, k')}{\mathrm{sn}\,(q, k')} \right\}, \quad . \quad (37)$$

$k'=\sin 86°$ approx. so q is found by inserting trial values obtained from pp. 302–303 of the Smithsonian Tables of Elliptic Functions by Adams and Hippisley. After some labour we find $q=0{\cdot}522$, so that $u=-iq =-i\times 0{\cdot}522$, $t=-3{\cdot}370$, $\alpha=+3{\cdot}370$, $\operatorname{sn}\beta=0{\cdot}545$.

§ 8. *Equipotentials and Lines of Force.*

Fig. 4 shows the arrangement of the equipotentials and lines of force in a system like the one just discussed.

Fig. 5 gives the equipotentials and lines of force of an actual two-dimensional Gerlach–Stern system, the angle of the wedge being 72°. The width and depth of the slot are made equal, both in figs. 4 and 5. In each case, also, the distance from the sharp edge of the plate or wedge to the front plane of the other pole-piece is made equal to half the width or depth of the slot. These diagrams were obtained experimentally by the method described in earlier papers.

Fig. 5.

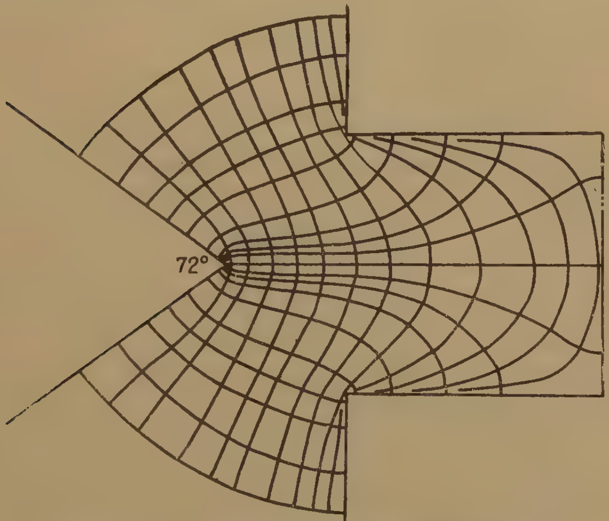

Field of force of a Gerlach-Stern magnet.

By inspection of these diagrams it is seen that along the line of symmetry drawn from the sharp edge to the middle of the bottom of the slot, the arrangement of lines of force and equipotentials is very much the same in the two cases. The fields are alike on this line but differ more and more as the lateral distance from the line of symmetry increases, except inside the slot.

In both figs. 4 and 5 it is seen that those lines of force which terminate on the sides or bottom of the slot begin at or very close to the tip of the wedge or sharp edge, respectively.

CIII. *A Note on a Particular Type of Asymptotic Series.*

By R. A. Rankin, Clare College, Cambridge *.

[Received February 26, 1945.]

The labour of computing new or untabulated functions can often be reduced by the use of asymptotic formulæ valid for certain ranges of the argument. In the following note I show how the useful range of application of a general class of asymptotic formulæ can be extended, by obtaining narrower bounds for the " remainder " or " error " term than those ordinarily used. The method is extremely simple, but is, so far as I am aware, new.

Suppose that, for x in the interval $x > a$, the function $f(x)$ possesses an alternating asymptotic series of the form

$$f(x) = \sum_{s=0}^{n-1} (-1)^s u_s(x) + (-1)^n \mathrm{R}_n(x), \quad . \quad . \quad . \quad . \quad . \quad . \quad (1)$$

where $u_s(x)$ and the remainder term $R_n(x)$ are positive functions of x. By this is meant that

$$\lim_{x\to\infty} \frac{\mathrm{R}_n(x)}{u_{n-1}(x)} = 0$$

for fixed $n \geqslant 1$. The series is said to be " strictly " asymptotic if, in addition,

$$0 \leqslant \mathrm{R}_n(x) \leqslant u_n(x) \quad . \quad . \quad . \quad . \quad . \quad . \quad . \quad . \quad . \quad . \quad (2)$$

for all x in the interval, and for each $n \geqslant 1$. It follows from (2), since $\mathrm{R}_n(x) = u_{n-1}(x) - \mathrm{R}_{n-1}(x)$, that

$$0 \leqslant \mathrm{R}_n(x) \leqslant u_{n-1}(x) \quad . \quad . \quad . \quad . \quad . \quad . \quad . \quad . \quad (3)$$

for $n \geqslant 1$. Inequalities of the types (2) and (3) are useful when asymptotic series are employed in numerical work.

If, however, $f(x)$ is expressible in the form

$$f(x) = \int_0^\infty \frac{\phi(t, x)}{1+t}\, dt,$$

it may be possible to find sharper inequalities for the remainder term than those given by (2) and (3) without introducing new functions. It is assumed here that $\phi(t, x)$ is not negative for any $x > a$, and that the function

$$u_\nu(x) = \int_0^\infty t^\nu \phi(t, x)\, dt \quad . \quad . \quad . \quad . \quad . \quad . \quad . \quad . \quad (4)$$

exists as a convergent integral for all $\nu \geqslant 0$.

When this is the case, the expansion (1) holds with $u_s(x)$ defined by means of (4), and the remainder term $\mathrm{R}_n(x)$ satisfies the inequalities

$$\mathrm{R}_n(x) \leqslant \tfrac{1}{2} u_{n-\frac{1}{2}}(x), \quad . \quad . \quad . \quad . \quad . \quad . \quad . \quad . \quad . \quad (5)$$

---

* Communicated by the Author.

and
$$R_n(x) \geqslant u_{n-\frac{1}{2}}(x) - \tfrac{1}{4}\{u_n(x)+u_{n-1}(x)\} \quad . \quad . \quad . \quad . \quad . \quad (6)$$
in addition to the usual inequalities (2) and (3) for $n \geqslant 1$. For certain values of n the right-hand side of (6) may not be positive. In this case (6) is trivial.

Since
$$\frac{1}{1+t} = \sum_{s=0}^{n-1} (-1)^s t^s + (-1)^n \frac{t^n}{1+t},$$
it is clear that (1) holds for all $x > a$, and that
$$R_n(x) = \int_0^\infty \frac{t^n \phi(t, x)}{1+t} dt. \quad . \quad . \quad . \quad . \quad . \quad . \quad . \quad . \quad (7)$$

The inequalities (2) and (3) follow from (4) and (7) since
$$\frac{1}{1+t} \leqslant 1, \qquad \frac{1}{1+t} \leqslant \frac{1}{t},$$
for $t \geqslant 0$. The new inequalities (5) and (6) are derived in a similar manner from
$$\frac{1}{1+t} \leqslant \frac{1}{2\sqrt{t}}, \quad . \quad . \quad . \quad . \quad . \quad . \quad . \quad . \quad . \quad (8)$$
and
$$\frac{1}{1+t} \geqslant \frac{1}{\sqrt{t}} - \frac{1}{4}\left(1+\frac{1}{t}\right). \quad . \quad . \quad . \quad . \quad . \quad . \quad . \quad . \quad (9)$$

Other bounds for $R_n(x)$ may, of course, be obtained by the choice of inequalities more complicated than (8) and (9). Thus, for example,
$$R_n(x) \leqslant \alpha^\alpha (1-\alpha)^{1-\alpha} u_{n-\alpha}(x) \qquad (0<\alpha<1)$$
follows from the inequality
$$1+t \geqslant t^\alpha \alpha^{-\alpha} (1-\alpha)^{\alpha-1}.$$
The particular case given by $\alpha = \frac{1}{2}$ is, however, the only one likely to be of practical use.

As an example of the above, consider the function $F(x)$ defined by
$$F(x) = \frac{1}{\sqrt{\pi}} \int_0^\infty \frac{y^{-\frac{1}{2}} e^{-xy}}{1+y^2} dy = \frac{1}{2\sqrt{\pi}} \int_0^\infty \frac{t^{-\frac{3}{4}} e^{-x\sqrt{t}}}{1+t} dt.$$
This function is related to the Fresnel integrals. We have
$$\phi(t, x) = \frac{1}{2\sqrt{\pi}} t^{-\frac{3}{4}} e^{-x\sqrt{t}},$$
and
$$u_n(x) = \frac{(4n)\,!}{(2n)\,!\; 2^{4n} x^{2n+\frac{1}{2}}}, \qquad u_{n-\frac{1}{2}}(x) = \frac{(4n-2)\,!}{(2n-1)\,!\; 2^{4n-2} x^{2n-\frac{1}{2}}}.$$

By means of the inqualities (5) and (6) it is possible to evaluate $F(x)$ to four figures of decimals for values of x as low as 7. Thus, for $x=7$, we obtain $F(7)=0{\cdot}3729$ correct to four places. More precisely, from (5 and (6) with $n=4$,
$$0{\cdot}372915 \leqslant F(7) \leqslant 0{\cdot}372933.$$

The inequalities (2) confine the error term to limits as close as this only when $x > 10$. For $x=7$ the best they give is
$$0{\cdot}372691 \leqslant F(7) \leqslant 0{\cdot}373210.$$

CIV. *The Use of the Impedance Concept as Applied to Wave Guides.*

By Gordon Williams and H. C. Bolton,
King's College, London *.

[Received June 7, 1945.]

Summary.

The analogy between Lecher lines and wave guides first suggested by Schelkunoff (1937) and later developed by Flint and Pincherle (1943) has been used to derive a wave-guide method for the measurement of the properties of dielectrics at very high frequencies. The experimental results support the theoretical conclusions obtained using the analogy.

Introduction.

Schelkunoff (1937) was the first to show that there are quantities in wave-guide theory which satisfy similar equations as do potential, current and impedance in line theory. Later (1938) he extended the impedance concept to other branches of physics. In 1943, Flint and Pincherle returned to its original application, and showed not only how it gave results already known from the wave theory, but also that its use suggested further experiments in guides.

For H waves, which are the easier of the two classes to treat, the following comparisons can be written

$$\left.\begin{array}{ll} \mathrm{R}\equiv 0 & \mathrm{G}\equiv g \\ \mathrm{L}\equiv\mu & \mathrm{C}\equiv\epsilon-\chi^2/\omega^2\mu \end{array}\right\} \quad . \quad . \quad . \quad . \quad . \quad . \quad . \quad . \quad (1)$$

The quantities taking the place of current and voltage do not possess such an immediate significance and have been omitted. The M.K.S. rationalized system of units is used and the definitions are those of Stratton (1941). R, G, L and C refer to the resistance, leakance, inductance and capacity of the line system, whereas g, μ and ϵ refer to the conductivity, permeability and real inductive capacity of the medium in the guide. χ is the constant characterizing the system down which the wave is propagated and $\omega=2\pi f$, where f is the frequency of the oscillations.

For E waves the equivalent quantities are :

$$\left.\begin{array}{ll} \mathrm{R}\equiv\dfrac{\chi^2 g}{g^2+\omega^2\epsilon^2} & \mathrm{G}\equiv g \\[2ex] \mathrm{L}\equiv\mu-\dfrac{\chi^2\epsilon}{g^2+\omega^2\epsilon^2} & \mathrm{C}\equiv\epsilon \end{array}\right\} \quad . \quad . \quad . \quad . \quad . \quad . \quad . \quad . \quad (2)$$

At first sight the expressions do not seem as simple as those for H waves ; it is to be noted especially that the expression equivalent to R is not zero. Because of the simplicity introduced into line theory when R is negligible compared with ωL, it seems desirable to find for E waves the conditions under which this inequality can be applied to the equivalent quantities. This implies that

---

* Communicated by Prof. H. T. Flint.

$$\chi^2 g \ll \omega(\mu g^2+\omega^2\mu\epsilon^2-\chi^2\epsilon). \quad . \quad . \quad . \quad . \quad . \quad . \quad . \quad . \quad (3)$$

The waves must be shorter than the cut-off wave-length of the guide, that is $\omega^2\mu\epsilon>\chi^2$.

If now we put $\omega^2\mu\epsilon=m\chi^2$, where $m>1$, the inequality (3) becomes

$$\frac{\omega^2\mu\epsilon}{m}g \ll \omega\left[\mu g^2+\frac{(m-1)\omega^2\mu\epsilon^2}{m}\right],$$

that is

$$1 \ll \frac{g}{\omega\epsilon}m+\frac{\omega\epsilon}{g}(m-1),$$

or

$$1 \ll mx+\frac{m-1}{x}, \quad . \quad . \quad . \quad . \quad . \quad . \quad . \quad . \quad (4)$$

where $x=g/\omega\epsilon$.

In order that this may be satisfied for all values of x, the minimum value of

$$y=mx+(m-1)/x \quad . \quad . \quad . \quad . \quad . \quad . \quad . \quad . \quad . \quad (5)$$

has to be much greater than unity. The value of $y_{\text{min.}}$ obtained from equation (5) is $2\sqrt{m(m-1)}$.

In normal wave-guide experiments, m is of the order of 2 or 3, from which it is seen that the inequality (4) cannot be satisfied for all values of x; so that, in general, when using the line analogy for E waves, we must retain the expression for R. The inequality (4) is, however, satisfied when $x \gg 1$ and when $x \ll 1$. The first condition implies that $g \gg \omega\epsilon$, which is not applicable in the case of normal dielectrics. The second means that $g \ll \omega\epsilon$, and this may or may not be satisfied in an actual experiment. In the anomalous dispersion region of polar dielectrics it is most likely not satisfied, since here g is large and ϵ is decreasing from its high " statical " value to its low " optical " value.

It is also seen that the quantity equivalent to L will depend upon the dielectric properties, ϵ and g, of the medium in the guide unless

$$\mu \gg \frac{\chi^2\epsilon}{g^2+\omega^2\epsilon^2},$$

that is

$$\mu g^2+\omega^2\mu\epsilon^2 \gg \chi^2\epsilon.$$

But we can again put

$$\omega^2\mu\epsilon=m\chi^2, \quad (m>1),$$

when we have

$$1+\frac{g^2}{\omega^2\epsilon^2} \gg \frac{1}{m}.$$

Since m can approximate to 1 we can neglect the unity term on the left-hand side and write the inequality as

$$g^2 \gg \omega^2 \epsilon^2 .$$

A condition similar to this has already been discussed.

In the preceding theory we have assumed the attenuation of the waves in passing down the tube to be due solely to the conductivity of the dielectric medium and have ignored any attenuation arising from the large, though still finite, value of the conductivity of the walls. This is, in effect, saying that the large value of the wall conductivity is taken to be infinite and, so far as is known, there are no dielectric experiments on wave guides where this is not taken to be the case. Recent results based on this assumption have been given by Lamont (1940), Roberts and Hippel (1940), Middleton (1943), Fejér and Scherrer (1943). The accuracy of dielectric measurements given at decimetre wave-lengths and shorter still, does not warrant making any correction for the conductivity of the metals commonly used, brass and copper. Indeed it is only recently, especially since the time of Knerr (1937) (who studied water using both a Lecher line and a free wave method), that the technique of using higher and higher frequencies has advanced so far as to allow dielectric measurements to be made in the decimetre and centimetre region using undamped waves. For instance, early experiments on water, those of Eckert (1913), Mobius (1920) and Tear (1923), though they bridged the gap between the "statical" and "optical" value of the dielectric constant, used damped waves; and the results of different observers do not agree. It is felt that the experiments on undamped waves in hollow tubes offer the best means of studying dielectric properties in the anomalous dispersion region: the wave-lengths are of the order of the dimensions of the apparatus, but diffraction and screening difficulties are avoided when the waves are completely contained in the tubes.

The Measurement of the Properties of Dielectrics.

The following method is discussed for H waves only, though it can be used for E waves with the limitations already mentioned. It is suggested as a simple and practicable means of obtaining the properties of substances at ultra high frequencies. It can be applied to both solids and liquids, using either transmission lines or wave guides, and will give the losses in the substance as well as its dielectric constant. The theory as it applies to lines will be given, before its application to wave guides is discussed.

Line Theory of the Method.

Referring to fig. 1, the lines are short-circuited and are immersed in the dielectric to the point A (a coaxial line is depicted in the diagram).

The impedance of the line beyond A is then measured using a convenient method. Let this impedance be $R_1 + jX_1$. It can also be written Z_0' tanh $P's$, where Z_0' is the characteristic impedance of this line and $P'=\alpha'+j\beta'$, its propagation constant.

Thus
$$R_1+jX_1=Z_0' \tanh P's'. \quad . \quad . \quad . \quad . \quad . \quad . \quad . \quad . \quad (6)$$

If now the short circuit is removed and the impedance as measured is R_2+jX_2 we have

$$R_2+jX_2=Z_0' \coth P's'. \quad . \quad . \quad . \quad . \quad . \quad . \quad . \quad . \quad (7)$$

In practice the stray displacement currents which exist beyond the end of the line in the latter case introduce large errors into the corresponding formula, that is, Z_0' coth $P's'$. (See Jackson and Huxley, 1944). In the case of wave guides it will not even be approximately true, due to the loss of energy by radiation from the open end of the guide. The difficulty can be overcome, however, by maintaining the short circuit and moving the dielectric a distance of a quarter wave-length along the line, fig. 2. Then from equations (6) and (7) we have the well-known equation

Fig. 1.

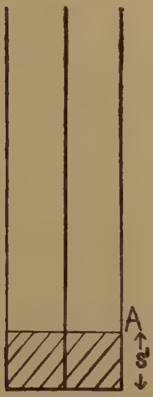

Fig. 2.

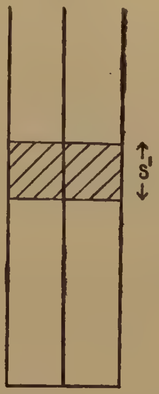

$$(R_1+jX_1)(R_2+jX_2)=(Z_0')^2, \quad . \quad . \quad . \quad . \quad . \quad . \quad . \quad (8)$$

from which the components, R_0' and X_0', of Z_0' can be determined. The calculation is simple since R_1, X_1, R_2 and X_2 are all numbers and will be expressed in terms of Z_0, the characteristic impedance of the air-filled line. The value of s' is not required.

If it can be assumed that the resistance of the lines is negligible, a condition which can be satisfied in practice, α' and β' are related to R_0' and X_0' by the simple equations :

$$\alpha'=\frac{\omega L}{X_0'(1+R_0'^2/X_0'^2)}, \quad . \quad . \quad . \quad . \quad . \quad . \quad . \quad . \quad (9)$$

and

$$\beta'=\frac{\omega L}{R_0'(1+X_0'^2/R_0'^2)}. \quad . \quad . \quad . \quad . \quad . \quad . \quad . \quad . \quad (10)$$

But for an air-filled line $Z_0=\sqrt{L/C}=cL$, since $c=1/\sqrt{LC}$, the latter being the velocity of electro-magnetic waves in free space.

Also $c=f\lambda_a$, λ_a being the wave-length of the oscillations in free space, so that

$$\alpha'=\frac{2\pi}{\lambda_a}\cdot\frac{Z_0}{X_0'(1+R_0'^2/X_0'^2)}, \quad . \; . \; . \; . \; . \; . \; . \quad (11)$$

$$\beta'=\frac{2\pi}{\lambda_a}\,\frac{Z_0}{R_0'(1+X_0'^2/R_0'^2)}. \quad . \; . \; . \; . \; . \; . \; . \quad (12)$$

But since R_0' and X_0' will have been obtained in the experiment in terms of Z_0, the absolute value of the latter quantity will not be required.

Having found α' and β', these values can be then used to give K, the dielectric constant, and g, the conductivity of the medium. It is more convenient to keep the real part (ϵ') and imaginary part (ϵ'') of the inductive capacity separate when we obtain

$$\beta'^2-\alpha'^2=\left(\frac{2\pi}{\lambda_a}\right)^2\frac{\epsilon'}{\epsilon_0}=\left(\frac{2\pi}{\lambda_a}\right)^2 K \quad . \; . \; . \; . \; . \; . \quad (13)$$

and

$$\epsilon''=g/\omega=2\alpha'\beta'/\omega^2\mu. \quad . \; . \; . \; . \; . \; . \; . \; . \quad (14)$$

The method outlined above measures the real and imaginary parts of the complex inductive capacity, as do also the condenser methods which are used at lower frequencies. When the approach to the problem is by wave methods, however, it is the refractive index that is stressed. Maxwell's relation, that the dielectric constant is the square of the index of refraction at any given frequency, is generalized, when losses are heavy by the relation $\epsilon^*=\epsilon_0 n^2(1-jk)^2$. This introduces the complex refractive index $n(1-jk)$; n is known as the refractive index defined as λ in air/λ in medium, and k is the absorption coefficient. We have

$$\epsilon^*=\epsilon'-j\epsilon''=\epsilon_0 n^2(1-jk)^2,$$

so that

$$K=\epsilon'/\epsilon_0=n^2(1-k^2). \quad . \; . \; . \; . \; . \; . \; . \; . \; . \quad (15)$$

Equation (15) must be remembered when comparing results of experiments in which the approaches are different—one from the condenser and the other from the wave standpoint.

If the dielectric is loss-free $\alpha'=0$, $X_0'=0$ and $R_0'=\omega L/\beta'=fL\lambda'$.

Equations (6) and (7) become

$$X_1=Z_0'\tan\beta's' \quad . \; . \; . \; . \; . \; . \; . \; . \quad (16)$$

and

$$X_2=-Z_0'\cot\beta's' \quad . \; . \; . \; . \; . \; . \; . \; . \quad (17)$$

respectively, so that

$$-X_1X_2=(Z_0')^2. \quad . \; . \; . \; . \; . \; . \; . \; . \quad (18)$$

Both X_1 and X_2 are measured in terms of Z_0, the characteristic impedance of the air-filled line. Then equation (18) becomes

$$-\left(\frac{X_1}{Z_0}\right)\left(\frac{X_2}{Z_0}\right)=\left(\frac{Z_0'}{Z_0}\right)^2=\left(\frac{\lambda'}{\lambda_a}\right)^2=\frac{1}{K}. \quad . \; . \; . \; . \quad (19)$$

Also, in the present case, one equation will suffice to give the dielectric constant. For example, equation (16) can be written as

$$\frac{X_1}{Z_0}=\frac{1}{\sqrt{K}}\tan\frac{2\pi}{\lambda_a}\sqrt{K}\,s', \quad . \; . \; . \; . \; . \; . \; . \quad (20)$$

and equation (17) as

$$\frac{X_2}{Z_0}=-\frac{1}{\sqrt{K}}\cot\frac{2\pi}{\lambda_a}\sqrt{K}s'. \qquad (21)$$

In either of these two equations, (20), (21), all the quantities are known except K, which can be calculated. For wave guides, it must be remembered that having obtained satisfactory values of λ' and K using equation (19) it does not follow that equations (16) and (17) are necessarily true. For instance, if

$$X_1=Z_0'\psi(\beta's') \quad \text{and} \quad X_2=-Z_0'/\psi(\beta's'),$$

where ψ is any function, equation (18) would be derived as before. The check on the analogy is given on solving equations (16) and (17) in the case of wave guides. If the value of K from these last two equations is the same as that from equation (19) then the analogy is verified.

Application to Wave Guides.

In order that the ideas may be applied to wave guides a method has to be evolved which will measure a quantity equivalent to impedance in the case of lines. The method suggested involves the use of a single movable probe which measures the potential difference in a line system (or its equivalent in a wave guide). A fixed probe can also be introduced into the guide, in a convenient position, to ensure that the output of the oscillator supplying energy is a constant, and that the effect of the movable probe on the wave pattern in the line or guide is negligible. These conditions will be satisfied if the reading on the meter attached to the fixed probe is a constant.

Fig. 3

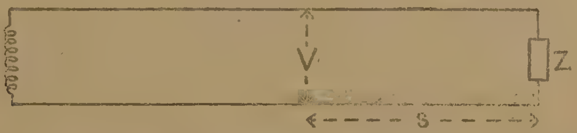

Referring to fig. 3, which represents a transmission line terminated by an impedance Z, it can be shown by the usual line theory that the potential difference is given by the equation

$$V=\frac{I_z Z_0}{\sinh r}\cosh(Ps+r), \qquad (22)$$

where I_z is the current through Z and r is a constant, Z_0 is the characteristic impedance of the line and $P=\alpha+j\beta$ is its propagation constant. r is related to Z by the equation

$$\frac{Z-Z_0}{Z+Z_0}=e^{-2r}, \qquad (23)$$

which represents the voltage reflection coefficient for Z. r is complex and is written in the form $a+jb$, so that from equation (23) it is seen that

$$Z=Z_0\coth(a+jb).$$

The real or resistive part of Z is thus

$$R=Z_0\frac{\sinh 2a}{\cosh 2a-\cos 2b}, \quad . \quad . \quad . \quad . \quad . \quad . \quad . \quad (24)$$

and the imaginary or reactive component of Z is

$$X=-Z_0\frac{\sin 2b}{\cosh 2a-\cos 2b}. \quad . \quad . \quad . \quad . \quad . \quad . \quad . \quad (25)$$

In practice it is the modulus of V which is measured. This is obtained from equation (22) and can be written

$$|V|^2=\frac{A}{2}[\cosh 2a+\cos 2(b+\beta s)], \quad . \quad . \quad . \quad . \quad . \quad (26)$$

where A is a constant for a given value of Z. This equation can be solved for a and b using a method described by Flint and Williams (1941).

The above reasoning applies in detail to wave guides, but here there may be some difficulty in interpreting the meaning of the term " characteristic impedance of a wave guide." This does not affect the method since the impedance concept simply represents another way of expressing the reflection of waves in a guide.

Thr introduction of the symbols a and b into wave guides is a departure from general practice, the usual procedure being to express the reflection coefficient in the guide as $\rho e^{j\phi}$, ρ being the fraction representing the percentage of amplitude reflected and ϕ the phase change on reflection. Hence $\rho=e^{-2a}$, $\phi=-2b$, and the modulus of V is given by

$$|V|^2=\frac{A}{4\rho}[1+\rho^2+2\rho\cos(2\beta s-\phi)]. \quad . \quad . \quad . \quad . \quad . \quad (27)$$

A/4ρ is a constant for any given " impedance."

In the practical work to be described later, the detector had a square law characteristic and it was equation (27) which was used to find ρ and ϕ, and hence the terminating " impedance." In terms of ρ, ϕ, equations (24) and (25) can be written

$$R=Z_0\frac{1-\rho^2}{1+\rho^2-2\rho\cos\phi} \quad . \quad . \quad . \quad . \quad . \quad . \quad . \quad (28)$$

$$X=Z_0\frac{2\rho\sin\phi}{1+\rho^2-2\rho\cos\phi}. \quad . \quad . \quad . \quad . \quad . \quad . \quad (29)$$

Application of Method.

The procedure adopted for wave guides is identical with that already described for lines. The guide is closed with a metal plate, which is a perfect reflector, and the " impedance " of the dielectric filled guide is measured with the dielectric in contact with the reflecting plate and also when it is moved a distance of one-quarter of a wave-length along the guide. A convenient method of measuring the " impedance " has been given.

The values of R_0' and X_0', which now refer to the dielectric-filled guide, can thus be determined in terms of Z_0, the " characteristic impedance" of the air-filled guide. The values of the attenuation constant (α_t') and phase constant (β_t') in the dielectric-filled guide are then obtained from equations similar to equations (11) and (12), no assumption regarding the value of Z_0 being necessary. The equivalent wave-guide expressions for H waves (which were used experimentally) are obtained from equations (11) and (12) by substituting λ_t, the wave-length in air in the guide, for λ_a. The value of the dielectric constant of the substance and its losses can then be calculated.

If the dielectric is loss free, equation (18) can be used to give the value of $\lambda_t'=2\pi/\beta_t'$, the wave-length in the dielectric in the guide. Again, the value of λ_t' may be obtained from equations (16) and (17) independently. For example, equation (16) can be written

$$Z_0 \cot \phi/2 = Z_0' \tan \beta_t' s', \quad \ldots \ldots \quad (30)$$

where $X_1=Z_0 \cot \phi/2$ is obtained from equation (29) by putting $\rho=1$. Now, substituting for Z_0 and Z_0', the equivalent wave-guide quantities $\mu\omega/\beta_t$ and $\mu\omega/\beta_t'$ respectively, we have

$$\frac{1}{\beta_t} \cot \phi/2 = \frac{1}{\beta_t'} \tan \beta_t' s', \quad (\alpha_t'=0),$$

that is,

$$\frac{\lambda_t}{\lambda_t'} \cot \phi/2 = \tan \frac{2\pi}{\lambda_t'} s'. \quad \ldots \ldots \quad (31)$$

This equation can readily be solved for λ_t' since ϕ, s' and λ_t are known. If λ_c is the cut-off wave-length for the air-filled guide we can write, for a substance having no losses,

$$\left(\frac{1}{\lambda_t'}\right)^2 = K\left(\frac{1}{\lambda_a}\right)^2 - \left(\frac{1}{\lambda_c}\right)^2, \quad \ldots \ldots \quad (32)$$

from which K can be calculated.

Experimental Results.

The method is most useful for solids and has been used to measure the properties of paraffin wax, distrene and ebonite. The results obtained for wax are given in detail to illustrate the use of the complete method.

An H_{10} wave was injected from a coaxial line resonator into a rectangular brass tube, of average cross-section, 6·97 and 3·50 cm., the air wave-length (λ_a) being 12·85 cm., and the wave-length (λ_t) in the tube 32·98 cm. A block of wax having a thickness of 1·05 cm. was first placed a distance of $\lambda_t/4=8{\cdot}25$ cm. from the short-circuiting plate at the end of the guide and a series of readings obtained using a probe detector at varying distances, *s*, from the front face of the block. The detector contained a coaxial tuning element and a crystal rectified the signal, the output being read on a microammeter. The results obtained are graphed in fig. 4.

The minimum reading is zero, showing that no losses were detected in the wax. It may have been that a thicker block of wax would show the losses: accordingly, a block, 3·21 cm. thick was made, but again no losses were observed and the dielectric constant was found to be substantially the same as for the thinner block. From equation (27) it is seen that the microammeter reading is a maximum when $\cos(2\beta_t s - \phi) = +1$, *i. e.*, $2\beta_t s - \phi = 2n\pi$ or $2s/\lambda_t = n + \phi/2\pi$, where n is an integer.

Fig. 4.

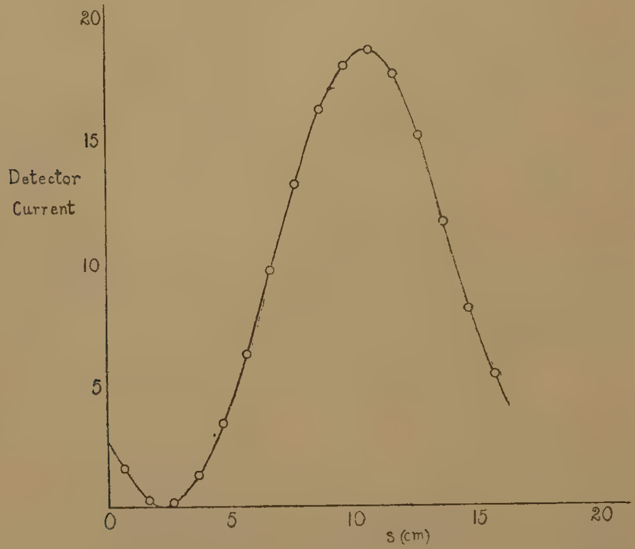

Fig. 5.

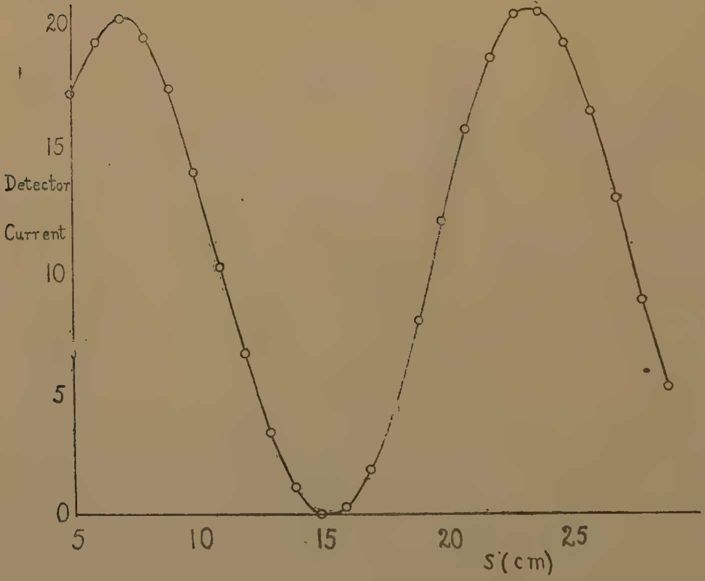

In the present case, $\lambda_t/2 = 16{\cdot}49$ cm. and the position of the maximum is given by $s = 10{\cdot}44$ cm. This gives a value for ϕ of 228° 0′, and, using equation (31), λ_t' is found to be 10·57 cm.

TABLE I.

Substance	Dielectric Constant
Paraffin Wax	2·32
Distrene	2·44
Ebonite	2·82

TABLE II.

Paraffin Wax.

$K=\epsilon/\epsilon_0$	λ_a	Authority
2–2·3	∞	Kaye and Laby, Tables.
2·22 2·21	15 cm.	Lamont.
2·32	13 cm.	Present Method.

TABLE III.

Distrene.

$K=\epsilon/\epsilon_0$	λ_a or f	Authority
2·6	60 c/s.	Plastics (1944)
2·55	$30 . 10^6$ c/s.	Plastics (1944).
2·47	15 cm.	Lamont.
2·41	10 cm.	Middleton.
2·44	13 cm.	Present Method.

TABLE IV.

Ebonite.

$K=\epsilon/\epsilon_0$	λ_a	Authority
2·7–2·9	∞	Kaye and Laby, Tables.
2·82	13 cm.	Present Method.

The wax was then pushed to the end of the guide and a further series of readings was obtained. These are shown in fig. 5.

The value of ϕ obtained from the positions of both the maximum and minimum is 154° 4′ which in equation (17) gives λ_t' as 10·67 cm.

Using both results in equation (18), λ_t' is 10·56 cm. These three values of λ_t' are experimentally independent and, substutiting their average in equation (32), the dielectric constant is calculated as 2·32. For the H_{10} wave, the cut-off air wave-length is twice the width of the tube in the x direction; here $\lambda_c=13{\cdot}94$ cm.

The results so far obtained, using the method, are given in Table I. As would be expected, the losses in each case are too small to be detected by the method.

Tables II., III., IV. compare the values of dielectric constants found by the present and other methods.

The accuracy of the values given by the present method depends upon the precision with which the curves can be obtained, in particular the positions of the maxima and minima relative to that of the front face of the dielectric block. In every case, several curves were plotted similar to figs. 4 and 5 and average values obtained. Considering the value of the wave-length in the dielectric in the guide, the maximum deviation of any single value from the average was 3 per cent.: this gives some idea of the order of accuracy expected in the final results.

Dielectric losses in solids due to permanent dipoles in their structure are almost certainly absent at these high frequencies as their "inner viscosity" is too high. The above method may be adapted for measuring the losses in liquids, however. On account of the difficulty of varying the thickness of the solid slab of dielectric the majority of experiments are resonance methods to find dielectric constant, *e. g.*, King (1937) and Kusters (1944) on Lecher lines, Lamont (1940), Middleton (1943), Fejér and Scherrer (1943) in hollow tubes. Standing wave methods were used by Velasco and Hutchinson (1939), and Roberts and Hippel (1940), the latter of whom have only announced their work in abstract form. The ideas underlying the present method are different again and the fact that different methods give results of the same order, remembering that all three substances can vary in purity and composition, is indication of the correctness of the Impedance Concept on which the present work is based.

References.

Eckert, *Ver. Deut. Phys. Ges.* xv. p. 307 (1913).
Fejér and Scherrer, *Helv. Phys. Acta.* xiv. p. 141 (A) (1941); xv. p. 645 (1943).
Flint and Pincherle, Proc. Phys. Soc. lv. p. 329 (1943).
Flint and Williams, Phil. Mag. xxxii. p. 489 (1941).
Jackson and Huxley, J. I. E. E. (Sept.) xci. pt. 3, p. 105 (1944).
King, Rev. Sci. Inst. viii. p. 201 (1937).
Knerr, Phys. Rev. lii. p. 1054 (1937).
Kusters, 'Wireless Engineer' (Jan.) xxi. p. 13 (1944).
Lamont, Phil. Mag. xxix. p. 521; xxx. p. 1 (1940).
Lamont, 'Wave Guides,' Methuen (1942).
Middleton, Phys. Rev. lxiii. p. 343 (1943).

Mobius, *Ann. der Phys.* lxii. p. 293 (1920).
Couzens and Wearmouth, ‘Plastics in the Radio Industry,’ Hulton Press (1944).
Roberts and Hippel, Phys. Rev. lvii. p. 1056 (A) (1940).
Schelkunoff, P. I. R. E. xxv. p. 1457 (1937).
Schelkunoff, B. S. T. J. xvii. p. 17 (1938).
Stratton, ‘Electromagnetic Theory’ (1941).
Tear, Phys. Rev. xxvii. p. 611 (1923).
Velasco and Hutchinson, Proc. Phys. Soc. li. p. 689 (1939).
“Wave Guide Discussion,” J. I. E. E. (Sept.) xci. pt. 3, p. 145 (1944).

CV. *Noticec respecting New Books.*

Physics and Experience. By Bertrand Russell. [Pp. 26.] (Cambridge University Press, 1946.) Price 1*s.* 6*d.*

The question propounded for discussion in this Henry Sidgwick lecture is: “Assuming physics to be, broadly speaking, true, can we know it to be true,” and, if so, “does this involve knowledge of other truths besides those of physics?” No clear-cut answer seems to be given to this question, but in the course of the discussion a brief but penetrating analysis is given of a number of problems which are fundamental and relevant. A consideration of the idealist and empirical theories of perception leads to a discussion of the relation between physical and mental occurrences, a mental occurrence being defined, after rejection of some of the current definitions, as one which can be known without inference. The causal status of percepts is discussed, and the relation between perceptual and physical space. How percepts, in which physical and mental overlap, can be a source of knowledge as to physical objects becomes the central question on which attention is focussed; but, after a statement that the principles justifying inference from percepts to physical objects have not been sufficiently studied, the lecture ends somewhat abruptly, with a summary, in which the conclusion seems to be that such inference cannot be precise, and that science largely consists of devices for overcoming the initial lack of precision. The attempt to deal adequately with so large a theme within the limits of a single lecture was, perhaps, foredoomed to failure. It is as though the lecturer, having guided his audience to a central issue, and roused their interest in what he might have to say on it, was given thirty seconds to state his conclusions—and was not quite ready to do so. It is a little tantalizing. And yet, how much is here! For, in a few effortless paragraphs, Russell seems to get nearer to the core of the problems touched upon than do others in as many laboured chapters. E. C. S.

The Advancement of Science. Vol. III., No. 11. [Pp. 225–281.] (British Association, November 1945.) Price 5*s.* 0*d.*

In the previous issue of this journal (May, 1945) a series of articles was begun under the general heading “Applications of Science.” It is intended to issue each of the articles in separate pamphlet form, as circumstances permit. The bulk of the present issue is made up of four further articles in the series, dealing with science in education (by A. E. E. McKenzie), producing oils (G. D. Hobson), plant breeding and genetics (P. S. Hudson), and science in building (J. L. Martin). The articles are similar in length, between 10,000 and 13,000 words, but very diverse in character. They are, in fact, individual studies of particular fields in which science is involved in one way or another.

McKenzie's article reviews the place that science occupies and might occupy in school, university and adult education, and sketches the kind of presentation of science, particularly in its historical, philosophical and sociological aspects, which might be appropriate in general education. The problem of what to leave out in present educational curricula is not faced, and it is perhaps too lightly assumed that an appreciation of scientific methods can be conveyed without the time and effort required to gain some mastery of the technical weapons. The specialist tendency to miss the major issues through undue concentration on details is, however, only too apparent, and it is not peculiar to any one branch of human activity or study; and those who wish to see "more science for the non-scientist," would do well to urge also "less science for the scientist." This negative is not so crudely stated, though it is perhaps implicit in the article, which contains much to provoke thought, and action, by any who are concerned with the teaching of science.

An enormous amount of information, perhaps too much, is packed into the article by Hobson on the production and preparation of oils. The recovery and uses of animal and vegetable oils and fats; the nature of oil pools; the drilling of wells; oil production and reserves; refining, cracking, hydrogenation; petroleum substitutes: these are a few of the topics surveyed. Those requiring the facts about oil in brief space could hardly be better served.

In contrast, Martin's article about science in building gives almost no factual information at all, but rather an analysis of what is required in buildings (warmth, light, freedom from noise), and of the questions involved in the choice of the materials and methods to be used in building. The general thesis is that "towns and buildings can be the means of enriching human life if we are prepared to recognize—and use— the knowledge that exists." The argument would be strengthened if more examples were given of the data provided by scientific investigation. In the article itself, the assertions, though no doubt fully justified, seem to lack illustrative backing. Fairly full references are, however, given, and with the proviso that a scientific knowledge of what is required in buildings and how to build goes but a small way to the actual provision of large numbers of houses, this article may be strongly commended to those directly and indirectly responsible for putting them up.

Hudson gives an admirable review of recent progress in "Plant breeding and genetics to-day," an article as easy to read as it would be to listen to a good talk. The article is not technical (there are, for example, no references), but there is no writing down; the background required in the reader is that which may be assumed as common to all those who have some familiarity with the studies of Darwin and Mendel on inheritance, and with the more recent work on chromosomes. Many fascinating examples are given of the successful use of hybridisation in the solution of economic problems. The final section deals with non-Mendelian inheritance and the "genetics controversy," in which, largely as a result of remarkable Russian work in recent years, some of the long-accepted principles of inheritance are again open to question.

A journal of this kind naturally falls mainly into the hands of the "converted," who will usually have ready access to other sources of information on the subjects with which these articles deal. If others, too, are induced to read only such of the articles, possibly when they are issued in pamphlet form, as appear to have a direct bearing on their own activities, an important advance will have been made by the British Association towards its primary objective, "to promote general interest in science and its applications."

E. C. S.

[The Editors do not hold themselves responsible for the views expressed by their correspondents.]

Fig. 5.

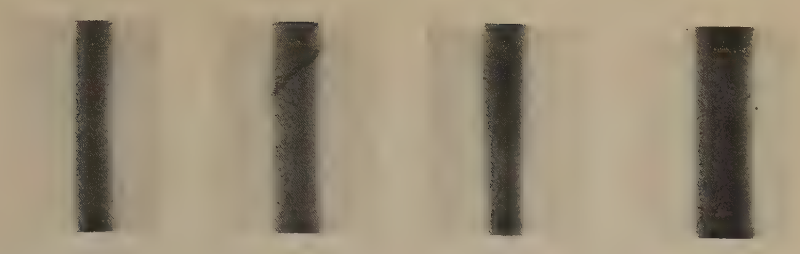

North (165)
East (255)
South (175)
West (260)

Fig. 6.

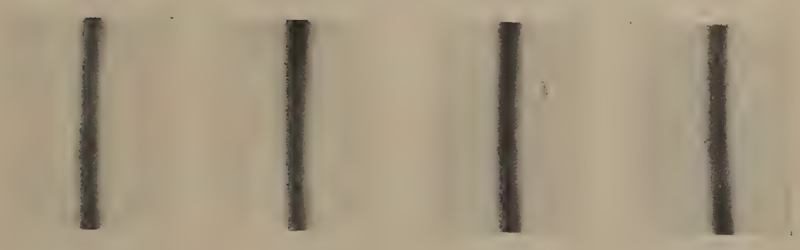

North (120)
East (120)
South (130)
West (120)

Fig. 7.

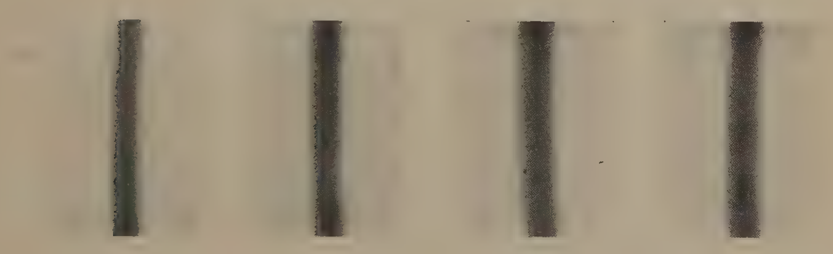

North (130)
East (160)
South (190)
West (165)

Fig. 8.

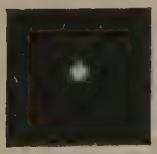

INDEX TO VOL. XXXVI.

ACCUMULATION of chance effects and the Gaussian frequency distribution, on the, 294.

—— of chance effects and the Gaussian frequency distribution, 428.

Addison (C. C.), the measurement of surface and interfacial tensions at fresh surfaces by the vibrating jet method, 73.

Aggregates in one- and two-dimensional random distributions. (Developability of silver specks of known dimensions and the size of photographic sensitiviry specks), 337.

—— in random distributions of points, probable number of, 319.

Archbold (J. W.), second note on condensation in the form of clouds and dew, 414.

Asymptotic series, a note on a particular type of, 860.

Bates (L. F.), the magnetic potentiometer study of permanent magnets, 297.

Behaviour of glass under impact and static loading, 777.

—— of liquids in a vibrating air column, 20.

—— of liquids in shear, 490.

Berg (W. F.), aggregates in one- and two-dimensional random distributions. (Developability of silver specks of known dimensions and the size of photographic sensitivity specks), 337.

Bickley (W. G.), notes on the evaluation of zeros and turning values of Bessel functions.—III. Interpolation by Taylor series, 131.

—— and Miller (J. C. P.), notes on the evaluation of zeros and turning values of Bessel functions. —I. Introductory, 121 ; II. The McMahon Series, 124.

Bickley (W. G.) and Miller (J. C. P.), notes on the evaluation of zeros and turning values of Bessel functions.—V. Checks, 206.

Bloch (A.), systems with gyroscopic coupling terms, 440.

Bolton (H. C.) and Williams (G.), the use of the impedance concept as applied to wave guides, 862.

Books, new :—Five-figure Logarithm Tables, 145 ; Prof. G. N. Watson, A Treatise on the Theory of Bessel Functions, 146 ; Mathematical Tables and other Aids to Computation, 147 ; E. Schrödinger, What is Life ? 147 ; Dr. M. Davidson, From Atoms to Stars, 149 ; Sound Insulation and Acoustics, 150 ; S. L. Green, An Introduction to Differential Equations, 150 ; N. E. Dorsey, The Velocity of Light, 151 ; F. Emde, Tables of Elementary Functions, 296 ; H. Brandenburg, Sechsstellige Trigonometrische Tafel, 296 ; R. Belcher and A. L. Godbert, Semi-Micro Quantitative Organic Analysis, 369 ; A. W. Stewart and C. L. Wilson, Recent Advances in Physical and Inorganic Chemistry, 370 ; Building Research Board's Report on the Lighting of Buildings, 441 ; A. Talalay and M. Magat, Synthetic Rubber from Alcohol, 442 ; The Advancement of Science (British Association), 514 ; C. W. Bunn, Chemical Crystallography, 586 ; Table of Arcsin x : prepared by the Mathematical Tables Project, 657 ; A. Weissberger, Physical Methods of Organic Chemistry, 658 ; R. E. Burk and O. Grummitt, Frontiers in Chemistry, 728 ; Dr. E. I. Rabinavitch, Photosynthesis and Related Processes, 728 ; Tables of

Associated Legendre Functions. Prepared by the Mathematical Tables Project, 729; F. B. Puddick, Currents in Aerials and High Frequency Networks, 730; Circular and Hyperbolic Functions (B. A. Mathematical Tables, Vol. I.); A. Wood, The Cavendish Laboratory, 802; Bertrand Russell, Physics and Experience, 873; The Advancement of Science, Vol. III. No. 11 (British Association), 873.

Booth (A. D.), an expression for following the process of refinement in X-ray structure analysis using Fourier Series, 609.

Bowden (S. T.) and Jones (W. J.), a power law of the viscosity of liquids, 705.

Brindley (G. W.), the effect of grain or particle size on X-ray reflections from mixed powders and alloys, considered in relation to the quantitative determination of crystalline substances by X-ray methods, 347.

Buckling of flat rectangular plywood plates, 659.

Burgess (R. E.), comments on Dr. Silberstein's paper in Phil. Mag. 1944, 143.

Butler (C. C.) and Rymer (T. B.), the precision of measurement of broad spectrum lines, with special reference to electron-diffraction photographs, 515.

—— ——, the technique of precise electron-diffraction measurements with polycrystalline specimens, 821.

Campbell's theorem of random fluctuations, an extension of, 688.

Chance effects and the Gaussian distribution, 184.

Change produced by spraying liquids with a jet of air, a note on the, 218.

Characteristic equation of a matrix, the application of the, to the evaluation of the range of frequencies for which currents are passed through networks with four or more terminals without attenuation, 255.

Chih-En (G.), a note on the change produced by spraying liquids with a jet of air, 218.

Christian (J. W.) and Hume-Rothery (W.), the equilibrium diagrams of certain alloys of iron, 835.

Coefficients for mid-internal numerical integration with central differences, 216.

Coleman (A. J.), phase space in Eddington's theory, 269.

Commutative functions, construction of groups of, 43.

Compatibility of stress and strain in yielded metals, 443.

Computation of the solution of Mathieu's equation, 403.

Condensation in the form of clouds and dew, second note on, 414.

Craggs (J. W.), heat conduction in semi-infinite cylinders, 220.

—— and Tranter (C. J.), the stress distribution in a long circular cylinder when a discontinuous pressure is applied to the curved surface, 241.

Crystalline sheen of moonstones, 719.

Dalzell (D. P.), a summary statement of the principles of measurement, 485.

Davy (N.), a closer approximation to the theory of the field of Gerlach-Stern magnets, 852.

Davy (N.), ten two-dimensional electrostatic problems, 153.

——, the two-dimensional electric field of a simple semi-infinite rectangular conductor, 694.

Demagnetizing factors for ellipsoids, 803.

Deutsch (W.) on the pseudo-plastic state, 115.

Dielectric constants of liquids flowing through narrow separations, on the change in the, 622.

Drainage of a vertical plate, 581.

Drew (H. D. K.), a relation between some natural constants and the lesser particles, 577.

Duncan (W. J.), factorization of a class of determinants and applications to dynamical strains, 615.

——, the principal directions of loading and the principal directions of forced oscillation at a point of an elastic body or system, 715.

Durant (N. J.), an application of the method of finite difference equations to a problem of bending moments.—Continuous beam of N equal spans under transverse loading and an axial force, 569.
——, struts of variable flexural rigidity, 572.
Eddington's theory, phase space in, 269.
Ede (A. J.), a new form of chart for determining temperatures in bodies of regular shape during heating or cooling, 845.
Edmunds (I. G.) and Owen (E. A.), study of the relative intensities of lines in fibre X-ray camera photographs, 54.
Ehrenberg (W.), entropy and irreversible processes, 250.
Electric intensity near an aerial cage, determination of, 758.
Electrical resonance, a new type of, 371.
Electromotive force of the selenium barrier-layer photo-cell, 279.
Electron-diffraction measurements with polycrystalline specimens, the technique of precise, 821.
Energies of uniformly accelerated particles in a gas, 185.
Energy and mechanical relations of the magnetic field, on the, 1.
Entropy and irreversible processes, 250.
Equations of plane plastic flow, a note on the, 629.
Equilibrium diagrams of certain alloys of iron, 835.
Expansion in series of the exact solution for compressible flow past a circular or an elliptic cylinder, 499.
Factorization of a class of determinants and applications to dynamical chains, 615.
Ferguson (A.), the Whipple collection of historic scientific instruments, 144.
Finite difference equations, an application of the method of, to a problem of bending moments.—Continuous beam of N equal spans under transverse bending and an axial force, 569.
Flint (H. T.), quantum equations and nuclear field theories, 635.
Freeman (G. F.), note on the Helmholtz make - and - break theorem and an application to the Wheatstone net, 541.
Friend (J. W.) and Hargreaves (W. D.), viscosity and the hydrogen bond. Hydroscyl and ortho effects, 731.
Gerlach-Stern magnets, a closer approximation to the theory of the field of, 852.
Goddard (L. S.), the accumulation of chance effects and the Gaussian frequency distribution, 428.
Green (A. E.) and Hearmon (R. F. S.), the buckling of flat rectangular plywood plates, 659.
Grimsey (A. H. R.) on the accumulation of chance effects and the Gaussian frequency distribution, 294.
Ground-water accumulation, theory of, 651.
Gyroscopic coupling terms, 223.
Haldane (J. B. S.), chance effects and the Gaussian distribution, 184.
Hammad (A.), the primary and secondary scattering of sunlight in a plane-stratified atmosphere of uniform composition.—Part II. Numerical tables and discussion of the directional distribution of the primary scattered light, 434.
Hargreaves (W. D.), a viscometer with constant working volume suitable for measurements over a wide range of viscosities, 756.
Hargreaves (W. D.) and Friend (J. N.), viscosity and the hydrogen bond. Hydroxyl and ortho effects, 731.
Haward (R. N.), the behaviour of glass under impact and static loading, 777.
Hearmon (R. F. S.) and Green (A. E.), the buckling of flat rectangular plywood plates, 659.
Heat conduction in elliptical cylinder and an analogous electromagnetic problem, 600.
—— —— in semi-infinite cylinders, 220.

Helmholtz make-and-break theorem and an application to the Wheatstone net, note on the, 541.
—— resonator, the application of the, to the measurement of sound absorption, 473.
Historical note on a paradox in electrodynamics, 32.
Hopkins (H. H.), monochromatic lens aberration theory, 546.
Houstoun (R. A.) and Howatson (A. F.), the electromotive force of the selenium barrier-layer photo-cell, 279.
Howatson (A. F.), the behaviour of liquids in a vibrating air column, 20.
—— and Houstoun (R. A.), the electromotive force of the selenium barrier-layer photo-cell, 279.
Hume-Rothery (W.) and Christian (J. W.), the equilibrium diagrams of certain alloys of iron, 835.
—— and Lonsdale (K.), the lattice spacing of rubidium between $-183°$ C. and $+19°$ C., 842.
—— ——, the lattice spacings of lithium at 20° C. and $-183°$ C., 799.
Impedance concept as applied to wave guides, the use of the, 862.
Intensities, relative, of lines in fibre X-ray camera photographs, study of the, 54.
Interferometry, new contributions to. Part V.—New multiple beam white light interference fringes and their applications, 225.
——. Part VI.—White light Fabry-Perot fringes, 236.
Ives (H. E.), derivation of the Lorentz transformations, 392.
Jaegar (J. C.) on thermal stresses in circular cylinders, 418.
——, switching problems and instantaneous impulses, 644.
Jefferson (H.), gyroscopic coupling terms, 223.
Jones (C. W.) and Miller (J. C. P.), notes on the evaluation of zero and turning values of Bessel functions.—IV. A new expansion, 200.
Jones (W. J.) and Bowden (S. T.), a power law of the viscosity of liquids, 705.
Kinematic relativity, 113.
—— ——: a reply to Prof. W. Wilson, 134.
—— ——, on the vectors and invariants of, 170.
Laminar flow in an incompressible boundary-layer with mainstream velocity $U \propto x^m$ or $U \propto e^{\alpha x}$, calculations concerning theoretical values of boundary-layer thickness and coefficients of friction and of heat transfer for steady two-dimensional, 587.
Lattice spacings of lithium at 20° C. and $-183°$ C., 799.
—— spacing of rubidium between $-183°$ C. and $+19°$ C., 842.
Lewis (T.), some criticisms of the theory of point electrons, 533.
Light-scattering, on the theory of, a note, 510.
Liquids in shear, the behaviour of, 490.
Livens (G. H.) on the energy and mechanical relations of the magnetic field, 1.
Lonsdale (K.) and Hume-Rothery (W.), the lattice spacings of lithium at 20° C. and $-183°$ C., 799.
—— ——, the lattice-spacing of rubidium between $-183°$ C. and $+19°$ C., 842.
Lorentz transformations, derivation of the, 392.
Lowry (H. V.), the application of the characteristic equation of a matrix to the evaluation of the range of frequencies for which currents are passed through networks with four or more terminals without attenuation, 255.
Löwy (H.), theory of ground-water accumulation, 651.
Magnetic potentiometer study of permanent magnets, 297.
Manwell (A. R.), expansion in series of the exact solution for compressible flow past a circular or an elliptic cylinder, 499.
McCormick (H.), the surface tension of molecular solutions, 288.
McLachlan (N. W.), computation of the solution of Mathieu's equation, 403.

McLachlan (N. W.), heat conduction in elliptical cylinder and an analogous electro-magnetic problem, 600.

Miller (J. C. P.) and Bickley (W. G.), notes on the evaluation of zeros and turning values of Bessel functions.—I. Introductory, 121.

—— ——. II. The McMahon Series, 124.

—— ——, notes on the evaluation of zeros and turning values of Bessel functions.—V. Checks, 206.

—— and Jones (C. W.), notes on the evaluation of zeros and turning values of Bessel functions.—IV. A new expansion, 200.

Milne (E. A.), kinematic relativity: a reply to Prof. W. Wilson, 134.

Monochromatic lens aberration theory, 546.

Multiple integral, a certain, 224.

Nelson (J. B.) and Riley (D. P.), orientation effect in powder photographs of graphite, 711.

Newing (R. A.), kinematic relativity, 113.

Oldroyd (J. G.), calculations concerning theoretical values of boundary-layer thickness and coefficients of friction and of heat transfer for steady two-dimensional laminar flow in an incompressible boundary layer with mainstream velocity $U \propto x^m$ or $U \propto e^{\alpha x}$, 587.

Orientation effect in powder photographs of graphite, 711.

Owen (E. A.) and Edmunds (I. G.), study of the relative intensities of lines in fibre X-ray camera photographs, 54.

Parthasarathy (S.), on the theory of light-scattering, a note, 510.

Phase space in Eddington's theory, 269.

Point electrons, some criticisms of the theory of, 533.

Precision of measurement of broad spectrum lines, with special reference to electron-diffraction photographs, 515.

Primary and secondary scattering of sunlight in a plane-stratified atmosphere of uniform composition.—Part II. Numerical tables and discussion of the directional distribution of the primary scattered light, 434.

Principal directions of loading and the principal directions of forced oscillation at a point of an elastic body or system, 715.

Principles of measurement, a summary statement of, 485.

Probable number of aggregates in random distributions of points, 319.

Pseudo-plastic state, on the, 115.

Quantum equations and nuclear field theories, 635.

Rankin (R. A.), a note on a particular type of asymptotic series, 860.

Raynor (G. V.), on the solid solutions of chromium and manganese in aluminium, 770.

Relation between some natural constants and the lesser particles, 577.

Richardson (E. G.), the behaviour of liquids in shear, 490.

Riley (D. P.) and Nelson (J. B.), orientation effect in powder photographs of graphite, 711.

Rivlin (R. S.), an extension of Campbell's theorem of random fluctuations, 688.

Roberts (J. E.), spectrum of radium (B and C) gamma-rays, 264.

Robertson (I. A.), an historical note on a paradox in electrodynamics, 32.

Rymer (T. B.) and Butler (C. C.), the precision of measurement of broad spectrum lines, with special reference to electron-diffraction photographs, 515.

—— ——, the technique of precise electron-diffraction measurements with polycrystalline specimens, 821.

Salzer (H. E.), coefficients for mid-interval numerical integration with central differences, 216.

Schneider (E. E.), a new type of electrical resonance, 371.

Sen (B.), direct determination of stresses from the stress equations in some two-dimensional problems of elasticity.—Part IV. Problems of wedges, 66.

——, stresses in an infinite plate due to isolated forces and couples acting near a circular hole, 211.

Silberstein (L.), construction of groups of commutative functions, 43.
——, the probable number of aggregates in random distributions of points, 319.
Silberstein's paper in Phil. Mag. 1944, comments on, 143.
Simmonds (J. C.), determination of the electric intensity near an aerial cage, 758.
Simpson (H.), a certain multiple integral, 224.
Singh (B. N.) and Singh (B. D.) on the change in the dielectric constants of liquids flowing through narrow separations, 622.
Sneddon (I. N.), a note on the equations of plane plastic flow, 629.
Solid solutions of chromium and man ganese in aluminium, on the, 770.
Spectrum of radium (B and C) gamma-rays, 264.
Spin in the universe, 101.
Stevenson (A. C.), tension of semi-infinite plate with notched boundary, 178.
Stoner (E. C.), the demagnetizing factors for ellipsoids, 803.
Stress distribution in a long circular cylinder when a discontinuous pressure is applied to the curved surface, 241.
Stresses, direct determination of, from the stress equations in some two-dimensional problems of elasticity.—Part IV. Problems of wedges, 66.
—— in an infinite plate due to isolated forces and couples acting near a circular hole, 211.
Struts of variable flexural rigidity, 572.
Surface tension of molecular solutions, 288.
Swainger (K. H.), compatibility of stress and strain in yielded metals, 443.
Switching problems and instantaneous impulses, 644.
Systems with gyroscopic coupling terms, 440.
Temperatures in bodies of regular shape during heating or cooling, a new form of chart for determining, 845
Ten two-dimensional electrostatic problems, 153.
Tension of semi-infinite plate with notched boundary, 178.
Tensions, the measurement of surface and interfacial, at fresh surfaces by the vibrating jet method, 73.
Thermal stresses in circular cylinders, 418.
Thosar (B. V.), crystalline sheen of moonstones, 719.
Tolansky (S.), new contributions to interferometry. Part V.—New multiple beam white light interference fringes and their applications, 225.
——. Part VI.—White light Fabry-Perot fringes, 236.
Tranter (C. J.) and Craggs (J. W.), the stress distribution in a long circular cylinder when a discontinuous pressure is applied to the curved surface, 241.
Tucker (W. S.), the application of the Helmholtz resonator to the measurement of sound absorption, 473.
Two-dimensional electric field of a single semi-infinite rectangular conductor, 694.
Viscometer with constant working volume suitable for measurements over a wide range of viscosities, 756.
Viscosity and the hydrogen bond. Hydroxyl and ortho effects, 731.
—— of liquids, a power law of the 705.
Whipple collection of historic scientific instruments, 144.
Whitrow (G. J.) on the vectors and invariants of kinematic relativity, 170.
Whittaker (E. T.), spin in the universe, 101.
Williams (G.) and Bolton (H. C.), the use of the impedance concept as applied to wave guides, 862.
Wyllie (G.), drainage of a vertical plate, 581.
X-ray reflections from mixed powders and alloys, the effect of grain or particle size on, considered in relation to the quantitative determination of crystalline substances by X-ray methods, 347.

X-ray structure analysis using Fourier series, an expression for following the process of refinement in, 609.

Yarnold (G. D.), the energies of uniformly accelerated particles in a gas, 185.

Zeros and turning values of Bessel functions, notes on the evaluation of.—I. Introductory, 121.

——. II. The McMahon Series, 124.

——. III. Interpolation by Taylor Series, 131.

——. IV. A new expansion, 200.

——. V. Checks, 206.

END OF THE THE THIRTY-SIXTH VOLUME.

PRINTED IN GREAT BRITAIN BY TAYLOR AND FRANCIS, LTD.
RED LION COURT, FLEET STREET, LONDON, E.C.4.

DATE DUE

UIC AUG 13 '02

UIC Rec

9/02/'02

FEB 18 2009

UIC-REC'D AUG 28 '02

DEMCO 38-297

BOUND BY
LINNEMANN
[illegible], MD.